KANSAS GEOLOGICAL SURVEY
OPEN-FILE REPORT 96-10

LITHOFACIES AND DIAGENSIS OF THE UPPER ORDOVICIAN VIOLA FORMATION ON THE CENTRAL KANSAS ARCH AND ADJACENT BASINS

by

K. David Newell

Disclaimer

The Kansas Geological Survey does not guarantee this document to be free from errors or inaccuracies and disclaims any responsibility or liability for interpretations based on data used in the production of this document or decisions based thereon. This report is intended to make results of research available at the earliest possible date, but is not intended to constitute final or formal publications.

Kansas Geological Survey
1930 Constant Avenue
University of Kansas
Lawrence, KS 66047-3726

ABSTRACT

K. David Newell, December 1995
University of Kansas

The Upper Ordovician Viola Formation, an important petroleum reservoir in the midcontinent, is a carbonate unit present over much of the subsurface in Kansas. The Viola is composed of two fining-upward sedimentary packages that are vertically separated from each other by a minor karstic surface representing a brief period of exposure. Each package represents a third-order sedimentary cycle and consists of a echinoderm-rich packstone overlain by a thicker lime mudstone. The echinoderm-rich grainstones and packstones were deposited in nearshore areas in agitated waters, but subsequently were bioturbated. Finer-grained facies were deposited in deeper, quiet waters, and locally contain storm-deposited carbonate sands. Subtle growth of the Central Kansas arch and Pratt anticline (structures transecting the depositional shelf) is indicated by packstones and grainstones being thicker over these arches, whereas finer-grained lithologies dominate adjacent basinal areas.

Diagenetic events and their progressions in both sedimentary packages are approximately similar. Original porosity in the packstones and grainstones was occluded early by syntaxial spar. The best present porosity is intercrystalline, moldic, and vuggy porosity developed in dolomitized mudstones and wackestones. Viola subunits are dolomitized near their pinchouts and along the crest of the Chautauqua and Central Kansas arches, but these subunits tend to be undolomitized where they underlie outliers of the overlying Maquoketa Shale. Recrystallized dolomite is common at the crests of these early Paleozoic arches, whereas unrecrystallized dolomite with pristine concentric zonation dominates flanking areas. Fluid inclusions, stratigraphic relationships, stoichiometry, and oxygen-isotopic data indicate that dolomite recrystallization was by hypersaline reflux at depths less than 100 m. Strontium isotopic data and crosscutting relationships of the dolomite with karstic breccias beneath unconformities at the top of the Viola indicate this recrystallization occurred in Silurian time.

Saddle dolomite precipitated in vugs and fractures during late-stage diagenesis. Fluid-inclusion temperatures in excess of that which could be expected by projected burial and normal geothermal gradients indicate that this saddle dolomite likely precipitated from hot brines derived from the Anadarko basin, probably during the Late Pennsylvanian to Early Permian Ouachita orogeny.

ACKNOWLEDGMENTS

Several individuals have been very helpful during my long process of study and research for this degree at the University of Kansas. I first want to gratefully acknowledge Drs. Paul Enos, Robert Goldstein, and John Doveton for their helpful suggestions with regard to my research, and for their many beneficial comments on the text and content of this dissertation. The thorough and detailed geologic editing by Dr. Enos greatly improved this text. I also thank him for returning to Lawrence from sabbatical in Europe for the Final Defense. Constructive criticism on the manuscript by Drs. Ernest Angino and William Johnson, also committee members, are also greatly appreciated.

Several individuals provided ancillary support to the research. These individuals include Robert Goldstein for Raman spectroscopy and helpful commentary and encouragement for fluid-inclusion work, Doug Walker for help in preparation of samples for isotopic analyses, Mike Magnuson for laboratory support and x-ray diffraction and SEM analyses, Dana Adkins-Heljeson and Alan Feltz for trouble-shooting problems with computer mapping, Janice Sorensen for help in library searches, Charles Ross for use of his computer program for conversion of geographic coordinates, Christopher Maples for use of facilities of the Geologic Investigations Section of the Kansas Geological Survey, John Charlton for some of the photographic developing, Bryan Stephens for instruction in the art of making thin sections, Larry Mason for search and retrieval of cores, Michael Lambert for help in obtaining well logs, Jack Wilson for facilitating donation of the Damac #1 Sandra Allen core, Ian Rowell for guidance in sample preparation, and LeaAnn Davidson for helping put the final version of the dissertation in order. The contributions of others are credited in the text.

I also want to thank Dr. Lee C. Gerhard and Dr. Lawrence Brady of the Kansas Geological Survey for their patience and indulgence in allowing me to temporarily pare my employment and responsibilities at that institution in order to finish the research and writing. I was also supported by the Department of Geology Shell Research Fellowship for a one-year leave-of-absence from the Survey. A travel grant from Graduate School of the University of Kansas also defrayed expenses during this leave-of-absence. Laboratory expenses for isotopic analyses were borne by the Kansas Geological Survey and the Geology Associates Program of the University of Kansas Department of Geology.

Several individuals have been supportive and encouraging. These individuals are: my parents, Robert H. and Mae L. Newell, my brother Keith D. Newell, my sister Joyce K. Byrer, and brother-in-law James Byrer; colleagues at the Kansas Geological Survey, including Howard Feldman, Evan Franseen, LeaAnn Davidson, Michael Lambert, Sara Marcus, Willard Guy, Lawrence Brady, Robert Sawin, Rex Buchanan, Christopher Maples, Dan Merriam, and Janice Sorensen; and other professional associates and friends, including Jack Wilson, Dr. J. Fred Stone, Dr. L.W. Slentz, and Dr. Ian Johnston and Barbara Johnston. The encouragement these people conveyed to me sustained my confidence and concentration through several trying but unrelated circumstances I experienced during my course of study at the University of Kansas.

TABLE OF CONTENTS

Abstract ii
Acknowledgments iii
List of Figures vii
List of Tables xx
List of Appendices xx

Chapter 1 -- Introduction 1

Chapter 2 -- Regional Geologic Setting 6
Regional Middle and Upper Ordovician Time-Rock Classification 6
The Tippecanoe Transgression 9
Middle and Late Ordovician Paleogeography and Climates 12
Plate Configuration and Associated Tectonic Events 12
Middle and Late Ordovician Climate 13

Chapter 3 -- Middle and Upper Ordovician Lithostratigraphy in the Midcontinent 19
Simpson Group 19
St. Peter Sandstone 19
Platteville Formation 25
Viola Formation 27
Maquoketa Formation 32

Chapter 4 -- Local Geologic Setting and Stratigraphy of Viola Formation 37
Structure, Thickness, and Relationship to Other Geologic Units 37

Chapter 5 -- Stratigraphic Framework of the Viola Limestone in Kansas 47
Previous Studies 47
Methods and Procedures 52
Results and Discussion 63
Subcrop Mapping 63
Regional Isopach Mapping 68
Basal Limestone 68
Lower Cherty Dolomitic Limestone 78
Upper Limestone 87
Upper Cherty Dolomitic Limestone 92
Discussion 95
Detailed Mapping over Pratt Anticline 96
Relationship of Viola Stratigraphy to Petroleum Production 114

Chapter 6 -- Thermal and Burial History of the Viola in the Study Area 125
Introduction 125
Data Constraints for Time-Temperature Index (TTI) Modeling 127
TTI Models and Results 136
Comparison of TTI Modeling to Organic Maturation Data 142
Rock-Eval Data 144
Vitrinite Reflectance Data 155
Comparison of TTI Modeling to Fluid-Inclusion Data 160

TABLE OF CONTENTS (con't.)

Summary 164

Chapter 7 -- Lithofacies of the Viola Formation 166
Introduction 166
Methods and Procedures 167
Basal Limestone 172
Observations 172
Interpretations 183
Lower Cherty Dolomitic Limestone 188
Observations 188
Interpretations 204
Upper Limestone 208
Observations 208
Interpretations 209
Upper Cherty Dolomitic Limestone 213
Observations 213
Interpretations 225
Upper Contact of the Viola 228
Observations 228
Interpretation 229
Discussion 234

Chapter 8 -- Diagenesis of the Viola Formation 240
Introduction 240
Dolomitization and Petrophysical Properties 241
Regional Distribution of Dolomite 244
Introduction 244
Dolomite in the Viola Subunits 250
Discussion 265
Diagenetic Sequences 269
Introduction 269
Methods and Procedures 271
Grain-Supported Lithologies 275
Mud-Supported Lithologies 275
Diagenetic Events 278
Bioturbation and Compaction 278
Observations 278
Interpretations 279
Early Moldic Porosity and Degrading Neomorphism 282
Observations 282
Interpretations 283
Spar Cementation and Early Bladed Cement 286
Observations 286
Interpretations 294
Silicification 296
Observations 296
Interpretations 303
Dolomitization 305
Observations 305

TABLE OF CONTENTS (con't.)

Interpretations 350
Brecciation 365
Observations 365
Interpretations 369
Calcitization of Dolomites ("Dedolomitization") 372
Observations 372
Interpretations 384
Vugs, Saddle Dolomite, and Other Late Vug-Filling Phases 387
Observations 387
Interpretations 408
Stylolitization and Associated Pyrite 415
Observations 415
Interpretations 416
Fracturing and Hydrocarbon Migration 419
Observations 419
Interpretations 420
Discussion 421

Chapter 9 -- Conclusions and Suggestions for Further Research 430
Conclusions 430
Suggestions for Further Research 434

References Cited 439

FIGURES

Figure 1.1 Stratigraphic column of the Devonian, Silurian, and part of the Ordovician Systems in Kansas. 2

Figure 1.2 Large-scale structural features in Kansas. 3

Figure 2.1 Generalized correlation chart for Middle and Upper Ordovician rocks in the midcontinent. 8

Figure 2.2 Schematic diagram of time-stratigraphic relationships of North American cratonic sequences. 10

Figure 2.3 Middle-Late Ordovician (Llandeilian-Caradocian) plate tectonic reconstruction. 14

Figure 2.4 Late Ordovician (Ashgillian) plate tectonic reconstruction. 15

Figure 3.1 Preserved dominant lithologies deposited during Chazyan-Blackriverian time. 24

Figure 3.2 Preserved dominant lithologies deposited during Rocklandian-Maysvillian time. 31

FIGURES (con't.)

Figure 3.3 Preserved dominant lithologies deposited during Richmondian time. 35

Figure 4.1 Producing oil and gas wells, past and present, from Upper Ordovician strata (Viola and Maquoketa formations) in Kansas. 38

Figure 4.2 Structure map at the base of the Viola (top of Simpson Group) in south-central Kansas. 40

Figure 4.3 Isopach map of Viola Formation in south-central Kansas study area. 42

Figure 4.4 A "worm's-eye view" or "lap-out" map illustrating units superjacent to Viola Formation in the study area. 45

Figure 5.1 Summary of informal stratigraphic subdivisions of Viola Formation in Kansas. 48

Figure 5.2 Characteristic geophysical log signatures of Viola subunits from two wells approximately 1900 ft (580 m) apart. 54

Figure 5.3 Base map showing location of regional cross-sections and detailed study area. 58

Figure 5.4 Well density used for isopach and subcrop mapping of Viola subunits. 60

Figure 5.5 Location of wells used in regional subcrop mapping and isopach mapping. 62

Figure 5.6 Subcrop map displaying which subunit of the Viola Formation is present at the top of the Viola Formation. 65

Figure 5.7 Regional isopachous map of the basal limestone of the Viola Formation. 70

Figure 5.8 A third-order trend surface fitted to the basal limestone isopach. 73

Figure 5.9 Goodness-of-fit statistic for varying orders of trend surfaces fitted to the basal limestone subunit and the lower cherty dolomitic limestone subunit of the Viola Formation. 74

Figure 5.10 Trend-surface residual map for the basal limestone of the Viola Formation. 77

Figure 5.11 Regional isopachous map of the lower cherty dolomitic limestone of the Viola Formation. 80

FIGURES (con't.)

Figure 5.12 Regional isopachous map of the lower cherty dolomitic limestone of the Viola Formation using only wells where this subunit is overlain by the upper limestone subunit. 83

Figure 5.13 Trend-surface residual map for the lower cherty dolomitic limestone of the Viola Formation. 86

Figure 5.14 Regional isopachous map of the upper limestone of the Viola Formation. 89

Figure 5.15 Regional isopachous map of the upper limestone of the Viola Formation using only wells where this subunit is overlain by the upper cherty dolomitic limestone subunit. 91

Figure 5.16 Regional isopachous map of the upper cherty dolomitic limestone of the Viola Formation. 94

Figure 5.17 An east-west stratigraphic cross-section of the Viola Formation with datum at the top of the Simpson Group. 98

Figure 5.18 Isopach of the basal limestone of the Viola Formation in an area straddling T.31S., T.32S. and R.14W., R.15W. 101

Figure 5.19 Isopach of the portion of the lower cherty dolomitic limestone above the basal limestone and "intermediate" limestone of the Viola Formation in an area straddling T.31S., T.32S. and R.14W., R.15W. 103

Figure 5.20 Isopach of the "intermediate" limestone of the Viola Formation in an area straddling T.31S., T.32S. and R.14W., R.15W. 106

Figure 5.21 Isopach of the portion of the lower cherty dolomitic limestone above the "intermediate" limestone and below the upper limestone of the Viola Formation in an area straddling T.31S., T.32S. and R.14W., R.15W. 108

Figure 5.22 Isopach of the upper limestone of the Viola Formation in an area straddling T.31S., T.32S. and R.14W., R.15W. 110

Figure 5.23 Development of the cross-section depicted in Figure 5.17. 112

Figure 5.24 Viola hydrocarbon production overlain onto the structure map at the base of the Viola. 116

Figure 5.25 Viola hydrocarbon production overlain onto the subcrop map displaying which subunit of the Viola Formation is present at the top of the Viola Formation. 119

Figure 5.26 Viola hydrocarbon production overlain onto the worm's-eye view map illustrating units superjacent to Viola Formation. 124

FIGURES (con't.)

Figure 6.1 Geothermal gradient map of Kansas based on bottom-hole temperatures from oil and gas tests. 130

Figure 6.2 Tectonic mobility diagram and temperature history of the stratigraphic column in McPherson County (T.19S., R.4W.). 134

Figure 6.3 A nomogram summarizing effects on calculated TTIs of the Simpson Group by varying combinations of geothermal gradient and Cretaceous cover in McPherson County. 138

Figure 6.4 A nomogram summarizing effects on calculated TTIs at the base of the Pennsylvanian section by varying combinations of geothermal gradient and Cretaceous cover in McPherson County. 139

Figure 6.5 Tectonic mobility diagram and temperature history of the stratigraphic column in Harper County (T.33S., R.7W.), at 25 °C/km geothermal gradient. 140

Figure 6.6 Tectonic mobility diagram and temperature history of the stratigraphic column in Harper County (T.33S., R.7W.), at 40 °C/km geothermal gradient. 141

Figure 6.7 Thermal maturation of Ordovician strata in north-central Kansas as expressed by Rock-Eval T_{max} data. 146

Figure 6.8 Thermal maturation of Ordovician strata in north-central Kansas as expressed by source-rock transformation ratios (TR). 148

Figure 6.9 Rock-Eval maturation parameters T_{max} and transformation ratio (TR) for wells in and near McPherson County, plotted by subsea depth. 151

Figure 6.10 Rock-Eval maturation parameters T_{max} and transformation ratio (TR) for wells in and near McPherson County, plotted by depth in relation to the basal Pennsylvanian unconformity. 153

Figure 6.11 Thermal maturation in Kansas as expressed by available published and unpublished vitrinite reflectance and conodont-alteration index (CAI) data. 157

Figure 6.12 Rock-Eval and vitrinite maturation profiles for two wells near McPherson County, Kansas. 158

Figure 6.13 Histograms of T_h and $Tm_{(ice)}$ measurements, together with fluid-inclusion assemblages for the samples of saddle dolomite for three localities in the study area. 162

Figure 7.1 Map of the study area showing disposition of cores studied. 171

FIGURES (con't.)

Figure 7.2 Photomicrograph of typical skeletal constituents packstones and grainstones in the basal limestone (3259 ft depth) from the Northern Natural Gas #1 Caldwell core in Rice County (2-T.20S.-R.8W.). 174

Figure 7.3 Polished slab of the basal limestone (3892.4 ft depth) from the Derby #1 Wood core in Reno County (36-T.22S.-R.5W.) showing bedding inclined approximately 20 degrees to the right. 176

Figure 7.4 Polished slab of the basal limestone (3837.6 ft depth) from the Derby #1 Rainbow core in Reno County (33-T.22S.-R.7W.) showing random orientation of fossil fragments. 177

Figure 7.5 Schematic diagram of ichnofabric indices 1 through 5. 178

Figure 7.6 Polished slab of the basal limestone subunit (3836.5 ft depth) from the Derby #1 Rainbow core in Reno County (33-T.24S.-R.5W.) showing fining-upward grain size in a lime packstone. 179

Figure 7.7 Polished slab of dolomitized stylolitic wackestone containing horizontal burrows filled with muddy crinoidal packstone from the Derby #1 Wood core (depth 3889.7 ft) in Reno County (36-T.22S.-R.5W.) 181

Figure 7.8 Polished slab showing the sharp contact between the basal limestone subunit of the Viola Formation and an olive-green siltstone in the underlying Middle Ordovician Simpson Group from the Champlin Oil #1 Kottman core (depth 3363 ft) in Rice County (19-T.19S.-R.8W.). 182

Figure 7.9 Polished slab showing the sharp contact between the basal limestone subunit of the Viola Formation and a sandy porous dolomite in the underlying Middle Ordovician Simpson Group from the Midcontinent Marine #1 South Hilger core (depth 4045.4 ft) in Reno County (9-T.26S.-R.4W.). 184

Figure 7.10 Polished core slabs showing the gradational contact between packstone of the basal limestone and wackestone of the dolomitic lower cherty dolomitic limestone (depths 3441-3443 ft) in the Damac #1 Sandra Allen core in McPherson County (7-T.17S.-R.3W.). 190

Figure 7.11 Dominant lithologies encountered in cores from the lower cherty dolomitic limestone subunit, superimposed on its isopachous map. 193

Figure 7.12 Stratigraphic cross-section (A-A') showing geometry of Viola subunits and stratigraphic position and lithology of cored intervals. 195

FIGURES (con't.)

Figure 7.13 Polished slab of dolomitized wackestone from a small outlier of the lower cherty dolomitic limestone on the crest of the Central Kansas arch, from the Derby Oil #8 Schrock core (depth 3830.3 ft) in Reno County (27-T.24S.-R.5W.). 196

Figure 7.14 Stratigraphic cross-section (B-B') showing geometry of Viola subunits and stratigraphic position and lithology of cored intervals. 198

Figure 7.15 Slabbed core of bryozoan-rich wackestone from the lower cherty dolomitic limestone, from the Sinclair #1 M. Binning core (depth 4483 ft) in Barber County (26-T.32S.-R.13W.). 200

Figure 7.16 Slabbed core of argillaceous wavy-laminated mudstone from the lower cherty dolomitic limestone subunit, from the Bunte Brothers and Shell #1 V. Sheppard core (depth 4310.1 ft) in Kingman County (10-T.27S.-R.10W.). 201

Figure 7.17 Slabbed core of argillaceous wavy-laminated mudstone from the lower cherty dolomitic limestone subunit showing thin bed of calcitic mudstone with a trilobite fragment, from the Bunte Brothers and Shell #1 V. Sheppard core (depth 4310.8 ft) in Kingman County (10-T.27S.-R.10W.). 202

Figure 7.18 Slabbed core of structureless dolomitized mudstone from the lower cherty dolomitic limestone at the Braden-Zenith ZU-3 well (depth 3775 ft) in Stafford County (11-T.24S.-R.11W.) 203

Figure 7.19 Photograph of abrupt contacts between the lower cherty dolomitic limestone and the base of the upper limestone in the Braden-Zenith ZU-1 core (depths 3829-3831 ft) and Braden-Zenith ZU-3 core (3773-3775 ft) in Stafford County (11-T.24S.-R.11W.). 205

Figure 7.20 Two slabbed cores from the upper limestone subunit from the Lario Oil & Gas #2 Randles core (depths 4740-4742 ft) in Barber County (34-T.32S.-R.12W.). 210

Figure 7.21 Slabbed core fragments (depths 4447-4450 ft) from the upper cherty dolomitic limestone subunit in the Sinclair-Prairie #1 Alice Oldfather core in Barber County (18-T.31S.-R.14W.) showing contorted bedding interpreted to be slumping. 215

Figure 7.22 Dominant lithologies of the upper cherty dolomitic limestone, superimposed on its isopachous map. 217

Figure 7.23 Slabbed core of wavy-bedded argillaceous lime mudstone in the upper cherty dolomitic limestone from the Sinclair-Prairie #1 DeGeer well (depths 4964-4965) in Barber County (34-T.32S.-R.15W.). 219

FIGURES (con't.)

Figure 7.24 Slabbed core of a dolomitized sparse wackestone in the upper cherty dolomitic limestone (depth 4440 ft) from the Sinclair-Prairie #1 Alice Oldfather core in Barber County (18-T.31S.-R.14W.). 220

Figure 7.25 Typical structureless dolomitized mudstone in the upper cherty dolomitic limestone, from the Braden-Zenith ZU-1 core (depth 3821 ft) from Stafford County (11-T.24S.-R.11W.). 221

Figure 7.26 Slabbed cores from the upper cherty dolomitic limestone in the Braden-Zenith ZU-1 core (depths 3810-3811.5 and 3816-17 ft) from Stafford County (11-T.24S.-R.11W.). 222

Figure 7.27 Polished slab of a cross-bedded, chertified packstone from the upper cherty dolomitic limestone subunit in the Braden-Zenith ZU-1 core (depth 3821 ft) from Stafford County (11-T.24S.-R.11W.). 223

Figure 7.28 Polished slab of a solution breccia developed in a dolomitized mudstone within the upper cherty dolomitic limestone (depth 3793) at the Braden Zenith ZU-1 core in Stafford County (11-T.24S.-R.11W.). 224

Figure 7.29 Breccia developed in the upper cherty dolomitic limestone immediately below the angular unconformity beneath the Devonian-Mississippian Chattanooga Shale at the Sinclair-Prairie #4 G. Oldfather well (4328 ft depth) in Barber County (7-T.31S.-R.14W.). 230

Figure 7.30 Polished slab showing contact of the Viola Formation (basal limestone subunit) with the overlying Maquoketa Formation (4029.2 ft depth) at the Midcontinent Marine #1 South Hilger well in Reno County (9-T.26S.-R.4W.). 231

Figure 7.31 Contact of the Viola Formation (lower cherty dolomitic limestone) with the overlying Maquoketa Formation (3439 ft depth) at the Damac #1 Sandra Allen well in northern McPherson County (7-T.17S.-R.3W.). 232

Figure 7.32 Polished slab (depth 3439.2 ft) from the Damac #1 Sandra Allen well (#2) in McPherson County (7-T.17S.-R.3W.) showing clay cutans around compressed peds developed in the lower cherty dolomitic limestone of the Viola. 233

Figure 7.33 Depositional model of the lithofacies of the Viola Formation. 236

Figure 8.1 Porosity-permeability crossplots for basal limestone and upper limestone subunits. 243

Figure 8.2 Porosity-permeability crossplot for upper and lower cherty dolomitic limestone subunits, together with data for the basal and upper limestone subunits. 245

FIGURES (con't.)

Figure 8.3 Limestone/dolomite ratio for entire Viola Formation (from Blair and Berendsen, 1988). 247

Figure 8.4 Davies's sample log of well cuttings from the Sunray DX #1 M. Gregg well. 249

Figure 8.5 Dominant lithology of Viola Formation basal limestone subunit from Davies's sample logs, superimposed on the isopachous map for this subunit. 252

Figure 8.6 Neutron-density crossplot of the basal limestone for wells in a line off the Chautauqua arch. 253

Figure 8.7 Neutron-density crossplot of the basal limestone for a second line of wells off the Chautauqua arch. 255

Figure 8.8 Dominant lithology of Viola Formation lower cherty dolomitic limestone subunit from Davies's sample logs, superimposed on the isopachous map for this subunit. 257

Figure 8.9 Dominant lithology of Viola Formation upper limestone subunit from Davies's sample logs, superimposed on the isopachous map for this subunit. 260

Figure 8.10 Neutron-density crossplot of the upper limestone for wells in a line off the Chautauqua arch. 262

Figure 8.11 Dominant lithology of Viola Formation upper cherty dolomitic limestone subunit from Davies's sample logs, superimposed on the isopachous map for this subunit. 264

Figure 8.12 Dominant lithology at the top of the Viola Formation, from Davies's sample logs, superimposed on the worm's-eye-view map. 267

Figure 8.13 Paragenetic sequence for grain-supported lithologies. 276

Figure 8.14 Paragenetic sequence for mud-supported lithologies. 277

Figure 8.15 Photomicrograph of typical skeletal constituents in packstones and grainstones in the basal limestone subunit (3363 ft depth) from the Champlin #1 Kottman core in Rice County (19-T.19S.-R.8W.). 280

Figure 8.16 Photomicrograph of partially dissolved micritized mollusk(?) fragment in a packstone in the basal limestone (3276.7 ft depth) from the Northern Natural Gas #1 Caldwell core in Rice County (2-T.20S.-R.8W.). 281

FIGURES (con't.)

Figure 8.17 Patchy development of degrading neomorphic spar associated with partial moldic porosity in a crinoid grain in the upper limestone (3703 ft depth) from the Shell #1 A.C. Brown core in Stafford County (2-T.24S.-R.11W.). 285

Figure 8.18 Photomicrograph of silicified brachiopod fragments with a bladed calcite spar developed on them, from the basal limestone (3259.8 ft depth) from the Northern Natural Gas #1 Caldwell core in Rice County (2-T.20S.-R.8W.). 287

Figure 8.19 Photomicrograph of late ferroan calcite spar cement in optical continuity with earlier nonferroan spar, from the basal limestone subunit (3360.5 ft depth) in the Champlin #1 Kottman core in Rice County (19-T.19S.-R.8W.). 289

Figure 8.20 Matched pair of photomicrographs of syntaxial spar in a mud-poor crinoidal packstone in the basal limestone subunit from the Champlin #1 Kottman core, depth 3359 ft, in Rice County (19-T.19S.-R.8W.). 291

Figure 8.21 Matched pair of photomicrographs of syntaxial spar in a mud-poor crinoidal packstone in the basal limestone subunit from the Northern Natural Gas #1 Caldwell core, depth 3259.75 ft, in Rice County (2-T.20S.-R.8W.). 293

Figure 8.22 Photomicrograph of silicified brachiopod fragments in a packstone in the basal limestone, from the Derby #1 Wood core (3891.6 ft depth) in Reno County (36-T.22S.-R.5W.). 298

Figure 8.23 Photomicrograph of interior of a chert nodule in the lower cherty dolomitic limestone (depth 3779.4 ft) from the Braden-Zenith ZU-3 core in Stafford County (11-T.24S.-R.11W.). 299

Figure 8.24 Photomicrograph of moldic porosity in an outlier of lower cherty dolomitic limestone (depth 3349-52.5 ft) in the Shell #4 Griffin 'B' core from McPherson County (11-T.19S.-R.2W.). 301

Figure 8.25 Polished slab of dolomitic fine-grained muddy packstone and brecciated chert from the lower cherty dolomitic limestone in the Braden-Zenith ZU-3 core (depth 3772 ft) in Stafford County (11-T.24S.-R.11W.). 302

Figure 8.26 Core slab of a chertified packstone in the upper cherty dolomitic limestone in the Braden-Zenith ZU-1 core in Stafford County (11-T.24S.-R.11W., depth 3824 ft). 303

FIGURES (con't.)

Figure 8.27 Photomicrograph of euhedral to subhedral dolomite (pale color) replacing echinoderm grains and syntaxial spar in a compacted muddy packstone in the basal limestone, from the Derby #1 Wood core (3899.5 ft depth) in Reno County (36-T.22S.-R.5W.). 307

Figure 8.28 Matched pair of photomicrographs of a patch of concentric dolomite in a crinoidal packstone in the basal limestone subunit, from the Derby #1 Wood core (3903.3 ft depth) in Reno County (36-T.22S.-R.5W.). 310

Figure 8.29 Matched pair of photomicrographs of a patch of collage dolomite in a crinoidal packstone in the basal limestone subunit, from the Derby #3 Lehman core (3403 ft depth) in Harvey County (13-T.22S.-R.2W.). 312

Figure 8.30 Matched pair of photomicrographs of collage dolomite with a thin concentric rim, in the upper cherty dolomitic limestone subunit, from the Braden-Zenith ZU-3 core (depth 3761 ft) in Stafford County (11-T.24S.-R.11W.). 314

Figure 8.31 Photomicrograph of a euhedral rhomb of replacive dolomite transecting the margin of an echinoderm and its syntaxial spar, from the basal limestone subunit (depth 3412 ft) in the Shell #1 Anderson core in McPherson County (30-T.19S.-R.1W.). 315

Figure 8.32 Matched pair of photomicrographs with of a mimetically dolomitized echinoderm packstone in the basal limestone, from the Midcontinent Marine #1 North Hilger core in Reno County (depth 4127.5 ft; 34-T.25S.-R.4W.). 318

Figure 8.33 Matched pair of photomicrographs of a mimetically dolomitized crinoidal packstone in the basal limestone subunit, showing banded dolomite cement, from the Midcontinent Marine #1 North Hilger core in Reno County (depth 4127.3 ft; 34-T.25S.-R.4W.). 321

Figure 8.34 Matched pair of photomicrographs of a patch of replacement dolomite in a mimetically dolomitized crinoidal packstone in the basal limestone subunit, thin section is from the Midcontinent Marine #1 North Hilger core in eastern Reno County (depth 4114.8 ft; 34-T.25S.-R.4W.). 323

Figure 8.35 Photomicrograph of undolomitized wackestone in lower cherty dolomitic limestone from Sinclair #1 Binning core (depth 4780 ft) in Barber County (26-T.32S.-R.13W.). 324

Figure 8.36 Photomicrograph of dolomitized wackestone in lower cherty dolomitic limestone from the Shell #6 Fleming core (depth 3394-87 ft) in McPherson County (11-T.24S.-R.2W.). 325

FIGURES (con't.)

Figure 8.37 Map illustrating internal texture of dolomite crystals in the basal limestone subunit, based on examination of thin sections at core localities. 328

Figure 8.38 Map illustrating internal texture of dolomite crystals in the lower cherty dolomitic limestone subunit, based on examination of thin sections at core localities. 330

Figure 8.39 Map illustrating internal texture of dolomite crystals in the upper limestone subunit, based on examination of thin sections at core localities. 332

Figure 8.40 Map illustrating internal texture of dolomite crystals in the upper limestone subunit, based on examination of thin sections at core localities. 334

Figure 8.41 Map illustrating internal texture of dolomite crystals at the top of the Viola, regardless of which subunit subcrops at that contact, based on examination of thin sections at core localities. 336

Figure 8.42 Diffractograms and associated stoichiometry determined for dolomite samples from the Viola Formation. 340

Figure 8.43 Histogram of $Tm_{(ice)}$ data from planar-p dolomite from the basal limestone subunit (Derby #1 Wood core; depth 3894.5 ft; 36-T.22S.-R.5W.) and planar-e dolomite from the upper cherty dolomitic limestone (E.H. Moore #2 R.F. Stewart core; depth 3785 ft; 12-T.24S.-R.11W.). 344

Figure 8.44 Secular variations in strontium isotopes for marine carbonate rocks through Phanerozoic time, with results from seven dolomite samples from the study area. 351

Figure 8.45 Crossplot of oxygen and carbon isotopes for Viola Formation dolomites and calcites. 352

Figure 8.46 Oxygen isotopic composition of dolomite as a function of temperature and the oxygen isotopic composition of the water from which it precipitated, plotted with data from Viola concentric dolomites. 363

Figure 8.47 Stratigraphic cross-section in the vicinity of the Braden-Zenith ZU-1, Braden-Zenith ZU-3, and Shell #1 A.C. Brown (2, 11-T.24S.-R.11W.) in Stafford County. 367

Figure 8.48 Photomicrograph of the upper surface of a breccia fragment and adjacent calcite spar from the intraformational breccia zone in the lower cherty dolomitic limestone in the Braden-Zenith ZU-3 core (3771.2 ft depth; 11-T.24S.-R.11W.) in Stafford County. 368

FIGURES (con't.)

Figure 8.49 Photomicrograph of the margin of a clast from a karstic breccia in the upper cherty dolomitic limestone immediately below the angular unconformity beneath the Devonian-Mississippian Chattanooga Shale at the Sinclair-Prairie #4 G. Oldfather well (4328 ft depth; 7-T.31S.-R.14W.) in Barber County. 370

Figure 8.50 Polished slab showing a completely calcitized dolomite ("dedolomite") from the Braden-Zenith ZU-3 core (depth 3779.3 ft; 11-T.24S.-R.11W.) in Stafford County. 373

Figure 8.51 Photomicrograph of a completely calcitized dolomite from the lower cherty dolomitic limestone in the Braden-Zenith ZU-3 core (depth 3779.3 ft; 11-T.24S.-R.11W.) in Stafford County. 374

Figure 8.52 Matched pair of photomicrographs of a completely calcitized dolomite with a grumeleuse texture, from the upper cherty dolomitic limestone in the Braden-Zenith ZU-1 core (depth 3815 ft; 11-T.24S.-R.11W.) in Stafford County. 378

Figure 8.53 Histogram of fluid-inclusion $Tm_{(ice)}$ temperatures for dedolomite having a grumeleuse texture, from the upper cherty dolomitic limestone (depth 3815 ft) from Braden-Zenith ZU-1 core (11-T.24S.-R.11W.) in Stafford County. 381

Figure 8.54 Photomicrograph of two-stage infill (nonferroan and ferroan calcite) of pseudomorphic calcite in a dolomite mold in the center of a crinoid columnal, from the basal limestone in the Northern Natural Gas #1 Caldwell core (3259.75 ft depth) in Rice County (2-T.20S.-R.8W.). 382

Figure 8.55 Photomicrograph of a blue ferroan dedolomite that is a patchy replacement in the centers of saddle dolomite crystals, from a packstone in the basal limestone from the Derby #1 Schrock core (depth 3842.1 ft) in Reno County (27-T.24S.-R.5W.). 383

Figure 8.56 Photomicrograph of the wall of the vug from the Derby #1 Wood core (depth 3894.5 ft; 36-T.22S.-R.5W.) in Reno County. 389

Figure 8.57 Photomicrograph of a euhedral quartz crystal from a vug in the basal limestone subunit from the Derby #1 Wood core (depth 3894.5 ft; 36-T.22S.-R.5W.) in Reno County. 390

Figure 8.58 Histograms of $Tm_{(ice)}$ data for fluid inclusions in vug quartz from the Derby #1 Wood core (depth 3894.5 ft; 36-T.22S.-R.5W.) in Reno County. 393

Figure 8.59 Histograms of homogenization temperatures, and a crossplot of T_h and $Tm_{(ice)}$ data for the euhedral quartz from a vug in the Derby #1 Wood core (depth 3894.5 ft; 36-T.22S.-R.5W.) in Reno County. 395

FIGURES (con't.)

Figure 8.60 Bivariate plot showing paleobarometric determinations versus change in volume from fluid inclusions from the euhedral quartz in a vug in the Derby #1 Wood core (depth 3894.5 ft; 36-T.22S.-R.5W.) in Reno County. 398

Figure 8.61 Crossplot and histograms of T_h and $Tm_{(ice)}$ measurements for saddle dolomite from the lower cherty dolomitic limestone subunit at the Damac #1 Sandra Allen core (depth 3438.1 ft; 7-T.17S.-R.3W.) in McPherson County. 404

Figure 8.62 Crossplot and histograms of T_h and $Tm_{(ice)}$ measurements for saddle dolomite from the basal limestone subunit at the Derby #1 Wood core (depth 3894.5 ft; 36-T.22S.-R.5W.) in Reno County. 405

Figure 8.63 Crossplot and histograms of T_h and $Tm_{(ice)}$ measurements for saddle dolomite from the basal limestone subunit at the Midcontinent Marine #1 South Hilger core (depth 4029 ft; 9-T.26S.-R.4W.) in Reno County. 406

Figure 8.64 Photomicrograph of dolomite rhombs associated with a stylolite from the upper limestone (depth 4310 ft) in the Bunte Bros. and Shell #1 V. Sheppard core in Kingman County (10-T.27S.-R.10W.). 417

Figure 8.65 Eight models, with their variations, hypothetically satisfy the necessary pumping mechanism and magnesium source for extensive dolomitization. 423

Figure VI.1 Porosity vs. thickness of the basal limestone and the portion of the lower cherty dolomitic limestone between the basal and "intermediate" limestone. 603

Figure VI.2 Porosity vs. thickness of the crinoidal limestones (basal, "intermediate", and upper limestones) from the small map area straddling T.31S., T.32S. and R.14W., R.15W. 604

Figure VI.3 Neutron-density crossplot of the basal limestone and upper limestone from wells shown from the small map area straddling T.31S., T.32S. and R.14W., R.15W. 606

Figure VI.4 Comparison of porous and nonporous crinoidal packstones from the upper limestone subunit from the small map area straddling T.31S., T.32S. and R.14W., R.15W. 607

Figure VI.5. Thin-section photomicrograph of porosity in a crinoidal packstone from the upper limestone subunit (4370-ft depth) in the Sinclair-Prairie #4 G. Oldfather well. 608

Plate 1. East -- west stratigraphic cross-section of Viola Formation. . . . . (in pocket)

FIGURES (con't.)

Plate 2. South-southwest -- north-northeast stratigraphic cross-section of Viola Formation. . . . . (in pocket)

TABLES

Table 5.1 A survey of literature on oil and gas fields that produce from Viola Formation in Kansas. 120

Table 6.1 Temperature and tectonic data used to construct tectonic mobility diagrams and TTI calculations. 132

Table 7.1 Cores used in this study, with location, depth, and Viola subunit. 168

Table 8.1 Summary of cathodoluminescence patterns observed in dolomite in selected cores from subunits in the Viola Formation, versus their dolomite content. 338

Table 8.2 Fluid-inclusion data from replacive dolomite rhombs (planar-p texture) and in the basal limestone subunit, and replacive dolomite rhombs (planar-e texture) from the upper cherty dolomitic limestone. 342

Table 8.3 Samples analyzed for strontium, oxygen, and carbon isotopic ratios. 346

Table 8.4 Fluid-inclusion data from a dedolomitic limestone having a grumeleuse texture, upper limestone subunit. 379

Table 8.5 Fluid-inclusion data from euhedral quartz crystals from a vug in the basal limestone subunit. 391

Table 8.6 Paleobarometric data from fluid inclusions in euhedral quartz crystals from a vug in the basal limestone subunit 396

Table 8.7 Fluid-inclusion data from saddle dolomites from three localities in the study area. 401

APPENDICES

Appendix I -- Tops of subunits of Viola Formation, south-central Kansas (taken from 1,709 Wireline logs). 474

Appendix II -- Rock-Eval maturation data for Ordovician strata in northeastern and north-central Kansas. 500

Appendix III -- Rock-Eval and vitrinite-reflectance maturation data for wells in and near McPherson County, Kansas. 506

APPENDICES (con't.)

Appendix IV -- Lithologic descriptions for Viola Cores. 511

Appendix V -- Lithology of subunits of Viola Formation, south-central Kansas (taken from Davies's sample logs). 591

Appendix VI -- Porosity - thickness relationships of Viola subunits on the Pratt anticline. 602

Appendix VII -- Requisite chemical and physical conditions necessary for regional dolomitization. 609

Chapter 1

INTRODUCTION

The Upper Ordovician Viola Formation, an important petroleum reservoir in the midcontinent, was deposited at the acme of the greatest inundation of epicontinental seas onto the craton in Phanerozoic history (Ross, 1976; Witzke, 1980). This unit is dominantly open-marine to restricted limestone or dolomite and lies between siliciclastics of the underlying Middle Ordovician Simpson Group and overlying Upper Ordovician Maquoketa Shale (Figure 1.1; Goebel, 1968a). It is present only in the subsurface in Kansas, with nearest outcrops being in the Arbuckle Mountains of southern Oklahoma. Stratigraphically equivalent carbonates also crop out on the northeastern flank of the Ozark uplift in eastern Missouri, where they are known as Kimmswick Limestone, and in palisades in the Upper Mississippi Valley in northeastern Iowa and southeastern Minnesota, where they are known as Galena Formation.

Subsurface extent of Viola Limestone in Kansas is largely governed by the pattern of uplifts and basins that formed in pre-Devonian and pre-Pennsylvanian time (Figure 1.2). It is absent in southeastern Kansas over a broad arch extending west-northwestward off the Ozark uplift because of erosion occurring prior to deposition of the Upper Devonian-Lower Mississippian Chattanooga Shale. Similarly, pre-Chattanooga erosion probably removed it from the Ancestral Central Kansas uplift, the predecessor to the Late Mississippian--Early Pennsylvanian Central Kansas uplift (Merriam, 1963). Erosion over the Late Mississippian--Early Pennsylvanian Nemaha uplift and Pratt anticline also locally removed Viola, as well as older Ordovician and Cambrian units, in northeastern and central Kansas. The Viola is preserved on the

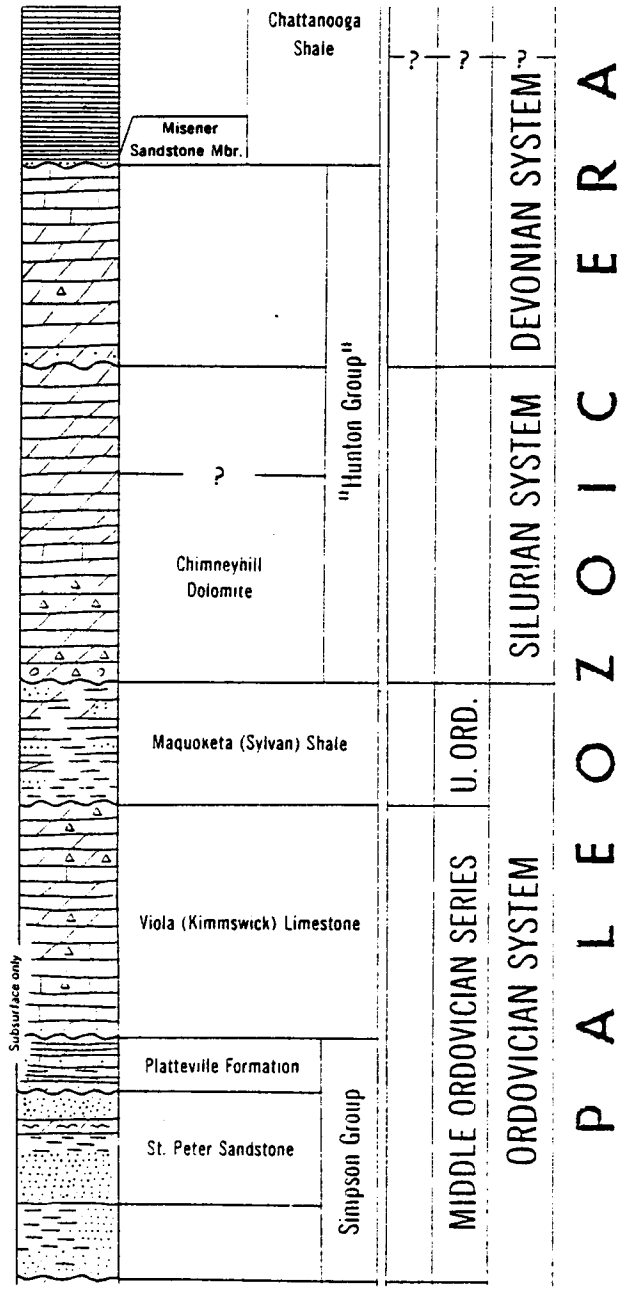

Figure 1.1 Stratigraphic column of the Devonian, Silurian, and part of the Ordovician Systems in Kansas (from Zeller, 1968). Silurian and Devonian "Hunton" carbonate rocks are present only in northeastern Kansas in the Forest City basin, Salina basin, and northern part of the Sedgwick basin (Merriam, 1963; Ireland, 1967). In more recent translations to global classification, Blackriverian and younger rocks (which includes the Viola Formation) are now classified as Upper Ordovician. These changes are expressed on recent COSUNA charts (Correlation of Stratigraphic Units of North America) by the American Association of Petroleum Geologists (see Salvador, 1985; Shaver and others, 1985).

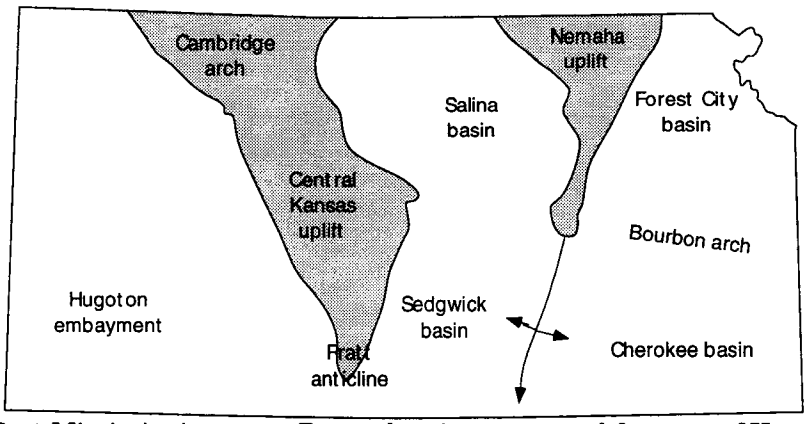

A. Post-Mississippian -- pre-Pennsylvanian structural features of Kansas

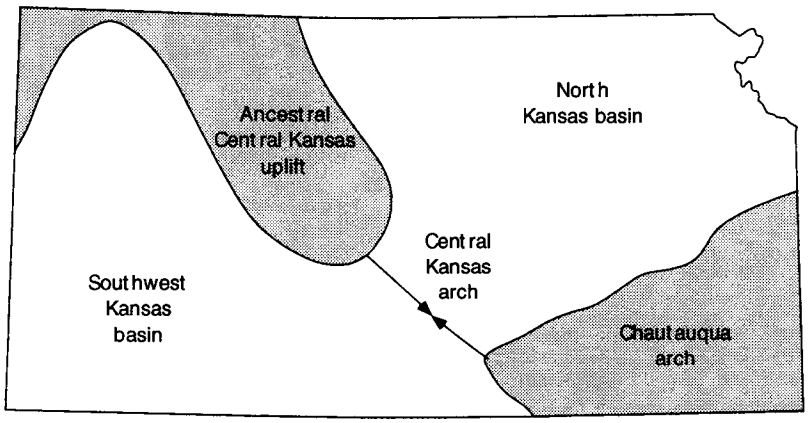

B. Post-Ordovician -- pre-Mississippian structural features of Kansas

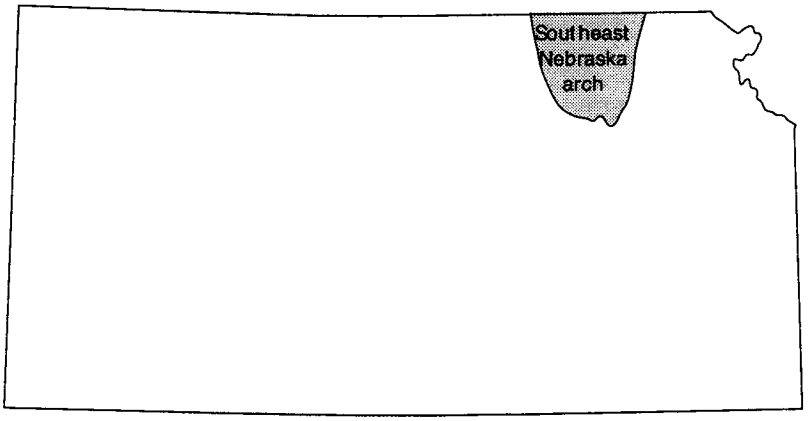

C. Post-Cambrian -- pre-Middle Ordovician structural features of Kansas

Figure 1.2 Large-scale structural features in Kansas: A - Pre-Desmoinesian -- post Mississippian features; B - Pre-Mississippian -- post-Ordovician; C - Post-Cambrian -- pre-Middle Ordovician (from Merriam, 1963).

flanks of these late Paleozoic uplifts and in the adjacent Salina, Forest City, and Sedgwick basins.

This study focuses on lithofacies and diagenesis of the Viola Formation in an early Paleozoic structural saddle between the Chautauqua arch and the Ancestral Central Kansas uplift -- a feature known as the Central Kansas arch (Figure 1.2; Merriam, 1963). The locus and thickness of depositional facies and early diagenesis could reveal possible growth of this structural saddle during Viola deposition; later diagenesis reflects subsequent burial and uplift. A synthesis of data from core examination, fluid-inclusion and cathodoluminescence petrography, organic geochemistry, stable isotopes, subsurface mapping, and well-log analysis provides an integrated picture of temperatures, depths, and environments of diagenesis that have affected this unit.

Prior studies that were the major impetus for work presented in this dissertation include a 1978 dissertation by Erhard Bornemann at Syracuse University (Bornemann, 1978) and a 1982 thesis at The University of Kansas by Patricia N. St. Clair (St. Clair, 1982). Both of these studies concentrated on Viola Formation in Pratt and Barber counties on the Pratt anticline, a complex uplift plunging southward off the Central Kansas uplift in south-central Kansas. Bornemann (1978) summarized spatial lithologic patterns in the Viola discernable from mathematically calibrated wireline logs. St. Clair (1982) petrographically examined the Viola and developed a local stratigraphic framework for the unit that confirmed results developed by Bornemann (1978). This study extends the lithostratigraphy developed by Bornemann (1978) and St. Clair (1982) northward onto the structural sag between the Chautauqua arch and Ancestral Central Kansas uplift and examines the sequence of diagenetic events that made the Viola an important petroleum reservoir in Kansas. An integrative study, it is hoped, will provide a more regional and precise understanding

and prediction of porosity development and diagenetic facies in this unit.

This study is structured as an approach that moves from the general to the specific, where the context of world-wide and continental Ordovician geology is first reviewed (Chapter 2), then midcontinent Ordovician stratigraphy is outlined (Chapter 3). The spatial relationships of the Viola to other stratigraphic formations within the study area are presented in Chapter 4. This information, in turn, provides a basis for the examination of the internal stratigraphy of the Viola and how each of its subunits thicken and thin over the study area (Chapter 5). The burial and thermal history are determined in Chapter 6. Lithology and interpreted depositional environments are presented in Chapter 7. In turn, the diagenesis of the Viola is examined and set in the context of its stratigraphic framework and burial history (Chapter 8).

Chapter 2

REGIONAL GEOLOGIC SETTING

Ordovician and regional geology that may influence spatial and temporal aspects of Viola deposition are examined in this section. A major marine transgression was responsible for the Viola Formation and its superjacent and subjacent units. Ordovician plate-tectonic configuration, regional tectonism, and climate at the time of Viola deposition were all controls. Regional correlations of stratigraphic units deposited during the Tippecanoe transgression represented by early work on the lithostratigraphy of the Viola define the stratigraphic setting.

REGIONAL MIDDLE AND UPPER ORDOVICIAN TIME-ROCK CLASSIFICATION

Time-rock classification of Ordovician stratigraphy is currently in a state of flux in that many North American stratigraphers are adopting a global system of classification that has largely developed from study of European outcrops (Keith, 1988a). In the translation to the global classification, the traditionally Middle Ordovician Champlainian Series time-rock classification (Figure 2.1) is split between the Middle and Upper Ordovician, with Blackriverian and younger rocks being classified as Upper Ordovician. The term "Trentonian" is also eliminated. These changes are expressed on recent COSUNA charts (Correlation of Stratigraphic Units of North America) by the American Association of Petroleum Geologists (see Salvador, 1985; Shaver and others, 1985). Use of the terms "Middle" and "Upper" Ordovician in

Figure 2.1 Generalized correlation chart for Middle and Upper Ordovician rocks in the midcontinent. The time-stratigraphic relationships at stage level are not precise in that there is contradictory evidence and uncertainty in lithologic and biostratigraphic correlations for many of these units (see text for discussion). Approximate chronologic dates are from Palmer (1983) and have uncertainties of 12 to 16 million years. A new Ordovician time scale by Sloan (1987) proposes dates of 478.3, 468.8, 464.3, 445.7, and 438.0 Ma as chronologic boundaries between the global series shown on the diagram. New British stages are from Fortey and others, 1991; correlation of North American stages and series to British series are from Sweet (1984) and Keith (1988a).

Generalized Correlation Chart for Middle and Upper Ordovician Rocks in the Midcontinent

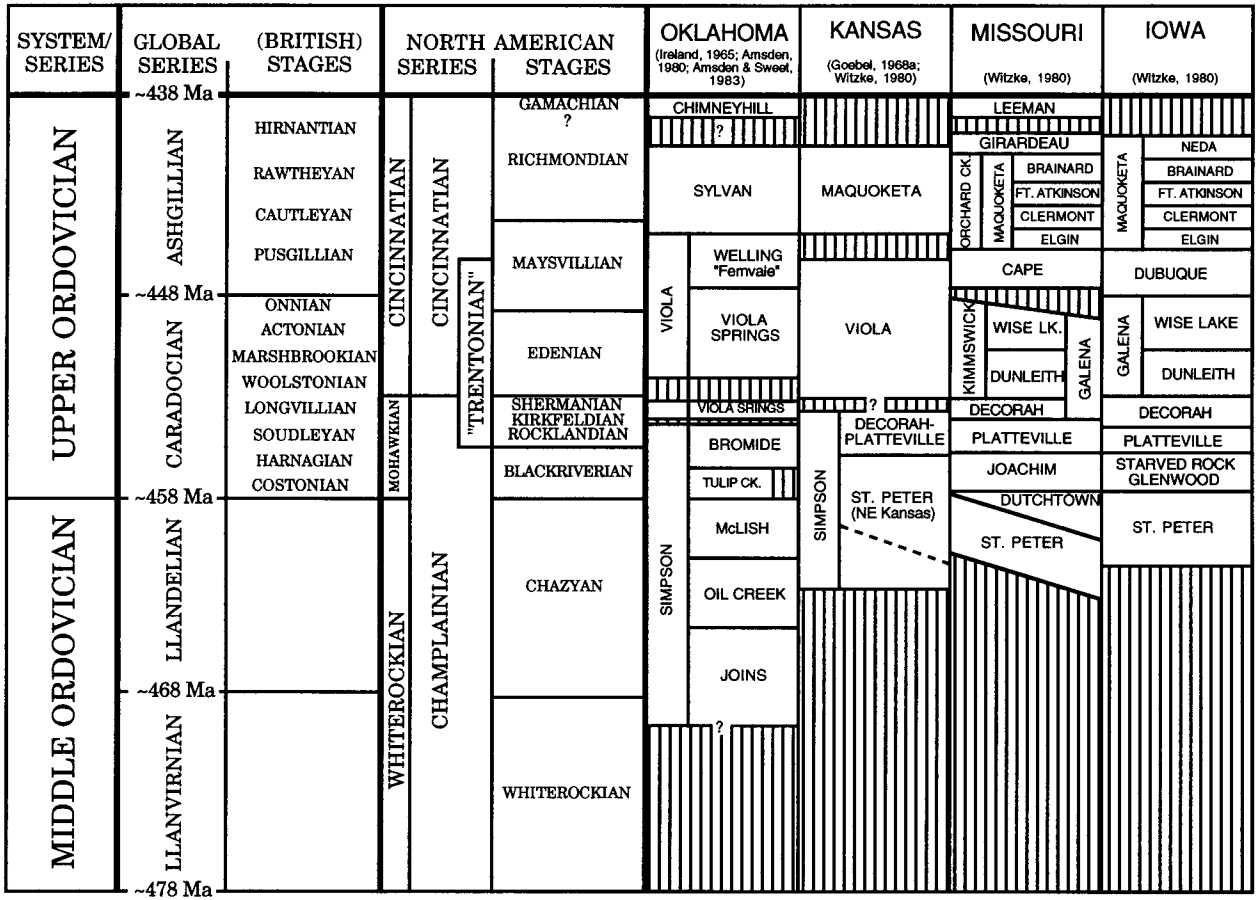

referencing older literature can be confusing in the context of this change, hence where possible either Series and Stage names will be used or literature citations will be translated to the newer time interpretation while putting the old usage with the citation.

Correlation problems occur in assigning unequivocal ages to Ordovician rocks in Oklahoma and Kansas due to disparities encountered in regional time-stratigraphic correlations between the Appalachians and the midcontinent (cf., Neuman, 1976); disagreement that seems inherent among work with separate fossil groups (cf., Schramm, 1965a; Berry, 1976; Cooper, 1976; Jaanusson, 1984); controversies with lithostratigraphic and biostratigraphic correlations between basin, basin-flank, and shelf localities (cf., Jaanusson, 1984); and lack of good collections and macrofossils from subsurface sections (Ireland, 1965). Time-rock correlations shown in Figure 2.1 are therefore approximate at least at stage level.

THE TIPPECANOE TRANSGRESSION

The Viola Limestone was deposited in an epeiric sea that was the product of the Tippecanoe transgression, which was the second great Paleozoic transgression on to the North American craton (Sloss, 1963, 1988; Figure 2.2). Inundation of the continent began in early Middle Ordovician time and reached its acme in the Late Ordovician, spreading over a wider area than any previous or subsequent epeiric sea (Sloss, 1963; Ross, 1976; Frazier and Schwimmer, 1987, p. 145). According to Ross (1976, p. 91), the Tippecanoe transgression constituted "the greatest inundation in North American history." Withdrawal of the Tippecanoe sea was complete by the Early Devonian (Sloss, 1963, 1988).

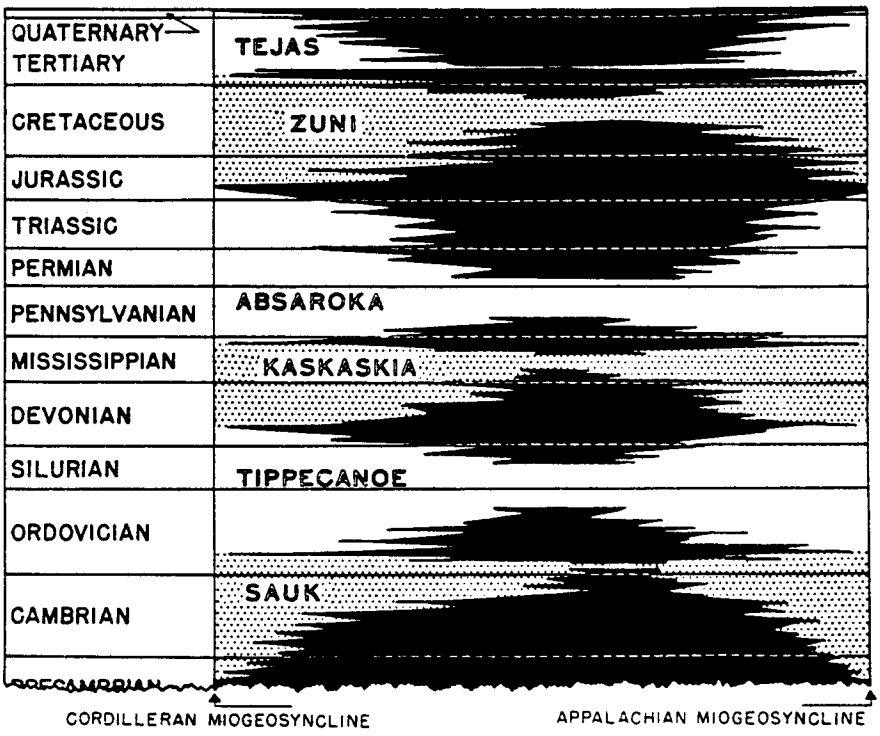

Figure 2.2 Schematic diagram of time-stratigraphic relationships of North American cratonic sequences (from Sloss, 1963). Black areas represent erosional or nondepositional hiatuses. White and stippled areas differentiate depositional episodes of separate sequences.

Sloss (1988) divided the Tippecanoe sequence into two subsequences -- Tippecanoe I (Middle and Late Ordovician) and Tippecanoe II (Early Silurian to Early Devonian). The top of the Tippecanoe I subsequence commonly is a subtle disconformity that may be related to a eustatic lowering of sea level caused by continental glaciation on the Gondwana supercontinent (Dennison, 1976; Sloss, 1988). Strata of the Tippecanoe II subsequence are not as widespread as those of the Tippecanoe I subsequence because the Tippecanoe II transgression was not as extensive as the Tippecanoe I transgression. The Tippecanoe II subsequence was also

subject to considerably more erosion during 40 million years of exposure prior to the subsequent Kaskaskia transgression (Sloss, 1988; Bunker and others, 1988).

The initial deposits of the Tippecanoe I transgression, like those of the preceding Sauk transgression, generally were texturally and mineralogically mature quartz sands that were deposited unconformably over a widespread erosional surface. The Simpson Group in Kansas is a product of this episode of detrital sedimentation (Leatherock, 1945; Merriam, 1963; Goebel, 1968a; Cole, 1975). This detrital sedimentation generally was followed by widespread carbonate deposition as sources for the detrital sedimentation were reduced in area and elevation by the rising seas. The Viola Limestone (subject of this research) and Maquoketa Formation are the products in Kansas of this carbonate depositional episode (Leatherock, 1945; Merriam, 1963; Goebel, 1968a).

Rocks deposited in Kansas during the Tippecanoe II transgression include undifferentiated Silurian and Devonian carbonates present in the Forest City and Salina basins that are commonly referred to by drillers as "Hunton limestone" (Goebel, 1968b). "Hunton" is a misnomer, however, because rocks by this name in Kansas, although carbonates, are not strictly time correlative to the type Hunton Group in the Anadarko basin of Oklahoma. The Kansas rocks are composed of Middle Silurian and Middle Devonian strata whereas the type Hunton is Silurian and Lower Devonian (Lee, 1943; Taylor, 1946; Hilpman, 1967; Goebel, 1968b), and possibly even Upper Ordovician (Amsden, 1980). The unconformity between the Silurian and Middle Devonian rocks in Kansas is very subtle and largely defined by biostratigraphic zonation. In places, this approximately 20-million-year gap in sedimentation is revealed only by the presence of a slightly sandy carbonate bed (Lee, 1943, 1956; Merriam, 1963). The Devonian limestones overlap underlying Silurian strata and lie disconformably on Middle and Upper Ordovician strata on the flanks of the Salina

basin (Lee, 1956).

MIDDLE AND LATE ORDOVICIAN PALEOGEOGRAPHY AND CLIMATES

Plate Configuration and Associated Tectonic Events

The cratonic margins of North America were tectonically quiescent during the early part of the Tippecanoe transgression. The craton underlying the northern midcontinent also remained stable throughout most of the transgression. Consequently, strata deposited are thin, are dominated by carbonates after inundation of sand-producing lowlands, and contain numerous minor unconformities. Ordovician strata thicken toward the margins of the craton and the record of sedimentation becomes progressively more complete. In Middle and Late Ordovician time, the Taconic orogeny in the eastern United States delivered increasing amounts of detritus westward onto the center of the craton and produced major paleogeographical changes during Late Ordovician time (Neuman, 1976, "late Middle Ordovician"). The Taconic orogeny reached its climactic phase in the southern Appalachians in post-Blackriverian time and in the Hudson valley region by Richmondian time (Rast, 1989). The detrital deposits in the Hudson valley region derived from the Taconic orogen, are known as the Taconic or Queenston clastic wedge. Thin shales intercalated with limestone, representing distal deposits of this detrital clastic wedge, reached their maximum lateral extent when they covered much of the present United States east of the Mississippi River in latest Ordovician (Richmondian) time (Sweet and Bergstrom, 1976; Frazier and Schwimmer, 1987, p. 146; Sloss, 1988).

Middle and Late Ordovician paleogeography from Scotese and McKerrow (1991; Figures 2.3, 2.4) puts North America (Laurentia) athwart the paleoequator,

with the study area being at approximately 20° S latitude. The Iapetus Ocean, east of the North American plate, started closing during Ordovician time and associated tectonism at the periphery of the craton accounts for the Taconic orogeny (Dewey and Bird, 1970; Rowley and Kidd, 1981; Rast, 1989). The latitude of the North American changed little during this closing; tectonic plates on the opposite side of the Iapetus Ocean (now composing most of present-day northern Europe) moved from higher to lower southern latitudes (Spjeldnaes, 1976; Scotese and McKerrow, 1991).

The Transcontinental arch was a major influence on the paleogeography of the Tippecanoe transgression on the North American craton (Ross, 1976; Witzke, 1980). This feature extended from New Mexico to central Minnesota as a low-lying upland. Many Middle Ordovician formations lap out against its flanks, but rising seas finally breached the arch in Late Ordovician time and it subsequently had no great paleogeographic influence (Ross, 1976, "late Middle Ordovician"). The Transcontinental arch was a contributor of siliciclastic sediment during Decorah-Platteville time, but continued marine transgression inundated it by the time of Viola deposition (Ross, 1976; Witzke, 1980; Bunker and others, 1988).

Middle and Late Ordovician Climate

Tropical conditions, with predominantly easterly trade winds, probably prevailed in Kansas during Middle and Late Ordovician time, due to its low-latitude position (Scotese and others, 1979). Westward-blowing winds also are indicated by the presence of bentonite ash beds extending into the upper Mississippi Valley from volcanic eruptions associated with the Taconic orogeny (Willman and Kolata, 1978; Kolata and others, 1983) and by generally westward paleocurrent directions in St. Peter Sandstone (Dapples, 1955; Dott and Roshardt, 1972). A humid climate and associated deep chemical weathering would account for abundant quartz sand,

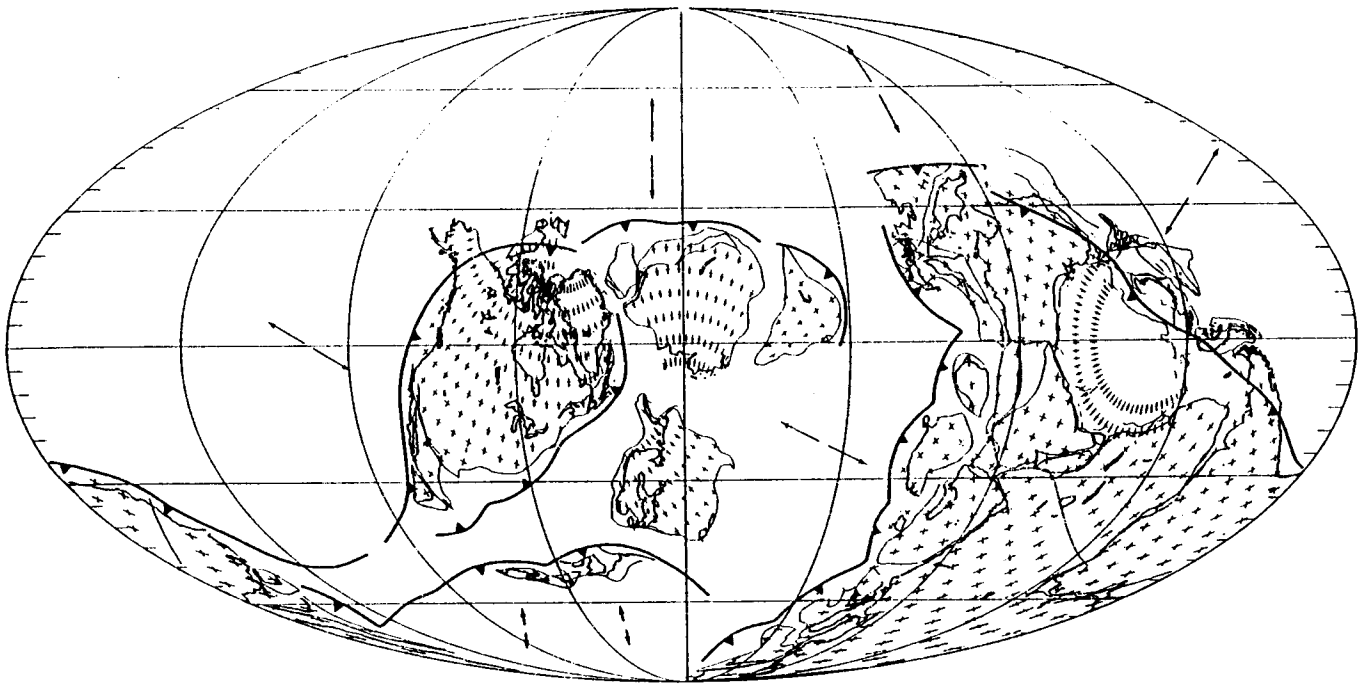

Figure 2.3 Middle-Late Ordovician (Llandeilian-Caradocian) plate tectonic reconstruction from Scotese and McKerrow (1991) based on paleomagnetic information, paleoclimatology, biogeography, and plate kinematics. Bold lines are subduction zones; divergent arrows indicate areas of probable plate divergence. Scotese and McKerrow (1991) estimate a +15-degree uncertainty in the latitudinal positions of the major continents, and a +30-degree uncertainty in their relative longitudinal positions. Llandelian to Caradocian time is approximately correlable to Chazyan to mid-Maysvillian time in North America (see Figure 2.1) -- a period of time during deposition of most of the Simpson and Viola.

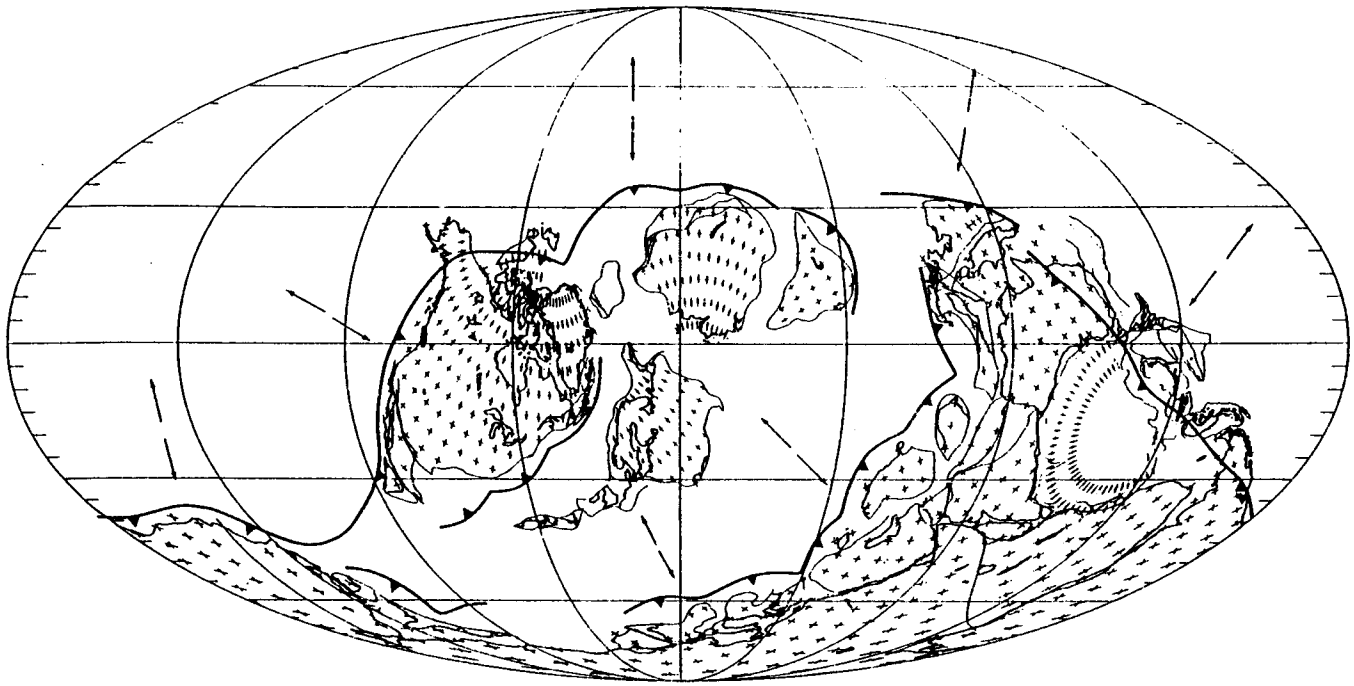

Figure 2.4 Late Ordovician (Ashgillian) plate tectonic reconstruction from Scotese and McKerrow (1991). Ashgillian time corresponds to mid-Maysvillian through Richmondian time in North America (see Figure 2.1) -- a period of time during deposition of the Maquoketa and end of Viola.

kaolinitic clay, and oölitic ironstones present in the Simpson (Witzke, 1980, 1990 ; Berendsen and others, 1992). Later, in the Late Ordovician, paleoclimate was probably tropical to warm-temperate and seasonally moist, based on a study of paleosols in the Upper Ordovician Juniata Formation in the Appalachian region (Driese and Foreman, 1992).

Paleogeographic reconstructions based on "climate-sensitive and latitudinally-related lithic indicators" presented in Witzke (1980) put the study area farther south of the paleoequator determined by Scotese and McKerrow (1991; Figures 2.3, 2.4). Witzke (1980) also inferred approximately 10 degrees southward motion of the North American craton with respect to the Ordovician equator from Middle to Late Ordovician (i.e., Chazyan to Richmondian) time -- movement that was not markedly expressed in paleogeographic reconstructions in Scotese and McKerrow (1991; Figures 2.3, 2.4). The net effect of this southward motion would be to move the study area out of the humid climate zone that characterizes oceanically influenced areas within 5 to 10 degrees of the equator. The midcontinent would be characterized by more arid climate if was approximately 30 degrees south of the equator by Late Ordovician (Edenian-Maysvillian) time (Witzke, 1990). Arid conditions are indicated by cyclic evaporites in the upper Red River Formation (Cincinnatian) of the Williston basin (see Fuller, 1961). Early paleomagnetic data, however, put the midcontinent very near the equator in Late Ordovician time (see McElhinny and Briden, 1971; McElhinny and Opdyke, 1973) and thus the presence of evaporites are an apparent contradiction to the humid climate that characterizes the equatorial zone. Ross (1976) recognized this paradox and attempted a compromise. He accepted the paleomagnetic position of the midcontinent being on the equator and no movement of Laurentia with respect to the Ordovician equator, but invoked a paleogeographic model in which vast areas of the shallow carbonate shelf in the midcontinent become periodically restricted and subject

to evaporite deposition due to glacial-eustatic lowering of sea-level. Rectifying paleomagnetic data with the rock record may be a matter of critically reevaluating the paleomagnetic data because a strong Permian-age episode of secondary magnetization affecting lower Paleozoic strata in the midcontinent has been only recognized in the last few years (McCabe and Elmore, 1989). Inasmuch as earlier paleomagnetic studies may have not recognized this potential complication, their paleogeographic reconstructions may have been slightly in error.

Glacial control of sea level during the Late Ordovician is implied by the presence of the Gondwana supercontinent in the vicinity of the South Pole at this time (McElhinny and Briden, 1971; see Figure 2.4), as well as by strong latitudinal differentiation of faunal habitats (Berry and Boucot, 1970). Glacial sedimentation is recorded in north Africa and South America (Fairbridge, 1971; Berry and Boucot, 1973; Allen, 1975; Dennison, 1976; Caputo and Crowell, 1985; Abed and others, 1993). Continental glaciation has been discussed as a possible cause of lowering of sea level, of attendant faunal changes at the end of Ashgillian (Richmondian) time (Sheehan, 1973, 1975; Dennison, 1976; McKerrow, 1979; Brenchley and Newall 1980, 1984; Fortey, 1984; Melchin and Mitchell, 1991), and of the unconformity forming the Ordovician-Silurian boundary worldwide (see Lenz, 1976; Brenchley and Newall, 1980, 1984; Brenchley and others, 1994).

Cyclicity in Cincinnatian strata in the Ohio Valley (Kope and Fairview formations; Jennette and Pryor, 1993) and North Dakota (upper Red River Formation; Ross, 1976) has been attributed to glacial pulses. However, presence of an ice cap at the South Pole earlier in the Ordovician (specifically during Caradocian time; i.e., during Viola deposition) is unclear because Gondwanaland may have been off the pole at that time (Fortey, 1984; cf., Figures 2.3, 2.4). Glacial episodes are nevertheless invoked to account for minor variations in sea level on the time scale of 0.1 to 1

million years recorded in Rocklandian- to Shermanian-age strata in the Mississippi Valley (Cisne and Gildner, 1988). These strata are probably chronostratigraphically equivalent to Decorah-Platteville and lower Viola rocks in Kansas.

Chapter 3

MIDDLE AND UPPER ORDOVICIAN LITHOSTRATIGRAPHY IN THE MIDCONTINENT

SIMPSON GROUP

St. Peter Sandstone

The basal transgressive sandstone of the Tippecanoe sequence is generally an extremely mature quartz arenite known throughout much of the central United States as the St. Peter Sandstone (Sloss, 1963; Adler, 1971; Frazier and Schwimmer, 1987, p. 138; see Figure 2.1). The St. Peter Sandstone is easily identified in the subsurface of northeastern Kansas (Leatherock, 1945; Cole, 1975) and is unconformably overlain by green shales, dolomites, limestones, and minor sandstones of the Platteville Formation in the Forest City basin (Leatherock, 1945; Cole, 1975). The St. Peter and the Platteville compose what is known as the Simpson Group or Simpson Sandstone in Kansas. The Simpson name is adopted from the Anadarko basin in Oklahoma (Goebel, 1968a).

Depositional mechanisms for St. Peter Sandstone have been postulated to be southwesterly moving longshore currents (Dapples, 1955; Amaral and Pryor, 1977). Eolian-to-shallow-marine transitional environments have also been interpreted (Dott and others, 1986). Autio (1985) identified eight lithofacies in the Simpson of central Kansas that occur in a gradually coarsening-upward sequence and proposed that this could result from either progradation of shoreline deposits over a lower-energy shelf deposits, or from a barrier island backstepping over a lagoonal sediments. Coalescent estuarine deposition was suggested by Esslinger (1983) for similar Simpson deposits in Oklahoma.

St. Peter Sandstone is generally recognized as a distinct entity only in northeastern Kansas and is thought to be correlative to the sandy lower part of the Simpson Group in the rest of Kansas (Goebel, 1968a). Dapples (1955) stated that slight uncertainties in correlation between Simpson Group of Oklahoma and St. Peter Sandstone of the northern midcontinent are encountered crossing the Nemaha uplift. East of this structural barrier, thin sands separated by thin shales grade into typical St. Peter sheet sandstones. Southwest of the Nemaha uplift, sand, shale, and carbonates of the Simpson occur, with the amount of shale in the Simpson increasing as the unit increases in thickness southward.

Lithologic correlations of the Simpson and St. Peter in Kansas to divisions of the Simpson in Oklahoma are equivocal. In ascending order, the Simpson Group in Oklahoma comprises the Joins, Oil Creek, McLish, Tulip Creek, and Bromide formations (Decker, 1933). Ireland (1965) regarded the St. Peter Sandstone in Kansas as an amalgamation of basal sandstones of the McLish, Tulip Creek, and possibly Oil Creek formations of Oklahoma and correlated the Bromide Formation with the Platteville Formation. Schramm (1964, 1965a), Statler (1965), and Doveton and others (1984, 1990) contended that the St. Peter Sandstone and the overlying Platteville Formation in Kansas are lithologic equivalents of just the McLish and Bromide formations. They extended the Oil Creek Formation into Kansas less than 5 miles (8 km) in Harper, Sumner, and Clark counties (Schramm, 1964, 1965b) and regarded the Tulip Creek as truncated by erosion and limited to central Oklahoma (see Figure 4.1 for location of Kansas counties).

Harris (1957) considered both Joins and Oil Creek formations in Oklahoma as Chazyan and the overlying McLish and Bromide formations as Blackriverian in age, based on ostracode faunas. A Chazyan age for the Joins and Oil Creek formations is also indicated by brachiopod fauna (Dapples, 1955) and other marine invertebrates

(Decker, 1952; Huffman and Starke, 1960; Harris, 1957). Schramm (1965a) reported that most paleontologists consider the McLish to be Chazyan in age, contrary to the ostracode data of Harris (1957) and lithologic correlations by Schramm himself. Ireland (1965) also considered the McLish as Chazyan but stated the overlying Bromide Formation is Blackriverian in age. Recent conodont data by Sweet (1992) also supports a Chazyan age for the McLish. The Tulip Creek Formation is stratigraphically between the McLish and the Bromide (Figure 2.1) and has been assigned either Chazyan and Blackriverian ages (Schramm, 1965a). The Tulip Creek is limited to the south-central part of Oklahoma (Ireland, 1965; Schramm, 1964, 1965b); in other regions of the state the Bromide Formation lies directly on McLish Formation.

A consensus of subsurface stratigraphers in Oklahoma considers the Bromide Formation to be younger than Chazyan; it is generally considered to be Blackriverian in age due to a close association with "Blackriverian" Decorah fauna of the upper Mississippi valley (as reported by Schramm, 1965a). A younger age is possible if a Trentonian age is accepted for the Decorah, as espoused by Kay (1937) and Templeton and Willman (1933). A Chazyan age for the Bromide is supported by Twenhofel and others (1954) and Dapples (1955).

According to Adkison (1972) the top of the Simpson Group in the Sedgwick basin and adjacent areas in south-central Kansas is identified in well cuttings by the first occurrence of sandy carbonates, sandstone, or shale below the relatively pure limestones and dolomites of the Viola Formation. Although some drillers prefer to identify the top of the Simpson at the first sandstone below the Viola, this is not the convention used in this report. Sandstone in the Simpson in Kansas is commonly loosely cemented, quartzose, dominantly fine- to medium-grained, and subangular to well-rounded, and generally found in the upper and middle part of the unit. Shales

are typically waxy in appearance, greenish gray to dark greenish gray, clayey, and well indurated. Sandy carbonate beds, where present, generally occur in the upper part of the group. Sandstone typically makes up about 20% of the Simpson; limestones and dolomites less than 20%, but percentages of these lithologies can vary greatly (Adkison, 1972).

Simpson rocks in Kansas are thickest (250 ft, 75 m) in Harper County near the Kansas-Oklahoma state line (Cole, 1965). The Simpson thickness in Kansas is only a fraction of that in Oklahoma, where it reaches 2,300 ft (700 m; Lee, 1956; Ireland, 1965). Northward onlap, thinning, and some truncation of individual units out of the Anadarko basin is indicated by regional lithologic correlations (Schramm, 1964; Ireland, 1965) and well-log analysis (Doveton and others, 1984). Locally thick deposits of Simpson occur in sporadically distributed sink holes and karst valleys developed on underlying Cambrian - Ordovician Arbuckle carbonate rocks (Leatherock, 1945; Lee and others, 1946; Merriam and Atkison, 1956; Ireland, 1965),

Units correlative to the Simpson include the Harding Sandstone in Colorado and Wyoming, the Fort Peña Formation of the Marathon uplift, the Swan Peak and Eureka formations of Utah and Nevada, and the Winnipeg Formation in the Williston basin (Ireland, 1965; Ross, 1976; Frazier and Schwimmer, 1987, p. 139; Witzke, 1980; Figure 3.1). The provenance for sandstones in the Simpson Group in Kansas and other parts of the midwestern United States is probably exposed granitic terranes of the Precambrian shield in the Great Lakes region, Ozark dome, and Transcontinental arch in addition to reworking of Upper Cambrian sandstones deposited during the Sauk transgression that flank these exposed basement terranes (Ireland, 1965; Ketner, 1968; Frazier and Schwimmer, 1987, p. 139; Witzke, 1980). Granitic rock exposed on the Southeast Nebraska arch (Lee, 1956; Witzke, 1980; Figure 1.2) may have locally contributed detrital material.

Figure 3.1 Preserved dominant lithologies deposited during Chazyan-Blackriverian time (from Cook and Bally, 1975; Ross, 1976). At this time, the Transcontinental arch was probably a low-lying peninsula separating waters of the encroaching Tippecanoe transgression. Westerly moving trade winds near the equator aid longshore currents in moving sand off the Precambrian shield into the midcontinent. Note that carbonate deposition characterizes the generally tectonically quiescent eastern flank of the North American craton except in extreme northeastern United States.

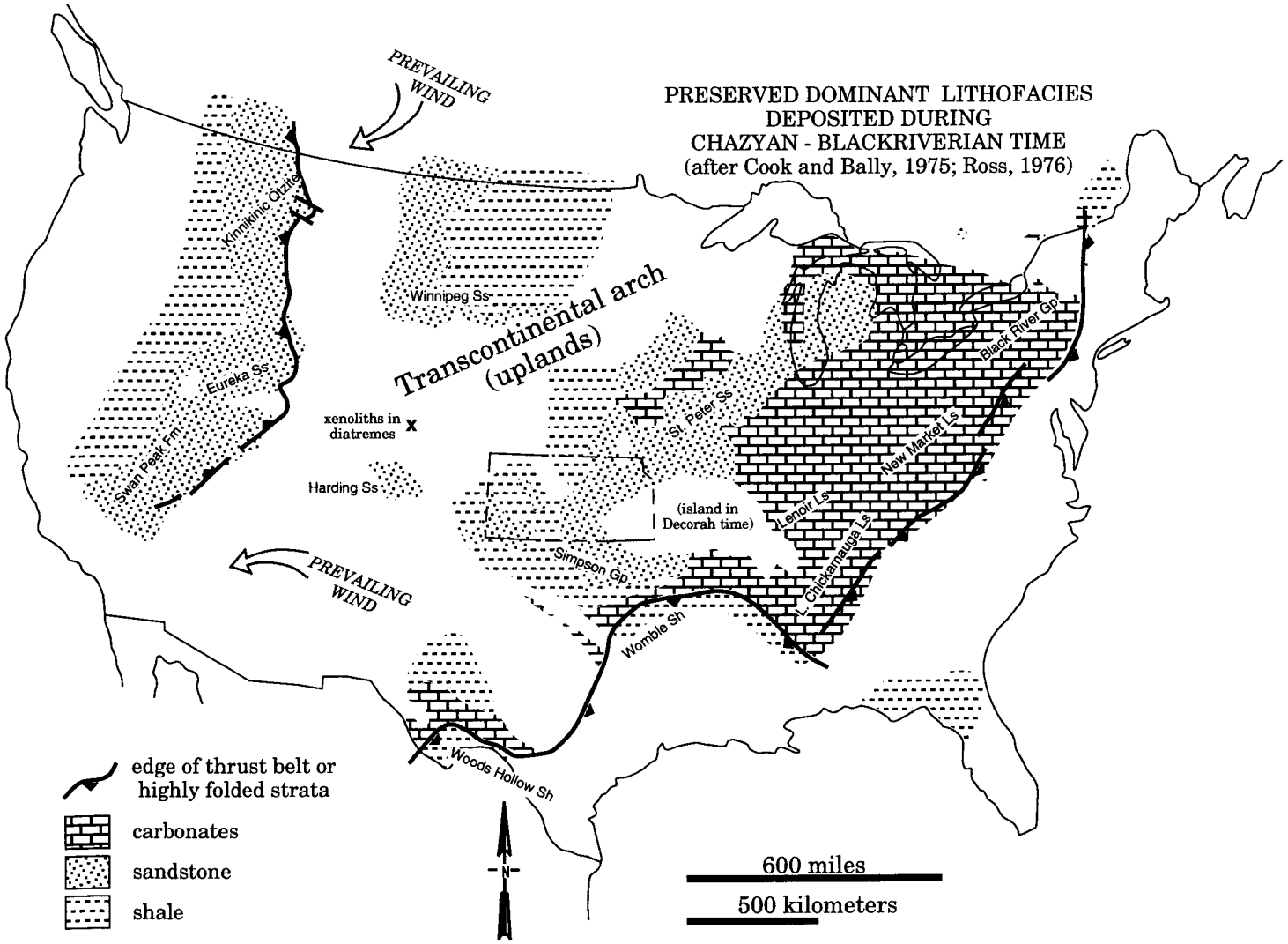
PREVAILING WIND
PRESERVED DOMINANT LITHOFACIES
DEPOSITED DURING
CHAZYAN - BLACKRIVERIAN TIME
(after Cook and Bally, 1975; Ross, 1976)
Kinniktinic Qtzite
Winnipeg Ss
Transcontinental arch
(uplands)
Eureka Ss
Swan Peak Fm
xenoliths in diatremes
Harding Ss
St. Peter Ss
Black River Gp
New Market Ls
Lenoir Ls
Chickamauga Ls
(island in Decorah time)
Simpson Gp
Womble Sh
Woods Hollow Sh
PREVAILING WIND
edge of thrust belt or highly folded strata
carbonates
sandstone
shale
N
600 miles
500 kilometers

Platteville Formation

The nature of the contact between the Platteville and underlying St. Peter Sandstone is problematical. Lee and others (1946) and Goebel (1968a) considered the Platteville to lie unconformably on the St. Peter Sandstone, but these conclusions were based solely on cuttings. Conversely, Witzke (1980) indicated that deposition was continuous from St. Peter to Decorah-Platteville time in Iowa. In Oklahoma, the Platteville-Decorah interval is not recognized, and erosion over an island situated over the present area of the Ozarks, western Missouri, and northeastern Oklahoma has eliminated strata near the top of the Simpson (Ireland, 1965, 1966; Statler, 1965).

In Kansas, the Platteville Formation consists of an upper dolomite, limestone, sandstone, and green shale, and a persistent lower dolomite, 5 to 35 ft (1.5 to 10.7 m) thick (Goebel, 1968a). According to Lee (1956) and Cole (1975), the Platteville is 100 ft (30.5 m) thick in northern Brown County (northeastern Kansas), but thins irregularly south and west until it is thin or absent southwest of Marion and Harvey counties, and west of Smith and Osborne counties. In these areas where the Platteville is thin, it is usually mapped as undifferentiated Simpson Group (Ireland, 1966; Witzke, 1980). The area where Platteville is thickest roughly comprises the old North Kansas basin of Rich (1933).

The detrital beds in the upper part of the Platteville are considered equivalent to the Decorah Formation of Iowa and Wisconsin (see Figure 2.1) although Decorah *per se* is not recognized on eastern flank of the Central Kansas uplift and in much of western Kansas (Leatherock, 1945; Ireland, 1966; Witzke, 1980). According to Lee (1943), strata equivalent to Decorah in the Forest City basin, where present, are characteristically sandy dolomites interstratified with dark and gray-green shale. Regionally, the Platteville-Decorah interval is lithologically quite variable and can contain shales, carbonates, and sandstones. In general, this interval increases in

thickness and shale content toward the Transcontinental arch, suggesting the arch as a source area (Witzke, 1980; Bunker and others, 1988).

Schramm (1965a) and Goebel (1968a) considered the upper part of the Simpson Group in Kansas (i.e., Platteville Formation) to be Blackriverian, whereas the lower part of the Simpson Group in Kansas is Chazyan. In studying conodonts, Sweet and Bergstrom (1976) and Sweet (1984) stated the Simpson Group in the subsurface of central Kansas and south-central Oklahoma is considerably older -- Whiterockian through earliest Blackriverian in age. As such, the Platteville-Decorah interval would be time-equivalent to the Bromide Formation of Oklahoma (Ireland, 1965). An early Trentonian to possible Blackriverian age is assigned to the Platteville-Decorah interval in Kansas by Twenhofel and others, 1954, Ireland, 1966; Witzke, 1980. If this age is accepted, the Platteville-Decorah interval would be time-equivalent to the Corbin Ranch Formation in Oklahoma (Ireland, 1966). Sweet and Bergstrom (1976) reported the rocks equivalent to the Decorah in central Kansas are younger than Blackriverian and contain Kirkfeldian conodont faunas.

The Decorah-Platteville interval greatly increases in thickness eastward into Iowa and Illinois, where it is differentiated into several members (Willman and Kolata, 1978). Several bentonite beds, which originated as ash-falls from distant volcanic eruptions associated with the Taconic orogeny, are present in the Decorah-Platteville interval in the upper Mississippi Valley. None have been detected in Kansas; however, Witzke (1980) reported one bentonite in the Decorah-Platteville interval extends to the margin of the Transcontinental arch in northern Iowa. Ireland (1966) also described a bentonite in the Decorah present as far west as southeastern Missouri. This may be a particularly extensive bed called the K-bentonite, which was deposited during Decorah-Platteville time, according to conodont age correlations in Huff and others (1992). Comparison of bentonites ages in Huff and others (1992) with

associated conodont zones (see Sweet, 1979, 1984) indicates that some bentonites also could be coeval with deposition of the lower part of the Viola in Kansas.

Relationship of Decorah to overlying Viola (Kimmswick) Limestone is obscure, the Decorah is commonly represented by slightly clastic or sandy and shaly member at the base of the Viola (Lee, 1943). Based on study of outcrops, Witzke (1980) reported a complex diachronous transition zone a few meters thick, rather than an unconformity, characterizes the upward change from the Decorah-Platteville interval to the Galena Formation (i.e., the Viola lithostratigraphic equivalent) in Iowa. This study also concluded that the shaly upper Decorah near the Transcontinental arch (e.g., western Iowa) is contemporaneous with pure carbonates of the Galena Formation away from the arch (e.g., northwestern Illinois). Older studies targeting Kansas (cf., Leatherock, 1945; Lee, 1956) and based principally on well cuttings and insoluble residues derived from well cuttings invoked the presence of unconformities not only between the Decorah/Platteville interval and the Viola, but between virtually all other Lower Paleozoic units.

VIOLA FORMATION

The thick and regionally persistent carbonate unit above the Platteville (or Decorah) Formation, and below the Maquoketa Shale is identified as either the Viola Limestone or Viola Formation (Goebel, 1968a; see Figures 1.1, 2.1). This unit is named for exposures near the village of Viola, near Bromide in Johnston County, Oklahoma (Taff, 1902, 1904). In 1890, the village of Viola was founded and named for Viola Jackson by her father, William H. Jackson, who was a territorial jurist for the Oklahoma Territory. Viola, Oklahoma was renamed Springbrook in 1906 and

subsequently went into decline and abandonment (Vickie Luster, Chickasha Council House and Museum, Tishomingo, OK, personal communication, December, 1995).

Maximum thickness of the Viola Formation in Kansas is approximately 325 ft (99 m) just south of the Nebraska state line in Jewell and Republic counties (Cole, 1975). The Viola is markedly thinner in Kansas than it is in Oklahoma, where it is 935 ft thick (286 m) in the subsurface north of the Wichita Mountains (Cram, 1930; Ireland, 1966).

Lithostratigraphic correlation of subdivisions of the Viola from Oklahoma northward into Kansas is not established because the lithology of the Viola in Kansas is more like that of Missouri and Iowa than that of the Arbuckle Mountains in Oklahoma (Ireland, 1966). Most likely only the lower part of the Viola in Oklahoma is preserved in Kansas (Adkison, 1972). A coarsely crystalline, non-siliceous limestone unit disconformably above the Viola in the Arbuckle Mountains of Oklahoma is referred to by some as the Fernvale Limestone (Wengerd, 1948; Ireland, 1966) but this unit is not formally recognized in Kansas (Goebel, 1968a), and may not have been deposited (Edson, 1929; Lee, 1943, 1956; Ireland, 1966). The name "Fernvale" is moribund in Oklahoma because rocks formerly identified as Fernvale in Oklahoma are older than the type section in central Tennessee (Alberstadt, 1973; Amsden, 1979). Amsden (1979) proposed to replace the name "Fernvale" in eastern Oklahoma with Welling Formation. The Corbin Ranch and Fite limestones, which are locally recognized, dense units at the base and top of the Viola, respectively, in Oklahoma, also are not recognized in Kansas (Ireland, 1966; Goebel, 1968a; Figure 2.1).

Paleontological age determinations on the Viola have varied for both Kansas and Oklahoma. The Viola in Oklahoma was once considered entirely Trentonian in age, but was subsequently considered to be late Blackriverian, Trentonian, and early Richmondian in age (Ireland, 1966). Sweet and Bergstrom (1976) described late

Shermanian and early Edenian conodont faunas in the Viola in the subsurface in northeastern Kansas. More recently, the Viola in southern Kansas has been considered to be late Edenian and early Maysvillian in age on the basis of conodonts (Sweet, 1992). Achritarchs and chitinozoans from a core taken in extreme southern Nemaha County (near the point common to Nemaha, Pottawatomie, and Jackson counties) indicates the Viola is Caradocian in age (Wright and Meyers, 1981).

Viola and lithostratigraphically equivalent carbonate deposits across the United States have traditionally been grouped into a generalized stage called the "Trentonian." The Trentonian stage is now considered roughly correlative to the Rocklandian, Kirkfeldian, Shermanian, Edenian, and early Maysvillian stages (Witzke, 1980; Figure 2.1). The Viola in Kansas is lithostratigraphically correlative to the Galena Group in Illinois, Wisconsin, Minnesota, Nebraska, and Iowa (Witzke, 1980); the Kimmswick Formation in Missouri and Arkansas (Lee, 1943; Leatherock, 1945); the Fremont Formation in Colorado (Ross, 1976; Witzke, 1980); the lower Big Horn Formation in Wyoming (Witzke, 1980); the Red River Formation in the Dakotas and Montana (Bunker and others, 1988); the Lexington Limestone in Kentucky (Frazier and Schwimmer, 1987, p. 145); the uppermost Chickamauga Limestone in Georgia, Alabama, and Tennessee (Frazier and Schwimmer, 1987, p. 145); and the Nashville Group in central Tennessee (Frazier and Schwimmer, 1987, p. 145; Figure 3.2). A deep-water equivalent of the Viola in the Ouachita Mountains of Oklahoma and Arkansas is the Big Fork Chert (Ireland, 1966; Lyons, 1966). The vast shallow-water carbonate shelf responsible for this depositional episode did not spread synchronously over the craton, therefore these units are not exact chronostratigraphic equivalents. For example, the Viola in Kansas includes younger strata than the Galena Group in Iowa and Illinois (Adler, 1971; Witzke, 1983; Bunker and others, 1988).

Figure 3.2 Preserved dominant lithologies deposited during Rocklandian-Maysvillian time (from Cook and Bally, 1975; Ross, 1976; Keith, 1988a). Continued transgression of the sea has Viola carbonates overstepping earlier siliciclastic deposition of the Simpson and St. Peter sandstones in the midcontinent. The Transcontinental arch was breached by the sea at this time and was probably expressed as a series of islands.

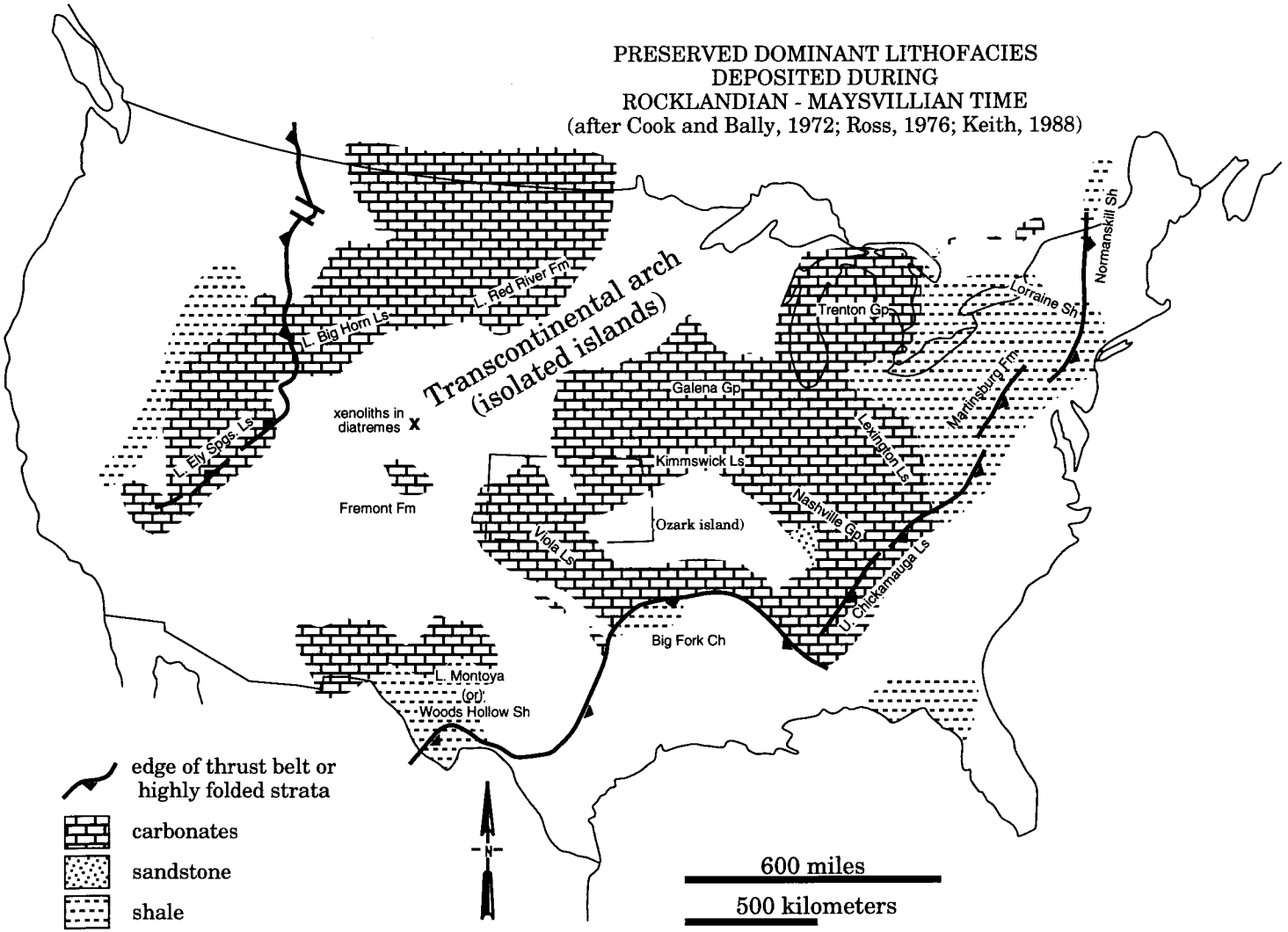
PRESERVED DOMINANT LITHOFACIES
DEPOSITED DURING
ROCKLANDIAN - MAYSVILLIAN TIME
(after Cook and Bally, 1972; Ross, 1976; Keith, 1988)
Transcontinental arch
(isolated islands)
L. Red River Fm
L. Big Horn Ls
L. Ely Springs Ls
xenoliths in diatremes
Fremont Fm
Galena Gp
Kimmswick Ls
(Ozark island)
Viola Ls
Trenton Gp
Lorraine Sh
Normanskill Sh
Martinsburg Fm
Lexington Ls
Nashville Gp
U. Ordovician Ls
Big Fork Ch
L. Montoya (pr)
Woods Hollow Sh
edge of thrust belt or highly folded strata
carbonates
sandstone
shale
N
600 miles
500 kilometers

MAQUOKETA FORMATION

The Viola is stratigraphically bracketed by detrital rocks of the subjacent Simpson Group and superjacent Maquoketa Formation. In northeastern Kansas, the Maquoketa is characteristically a greenish-gray, silty, dolomitic shale or a cherty, silty dolomite. It becomes more argillaceous and less cherty and dolomitic in southern Kansas (Goebel, 1968a). Taylor (1947a), Lee (1956), and Adkison (1972) all recorded a westward increase in carbonate rocks in this unit and noted that the upper part of the Viola in south-central Kansas may be indistinguishable from the Maquoketa due to this increase in carbonate percentage. The Maquoketa in Kansas is interpreted to be separated by slightly angular unconformities from underlying Viola Limestone and overlying Silurian rocks (Goebel, 1968a; Figure 2.1). Wright and Meyers (1981) observed a pyrite-laden clastic zone between the Maquoketa and Viola in the Forest City basin in northeastern Kansas and interpreted the contact as an unconformity. Witzke (1980) recognized a regionally persistent corrosion surface at the base of the Maquoketa in the midcontinent (including Oklahoma, Missouri, and Illinois) that is characterized by phosphatic pellets, pyrite, and phosphatic diminutive fossils. This phosphatization is an early diagenetic process related to upwelling of deeper anoxic water that dominated deposition in the Mississippi Valley region during Late Ordovician time (Witzke, 1980; Carozzi, 1989, p. 495). Phosphatic zones at the base of the Maquoketa are not the norm in Kansas (Lee, 1956; Adkison, 1972; Wright and Meyers, 1981).

There is general agreement that the Maquoketa is Late Ordovician (Cincinnatian) in age, although its precise position within this series is subject to uncertainty (Ireland, 1966; Amsden, 1980). The Maquoketa is considered to be Richmondian in age in Oklahoma and Kansas (Ireland, 1966). However, Sweet and

Bergstrom (1976) found it also contains late Maysvillian conodont faunas in central Kansas. The phosphorite at the base of the Maquoketa in Iowa is considered by Witzke (1980) to be a diachronous unit but the fossils found in the phosphorite are all of Edenian-Maysvillian age (Witzke, 1980). Wright and Meyers (1981) in their study of achritarchs and chitinozoans in a core from extreme southern Nemaha County, Kansas, indicated a Caradocian to Ashgillian age for the Maquoketa Shale. Ashgillian chitinozoans were recovered from this unit in Oklahoma (Jenkins, 1970).

Maximum reported thickness of the Maquoketa Shale is approximately 170 ft (52 m) in east-central Kansas (McPherson and Ellsworth counties) (Cole, 1965). The Maquoketa Shale extends over much of Iowa, Wisconsin, Nebraska, northern Missouri, southeastern Wisconsin, and Illinois (Witzke, 1980). It is correlative to the Sylvan Shale of Oklahoma based on similar lithology and stratigraphic position (Lee, 1943, 1956; Taylor, 1947a; Ireland, 1966; Cole, 1975). Regionally, it is chronostratigraphically equivalent to the upper Red River Formation of the Williston basin of Montana (Witzke, 1980), the Priest Canyon Formation in Colorado (Witzke, 1980), the Stony Mountain Formation of North and South Dakota (Witzke, 1980), and the upper Big Horn Formation in Wyoming (Witzke, 1980; Figure 3.3). The Polk Creek Shale in the Ouachita Mountains of Oklahoma and the Maravillas Limestone in the Marathon region of Texas are probably deep-water facies deposited during Maquoketa time (Ireland, 1966).

Marginal-marine and terrestrial detrital rocks were deposited contemporaneously with the Maquoketa Shale in the eastern United States, reflecting the increasing influence of the Taconic orogeny as a generator of detritus during Late Ordovician time (Dennison, 1976; Keith, 1988a). Largely nonmarine shales and sandstones of the Juniata Formation in Ohio, Virginia, and Pennsylvania, and the Queenston Formation in New York are temporal equivalents of the Maquoketa in the

Figure 3.3 Preserved dominant lithologies deposited during Richmondian time (from Cook and Bally, 1975; Ross, 1976; Keith, 1988a). A combination of regression and later erosion limits the distribution of these strata relative to that deposited earlier in the Tippecanoe transgression. Note that the carbonate deposition in the midcontinent has largely been replaced by fine-grained siliciclastic material ultimately derived from the rising Taconic highlands in the northeastern United States. These fine-grained siliciclastics are expressed as the Maquoketa and Sylvan shales in the midcontinent. Carbonates of the Richmond Group in the vicinity of the Ohio Valley are both argillaceous carbonates and mixed shales and carbonates that were deposited on shallow shelf west of the Taconic uplands (Keith, 1988a). Basinal conditions prevailed farther west where Maquoketa Shale was deposited (Carozzi, 1989, p. 494-495). Shoaling in the vicinity of the Transcontinental arch is expressed by carbonate deposition.

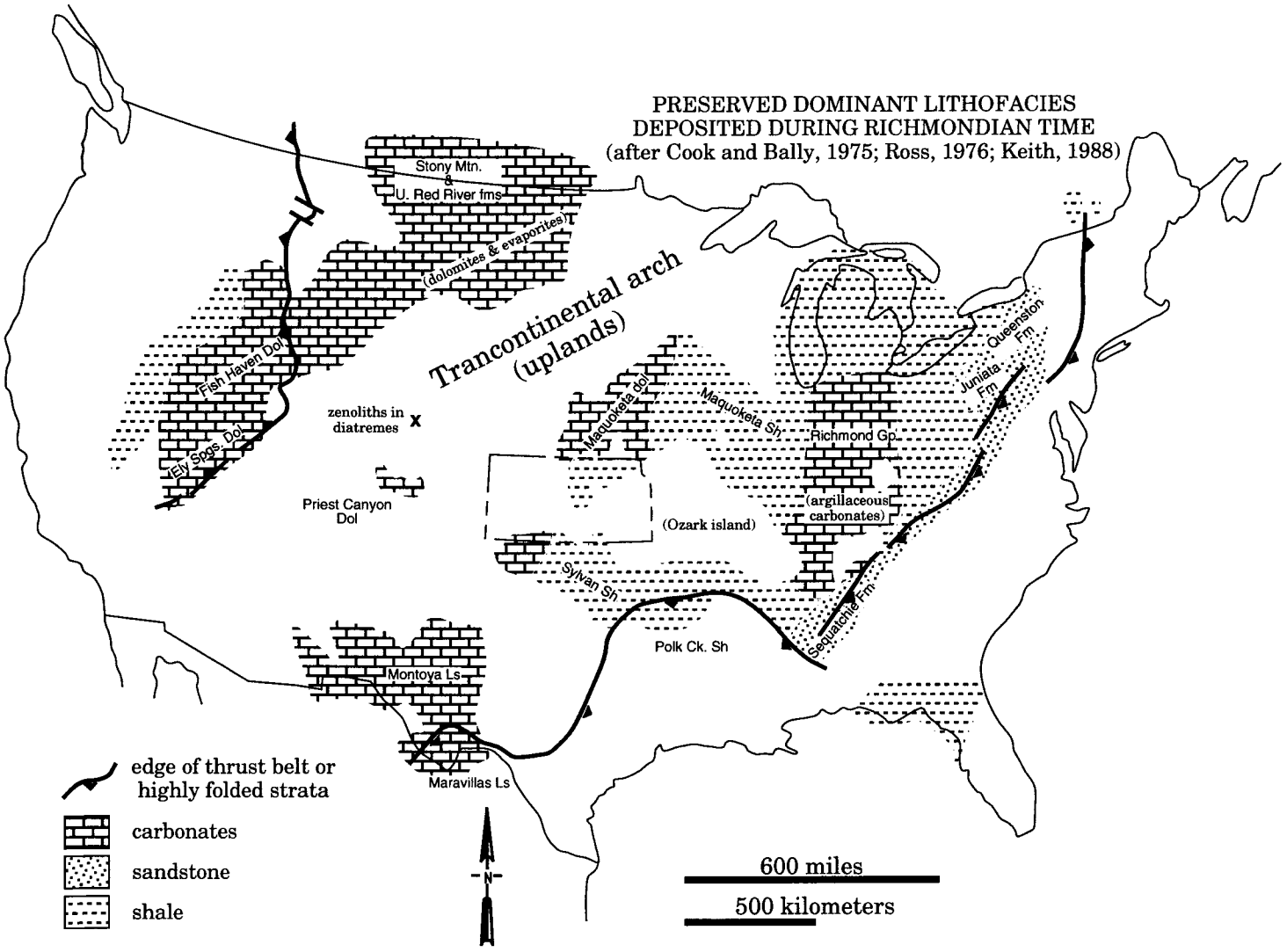
PRESERVED DOMINANT LITHOFACIES
DEPOSITED DURING RICHMONDIAN TIME
(after Cook and Bally, 1975; Ross, 1976; Keith, 1988)
Stony Mtn.
&
U. Red River fms
(dolomites & evaporites)
Trancontinental arch
(uplands)
Fish Haven Dol
Ely Spgs. Dol
zenoliths in
diatremes
Priest Canyon
Dol
Maquoketa dol
Maquoketa Sh
Richmond Gp
(argillaceous
carbonates)
(Ozark island)
Queenston
Fm
Juniata
Fm
Sylvan Sh
Sequatchie Fm
Polk Ck. Sh
Montoya Ls
Maravillas Ls
edge of thrust belt or
highly folded strata
carbonates
sandstone
shale
N
600 miles
500 kilometers

midcontinent (Dennison, 1976; Frazier and Schwimmer, 1987, p. 146; Keith, 1988a).

Chapter 4

LOCAL GEOLOGIC SETTING AND STRATIGRAPHY OF VIOLA FORMATION

STRUCTURE, THICKNESS, AND RELATIONSHIP TO OTHER GEOLOGIC UNITS

Information on the geologic structure and thickness of the Viola Formation in Kansas is primarily based on drilling of wells for exploration and development of petroleum (Figure 4.1). Local structure of the Viola can be quite complicated due to anticlines and synclines with amplitudes of several tens to hundreds of meters, and wavelengths of generally less than 5 km. Most of these structures were formed during Late Mississippian -- Early Pennsylvanian time (Merriam, 1963; Atkison, 1972; Newell and others, 1987) and some of the anticlines are the locus of oil and gas fields. Subsea depths of the Viola Formation are approximately -2,000 ft (-610 m) at the structural sag between the ancestral Central Kansas uplift and the Chautauqua arch, deepening southward to approximately -4,000 ft (-1,220 m) at the Kansas-Oklahoma state line (Adkison, 1972; Figure 4.2).

Comparison of the present-day structure map of the Viola (Figure 4.2) with the Viola isopach map (Figure 4.3) indicates the early Paleozoic structural sag between the ancestral Central Kansas uplift and the Chautauqua arch (located in Kingman and Reno counties) is approximately 40 miles (65 km) south of the broad, unnamed late Paleozoic arch between the Salina and Sedgwick basins (located in Rice, McPherson, and Marion counties). Local thinning of the Viola occurs along the axis of the structurally complex Pratt anticline and Nemaha uplift. South of the Kansas-Oklahoma state line, the Viola thickens markedly into the Anadarko basin

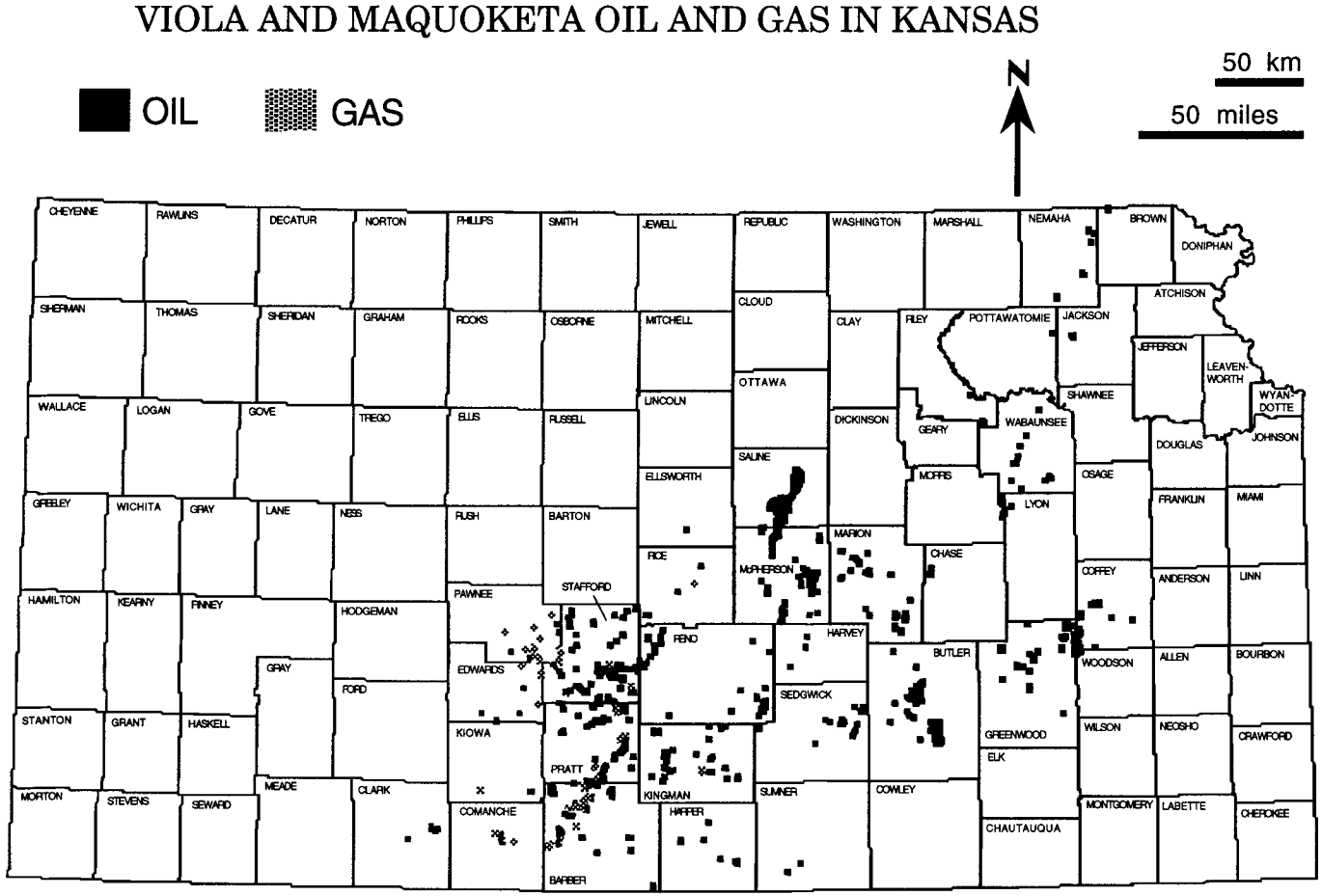

Figure 4.1 Producing oil and gas wells, past and present, from Upper Ordovician strata (Viola and Maquoketa formations) in Kansas (from Newell and others, 1987). As of 1988, fifty-seven oil fields in Kansas produced solely from the Viola and another two hundred fields have Viola petroleum as a component of their production (Appendix E, Kansas Geological Survey and Tertiary Oil Recovery Project, 1991).

Figure 4.2 Structure map at the base of the Viola (top of Simpson Group) in south-central Kansas (from Adkison, 1972). Most local structures with closures of less than 100 ft (30 m) cannot be expressed at this scale.

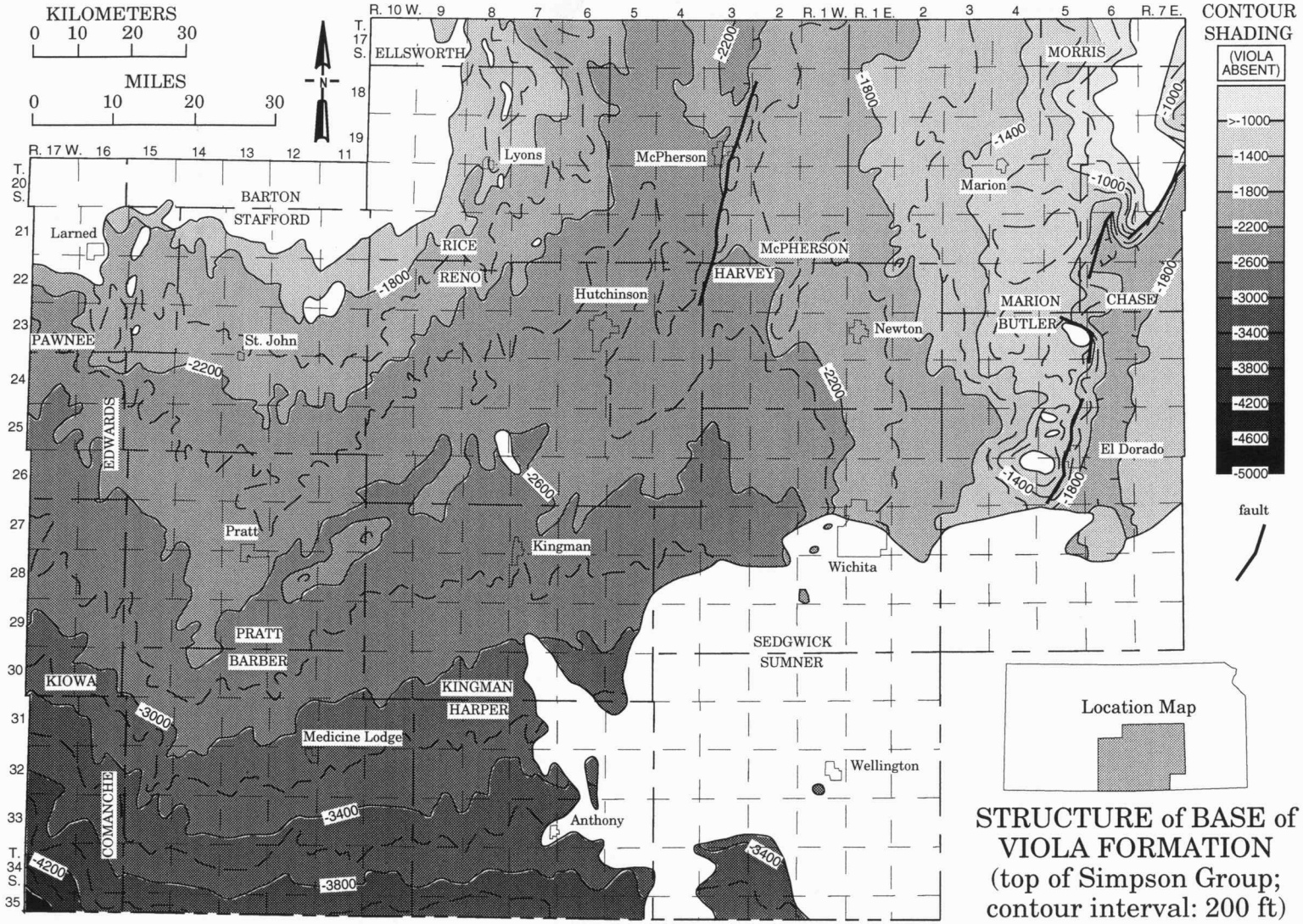

STRUCTURE of BASE of VIOLA FORMATION
(top of Simpson Group; contour interval: 200 ft)

Figure 4.3 Isopach map of Viola Formation in south-central Kansas study area from Adkison (1972), Cole (1975), and data from this study.

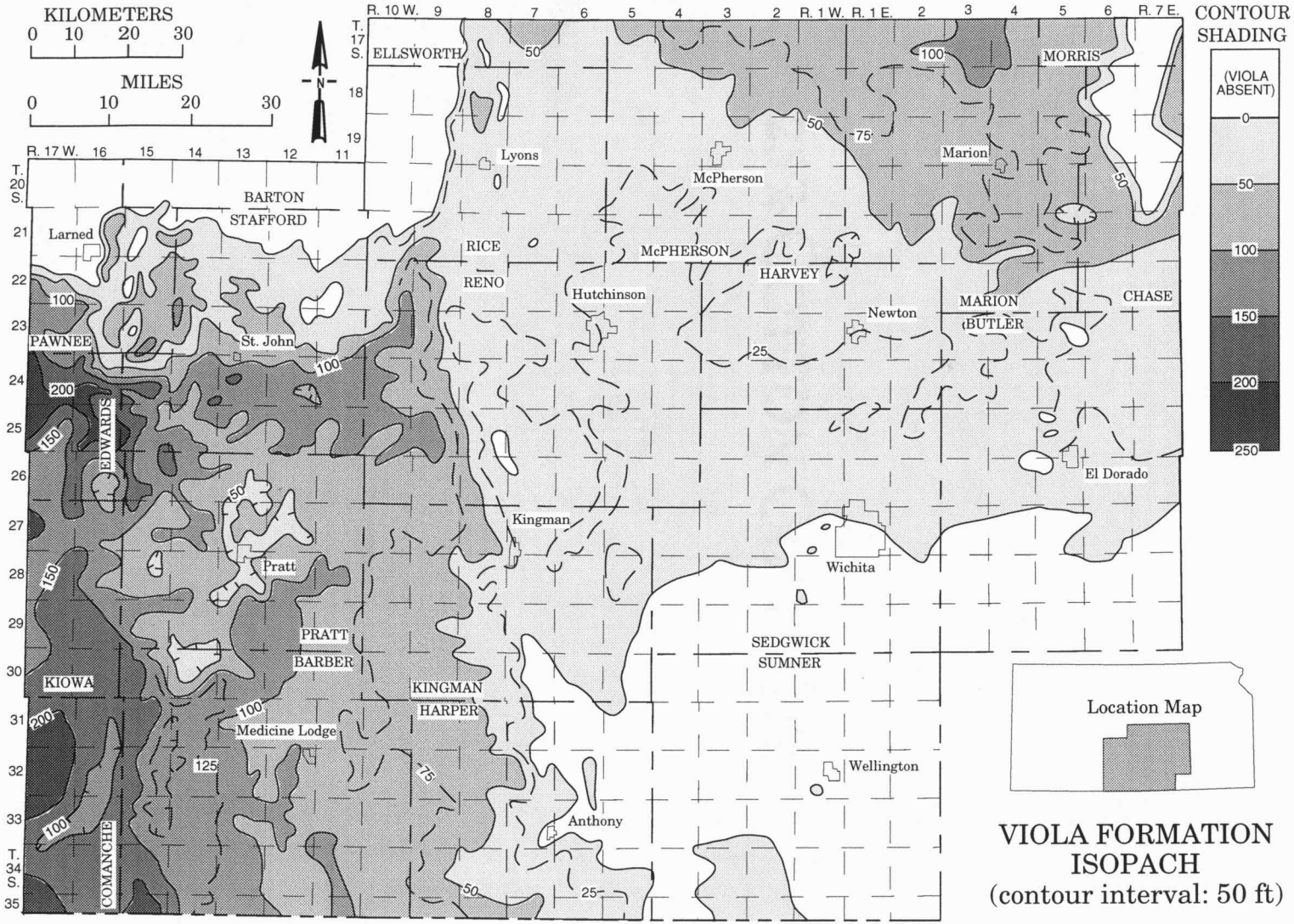

VIOLA FORMATION
ISOPACH
(contour interval: 50 ft)

(Chenoweth, 1966).

Minor erosion prior to deposition of Silurian and Devonian ("Hunton") carbonates and more marked uplift and erosion prior to deposition of the Upper Devonian -- Lower Mississippian Chattanooga Shale beveled Viola and other Ordovician units in the structural sag between the Ancestral Central Kansas uplift and the Chautauqua arch. In McPherson, Marion, and Rice counties, the Chattanooga Shale occupies a broad paleo-valley that cuts down to the Viola and even into the Simpson Group in some localities; hence, over much of central Kansas, Chattanooga Shale lies directly on the Viola Formation instead of on Maquoketa Shale. Lee (1956) dubbed this valley the "McPherson valley"; in its axis Chattanooga Shale is as thick as 275 ft (75 m).

The Simpson Group is universally present below the Viola in central and southern Kansas, but the configuration of stratigraphic units directly above the Viola is more complicated (Figure 4.4). Isolated areas where Viola underlies Chattanooga Shale in McPherson and Marion counties are along the axis of the McPherson valley. Farther west along the south-plunging Pratt anticline, the Chattanooga Shale *per se* is not present but is replaced by coarser-grained facies. These sandstones and siltstones may be equivalent to the entire Chattanooga Shale or just to the Misener sandstone member present in places at its base (Adkison, 1972). Inasmuch as these deposits are relatively thin (less than 50 ft [15 m]) and Chattanooga Shale is not present directly above these strata, they also may be sandy deposits developed above younger unconformities either at the base of the Mississippian carbonate section or even at the base of the Pennsylvanian System (McCaleb and Wheeler, 1965). Conodonts recovered from shale, shaly limestone, and sandstone in a core from Edwards County just west of the study area indicate the siliciclastic rocks at this locality are Mississippian (Kinderhookian) in age and therefore are time-equivalent to Chattanooga Shale,

Figure 4.4 A "worm's-eye view" or "lap-out" map illustrating units superjacent to Viola Formation in the study area. Area north of T.27S. and east of R.11W. is taken from Newell (1986; 1987a, b). The remaining area is from Adkison (1972). Upper Devonian -- Mississippian siliciclastic strata present in the western part of the map area are, in part, Mississippian (Kinderhookian) in age and therefore are time-equivalent to Chattanooga Shale, Sedalia Dolomite, or Gilmore City Limestone (Goebel, 1968c; see text for discussion).

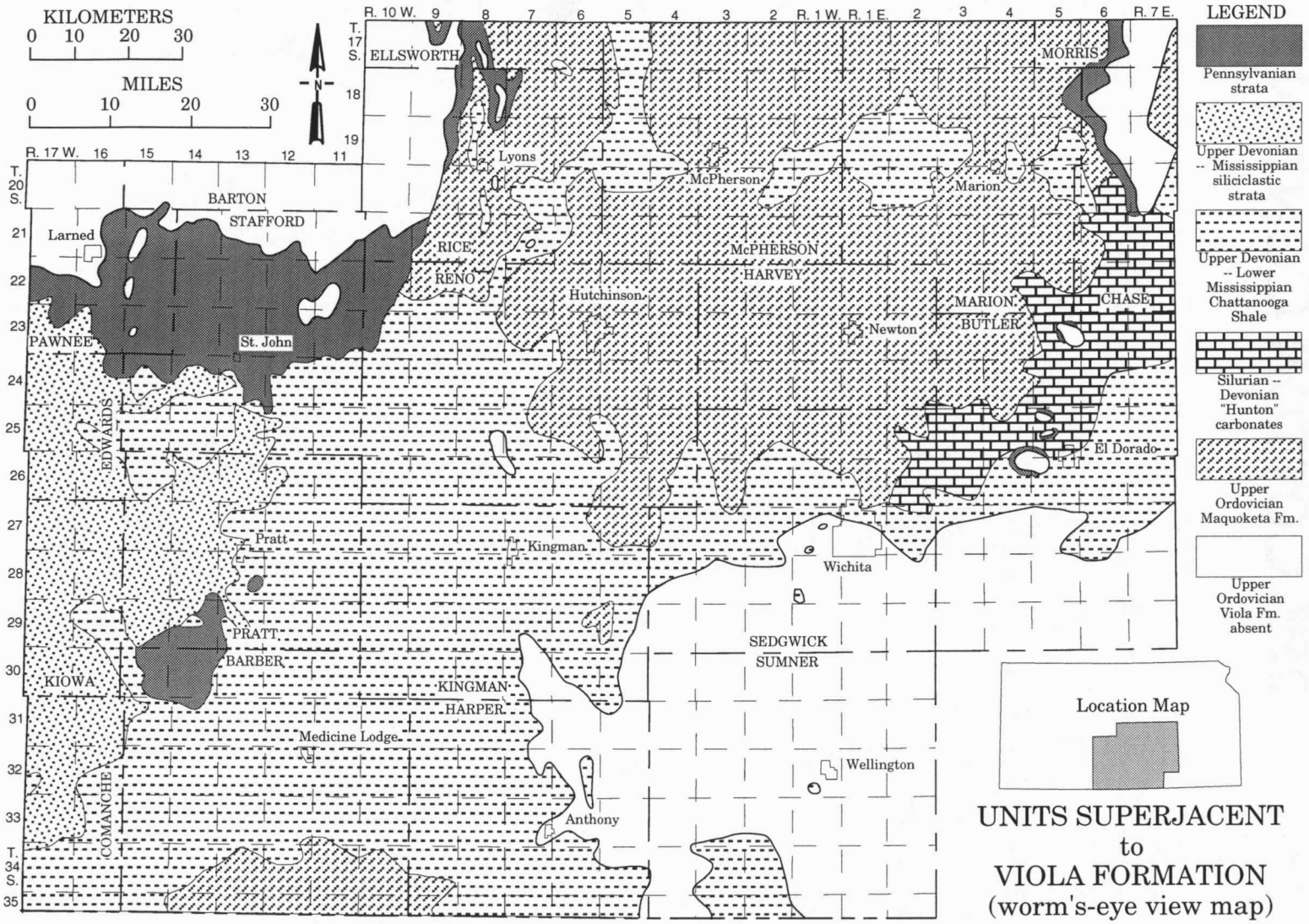
KILOMETERS
0 10 20 30
MILES
0 10 20 30
N
R. 10 W. 9 8 7 6 5 4 3 2 R. 1 W. R. 1 E. 2 3 4 5 6 R. 7 E.
R. 17 W. 16 15 14 13 12 11
T. 17 S.
18
19
T. 20 S.
21
22
23
24
25
26
27
28
29
30
31
32
33
T. 34 S.
35
ELLSWORTH
MORRIS
Lyons
McPherson
Marion
BARTON
STAFFORD
Larned
RICE
McPHERSON
HARVEY
RENO
Hutchinson
MARION
CHASE
BUTLER
Newton
PAWNEE
St. John
EDWARDS
El Dorado
Pratt
Kingman
Wichita
PRATT
BARBER
SEDGWICK
SUMNER
KIOWA
KINGMAN
HARPER
Medicine Lodge
Wellington
COMANCHE
Anthony
LEGEND
Pennsylvanian strata
Upper Devonian -- Mississippian siliciclastic strata
Upper Devonian -- Lower Mississippian Chattanooga Shale
Silurian -- Devonian "Hunton" carbonates
Upper Ordovician Maquoketa Fm.
Upper Ordovician Viola Fm. absent
Location Map
UNITS SUPERJACENT
to
VIOLA FORMATION
(worm's-eye view map)

Sedalia Dolomite, or Gilmore City Limestone (Goebel, 1968c).

Areas where Pennsylvanian strata lie on Viola (Figure 4.4) are where Viola has been beveled by late Mississippian -- early Pennsylvanian erosion. These areas are characteristically over structural highs on the Pratt anticline and along the flanks of the Central Kansas uplift (Adkison, 1972) and smaller but complex anticlinal closures on the Nemaha uplift such as the El Dorado anticline in Butler County (see Biederman, 1966). Adkison (1972) reported the greatest thickness of residual chert (50 to 100 feet; 15 to 30 m) in central and northern Stafford County is where the Viola subcrops beneath the basal Pennsylvanian unconformity on the southern margin of the Central Kansas uplift (Figure 4.4).

Chapter 5

STRATIGRAPHIC FRAMEWORK OF THE VIOLA FORMATION IN KANSAS

PREVIOUS STUDIES

Several informal stratigraphic divisions of the Viola Limestone have been proposed in Kansas (Figure 5.1). Most of these divisions are based on study of well cuttings and insoluble residues derived from well cuttings, principally characteristics of chert. In addition, most were made prior to the advent of modern carbonate petrography and modern wireline well-log suites (principally gamma ray, neutron porosity, and density logs), hence difficulties can occur in correlating from a well that has been stratigraphically subdivided according to cuttings to a subsequently drilled well nearby with geophysical logs.

Lee (1943) first subdivided the Viola in the Forest City basin of northeastern Kansas into three intervals -- an upper non-cherty dolomitic limestone, a middle cherty member, and a basal sparsely cherty limestone. The middle cherty member is divisible into three units; the middle one is non-cherty). These three zones were tentatively correlated by Lee (1943) to three zones defined by McQueen and Greene (1938) in the Kimmswick Formation in the subsurface in northwestern Missouri. Lee (1943) noted that the Viola is predominantly a dolomite in the northeast, but grades to limestone (from top to base) toward south-central Kansas. An absence of argillaceous impurities was also noted. After extending his study of Paleozoic rock units to the Salina basin of north-central Kansas, Wallace Lee stated that Viola Formation in Kansas "does not lend itself to accurate regional zoning" (Lee, 1956, p. 36). Taylor (1947b) and Ver Wiebe (1947, 1948) subdivided the Viola primarily by abundance and

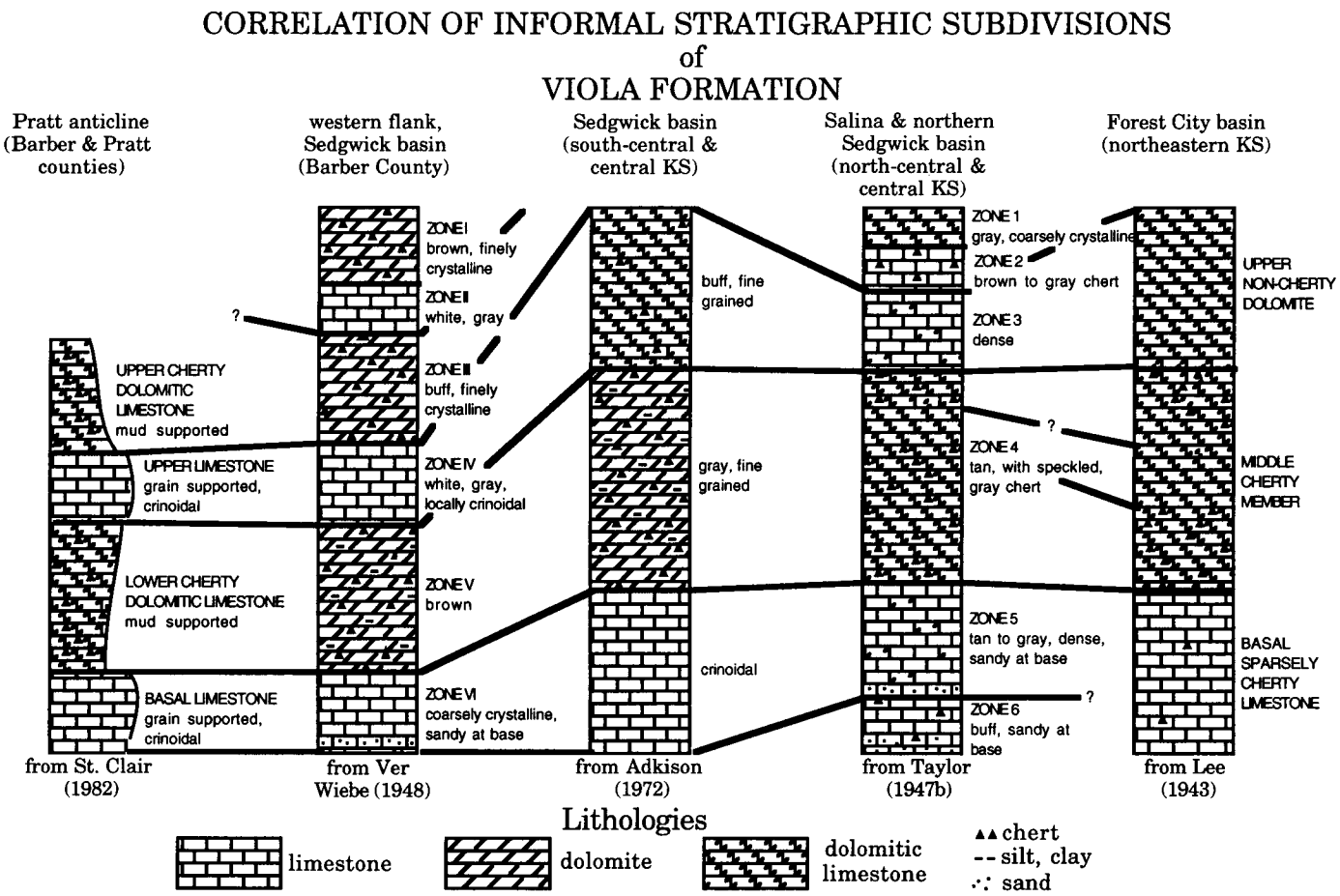

Figure 5.1 Summary of informal stratigraphic subdivisions of Viola Formation in Kansas (no vertical scale). Correlation of stratigraphic units by Lee (1943) and Taylor (1947b) is from Taylor (1947b). Correlation of Ver Wiebe (1948) to Adkison (1972) is from Adkison (1972). Correlation of stratigraphic units by St. Clair (1982) to Ver Wiebe (1948), and Adkison (1972) to Taylor (1948b) are from this study. See text for discussion on these informal units. No vertical scale is available for this conceptual correlation chart because original studies did not detail either thicknesses or specific localities within their study area.

characteristics of chert, which Lee (1943, 1956) maintained can be extremely variable over distances of less than 15 km. The lack of continuity in the presence and position of the cherty zones suggests intraformational unconformities, but no breaks in sedimentation were discernable (Lee, 1956).

Taylor (1947b) divided the Viola in the northern Sedgwick basin (central Kansas) and Salina basin (north-central Kansas) into six informal members. From base to top, these include: zone 6 (basal clastic member) -- a sandy, cherty limestone, 0 to 20 ft [0 to 6 m] thick), zone 5 (lower limestone member) -- brown or gray crystalline limestone with small amounts of dolomite and insoluble material, 0 to 50 ft [0 to 15 m] thick), zone 4 (middle cherty member) -- tan crystalline limestone, dolomitized in places with insoluble residues of dark-speckled, microfossiliferous rough and smooth chert, 0 to 100 ft [0 to 30 m] thick), zone 3 (middle limestone member) -- tan or gray dense to finely crystalline limestone with minor dolomite and little insoluble residue, 0 to 40 ft [0 to 12 m] thick), zone 2 (upper cherty limestone member) -- finely crystalline limestone containing large amounts of microfossiliferous, brown or gray, conchoidal, smooth chert, 0 to 25 ft [0 to 8 m] thick), and zone 1 (upper limestone member) -- a gray coarsely crystalline dolomitic limestone containing abundant coarse dolomite rhombs, 0 to 20 ft [0 to 6 m] thick). Taylor (1947b) stated that the basal clastic member (zone 6) is present only in north-central Kansas and may represent beds correlative to the Decorah-Platteville interval in northeastern Kansas. The lower limestone member (zone 5) is the most widespread of all the Viola zones. This zone and the superjacent middle cherty member (zone 4) are more dolomitic toward the south. Zones 4, 3, 2, and 1 are recognized only in the Salina basin and are successively more geographically limited to the north due to offlap (Taylor, 1947b). Zone 1 may represent dolomitization immediately beneath an unconformity at the base of the Maquoketa-Sylvan Shale, hence this zone may cross-cut lower stratigraphic

zones. Taylor (1947b) considered zone 4 equivalent to the middle cherty member of Lee (1943); zone 3 equivalent to the upper non-cherty member; and zone 5 (and possibly zone 6) equivalent to the lower sparsely cherty limestone (Taylor, 1947b; Figure 5.1). Taylor (1947b) inferred breaks in sedimentation above and below zone 4 on the basis of isopach mapping.

Ver Wiebe (1947, 1948), working in Barber County, and the western portion of the Sedgwick basin and northern part of the Hugoton embayment west of the Central Kansas uplift, informally split the Viola into six zones. From base to top, these include: zone VI -- white, coarsely crystalline limestone averaging 20 ft (6 m) thick; zone V -- dolomitic and cherty argillite with stony to smokey, dark-gray chert averaging 70 ft (21 m) thick; zone IV -- white to gray limestone with brown spots, locally crinoidal, averaging 30 ft (9 m) thick; zone III -- finely crystalline, cherty dolomite with tripolitic chert, averaging 50 ft (15 m) thick; zone II -- white to gray limestone with brown spots, similar to zone IV, averaging 20 ft (6 m) thick, and zone I -- finely crystalline, cherty dolomite averaging 30 ft (9 m) thick.

Ver Wiebe (1948) stated that zone VI is present over the entire Barber-County study area. He also maintained that zone V is similarly widespread and is mistakenly identified "by many" as Maquoketa. Zones IV through I are variably present, depending on the severity of erosion beneath the basal Pennsylvanian angular unconformity. Zones II and I are present only in the deepest structural lows or in areas well off the flanks of the Pratt anticline.

Cole (1975) recorded an informal stratigraphy of the Viola proposed by R.A. Carmody in 1958 by verbal communication. In central, southern, and southwestern Kansas, the Viola can be divided, from base to top into: Viola A -- fairly thin, non-cherty dolomite or limestone; Viola B -- thick, cherty dolomite; Viola C -- thin limestone, commonly absent; and Viola D -- dolomitic shale to dolomite. The relation

of this informal stratigraphy to those developed by the researchers above is unclear but observations in this study indicate the Viola A could be equivalent to zone VI of Ver Wiebe (1947, 1948) and zone 5 of Taylor (1947b), whereas Viola B could be equivalent to zone V of Ver Wiebe (1947, 1948) and zone 4 of Taylor (1947b).

Adkison (1972) inspected well cuttings of Ordovician rocks in the Sedgwick basin and recognized a tripartite stratigraphic architecture in the Viola: a basal light gray to buff, medium- to coarse-crystalline crinoidal limestone, 5 to 30 ft (1.5 to 9 m) thick, cross-bedded and dolomitized in places and overlain by gray to brownish gray, cherty, silty, fine- to very fine-grained dolomite, 15 to 60 ft (4.5 to 18 m) thick. The upper part of Viola consists mainly of light-gray to buff, fine- to medium-crystalline limestone and dolomite that is cherty or silty, or both. Chert is most abundant in an area extending southward from the Central Kansas uplift for about 60 mi (100 km). The basal crinoidal limestone is the most widespread of all the units traced by Adkison (1972). Adkison (1972) correlated his middle silty, dolomite unit to zone V of Ver Wiebe (1947, 1948), hence zone VI of Ver Wiebe (1947, 1948) would be equivalent to the basal crinoidal limestone unit (Figure 5.1).

Studies at the University of Kansas, Kansas Geological Survey, and Syracuse University (St. Clair, 1982, 1985; Bornemann, 1979; Bornemann and others, 1982; Bornemann and Doveton, 1983) eclectically utilized cuttings, cores, and, for the first time, wireline logs to subdivide the Viola on the western flank of the Sedgwick basin in Barber and Pratt counties. The Viola is divided into four mappable informal units. From base to top, these are: basal limestone, 5 to 25 ft (2 to 8 m) thick; lower cherty dolomitic limestone, 10 to 104 ft (3 to 32 m) thick; upper limestone, 4 to 32 ft (1 to 10 m) thick; and upper cherty dolomitic limestone, 4 to 48 ft (1 to 15 m) thick. The limestones are low-porosity crinoidal packstones, whereas the cherty dolomites generally are mixed-skeletal dolomitized wackestones and mudstones with nodular

chert (St. Clair, 1982, 1985). St. Clair did not correlate this informal stratigraphy with previous studies, but her four units are probably equivalent to zones VI, V, IV, and III of Ver Wiebe (1947, 1948; Figure 5.1).

METHODS AND PROCEDURES

In order to better understand the spatial distribution and thickness of subunits within the Viola Formation, several regional and local stratigraphic cross-sections were assembled to trace the subsurface distribution of the four Viola subunits defined by St Clair (1982, 1985). The stratigraphic datum for these cross-sections was the contact between the Viola Formation and the underlying Simpson Group (i.e., the top of the Simpson Group). The advantage of using this contact as a datum is that it is present over the entire study area and it has comparatively little local or differential erosion associated with it, inasmuch as the Simpson stays relatively constant in thickness. Thin shale beds at or near the top of the Simpson also persist over wide areas (up to 10 or more townships), thereby indicating the contact between the Simpson and the overlying Viola was not subject to appreciable erosion. Conversely, as indicated by the worm's eye view map (Figure 4.4) and local subcrop maps of units above the Viola Formation (Newell, 1987a, b), unconformities of varying ages bevel the top of the Viola, hence using the top of the Viola as a datum would subject stratigraphic correlations within the Viola to unnecessary complications.

An example of the correlation of the four Viola subunits defined by St Clair (1982) to geophysical logs is shown in Figure 5.2. Resistivity and newer porosity-specific tools such as the density and neutron logs respond to the relatively high and low porosities that respectively typify the cherty dolomites and the limestones that

Figure 5.2 Characteristic geophysical log signatures of Viola subunits from two wells approximately 1900 ft (580 m) apart. The Sinclair-Prairie #1 Eva DeGeer log (taken from St. Clair, 1982) is a typical older electrical log run in 1947 whereas the newer Vincent Oil #1 DeGeer log, which illustrates the corresponding response of the neutron porosity, density porosity, and gamma ray tools, was run in 1983. The apparent downward offset of the trace of the lateral log versus the normal resistivity log on the Eva DeGeer well is an artifact of the spacing of the electrodes on these respective tools (see Schlumberger, 1987, p. 69-74). Lime grainstones (basal limestone and upper limestone) are typically nonporous and have high resistivities whereas dolomitic mudstones (lower cherty dolomitic limestone and upper cherty dolomitic limestone) have higher porosities and lesser resistivities. Log depths are in feet.

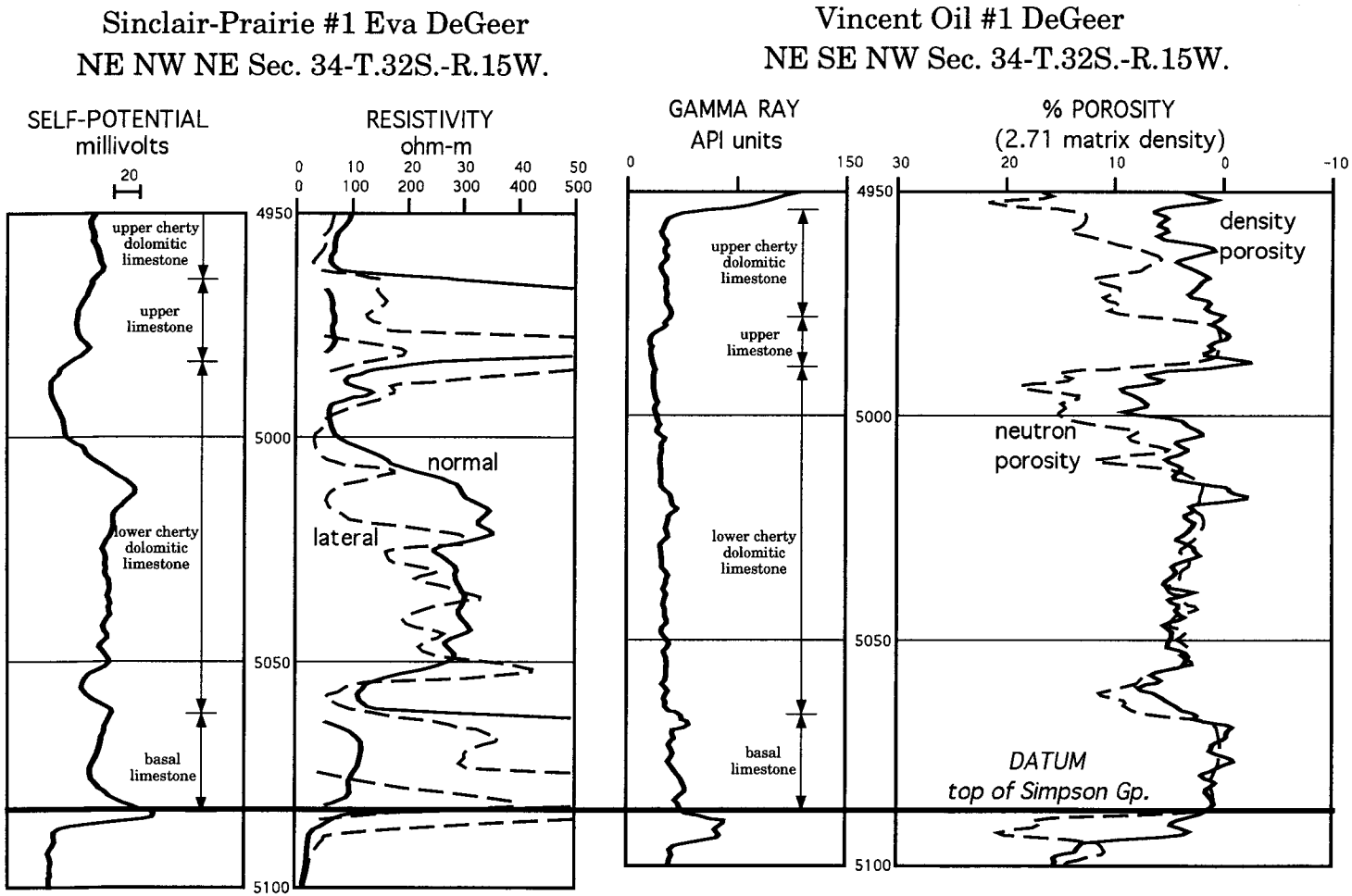

CHARACTERISTIC GEOPHYSICAL LOG SIGNATURES of VIOLA SUBUNITS

make up the informal stratigraphy of the Viola. The basal limestone and upper limestone are typically nonporous and their lack of porosity is particularly evident by marked rightward deflections with neutron and resistivity logs. Minor deflection of the density log is also evident. Conversely, porosity in the cherty dolomitic limestones is expressed by low resistivity and leftward deflection of the neutron log. The lesser response of the density log to porosity in the cherty dolomitic limestones, as compared to the marked response of the neutron log, reflects the greater density of the mineral dolomite (2.876 grams/cc) as compared to calcite (2.710 grams/cc) (Asquith with Gibson, 1982, p. 67; Doveton, 1986, p. 267). SP (self-potential; spontaneous potential) and gamma ray logs are not very useful for identifying the Viola subunits (Figure 5.2). Correlation of the Viola subunits to geophysical logs was aided comparing sample logs of cuttings and selected cores with their associated geophysical logs, or with very nearby wells with geophysical logs.

Drill cuttings (lithologic sample) logs are useful as a general guide to understanding stratigraphic correlations, but they are not practical for detailed stratigraphic correlations of units within the Viola (with perhaps the exception of the basal limestone unit). Nonporous crinoidal grainstones and packstones that characterize the basal limestone and upper limestone of St. Clair (1982, 1985) are usually identified as "white, crystalline" or "tight" limestones in sample logs based on cuttings. Cherty dolomitic limestones typifying the lower and upper cherty dolomitic limestones are usually identified as "gray, microcrystalline", "porous", or "cherty dolomite".

Initial examination of widespread cores, cuttings sample logs and nearby geophysical logs, indicates that the internal subunits of the Viola Formation are consistently correlatable over the study area. The crinoidal packstones (the basal limestone and upper limestone documented by St. Clair) are, as a general rule, less

porous than the upper and lower cherty dolomitic limestones. Two long-distance stratigraphic cross-sections (Plates 1, 2) illustrate the widespread nature of the subunits of the Viola (see location of these cross sections in Figure 5.3). Several other regional cross sections are archived at the Kansas Geological Survey.

The cross sections in Plates 1 and 2 and others, were used as reference correlations for inspection of several hundred well logs for regional geologic mapping of the Viola subunits. A spreadsheet database in Lotus 1-2-3 (by Lotus Development Corporation of Cambridge, MA) of 1709 well logs was compiled with interpretation of geophysical logs available in the Kansas Geological Survey Well Data Library (see Appendix I). Operator, well name, datum elevation (i.e., usually kelly bushing elevation but with some wells drill floor or surface elevations were used as datums), and legal description (i.e., section-township-range and spot location) for each of these wells were recorded in this database, in addition to geologic information on the depths of the tops of the four Viola subunits defined by St. Clair (1982) and the underlying Simpson Group. Spatial density of wells used in the database varied according to the geologic complexity of the area. A maximum density of 36 wells per township (1 well per section) was used over the structurally complex Pratt anticline in south-central Kansas (Figure 1.2). Lesser densities of 9 wells per township (1 well per 4 sections) and 4 wells per township (1 well per 9 sections) were used in less structurally deformed areas to the north and east of the Pratt anticline (Figure 5.4). The locations of wells used in the database and resultant maps are shown in Figure 5.5.

While entering information into this database, a subcrop map (Figure 5.6) was drawn showing which of the four informal subunits was present at the top of the Viola Formation. Original map scale was 1:250,000 (1 inch equals approximately 4 miles; 1 cm equals 2.5 km). Isopach maps of the four subunits, derived from data presented in Appendix I, are displayed in Figures 5.7, 5.11, 5.14, and 5.16. These maps were

Figure 5.3 Base map showing location of regional cross-sections (see Plates 1 [A-A'] and 2 [B-B']) and detailed study area featured in Figures 5.15, 5.16, 5.17, 5.18, and 5.19.

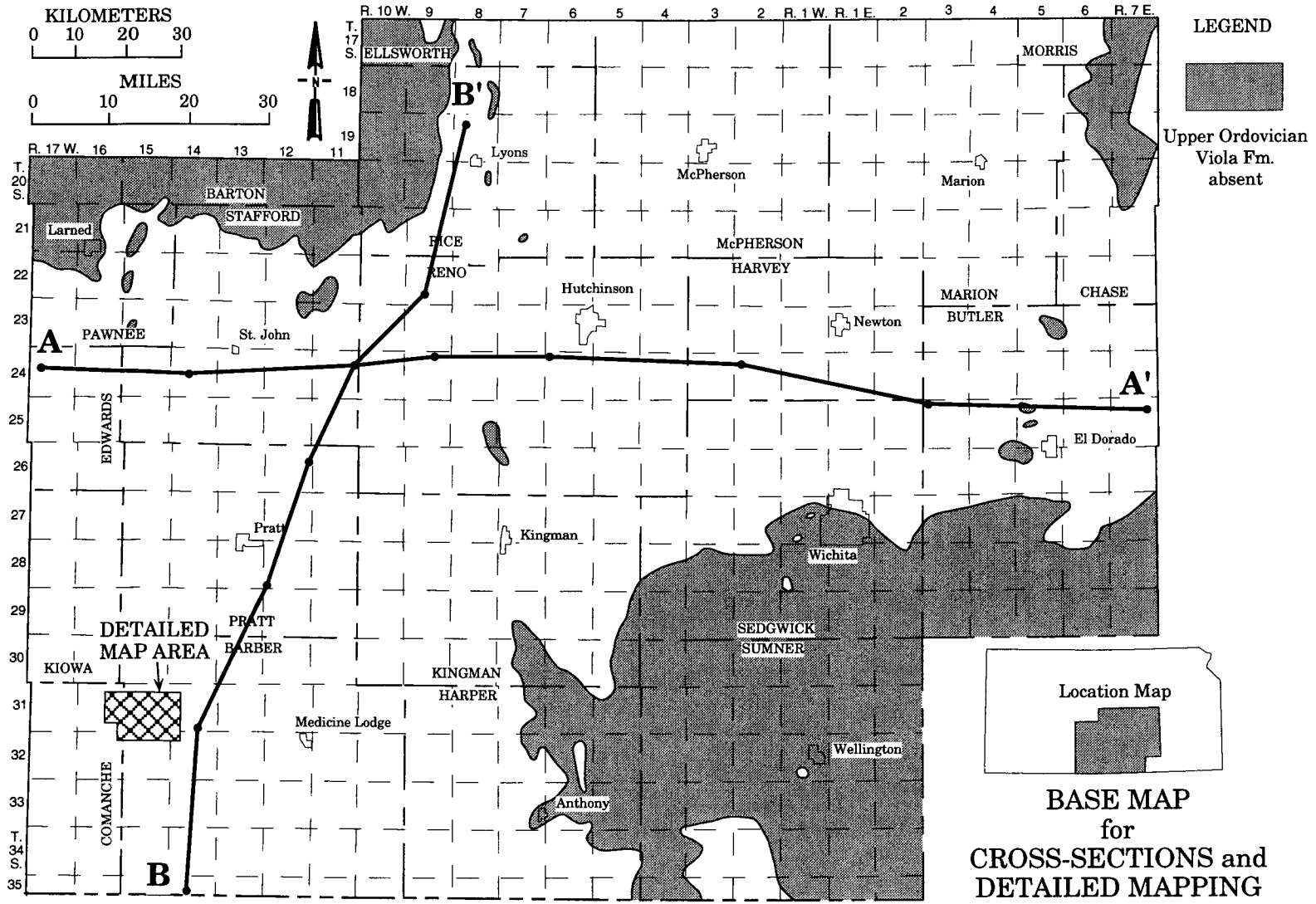
KILOMETERS
0 10 20 30
MILES
0 10 20 30
N
R. 10 W. 9 8 7 6 5 4 3 2 R. 1 W. R. 1 E. 2 3 4 5 6 R. 7 E.
R. 17 W. 16 15 14 13 12 11
T. 17 S.
T. 20 S.
T. 34 S.
ELLSWORTH
MORRIS
BARTON
STAFFORD
Larned
Lyons
McPherson
Marion
RICE
RENO
McPHERSON
HARVEY
Hutchinson
Newton
MARION
BUTLER
CHASE
PAWNEE
St. John
EDWARDS
El Dorado
Pratt
Kingman
Wichita
SEDGWICK
SUMNER
DETAILED
MAP AREA
PRATT
BARBER
KIOWA
KINGMAN
HARPER
Medicine Lodge
Wellington
COMANCHE
Anthony
A
A'
B
B'
LEGEND
Upper Ordovician
Viola Fm.
absent
Location Map
BASE MAP
for
CROSS-SECTIONS and
DETAILED MAPPING

Figure 5.4 Well density used for isopach and subcrop mapping of Viola subunits. The differing densities were necessary for understanding the geologic complexity of the study area. The greatest density of coverage was necessary in the relatively geologic complex area of the Pratt anticline in Barber, Comanche, Kiowa, and Pratt counties.

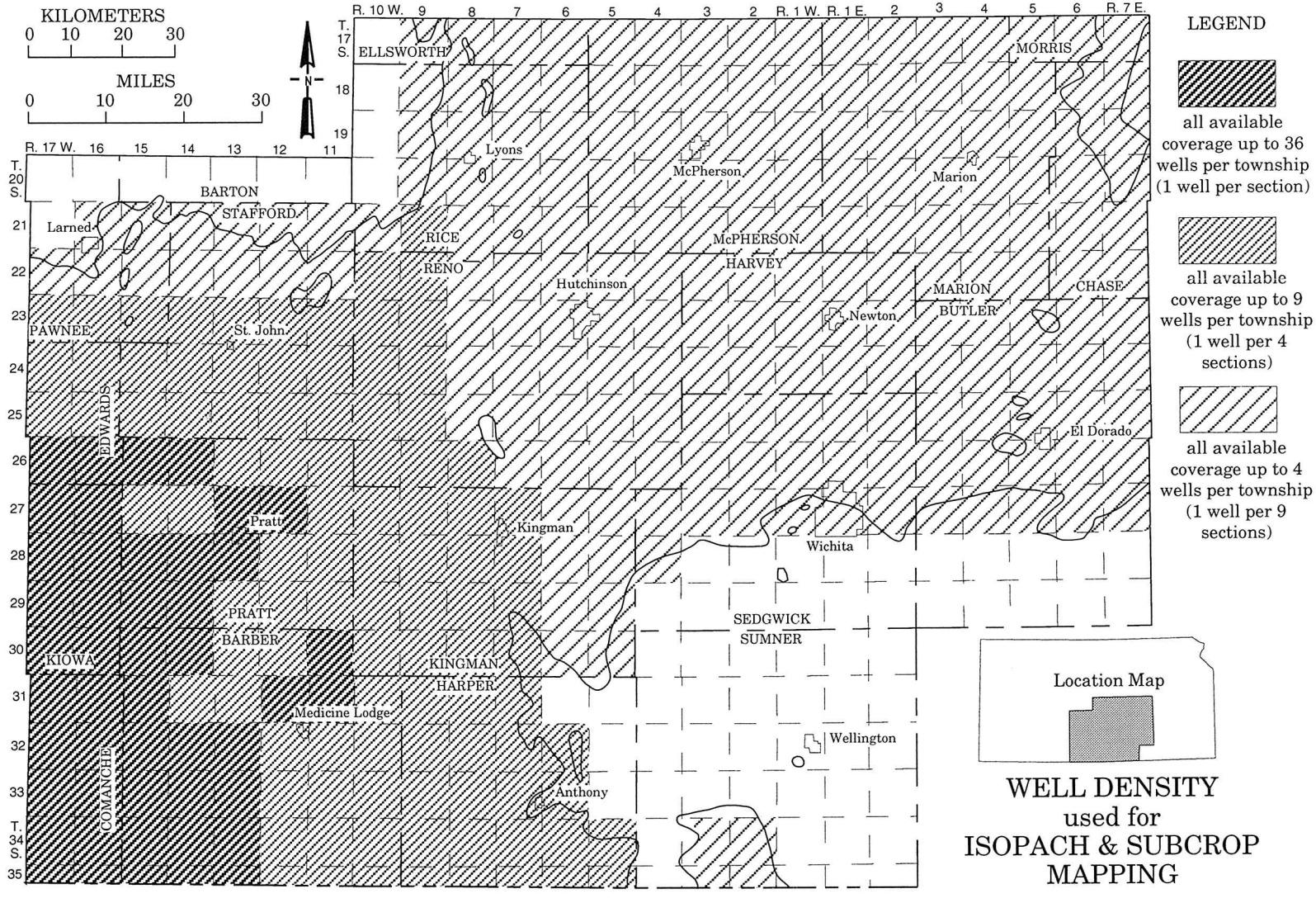

WELL DENSITY
used for
ISOPACH & SUBCROP
MAPPING

Figure 5.5 Location of wells used in regional subcrop mapping (Figure 5.6) and isopach mapping (Figures 5.7, 5.11, 5.14, 5.16). A total of 1709 wells are were used for this mapping (Appendix I).

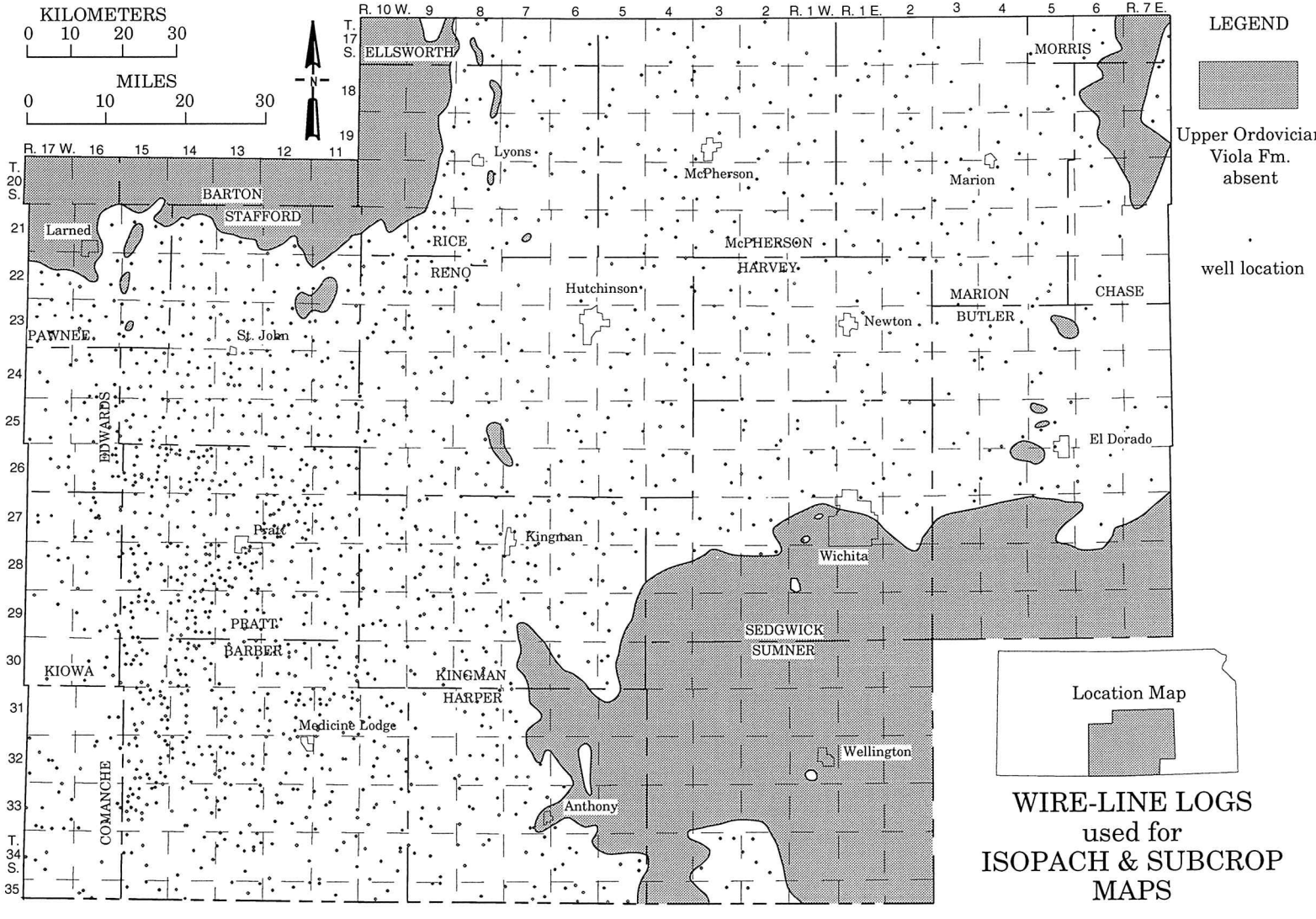
KILOMETERS
0 10 20 30
MILES
0 10 20 30
N
R. 10 W. 9 8 7 6 5 4 3 2 R. 1 W. R. 1 E. 2 3 4 5 6 R. 7 E.
R. 17 W. 16 15 14 13 12 11
T. 17 S.
T. 20 S.
T. 34 S.
18
19
21
22
23
24
25
26
27
28
29
30
31
32
33
35
ELLSWORTH
MORRIS
Lyons
McPherson
Marion
BARTON
STAFFORD
Larned
RICE
RENO
McPHERSON
HARVEY
Hutchinson
MARION
CHASE
BUTLER
Newton
PAWNEE
St. John
EDWARDS
El Dorado
Pratt
Kingman
Wichita
PRATT
BARBER
SEDGWICK
SUMNER
KIOWA
KINGMAN
HARPER
Medicine Lodge
Wellington
COMANCHE
Anthony
LEGEND
Upper Ordovician Viola Fm. absent
well location
Location Map
WIRE-LINE LOGS
used for
ISOPACH & SUBCROP
MAPS

produced using Surface III, a contouring program developed by the Kansas Geological Survey (Lawrence, KS). Translation of legal locations for each well to latitude-longitude measurements used in mapping was done with a conversion program "LEO II" (Ross, 1991). Graphical output from Surface III was sent to the Macintosh graphics program "Canvas" (Deneba Software, San Diego, CA). "Canvas" and "Aldus SuperPaint" (Silicon Beach Software, San Diego, CA) are used for drafting most of the illustrations in this dissertation.

The Surface III program was run on a Macintosh computer. Surface III, like most computer-contouring programs, takes irregularly spaced data (well locations, in this case) and creates a regularly-spaced network of values (an orthogonal grid). Contour maps are in turn created by "weaving" contour lines through this grid (Davis, 1976, 1987; Sampson, 1988). The mathematically-derived orthogonal grid of values is constructed for the practical reason in that it is easier to draw contour lines through an array of regularly-spaced grid values than through an irregular spacing represented by the original values. Although minor errors can result from this method in that the contours may not honor all control points, the regional mapping for which Surface III was used in this case also is inherently an approximation. Local variations generally represent details much too fine to display on the map anyway.

RESULTS AND DISCUSSION

Subcrop Mapping

The subcrop map of Viola subunits (Figure 5.6) shows that the Viola Formation is eroded down to its lowermost informally identified subunit, the basal limestone, over the north-northwest--south-southeast trending crest of the Central Kansas arch that

Figure 5.6 Subcrop map displaying which subunit of the Viola Formation is present at the top of the Viola Formation. The unconformity beveling the Viola Formation varies over the study area. The worm's-eye-view map (Figure 4.4), complements this map by illustrating the rock unit superjacent to the Viola Formation. The north-northwest--south-southeast trending crest of the Central Kansas arch (northwestern Sedgwick, eastern Rice, and eastern Reno counties) is illustrated by the presence of the lowermost subunit of the Viola, the basal limestone, being present at the top of the Viola Formation.

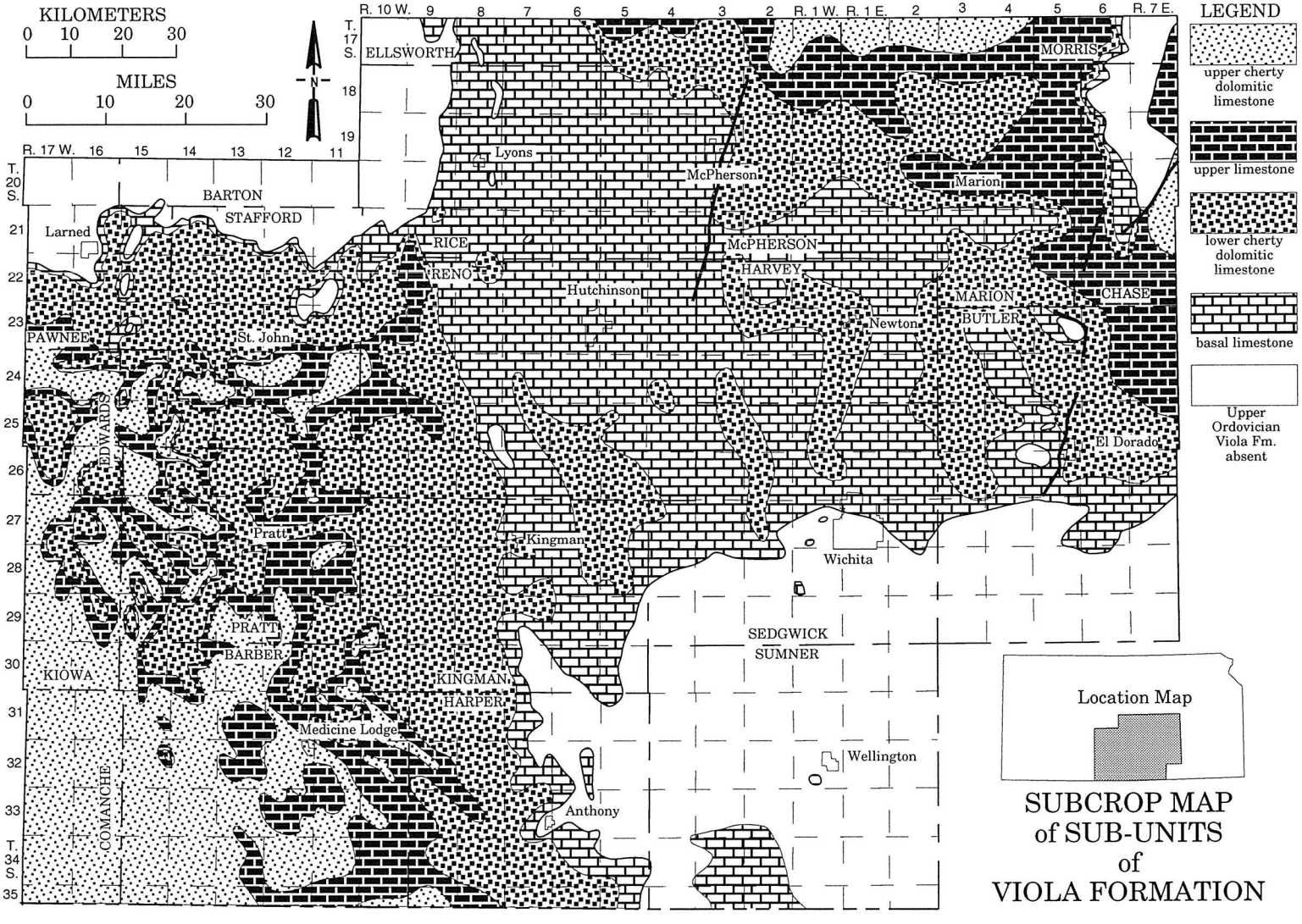
KILOMETERS
0 10 20 30
MILES
0 10 20 30
N
R. 10 W. 9 8 7 6 5 4 3 2 R. 1 W. R. 1 E. 2 3 4 5 6 R. 7 E.
R. 17 W. 16 15 14 13 12 11
T. 17 S.
T. 20 S.
T. 34 S.
18
19
21
22
23
24
25
26
27
28
29
30
31
32
33
35
ELLSWORTH
MORRIS
Lyons
McPherson
Marion
BARTON
STAFFORD
Larned
RICE
RENO
McPHERSON
HARVEY
Hutchinson
MARION
CHASE
Newton
BUTLER
PAWNEE
St. John
EDWARDS
El Dorado
Pratt
Kingman
Wichita
PRATT
BARBER
SEDGWICK
SUMNER
KIOWA
KINGMAN
HARPER
Medicine Lodge
COMANCHE
Wellington
Anthony
LEGEND
upper cherty dolomitic limestone
upper limestone
lower cherty dolomitic limestone
basal limestone
Upper Ordovician Viola Fm. absent
Location Map
SUBCROP MAP
of SUB-UNITS
of
VIOLA FORMATION

extends through southwestern Rice, northeastern Reno, and northwestern Sedgwick counties. Successively younger subunits are arrayed in a generally symmetric pattern along the northeastern and southwestern flanks of the arch. Comparison of this erosional pattern with that of the worm's-eye view map (Figure 4.4) indicates that much of the erosion accounting for the subcrop pattern on the northeastern flank of the arch (i.e., the general area encompassing northern Butler, Chase, Harvey, Marion, McPherson, Rice, and northern Sedgwick counties) occurred before deposition of the Upper Ordovician Maquoketa Formation because the truncated Viola subunits underlie the Maquoketa in this region. The arch was thus active during Ordovician time prior to deposition of the Maquoketa Formation. A subtle angular unconformity separates the Viola from the overlying Maquoketa Formation. Uplift of the Central Kansas arch and concomitant subsidence of the North Kansas basin may have even begun prior to deposition of the Viola Formation because Lee (1949) noted that the underlying Platteville Formation of the Simpson Group gradually thickens to the center of the North Kansas basin. Adkison (1972) noted the absence of carbonates in the Simpson Group over the arch together with their increased presence along the flank and also attributed this to slight movement of the arch in possibly an entirely marine environment during Simpson deposition.

The subcrop map (Figure 5.6) reveals a complex group of northwest-southeast trending, township-size uplifts on the southwestern flank of the Central Kansas arch (i.e., in the area of Edwards, Pratt, northern and eastern Barber, and western Harper County). The amoeboid appearance of some of these features can also be the result of differential erosion and relief on the unconformity at the base of the Chattanooga Shale in combination with low angles of dip the subunits of the Viola have in relation to this unconformity. Although location of faults are difficult to define precisely with present control, they may be present in this region of uplifts where there are close-

spaced changes in the subcrop pattern. The Viola unconformably underlies the Upper Devonian -- Lower Mississippian Chattanooga Shale over most of this region, so the subtle tectonic movement responsible for these structures can only be assigned a pre-Late Devonian -- post-Middle Ordovician age. Minor Late Mississippian to Early Pennsylvanian faulting along the north-south-trending Pratt anticline in northwestern Barber and southwestern Pratt counties is indicated by Pennsylvanian strata being directly superjacent to the Viola (Figure 4.4). Average throw of major faults paralleling the north-northeast--south-southwest-trending Pratt anticline in Pratt County is 150 ft (45 m; Brewer, 1959).

The north-south trending Voshell fault in McPherson County is also illustrated on the Viola subcrop map (Figure 5.6). This fault is located on the western flank of the McPherson anticline (Hiestand, 1933) or Voshell anticline (Berendsen and Blair (1986), a pronounced structure with separate culminations that are the loci for a series of oil and gas fields (Newell and others, 1987). Present offset of this fault is down to the west. Mississippian strata are offset approximately 400 ft (125 m; Berendsen and Blair, 1986). Although major movement on this fault occurred in Late Mississippian to Early Pennsylvanian time (Hiestand, 1933; Jewett, 1951; Merriam, 1963), the presence of younger subunits of the Viola on the eastern side of this fault indicates that it may have an earlier history of movement that is the reverse (i.e., down to the east) of the dominant direction of movement in late Paleozoic time. Similarly, the preservation of Silurian -- Devonian "Hunton" carbonates only to the east of this fault, as shown in a sub-Chattanooga Shale subcrop map (Newell, 1987b) also implies that this fault may have had an early history of down-to-the-east movement.

Regional Isopach Mapping

Basal Limestone

An isopach of the basal limestone subunit (Figure 5.7) reveals this subunit is thickest in the northern part of the study area in the vicinity of Harvey, Marion, McPherson, and Rice counties. Notwithstanding possible erosional beveling at the base of the Maquoketa Formation, it is nearly 60 ft (18 m) thick in Rice County. Minor thickening is also evident in Pawnee and Edwards counties just south of the Central Kansas uplift. The marked thickening of this subunit in this vicinity of the crest of the Central Kansas arch and immediately to the north indicates the persistence of depositional conditions that encouraged accumulation of crinoid and bryozoan fragments. Southwest of its present-day subcrop, the basal limestone subunit (see Figures 5.6, 5.7) is considerably thinner (10 to 20 ft; 3 to 6 m), possibly signifying conditions for development of crinoid and bryozoan packstones were less intense or long-lived.

Depositional conditions for the basal limestone subunit are discussed in detail in the lithofacies chapter (Chapter 7), but relatively shallow-water conditions are indicated for the packstones that dominate the basal and upper limestones. Relatively deeper water influences deposition in the intervening cherty dolomitic limestone subunits. The thickening of the packstone-dominated subunits on-structure, and the thickening of the mudstone-dominated subunits off-structure pattern is consistent with the probable deeper and more open-water conditions that would be expected off the Central Kansas arch and, in general, farther south toward the continental margin and ancestral Anadarko basin (Figure 2.3).

Another cogent feature of the isopach of the basal limestone is a zone of thin areas less than 10 ft [3 m] thick, NNE-SSW trending, extending from northern Pratt County to northeastern Kiowa County. This trend spatially coincides with the

Figure 5.7 Regional isopach map of the basal limestone of the Viola Formation. This map and the other isopach maps at this scale were constructed using a 49 X 38 grid -- each grid cell approximately corresponds to an area of one-quarter township. Grid nodes were calculated by linear projection (Davis, 1987) and a nearest-neighbor search of for the eight closest points to the grid node being estimated. The subcrop of the basal limestone (taken from Figure 5.6) is shown in gray tone. The basal limestone is relatively thick on top of the Central Kansas arch and directly north of its subcrop (i.e., Marion, McPherson, and Rice counties), thereby indicating the presence of shallow-water shoals on top of the arch and on the northern flank of the ancestral Anadarko basin.

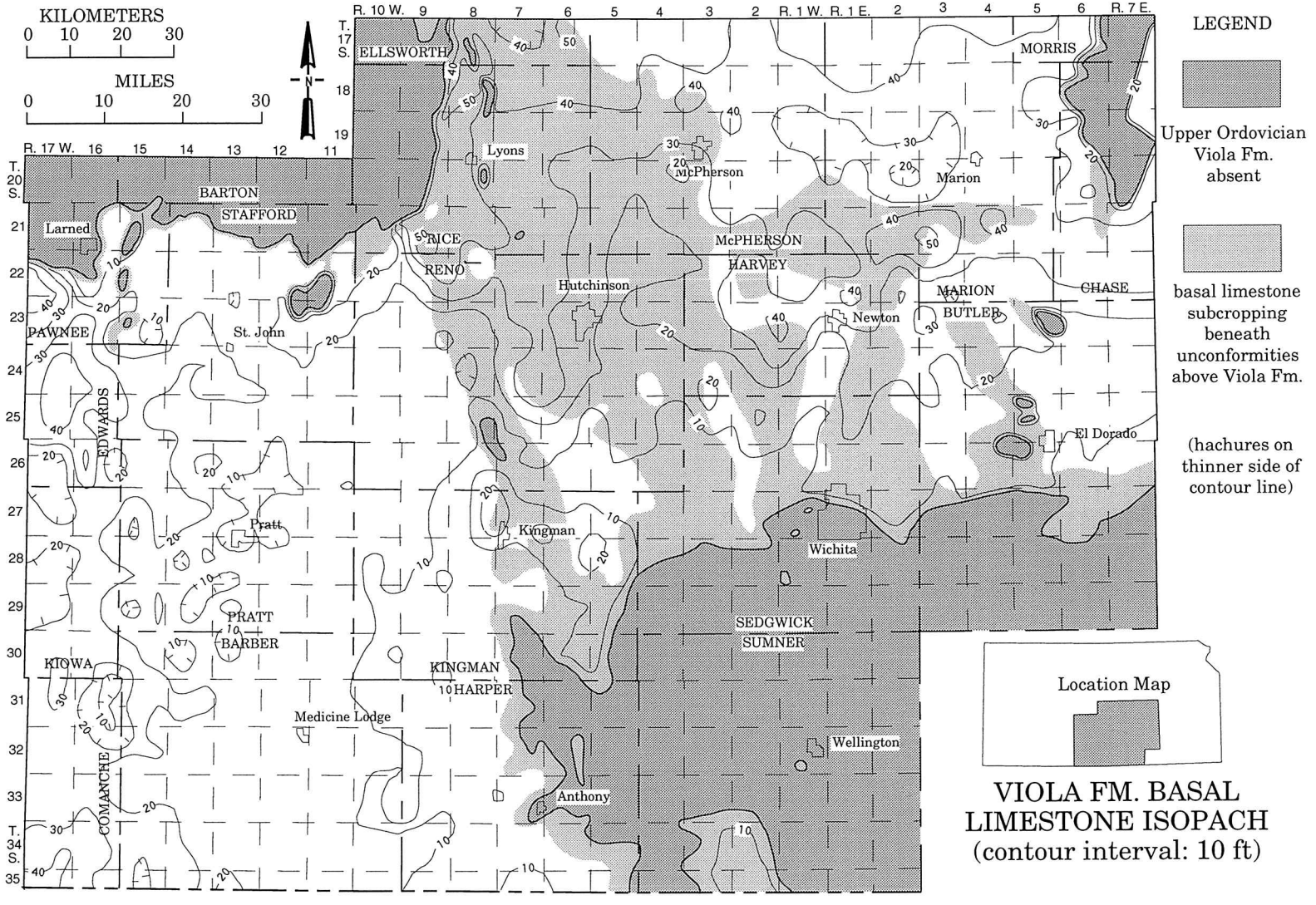

VIOLA FM. BASAL LIMESTONE ISOPACH
(contour interval: 10 ft)

present-day trend of the Pratt anticline (Merriam, 1963; Figures 1.2, 4.2) and indicates that, contrary to the regional thickening present on the northern flank of the Central Kansas arch, the basal limestone may display thinning over sharper and more localized structures that probably were active during its deposition. The Pratt anticline may be a Late-Mississippian -- Early-Pennsylvanian manifestation of a long-lived zone of structural weakness that coincides with the western flank of the 1100-Ma Midcontinent Rift System (cf., Van Schmus and others, 1982; Dickas, 1986) and with one of several NNE-SSW trending magnetic lineations evident in the Precambrian basement (Yarger, 1981, 1983). Subtle NNE-SSW trends in chert content and porosity of the Viola Formation in this area have also been noted by Doveton and Bornemann (1981), Bornemann and others (1982), and Bornemann and Doveton (1983). The NW-SE orientation of the individual thin areas along a NNE-SSW trend produces a left-stepping *en echelon* pattern that is compatible with left-lateral movement along this long-lived zone of structural weakness.

A trend-surface fitted to the basal limestone isopach is shown in Figure 5.8. Trend surfaces are mathematically derived polynomial surfaces that represent a best fit to a surface in question -- in this case the isopach map of the basal limestone. Trend-surface analysis is useful to separate regional trends from local trends (Doveton and Bornemann, 1981; Davis, 1986, p. 405). The order of the trend surface corresponds to its increasing complexity. A first-order trend surface is a plane, a second-order trend surface has one curve (or fold) in it. Higher-order surfaces are increasingly more complex and will increasingly better fit the surface to which they are compared, but eventually successively higher-order surfaces will only marginally improve the fit (Doveton and Bornemann, 1981; Davis, 1986, p. 419). Goodness-of-fit statistics for several trend surfaces fitted to the basal limestone isopach are shown in Figure 5.9. According to Davis (1986, p. 418-419), the interpretation of goodness-of-fit

Figure 5.8 A third-order trend surface fitted to the basal limestone isopach depicted in Figure 5.7.

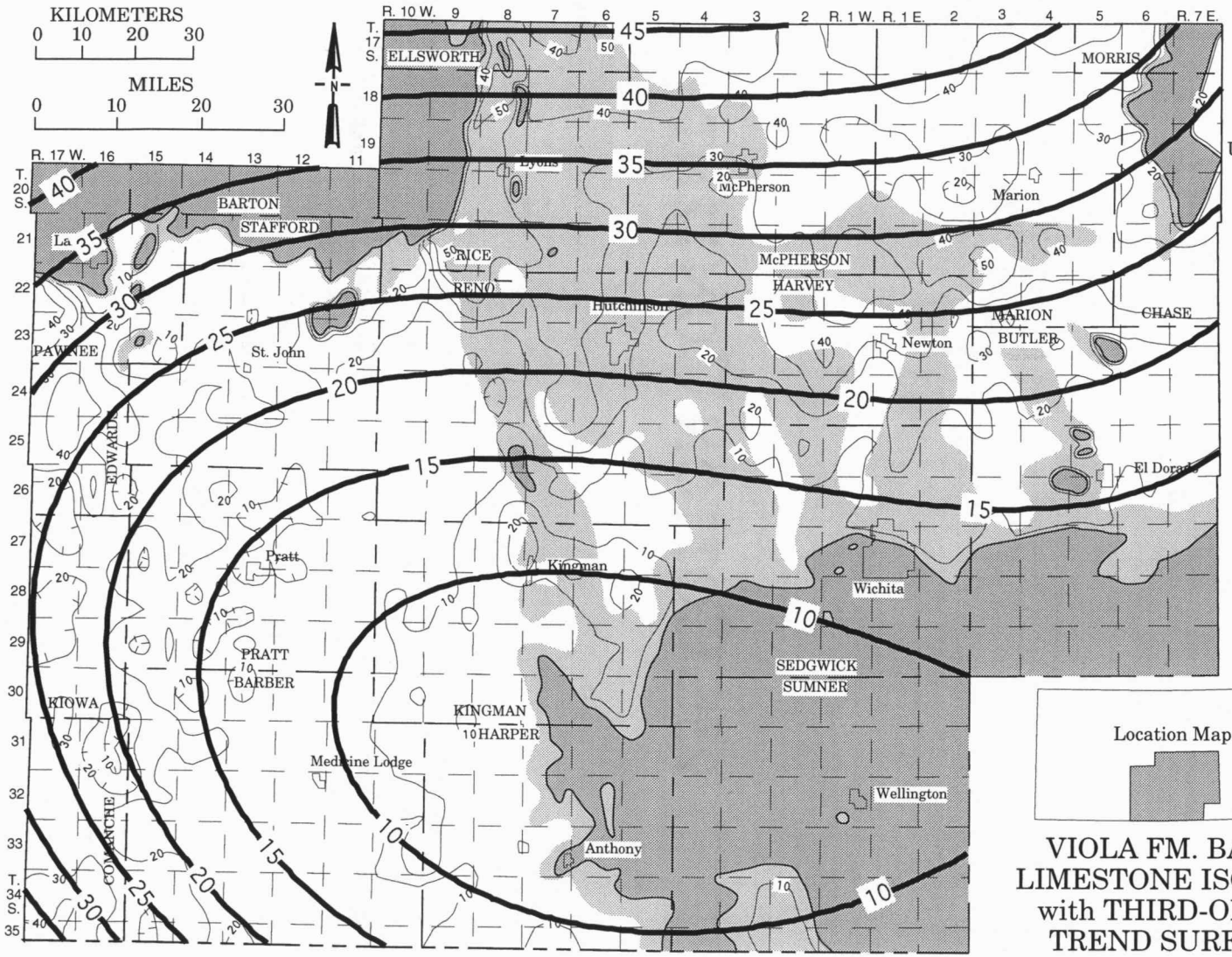

LEGEND

Upper Ordovician Viola Fm. absent

basal limestone subcropping beneath unconformities above Viola Fm.

(hachures on thinner side of contour line)

Location Map

VIOLA FM. BASAL LIMESTONE ISOPACH with THIRD-ORDER TREND SURFACE

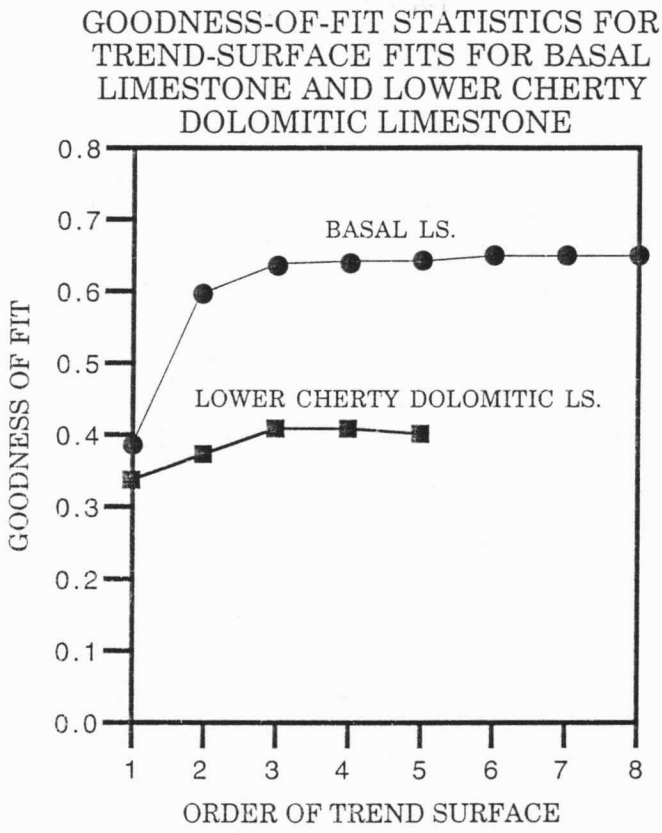

Figure 5.9 Goodness-of-fit statistic for varying orders of trend surfaces fitted to the basal limestone subunit and the lower cherty dolomitic limestone subunit of the Viola Formation. Higher-order trend surfaces could not be computed for the lower cherty dolomitic limestone subunit due to insufficient distribution of data over the study area.

statistics is somewhat arbitrary, but his experience with trend-surfaces of geologic structures indicates that correlations of less than 0.3 provide a "poor fit", whereas those higher than 0.7 conform closely to the original data points. Higher-order surfaces yield little additional information with regard to removing a regional trend from the original data. Curiously, with the basal limestone, a reasonably acceptable fit (0.59 goodness of fit) for trend-surface analysis was obtained with a second-order trend surface. The third-order surface showed marginal improvement (0.64 goodness of fit), and higher-order surfaces were characterized with only triflingly better fits

(Figure 5.9). Subtraction of the trend-surface from the contoured surface being studied yields a trend-surface residual map which should ideally enhance small-scale features by removing a regional trend. The third-order surface was used in the analysis of the isopach of the basal limestone (Figure 5.8) but it and its pattern of residuals closely resemble those generated with the second-order trend surface.

The trend-surface residual map for the basal limestone (Figure 5.10) enhances two areas, both characterized by residuals in excess of 5 ft (1.5 m), where the basal limestone of the Viola is relatively thick. One area extends south-southeastward off the eastern margin of the Central Kansas uplift through Rice County, north-central Reno County, and into eastern Kingman County. Another trends ENE-WSW and extends from Harvey County into southern Chase County. These thick areas are interpreted to be shoal complexes of crinoid debris that developed atop a broad bathymetric high caused by subtle uplift of the Central Kansas arch during deposition. Several areas of negative residual values are interspersed among the positive anomalies, but these negative anomalies may be due to erosion of the basal limestone along the crest of the arch. In some areas the basal limestone is beveled at the top of the Viola (Figures 5.6, 5.7).

The previously discussed left-stepping *en echelon* areas of local thinning along the crest of the Pratt anticline are accentuated by the residual map and are characterized by a NNE-SSW trending series of negative residual anomalies. A N-S trending group of similar-sized negative anomalies are accentuated in the residual map along the N-S line separating R.15W. and R.16W. Correlation of well logs in this region indicates this area is a down-to-the-west flexure zone that influenced deposition of the basal limestone and the overlying lower cherty dolomite. A marked change in lithology along this N-S line is also expressed in the Simpson Group, where the Simpson is dominated by carbonates to the west, and siliciclastics to the east of this

Figure 5.10 Trend-surface residual map for the basal limestone of the Viola Formation. This map enhances local features of the isopach and is obtained by subtraction of the third-order trend surface from the basal limestone isopach (see Figure 5.8).

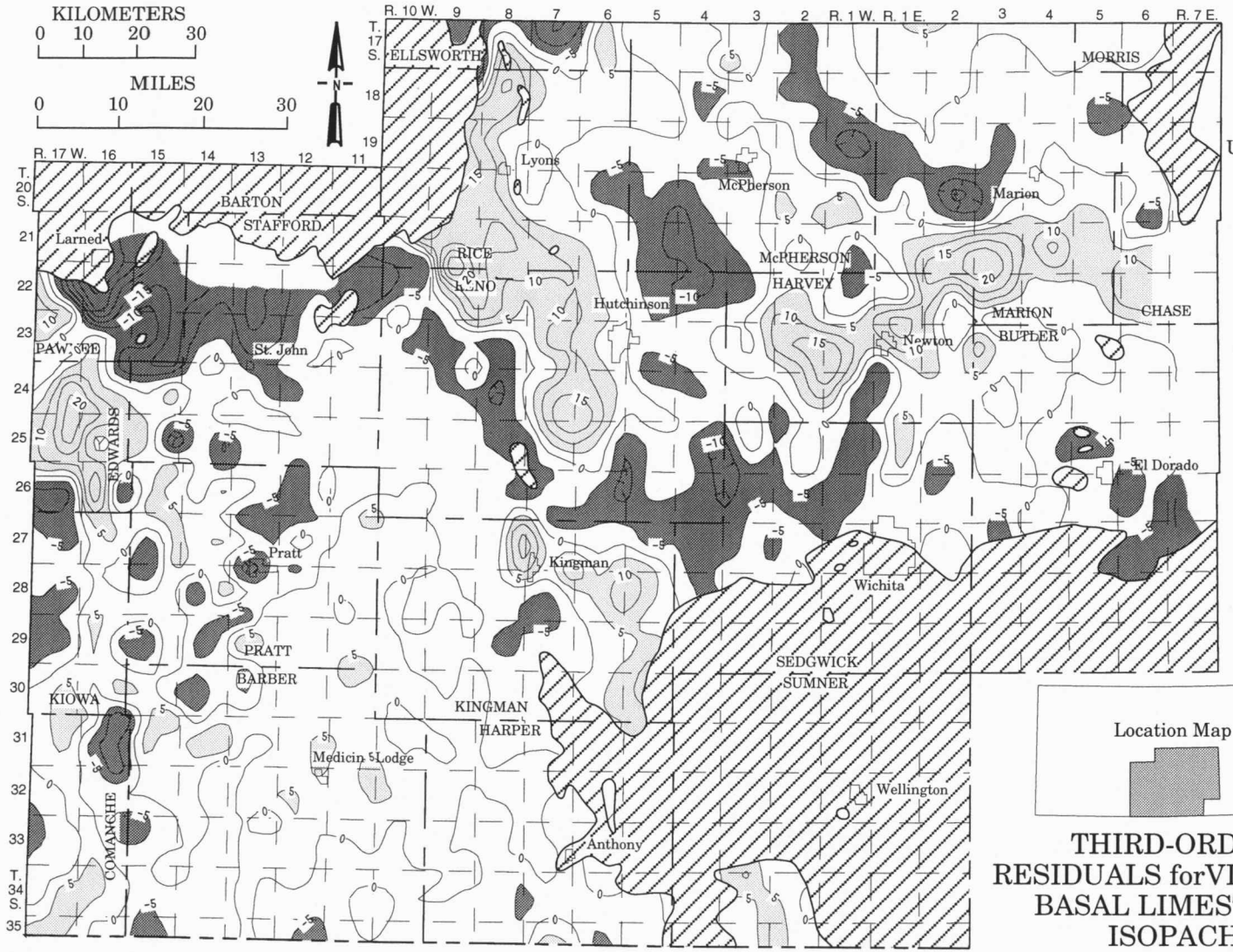

THIRD-ORDER RESIDUALS for VIOLA FM. BASAL LIMESTONE ISOPACH

line (Doveton and others, 1990). This zone of flexure will subsequently be examined in detail.

Lower Cherty Dolomitic Limestone

The isopachous map of the lower cherty dolomitic limestone (Figure 5.11), the subunit immediately above the basal limestone subunit, indicates the thickness of this subunit is more variable than that of the basal limestone. Many areas of local thinning, including those evident over the Pratt anticline, are due to local uplift and truncation of this subunit at unconformities above the Viola Formation. This subunit is largely absent over the Central Kansas arch but scattered outliers present in Harvey, eastern Reno, and Sedgwick counties indicate that it probably was deposited contiguously over the arch and subsequently eroded. In general, in areas where it was not subject to beveling at the top of the Viola, it thickens westward off the Central Kansas arch, indicating that the arch was active during deposition of this part of the Viola Formation. An area of marked westward thickening is evident along a N-S line roughly corresponding to the eastern border of Comanche, Edwards, and Kiowa counties (i.e., along the boundary between the R.15W. - R.16W. tiers of townships). This same area is also detected on the trend-surface residual map for the basal limestone (Figure 5.10). Marked isopach thinning is evident in a NE-SW trend across central Pratt County. This area is where the lower cherty dolomitic limestone subcrops at the unconformity beneath the Chattanooga Shale and the younger unconformity at the base of the Pennsylvanian System (Figures 4.4, 5.6). Abnormal thicknesses of detrital chert are present in these locations at the top of the Viola Formation (see Adkison, 1972; Bornemann and Doveton, 1983) and probably represent insoluble material left after dissolution of surrounding carbonate rocks.

The isopach of the lower cherty dolomite abruptly thins to a NNW-SSE-trending 0-line extending from northwestern Reno County to central Harper County

Figure 5.11 Regional isopachous map of the lower cherty dolomitic limestone of the Viola Formation. The limits (0 line) and subcrop of the lower cherty dolomitic limestone (taken from Figure 5.6) is shown in gray tone.

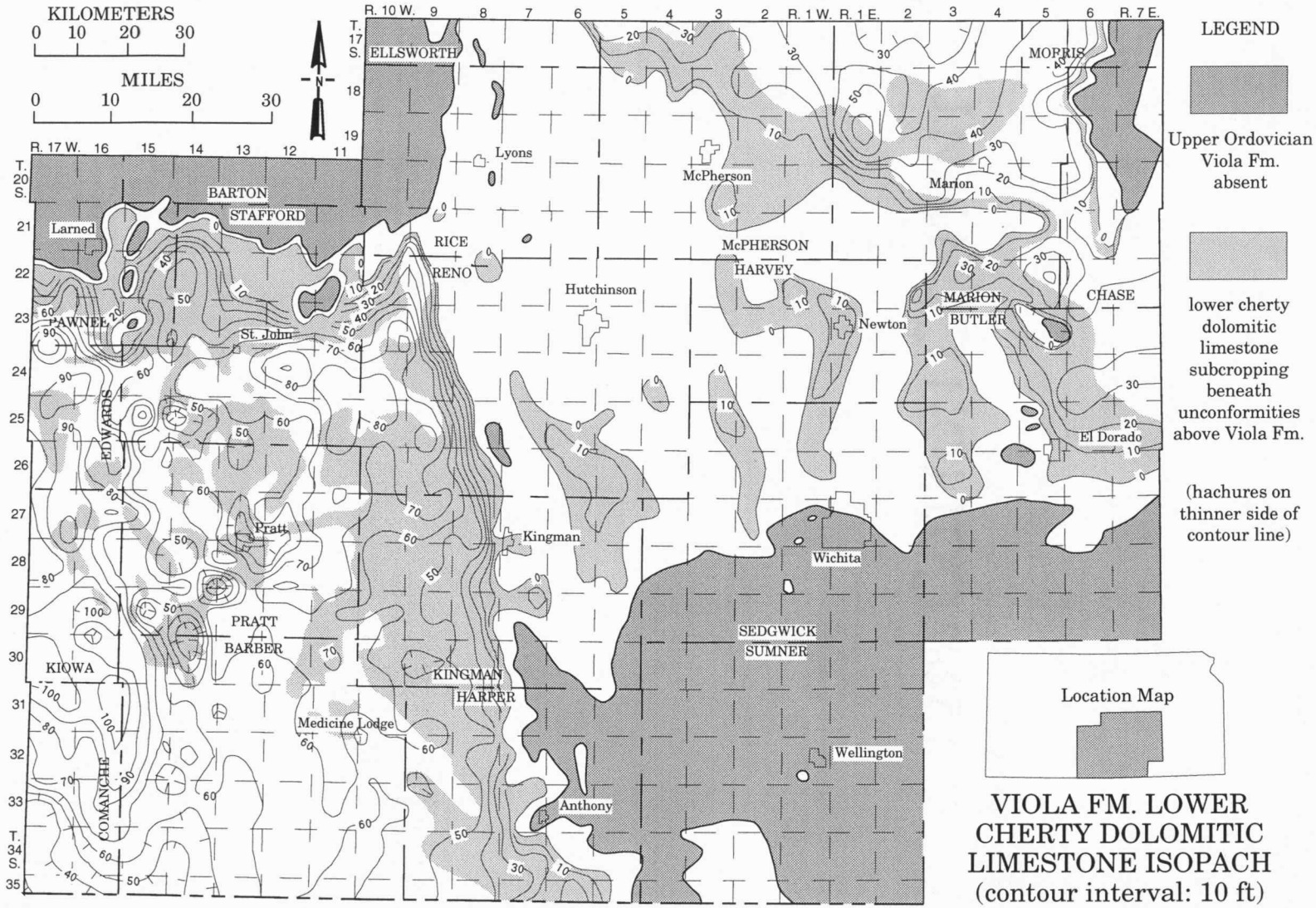

VIOLA FM. LOWER CHERTY DOLOMITIC LIMESTONE ISOPACH
(contour interval: 10 ft)

(Figure 5.11). This is an area where residual chert would be expected to build up in a manner similar to that noted along the Pratt anticline and at the southern end of the Central Kansas uplift. However, no residual chert is present in this area (Adkison, 1972) despite indications from well-log analysis (Bornemann, 1979; Bornemann and others, 1982; Bornemann and Doveton, 1983) that chert is present within the Viola in this area in proportion similar to that on the Pratt anticline. Speculatively, this chert could have been eroded and comminuted into sand that now is included in the Misener sandstone, the transgressive quartz-dominated sandstone at the base of the Chattanooga Shale (cf., Kuykendall and Fritz, 1993). Mapping by Newell (1989), however, shows Misener sandstone is largely absent in southwestern Reno County along the subcrop trend of the lower cherty dolomitic limestone, hence the problem of why there is no significant residual chert along the southwestern flank of the Central Kansas arch awaits future study.

A more detailed examination of the original thickness of the lower cherty dolomitic limestone is possible by ignoring any data point where this subunit subcrops directly beneath any post-Viola unconformity. Figure 5.12 is an isopachous map that was constructed using only wells where the upper limestone is present directly above the lower cherty dolomitic limestone, thereby ignoring post-Viola erosion of the lower cherty dolomitic limestone. A NW-SE trend of thin and thick areas in the isopachous map is discernible in the northeastern part of the study area in Morris and Marion counties, and in the western part of the study area in western Reno and Stafford counties. The lower cherty dolomitic limestone subunit is relatively thin (60 ft [18m] or less) in much of western Pratt, Barber, and Stafford counties (Figure 5.12). As with the basal limestone, a marked thickening occurs west of a N-S line roughly corresponding to the eastern border of Comanche, Edwards, and Kiowa counties (i.e., along the boundary between the R.15W. - R.16W. tiers of townships), thereby

Figure 5.12 Regional isopachous map of the lower cherty dolomitic limestone of the Viola Formation using only wells where this subunit is overlain by the upper limestone subunit. Effects of post-Viola erosion are therefore ignored by this technique, however, some areas without a sufficient density of data points are not contourable. A third-order trend-surface for this isopachous map is superimposed in heavy lines.

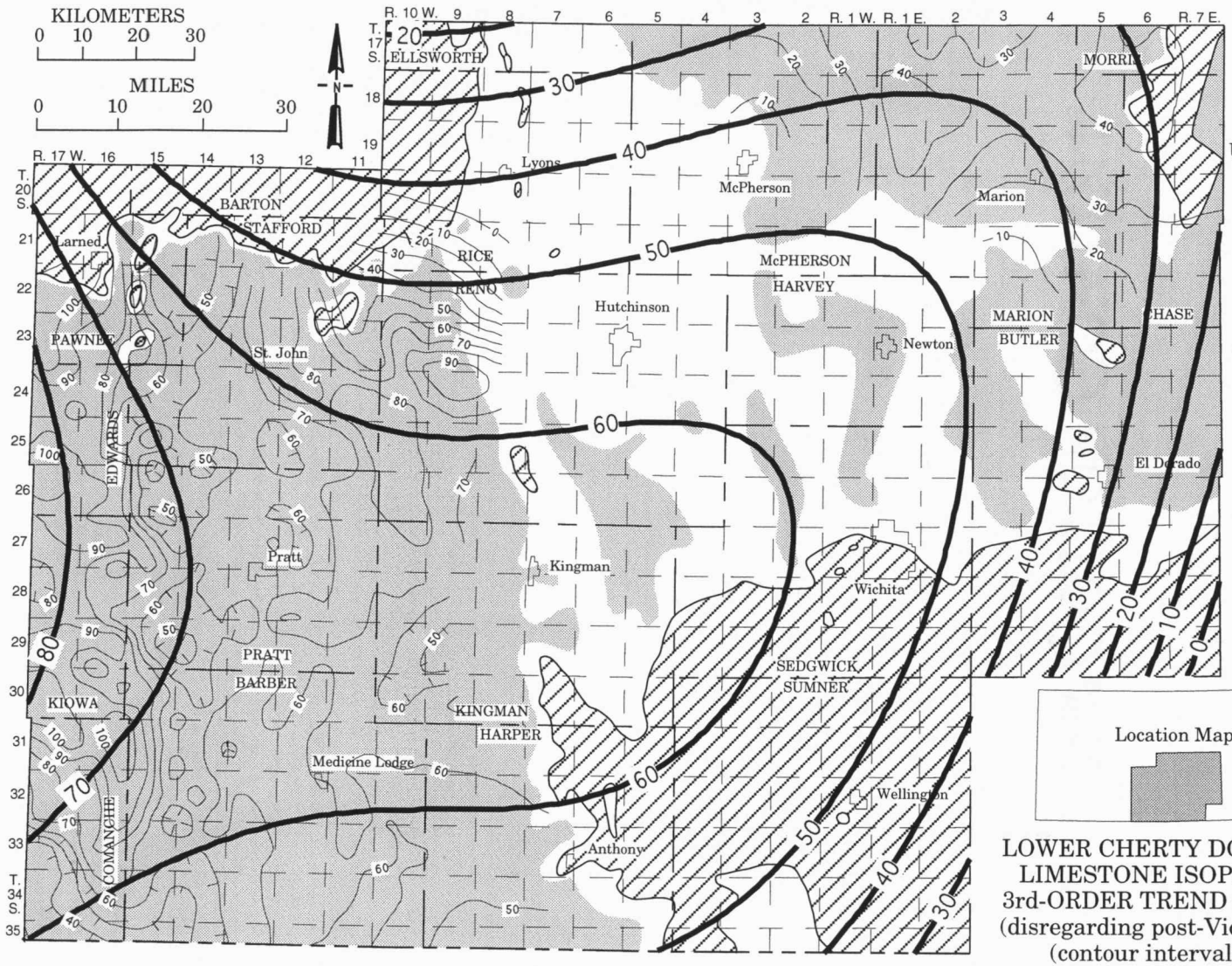

LOWER CHERTY DOLOMITIC LIMESTONE ISOPACH and 3rd-ORDER TREND SURFACE
(disregarding post-Viola erosion)
(contour interval: 10 ft)

indicating the western flank of the Pratt anticline was an active tectonic element during deposition of the lower cherty dolomitic limestone. Conversely, the left-stepping *en echelon* pattern of isopach thins on the eastern flank of the Pratt anticline, which is well developed in the isopach of the basal limestone (Figures 5.7, 5.10), is not as well expressed and indicates that this feature was less active during deposition of the lower cherty dolomitic limestone subunit, or that lithologies in this subunit are not sensitive to bathymetric changes.

A third-order trend surface is superimposed on the isopach of the lower cherty dolomitic limestone in Figure 5.12. Goodness-of-fit for this and other trend surfaces for this subunit is less than for the basal limestone (Figure 5.9), probably because of greater local thickness variations in the lower cherty dolomitic limestone and the lack of data in areas where the lower cherty dolomitic limestone is either not present or where it subcrops at the top of the Viola Formation. The axis of the trend surface is spatially coincident with the outliers of the lower cherty dolomitic limestone on the crest of the Central Kansas arch in Harvey, Kingman, and Sedgwick counties (although these outliers did not affect the trend surface), suggesting that this area was where the sea was deepest along the crest of the arch.

The trend-surface residual map for the lower cherty dolomitic limestone (Figure 5.13) accentuates the thinning of this subunit over a broad area on top of the Pratt anticline in western Pratt and northwestern Barber counties. Similarly, the marked westward thickening off the Pratt anticline along the eastern side of Pawnee, Edwards, Kiowa, and Comanche counties is also emphasized by positive trend-surface residuals. These features indicate the western flank of the Pratt anticline was active during deposition of this subunit and that it may have been a flexure with subtle, recurrent movement along basement faults.

The upper limestone and upper cherty dolomitic limestone subunits were not

Figure 5.13 Trend-surface residual map for the lower cherty dolomitic limestone of the Viola Formation. This map enhances local features of the isopach and is obtained by subtraction of the third-order trend surface from the isopachous map in Figure 5.12.

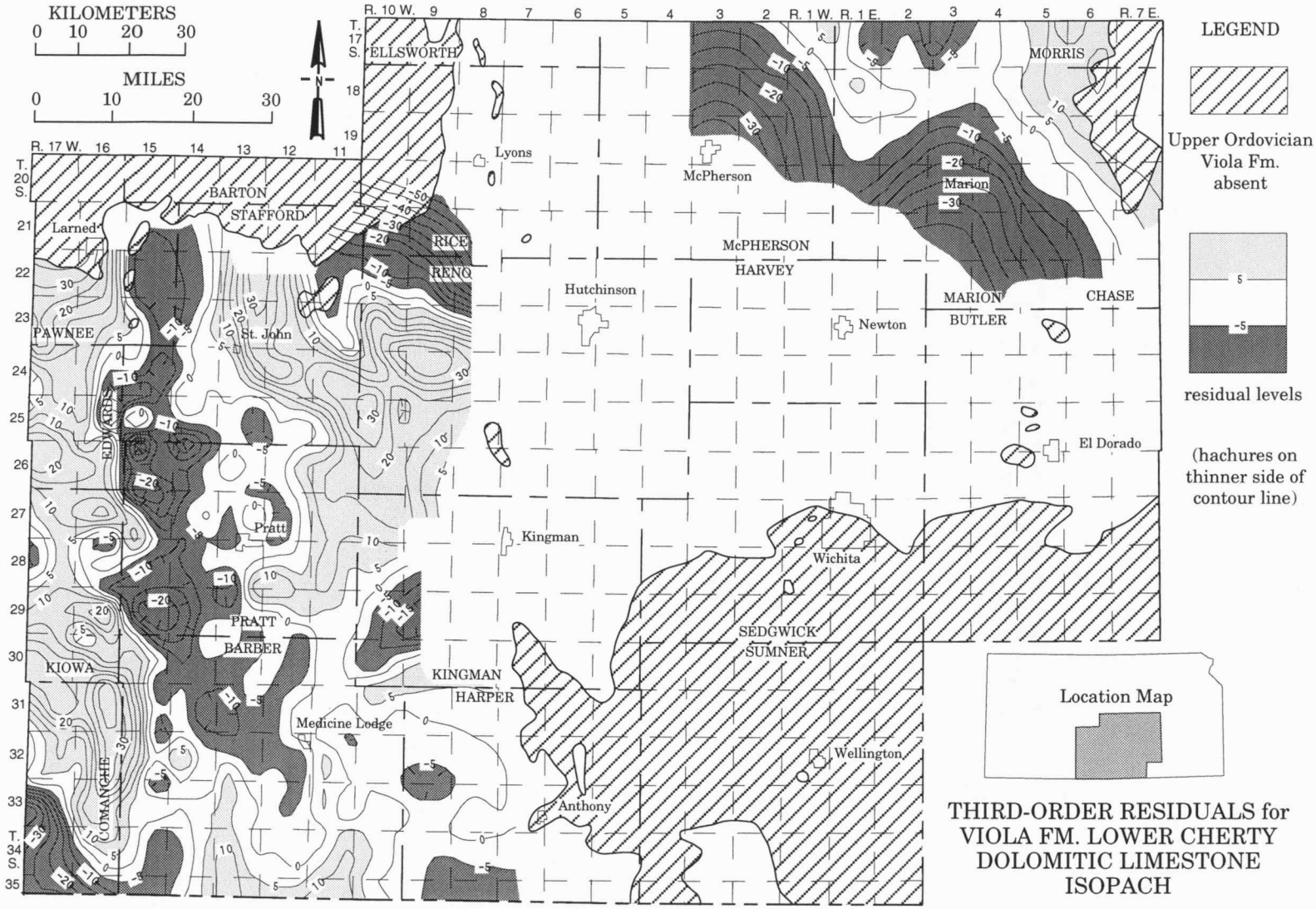

THIRD-ORDER RESIDUALS for
VIOLA FM. LOWER CHERTY
DOLOMITIC LIMESTONE
ISOPACH

amenable to trend-surface analysis, because they were subjected to more post-depositional erosion at unconformities above the Viola Formation. Application of a trend surface to isopach maps with geometries that are largely the product of erosion will not yield valid information on depositional patterns.

Upper Limestone

The distribution and thickness of the upper limestone of the Viola Formation (Figure 5.14) is mostly controlled by erosion along unconformities at the base of the Maquoketa Formation, Chattanooga Formation, and Pennsylvanian System (see Figures 4.4, 5.6). Scattered areas where it is in excess of 30 ft (9 m) thick and still overlain by the upper cherty dolomitic limestone of the Viola Formation are present in Edwards and southern Stafford counties, immediately south of the Central Kansas uplift. These areas are interpreted to be remnants of shoals developed in shallow water near the broad crests of the Central Kansas arch and ancestral Central Kansas uplift. Westward thickening near the western margin of the study area is also evident and may possibly indicate development of persistent shoaling conditions to the west.

An isopachous map made using only data points where the upper limestone is overlain by the upper cherty dolomitic limestone (Figure 5.15) eliminates the local effects of post-Viola erosion on the spatial distribution of the upper limestone. Areas of thick upper limestone are locally present on the Pratt anticline in northwestern Pratt and southwestern Stafford counties -- areas where the underlying lower cherty dolomitic limestone is relatively thin (see Figure 5.12). These thick areas probably represent a trend of crinoidal shoals that developed in relatively shallow and agitated water over the Pratt anticline and on the southern flank of the Central Kansas uplift. An arcuate pattern of these shoals, concave westward, extends from southwestern Edwards County to north-central Barber County. Although isopach trends such as this are extrapolated over areas where the upper limestone is now not present or

Figure 5.14 Regional isopachous map of the upper limestone of the Viola Formation. The limits (0 line) and subcrop of the upper limestone (taken from Figure 5.6) is shown in gray tone.

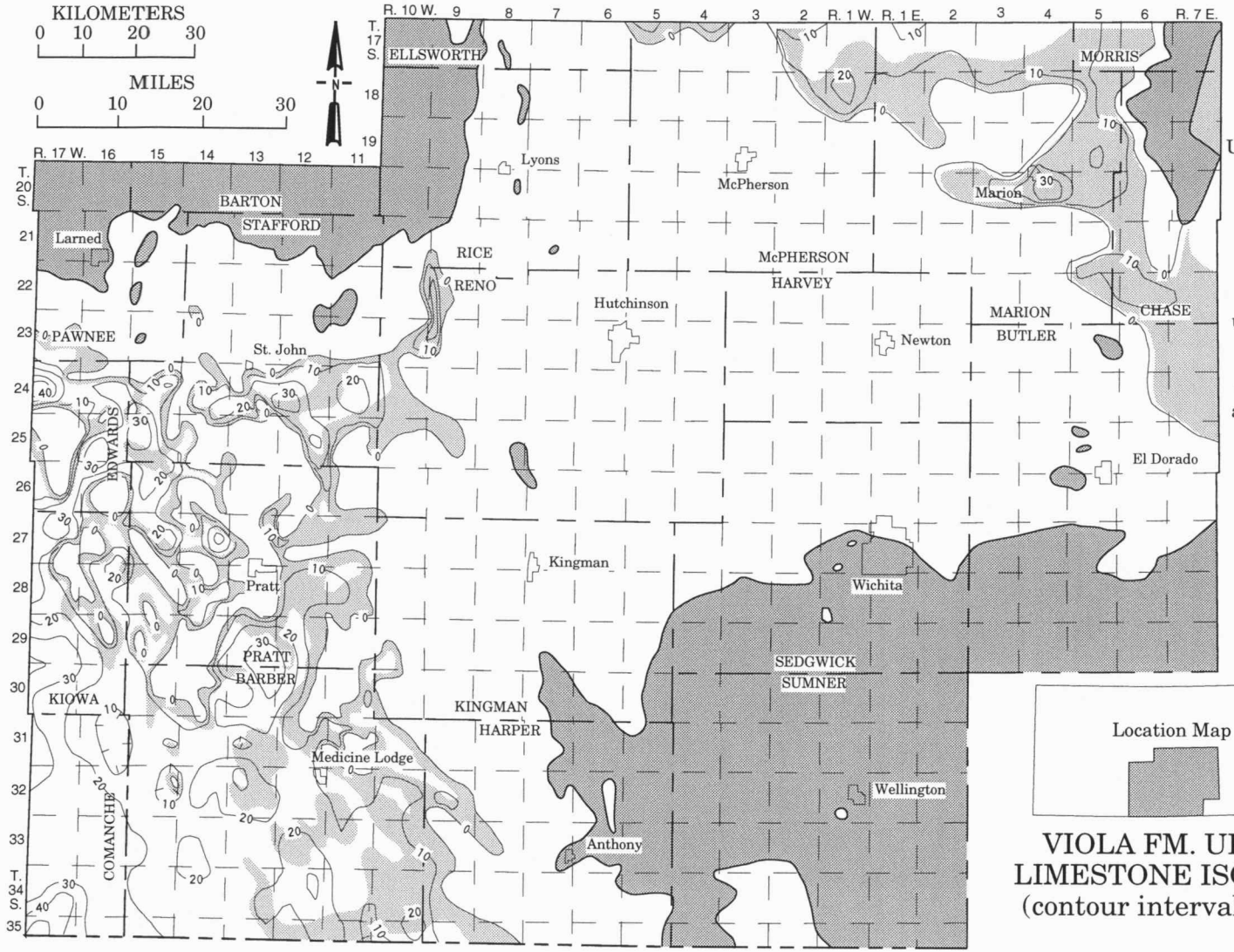

VIOLA FM. UPPER LIMESTONE ISOPACH
(contour interval: 10 ft)

Figure 5.15 Regional isopachous map of the upper limestone of the Viola Formation using only wells where this subunit is overlain by the upper cherty dolomitic limestone subunit. Effects of post-Viola erosion are therefore ignored by this technique, however, some areas without a sufficient density of data points are not contourable.

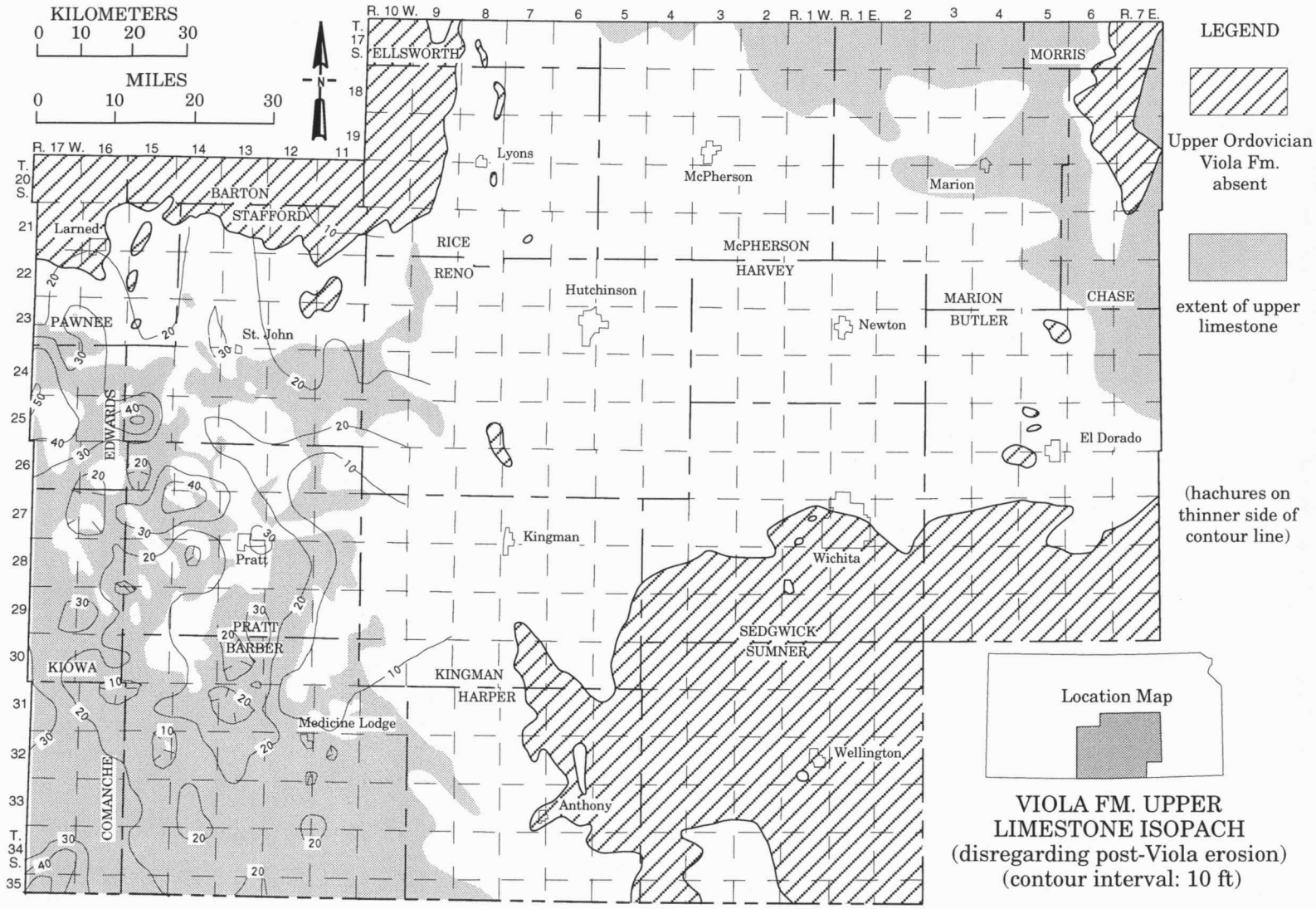

VIOLA FM. UPPER LIMESTONE ISOPACH
(disregarding post-Viola erosion)
(contour interval: 10 ft)

where there are no data, the computer contouring process is not directionally biased due to the orthogonal equidimensional grid utilized to construct the contours. Any trends that are evident by machine contouring are therefore not artifacts of the contouring process.

Upper Cherty Dolomitic Limestone

The thickness and distribution of the uppermost subunit of the Viola Formation, the upper cherty dolomitic limestone (Figure 5.16) are entirely controlled by erosion along unconformities present above the Viola Formation, hence its present residual geometry gives no hints to its depositional geometry. Areas of drastic changes in thickness, as indicated by closely spaced isopach lines, are due to local structures truncated by the marked angular unconformity at the base of the Pennsylvanian System in Kansas. Both NE-SW and NW-SE trends are developed, which are evident by the pattern of the contours and subcrop limits (0 line). The NW-SE trends developed in northeastern Barber County are subjacent to the unconformity at the base of the Chattanooga Shale (Figure 4.4), hence they are pre Late-Devonian in age. Farther north in Edwards and northern Kiowa counties, the precise age of the strata above the Viola is unclear (see earlier discussions), therefore trends in these later localities may be attributable to structural movements and subsequent erosion as late as Late Mississippian time.

The top of the Viola where the upper cherty dolomitic limestone is present is not characterized by an abundance of residual chert, according to maps showing chert thickness in Adkison (1972). This lack of residual chert may indicate that this subunit, although universally truncated and eroded at its top, is generally not subject to deep weathering and erosion and that the preserved thickness of this subunit is nearly its original thickness. Alternately, the abundance of chert in this subunit may be considerably less than that of the lower cherty dolomitic limestone. Scattered areas

Figure 5.16 Regional isopachous map of the upper cherty dolomitic limestone of the Viola Formation. The limits (0 line) and subcrop of the upper cherty dolomitic limestone (taken from Figure 5.6) is shown in gray tone.

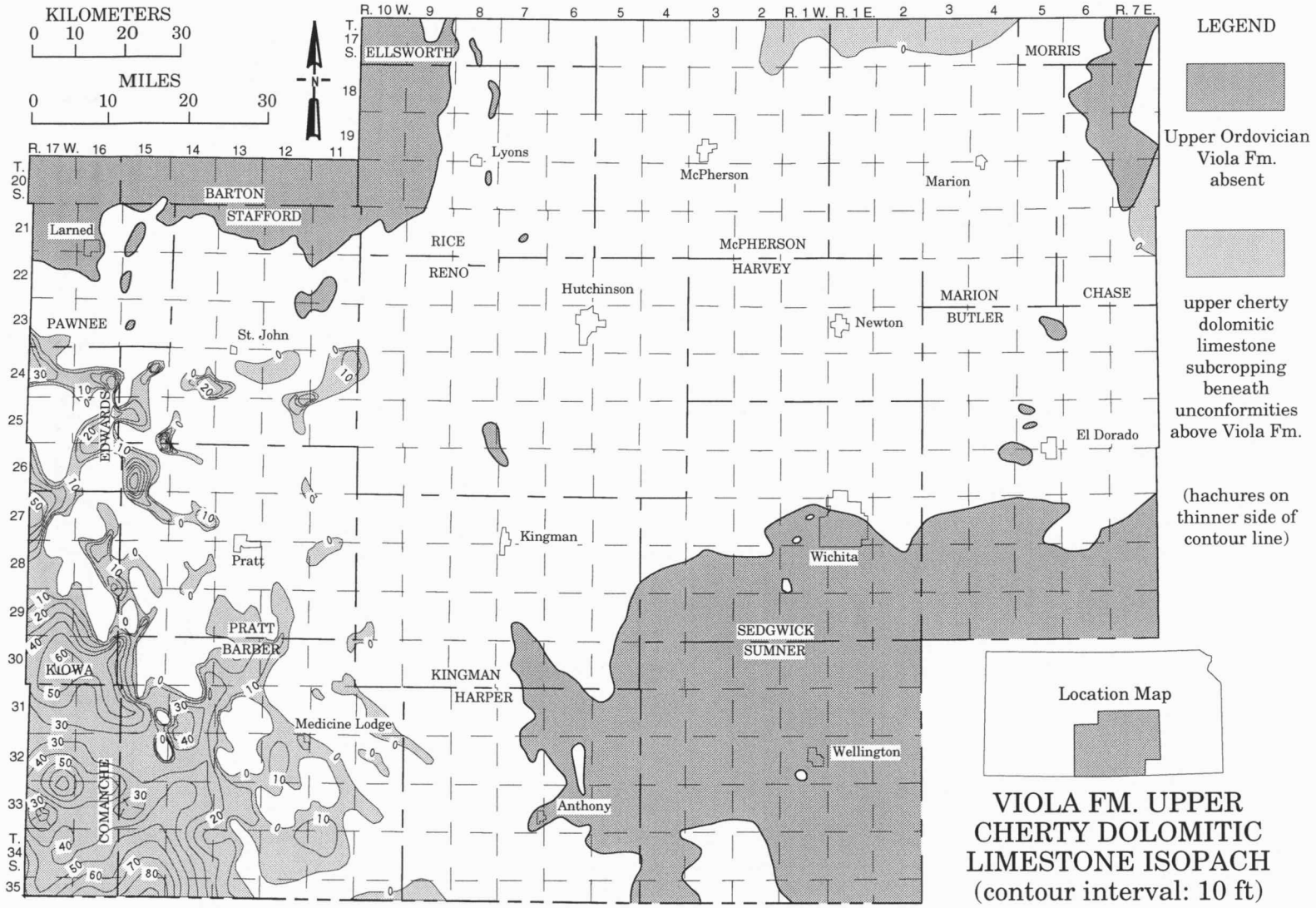

VIOLA FM. UPPER CHERTY DOLOMITIC LIMESTONE ISOPACH
(contour interval: 10 ft)

where residual chert is less than 50 ft (15 m) thick are present in northern and western Barber County, eastern Kiowa County, and eastern Edwards County according to maps presented in Adkison (1972). These areas are just beyond the present subcrop limit of the upper cherty dolomitic limestone and may represent residual chert derived from its complete dissolution. The spatial distribution of chert in the upper cherty dolomitic limestone, like that of the lower cherty dolomitic limestone, may be a worthwhile future study by lithologic analysis with well logs.

Discussion

Comparison of the isopachous map of the basal limestone (Figure 5.7) with the subcrop map for the Viola subunits (Figure 5.6) and the worm's-eye-view map (Figure 4.4) indicates that the trend of the broad crest of the Central Kansas arch may have rotated clockwise and moved approximately 70 miles (110 km) southwestward subsequent to deposition of the Viola Formation. The crest of the arch during deposition of the basal limestone subunit (see Figure 5.7), as indicated by areas of its maximum thickness, trends approximately east-west from central Rice County to southern Chase County. The subcrop pattern of this subunit and the overall pattern of thinning for the entire Viola Formation (see Figure 4.3) indicate the subsequent crest of the Central Kansas arch trended approximately NW-SE from southeastern Rice County through central Sedgwick County. Subsequent removal of the Upper Ordovician Maquoketa Formation, as indicated by the worm's-eye view map (Figure 4.4), suggests a crest even farther south by post Late-Ordovician -- pre Late-Devonian time (prior to deposition of the Chattanooga Shale). This latest structural axis (albeit poorly defined) extends NNW-SSE from northern Stafford County to eastern Harper County. The reasons for the apparent shifts of the crest of the arch are not clear; perhaps they are manifestations within the craton of stresses due to the convergent plate boundary developed on the southeastern margin of the North American

(Laurentian) craton during Ordovician time (Figures 2.3, 2.4).

Detailed Mapping over Pratt Anticline

Local anomalies detected by correlations of geophysical log and isopachous mapping warranted detailed analysis of a small area on the Pratt anticline along the N-S zone of flexure detected in the trend-surface residual map of the basal limestone (Figure 5.10) and the isopach of the lower cherty dolomite (Figure 5.11). The area selected covers approximately one and one-half townships (51 square mi; 132 square km) and encompasses parts of T.31S., T.32S. and R.14W. and R.15W. (Figure 5.3). An east-west stratigraphic cross section across this area (Figure 5.17) shows the upper limestone subunit apparently bifurcates on the west flank of the Pratt anticline (i.e., west of the Graybol #1 Hull well) and a westward-thickening wedge of fine-grained dolomite is present between these two limestone beds. Nearby cross sections drawn parallel to the one shown in Figure 5.17 also indicate this extra limestone, identified here as the "intermediate limestone", converges to, or is truncated at the base of the upper limestone subunit. For purposes of regional mapping the thin "intermediate limestone" was included within the lower cherty dolomitic limestone subunit.

A westward-thickening wedge of porous dolomitic limestone lies between the "intermediate" and upper limestones. This wedge of porous dolomitic limestone is in the upper part of the lower cherty dolomitic limestone and accounts the westward thickening of this Viola subunit. The thinning of the lower part of the lower cherty dolomitic limestone between the "intermediate limestone" and the basal limestone west of Graybol #1 Hull is enigmatic. Reversal of the relative structural subsidence of the west flank of the Pratt anticline relative to its crest, in which the west flank is temporarily uplifted to account for the thinning in this stratigraphic interval, is considered unlikely because this operation invokes relatively complex structural

Figure 5.17 An east-west stratigraphic cross-section of the Viola Formation with datum at the top of the Simpson Group. The basal, "intermediate", and upper limestones of the Viola Formation are relatively nonporous crinoidal packstones and grainstones that are interbedded between thicker cherty dolomitic limestones, which are primarily dolomitized mudstones and wackestones. Location of the cross section is on Figures 5.18 through 5.22.

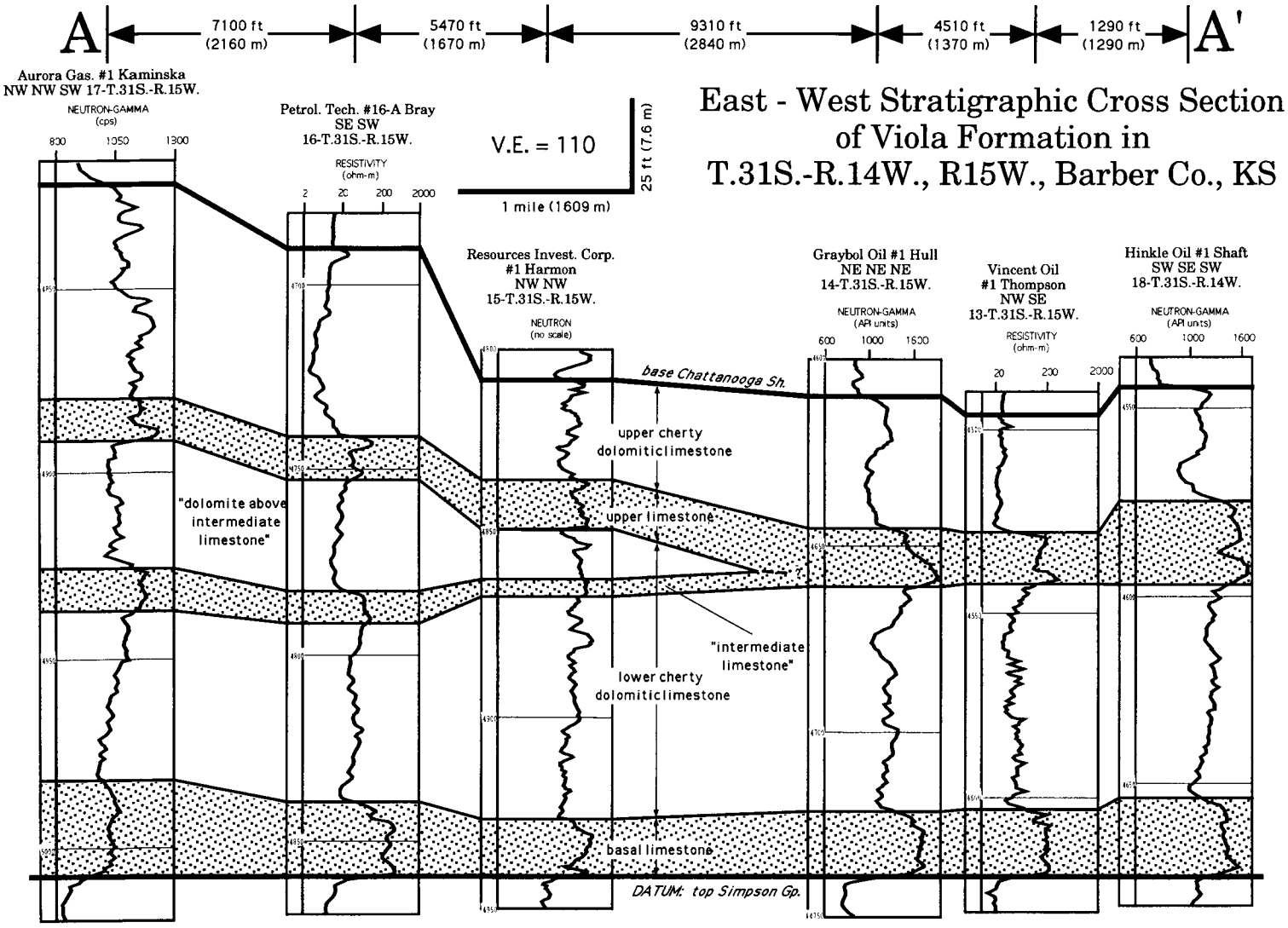
A
7100 ft (2160 m)
5470 ft (1670 m)
9310 ft (2840 m)
4510 ft (1370 m)
1290 ft (1290 m)
A'
Aurora Gas. #1 Kaminska
NW NW SW 17-T.31S.-R.15W.
NEUTRON-GAMMA (cps)
800 1050 1300
Petrol. Tech. #16-A Bray
SE SW
16-T.31S.-R.15W.
RESISTIVITY (ohm-m)
2 20 200 2000
V.E. = 110
25 ft (7.6 m)
1 mile (1609 m)
East - West Stratigraphic Cross Section
of Viola Formation in
T.31S.-R.14W., R15W., Barber Co., KS
Resources Invest. Corp.
#1 Harmon
NW NW
15-T.31S.-R.15W.
NEUTRON (no scale)
Graybol Oil #1 Hull
NE NE NE
14-T.31S.-R.15W.
NEUTRON-GAMMA (API units)
600 1000 1600
Vincent Oil
#1 Thompson
NW SE
13-T.31S.-R.15W.
RESISTIVITY (ohm-m)
20 200 2000
Hinkle Oil #1 Shaft
SW SE SW
18-T.31S.-R.14W.
NEUTRON-GAMMA (API units)
600 1000 1600
base Chattanooga Sh.
upper cherty dolomiticlimestone
upper limestone
"dolomite above intermediate limestone"
"intermediate limestone"
lower cherty dolomiticlimestone
basal limestone
DATUM: top Simpson Gp.

movements. A simpler scenario could be that this thinning may be basinward depositional thinning of the lower cherty dolomitic limestone. The "intermediate limestone" could therefore represent either a regressive limestone deposited during a brief drop in sea level, or a transgressive limestone deposited during the subsequent sea-level rise. Cores are not available to clarify which alternative is more likely, but cores 50 miles (80 km) to the north in the Zenith-Peace Creek oil field (e.g., Braden-Zenith ZU-1 and ZU-3; discussed in Chapter 7) contain karstic breccias at the top of the lower cherty dolomitic limestone. These karstic breccias possibly indicate a period of emergence during Viola deposition, and are at the stratigraphic level that would correspond to the sea-level drop necessary for the depositional-thinning scenario.

Detailed isopach maps of the basal limestone, the lower cherty dolomitic limestone below the "intermediate limestone", the "intermediate limestone", the wedge of cherty dolomitic limestone between the "intermediate" and upper limestones, and the upper limestone are presented in Figures 5.18, 5.19, 5.20, 5.21, and 5.22. All available geophysical logs were used in making these isopach maps; however, the more dense well control is on the eastern margin of the map area, which includes the western edge of the Skinner field. This multipay field (Beene, 1993) produces minor Viola oil and gas from the upper cherty dolomitic limestone where this subunit is truncated and sealed by the overlying Chattanooga Shale.

Thickness of each of the Viola beds varies considerably over the study area; however, thickness trends could be reasonably discerned and mapped. A general NW-SE grain is interpreted for the basal limestone (Figure 5.18), but localized thinning occurs over anticlinal crests present in sections 12 and 13, T.31S.-R.15W. The large lobate feature at the center of the map may be related to currents at the time of deposition. The isopach of the overlying cherty dolomite interbedded between the basal limestone and the "intermediate" limestone (Figure 5.19) shows no marked

Figure 5.18 Isopach of the basal limestone of the Viola Formation in an area straddling T.31S., T.32S. and R.14W., R.15W. Location of this map area is also on the regional base map in Figure 5.5.

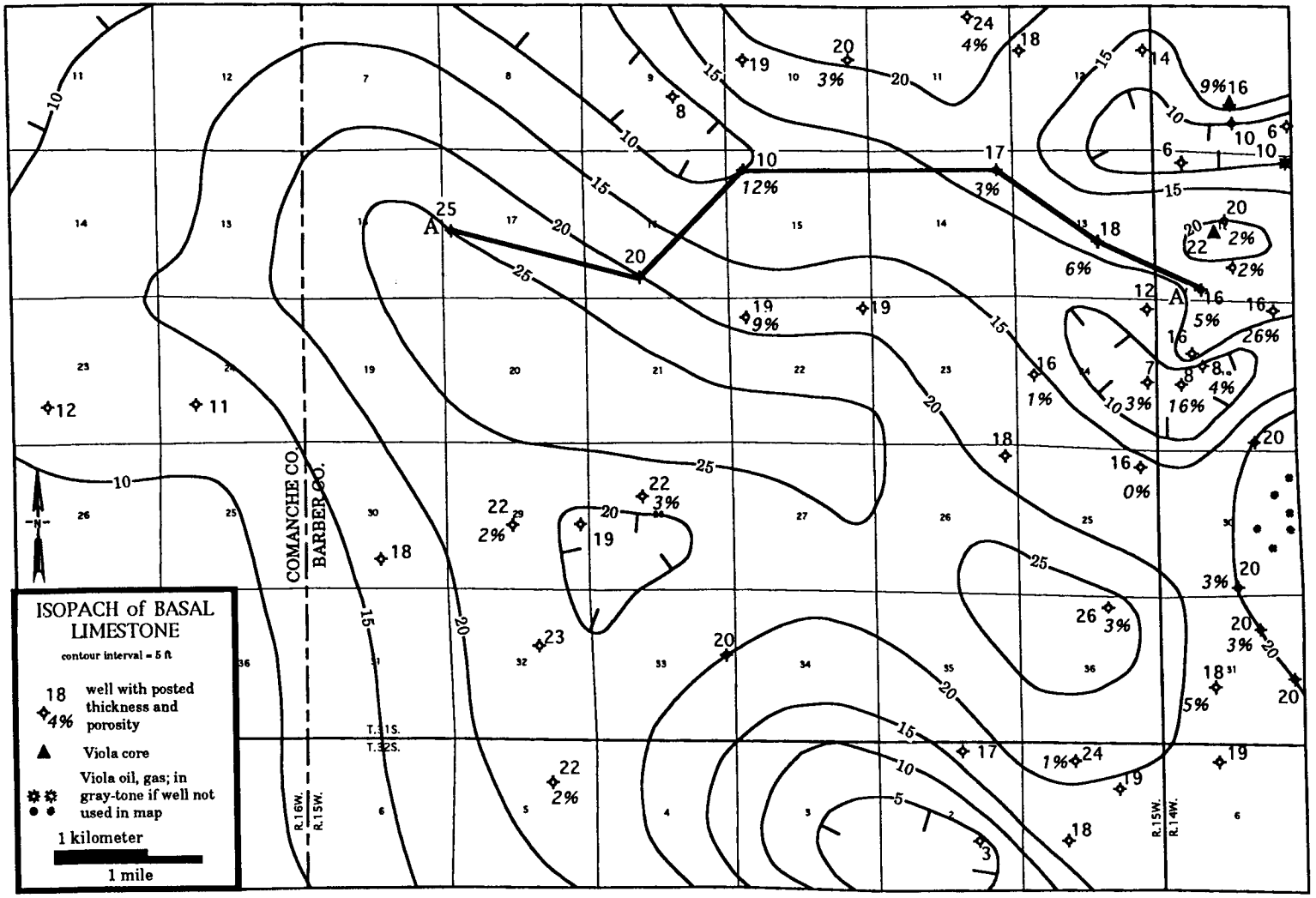
ISOPACH of BASAL LIMESTONE
contour interval = 5 ft
well with posted thickness and porosity
Viola core
Viola oil, gas; in gray-tone if well not used in map
1 kilometer
1 mile
COMANCHE CO.
BARBER CO.
T.31S.
T.32S.
R.16W.
R.15W.
R.14W.
A
A'

Figure 5.19 Isopach of the portion of the lower cherty dolomitic limestone above the basal limestone and "intermediate" limestone of the Viola Formation in an area straddling T.31S., T.32S. and R.14W., R.15W. Location of this map area is also on the regional base map in Figure 5.5.

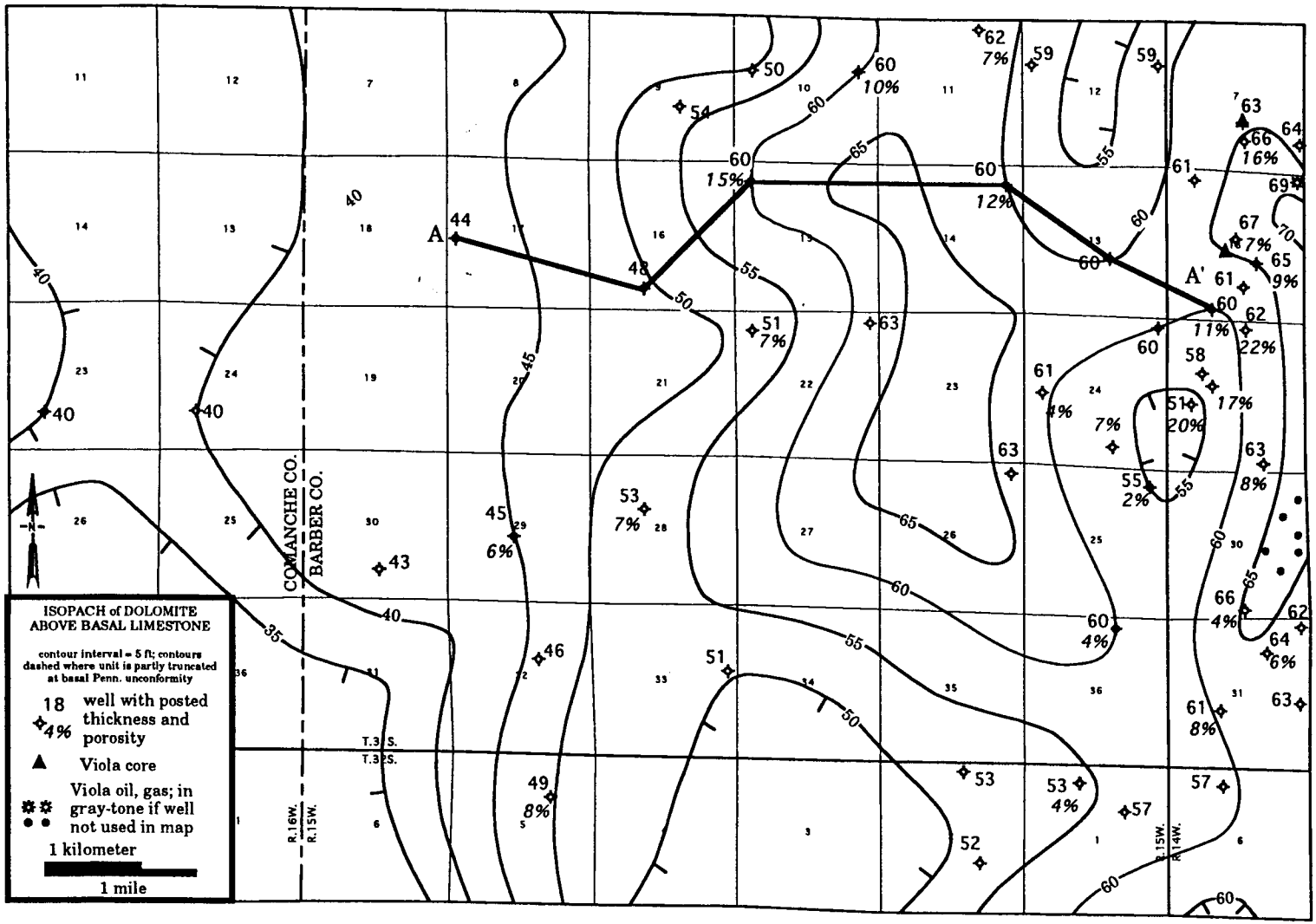
ISOPACH of DOLOMITE ABOVE BASAL LIMESTONE
contour interval = 5 ft; contours dashed where unit is partly truncated at basal Penn. unconformity
18 4% well with posted thickness and porosity
Viola core
Viola oil, gas; in gray-tone if well not used in map
1 kilometer
1 mile
COMANCHE CO.
BARBER CO.
A
A'
T.33S.
T.32S.
R.16W.
R.15W.
R.14W.

trends, nevertheless there is a general thinning to the west of approximately 25 ft (8 m). The overlying "intermediate" limestone (Figure 5.20), which converges to the upper limestone along a sinuous north-south trending boundary, shows virtually no trends in thickness with present distribution of data. The wedge of cherty dolomitic limestone above the "intermediate" limestone markedly thickens to the west (Figure 5.21), although at a rate of thickening of 25 to 30 ft per mile (5 to 10 m per km), the angle of convergence (the apical angle of the wedge) is less than one degree. Lobate features, similar to that interpreted for the basal limestone, are evident in the isopach for the upper limestone (Figure 5.22), but the data are best accommodated by NE-SW trends. Inasmuch as the basal and upper limestones are crinoidal grainstones and packstones showing evidence of high-energy depositional conditions (St. Clair, 1982, 1985), these lobate features could be current formed.

The wedge of porous dolomitic limestone in the upper part of the lower cherty dolomitic limestone subunit (i.e., the dolomitic limestone between the "intermediate" limestone bed and the base of the upper limestone subunit) provides an intriguing relationship that hints at the depositional environment and geometry of the Viola at this locality. Inasmuch as this wedge (see Figure 5.17) abruptly thickens on the western flank of the Pratt anticline, accommodation space for it was likely created by tectonic movement during deposition. Present-day geometry along the cross section depicted in Figure 5.17 (also see Figure 5.23, part E) also indicates a flexure at the eastern limit of the wedge in that the three wells in the western half of the cross section have dropped down as a unit relative to wells farther east. If the crinoidal limestones represent high-energy shoaling conditions, it is likely that the dolomitic wedge represents lime muds that may have been deposited in quieter, deeper waters toward the ancestral Anadarko basin and continental margin farther south. Unfortunately, no core is available to confirm this model. However, the geometry of

Figure 5.20 Isopach of the "intermediate" limestone of the Viola Formation in an area straddling T.31S., T.32S. and R.14W., R.15W. Location of this map area is also on the regional base map in Figure 5.5.

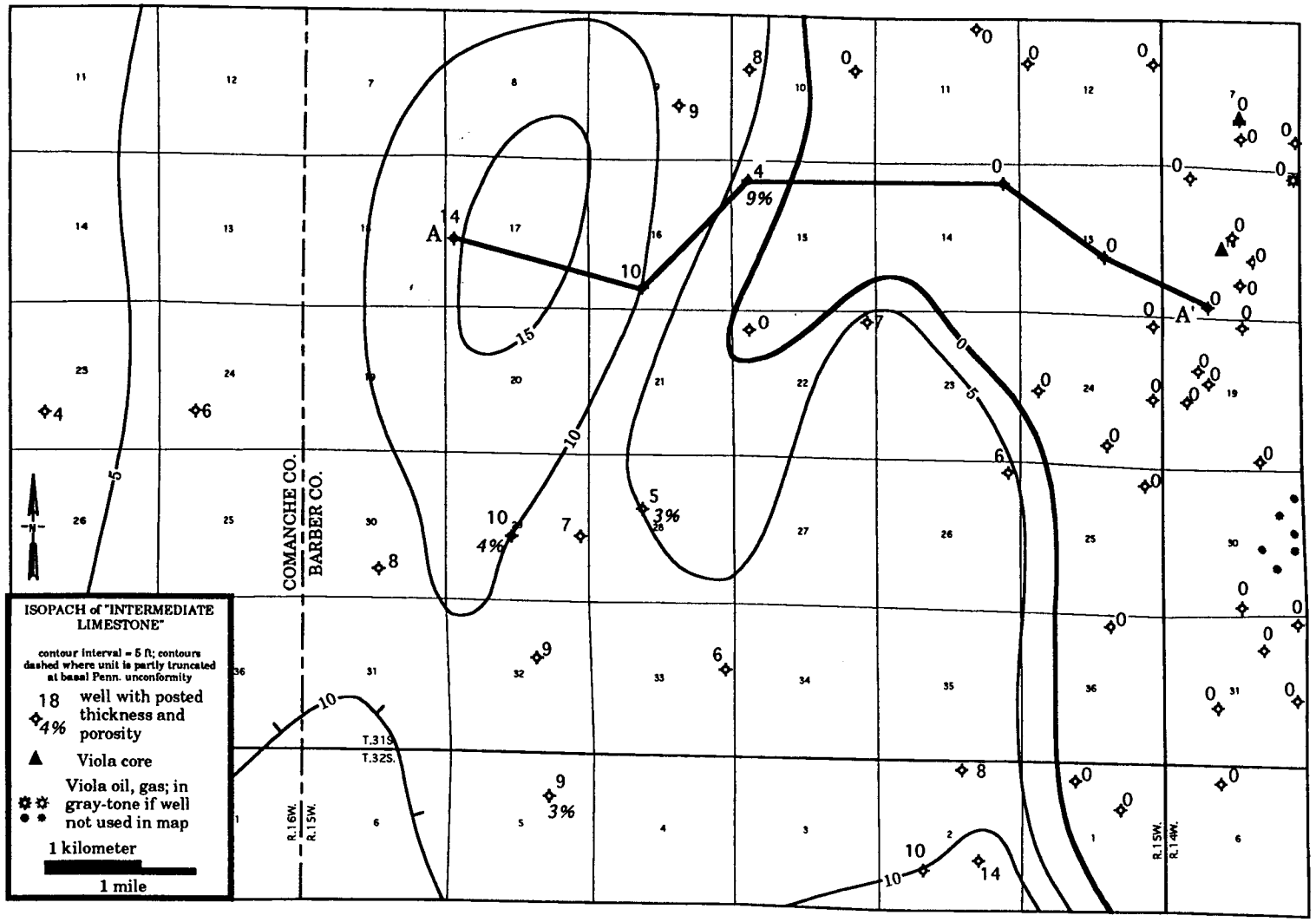
ISOPACH of "INTERMEDIATE LIMESTONE"
contour interval = 5 ft; contours dashed where unit is partly truncated at basal Penn. unconformity
18 well with posted thickness and porosity
4%
Viola core
Viola oil, gas; in gray-tone if well not used in map
1 kilometer
1 mile
COMANCHE CO.
BARBER CO.
A
A'
T.31S.
T.32S.
R.16W.
R.15W.
R.15W.
R.14W.
9%
4%
3%

Figure 5.21 Isopach of the portion of the lower cherty dolomitic limestone above the "intermediate" limestone and below the upper limestone of the Viola Formation in an area straddling T.31S., T.32S. and R.14W., R.15W. Location of this map area is also on the regional base map in Figure 5.5.

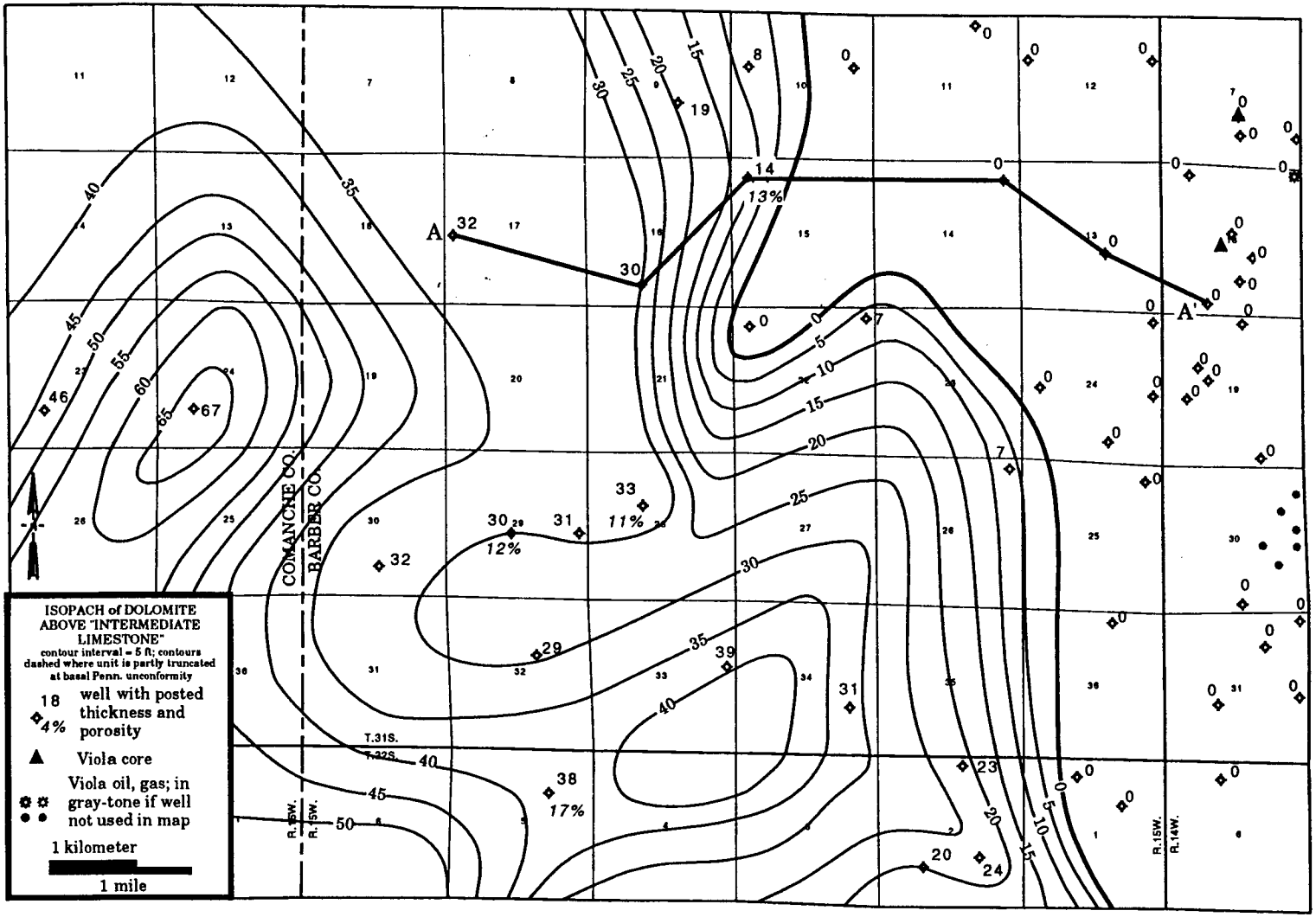
ISOPACH of DOLOMITE ABOVE "INTERMEDIATE LIMESTONE"
contour interval = 5 ft; contours dashed where unit is partly truncated at basal Penn. unconformity
18 4% well with posted thickness and porosity
Viola core
Viola oil, gas; in gray-tone if well not used in map
1 kilometer
1 mile
COMANCHE CO.
BARBER CO.
A
A'
T.31S.
T.32S.
R.15W.
R.14W.

Figure 5.22 Isopach of the upper limestone of the Viola Formation in an area straddling T.31S., T.32S. and R.14W., R.15W. Location of this map area is also on the regional base map in Figure 5.5.

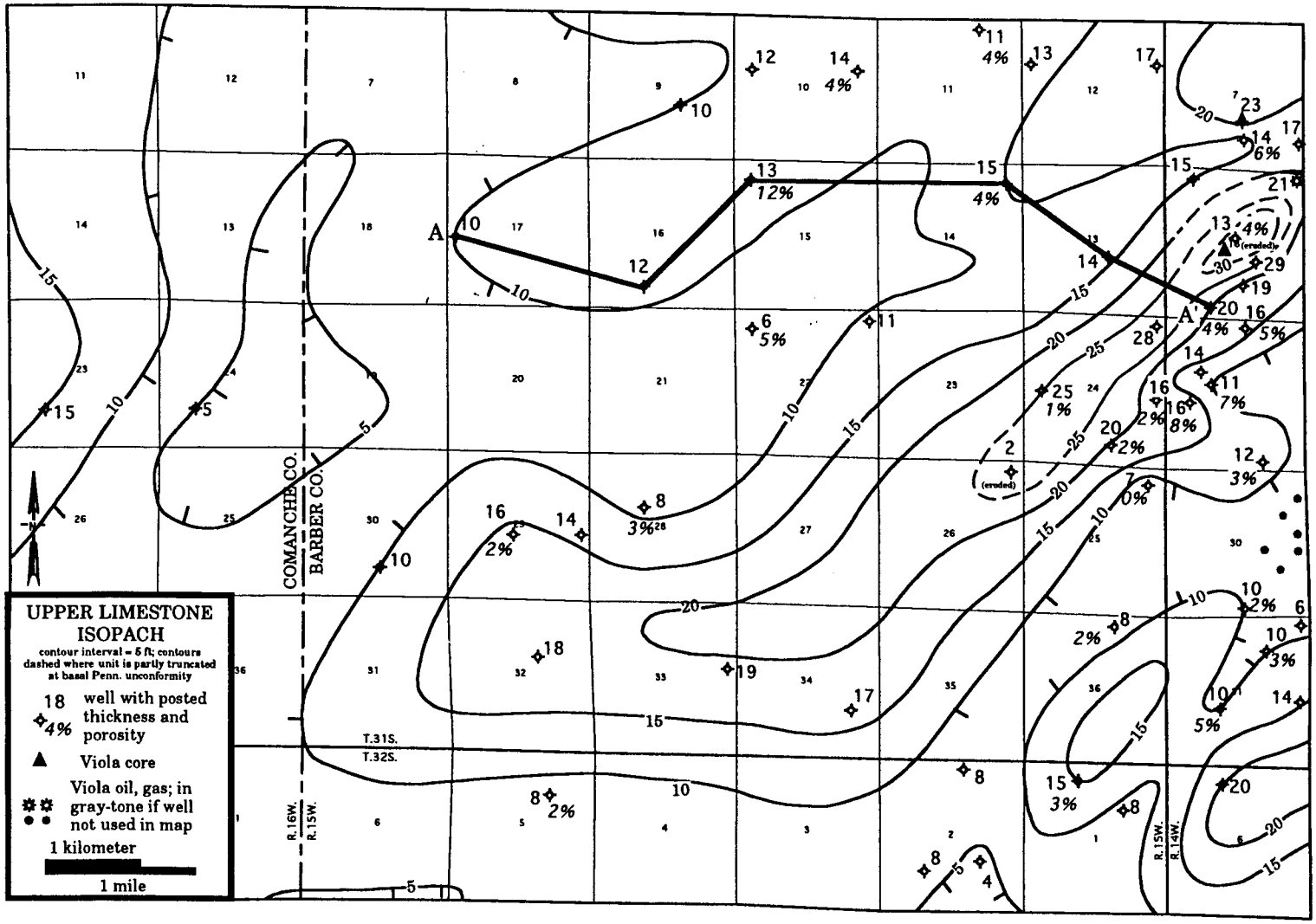
UPPER LIMESTONE ISOPACH
contour interval = 5 ft; contours dashed where unit is partly truncated at basal Penn. unconformity
18 4% well with posted thickness and porosity
Viola core
Viola oil, gas; in gray-tone if well not used in map
1 kilometer
1 mile
COMANCHE CO.
BARBER CO.
A
A'
T.31S.
T.32S.
R.16W.
R.15W.
R.14W.

Figure 5.23 Development of the cross-section depicted in Figure 5.17. Vertical exaggeration is 110, identical to that for Figure 5.17. This cross-section straddles the Pratt anticline. Early movement on the Pratt anticline (the crest of which is approximately located at the easternmost well in the cross-section) affected the depositional geometries within the Viola Limestone. Stippled pattern denotes crinoidal packstones and grainstones.

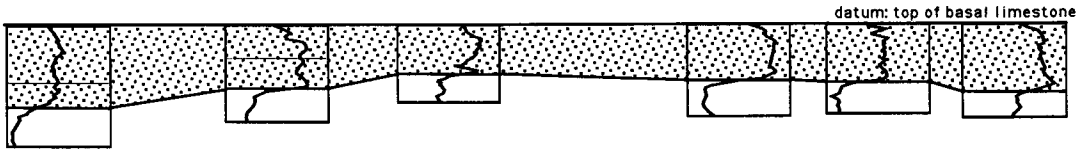

A. At end of deposition of grainstones and packstones of the basal limestone -- shoals of coarse-grained crinoidal debris and shell fragments are deposited in shallow, agitated water during initial transgression responsible for the Viola Formation.

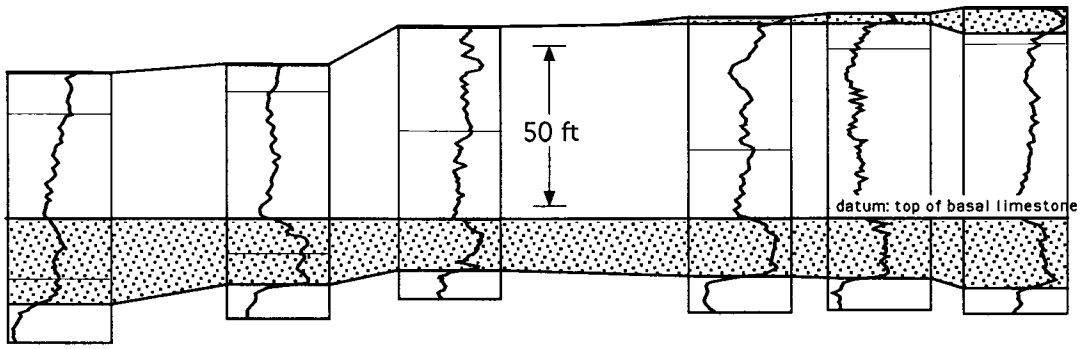

B. During deposition of grainstones and packstones of the upper limestone -- lower-energy depositional environments prevail after deposition of grainstones and packstones of basal limestone, and finer grained lime muds and sparse skeletal debris of the lower cherty dolomitic limestone are deposited. A westward-facing depositional slope developed as shoals of crinoidal debris and shell fragments of the upper limestone prograde westward.

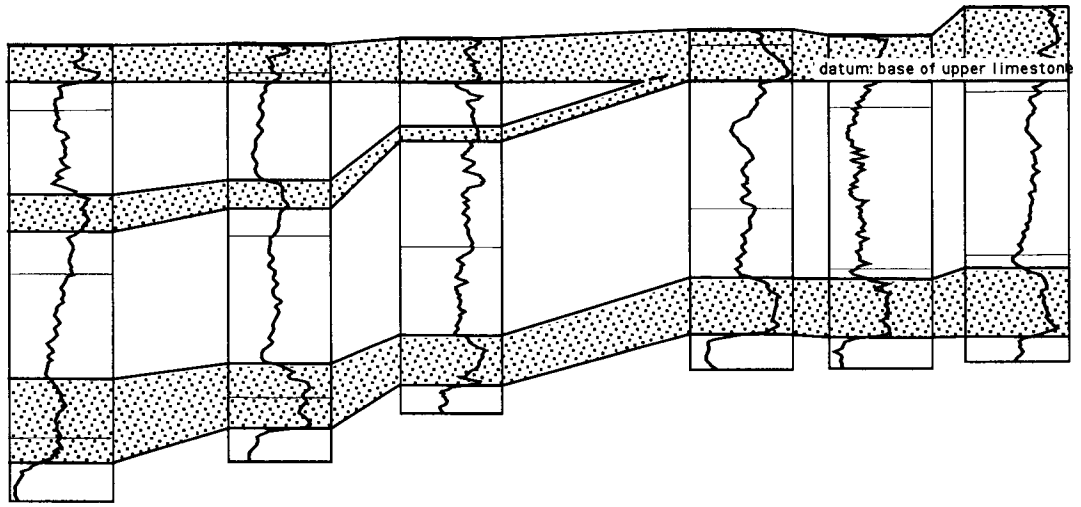

C. At end of deposition of grainstones and packstones of the upper limestone -- downslope movement of coarse-grained skeletal debris from shallow-water shoals create the "intermediate limestone". Lime muds and sparse skeletal debris subsequently dominate in western part of section, possibly due to persistent deeper water caused by local tectonic subsidence (expressed with westernmost three wells). Shoals of coarse-grained crinoidal debris and shell fragments of the upper limestone eventually prograde westward over this westward-thickening wedge of relatively deeper-water deposits.

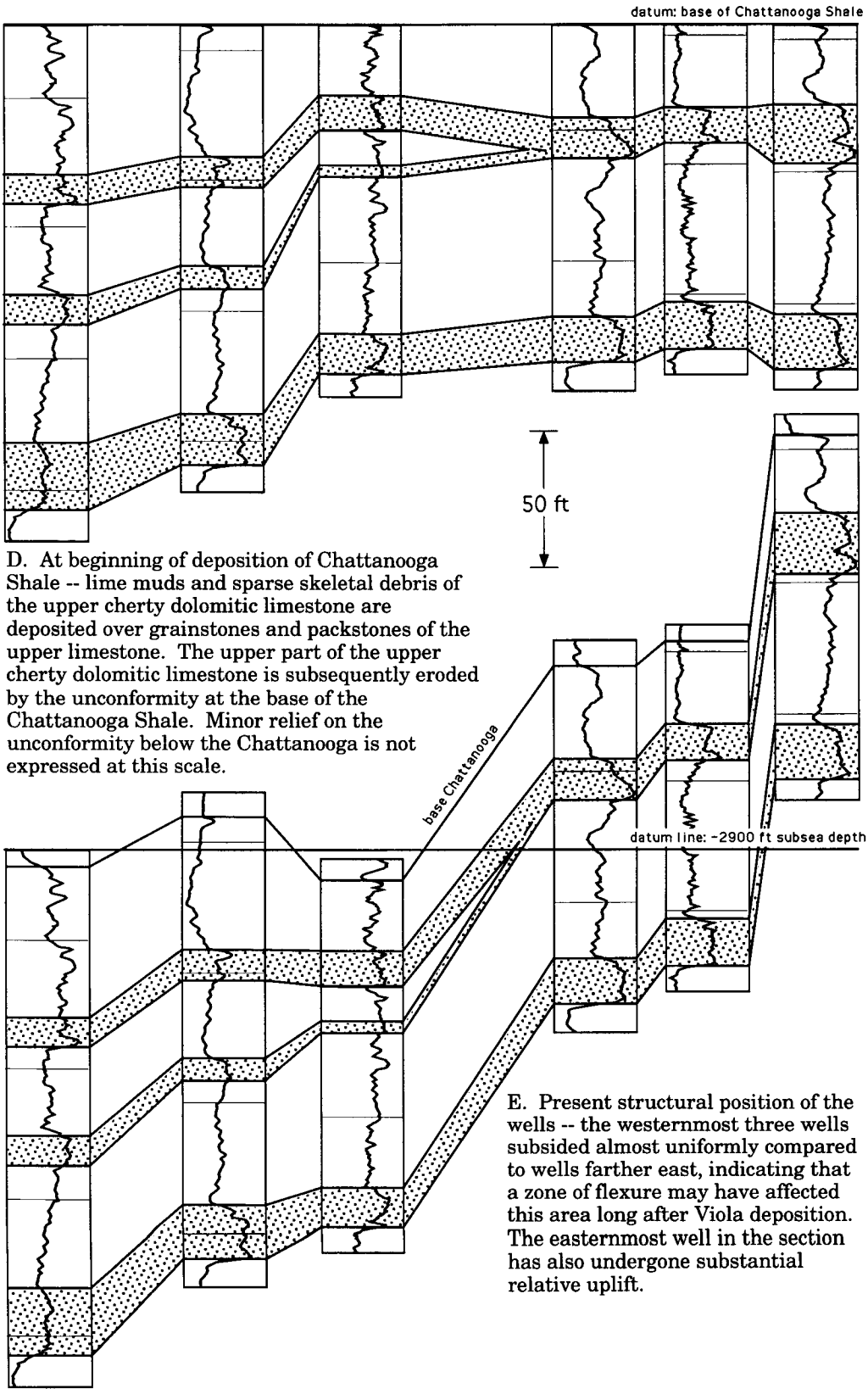

D. At beginning of deposition of Chattanooga Shale -- lime muds and sparse skeletal debris of the upper cherty dolomitic limestone are deposited over grainstones and packstones of the upper limestone. The upper part of the upper cherty dolomitic limestone is subsequently eroded by the unconformity at the base of the Chattanooga Shale. Minor relief on the unconformity below the Chattanooga is not expressed at this scale.

E. Present structural position of the wells -- the westernmost three wells subsided almost uniformly compared to wells farther east, indicating that a zone of flexure may have affected this area long after Viola deposition. The easternmost well in the section has also undergone substantial relative uplift.

this wedge that lies between these crinoidal limestones suggests that the shallow-water, high-energy conditions responsible for accumulation of the crinoidal grainstones and packstones were interrupted by the relative subsidence of the western flank of the Pratt anticline (see Figure 5.23). The thickness of the wedge (approximately 60 feet, 18 m) could represent the maximum water depth seaward of the crinoidal shoals, provided sea-level remained constant while it was being deposited. The low apical angle of the wedge (less than one degree) also implies that the Viola shelf is best characterized as a ramp (Ahr, 1973; Wilson, 1975, p. 21-22) where no drastic change in slope existed. The Pratt anticline would represent minor local relief on this vast shelf, with more open water present farther south in the ancestral Anadarko basin in Oklahoma. Facies patterns are likely to be wide and irregular on a carbonate ramp (Wilson, 1975, p. 21).

RELATIONSHIP OF VIOLA STRATIGRAPHY TO PETROLEUM PRODUCTION

Stratigraphic and structural controls of Viola petroleum production within the study area are evident in comparisons of production with the regional-structure (Figure 5.24), subcrop (Figure 5.25), and worm's-eye-view maps (Figure 5.26). Two northeast-southwest trends of Viola petroleum production obliquely cut across the trend of the south-plunging Pratt anticline (Figure 5.24). One production trend extends from central Stafford County to northwestern Reno County; the other trend stretches from west-central Barber County to east-central Pratt County. This pattern of petroleum production indicates that the Pratt anticline is not a major control of the distribution of Viola petroleum production. Both production trends are represented by

Figure 5.24 Viola hydrocarbon production overlain onto the structure map at the base of the Viola (see Figure 4.2). Each square represents one producing well. Production maps were taken from Newell and others (1987). See text for discussion.

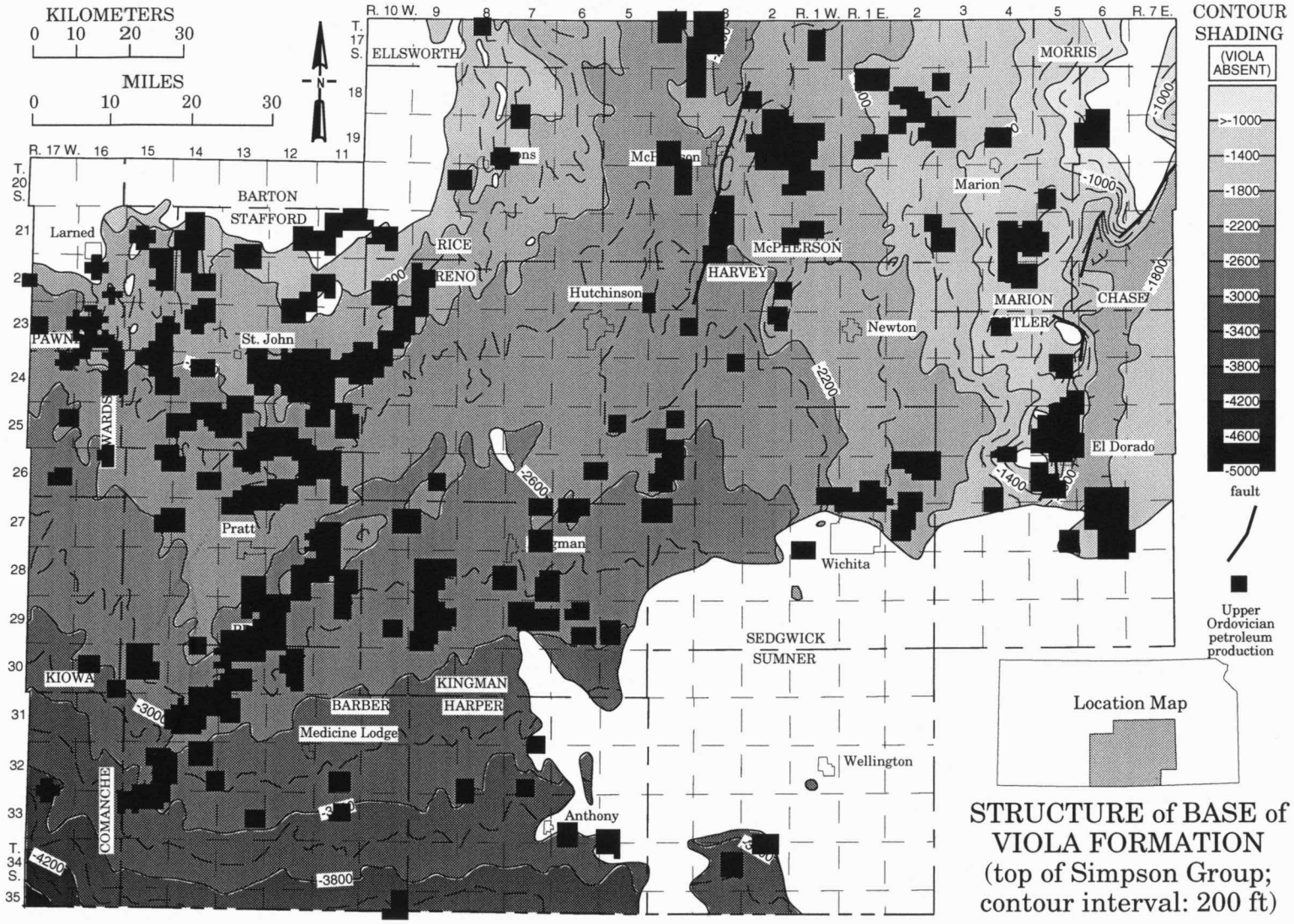

STRUCTURE of BASE of VIOLA FORMATION
(top of Simpson Group; contour interval: 200 ft)

a variety of types of traps (Newell and others, 1987). The production along the northeastern part of the northern trend (T.22-23S., R.9-11W.) is stratigraphically entrapped oil in the Zenith-Peace Creek field where Viola reservoirs are truncated by the basal Pennsylvanian and pre-Chattanooga unconformities (Imbt, 1941; Paddleford, 1941; Kornfeld, 1943; Newell and others, 1991). The northeastern end of the southerly trend (T.28S., R.11W.) is the Cunningham field, which is a combination structural-stratigraphic trap that produces gas (Rutledge and Bryant, 1937; Page, 1940).

The two production trends that obliquely cross the Pratt anticline are spatially associated with broad southwest-plunging synclines expressed on the subcrop map (Figures 5.6, 5.25). Both of these synclines have significant thicknesses of the upper cherty dolomitic limestone preserved in them, which constitutes the primary Viola reservoir in these production trends. A survey of Viola petroleum production within and near the study area (Table 5.1), also indicates that dolomite is the dominant reservoir rock in the Viola. The spatial association of production with the subcrop pattern of the Viola subunits implies that the distribution of reservoir rock at the top of the Viola significantly controls migration and accumulation of hydrocarbons within this unit in south-central Kansas, and that hydrocarbons migrating up the plunge of the Pratt anticline could have been shunted off its crest, but still up dip, along the subcrop limit of the porous upper cherty dolomite.

The principal controls on the distribution of Viola petroleum production elsewhere in the study area is unclear. Most fields appear to be associated with the subcrop of the cherty dolomitic subunits rather than the limestone subunits (see Figure 5.25). An exception to this is a diffuse group of fields that produce from the basal limestone subunit along the southerly pinchout of the Viola -- an area extending from southeastern Kingman County to east-central Butler County.

Viola production superimposed on the worm's-eye-view map (Figure 5.26)

Figure 5.25 Viola hydrocarbon production overlain onto the subcrop map displaying which subunit of the Viola Formation is present at the top of the Viola Formation (see Figure 5.6). Two broad southwesterly plunging synclines, respectively extending southwestward from T.22S.-R.9W. and T.27S.-R.11W., are the locus for two production trends of Viola oil and gas. Most Viola oil and gas fields are associated with subcrops of the upper cherty dolomitic limestone and the lower chert dolomitic limestone. See text for discussion.

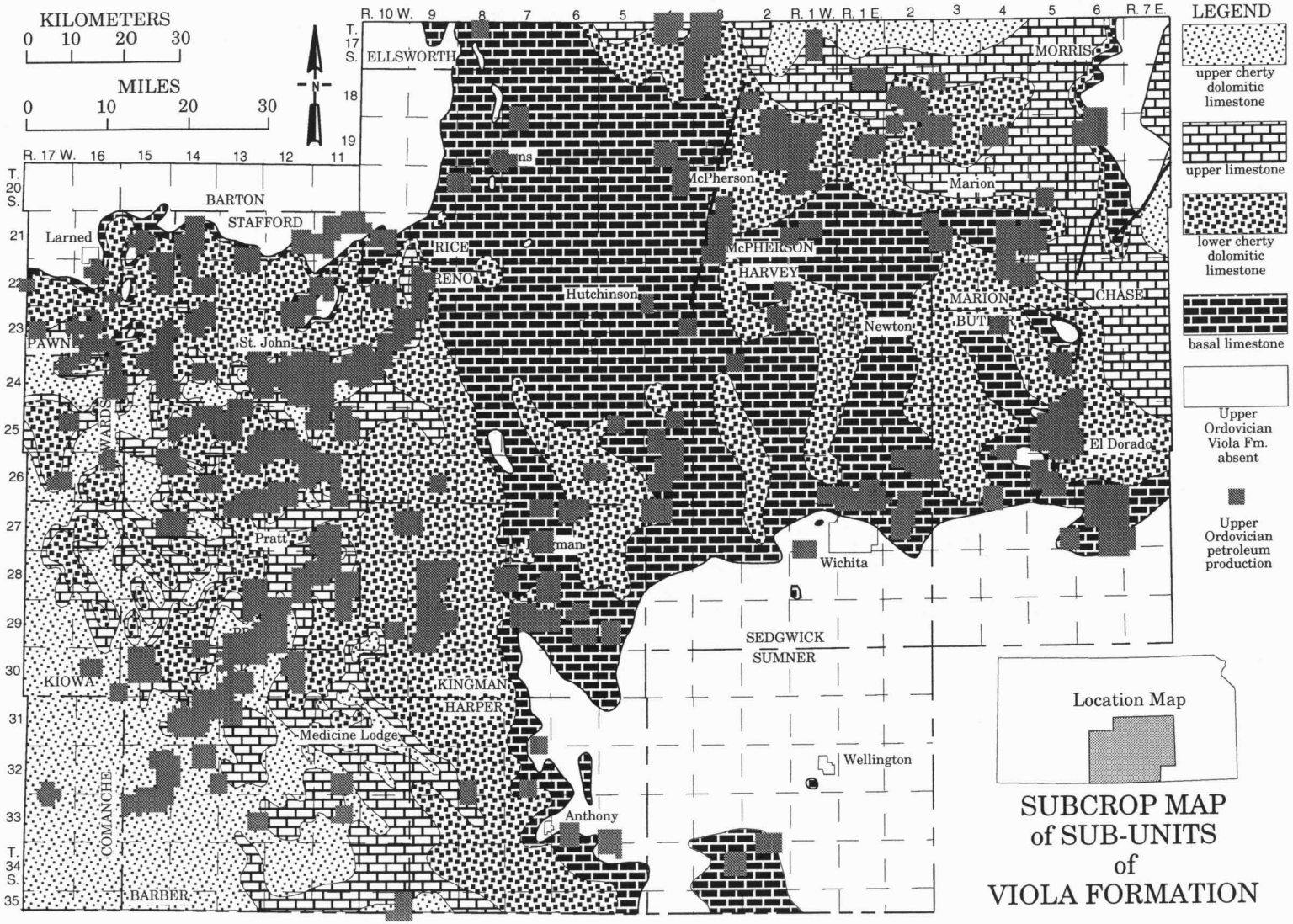
KILOMETERS
0 10 20 30
MILES
0 10 20 30
N
R. 10 W. 9 8 7 6 5 4 3 2 R. 1 W. R. 1 E. 2 3 4 5 6 R. 7 E.
R. 17 W. 16 15 14 13 12 11
T. 17 S.
T. 20 S.
T. 34 S.
ELLSWORTH
MORRIS
McPherson
Marion
BARTON
STAFFORD
Larned
RICE
McPHERSON
HARVEY
RENO
Hutchinson
Newton
MARION
BUTLER
CHASE
PAWNEE
St. John
WARD
El Dorado
Pratt
Wichita
SEDGWICK
SUMNER
KIOWA
KINGMAN
HARPER
Medicine Lodge
Wellington
Anthony
COMANCHE
BARBER
LEGEND
upper cherty dolomitic limestone
upper limestone
lower cherty dolomitic limestone
basal limestone
Upper Ordovician Viola Fm. absent
Upper Ordovician petroleum production
Location Map
SUBCROP MAP
of SUB-UNITS
of
VIOLA FORMATION

Table 5.1 A survey of literature on oil and gas fields that produce from Viola Formation in south-central Kansas.

FIELD NAME	LOCATION (COUNTY)	TYPE of TRAP	TYPE of PAY	RESERVOIR LITHOLOGY	REFERENCE
Alameda	T.28S., R.7W. (Kingman)	structural	oil	med.-grained vuggy dolomite	King (1965a,b)
Albion, Albion North	T.26S., R.6W. (Reno)	stratigraphic	oil	fractured, vuggy dolomite	Oros (1965)
Cairo North	T.28S., R.11W. (Pratt)	stratigraphic	oil	med.-grained cherty dolomite	Thompson (1955)
Cunningham	T.27-28S., R.11-12W. (Kingman, Pratt)	struct./strat.	gas	porous dolomite	Rutledge and Bryant (1937) Page (1940) Skelly Oil Co. Geol. Dept. (1956)
Deerhead	T.32S., R.15W. (Barber)	stratigraphic	oil, gas	med.-grained dolomite, coarse-grained limestone	Tucker (1956)
El Dorado	T.25S., R.5E. (Butler)	structural	oil, gas	cherty dolomitic limestone	Reeves (1929) Biedermam (1966)
Enlow	T.24S., R.16W. (Edwards)	structural	oil	vuggy med.-crystalline limestone	Sheats (1956)
Jem	T.30S., R.13W. (Barber)	stratigraphic	oil	chert breccia, dolomite	Brown and Banta (1993)
Lerado	T.26S., R.9W. (Reno)	structural	oil	med.-crystalline dolomite	McGinness (1965) Steincamp (1965)
Lerado Southwest	T.26S., R.9W. (Reno)	structural	oil	med.-crystalline dolomite	McGinness (1965)
Lindsborg	T.16-17S., R.3-4W. (McPherson, Saline)	struct./strat.	oil	coarse-crystalline limestone	Newell (1990)
Nescatunga	T.32S., R.18W. (Comanche)	structural	gas	vuggy cherty dolomite	Capps (1965)
Rhodes	T.33S., R.11W. (Comanche)	stratigraphic	oil	(not specified)	Clark (1956)
Skully	T.18S., R.1E. (Marion)	structural	oil	dolomite	Salgat (1983)
Sullivan	T.32S., R.8-9W. (Harper)	struct./strat.	oil show	sucrosic dolomite	Erlenwein (1985)
Valley Center	T.25-26S., R.1W., R.1E. (Sedgwick)	structural	oil	vuggy coarse-crystalline dolomite	Wright (1960)

Table 5.1 (continued). A survey of literature on oil and gas fields that produce from Viola Formation in south-central Kansas.

FIELD NAME	LOCATION (COUNTY)	TYPE of TRAP	TYPE of PAY	RESERVOIR LITHOLOGY	REFERENCE
Willowdale	T.21S., R.9W. (Kingman)	structural	oil	cherty med.-crystalline dolomite	Cruce (1956)
Zenith-Peace Creek	T.23S., R.10-11W. (Reno, Stafford)	stratigraphic	oil	cherty sucrosic dolomite	Imbt (1941) Paddleford (1941) Kornfeld (1943) Newell and others (1991)

shows no obvious correlation with the pattern of units superjacent to the Viola Formation. However, Mississippian siliciclastic strata off the west flank of the Pratt anticline in eastern Edwards, eastern Kiowa, northern Comanche, and western Pratt counties has little associated Viola production, which may mean that this unit is not a good seal to any Viola reservoir bed directly beneath it.

Figure 5.26 Viola hydrocarbon production overlain onto the worm's-eye view map illustrating units superjacent to Viola Formation (see Figure 4.4). No close association of the production trends with the map pattern is evident. See text for discussion.

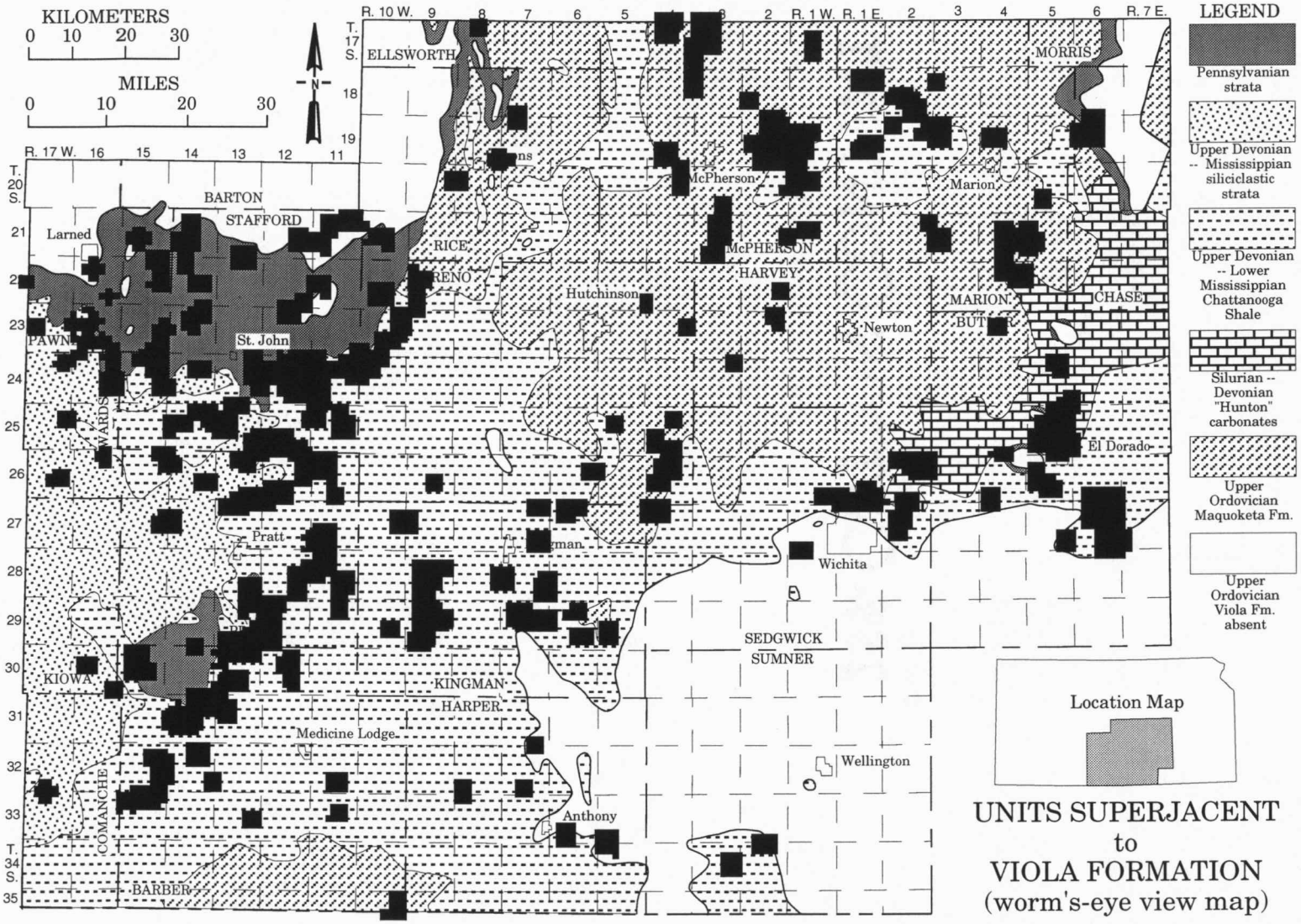

UNITS SUPERJACENT
to
VIOLA FORMATION
(worm's-eye view map)

Chapter 6

THERMAL AND BURIAL HISTORY OF THE VIOLA IN THE STUDY AREA

INTRODUCTION

The thermal and burial history of the Viola is reviewed in this section in order to understand how the present geometry of the Viola evolved, and what geologic events may be critical to its observed diagenetic features. The results of several models in which maturation occurs strictly by burial heating are compared to directly observed maturation measurements and fluid-inclusion homogenization temperatures. Inadequacies of the burial models are then considered in the context of geologic processes or amended modeling parameters that may account for the differences in theoretical and observed maturation.

The inferred thermal and burial history of the Viola in the study area can be modeled using available isopach and temperature data. In turn, these models can be compared to maturation indicated by organic material within the rocks to test the model. If there is reasonable agreement between the models and the directly-observed maturation, confidence in the thermal history conjured by the models is increased considerably. However, even though there may be good agreement between the results of the theoretical models and the analyses from the rocks themselves, the models are not unique solutions because similar modeling results could possibly be reproduced by adjusting model parameters, provided the adjustments are within the range of variability allowed by the geology. With this in mind, the maturation modeling is performed by varying certain parameters, principally geothermal gradient and thickness of Cretaceous strata. In addition to gaining an understanding on how

sensitive the results are to changes in these parameters, the models can then be evaluated in the context of what is geologically most likely or reasonable.

The thermal history of Viola Formation in the study area is initially assessed with time-temperature index modeling. This type of construct traces the history of subsidence and uplift of the Viola after deposition. The inferred thermal history can, in turn, be a useful tool for comparison to thermal parameters measured with fluid inclusions and organic maturation indicators. A time-temperature index (TTI) model (Waples, 1980; 1981, p. 95), based on work by Lopatin (1971), takes into account both time and temperature in calculating a cumulative thermal maturity for organic matter contained in sediments. This technique assumes that the rates of numerous chemical reactions involved in the conversion of organic matter (i.e., kerogen) to petroleum can be mathematically approximated by that of a first-order chemical reaction in which the rate of maturation of organic matter roughly doubles for every 10 °C rise in temperature. The Lopatin technique generates a dimensionless number, called the "time-temperature index" (TTI) that can be empirically correlated to stages of oil and gas generation (cf., Waples, 1981, p. 102). The graphical history of subsidence and uplift used to calculate the TTI can also be utilized to infer the maximum temperature and subsidence a given stratigraphic interval has experienced and the time at which various levels of maturation were achieved.

TTI calculations by the Lopatin technique are essentially one-dimensional in that the tectonic and thermal model on which those calculations are based are applicable only to a single geographic locality -- usually one well. The spatial variability of maturation over a given region or basin, however, can be determined by performing TTI calculations for several wells or locations in a study area. For this purpose, two localities were selected in the study area: a location at the north end of the study area at the crest of the Central Kansas arch in western McPherson County

(T.19S., R.4W.), and a location at the southern part of the study area in southern Harper County (T.33S., R.7W.) where the Viola is near its present maximum depth in the study area.

The TTI calculation carries with it several assumptions. Various refinements and complications can be added to the calculation procedures, such as decompacting the sedimentary column and taking into account heat flow and thermal conductivity in the determination of the geothermal gradient (cf., Woods and others, 1988). More precise answers may be derived by these more sophisticated procedures, but only limited organic and thermal maturation data are available with which to compare the results of such elaborate modeling. The models presented in this report are uncomplicated, using reasonable assumptions of geothermal gradients and stratigraphic thicknesses to provide approximate answers to the following questions: a) what is the maximum temperature and depth to which the Viola in the study area has been subjected?; b) when did the Viola experience these conditions?; c) how well do direct maturation indicators such as vitrinite reflectance, Rock-Eval data, and fluid-inclusion homogenization temperatures compare to the thermal maturity indicated by the TTI modeling; d) are additional thermal events necessary to better correlate the TTI modeling to the direct maturation indicators?

DATA CONSTRAINTS FOR TIME-TEMPERATURE INDEX (TTI) MODELING

An approximate thermal history at a given locality can be established by assuming a geothermal gradient and an ambient surface temperature, both of which may vary over geologic time. The tectonic history is depicted by plotting subsidence and uplift of various strata against time. The amount of subsidence a given rock unit

has experienced is determined by thicknesses and ages of strata above that unit. Uplift can be evaluated by estimating erosion that has occurred at major unconformities.

Few data are available to precisely ascertain even present-day geothermal gradients in Kansas (Stavnes, 1982), and uncertainty increases when considering how the thermal regime may have changed during Phanerozoic time. For Mesozoic strata, and certainly for older Paleozoic strata such as the Viola, the variation of heat flow with time is the single most important source of uncertainty in these types of maturation calculations (Gretener and Curtis, 1982). However, a simple model assuming a constant geothermal gradient approximately equal to that of the present is a reasonable starting point. Ephemerally higher geothermal gradients may have occurred in the past. For example, the passing of a mantle plume in Cretaceous time could have been responsible for kimberlitic intrusive activity in Kansas (Steeples, 1989) and may have raised heat flow and thus temporarily increased the regional geothermal gradient. Thermal effects inboard in the craton due to rifting in the Oklahoma aulacogen in early Paleozoic time (Late Cambrian through Ordovician periods; Feinstein, 1981) or the Ouachita orogeny in Late Pennsylvanian time (Garner and Turcotte, 1984; Houseknecht and others, 1992; Spötl and others, 1994) may have been significant. Unfortunately, there currently is little evidence to evaluate the influence of these possible short-lived thermal events in the midcontinent. Similarly, the intensity and extent of regional lateral updip (advective) flow of heated brine from the Ouachita orogen in late Paleozoic time may also be important (Barker and others, 1992; Ge and Garven, 1992). Advective flow from the Ouachita orogen was shown by Wojcik and others (1992, 1994) to affect Pennsylvanian strata in southeastern Kansas. In addition, a strong Permian-age episode of secondary magnetization that affects lower Paleozoic strata in the midcontinent has been recognized in the last few years

(see McCabe and Elmore (1989)). This episode of remagnetization may, in part, be caused by addition of diagenetic minerals precipitated from chemically active and perhaps hot fluids expelled from the Ouachita orogen (Elmore and others, 1989; McCabe and Elmore, 1989).

Geothermal gradients can be calculated from temperature and depth information included on most wireline logging runs in wells drilled for oil and gas. Although bottom-hole temperatures (BHTs) from wireline logs are routinely recorded in these tests, only rarely does sufficient time elapse for drill-hole temperatures to equilibrate with the surrounding rocks (Ball, 1982). BHT measurements must therefore be used with caution, or corrected. Even after correction, the geothermal gradient calculated with BHT data is a two-point approximation from surface temperature and the BHT over the entire thickness of rock considered, hence vertical variations in the gradient due to differing thermal conductivities of rocks penetrated in the well are not recognized (Förster and Merriam, 1993).

Stavnes (1982) constructed geothermal gradient maps of the state based on BHTs from 42,348 wells deeper than 1000 ft (305 m) (see Figure 6.1) and found that although BHTs may not precisely determine the geothermal gradient at any given locality, they were helpful for revealing relative spatial variations of the geothermal gradient. Temperature profiles on 144 wells were logged by Stavnes to supplement the information derived from the BHT data, but the spacing of the temperature-logged wells left large areas of the state not covered. Maps presented in Stavnes (1982) and Stavnes and Steeples (1982), and from the Geothermal Survey of North America (American Association of Petroleum Geologists, 1976) indicate the geothermal gradient in the northern part of the study area is approximately 25 °C/km, but nearby wells that have been thermally logged indicate a gradient of approximately 30 °C/km. The geothermal gradient in the southern part of the study area is more enigmatic in that

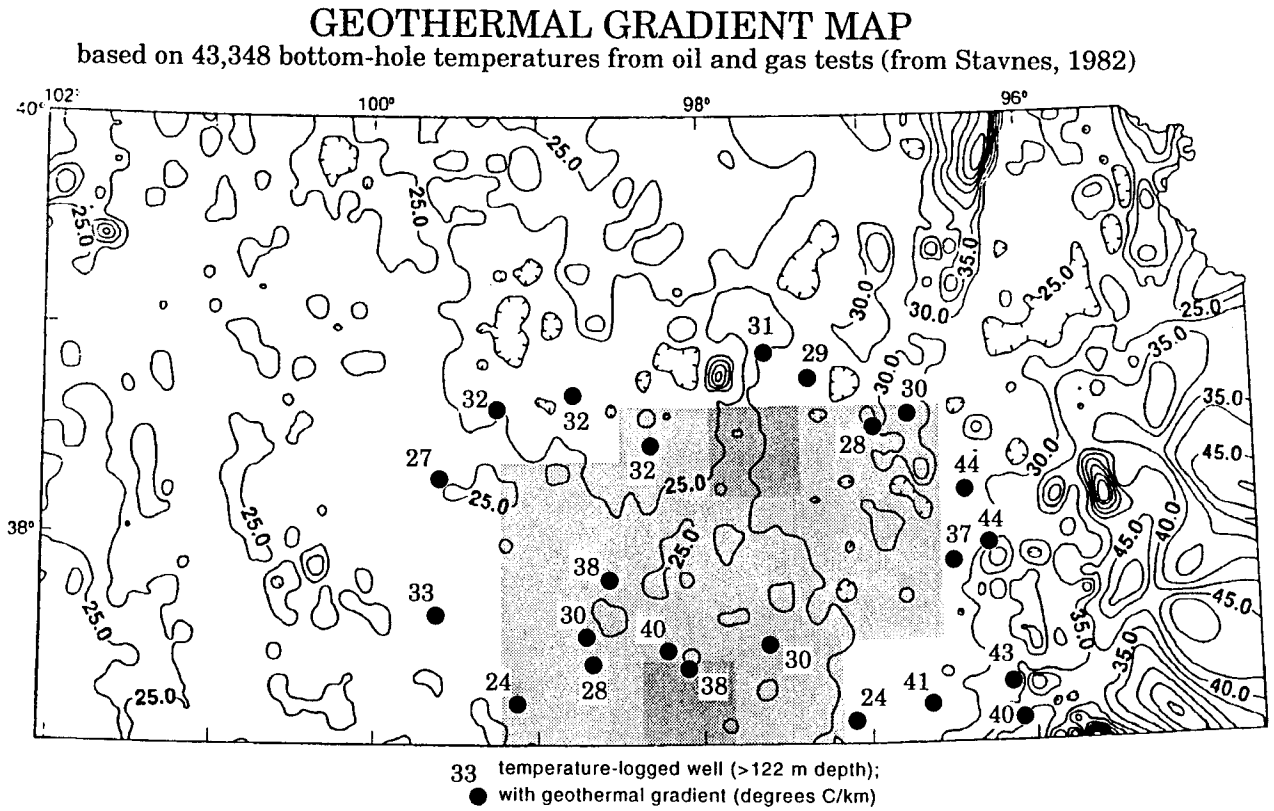

Figure 6.1 Geothermal gradient map of Kansas based on bottom-hole temperatures from oil and gas tests (from Stavnes, 1982). Isopleths are at intervals of 5 °C/km. Temperature-logged wells in the vicinity of the study area (shaded) are superimposed. McPherson and Harper counties, the two localities modeled for thermal maturation, are shaded darker. Generally higher geothermal gradients in the eastern Kansas are attributable to data derived from many relatively shallow wells that were drilled only into Pennsylvanian strata. These strata are characterized by relatively low thermal conductivity, hence temperatures will rise relatively rapidly with depth, and consequently a bottom-hole-temperature from shallow wells such as these would yield an anomalously high geothermal gradient (Förster and Merriam, 1993).

BHTs indicate it is approximately 25 °C/km, but nearby wells that have been thermally logged indicate gradients as high as 40 °C/km (see Figure 6.1). Because of these uncertainties in the geothermal gradients, maturation models presented in this study were calculated using gradients ranging between 20 and 50 °C/km.

Surface temperature and its variation during Phanerozoic time plays a subsidiary roll in the determination of the geothermal gradient. Changes in surface temperature with every geologic period were estimated from climatological information and plate-tectonic reconstructions presented in Habicht (1979) (Table 6.1, Figure 6.2). These mean surface temperatures vary between 14 °C in late Tertiary time and 30 °C during the Permian. The present mean surface temperature in Kansas is approximately 12 °C (54 °F; Kansas State Board of Agriculture, 1985).

The tectonic history for both the northern and southern modeling locales are summarized in Table 6.1. Uncertainties in reconstructing the history of subsidence and uplift primarily stem from the numerous unconformities that are characteristically present in cratonic sedimentary strata. Phanerozoic time in this part of the midcontinent has been dominated by erosion and nondeposition; Förster and Merriam (1994, in press) estimated that 88% of Phanerozoic time is not recorded by rocks preserved in the Cherokee basin of southeastern Kansas. Elsewhere in Kansas, 50 to 85% of Phanerozoic geologic time is represented by unconformities (Merriam, 1963). Although the incomplete nature of the geologic record poses problems for paleotectonic reconstructions, lower Paleozoic units (i.e., Arbuckle, Simpson, Viola, Maquoketa, "Hunton", Chattanooga, and Mississippian strata) are characterized by only mild deformation with relative dips between units varying less than 5 degrees (Lee, 1956). The thinness of these units compared to their areal extent also suggests that significant differential subsidence and uplift were not the norm during the early Paleozoic and that the maximum preserved thickness of individual units is probably

Table 6.1 Stratigraphic and temperature data for TTI modeling.

AVERAGE SURFACE TEMPERATURE (from Habicht, 1979)

AGE	**MEAN SURFACE TEMP. (°C)**		**AGE**	**MEAN SURFACE TEMP. (°C)**	
Present	12	(@ 0 Ma)	Permian	30	(@ 270 Ma)
Late Tertiary	14	(@ 5 Ma)	Carboniferous	24	(@ 325 Ma)
Early Tertiary	18	(@ 40 Ma)	Devonian	26	(@ 385 Ma)
Cretaceous	20	(@ 103 Ma)	Silurian	27	(@ 425 Ma)
Jurassic	24	(@ 175 Ma)	Ordovician	20	(@ 470 Ma)
Triassic	29	(@ 230 Ma)	Cambrian	26	(@ 545 Ma)

SUBSIDENCE AND UPLIFT OF BASEMENT IN WESTERN McPHERSON COUNTY (in feet). Absolute ages of strata are from Haq and Van Eysinga (1987).

AGE (and unit)	**Ma**	**SUBSIDENCE (ft)**	**UPLIFT (ft)**
Cambrian - Ordovician (Arbuckle)	524-478	550	----
	478-466	----	50
Ordovician (Simpson)	466-446	200	----
Ordovician (Viola, Maquoketa)	446-440	50	----
Silurian ("Hunton")	440-422	250	----
	422-388	----	----
Devonian ("Hunton")	388-376	50	----
	376-368	----	300
Devonian - Miss. (Chattanooga)	368-340	350	----
Mississippian	340-326	325	----
	326-310	----	100
Pennsylvanian (Desmoinesian) strata	310-306	300	----
Pennsylvanian (Missourian) strata	306-302	325	----
Pennsylvanian (Virgilian) strata	302-290	1000	----
Permian	290-250	2250	----
	250-140	----	550
Cretaceous	140- 68	1500	----
	68- 0	----	1950

Table 6.1 (continued). Stratigraphic and temperature data for TTI modeling.

SUBSIDENCE AND UPLIFT OF BASEMENT IN CENTRAL HARPER COUNTY (in feet). Absolute ages of strata are from Haq and Van Eysinga (1987).

AGE (and unit)	**Ma**	**SUBSIDENCE (ft)**	**UPLIFT (ft)**
Cambrian - Ordovician (Arbuckle)	524-478	1050	----
	478-466	----	50
Ordovician (Simpson, Viola)	466-446	150	----
Ordovician (Maquoketa)	446-440	----	----
Silurian ("Hunton")	440-422	----	----
	422-388	----	----
Devonian ("Hunton")	388-376	----	----
	376-368	----	50
Devonian - Miss. (Chattanooga)	368-340	125	----
Mississippian	340-326	325	----
	326-324	----	100
Pennsylvanian (Morrowan-Atokan) strata	324-310	325	----
Pennsylvanian (Desmoin.-Virgil.) strata	310-290	1775	----
Permian	290-250	2875	----
	250-140	----	175
Cretaceous	140- 68	500	----
	68- 0	----	600

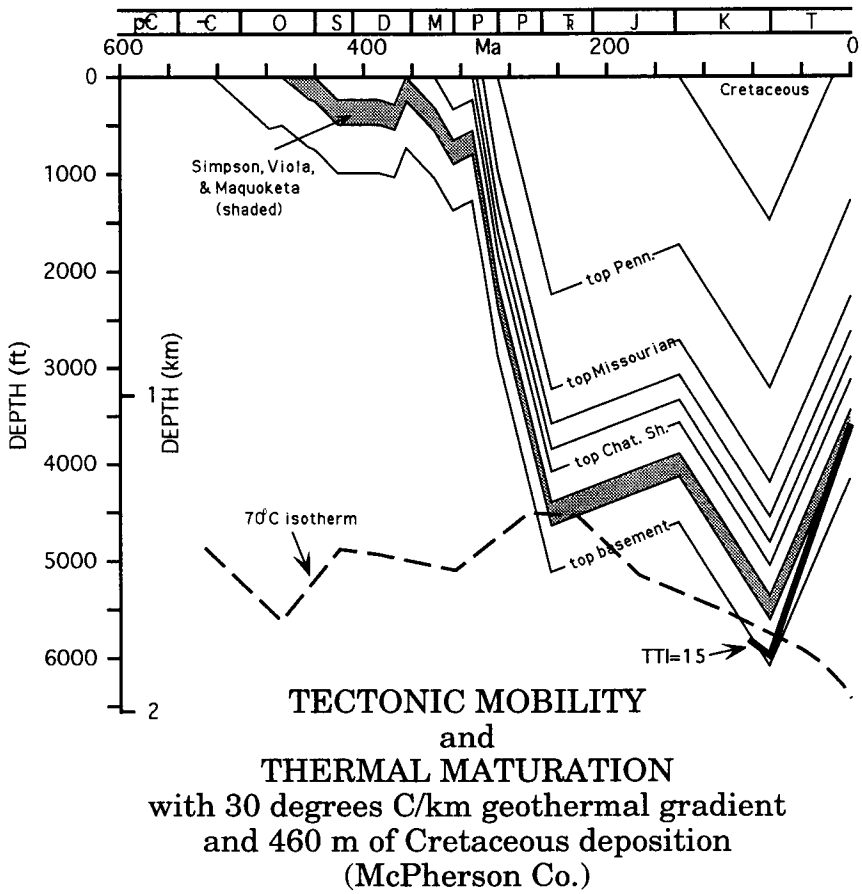

Figure 6.2 Tectonic mobility diagram and temperature history of the stratigraphic column in McPherson County (T.19S., R.4W.), using data presented in Table 6.1. A 30 °C/km geothermal gradient would cause the Viola (shaded) to experience a maximum temperature of 70 °C at the end of Permian time, however, thicknesses of Cretaceous rock in excess of 1900 ft (580 m) will cause slightly greater temperatures to be experience by the Viola at the end of Cretaceous time (see text for discussion). The depth fluctuations of the 70 °C isotherm over time are caused by variations in surface temperature (see data in Table 6.1). Although geothermal gradient is assumed to be constant in this model, a geothermal gradient that varies with time would also affect the depth at which a given isotherm occurs. TTI = 15 is the beginning of significant oil generation (i.e., top of the oil window).

close to the original thickness, discounting compaction. Unless considerable uplift and erosion occurs, gaps in sedimentation during deposition of a geologic formation spanning several million years of time are relatively inconsequential for purposes of TTI calculations. The thicknesses of the lower Paleozoic units also do not indicate significant burial (i.e., greater than 1 km) before Pennsylvanian time and as a result maturation experienced by the Viola during early Paleozoic time was minimal.

Subsidence in Pennsylvanian time is less difficult to estimate because most of the strata deposited during this period are still present. Permian subsidence, however, is more difficult to estimate because these strata are less well preserved, having been subject to erosion and uplift both before and after deposition of Cretaceous strata. Original thickness of the Permian rocks was estimated by summing restored isopachs presented in McKee and others (1967).

Original thickness of Mesozoic strata is even harder to estimate, because these rocks have mostly been eroded in the study area. Thin Jurassic and Triassic units are present in western Kansas and eastern Colorado (Merriam, 1963), but these units are inferred not to have been deposited farther east. A northwestwardly thickening wedge of Cretaceous strata is preserved in western Kansas as a remnant of a broad seaway through the west-central United States and Canada. The eastern margin of this seaway has been eroded so estimates of the amount of Cretaceous strata once deposited over the study area largely depend on eastward projection of thicknesses across nearly the entire state. Cretaceous rocks reach 3000 ft (920 m) in thickness in extreme northwestern Kansas, but are completely eroded in the eastern and south-central parts of the state (Merriam, 1963). Graphical projection of Cretaceous thicknesses in regional cross-sections presented in Merriam (1963) across the state to the modeling location in McPherson County indicate Cretaceous strata deposited in McPherson county were at least 1500 ft (460 m) but probably did not exceed 3000 ft

(920 m). The thickness of Cretaceous strata deposited in southern and southeastern Kansas was presumably less than in McPherson County because this area was on the flank of the Ozark dome, which probably remained a positive element during Mesozoic time. Barker and others (1992) assumed significant uplift and erosion of Pennsylvanian and Permian strata occurred in southeastern Kansas before deposition of any Cretaceous strata, and they estimated less than 300 ft (90 m) of Mesozoic and Cenozoic rock were deposited in southeastern Kansas. Thermal modeling presented in Förster and Merriam (in press) assumed 400 ft (125 m) of Cretaceous strata in the Cherokee basin, from projection of thicknesses of Cretaceous strata to a 0-line on the flank of the Ozark dome. With the same assumption of a continuum of southeastward decreasing thicknesses of Cretaceous strata, 500 ft (150 m) of Cretaceous strata is estimated to have been deposited at the modeling locality in Harper County. Erosion of Cretaceous strata is assumed to have been initiated at the beginning of the Laramide orogeny in Late Cretaceous - Early Tertiary time and this erosion is assumed to be continuous to the present. In Tertiary time an apron of clastic debris was shed off the Rocky Mountains and is manifest as the Ogallala Formation, which covers much of the Great Plains and the western third of Kansas. A convergence map in Merriam (1963) showing restored thicknesses of the Ogallala Formation in Kansas indicates this unit was probably considerably less than 100 ft (30 m) thick in central Kansas, and it is therefore considered unimportant with respect to TTI modeling.

TTI MODELS AND RESULTS

The tectonic mobility diagram and temperature history for the stratigraphic column in the northern part of the study area (McPherson County) (Figure 6.2)

illustrates the sequential interaction of subsidence, uplift, and temperature variations for several stratigraphic horizons, and the resultant thermal maturation. This particular model assumes a 30 °C/km constant geothermal gradient and 1500 ft (460 m) of Cretaceous strata, but other models were also tested with different thicknesses of Cretaceous strata and different geothermal gradients. According to this model, the Viola Formation reached a maximum temperature of 70 °C at the end of the Permian. A higher geothermal gradient of 40 °C would have subjected the Viola to a maximum temperature of 85 °C at the end of the Permian, and again at the end of the Cretaceous just before the post-Laramide uplift and erosion. A high-end estimate of 3000 ft (920 m) of Cretaceous strata, in conjunction with a 30 °C/km gradient, at this locality would have subjected the Viola to a maximum temperature at the end of the Cretaceous of 85 °C for and 105 °C for a 40 °C/km gradient.

The top of the oil window (i.e., beginning of significant oil generation; TTI = 15) would have reached the Simpson Group, which underlies the Viola, in Late Tertiary time (Figure 6.2), assuming a 30 °C/km gradient and 1500 ft (460 m) of Cretaceous deposition. The Viola would therefore be marginally mature with respect to oil generation. As previously discussed, the maturation and temperature the Viola Formation in the northern part of the study area would experience primarily depends on the interplay between geothermal gradient and Cretaceous cover. The results of several TTI models varying each of these geologic conditions are diagrammatically expressed in nomograms (Figures 6.3, 6.4) that show the TTI calculated for the top of the Simpson Group (i.e., near base Viola Formation) and the base of the Pennsylvanian section for different combinations of geothermal gradient and Cretaceous cover. Figures 6.3 and 6.4 indicate the calculated maturation is slightly more sensitive to the geothermal gradient than to the thickness of Cretaceous rocks. Most combinations of likely geothermal gradients and Cretaceous thicknesses at this

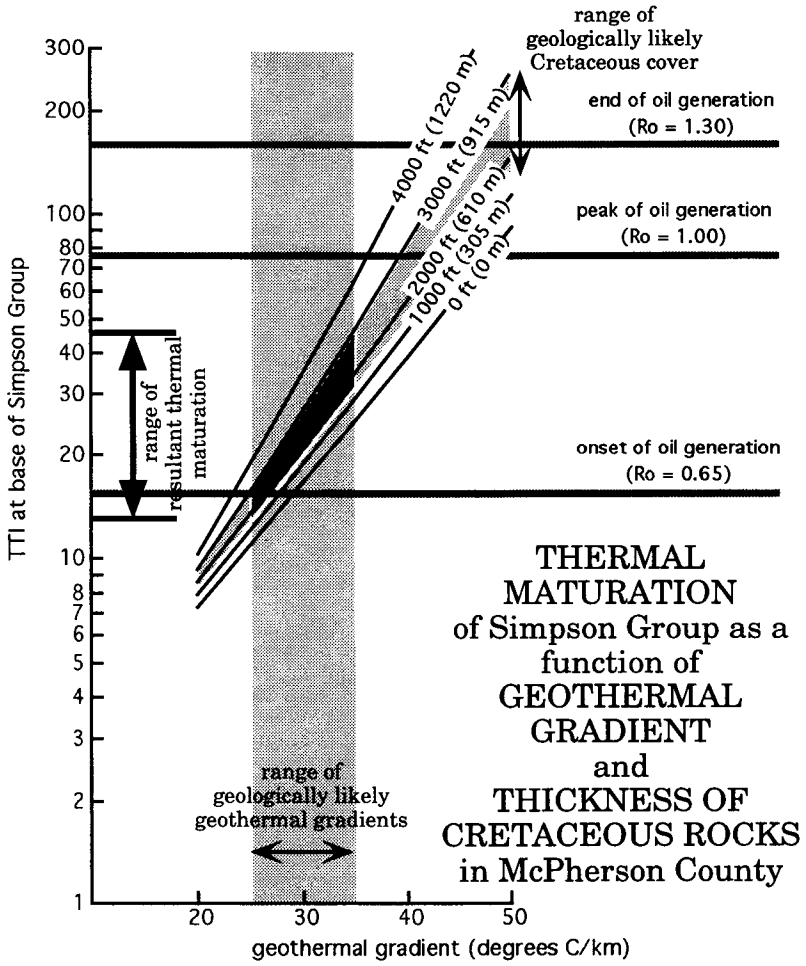

Figure 6.3 A nomogram summarizing effects on calculated TTIs of the Simpson Group by varying combinations of geothermal gradient and Cretaceous cover in McPherson County. The TTI is determined by assuming a geothermal gradient at the base of the diagram, extending this gradient in a vertical line to the assumed amount of Cretaceous rocks that were deposited. The resultant TTI is then determined by extending a horizontal line left from the point determined by the intersection of lines depicting the geothermal gradient and Cretaceous cover. Most combinations of likely geothermal gradients and Cretaceous cover would put the Simpson and Viola into initial stages of oil generation.

location will put the Simpson Group into the oil window (i.e., TTIs greater than 15) but below the peak of oil generation (TTI = 75; cf., Waples, 1981, p. 102) (see Figure 6.3) whereas the Pennsylvanian section would be in initial stages of oil generation (see Figure 6.4).

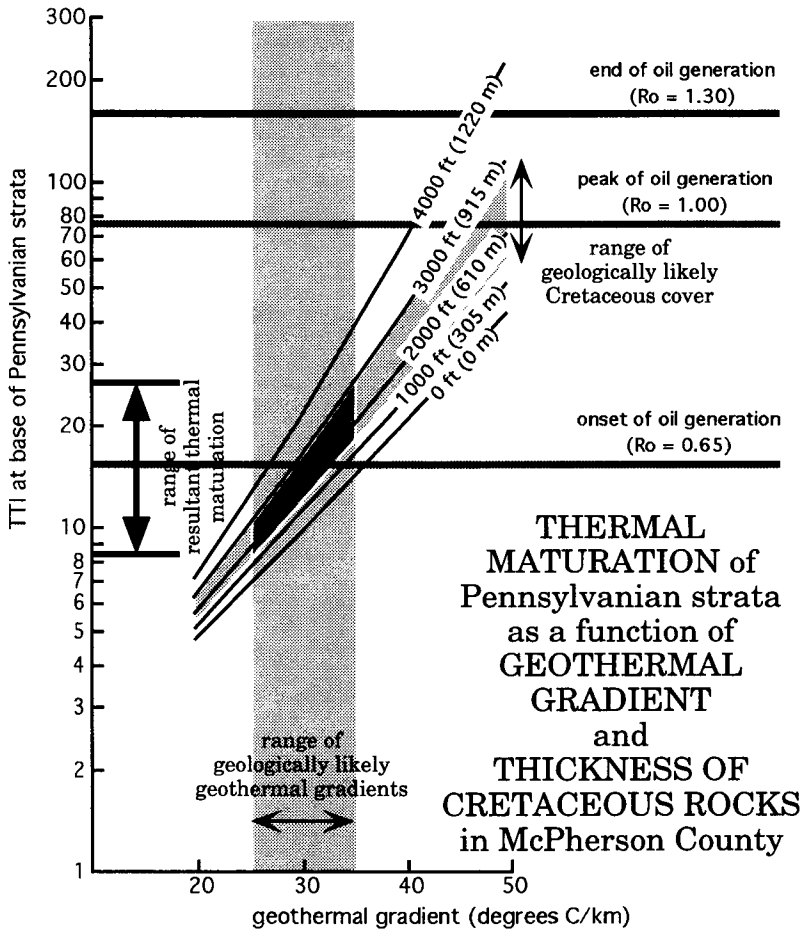

Figure 6.4 A nomogram summarizing effects on calculated TTIs at the base of the Pennsylvanian section by varying combinations of geothermal gradient and Cretaceous cover in McPherson County. See Figure 6.3 for instructions. Most combinations of likely geothermal gradients and Cretaceous cover indicate the base of the Pennsylvanian section will be immature to only marginally mature with respect to significant oil generation.

There is less uncertainty in the range of Cretaceous cover that could be expected at the locality modeled farther south in Harper County, hence the cardinal control of expected maturation in that area is geothermal gradient. Two models, shown in Figures 6.5 and 6.6, respectively assume constant geothermal gradients of 25 °C/km and 40 °C/km -- the extremes in the modern geothermal gradient indicated by

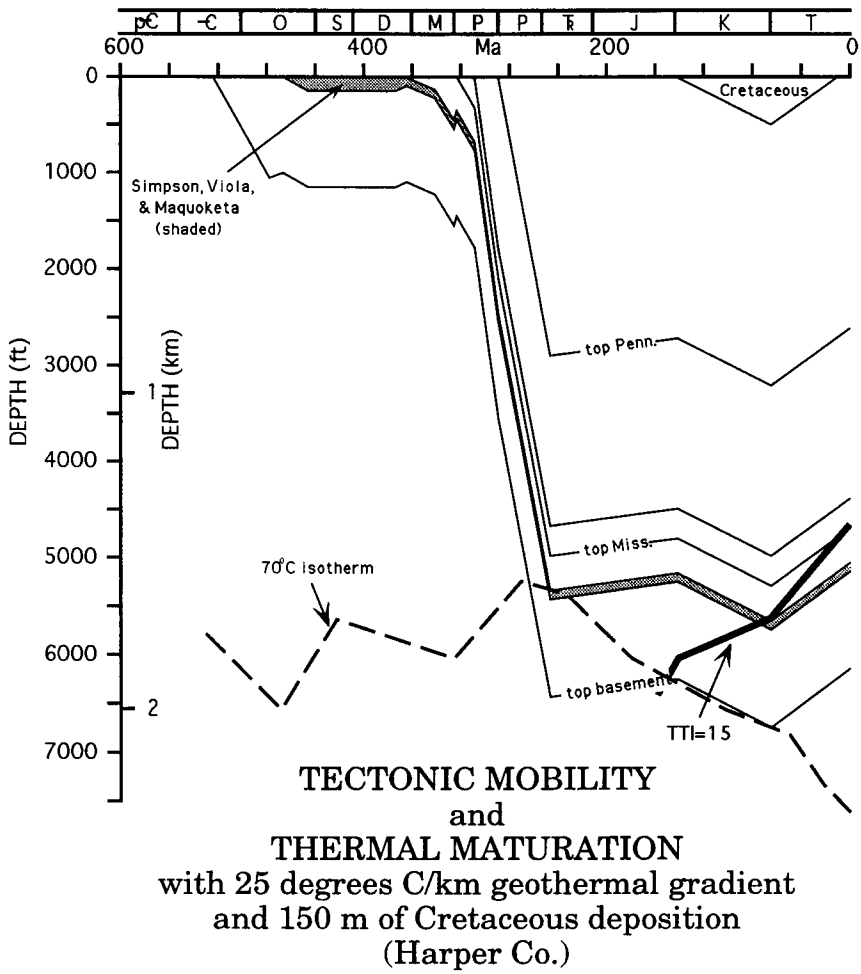

Figure 6.5 Tectonic mobility diagram and temperature history of the stratigraphic column in Harper County (T.33S., R.7W.), using data presented in Table 6.1. A 25 °C/km geothermal gradient would cause the Viola to experience a maximum temperature of 70 °C at the end of Permian time, despite it being buried deeper than the locality modeled in McPherson County. Cretaceous deposition in Harper County was assumed to be about one-third that assumed at McPherson County. TTI = 15 is the beginning of significant oil generation (i.e., top of the oil window).

the BHTs and the temperature-logged wells respectively (see Figure 6.1). Cretaceous deposition in both models is assumed to be 500 ft (150 m) since this locality is near the eastern margin of the Cretaceous Seaway. According to the model that is based on a geothermal gradient of 25 °C/km (Figure 6.5), the Viola Formation would reach a

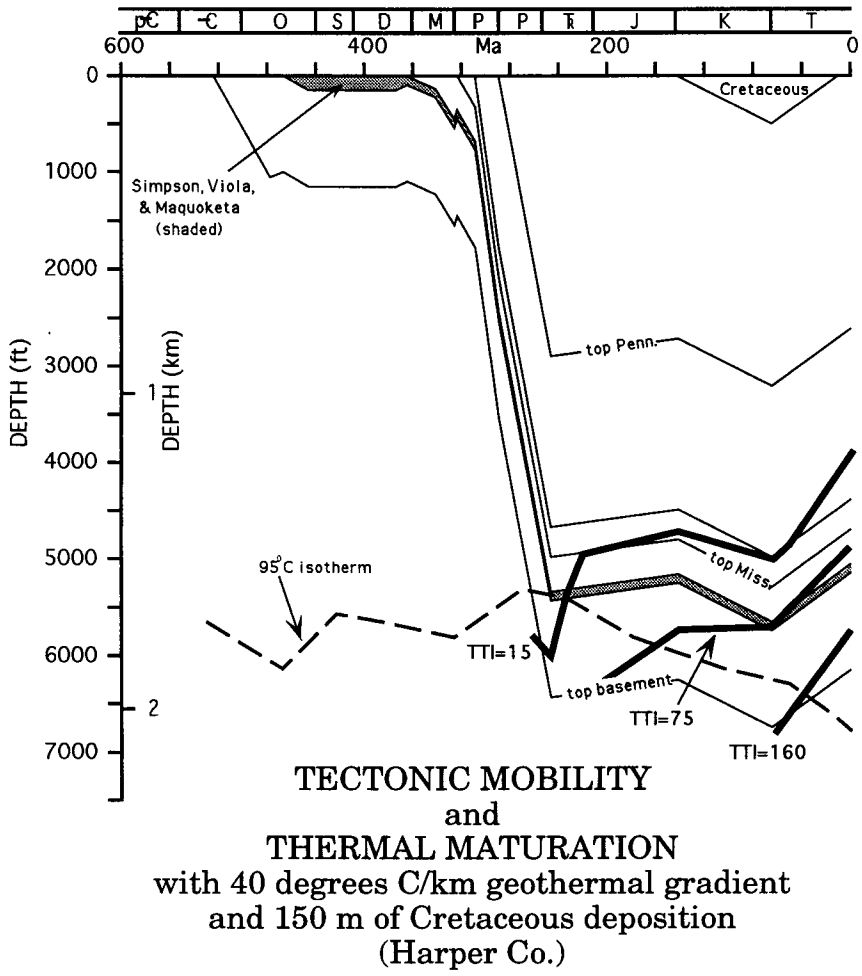

Figure 6.6 Tectonic mobility diagram and temperature history of the stratigraphic column in Harper County (T.33S., R.7W.), using data presented in Table 6.1. A 40 °C/km geothermal gradient would cause the Viola to experience a maximum temperature of 95 °C at the end of Permian time. Cretaceous deposition is assumed to be significantly thinner in Harper County than at McPherson County. TTI = 15 is the beginning of significant oil generation (i.e., top of the oil window); TTI = 75 represents peak oil generation; TTI = 160 is the end of significant oil generation (i.e., base of the oil window).

maximum temperature of 70 °C at the end of the Permian. Although present depth to the Viola Formation is approximately 1200 ft (370 m) deeper in Harper County than at the locality modeled in McPherson County, the lower geothermal gradient and inferred

thinner Cretaceous cover in Harper County accounts for the comparable maximum temperature modeled here for the Viola.

At the location modeled in Harper County, the top of the oil window (i.e., beginning of significant oil generation; TTI = 15) would reach the Simpson Group in Late Cretaceous time and would extend into the lower part of the Pennsylvanian System (Figure 6.5), if the low-end 25 °C/km geothermal gradient is assumed. Present thermal maturity of the Ordovician section would be TTI = 18, which is still only in initial stages of oil generation.

Using the higher geothermal gradient of 40 °C/km (Figure 6.6) in Harper County, the Viola would reach a maximum temperature of 95 °C at the end of Permian time. The top of the oil window (i.e., beginning of significant oil generation; TTI = 15) would reach the Simpson Group in Triassic time (238 Ma) and would extend well into the Pennsylvanian System (Figure 6.6). Present thermal maturity of the Ordovician section would be TTI = 87, which is past peak oil generation (TTI = 75). Maturity at the base of the Pennsylvanian System is TTI = 66, which is near peak oil generation.

COMPARISON OF TTI MODELING TO ORGANIC MATURATION DATA

The inferred thermal history of Viola Formation in the study area can be compared to maturation indicated by organic material within the rocks. Most Lower Paleozoic shelf limestones in Kansas, including the Viola Formation, are low in organic content, hence relatively organic-rich units that stratigraphically bracket the Viola (e.g., dark shales from the Middle Ordovician Simpson Group, the Upper Ordovician Maquoketa Shale, and the Devonian-Mississippian Chattanooga Shale) have to suffice to infer the maturation of the Viola. The most common data available for these

purposes are vitrinite reflectance and Rock-Eval pyrolysis. Unfortunately, few non-proprietary maturation data are available for wells drilled in the study area, and it is therefore difficult to assess the spatial and stratigraphic variability of thermal maturation and its history in great detail. Most data are available for the area modeled in McPherson County. Notwithstanding the difficulties and uncertainties with these types of analyses, enough organic maturation data exist to at least assess the validity of the maturation models and the TTIs calculated from them.

Small commercial accumulations of a geochemically distinct group of oils that are generated by Ordovician strata are present in the southern end of the Salina basin and along the axis of the Forest City basin (see Martin and others, 1963; Hatch and others, 1987; Longman and Palmer, 1987; Newell and others, 1987b; Newell, 1990). The main characteristics of these oils are a strong odd-over-even preference in *n*-alkanes in the C_{11}-C_{20} range, low amounts of C_{19+} *n*-alkanes, and only minor amounts of acyclic isoprenoids. World-wide sampling of oils and source rocks indicates that this group of oils are only associated with Ordovician-age source rocks and have probably been derived in part from the fossil alga *Gloeocapsomorpha priscae* (Fowler and Douglas, 1984; Reed and others, 1986; Hoffman and others, 1987; Jacobson and others, 1988). The fields containing this Ordovician oil in the Forest City basin and in the southern end of the Salina basin are located in production trends that are structurally separated from contiguous production trends extending northward out of the Anadarko and Arkoma basins (Newell and others, 1987a, b; Jenden and others, 1988), hence they are not likely the result of long-distance buoyant migration out of the Anadarko basin (cf., Gussow, 1954; Price, 1980). The presence of oils generated from Ordovician strata in the northern part of the study area indicate thermal maturity of the Ordovician section in this area is at least TTI = 15 (onset of significant oil generation) or greater.

Rock-Eval Data

Direct assessment of the thermal maturity of Lower Paleozoic rocks such as the Simpson Group, Viola Formation, and Maquoketa Shale by vitrinite reflectance is not feasible because vitrinite, a product of land plants, is not present in pre-Silurian rocks (Hunt, 1979, p. 332). Nevertheless, maturation of Lower Paleozoic strata can be semi-quantitatively evaluated using Rock-Eval pyrolysis data. Four basic parameters (S_1, S_2, S_3, and T_{max}) are obtained by Rock-Eval pyrolysis (Espitalié and others, 1977). S_1 (expressed as mg HC/g rock, or the equivalent measure of kg HC/metric ton rock) measures free or adsorbed hydrocarbons present in the rock. S_2 (expressed as mg HC/g rock, or kg HC/metric ton rock) measures pyrolitic hydrocarbons derived from thermal breakdown of kerogens. The temperature (°C) at which maximum pyrolitic hydrocarbon yield occurs is T_{max}. S_3 (expressed as mg CO_2/g rock, or kg CO_2/metric ton rock) measures pyrolitic carbon dioxide yielded by the sample.

Several ratios of these Rock-Eval parameters can be used as approximate measures to ascertain both quality of organic matter and its maturation (see Espitalié and others, 1977). Genetic potential ($S_1 + S_2$) indicates overall ability of the rock to generate hydrocarbons. The ratio of S_1 to the genetic potential ($S_1/[S_1 + S_2]$) defines the transformation ratio (TR), also called productivity index (Peters, 1986). The TR increases with thermal maturation until expulsion of hydrocarbons take place. T_{max} also increases with thermal maturation. According to Tissot and Welte (1984, p. 522) and Peters (1986), the oil window corresponds to a TR range between 0.1 to 0.4. The oil window according to T_{max} lies between 435 and 470 °C, with the caveat that T_{max} values signaling the beginning of significant oil generation may vary according to the type of organic matter (Peters, 1986).

T_{max} and TR data for north-central Kansas are shown in Figures 6.7 and 6.8, respectively, and summarized in Appendix II. These new data apply to the locality

Figure 6.7 Thermal maturation of Ordovician strata in north-central Kansas as expressed by Rock-Eval T_{max} data. Most of these samples (listed in Appendix II) were collected by the writer and were analyzed either by Sohio, Brown and Root, DGSI, and the USGS. The temperature ranges of the T_{max} data (measured in °C) indicate Ordovician strata in Kansas are immature to marginally mature with respect to significant petroleum generation. These levels of thermal maturity corroborate the maturity indicated with TTI modeling.

T_{max} DATA for Ordovician strata in north-central Kansas

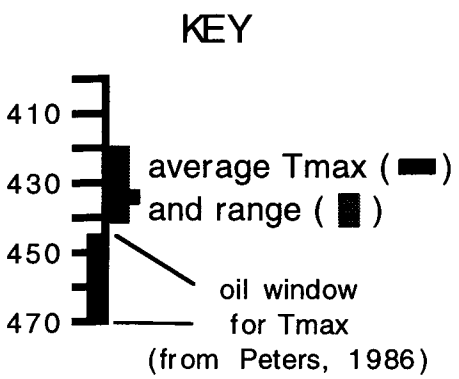

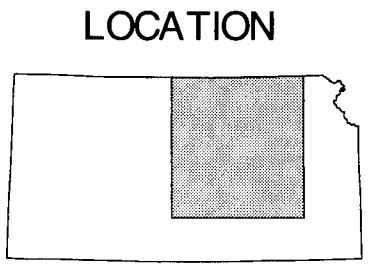

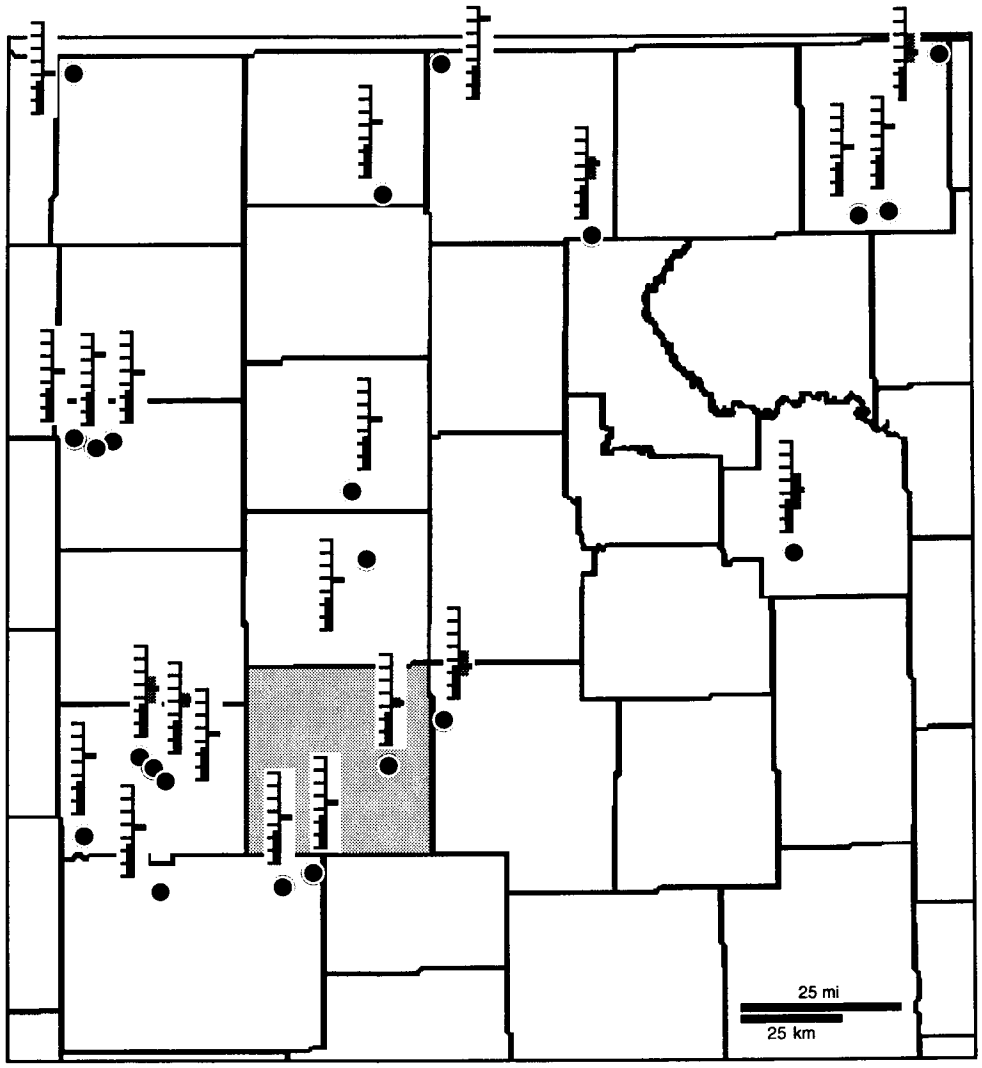

Figure 6.8 Thermal maturation of Ordovician strata in north-central Kansas as expressed by source-rock transformation ratios (TR). Most of these samples (listed in Appendix II) were collected by the writer and were analyzed either by Sohio, Brown and Root, DGSI, and the USGS. Although sightly higher thermal maturities are indicated by the TR data than with the T_{max} data, most Ordovician strata in Kansas are immature to marginally mature with respect to significant petroleum generation. These levels of thermal maturity corroborate the maturity indicated with TTI modeling.

TRANSFORMATION-RATIO DATA for Ordovician strata in north-central Kansas

KEY

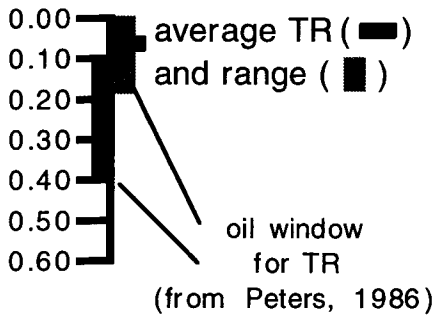

LOCATION

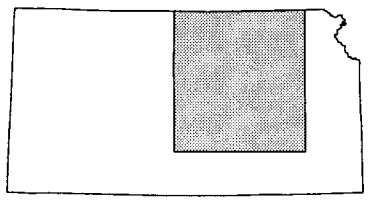

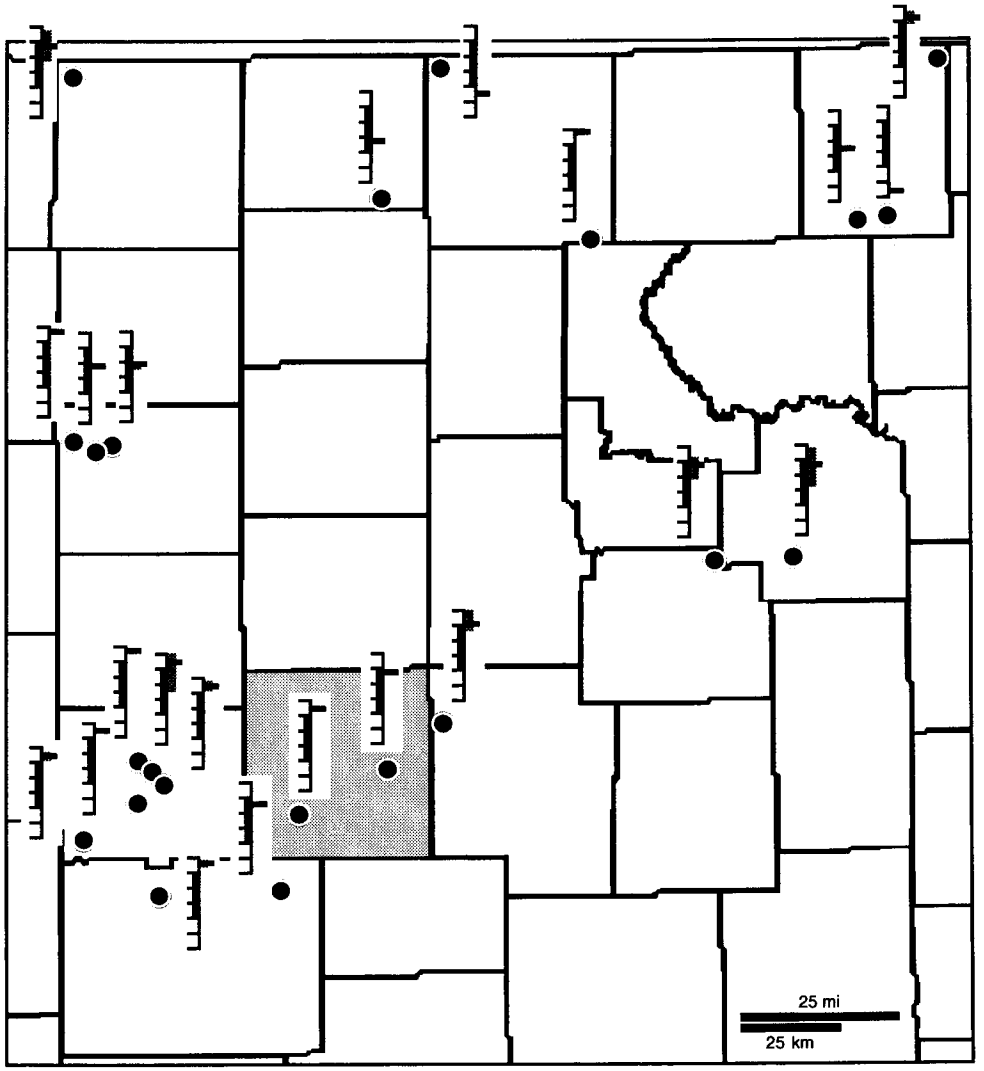

modeled in McPherson County. No data are available close to the locality modeled in Harper County. Notwithstanding considerable scatter that is characteristic of Rock-Eval data, these results indicate that Ordovician strata in Kansas are immature or are in early stages of oil generation. Comparison of the T_{max} and TR data sets in Figures 6.7 and 6.8 indicate slightly higher maturities are registered by the TR data, but nevertheless, maturities approximately at the onset of oil generation are likely. These observations can be accommodated by the results obtained by thermal modeling, but only if relatively cool geothermal gradients of 25 to 30 °C/km are used (see Figure 6.3).

A general increase in the maturation parameters, T_{max} and TR, with depth is evident for several wells in the vicinity of McPherson County (Figure 6.9; Appendix III. The TR data are characterized by more scatter than the T_{max} data, but some of the anomalously high TR values could be due the presence of migrated hydrocarbons, which would inordinately augment the S_1 peak during pyrolysis (see Clementz, 1979; Peters, 1986). No wells have maturation significantly into the oil-generation window, but variations in levels of maturation are evident between wells, and with depth for each well. Displaying maturation data according to depth relative to the basal Pennsylvanian unconformity (Figure 6.10) removes effects of post-Pennsylvanian structural complications on the vertical profiles (see Wojcik and others, 1994). Differences in maturation at similar levels relative to the basal Pennsylvanian unconformity are still evident though. Inasmuch as there are not significant differences in age of the strata relative to the basal Pennsylvanian unconformity for the wells considered in McPherson County, the differences in maturity shown by different wells at a given level in relation to the basal Pennsylvanian unconformity are most likely due to a variation in thermal history experienced at each locality. For example, the T_{max} values at the Diamond-Shamrock #1-9 Skully well indicate consistently greater maturation than those recorded at the nearby Walker #1 Unruh

Figure 6.9 Rock-Eval maturation parameters T_{max} and transformation ratio (TR) for wells in and near McPherson County, plotted by subsea depth. Marginal maturities are indicated by both parameters. Anomalously high TR values are probably due to excess hydrocarbons that may have migrated into the source rock. Lines connect analyses from selected wells.

ROCK-EVAL MATURATION PROFILES (BY SUBSEA DATUM)
McPherson County Vicinity

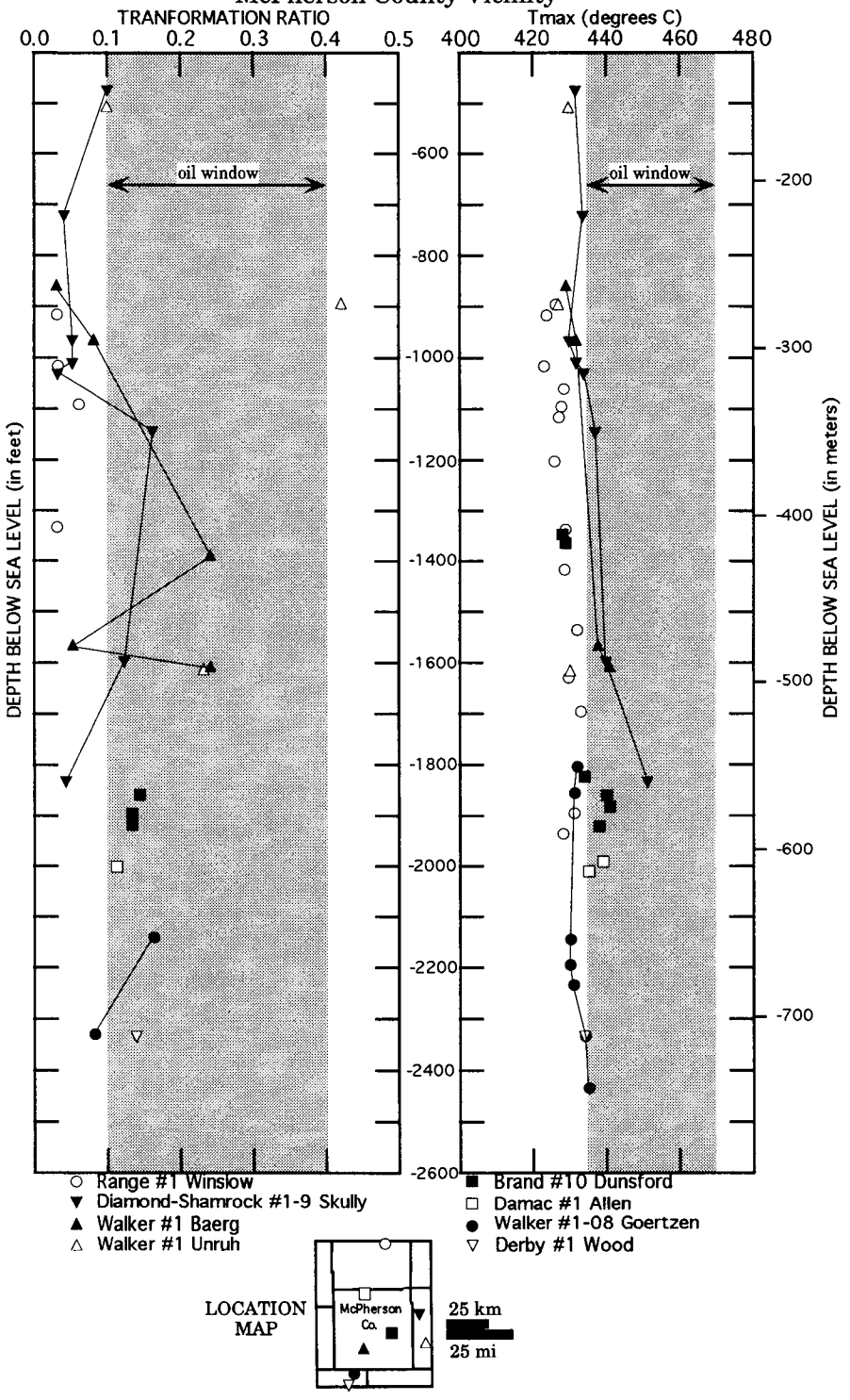

Figure 6.10 Rock-Eval maturation parameters T_{max} and transformation ratio (TR) for wells in and near McPherson County, plotted by depth in relation to the basal Pennsylvanian unconformity. Comparison of this figure with the data arrayed according to subsea depth (Figure 6.9) indicates that maturation at a given stratigraphic level is not solely a function of depth, therefore locally higher geothermal gradients may account for some wells (e.g., Diamond-Shamrock #1-9 Skully and Walker #1 Baerg) having more mature rocks at relatively shallow depths. Lines connect analyses from selected wells.

ROCK-EVAL MATURATION PROFILES
(BY DATUM at BASAL PENNSYLVANIAN UNCONFORMITY)
McPherson County Vicinity

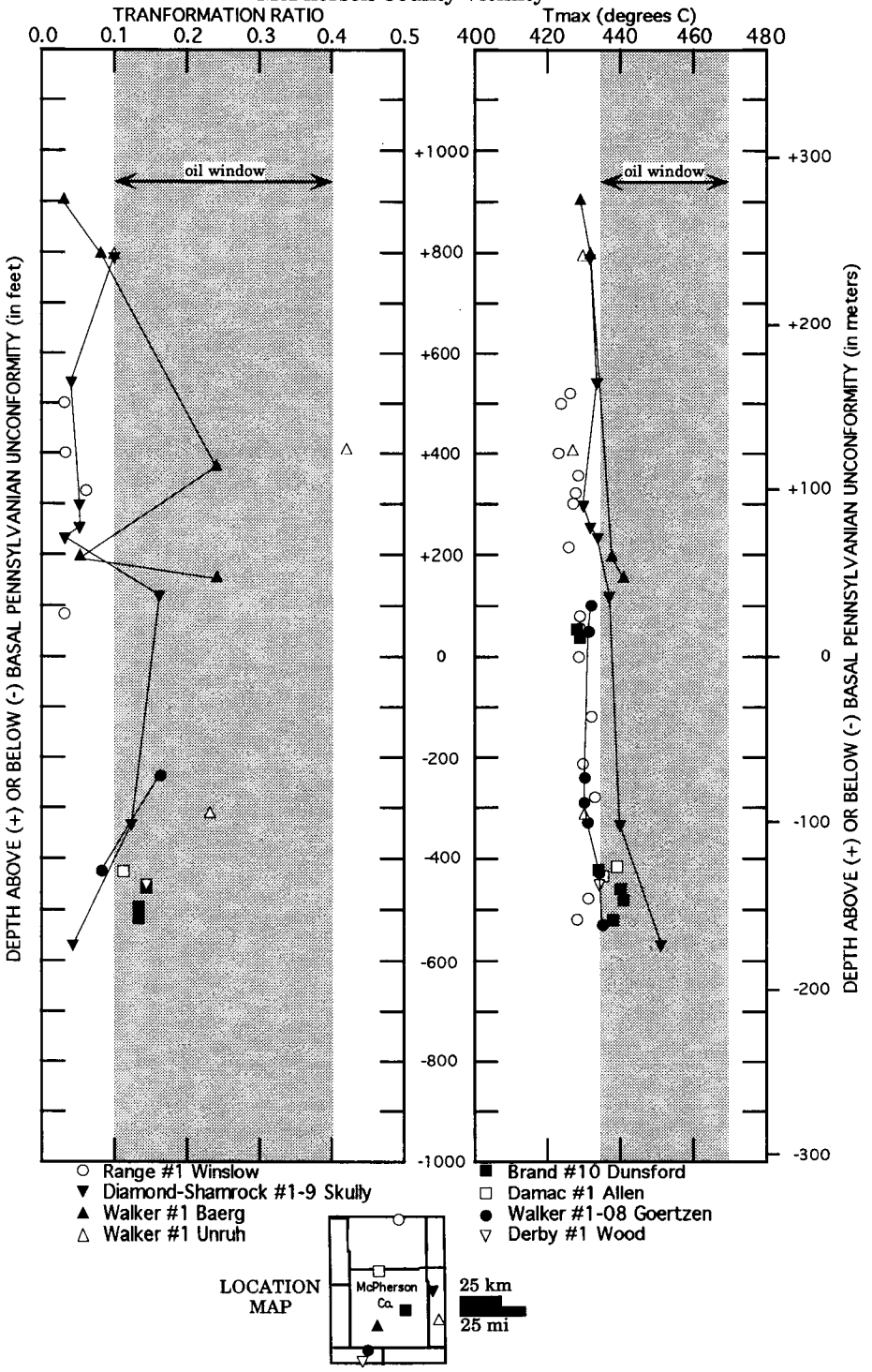

well even though the effects of depth and stratigraphy are largely removed by plotting their maturation profiles in relation to the basal Pennsylvanian unconformity (Figure 6.10). Inasmuch as thermal conductivities at both wells are similar due to their nearly identical stratigraphy, a locally higher heat flow or localized advective heat transport would be the most likely explanation for the greater maturation at the Diamond-Shamrock #1-9 Skully well.

Inferences on the method of heat transfer may also be made with the data available in Figures 6.9 and 6.10. If vertical conduction of heat through the stratigraphic column were the sole means by which maturation occurred in these rocks, consistent increases of maturation with depth would be expected. However, maturity in each well does not necessarily increase with greater depth. Anomalous increases in maturation with depth are present, such as with the relatively high T_{max} values recorded below -300 ft (-90 m) at the Diamond-Shamrock #1-9 Skully (Figure 6.10). Local decreases in maturation with depth also occur in nearly all of the wells. Some of these anomalies could be due to expected scatter in the data by sampling problems or laboratory technique, but heating caused by movement of hot fluids through the stratigraphic column may also cause these anomalies. Heating of rocks in and near such hot fluids, and a lack of heating of rocks thermally protected by impermeable strata, would cause both vertical and geographic variations in maturation. In particular, advection (the general lateral flow of fluids, commonly along stratigraphically controlled carrier units, but also vertically through fractures or stratigraphic discontinuities) could account for the anomalous jumps in maturation with depth and irregularities in the maturation profiles of individual wells, as well as different wells yielding different baseline value of maturation.

Vitrinite Reflectance Data

Vitrinite is an organic maceral derived from the tissue of terrestrial plants (Tissot and Welte, 1984, p. 139). With increasing thermal maturity vitrinite undergoes progressive irreversible graphitization and consequently its reflectivity increases. Vitrinite reflectance (R_o) is the most commonly used quantitative thermal maturation indicator in the oil industry. Several scales correlating R_o to stages of oil generation exist (cf., Héroux and others, 1979; Waples, 1980; Dow and O'Connor, 1982; van Gijzel, 1982; Tissot and Welte, 1984, p. 71). In general, R_o from 0.5 to 1.4% corresponds to the range of maturation in which oil is generated, with the peak of oil generation occurring about 1.0% R_o. Assessment of maturation of the Viola in terms of R_o cannot be directly done because vitrinite, a product of land plants, is not present in pre-Silurian rocks (Hunt, 1979, p. 332). Nevertheless, the R_o scale is a standard to which various types of maturation data can be compared.

Published (Jenden and others, 1988) and new R_o maturation data (see Appendix III) for strata in the vicinity of McPherson County shows that Pennsylvanian shales register marginal maturity, with nearby R_o values ranging between 0.54 to 0.69% (Figure 6.11). Maturation in the vicinity of Harper County is slightly greater, with R_o values ranging between 0.64 to 0.75% in the Pennsylvanian section (Figure 6.11).

The vitrinite-depth profiles (Figure 6.12), and the T_{max}-depth and TR-depth profiles (Figures 6.9, 6.10) contain scatter. However, uneven heating of the stratigraphic column cannot be ruled out either. As with the depth profiles of Rock-Eval data in Figure 6.10, anomalous zones of apparently higher maturation sandwiched between strata with lower maturation could be due to lateral movement of heated fluids along thin stratigraphic intervals.

According to a TTI-to-R_o correlation in Waples (1980), an R_o ranging between

Figure 6.11 Thermal maturation in Kansas as expressed by available published (Jenden and others, 1988; Barker and others, 1992) and unpublished vitrinite reflectance and conodont-alteration index (CAI) data available at the Kansas Geological Survey (see Appendix III). Conodont alteration index (CAI) is a coloration scale applied to the progressive darkening of conodonts with thermal maturation, and can be related to vitrinite reflectance by the conversion in the legend. VRE (vitrinite-reflectance equivalent) data are from Barker and others (1992), and is based on correlation of T_{max} data with vitrinite reflectance data from Pennsylvanian rocks in the Cherokee basin. McPherson and Harper counties are shaded.

THERMAL MATURATION IN KANSAS

vitrinite reflectance (R_o) and vitrinite-reflectance equivalent data

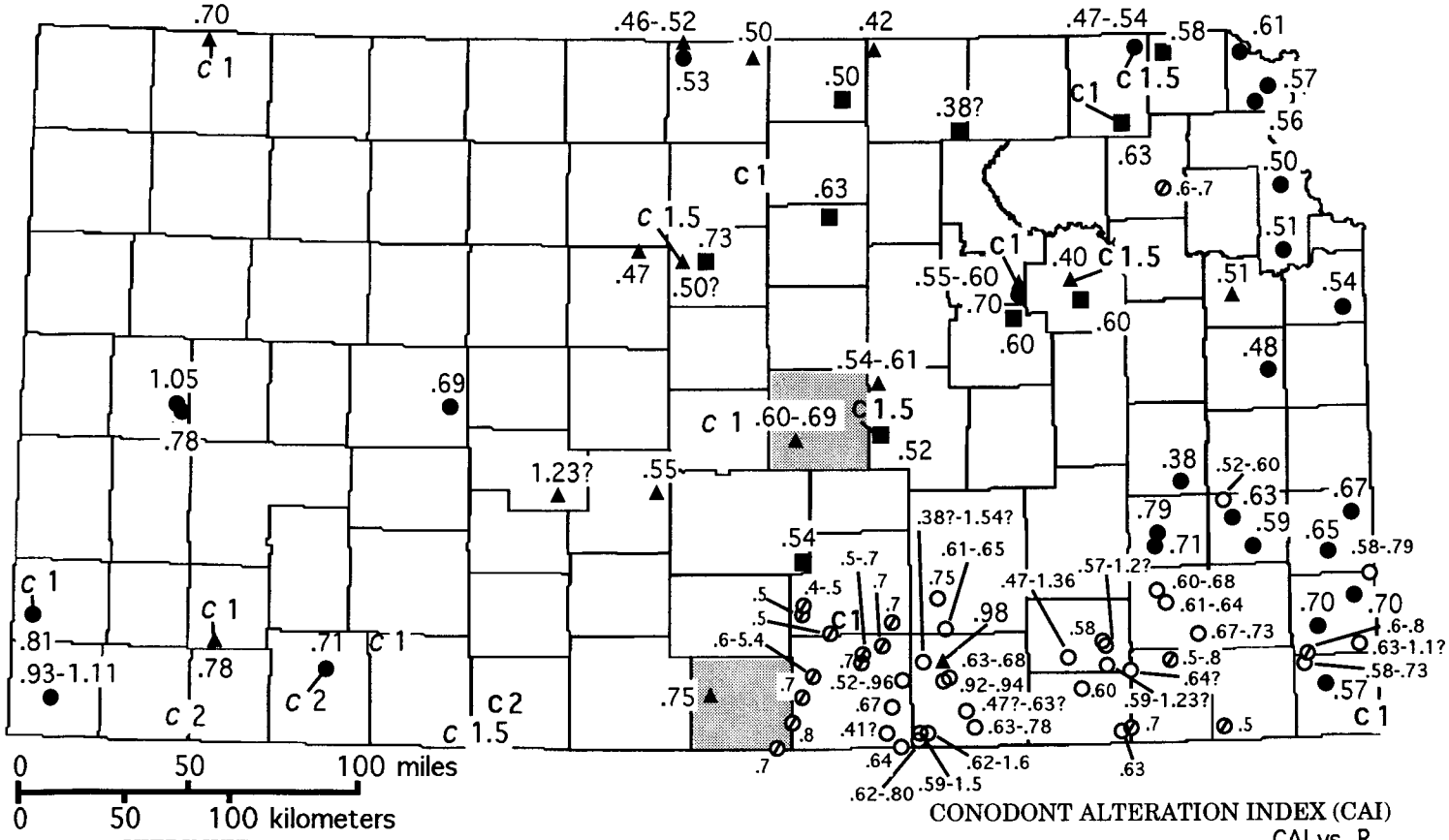

VITRINITE MATURATION MEASUREMENTS

- ▲ Pennsylvanian (post Desmoinesian)
- ● Pennsylvanian (Desmoinesian and older)
- ■ Devonian-Mississippian Chattanooga Sh.

Undifferentiated Pennsylvanian (from Barker and others, 1992)

- O R_o measurement
- Ø R_o equivalent data

CONODONT ALTERATION INDEX (CAI)

- C Pennsylvanian
- C Pre-Pennsylvanian

CAI vs. R_o (from Harris, 1979)

1	<0.8%
1.5	0.7 - 0.85%
2	0.85 - 1.3%

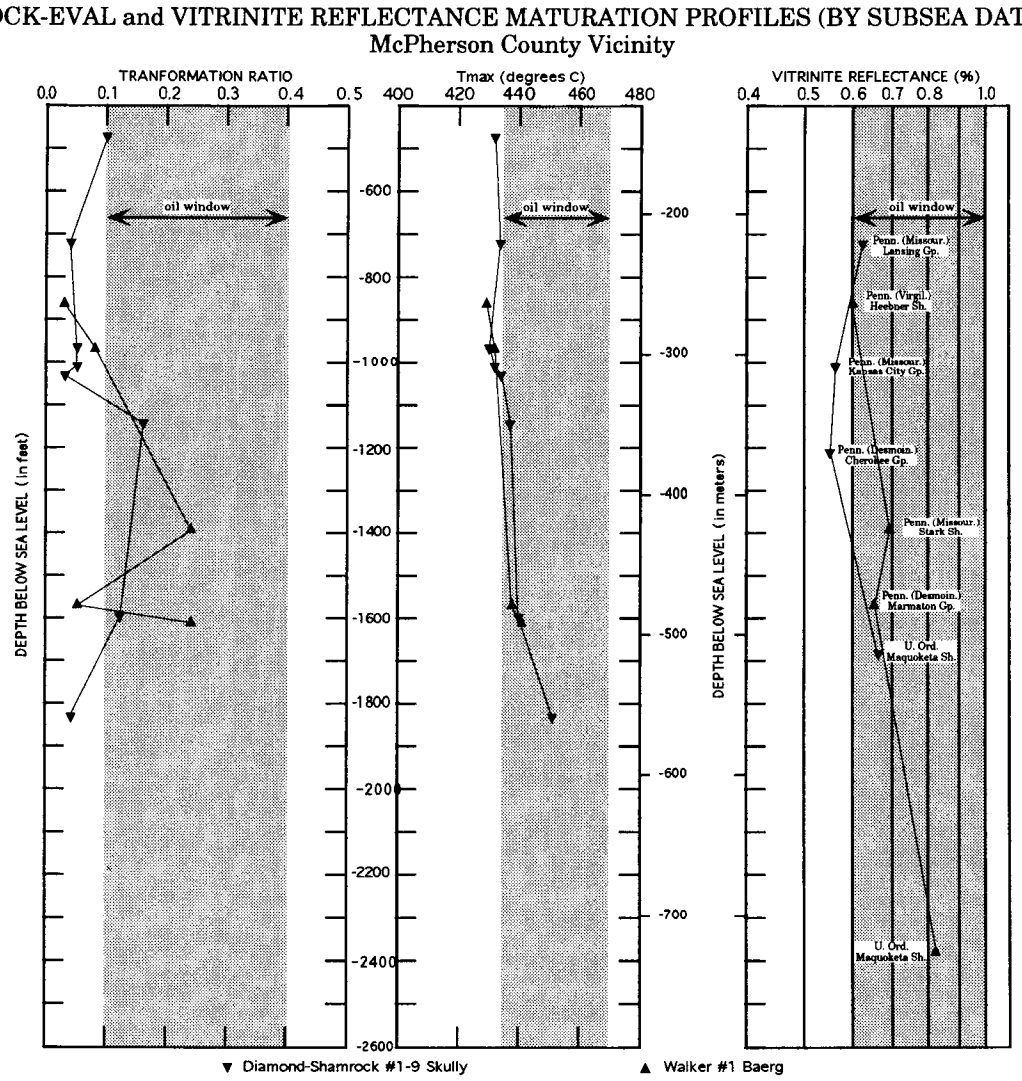

Figure 6.12 Rock-Eval and vitrinite maturation profiles for two wells near McPherson County, Kansas (refer to Figures 6.9, 6.10, and Appendix III for locations). Relative immaturity with respect to oil generation is indicated for both wells, but the vitrinite data, despite scatter, generally agrees with Rock-Eval results. Reflectance values for Ordovician strata is on vitrinite-like organic material.

0.6 to 0.7% corresponds to a TTI range from 10 to 20. The maturation based on R_o values is compatible with the range of calculated TTIs, given likely geothermal gradients and Cretaceous cover at the modeling locality in McPherson County (see Figures 6.3, 6.4). If the high end of the R_o range is accepted for the base of the Pennsylvanian System, (i.e., 0.7% R_o, which corresponds to TTI = 20), and the thickness of Cretaceous rocks is kept at 1500 ft (460 m; see Figure 6.2), a geothermal gradient of 37 °C/km would be necessary to account for this apparent maturation (see Figure 6.4). A 37 °C/km geothermal gradient would subject the Viola to a maximum temperature of 80 °C at the end of Permian time. A geothermal gradient of 37 °C/km is higher than the range likely for this area (i.e., 25-35 °C/km, based on local measurements; see Figures 6.1, 6.4). Greater Cretaceous burial can be invoked to compensate for the geothermal gradient, but the maximum likely Cretaceous thickness of 3000 ft (915 m) would reduce the necessary geothermal gradient to only 32 °C/km -- within the acceptable range of geothermal gradients, but still on the high end (Figure 6.4). A geothermal gradient of 32 °C/km in conjunction with 3000 ft (915 m) Cretaceous burial would subject the Viola to a maximum burial temperature of 90 °C at the end of Cretaceous time. Inasmuch as both geothermal gradient and Cretaceous burial have to be maximized in a model that assumes simple burial heating and constant heat flow, there is a nagging possibility that this type of model may be inadequate to explain the maturation observed.

The greatest vitrinite-reflectance value (0.75% R_o) for Pennsylvanian strata nearest the locality modeled in Harper County (Figure 6.11) corresponds to TTI = 25 (see Waples, 1980). A calculated TTI of 18 (approximately 0.68% R_o according to Waples, 1980) for the base of the Pennsylvanian section using the 25 °C/km geothermal gradient (see Figure 6.5) indicates this geothermal gradient may be too low. A geothermal gradient of approximately 30 °C/km at this locality would reconcile

calculated and observed maturities. Conversely, a 40 °C/km geothermal gradient (see Figure 6.6) is too high, in that maturation at the base of the Pennsylvanian section (TTI = 66) with this higher geothermal gradient would be equivalent to 0.97% R_o. These models predict that the maximum temperature experienced by the Viola in Harper County most likely was between 70 ° and 90 °C.

Characterization of maturation for this entire area by a single R_o value may be misleading in that detailed work by Barker and others (1992) and Walton and others (1995) in the Cherokee basin of southeastern Kansas has revealed marked spatial variations in maturation that indicate local "warm spots". These warm spots are suggested to have formed by upward flow of warm waters through fractures into the Pennsylvanian section (Barker and others, 1992) and have caused maturities in these rocks in excess of 1.0% R_o in some wells. Lateral, updip (advective) flow of these warm waters out of the Anadarko and Arkoma basins is surmised to have occurred (Barker and others, 1992; Ge and Garven, 1992; Wojcik and others, 1992, 1994; Spötl and others, 1994; Walton and others, 1995) in late Paleozoic time.

The process of advection and its effect on maturation cannot be adequately modeled by TTI calculations. Nevertheless, the TTI models are useful in that by their very inadequacy to explain observed characteristics of present-day maturation, they reveal that heat-transfer processes other than conduction may have once been active in southern Kansas.

COMPARISON OF TTI MODELING TO FLUID-INCLUSION DATA

Fluid-inclusion homogenization temperatures (T_h) can also test the conductive heating scenario depicted in the TTI calculations. Fluid-inclusion T_hs presented here

are not corrected for pressure and therefore represent minimum temperatures of entrapment (see Roedder, 1984, p. 254-255; Goldstein and Reynolds, 1994, p. 27, 128). These T_hs can be compared to the maximum burial temperature modeled for the Viola. To this goal, T_hs from saddle dolomites from three cores penetrating the Viola (e.g., Damac #1 Sandra Allen in northern McPherson County, Derby #1 Wood in northern Reno County, and Midcontinent Marine #1 South Hilger in southern Reno County were measured (Figure 6.13). Complete results of these analyses (Table 8.7) and additional implications are deferred to the discussion titled "Vugs, Saddle Dolomite, and Other Late Vug-Filling Phases" in Chapter 8.

Saddle dolomite contains abundant fluid inclusions that are varyingly concentrated in density in zones parallel to crystal faces. These zones therefore define growth bands that contain primary fluid inclusions (see Goldstein and Reynolds, 1994, p. 14-15). All inclusions observed in the saddle dolomites are two-phase, with very consistent liquid-to-vapor ratios, despite differences in sizes of the inclusions. T_h values overlap for all three samples (Figure 6.13); the range spans about 40 °C with maximum values of 135 to 140 °C for primary inclusions. This broad span in T_h for these samples indicates that the inclusions may not have been entrapped during a single thermal event. Goldstein and Reynolds (1994, p. 127) stated that approximately 90% of the fluid inclusions in a given assemblage derived from a single thermal event should fall within a temperature interval of 10 to 15 °C. Fluid-inclusion assemblages, defined in this case as a group of closely associated inclusions along a growth band, have T_h ranges that generally are smaller than the range defined by all the fluid-inclusion assemblages recorded at a given locality (Figure 6.13, Table 8.7). Most fluid-inclusion assemblages have ranges in T_h that are within the temperature interval of 10 to 15 °C, as determined by Goldstein and Reynolds (1994). A minimum estimate of the temperature experienced can be inferred as being the highest-temperature T_h from

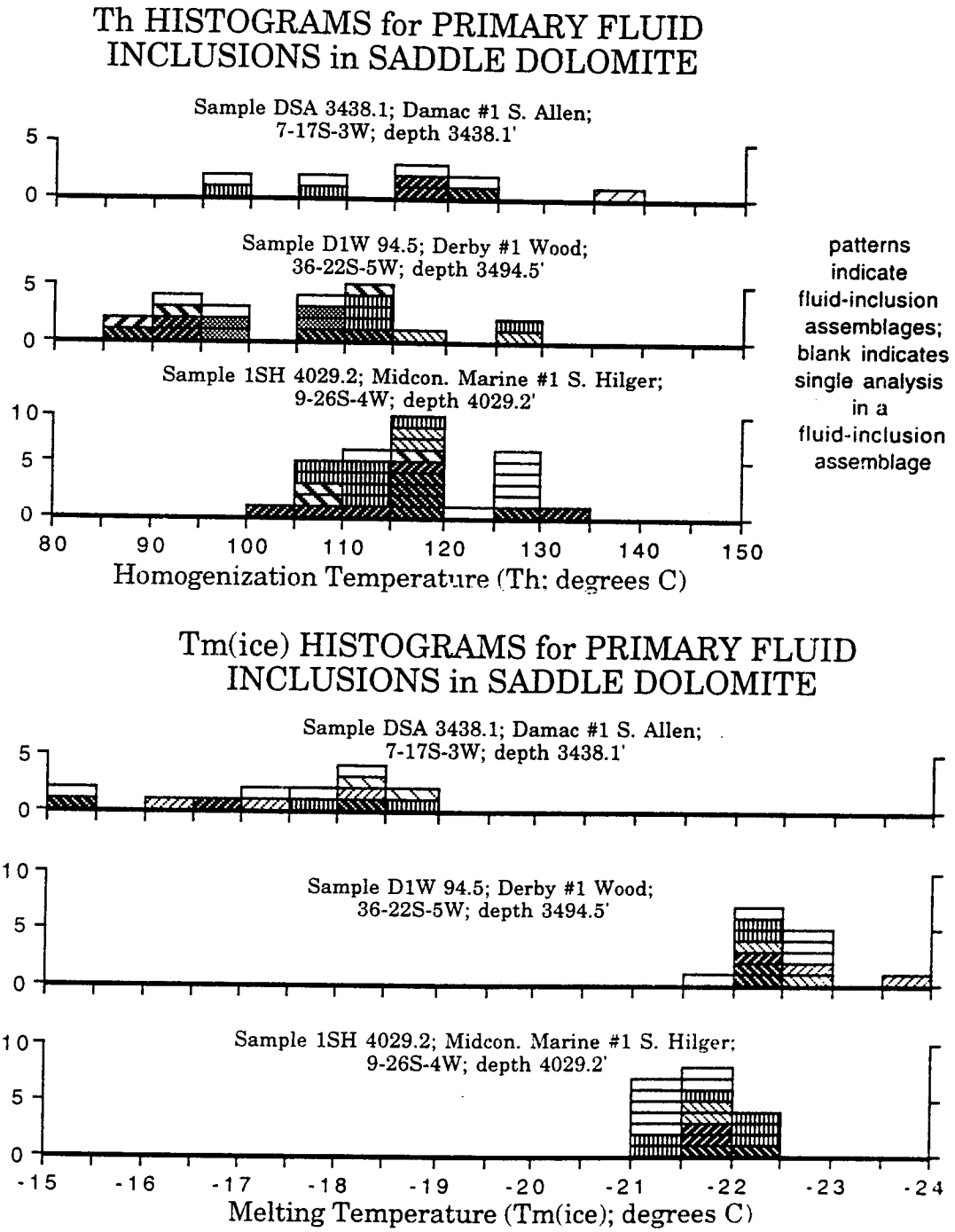

Figure 6.13 Histograms of T_h and $Tm_{(ice)}$ measurements, together with fluid-inclusion assemblages for the samples of saddle dolomite for three localities in the study area. See Table 8.7 for a listing of this data, and Figures 8.61, 8.62, and 8.63 for histograms and crossplots for each sample locality. A measurement from an "isolated" inclusion represents a single measurement obtained from a fluid-inclusion assemblage.

a consistent fluid-inclusion assemblage (Goldstein and Reynolds, 1994, p. 139). In the case of the Viola, this temperature is estimated to be 125 to 130 °C for the Midcontinent Marine #1 South Hilger well and the Derby #1 Wood well, and 115 to 120 °C for the Damac #1 Allen well. Although higher T_hs are recorded for other fluid-inclusion assemblages in the histograms in Figure 6.13, these T_hs are either singular determinations from an assemblage, or they are from assemblages that have a broad spread of T_hs, thus some uncertainty is attached to their use as a minimum estimate of temperature experienced by these rocks.

Even though T_h values are not corrected for pressure and therefore represent minimum temperatures of entrapment (see Roedder, 1984, p. 254-255; Goldstein and Reynolds, 1994, p. 27, 128), the T_h values are approximately 15 to 50 °C greater than maximum temperatures inferred for the Viola based on its burial history and current geothermal gradients (i.e., 70 to 90 °C, see prior discussions). The maximum recorded T_h of 139 °C from a primary fluid inclusion at the Damac #1 Sandra Allen well (Figure 6.13, Table 8.7) represents a temperature 49 to 69 °C in excess of the maximum inferred burial temperature at that locality. An analysis in the context of the TTI model for McPherson County (Figure 6.2) aids in ascertaining the cause of this thermal discrepancy. Even if the moderately "cool" temperature of 112 °C (the average T_h from the Damac #1 Sandra Allen core in northern McPherson County) is conservatively taken as the maximum temperature experienced at that locality when the Viola was at its inferred maximum depth of 4500 ft (1.37 km) during Late Pennsylvanian -- Early Permian time (the time most likely for mineralization), the resulting geothermal gradient would have to be 68 °C/km! This geothermal gradient is approximately twice the present-day gradient and is well in excess of any gradient that can be modeled from simple burial heating to accommodate the maximum organic maturation observed at that locality (Figure 6.3). The temperatures recorded by the

saddle dolomites therefore have to represent one or more ephemeral thermal events -- either a thermal pulse(s) heating the entire stratigraphic column, or advective fluid flow(s) out of the Ouachita foreland basin, as suggested by Leach and Rowan (1986). Organic maturation indicators that erratically vary with depth at a given locality suggest that advective fluid flow is the more likely alternative.

Highest modal T_hs (125-130 °C) occur at the Midcontinent Marine #1 South Hilger core, the most southerly and deeply buried sample. The shallowest and most northerly sample, from the Damac #1 Sandra Allen core, however, does not conversely record the lowest modal T_h value of all the samples analyzed (Figure 6.13). Inasmuch as there is no correspondence between burial depth and modal T_h, a simple model that invokes a linear increase in temperature with depth is probably not accurate to depict the burial and thermal history of the Viola.

SUMMARY

TTI modeling and organic maturation measurements generally indicate the Viola would be in initial stages of oil generation if it were a petroleum source rock. Theoretical maturation from TTI modeling can match maturation indicated by analyses of organic material for Paleozoic rocks in the study area, but geothermal gradients and Cretaceous thicknesses have to be maximized. If geologically unreasonable assumptions such as extreme geothermal gradients or excessive subsidence or uplift have to be invoked to achieve an agreement with laboratory results, chances are greater that the assumptions of the models are incorrect and have to be reassessed. TTI models implicitly assume a vertical transfer of heat by conduction in the rock column and cannot account for uneven heating of the

stratigraphic column by heated brines moving by advection.

Organic-maturation parameters and maturation profiles in individual wells reveal well-to-well variations in maturation, erratic increases of maturation parameters with depth in individual wells, and even decreases of maturation with depth. These anomalies indicate nonuniform heating of the rock column and thermal regimes that vary over short distances. In addition, fluid-inclusion homogenization temperatures in saddle dolomites in the Viola are well in excess of that predicted by simple burial heating with a constant geothermal gradient. These homogenization temperatures also do not correspond to paleoburial depths. Advective heating by vertical and lateral movement of formation waters may best account for these thermal anomalies and overall thermal maturity of the Viola.

Chapter 7

LITHOFACIES OF VIOLA LIMESTONE

INTRODUCTION

Lithologies in the Viola indicate depositional settings and stratigraphic relationships. Amalgamated depositional settings produce a general model for the depositional history of the Viola Formation in a regional and global context. Diagenesis (see Chapter 8) locally affects the general physical characteristics of the lithology discussed, affects the preservation of depositional textures, and can even aid in the depositional interpretation. It is perhaps paradoxical that the definition of the Viola subunits is based on diagenetic features (chert, limestone, and dolomite), rather than strictly depositional features. However, many diagenetic features in the Viola are strongly fabric-selective, in that the lower and upper cherty dolomitic limestones, as initially identified in Barber and Pratt Counties by St. Clair (1982), are principally heavily dolomitized and silicified lime mudstones and subsidiary wackestones. Similarly, the basal and upper limestone subunits are dominantly skeletal packstones and subordinate grainstones that are heavily cemented with calcite. The identification of lithologic units partly by diagenetic features (rather than strictly depositional features) is a common and even permissible practice, but can lead to confusion as the lithologic correlations are extended beyond the area in which these subunits were initially defined. Furthermore, it introduces the nagging possibility that the boundaries of the subunit defined by such diagenetic features can be diachronous, or simply not follow the stratigraphic boundaries based strictly on depositional textures. Although the cherty dolomitic subunits of the Viola display varying degrees of

dolomitization and silicification over the study area (see Chapter 8), their identification by well logs and cuttings descriptions is still relatively easy, principally because the stratigraphically adjacent lime packstone subunits remain relatively nonporous, calcitic, and "coarsely crystalline" (primarily due to the presence of crinoidal debris). In areas where the "basal limestone" subunit is heavily dolomitized, the Viola is truncated by overlying unconformities to such an extent that none of the overlying cherty dolomitic limestones are present, and no stratigraphic confusion thus occurs. Although it may be politic to rename the Viola subunits according to their depositional characteristics (i.e., "basal limestone" becomes "basal packstone", "lower cherty dolomitic limestone" becomes "lower mudstone/wackestone", etc.), precedence has been set in several publications (see Bornemann and others, 1982; Bornemann and Doveton, 1983; St. Clair, 1985), and the addition of a new informal stratigraphic nomenclature for the Viola at this point would be needlessly confusing.

METHODS AND PROCEDURES

Forty cores from south-central Kansas were slabbed and examined with approximately 350 thin sections for this study (Table 7.1, Figure 7.1, Appendix IV). For convenience, the well numbers in Table 7.1 and Figure 7.1 will be displayed in parentheses and italics after each well name in the text and figure captions. Nine of these cores and 133 thin sections were used by St. Clair (1982); these were reexamined and the results put in a format with that used with other cores in this study. All of the cores were obtained from the Earth Materials Repository at the Kansas Geological Survey of The University of Kansas in Lawrence, Kansas (Table 7.1). No single core completely sampled all four subunits of the Viola, and only where the Viola was very

Table 7.1 Cores used in this study. The numbers at the left correspond to the numbers adjacent to the symbols on the map in Figure 7.1. The Viola subunit cored is expressed by the numbers at the right of the table; a subunit not cored is indicated by a dash [-] in the appropriate numerical position: 1 - basal limestone, 2 - lower cherty dolomitic limestone, 3 - upper limestone, 4 - upper cherty dolomitic limestone.

#	OPERATOR & WELL	COUNTY	LOCATION	DEPTH (ft)	SUBUNIT
1	Carter #2 Kansas Exploration	Mitchell	SE SW 20-09S-07W	3495-3505 3547-3561	-23-
2	Damac #1 Sandra Allen	McPherson	SW 7-17S-03W	3437-3444	12--
3	Shell #1 Anderson	McPherson	SE SE NW 30-19S-01W	3409-3414	12--
4	Shell #4 Hill	McPherson	NE 10-19S-02W	3402-3408	12--
5	Shell #4 Hull	McPherson	NE SW 11-19S-02W	3364-3366	-2--
6	Shell #6 Decker	McPherson	SW 11-19S-02W	3367-3369	-2--
7	Shell #6 Fleming	McPherson	E2 NW 11-19S-02W	3388-3397	-2--
8	Stanolind #3 Lovett	McPherson	SE SW 11-19S-02W	3392-3407	-2--
9	Shell #4 Griffin 'B'	McPherson	W2 W2 NE 11-19S-02W	3350-3355	-2--
10	Champlin #8 Speck	Rice	NW NW 18-19S-08W	3410-3411	1---
11	Champlin #1 Kottman	Rice	NE SW 19-19S-08W	3758-3763	1---
12	Northern Natural Gas #1 Caldwell	Rice	NE NE 2-20S-08W	3258-3286	1---
13	Bell-Shell #1-A Timbers	Rice	NW NW NE 8-21S-08W	3395-3469	1---
14	Derby #3 Lehman	Harvey	SW SE NW 13-22S-02W	3407-3416	1---
15	Derby #1 Wood	Reno	NE 36-22S-05W	3889-3904	1---
16	Derby #1 Rainbow	Reno	NW NW SE 33-22S-07W	3836-3838	1---
17	Derby #8 Schrock	Reno	SE SW 27-24S-05W	3828-3845	12--
18	Shell #1 A.C. Brown	Stafford	SW NW SW 2-24S-11W	3704-3715	---4
19	Braden-Zenith #1 Zenith Unit	Stafford	SW SE SW 11-24S-11W	3783-3801 3810-3845	-234
20	Braden-Zenith #3 Zenith Unit	Stafford	SW NW NE 11-24S-11W	3756-3785	-234
21	E.H. Moore #2 R.F. Stewart	Stafford	S2 SE SW 12-24S-11W	3777-3788	---4
22	E.H. Moore #3 R.F. Stewart	Stafford	S2 NE SW 12-24S-11W	3767-3770 3777-3779 3789-3793	---4
23	E.H. Moore #4 R.F. Stewart	Stafford	S2 SW SE 12-24S-11W	3769-3781	---4
24	E.H. Moore #1 N.W. Johnson	Stafford	SW NW NE 13-24S-11W	3789-3798	---4
25	E.H. Moore #3 N.W. Johnson	Stafford	SW NE NE 13-24S-11W	3789-3792	---4
26	E.H. Moore #5 N.W. Johnson	Stafford	N2 NE NE 13-24S-11W	3775-3777	---4
27	E.H. Moore #4 J.K. Johnson	Stafford	NE SW NE 13-24S-11W	3792-3795	---4
28	Midcontinent Marine #1 North Hilger	Reno	SW NW 34-25S-04W	4125-4141	1---

Table 7.1 (continued). Cores used in this study.

#	OPERATOR & WELL	COUNTY	LOCATION	DEPTH (ft)	SUBUNIT
29	Midcontinent Marine #1 South Hilger	Reno	W2 SW SW 9-26S-04W	4029-4046	1---
30	Bunte Bros. & Shell #1 V. Sheppard	Kingman	SE SE SE 10-27S-10W	4308-4314	-2--
31	Palmer & Colorado O&G #2 Grier	Pratt	NE NE NE 25-27S-13W	4296-4300 4306-4310	12--
32	Sinclair-Prairie #1 Blurton	Pratt	NE SE SW 22-28S-12W	4298-4307	--3-
33	Bridgeport #1 Brown "I"	Pratt	NE NW 25-29S-13W	4576-4585 4428-4446	1---
34	Sinclair-Prairie #4 G. Oldfather	Barber	SW NW SE 7-31S-14W	4327-4329 4363-4364 4370-4392	1234
35	Sinclair-Prairie #1 A. Oldfather	Barber	NE NE SW 18-31S-14W	4427-4467 4546-4557	1-34
36	Lario Oil & Gas #2 Randles	Barber	NE NE 34-32S-12W	4734-4744	1---
37	Sinclair #1 M. Binning	Barber	SE SE SW 26-32S-13W	4772-4790 4854-4859	-23-
38	Carter #1 Lytle	Barber	NE NW 6-32S-14W	4740-4747	--3-
39	Sinclair-Prairie #1 DeGeer	Barber	NE NW NE 34-32S-15W	4960-4971 4975-4986 4989-4991 5045-5060 5082-5088	1234
40	Sinclair #1 Alice Gentry	Barber	NE NE 1-33S-15W	5106-5141 5220-5228	1--4

Figure 7.1 Map of the study area showing disposition of cores studied. Numbers correspond to the listing of cores in Table 7.1. Core descriptions are in Appendix IV. For convenience, the well numbers shown in Table 7.1 and this figure will be displayed in parentheses and italics after each well name in the text and figure captions. One core, the Carter #2 Kansas Exploration (*#1*), is approximately 45 miles (70 km) north of the study area. Two cross-sections (A-A' and B-B') are shown in Figures 7.12 and 7.14.

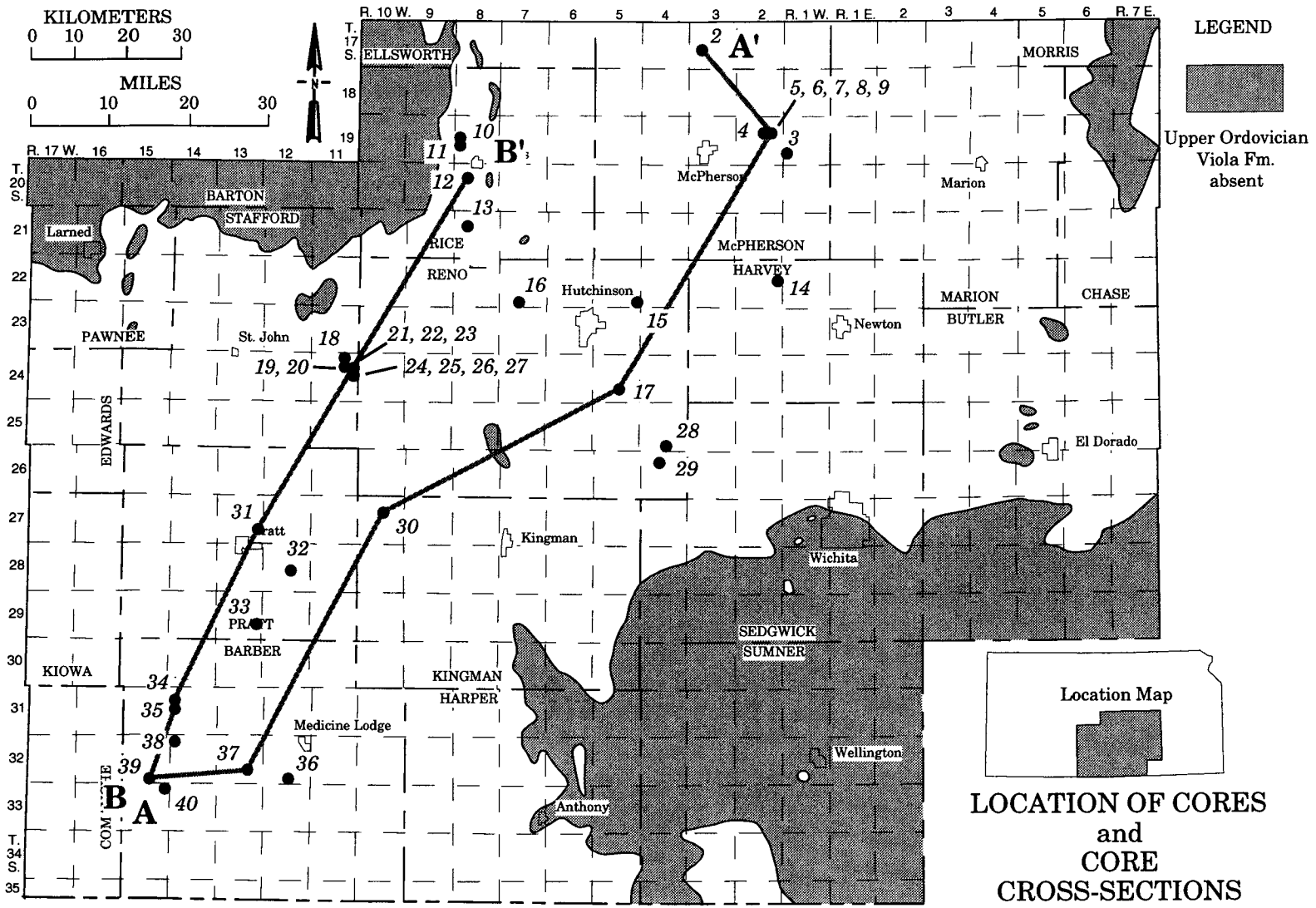
KILOMETERS
0 10 20 30
MILES
0 10 20 30
N
R. 10 W. 9 8 7 6 5 4 3 2 R. 1 W. R. 1 E. 2 3 4 5 6 R. 7 E.
R. 17 W. 16 15 14 13 12 11
T. 17 S.
T. 20 S.
T. 34 S.
ELLSWORTH
MORRIS
BARTON
STAFFORD
Larned
RICE
RENO
McPherson
Marion
McPHERSON
HARVEY
MARION
BUTLER
CHASE
Hutchinson
Newton
El Dorado
PAWNEE
St. John
EDWARDS
Kingman
Wichita
SEDGWICK
SUMNER
PRATT
BARBER
KIOWA
KINGMAN
HARPER
Medicine Lodge
COMANCHE
Wellington
Anthony
A
A'
B
B'
2
5, 6, 7, 8, 9
4
3
10
11
12
13
16
14
15
18
21, 22, 23
19, 20
24, 25, 26, 27
17
28
29
31
30
32
33
34
35
38
37
36
39
40
LEGEND
Upper Ordovician
Viola Fm.
absent
Location Map
LOCATION OF CORES
and
CORE
CROSS-SECTIONS

thin and eroded down to the basal limestone member over the Central Kansas arch was the Viola completely recovered. The subunits were determined by correlation to nearby well logs and by relative position of the core within the Viola Formation.

Core descriptions (Appendix IV) utilized the carbonate-rock classification of Dunham (1960), with the grain-size scale for constituent particles following that of Swanson (1981) (see introduction in Appendix IV). Swanson (1981) uses the Wentworth (1922) size scale except that the subdivision of mud and silt is at 20 μm rather than at 4 μm. Porosity nomenclature of Choquette and Pray (1970) is used. Dolomite textures follow the terminology of Sibley and Gregg (1987). Most mineral and porosity percentages are estimated with the comparator charts in Scholle (1978; p. x). Rock-color descriptions use the color reference chart by the Geological Society of America (GSA Rock-Color Chart Committee, 1984). Alizarin Red-S and potassium ferricyanide stains (Dickson, 1965, 1966) were used for detection of calcium carbonate and iron, respectively in selected core slabs and thin sections. Potassium ferricyanide staining can detect FeO as low as 0.5% in carbonate minerals (Lindholm and Finkelman, 1972). Thin sections were doubly polished, prepared using cold techniques and epoxy sensitive to ultraviolet-light to avoid thermal reequilibration of fluid inclusions during laboratory preparation.

BASAL LIMESTONE

Observations

The basal limestone subunit is dominantly composed of medium- to massive-bedded, gray to light-gray lime packstones with minor interbedded lime wackestones and grainstones. Packstones and grainstones compose approximately 80% of the core

footage observed in the basal limestone, with wackestones and a few lime mudstones constituting the remaining 20%. Most of the packstones are almost mud free with approximately 2-5% lime mud. Grainstones are present in the basal limestone but compose less than 5% of the grain-supported lithologies. Some packstones in this subunit are pale red to pinkish gray (cf., Northern Natural Gas #1 Caldwell; *#12*, 3258-3268 ft depth), but no consistent pattern in coloration was noticed with respect to locality or stratigraphic position.

The major allochemical constituents of the grain-supported lithologies are echinoderm fragments (mostly crinoid ossicles) that comprise 50-95% of all allochems, and brachiopod shell fragments (5-40% of all allochems) (see Figure 7.2). Brachiopod shell fragments are commonly the largest grains in the packstones and grainstones, reaching 1 to 4 cm in length. These fragments generally have thick, sturdy walls. Most larger skeletal grains show rounding at edges that is indicative of abrasion. Fragments of fenestrate and ramose bryozoans and mollusk shells (commonly spar-filled molds) may constitute from 5 to 15% of all allochems. Trilobite, ostracode, gastropod, and unidentifiable shell debris generally make up less than 5% of all allochems. Finely comminuted phosphatic shell debris, fragments of horn corals, and dasycladacean(?) algal grains are rare. Oöids and coated grains are very rare, and intraclasts are uncommon. Isolated peloids were rarely observed, but are numerous in some burrows, suggesting they are fecal pellets.

As a rule, packstones and grainstones of the basal and upper limestones have low porosities because they are tightly cemented by calcite spar growing in optical continuity with the abundant crinoidal debris. Dolomite, typically isolated rhombs, occurs within allochems, especially bryozoan fragments. Partial silicification of brachiopod shells is common.

Most of the packstones and grainstones are coarse-grained with poor to

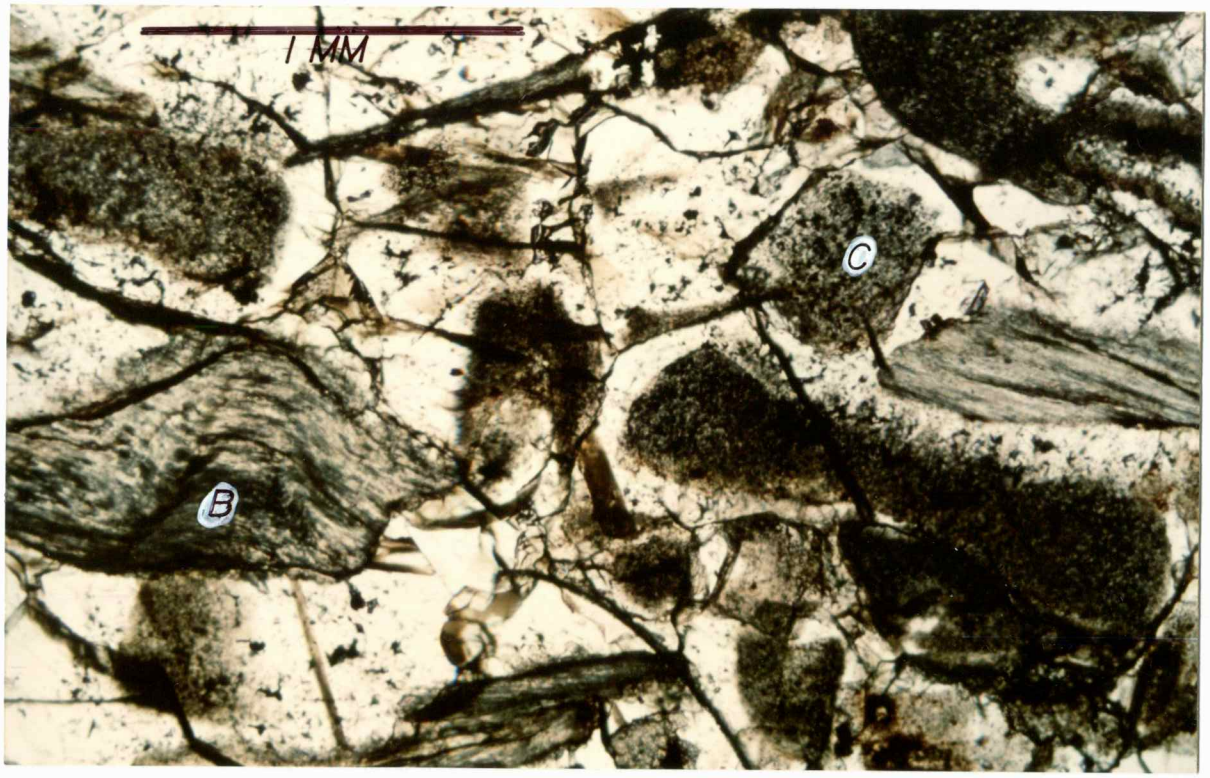

Figure 7.2 Photomicrograph of typical skeletal constituents in packstones and grainstones in the basal limestone (3259 ft depth) from the Northern Natural Gas #1 Caldwell core (#12) in Rice County (2-T.20S.-R.8W.). Syntaxial spar on crinoid fragments (**C**) is the major cement. This cement commonly envelopes other skeletal grains such as brachiopod fragments. Note thick-shelled brachiopod fragments (**B**) are rounded.

moderate sorting. Although variations in particle size occur within the packstones, bedding is commonly vague and difficult to discern. If bedding is evident, it is commonly defined only by a subparallel disposition of elongate shell fragments or by thin, slightly muddy layers. Cherty zones and stylolites, commonly developed within thinner, slightly muddier intervals in the packstones, also aid in defining bedding. Slightly silty and clayey beds are commonly evident as "horsetail" partings (cf., Derby #3 Lehman; *#14*, 3409-3416 ft depth; Appendix IV). Most bedding observed is in stratigraphic intervals less than 2 ft (0.6 m) thick with internal stratification inclined 5 to 25 degrees, indicating cross-stratification (cf., Derby #1 Woods, *#15*, 3900-3901 ft depth; Champlin #1 Kottman, *#11*, 3761-3763 ft depth, Appendix IV; see Figure 7.3). Cross-bedding was also observed in crinoidal grainstones in the Viola by Adkison (1972). Although St. Clair (1982) did not specifically identify cross-stratification in Pratt and Barber counties, inclined bedding is present in several cores used in her study. This inclined bedding is interpreted to be cross-stratification in this study. Inclined bedding is observable in approximately 20% of the core footage inspected in the basal and upper limestones.

Bioturbation is indicated by the lack of well-developed bedding, random orientations of flat skeletal fragments, and an overall clotted and churned appearance of the rock (Figure 7.4). Individual burrows are typically vertical, are approximately 1 cm in width and 3 to 5 cm in length, and contain slightly greater amounts of clays, lime muds, or dolomite than the surrounding packstone. The lack of bedding in some of the crinoidal packstones and grainstones may be due to extreme bioturbation, with individual burrows being unrecognizable. Overall, the level of bioturbation in the basal limestone corresponds to "ichnofabric index 5" with a subsidiary occurrence of "ichnofabric index 6" (Droser and Bottjer, 1988; Figure 7.5). In ichnofabric index 5 original bedding is completely disturbed, but individual burrows are still visible;

Figure 7.3 Polished slab of the basal limestone (3892.4 ft depth) from the Derby #1 Wood core (*#15*) in northeastern Reno County (36-T.22S.-R.5W.) showing bedding inclined approximately 20 degrees to the right. This inclination, largely defined by a subparallel orientation of flat shell fragments, is interpreted as cross-stratification.

ichnofabric index 6 means complete homogenization.

Skeletal grains in the coarser-grained lithologies of the Viola commonly have a rind of fine-grained carbonate, a micrite envelope, 20 μm thick or less, that cross-cuts and obfuscates the original internal texture of the grain. In some grains (mostly bladed fragments probably derived from mollusks) the skeletal core is dissolved away

Figure 7.4 Polished slab of the basal limestone (3837.6 ft depth) from the Derby #1 Rainbow core (*#16*) in northern Reno County (33-T.22S.-R.7W.) showing random orientation of fossil fragments -- a common type bedding observed in both the basal and upper limestone subunits. This bedding is interpreted as bioturbation of the sediment.

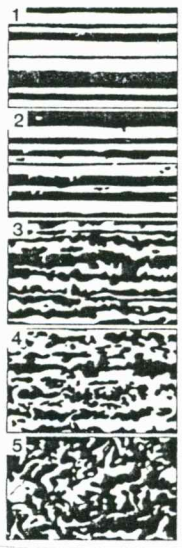

Figure 7.5 Schematic diagram of ichnofabric indices 1 through 5. Ichnofabric index 1: no bioturbation, all original sedimentary structures preserved; ichnofabric index 2: discrete isolated trace fossils, up to 10% of original bedding disturbed; ichnofabric index 3: 10%-40% of original bedding disturbed; ichnofabric index 4: last vestiges of bedding discernable, 40%-60% of original bedding disturbed; ichnofabric index 5: bedding is completely disturbed, but burrows are still discrete. Ichnofabric index 6, for which a schematic diagram cannot be made, represents completely homogenized sediment (from Droser and Bottjer, 1988).

leaving only the peripheral micrite. High magnification indicates this material is a fine-grained mosaic of equant calcite. Micritization of fossil fragments in the wackestones and mudstones of the lower and upper cherty dolomitic limestones is manifest by a slight darkening at the edges of some fragments, but in general, micrite rims are not as well developed as they are in the grain-supported lithologies in the basal and upper limestones.

Rarely, graded bedding is present in the basal limestone subunit. An example is a muddy graded packstone bed in the Derby #1 Rainbow core (*#16*) in northern Reno County (Figure 7.6). This bed has an erosional base and is 2 in (5 cm) thick. It is

Figure 7.6 Polished slab of the basal limestone subunit (3836.5 ft depth) from the Derby #1 Rainbow core (*#16*) in northern Reno County (33-T.24S.-R.5W.) showing fining-upward grain size in a lime packstone. This thin bed is interpreted to be the result of storm deposition.

enveloped by structureless, probably bioturbated, packstones. Overall mud content increases upward with a coinciding decrease in grain-size of the skeletal debris. Mud is also perched on individual skeletal grains. Similar features are present in the upper limestone subunit of the Viola Formation (see below).

Wackestones, and rarely lime mudstones, in the basal limestone subunit are

present as beds ½ to 2 ft (15 to 60 cm) thick within thicker sequences of packstones and grainstones (Figure 7.7). Boundaries between the wackestones and packstones are commonly gradational over less than 1 in (1 to 2 cm), or are stylolites. Composition of skeletal grains in the wackestones is not significantly different from that of the adjacent grain-supported lithologies and consists mostly of crinoid ossicles and, to a lesser extent, large (1-2 cm), thick brachiopod shell fragments and unidentifiable shell fragments. Vague laminations, vertical burrows (commonly dolomitized), or mottling (possibly due to extreme bioturbation) are commonly the only textures observable. Clay content in the wackestones is estimated at 10 to 15%, and stylolites are more abundant than in adjacent lime packstones. Color of the wackestones is commonly identical to or slightly darker than that of the accompanying packstones and grainstones. Wackestones are commonly more dolomitized. Comparison of the stratigraphic succession of closely spaced cores indicate the stratigraphic positions of the wackestone beds within the packstone-dominated basal limestone are not consistent; this suggests that the wackestones reflect local rather than regional changes in depositional environments.

The basal limestone, as its name implies, is the lowermost identifiable subunit of the Viola Limestone. Several cores (e.g., Midcontinent Marine #1 South Hilger, *#29*; Midcontinent Marine #1 North Hilger, *#28*; Derby #8 Schrock, *#17*; Derby #1 Wood, *#15*; Champlin #1 Kottman, *#11*; Northern Natural Gas #1 Caldwell, *#12*; and others) cut the contact between this subunit and the Simpson below. The Viola-Simpson contact in all cases is nearly planar and locally stylolitic. Erosion of the Simpson is demonstrated by truncation of burrows, carbonate grains, thin laminations, and other structures typically observable only in thin section (Figure 7.8).

Well-rounded, medium-sand quartz grains are commonly in the Viola up to a few centimeters above the contact and may locally constitute up to 20% of the rock.

Figure 7.7 Polished slab of dolomitized stylolitic wackestone containing horizontal burrows filled with muddy crinoidal packstone. Wackestones comprise approximately 20 percent of the basal limestone subunit. Lime mudstones are only rarely present. Sample is a thin wackestone locally present in the basal-limestone packstones from the Derby #1 Wood core (#*15*; depth 3889.7 ft) in northeastern Reno County (36-T.22S.-R.5W.).

Figure 7.8 Polished slab showing the sharp contact between the basal limestone subunit of the Viola Formation and an olive-green siltstone in the underlying Middle Ordovician Simpson Group. A hardground is observable in thin section (Figure 8.15) in the crinoidal-brachiopod packstone of the Viola Formation 2-3 cm above the contact. Burrows in the olive-green siltstone of the Simpson Group are filled with silt and floating sand grains. These burrows are truncated by the Viola-Simpson contact. Sample is from the Champlin Oil #1 Kottman core (#*11*, depth 3363 ft) in central Rice County (19-T.19S.-R.8W.).

Medium- and fine-grained, well-rounded, phosphatic grains, also reworked from the Simpson, are locally present near the contact (e.g., Derby Oil #1 Rainbow, (*#16*). In one well (Midcontinent Marine #1 South Hilger, *#29*), bird's eye (fenestral) porosity is present for 10 cm above the Simpson-Viola contact in a dolomitized crinoidal wackestone (Figure 7.9). Crinoidal packstone typical of the basal limestone is present above this wackestone at this locality.

Interpretations

Lee (1983) noted a similarly sharp, truncating contact between the Viola-equivalent Kimmswick Limestone and the underlying Middle Ordovician Plattin Group in north-central Arkansas. He referred to this contact as being "welded" (i.e., tightly cemented) and pitted, with minute depressions filled with overlying the Kimmswick Limestone. Lee (1983) concluded the contact implies that the Simpson was at least partially lithified and subaerially or subaqueously eroded prior to deposition of the overlying Viola. The surface between the Simpson and the Viola would generally be termed a disconformity in the denotation of Grabau (1905), that is, "a surface of unconformity separating essentially parallel strata". This surface would be a paraconformity to Dunbar and Rodgers (1957, p. 117) in that there is little physical evidence other than a difference in age between the strata, notwithstanding the grain truncations seen in thin section and the upward change in lithology from sandstone to carbonate rock. The well-rounded medium-sand quartz grains and the medium- and fine-grained, well-rounded, phosphatic grains commonly present in the basal limestone subunit just above this unconformity are characteristic material reworked from the Simpson.

The bird's eye (fenestral) porosity near the base of the Viola is indicative of an upper intertidal or supratidal depositional environment (Shinn, 1968). These

Figure 7.9 Polished slab showing the sharp contact (see arrows) between the basal limestone subunit of the Viola Formation and a sandy porous dolomite in the underlying Middle Ordovician Simpson Group. The Viola in this sample consists of dolomitized mudstone with vugular and solution-enlarged fenestral porosity. The mudstone at the base of the basal limestone subunit makes a gradational transition to packstone (not shown) a few centimeters above the contact. Sample is from the Midcontinent Marine #1 South Hilger core (#*29*, depth 4045.4 ft) in southeastern Reno County (9-T.26S.-R.4W.).

conditions were relatively short-lived and subsequent open-marine conditions are indicated by the abundance and diversity of stenohaline biotic constituents in the packstones and grainstones of the basal limestone subunit. The light gray and local red to pink coloration of these rocks indicate well-oxygenated conditions. The coarse grain size, the abrasion of the larger grains, local cross-bedding, and the low percentage of mud suggest moderate to high depositional energies in which currents reworked the original sediments and washed finer grained material away. The stratigraphic position of the packstones and grainstones directly above thin, locally developed supratidal facies suggests a nearshore, possibly shoreface depositional environment or a nearshore complex of shoals of skeletal debris. Amsden and Sweet (1983) interpreted the depositional setting of the Ordovician Welling Formation in northeastern Oklahoma to be shallow, clear to only slightly turbid, warm, tropical to subtropical water. The faunal assemblages were considered essentially life assemblages. The uniform composition and good preservation of the skeletal material indicated minimal transport (Amsden and Sweet, 1983). Subcrop maps presented in their report indicate the Welling Formation may be the lithologic correlative to the basal limestone subunit in Kansas.

Lobate submarine shoals of skeletal debris (see Figure 5.18), possibly shaped by storm currents, probably coalesced to form the virtually continuous and widespread basal limestone. The abundance of burrowing indicates that, even though currents may have been important in the initial deposition of the sediments composing this subunit, long periods of time may have transpired without currents that could remobilize these sediments. During the period of time without significant currents, an active benthic infauna reworked and largely destroyed the original depositional textures. Tidal currents, with virtually constant activity, therefore may not have been a major part of the depositional dynamics of these sediments.

Skeletal debris in the basal limestone is dominated by sessile benthonic organisms -- principally brachiopods, bryozoans, and crinoids. Feldman and others (1993), in a study of similar cross-bedded grainstones of sessile-benthonic skeletal debris of Carboniferous age, concluded that the cross-bedding was probably produced only during rare episodes of sediment reworking, because these fauna require long periods of sediment stability in order to thrive.

The lack of oöids or oölitic coatings on grains derived from shallow, open-marine biota also may be a clue to the depositional dynamics. Growth of oöids is dependent on many factors, including seawater chemistry, sedimentation rate, and hydraulic conditions (cf., Bathurst, 1976, p. 295-305; Sumner and Grotzinger, 1993). The virtual lack of oöids in the basal limestone argues for either infrequent movement of sediment, thereby precluding the agitation necessary for oöid development, or a sedimentation rate so high that early burial precluded any grains being oölitically coated, or both. The abundance of burrows also argues for prolonged sediment stability because a high sedimentation rate would tend to bury current-related sedimentary structures before they were destroyed by an active infauna.

Micrite envelopes observed on skeletal grains in the basal and upper limestones are common in modern and ancient carbonate sediments, and are interpreted to represent filled borings made by endolithic algae and fungi (Bathurst, 1966; Bathurst, 1976, p. 381-394). The common occurrence of micrite envelopes associated with skeletal grains deposited in the photic zone in Holocene carbonate sediments (generally at depths less than 40 m, and typically less that 15-18 m; see Swinchatt, 1969) allows cautious speculation that the basal and upper limestones of the Viola were probably deposited in relatively shallow water.

Paleobathymetric interpretations based on endolithic microorganisms can be fraught with uncertainty in that well-developed photosynthetic endolithic chlorophytes

have been recovered from depths as great as 370 m (Lukas, 1978; LeCampion-Alsumard and others, 1982) and endolithic fungi can be active below the photic zone (Zeff and Perkins, 1979). Environmental factors other than the depth of penetration of sunlight in water may therefore control the vitality of endolithic microorganisms recorded in the Viola.

The rare graded beds in the basal limestone subunit, such as the one described from the Derby #1 Rainbow core (*#16*) in Figure 7.6, are interpreted to be the product of storm deposition. Storm deposits have also been described elsewhere in the Ordovician System (see Kuhnhenn and Carozzi, 1977; Kreisa, 1981; Delgado, 1983; Bakush and Carozzi, 1986; Gardiner-Kuserk, 1988; Fara and Keith, 1988). Kuhnhenn and Carozzi (1977), Bakush and Carozzi (1986), and Carozzi (1989, p. 59) describe thin but extensive storm beds (average 7 cm thickness) that irregularly interrupt normally bioturbated skeletal packstones and grainstones in the Ordovician Platteville and Galena groups of northwestern Illinois. These beds commonly have sharp and irregular basal contacts, internal imbrication and incipient graded bedding of skeletal grains. Although comparable beds are present in the basal and upper limestone subunits of the Viola, they are not nearly as common. Mechanically entrained carbonate mud within the packstone storm layers, and an upward gradation to laminated and rippled mudstone are also common features in storm deposits (Aigner, 1982), but if this fine-grained material is not available to be worked into the storm deposit (as is perhaps the case in this study area), these features would be absent.

The thin wackestones interbedded with the packstones are interpreted to represent sheltered areas where quiet-water conditions dominated -- perhaps in bathymetric lows between the shoals of skeletal debris. The marine fauna similar to that of the adjacent packstones indicates that normal marine conditions prevailed during deposition of the wackestones.

The entire sequence of lithologies within the basal limestone indicates deposition on an unconformity that developed during a probable brief period of subaerial exposure at the end of Simpson deposition. Supratidal conditions occurred briefly, followed by subtidal deposits as seas transgressed this surface and gradually deepened. While the sea was relatively shallow, extensive beds of crinoidal debris were deposited across the shelf in southern Kansas, but deposition eventually did not keep up with rising sea level. Mud-free depositional environments on the shallow, well-washed, coarse-grained skeletal shoals were eventually succeeded by deeper water, lower energy depositional environments in which mud-supported sediments were dominant. The stratigraphic transition to the upper cherty dolomitic limestone represents a continued deepening of the sea, together with a concomitant abatement of the strength of storm, tidal, and wave-generated currents. Depositional environments responsible for packstone and grainstones in the basal limestone subunit were more persistent and favorable atop the broad Central Kansas arch, but eventually even this structural and possible bathymetric high was sufficiently inundated to drown the shoals.

LOWER CHERTY DOLOMITIC LIMESTONE

Observations

The contact of the basal limestone with the overlying lower cherty dolomitic limestone is problematical because few cores unequivocally straddle this stratigraphic boundary, and the few that do are mostly rubble or rock fragments representing incomplete recoveries in which the contact is not directly observable. This contact is also troublesome to pick because it is a carbonate-to-carbonate contact and it is

difficult to unequivocally discern from merely a local alternation of wackestone and grainstone within the basal limestone, because thin beds (1-2 in; 2-5 cm) of packstone and wackestone are also present in the upper part of the basal limestone in several wells. Notwithstanding these difficulties, three cores in McPherson County (Damac #1 Sandra Allen, *#2*; Shell #1 Anderson, *#3*; and Derby #8 Schrock, *#17*; Table 7.1, Figure 7.1) apparently include this contact, based on regional correlations with wireline logs. The contact between the basal limestone and the lower cherty dolomitic limestone appears to be gradational, occurring over a few centimeters in the Shell #1 Anderson (*#3*) and Damac #1 Sandra Allen (*#2*) wells (see Figure 7.10). In the nearby Derby #8 Schrock (*#17*) well, it is a stylolitized contact. The lower few centimeters of the wackestones of the overlying lower cherty dolomitic limestone in the Damac #1 Sandra Allen core (*#2*) (Figure 7.10) contain skeletal grains in matrix support and slightly deformed packstone intraclasts.

The lower cherty dolomitic limestone is dominantly composed of mudstone and minor wackestone. Nodular and bedded chert are universally present in this subunit regardless of the degree of dolomitization. Although this subunit is commonly dolomitic, the degree of dolomitization varies, and in some localities (see Chapter 8) dolomitization is minor. Dolomite appears more common toward the upper part.

Fossiliferous wackestones, commonly dolomitized, are the second most common lithology, comprising approximately 30% of the core footage inspected in this subunit. Differentiation of wackestone and mudstone lithologies by inspection of cuttings and cuttings descriptions is difficult because of the small size of the cuttings and problems with cavings, so cores are the principal means by which lithologies and depositional patterns can be determined. Unfortunately, core coverage, both stratigraphically and spatially, is uneven and sparse, therefore complete confidence in understanding the lithologic characteristics is difficult. Nevertheless, possible trends can be discerned.

Figure 7.10 Polished core slabs showing the gradational contact between packstone of the basal limestone and wackestone of the dolomitic lower cherty dolomitic limestone (depths 3441-3443 ft) in the Damac #1 Sandra Allen core (#2) in northern McPherson County (7-T.17S.-R.3W.). Packstone is lighter colored and calcitic whereas the interbedded wackestone is darker colored and dolomitic (see strip stained by Alizarin Red-S along side of core). Crinoid fragments typical of packstones in the basal limestone are reworked (probably by bioturbation) into the lower part of the wackestone. The wackestone is interpreted to be at the base of the lower cherty dolomitic limestone subunit. Small divisions of scale are centimeters.

The spatial distribution of the depositional textures encountered in cores from the lower cherty dolomitic limestone subunit (Figure 7.11) indicates fossiliferous wackestones are more common near the crest of the Central Kansas arch. Argillaceous wackestones compose most of this subunit in McPherson County (e.g., Damac #1 Sandra Allen, *#2*; Shell #1 Anderson, *#3*; Shell #4 Hill, *#4*; Shell #6 Decker, *#6*; Stanolind #3 Lovett, *#8*; and Shell #4 Griffin 'B', *#9*). These localities are on the northern flank of the Central Kansas arch, but near its crest (see Table 7.1; Figures 7.1, 7.12). One core recovering wackestone (i.e., Derby #8 Schrock [*#17*] in T.24S.-R.5W.), taken from a small outlier of the lower cherty dolomitic limestone subunit in eastern Reno County that is too small to show on isopach maps of this subunit, lies on the crest (Figures 7.11, 7.12). This wackestone (Figure 7.13) has approximately 10% cement-reduced moldic porosity after mollusk and brachiopod shells. It is not argillaceous, but only 4 ft (1 m) of this subunit is preserved at this locality.

Erosion or non-deposition has left only isolated outliers of the basal part of the lower cherty dolomitic limestone on the Central Kansas arch (see Figures 5.6, 5.11) so the apparent prevalence of wackestones on the arch may just be an artifact of the preservation of the basal part of this subunit rather than a spatially significant change in lithofacies. However, stratigraphic cross-sections in Figures 7.12 and 7.14 show that in wells to the south off the Central Kansas arch (i.e., Sinclair-Prairie #1 DeGeer, *#39*; Sinclair-Prairie #4 G. Oldfather, *#34*; and Palmer & Colorado Oil and Gas #2 Grier, *#31*), mudstones are in positions stratigraphically equivalent to the wackestones on the arch, therefore this apparent change in lithofacies may indeed be real.

Wackestones are also present in some wells near the top of the lower cherty dolomitic limestone subunit, approximately a meter or so below its contact with the upper limestone subunit (e.g., Sinclair #1 Binning, *#37*, see Figure 7.12; Sinclair-Prairie #4 G. Oldfather, *#34*, see Figure 7.14). Mudstones appear to be the norm in

Figure 7.11 Dominant lithologies encountered in cores from the lower cherty dolomitic limestone subunit, superimposed on its isopachous map (Figure 5.11). Argillaceous wackestones are present are closer to the crest of the Central Kansas arch, whereas farther off the arch lime mudstones dominate. Refer to Appendix IV for core descriptions.

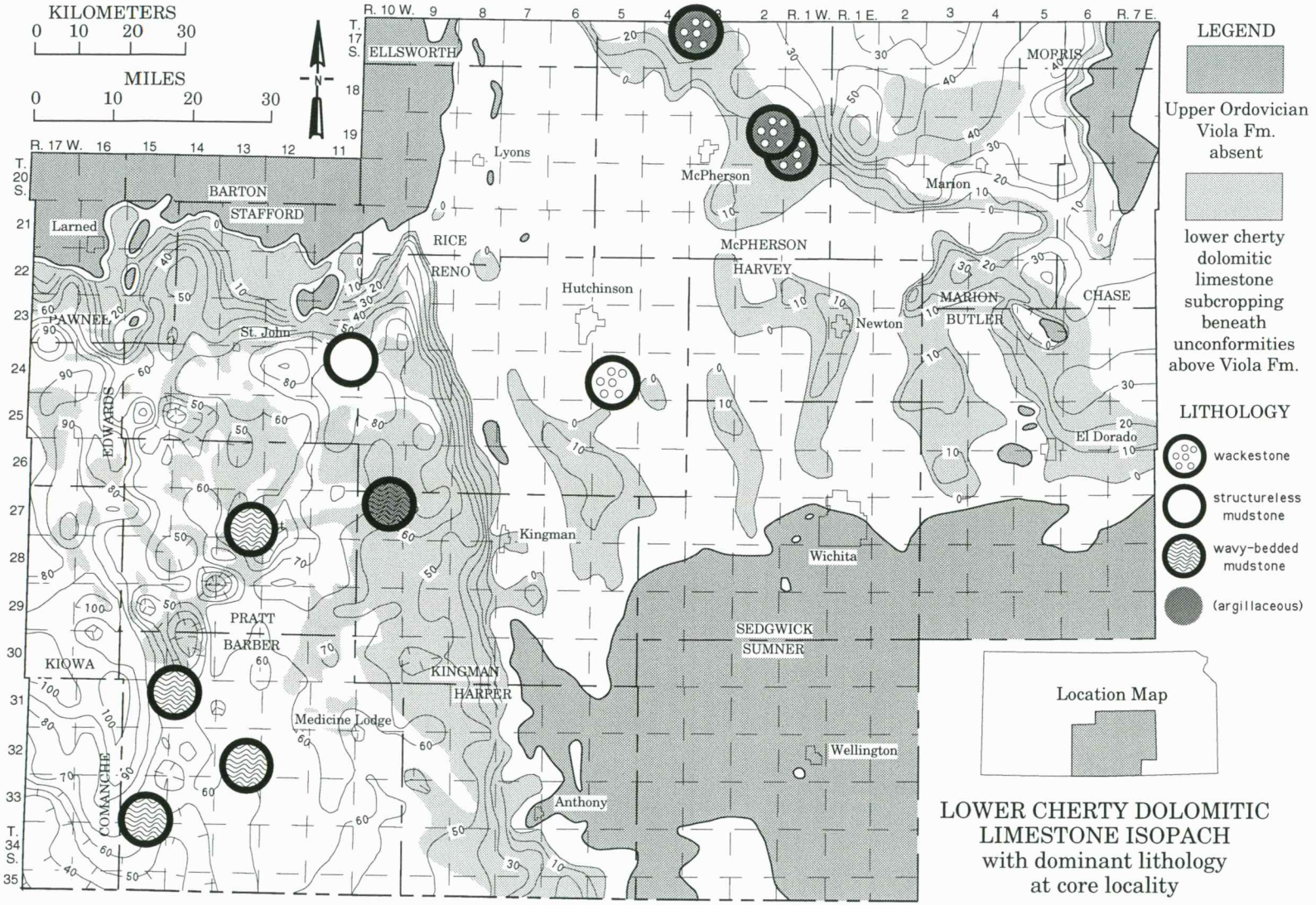

LOWER CHERTY DOLOMITIC LIMESTONE ISOPACH
with dominant lithology
at core locality

Figure 7.12 Stratigraphic cross-section (A-A') showing geometry of Viola subunits and stratigraphic position and lithology of cored intervals. Thickening of basal limestone subunit at the right of the cross-section is due to well-developed and extended shoaling conditions on and near the crest of the Central Kansas arch. Wackestones dominate in the lower cherty dolomitic limestone subunit at this locality whereas farther off the arch (to the left) mudstones are present in equivalent stratigraphic positions. Interpolation of thicknesses of subunits between wells is based on regional isopach maps presented in Figures 5.7, 5.11, 5.14, and 5.16. Thinning of the Viola Formation by apparent erosion at the base of the Maquoketa and Chattanooga shales can reflect either erosion in valleys (e.g., center of cross-section where the Chattanooga Shale lies directly on Simpson Group) or beveling at the tops of structures. See Figure 7.1 for location of wells used in the cross section. Numbers beneath wells refer to the well numbers used in Figure 7.1 and Table 7.1. Wells 4 and 7 are separated 2000 ft (600 m).

NORTHEAST-SOUTHWEST STRATIGRAPHIC CROSS-SECTION of VIOLA FORMATION with CORED INTERVALS and LITHOLOGY of CORES

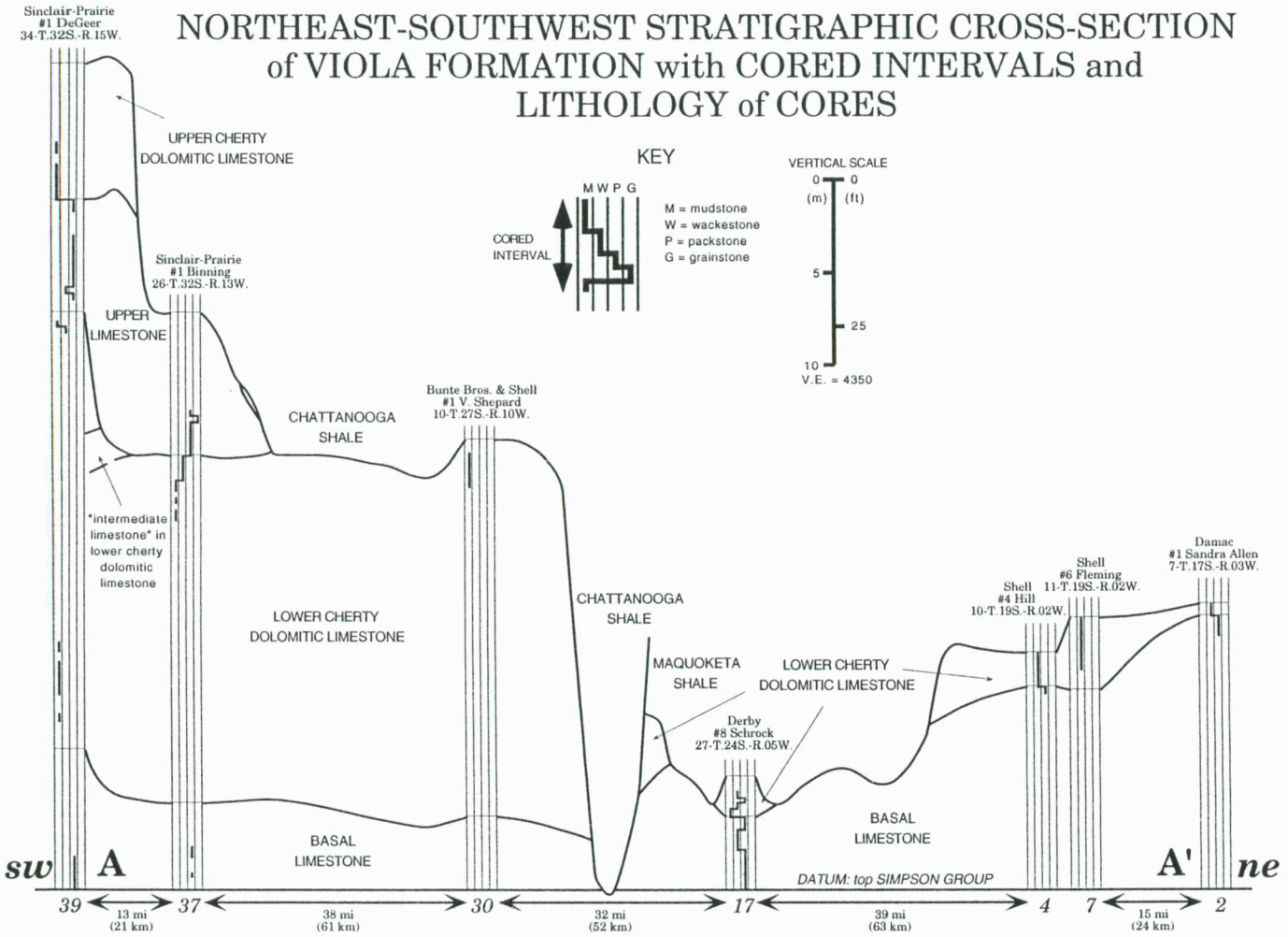

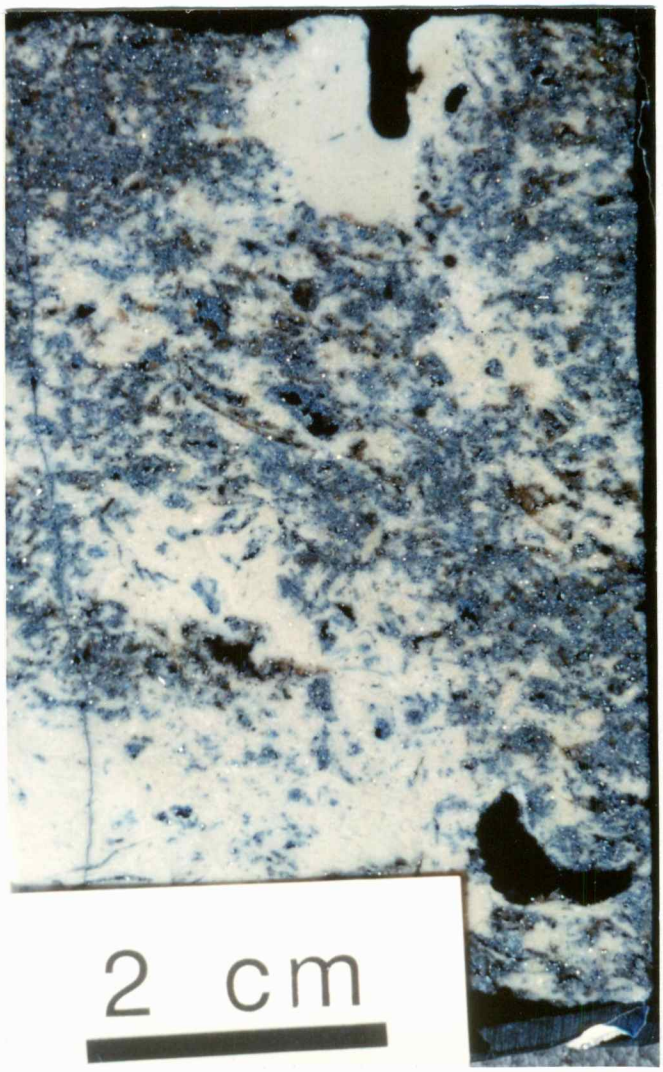

Figure 7.13 Polished slab of dolomitized wackestone from a small outlier of the lower cherty dolomitic limestone on the crest of the Central Kansas arch. The appearance of churned bedding in this sample may be due to bioturbation. Approximately 10% moldic porosity, after mollusk shells, is accentuated by blue epoxy infused into the sample. Sample is from the Derby Oil #8 Schrock core (#*17*, depth 3830.3 ft) in eastern Reno County (27-T.24S.-R.5W.).

the middle of this subunit according to descriptions of cuttings (St. Clair, 1982) but unfortunately no cores are available for unequivocal substantiation of this.

The wackestones in the lower cherty dolomitic limestone are commonly pale brown to dark gray and are generally darker colored than underlying packstones in

Figure 7.14 Stratigraphic cross-section (B-B') showing geometry of Viola subunits and stratigraphic position and lithology of cored intervals. Thickening of basal limestone subunit at the right of the cross-section is due to well-developed shoaling conditions near the crest of the Central Kansas arch. The presence of the upper limestone subunit (based on regional mapping using wireline logs and cuttings) on a relatively thin interval of lower cherty dolomitic limestone between the Braden-Zenith ZU-1 well (*#19*) and the Northern Natural Gas #1 Caldwell well (*#12*) suggests an unconformity may be present between these two subunits. Packstones developed in the upper cherty dolomitic limestone subunit at the Braden-Zenith ZU-1 well (*#19*) suggested intermittent shallow-water conditions developed atop the Central Kansas arch; however, mud-supported lithologies dominate the upper cherty dolomitic limestone off the Central Kansas arch (i.e., Sinclair-Prairie #1 Alice Oldfather [*#35*] and #1 DeGeer [*#39*] wells). Interpolation of thicknesses of subunits between wells is based on regional isopach maps presented in Figures 5.7, 5.11, 5.14, and 5.16. Thinning of the Viola Formation by apparent erosion at the base of Pennsylvanian strata and the Maquoketa and Chattanooga shales can reflect either erosion in valleys or beveling at the tops of structures. See Figure 7.1 for location of wells used in the cross section. Numbers beneath wells refer to the well numbers used in Figure 7.1 and Table 7.1. Wells 24 and 25 are separated 4800 ft (1450 m).

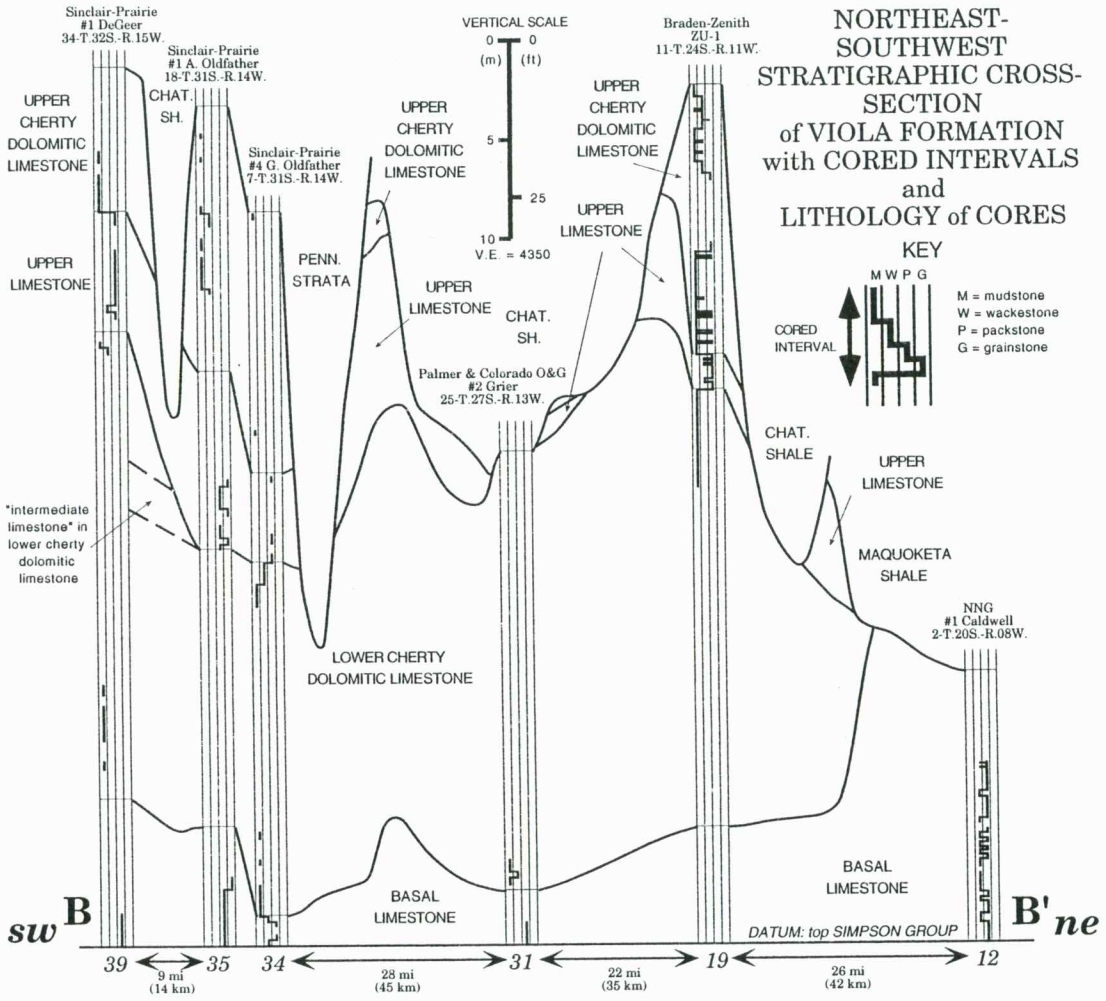
NORTHEAST-SOUTHWEST STRATIGRAPHIC CROSS-SECTION of VIOLA FORMATION with CORED INTERVALS and LITHOLOGY of CORES
KEY
M W P G
M = mudstone
W = wackestone
P = packstone
G = grainstone
CORED INTERVAL
VERTICAL SCALE
0 0
(m) (ft)
5
25
10
V.E. = 4350
Sinclair-Prairie #1 DeGeer 34-T.32S.-R.15W.
Sinclair-Prairie #1 A. Oldfather 18-T.31S.-R.14W.
Sinclair-Prairie #4 G. Oldfather 7-T.31S.-R.14W.
Palmer & Colorado O&G #2 Grier 25-T.27S.-R.13W.
Braden-Zenith ZU-1 11-T.24S.-R.11W.
NNG #1 Caldwell 2-T.20S.-R.08W.
UPPER CHERTY DOLOMITIC LIMESTONE
UPPER LIMESTONE
CHAT. SH.
PENN. STRATA
LOWER CHERTY DOLOMITIC LIMESTONE
CHAT. SHALE
MAQUOKETA SHALE
BASAL LIMESTONE
"intermediate limestone" in lower cherty dolomitic limestone
sw B
B' ne
DATUM: top SIMPSON GROUP
39
9 mi (14 km)
35
34
28 mi (45 km)
31
22 mi (35 km)
19
26 mi (42 km)
12

the basal limestone subunit. The most common skeletal fragments are crinoid columnals but bryozoan fragments are locally abundant (Figure 7.15). Other skeletal fragments, in decreasing order of abundance, include brachiopods and unidentified mollusk shells, fenestral and ramose bryozoan fragments, fine-grained phosphatic debris, and trilobite fragments. Sponge spicules, ostracodes, gastropod, and algae fragments can be seen in thin sections but are uncommon. Shell debris are usually thin and delicate, showing little wear. Intraclasts of mudstone are rare (see Figure 7.15). Micrite envelopes are rarely present.

Silicification is preferentially concentrated in skeletal fragments -- crinoid columnals, brachiopod shells, and less commonly in bryozoan fragments. Moldic and vugular porosity are as high as 25% by visual estimate in this subunit (see Figure 7.13). Intercrystalline porosity associated with dolomitization is very common throughout the lower cherty dolomitic limestone and can comprise up to 30% volume.

Although wackestones are the dominant lithology of the lower cherty dolomitic limestone over the Central Kansas arch, lime mudstones appear to be more common off the arch (see Figures 7.11, 7.12, 7.14). Mudstones composing this subunit are generally characterized by either wavy-laminated bedding (Figures 7.16, 7.17), or are structureless (see Figure 7.18), as in the Braden-Zenith ZU-1 (*#19*) and Braden-Zenith ZU-3 (*#20*) cores in eastern Stafford County on the flanks of the present-day Central Kansas uplift. The wavy laminations are defined by either slight variation of dolomite crystal sizes, probably reflecting variations in original grain size, or by variable clay content in the argillaceous mudstones. Laminations are continuous with little evidence of disruption except by soft-sediment deformation and minor burrowing (see Figure 7.16). Amplitudes of the wavy beds are typically less than 2 inches (2-3 cm), with wavelengths of 0.6 to 1 ft (20-30 cm). Some beds are graded. These graded beds vary from less than 0.5 in (1 cm) to approximately 2 in (5 cm) in thickness, with

Figure 7.15 Slabbed core of bryozoan-rich wackestone from the lower cherty dolomitic limestone. Crinoid columnals (**C**) and intraclasts of mudstone (**M**) are also present (see arrows). This wackestone is 4 ft (1.2 m) below the base of the upper limestone subunit (dominantly lime packstone) and 1 ft (0.3 m) above a section of lime mudstone, and may represent shallowing of water depth and a concomitant slight increase in depositional energy near the end of deposition of the lower cherty dolomitic limestone. Sample is from the Sinclair #1 M. Binning core (#37, depth 4483 ft) in central Barber County (26-T.32S.-R.13W.).

argillaceous material concentrated in the finer portions of the bed (Figure 7.16).

Discrete, isolated vertical burrows are present but not common, so the majority of the wavy bedded mudstones can be characterized as ichnofabric index 2 (Droser and Bottjer (1988) (see Figure 7.5). Stylolites also disrupt bedding and are typically concentrated in the argillaceous mudstones, especially in clay-rich zones. Clays can also be concentrated along the stylolites. Whispy, discontinuous clayey zones that

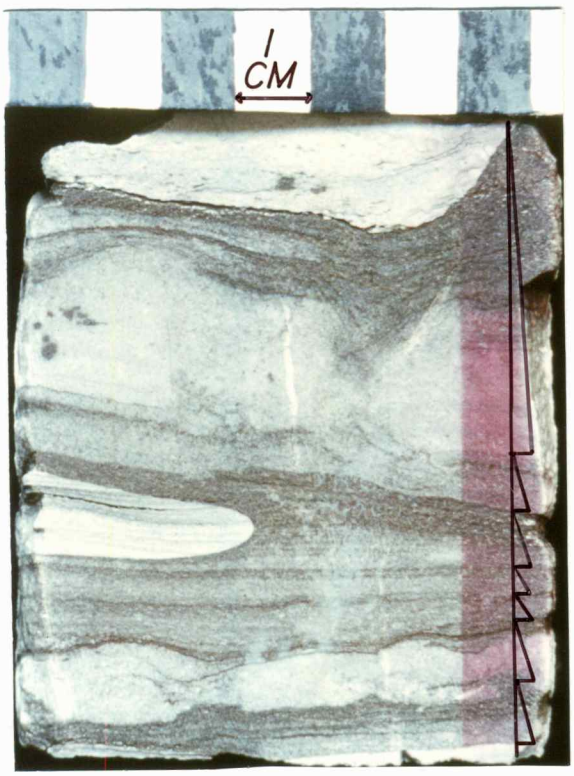

Figure 7.16 Slabbed core of argillaceous wavy-laminated mudstone from the lower cherty dolomitic limestone subunit. Silty and clayey laminations are generally continuous through the mudstone, showing little evidence up disruption (i.e., cracking, rip-up clasts, etc.) except for soft-sediment deformation. Minor soft-sediment deformation or possibly a tangential cut of a burrow is in the upper half of this sample. Graded beds, shown by triangles with apices at the finer grained portion of the bed, are also present. Laminations extend through a chert nodule at lower left. Alizarin Red-S stain indicates dolomite is concentrated within the more argillaceous layers whereas cleaner portions of the rock are limestone. Sample is from the Bunte Brothers and Shell #1 V. Sheppard core (*#30*, depth 4310.1 ft) in northwestern Kingman County (10-T.27S.-R.10W.).

commonly fan out laterally and dissipate in one direction (descriptively identified as "horsetail stylolites" or "discontinuous seams" of Wanless (1979)), are also common. Interpretation of depositional environments is hampered by this type of dissolution feature because primary sedimentary structures can be distorted (see Wanless, 1979). Stylolitization, however, is not as common in this subunit as in the basal limestone.

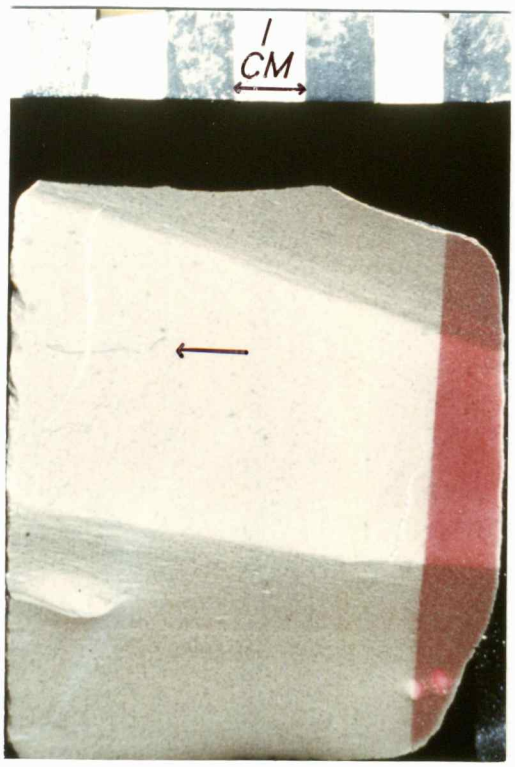

Figure 7.17 Slabbed core of argillaceous wavy-laminated mudstone from the lower cherty dolomitic limestone subunit showing thin bed of calcitic mudstone with a trilobite fragment (arrow). Few fossils are present in the mudstones of this subunit in the Viola Formation. Sample is from the Bunte Brothers and Shell #1 V. Sheppard core (*#30*, depth 4310.8 ft) in northwestern Kingman County (10-T.27S.-R.10W.).

The laminated mudstones typically contain few, if any, macroscopic fossils. Microscopic phosphatic shell debris is common, however. Identifiable shell fragments are rare; they may include crinoid columnals, bryozoans, trilobites, and delicate mollusk and brachiopod shells (see Figure 7.17). Structureless mudstones also rarely contain fossils, although where the structureless mudstones are most common, in the Braden-Zenith ZU-1 (*#19*) and ZU-3 (*#20*) wells in eastern Stafford County, they have been heavily dolomitized. This dolomitization or prior dissolution events may have destroyed fossils (Figure 7.18) because molds of bladed shell fragments (probably

Figure 7.18 Slabbed core of structureless dolomitized mudstone from the lower cherty dolomitic limestone at the Braden-Zenith ZU-3 well (#*20*, depth 3775 ft) in eastern Stafford County (11-T.24S.-R.11W.) showing thin horizontal zones of intercrystalline porosity that may be related to original bedding. Porous zones are darker than nonporous zones due to oil staining. Minor fracture porosity is also evident.

mollusks) are present.

Nodular chert is abundant within the mudstones of the lower cherty dolomitic limestone. Most nodules are oriented parallel to bedding in the wavy-bedded mudstones but are more randomly oriented in the structureless mudstones. In general, chert nodules are lighter colored than the surrounding mudstone. In argillaceous wavy-bedded mudstones, clayey laminations extend through some nodules (see Figure 7.16), and supratenuous folds, where fine laminations in the adjacent mudstone thin and drape over nodules, are also observable (St. Clair, 1982). Some chert nodules have lighter-colored peripheral rinds but no pattern to the stratigraphic distribution of this type of nodule could be discerned. However, chert nodules with lighter-colored rinds in the Braden-Zenith ZU-1 (*#19*) and Braden-Zenith ZU-3 (*#20*) wells in eastern Stafford County were only present below a brecciated zone at the base of the upper limestone (Figure 7.19), whereas chert nodules a few feet above in the upper cherty dolomitic limestone display no such rind.

Interpretations

Slightly deformed packstone intraclasts and floating skeletal grains typical of the basal-limestone packstones indicate that the basal limestone was not completely lithified before deposition of the overlying lower cherty dolomitic limestone. Thin beds of wackestone interbedded with packstones in the upper part of the basal limestone in several wells signifies that although energy conditions may have changed frequently. The transitional contact between the basal limestone subunit and the lower cherty dolomitic limestone subunit therefore records nominally continuous deposition.

Quiet-water deposition is indicated by the fine-grained nature of the wavy-bedded mudstones in this Viola subunit. Lack of abundant intraclasts and the presence of delicate, paper-thin shells in the mudstone indicate that strong currents

Figure 7.19 Slabbed cores showing abrupt contacts between the lower cherty dolomitic limestone and the base of the upper limestone in the Braden-Zenith ZU-1 (left side; *#19*, depths 3829-3831 ft) core and Braden-Zenith ZU-3 (right side; *#20*, depths 3773-3775 ft) core in eastern Stafford County (11-T.24S.-R.11W.). Approximately 3900 ft (1200 m) separates the wells. The uppermost fragment (light colored) in each core is the lowest occurrence of packstone in the upper limestone subunit. A brecciated zone is relatively well-developed in the Braden-Zenith ZU-3 core (*#20*) (right) at top of the lower cherty dolomitic limestone subunit at 3774 ft. This brecciated zone is not as pronounced in the Braden-Zenith ZU-1 core (*#19*) (left) but is nevertheless expressed as a thin zone of clasts in the lowermost core fragment on the left (depth 3831 ft). Note chert fragments with light-colored rind below the upper limestone (arrows). The brecciated zone in both wells is interpreted to represent a brief period of subaerial exposure that occurred before deposition of the upper limestone. Small divisions of scale are centimeters.

were not the norm during deposition of this unit. The presence of thin beds displaying fine grading is evidence that occasional gravity currents brought influxes of fine-grained sediment into this quiet-water environment. The common preservation of these graded beds indicates that the normal depositional environment was probably below fairweather wave base but above maximum (and possibly mean) storm wave base. Water depth is not determinable, but the lateral continuity of the laminations, the lack of current-generated structures (i.e., ripples, cross-stratification), and the absence of exposure features (i.e., fenestral porosity, desiccation cracks, etc.) indicate a continual subtidal depositional environment. The relatively dark coloration of these rocks (medium and dark grays as opposed to light grays for the basal limestone subunit) implies less oxygenation of the water column and in pore waters. The general lack of micrite envelopes on skeletal grains argues for its deposition below the photic zone. The lack of fossil debris and burrowing in the wavy-bedded mudstones implies a stressed environment possibly due to abnormal salinity, lack of nutrients, anoxia, or temperature extremes. Vertical and lateral transitions to lithofacies characteristic of bathymetric barriers such as shoals, barrier islands, or reefs are often diagnostic in interpreting such restricted environments (Enos, 1983). However, such barrier facies are not evident in the Viola in either Kansas or Oklahoma. St. Clair (1982) invoked a facies transition to shoals of packstones and grainstones characteristic of the basal and upper limestones as being culpable for the restricted environment she interpreted for the lower cherty dolomitic limestone. However, regional mapping indicates that although these crinoidal shoals may be in part a facies transition to the mudstones of the lower cherty dolomitic limestone, these shoals are principally developed shoreward of these mudstones and in relatively shallow water over subtle structures such as the Pratt anticline and Central Kansas arch. The chief factor in the restriction may have been the damping effect of the shallow,

expansive Viola shelf itself, in which long residence time of water on the shelf could lead to nutrient depletion (cf., Enos, 1983). Even on the relatively steep and tectonically downdropped west flank of the Pratt anticline, mapping (see Figure 5.21) and cross-sections (see Figures 5.17, 5.23) presented in this study indicate water depths were probably at most 60 ft (18 m), with bathymetric slopes of less than one degree. Lesser slopes and depths would be expected elsewhere on the shelf.

Structureless mudstones observed at the Braden-Zenith ZU-1 (*#19*) and ZU-3 (*#20*) wells in eastern Stafford County were not observed elsewhere, so the original vertical and lateral extent of this facies is unknown. The lighter color of the structureless mudstones implies a more oxygenated environment than with the wavy-bedded mudstones. The lack of coherent bedding, and the random orientation of chert nodules in these rocks may indicate extreme bioturbation in which the sediment has been completely homogenized (i.e., ichnofabric index 6 of Droser and Bottjer (1988)). Although quiet-water deposition without subaerial exposure is indicated by the structureless mudstones, water may have been sufficiently shallow or oxygenated to support abundant burrowing benthic fauna.

The wackestone facies and the diverse marine fauna it contains implies more normal levels of oxygenation and salinity; however, currents were not sufficiently strong to wash away most mud as on the crinoid shoals. The fact that wackestones are common on the Central Kansas arch directly above the basal limestone implies, as stated in Walther's Law (Walther, 1894), a slightly deeper, quieter, and possibly more turbid-water depositional environment was adjacent to the crinoid shoals.

The argillaceous mudstones and wackestones are principally located on the flanks of the Central Kansas arch whereas less argillaceous mudstones are present away from the arch (Figure 7.11), hence the structurally higher extensions of the Central Kansas arch (i.e., the Chautauqua arch in southeastern Kansas and the

Ancestral Central Kansas uplift in north-central Kansas) could have contributed the fine-grained siliciclastic sediment to the Viola. These clays and silts could have been eroded from the Simpson Group where it is truncated beneath the Chattanooga Shale in southeastern Kansas, or from Precambrian rocks and the Simpson Group where they are absent or subcropping beneath Pennsylvanian strata on the present-day Central Kansas uplift.

The continuous deposition between the basal limestone and the lower cherty dolomitic limestone, and the inferred deeper-water conditions that influenced the lower cherty dolomitic limestone indicates that most likely sedimentation in the shoal environment that characterizes the basal limestone subunit was not able to keep up with a relative rise in sea level. As the sea floor sank below fairweather wave base, quiet-water deposition, characterized by wackestones and mudstones, prevailed on the Viola shelf.

UPPER LIMESTONE

Observations

The contact at the base of the upper limestone was recovered by two cores in eastern Stafford County (i.e., Braden-Zenith ZU-1 [*#19*] and ZU-3 [*#20*]). In the ZU-3 well (*#20*), the contact is directly above a breccia, approximately ½-ft (15-cm) thick, composed of pebble- and cobble-sized chert fragments and "fitted" clasts of dolomitized mudstone in a coarsely-crystalline matrix of calcite spar (Figure 7.19). This brecciation grades downward into unaltered, wavy-bedded dolomitic mudstone in the lower cherty dolomitic limestone. At nearby Braden-Zenith ZU-1 (*#19*), the brecciation is not as well developed but a thin zone of incipient brecciation is present in which

clasts display a fitted fabric (Figure 7.19). The brecciation at Braden-Zenith ZU-1 (*#19*) is approximately 1 ft (25 cm) below the lowermost packstone characteristic of the upper limestone subunit, and grades upward and downward into unbrecciated laminated dolomite.

The upper limestone is virtually identical to the basal limestone in that both of these subunits are dominated by packstones and grainstones composed of crinoid columnals, bryozoans, and shell fragments. These grains commonly display peripheral micritization. Both subunits are typically nonporous, being tightly cemented by sparry calcite. Tilted bedding, indicative of cross-stratification, is present in approximately 55% of the core described in the upper limestone. Grain-supported lithologies in both subunits commonly display varying degrees of bioturbation that are commonly manifest in thin sections as a random orientation of skeletal grains and on larger polished slabs as either structureless bedding, or beds that are churned or appear clotted (i.e., ichnofabric index 5; Droser and Bottjer, 1988; Figure 7.20). Other than their stratigraphic position within the Viola Formation, no significant dissimilarities were noted in the texture and biotic constituents of the upper limestone and basal limestone that would aid in differentiating differences in the depositional environments of these two units.

Interpretations

The brecciated zone at the top of the lower cherty dolomite indicates a period of dissolution prior to deposition of the upper limestone subunit in which the seas probably retreated and the lower cherty dolomitic limestone was subject to erosion and a flux of fresh water. The geographical extent of this minor unconformity is unclear because the two cores in which this unconformity was observed (Braden-Zenith ZU-1 [*#19*] and ZU-3 [*#20*]) are from a locality situated near the crests of the Central

Figure 7.20 Two slabbed cores from the upper limestone subunit from the Lario Oil & Gas #2 Randles core (*#19*, depths 4740-4742 ft) in central Barber County (34-T.32S.-R.12W.). The core slab to the left displays the "clotted" texture that is typical of extensively bioturbated packstones whereas the core segment on the right is cross-stratified. A vestige of cross stratification is preserved in the upper half of the left core. Small divisions in scale are centimeters.

Kansas arch and Pratt anticline -- areas where local subaerial exposure may likely have resulted from minor tectonic uplift. Lack of angular relationships between the subunits above and below this surface, and the possible local extent of this unconformity indicates that the subaerial exposure associated with it was probably short lived. The relationship of this minor unconformity to the stratigraphic boundary between the lower cherty dolomitic limestone and the upper limestone elsewhere in the study area is presently unclear.

The brecciation at the base of the upper limestone observed at the Braden-Zenith ZU-1 (*#19*) and ZU-3 (*#20*) wells in eastern Stafford County (see Figure 7.19) is characteristic of a carbonate-rock dissolution feature dubbed "intrastratal karst" (Quinlan, 1972) or "intraformational breccias" (Mussman and Read, 1986), in which dissolution and collapse of the underlying dolomitic mudstone occurred. The consistent stratigraphic position of the brecciation in the two wells indicates that dissolution processes at the upper part of the phreatic zone (i.e. water table) could have been responsible. A similar stratal distribution of more pronounced karstic features has been observed in the Lower Ordovician Ellenburger Group in the Permian basin of west Texas by Kerans (1988). The lighter-colored peripheral zones in chert nodules in the lower cherty dolomitic limestone just below this brecciated zone (see Figure 7.19) may be a leaching phenomenon attributable to a flux of fresh water associated with this possible exposure surface. Chert nodules a few feet above the breccia in the upper cherty dolomitic limestone display no such rind.

Their identical lithologic characteristics indicate that both the basal limestone and upper limestone subunits represent similar depositional environments -- open-marine, shoaling conditions that were subject to relatively high-energy currents. Extensive bioturbation of both subunits indicates that a benthic infauna was able to rework these sediments for long periods of time after their initial deposition and that

hydrodynamic reworking of these sediments may have been relatively infrequent.

Both the basal limestone and the upper limestone subunits are thickest atop structural highs. The locus of deposition for the basal limestone is the crest of the Central Kansas arch whereas the northern (structurally highest) portion of the Pratt anticline is where the upper limestone is thickest. The fact that both of these subunits, which were deposited in shallow-water conditions probably at or near normal wave-base, are thickest atop these structural highs implies that accommodation space was continually made available atop these structures in order that these thicknesses of shallow-water sediments could be preserved. The rate of creation of this accommodation space also nearly matched the sedimentation rate. The accommodation space was made by a gradual rise in sea level during the deposition of these two subunits or by regional subsidence of an area encompassing the Central Kansas arch and Pratt anticline.

A rough estimate for depth of wave base for both the basal limestone and the upper limestone subunits would be the vertical difference in thickness of the packstone between where each of these subunits are thickest on-structure and where they are thinnest off-structure. For example, in Figure 7.14, the Northern Natural Gas #1 Caldwell well (*#12*), which is situated near the crest of the Central Kansas arch, contains a section of basal limestone that is 35 ft (10.5 m) thicker than at the Sinclair-Prairie #4 G. Oldfather well (*#34*), notwithstanding erosion. If the top of the packstone sequence in each well is approximately the same age, and if the top of the packstone at the Northern Natural Gas #1 Caldwell well (*#12*) was at sea level, then the vertical difference between the respective packstone tops would be a minimum estimate for both the depth of wave base and water depth. In the case of the basal limestone subunit, a minimum estimate of depth of wave base is 40 ft (12 m), based on differences in the maximum and minimum contours on the isopachous map (Figure

5.7). By this same method, the upper limestone has a minimum depth of wave base of 30 ft (9 m) (see Figure 5.15). In actuality, time lines most likely do not coincide with either the top or the base of the basal limestone subunit, nor is it likely that depositional rates at all localities are identical, therefore the estimate of the depth of wavebase by this method is perhaps hazardous.

The abrupt base of the upper limestone and the associated solution features and brecciation in the lower cherty dolomitic limestone directly underlying it indicate a hiatus due to a relative fall in sea level after deposition of the lower cherty dolomitic limestone. In turn, the packstones of the upper limestone represent intertidal-to-subtidal transgressive deposits occurring with the return of marine conditions. Any sediments representing supratidal deposition in the initial stages of this marine transgression were probably largely destroyed in the subsequent high-energy shoal environments.

UPPER CHERTY DOLOMITIC LIMESTONE

Observations

The basal contact of the upper cherty dolomitic limestone is represented in the Braden-Zenith ZU-1 (*#19*) and Braden-Zenith ZU-3 (*#20*) cores from eastern Stafford County. The contact is difficult to pick precisely because the packstones that typify the subjacent upper limestone subunit do not change abruptly upward to the cherty mudstones characteristic of the upper cherty limestone subunit; rather interbedding of the two lithologies occurs over a zone several feet thick -- a motif similar to that seen with the basal limestone and overlying lower cherty dolomitic limestone. For example, several thin (1-3 in; 2-7 cm) chertified packstone beds with imbricated skeletal grains

occur over a 4-ft (1-m) zone (3821-3825 ft depth) in the Braden-Zenith ZU-3 (*#20*) well near the base of a sequence of dolomitized mudstones that are identified as the upper cherty dolomitic limestone subunit (see Appendix IV). Thin chertified packstones are also found up to 3.5 ft (1 m) above the top of the 5-ft-thick (1.5-m) packstone bed representing the upper limestone in the nearby Braden-Zenith ZU-1 core (*#19*).

The contact of the upper cherty dolomitic limestone and the underlying upper limestone is not recovered in cores elsewhere, but a 3-ft-thick (1-m) zone of contorted bedding is present in the lower part of the upper cherty dolomitic limestone in the Sinclair-Prairie #1 Alice Oldfather core (*#35*) in western Barber County (see Figure 7.21; Appendix IV). A 5-ft (1.5 m) gap in which no core was recovered is present between this contorted zone and packstones below, which are identified as the upper limestone subunit. The lowermost core fragment in the contorted zone includes a crinoidal wackestone that may represent the top of the underlying upper limestone.

A closely controlled determination of lithofacies in the upper cherty dolomitic limestone is hindered by a limited stratigraphic and geographic distribution of cores and by the multiple erosional events that have removed much of this subunit from the Central Kansas arch and Pratt anticline. Nevertheless, the few cores that penetrate this subunit (see Appendix IV; Figure 7.22) provide insight into the depositional environments near the end of Viola deposition. A summary of the spatial distribution of rock types encountered in the upper cherty dolomitic limestone (Figure 7.22) indicates that wavy-bedded argillaceous mudstones with minor wackestones comprise this subunit in the limited area where it has been cored in the southern part of the study area (i.e., western Barber County). Homogeneous mudstones characterize this subunit in the single core farther north in eastern Stafford County.

Argillaceous mudstones in the upper cherty dolomitic limestone are similar to those present in the lower cherty dolomitic limestone in that they are characterized by

Figure 7.21 Slabbed core fragments (4447-4450 ft depths) from the upper cherty dolomitic limestone subunit in the Sinclair-Prairie #1 Alice Oldfather core (*#35*) in northwestern Barber County (18-T.31S.-R.14W.) showing contorted bedding interpreted to be slumping. Each fragment is a dolomitized mudstone and represents one foot of core, however, a crinoidal wackestone with intraclasts of mudstone in the lower half of the lowermost fragment (4450 ft depth) may represent a transitional facies above the underlying upper limestone subunit. If the upper limestone subunit was also involved in this slumping, both the upper limestone and the upper cherty dolomitic limestone represent a continuous depositional episode. Small divisions of scale are in centimeters.

Figure 7.22 Dominant lithologies of the upper cherty dolomitic limestone, superimposed on its isopachous map (see Figure 5.15). Argillaceous mudstones are principally limited to the southern part of the study area, indicating that the Chautauqua arch, but not the Ancestral Central Kansas uplift, was probably contributing fine-grained siliciclastic sediments to this unit. Refer to Appendix IV for core descriptions.

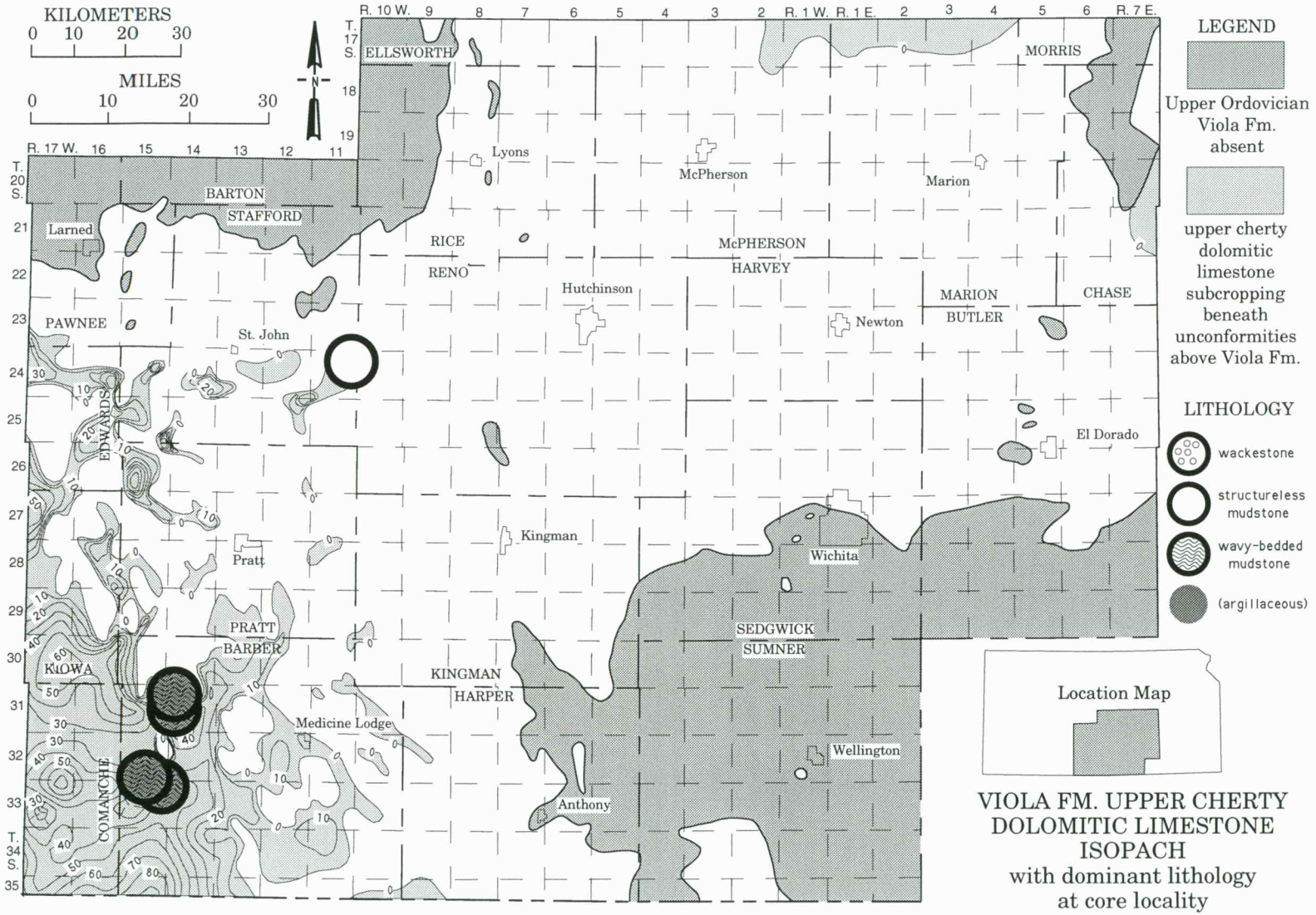

VIOLA FM. UPPER CHERTY DOLOMITIC LIMESTONE ISOPACH
with dominant lithology at core locality

wavy bedding, nodular chert, and few fossils (although fossils appear to be slightly more common than in the lower cherty dolomitic limestone; see Figure 7.23). Laminations are commonly defined by thin (0.5-1 in; 1-3 cm) clayey or silty layers and slight changes in the size of dolomite crystals. Amplitudes of the wavy beds are generally less than 2 in (2-3 cm), with projected wavelengths of approximately a foot (25 cm).

The sparse (less than 5%) skeletal debris in the mudstones typically consists of paper-thin, brachiopod and mollusk shells and finely comminuted phosphatic shell fragments. Skeletal debris is locally sufficiently abundant to classify the rock as a wackestone (Figure 7.24). Core control is not sufficient to determine stratigraphic extent of these wackestones. In western Barber County, thin wackestones occur in the middle of the upper cherty dolomitic limestone in the Sinclair-Prairie #1 A. Oldfather well (*#35*, see Figure 7.14, Appendix IV) and at its base in the nearby Sinclair #1 Alice Gentry well (*#40*, see Appendix IV).

Isolated vertical burrows are not common, but they are locally abundant (see Figure 7.24). The majority of the wavy-bedded mudstones and wackestones observed in western Barber County have an ichnofabric index of 2 (Droser and Bottjer, 1988).

The upper cherty dolomitic limestone changes lithologic character between Barber County and farther north in Stafford County. The majority of fine-grained strata in this subunit at Stafford County in the Braden-Zenith ZU-1 (*#19*) and ZU-3 (*#20*) cores is characterized by homogeneous beds, possibly indicative of intense burrowing (Figure 7.25). Mudstones at the Braden-Zenith ZU-1 (*#19*) and ZU-3 (*#20*) wells typically contain little clay. The upper cherty dolomitic limestone in the Braden-Zenith ZU-1 well (*#19*) also contains several thin wackestone and packstone beds (Figure 7.14). These packstones in the Braden-Zenith ZU-1 well (*#19*) and the nearby Braden-Zenith ZU-3 well (*#20*) are distinctive in that they display graded bedding

Figure 7.23 Slabbed core of wavy-bedded argillaceous lime mudstone in the upper cherty dolomitic limestone from the Sinclair-Prairie #1 DeGeer well (#*39*, depths 4964-4965) in Barber County (34-T.32S.-R.15W.). The minor amount of delicate molluscan shell debris almost qualifies these rocks as being sparse wackestones. Both rocks are totally dolomitized. In the 4464-ft slab argillaceous material is concentrated in a thin laminated zone in the middle of the sample. Light-colored areas in the 4465-ft sample are slightly chertified zones and horizontal burrows.

(Figure 7.26). Other thin packstone beds within the upper cherty dolomitic limestone at this locality are relatively fine-grained, cross-bedded, and contain abundant mollusk and brachiopod shells (Figure 7.27) that show little wear. A few skeletal fragments with micrite rims are present in graded grainstones contained within the upper cherty dolomitic limestone (Figure 7.26).

Geophysical well logs of the upper cherty dolomitic limestone in the vicinity of the southern flank of the Ancestral Central Kansas uplift (i.e., Edwards, Stafford, and Pawnee counties) typically show several non-porous intervals that are identified in cuttings as "coarse crystalline limestone". These intervals are probably crinoidal

Figure 7.24 Slabbed core of a dolomitized sparse wackestone in the upper cherty dolomitic limestone (depth 4440 ft) from the Sinclair-Prairie #1 Alice Oldfather core (*#35*) in northwestern Barber County (18-T.31S.-R.14W.). Fine-grained skeletal debris in this sample includes crinoid columnals and black phosphatic brachiopod(?) shell fragments. Moldic porosity (approximately 2-3%), after mollusk shells, is also present. Vertical burrowing has disrupted some of the lamination. Slightly darker colored laminations are more pronounced than usual due to minor oil staining. Although this sample is a wackestone with greater than 10% fossil debris, the wavy-bedding, nodular chert, and fine-grained laminae are typical of wavy bedded mudstones in the upper cherty dolomitic limestone.

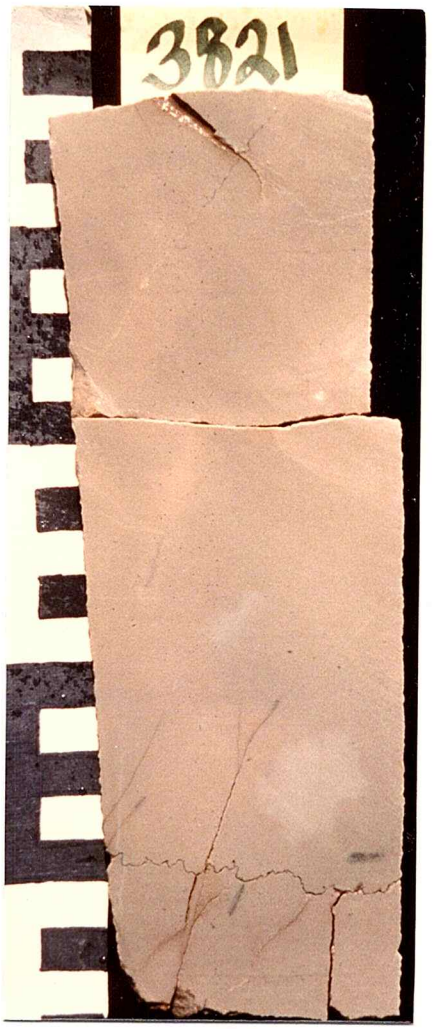

Figure 7.25 Typical structureless dolomitized mudstone in the upper cherty dolomitic limestone, from the Braden-Zenith ZU-1 core (*#19*, depth 3821 ft) from eastern Stafford County (11-T.24S.-R.11W.). Minor intercrystalline (<5%) and fracture porosity is present in this sample. A stylolite that cross-cuts a near vertical fracture is present near the base of the sample. Small divisions of scale are centimeters.

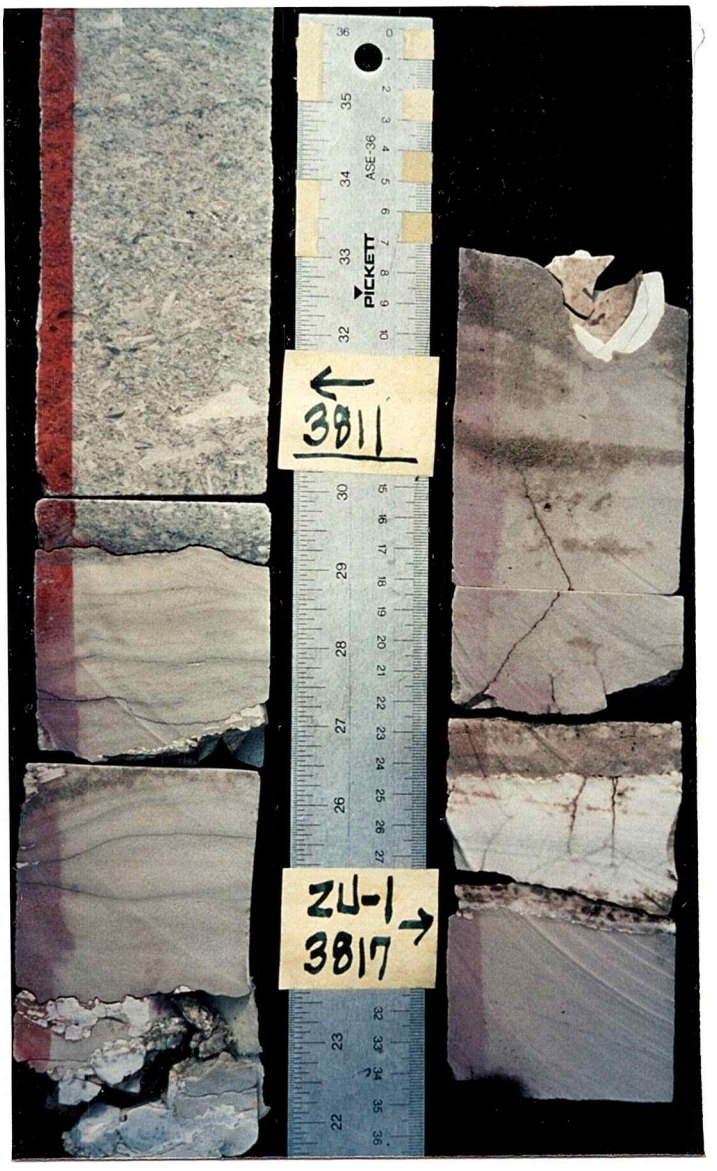

Figure 7.26 Slabbed cores from the upper cherty dolomitic limestone in the Braden-Zenith ZU-1 core (#*19*, depths 3810-3811.5 and 3816-17 ft) from eastern Stafford County (11-T.24S.-R.11W.). The coarse-grained bryozoan-rich packstone (3811 ft, to top of core) displays graded bedding and an erosional base, indicating it was probably deposited by a density current in a single depositional episode. Immediately below the graded packstone is a thin, wavy-bedded, dolomitized mudstone with laminations suggesting small-scale hummocky cross-stratification, which may be a feature of storm deposition. Inasmuch as muds do not tend to display cross-stratification, the presence of this bedding feature also implies that mudstone may have originally been pelletal silt or sand before the finer features of the rock were destroyed by dolomitization. The core on the right side of the photograph illustrates the homogeneous (structureless) bedding that typifies most of the upper cherty dolomitic limestone at this locality. Marks on ruler are inches (left) and centimeters (right).

Figure 7.27 Polished slab of a cross-bedded, chertified packstone from the upper cherty dolomitic limestone subunit in the Braden-Zenith ZU-1 core (*#19*, depth 3821 ft) from eastern Stafford County (11-T.24S.-R.11W.). Microscopic examination indicates little wear on the skeletal fragments, indicating the event that deposited this bed (probably a storm) was not long-lived or exceedingly intense. This bed occurs approximately 10 ft (3 m) below the graded packstone illustrated in Figure 7.26.

packstone or grainstone beds. These beds are less well-developed farther south, because fine-grained cherty dolomites are more the norm in this subunit in Kiowa, Pratt, Comanche, and Barber counties.

A breccia, similar to that observed in the lower cherty dolomitic limestone immediately below the upper limestone in the Braden-Zenith ZU-3 core (*#20*) (Figure 7.19), is also present in the upper cherty dolomitic limestone at the Braden-Zenith ZU-1 core (*#19*) at 3793 ft (Figure 7.28). This breccia is approximately 4 inches (10 cm)

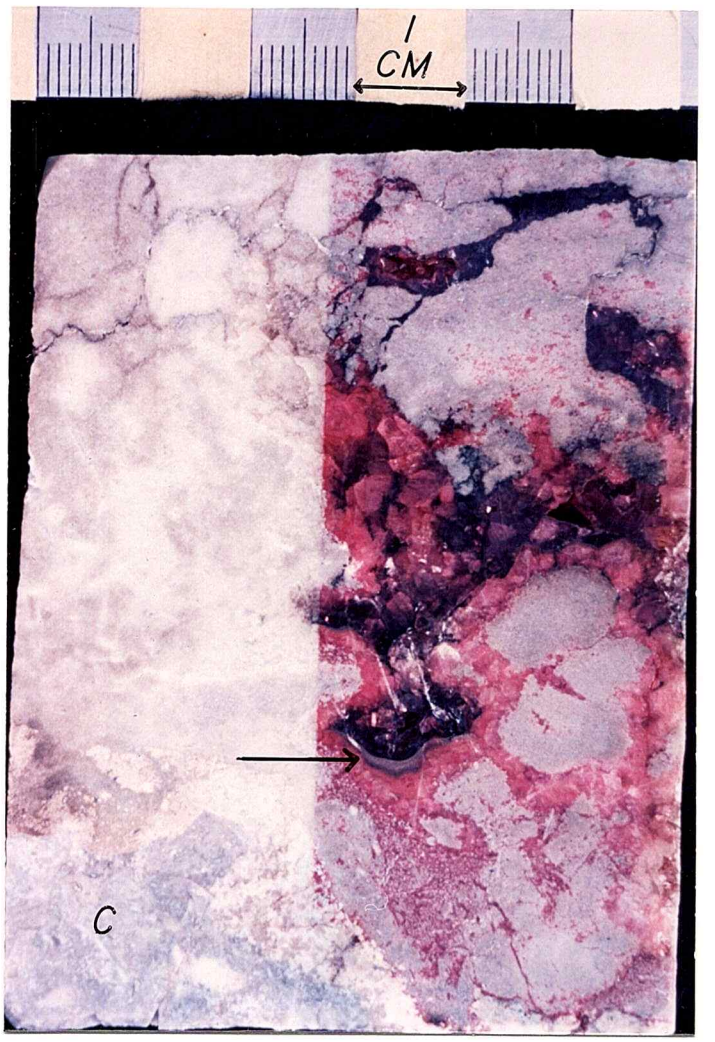

Figure 7.28 Polished slab of a solution breccia developed in a dolomitized mudstone within the upper cherty dolomitic limestone (depth 3793 ft) at the Braden Zenith ZU-1 core (*#19*) in eastern Stafford County (11-T.24S.-R.11W.). Right half of the sample is stained by potassium ferricyanide and Alizarin Red-S. Two generations of calcite cement infills the void between breccia clasts -- a cloudy, coarsely crystalline spar, then a clear, coarsely crystalline spar. Internal sediment (arrow) is present between the two cements. The upper part of a chert clast (**C**, truncated at the base of the sample) consists of an ostracode grainstone. Note that individual dolomite clasts have ill-defined margins. Thin-section analysis indicates this is due to euhedral dolomite rhombs protruding into, and floating within, the interstitial spar.

thick, contains angular, cobble-size clasts in a fitted fabric, and displays abundant coarse interstitial spar cement.

Interpretations

The transitional nature of the contact between the upper limestone and the upper cherty dolomitic limestone, as exemplified by the Braden-Zenith ZU-1 (*#19*) and ZU-3 (*#20*) cores (see Appendix IV) implies sea level gradually rose. The resultant deeper water and lower-energy depositional environments were less conducive to the development of shoals and banks of skeletal debris. In all probability, the transition from the upper limestone to the upper cherty dolomitic limestone was similar to that from the basal limestone to the lower cherty dolomitic limestone, essentially continuous deposition.

The contorted bedding in the Sinclair-Prairie #1 Alice Oldfather core (*#35*) in western Barber County (see Figure 7.21; Appendix IV) is interpreted to be a slump feature. It is present very near the base of the upper cherty dolomitic limestone. Inasmuch as the lowermost core fragment in this feature includes a crinoidal wackestone that may represent the top of the underlying upper limestone, this slumping can be taken as additional evidence that deposition was continuous between the upper limestone and the upper cherty dolomitic limestone.

The distribution of argillaceous facies in this subunit (Figure 7.22) indicates that the Chautauqua arch in southeastern Kansas (see Figure 1.2) may have been a positive structural element that was undergoing erosion toward the end of Viola deposition. The siliciclastic mud incorporated into the argillaceous mudstones might have been transported as suspended load in near-surface, turbulent waters. The absence of argillaceous beds in the upper cherty dolomitic limestone farther north in an outlier in eastern Stafford County indicates that at this time the Ancestral Central

Kansas uplift may have not been actively eroding and contributing fine-grained siliciclastic material to the Viola. A southerly shift of the crest of the Central Kansas arch was inferred by comparison of the isopach of the basal limestone (Figure 5.7) with the subcrop (Figure 5.6) and worm's-eye-view maps (Figure 4.4; see discussion at end of section on regional mapping). The contribution of siliciclastics to the upper cherty dolomitic limestone subunit from the south and east, together with the apparent lack of contribution from the Ancestral Central Kansas uplift in the north and west, is consistent with the interpretation that the Chautauqua arch was the dominant tectonic feature near the close of Viola deposition.

As water depths increased and wave action concomitantly decreased, lime mudstone became the dominant lithology over the wackestones and thin beds of packstones that characterize the lower part of the upper cherty dolomitic limestone. The thin graded wackestones and packstones in the northern part of the study area probably signal the proximity of crinoid-bryozoan shoals that typify deposition in the upper limestone subunit. The thin wackestones and packstones within the upper cherty dolomitic limestone are interpreted to represent shedding of coarse-grained skeletal debris from shoals into adjacent deeper waters by density currents, possibly during storms. Imbrication of shell fragments in the thin packstones also may indicate episodic current activity. Skeletal fragments with micrite rims present in graded grainstones contained within the upper cherty dolomitic limestone (Figure 7.26) were presumably washed in from shallower water by storms.

The "coarse crystalline limestone" beds that correlate to non-porous zones in the upper cherty dolomitic limestone in Edwards, Pawnee, and Stafford counties are probably crinoidal packstones or grainstones that either represent minor shoals, or perhaps tongues of coarse-grained debris shed off into relatively deeper water from nearby shoals. Their absence farther south suggests concomitant minor uplift of the

southern flank of the Ancestral Central Kansas uplift and the northern part of the Pratt anticline during deposition of the upper cherty dolomitic limestone. Detailed mapping of the stratigraphic distribution of these beds in the inliers of upper cherty dolomitic limestone in Edwards, Stafford, and Pawnee counties and to the west may give more detailed insight into the facies, depositional environments, and paleocurrents in the basin near the close of Viola deposition.

Graded bedding in the packstones (Figure 7.26) implies deposition above storm wave-base (cf., Leckie and Krystinik, 1989, Table 1; Jennette and Pryor, 1993), whereas the presence of small-scale hummocky cross-stratification (Figure 7.26) indicates rapid deposition from suspension during conditions of decreasing oscillatory or unidirectional currents (Harms and others, 1975; Duke, 1990; Duke and others, 1991). Depositional structures such as ripple-drift cross-lamination and asymmetric small-scale hummocky cross-stratification have been used as diagnostic features for "distal" deposition by storms in siltstones in Upper Ordovician (Cincinnatian) strata of southwestern Ohio (Jennette and Pryor, 1993).

The dominance of structureless mudstones near the crest of the Central Kansas arch and wavy-bedded mudstones away from the arch (Figure 7.22) suggests a subtle influence of the arch during deposition of both the lower and upper cherty dolomitic limestone subunits. More intense bioturbation could have been characteristic of the relatively shallower or more nutrient-rich depositional environments near the crest of the arch, whereas less bioturbation may have occurred in relatively deeper water farther in the basin. Other alternatives may also be possible in that the structureless mudstones near the crest of the arch perhaps could represent more rapid deposition. More detailed correlations and mapping focusing on the internal stratigraphy of both cherty dolomitic limestones may lend insight to the interplay of tectonics and sedimentation during deposition of these two subunits.

The breccia described in Braden-Zenith ZU-1 (*#19*) (Figure 7.28), like similar breccias described near the top of the lower cherty dolomitic limestone (see previous discussion) is another "intrastratal karst" (Quinlan, 1972) or "intraformational breccias" (Mussman and Read, 1986). It possibly signifies that the upper cherty dolomitic limestone in the vicinity of the Ancestral Central Kansas uplift was occasionally exposed and chemically weathered. Inasmuch as these solution breccias were not observed elsewhere (partly due to lack of adequate core control), it is unclear whether this feature represents local tectonic uplift or a more regional uplift or sea-level drop.

UPPER CONTACT OF THE VIOLA

Observations

Several slightly angular unconformities separate the Viola Formation from overlying rock units. The worm's-eye-view map (Figure 4.4) shows that the ages of the rock immediately above the Viola range from Late Ordovician for the Maquoketa Formation to Early Pennsylvanian. The subcrop map (Figure 5.6) shows that any of the Viola subunits may be present at the top of the Viola, depending to the degree to which the Viola is beveled by these unconformities. Generally, the Viola displays no marked effects associated with these angular unconformities except in the vicinity of the southern flank of the Central Kansas uplift where residual chert breccias are commonly present immediately below the basal Pennsylvanian angular unconformity (Adkison, 1972; Bornemann and others, 1982; Bornemann and Doveton, 1983). In all cases where cores recovered the upper contact of the Viola in the study area the contact is sharp and abrupt. Locally, breccia is present just below the contact with the

Chattanooga Shale in Barber County (Figure 7.29).

The contact between the Viola and the Maquoketa on top of the Central Kansas arch shows marked evidence of interrupted deposition and early lithification of the Viola. Individual grains in a packstone bed of the basal limestone are truncated and packstone lithoclasts of the basal limestone are present in the silty dolomitic mudstone of the Maquoketa Formation at the Midcontinent Marine #1 South Hilger well (#29) in southeastern Reno County (Figure 7.30). This locality is near the downdip limit of the Maquoketa on the southwestern flank of the Central Kansas arch. Secondary pyrite mineralization is common along this contact at this locality.

Farther up on the northern flank of the arch at the Damac #1 Sandra Allen well (#2) in northern McPherson County, clays and blocky structures atypical of any lithology encountered elsewhere in the study are developed in the lower cherty dolomitic limestone just below the upper contact of the Viola (Figures 7.31, 7.32). Lithoclasts of packstone and wackestone that were derived from the basal limestone and lower cherty dolomitic limestone subunits are also present in the Maquoketa Formation immediately above the contact (Figure 7.32).

Interpretation

The contact at the Damac #1 Sandra Allen well (#2) in northern McPherson County is interpreted to be a thin soil zone developed on the lower cherty dolomitic limestone directly beneath the Maquoketa Formation (Figures 7.31, 7.32). Approximately 2 in (5 cm) below the contact are clayey cutans (veneers of clay approximately 1 mm thick; see Retallack, 1988), which are developed between structures that are interpreted to be compressed peds. Peds are aggregates or weak lumps of soil (cf. Retallack, 1988). In this case, they are subangular and blocky, 0.5 to 1 cm in size. Pedotubules (irregularly shaped structures filled with material foreign to

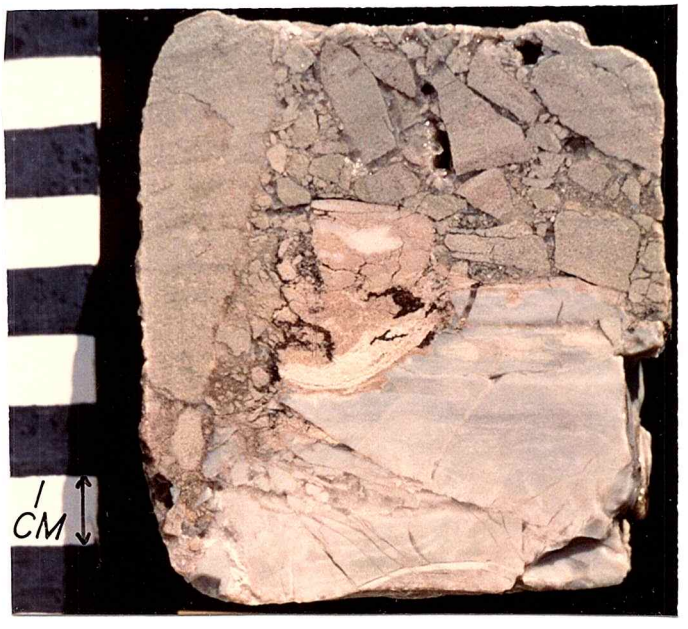

Figure 7.29 Breccia developed in the upper cherty dolomitic limestone immediately below the angular unconformity beneath the Devonian-Mississippian Chattanooga Shale at the Sinclair-Prairie #4 G. Oldfather well (*#34*, 4328 ft depth) in Barber County (7-T.31S.-R.14W.). Clasts of dolomitic mudstone and chert are set in a matrix of calcite spar. Chertification and dolomitization of the mudstone occurred before the brecciation.

the rock itself; Retallack, 1988), 1 to 4 cm in diameter, are also present and filled with light-brown clay. The presence of cutans, peds, and pedotubules in a zone in which the parent material is slightly weathered indicates this is a poorly developed paleosol (i.e., an *inceptisol* according to Retallack, 1988).

Incipient soil development at the top of the Viola on the Central Kansas arch observed in this study implies a brief period of subaerial exposure before Maquoketa deposition. Lithoclasts of packstone derived from the basal limestone subunit and wackestone derived from the lower cherty dolomitic limestone subunit found within the Maquoketa just above its basal contact with the Viola indicate early lithification before the transgression responsible for the Maquoketa Formation.

Figure 7.30 Polished slab showing contact (arrow) of the Viola Formation (basal limestone subunit) with the overlying Maquoketa Formation (4029.2 ft depth) at the Midcontinent Marine #1 South Hilger well (#*29*) in southeastern Reno County (9-T.26S.-R.4W.). At this locality silty dolomitic shale (dark brown) of the Maquoketa Formation overlies dolomitized lime packstone (gray) of the Viola Formation. Secondary pyrite mineralization permeates the contact, and a lithoclast of packstone (**L**) immediately above the contact (see arrow).

Figure 7.31 Contact of the Viola Formation (lower cherty dolomitic limestone) with the overlying Maquoketa Formation (3439 ft depth) at the Damac #1 Sandra Allen well (#2) in northern McPherson County (7-T.17S.-R.3W.). The contact of the Viola with the Maquoketa is at **A**. Lithoclasts of chertified packstone overlie this contact (**B**). Secondary pyrite (**C**) is also along the contact. Below the contact are clay cutans (see Retallack, 1988), which are developed between structures that are interpreted to be compressed peds (**D**), and pedotubules filled with clay (**E**). The cutans, peds, and pedotubules indicate the B horizon of a poorly developed paleosol, an *inceptisol* of Retallack (1988). Small divisions of scale are in centimeters.

Figure 7.32 Polished slab (depth 3439.2 ft) from the Damac #1 Sandra Allen well (#2) in northern McPherson County (7-T.17S.-R.3W.) showing clay cutans (**C**)(also see **D** in Figure 7.31) around compressed peds (**P**) developed in the lower cherty dolomitic limestone of the Viola.

The pyrite-rich zone in the Midcontinent Marine #1 South Hilger well (*#29*) in southeastern Reno County (Figure 7.30) is consistent with observations by Wright and Meyers (1981) who noted a pyrite-laden clastic zone between the Maquoketa and Viola in the Forest City basin in northeastern Kansas. Wright and Meyers (1981) also interpreted the contact as an unconformity.

The breccia in the upper cherty dolomitic limestone immediately below the angular unconformity beneath the Chattanooga Shale at the Sinclair-Prairie #4 G. Oldfather well (*#34*) in Barber County is interpreted to be a karstic breccia associated with periods of exposure prior to deposition of the Chattanooga Shale. The angular and fitted clasts of dolomitic lime mudstone set in a matrix of calcite spar is similar to the intraformational breccias observed in the Braden-Zenith ZU-1 (*#19*) and Braden-Zenith ZU-3 (*#20*) cores (Figures 7.19, 7.28, 7.29). The calcite spar cementing the clasts contains no dolomite, which implies that the dolomitization occurred before significant burial.

The slight angular unconformity that separates the Viola from the overlying Upper Ordovician Maquoketa Shale corresponds to a period of subaerial exposure. Localized soil development and dolomite-clast solution breccias occurring just below this unconformity and lithoclasts of Viola packstones incorporated in the basal Maquoketa indicate the Viola was lithified and dolomitized before the Maquoketa was deposited.

DISCUSSION

A generalized depositional model by St. Clair (1982) envisaged the packstones and grainstones of the basal limestone as representing the most open-marine and high-energy depositional environments. Landward of this facies belt of well-washed shoals would be semi-restricted areas of shallower water in which wackestones were

synchronously being deposited. Farther landward in yet shallower water would be the more restricted and quieter depositional environment of the mudstone facies that characterizes the lower cherty dolomitic limestone subunit. The skeletal shoals would buffer waves and currents of the open sea, and to the lee of these shoals would be the quiet-water, biotically stressed environments. Similar depositional relationships were inferred for the grain-dominated facies of the upper limestone and the mud-dominated facies of the upper cherty dolomitic limestone.

Vertical and lateral stratigraphic relationships and faunal content suggest that the packstones and grainstones of the basal and upper limestone subunits are the product of a nearshore facies belt of shoal and shoreface carbonate sands with only a narrow, poorly developed area of lagoonal and peritidal sediments behind it (Figure 7.33). In slightly deeper waters between the shoals and farther offshore, skeletal debris derived from the shoals, possibly during storms, was mixed with indigenous mudstone to form wackestones. Farther seaward, in deeper, quieter water mudstones dominated. The bathymetric position of the mudstones may have also influenced the degree of bioturbation; in relatively shallower and more oxygenated waters within the mudstone facies belt, intense bioturbation destroyed much of the original bedding of the mudstones. Farther into the basin, deeper and less-oxygenated waters could not support a thriving infauna; laminated mudstones were consequently preserved. Erosion on top of the broad tectonic arches adjacent to the basin provided a variable component of argillaceous material in the basinal depositional environments. Further studies of the available biotic constituents in the mudstones and associated wackestones may establish if environments associated with these lithologies were significantly stressed, although the limited core available may prohibit obtaining sufficient sampling populations. Size determinations of selected biotic constituents may be also be useful for determining the biotic productivity of these environments.

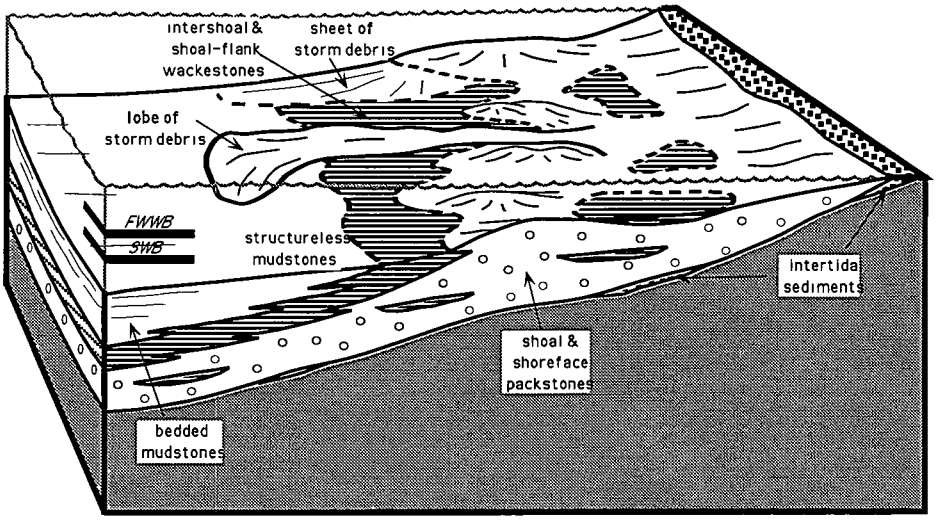

DEPOSITIONAL MODEL of VIOLA FORMATION

Figure 7.33 Depositional model of the lithofacies of the Viola Formation. A narrow intertidal zone (stippled) is landward of a shoreface-shoal complex of skeletal sands (open-circle pattern). Offshore of the skeletal sands, and in intershoal areas, are deeper, quieter waters in which wackestones (lined) are being deposited. Farther offshore, mudstones dominate. Lobes (mass-transport deposits) and sheets of skeletal sands deposited by storms extend into the mudstone facies of the basin. Normally, a burrowing infauna destroys bedding in both the shoreface-shoal complex and in the nearby wackestones and mudstones. Original bedding laminations have the highest potential of being preserved in mudstones deposited in the deepest waters. In a transgressive sequence, sediments from the narrow, sheltered intertidal zone are reworked and largely destroyed by waves and currents in the higher-energy shoreface-shoal complex. FWWB is fair-weather wave base; SWB is storm wave base.

The general model depicted in Figure 7.33 resembles the facies belts portrayed in humid carbonate-ramp depositional-sequence model presented in Handford and Loucks (1993) except in the Viola model more lateral continuity of individual lithofacies is indicated, and mud-supported lithofacies characteristic of offshore depositional environments do not markedly thin basinward. These characteristics may indicate relatively sluggish rates of sea-level rise in the Viola. In this model, a narrow intertidal zone was present on the landward side of a shoreface-shoal complex of

skeletal sands. A depositional record of this intertidal zone, however, was only rarely preserved in the transgressive deposits of the Viola Formation because the intertidal sediments were reworked by waves and currents that dominated in the shoreward part of the shoreface-shoal complex. The shoreface-shoal complex was responsible for the packstones and grainstones that typify the basal and upper limestone subunits. Skeletal sand washed off the shoals into muddy, deeper swales adjacent to and within the shoal complex. If sufficiently thick, these sands could be preserved as graded or cross-bedded packstone beds within a mudstone-dominated sequence. Bioturbation could also mix these coarser grained beds with the surrounding carbonate muds, thereby forming wackestones. Farther offshore, mudstones dominated. Once deposited, skeletal sands were bioturbated, as were the lime muds in deeper water, until their original bedding was destroyed. In deepest waters, bioturbation was less intense and bedding laminations were therefore preserved in the mudstones. Lobes of skeletal sands deposited by storms locally extended into the lime-mudstone depositional environments farther in the basin.

Two similar upward-deepening depositional cycles can be discerned in the Viola Formation. These cycles are defined by the basal limestone subunit and lower cherty dolomitic limestone subunit, followed by the upper limestone subunit and the upper cherty dolomitic limestone subunit. An hiatus, reflecting a brief drop in relative sea level separates these cycles. The hiatus is expressed by incipient karstification at the top of the lower cherty dolomitic limestone in the northern part of the study area. Both of the cycles are extensive, being present on structural highs, such as the Pratt anticline and Central Kansas arch, as well as adjacent basinal areas. Although these two cycles are spread across the entire study area, the geographic area studied is still too limited to determine if these cycles reflect changes in eustatic sea level, or just relative sea level due to tectonic movements of the continental margin of the

Laurentian plate.

The magnitude of relative sea-level fluctuation is unclear because it is difficult to precisely estimate the water depths that are responsible for the facies changes represented by the Viola subunits. The basal and upper limestone subunits, however, probably represent deposition near sea level, probably at or above fair-weather wave base, and certainly above storm-wave base. Mapping on the Pratt anticline indicates that the western flank of this anticline, where lime muds were deposited, was downdropped 60 ft (20 m) relative to its crest, where skeletal sands were deposited. This indicates that perhaps a water depth of not more that 60 ft (20 m) is sufficient to induce the consistent quiet-water conditions favorable for development of the facies represented by the upper and lower cherty dolomitic limestone subunits. If 60 ft (20 m) approximates the relative magnitude of sea-level fluctuation during Viola deposition it is appreciably less than the eustatic fluctuations caused by glacial pulses during the Holocene (approximately 325-350 ft [100-110 m]; Flint, 1971, p. 321; Williams, 1988) and those inferred for cyclothems in the Pennsylvanian System in Kansas (approximately 230 ft [70 m]; Heckel, 1977; Watney and others, 1991).

The duration of the cycles of the Viola Formation is difficult to estimate precisely. The late Edenian and early Maysvillian age of the Viola on the basis of conodonts (see Sweet, 1992) covers a span of time of approximately 5 m.y. (see Figure 2.1), therefore an estimate of 2.5 m.y. duration for each cycle is indicated. According to periodicity scales in Vail and others (1977) and Van Wagoner and others (1990), these would be third-order cycles (i.e., 1 to 10 m.y.). The period for a third-order cycle is excessively long for a glacial-eustatic driving mechanism, and tectonic or other eustatic processes are usually suggested as the ultimate driving mechanisms for such cycles (Goldhammer and others, 1991).

Withdrawal and recharge of water in the world ocean by alternate

accumulation and melting of continental ice caps has been invoked to explain fourth-order cycles (0.1 to 1 m.y.; Vail and others, 1977; Van Wagoner and others, 1990), but short third-order cycles of 1- to 2-m.y. duration can also be explained by either glacial-eustacy and changes in volume of mid-oceanic ridges (Miall, 1984; p. 346, 357). Continental glaciation in the Late Ordovician may have started as early as late Caradocian time (Bennacef and others, 1971), and hence would be contemporaneous with Viola deposition (see Figure 2.1).

Fourth-order cycles are likely imbedded within each Viola subunit, but present core control makes differentiation of these cycles from spurious episodic events such as storm deposition or tectonism extremely difficult. Correlation of fining- or coarsening-upward bedding in the basal and upper limestones in the study area, even in localities with close well control, could not be done with any confidence. Similarly, comparison of cores of the lower and upper cherty dolomitic limestone subunits between closely spaced wells such as the Braden-Zenith ZU-1 (*#19*) and Braden-Zenith ZU-3 (*#20*) wells (separated by 3900 ft [1200 m]) indicates no consistent correlation of bedding packages within these Viola subunits.

A minimum averaged rate of deposition of 0.6 in/1000 yr. (150 mm/1000 yr.) for the sequence comprising the basal limestone and the lower cherty dolomitic limestone can be calculated by dividing the maximum combined isopach of both subunits (i.e., 130 ft [40 m] at T.25S.-R.17W.; see Figures 5.7, 5.11) by 2.5 m.y. This rate is compatible with other rates of deposition for platform carbonates in the geologic record (Enos, 1991, Table 3). Relatively deep erosion at the top of the Viola precludes calculation of an average rate of deposition for the sequence comprising the upper limestone and upper cherty dolomitic limestone.

Chapter 8

DIAGENESIS OF THE VIOLA FORMATION

INTRODUCTION

The first section of this chapter, "Dolomitization and Petrophysical Properties of the Viola Formation" examines the correspondence of porosity and permeability with the degree of dolomitization in the Viola subunits. The presence of dolomite in the Viola subunits affects its porosity and permeability, and these petrophysical characteristics vary with the extent of dolomitization. An alternate approach to porosity development in the Viola subunits is also presented in Appendix VI, where an apparent variation of porosity with thickness in the basal and upper limestone subunits is examined.

Core and log analyses hint that the distribution of dolomite in the Viola Formation is variable. As a follow-on, the spatial and stratigraphic distribution of dolomite in the Viola subunits is explored in detail using logs of drill cuttings in the section titled "Regional Distribution of Dolomite". Resultant maps of dolomite distribution in the Viola subunits are also supplemented by wireline well-log analyses in key geographic localities. The patterns of dolomitization in the Viola subunits also are compared to tectonic features present during and after deposition of the Viola, and to the stratigraphic framework developed in previous chapters. The comparison of the distribution of dolomite to tectonic features and the stratigraphic framework gives potentially important clues to the timing and movement of dolomitizing fluids and ultimately to the diagenetic environments responsible for the dolomitization.

The next section of this chapter, "Diagenetic Sequences", summarizes the

sequence of diagenetic events in grain-supported versus mud-supported lithologies in the Viola. Pertinent petrographic and stable-isotope data that aid in understanding the relative timing and interpreted environment of the major diagenetic events that have affected the Viola are discussed and summarized in the following section titled "Diagenetic Events".

A summary and interpretation of the results of the isotopic analyses and the petrographic observations and stratigraphic relationships are presented in "Discussion", the final part of this chapter. Most emphasis is directed to the timing and environment(s) of dolomitization, inasmuch as this geologic process has profound effects on reservoir characteristics of the Viola Formation, as well as other prominent carbonate reservoir rocks in the midcontinent.

DOLOMITIZATION AND PETROPHYSICAL PROPERTIES

Estimations of porosity and dolomite content in core descriptions (Appendix IV) indicate that porosity is best developed where the Viola subunits have been dolomitized. Core analyses for porosity and permeability can also be compared with the degree of dolomitization recorded during core descriptions. Crossplotted porosity and permeability information for the basal and upper limestones from the Northern Natural Gas #1 Caldwell (2-T.20S.-R.8W.), Braden-Zenith ZU-1 (11-T.24S.-R.11W.), and Braden-Zenith ZU-3 (11-T.24S.-R.11W.; see Figure 8.1A, B) indicates that partly dolomitized rocks within the basal and upper limestone subunits generally have greater porosity than those that are undolomitized. Permeability apparently is not significantly changed with dolomitization in these grain-supported lithologies. A breakdown of lithologies of these cores according to whether the sample analyzed is a

Figure 8.1 Porosity-permeability crossplots for basal limestone and upper limestone subunits, from cores obtained from NNG #1 Caldwell (*#12*, 2-T.20S.-R.8W.), Braden-Zenith ZU-1 (*#19*, 11-T.24S.-R.11W.), and Braden-Zenith ZU-3 (*#20*, 11-T.24S.-R.11W.), and Champlin #8 Speck (*#10*, 18-T.20S.-R.8W.). Samples in the upper diagram (A) are differentiated by presence of dolomitization, according to core descriptions in Appendix IV. No more than 25% dolomite was noted in any of the samples. Samples in the lower diagram (B) are differentiated, by use of core descriptions, as being either grain-supported (i.e., packstone or grainstone) or mud-supported (i.e., wackestone or mudstone). Each data point represents analyses for one foot of core. Wackestones generally have less porosity, but show no more propensity to be dolomitized than the packstones. Petrophysical data were obtained by Core Laboratories, Inc. (Dallas, TX) and are archived in files at the Kansas Geological Survey. Any sample below the detection limit of 0.1 millidarcies is displayed at the base of the graph.

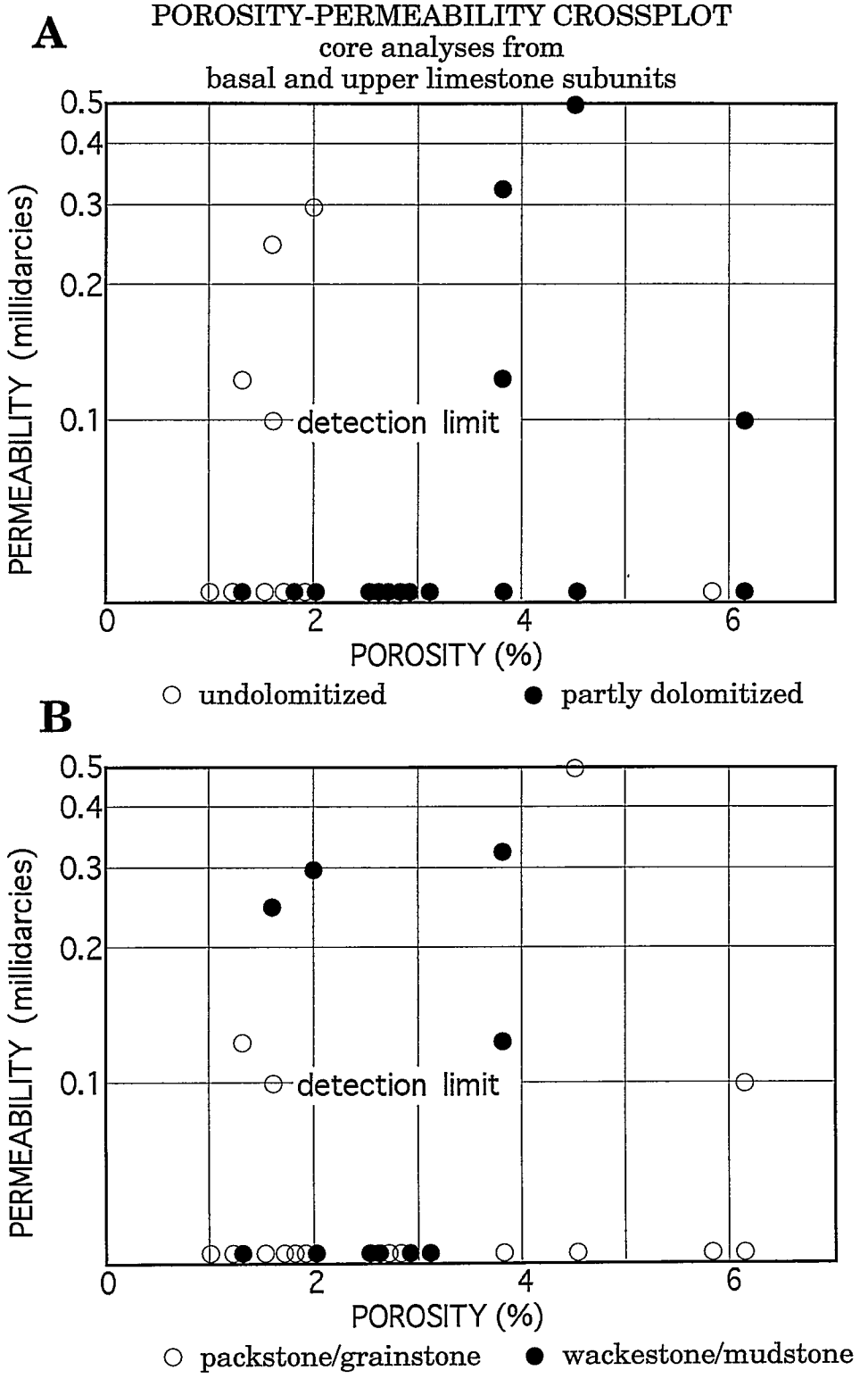
A
POROSITY-PERMEABILITY CROSSPLOT
core analyses from
basal and upper limestone subunits
PERMEABILITY (millidarcies)
0.5
0.4
0.3
0.2
0.1
detection limit
0
2
4
6
POROSITY (%)
○ undolomitized
● partly dolomitized
B
PERMEABILITY (millidarcies)
0.5
0.4
0.3
0.2
0.1
detection limit
0
2
4
6
POROSITY (%)
○ packstone/grainstone
● wackestone/mudstone

mud-poor packstone/grainstone versus a wackestone (Figure 8.1A) also indicates wackestones in the basal and upper limestone subunits have no more marked propensity to be dolomitized than the grain-supported carbonates.

Comparison of core-derived porosity and permeability data of the basal and upper limestones with that of the lower and upper cherty dolomitic limestones (Figure 8.2) indicate that the basal and upper limestones are relatively nonporous and impermeable. Samples with less than 6% porosity generally have less than 1 millidarcy permeability.

Significantly dolomitized mudstones and wackestones (Figure 8.2) generally have significant porosity, either intercrystalline, vuggy, or moldic (Appendix IV). Intercrystalline porosity is usually microscopic and developed between dolomite rhombs. Molds are mostly megascopic, commonly after mollusk fragments. Illustrations of typical pore types are presented in the section on diagenetic events.

REGIONAL DISTRIBUTION OF DOLOMITE

Introduction

A map of the limestone/dolomite ratio for the entire Viola Formation over the state of Kansas, from Blair and Berendsen (1988), shows a heavily dolomitized area immediately north and west of the Chautauqua arch (Figure 8.3). The spatial association of this dolomite with the Chautauqua arch implies the arch exerted control in the genesis of much of the dolomite in the Viola. The Ancestral Central Kansas uplift does not have a similar aureole of dolomite associated with it, therefore implying that it did not localize dolomitizing fluids and possibly was not a major uplift preceding or contemporaneous with Viola dolomitization.

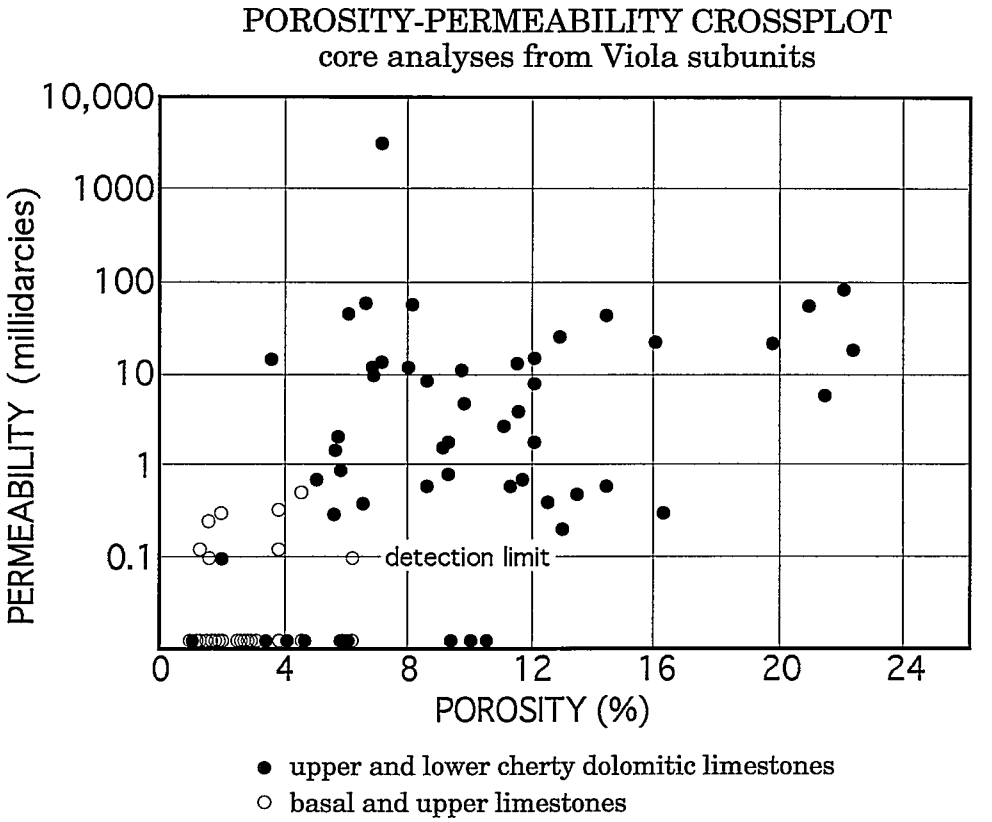

Figure 8.2 Porosity-permeability crossplot for upper and lower cherty dolomitic limestone subunits, from cores obtained from Braden-Zenith ZU-1 (*#19*, 11-T.24S.-R.11W.), and Braden-Zenith ZU-3 (*#20*, 11-T.24S.-R.11W.), together with data from Figure 8.1 for the basal and upper limestone subunits. Petrophysical data were obtained by Core Laboratories, Inc. (Dallas, TX) and are archived in files at the Kansas Geological Survey. Any sample below the detection limit of 0.1 millidarcies is displayed at the base of the graph. An increase in permeability with dolomitization, without an attendant increase in porosity is probably due to the euhedral shape and uniform size of the dolomite rhombs (see Wardlaw, 1976). See text for discussion.

The limestone/dolomite-ratio map (Figure 8.3) was constructed using a ratio of the total footage of the Viola that could be classified as either dolomite or limestone. Rather than an expression of the total thickness of dolomite within the entire Viola Formation, this map also reflects the thickness and distribution of its subunits. For example, the east-west trend of dolomite extending across southern Stafford County and a northeast-southwest trend of dolomite in eastern McPherson County are

Figure 8.3 Limestone/dolomite ratio for entire Viola Formation (from Blair and Berendsen, 1988). This map is based on a control of one well per township. Well-cuttings sample logs, supplemented with visual inspection of offsets of curves in neutron-density logs, provided an approximate stratigraphic determination of dolomite versus limestone. One well per township was used in producing the map; no record is available for petrophysical parameters used (Pieter Berendsen, Kansas Geological Survey, Lawrence, KS, personal communication, December, 1994).

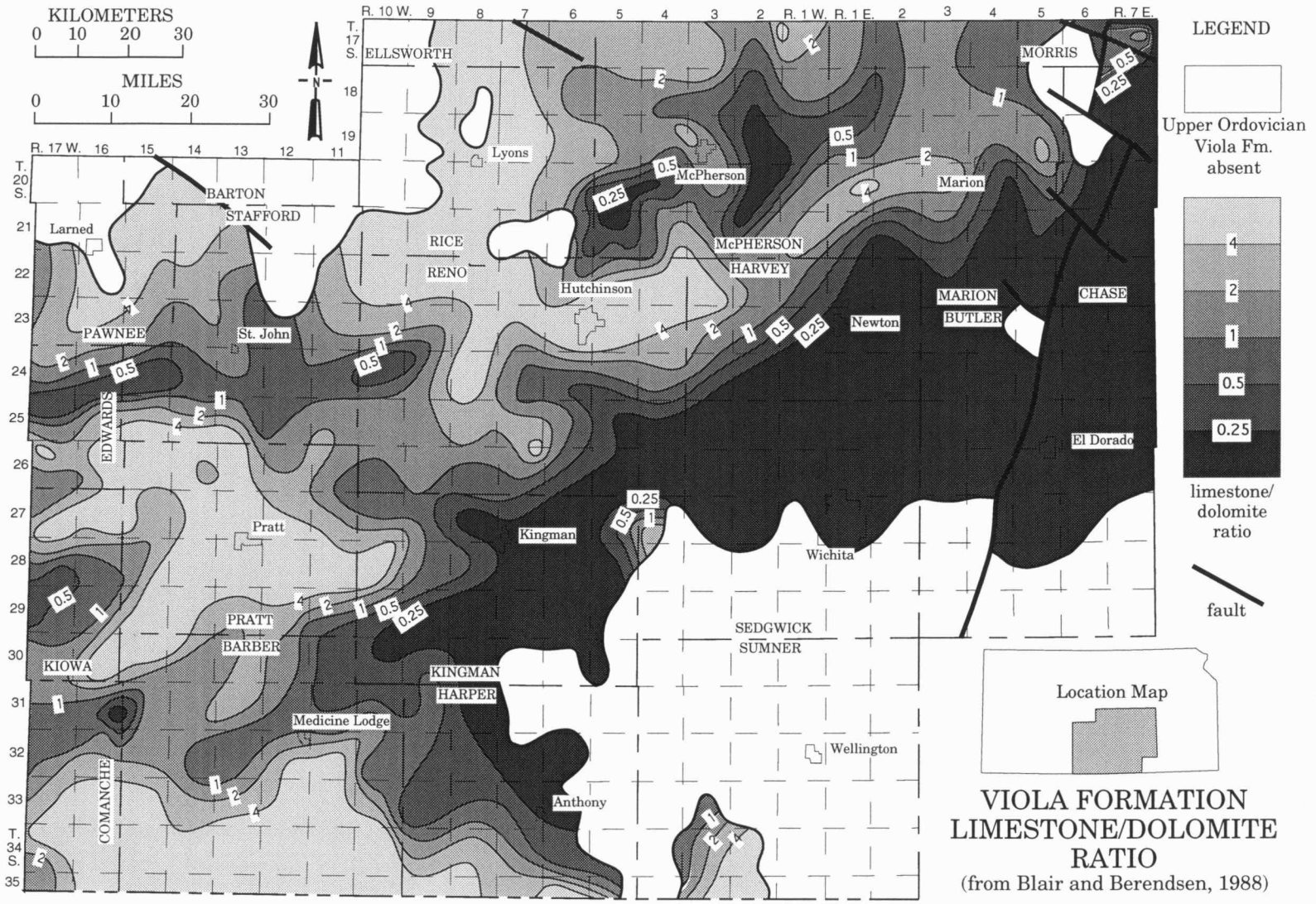

VIOLA FORMATION LIMESTONE/DOLOMITE RATIO

(from Blair and Berendsen, 1988)

probably due to the presence of synclines in these localities in which significant thicknesses of the cherty dolomitic limestone subunits are preserved (see subcrop map in Figure 5.6).

In order to better understand the pattern of dolomitization within the Viola subunits, the general lithology of the subunits was compiled from a series of well-cuttings logs commercially produced by J.D. Davies, which are on file in the Geoscience Data Library at the Kansas Geological Survey (Lawrence, KS). Use of this particular genre of logs (see Figure 8.4) reduces possible inconsistencies and biases inherent in utilizing observations by several different wellsite geologists. Hundreds of these logs are available, so detailed coverage of a large region can be quickly assembled. Wherever possible, only Davies's logs associated with the wells used to create the isopach maps of the Viola subunits were utilized (see Appendix I), thereby enabling a reasonable correlation, by depth, of Viola subunits to the lithology recorded on the Davies's logs. The lithologies of each of the Viola subunits were interpreted to be either limestone, limestone with minor dolomite, dolomite with minor limestone, dolomite, or chert/chert breccia. Results are compiled in Appendix V. Inasmuch as chert is a universal accessory in the lower and upper cherty dolomitic limestone subunits, its presence was not specifically noted, unless it was the sole lithology. Symbols signifying the respective lithologies were in turn superimposed at the well locations on the isopach maps of the individual Viola subunits.

Wireline logs are also used to determine the extent of dolomite and porosity. Neutron-density crossplots (see Schlumberger, 1987, p. 56) are the chief method employed. Lithology can be determined by the neutron-density crossplot method in rocks that can be nominally characterized as simple binary mineralogical compositions of either calcite versus dolomite, calcite versus quartz, or quartz versus dolomite. Lithologic determination of a mixture of quartz, dolomite, and calcite; and more

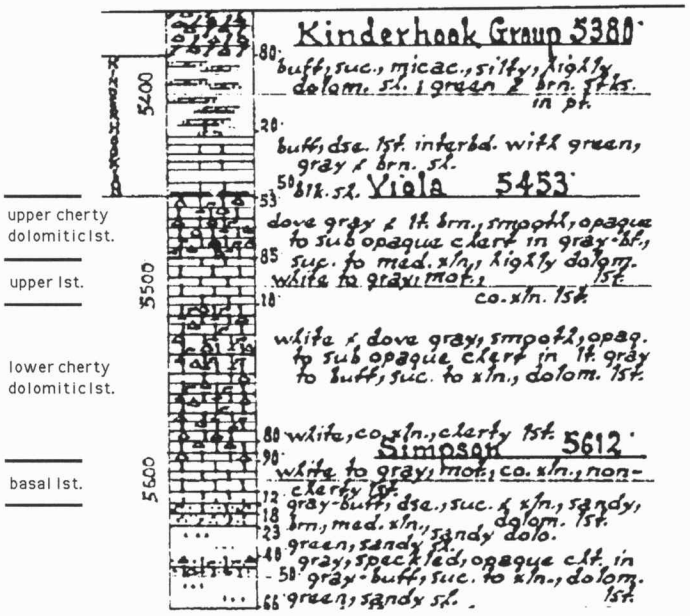

Davies sample log of
Sunray DX #1 M. Gregg
(NW SE, sec. 31-T.33S.-R.16W.)
(with Viola subunits interpreted at left)

Figure 8.4 Davies's sample log of well cuttings from the Sunray DX #1 M. Gregg well (NW SE, 31-T.33S.-R.16W.). The four Viola subunits are distinguishable at left on this log. Lithologies for the Viola subunits were interpreted from several hundred sample logs produced by J.D. Davies in south-central Kansas (see Appendix V). Depths are in feet.

complex mineralogical mixtures by this crossplot method, however, can yield ambiguous results. For example, Doveton (1994, p. 69-70) illustrated that the neutron-density response of cherty dolomites (such as those present in the lower and upper cherty dolomitic limestone subunits) in the Viola Formation somewhat mimics that of pure limestone. Inasmuch as they yield ambiguous lithologic determinations, neutron-density crossplots are not applied to the lower cherty dolomitic limestone and upper cherty dolomitic limestone subunits. Less ambiguity is attendant to log analyses of the basal and upper limestones. Examination of cores (Appendix IV) from

the basal and upper limestone subunits in the study area indicates that quartz and chert are not major components of the basal and upper limestone subunits. The method of the neutron-density crossplot will be useful in examining lithology for these subunits because their lithology only varies between pure limestone and pure dolomite. In turn, porosity can be examined simultaneously with the extent of dolomitization.

Dolomite in the Viola Subunits

The lithology of the basal limestone subunit (Figure 8.5), as distinguished by well cuttings compiled by Davies's logs, reveals extensive dolomitization on the north flank of the Chautauqua arch and confirms the pattern revealed in the map of the limestone/dolomite ratio for the Viola (Figure 8.3). The transition to undolomitized limestone is also abrupt, and only isolated areas of dolomite occur elsewhere. In the northern part of the study area (i.e., McPherson and Marion counties) the off-arch transition from dolomite to limestone occurs close to where this subunit subcrops at the top of the Viola Formation. A weaker trend of dolomitization is also manifest on the western flank of the Pratt anticline in Kiowa, western Pratt, and southeastern Edwards counties, but dolomitization is minor on the Pratt anticline.

A neutron-density crossplot of the basal limestone subunit (Figure 8.6) from a line of wells along the crest of the Central Kansas arch (line a-a', see Figure 8.5) confirms the pattern of decreasing dolomitization away from the updip pinchout of this subunit on the Chautauqua arch. A corresponding decrease in porosity is attendant with the decrease in dolomite. A similar but less pronounced pattern of decreasing dolomitization away from the Chautauqua arch is displayed by a second line of wells (see Figure 8.7) extending westward off the Chautauqua arch (line b-b', see Figure 8.5) in Harper, Barber, and Comanche counties.

The lower cherty dolomitic limestone subunit is more heavily dolomitized along

Figure 8.5 Dominant lithology of Viola Formation basal limestone subunit from Davies's sample logs, superimposed on the isopachous map for this subunit (see Figure 5.7). Lines a-a' and b-b' are the wells used in lithologic determinations by neutron-density crossplots (Figures 8.6, 8.7). See text for discussion. In order that no confusion results with these lithologic determinations versus the informal nomenclature of the Viola subunits, this study follows the precedence of subunit names given in earlier studies (see Bornemann and others, 1982; Bornemann and Doveton, 1983; St. Clair, 1985), thus "basal limestone" refers to the name of the subunit and not necessarily its lithology (see Introduction, Chapter 7).

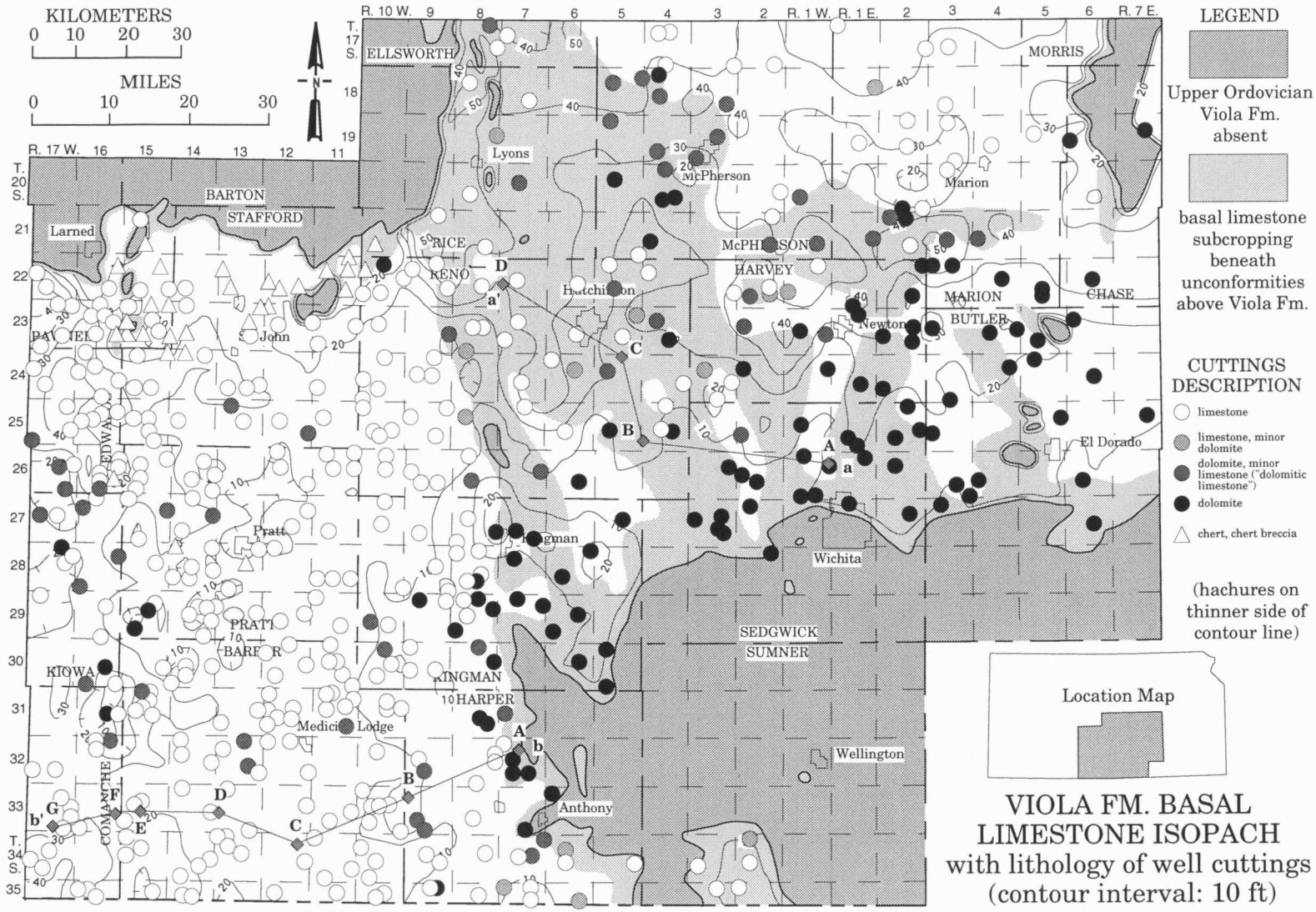

VIOLA FM. BASAL LIMESTONE ISOPACH
with lithology of well cuttings
(contour interval: 10 ft)

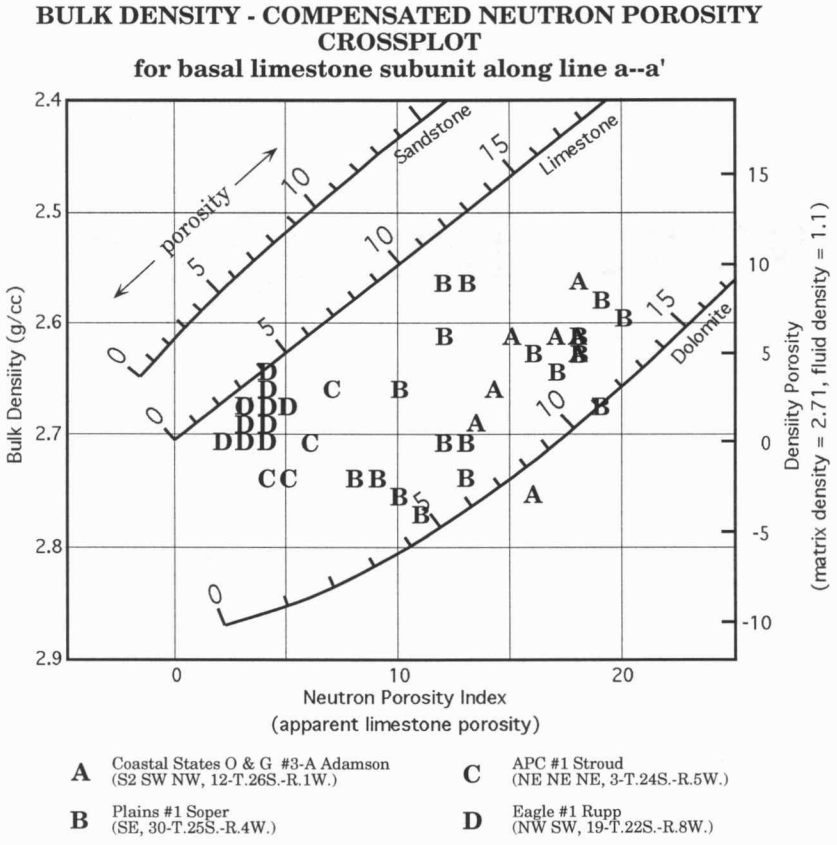

Figure 8.6 Neutron-density crossplot of the basal limestone for wells in a line along the crest of the Chautauqua arch (see line a-a' in Figure 8.5). A decrease in dolomite and porosity away from the subcrop limit on the flank of the arch is evident (i.e., from A toward D). Each letter, which corresponds to the well in the legend, represents a porosity determination by bulk-density and neutron logs for a 2-ft thickness interval. Compositional lines are from Schlumberger (1987, p. 56).

its subcrop on both the northeast and southwest flank of the Central Kansas arch (i.e., respectively western Reno, western Kingman, and western Harper counties; and Marion, Butler, and McPherson counties; Figure 8.8). It is less dolomitic farther from the arch in Comanche and western Barber counties. Chert and chert breccia dominate along the southern flank of the Central Kansas uplift in Stafford and Pawnee counties where this subunit has undergone extensive dissolution beneath the basal

Figure 8.7 Neutron-density crossplot of the basal limestone for wells in a line on the flank of the Chautauqua arch (see line b-b' in Figure 8.5). Dolomitization is not as intense as along line a-a' (see Figures 8.5, 8.6) but nevertheless a decrease in dolomite and porosity away from the subcrop limit on the flank of the arch is evident (i.e., from A toward G). Each letter, which corresponds to the well in the legend, represents a porosity determination by bulk-density and neutron logs for a 2-ft thickness interval. Compositional lines are from Schlumberger (1987, p. 56).

BULK DENSITY - COMPENSATED NEUTRON POROSITY CROSSPLOTS
for basal limestone subunit along line b--b'

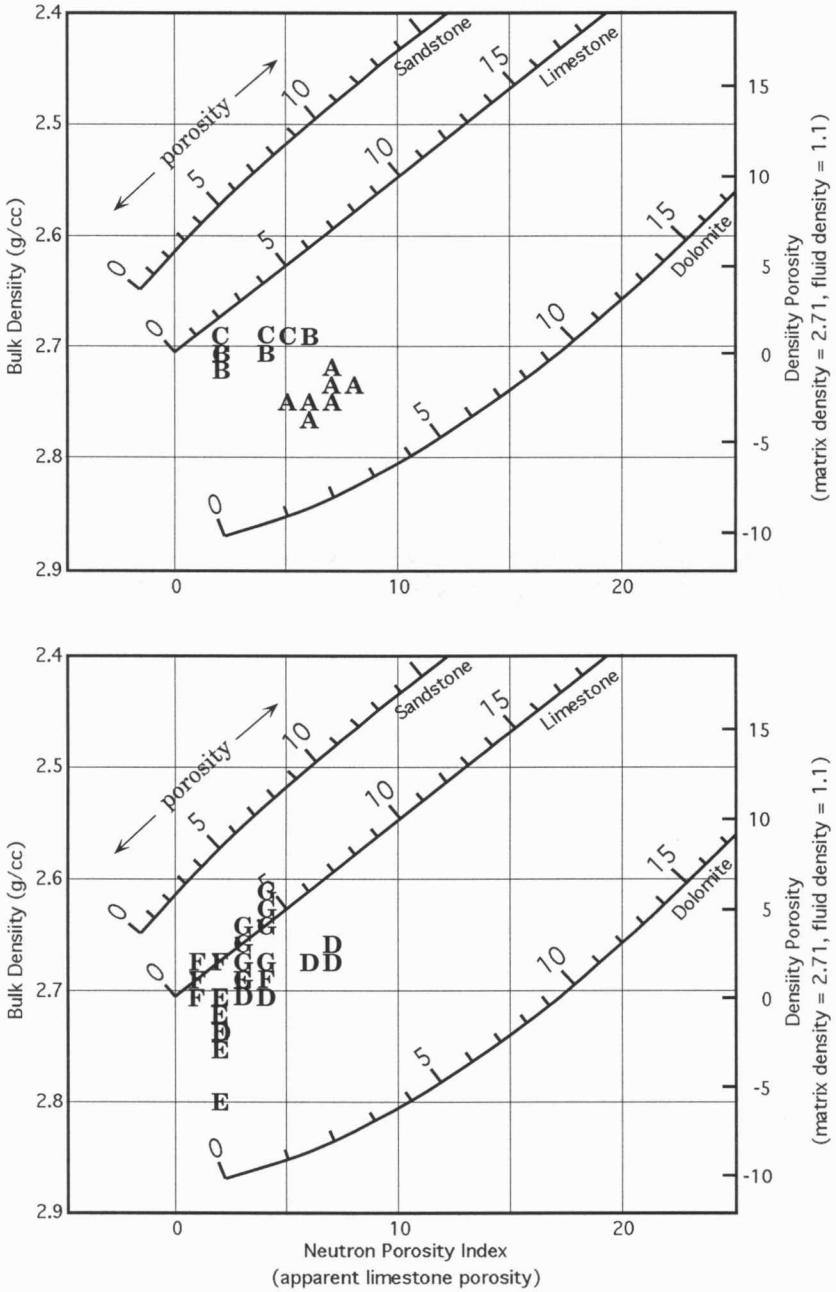

A Texas Oil #3 Zuercher (NE SW, 9-T.32S.-R.7W.)

B Banders #7 Grosnick (SW SW, 7-T.33S.-R.9W.)

C Cross Continental Res. #1-11 Andrews (NW SW, 11-T.34S.-R.12W.)

D McElvain #1 Bell (NE NW, 19-T.33S.-R.13W.)

E Petrosil #1 Beck (NW SE, 21-T.33S.-R.15W.)

F NCRA #1 Merrill (E2 NE NE, 24-T.33S.-R.16W.)

G Gould #1 Carlile (SE SW, 34-T.33S.-R.17W.)

Figure 8.8 Dominant lithology of Viola Formation lower cherty dolomitic limestone subunit from Davies's sample logs, superimposed on the isopachous map for this subunit (Figure 5.11). See text for discussion. In order that no confusion results with these lithologic determinations versus the informal nomenclature of the Viola subunits, this study follows the precedence of subunit names given in earlier studies (see Bornemann and others, 1982; Bornemann and Doveton, 1983; St. Clair, 1985), thus "lower cherty dolomitic limestone" refers to the name of this subunit and not necessarily its lithology (see Introduction, Chapter 7).

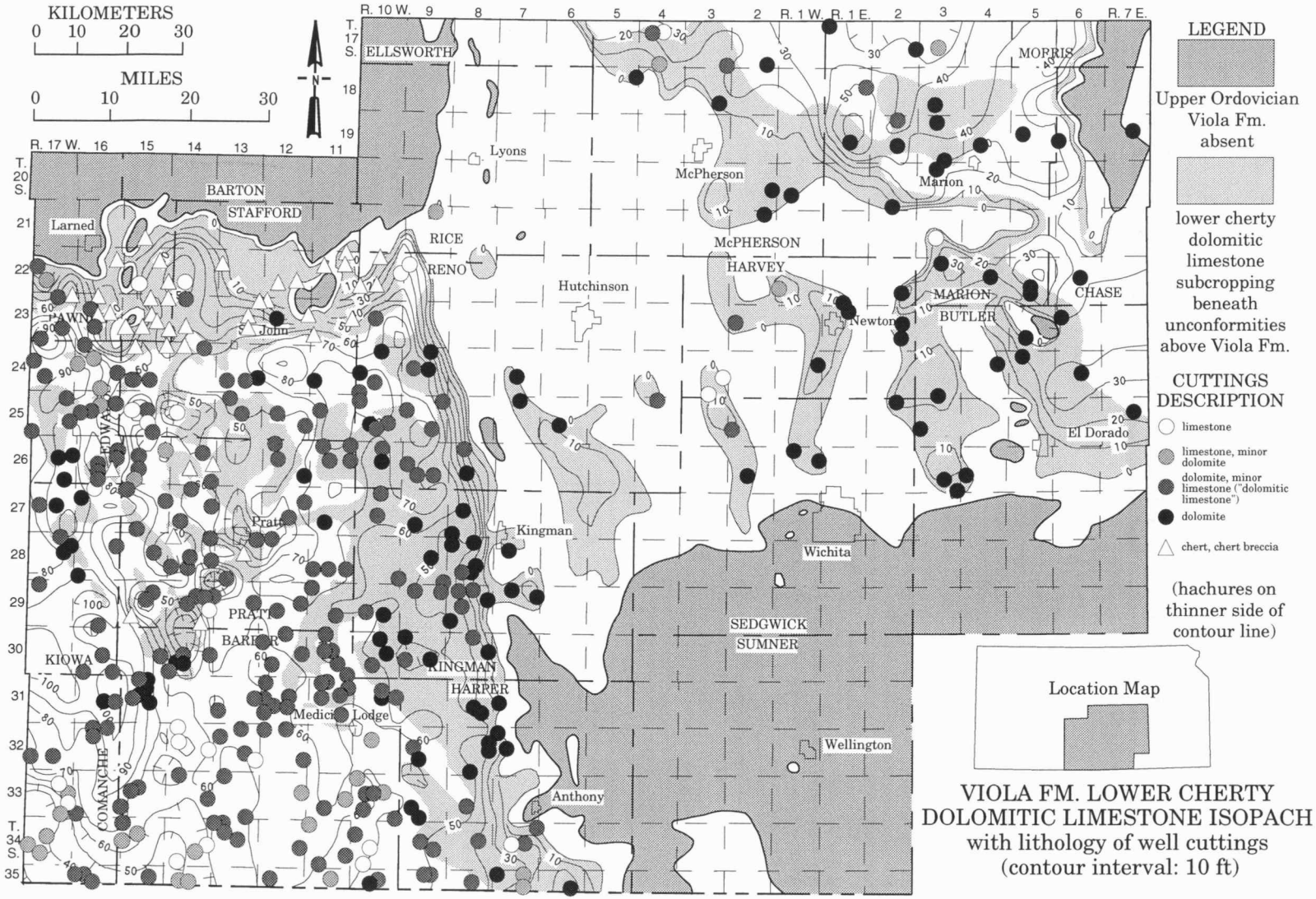

VIOLA FM. LOWER CHERTY DOLOMITIC LIMESTONE ISOPACH
with lithology of well cuttings
(contour interval: 10 ft)

Pennsylvanian unconformity.

Dolomite in the upper limestone subunit (Figure 8.9) is more erratically distributed than in the lower cherty dolomite and basal limestone subunits, but in a pattern similar to the basal limestone subunit; dolomite appears to be concentrated near the updip limits of this subunit as it pinches out on the flank of the Central Kansas and Chautauqua arches. In part, this pattern may be an artifact of the sampling process because cuttings samples are usually taken at 10-ft (3 m) intervals, therefore where this subunit is relatively thin (i.e., less than 10-feet [3 m] thick), the sample may actually contain more of the superjacent upper cherty dolomitic limestone or the subjacent lower cherty dolomitic limestone. Nevertheless, the pattern of dolomite on the updip flanks of the arch is still present where this subunit exceeds 10 ft (3 m) in thickness, hence the pattern evident on the map is probably real. Neutron-density crossplots of the upper limestone subunit (Figure 8.10) along the b-b' line of wells (see Figures 8.5, 8.9) confirms, in general, there is more dolomite in this subunit closer to its pinchout, although the downflank decrease is not as consistent as in the basal limestone subunit. Comparison of the dolomitization in the upper limestone with that of the basal limestone subunits in a given well (i.e., contrast Figure 8.10 with Figure 8.7) yields no consistent relationship.

The pattern of dolomitization is somewhat ambiguous in the upper cherty dolomitic limestone (Figure 8.11) because this subunit is the most geographically limited of all the Viola subunits. Although it is dominantly dolomitic (as its name implies), small areas are relatively free of dolomite (e.g., a group of four wells recorded as "limestone" in southwestern Stafford County; another group of seven wells in southern Barber County). The reason for these dolomite-free areas is presently unknown. Data coverage is not sufficient to reveal if there is an updip increase in dolomite near its pinchout on the flank of the Central Kansas arch or the Pratt

Figure 8.9 Dominant lithology of Viola Formation upper limestone subunit from Davies's sample logs, superimposed on the isopachous map for this subunit (Figure 5.14). See text for discussion. In order that no confusion results with these lithologic determinations versus the informal nomenclature of the Viola subunits, this study follows the precedence of subunit names given in earlier studies (see Bornemann and others, 1982; Bornemann and Doveton, 1983; St. Clair, 1985), thus "upper limestone" refers to the name of this subunit and not necessarily its lithology (see Introduction, Chapter 7).

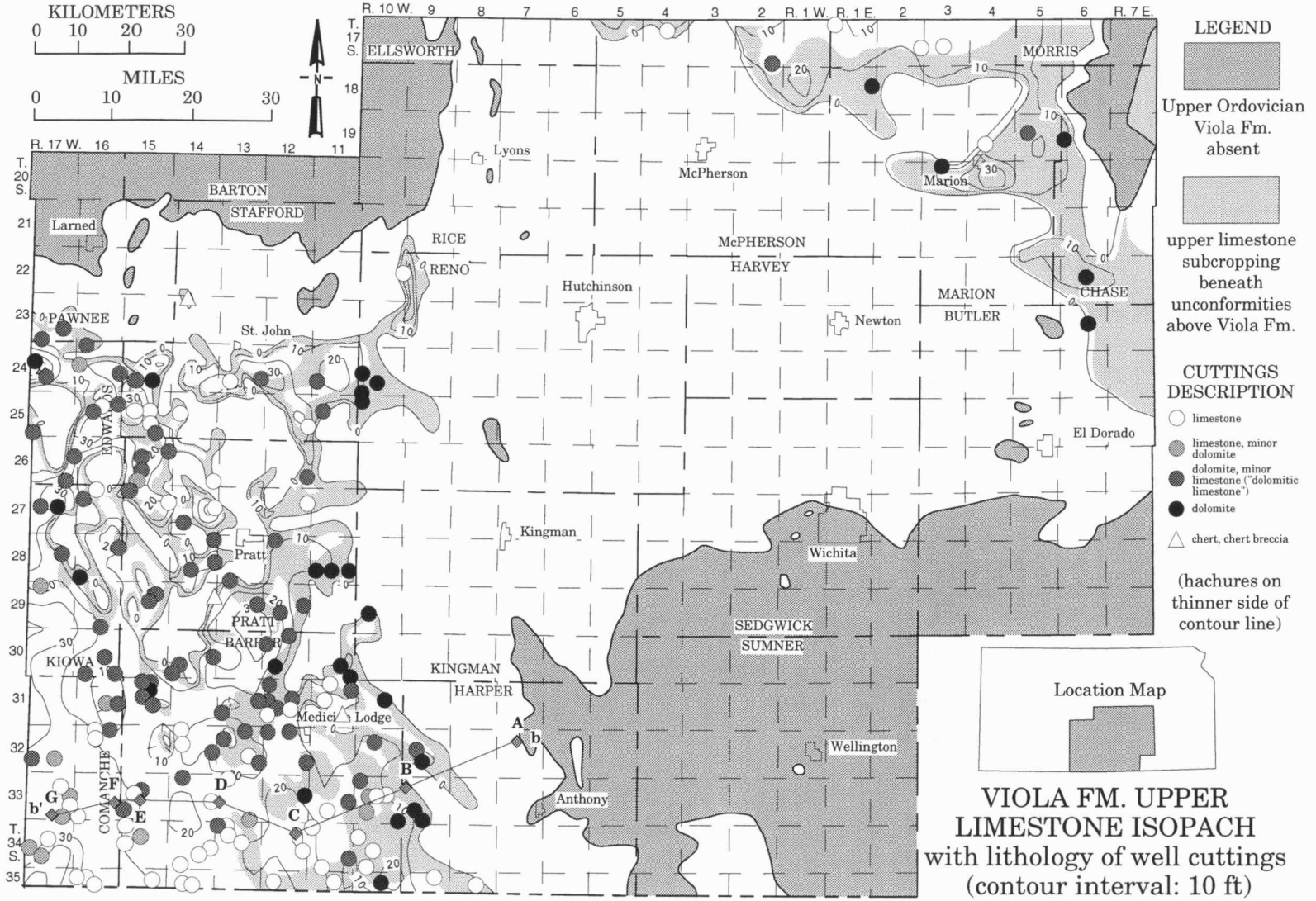

VIOLA FM. UPPER LIMESTONE ISOPACH
with lithology of well cuttings
(contour interval: 10 ft)

Figure 8.10 Neutron-density crossplot of the upper limestone for wells in a line on the flank of the Chautauqua arch (line b-b' in Figure 8.9). A general decrease in dolomite and porosity away from the subcrop limit on the flank of the arch is evident (i.e., B toward G), but some localities away from the subcrop limit display slight dolomitization. Each letter, which corresponds to the well in the legend, represents a porosity determination by bulk-density and neutron logs for a 2-ft thickness interval. Compositional lines are from Schlumberger (1987, p. 56).

BULK DENSITY - COMPENSATED NEUTRON POROSITY CROSSPLOTS
for upper limestone subunit along line b--b'

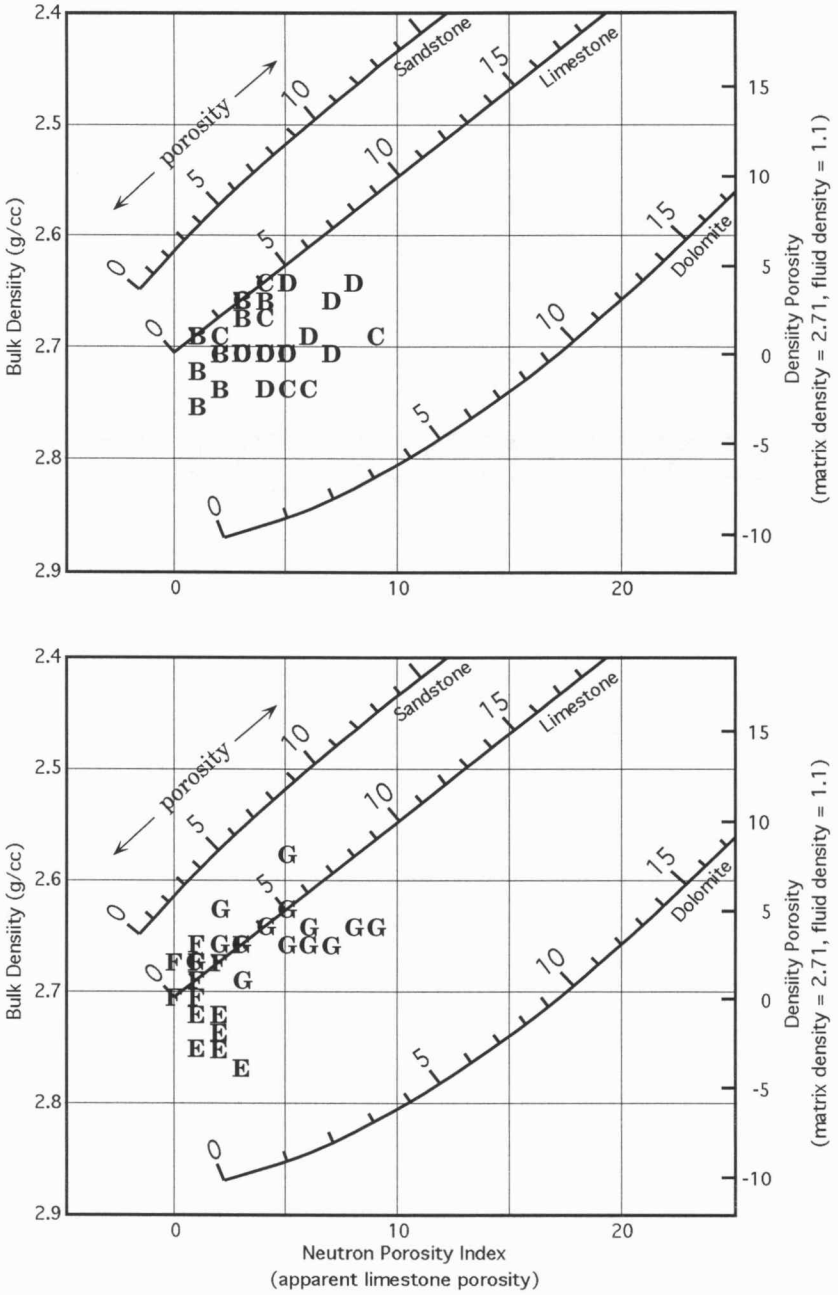

A Texas Oil #3 Zuercher (NE SW, 9-T.32S.-R.7W.)

B Banders #7 Grosnick (SW SW, 7-T.33S.-R.9W.)

C Cross Continental Res. #1-11 Andrews (NW SW, 11-T.34S.-R.12W.)

D McElvain #1 Bell (NE NW, 19-T.33S.-R.13W.)

E Petrosil #1 Beck (NW SE, 21-T.33S.-R.15W.)

F NCRA #1 Merrill (E2 NE NE, 24-T.33S.-R.16W.)

G Gould #1 Carlile (SE SW, 34-T.33S.-R.17W.)

Figure 8.11 Dominant lithology of Viola Formation upper cherty dolomitic limestone subunit from Davies's sample logs, superimposed on the isopachous map for this subunit (see Figure 5.16). See text for discussion. In order that no confusion results with these lithologic determinations versus the informal nomenclature of the Viola subunits, this study follows the precedence of subunit names given in earlier studies (see Bornemann and others, 1982; Bornemann and Doveton, 1983; St. Clair, 1985), thus "upper cherty dolomitic limestone" refers to the name of the subunit and not necessarily its lithology (see Introduction, Chapter 7).

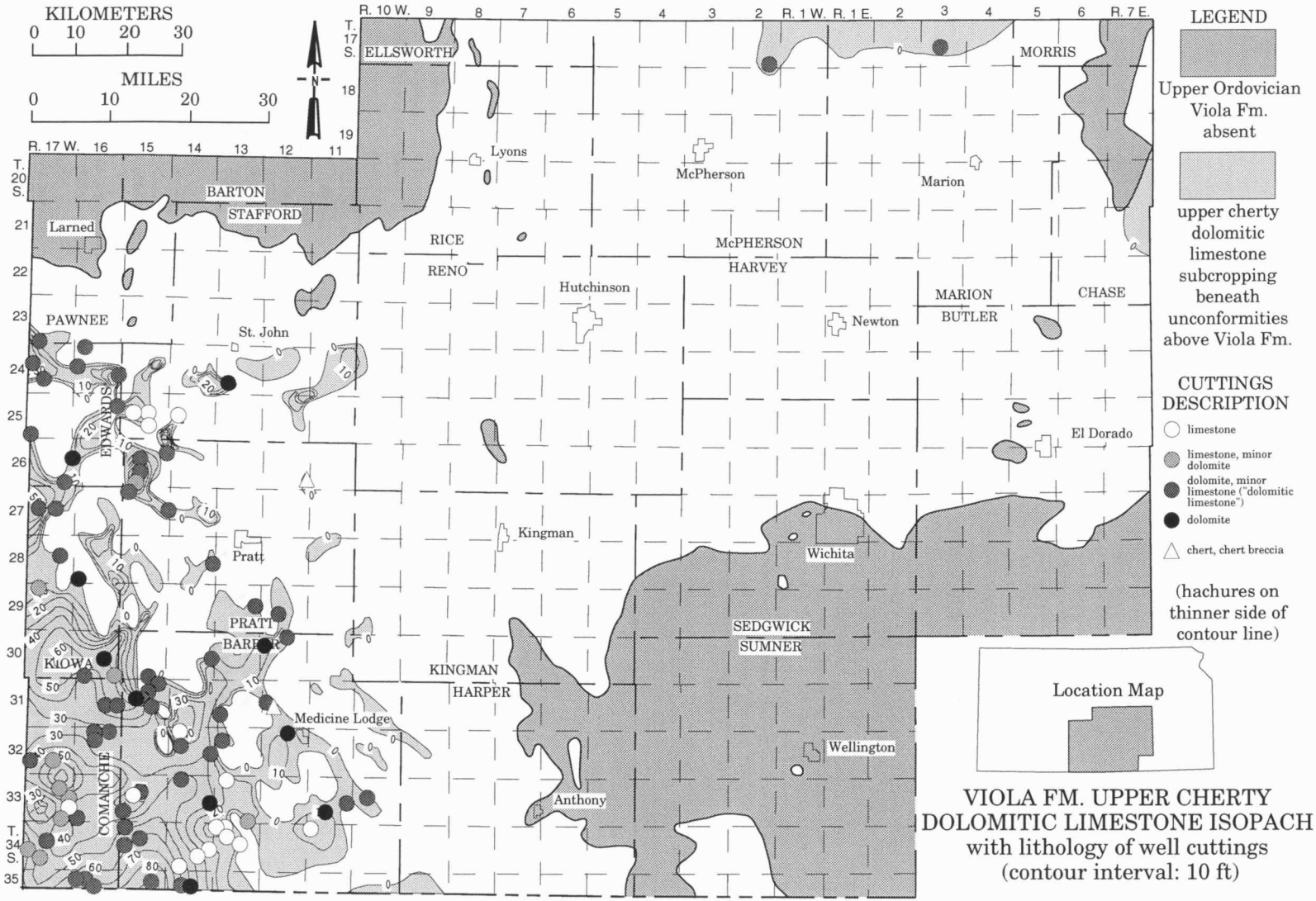

VIOLA FM. UPPER CHERTY DOLOMITIC LIMESTONE ISOPACH
with lithology of well cuttings
(contour interval: 10 ft)

anticline.

Inasmuch as the pattern of dolomitization in the Viola subunits may be, in part, controlled by the Central Kansas arch and the Chautauqua arch, the pattern of dolomitization can also be examined by a hybrid map (Figure 8.12) in which the lithology at the top of the Viola is superimposed upon a map of rock units overlying the Viola (i.e., a worm's-eye-view map; Figure 4.4). The presence of dolomite or limestone at the top of the Viola is roughly correlative to which subunit subcrops beneath the various unconformities that bevel the top of the Viola, but as the maps presented in this section have shown, the degree to which these subunits are dolomitized can vary across the study area. Figure 8.12 shows that dolomite at the top of the Viola is more or less omnipresent throughout the study area. Although there is much scatter to the data, wells recording "limestone" may be more common beneath the Maquoketa Shale where it is preserved in an off-arch position in southern Barber County. Limestone also is more common where the Maquoketa Shale is present off the northern flank of the Central Kansas and Chautauqua arches (i.e., Rice, Harvey, Reno, McPherson, and Marion counties). The spatial distribution of other younger shales that directly overlie the Viola Formation, such as the Chattanooga Shale, apparently do not correlate to the pattern of dolomitization in the Viola.

Discussion

Although the regional pattern of dolomitization is most probably a composite of several dolomitizing events, it suggests that the major event(s) responsible for the dolomitization relate to early Paleozoic tectonic features, specifically the Chautauqua arch and its northwestward extension, the Central Kansas arch. Furthermore, the increase in dolomite toward the crest of these arches is not primarily due to spatial

Figure 8.12 Dominant lithology at the top of the Viola Formation, from Davies's sample logs, superimposed on the worm's-eye-view map (see Figure 4.4). Limestone may be preferentially preserved below the Maquoketa Shale. See text for discussion.

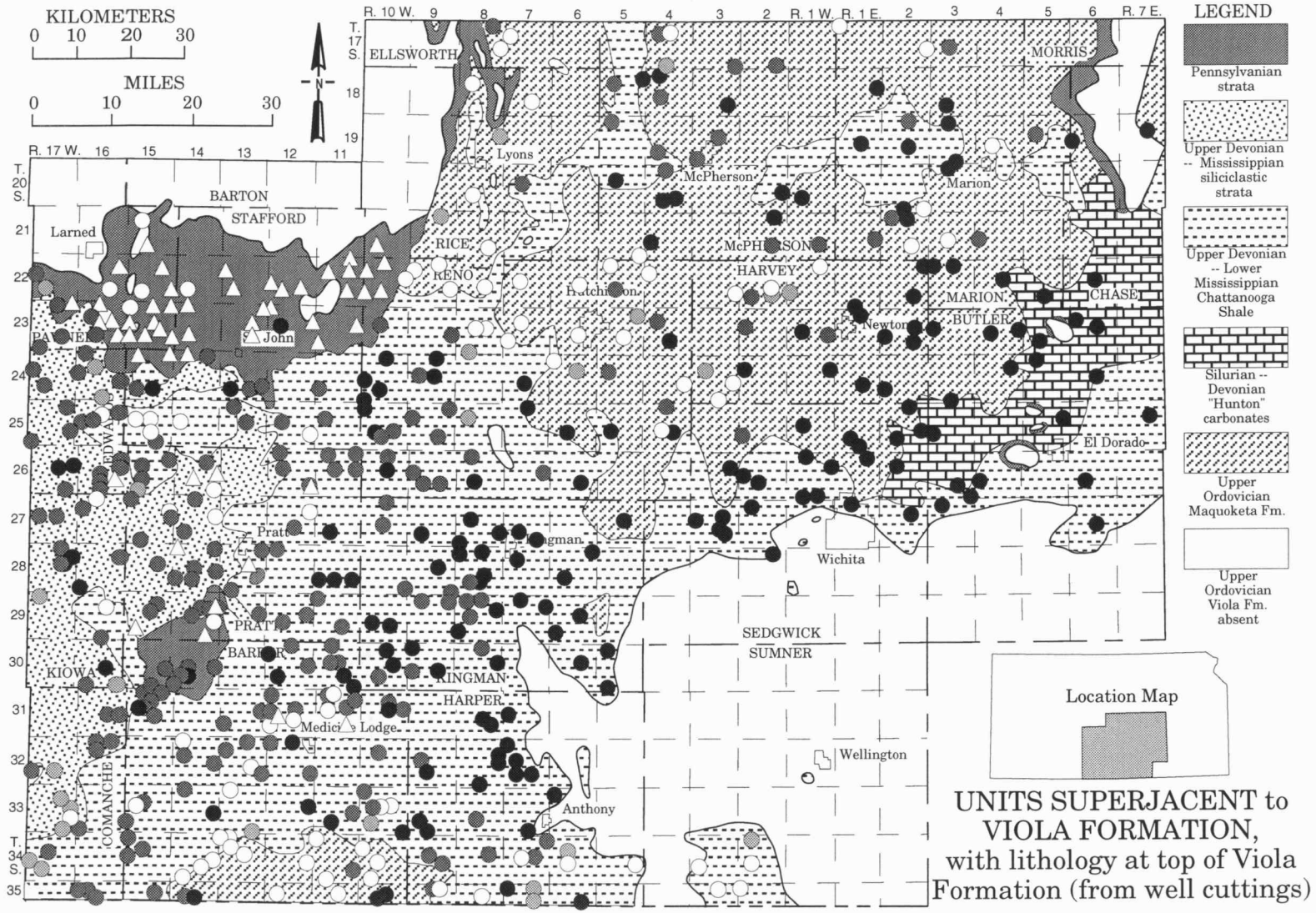

UNITS SUPERJACENT to VIOLA FORMATION, with lithology at top of Viola Formation (from well cuttings)

variation of lithology and its susceptibility to dolomitization, because all Viola subunits show some increase in dolomitization toward the crest of the arch (see Figures 8.5, 8.8, 8.9, and 8.11). No significant dolomitization is spatially associated with the Ancestral Central Kansas uplift; however, localized dolomitization is present over the Pratt anticline and its west flank.

The general increase in porosity attendant with dolomitization could also account for several Viola oil and gas fields on the northern flank of the Chautauqua arch (see Figures 5.24, 5.25, 5.26). Subcrop mapping (see Figure 5.6) indicates these fields are where the basal limestone subunit has been dolomitized.

Although this pattern of limestone being preferentially preserved under the Maquoketa Shale (Figure 8.12) may be illusory, it suggests that the Maquoketa may have impeded downward flow of dolomitizing fluids into the subjacent Viola Formation. Later shales that directly overlie the Viola Formation, such as the Chattanooga Shale, apparently do not correlate to the pattern of dolomitization in the Viola. This may be a key to the timing of dolomitization, in that it implies the Upper Ordovician Maquoketa Shale was extant during dolomitization, but not the Devonian-Mississippian Chattanooga Shale. Although structural development of the Chautauqua and Central Kansas arches continued into Late Mississippian time when the Sedgwick and Cherokee basins formed (Merriam, 1963), isopach maps of the Upper Devonian-Lower Mississippian Chattanooga Shale and its stratigraphic subdivisions in Lambert (1992a, b) suggest these arches were not active during deposition of the Chattanooga Shale. The demise of the Chautauqua and Central Kansas arches as positive structural elements, however, does not unequivocally bracket the timing of dolomitization in the Viola. The subcrop pattern, which defines these arches, may simply have channeled cross-formational movement of dolomitizing fluids into the top of the Viola Formation.

DIAGENETIC SEQUENCES

Introduction

All the diagenetic features and the spatial relationships that define their relative chronologic sequence are not present in any individual thin section. The relative timing of two diagenetic events may be equivocal due either to a lack of cross-cutting relationships between the two events or ambiguous relationships that may reflect overlap in time. Relative timing of diagenetic events for each Viola subunit was established by petrographically determining the sequence of diagenetic events first for each thin section, where possible, and then determining a composite of these events from several thin sections at a core locality. A composite diagenetic sequence for the subunit at that core locality was compared to the diagenetic sequence in nearby cores. Although minor variations occur, no significant differences in the diagenetic events for a given subunit were detectable over the entire study area.

The knowledge gained by the above approach has to be tempered with the cautionary note that in a subsurface study, evidence of critical stratigraphic relationships between samples and cores, such as the presence of unconformities or hardgrounds, can be missing. In some wells only core fragments are available for inspection rather than continuous cores. Although well-to-well correlations of rock units by wireline logs provide stratigraphic control, the benefits of continuous or closely spaced outcrops is not available in a subsurface study, hence there is a possibility that stratigraphic discontinuities and thin beds can go unrecognized.

Determining the timing of dolomitization relative to other diagenetic events also presents problems. Both the rhombohedral habit of dolomite crystals in secondary dolomites and the replacement of pre-existing limestones with preservation of original

depositional textures make it difficult to place dolomitization in sequence with other diagenetic events (Davies, 1979). Extensive dolomitization can completely obscure all prior depositional and diagenetic textures and therefore appear to be the only diagenetic event.

Thin-section petrography indicates grain-supported lithologies of the Viola (i.e., the basal limestone, upper limestone, and localized packstone beds in the upper cherty dolomitic limestone) have similar sequences of diagenetic events. The mudstones and wackestones of the lower cherty dolomitic limestone also display nearly comparable successions of diagenetic events with similar lithologies in the upper cherty dolomitic limestone. This is not surprising considering that depositional environments and lithofacies of the basal limestone and lower cherty dolomitic limestone subunits are analogous to the upper limestone and upper cherty dolomitic limestone subunits. Diagenetic patterns such as the locus of porosity development and cementation (cf., Choquette and Pray, 1970; Bathurst, 1976; Schneidermann and Harris, 1985) can also be inherited from depositional fabrics.

Inasmuch as diagenetic features in the Viola subunits are similar, this part of the diagenesis chapter and the next part, "Diagenetic Events", report diagenesis in the major lithofacies by a process-by-process basis. Descriptions of the diagenetic characteristics are presented in the approximate order in which they occurred, and petrographic observations that aid in determining their chronology are presented and discussed. Fluid-inclusion data, stable isotopes, and cathodoluminescence petrography that augment understanding of the diagenetic environments are also presented, where applicable. Lastly, interpretations of the various diagenetic environments are advanced and discussed with respect to the larger context of the regional stratigraphy, depositional environments, timing, and burial history.

Methods and Procedures

For fluid-inclusion microscopy, doubly polished sections were made using cold techniques and ultraviolet-light-sensitive epoxy to avoid thermal reequilibration of fluid inclusions during sample preparation. Homogenization temperatures (T_h) of inclusions were determined using a Fluid, Inc. adapted U.S.G.S. gas-flow heating/freezing stage attached to an optical microscope. Freezing runs to determine salinity of inclusions by final melting temperatures of the ice phase(s) ($Tm_{(ice)}$) were made after T_hs were determined by heating runs. The method of "cycling", which exploits the metastable phase behavior of the liquid (Goldstein and Reynolds, 1994, p. 93-95, 105-109), was utilized to determine T_h and $Tm_{(ice)}$. Fluorescence of inclusions, which can reveal the presence of hydrocarbons, was observed with epifluorescence illumination (Burruss, 1991) using blue light and long-wavelength ultraviolet light. Where necessary, nucleation of bubbles in all-liquid fluid inclusions was induced by storing samples in a household freezer for several days. After T_h determinations were made, low-temperature heating in an oven (usually 6 hours at 200 °C) forced sufficient stretching of the remaining all-liquid inclusions to create a permanent bubble that aided in $Tm_{(ice)}$ determinations. Crushing of fluid inclusions to determine their internal pressure at room temperature was accomplished using a crushing stage made out of glass plates and tape, the design of which is outlined in Goldstein and Reynolds (1994, p. 75) and Roedder (1970). Crushing of fluid inclusions was recorded on a high-resolution videotape system ("super VHS"); stop-action features were utilized for measuring dimensions of bubbles before and after crushing. The emersion medium generally was glycerine, but kerosene and mineral oil were also used.

Thin-section petrography was further supplemented by cathodoluminescence petrography. Zonation in cements in polished thin sections can be revealed with a luminoscope, in this study a Technosyn Cold Cathode Luminescence Model 8200 Mk II.

Dolomite crystals in the Viola are generally dull brown to red under cathodoluminescence, with zonation and replacement features being defined by changes in brightness, but iron-rich varieties like saddle dolomite are typically nonluminescent. Calcite is generally a bright orange to yellow, but iron-rich varieties, as revealed by staining, are also dully luminescent to nonluminescent. Cathodoluminescence intensity in carbonate minerals is accepted as due to the ratio of trace-element "activators" that cause luminescence (commonly Mn^{2+}), and "quenchers" (commonly Fe^{2+}) that inhibit it (cf., Frank and others, 1982; Hemming and others, 1989; Machel and others, 1991). Cathodoluminescence zonation in calcite cements and dolomite have been interpreted principally in the context of the Eh, or degree of oxygenation of the precipitating fluid, which in turn, controls incorporation of Fe and Mn into the crystal lattice (cf., Meyers, 1974, 1978; Kaufman and others, 1988). Although the interplay of Mn^{2+} and Fe^{2+} may be the most common control of cathodoluminescence in calcite and dolomite, many different elements can function as activators and quenchers (Machel and others, 1991). In addition, a plethora of chemical, biological, and environmental factors may govern the incorporation of these various activators and quenchers in carbonate minerals (Machel and Burton, 1991). Interpretation of cathodoluminescence of a calcite or dolomite in the context of the chemistry of the water from which these minerals precipitated is therefore fraught with potential pitfalls that can only be avoided with further research in cathodoluminescence and with detailed chemical analyses. Although cathodoluminescence may not be a definitive analytical tool for chemical composition of carbonates, it still reveals features related to growth zonation, recrystallization, dissolution, and ultimately cement stratigraphy.

X-ray analysis of dolomite was performed on a Philips diffractometer with a Radix automation upgrade. The diffractometer was operated at 40 milliamps and

50kV, with a 1° divergence slit and a 0.2 scattering slit. Scan rates varied between 6.7 minutes per degree (0.01 degree steps with 4 seconds of counting for each step) and 1 hour, 7 minutes per degree (0.005 degree steps with 20 seconds of counting for each step), but differences in results were minimal within this range. Cu $K\alpha$ radiation was selected with a graphite monochromator. All dolomite samples analyzed were spiked with approximately 50 wt. % of reagent-grade NaCl as internal standard.

Samples selected for stable-isotope and x-ray analyses were obtained from polished or stained thin-section billets. The fine-grained and homogeneous nature of most of the dolomites allowed bulk sampling simply by a 3/16" masonry bit on a hand drill, but finer sampling of cement phases in calcite grainstones and saddle dolomites was done using a dental drill under a binocular microscope. Samples were ground to less than 75 μm (200 mesh sieve).

Extraneous calcite was eliminated from dolomite samples prepared for isotope and x-ray analyses by placing the powdered samples in plastic centrifuge tubes and washing the samples in 1% acetic acid for 3 minutes. In order to ensure complete reaction of the calcite with the acid, the centrifuge tubes were shaken, placed in an ultrasonic bath, and centrifuged again. If no gas bubbles were present in the powder after centrifuging, the supernatant liquid was then decanted off the settled powder. If gas bubbles were present, indicating the presence of undigested calcite, the procedure of shaking and placing the sample in an ultrasonic bath was repeated. After decanting, the sample was successively washed with deionized distilled water, centrifuged, decanted three times, and air dried.

All samples prepared for isotopic analysis for Sr were dissolved in 3.5 N nitric acid and subsequently heated to assure complete dissolution of the dolomite. The sample was then centrifuged and the supernatant liquid pipetted off in order to rid the sample of insoluble residue. The supernatant liquid was purified of Sr by four

successive filterings of 3.5 N nitric acid through a Sr-specific resin column (filled with SR-Spec (®) resin by EIChroM Industries, Inc., Darien, IL). The Sr was eliminated from the resin by eluting the resin twice with deionized water. The water was evaporated with a gather of phosphoric acid.

Strontium isotopic analyses were performed at Massachusetts Institute of Technology by Dr. Drew Coleman. All samples and standards were loaded on single Re filaments with 1 μL each of 1M H_3PO_4 and TaCl. Samples were analyzed on a VG Sector 54 mass spectrometer in three-cycle, dynamic multicollector mode with an ^{88}Sr ion-beam intensity of 3V. All data are normalized to $^{86}Sr/^{88}Sr = 0.1194$ using an exponential fractionation law. The mean $^{87}Sr/^{86}Sr$ ratio of 3V NBS-987 standards run since installation of new collectors is 0.710243 ± 0.000012 (standard error (2σ) external reproducibility absolute, n = 6).

Oxygen and carbon isotopic analyses were performed by Benedum Stable Isotope Laboratory at Brown University under supervision by Dr. Robert Fifer. Organic material was removed by vacuum roasting samples for 1 hour at 300 °C. Calcite samples were reacted with 100% H_3PO_4 at 90 °C for 15 minutes, and the resultant CO_2 was analyzed by a VG SIRA-24 mass spectrometer for both oxygen and carbon isotopic ratios. Dolomites were reacted at the same temperature as the calcites, but for 40 minutes with a 20-minute pump-out period to remove residual gas. No correction was applied for dolomite fractionation in H_3PO_4. Isotopic data are reported in per mil (‰) PDB (see Craig, 1957). External precision on standards was 0.09 ‰ for oxygen and 0.17 ‰ for carbon.

Grain-Supported Lithologies

The diagenetic sequence for the grain-supported lithologies (i.e., most beds in the basal limestone, upper limestone, and localized packstones in the upper cherty

dolomitic limestone) (Figure 8.13) was determined from thin sections from 24 cores (see Figure 7.1 and Table 7.1). The sequence of major diagenetic events in the basal limestone is similar to the upper limestone. Although quantitatively insignificant, degrading neomorphism (Folk, 1965) of crinoid fragments is slightly more prevalent in the upper limestone subunit and miscellaneous packstones in the upper cherty dolomitic limestone than it is in the basal limestone subunit (Figure 8.13). Dolomitization affects all grain-supported lithologies in the Viola to a minor degree; the basal limestone subunit on the north flank of the Chautauqua arch is completely mimetically dolomitized. Calcitization of dolomites (i.e., "dedolomitization") occurs in both the basal and upper limestones, but it is more prevalent in the upper limestone, and the calcite is not ferroan calcite as it is in the basal limestone.

Mud-Supported Lithologies

The diagenetic sequence for the mud-supported lithologies (i.e., most beds in the lower cherty dolomitic limestone and upper cherty dolomitic limestone) (Figure 8.14) was determined from thin sections from 28 cores (see Figure 7.1 and Table 7.1). The sequence of diagenetic events in mud-supported lithologies is almost identical, except the upper cherty dolomitic limestone is slightly more complex. Specifically, the upper cherty dolomitic limestone displays additional events of silicification, karstic brecciation, and dedolomitization.

An episode of dissolution occurred before dolomitization in the lower and upper cherty dolomitic limestone. Chert nodules and silicified fossils adjacent to pore space commonly have a ragged or eroded appearance, indicating that the silica has been partly dissolved. Euhedral rhombs of dolomite also commonly extend into these molds and small vugs and are generally slightly larger than adjacent rhombs in the rock matrix. The euhedral nature of the dolomite and the slight enlargement of dolomite

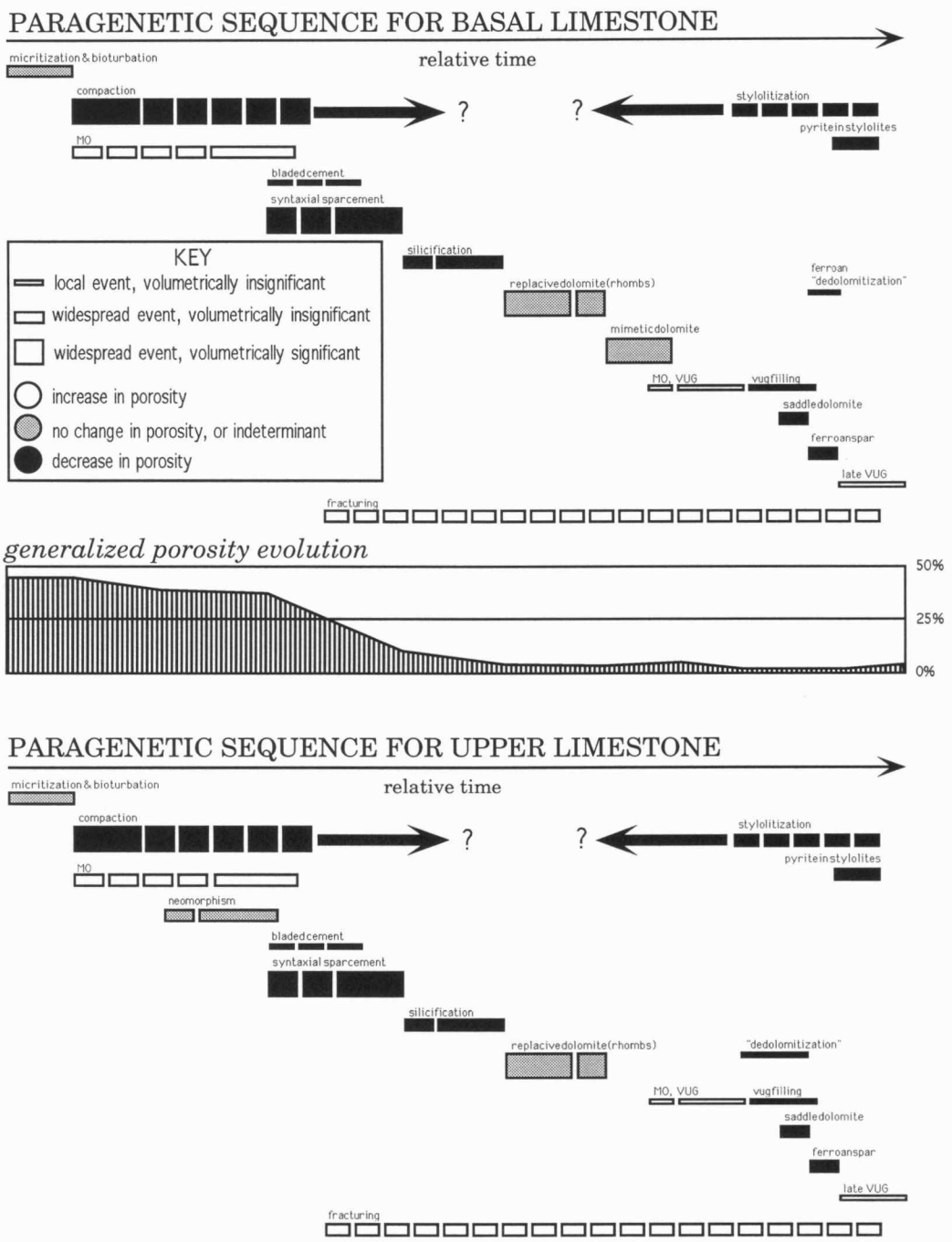

Figure 8.13 Paragenetic sequence for grain-supported lithologies in the basal limestone subunit, the upper limestone subunit, and localized packstones beds in the upper cherty dolomitic limestone subunit observed in wells eastern Stafford County (i.e., cores *#18* through *#27*) This sequence represents an eclectic summary of diagenetic features seen in several cores in the study area (see text for discussion). Initial average primary porosity of grainstones and packstones in the basal limestone and upper limestone subunits is estimated to be 45%, approximately that determined for modern sediments by Enos and Sawatsky (1981).

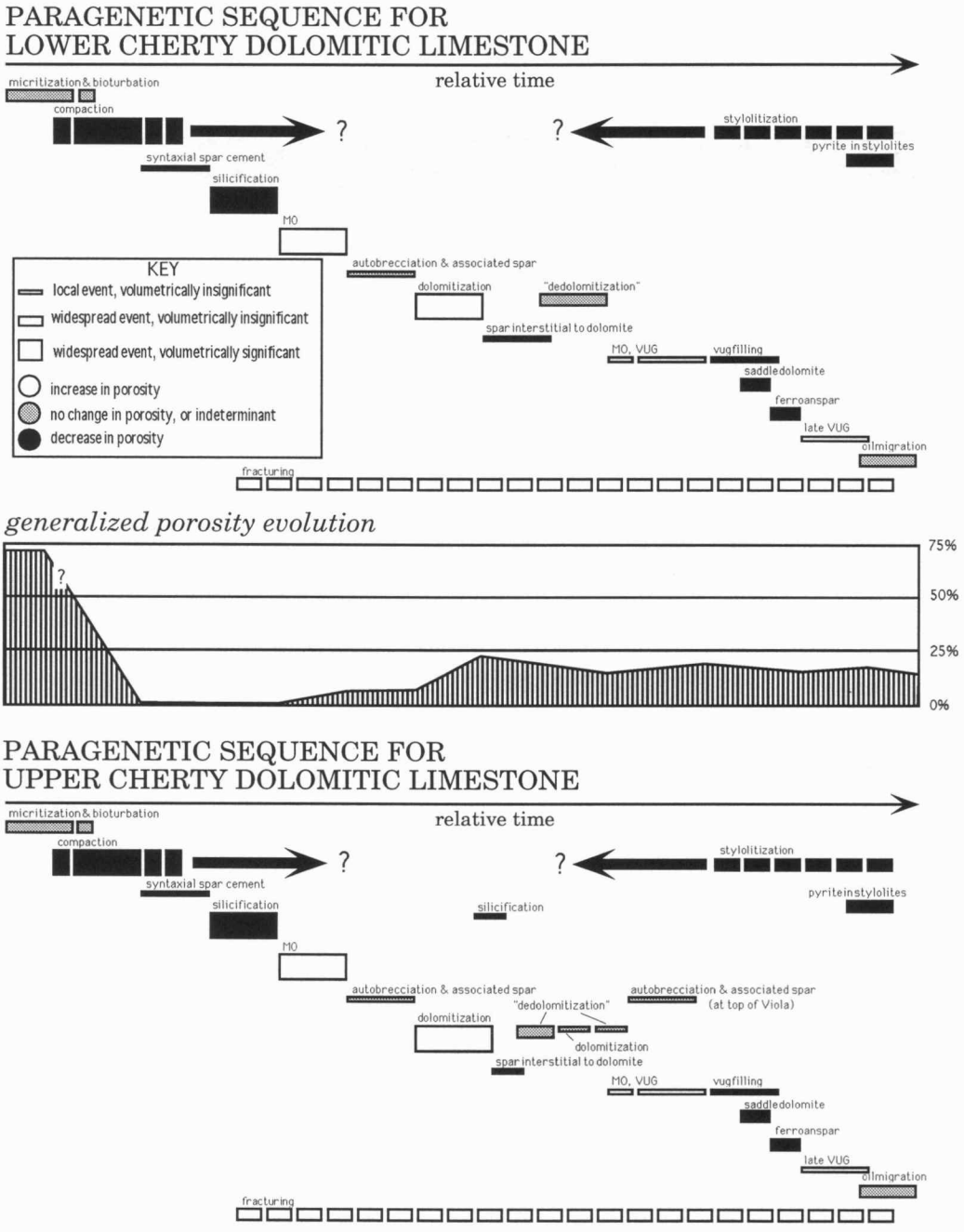

Figure 8.14 Paragenetic sequence for mud-supported lithologies in the lower cherty dolomitic limestone subunit and the upper cherty dolomitic limestone subunit. This sequence represents an eclectic summary of diagenetic features seen in several cores in the study area (see text for discussion). Initial average porosity in carbonate muds is assumed to be approximately 70% as per determinations by Enos and Sawatsky (1981), but this porosity probably drops drastically with early compaction and cementation (see Enos, 1988).

crystals within the vug also indicate the vug or mold existed before the dolomite. This episode of dissolution prior to dolomitization is not expressed in the paragenetic sequence in the basal and upper limestones.

A coarse-grained poikilitic calcite spar locally occurs in the lower cherty dolomitic limestone at the Braden-Zenith wells in eastern Stafford County. This spar completely occludes the intercrystalline porosity of the lower cherty dolomitic limestone. Exemplifying this texture, in the Braden-Zenith ZU-1 core (*#19*) at 3977 ft depth (see Appendix IV) large (~1 cm) nonferroan calcite crystals poikilitically enclose a mesh of dolomite crystals. The relationship of this spar to that of other spar generations (i.e., the early spar filling shelter porosity, spar in calcitized dolomites) is unknown, because no cross-cutting relationships with these other phases were observed. Under cathodoluminescence, the poikilitic calcite has dull luminescence with no evident zonation, so its pattern of precipitation is difficult to discern.

DIAGENETIC EVENTS

Bioturbation and Compaction

Observations

By a liberal definition, bioturbation can also be considered a post-depositional, pre-burial diagenetic event (cf., Ginsburg, 1957). Depositional implications of bioturbation of the Viola subunits are discussed in Chapter 7. Burrows are a locus of dolomitization in otherwise undolomitized rock in both grain-supported and mud-supported lithologies.

A major diagenetic event commonly observed in packstones and grainstones of the basal and upper limestone is compaction. Mechanical compaction is expressed

principally as broken grains, but it is not common. Chemical compaction is more common and manifests itself as overly close packing of grains and slight embayments where grains contact each other. In cases of extreme compaction, a fitted fabric (Buxton and Sibley, 1981) results where grain-to-grain contacts are sutured. Large portions of each grain may be missing, with no primary interparticle pore space is preserved between grains. Compaction by pressure solution is more common in the muddier packstones than in the cleaner packstones and grainstones (Figure 8.15). While fossil fragments in grain-supported lithologies may have sutured contacts with each other, the interface between spar cements nucleated on adjacent fossil fragments is planar in most cases, thereby indicating that the spar cement succeeded the early compaction. As a counter example, however, calcite-spar infill of the intraparticle porosity is interpreted to have prevented the delicate particle in Figure 8.16 (a micrite envelope after a mollusk(?) fragment) from being crushed by compaction.

Early compaction is difficult to discern in the mud-supported lithologies, although fossil grain contacts in wackestones may display minor embayments. Stylolites are generally present, particularly in argillaceous zones, but these generally cross-cut all other diagenetic features and are thus considered as later diagenetic features.

Interpretations

Some compaction prior to cementation in packstones and grainstones is indicated by fossil fragments being sutured where they are contacting each other, whereas their interparticle cements have planar intercrystalline boundaries. However, other observations of micrite envelopes being protected from crushing by spar infill argue that spar infill occurred before significant compaction (Figure 8.16). Some compaction is therefore probably penecontemporaneous with spar cementation. Microstylolites and grain-to-grain suturing have been noted at depths as shallow as

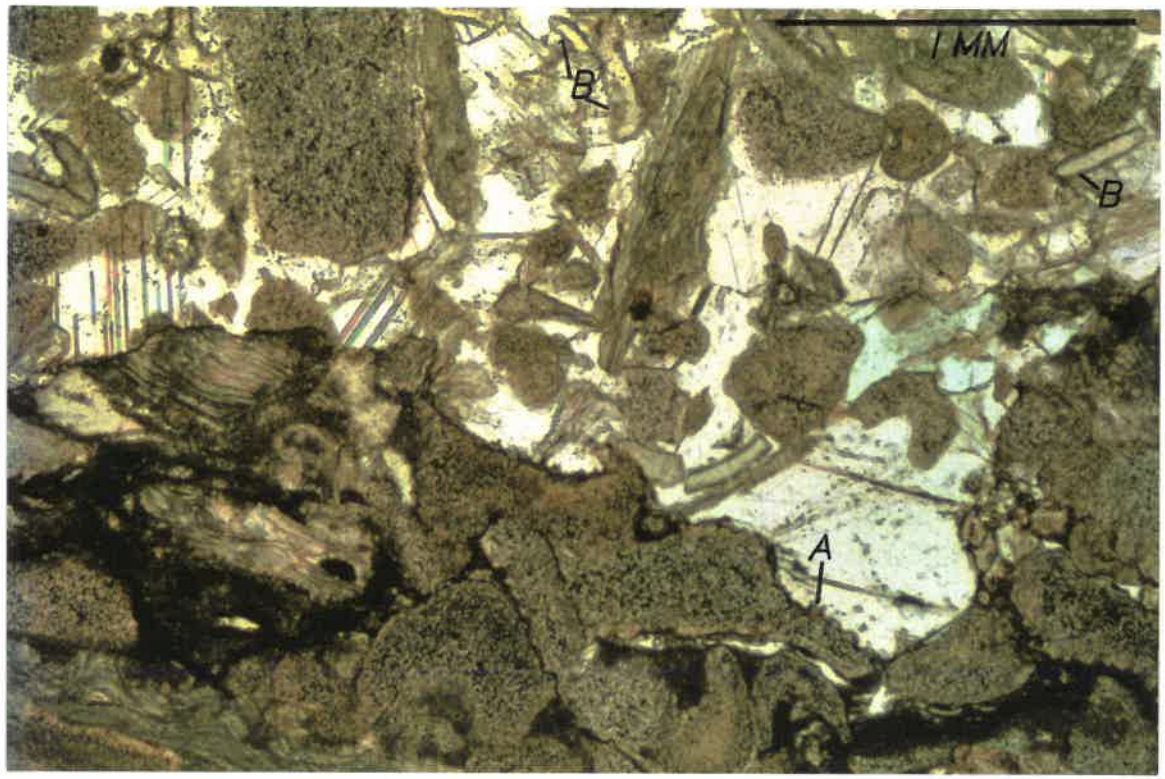

Figure 8.15 Photomicrograph of typical skeletal constituents in packstones and grainstones in the basal limestone subunit (3363 ft depth) from the Champlin #1 Kottman core (*#11*) in Rice County (19-T.19S.-R.8W.). A hardground (**A**) separates a compacted muddy crinoidal packstone (below) from a relatively uncompacted, spar-cemented crinoidal grainstone (above). Several skeletal grains in the relatively uncompacted grainstone have micrite envelopes (**B**). Interstitial mud is interpreted to have inhibited growth of early spar in the underlying packstone, thereby allowing subsequent compaction to occur.

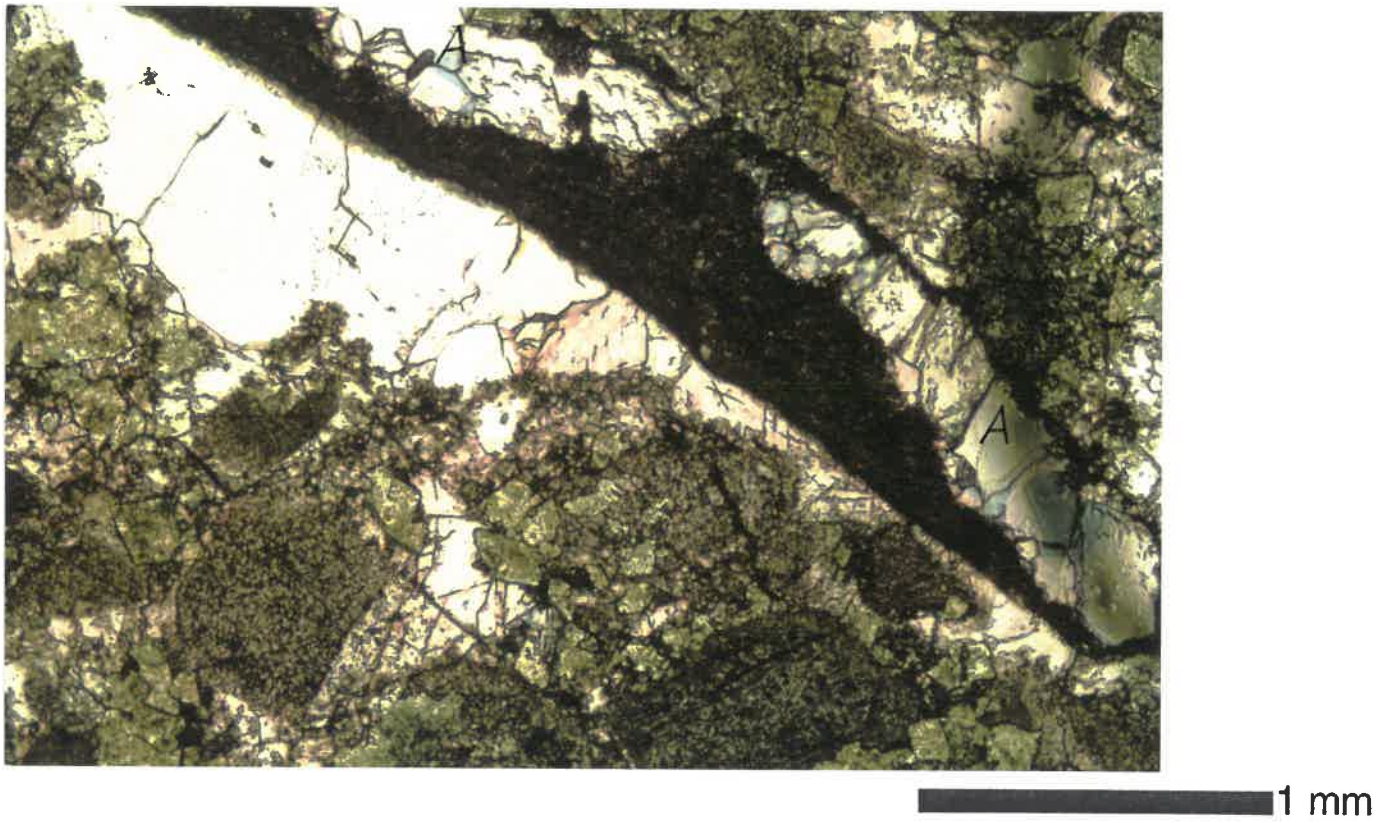

Figure 8.16 Photomicrograph of partially dissolved, micritized mollusk(?) fragment in a packstone in the basal limestone (3276.7 ft depth) from the Northern Natural Gas #1 Caldwell core (*#12*) in Rice County (2-T.20S.-R.8W.). Early calcite-spar infill of the moldic porosity is interpreted to have prevented this delicate particle from being crushed by compaction shortly after burial. A minor dissolution event prior to spar cementation is indicated by cement-filled partial-moldic porosity in approximately 1% of the allochems (**A**).

approximately 100 m (Bathurst, 1976, p. 473; James and Bone, 1989) -- consistent with compaction at least starting with shallow-burial for the grain-supported lithologies. Nevertheless, mechanical and chemical compaction are ongoing processes in a sedimentary column, hence determining the timing of compaction and stylolitization relative to other diagenetic events is difficult.

Compaction by pressure solution is more common in muddier packstones than in cleaner packstones and grainstones; mud probably inhibited nucleation and growth of sparry cement, particularly the syntaxial variety that grows on crinoidal debris. Buxton and Sibley (1981) noted a somewhat similar relationship in which Devonian packstones, wackestones, and sparsely-cemented crinoidal grainstones more commonly have fitted fabrics than well-cemented crinoidal grainstones.

Early Moldic Porosity and Degrading Neomorphism

Observations

Minor dissolution prior to spar cementation is indicated by spar-filled partial moldic porosity in skeletal grains in the basal limestone subunit (see Figure VI.5 in Appendix VI). Molds after mollusks(?), leaving only their micrite envelopes, are an extreme example of this dissolution event (Figure 8.16). The partial moldic pores, commonly 100 to 200 μm in size, are present in less than 1% of the skeletal grains in the grainstones and packstones of the basal limestone subunit. Similar spar-filled pores are slightly more common in echinoderm grains in packstones and grainstones in the upper limestone and upper cherty dolomitic limestone subunits. Visual estimates of compositions of the upper limestone and upper cherty dolomitic limestone indicated these subunits do not respectively have significant differences with the compositions of the basal limestone and lower cherty dolomitic limestones, hence a slightly different chemical history may be indicated for the upper limestone and upper cherty dolomitic

limestones. Patches of degrading neomorphic(?) spar (Folk, 1965) (Figure 8.17) are spatially associated with moldic porosity in crinoid fragments in the upper limestone, but they are rare in crinoids fragments in the basal limestone. The dissolution features and sparry patches observed in echinoderm fragments in the grain-supported lithologies of the Viola were not observed in echinoderm fragments in the mud-supported lithologies.

Interpretations

Folk (1965) originally defined degrading neomorphism as a process by which coarser crystalline carbonate crystals are replaced by finer crystalline mosaics of the without evidence of the formation of visible porosity as an intermediate step. The actual nature of the process is obscure, but it is more easily recognizable in crinoid fragments (Figure 8.17), in that crinoids fragments are composed of large single crystals or numerous minuscule crystals having nearly identical optical orientation (Towe, 1967).

Wholesale leaching and neomorphism of crinoid grains observed by Dorobek (1983) are characteristics of early diagenesis by waters undersaturated with respect to high-magnesium calcite. The uncommon selective leaching of crinoid grains in the grain-supported lithologies of the Viola Formation suggests pore waters were not nearly as undersaturated. The spotty leaching of the echinoderm grains could be explained by slight variations in magnesium content within the skeleton, which would cause differences in solubility. Intraskeletal variations in chemistry are seen in modern echinoderms (Weber, 1969) and should probably be expected in their ancient counterparts. Other factors affecting solubility on the microscopic scale in crinoid grains include trapped organic matter, differences in skeletal microstructure, and the surface area of the grain that may have been exposed to diagenetic fluids (Mackenzie and others, 1983; Walter, 1983; Dorobek, 1987). Degrading neomorphism and leaching

Figure 8.17a, 8.17b Matched pair of photomicrographs with plane-polarized light (8.17a) and crossed polars (8.17b). Patchy development of degrading neomorphic spar (**N**) associated with partial moldic porosity (**P**) in a crinoid grain in the upper limestone subunit (3703 ft depth) from the Shell #1 A.C. Brown core (*#18*) in Stafford County (2-T.24S.-R.11W.). Patchy development of irregular-sized granular spar in a coarser grained host, with curved and wavy crystal boundaries are characteristics of degrading neomorphic spar (Folk, 1965). Crinoid grain is at extinction in 8.17b. Thin section has been stained by potassium ferricyanide and Alizarin Red-S.

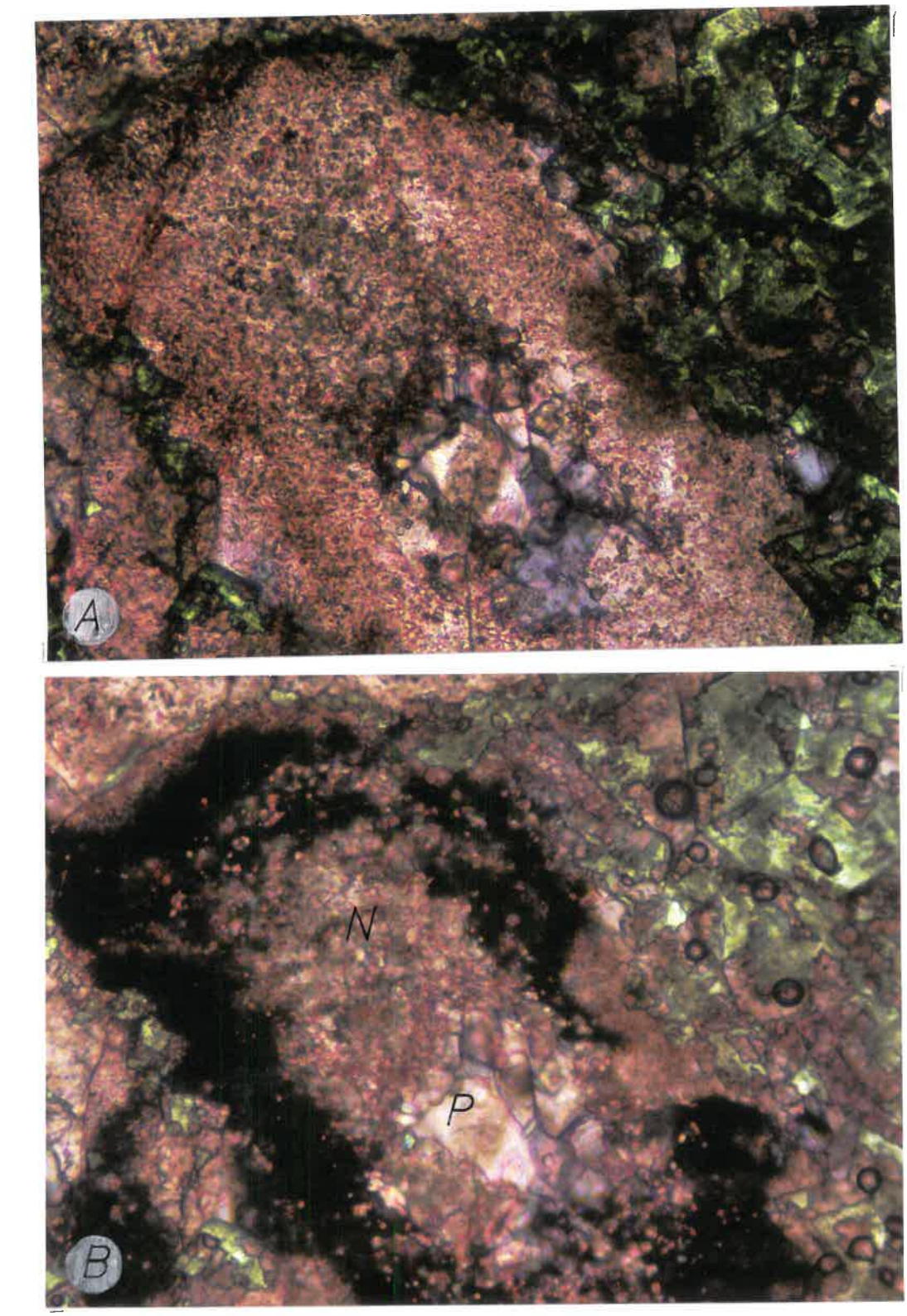
A
N
P
B
0.5 mm

of crinoid grains are more common in the upper limestone subunit and locally in the upper cherty dolomitic limestone, hence these rocks may have been subjected to slightly less saturated waters than the basal limestone subunit.

Spar Cementation and Early Bladed Cement

Observations

The infill of pore space by sparry calcite cement is the major diagenetic event that effectively destroys the primary porosity of the packstones and grainstones in the basal limestone subunit. Typically this spar is equant and ranges in size from 100 to 500 μm and can compose up to 45% of the packstones and grainstones -- essentially all of the estimated original interparticle porosity. It is largely confined to primary shelter and interparticle pores, although minor intraparticle and partial moldic porosity within the particle is also occluded by this cement. Most commonly it is in optical continuity with nearby echinoderm fragments, therefore representing a syntaxial overgrowth on the single-crystal substrates of these grains.

The syntaxial sparry cement commonly envelopes or borders non-crinoidal, polycrystalline grains such as brachiopod fragments (Figure 8.18). Rarely, however, finely crystalline, isopachous bladed cements, commonly 25 to 50 μm in length, are developed on these grains prior to the enveloping spar. Cathodoluminescence reveals that zonation in these isopachous bladed cements, if present, is commonly identical to early zonation in nearby syntaxial cements. The bladed cements and syntaxial cements typically have straight cleavage planes and uniform extinction. Carbonate mud locally perched on the upper side of grains in the packstones may locally inhibit overgrowth of syntaxial and bladed cements on some allochems, whereas the relatively mud-free undersides of these same grains may have well-developed sparry overgrowths. Although this may superficially resemble pendant cement, other nearby

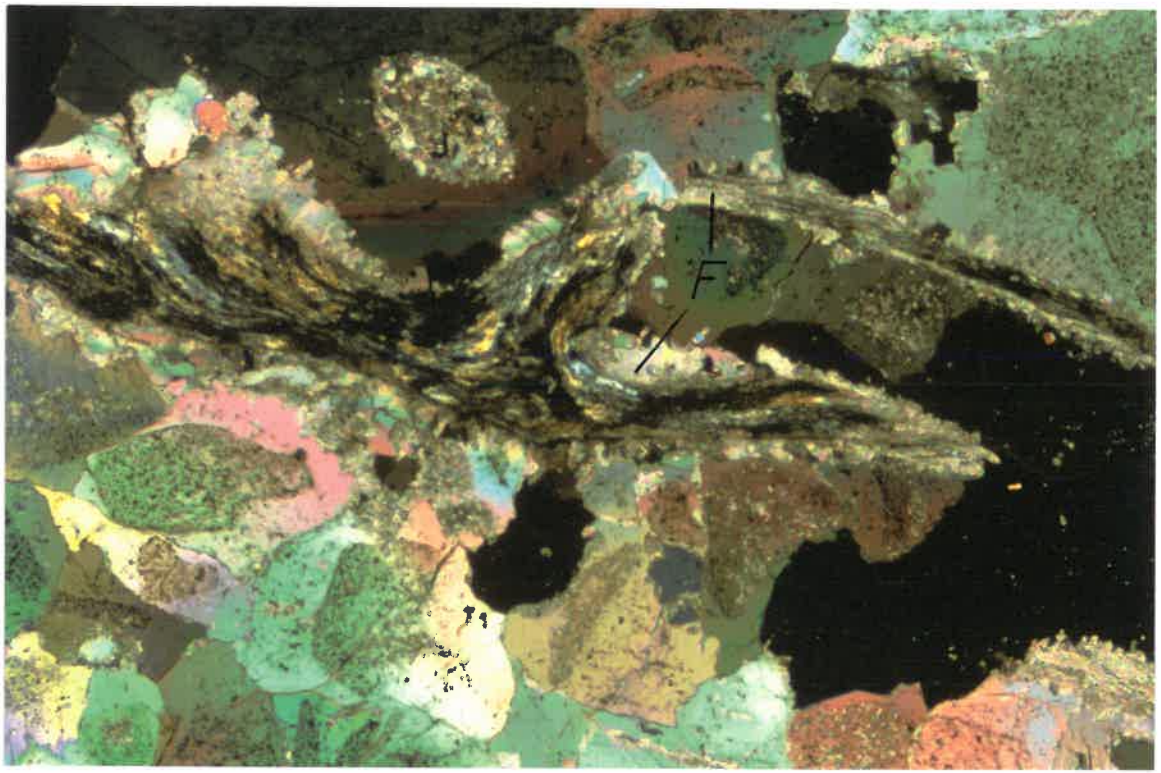

Figure 8.18 Photomicrograph (with crossed polars) of silicified brachiopod fragments (**F**) with a bladed calcite spar developed on them. Remaining interparticle pore space is occluded by syntaxial spar overgrowths growing on nearby echinoderm fragments. Basal limestone subunit (3259.8 ft depth) from the Northern Natural Gas #1 Caldwell core (*#12*) in Rice County (2-T.20S.-R.8W.).

grains without a dusting of mud on their upper surfaces almost always have syntaxial or bladed overgrowths developed equally both underneath and above.

Staining for iron with potassium ferricyanide indicates that the bladed and equant spar is mostly nonferroan; however, late-stage spar that fills remaining pore space (commonly center-pore positions) can be iron-rich (Figure 8.19). Late-stage ferroan spar is volumetrically insignificant. If present, it typically represents less than 1% of the intergranular spar and is commonly precipitated in fractures.

Examination of the packstone and grainstone lithologies by cathodoluminescence reveals their sparry cements have inconsistent patterns of internal zonation. Although cement stratigraphies may be consistent for all thin sections from a core that penetrates a given subunit, correlation of cement stratigraphies between wells in that subunit of the Viola is difficult. For example, the cathodoluminescence pattern of syntaxial spar in crinoidal packstones of the basal limestone subunit in the Champlin #1 Kottman well (*#11*; Figure 8.20) and the Northern Natural Gas #1 Caldwell well (*#12*; Figure 8.21), two wells within 5½ miles (9 km) of each other, are dissimilar. Cathodoluminescence also reveals that syntaxial spar in the latter core has an imbedded dissolution zone in which early spar has been partly dissolved and replaced by later spar that is in optical continuity with the earlier spar (Figure 8.21). As with the cement stratigraphies revealed by cathodoluminescence, no consistent pattern of dissolution is evident for any geographic area. However, the cement that commonly follows the dissolution event is typically nonluminescent. Staining with potassium ferricyanide reveals that this cement is commonly iron-rich. Partial moldic porosity within crinoid grains is also commonly filled by this nonluminescent cement.

Macroscopic interparticle porosity generally is not present in mudstones or wackestones, hence the early episode of spar cementation seen in the packstones and

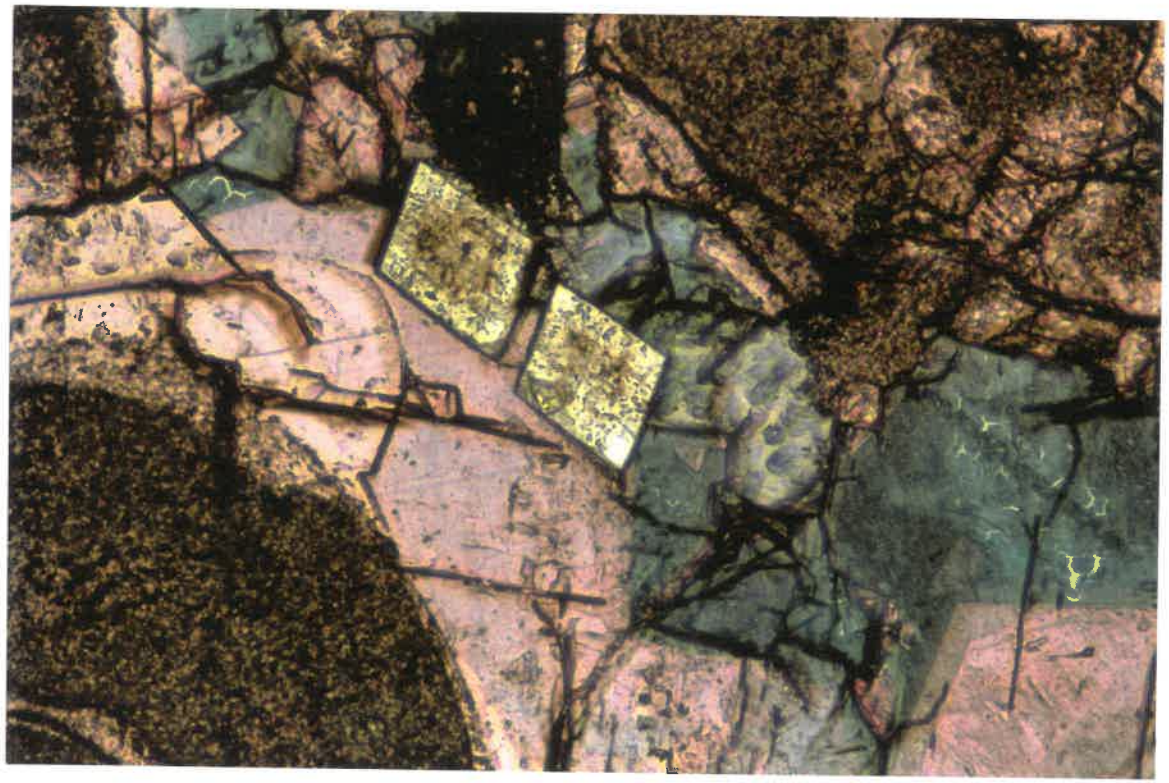

Figure 8.19 Photomicrograph of late ferroan calcite spar cement (blue) in optical continuity with earlier nonferroan spar (pink). The nonferroan and ferroan calcite-spar cements are in optical continuity with the crinoid columnal in the lower left of the photograph. Two rhombs of saddle(?) dolomite, as indicated by their curved crystal faces, "float" in the spar, and therefore succeed the ferroan calcite. Thin section is stained with a combination of Alizarin Red-S and potassium ferricyanide and is from the basal limestone subunit (3360.5 ft depth) in the Champlin #1 Kottman core (*#11*) in Rice County (19-T.19S.-R.8W.).

Figure 8.20a, 8.20b Matched pair of photomicrographs of syntaxial spar in a mud-poor crinoidal packstone in the basal limestone subunit, in plane-polarized light (8.20a) and with cathodoluminescence (8.20b). The stratigraphic pattern of moderate luminescence (**M**) growing outward to dull luminescence (**D**), then moderately bright luminescence (**L**) in the large pore is not developed in this subunit in a well 5½ mi (9 km) away (see Figure 8.21). Thin section is from the Champlin #1 Kottman core (*#11*), depth 3359 ft, in Rice County (19-T.19S.-R.8W.).

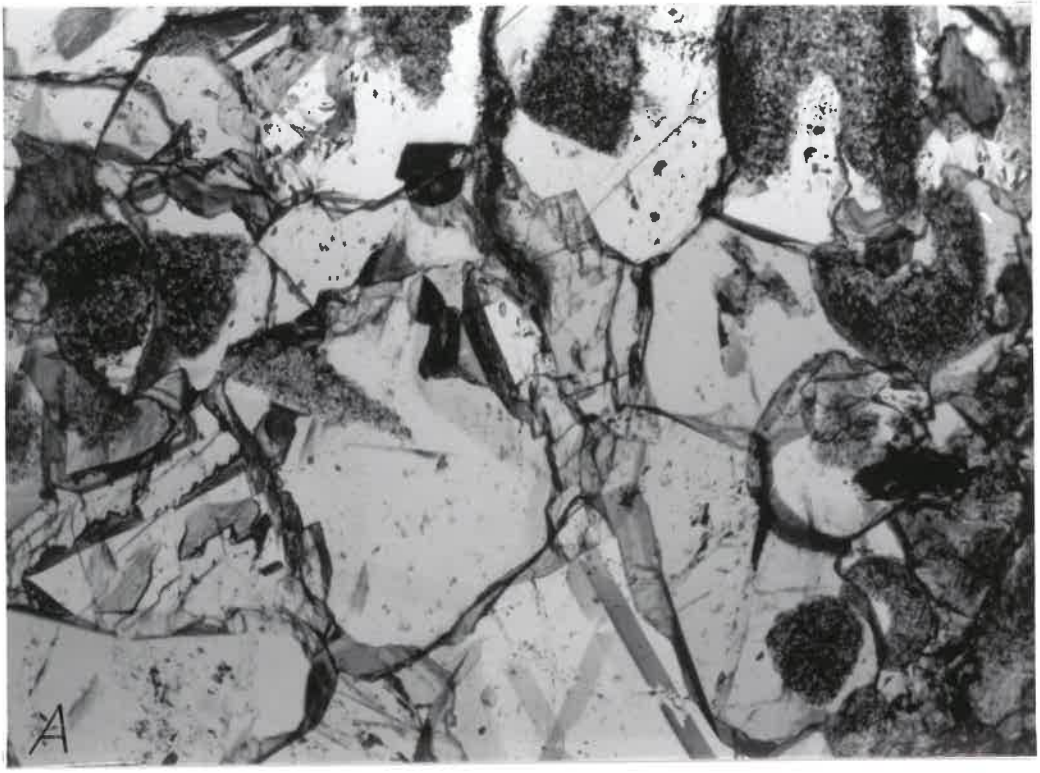
A

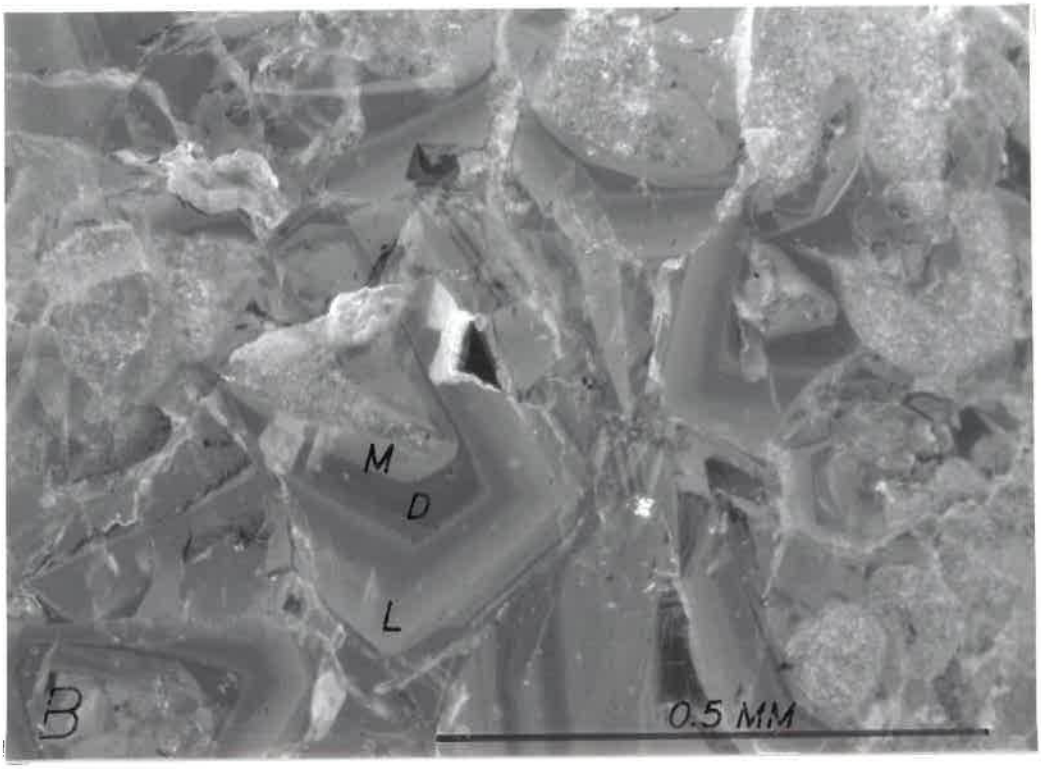
M
D
L
B
0.5 MM

Figure 8.21a, 8.21b Matched pair of photomicrographs of syntaxial spar in a mud-poor crinoidal packstone in the basal limestone subunit, in plane-polarized light (8.21a) and with cathodoluminescence (8.21b). The cement stratigraphy of this sample consists of a moderately luminescent cement (**M**) that grades outward to a slightly duller cement (**D**). In turn this is followed by a banded zone of dark and brightly luminescent cement (**L**). An irregular dissolution surface truncates these earlier cements and is followed by a nonluminescent cement (**N**). Another dissolution surface (**S**) separates the dull cement from the banded cement. The stratigraphy of this syntaxial cement is notably different from the nearby Champlin #1 Kottman core (see Figure 8.20). Thin section is from the Northern Natural Gas #1 Caldwell core (*#12*), depth 3259.75 ft, in Rice County (2-T.20S.-R.8W.).

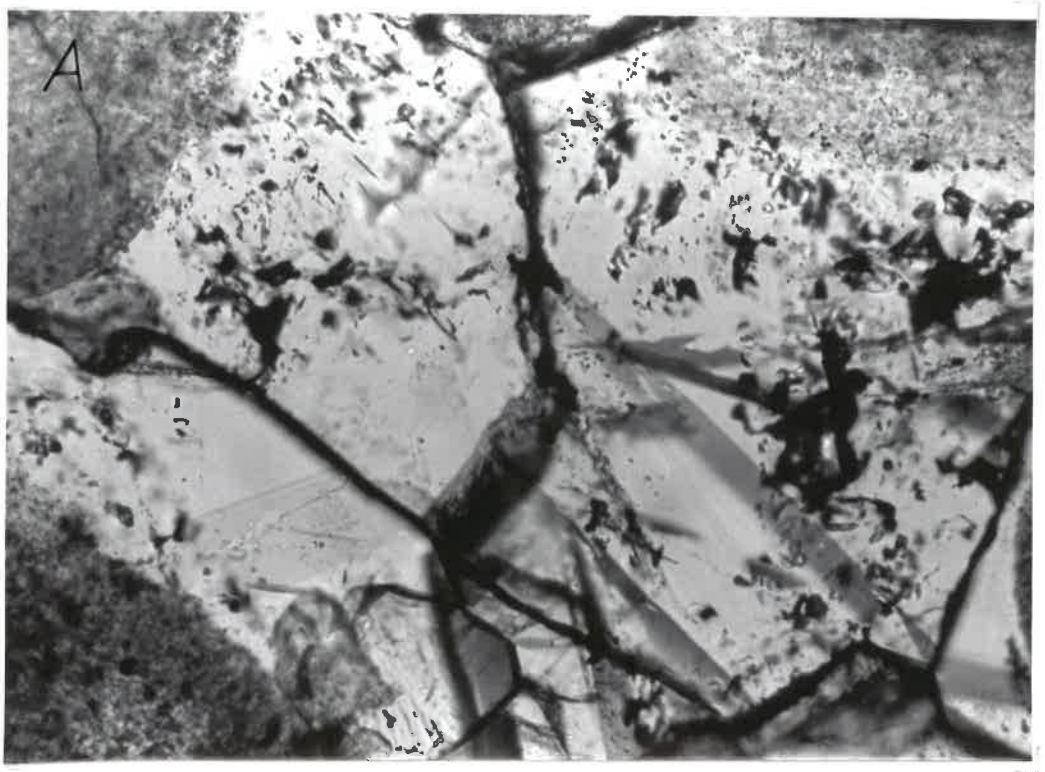
A

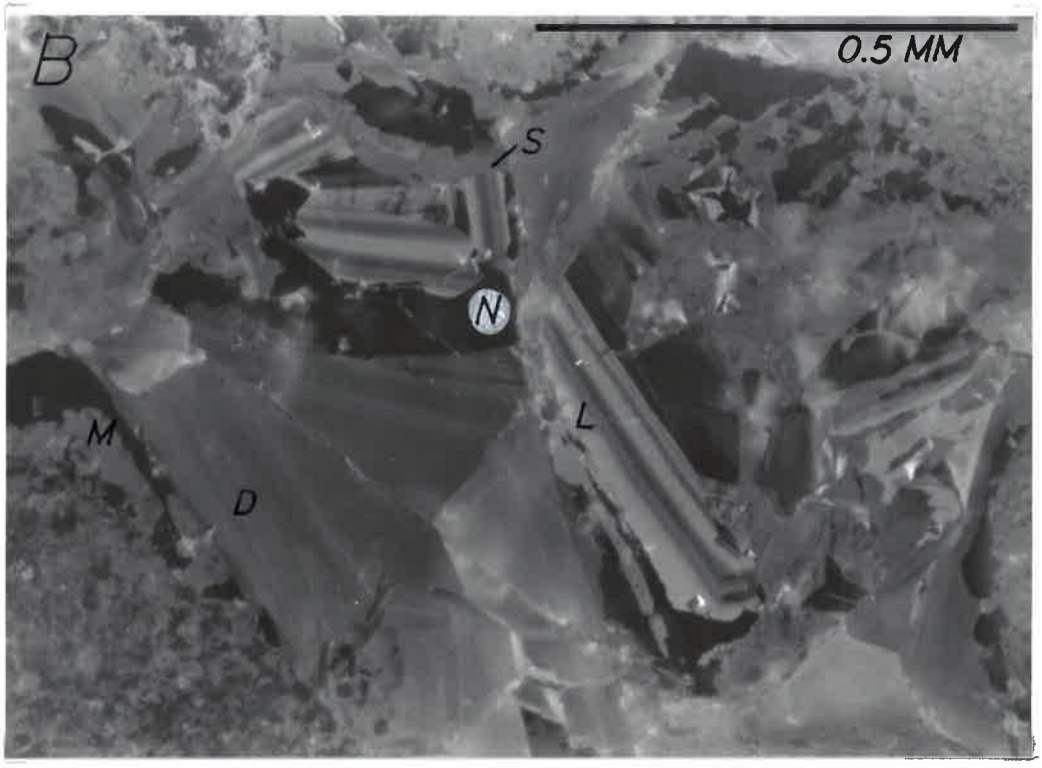
B
0.5 MM
S
N
M
D
L

grainstones of the basal limestone subunit is not recorded in the mud-supported lithologies of the lower and upper cherty dolomitic limestone. Rarely, however, minor shelter porosity beneath two adjacent crinoid grains will be filled by nonferroan, syntaxial spar.

Interpretations

Bladed isopachous cement in the grain-supported lithologies is consistent with, but not necessarily diagnostic of marine phreatic diagenetic environments (Harris and others, 1985). The diagenetic environment that produces syntaxial sparry overgrowths on the crinoid fragments and associated pore-filling equant spar is less certain. Longman (1980) maintains that syntaxial overgrowths on echinoderms are principally formed in freshwater diagenetic environments, but these overgrowths can also be marine in origin (Cantrell and Walker, 1985; Harris and others, 1985; Dorobek, 1987). Crystal habit and composition of cements depend on many factors, but a general relationship established by Folk (1974) indicates the bladed cement was probably low-magnesium calcite, because high-magnesium calcite tends to have an acicular crystal habit. The lack of iron in most of the spar indicates that the diagenetic environment was well oxygenated, for Fe^{+2} is not favored for incorporation into the calcite crystallographic lattice in oxidizing conditions (Evamy, 1969; Meyers and Lohmann, 1980).

The cathodoluminescence pattern of the syntaxial cements indicates they persisted growing as the diagenetic environment changed, and thus a variety of diagenetic environments are encompassed and recorded by these cements. Dissolution events that occurred during growth of the syntaxial cements record fluxes of water undersaturated with respect to calcite. The difficulties in correlation of these dissolution events and the associated cement stratigraphies implies that although the packstones and grainstones in the basal and upper limestone subunits of the Viola

are laterally contiguous for long distances, the diagenetic environments are more localized. Perhaps the tops of shoals or lobes of these carbonate sand bodies were occasionally exposed during minor drops in sea level, and meteoric waters were either locally established as lenses or mixed with seawater to produce laterally variable diagenetic environments. Early cementation of a laterally diachronously exposed sheet of carbonate sand would also yield apparently inconsistent cement stratigraphies, particularly if well spacing is sparse.

A marine to shallow-burial origin for the bladed and syntaxial cements is implied by their being first-generation cements in a marine-deposited unit. The lack of significant degrading neomorphism and grain dissolution also militates against a freshwater diagenetic environment set forth by Longman (1980) for syntaxial overgrowths on crinoid grains. The bladed cement probably nucleated on polycrystalline substrates (principally brachiopod fragments or heavily micritized surfaces) either prior to or, as revealed by cathodoluminescence in some cases, contemporaneously with early stages of the volumetrically more significant syntaxial cement. The lesser compaction observed in spar-cemented grainstones, as opposed to the muddier packstones (Figure 8.15), implies that the bladed and syntaxial spar cements probably precipitated shortly after deposition and prior to significant burial. Spar infill within delicate but uncrushed micrite envelopes also suggests some cementation occurred before or during compaction of the sediments (Figure 8.16). Minor chemical compaction, however, occurred before some spar cementation because although two adjacent echinoderm fragments may have a sutured boundary between them, their respective syntaxial cements were characterized by a straight compromise growth boundary in some thin sections.

Thick micrite envelopes or a thin layer of carbonate mud on the upper surface of echinoderm fragments probably inhibited nucleation and growth of syntaxial spar

in the packstones and grainstones of the basal limestone and upper limestone subunits (St. Clair, 1982). Lucia (1962) and Evamy and Shearman (1965) noted similar features in their studies of crinoidal packstones.

The presence of plastically deformed packstone lithoclasts just above the base of the lower cherty dolomitic limestone subunit (see Figure 7.10) implies that the underlying basal limestone subunit had experienced early but minor cementation shortly after deposition. The presence of broken, but not plastically deformed, silicified packstone lithoclasts in the Maquoketa Shale (see Figure 7.31), however, indicate the process of lithification of the basal limestone subunit was farther advanced, probably to the silicification stage (see Figure 8.13) by the time the overlying Maquoketa was deposited.

The ferroan spar in center-pore positions that is in optical continuity with the earlier nonferroan spar suggests a later stage of cementation that was characterized by a reducing environment, possibly with deep burial. Continuous growth of spar as diagenetic conditions suddenly became more reducing is not necessary. Instead, a gap in time could have occurred between deposition of the Fe-poor and Fe-rich spars, with the Fe-rich spar conveniently building upon the crystallographic foundation of the Fe-poor spar. The volumetric insignificance of the ferroan spar (approximately 1% of the total spar) indicates that oxygenated conditions dominated the occlusion of porosity in the grain-supported lithologies of the basal limestone, and these rocks were almost completely cemented before being introduced to a reducing environment.

Silicification

Observations

Although quantitatively insignificant (<1%), fine-crystalline quartz and chalcedony selectively replace a few skeletal grains in the basal and upper limestones.

Brachiopod fragments are the most commonly replaced grain, with their microstructure being preserved in detail (Figure 8.22). Rarely, bladed quartz cement is developed on silicified brachiopod fragments. Crinoid grains also can be partly silicified, but their microstructure tends to be obliterated by the silicification. The timing of the silicification in the basal and upper limestone with respect to the other major diagenetic events is equivocal, partly due to its being present largely only as a replacement wholly within fossil grains. However, in some grains silicification extends beyond the boundary of the grain it replaces and encroaches into the adjacent spar cement; therefore, it appears to chronologically follow the spar cement. In rare instances, a thin streak of chert was observed sandwiched between two spar crystals, which is additional evidence that chertification succeeds spar cementation. However, broken grains, with both grain fragments equally silicified, but separated by spar cement (Figure 8.22) is evidence that some silicification may have occurred prior to, or contemporaneous with, spar cementation. No strong geographic or stratigraphic trends in the amount of silicification are evident in the basal or upper limestone in the study area, although cores from near the pinchout of the basal limestone subunit on the Chautauqua arch (i.e., Midcontinent Marine #1 North Hilger (#*28*; 34-T.25S.-R.4W.) and #1 South Hilger (#*29;* 9-T.26S.-R.4W.) display slightly more silicification than wells elsewhere. With cathodoluminescence, silicified areas in the Viola are typically very light blue.

In contrast to its volumetric insignificance in the grain-supported lithologies of the Viola, silicification, manifest by bedded and nodular chert, is a volumetrically major diagenetic event in the mud-supported lithologies. Microfossil debris and depositional textures are commonly exquisitely preserved in these chert nodules, whereas no trace of these features may be present in the surrounding dolomitized rock (Figure 8.23). In addition, packing of the microfossil debris within the chert

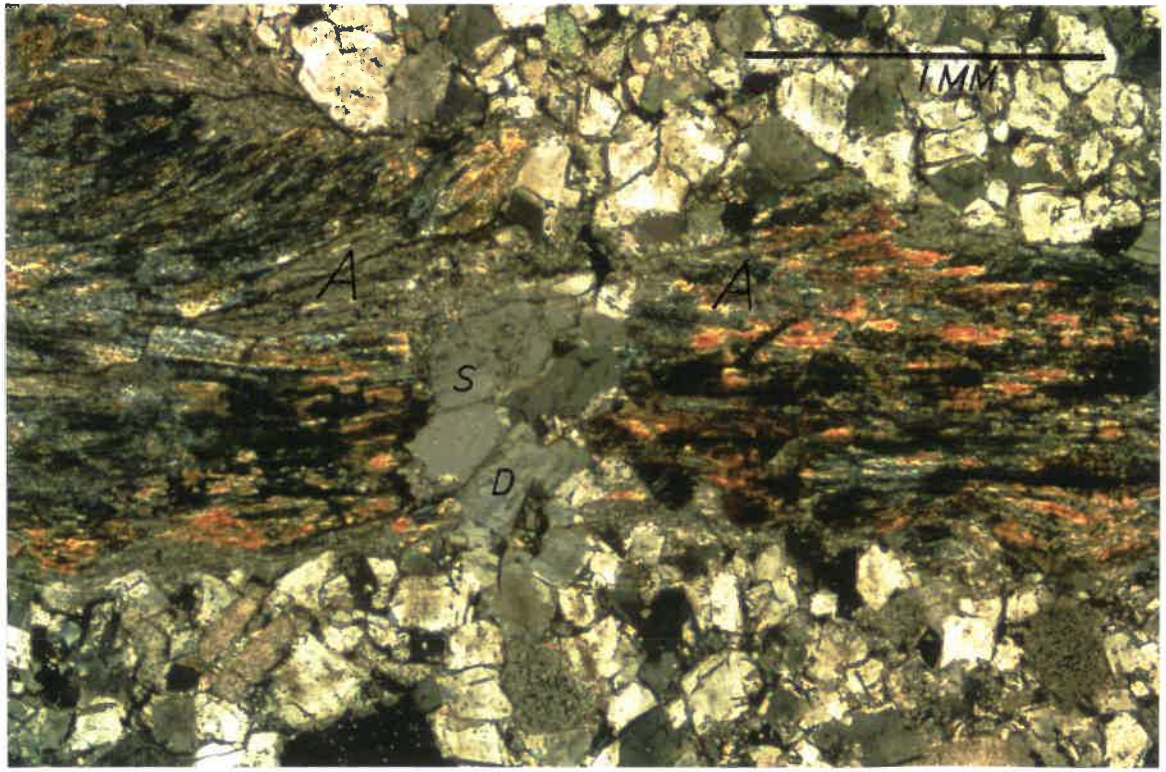

Figure 8.22 Photomicrograph (with crossed polars) of silicified brachiopod fragments (**A**) in a packstone in the basal limestone. Calcite spar (**S**) with a dolomite crystal (**D**) (both at partial extinction) is present in the gap between the two silicified fragments, formerly a single shell. Thin section is from the Derby #1 Wood core (#*15*, 3891.6 ft depth) in northeastern Reno County (36-T.22S.-R.5W.).

Figure 8.23 Photomicrograph of interior of a chert nodule in the lower cherty dolomitic limestone (depth 3779.4 ft) from the Braden-Zenith ZU-3 core (*#20*) in eastern Stafford County (11-T.24S.-R.11W.). Light-colored arcuate fossil fragment in center of the photograph is an ostracode. Other materials include unidentified phosphatic shell fragments, other ostracode fragments, and organic macerals. Rock surrounding the chert nodule is dolomitized. In contrast to the chert nodule, no original depositional texture is preserved in these dolomitized areas. The chert is therefore interpreted to precede the dolomite.

nodules is typically loose and with little breakage, indicating minimal compaction before these rocks were silicified. Small (10 to 20 μm), isolated euhedral dolomite rhombs are commonly present in the chert nodules. Some chert nodules have microscopic moldic porosity after siliceous sponge spicules. Silica replaces fossils, mostly brachiopod shells fragments (Figure 8.24) in wackestones and mudstones of the lower and upper cherty dolomitic limestone. Due to absence of cross-cutting relationships, it is difficult to tell if this is the same episode of silicification that accounts for the chert nodules in these subunits.

Chert nodules are universally present and common in both the lower cherty dolomitic limestone and upper cherty dolomitic limestone subunits. No appreciable geographic variations in the chert within these subunits could be discerned from inspection of cuttings logs and cores, although in the lower cherty dolomitic limestone residual chert is concentrated by dissolution of accompanying carbonate rock locally on the Pratt anticline and on the southern flank of the Central Kansas uplift (Adkison, 1972; Bornemann and others, 1982; Bornemann and Doveton, 1983; Figure 8.8).

In the Braden-Zenith ZU-1 (*#19*) and ZU-3 (*#20*) cores in eastern Stafford County, chert nodules are broken in the thin intraformational breccia zones at the top of the lower cherty dolomitic limestone, approximately 3 ft (1 m) beneath the upper limestone subunit. In these intraformational breccias the chert nodules display sharp, conchoidal margins (Figures 7.19, 8.25) but the interbedded dolomitic mudstone, despite also being brecciated, displays a crumbly texture (Figure 8.25) indicating it was not well lithified when the chert nodule was broken. Chert in the upper cherty dolomitic limestone also appears to be very early in that it breaks sharply, but the surrounding carbonate sediment (probably lime muds) were still plastic and were injected into fractures within the chert (Figure 8.26).

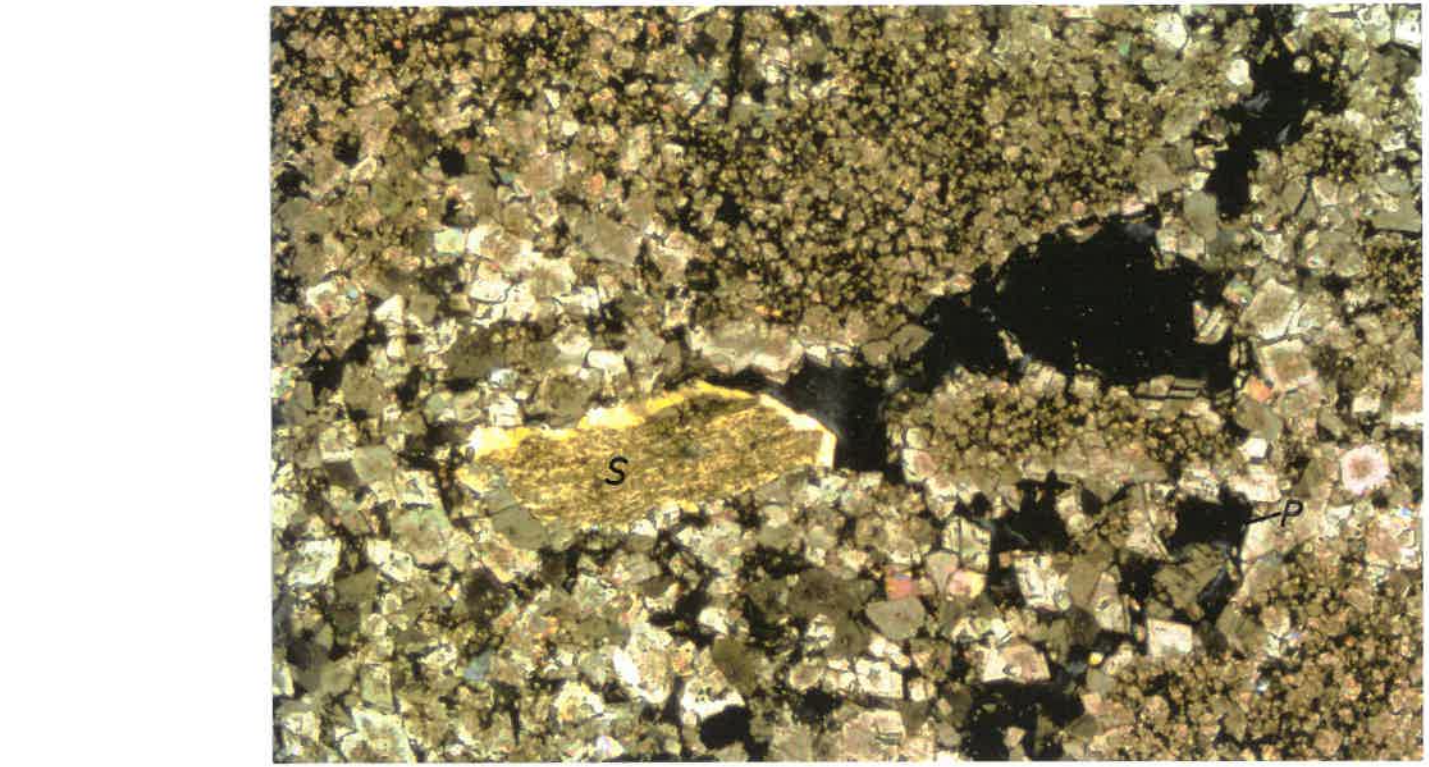

Figure 8.24 Photomicrograph (crossed polars) of moldic porosity in an outlier of lower cherty dolomitic limestone (depth 3349-52.5 ft) in the Shell #4 Griffin 'B' core (#9) from eastern McPherson County (11-T.19S.-R.2W.). Early silicification preserves the interior texture of part of a brachiopod shell (S). The right-hand side of the shell is expressed as a mold. This part may have not been silicified, and was subsequently dissolved. The resulting mold was also slightly enlarged and a clear quartz cement grew on the upper surface of the brachiopod and its side open to the mold; the rock was then dolomitized. Intercrystalline porosity (P) is expressed as dark areas between the rhombs.

Figure 8.25 Polished slab of dolomitic fine-grained muddy packstone and brecciated chert from the lower cherty dolomitic limestone in the Braden-Zenith ZU-3 core (*#20*, depth 3772 ft) in eastern Stafford County (11-T.24S.-R.11W.). The brecciated zone is interpreted to represent a brief period of dissolution that occurred before deposition of the upper limestone subunit (see Chapter 7). Two stages of lithification (**A** & **B**) may be indicated by the light blue and white zones in the chert. Very early lithification of the chert is revealed by the relationship between it and the superjacent fine-grained packstone. Vertical fractures in the chert are partly filled by sediment derived from the packstones above. Small "overhead stopes" (**S**) in the packstone (caused by crumbling of the packstone and its particles falling into voids created by the fractures) are now filled with calcite spar. Left side of slab has been stained by potassium ferricyanide and Alizarin Red-S.

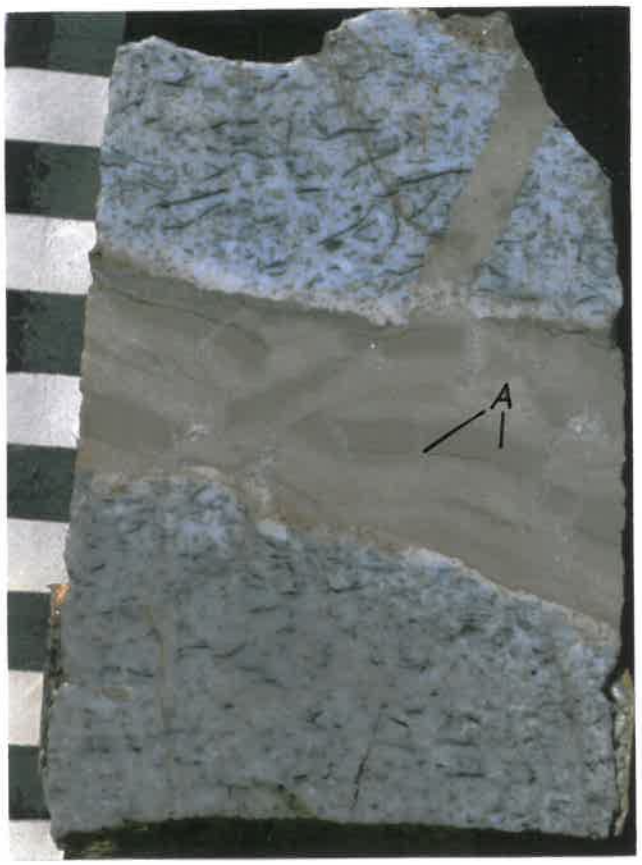

Figure 8.26 Core slab of a chertified packstone in the upper cherty dolomitic limestone in the Braden-Zenith ZU-1 core (*#19*) in eastern Stafford County (11-T.24S.-R.11W., depth 3824 ft). A semilithified dolomitized mudstone is plastically deformed and injected into a fracture in the chertified packstone. Spar-filled fractures (**A**) are also developed between intraclasts that were formed from a thin bed that was slightly more lithified than the surrounding mud. Textural relationships indicate early formation and lithification of chert in this unit. Scale divisions are in centimeters.

Interpretations

The diagenetic environment and source of the replacive silicification in the Viola Formation remains obscure. Dissolution of biogenic silica, such as sponge spicules is a possible source for the silica. For replacement of calcitic fossils, the diagenetic waters must be chemically supersaturated with respect to amorphous silica

and undersaturated with respect to calcite. The concentration of silica in solution is favored by a very high pH (>10), and its precipitation could then be caused by a drop in the pH to neutral levels (Berner, 1971, p. 164). Inasmuch as silicification is not prevalent in the basal and upper limestones, perhaps the diagenetic environment for this replacement reflects local lithologic control on a microscopic scale.

It is unclear if the replacement silicification in the skeletal packstones and grainstones of the basal and upper limestones, and the nodular cherts in the mudstones and wackestones of the lower and upper cherty dolomitic limestones, occur in a similar diagenetic environment. Dorobek (1987) hypothesized that possible sources for silica in cherty limestones could be dissolution of sponge spicules, clay-mineral diagenetic reactions, or pressure solution of quartz grains. The latter two processes may have been important for the minor silicification observed in the Viola basal limestone, but silica-bearing solutions also may have been expelled from subjacent shales and sandstones in the Simpson Group. Locally, clay-mineral reactions in the overlying Maquoketa Shale may have been a source of silica, but the Upper Ordovician strata in Kansas was subject to sufficient burial or heating soon after deposition for these types of reactions to have occurred to any great extent (see Chapter 6). Molds of spicules preserved in chert nodules in the lower and upper cherty dolomitic limestones suggest that remobilized biogenic silica may be the dominant process responsible for the chert. St. Clair (1982) speculated that the dominance of chert nodules in the wackestones and mudstones of the lower and upper cherty dolomitic limestones, as compared to their rarity in the packstones and grainstones in the basal and upper limestones, reflects a local source of silica. She suggested that the mudstones and wackestones may have had greater permeability and porosity than the packstones and grainstones at the time of silicification. The calcite spar in the basal and upper limestones probably occluded the porosity of the

grain-supported lithologies early and thus reduced their permeability.

The small euhedral dolomite crystals in the chert nodules of the lower and upper cherty dolomitic limestones are very common in nodular cherts in other units where the surrounding carbonate is extensively dolomitized (Knauth, 1979). Knauth (1979) speculated that dolomite is not as readily replaced by silica as calcium carbonate and that silicification occurred with or after the dolomitization. He adopted a mixing-zone model (Badiozamani, 1973), in which seawater and meteoric water mingle along coastal areas, to explain the penecontemporaneous dolomitization and silicification. Others (cf., Wise and Weaver, 1974; Baker and Kastner, 1981; Mišík, 1993) suggested that dolomite rhombs within chert nodules may be related to localized diagenetic environments within the nodule. A study of the oxygen isotopes of the chert and its included dolomite and a comparison with the surrounding dolomites is a possible avenue of further investigation.

The preservation of relatively uncompacted depositional textures in chert nodules, the virtual exclusion of any other diagenetic process in chertified areas, and the tendency of the nodules to fracture when the surrounding sediment either disaggregates (Figure 8.25) or deforms plastically (Figure 8.26), indicates the chert in the Viola is an early diagenetic phenomenon. Considering that the fracturing of the chert in the lower cherty dolomitic limestone shown in Figure 8.25 is probably from karstic dissolution immediately before deposition of the upper limestone subunit, the precipitation and lithification of the chert probably occurred very shortly after deposition.

Dolomitization

Observations

Dolomitization is the second-most volumetrically significant diagenetic event

(after cementation by sparry calcite) to affect the grain-supported lithologies of the basal and upper limestones. Outside of the heavily dolomitized area immediately north of the Chautauqua arch (which will be discussed later; see Figure 8.5) dolomite constitutes at most 25% of the basal limestone; the norm is estimated at 1 to 10%. A similar ratio characterizes the upper limestone subunit and local packstone beds in the upper cherty dolomitic limestone subunit. No consistent change in dolomite content occurs stratigraphically within the basal and upper limestones; however, depositional texture strongly controls the dolomitization, in that packstones and grainstones are commonly less dolomitized than interbedded wackestones. Differences in the average sizes of dolomite crystals also correspond to the depositional texture of the rock in that dolomite rhombs range in size from 50 to 100 μm in mud-supported lithologies, whereas in grain-supported lithologies they are larger, commonly 200 to 500 μm. The change in size can occur abruptly -- within a centimeter or across a stylolite. Burrows, particularly if their fill is finer grained than surrounding rock, commonly are preferentially dolomitized. Bryozoans generally have more dolomite rhombs concentrated in them than other allochems (St. Clair, 1982).

Dolomite in the basal and upper limestone is mostly replacive, in that discrete euhedral to subhedral rhombs commonly cross-cut and replace previous fabric elements (i.e., typically planar-p texture in Sibley and Gregg, 1987) (Figure 8.27). Most dolomite rhombs in both mud- and grain-supported lithologies have cloudy (inclusion-rich) centers and clear rims, but strong concentric zonation defined by inclusions within the dolomite rhomb is not typical. Additional cloudy-to-clear growth bands commonly are present and they may vary in number even in the same core.

Cathodoluminescence of dolomite rhombs reveals striking differences in their internal structure, regardless of whether the dolomite is in grain-supported or mud-

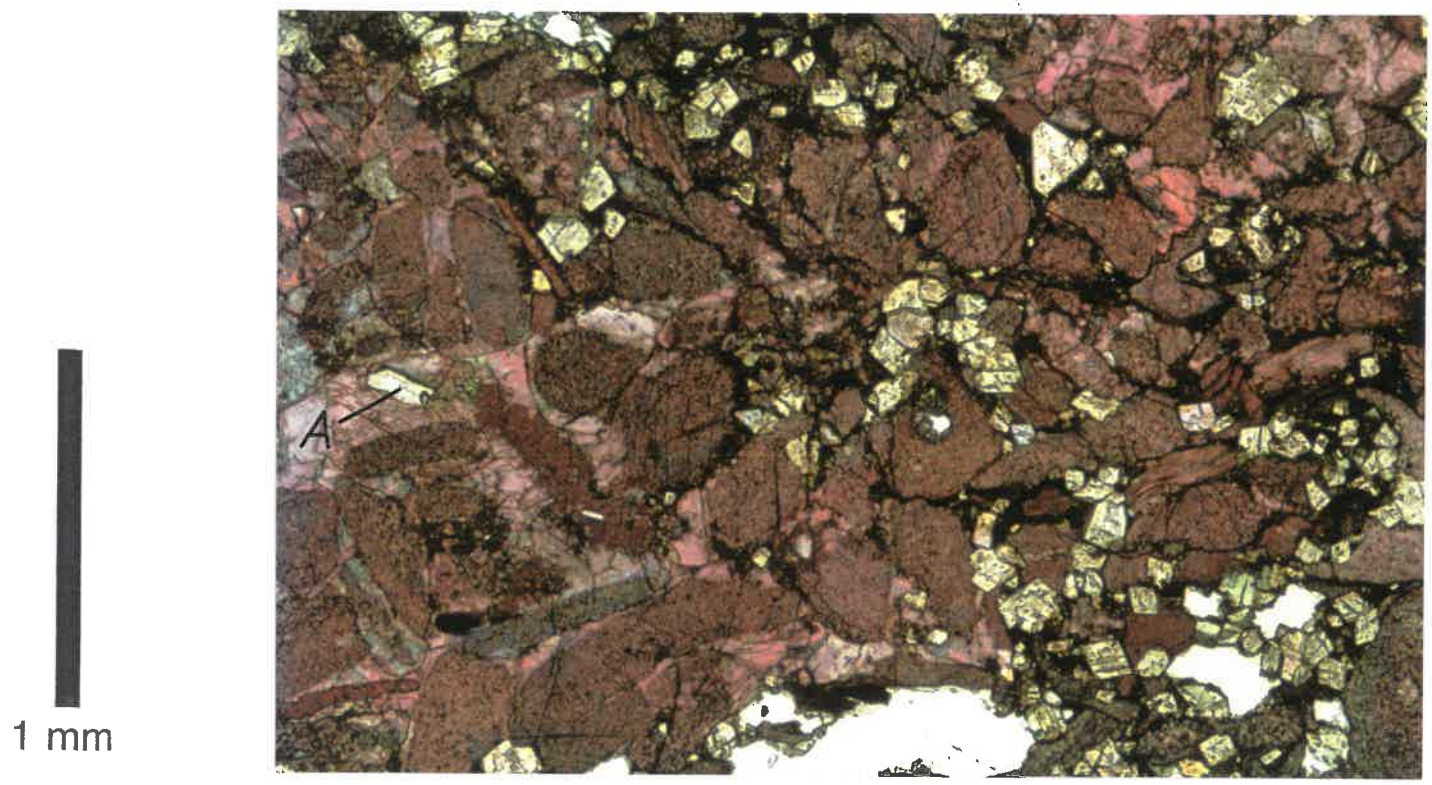

Figure 8.27 Photomicrograph of euhedral to subhedral dolomite (pale color) replacing echinoderm grains and syntaxial spar in a compacted muddy packstone in the basal limestone. Dark residue between clasts is mud. Dolomite rhombs crosscut sutured contacts between the echinoderm grains, and are interpreted to postdate the spar and compaction. The echinoderm grains in the left of the photograph developed syntaxial spar and compacted less than those on the right. Dolomite also is concentrated in areas where there is less spar. Minor suturing by dissolution is evident on the margins of some dolomite rhombs, but generally to a lesser extent than the surrounding calcite. Dolomite is wholly contained within the spar in the left side of the photograph (**A**). Thin section is stained with Alizarin Red-S and potassium ferricyanide; taken from the Derby #1 Wood core (*#15*, 3899.5 ft depth) in northeastern Reno County (36-T.22S.-R.5W.).

supported lithologies. The simplest internal structure observed for replacive dolomites is a concentric structure (Figure 8.28) in which growth zones within the rhomb are developed parallel to its crystal faces. Another texture observable in cathodoluminescence is more heterogeneous, with the dolomite crystal exhibiting a complex patchwork texture rather than zonation (Figure 8.29). For descriptive purposes, dolomite characterized by this type of complex cathodoluminescent pattern is identified in this report as "collage dolomite". With present core coverage and spacing, there is no apparent correlation of zones in the concentric dolomite between wells. Likewise, the collage texture is rarely consistent with its cathodoluminescence intensity and granularity from well to well and even within a given core. Such changes are not related to subunit boundaries. The two types of internal structure (i.e., "concentric" and "collage") show little intergradation in the study area, although some concentric dolomite crystals display volumetrically insignificant isolated patches or specks of dolomite with either darker or lighter cathodoluminescence (Figure 8.28) that cut across the concentric zonation. Most dolomite crystals with the collage textures have a thin concentric rim (Figure 8.30).

The relative timing of the dolomitization in the basal and upper limestone is difficult to ascertain because of the ubiquitous euhedral habit of the dolomite crystals and their occurrence as a replacement. However, the dolomite probably postdates the interparticle syntaxial cement because crystals of dolomite commonly "float" in spar cement; that is, they are contained entirely within the spar and not attached to or near a substrate (Figure 8.27). Dolomite rhombs cross-cut echinoderm fragments and their syntaxial spar (Figure 8.31). This relationship, however, could be interpreted as subsequent growth of spar around a dolomite rhomb that nucleated in the echinoderm fragment and protruded into adjacent pore space.

The relationship of the replacive dolomite to the chert aids in determining

Figure 8.28a, 8.28b Matched pair of photomicrographs of a patch of dolomite in a mud-poor crinoidal packstone in the basal limestone subunit, in plane polarized light (8.28a) and with cathodoluminescence (8.28b). This dolomite typifies a "concentric" internal structure. Bright specks within each dolomite are interpreted as representing small areas that have been recrystallized or replaced. Thin section is from the Derby #1 Wood core (*#15*, 3903.3 ft depth) in northeastern Reno County (36-T.22S.-R.5W.).

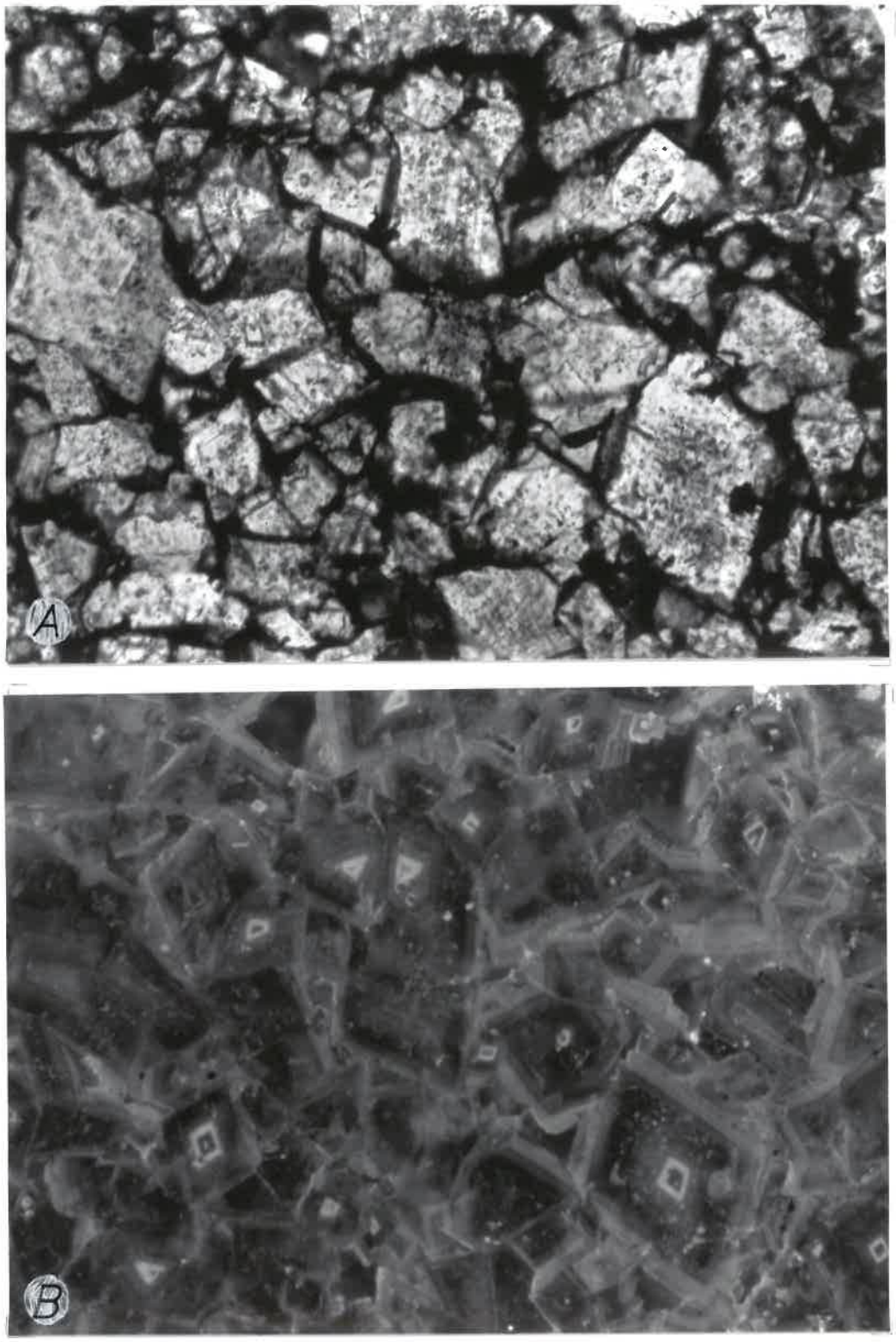
A
B
0.5 mm

Figure 8.29a, 8.29b Matched pair of photomicrographs of a patch of dolomite in a crinoidal packstone in the basal limestone subunit, in plane polarized light (8.29a) and with cathodoluminescence (8.29b). This dolomite typifies a "collage" internal structure. The core sample was taken 1.9 mi (3.1 km) north of the core sample shown in Figure 8.28, where dolomite in the same Viola subunit displays a concentric structure. Thin section is from the Derby #3 Lehman core (#*14*, 3412.3 ft depth) in northern Harvey County (13-T.22S.-R.2W.).

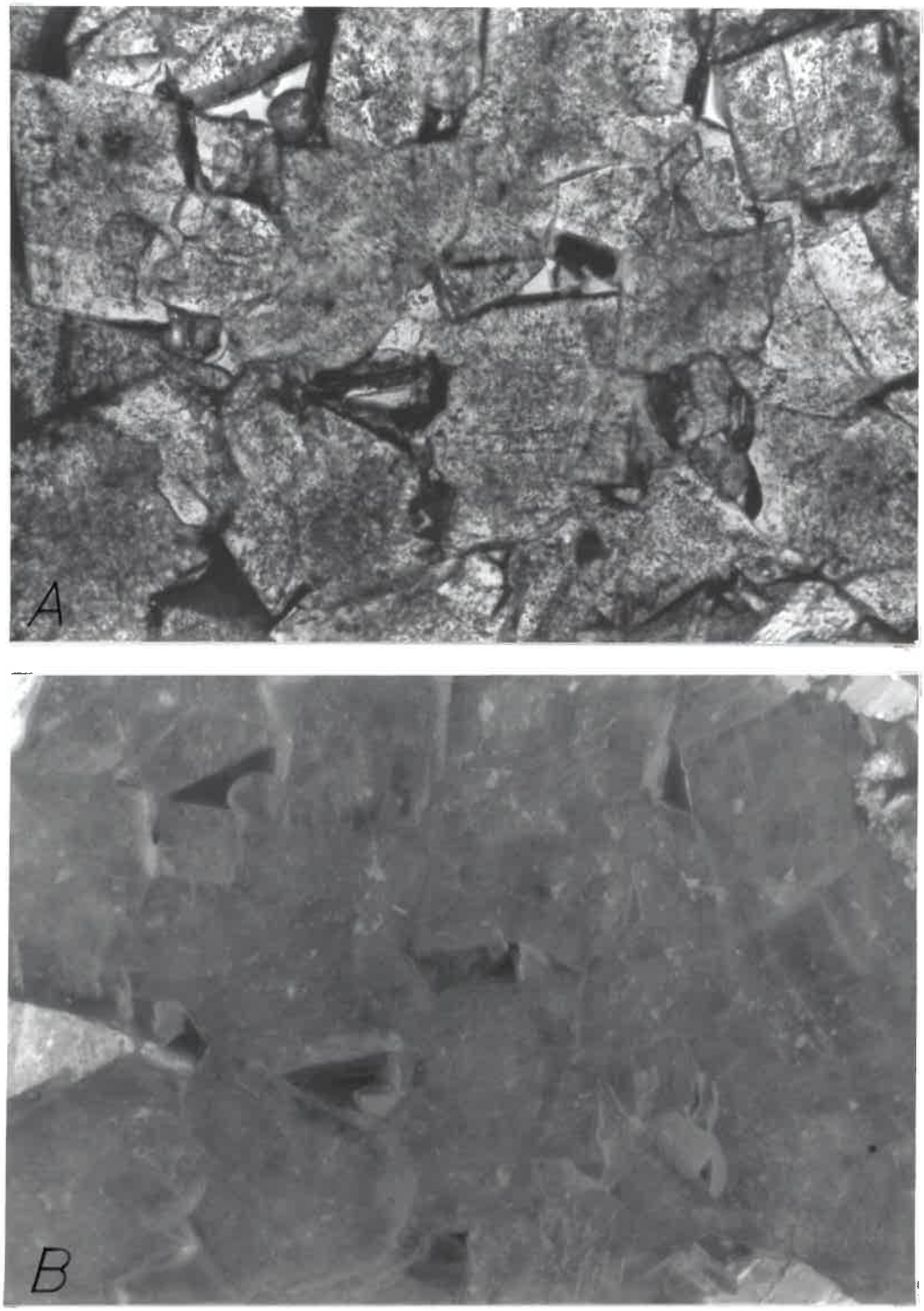
A
B
0.5 mm

Figure 8.30a, 8.30b Matched pair of photomicrographs of dolomite in the upper cherty dolomitic limestone subunit, in plane polarized light (8.30a) and with cathodoluminescence (8.30b). This dolomite typifies a collage internal structure, but with a thin concentric rim. Thin section is from the Braden-Zenith ZU-3 core (#*20*, depth 3761 ft) in eastern Stafford County (11-T.24S.-R.11W.).

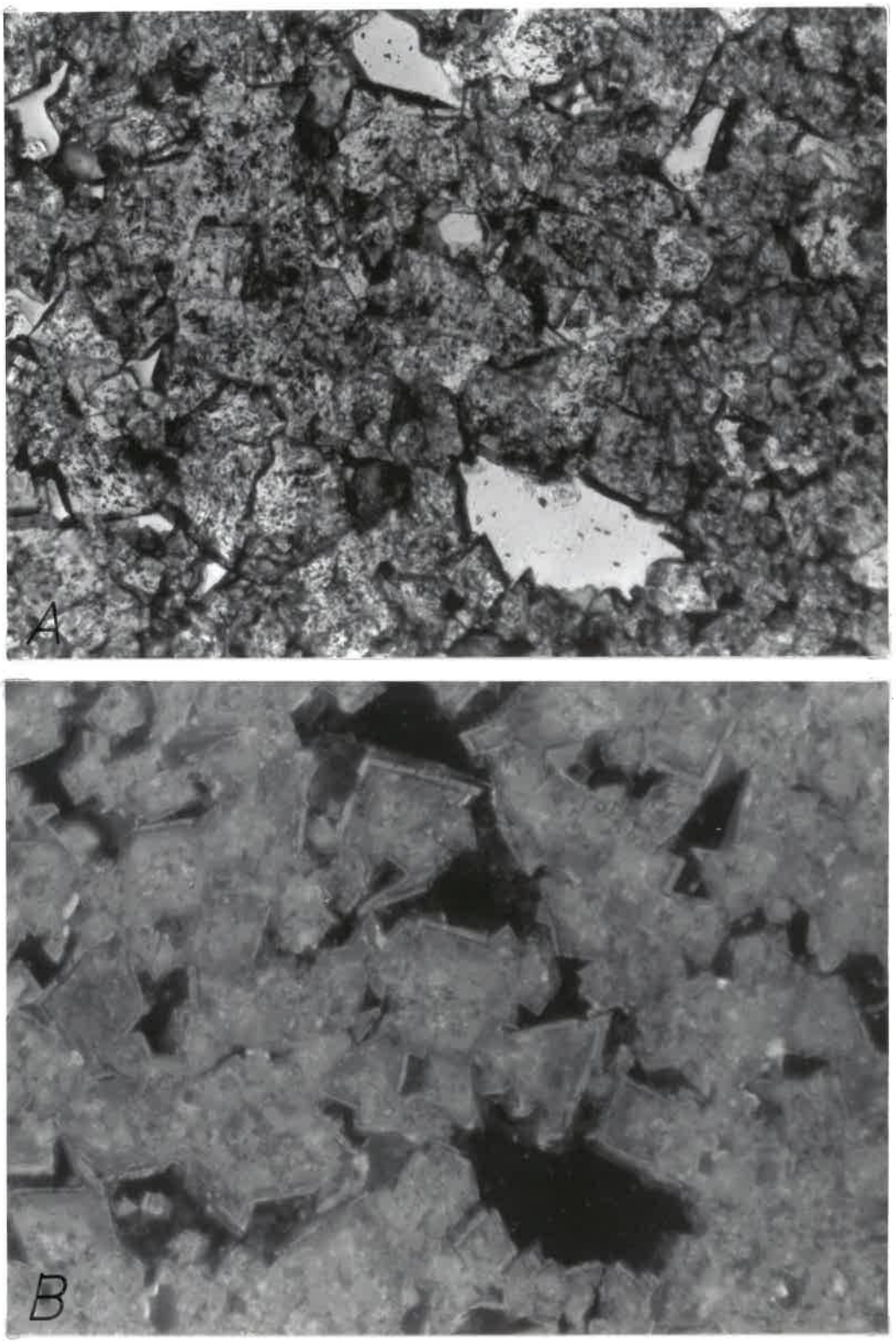
A
B
0.5 mm

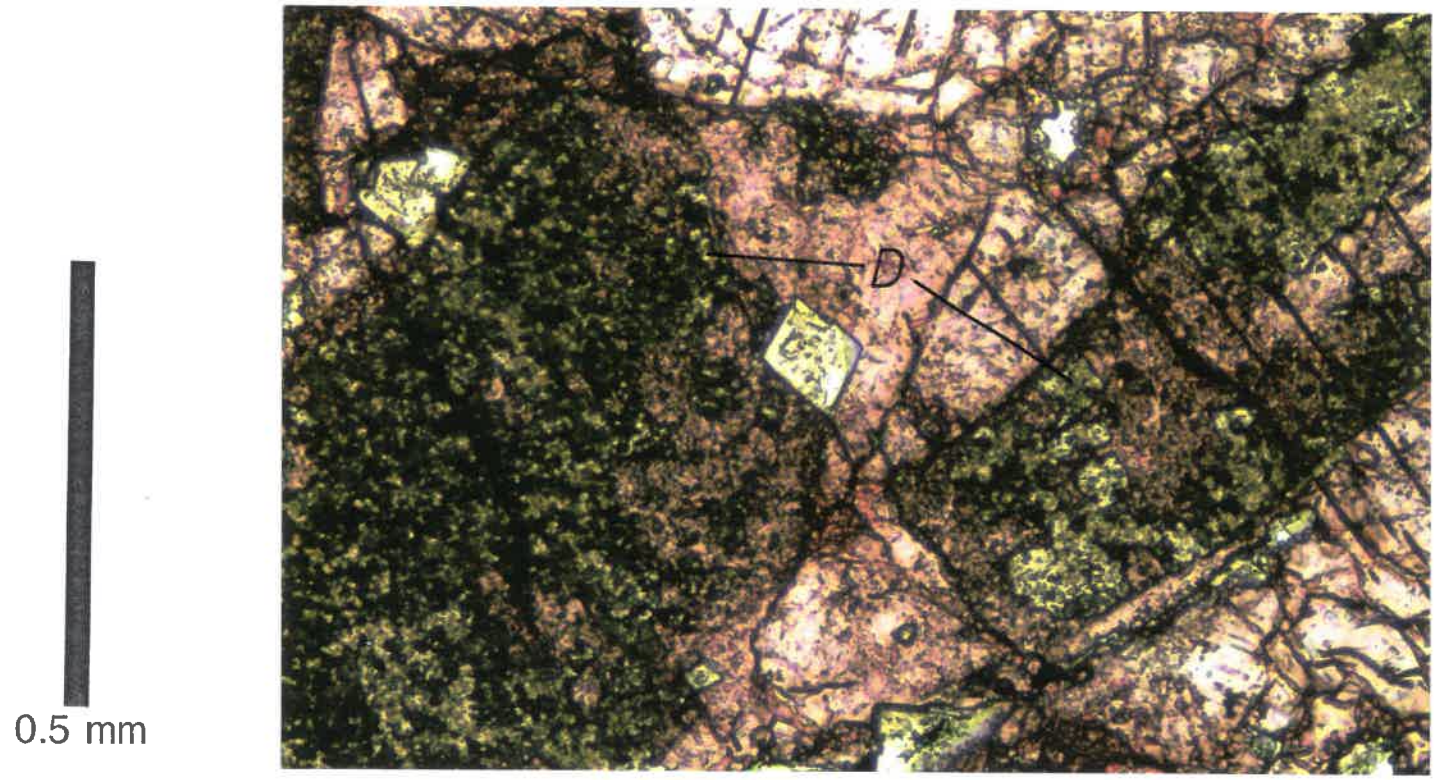

Figure 8.31 Photomicrograph of a euhedral rhomb of replacive dolomite (center) transecting the margin of an echinoderm and its syntaxial spar. Sample is from a packstone (depth 3412 ft) in the basal limestone from the Shell #1 Anderson core (#3) in eastern McPherson County (30-T.19S.-R.1W.). Echinoderm fragments are also partly replaced by a mimetic dolomite (**D**), which occurs in irregularly shaped patches within the grain. Thin section is stained with Alizarin Red-S and potassium ferricyanide.

where dolomitization falls within the paragenetic sequence. Silicified brachiopod fragments were never seen with dolomite rhombs (or ghosts of dolomite rhombs) within them, whereas nearby unsilicified brachiopod fragments locally contain dolomite rhombs. This observation suggests that the silicification occurred before the dolomitization and that the dolomite could not replace silica as easily as calcite. An analogous relationship is shown in Figure 8.22, in which a relatively dense concentration of dolomite surrounds silicified brachiopod fragments, but no dolomite rhombs are present within the brachiopod fragments. The syntaxial calcite spar is interpreted to generally precede silicification as discussed above. In turn, silicification apparently precedes dolomitization (Figure 8.22).

Virtually complete dolomitization of the basal limestone subunit on the northern flank of the Chautauqua arch is indicated by the regional distribution of dolomite shown in Figures 8.3 and 8.5. Four cores in this region recover dolomitized packstones and grainstones from the basal limestone subunit in this heavily dolomitized area: Shell #1 Anderson (*#3*) in 30-T.19S.-R.1W., Shell #4 Hill (*#4*) in 10-T.19S.-R.2W., Midcontinent Marine #1 North Hilger (*#28*) in 34-T.25S.-R.4W., and Midcontinent Marine #1 South Hilger (*#29*) in 9-T.26S.-R.4W. (see Appendix IV). In these cores the most abundant dolomite is a mimetic dolomite, in which the depositional texture of the rock and the internal structure of its constituent grains, are preserved (Figures 8.31, 8.32). Regional mapping indicates the dolomitization boundary is irregular and somewhat abrupt, because wells 6 to 8 mi (9 to 12 km) distant from each other show drastic differences in the degree of dolomitization in their cuttings (see Figure 8.5).

Mimetic dolomitization similar to that in the basal limestone subunit was not observed in the upper limestone subunit. However, this may reflect a sampling problem because no cores are available near the updip pinchout of the upper

Figure 8.32a, 8.32b Matched pair of photomicrographs with plane-polarized light (8.32a) and crossed polars (8.32b) of a mimetically dolomitized echinoderm packstone in the basal limestone. Sample is from the Midcontinent Marine #1 North Hilger core (*#28*) in eastern Reno County (depth 4127.5 ft, 34-T.25S.-R.4W.). The packstone is from the area north of the Chautauqua arch where the basal limestone is extensively dolomitized (see Figure 8.5). Plane-polarized light (above) shows echinoderm fragments (**E**) and their syntaxial cement (**C**). The view below, with crossed-polars, shows a crinoid fragment (center) and its syntaxial cement at extinction. Small rhombs of dolomite in the crinoid fragment, however, are not in optical continuity with it.

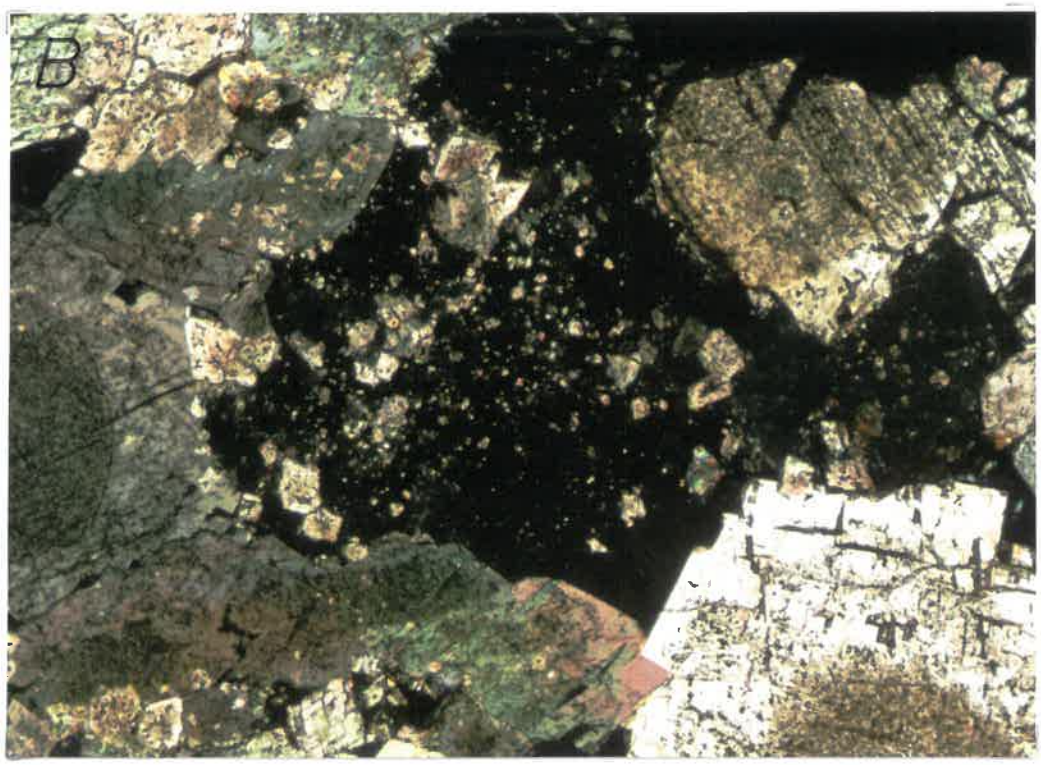

1 mm

limestone where it is dominantly dolomite (Figures 8.9, 8.10).

Under cathodoluminescence, the mimetic dolomite is complex -- characterized by fine-grained replacement of existing allochems and finely zoned cements (Figure 8.33). In the vicinity of the crest of the Chautauqua arch where the Midcontinent Marine #1 North Hilger (*#28*, 34-T.25S.-R.4W.), and Midcontinent Marine #1 South Hilger (*#29*, 9-T.26S.-R.4W.) are located, isolated rhombs of dolomite within the mimetically dolomitized packstones and grainstones of the basal limestone resemble those previously described as having a collage texture, but with thin concentrically zoned margins (Figure 8.34). Farther north, however, rhombs of collage dolomite in mimetic dolomite at the Shell #1 Anderson (*#3*, 30-T.19S.-R.1W.) and Shell #4 Hill (*#4*, 10-T.19S.-R.2W.) have no peripheral concentric zones.

Dolomitization of the lower and upper cherty dolomitic limestones (Figures 8.8, 8.11) is more widespread than in the basal and upper limestones (Figures 8.5, 8.9). The dolomitic limestone subunits are most heavily dolomitized where they pinch out on the flank of the Central Kansas and Chautauqua arches. Both of these subunits are least dolomitized in the extreme southwestern part of the study area where they are farthest from the crests of these arches (Figures 8.8, 8.11). In the regions where these two subunits are not heavily dolomitized, very fine-grained calcite within the lime-mud matrix is the major agent of lithification (Figure 8.35). Depositional textures are preserved. Any dolomite is present is replacive, with crystals being well-formed but isolated (planar-p texture according to Sibley and Gregg, 1987). If present, dolomite is typically concentrated within burrows. Individual crystals are typically aligned parallel to the margins of the burrow.

Dolomite in the cherty dolomitic limestones typically consists of an interlocking mesh of euhedral and subhedral crystals (planar-s texture in Sibley and Gregg, 1987), with individual rhombs 50 to 125 μm in size (Figure 8.36). This texture

Figure 8.33a, 8.33b Matched pair of photomicrographs of a mimetically dolomitized crinoidal packstone in the basal limestone subunit, in plane polarized light (8.33a) and with cathodoluminescence (8.33b). The crinoid grain (**C**) is replaced by a dolomite with a fine-grained, snowy-appearing pattern of varying luminescence, whereas its syntaxial rim is constructed of brightly banded dolomitic cement (**D**). Thin section is from the Midcontinent Marine #1 North Hilger core (#*28*) in eastern Reno County (depth 4127.3 ft, 34-T.25S.-R.4W.).

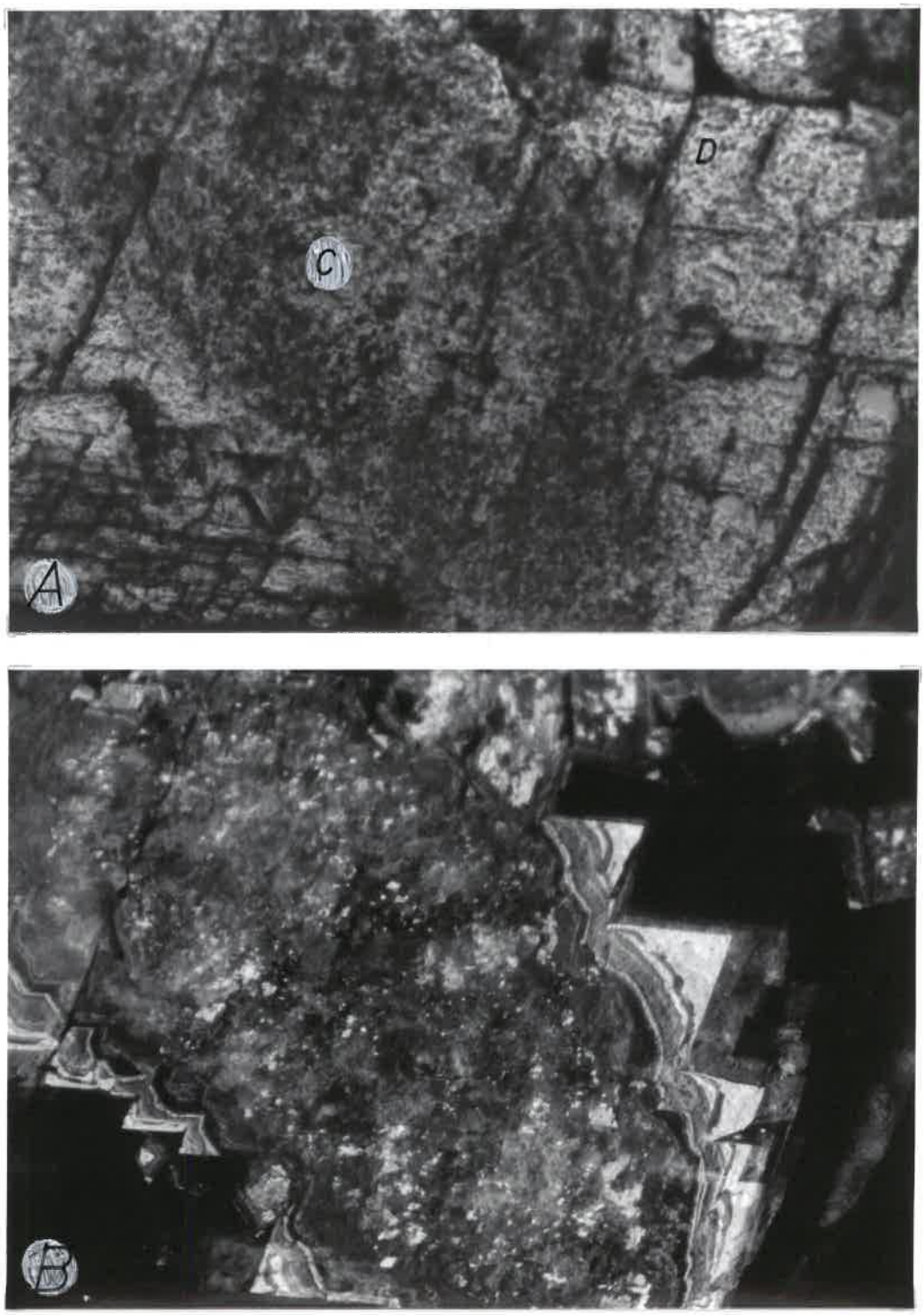

0.5 mm

Figure 8.34a, 8.34b Matched pair of photomicrographs of a patch of replacement dolomite in a mimetically dolomitized crinoidal packstone in the basal limestone subunit, in plane polarized light (8.34a) and with cathodoluminescence (8.34b). Bright zones within the rhombs are recrystallized patches. Thin section is from the Midcontinent Marine #1 North Hilger core (#*28*) in eastern Reno County (depth 4114.8 ft, 34-T.25S.-R.4W.).

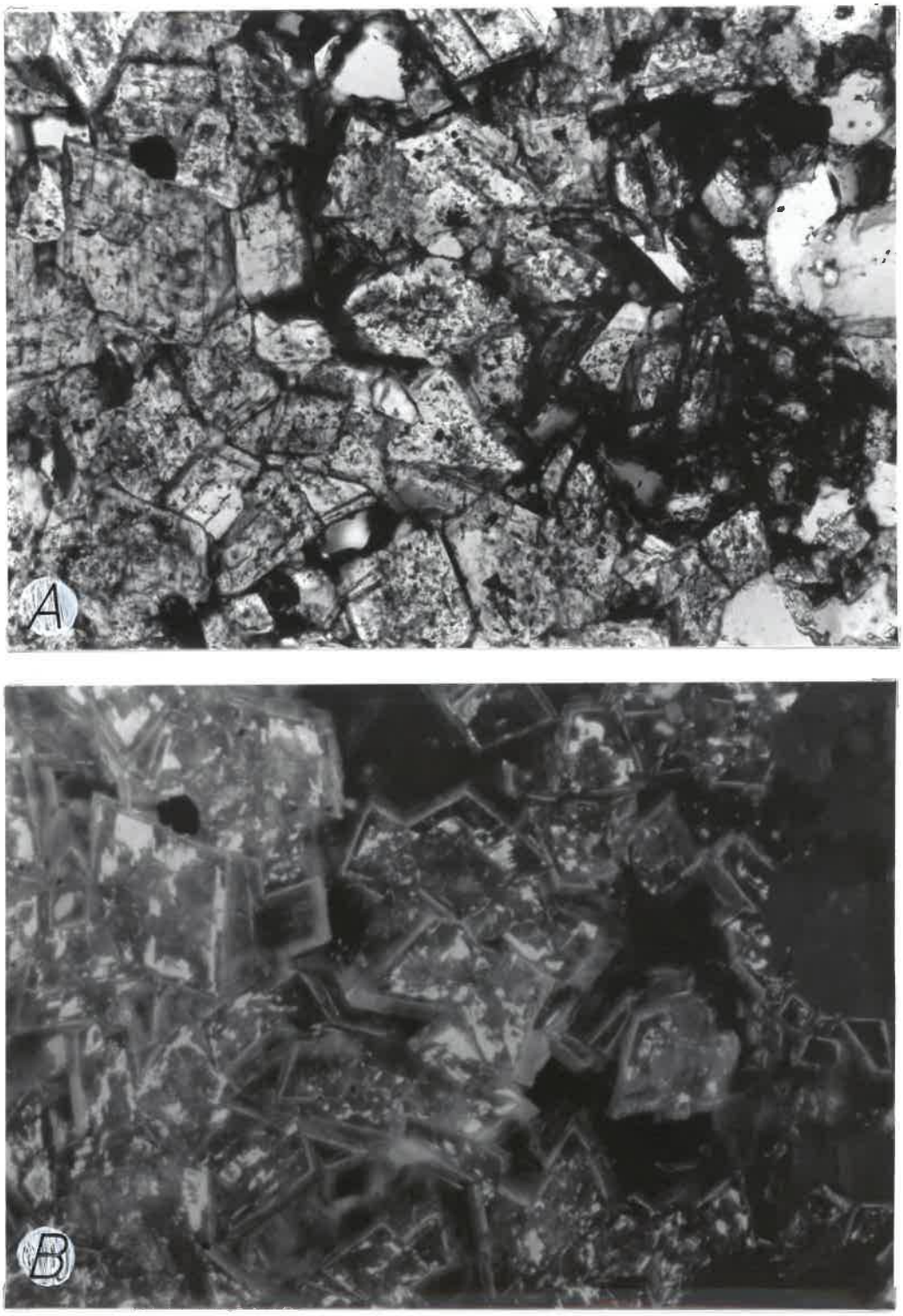
A
B
0.5 mm

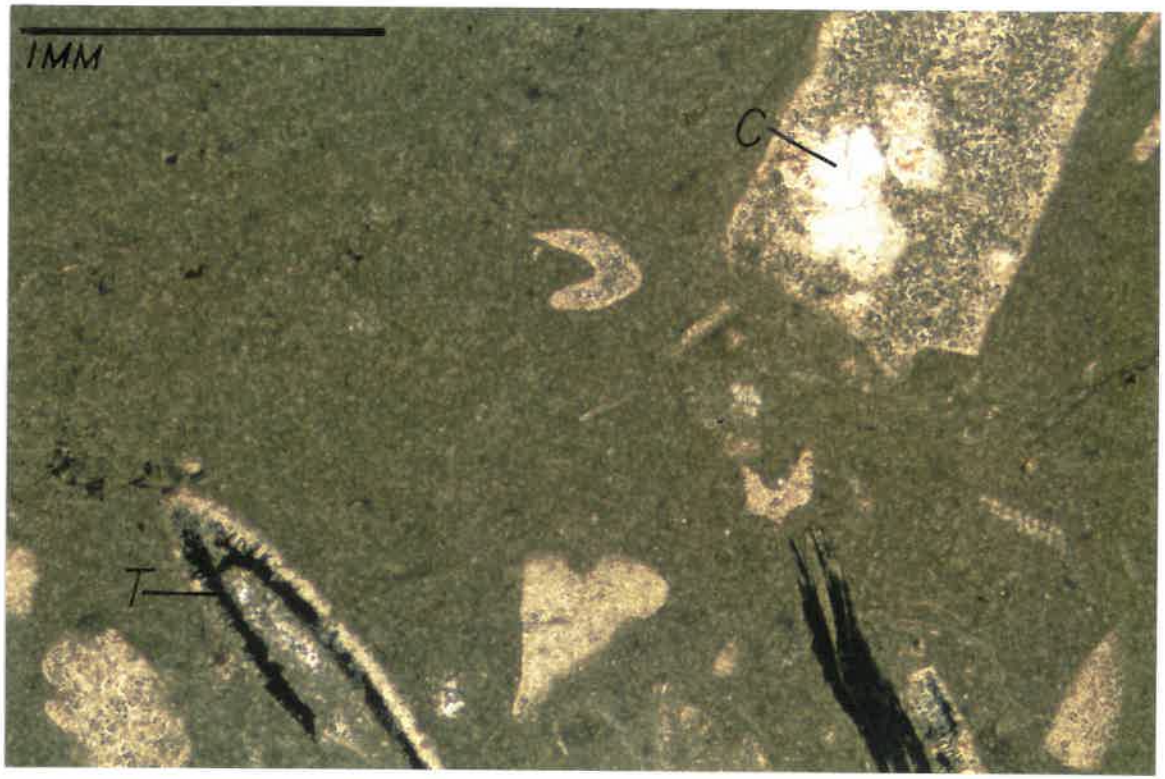

Figure 8.35 Photomicrograph of undolomitized wackestone in lower cherty dolomitic limestone from Sinclair #1 Binning core (#37, depth 4780 ft) in central Barber County (26-T.32S.-R.13W.). No peripheral micritization of the fossil fragments is evident. Dark material in the trilobite fragment (**T**) is fine-grained pyrite. Light-colored zone (**C**) in crinoid fragment is replaced by chert.

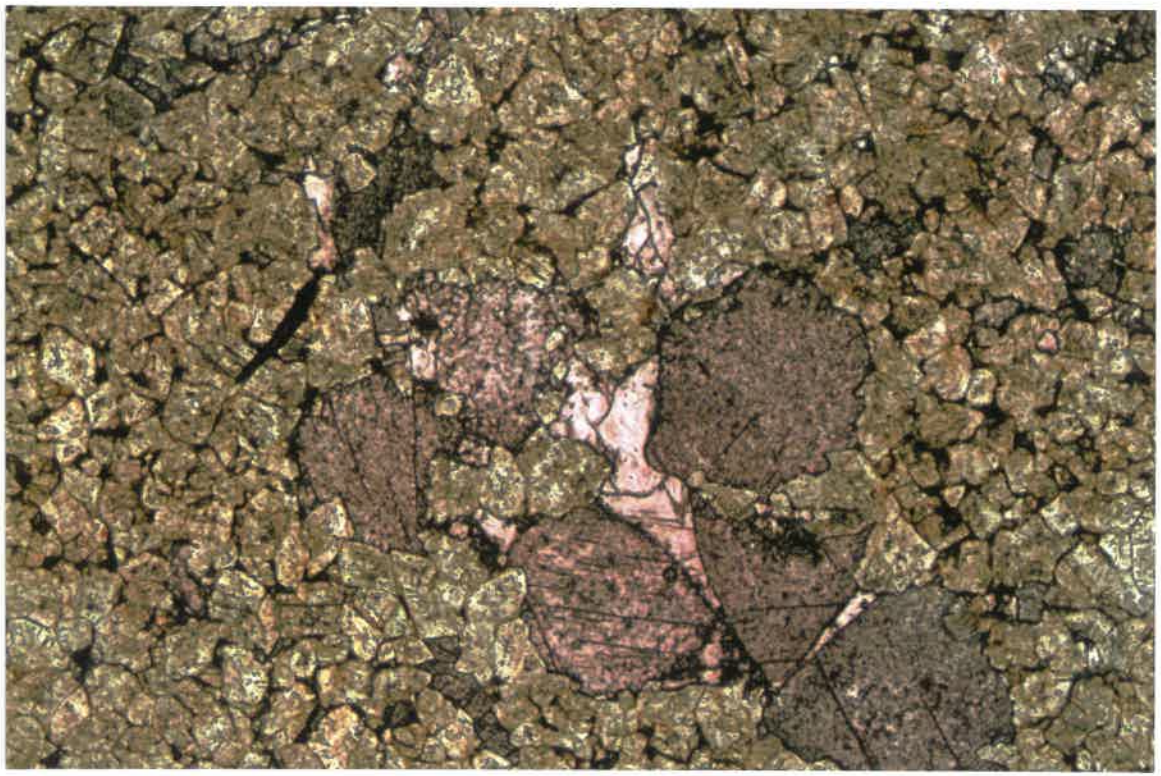

Figure 8.36 Photomicrograph of dolomitized wackestone in lower cherty dolomitic limestone from the Shell #6 Fleming core (#7, depth 3394-97 ft) in eastern McPherson County (11-T.24S.-R.2W.). Two undolomitized crinoid grains (pink), and an isolated area of spar-filled porosity between them, are cross-cut by dolomite with planar-s texture (see Sibley and Gregg, 1987). Thin section is stained with Alizarin Red-S and potassium ferricyanide.

is similar to the dolomitic texture present in the muddier lithologies of the underlying basal and upper limestones, but finer details may be lost or obscured. Calcite cement, infilling an isolated pocket of primary shelter porosity present between adjacent fossil fragments (Figure 8.36), is crosscut by dolomite (Figure 8.36), hence the dolomitization in the lower cherty dolomitic limestone, like the dolomitization in the basal limestone, is after a minor episode of calcite cementation. Intercrystalline porosity and subsidiary moldic porosity in the lower and upper cherty dolomitic limestones generally comprise from 5 to 15% of the rock volume (see Figure 7.13). Where significant moldic and intercrystalline porosity is present, the dolomite crystals are euhedral -- the planar-e texture of Sibley and Gregg (1987). In some samples the dolomite is ferroan, as revealed with staining by potassium ferricyanide, but no regional trends in iron content were discerned with the present core coverage.

None of the four Viola subunits can be characterized by a single type of dolomite. However, the subunits are dominated by one of these three types of dolomite within certain regions. Mimetic dolomite characterizes the basal limestone subunit near its truncated margin near the crest of the Chautauqua arch (Figure 8.37). On the Central Kansas arch, and on isolated areas on the Pratt anticline, collage dolomite dominates. Dolomite with concentric texture characterizes the basal limestone subunit where it is least dolomitized (generally in areas down the flanks of the Chautauqua arch and Pratt anticline). A similar pattern can be discerned for the lower cherty dolomitic limestone subunit (Figure 8.38) in that near its truncated margin on the Central Kansas arch, dolomite crystals have a collage internal texture, but farther off structure, the dolomite is concentrically zoned. Limited core control hinders perception of any pattern with dolomite internal textures in the upper limestone subunit (Figure 8.39) and the upper cherty dolomitic limestone subunit (Figure 8.40); however, available data do not contradict the patterns discerned in the

Figure 8.37 Map illustrating internal texture of dolomite crystals in the basal limestone subunit, based on examination of thin sections at core localities (see Figure 7.1). Symbols for internal texture of dolomite are superimposed on the map from Figure 8.5, showing the dominant lithology of this subunit based on Davies's sample logs. See text for discussion.

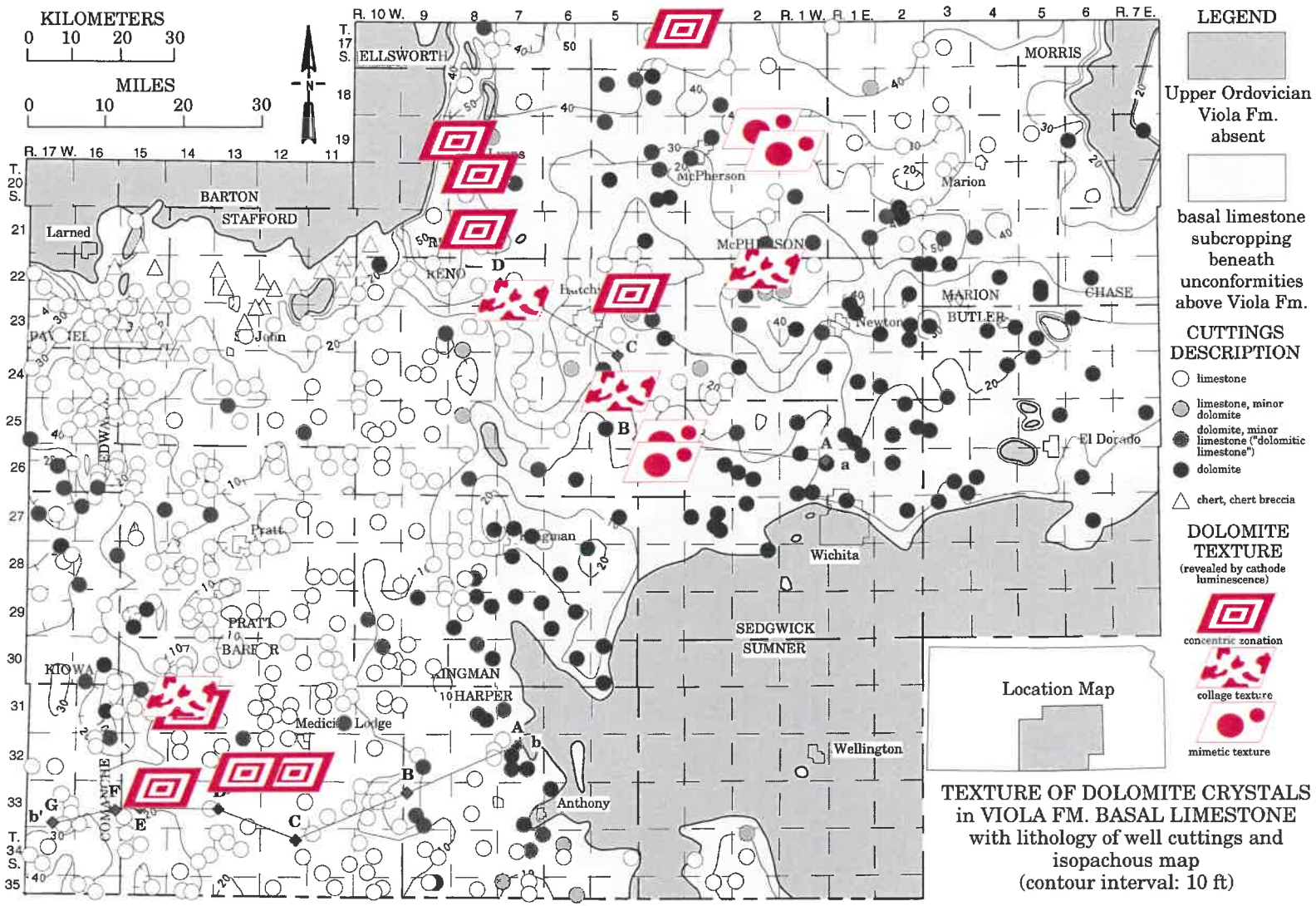

TEXTURE OF DOLOMITE CRYSTALS in VIOLA FM. BASAL LIMESTONE with lithology of well cuttings and isopachous map (contour interval: 10 ft)

Figure 8.38 Map illustrating internal texture of dolomite crystals in the lower cherty dolomitic limestone subunit, based on examination of thin sections at core localities (see Figure 7.1). Symbols for internal texture of dolomite are superimposed on the map from Figure 8.8, showing the dominant lithology of this subunit based on Davies's sample logs. See text for discussion.

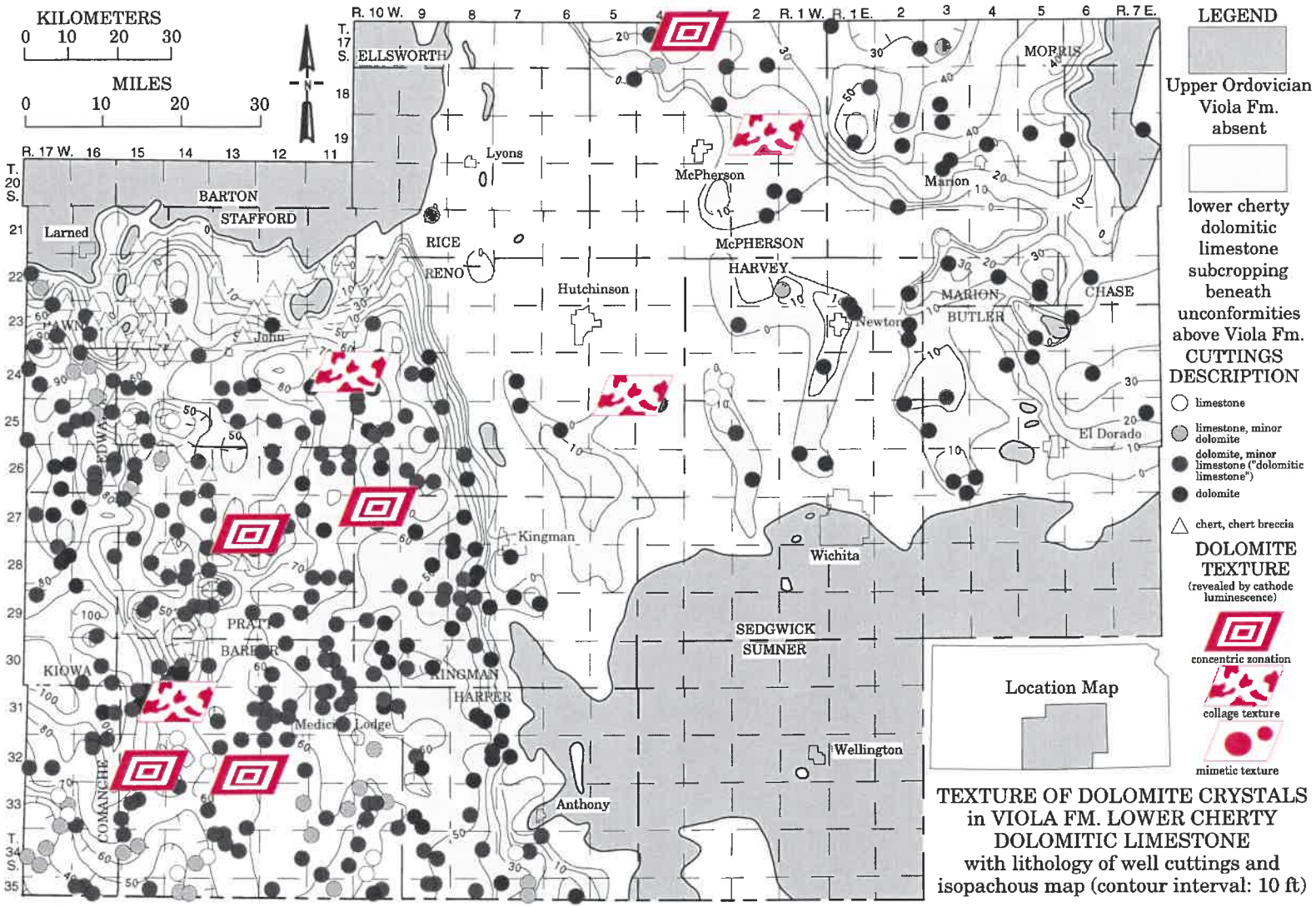

TEXTURE OF DOLOMITE CRYSTALS in VIOLA FM. LOWER CHERTY DOLOMITIC LIMESTONE with lithology of well cuttings and isopachous map (contour interval: 10 ft)

Figure 8.39 Map illustrating internal texture of dolomite crystals in the upper limestone subunit, based on examination of thin sections at core localities (see Figure 7.1). Symbols for internal texture of dolomite are superimposed on the map from Figure 8.9, showing the dominant lithology of this subunit based on Davies's sample logs. See text for discussion.

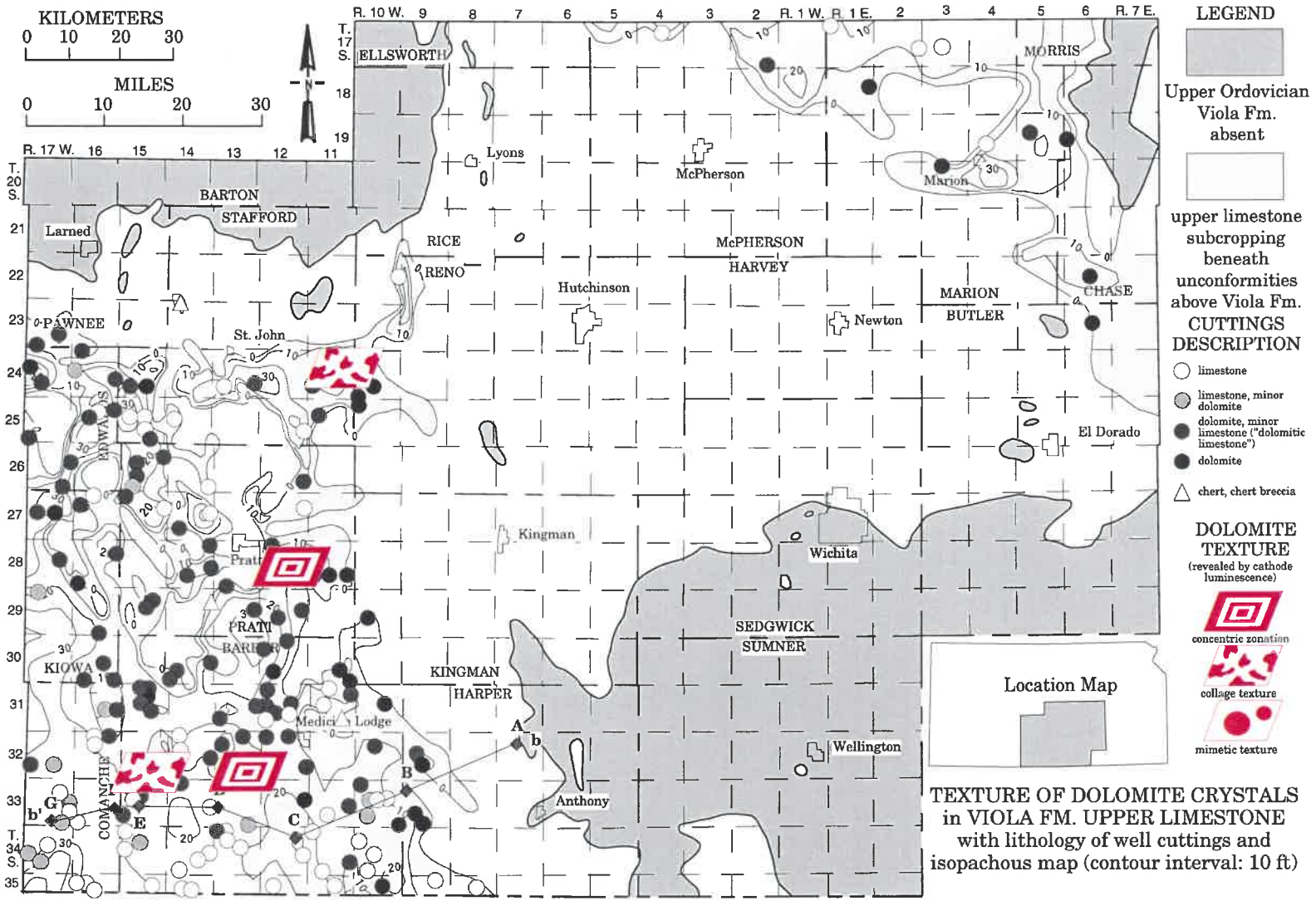

TEXTURE OF DOLOMITE CRYSTALS in VIOLA FM. UPPER LIMESTONE with lithology of well cuttings and isopachous map (contour interval: 10 ft)

Figure 8.40 Map illustrating internal texture of dolomite crystals in the upper cherty dolomitic limestone subunit, based on examination of thin sections at core localities (see Figure 7.1). Symbols for internal texture of dolomite are superimposed on the map from Figure 8.11, showing the dominant lithology of this subunit based on Davies's sample logs. See text for discussion.

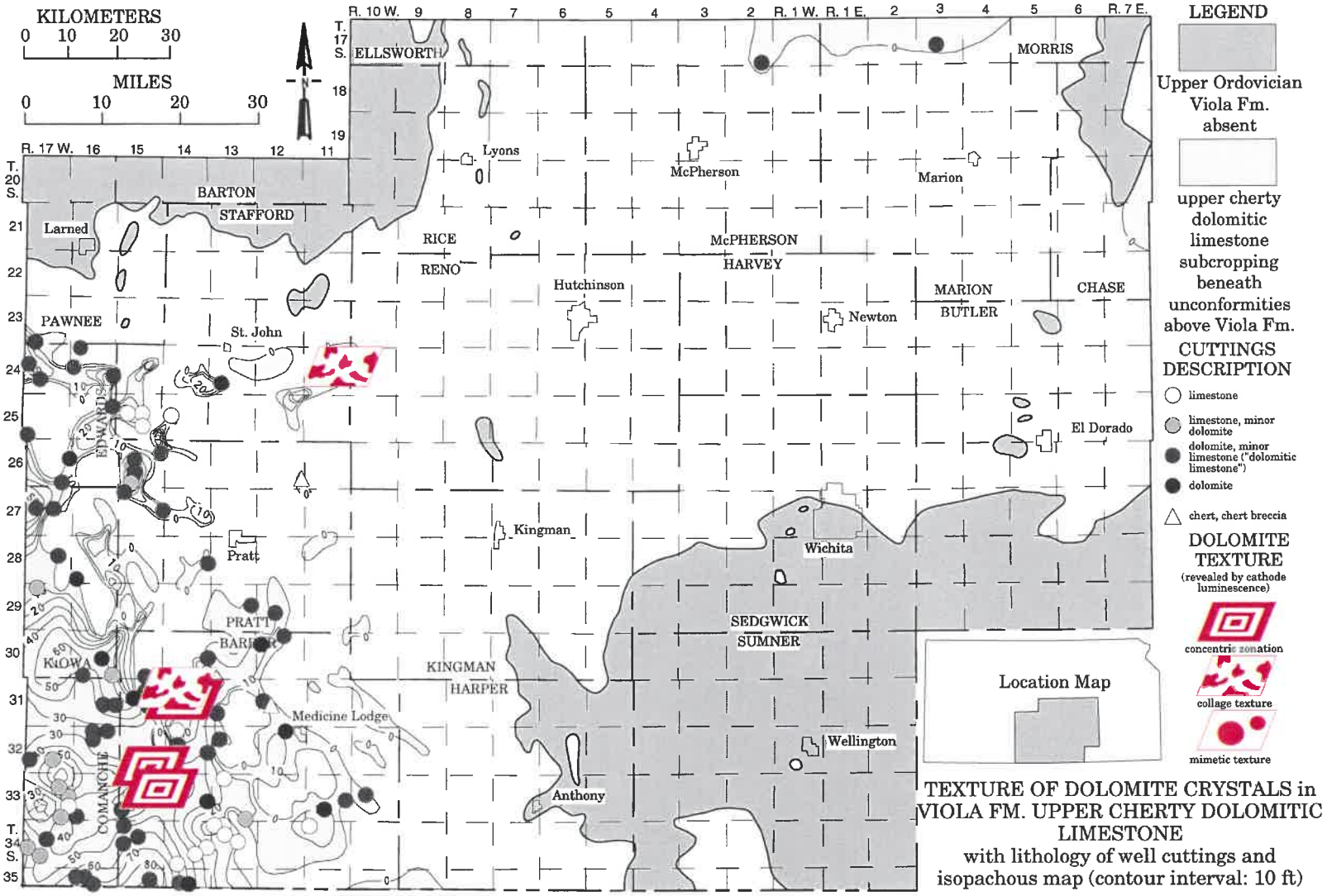

TEXTURE OF DOLOMITE CRYSTALS in VIOLA FM. UPPER CHERTY DOLOMITIC LIMESTONE
with lithology of well cuttings and isopachous map (contour interval: 10 ft)

more extensive lower cherty dolomitic limestone subunit and the basal limestone subunit. An eclectic map (Figure 8.41) illustrating the type of internal texture of dolomite present at the top of the Viola, regardless of which subunit subcrops at that surface, indicates that mimetic and collage dolomite are spatially associated with the Chautauqua arch, but farther down flank concentric textures dominate. Internal textures appear independent of the rock unit overlying the Viola.

Comparing the internal texture of dolomite with the abundance of dolomite (Table 8.1) indicates that concentric dolomites dominate where the basal limestone subunit is lightly dolomitized. Conversely, mimetic dolomite characterizes this subunit where it is heavily dolomitized. In the overlying lower cherty dolomitic limestone subunit, collage dolomite dominates where that subunit is heavily dolomitized, whereas concentric dolomite texture are present with all abundances of dolomite. Too little data are available for reliable observations for the upper limestone subunit and the upper cherty dolomitic limestone subunit.

Analysis of five samples of dolomite by x-ray diffraction yields information regarding their stoichiometry. The presence of excess calcium in dolomite causes an expansion of its crystal lattice, detectable by a precisely measurable shift in position of the $d_{[104]}$ x-ray peak, particularly with the inclusion of an internal standard (Goldsmith and Graf, 1958a; Blatt and others, 1980, p. 510-512). The stoichiometry determination depends on stoichiometric calibrations to the position of the diffraction peak. For dolomite, Goldsmith and Graf (1958a) determined lattice baseline values of 2.886 Å for 50.0% $CaCO_3$ and 2.901 Å for 55.0% $CaCO_3$. Using these values, Lumsden (1979) presented a linear equation by which N_{CaCO3} (the mole % $CaCO_3$ in dolomite) can be calculated:

Figure 8.41 Map illustrating internal texture of dolomite crystals at the top of the Viola, regardless of which subunit subcrops at that contact, based on examination of thin sections at core localities (see Figure 7.1). Symbols for internal texture of dolomite are superimposed on the worm's-eye-view map (Figure 8.12), showing the dominant lithology based on Davies's sample logs. Refer to Figures 8.37 to 8.40 for explanation of lithology and dolomite symbols. See text for discussion.

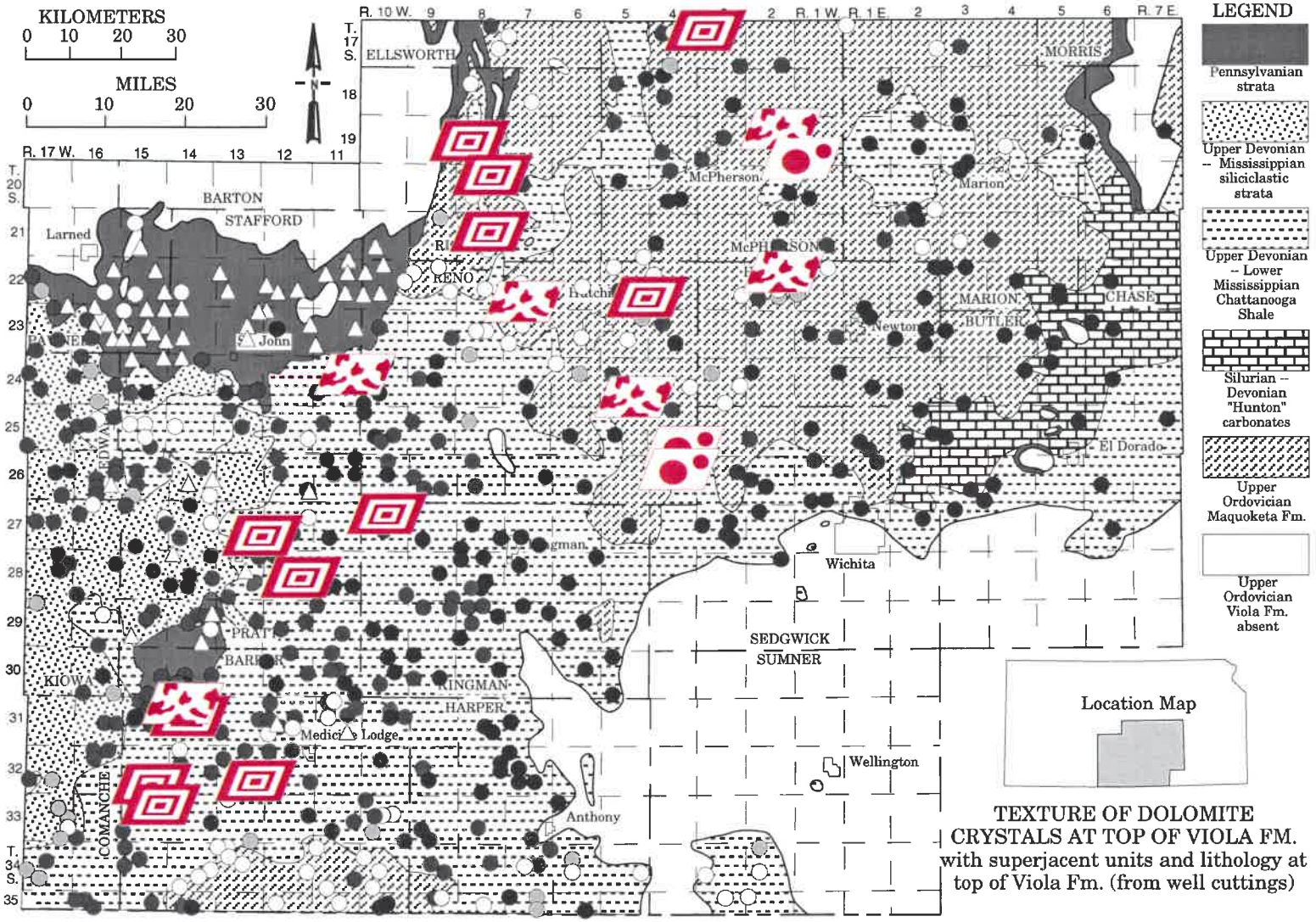

TEXTURE OF DOLOMITE CRYSTALS AT TOP OF VIOLA FM. with superjacent units and lithology at top of Viola Fm. (from well cuttings)

Table 8.1 Summary of cathodoluminescence patterns observed in dolomite in selected cores from subunits in the Viola Formation, versus their dolomite content (from Appendix IV). One observation constitutes a single core in a given Viola subunit. Number in italics indicates the core locality (see Table 7.1). Maps of the cathodoluminescence data are in Figures 8.37, 8.38, 8.39, and 8.40. See text for discussion.

UPPER CHERTY DOLOMITIC LIMESTONE SUBUNIT (5 observations)

	DOLOMITE CONTENT			
	<25%	≥25%-<50%	≥50%-<75%	≥75%
TEXTURE				
Mimetic	----	----	----	----
Collage	----	**1** *(#34)*	----	**1** *(#19)*
Concentric	----	**1** *(#40)*	----	**2** *(#35, 39)*

(no dolomite present in *#38*)

UPPER LIMESTONE SUBUNIT (4 observations)

	DOLOMITE CONTENT			
	<25%	≥25%-<50%	≥50%-<75%	≥75%
TEXTURE				
Mimetic	----	----	----	----
Collage	**1** *(#19)*	**1** *(#34)*	----	----
Concentric	**1** *(#37)*	**1** *(#32)*	----	----

(no dolomite present in *#33, 38*)

LOWER CHERTY DOLOMITIC LIMESTONE SUBUNIT (9 observations)

	DOLOMITE CONTENT			
	<25%	≥25%-<50%	≥50%-<75%	≥75%
TEXTURE				
Mimetic	----	----	----	----
Collage	----	----	----	**4** *(#6, 17, 19, 34)*
Concentric	**1** *(#37)*	**1** *(#30)*	**2** *(#2, 31)*	**1** *(#39)*

BASAL LIMESTONE SUBUNIT (17 observations)

	DOLOMITE CONTENT			
	<25%	≥25%-<50%	≥50%-<75%	≥75%
TEXTURE				
Mimetic	----	----	----	**4** *(#3, 4, 28, 29)*
Collage	**2** *(#14, 16)*	**1** *(#17)*	----	**1** *(#34)*
Concentric	**8** *(#2, 11, 12, 15, 35, 36, 37, 40)*	**1** *(#13)*	----	----

$$N_{CaCO3} = 333.33\ d_{[104]} - 911.99$$

where $d_{[104]}$ is the d-spacing of the $d_{[104]}$ diffraction plane (in Å), which is calculated from the Bragg law:

$$n\lambda = 2d\ \sin\theta$$

where d is the spacing of the reflecting planes (in Å), θ is the angle of reflection, and λ is the wavelength of the incoming radiation (i.e., 1.5406 Å for Cu $K\alpha$ x-rays when the halite standard $d_{[200]}$ peak [2.813 Å] is set to 31.690° 2θ) and n is the order of the diffracted wave (i.e., 1, 2, 3, etc.; but equals 1 in this case) (Nuffield, 1966, p. 4, 34).

Substitution of ions other than Ca^{+2}, such as Fe^{+2}, can expand the crystal lattice of dolomite and affect the position of the $d_{[104]}$ peak. Goldsmith and Graf (1958b) report that up to 3 mole % $FeCO_3$ in dolomite is necessary to produce a change detectable by x-ray diffraction. The Viola dolomites analyzed are essentially iron-free as indicated by staining with potassium ferricyanide with both the methods of Dickson (1966), and Adams and others (1984). Staining by this solution requires the presence of at least 0.5% FeO (Lindholm and Finkelman, 1972).

The five samples analyzed by x-ray diffraction represent the major types of dolomite detected in the Viola by petrography, with two samples being concentric dolomite, two being collage, and one being mimetic (Figure 8.42). Diffraction data, according to the equations above, indicate the two collage dolomites from the upper cherty dolomitic limestone subunit (samples ZU13789.1, 4RFS73M) are nearly stoichiometric, having respectively 52.2% and 51.6% calcium. The mimetic dolomite from the basal limestone subunit (sample 1SH4042.2) is likewise nearly stoichiometric with 51.3% calcium. The concentric dolomites, one from the basal limestone subunit

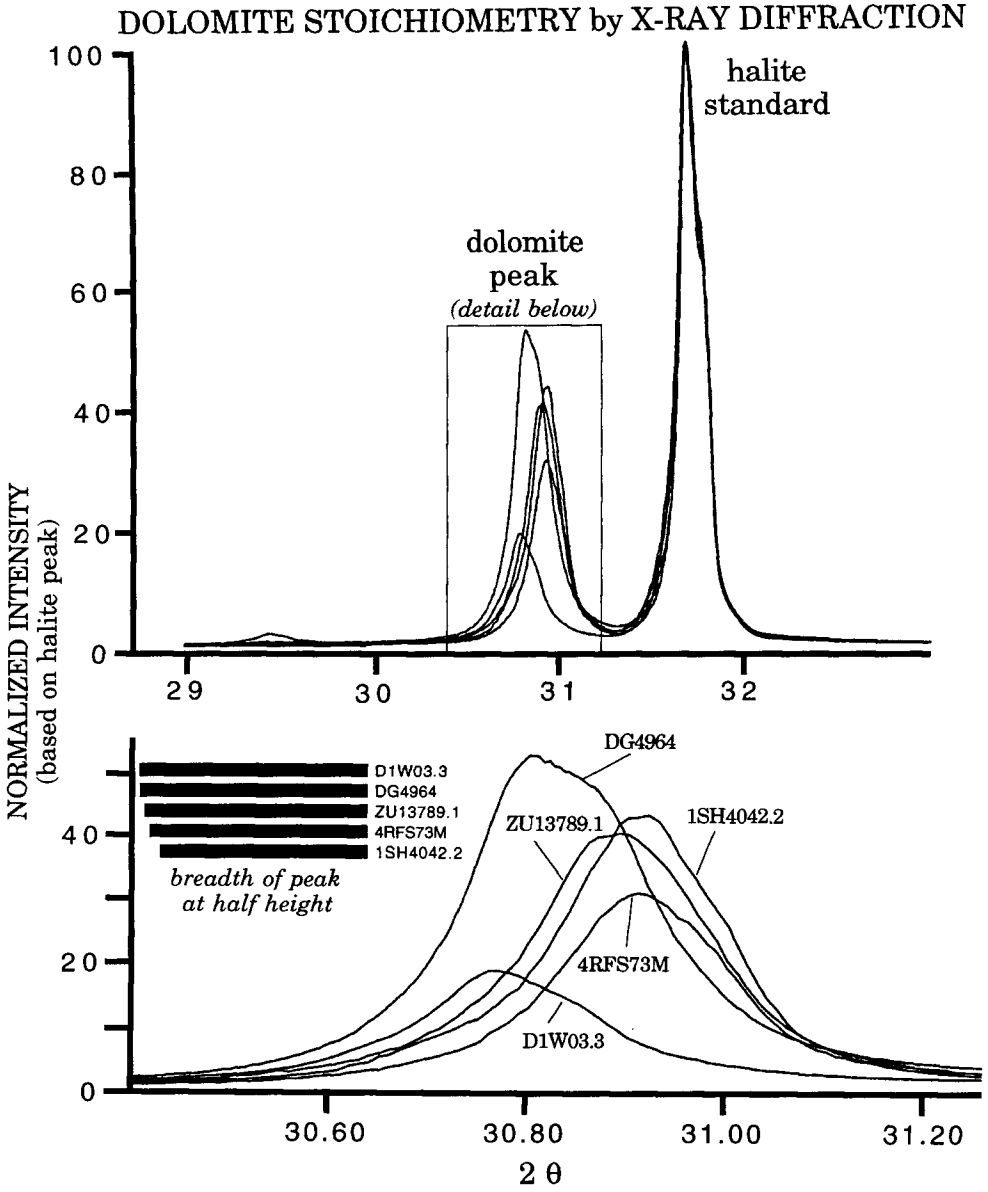

sample	well	subunit	dolomite type	2 θ	d-space	Ca (%)
D1W03.3	Derby #1 Wood depth 3903.3'; 36-22S-02W	basal limestone	concentric	30.760	2.9044	56.1
DG4964	Sinclair-Prairie #1 DeGeer depth 4964'; 6-32S-14W	upper cherty dolomite	concentric	30.800	2.9007	54.9
ZU13789.1	Braden-Zenith ZU-1 depth 3789'; 11-24S-11W	upper cherty dolomite	collage	30.889	2.8925	52.2
4RFS73M	E.H. Moore #4 R.F. Stewart depth 3773'; 12-24S-11W	upper cherty dolomite	collage	30.909	2.8907	51.6
1SH4042.2	Midcon. Marine #1 South Hilger depth 4042.2'; 9-26S-04W	basal limestone	mimetic	30.920	2.8898	51.3

Figure 8.42 Diffractograms and associated stoichiometry determined for dolomite samples from the Viola Formation. Dolomites with concentric internal texture are distinctly calcian whereas collage and mimetic dolomites are nearly stoichiometric.

(sample D1W03.3) and one from the upper cherty dolomitic limestone subunit (sample DG4964), are nonstoichiometric, respectively containing 56.1% and 54.9% calcium. Shoulders on the right side of these peaks indicate some parts of the concentric dolomites are slightly more stoichiometric (Figure 8.42).

Reconnaissance fluid-inclusion data obtained from rhombs of replacive planar-p dolomite in the basal limestone and replacive planar-e dolomite in the upper cherty dolomitic limestone (Table 8.2, Figure 8.43) show widely varying $Tm_{(ice)}$ values. Both of these dolomites have inclusion-rich cores surrounded by clearer rims, with the boundary between the core and the rim being sharp and parallel to the crystal faces. These textural features are consistent with these inclusions being primary in origin, according to criteria presented in Goldstein and Reynolds (1994, p. 14-15). $Tm_{(ice)}$ values for the planar-p sample from the basal limestone range from -0.6 to -20.9 °C (i.e., 1.05 to 22.98 wt. % NaCl equivalent by a conversion in Bodnar, 1992), with a modal concentration of -3.0 to -4.0 °C (4.96 to 6.45 wt. % NaCl equivalent). The planar-e dolomite from the upper cherty dolomitic limestone shows less variation in $Tm_{(ice)}$, with seven $Tm_{(ice)}$ determinations ranging from -17.0 to -18.2 °C (20.22 to 21.11 wt. % NaCl equivalent).

The planar-p dolomite is a concentric dolomite (Figure 8.28) whereas the planar-e dolomite is characterized by a collage texture surrounded by a thin concentric rim. It is impossible to distinguish many useful "fluid-inclusion assemblages" (see Goldstein and Reynolds, 1994, p. 87) in the collage dolomite due to its complex internal structure, although in transmitted light, crystals of this type of dolomite have cloudy centers identical to that of the concentric dolomite. It is conceivable that a process of dolomite recrystallization and subsequent precipitation of a clear rim of dolomite could replicate the cloudy-core, clear-rim texture in the collage dolomites. Fluid inclusions in such a dolomite would be primary to the

Table 8.2 Fluid-inclusion data from dolomite rhombs (planar-p texture with concentric texture under cathodoluminescence) from the basal limestone subunit in the Derby #1 Wood core (*#15*) in Reno County -- thin section D1W94.5 (NE, 36-T.22S.-R.5W.; depth 3894.5 ft), and from dolomite rhombs (planar-e texture with recrystallized texture under cathodoluminescence) from the upper cherty dolomitic limestone from the E.H. Moore #2 R.F. Stewart core (*#21*) in Stafford County -- thin section 2RFS 85K (SW, 12-T.24S.-R.11W.; depth 3785 ft). T_h, $Tm_{(ice)}$, T_e, and T_n are homogenization temperature, final melting temperature of ice, eutectic temperature, and nucleation temperature. L:V is liquid:vapor ratio. Fluid-inclusions are cataloged under the association column, in which each inclusion is identified with chip/view/crystal/assemblage. "Chip" identifies the chip cut from the thin section; "view" is the arbitrary location within that chip (usually a field of view through the microscope); "crystal" identifies the crystal holding the inclusion; "assemblage" identifies the fluid-inclusion assemblage (groups of genetically related inclusions in close proximity to each other). If an inclusion is isolated, the assemblage category will be blank. Even though the crystal number may be similar with two or more inclusions, if the chip and/or view designation is different, then the crystals are different. Uncertainty (±) in measurement of T_h and $Tm_{(ice)}$ reflects the precision arbitrarily achieved by the operator using cycling technique (see Goldstein and Reynolds, 1994, p. 93-95, 105-109). $Tm_{(ice)}$ data in this table are displayed in Figure 8.43.

ASSOCIATION chip/view/ crystal/asmblg.	T_h °C	$Tm_{(ice)}$ °C	T_e °C	T_n °C	L:V	NOTES*
thin section 2RFS 85K, E.H. Moore #2 R.F. Stewart, upper cherty dolomitic limestone						
1/A/1/	103.6	-17.5	----	----	7:1	
1/B/1/	84.1 ± 0.3	-18.2	----	-65	15:1	
1/B/2/a	----	-18.2	----	~ -72	----	adj. to below
1/B/2/a	----	-17.8	----	~ -69	----	adj. to above
1/D/1/	63.0 ± 0.3	----	----	----	15:1	
2/C/1/	94.9	-17.9	----	~ -70	16:1	
2/G/1/b	88.5	-17.6	----	~ -62	10:1	
2/G/1/b	----	-17.0	----	~ -68	8:1	
thin section D1W94.5, from Derby #1 Wood, basal limestone						
1/B/1/a	108.3	----	----	----	----	adj. to below
1/B/1/a	----	-0.6	----	----	----	leaked?
1/B/1/	111.5	----	----	----	----	
1/B1/1/	----	-16.2	~ -30	----	----	secondary
1/B1/1/	----	-2.2	----	----	----	secondary
1/B1/1/	----	-3.0	----	----	----	
1/B1/2/b	122.8	-3.5	----	----	----	adj. to below
1/B1/2/b	119.1	----	----	----	----	adj. to above
2/C/1/	----	-20.9	----	----	10:1	
2/C/2/	----	-7.1	----	----	----	
3/D/1/c	111.5	----	----	----	----	secondary
3/D/1/c	118.9	----	----	----	12:1	secondary
3/D/1/c	112.8	-2.2	----	----	20:1	secondary
3/D/1/c	103.4	----	----	----	----	secondary
3/D/1/	~ 130	-17.7	----	----	----	secondary
3/D/1/	----	-6.5	----	----	----	secondary
3/D/1/	107.0	----	----	----	9:1	
3/D'/1/	112.8	-2.1	----	----	----	
3/D'/1/	----	-1.2	----	----	5:1	
4/F''/1/d	110.1 ± 0.1	-16.6	~ -35	----	----	secondary?
4/F''/1/d	78.2	-11.2	----	----	----	secondary?

Table 8.2 (continued). Fluid-inclusion data from dolomite rhombs.

ASSOCIATION chip/view/ cryst./asmblg.	T_h °C	$Tm_{(ice)}$ °C	T_e °C	T_n °C	L:V	NOTES*
thin section D1W94.5, from Derby #1 Wood, basal limestone (continued)						
4/F'''/1/e	111.1	-3.2	----	----	----	
4/F'''/1/e	163.2	-3.4	----	----	----	
4/F'''/1/e	----	-3.4	----	----	----	
5/G/1/	118.4 ± 0.1	-10.9	----	----	10:1	
5/G/2/	122.6	----	----	----	----	
5/G/3/f	88.2 ± 0.1	----	----	----	----	secondary
5/G/3/f	143.5 ± 0.2	----	----	----	----	secondary
5/G/4/	118.1 ± 0.1	----	----	----	----	
5/G/5/	89.0	-1.1	----	----	----	

*Fluid inclusions are primary unless noted otherwise; adj. = adjacent

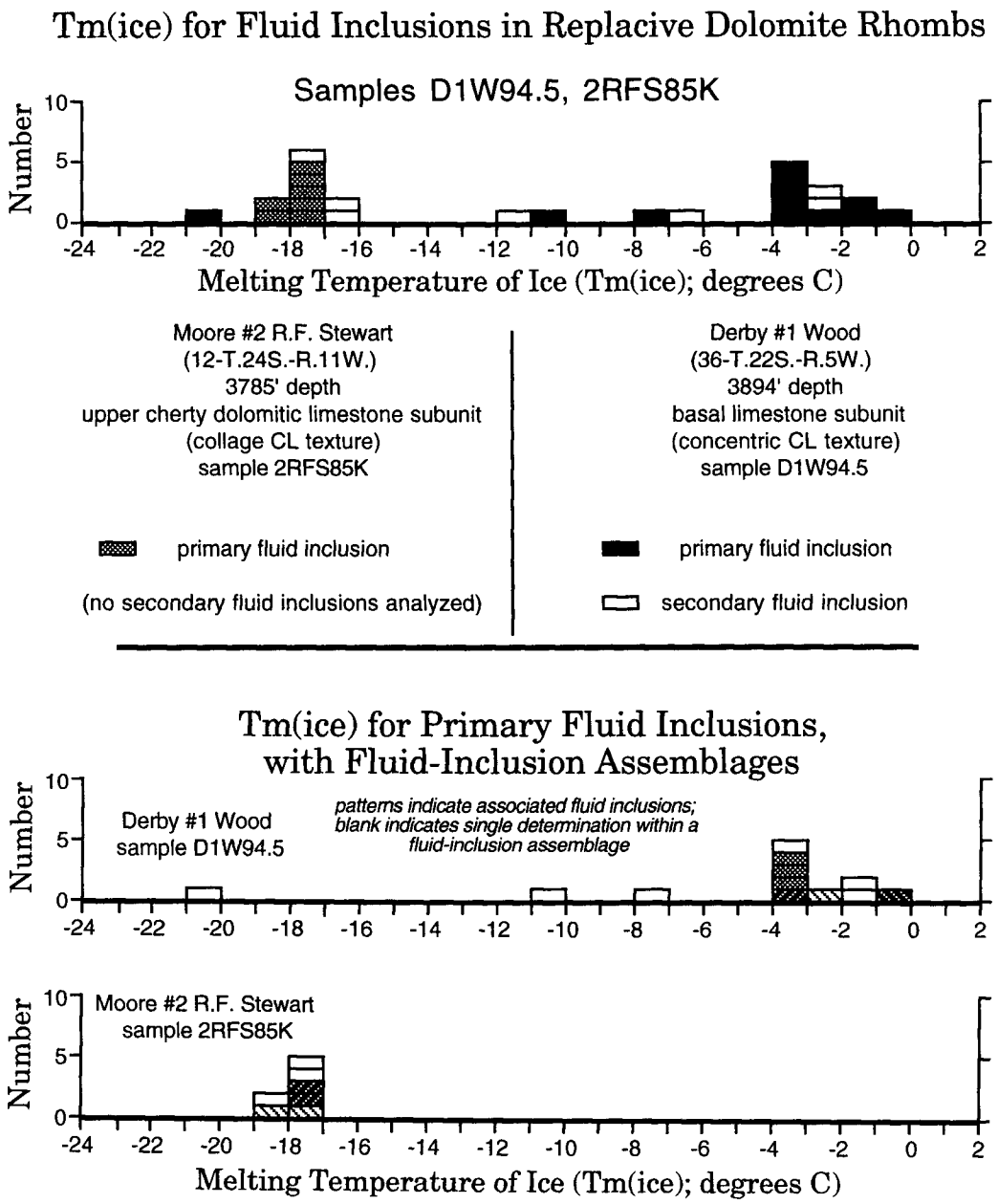

Figure 8.43 Histogram of $Tm_{(ice)}$ data from planar-p dolomite from the basal limestone subunit and planar-e dolomite from the upper cherty dolomitic limestone (see Table 8.2). The planar-p dolomite is from the Derby #1 Wood core (*#15*) depth 3894.5 ft, 36-T.22S.-R.5W.) in Reno County. The planar-e dolomite is from the E.H. Moore #2 R.F. Stewart core in eastern Stafford County (depth 3785 ft, 12-T.24S.-R.11W.). For comparison, seawater has a $Tm_{(ice)}$ of -1.9 °C. A measurement from an "isolated" inclusion represents a single measurement obtained from a fluid-inclusion assemblage. See text for discussion.

recrystallized dolomite, but not to the dolomite that preceded the recrystallization. Fluid inclusions within the cloudy centers of both types of dolomite are typically composed of two-phase inclusions with nearly consistent liquid-to-vapor ratios, but all-liquid inclusions are also present. The all-liquid inclusions are not obviously paired or in line with two-phase inclusions, thereby indicating the all-liquid inclusions did not originate by a process of "necking down", a process, by which a fluid inclusion is segmented into smaller inclusions by a change in shape to reduce its internal surface area (see Goldstein and Reynolds, 1994, p. 47). The all-liquid inclusions in the samples of concentric and collage dolomite could be metastable inclusions in which the gas bubble has failed to nucleate, but placing the sample in a household freezer overnight did not appreciably increase the proportion of inclusions with bubbles. Inasmuch as these all-liquid inclusions are comparable in size to the two-phase inclusions, and they vary in size and shape as do the two-phase inclusions, metastability is unlikely. After heating runs to determine T_h, heating was necessary to induce leakage in the all-liquid inclusions in samples of both types of dolomite in order to create bubbles for $Tm_{(ice)}$ measurements, but unfortunately no record was kept of which inclusions were all-liquid before heating.

Correlation of the inclusions in the concentric dolomite to specific cathodoluminescent zones is difficult, partly because inclusions are not strongly distributed in concentric zones and partly because of uncertainty inherent in correlating a surface phenomenon (cathodoluminescence) with inclusions that are present deeper within the crystal. The widely varying $Tm_{(ice)}$ measurements for this sample may indicate that some secondary inclusions may have been misidentified as primary inclusions, or leakage and refilling of primary inclusions may have occurred.

Seven samples of dolomite were selected for strontium isotope determinations (Table 8.3; Figure 8.44). Near the crest of the Chautauqua arch where the basal

Table 8.3 Samples analyzed for strontium, oxygen, and carbon isotopic ratios. See text for discussion.

WELL, LOCATION, DEPTH, and VIOLA SUBUNIT	SAMPLE #	$^{87}Sr/^{86}Sr$ ratio	$\delta^{18}O$ ‰ PDB	$\delta^{13}C$ ‰ PDB	NOTES
Damac #1 S. Allen 7-T.17S.-R.03W. 3428.1' Maquoketa Fm.	DSA3438.1	------	-2.33	+0.81	dolomite
Shell #1 Anderson 30-T.19S.-R.01W. 3409' basal limestone	SA3409	------	-3.11	-0.55	mimetic dolomite
NNG #1 Caldwell 2-T.20S.-R.08W. 3259.75' basal limestone	NNC3259.75	------	-5.88	+0.82	interparticle calcite spar in packstone
Derby #1 Wood 36-T.22S.-R.05W. 3894.5' basal limestone	D1W94.5	0.709033 ± 0.000013	-5.79	-1.29	saddle dolomite in vug
Derby #1 Wood 36-T.22S.-R.05W. 3903.3' basal limestone	D1W03.3	0.708032 ± 0.000011	-2.27	-0.14	replacive dolomite with concentric CL pattern
Braden-Zenith ZU-1 11-T.24S.-R.11W. 3784' upper cherty dolomite	ZU13784	------	-4.62	-1.26	replacive dolomite with collage CL pattern
Braden-Zenith ZU-1 11-T.24S.-R.11W. 3789.1' upper cherty dolomite	ZU13789.1	0.709018 ± 0.000011	-4.22	-1.40	replacive dolomite with collage CL pattern

Table 8.3 (continued) Samples analyzed for strontium, oxygen, and carbon isotopic ratios.

WELL, LOCATION, DEPTH, and VIOLA SUBUNIT	SAMPLE #	$^{87}Sr/^{86}Sr$ ratio	$\delta^{18}O$ ‰ PDB	$\delta^{13}C$ ‰ PDB	NOTES
Braden-Zenith ZU-1 11-T.24S.-R.11W. 3793' upper cherty dolomite	ZU13793	------	-5.52	-5.38	cloudy spar in intraformational breccia (before clear spar below)
Braden-Zenith ZU-1 11-T.24S.-R.11W. 3793' upper cherty dolomite	ZU13793	------	-2.41	-9.83	clear spar in intraformational breccia (follows cloudy spar above)
Braden-Zenith ZU-1 11-T.24S.-R.11W. 3813' upper cherty dolomite	ZU13813	------	-4.90	-1.17	replacive dolomite with collage CL pattern
Braden-Zenith ZU-1 11-T.24S.-R.11W. 3837' lower cherty dolomite	ZU13837	------	-3.78	-0.68	replacive dolomite with collage CL pattern
Braden-Zenith ZU-3 11-T.24S.-R.11W. 3760.2' upper cherty dolomite	ZU33760.2	------	-4.34	-1.17	replacive dolomite with collage CL pattern
Braden-Zenith ZU-3 11-T.24S.-R.11W. 3771.6' lower cherty dolomite	ZU33771.6	------	-6.21	-6.16	spar in intraformational breccia
Braden-Zenith ZU-3 11-T.24S.-R.11W. 3784.5' lower cherty dolomite	ZU33784.5	0.708603 ± 0.000013	-3.77	-0.89	replacive dolomite with collage CL pattern
E.H. Moore #4 R.F. Stewart 12-T.24S.-R.11W. 3771' upper cherty dolomite	4RFS71F	------	-6.28	-0.80	interparticle calcite spar in packstone

Table 8.3 (continued) Samples analyzed for strontium, oxygen, and carbon isotopic ratios.

WELL, LOCATION, DEPTH, and VIOLA SUBUNIT	SAMPLE #	$^{87}Sr/^{86}Sr$ ratio	$\delta^{18}O$ ‰ PDB	$\delta^{13}C$ ‰ PDB	NOTES
E.H. Moore #4 R.F. Stewart 12-T.24S.-R.11W. 3773' upper cherty dolomite	4RFS73M	------	-3.57	-0.96	replacive dolomite with collage CL pattern
Midcontinent Marine #1 North Hilger 34-T.25S.-R.04W. 4132.7' basal limestone	1NH4132.7	0.708768 ± 0.000013	-4.98	-0.65	mimetic dolomite
Midcontinent Marine #1 North Hilger 34-T.25S.-R.04W. 4135.4' basal limestone	1NH4135.4	------	-5.15	-1.29	mimetic dolomite
Midcontinent Marine #1 South Hilger 9-T.26S.-R.04W. 4031.9' basal limestone	1SH4031.9	------	-5.62	-1.38	mimetic dolomite
Midcontinent Marine #1 South Hilger 9-T.26S.-R.04W. 4042.2' basal limestone	1SH4042.2	0.708618 ± 0.000010	-5.11	-0.72	mimetic dolomite
Sinclair-Prairie #4 G. Oldfather 7-T.31S.-R.14W. 4328' upper cherty dolomite	4GO4328	0.708887 ± 0.000009	-3.21	+0.34	replacive dolomite with collage CL pattern

Table 8.3 (continued) Samples analyzed for strontium, oxygen, and carbon isotopic ratios.

WELL, LOCATION, DEPTH, and VIOLA SUBUNIT	SAMPLE #	$^{87}Sr/^{86}Sr$ ratio	$\delta^{18}O$ ‰ PDB	$\delta^{13}C$ ‰ PDB	NOTES
Sinclair-Prairie #4 G. Oldfather 7-T.31S.-R.14W. 4328' upper cherty dolomite	4GO4328	------	-8.93	-1.45	spar in intraformational breccia
Sinclair-Prairie #4 G. Oldfather 7-T.31S.-R.14W. 4438' lower cherty dolomite	4GO4438	------	-3.71	-0.50	replacive dolomite with concentric CL pattern
Sinclair-Prairie #4 G. Oldfather 7-T.31S.-R.14W. 4442' basal limestone	4GO4442	------	-6.67	-1.06	saddle dolomite in vug
Sinclair-Prairie #1 A. Oldfather 18-T.31S.-R.14W. 4429' upper cherty dolomite	1AO4429	------	-3.96	+0.13	replacive dolomite with concentric CL pattern
Sinclair-Prairie #1 DeGeer 34-T.32S.-R.15W. 4964' upper cherty dolomite	1DG4964	------	-2.49	-0.13	replacive dolomite with concentric CL pattern
Sinclair-Prairie #1 DeGeer 34-T.32S.-R.15W. 4990' lower cherty dolomite	1DG4990	------	-3.57	-0.36	replacive dolomite with concentric CL pattern

limestone subunit is completely altered by mimetic dolomitization, two samples (1SH4042.2 and 1NH4132.7) register ratios of 0.708618 and 0.708768, respectively. Two samples of collage dolomite (ZU13789.1 and 4GO4328) from the upper cherty dolomitic limestone, taken just below the unconformity beveling the top of the Viola Formation (subjacent to the Upper Devonian - Lower Mississippian Chattanooga Shale), have ratios of 0.709018 and 0.708887 respectively. A lower ratio of 0.708603 is from another collage dolomite taken from the lower cherty dolomitic limestone. The lowest ratio of 0.708032 is from a concentric dolomite (D1W03.3) from the basal limestone subunit on the Central Kansas arch.

Twenty-seven samples (20 dolomite, 6 calcite) were selected for carbon and oxygen isotope analyses (Table 8.3). A crossplot of carbon and oxygen isotopic data (Figure 8.45) shows that dolomites within the Viola overlap in their carbon and oxygen isotopic ranges, but in general, oxygen and carbon isotope ratios for concentric dolomites (mean $\delta^{18}O$ = -3.20 ‰ PDB; mean $\delta^{13}C$ = -0.40 ‰ PDB) are more positive than the ratios in collage dolomites (mean $\delta^{18}O$ = -4.05 ‰ PDB; mean $\delta^{13}C$ = -0.90 ‰ PDB) and mimetic dolomites (mean $\delta^{18}O$ = -4.79 ‰ PDB; mean $\delta^{13}C$ = -0.92 ‰ PDB).

Interpretations

Inasmuch as the boundaries between individual luminescent patches within the collage dolomites are abrupt rather than gradational, and the patches are irregularly shaped, a recrystallization process is suggested. Partial recrystallization of a preexisting dolomite by another type of dolomite can take on a variety of appearances, with the recrystallized zones being either zone-selective or nonselective, marginal or internal to the original crystal, or with varying combinations of the preceding characteristics (Nielson and others, 1994). Considering their complex appearance, the collage dolomites may represent wholesale replacement of a previous dolomite, which could perhaps be the concentric dolomite. In any event, the salinities

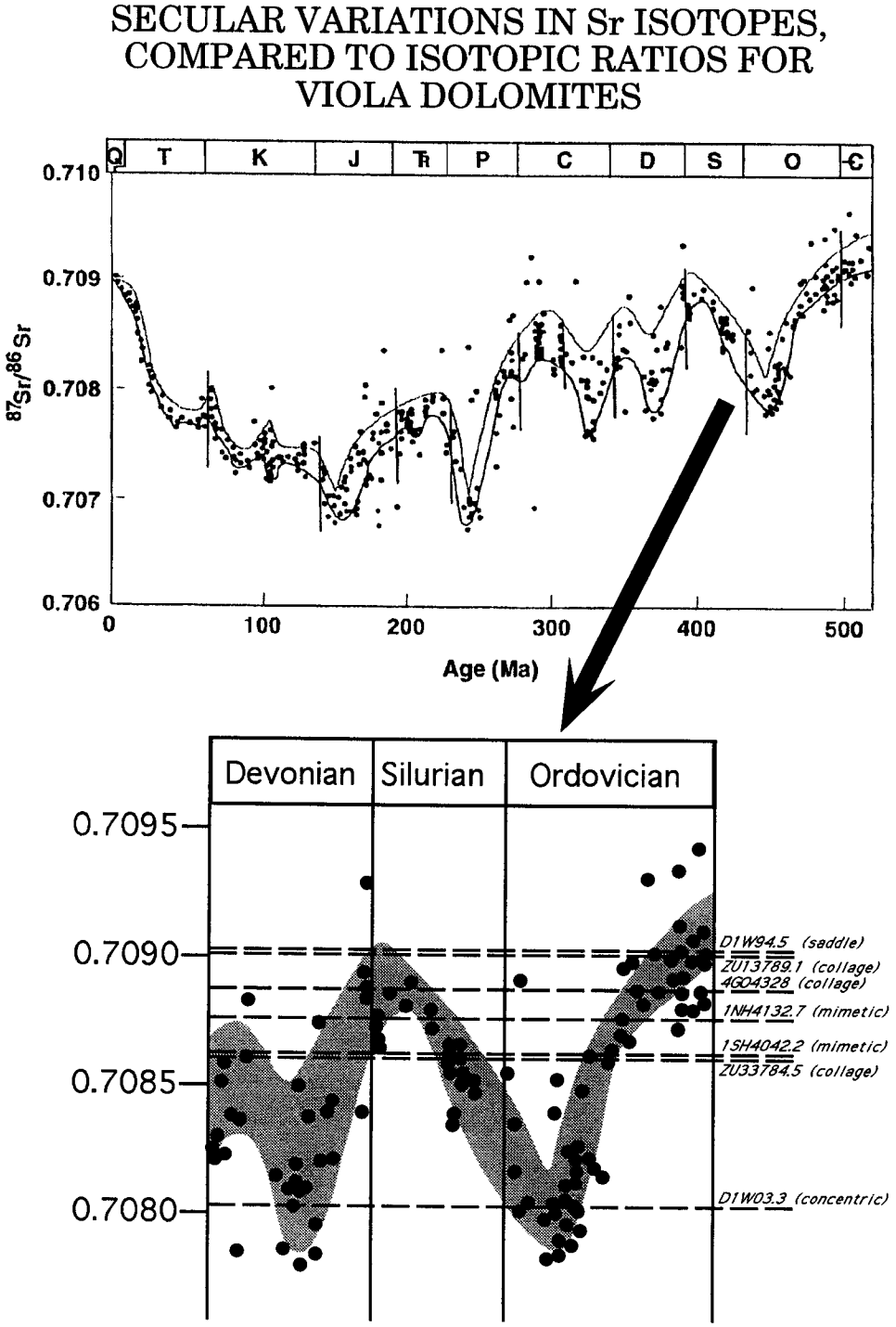

Figure 8.44 Secular variations in strontium isotopes for marine carbonate rocks through Phanerozoic time, with results from seven dolomite samples from the study area. See Table 8.3 for a listing of this data.

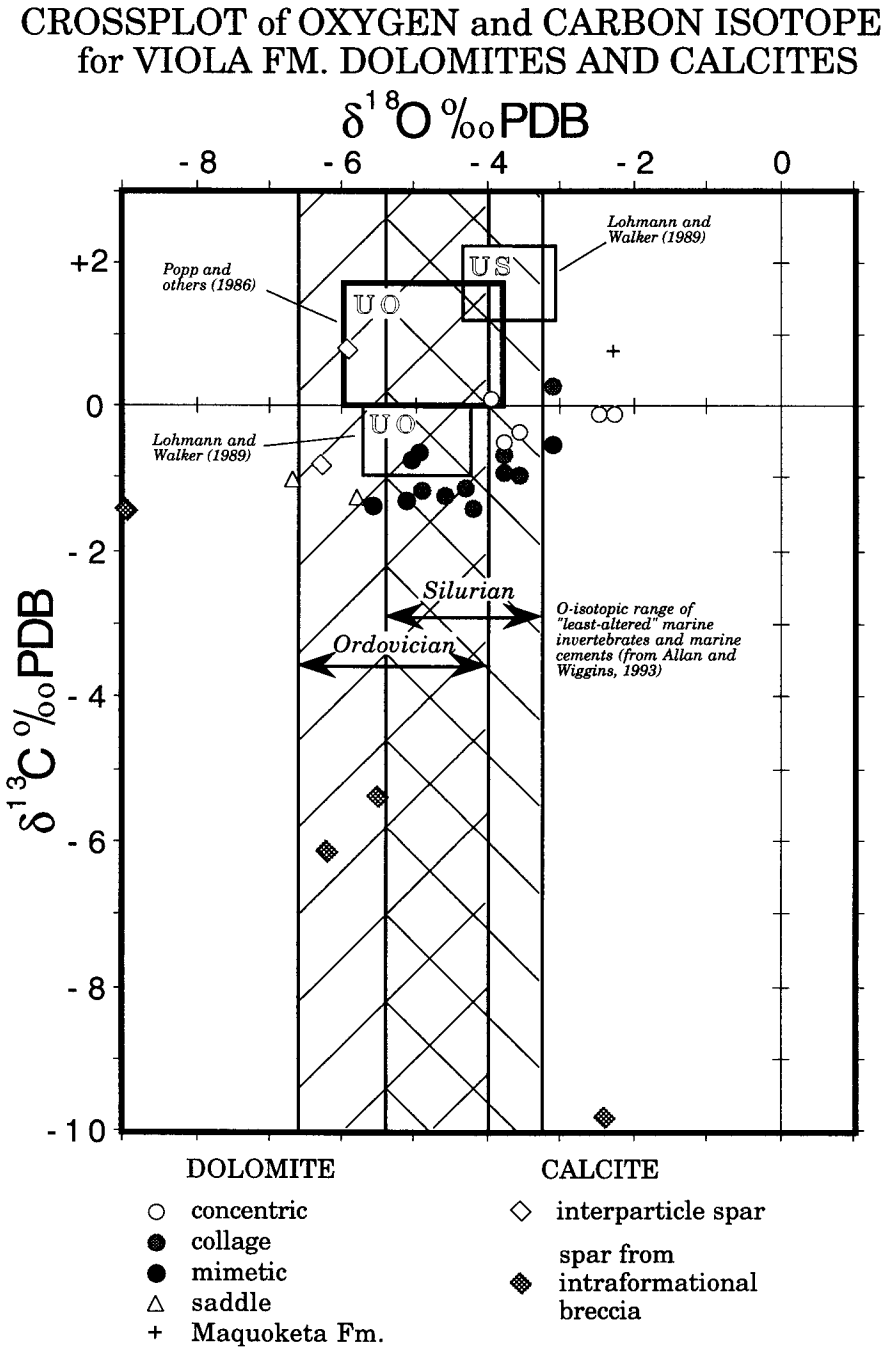

Figure 8.45 Crossplot of oxygen and carbon isotopes for Viola Formation dolomites and calcites. A listing of this data is in Table 8.3. Primary marine calcite baseline from Popp and others (1986) is based on the nonluminescent portion of brachiopods; baseline from Lohmann and Walker (1989) is based on marine cements. UO is "Upper Ordovician"; US is "Upper Silurian". See text for discussion.

recorded by their fluid inclusions (Figure 8.43, Table 8.2) indicate that these two dolomites did not merely originate as two separate morphologies from the same event. Application of Occam's razor suggests that the concentric dolomite precedes the collage dolomite, because the concentric dolomite has a simpler structure that would be obliterated by the process of recrystallization represented by the collage dolomite. Unfortunately, no transition varieties of dolomite were observed between the collage and concentric dolomites (for example, dolomites with concentric internal zonation gradually obliterated by an increasing concentration of brightly luminescent specks), however, the presence of a few specks of dolomite with markedly different cathodoluminescence apparently truncating the layers within the concentric dolomites (Figure 8.28) suggests that minor recrystallization followed the precipitation of the concentric dolomites. Although thin concentric rims were observed on collage dolomites, none of these rims displayed the succession of zones present within the nearest concentric dolomites, hence the recrystallization event(s) responsible for the collage dolomites may have interrupted the latter stages of a longer process that produced the concentric dolomites.

The temporal relationship of the mimetic dolomite to the other two types of dolomite is a conundrum. No concentric dolomite was observed in the localities where the basal limestone subunit was mimetically dolomitized, however, isolated rhombs of dolomite with collage textures were rarely observed (Figure 8.32). Dolomite rhombs with collage textures located within the mimetic dolomite does not necessarily elucidate the relative timing of these two types of dolomite. Conceivably, local impurities or local distortions in the crystal lattice of the mimetic dolomite or its calcite predecessor could have been loci for precipitation of small isolated dolomite crystals having collage textures, but this does not necessarily indicate that the isolated collage crystals within the mimetic dolomite are contemporaneous with

collage dolomites elsewhere. Even if they are bona fide collage dolomites, the isolated rhombs could just as well have been from a generation of dolomite that either preceded or succeeded the mimetic dolomite.

The fine-grained nature of the lower and upper cherty dolomitic limestone subunits probably rendered them more susceptible to dolomitization than the basal and upper limestones with their coarse-grained cements and echinoderm clasts essentially composed of large crystals of calcite. Early spar cementation and a concomitant decrease in porosity of the packstones and grainstones of the basal and upper limestone subunits could have rendered these subunits less permeable to subsequent dolomitizing fluids. Early cementation of crinoidal calcarenites and the susceptibility of fine-grained carbonate sediments to chemical change, was invoked by Murray and Lucia (1967) to account for fabric-selective dolomitization of mudstones in the Mississippian Turner Valley Formation in Alberta, Canada.

In updip areas near the pinchout of the Viola on the Chautauqua arch (cf., Figures 8.5, 8.9), the extensive dolomitization of the basal limestone subunit indicates that, despite its early cementation by calcite spar, sufficient fluid was able to enter this subunit to dolomitize it by both replacement and cementation (Figures 8.33, 8.34). The general pattern of limestones being present in downflank positions off the Chautauqua arch and Pratt anticline, together with its preservation beneath outliers of Maquoketa Shale (see Figures 8.5, 8.8, 8.9, 8.11) implies downdip movement of dolomitizing fluids some time after deposition of the Maquoketa Shale.

Cathodoluminescence maps (Figures 8.37 to 8.41) indicate the crest of the Chautauqua arch was the locus of particularly severe diagenesis inasmuch as dolomite with concentric internal texture is only present off the crests of these uplifts, whereas collage and mimetic patterns characterize dolomite present on the crests. X-ray analysis reveals that mimetic and collage dolomites are nearly stoichiometric

(Figure 8.42) whereas concentric dolomites are distinctly calcian, or nonstoichiometric. The chemistry of the dolomite has implications for the mechanism of dolomitization. Nielson and others (1994) note that recrystallization of dolomite in carbonate rocks is common and could be the result of several driving forces, including: a) lowering of free energy in which poorly ordered and nonstoichiometric dolomite recrystallizes to more ideal stoichiometry and ordering (Katz and Matthews, 1977; Reeder, 1981; Gregg and Sibley, 1984; Sibley, 1990), b) reduction in surface energy in which finely crystalline mosaics recrystallize to coarser grained crystals (Gregg and Sibley, 1984; Gregg and Shelton, 1984; Gregg and others, 1992); and c) reduction in crystal defects (Sibley, 1990). Such recrystallization in dolomite can go unrecognized if only ordinary transmitted-light petrographic techniques are employed (Nielson and others, 1994). The recrystallization of a calcian dolomite to a more stoichiometric dolomite is a convenient driving force for the collage dolomites in the Viola. Overall uniformity of size of the crystals in the collage and concentric dolomites rules out reduction in surface energy a major force in the recrystallization of the dolomite preceding the collage dolomites, for the concentric dolomites would also have been expected to be recrystallized as extensively as the collage dolomites. The spotty cathodoluminescence within individual crystals of collage dolomite implies that their surface energy may have even increased with the process of recrystallization. Reduction in crystal defects or the tendency to increase ordering within the crystal may be a possible driving mechanism, but further work is necessary to determine if differences are present with the types of dolomite observed. A ratio of the height of the $d_{[015]}$ peak (an ordering peak only specific to dolomite) to the height of the $d_{[110]}$ peak (a diffraction peak common to both calcite and dolomite) is suggested by Hardy and Tucker (1988, p. 222-224) as a means to measure ordering within a dolomite, but these measurements were not made on the Viola dolomites. Diffraction peaks

broaden in dolomite as ordering decreases (Schneider, 1976). A measure of the breadth of a diffraction peak is its width at half-height (Cullity, 1956, p. 411). Breadth measurements on the $d_{[104]}$ peak of the Viola dolomites indicate that the concentric (calcian) dolomites may be less well-ordered than the collage and mimetic (stoichiometric) dolomites (Figure 8.42). The tendency to increase ordering therefore cannot be ruled out as a driving force for the dolomite recrystallization in the Viola.

The reason why this recrystallization is concentrated on the crest of the Chautauqua arch and Pratt anticline is still unclear. These structurally high localities possibly would undergo diagenesis more frequently by near-surface fluids than areas farther downdip. Alternatively, the recrystallization and stoichiometry of the resultant dolomite may also be a result of the dolomitizing fluid itself. Dolomite with nearly stoichiometric composition (i.e., $Ca_{0.50}$ $Mg_{0.50}$) is associated with evaporite depositional settings (Goldsmith and Graf, 1958b; Morrow, 1982b). Hypersaline water derived from evaporative concentration of seawater becomes enriched in magnesium relative to calcium because of the removal of Ca^{+2} by precipitation of calcite and gypsum (Goldsmith and Graf, 1958b; Füchtbauer, 1974, p. 309; Lumsden and Chimahusky, 1980; Sperber and others, 1984). Conversely, dolomitization in low-permeability micritic sediment in more normal marine depositional settings will deplete the local supply of magnesium and nonstoichiometric dolomite will tend to precipitate (Sperber and others, 1984). By this provisional model, perhaps the nonstoichiometric dolomites with the concentric textures are the result of an early stage of dolomitization, whereas the stoichiometric dolomites with the collage and mimetic textures may be the result of a later stage of dolomitization that perhaps recrystallized some of the earlier concentric dolomites.

If the preliminary fluid-inclusion determinations are valid, the fluid precipitating the collage dolomites was hypersaline. Salinity of the fluid precipitating

the concentric dolomite is still not pinned down, but it could have ranged from dilute seawater to mildly hypersaline brines, possibly in a mixing zone. The presence of liquid-filled primary inclusions in both the concentric and collage replacive dolomites indicate both types of dolomite formed below about 50 °C and then partially reequilibrated to higher temperatures with subsequent heating, or they possibly precipitated over a wide range of temperatures (see Goldstein and Reynolds, 1994, p. 152). $Tm_{(ice)}$ measurements were made only on fluid inclusions that had bubbles present after the heating runs were performed to measure T_h, and it is not known if some of these inclusions were entirely liquid-filled prior to the heating runs. All-liquid primary fluid inclusions, however, would most likely be representative of the original precipitating liquid, whereas two-phase inclusions run the danger of having been refilled with waters with different salinities during later diagenesis. Although the petrographic characteristics of the fluid-inclusion assemblages from the Derby #1 Wood core (*#15*) and the E.H. Moore #2 R.F. Stewart core (*#21*) (Table 8.2) are consistent with low-temperature precipitation in shallow burial environments, the wide spread in T_h measurements are also indicative of higher-temperature reequilibration or precipitation with widely varying conditions. The upper part of the T_h ranges obtained from both types of dolomite still exceeds the maximum temperature expected by burial curves (see Chapter 6), hence advective heating or transiently high geothermal gradients could have affected these samples, and leakage and refilling could have affected the original fluid compositions.

The timing of dolomitization is indicated by the strontium-isotope data. The $^{87}Sr/^{86}Sr$ ratio of a marine carbonate mineral is identical to that ratio in the water from which that mineral precipitated, because no significant isotopic fractionation occurs with precipitation (Veizer and Compston, 1974). A standard reference curve for secular variations of the $^{87}Sr/^{86}Sr$ ratio of seawater and associated marine

carbonates over Phanerozoic time was documented by Burke and others (1982; see Figure 8.44). Secular variations in strontium isotopes can be used in some circumstances as a chronostratigraphic tool for carbonate precipitation and diagenesis. Fortunately, $^{87}Sr/^{86}Sr$ ratios for seawater changed drastically between Late Ordovician time (~0.708) and Late Silurian time (~0.709), therefore determining the $^{87}Sr/^{86}Sr$ ratio of the dolomite in the Viola may ascertain its timing, or at least test the hypothesis derived from petrographic and stratigraphic observations that most of the dolomite could be attributed to a pre-Devonian event.

A possible complication that hinders the use of $^{87}Sr/^{86}Sr$ ratios is the incorporation of excess ^{87}Sr into carbonate minerals from radioactive decay of ^{87}Rb in closely associated detrital siliciclastic sediments. For example, Simo and others (1994) reported that significant contamination, possibly by submicroscopic clays with a high content of radiogenically derived ^{87}Sr, elevated the $^{87}Sr/^{86}Sr$ ratios of Middle Ordovician dolomite from an 'initial' composition (~0.7085) to values as great as 0.7133. Despite appearing relatively free of impurities, some marine carbonate rocks containing just a few modal percent of clay minerals may have their $^{87}Sr/^{86}Sr$ ratios significantly affected by radiogenic ^{87}Sr being leached from these clay minerals during analysis or by chemical exchanges during diagenesis (DePaolo and others, 1983; Kralik, 1984; Banner, 1988; Winter, 1995). Notwithstanding these possible difficulties, the Viola is generally a very pure carbonate, with little or no clay- to sand-size siliciclastic grains, save that which is concentrated in stylolites and at the very base of the unit just above the Simpson Group. No Rb determinations therefore supplemented the Sr isotopic determinations. Results of the isotopic analyses (Table 8.3) also did not indicate the presence of excess ^{87}Sr so a correction for Rb probably is not necessary.

Results of the analyses (Table 8.3) are consistent with major dolomitization of

the Viola occurring from a fluid containing strontium derived from Silurian seawater (Figure 8.44). The two samples of mimetically dolomitized basal limestone (1SH4042.2 and 1NH4132.7) from near the crest of the Chautauqua arch have ratios corresponding to Sr isotopic values occurring in marine carbonates during Early Silurian time (Figure 8.44). The two samples of collage dolomite (ZU13789.1 and 4GO4328) from the upper cherty dolomitic limestone have ratios consistent with dolomitization by Late Silurian marine waters. These ratios are slightly higher than the ratios recorded for the mimetic dolomite. The relative age of the mimetic dolomite in the basal limestone subunit and the replacive dolomite in the lower and upper cherty dolomites could not be determined with present petrographic data, but the higher isotopic ratios of the collage dolomite at least in the upper cherty dolomitic limestone are consistent with dolomitization affecting these rocks later than the mimetic dolomite, but still in Silurian time.

Mixing of Ordovician and Silurian strontium during diagenesis cannot be ruled out as a process that may have modified the isotopic ratios of the mimetic dolomite. This may have occurred with a sample of replacive dolomite analyzed from the lower cherty dolomitic limestone (ZU33784.5), which records a ratio of 0.708603. Although this sample records a value consistent with Early Silurian marine waters, it may also represent mixing of solutes derived from dissolved Ordovician carbonates (having a ratio of ~0.708) and Silurian marine-derived waters (having a ratio of ~0.709), or mixing of a Silurian marine-derived water with Ordovician connate water. Dolomitizing fluids entering the Viola Formation from above is consistent with samples at the top of the Viola having a higher Sr-isotopic ratio than those farther down within the formation.

The one sample of concentric dolomite from the basal limestone (D1W03.3) has a relatively low isotopic ratio (0.708032). Comparison to secular variations in Sr

isotopes for geologic time (Figure 8.44) indicate that this ratio is consistent with early dolomitization before Silurian time, possibly from Late Ordovician seawater-derived fluids.

The oxygen and carbon isotopes give information that aids in determining the diagenetic environment of dolomitization. The oxygen isotopic ratio of a carbonate mineral principally depends on the temperature of precipitation and isotopic ratio of the fluid from which it precipitates. In the case of a diagenetic mineral such as dolomite, the amount of interaction between the fluid and host rock may affect the ratio (Anderson and Arthur, 1983; Land, 1983). High temperatures and dilution by meteoric water, which is typically isotopically negative, will generate carbonate minerals with negative $\delta^{18}O$ isotopic values. Conversely, carbonates precipitated under the influence of lower temperatures or hypersalinity will have more positive oxygen signatures relative to normal marine waters (Anderson and Arthur, 1983; Allan and Wiggins, 1993). Carbon isotopic ratios principally reflect the interplay of very light dissolved carbonate (ranging from about -15 to -35 $\delta^{13}C$ ‰ PDB; usually derived from oxidation of organic material) and skeletal carbonate material (ranging from about +3 to -5 $\delta^{13}C$ ‰ PDB) (Allan and Wiggins, 1993). For later diagenetic phases such as dolomite, interaction with host rock for carbon isotopes can be much more important than with oxygen isotopes, because the reservoir for carbon in the precipitating fluid (dissolved CO_2) is smaller than that for oxygen (dissolved CO_2 and H_2O) (Lohmann, 1983). Carbonate minerals precipitated in proximity to organic material undergoing methanogenic reactions also can incorporate coproduced CO_2 that is isotopically heavy and thus have $\delta^{13}C$ ranging between +5 to +20 ‰ PDB, but this is uncommon (Allan and Wiggins, 1993).

Secular variations in oxygen and carbon isotopes for marine carbonates have been recorded over geologic time by analyzing diagenetically unaltered marine

invertebrate fossils and marine calcium-carbonate cements (cf., Popp and others, 1986; Veizer and others, 1986; Lohmann and Walker, 1989). These studies provide baseline values for marine calcium carbonate by which other carbonate samples can be compared. Recognizing that minor discrepancies occur for given geologic periods, Allan and Wiggins (1993) surveyed data for carbon and oxygen isotope values for marine calcium carbonates based on 12 papers focused on the Ordovician period, and 9 focused on the Silurian period. Their proposed baseline ranges for the oxygen isotopes for primary marine calcium carbonates from both these periods are shown in Figure 8.45, as are other baselines based on the nonluminescent portion of brachiopods (Popp and others, 1986) and pristine marine cements (Lohmann and Walker, 1989).

In order to relate dolomite to these baselines, an relationship of dolomite to co-precipitated calcite is needed. A precise dolomite fractionation factor remains unknown, but experimental evidence indicates dolomite, at surface temperature (approximately 25 °C) will be enriched 3 to 6 ‰ in ^{18}O with respect to co-precipitated calcite (i.e., $\delta_{dolomite} - \delta_{calcite} = 3$ to 6 ‰) (Land, 1980, 1983a), however, Holocene examples suggest $\delta_{dolomite} - \delta_{calcite} = 2$ to 4 ‰ (Land, 1980, 1983a). Fractionation of calcite (PDB standard) with respect to water (SMOW standard) at 25 °C is approximately -2 ‰ (O'Neil and others, 1969; Land, 1983a). In other words, for example, a calcite cement having -2 ‰ $\delta^{18}O$ PDB would precipitate from a water having 0 ‰ $\delta^{18}O$ SMOW. Note that the oxygen isotopic standard for water is reported using the SMOW standard (Standard Mean Ocean Water) whereas carbonates are reported with the PBB standard (Peedee Formation Belemnite); the two standards are mathematically related by the equations:

$$\delta^{18}O(\text{SMOW scale}) = [(1.03086) * \delta^{18}O(\text{PDB scale})] + 30.86$$

$$\delta^{18}O(\text{PDB scale}) = [(0.97006) * \delta^{18}O(\text{SMOW scale})] - 29.94$$

Oxygen isotopic data from the Viola dolomites are generally within the range of both the Ordovician and Silurian baselines shown in Figure 8.45, considering that the dolomites might be approximately 2 to 4 ‰ more positive in $\delta^{18}O$ relative to the calcites upon which these baselines are determined. The concentric dolomite samples generally have the most positive oxygen-isotopic values, but considering fractionation factors, hypersaline fluid is not indicated for its precipitation even for the Ordovician Period. Successively more negative isotopic signatures characterize the collage and mimetic dolomites.

Another way to examine the isotopic data in the context of the precipitating fluid is to plot the isotopic data for the dolomites on the graphical solution to the dolomite-water fractionation equation presented in Land (1980; 1983a, b). Using this graph (Figure 8.46), a range for the oxygen-isotopic composition of the dolomitizing fluid can be inferred by using the $\delta^{18}O$ values of the dolomite and an estimated temperature of precipitation. The temperature for at least some of the concentric and collage dolomites is less than about 50 °C, based on fluid-inclusion assemblages. Ambient surface temperatures during the Ordovician and Silurian were 20 °C and 27 °C respectively (Table 6.1), and burial during dolomitization was no more than 500 ft (150 m; Figures 6.5, 6.6). Geothermal gradient, based on present-day data (Figures 6.1, 6.3, 6.4), is estimated to be between 25 and 35 °C/km. Likely temperature of precipitation is then bracketed between 20 °C near-surface temperature during Ordovician time, and 32 °C using 27 °C surface temperature in the Silurian in combination with 150 m maximum burial at 35 °C/km geothermal gradient. The resultant isotopic range of the precipitating fluid is between -7 and -3 ‰ $\delta^{18}O$ SMOW (Figure 8.46). Ordovician seawater would have a likely composition of -4.6 to -2.0 ‰ $\delta^{18}O$ SMOW, if the range of -6.6 to -4.0 ‰ $\delta^{18}O$ PDB for "least-altered" marine invertebrates and marine cements (from Allan and Wiggins, 1983) is accepted and

OXYGEN ISOTOPIC COMPOSITION of DOLOMITE as a FUNCTION of TEMPERATURE and OXYGEN ISOTOPIC COMPOSITION of WATER

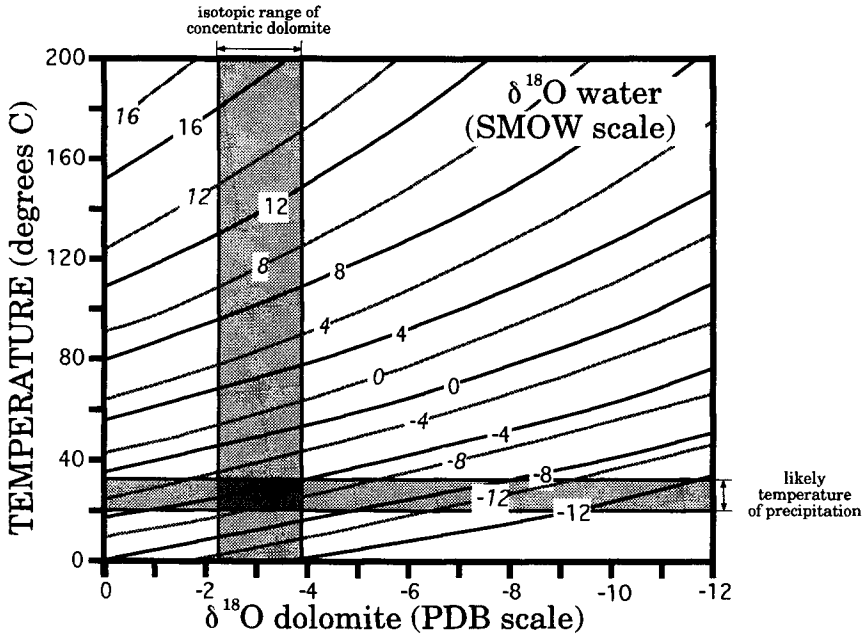

Figure 8.46 Oxygen isotopic composition of dolomite as a function of temperature and oxygen isotopic composition of the water from which it precipitated, plotted with data from Viola concentric dolomites. The upper diagram is a graphical solution to the fractionation equation in Land (1983a):

$$10^3 \ln\alpha_{\text{dolomite-water}} = [3.2 * 10^6 T(^\circ K)^{-2}] - 3.3$$

where

$$\alpha_{\text{dolomite-water}} = 1000 + \delta^{18}O_{(\text{dolomite})}/1000 + \delta^{18}O_{(\text{water})}.$$

The lighter lines represent the graphical solution to a different fractionation equation from Northrop and Clayton (1966):

$$10^3 \ln\alpha_{\text{dolomite-water}} = [3.2 * 10^6 T(^\circ K)^{-2}] - 1.5$$

Both solutions are shown for sake of diversity and possible range of solutions because the relationship between $\delta^{18}O_{\text{water}}$, $\delta^{18}O_{\text{dolomite}}$, and temperature is imperfectly known (Land, 1983a). Ordovician seawater concentrated by evaporation would be expected to have an oxygen isotopic signature more positive than -4.6 to -2.0 $\delta^{18}O$ (SMOW), according to fractionation factors estimated for dolomite by Land (1980, 1983a). Probable temperatures of precipitation are less than 50 °C according to fluid-inclusion characteristics and projected near-surface temperatures in the Ordovician (see Table 6-1). Seawater from which the concentric dolomites precipitated probably had an isotopic composition of -7 to -3 $\delta^{18}O$ (SMOW) according to the fractionation equation in Land (1983a). Slightly more negative results are obtained using the Northrop and Clayton (1966) equation (-9 to -4 $\delta^{18}O$ (SMOW)). See text for discussion.

converted using the -2 ‰ fractionation factor discussed above. Hypersalinity, which would produce $\delta^{18}O$ SMOW values more positive than -4.6 to -2.0 ‰, seems ruled out by the oxygen isotopes of the concentric dolomites. Reconnaissance fluid-inclusion evidence for the concentric dolomites possibly indicates a moderate degree of hypersalinity, but some $Tm_{(ice)}$ values indicate lesser salinities (Figure 8.43). Some of the more saline fluid inclusions, although primary, could have been refilled with more saline formation waters during later burial. Due to the relatively pristine condition of the concentric dolomites and their lack of recrystallization, a more detailed fluid-inclusion study of the concentric dolomites may have much potential to better define their environment of formation, but a mixing zone environment possibly is indicated with present data.

The mimetic and collage dolomites, which are isotopically more negative than the concentric dolomites, would have to precipitate from water even more depleted in ^{18}O. Water significantly depleted in ^{18}O is not consistent with hypersalinity. Preliminary fluid-inclusion data from a collage dolomite (Figure 8.43), together with its stoichiometric composition, however, suggests hypersalinity during its precipitation. Nevertheless, a hypersaline origin cannot be discounted based on the isotopic data. Increases in temperature and relative humidity, and periodic flushing by either, or both, fresh water and marine water could explain a lack of significant isotopic enrichment normally associated with hypersalinity (Lloyd, 1966). Post-depositional processes may also may change the isotopic values. The oxygen-isotopic signatures of the collage and mimetic dolomites in the Viola are inherently less definitive than in the concentric dolomites, in that recrystallization may have readjusted their isotopic compositions. Land (1983a) maintains that few ancient dolomites have isotopic compositions "consistent with formation from a surficial hypersaline fluid in a single event", and asserts that dolomite "more depleted than

about -2 ‰ must have either formed from or been affected by water depleted in ^{18}O with respect to seawater, or by elevated temperature". Although hypersalinity is not consistent with the isotopic data, the potential effects of recrystallization makes discerning the influence of meteoric water, as in a mixing-zone, problematic.

Brecciation

Observations

Intraformational breccias are present in eastern Stafford County in the Braden-Zenith ZU-1 core (*#19*, depth 3831 ft) and ZU-3 core (*#20*, 3774 ft) near the top of the lower cherty dolomitic limestone (see Figure 7.19). These intraformational breccias are correlatives (Figure 8.47). Intraformational breccias are also present in the upper cherty dolomitic limestone (see Figures 7.28, 7.29) and generally have coarse-grained calcite spar interstitial to the breccia clasts.

Close examination of the margins of the clasts in these intraformational breccias reveals key details regarding the timing of brecciation versus dolomitization. The walls of dolomitic mudstone clasts in the intraformational breccia beds near the top of the lower cherty dolomitic limestone in the Braden-Zenith cores (*#19*, *#20*) (see Figures 7.19, 8.48) are composed of euhedral dolomite crystals that protrude into the calcite spar in the matrix of these breccias. Dolomite rhombs also float in the calcite spar near the margins of the clasts. Consequently, to the naked eye, the margins of the clasts have a fuzzy appearance. A breccia in the upper cherty dolomitic limestone in the Braden-Zenith ZU-1 core (*#19*), shown in Figure 7.28, has similar characteristics. Chert clasts in these intraformational breccias, however, have very sharp boundaries (Figure 8.25).

Textural characteristics differ in an intraformational breccia developed in the upper cherty dolomitic limestone immediately below the angular unconformity

Figure 8.47 Stratigraphic cross-section in the vicinity of the Braden-Zenith ZU-1, Braden-Zenith ZU-3, and Shell #1 A.C. Brown (2, 11-T.24S.-R.11W.) in eastern Stafford County. Datum of cross-section is the top of the lower Misener sandstone, a sandstone with a nearly horizontal top, at or near the base of the Devonian-Mississippian Chattanooga Shale. Depositional textures observed at these three cores (see Appendix IV) are shown by the line to the right of the well column. Correlation lines and intermediate wells are from formation tops identified from inspection of well cuttings, scout cards, and drillers' logs in Newell (1991). Viola producing zones in this oil field (Zenith field) are dolomitized mudstones. A thick nonporous packstone locally present in the upper cherty dolomitic limestone subunit forms the upper seal to the "1st Viola" pay zone. Intraformational breccias and partially to completely calcitized dolomite (dedolomite) zones seen in core are displayed to the right of each well column. Calcitized dolomites are present in both the lower and upper cherty dolomites in the Viola. Although they are found in general stratigraphic horizons (i.e., below the upper limestone and perhaps just below the unconformity at the base of the Chattanooga Formation), well-to-well correlation of these calcitized zones is not feasible. Downdip seepage of meteoric water from either the basal Pennsylvanian unconformity or the unconformity at the base of the Devonian-Mississippian Chattanooga Shale is interpreted to cause the dedolomitization present at this locality.

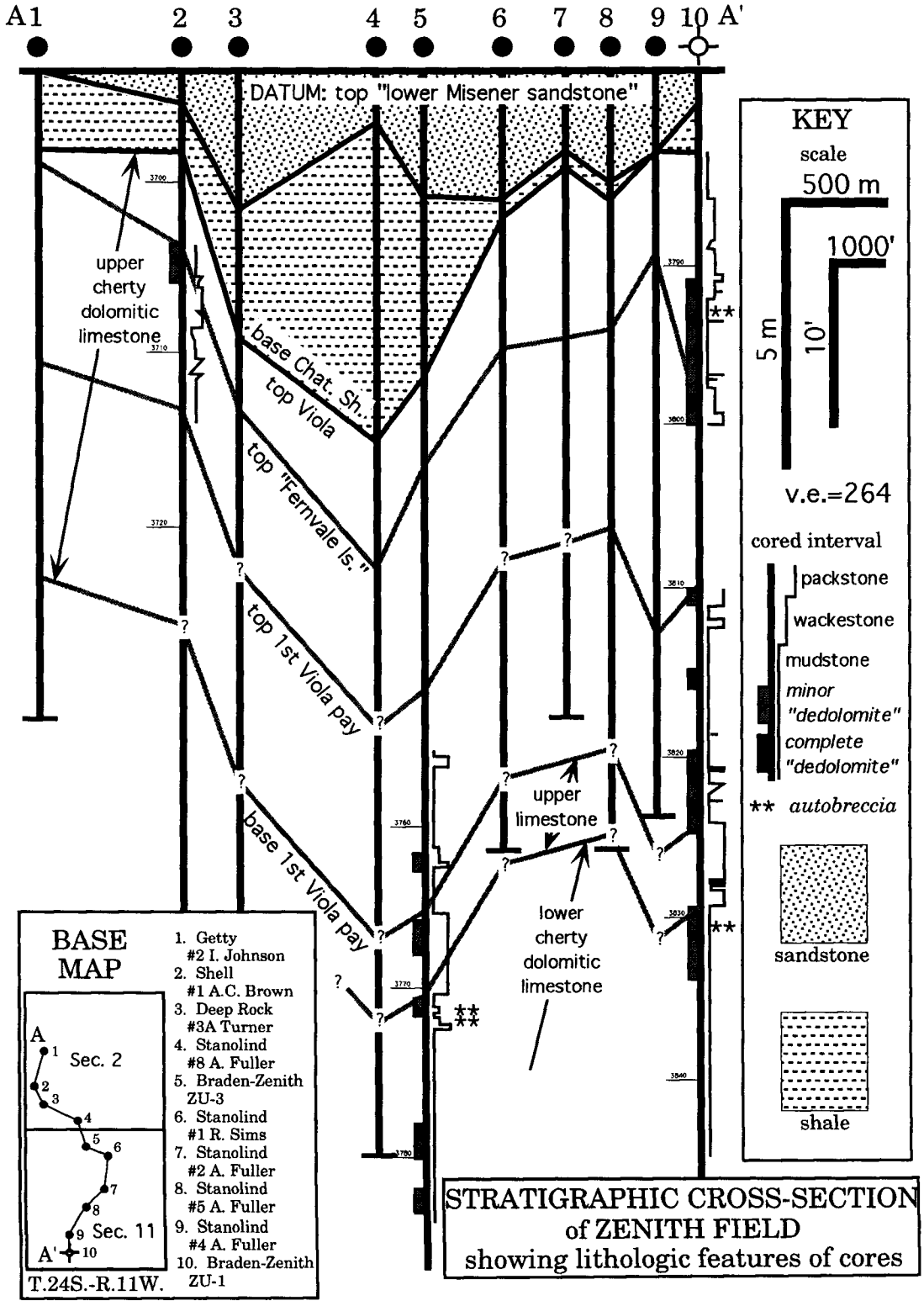

STRATIGRAPHIC CROSS-SECTION of ZENITH FIELD showing lithologic features of cores

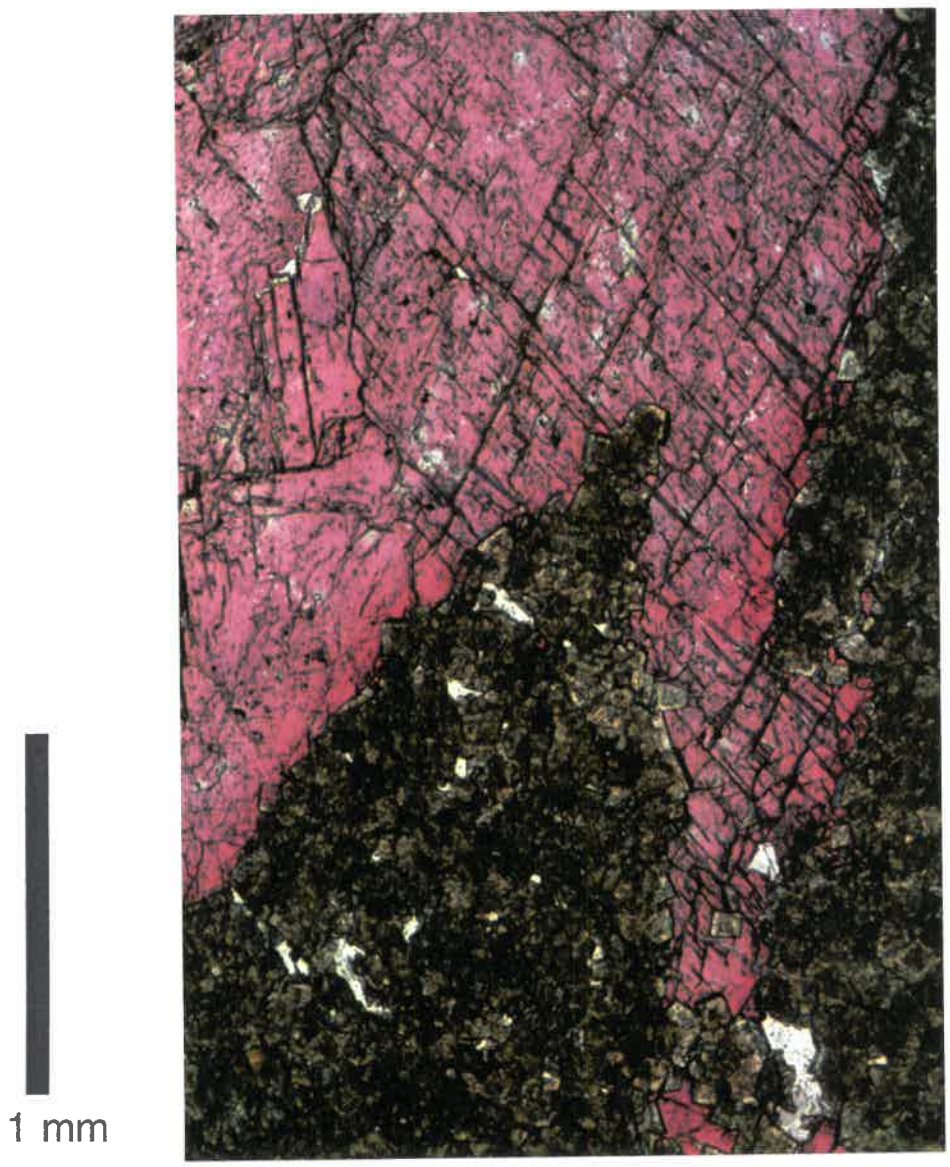

Figure 8.48 Photomicrograph of the upper surface of a breccia fragment and adjacent calcite spar from the intraformational breccia zone in the lower cherty dolomitic limestone in the Braden-Zenith ZU-3 core (#*20*) in eastern Stafford County (3771.2 ft depth, 11-T.24S.-R.11W.). A core slab of this intraformational breccia is shown in Figure 7.19. Note that the dolomite rhombs are euhedral and extend out into the spar. Isolated rhombs are also contained wholly within the calcite spar near the boundary of the clast. Brecciation is interpreted to have occurred before dolomitization. This texture contrasts with the sharp clast margins in another intraformational breccia at the Sinclair-Prairie #4 G. Oldfather well (#*34*, 4328 ft depth) in Barber County (7-T.31S.-R.14W.), shown in Figure 7.29 (hand-specimen) and Figure 8.49 (microscopic view). See text for discussion.

beneath the Devonian-Mississippian Chattanooga Shale at the Sinclair-Prairie #4 G. Oldfather well (*#34*, 4328 ft depth) in Barber County (7-T.31S.-R.14W.). This intraformational breccia is composed of clasts of dolomitic mudstone and chert set in a matrix of calcite spar (see Figure 7.29), but the margins of the dolomite clasts are sharp, and some dolomite rhombs are broken (Figure 8.49). A similar texture is developed in an intraformational breccia in the lower cherty dolomitic limestone in the Palmer & Colorado Oil & Gas #2 Grier core (*#31*) from Pratt County. The intraformational breccia in this core is approximately 2 inches (5 cm) thick and is immediately below the unconformity at the base of the Devonian-Mississippian Chattanooga Shale.

Chert breccias due to dissolution of the surrounding carbonate are represented by the thick accumulations of chert where the Viola subcrops beneath Pennsylvanian strata on the southern end of the Central Kansas uplift (Figures 8.5, 8.8, 8.9, 8.11, 8.12). Core bits are torn up by this type of rock and drillers are thus loath to core in it, therefore none of this material was available for examination by core.

Four spar samples from intraformational breccias in the Viola display a wide range of carbon and oxygen isotopic ratios (Table 8.3, Figure 8.45); the most negative $\delta^{18}O$ value, -8.93 ‰ PDB, is from the breccia in the upper cherty dolomitic limestone subunit at the Sinclair-Prairie #4 G. Oldfather core (#34, 4328 ft depth) in Barber County (7-T.31S.-R.14W.). This breccia, shown in Figure 7.29, is present immediately below the angular unconformity beneath the Devonian-Mississippian Chattanooga Shale. These spars register the most negative $\delta^{13}C$ values of all the Viola samples analyzed (Table 8.3, Figure 8.45).

Interpretations

The intraformational breccia in the lower cherty dolomitic limestone in the Braden-Zenith cores (Figures 7.19, 8.47, 8.48) is interpreted to have occurred by

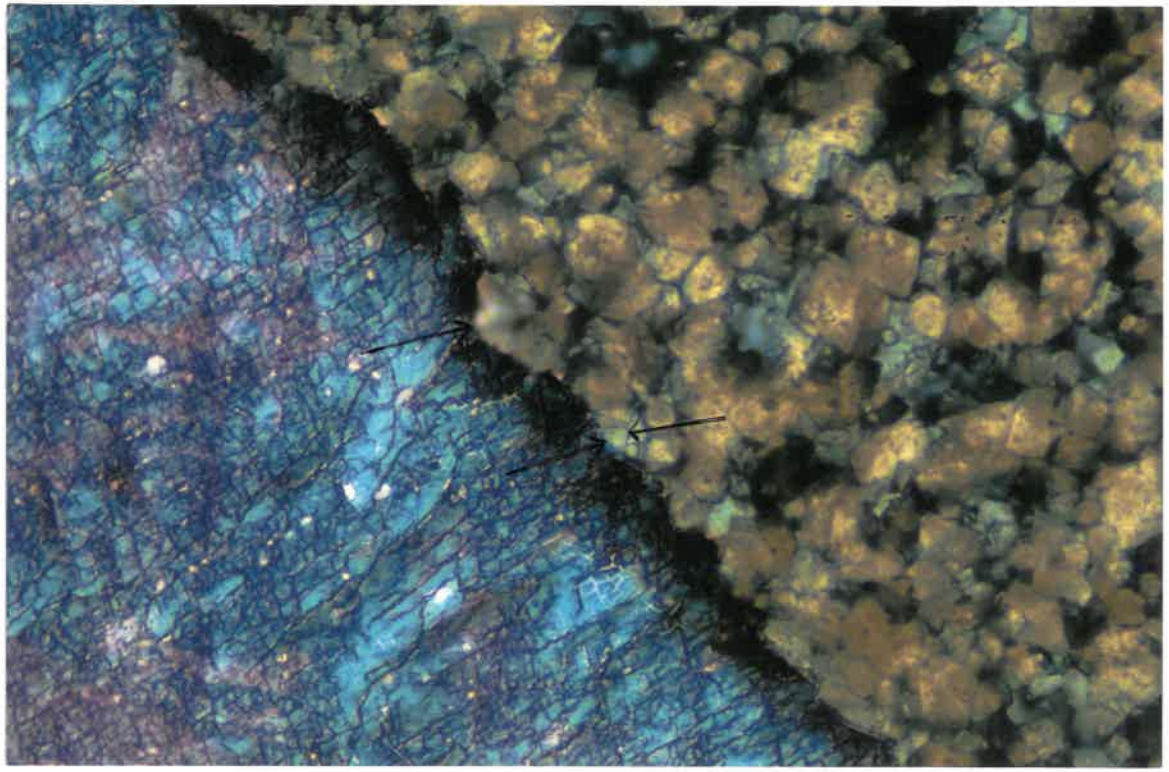

Figure 8.49 Photomicrograph of the margin of a clast from an intraformational breccia in the upper cherty dolomitic limestone immediately below the angular unconformity beneath the Devonian-Mississippian Chattanooga Shale at the Sinclair-Prairie #4 G. Oldfather well (#*34*, 4328 ft depth) in Barber County (7-T.31S.-R.14W.). Clasts of dolomitic mudstone and chert are set in a matrix of calcite spar. The margin of the clast is sharp and shows some dolomite rhombs that appear broken (arrow) -- crosscutting relationships that indicate dolomitization of the mudstone occurred before brecciation. Dark band at contact is a shadow developed due to differential etching of the dolomite and calcite, in combination with a condenser lens focusing the light. A cut slab of this breccia is shown in Figure 7.29. Thin section is stained with a combination of potassium ferricyanide and Alizarin Red-S. The calcite spar is ferroan, hence the deep blue stain.

dissolution processes during a brief period of subaerial exposure prior to deposition of the upper limestone subunit (see Chapter 7). The protruding euhedral dolomite rhombs at the edges of these clasts and the euhedral rhombs floating in the adjacent interstitial spar suggest that dolomitization occurred after brecciation. Intraformational breccias in separate localities in both the lower and upper cherty dolomitic limestones (i.e., Sinclair-Prairie #4 G. Oldfather well [*#34*] and Palmer & Colorado Oil & Gas #2 Grier core [*#31*]) have sharp clast margins that indicate that the brecciation occurred after dolomitization. Both breccias are present immediately below the unconformity at the Devonian-Mississippian Chattanooga Shale and are probably caused by exposure prior to deposition of the Chattanooga Shale. Major dolomitization of both the lower and upper cherty dolomitic limestones of the Viola therefore occurred before the Viola was beveled by the sub-Chattanooga unconformity. The Chattanooga Shale in Kansas is considered Late Devonian in age (Goebel, 1968b) but conodont biostratigraphy by Amsden and Klapper (1972) date the Misener sandstone (at the base of the correlative Woodford Shale) in north-central Oklahoma as Middle to Late Devonian (Givetian to early Famennian) in age. The timing of dolomitization of the Viola can therefore be bracketed between Late Ordovician and Middle to Late Devonian time by its relationship to these karstic breccias. Furthermore, regional mapping (see Figure 8.12 and associated discussion in text) indicates that the Maquoketa Shale may have protected the Viola from downward movement of dolomitizing fluids off the Chautauqua and Central Kansas arches, therefore the Maquoketa Shale was probably deposited before dolomitization of the Viola. Tectonic mobility diagrams illustrating the post-depositional history of the Viola (Figures 6.2, 6.5, 6.6) indicate the Viola probably was not buried more than 500 ft (150 m) before its exposure prior to deposition of the Chattanooga Shale.

The wide range in oxygen isotopic ratios for the interstitial spar from the

intraformational breccias probably reflects variable mixtures of a component of fresh-water bicarbonate with that remobilized from nearby dissolved limestone and dolomite. Three very negative $\delta^{13}C$ values (-5.38, -6.16, and -9.83 ‰ PDB) from the spar in intraformational breccias probably record the interaction of light carbon derived from oxidation of organic material.

Calcitization of Dolomites ("Dedolomitization")

Observations

Calcitization of dolomite ("dedolomitization") most prominently affects the Viola in the area of the Zenith-Peace Creek field in eastern Stafford County, although this may be an artifact of available core coverage. Stratigraphic correlation of the cores taken in that area (Figure 8.47) indicates that calcitized zones are present in both the lower and upper cherty dolomitic limestones, but well-to-well correlation of the calcitized zones is not possible. This calcitization is commonly expressed by the interiors of individual dolomite crystals being replaced by nonferroan calcite, but it also can be extreme, with all dolomite crystals being completely calcitized. One such zone in the lower cherty dolomitic limestone in the Braden-Zenith ZU-3 core (*#20*) at 3779 ft (Figures 8.47, 8.50) is approximately 2-3 inches (5 to 8 cm) thick and grades into partially calcitized dolomite (i.e., dolomite rhombs with calcitized cores) and then unaltered dolomite within a few centimeters. Microscopically, this completely calcitized dolomite is translucent but has a clotted appearance -- a characteristic "grumeleuse" texture (see Evamy, 1967) (Figure 8.51). The term "structure grumeleuse" was originally introduced by Cayeux (1935, p. 271) who described a clotted texture in limestone that he thought most likely evolved by growth of calcite crystals in an originally homogeneous micrite, however, the texture can be generated by other diagenetic processes (Bathurst, 1976, p. 511-513). Evamy (1967) stated that

Figure 8.50 Polished slab showing a completely calcitized dolomite (dedolomite) from the Braden-Zenith ZU-3 core (#*20*, depth 3779.3 ft, 11-T.24S.-R.11W.) in eastern Stafford County. The right half of the slab is stained with a combination of potassium ferricyanide and Alizarin Red-S. Ferroan calcite (**C**) shows up as specks of blue coloration interstitial to nonferroan calcite, and as a fracture fill (**F**). A fractured chert nodule with a lighter-colored rind dominates the lower part of the sample. The calcitized dolomite shown here is developed in an otherwise dolomitic mudstone. It is approximately 2 to 3 inches (5 to 8 cm) thick and grades into partially calcitized, then unaltered dolomite within a few centimeters. See Figure 8.51 for a microscopic view of this sample.

Figure 8.51 Photomicrograph of a completely calcitized dolomite from the lower cherty dolomitic limestone in the Braden-Zenith ZU-3 core (#*20*, depth 3779.3 ft) in eastern Stafford County (11-T.24S.-R.11W.). Note the rhombic form of a erstwhile dolomite crystal (**D**) at the center of the photograph. The texture preserved here is called a "grumeleuse" texture (Evamy, 1967), created when dolomite rhombs with dark (inclusion-rich) centers and clear (inclusion-free) rims are calcitized. A hand-specimen of this sample is shown in Figure 8.50. Thin section is stained with potassium ferricyanide and Alizarin Red-S.

this texture is also created when dolomite rhombs with dark centers rich in inclusions and clear rims are calcitized. Ghosts of dolomite rhombs are still preserved in the completely calcitized dolomite but margins of most of the constituent calcite crystals are anhedral, reminiscent of a neomorphic diagenetic fabric. Completely calcitized dolomite in the upper cherty dolomitic limestone at 3799- and 3815-ft depths at the Braden-Zenith ZU-1 well (Figure 8.47) have similar textures. Cathodoluminescence reveals rare remnants of the original dolomite in thin-sections of the rocks with grumeleuse texture. The surrounding calcite is either nonluminescent or luminesces yellow, whereas the dolomite luminesces dull red to brown. These remnants typically are isolated within a single crystal and have a fluted, corroded appearance.

One thin section from the E.H. Moore #4 R.F. Stewart core (3769 ft depth) in the Zenith field in eastern Stafford County displays partly calcitized rhombs of dolomite superimposed upon relict rhombic-shaped patches of calcite with grumeleuse texture. This is an isolated occurrence of this type of texture in the upper cherty dolomitic limestone that indicates a minor second cycle of dolomitization and subsequent calcitization.

It is difficult to determine unequivocally if fluid inclusions in a completely calcitized dolomite with a grumeleuse texture are primary. Crystal faces are typically curved and wavy (i.e., anhedral in form), the texture is equigranular, and zones of primary inclusions parallel to crystal faces are virtually nonexistent. Well-formed rhombic pseudomorphs of calcite after euhedral dolomite crystals are only rarely observed, and even more rarely is a clot of fluid inclusions fortuitously in the center of such a crystal. Many clots of inclusions are observable though and even if they originated as part of a cloudy center of a dolomite crystal, they are no longer primary inclusions indigenous to the original dolomite. It is difficult to petrographically identify and segregate fluid inclusions to the various generations of calcite that may

be present in a completely calcitized dolomite. The calcitization process also appears complex. Cathodoluminescent zonation within the completely calcitized dolomites is rarely parallel to remnant boundaries of the earlier dolomite rhombs (Figure 8.52). In the case of one Viola dedolomite, an interstitial ferroan spar is distributed throughout the nonferroan calcite (Figure 8.50). At least two generations of calcite may be reflected by the fluid-inclusion data obtained from the calcite with the grumeleuse texture (Table 8.4) from the upper limestone subunit (depth 3815 ft; see Figure 8.47 in the Braden-Zenith ZU-1 core (*#19*).

Although definition of fluid-inclusion assemblages as defined in Goldstein and Reynolds (1994, p. 87) cannot be accomplished with present petrographic samples from the completely calcitized dolomites with the grumeleuse textures, $Tm_{(ice)}$ determinations still provide a record of the salinities of some of the waters that have coursed through these rocks during and after destruction of the dolomite. A broad bimodal distribution of salinities, as shown by $Tm_{(ice)}$ determinations in Figure 8.53, has a saline group ($Tm_{(ice)}$ = -16 to -22 °C) and a less saline mode ($Tm_{(ice)}$ = -1.0 to -1.4 °C). Most notably, two fluid inclusions had $Tm_{(ice)}$ of 0.1 °C -- essentially that of fresh water. Homogenization temperatures (T_h) are not recorded for this sample because the core was heated to 200 °C for determination of residual-fluid saturation (Lynn Antwine, Core Laboratories, Oklahoma City, OK, personal communication, July, 1993; see procedures in Keelan, 1977) thereby causing stretching and leakage of the fluid inclusions. Some all-liquid inclusions are preserved in the sample, but they may be due to necking down of the inclusion, leakage and refilling, or metastability of the fluid phase after heating.

Partial calcitization of dolomite is common in the upper limestone but rare in the basal limestone of the Viola. It was observed in the basal limestone in only two thin sections from the Northern Natural Gas #1 Caldwell core (*#12*) (Figure 8.54) in

Figure 8.52a, 8.52b Matched pair of photomicrographs of a completely calcitized dolomite with a grumeleuse texture. Cathodoluminescent zones in 8.52b do not correspond to the rhombic outlines (**A**) of former dolomite crystals in 8.52a. Sample is from the lower cherty dolomitic limestone in the Braden-Zenith ZU-1 core (#*19*, depth 3815 ft) in eastern Stafford County (11-T.24S.-R.11W.).

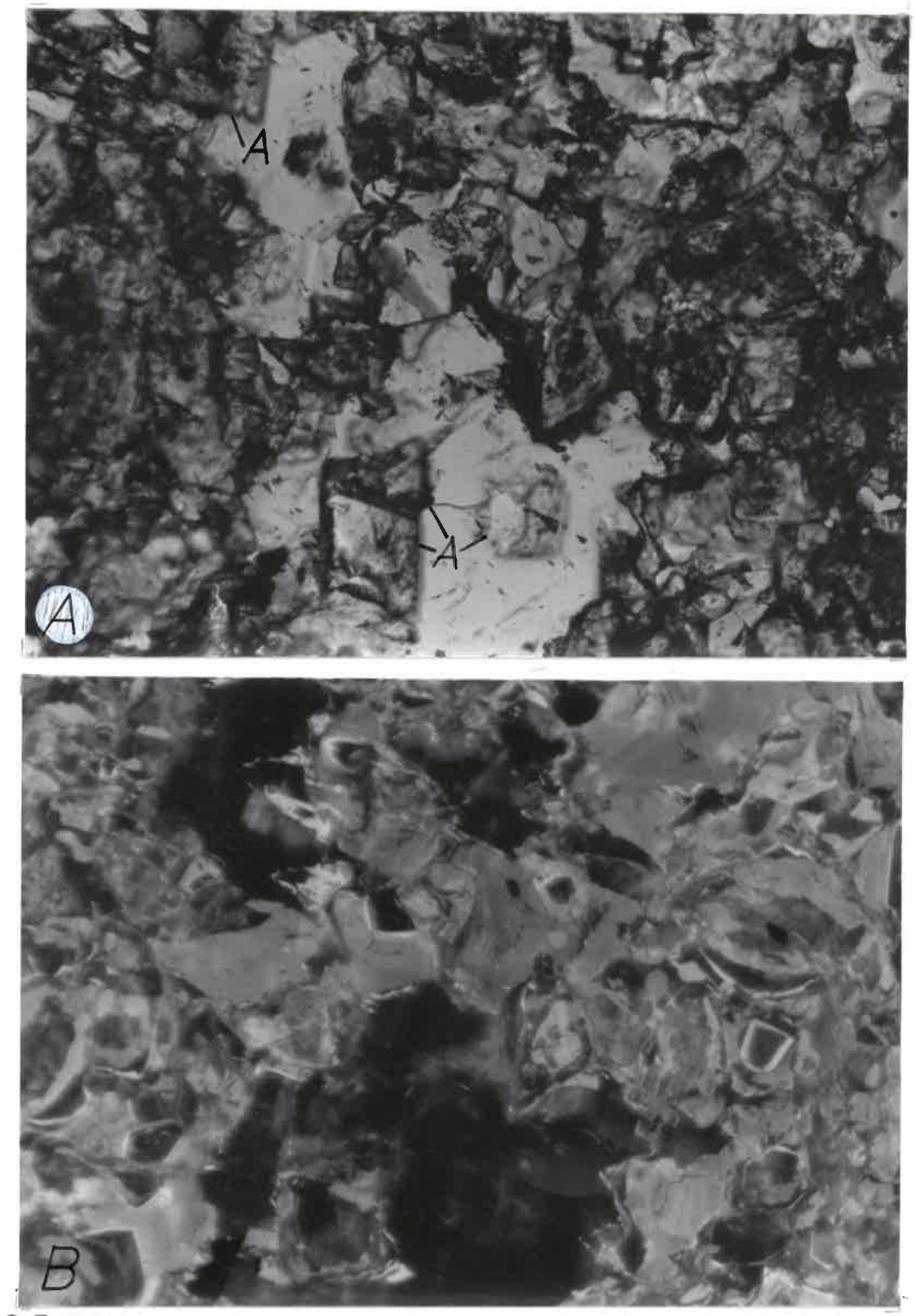
A
A
A
B
0.5 mm

Table 8.4 Fluid-inclusion data from a "dedolomitic" limestone having a "grumeleuse" texture -- thin section ZU-1 3815, from Braden-Zenith ZU-1 (*#19*; SW SE SW, 11-T.24S.-R.11W.; depth 3815 ft; Stafford County); upper cherty dolomitic limestone subunit. $Tm_{(ice)}$, T_e, and T_n are final melting temperature of ice, eutectic temperature, and nucleation temperature. T_h measurements were not made because the sample was heated during core analysis. Definition of fluid-inclusion assemblages, or groups of contemporaneously created primary fluid inclusions, is difficult in a rock with such a complex structure (see text for discussion), hence the association column only indicates the chip and crystal in which the fluid inclusions are found. If the fluid inclusion is isolated, or in a small grouping or "clot", it it designated as such in the notes column. Inclusions of obvious secondary origin were not analyzed. The $Tm_{(ice)}$ data are illustrated in Figure 8.53.

ASSOCIATION chip/crystal	$Tm_{(ice)}$ °C	T_e °C	T_n °C	NOTES*
F/5	-16.3	~ -29	----	isolated
F/1	-17.5	----	~ -73	isolated
F/1	-21.1	----	~ -78	isolated
F/3	----	~ -32	----	in "clot"
F/3	-19.7	----	~ -87	in "clot"
F/3	-20.4 ± 0.2	----	----	in "clot"
F/3	-20.8	----	~ -80	in "clot"
F'/1	-20.6	----	~ -83	in "clot"
G/3	-1.3	----	-39.1	in "clot"
G/3	-1.3	----	----	in "clot"
G/6	-1.0	----	~ -43	in "clot"
G/6	-1.1	----	-46.2	in "clot"
G/6	-1.2	----	-43.4	isolated
G/6	-1.3	----	----	in "clot"
G/6	-1.4	----	~ -51	in "clot"
G/2	-16.7	----	-67.4	in "clot"
G/1	-21.7	----	~ -74	in "clot"
G/4	-21.8	----	-67.5	in "clot"
G'/3	-1.1	----	-39.6	isolated
G'/3	-1.1	----	----	isolated
H/4	0.1	----	-45.6	isolated
H/5	0.1	----	~ -47	isolated
H/1	-2.3	----	-45.9	in "clot"
H/1	-2.9	----	~ -53	in "clot"
H/1	-3.9	----	~ -62	in "clot"
H/2	-3.0	----	~ -58	isolated
H/3	-11.4	~ -28	~ -67	isolated
H/7	-11.9	~ -28	-61.4	isolated
I/4	-21.6	----	~ -75	isolated

Table 8.4 (continued) Fluid-inclusion data from a "dedolomitic" limestone having a "grumeleuse" texture.

ASSOCIATION chip/crystal	$Tm_{(ice)}$ °C	T_e °C	T_n °C	NOTES*
I/5	-17.1	----	~ -68	isolated

*a fluid inclusion is noted as "in clot" if it is in a bundle or clot of fluid inclusions in or near the center of a rhombic crystal; "isolated", if it is by itself but approximately parallel to a crystal wall.

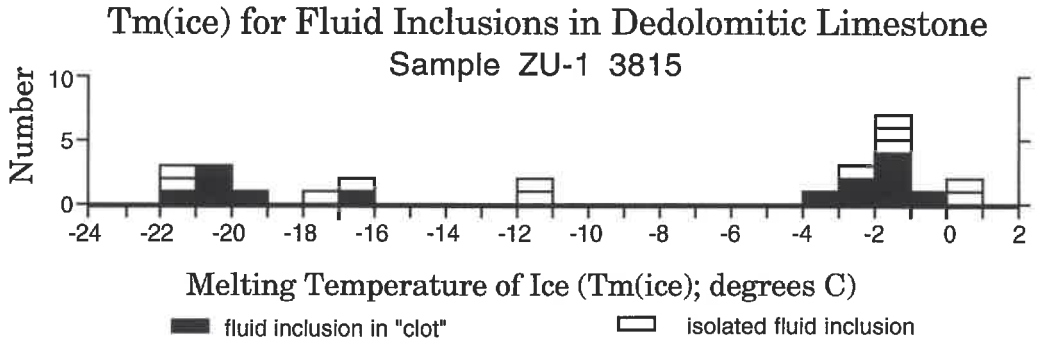

Figure 8.53 Histogram of fluid-inclusion $Tm_{(ice)}$ temperatures for dedolomite having a grumeleuse texture (see Evamy, 1967) from the upper cherty dolomitic limestone (depth 3815 ft) from Braden-Zenith ZU-1 core (*#19*) in eastern Stafford County (11-T.24S.-R.11W.; see Table 8.4). Homogenization temperatures (T_h) are not recorded because this sample had been heated to 200 °C for determination of residual-fluid saturation (Lynn Antwine, Core Laboratories, Oklahoma City, OK, personal communication, July, 1993; see procedures in Keelan (1977)), probably causing stretching and leakage of the fluid inclusions. See text for discussion.

central Rice County. In the Derby #8 Schrock core (*#17*) well in eastern Reno County, 30 mi (48 km) southeast, only two of eight thin sections taken in the basal limestone subunit (i.e., at depths 3836.9 and 3842.1 ft) display partially calcitized textures. Partial calcitization occurs in and is manifest by patchy replacement of approximately 1% of the dolomite rhombs, including saddle dolomite, by ferroan calcite (Figure 8.55). This calcite stains a lighter blue than the ferroan calcite in optical continuity with the nonferroan interparticle syntaxial spar, hence it may not be contemporaneous with this late ferroan spar. The ferroan calcitization is obviously later than the saddle dolomite, but temporal relationships to other diagenetic features in the rock is obscure.

Euhedral rhombs of ferroan calcite are locally present within crinoid ossicles in cores from the upper cherty dolomitic limestone in the Zenith field (e.g., the Shell #1 A.C. Brown core [*#18*], the Stewart cores [*#21, 22*] and the Johnson cores [*#24, 26, 26, 27*]), and rarely in the Sinclair-Prairie #4 G. Oldfather (*#34*; depth 4370 ft) and

Figure 8.54 Photomicrograph of two-stage infill of nonferroan (pink) and ferroan (blue) calcite in a mold after a dolomite crystal in the center of a crinoid columnal. Partially replaced (**P**) and undissolved dolomite rhombs (**U**) are in nearby crinoid fragments. Thin section is from the basal limestone in the Northern Natural Gas #1 Caldwell core (*#12*, 3259.75 ft depth) in Rice County (2-T.20S.-R.8W.). Thin section has been stained by Alizarin Red-S and potassium ferricyanide.

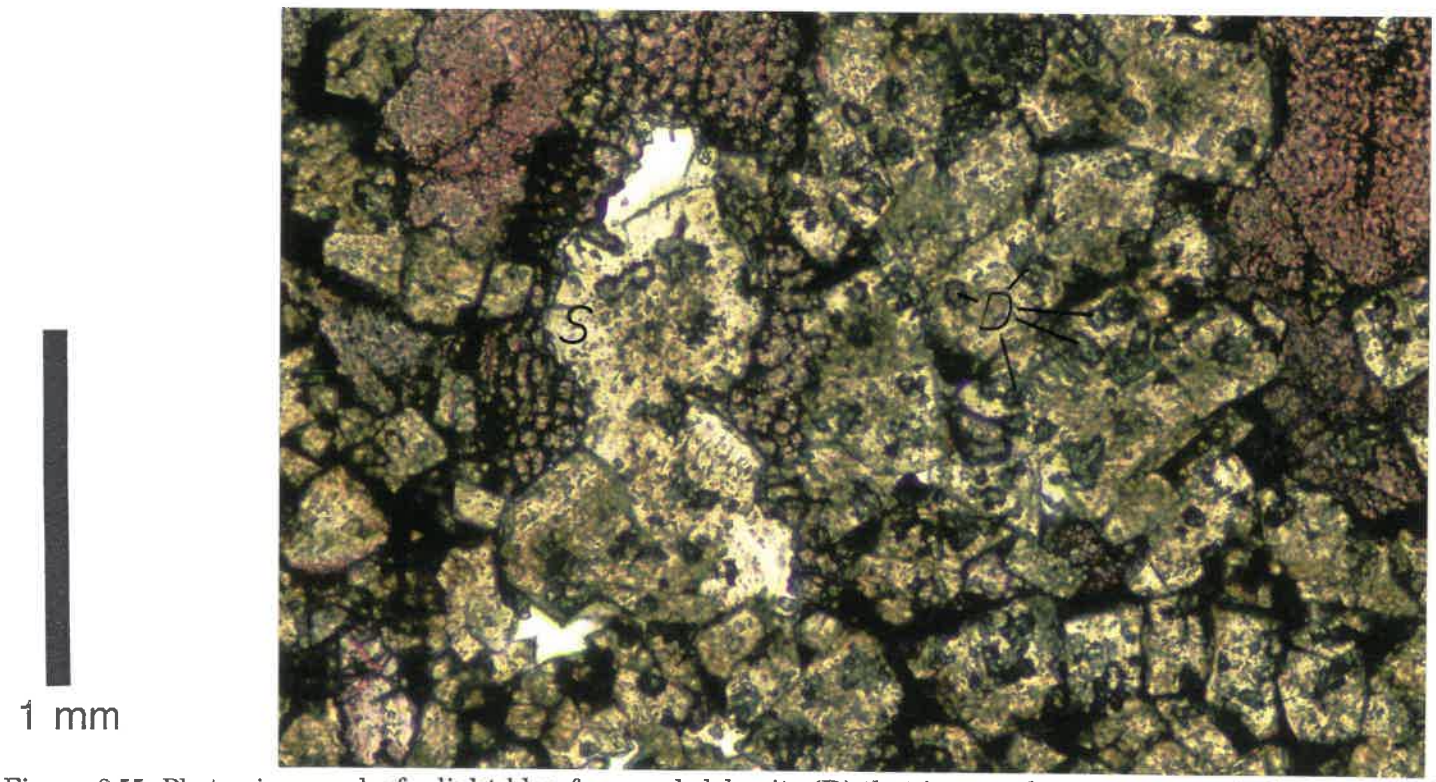

Figure 8.55 Photomicrograph of a light blue ferroan dedolomite (**D**) that is a patchy replacement in the centers of several dolomite crystals, including saddle dolomite (**S**) partly filling a small vug developed in a bryozoan. Sample is from a packstone in the basal limestone from the Derby #1 Schrock core (*#17*, depth 3842.1 ft) in eastern Reno County (27-T.24S.-R.5W.). Thin section is stained with Alizarin Red-S and potassium ferricyanide.

the #1 A. Oldfather (*#35*; depth 4546 ft). Although dolomite rhombs are commonly present in crinoid columnals in other cores, with present sample coverage it is difficult to determine if these calcite rhombs are dedolomitic calcite or a primary calcite (see discussion in Perkins, 1968).

Interpretations

The calcitization of dolomite is essentially the reverse of the dolomitization reaction

$$CaMg(CO_3)_2 + Ca^{2+} \rightleftharpoons 2CaCO_3 + Mg^{2+}$$

This reaction proceeds to the right when the activity ratio (Mg^{2+}/Ca^{2+}) is less than 1 (Abbott, 1974). Additional requirements for dedolomitization include adequate time for the solution-precipitation process to ensue and sufficient permeability and water flow for transporting Ca^{2+} to the reaction site and Mg^{2+} from it. A source of calcium is needed in order to maintain a low Mg/Ca ratio, which Back and others (1983) envisaged being supplied by the dissolution of gypsum ($CaSO_4 \cdot 2H_2O$), most likely by meteoric waters. Excess carbonate ions from the dissolution of dolomite will be removed by concomitant precipitation of calcite (i.e., the dedolomite).

Experimental duplication of the dedolomitization reaction by de Groot (1967) required temperature below 50 °C and partial pressures of CO_2 below 0.5 atm -- conditions fulfilled only in near-surface environments. Subsequent experimental work by Kastner (1982) indicates that calcitization of dolomite can take place at temperatures up to 200 °C. Similarly, the dedolomitization reaction was once thought to be only possible in the presence of sulfate in solution (Plummer, 1977; Wigley and others, 1978; Plummer and Back, 1980), however, Back and others (1983) clarified that the sulfate is a consequence of the dissolution of gypsum (which supplies calcium

in many circumstances of calcitization) and not a primary cause of the calcitization.

Calcitization of dolomite has been documented to be a diagenetic product in near-surface environments and is associated with Holocene near-surface chemical weathering (Chafetz, 1972; Al-Hashimi and Hemingway, 1973) and erosional unconformities in the subsurface (Schmidt, 1965; Goldberg, 1967; Braun and Friedman, 1970). It can also occur in a variety of deeper subsurface environments such as in downdip localities in a fresh-water aquifer (Back and others, 1983), along fault zones carrying fresh water (Abbott, 1974; Longman and Mench, 1978), and in other environments associated with calcium-rich brines (Land and Prezbindowski, 1981; Budai and others, 1984).

Fluid-inclusion $Tm_{(ice)}$-determinations from the dedolomite sample from the upper cherty dolomitic limestone from the Braden-Zenith ZU-1 core (*#19*) (Table 8.4; Figure 8.53) record more than one event of calcite precipitation. As mentioned earlier, it is difficult to distinguish phases of calcite precipitation and fluid-inclusion assemblages in a calcitized dolomite with a grumeleuse texture. Nevertheless, the presence of nearly fresh-water fluid inclusions is consistent with the influence of fresh water, or fresh water diluting saline water, in the calcitization of dolomite. The presence of fresh-water inclusions in the dedolomite (Table 8.4) indicates that the dedolomite precipitated before the rock was buried so deeply as to not be affected by near-surface processes. This confirms that dolomitization occurred also before the Viola was deeply buried.

The geologic history of Kansas (Merriam, 1963) indicates that the Viola in the study area was under the probable influence of fresh water when it was beveled at five major unconformities during the Paleozoic before being deeply and permanently buried in Pennsylvanian time. The periods of erosion associated with these unconformities occurred in Late Ordovician time (before deposition of the Maquoketa

Shale), in Late Ordovician - Early Silurian time (before deposition of the lower part of the Silurian-Devonian "Hunton" group), in Late Silurian time (before deposition of the upper part of the Silurian-Devonian "Hunton" group), in Late Devonian time (before deposition of the Devonian-Mississippian Chattanooga Shale), and in Late Mississippian - Early Pennsylvanian time (before deposition of the Pennsylvanian System). The exposure event prior to deposition of the Maquoketa Shale is probably not significant to the dedolomitization in the Viola because no calcitized dolomite was observed in the soil zone present immediately below the Maquoketa at the Damac #1 Sandra Allen core (#2) in McPherson County (see Figure 6.31). Regional mapping (Figure 8.12) indicates that the Maquoketa Shale may have been impermeable barrier to downward movement of dolomitizing fluids off the Chautauqua and Central Kansas arches, ergo, the dolomitization (and hence dedolomitization) most likely occurred after the exposure event expressed by the unconformity between the Viola and the Maquoketa.

Bushnag (1989) states calcitization of dolomite is common in the southern end of the Cunningham field (T.27S.-R.10W., T.28S.-R.11W.; northwestern Kingman County) in strata interpreted in this report to be the lower cherty dolomitic limestone subunit. Cursory core descriptions in Bushnag (1989) indicate that calcitization affects at most 50% of the dolomite in core samples obtained from this petroleum field cum gas-storage area. The lower cherty dolomitic limestone at the Cunningham field (Bushnag, 1989) and the lower and upper cherty dolomitic limestones at the Braden-Zenith wells in eastern Stafford County (this study) are the Viola subunits that subcrop at the top of the Viola (see Figure 5.6). The Upper Devonian-Lower Mississippian Chattanooga Shale overlies the Viola at both the Cunningham field and the Braden-Zenith locality (see Figure 4.4), hence the exposure event prior to deposition of the Chattanooga Shale may be responsible for the majority of the

calcitization of dolomite in the Viola.

Unlike the calcitization of dolomite in the vicinity of the Braden-Zenith ZU-1 and ZU-3 wells, the calcitization of the dolomite in the basal limestone subunit is not the product of near-surface processes. The timing for this ferroan dedolomitic calcite is late, inasmuch as it replaces saddle dolomite as well as earlier generations of dolomite. The ferroan calcite that replaces the interior of the dolomite in the Derby #8 Schrock core (*#17*) (Figure 8.55) precipitated under reducing conditions, which are characteristic of deep subsurface environments, but also occur in stagnant meteoric waters.

The ferroan calcite following nonferroan calcite and the crystal form of the calcite defined by staining of the thin section from the Northern Natural Gas #1 Caldwell core (*#12*) implies that the calcite shown in Figure 8.54 probably filled a mold after dolomite. This is not concomitant dissolution and precipitation as expressed by the dedolomitization reaction given above, nevertheless, such a two-step process is now included as a type of dedolomitization (James and others, 1993).

Vugs, Saddle Dolomite, and Other Late, Vug-Filling Phases

Observations

Irregularly shaped vugs, 0.5 to 2 in (1 to 5 cm) in size are sparse in the basal limestone subunit (i.e., one or two vugs may be present over 10 to 15 ft [3 to 5 m] of core). Most vugs are filled by secondary mineralization, but others have no mineralization and remain as open cavities. The sequence of cements filling vugs also varies; for example, vugs in the Northern Natural Gas #1 Caldwell core in central Rice County (*#12*; 2-T.25S.-R.8W.) are generally filled with coarsely crystalline saddle dolomite followed by coarsely crystalline equant ferroan calcite spar, but a few vugs have ferroan calcite spar preceding the saddle dolomite.

The sequence of minerals filling a vug in the basal limestone subunit at the Derby #1 Wood core in northeastern Reno County (*#15*; depth 3894.5 ft; 36-T.22S.-R.5W.) starts with very coarsely crystalline (1-2 mm) euhedral quartz, then very coarsely crystalline (1-2 mm) saddle dolomite. Remaining porosity in the vug is mostly occluded by extremely coarse (5-10 mm) calcite spar. The vug containing the quartz occurred after dolomitization, because dolomite rhombs in the rock matrix along the side of the vug are truncated or corroded (Figure 8.56). Euhedral quartz crystals have two growth bands that contain thin acicular microcrystals (10-100 μm in length) that were identified as either gypsum or anhydrite by electron microscopic analysis (Mike Magnuson, Kansas Geological Survey, Lawrence, KS, personal communication, August, 1992). Subsequent analysis by Raman microprobe (Robert Goldstein, University of Kansas, Lawrence, KS, personal communication, March, 1993) confirmed this mineral as anhydrite. The two anhydrite-rich zones are separated and followed by thin zones of primary inclusions that are free of anhydrite (Figure 8.57). One other vug with quartz containing acicular anhydrite was discovered in the study area in the Palmer & Colorado Oil and Gas #2 Grier core (*#31*, depth 4296.6 ft) in Pratt County. Primary fluid inclusions within the growth zones generally have inconsistent vapor-to-liquid ratios, but all-liquid inclusions and inclusions containing almost all gas are still common (see T_h and $Tm_{(ice)}$ data in Table 8.5). The inclusions vary in size. All-liquid inclusions were not aligned or petrographically paired with vapor-rich inclusions, thereby indicating that they were not products of necking down or segmentation of larger inclusions after a phase change. Salinities also vary widely from zone to zone and somewhat within each zone, with the inner thin primary zone (Figure 8.58) recording nearly fresh-water values. Histograms of T_h data and a crossplot of T_h and $Tm_{(ice)}$ data (Figure 8.59) show a wide range of homogenization temperatures, with the lowest T_h being 34.9 °C

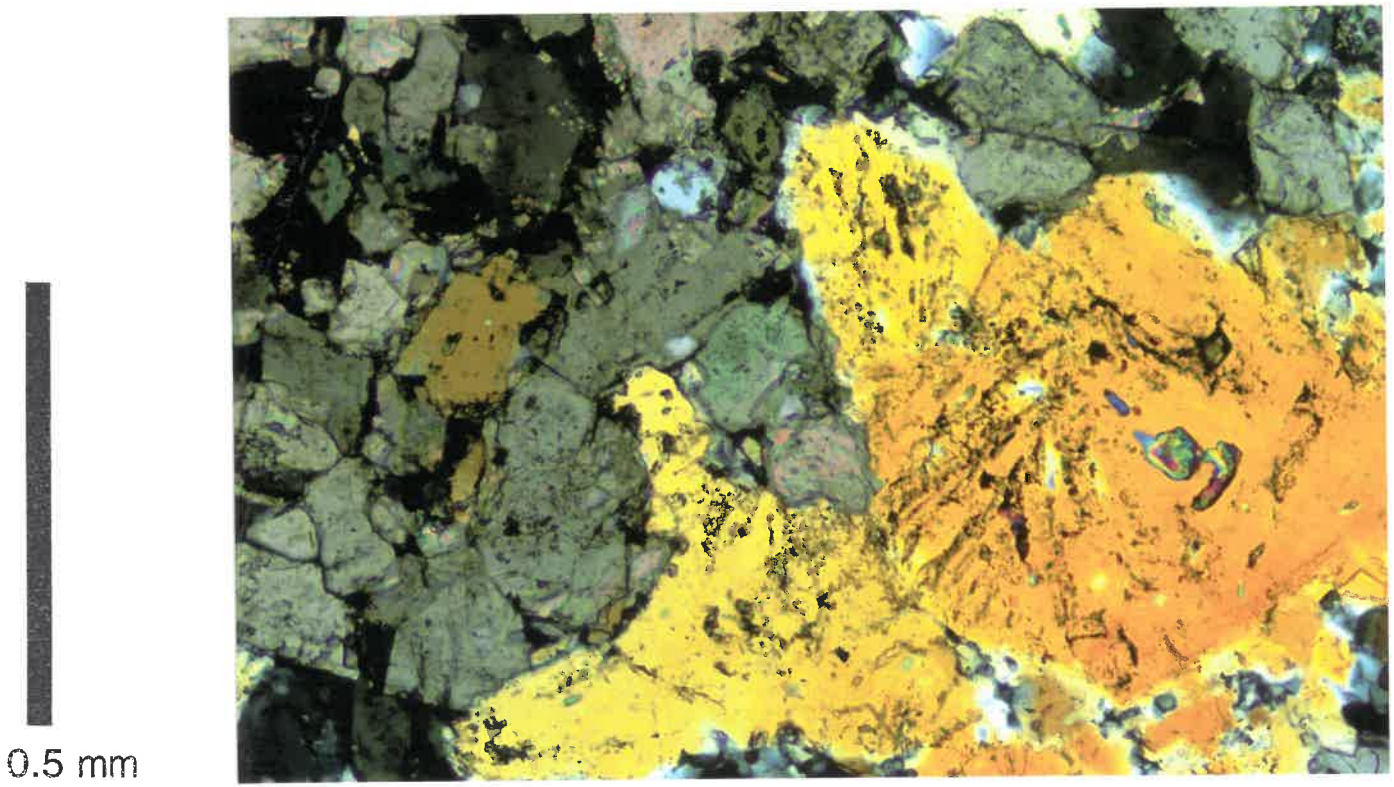

Figure 8.56 Photomicrograph of the wall of the vug from the Derby #1 Wood core (#*15*, depth 3894.5 ft, 36-T.22S.-R.5W.) in Reno County. Dolomite rhombs in the rock matrix are truncated and corroded, indicating that dolomitization occurred before vug formation. Quartz (yellow) partly filling this vug is the same generation of quartz shown in Figure 8.57.

Figure 8.57 Photomicrograph of a euhedral quartz crystal from a vug in the basal limestone subunit from the Derby #1 Wood core (*#15*, depth 3894.5 ft, 36-T.22S.-R.5W.) in Reno County. Four zones are present in this crystal, from core to edge these zones are: an inner zone containing small crystal "sprays" of anhydrite (**AN**) (i.e., "inner anhydrite-rich zone"; **A**), a thin zone of abundant primary fluid inclusions with no anhydrite (i.e., "inner thin primary zone"; **B**), an outer anhydrite-containing zone (i.e., "outer anhydrite-rich zone"; **C**), and an outer thin zone of primary inclusions without anhydrite (i.e., "outer thin primary zone"; **D**). The outer thin primary zone, unlike the concentrically-oriented inner thin primary zone, is not common present beneath all crystal faces. Fluid inclusions analyzed from quartz crystals in this vug have widely varying salinities (see text for discussion). A large saddle dolomite crystal is to the right of the quartz crystal.

Table 8.5 Fluid-inclusion data from euhedral quartz in vug-fill in the Derby #1 Wood core -- thin section D1W94.5 (*#15*; NE, 36-T.22S.-R.5W.; depth 3894.5 ft; Reno County). T_h, $Tm_{(ice)}$, T_e, and T_n are homogenization temperature, final melting temperature of ice, eutectic temperature, and nucleation temperature. L:V is liquid:vapor ratio. Fluid-inclusion assemblages (groups of genetically related inclusions) are designated by the code in the "notes" column, as to what zone they are found (see text for discussion). Uncertainty (±) in measurement of T_h and $Tm_{(ice)}$ reflects the precision achieved by the "cycling" technique (see Goldstein and Reynolds, 1994, p. 93-95, 105-109). Data in this table are displayed in Figures 8.58 and 8.59.

ASSOCIATION chip/crystal	T_h °C	$Tm_{(ice)}$ °C	T_e °C	T_n °C	L:V	NOTES*
A/1	168.5 ± 0.2	----	----	----	----	4
A/1	----	-20.5	----	~ -77	----	4
A/1	----	-21.9	----	----	----	4
A/1	38.3 ± 0.1	----	----	----	----	3
A/1	----	-9.8	----	----	----	3, secondary
A/1	----	-11.6	----	~ -55	----	3
A/1	----	-17.8	----	----	----	3, secondary
B/1	52.7	-22.1	~ -46	~ -65	12:1	3
B/1	45.0 ± 0.1	-20.4	~ -46	~ -85	20:1	3, secondary
B/1	----	-20.3	----	----	20:1	3, secondary
B/1	60.4 ± 0.2	----	----	----	----	3
B/1	84.3 ± 0.4	----	----	----	----	3
B/1	107.7 ± 0.2	----	----	----	----	3, secondary
B/1	74.9 ± 0.1	----	----	----	----	3
B/1	75.9 ± 0.1	----	----	----	----	3
B/1	34.9	----	----	----	50:1	3
B/1	----	-19.0	----	~ -69	9:1	4
B/1	----	-7.5	----	----	----	3, secondary
B/1	----	-16.0	----	~ -47	----	3
B/1	----	-12.1	----	----	----	3, secondary
B/1	----	-9.9	----	~ -54	----	3
B'/1	115.7	-12.0	----	----	18:1	3, secondary
B'/1	47.7	----	----	----	25:1	3, secondary
B'/1	85.6	-12.7	----	----	20:1	4
C/1	52.8	-20.7	~ -53	~ -64	16:1	3
C/1	60.8	----	----	----	----	3, secondary
C/1	89.4	----	----	----	----	3, secondary
C/1	55.5	----	~ -47	~ -75	25:1	1, secondary
C/1	----	-18.8	----	~ -71	----	1, secondary
C/1	----	-20.5	----	~ -71	----	1
C/1	71.0	----	----	----	15:1	1
C/1	----	-21.4	----	~ -58	16:1	1, secondary
C/1	72.6	-21.7	----	~ -75	25:1	1, secondary
C/1	53.0 ± 0.5	----	----	~ -73	16:1	1, secondary
C/1	79.9 ± 0.5	----	----	----	12:1	1, secondary
C/1	35.5 ± 0.5	-20.5	----	~ -78	30:1	1
C/1	68.8	----	----	----	12:1	1, secondary
C/1	90.3	-21.9	~ -43	~ -75	20:1	1
C/1	----	----	----	~ -67	liq.	1
C/1	77.8	----	----	~ -69	20:1	1
C/1	89.9	----	----	~ -73	20:1	1
C/1	92.5 ± 0.5	-20.3	~ -48	~ -62	15:1	1, secondary
C/1	90.0 ± 0.5	-15.1	~ -47	----	4:1	1
C/1	68.3	----	~ -46	----	25:1	2
C/1	----	-0.3	----	----	20:1	2
C/1	----	-2.0	~ -44	----	20:1	2
D/1	38.7	-22.0	~ -44	~ -64	50:1	3, secondary
D/1	----	-22.6	----	~ -54	liq.	3, secondary
D/1	----	-15.5	----	~ -55	liq.	3, secondary
D/1	----	----	----	~ -48	liq.	3

Table 8.5 (continued) Fluid-inclusion data euhedral quartz in vug-fill.

ASSOCIATION chip/crystal	T_h °C	$Tm_{(ice)}$ °C	T_e °C	T_n °C	L:V	NOTES*
D/1	39.1 ± 0.5	----	----	----	35:1	3
D/1	107.0 ± 0.2	----	----	----	10:1	3
D/1	73.0 ± 1.0	----	----	----	25:1	3
D/1	46.5 ± 0.7	----	----	~ -59	30:1	3, secondary
D/1	68.1	----	----	----	20:1	3
D/1	41.4	----	----	----	30:1	3, secondary
D/1	67.5	----	----	----	20:1	3
D/1	74.4	-19.5	----	~ -76	15:1	4
D/1	----	-18.8	----	~ -69	liq.	4
D/1	44.6	-23.4	----	~ -57	33:1	4
D/1	42.9	----	----	~ -76	25:1	4
D/1	45.5 ± 0.3	----	----	~ -67	10:1	4
D/1	----	-19.3	----	~ -70	liq.	4
E/1	95.5	-21.9	~ -44	~ -86	8:1	3
E/1	79.0 ± 0.5	-17.0	~ -39	~ -74	9:1	3
E/1	----	-17.7	~ -43	~ -67	liq.	1
E/1	121.6	-1.7	----	~ -34	10:1	2
E/1	60.9	-17.6	~ -48	~ -64	18:1	3
E/1	40.1	----	----	~ -49	35:1	3, secondary
E/1	----	-14.7	----	~ -37	liq.	3
E/1	----	-10.9	~ -33	~ -49	liq.	3, secondary
E/1	----	-0.9	----	----	----	2
E/1	----	-17.6	----	~ -60	----	4
F/1	94.1 ± 0.5	-12.3	----	~ -49	12:1	1, secondary
F/1	97.1 ± 0.5	-14.5	~ -47	~ -49	18:1	1, secondary
F/1	107.5 ± 0.2	----	----	----	10:1	1, secondary
F/1	109.6 ± 0.3	----	----	~ -39	6:1	1, secondary
F/1	58.9	-21.8	~ -45	~ -64	25:1	1
F/1	----	-0.7	----	~ -32	7:1	1, secomdary
F/1	80.4	-9.1	----	~ -50	17:1	1, secondary
F/1	65.2	-21.3	~ -48	~ -66	40:1	1
F/1	42.2 ± 0.2	-11.7	~ -35	~ -48	35:1	1, secondary
F/1	----	-0.1	----	~ -44	----	1, secondary
F/1	59.4	----	----	----	25:1	1
F/1	70.2	----	----	----	10:1	3
F/1	88.4 ± 0.3	----	----	----	10:1	3
F/1	94.7 ± 0.3	----	----	----	10:1	3, secondary
F/1	97.7 ± 0.1	----	----	----	15:1	3
F/1	108.9 ± 0.1	-7.7	~ -32	~ -52	12:1	3
F/1	----	-14.0	----	----	3:1	3
F/1	50.3 ± 0.2	-14.5	~ -35	~ -70	20:1	3

*1 = inner anhydrite-rich zone; 2 = inner, thin primary zone; 3 = outer anhydrite-rich zone; 4 = outer, thin primary zone. Fluid inclusions are primary unless noted otherwise.

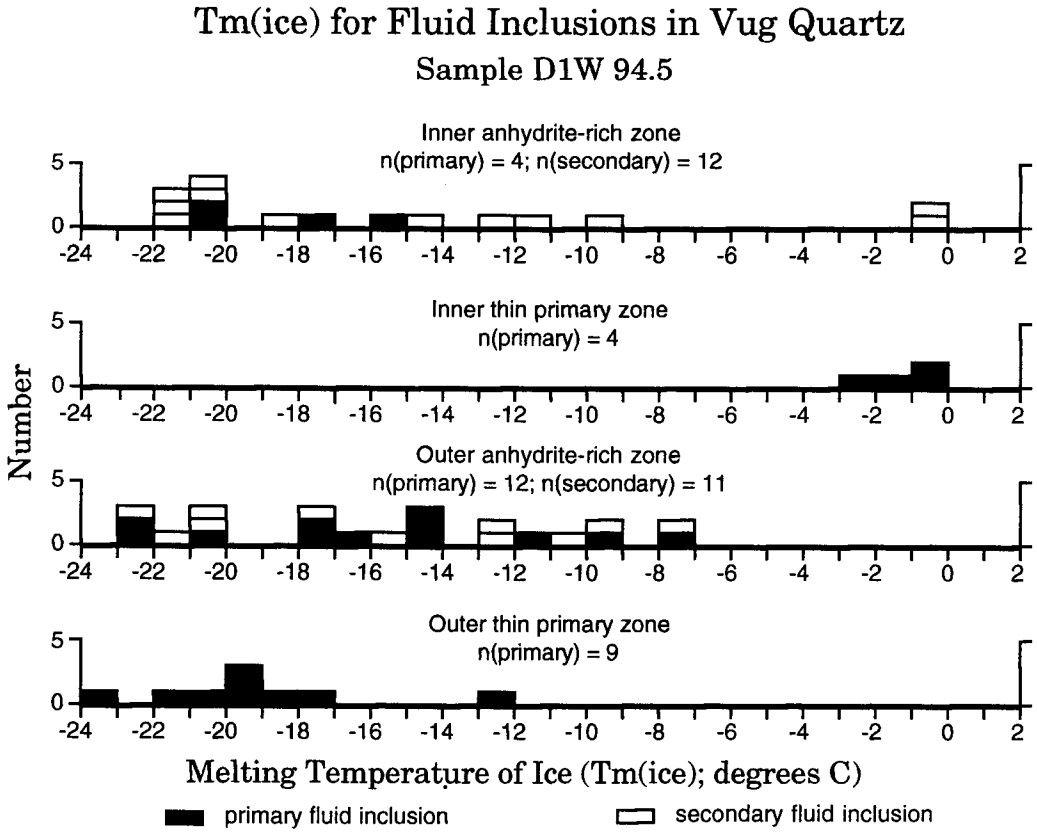

Figure 8.58 Histograms of $Tm_{(ice)}$ data for fluid inclusions in vug quartz from the Derby #1 Wood core (*#15*, depth 3894.5 ft, 36-T.22S.-R.5W.) in Reno County. A wide range of salinities is indicated, with some fluid inclusions in the "inner thin primary zone" being relatively fresh (near 0 °C) and to 23 wt. % NaCl equivalent (~ -21 °C). These varying salinities are indicative that the Viola was subject to fluxes of both hypersaline and nearly-fresh water, with implied shallow burial. See Table 8.5 for a listing of this data.

in the outer anhydrite-rich zone. A rough negative correlation of primary-inclusion T_h with $Tm_{(ice)}$ (i.e., higher T_h with lower $Tm_{(ice)}$) is evident (Figure 8.59). Microthermometry of fluid inclusions in saddle dolomite from this same vug are discussed below in a comparison to saddle dolomites from other localities in the study area.

Crushing the euhedral quartz crystals from the vug in the Derby #1 Wood core (Table 8.6; Figure 8.60) yields fluid inclusions exhibiting two types of behaviors --

Figure 8.59 Histograms of homogenization temperatures, and a crossplot of T_h and $Tm_{(ice)}$ data for the euhedral quartz from a vug in the Derby #1 Wood core (*#15*, depth 3894.5 ft, 36-T.22S.-R.5W.) in Reno County. The wide range of homogenization temperatures is indicative of heterogeneous entrapment. See Table 8.5 for a listing of this data. See text for discussion.

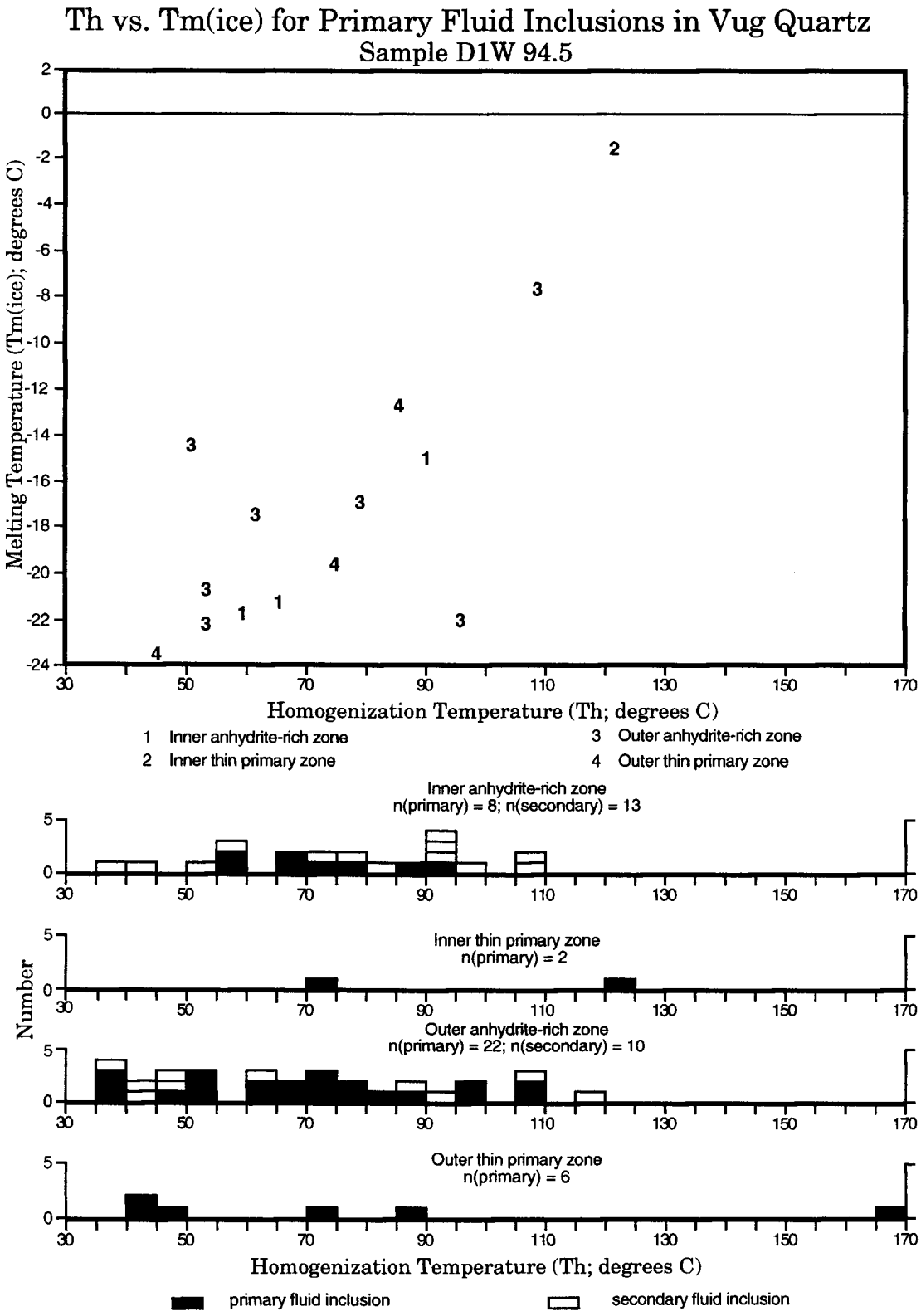
Th vs. Tm(ice) for Primary Fluid Inclusions in Vug Quartz
Sample D1W 94.5
Melting Temperature (Tm(ice); degrees C)
Homogenization Temperature (Th; degrees C)
1 Inner anhydrite-rich zone
2 Inner thin primary zone
3 Outer anhydrite-rich zone
4 Outer thin primary zone
Inner anhydrite-rich zone
n(primary) = 8; n(secondary) = 13
Inner thin primary zone
n(primary) = 2
Outer anhydrite-rich zone
n(primary) = 22; n(secondary) = 10
Outer thin primary zone
n(primary) = 6
Number
Homogenization Temperature (Th; degrees C)
primary fluid inclusion
secondary fluid inclusion

Table 8.6 Paleobarometry of fluid inclusions in euhedral quartz from a vug in the Derby #1 Wood core -- thin section D1W94.5 (*#15*; NE, 36-T.22S.-R.5W.; depth 3894.5 ft; Reno County). Uncertainty (±) in pressure and depth calculations are based on a plausible measurement error of 0.5 mm on the video screen (equivalent to 2.2 μm) for the size of the bubble both before and after the crushing run. This measurement error generally increases for the smaller bubbles, and is a function of the size of the bubble before and after crushing, and the shape of the bubble. The calculated hydrostatic depth based on saline water assumes a density of water of 1.19 grams per CC, equivalent to 23 wt. % NaCl. See text for discussion. Data in this table are displayed in Figure 8.60.

RUN #	INCLUSION VOLUME (μm^3) before crush	after crush	change in volume	CALCULATED PRESSURE (atm.)	HYDROSTATIC DEPTH (meters) fresh	saline	NOTES
chip 1	542.7	3,973.5	3,430.8	7.3 ± 0.9	67 ± 9	57 ± 8	
chip 2	150.5	224.1	73.6	1.5 ± 0.2	5 ± 3	4 ± 3	
chip 2	89.9	237.5	147.5	2.6 ± 0.6	17 ± 6	15 ± 5	
chip 2	75.6	236.0	160.5	3.1 ± 0.7	23 ± 7	19 ± 4	
chip 2	1,105.5	332.4	-773.1	0.3 ± 0.0	-7 ± 0	-6 ± 0	bubble shrinks
chip 2	1,040.5	322.3	-718.2	0.3 ± 0.0	-7 ± 0	-6 ± 0	bubble shrinks
chip 3	32.5	232.0	199.5	7.1 ± 2.1	65 ± 22	56 ± 19	
chip 4	190.7	462.4	271.8	2.4 ± 0.5	15 ± 5	13 ± 4	
chip 4	200.7	59.4	-141.3	0.3 ± 0.1	-7 ± 1	-6 ± 1	bubble shrinks
chip 4	474.9	305.9	-169.0	0.6 ± 0.0	-4 ± 1	-3 ± 1	bubble shrinks
chip 5	5.6	22.8	17.3	4.1 ± 2.6	33 ± 27	28 ± 25	
chip 5	182.7	1,204.3	1,021.6	6.6 ± 1.0	59 ± 11	51 ± 9	
chip 5	9.6	1.2	-8.4	0.1 ± 0.0	-9 ± 1	-8 ± 1	bubble shrinks
chip 6	32.5	356.8	324.3	11.0 ± 3.0	106 ± 32	90 ± 28	break not directly observed
chip 6	7.8	31.4	23.6	4.0 ± 2.3	32 ± 24	27 ± 21	
chip 6	257.8	338.1	80.3	1.3 ± 0.2	3 ± 3	3 ± 2	
chip 7	128.1	170.6	42.5	1.3 ± 0.3	4 ± 3	3 ± 3	measurement difficult
chip 9	874.4	1,293.8	419.4	1.5 ± 0.1	5 ± 2	4 ± 2	
chip 9	411.1	877.9	466.9	2.1 ± 0.3	12 ± 3	10 ± 3	
chip 9	19,268.2	28,953.6	9,685.5	1.5 ± 0.1	5 ± 1	5 ± 1	
chip 11	303.5	535.2	231.8	1.8 ± 0.3	8 ± 2	7 ± 2	
chip 12	93.7	305.9	212.3	3.3 ± 0.5	24 ± 6	21 ± 6	
chip 12	1,187.5	474.9	-712.6	0.4 ± 0.1	-6 ± 0	-5 ± 0	bubble shrinks
chip 12	65.0	9.6	-55.4	0.1 ± 0.0	-9 ± 1	-8 ± 0	bubble shrinks
chip 12	32.5	9.6	-22.9	0.3 ± 0.1	-7 ± 2	-6 ± 1	bubble shrinks
chip 14	42.8	1.2	-41.6	0.0 ± 0.0	-10 ± 0	-9 ± 0	bubble shrinks
chip 14	19.7	9.6	-10.0	0.5 ± 0.2	-5 ± 2	-5 ± 1	bubble shrinks

Table 8.6 (continued) Paleobarometry of fluid inclusions in euhedral quartz from a vug in the Derby #1 Wood core.

RUN #	INCLUSION VOLUME (μm^3) before crush	after crush	change in volume	CALCULATED PRESSURE (atm.)	HYDROSTATIC DEPTH (meters) fresh	saline	NOTES
chip 14	474.9	979.1	504.2	2.1 ± 0.2	11 ± 3	10 ± 2	
chip 15	8.9	24.1	15.2	2.7 ± 2.6	18 ± 17	15 ± 15	
chip 15	20.9	2.9	-18.0	0.1 ± 0.0	-9 ± 1	-8 ± 0	bubble shrinks
chip 16	2.9	32.5	29.7	11.4 ± 8.6	110 ± 92	94 ± 78	

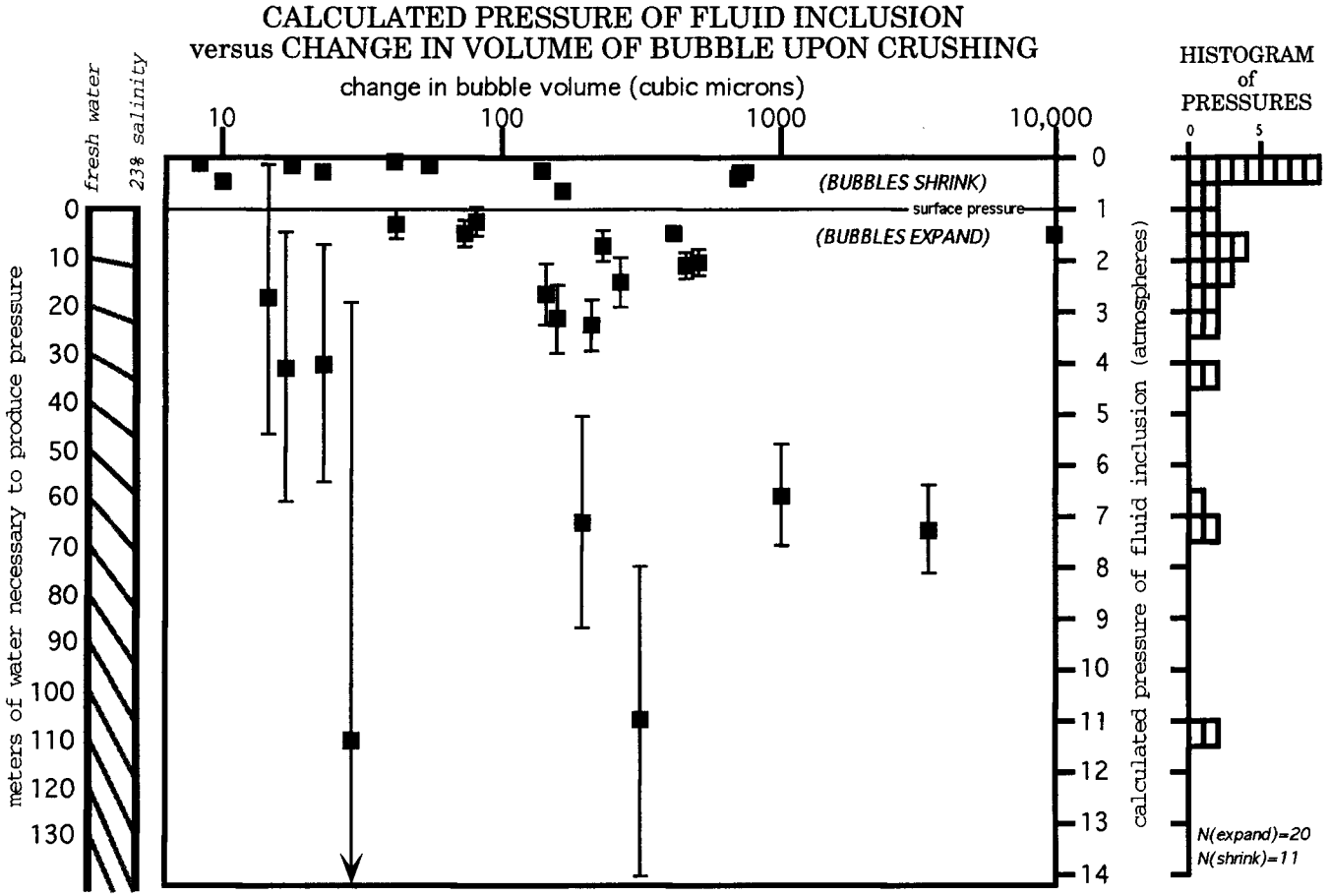

Figure 8.60 Bivariate plot showing paleobarometric determinations versus change in volume from fluid inclusions from the euhedral quartz in a vug in the Derby #1 Wood core (*#15*, depth 3894.5 ft, 36-T.22S.-R.5W.) in Reno County. Error bars on each symbol are explained in Table 8.6. See Table 8.6 for a listing of this data. See text for discussion.

a group of inclusions with bubbles that shrink once the inclusion is open to atmospheric pressure and another group in which the bubbles expand. Bubbles that shrink are under less-than-atmospheric pressure. Petrographically these are elongate inclusions aligned along deformation lamellae, characteristics suggesting a secondary origin. The pressures obtained from the bubbles that expand range from 1.3 to 11.4 atmospheres (atm), with a dominant mode at 1.5 to 2.0 atm and a minor mode at 6.5 to 7.0 atm. The calculated thicknesses of water columns necessary to account for these pressures depend on the density of the water enclosing the bubble as the inclusion was formed, assuming that the bubble was entrapped under hydrostatic conditions. Salinities obtained for fluid inclusions in the quartz (Table 8.5) range from nearly fresh water (density = 1.00 grams/cc) to 23 wt. % NaCl equivalent (density = 1.19 grams/cc), therefore these two extremes were used in calculating the thickness of the water columns. The resultant water columns (Table 8.6) are all less than 110 m. The bubbles within quartz grains crushed when immersed in kerosene dissolved within seconds, indicating the fluid inclusions contain methane or other organic gases (see Roedder, 1984, p. 218).

Vugs in the lower and upper cherty dolomite are similar in size to those in the basal limestone subunit. Some smaller vugs are recognizable as solution-enlarged molds after fossil fragments (see Figure 7.13), but nearly all the larger ones have no recognizable precursor. The sequence of mineralization within the vugs varies, but coarsely crystalline saddle dolomite followed by coarsely crystalline, equant calcite spar is a common motif. Sphalerite is present in a vug along a stylolite in the Shell #6 Decker (*#6*) core in eastern McPherson County (11-T.19S.-R.2W.). This sphalerite is medium crystalline (250 μm) and precipitated in the vug subsequent to quartz and saddle dolomite. The sphalerite is volumetrically insignificant, less than 1% of the vug fill, and contains no primary fluid inclusions.

Saddle dolomite fills other porosity such as fracture, moldic, and intercrystalline porosity, and is present in trace amounts in most thin sections. It also replaces, crosscuts depositional and earlier diagenetic features, including the late ferroan spar (Figure 8.18). It is generally coarsely to very coarsely crystalline, has a sweeping or undulatory extinction pattern, and curved crystal faces and cleavage. It is mostly ferroan; differences in staining with potassium ferricyanide define compositional growth bands. Saddle dolomite in the Viola does not luminesce, probably because of its iron content.

Saddle dolomite contains abundant fluid inclusions that are varyingly concentrated in zones parallel to crystal faces. These zones define growth bands that contain primary fluid inclusions (see Goldstein and Reynolds, 1994, p. 14-15). All fluid inclusions observed in the saddle dolomites are two-phase, with very consistent liquid-to-vapor ratios, despite differences in sizes of the inclusions.

T_h and $Tm_{(ice)}$ measurements (Table 8.7) were taken for primary fluid inclusions from saddle dolomite in three widely separated cores in central Kansas (e.g., Damac #1 Sandra Allen (*#2*) in northern McPherson County (Figure 8.61), Derby #1 Wood (*#15*) in northern Reno County (Figure 8.62), and Midcontinent Marine #1 South Hilger (*#29*) in southern Reno County (Figure 8.63). The data from the Derby #1 Wood core are from the same vug that holds the euhedral quartz discussed earlier; the saddle dolomite was precipitated following the quartz. Inasmuch as the T_hs are not corrected for pressure, they represent minimum entrapment temperatures (Goldstein and Reynolds, 1994, p. 27).

The fluid inclusions that were measured were classified according to their fluid-inclusion assemblages, defined in this case as a group of closely associated inclusions along a growth band. All inclusions observed in the saddle dolomites are two-phase, with very consistent liquid-to-vapor ratios. A variety of sizes of fluid

Table 8.7 Fluid-inclusion data from saddle dolomites -- thin section DSA3438.1, from Damac #1 Sandra Allen (*#2*; SW, 7-T.17S.-R.3W.; depth 3438.1 ft; McPherson County); thin section D1W94.5, from Derby #1 Wood (*#15*, NE, 36-T.22S.-R.5W.; depth 3894.5 ft; Reno County); and thin section 1SH4029.5 from Midcontinent Marine #1 South Hilger (*#29*, W2 SW SW, 9-T.26S.-R.4W.; depth 4029.5 ft; Reno County. $Tm_{(ice)}$, T_e, and T_n are final melting temperature of ice, eutectic temperature, and nucleation temperature. Fluid-inclusions are cataloged under the "association" column, in which each inclusion is identified with chip/view/crystal/assemblage. "Chip" identifies the chip cut from the thin section; "view" is the arbitrary location within that chip (usually a field of view through the microscope); "crystal" identifies the crystal holding the inclusion; "assemblage" identifies the fluid-inclusion assemblage (groups of genetically related inclusions in close proximity to each other). If an inclusion is isolated, the assemblage category will be blank. Even though the crystal number may be similar with two or more inclusions, if the chip and/or view designation is different, then the crystals are different. Uncertainty (±) in measurement of T_h and $Tm_{(ice)}$ reflects the precision achieved by the "cycling" technique (see Goldstein and Reynolds, 1994, p. 93-95, 105-109). Data from this table are displayed in Figures 6.13, 8.61, 8.62, and 8.63.

ASSOCIATION chip/view/ crystal/asmblg.	T_h °C	$Tm_{(ice)}$ °C	T_e °C	T_n °C	NOTES*
thin section DSA3438.1, from Damac #1 Sandra Allen					
1/A/1/	119.0	-17.2	----	~ -75	
1/A/1/a	120.0 ± 0.2	----	----	~ -66	
1/A/1/a	----	-18.2	----	----	
1/A/1/a	----	-15.4	----	~ -74	
1/B/1/b	119.4 ± 0.2	----	----	----	
1/B/1/b	117.0	-16.9	----	~ -80	
1/B/1/	104.9 ± 0.1	-7.7	----	----	secondary
1/B/1/	108.2 ± 0.1	----	----	----	
1/B/1/	117.2 ± 0.1	-2.0	----	~ -47	secondary
1/B/2/	108.8	----	----	----	secondary
1/B/3/	120.2 ± 0.1	-15.4	----	~ -79	
1/C/1/c	98.2 ± 0.2	-18.7	----	~ -82	
1/C/1/c	108.9 ± 0.1	-17.6	----	~ -84	
1/C/2/	----	-17.8	----	----	
1/C/3/	----	-18.3	----	~ -90	
1/C/4/d	139.0 ± 0.4	-16.0	----	----	secondary?
1/C/4/d	----	-18.2	----	~ -79	
1/C/4/d	----	-17.0	----	~ -73	
1/C/4/e	----	-18.4	----	----	
1/C/4/e	----	-18.9	----	----	
1/C/4/	97.5 ± 0.1	----	----	----	
thin section D1W94.5, from Derby #1 Wood					
1/A/1/a	111.4	----	----	----	secondary
1/A/1/a	129.2	----	----	----	secondary
1/A/1/	95.6	----	----	----	
1/A/1/b	109.1	----	----	----	
1/A/1/b	107.6	----	----	----	
1/A/1/b	95.6	----	----	----	
1/A/1/b	97.9	----	----	----	
1/B/1/c	----	-22.4	----	----	
1/B/1/c	109.7	-22.2	----	----	
1/B/1/c	87.9	----	----	----	
1/B/1/c	111.0	----	----	----	
1/B/1/	94.1	----	----	----	secondary
1/B/1/	----	-22.5	----	----	
1/B/1/	----	-22.8	----	----	

Table 8.7 (continued) Fluid-inclusion data from saddle dolomites.

ASSOCIATION chip/view crystal/asmblg.	T_h °C	$Tm_{(ice)}$ °C	T_e °C	T_n °C	NOTES*
thin section D1W94.5, from Derby #1 Wood					
1/B/1/	102.5	----	----	----	secondary
1/B/1/	90.3	----	----	----	
1/B/1/	76.9	----	----	----	secondary
1/B/1/	106.2	----	----	----	
1/B/1/	122.9	----	----	----	secondary
1/B/1/	156.3 ± 3.8	-20.0	----	----	secondary
1/B/1/d	92.1	-22.2	~ -42	----	
1/B/1/d	92.1	----	----	----	
1/B/1/	----	-21.8	~ -42	----	secondary
1/B/2/	173.4 ± 0.1	-21.9	----	----	sec., leaked(?)
2/A/1/e	126.6	-22.1	----	----	
2/A/1/e	116.7	-22.5	----	----	
2/B/1/f	110.1	----	----	----	
2/B/1/f	94.8	----	----	----	
3/BD4/1/	102.7	----	----	----	secondary
3/BD4/1/g	113.7	----	----	----	
3/BD4/1/g	125.6	-22.1	----	----	
3/BD4/1/g	113.9	-22.4	----	----	
3/BD4/1/g	110.8	----	----	----	
3/BD4/1/	114.4	----	----	----	secondary
3/BD4/1/	----	-22.6	----	----	
3/BD4/1/	----	-21.6	----	----	
3/BD5/1/	119.7	-22.8	----	----	secondary
3/BD5/1/h	79.4	-22.6	~ -42	----	secondary
3/BD5/1/h	79.4	----	----	----	secondary
3/BD5/1/i	88.0	----	----	----	
3/BD5/1/i	----	-23.6	----	----	
3/BD5/1/i	----	-22.5	----	----	
4/A/1/	----	-22.0	----	----	
thin section 1SH4029.5 from Midcontinent Marine #1 South Hilger					
1/A/1/a	127.8 ± 0.2	-22.2	----	~ -88	
1/A/1/a	118.3 ± 0.1	-21.5	----	~ -84	
1/A/1/a	118.1	----	----	~ -69	
1/A/1/a	118.0 ± 0.1	----	----	~ -81	
1/A/1/a	119.4	----	----	----	
1/A/1/	118.9	----	----	----	secondary
1/A/1/	152.5	-21.5	----	~ -61	secondary
1/A/1/b	119.7 ± 0.1	-21.5	----	~ -75	
1/A/1/b	104.5 ± 0.1	----	----	----	
1/A/1/b	113.4 ± 0.1	----	----	----	
1/A/1/b	106.2 ± 0.1	----	----	----	
1/A/1/b	133.9 ± 0.1	-21.5	----	----	
1/A/1/c	106.1 ± 0.3	----	----	----	
1/A/1/c	109.9	----	----	----	
1/A/1/c	119.9	----	----	----	
1/A/1/	129.1 ± 0.1	-21.7	----	----	
1/A/1/	128.5 ± 0.1	-21.9	----	~ -84	
1/A/2/d	117.5	-21.6	~ -35	~ -89	
1/A/2/d	118.1	-21.5	----	~ -84	
1/A/2/	113.9	-21.4	~ -34	~ -79	
1/A/2/e	129.2 ± 0.2	-21.8	----	~ -80	secondary
1/A/2/e	130.1	-21.8	----	~ -81	secondary?
1/B/1/	127.9	----	----	----	secondary?
1/B/1/f	111.6	-21.1	----	~ -88	
1/B/1/f	118.1	-22.2	----	~ -60	
1/B/1/f	107.5 ± 0.1	-22.2	----	~ -89	
1/B/1/f	113.6 ± 0.1	-22.0	----	~ -82	
1/B/1/f	112.4	-21.4	----	~ -87	

Table 8.7 (continued) Fluid-inclusion data from saddle dolomites.

ASSOCIATION chip/view crystal/asmblg.	T_h °C	$Tm_{(ice)}$ °C	T_e °C	T_n °C	NOTES*
thin section 1SH4029.5 from Midcontinent Marine #1 South Hilger (continued)					
1/B/1/f	109.6	----	----	----	
1/B/1/f	110.7	-21.7	----	~ -86	
1/B/1/	127.6 ± 0.1	-21.4	~ -32	~ -87	
1/B/1/	125.8	-21.4	----	~ -86	
1/B/1/	120.6	-21.3	----	~ -69	
1/B/1/	128.0 ± 0.1	-21.3	----	~ -86	

*fluid inclusions are primary unless noted otherwise

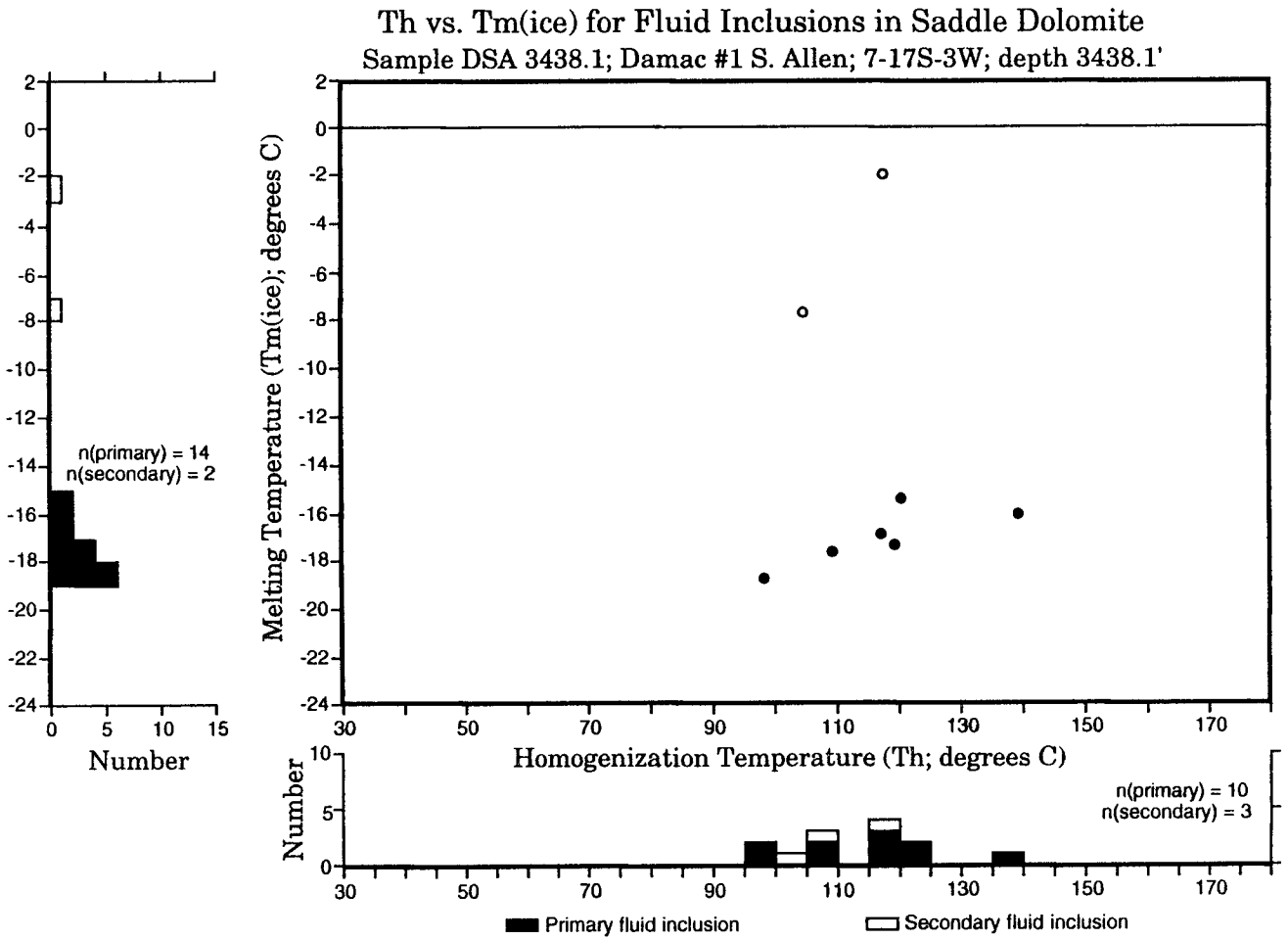

Figure 8.61 Crossplot and histograms of T_h and $Tm_{(ice)}$ measurements for saddle dolomite in moldic porosity from the lower cherty dolomitic limestone subunit at the Damac #1 Sandra Allen core (#2, depth 3438.1 ft, 7-T.17S.-R.3W.) in northern McPherson County. See Table 8.7 for a listing of this data.

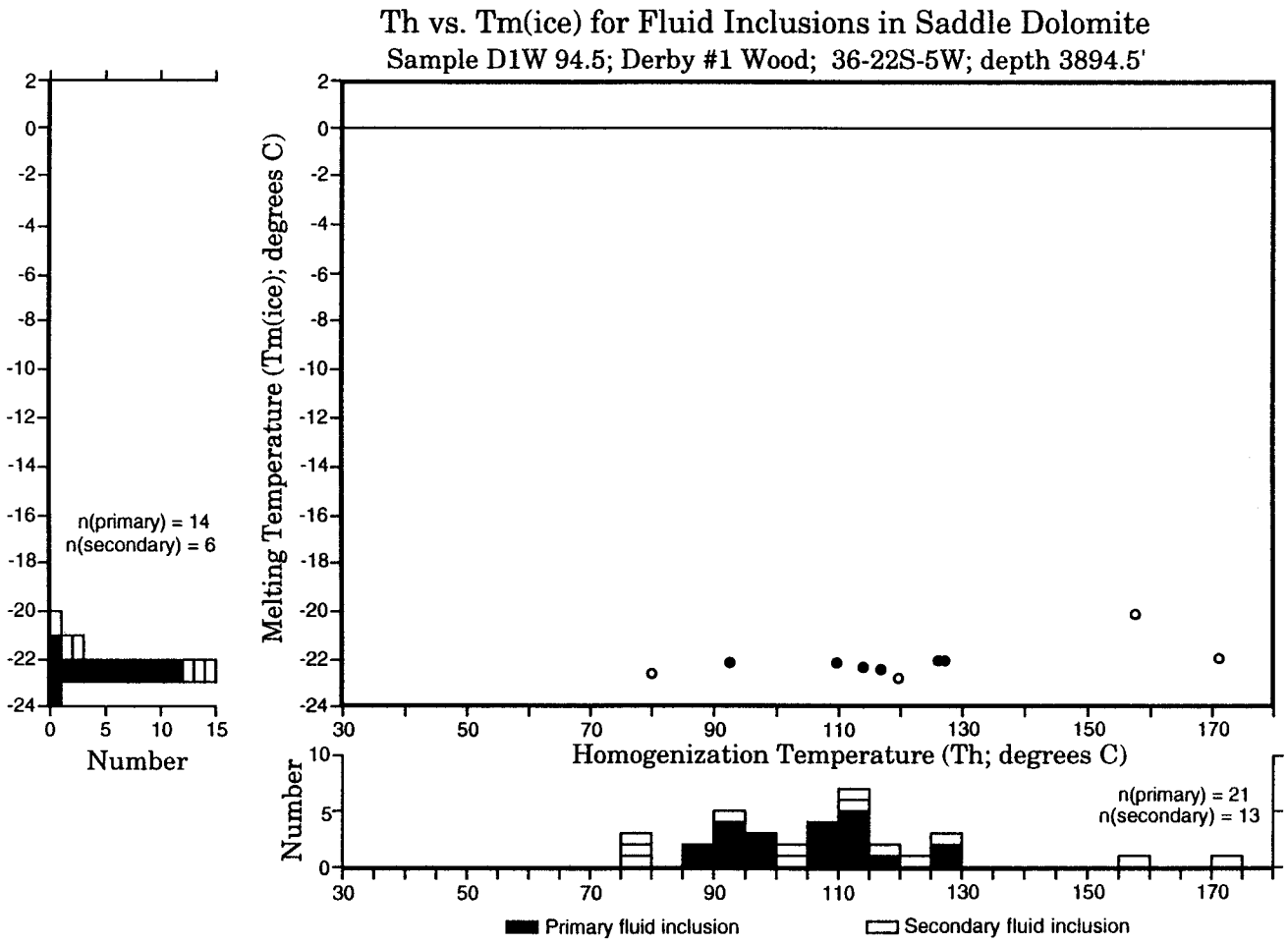

Figure 8.62 Crossplot and histograms of T_h and $Tm_{(ice)}$ measurements for saddle dolomite in vuggy porosity from the basal limestone subunit at the Derby #1 Wood core (*#15*, depth 3894.5 ft, 36-T.22S.-R.5W.) in northern Reno County. See Table 8.7 for a listing of this data.

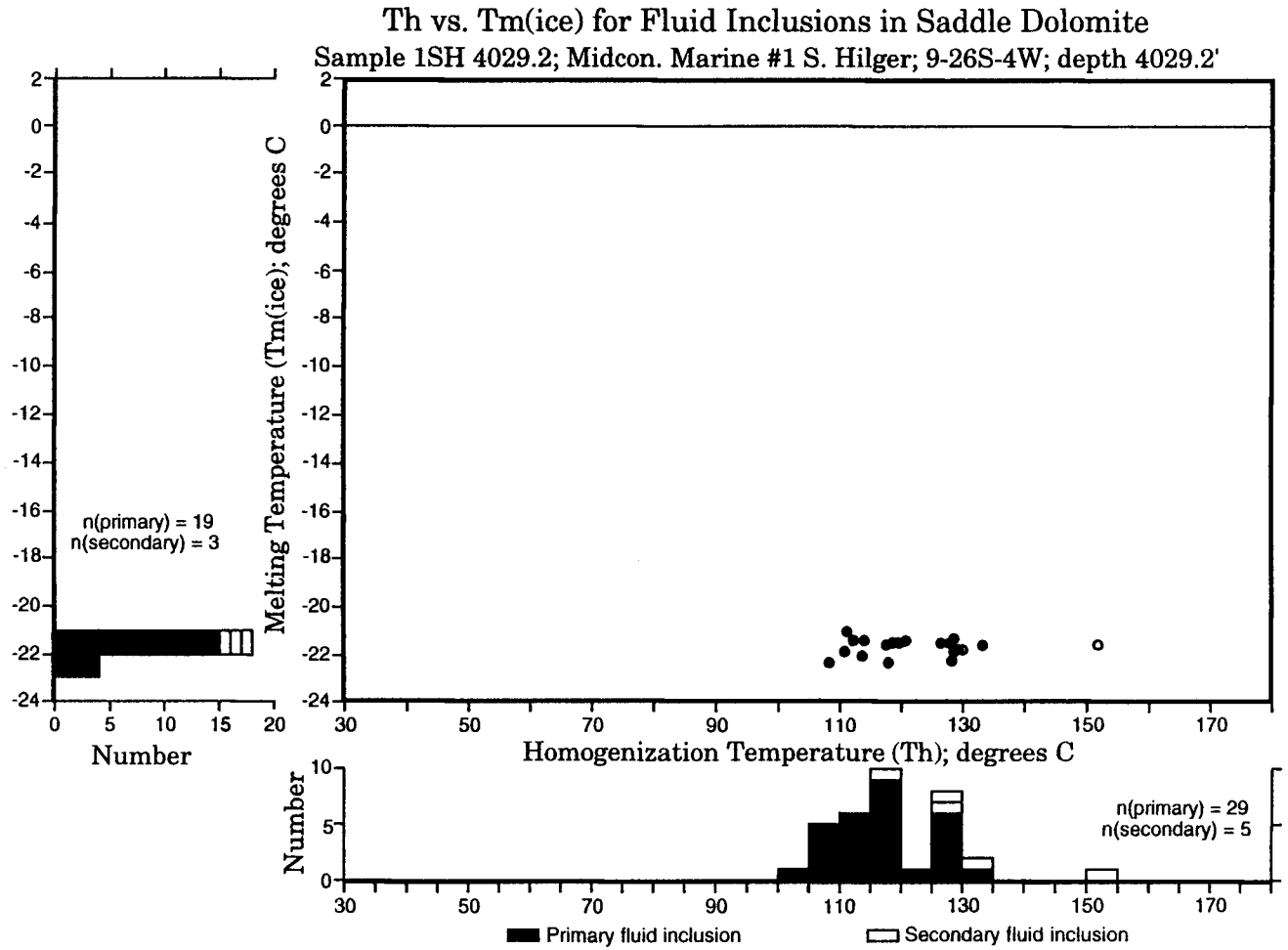

Figure 8.63 Crossplot and histograms of T_h and $Tm_{(ice)}$ measurements for saddle dolomite in vuggy porosity from the basal limestone subunit at the Midcontinent Marine #1 South Hilger core (*#29*, depth 4029 ft, 9-T.26S.-R.4W.) in southeastern Reno County. See Table 8.7 for a listing of this data.

inclusions are also present. T_h values obtained from these inclusions (Figure 6.13) are discussed in Chapter 6 in the section titled "Comparison of TTI Modeling to Fluid-Inclusion Homogenization Temperatures". The ranges in T_hs for individual fluid-inclusion assemblages generally are smaller than the range defined by all the fluid-inclusion assemblages measured at a given locality (Figure 6.13, Table 8.7; see discussion in Chapter 6). The $Tm_{(ice)}$ measurements for two of the Viola samples have relatively narrow ranges of approximately 2 °C), but the northernmost sample (Damac #1 Sandra Allen, [*#2*]) has a broader $Tm_{(ice)}$ range of 3.5 °C (see Table 8.7) and also records the least saline fluid inclusions of all the samples analyzed. Salinities average -17.5 °C (20.6 wt. % NaCl equivalent) for the #1 Sandra Allen sample, -21.6 °C (23.4 wt. % NaCl equivalent) for the Derby #1 Wood sample (*#15*), and -22.3 °C (23.9 wt. % NaCl equivalent) for the #1 South Hilger sample (*#29*) (Figure 6.13).

A weak covariance of T_h and $Tm_{(ice)}$ for the Damac #1 Sandra Allen (*#2*) sample (Figure 8.61) and a broad range of $Tm_{(ice)}$ values recorded by this single fluid-inclusion assemblage (see Figure 6.13) suggests that some leakage and refilling of its inclusions may have occurred. One fluid-inclusion assemblage from this sample (assemblage 1/A/1/; see Table 8.7) records $Tm_{(ice)}$ values that vary by 2.8 °C, as compared to the range of 3.5 °C for $Tm_{(ice)}$ in the entire sample. Insufficient data are available on the T_h range of this particular fluid-inclusion assemblage to corroborate that this assemblage has been affected by leakage and refilling (see Figure 6.13), so evidence for leakage and reequilibration is equivocal. Significant leakage and refilling, or reequilibration of fluid inclusions is not indicated for the other two samples because their fluid-inclusion assemblages have relatively narrow ranges of $Tm_{(ice)}$ and T_h (commonly <20 °C). If approximately 90% of the fluid inclusions in a given assemblage have T_hs within a temperature range of 10 to 15 °C, then that assemblage was probably derived from a single thermal event (Goldstein and

Reynolds, 1994, p. 127). The fluid-inclusion assemblages in the saddle dolomites fit this rule, therefore their T_hs represent the minimum temperatures at which the saddle dolomite precipitated.

Eutectic temperatures (T_e) for fluid inclusions in the saddle dolomite range from -32 to -42 °C (Table 8.7). Ideally, T_e reflects the composition of the fluid inclusion, but the presence of metastable phases, extra chemical species, and difficult observing conditions (i.e., small size of the inclusion, bad optics) cause imprecision (Goldstein and Reynolds, 1994, p. 98-99). Notwithstanding these difficulties, the T_e range corresponds to stable and metastable products observed with the $NaCl$-$MgCl_2$-H_2O system (see Goldstein and Reynolds, 1994, p. 99). This particular chemical system is unlikely for saddle dolomites inasmuch as prior studies in this region (Wojcik and others, 1992, 1994) indicate $NaCl$-$CaCl_2$-H_2O chemical systems are dominant. The T_e range as it currently stands is not particularly diagnostic, therefore confirmation of this chemical system will require more detailed analytical methods.

The Sr isotopes of one saddle dolomite (D1W94.5) registered a ratio of 0.709033 (Table 8.3). This and another saddle dolomite, both obtained from the basal limestone subunit, have markedly negative $\delta^{18}O$ values (-6.67 and -5.79 ‰ PDB) relative to other Viola dolomites (Figure 8.45).

Interpretations

Some vugs in the Viola are filled by secondary minerals; others remain as open cavities. This may indicate more than one dissolution event, but it could merely mean erratic subsequent mineralization. The varying sequence of cements filling the vugs could also indicate they were formed and filled at different times, or that late-stage cementation conditions varied over the study area.

Although the vug filling of euhedral quartz in the Derby #1 Wood core (*#15*) is unique, it has far-reaching implications for the environment and timing of diagenesis

in the Viola Formation. The widely varying vapor-to-liquid ratios, the large proportion of inclusions with high vapor-to-liquid ratios, and the lack of petrographic evidence for necking of inclusions implies either a vadose environment, or heterogeneous entrapment. Heterogeneous entrapment (Goldstein and Reynolds, 1994, p. 44) is any process by which inclusions trap both liquid and free gas at the time of their formation. Paleobarometric determinations (Table 8.6, Figure 8.60), which indicate that these inclusions are not at 1 atm pressure, rule out a vadose environment. The bimodality of the paleobarometric determinations could indicate separate conditions of entrapment corresponding to the two anhydrite-rich growth phases in the quartz. Hydrostatic depths obtained from these inclusion pressures indicate water columns generally less than 100 m, therefore the inclusions formed before the significant burial that started in Late Mississippian time (see Figure 6.2). The vug containing the euhedral quartz crosscuts concentric dolomite rhombs (Figure 8.56), so the dolomite also formed before significant burial of the Viola. This is consistent with conclusions reached from dedolomite relations. Arguments presented earlier on karstic brecciation, calcitization of dolomite, and regional distribution of dolomite suggest that most of the dolomite in the Viola formed after deposition of the Maquoketa Formation, which is 100 ft (30 m) thick at the Derby #1 Wood locality. Several paleobarometric determinations indicate lesser depths, but the discrepancy is not serious because the paleobarometric determinations are hydrostatic pressures, and the top of the water table may be considerably below the surface of the ground, particularly during arid conditions.

Most of the inclusions having less than 1 atm pressure (Figure 8.60, Table 8.6) are recognized as secondary inclusions arrayed along deformation planes in the quartz. These healed fractures probably formed at significant depth and high temperature. The liquid within their inclusions thermally contracted upon cooling.

Any bubble within an inclusion will expand to compensate for the tensile stress in the inclusion caused by the shrinkage of the liquid, thereby causing the bubble to be under less than 1 atm pressure at surface temperature (Roedder, 1984, p. 59). Entrapment of a gas-deficient aqueous liquid at elevated temperatures is indicated (Goldstein and Reynolds, 1994, p. 80).

The range of salinities recorded by the fluid inclusions in the quartz, and the successive zones of anhydrite within the quartz (Figure 8.58) indicate occasional fresh water interspersed with hypersaline water. The inconsistent vapor-to-liquid ratios caused by the heterogeneous entrapment of the fluid inclusions no doubt causes the wide range in T_h values (Figure 8.59). The apparent correspondence of higher salinities (lower $Tm_{(ice)}$ values) to lower homogenization temperatures (Figure 8.59) is puzzling, but this may only be an artifact of the fortuitous positions of the two data points above -10 °C ($Tm_{(ice)}$). The presence of numerous all-liquid primary fluid inclusions of various sizes in the quartz is indicative of entrapment at temperatures less than about 50 °C (Goldstein and Reynolds, 1994, p. 94).

The euhedral quartz in the vug in the Derby #1 Wood core (*#15*) records fluctuating fresh-water and hypersaline diagenetic conditions. The implication is that the Viola Formation was still near the surface where fluxes of fresh water could occasionally affect it. The anhydrite and the high salinities recorded in the fluid inclusions also indicate the occasional influence of evaporitic environments and associated hypersaline groundwaters, even though no bedded anhydrite or halite is preserved in Lower Paleozoic rocks in this part of the midcontinent. The only extensive evaporites in the rock column are in Lower Permian rocks (Merriam, 1963; Zeller, 1968), which were deposited long after growth of the quartz, when the Viola was buried to at least 4500 ft (1400 m) (see Figure 6.5).

Inasmuch as the euhedral quartz precedes saddle dolomite in the same vug,

the quartz is one of the last diagenetic features in the Viola influenced by near-surface processes before permanent deep burial of the Viola in Early Pennsylvanian time. An interesting caveat in the relationship of the quartz to the succeeding saddle dolomite is that low-temperature fluid inclusions in quartz are evidently not as prone to reequilibration (but not necessarily immune either) when subject to higher temperatures (see Bodnar and Bethke, 1984). Conversely, fluid inclusions in softer, more cleavage-prone minerals such as calcite tend to reequilibrate at higher temperatures and thus approach the maximum temperature subsequently experienced by the rock (see Goldstein, 1986; Prezbindowski and Larese, 1987; Prezbindowski and Tapp, 1991).

Coarsely crystalline ferroan saddle dolomite in vugs, fractures, and other available porosity is consistent with late-diagenetic passive precipitation. Radke and Mathis (1980) suggest that saddle dolomite is a high-temperature mineral that crystallizes between 60 and 150 °C. Synonyms, according to Radke and Mathis (1980) and Morrow (1982b), include "pearl spar", "late ferroan dolomite", "white sparry dolomite", "saddle-shaped dolomite", "baroque dolomite", "hydrothermal dolomite", "megacrystalline white dolomite", and "gangue dolomite". Minerals customarily associated with saddle dolomite include the sulfide minerals, sphalerite and pyrite, which indicate reducing diagenetic conditions. Ferroan banding in the saddle dolomites, however, indicate Eh fluctuations during its precipitation.

Saddle dolomite is considered a subset of a class of burial dolomite called "late dolomite cement", or "LDC" (Leach and others, 1991). LDC is associated with Mississippi Valley-type (MVT) mineralization, present throughout southeastern Missouri and west into Kansas and Oklahoma in Paleozoic strata (Leach and others, 1991). Northward advective migration of hot brines (80 to 180 °C, with 120 °C modal temperature) out of the Arkoma and Anadarko basins in Late Pennsylvanian -- Early

Permian time is an accepted origin (Leach and Rowan, 1986; Gregg and Shelton, 1990; Wojcik, 1991). MVT mineralization is also linked to deep-burial diagenesis by similarities in fluid-inclusion microthermometry, geologic relationships, and the common presence of associated hydrocarbons (Grover and Read, 1983).

The homogenization temperatures (T_h) obtained from the saddle dolomites in the study area (88 to 133 °C range; Figure 6.13) are 15 to 25 °C cooler than the temperatures of the late-stage cements reported for Pennsylvanian strata by Wojcik and others (1992, 1994). Nevertheless, these temperatures, like the temperatures obtained by Wojcik and others (1992, 1994), exceed that expected by heating by simple burial. Wojcik and others (1992) reported fluid-inclusion homogenization temperatures (T_h) for late-stage saddle dolomite in the Upper Pennsylvanian (Missourian) Hertha Limestone in southeastern Kansas (i.e., Elk, Chautauqua, and Cowley counties) range from ~97 to 158 °C, with a mode at 130-135 °C. Final melting temperatures of ice ($Tm_{(ice)}$) have a narrow range with a mean at -18.5 °C, indicating the dolomite precipitated from a fluid of 21.3 wt. % NaCl equivalent according to the conversion of Bodnar (1992). Elaborative findings presented in Wojcik and others (1994) described a more detailed fluid history in which the highest temperatures (by T_h) affecting Upper Pennsylvanian strata range between 85 and 150 °C. Fluid inclusions recording this temperature range are characterized by a NaCl brine with salinity ranging between 19 and 21 wt. % NaCl equivalent. Wojcik and others (1994) also raised the possibility that this brine could be the latter stages of a progressively changing diagenetic system in which mixing occurred with a slightly older Na-Ca-Cl brine, characterized by T_hs varying between 85 and 130 °C, and salinities ranging between 19 and 25 wt. % NaCl equivalent. T_h and salinity results obtained by Wojcik and others (1994) agree with fluid-inclusion data obtained on disseminated sphalerite from Pennsylvanian rocks in the Cherokee basin (see Coveney and others, 1987; Blash

and Coveney, 1988). The significance of these high-temperature fluid inclusions is that they are from 20 to 60 °C in excess of that predicted by maximum-burial temperatures (Wojcik and others, 1994). Advective heat transfer by long-distance movement of heated brines out of the Ouachita orogen in Late Permian time was invoked to account for the elevated temperatures recorded by the fluid inclusions, with the likely carrier beds being porous zones along and below the regional basal Pennsylvanian angular unconformity (Wojcik, 1991; Wojcik and others, 1994).

Ideally, T_h analyses of geographically scattered saddle dolomites and other associated late-stage minerals should be sufficient to map the thermal fingerprint of the advective movement of heated fluids northward out of the Ouachita orogen. Such a fingerprint should be characterized by a general southward increase in entrapment temperatures. The construction of such a map is fraught with difficulties in that the late-stage minerals have to be demonstrably penecontemporaneous, and post-entrapment changes of fluid inclusions have to be assessed (e.g., Goldstein, 1986; Prezbindowski and Larese, 1987; Prezbindowski and Tapp, 1991). Ephemeral fluctuations in temperature during mineralization may add possibly insurmountable complications. For example, Garven and others (1993) modeled that fluid temperatures would transiently vary between 90 and 135 °C for Mississippian strata in the Tri-State ore district in northeastern Oklahoma. Notwithstanding work by Leach and Rowan (1986), a decrease in temperature of late-stage mineralization northward from the Ouachita orogen has not been convincingly demonstrated to date, probably because of such difficulties. Leach and Rowan (1986) suggested an overall lateral temperature decrease of 0.09 °C/km, based on T_h data for sphalerite fluid-inclusions in several Ozark MVT districts that were plotted against their distance from the Ouachita foldbelt. Gregg and others (1992) and Shelton and others (1992), however, disputed this model and instead invoked a more complicated flow pattern

based on trace elements, stable isotopes, and microthermometry of fluid inclusions in replacement dolomites and late-stage dolomite cements. In any case, the present study area spans a north-south distance of 175 km, which would correspond to only a 16 °C-temperature change according to gradient data in Leach and Rowan (1986), so a larger geographic area may be needed to define a cooling trend out of the Anadarko basin even if their scenario of a single mineralization episode from a single basin source is accepted.

Mapping variations in salinity may have better utility for understanding effects of advective flow because $Tm_{(ice)}$ appears to be less variable within a given sample than T_h (see Figures 8.61, 8.62, 8.63). Some MVT-mineralization models suggest that the salinity of brines should decrease over time as brines migrate onto the cratonic shelves from adjacent basins (Garven and Freeze, 1984a, b; Deming and Nunn, 1991). Mixing with relatively dilute waters at the periphery of the basin may be why the northernmost sample from the #1 Sandra Allen core (#2) in McPherson County is the least saline of those analyzed, but it may also be due to the late incursion of freshwater into the formation, as predicted by these models. Internal variations in the salinity of fluid inclusions in successive growth stages in individual crystals may also be useful for understanding histories of fluid flow, particularly if a regional correlation of these growth stages can be established. Long-range correlations of banding in dolomite cements through several MVT ore districts (Ebers and Kopp, 1979; Calder and others, 1984; Gregg, 1985; Voss and Hagni, 1985; Rowan, 1986) suggest this type of regional correlation may be possible.

The $\delta^{18}O$ values (-6.67 and -5.79 ‰ PDB) obtained for the two saddle dolomite samples (Table, 8.7, Figure 8.45) are compatible with high-temperature precipitation typical for saddle dolomite (Allan and Wiggins, 1993). The oxygen-isotopic values of these samples are within the range reported by Wojcik and others (1992) for saddle

dolomites from Pennsylvanian (Desmoinesian) limestones in southeastern Kansas; however, carbon isotopic ratios for the Pennsylvanian saddle dolomites were significantly higher (+3 to +7 $\delta^{13}C$ ‰ PDB) than the values obtained in this study (i.e., -1.06 and -1.29 ‰ PDB).

The relatively high Sr value (0.709033) for saddle dolomite (Table 8.7, Figure 8.44) is consistent with the incorporation of radiogenic Sr that commonly characterizes basinal brines and associated burial dolomite. The radiogenic Sr is attributed to interaction of the allochthonous basinal brines with K-feldspars in siliciclastic sediments and basement rocks (Allan and Wiggins, 1993, p. 95).

Stylolitization and Associated Pyrite

Observations

Euhedral pyrite cubes, up to 1 cm in size, typically are present along stylolites and can locally replace limestone immediately adjacent to the stylolites. Secondary pyrite, generally massive, commonly permeates the upper contact of the Viola where it is beveled and overlain by the Maquoketa Shale (see Figures 7.30, 7.31). Stylolites and associated pyrite mineralization cuts most other fabric elements in the Viola, including some vugs.

The dolomitized mudstones, prevalent in the lower and upper cherty dolomitic limestones, are typically the least stylolitized lithology, particularly if they contain little clay. If dissolution features are developed in these dolomitized mudstones, they are typically concentrated along clayey zones and are poorly developed, with small amplitudes. Horsetail stylolites are typical dissolution features in the dolomitized mudstones.

Stylolites are least common in dolomitized mudstones and wackestones, and they are most common in undolomitized clayey wackestones. Undolomitized

packstones in the basal and upper limestone subunits have concentrations of stylolites that are intermediate to these two lithologies (see Appendix IV). Stylolites in the relatively undolomitized packstones and grainstones of the basal and upper limestones typically have amplitudes of approximately 1 cm.

Replacive ferroan dolomite rhombs, 75 to 150 μm in size, are locally concentrated in and adjacent to some stylolites in relatively undolomitized strata (Figure 8.64). The concentration of dolomite rhombs typically decreases away from the stylolite within a couple of centimeters.

Interpretations

The euhedral pyrite concentrated in and near stylolites indicates the pyrite is the product of late-stage mineralization by solutes concentrated by and probably moving along the stylolite. If the stylolite was merely accumulating the pyrite as a residual material, in essence "sweeping" it from the rock, as constituent carbonate minerals dissolved along the stylolite, the pyrite would be expected to have corrosion features and would not appear euhedral where it extends into the rock adjoining the stylolite. The reducing environment necessary for its precipitation, and its association with stylolites, indicates the pyrite probably originated away from the oxidizing surface and near-surface environments, but not necessarily in the deep subsurface.

The presence of stylolites in the Viola is unremarkable because most carbonate rocks have them in varying abundances. Stylolites are simply a pressure-dissolution phenomenon (Bathurst, 1987) in response to gravitational loading or tectonic forces (Engelder and others, 1981), and as such they are the result of similar processes that caused the grain-to-grain suturing observed in early compaction of the packstones and grainstones prevalent in the basal and upper limestones.

The general prevalence of stylolites in extensively cemented limestones has been attributed by Railsback (1993a) to: (1) stylolites generating the solutes that

Figure 8.64 Photomicrograph of dolomite rhombs associated with a stylolite (arrow) from the upper limestone (depth 4310 ft) in the Bunte Bros. and Shell #1 V. Sheppard core (#30) in Kingman County (10-T.27S.-R.10W.). Note concentration of dolomite decreases away from the stylolite. Thin section has been stained with Alizarin Red-S.

precipitated as cements nearby, (2) the characteristic that well-cemented rocks typically dissolve along discrete surfaces (whereas less cemented rocks undergo dissolution at grain-to-grain contacts) (cf., Buxton and Sibley, 1981), and (3) the complex interaction of less pressure-soluble components (principally $CaCO_3$ cements and bryozoans) with more pressure-soluble components (principally non-bryozoan skeletal grains and non-$CaCO_3$ components). The amount of overburden necessary to cause significant pressure-dissolution in carbonate rocks such as bedding-parallel stylolites is difficult to precisely estimate, although such features may have developed in other well-cemented packstones and grainstones at minimum depths from 300 to 1000 m (Railsback, 1993b). Nevertheless, the specific burial depth cannot be estimated. Studies of chalks and micritic limestones from deep-sea cores suggest pressure solution and concomitant reprecipitation of calcite become important diagenetic processes after 50 to 200 m of burial in seawater (Garrison, 1981).

The lesser abundance of stylolites in dolomite, according to Railsback (1993a), may be attributable to dolomite having a lower susceptibility to pressure dissolution than calcite. Isolated euhedral dolomite rhombs in and near stylolites are prominent in several cores in relatively undolomitized sections in the upper and lower cherty dolomitic limestone subunits (see Appendix IV). Although the concentration of dolomite as refractory material from rock that was dissolved along these seams is possible, some corrosion of the rhombs in the stylolites would be expected. Freeman (1966) argued that the euhedral shape of dolomite rhombs in the Middle Ordovician Plattin Limestone of northern Arkansas and the uniform concentration of dolomite in stylolites, regardless of how well-developed the stylolite is, indicates a post-lithification origin. Wanless (1979), however, maintains that the cause of stylolites and dolomites are related, with the dolomite being a response to the same stresses that cause pressure solution. Although mass-balance calculations (Morrow, 1982b;

Land, 1982) indicate that clays along stylolites cannot expel sufficient Mg to cause regionally significant dolomitization, minor dolomite in and near stylolites still may be generated by this process.

No significant amount of clay is present in the stylolite in Figure 8.64, so clay minerals were probably not the source for the Mg necessary for dolomitization. Nevertheless, clay content could be greater along this stylolite just beyond the core. The decrease of dolomite away from the stylolite implies that the stylolite may have acted as a conduit for dolomitizing fluids that dispersed into the rock adjacent to the stylolite, rather than the stylolite sweeping the dolomite from the rock. Subtle dissolution can extend several centimeters beyond a stylolite though (McNeice, 1986), hence the observed decrease of dolomite away from the seam still may be nefariously related to dissolution, but the lack of corrosion features on the dolomite crystals in Figure 8.64 militates against this process for this specific case.

Fracturing and Hydrocarbon Migration

Observations

Fractures in the Viola, like the vugs, have a variety of cements precipitated in them. Most fractures are vertical to nearly vertical and are less than 2 mm wide. Most commonly, the fill is by one mineral, typically nonferroan calcite, but ferroan calcite (Figure 8.50), saddle dolomite, and quartz may also be present. Chert nodules commonly are cut by numerous closely spaced open fractures and may have a shattered appearance. If no cement is present in the fractures these chert nodules easily disintegrate upon handling. It is unknown if the fracturing of the chert in this latter case is an artifact of coring.

Oil staining in the Viola is common; mostly in cores that were taken in or near known Viola oil fields (e.g., Braden-Zenith ZU-1 [*#19*], Braden-Zenith ZU-3 [*#20*],

Midcontinent Marine #1 North Hilger [*#28*], Midcontinent Marine #1 South Hilger [*#29*]; see Appendix IV). This oil commonly stains any available pore space, including open fractures and some stylolites. Inspection by fluorescent light did not reveal any hydrocarbons in fluid inclusions present in diagenetic minerals.

Interpretation

The lack of a consistent fracture-filling mineral may indicate that fracturing occurred several times during the diagenesis of the Viola, hence several fracturing events could have occurred sporadically over the diagenetic history of the Viola (see Figures 8.13, 8.14). Core coverage is not adequate to identify any specific set of fractures with any particular geologic event, and local variations in cementation may merely give the appearance that fracturing occurred at several different times.

Crude oil was interpreted as being introduced to the Viola relatively late because it is present in a variety of late diagenetic features such as vugs, intercrystalline dolomitic porosity, and stylolites. Saddle dolomites and other minerals characteristic of MVT mineralization can contain hydrocarbons (Burruss, 1981), so a diligent search of the saddle dolomites may reveal some oil-filled fluid inclusions. However, the general lack of oil in fluid inclusions in the diagenetic minerals of the Viola also argues for its late introduction to the rocks in this study area. Sufficient thermal maturation for generation of hydrocarbons in Ordovician rocks in the study area should have occurred after their relatively deep burial in Pennsylvanian and Permian time, and direct maturation indicators suggest these rocks are now only in initial stages of hydrocarbon generation (see Chapter 6). Major migration of hydrocarbons out of thermally mature strata in the Anadarko basin of Oklahoma is interpreted to have occurred after the present geometry of most major uplifts and basins in the midcontinent was established (Figure 1.2A), that is, during Pennsylvanian and Permian time with the Ouachita orogeny (Walters, 1958; Price,

1980; Filipek, 1992), although relatively minor local generation also occurred (Newell and others 1987b, 1990; Hatch and others, 1987; Jenden and others, 1988). The relative timing of diagenetic events and the tentative correlation of dolomitization and calcitization to Paleozoic exposure events indicates most of the diagenetic evolution of the Viola occurred in Paleozoic time before this major episode of hydrocarbon migration.

DISCUSSION

The early diagenetic events that occurred on or directly under the seafloor include bioturbation and micritization. These shallow diagenetic processes are characteristic to the eogenetic diagenetic zone of Choquette and Pray (1970). Later diagenetic events, including early spar cementation, compaction, silicification, and dolomitization, were still within the influence of the surface, hence these processes fall into the realm of the eogenetic diagenetic environment of Choquette and Pray (1970). The mesogenetic environment, away from the direct influence of the surface, is responsible for precipitation of saddle dolomite and most of the ferroan calcite precipitation, and the migration of hydrocarbons. The telogenetic diagenetic environment of Choquette and Pray (1970) is manifest by karstic brecciation, vugs, early quartz mineralization in vugs, and calcitization of dolomites. All of these telogenetic events followed lithification and some burial, by definition, but preceded deep burial of the Viola in Pennsylvanian and Permian time.

Indications of the timing and environment of the replacive and mimetic dolomitization within the Viola can be garnered by the geometry of the dolomitization and its relative timing with respect to the other major diagenetic events affecting the

Viola Formation. First, some background is necessary regarding the process of dolomitization. The two major requirements envisaged for extensive dolomitization are a pumping mechanism by which large volumes of water can be moved through the dolomitizing environment to bring in Mg^{2+} and simultaneously remove Ca^{2+}; and a sufficient source of Mg (see Appendix VII). Seawater is one of the few fluids that volumetrically satisfies the need for the copious amounts of water and Mg required for extensive dolomitization, particularly those that formed in the shallow-burial realm (Land, 1980, 1985; Morrow, 1982b; Machel and Mountjoy, 1986).

Tucker (1990, p. 336) suggested eight models, with variations thereof, to hypothetically satisfy the necessary pumping mechanism and magnesium source for extensive dolomitization (Figure 8.65). The primary models are: sabkha/evaporative (Figure 8.65A), seepage-reflux (Figure 8.65B), falling sea-level/evaporative drawdown (Figure 8.65C), mixing-zone, unconfined coastal aquifer (Figure 8.65D), mixing-zone, deep confined aquifer (Figure 8.65E), Coorong-type (Figure 8.65F), Kohout convection (Figure 8.65G), and burial compaction (Figure 8.65H). The fluid by which the sabkha/evaporative model (Figure 8.65A) dolomitizes is seawater concentrated by evaporation; movement of hypersaline brines by density or a fall in base level drive the seepage-reflux (Figure 8.65B) and falling sea-level/evaporative drawdown models respectively (Figure 8.65C); mixing of fresh water with seawater or hypersaline brines in different geological settings define the mixing-zone, unconfined coastal aquifer (Figure 8.65D), mixing-zone, deep confined aquifer (Figure 8.65E), and Coorong-type models (Figure 8.65F); seawater is driven by geothermal convection in the Kohout model (Figure 8.65G); and the expulsion of deep basinal brines by lithologic loading constitutes burial compaction (Figure 8.65H).

Several of these models can be eliminated because they do not fit depositional or diagenetic parameters for the Viola Formation. The sabkha/evaporation model

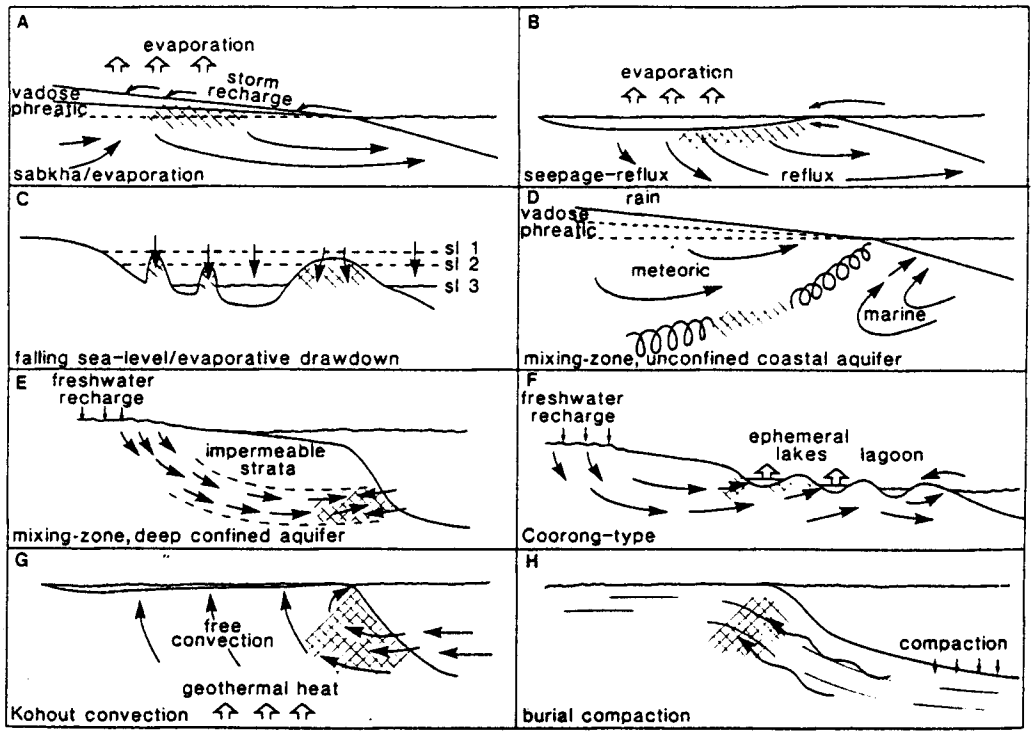

Figure 8.65 Eight models, with their variations, hypothetically satisfy the necessary pumping mechanism and magnesium source for extensive dolomitization (from Tucker, 1990, p. 366 [after Land, 1985]). The primary models are: sabkha/evaporative (A), seepage-reflux (B), falling sea-level/evaporative drawdown (C), mixing-zone, unconfined coastal aquifer (D), mixing-zone, deep confined aquifer (E), Coorong-type (F), Kohout convection (G), and burial compaction (H).

(Figure 8.65A) incorporates the concept that dolomite can form by evaporation of seawater in mostly supratidal marginal-marine settings such as modern sabkhas. Notwithstanding minor fenestral porosity observed in one core at the base of the Viola Formation (Figure 7.9), the absence of lithologic features associated with subaerial exposure during deposition (i.e., mudcracks, fenestral porosity, tidal channels, stressed biota, casts of evaporite minerals, etc.) eliminates the sabkha/evaporite model (Figure 8.65A) as a cause for extensive dolomitization in the Viola. Primary

microcrystalline laminated dolomites are also typical of this environment of dolomitization (Shinn and others, 1965; Davies, 1979; and others). Although dolomite in the Viola Formation is not microcrystalline nor laminated, recrystallization could have enhanced the size of the dolomite crystals and obscured original depositional textures.

The lack of evidence of a widely fluctuating sea level during and shortly after Viola deposition militates against the falling sea-level/evaporative drawdown model (Figure 8.65C). The only significant drop in sea level indicated in the Viola Formation was immediately prior to deposition of the upper limestone subunit. This drop in sea level accounts for the intraformational breccias in the lower cherty dolomitic limestone at the Zenith field (Figures 7.19, 8.47), but it precedes dolomitization as evidenced by the textural relationship of the dolomite rhombs to the interparticle calcite (Figure 8.48).

The presence of regionally impermeable beds eliminates the model for the mixing zone in the unconfined coastal aquifer (Figure 8.65D). The basal and upper limestones were lithified mostly by calcite spar very early and probably operated as relatively impermeable confining beds shortly after deposition.

The Coorong-type model (Figure 8.65F) involves periodic recharge of ephemeral alkaline lakes by a combination groundwater and seawater (Von der Borch and Jones, 1976). Dolomite is precipitated by both evaporative processes and mixing of the groundwater and seawater. This model requires a facies mosaic of lacustrine and near-shore depositional environments; thus it is not amenable to the regionally extensive pattern of dolomitization in the widespread subtidal environments that characterize the Viola.

The Kohout convection model (Kohout, 1967) (Figure 8.65G) proposes large-scale, geothermal-driven circulation of water into carbonate platform-margins. Simms

(1984) recognized that this model could be a pumping mechanism for water involved with dolomitization. Land (1985) further fortified the viability of this model with geochemical arguments that relatively pristine seawater, unaltered by concentration or dilution, could be a dolomitizing fluid. Dolomite precipitated with this type of pumping mechanism should contain only slightly altered seawater. With respect to its application to the Viola however, the low relief of the sea floor and the extensive area of the Viola carbonate shelf does not provide a steep platform-margin necessary for intake of cold seawater. The Viola is relatively thin and only slight geothermal temperature differential would exist across it to drive the flux of seawater necessary for this type of dolomitization. The dilute and hypersaline brines recorded in fluid inclusions in the Viola dolomite are also not compatible with this model. Cander and others (1988) discounted a Kohout convection model for regional dolomite in the Burlington-Keokuk Formation (Mississippian) in western Illinois and eastern Missouri for similar reasons.

Inasmuch as major dolomitization of the Viola had to occur before its deep burial in Pennsylvanian and Permian time (as indicated by the dolomitization occurring before the karstic brecciation associated with the unconformity at the base of the Chattanooga Shale; see Figure 8.49 and associated discussion), the burial-compaction model (Figure 8.65H) is not likely. However, saddle dolomites in the Viola fit this particular model.

By process of elimination, the most likely models to account for the extensive dolomitization of the lower and upper cherty dolomitic limestones, and of the basal limestone near the crest of the Chautauqua and Central Kansas arches, are the seepage-reflux model (Figure 8.65B) and the confined aquifer mixing-zone model (Figure 8.65E). According to the regional pattern of dolomitization (Figures 8.3, 8.5, 8.8, 8.9, 8.11), the likely source area for the dolomitizing fluids include the crest of the

Chautauqua-Central Kansas arches, and local structural highs along the Pratt anticline.

In the mixing-zone model, dolomitization occurs where fresh and saline (marine) waters mix in aquifers in proportions such that the pore fluids are undersaturated with respect to calcium carbonate but supersaturated with respect to dolomite (Badiozamani, 1973; Land, 1973; Magaritz and others, 1980). Seawater supplies the necessary Mg, and a hydrodynamic head from a freshwater lens forces meteoric water to move seaward and mix with seawater along a diffuse hydrologic interface. The proportion of mixing necessary for dolomitization theoretically depends on the stoichiometry of the resultant dolomite and the partial pressure of CO_2 during dolomitization (cf., Badiozamani, 1973; Wigley and Plummer, 1976; Hardie, 1987). The dolomitization window of seawater mixed with fresh water ranges from 5% to 50% by calculations in Badiozamani (1973), 30% to 40% by Hardie (1987), and 35% to 75% by Wigley and Plummer (1976). Problems cited for mixing-zone dolomitization include a chemical precipitation or nucleation problem in that seawater by itself is more supersaturated with respect to dolomite than any seawater-fresh water mixture, and few modern mixing zones are documented as containing newly precipitated dolomite (Allan and Wiggins, 1993, p. 4). Purser and others (1994b) note that the mixing zone has an oblique geometry that is difficult to reconcile with seemingly homogeneous dolomitized platforms.

Prior studies of the Viola (St. Clair, 1982; Bushnag, 1989) favored a mixing-zone model over a seepage-reflux model because of the absence of evaporite minerals or their pseudomorphs, or of collapse breccias that would hint at the former presence of bedded evaporites in the Viola. Mixing-zone dolomitization would presumably be dominant during times of sea-level fall when meteoric recharge from exposed terrain would force connate-marine waters seaward or farther downdip. Transgression would

also create a dynamic mixing-zone environment as long as exposed land areas that are the sources of the meteoric waters were not submerged. Crests of structures that were topographic or bathymetric highs during or shortly after deposition would be more prone to this type of dolomitization. However, a similar pattern would also result from the downward movement of dense hypersaline brines.

Fluid-inclusion data presently cannot eliminate either of these models for the concentric dolomite, for salinities recorded by primary(?) fluid inclusions in the concentric dolomite range from a blend of fresh water and seawater, to moderately hypersaline water (Figure 8.43). Oxygen isotopic data from the concentric dolomites do not show enrichment in ^{18}O that would be expected with hypersalinity; this is consistent with a mixing-zone environment.

Hypersalinity recorded in primary(?) fluid inclusions in the collage dolomite argues that seepage-reflux of hypersaline water may be the dominant process responsible for these later dolomites, but their oxygen isotopes are too negative for hypersaline waters at near-surface temperatures. Nevertheless, complications with occasional fluxes of freshwater and seawater at deposition (see Lloyd, 1966) and recrystallization of the dolomite in the subsurface (see Land, 1983a) could significantly alter the expected ^{18}O enrichment that would be expected with hypersalinity. The chemistry of the collage and mimetic dolomites have nearly ideal stoichiometry that would be expected from dolomitization associated with evaporites. No evaporites are associated with the collage and mimetic dolomites in the Viola. This is a problem for the hypersaline model, but since these dolomites may be derived from dolomitization occurring in Silurian time, hypersaline brines could have seeped into the Viola from overlying strata.

Anhydrite inclusions in the quartz vug-fill in the Derby #1 Wood core are telltale evidence that evaporites may have been associated with the Viola, and that

hypersaline brines have at least migrated through this unit. Even though evaporites are not present in the Viola, they could have been present in rock units deposited above the Viola, and subsequently destroyed by any of the several exposure events that occurred between deposition of the Upper Ordovician Maquoketa Shale and the Upper Devonian-Lower Mississippian Chattanooga Shale. Strontium isotopes suggest candidate time-intervals for hypersaline dolomitization of the Viola may be latest Ordovician and Silurian time. Speculatively, the concentric dolomite may be attributable to the former time interval, whereas the recrystallized and mimetic dolomites may be attributable to the latter.

The lower part of the "Hunton" group in Kansas was deposited during the Silurian (Goebel, 1968b). Beardall and Al-Shaieb (1984), Al-Shaieb and others (1993) and Fritz and Medlock (1993) reported the Silurian Henryhouse Formation of the Hunton Group in Oklahoma (see Figure 2.1) contains anhydrite nodules. Al-Shaieb and others (1993) specifically interpreted three types of dolomite in the Henryhouse Formation: (1) brownish, cloudy, hypidiotopic dolomite that formed shortly after deposition from hypersaline brines; (2) white or limpid idiotopic dolomite that formed after the hypersaline dolomite due to mixing of meteoric water and seawater; and (3) mold-, vug-, and fracture-filling saddle dolomite. A similar progression of dolomites formed respectively from hypersaline brines, mixed marine and fresh waters, and deep burial was invoked by Fritz and Medlock (1993) to account for dolomitization in the Henryhouse Formation.

The Silurian part of the Hunton Group in Oklahoma (the Henryhouse and Chimneyhill formations) is mostly dolomite (Amsden, 1980). Amsden (1980) reported the geographic distribution of dolomite defined in the Silurian part of the Hunton Group in Oklahoma is imprinted on the underlying Upper Ordovician Keel Formation, an oölitic carbonate unit locally present above the Upper Ordovician Sylvan Shale

(see Figure 2.1). He interpreted the Keel dolomite as "emplaced" before deposition of the Frisco Formation, dated as Middle Early Devonian (Siegenian) in age. Goebel (1968b, p. 15) reported the lower part of the "Hunton" in Kansas, identified as the Chimneyhill Formation, is dominantly fine- to coarse-crystalline, vuggy dolomite, which is "no younger than Mid-Silurian" in age. The upper part of the "Hunton" in Kansas is "no older than Mid-Devonian" in age (Goebel, 1968b, p. 15) and is mostly composed of white lithographic limestone that is not considered part of the underlying Chimneyhill Formation.

The influence of possible hypersaline and mixed-water dolomitization in the Silurian part of the Hunton Group of Oklahoma and its imprint on the underlying Upper Ordovician strata suggests a similar relationship may exist in Kansas between the dolomite in the Silurian part of the "Hunton" and the underlying Viola and Maquoketa formations. Dolomitization may particularly affect the Viola Formation in areas where the overlying Maquoketa Shale was removed by erosion over the crests of regional uplifts. The pattern of dolomitization along the crest of the Chautauqua arch and locally along the Pratt anticline is consistent with this model. A comparative geochemical and petrographic study of the dolomite in the "Hunton" and Upper Ordovician units in Kansas may therefore reveal similar patterns, which could indicate a common mechanism of dolomitization. The possibility of a genetic link between dolomite in Silurian and Ordovician rocks in the Michigan basin was suggested by Coniglio and others (1994) to be worthy of further study, in that these dolomites have similar oxygen and carbon isotopic compositions (see O'Shea and others, 1988), and strontium isotopic ratios (see Granath, 1991). Sulfur and oxygen isotopic values of anhydrites in these two rock systems in the Michigan basin are also similar (Fritz and others, 1988).

Chapter 9

CONCLUSIONS AND SUGGESTIONS FOR FURTHER RESEARCH

CONCLUSIONS

1. The Viola is divided into four mappable informal subunits. From base to top, these are: basal limestone, lower cherty dolomitic limestone, upper limestone, and upper cherty dolomitic limestone. These subunits were originally defined by St. Clair (1982) in a two-county area, but they are recognizable across much of central Kansas. The limestones are low-porosity crinoidal packstones, whereas the cherty dolomitic limestones generally are porous, mixed-skeletal dolomitized wackestones and mudstones with nodular chert.

2. The Viola Formation is eroded down to the basal limestone subunit over the crest of the Central Kansas arch and is missing on the crests of the Chautauqua arch and Ancestral Central Kansas uplift. Successively younger subunits are arrayed in a generally symmetric pattern along the northeastern and southwestern flanks of the Central Kansas arch. Much of the erosion on the northeastern flank of the arch occurred before deposition of the Upper Ordovician Maquoketa Formation, whereas later pre-Devonian erosional events account for the subcrop pattern on the southwestern flank.

3. A subtle angular unconformity with a poorly developed subaerial exposure surface separates the Viola from the overlying Maquoketa Formation. The contact with the underlying Simpson Group is more subtle, commonly a stylolitic contact or abrupt knife-edge change in lithology from silty shale to carbonate. Although no subaerial exposure surface is developed on the Simpson, it was lithified before the

Viola was deposited.

4. The Central Kansas arch and Pratt anticline were active during Viola deposition and locally influenced the thickness of Viola subunits deposited on them. The basal and upper limestones, dominantly grain-supported lithologies, generally thicken on the crests of these uplifts, whereas the lower and upper cherty dolomitic limestones, dominantly mud-supported lithologies, are thickest on the flanks of these uplifts and in adjacent basins. A group of left-stepping, *en echelon* isopachous thins developed along the Pratt anticline are compatible with left-lateral movement along this long-lived zone of structural weakness.

5. The basal and upper limestones are characterized by lobe-like thick areas that indicate these units are not strictly sheet deposits, but rather they may be coalesced shoals of carbonate sand.

6. A shoreface-shoal complex was responsible for the packstones and grainstones typifying the basal and upper limestone subunits. Storm currents may have been responsible for initial deposition of these sediments, but burrowing subsequently destroyed much of their original depositional textures. Long periods of time may have transpired without the influence of strong or repetitive currents on the seafloor.

7. Quiet-water deposition is indicated by the fine-grained nature and delicate infauna of the mudstones in the lower and upper cherty dolomitic limestones. These units are interpreted to have been deposited in deeper subtidal environments basinward of the shoreface-shoal complexes responsible for the basal and upper limestones. Thin, graded beds within these subunits indicate occasional gravity currents possibly generated by storms.

8. Depositional geometries of the Viola Formation indicate that it was a carbonate ramp, open to the south, with depositional slopes of less than one degree.

9. Continuous deposition is indicated between the basal limestone and the overlying lower cherty dolomitic limestone, and between the upper limestone and upper cherty dolomitic limestone, but a minor unconformity with associated intrastratal karstic brecciation separates lower cherty dolomitic limestone from the overlying upper limestone. Two depositional cycles therefore compose the Viola, each cycle being approximately 2.5 m.y. duration. These cycles would be third-order cycles according to published periodicity scales.

10. Petroleum production in the Viola Formation is dominantly from porous dolomite in the lower and upper cherty dolomitic limestones. Production trends are oriented obliquely across the Pratt anticline and are spatially associated with broad southwest-plunging synclines expressed by subcrop patterns of the Viola subunits. Dolomitized basal limestone serves as the reservoir rock in a separate production trend near the pinchout of this subunit on the flanks of the Chautauqua arch. Approximately 5 to 6% porosity has to be developed before significant permeability is manifest in any Viola subunit. Intercrystalline, vuggy, and moldic porosity dominate where the Viola is heavily dolomitized.

11. The erratic increase and decrease of organic maturation with depth, and variations in maturation of the same strata between nearby wells suggest that heating of the rock column may not have been controlled strictly by a regionally consistent geothermal gradient. Advective flow of heated waters may account for this pattern of maturation. Homogenization temperatures from saddle dolomites in the Viola range from 88 to 133 °C -- temperatures that exceed heating by simple burial. These temperatures probably represent either thermal pulses heating the entire stratigraphic column or advective flow of heated brines out of the Anadarko basin, mostly likely in Late Pennsylvanian -- Early Permian time.

12. Echinoderm-rich packstones and grainstones in the basal and upper

limestones display similar paragenetic sequences. Early syntaxial spar cements occluded much of their original interparticle porosity. Minor silicification and replacive dolomitization followed. The basal limestone is mimetically dolomitized near its pinchout on the Chautauqua arch, but little dolomite is present at its pinchout on the flank of the Central Kansas uplift. Local dissolution after dolomitization created vugs that were subsequently filled with quartz, saddle dolomite, and calcite.

13. A similar paragenetic sequence is indicated for the lower and upper cherty dolomitic limestones, however, replacive dolomitization was the dominant diagenetic event. Silicification was more intense than in the grain-support lithologies; chert formed early, before surrounding sediments were completely lithified.

14. All four Viola subunits are more heavily dolomitized where they subcrop on flank of the Chautauqua arch, but they are less dolomitic away from the arch. The Viola is intensely dolomitized immediately north and west of the Chautauqua arch. This spatial association implies that the Chautauqua arch controlled the genesis of this dolomite. Dolomitization was reduced beneath outliers of Maquoketa Shale; this pattern suggests downward movement of dolomitizing fluids after deposition of the Maquoketa.

15. Cathodoluminescence petrography indicates dolomite at the crests of the Chautauqua and Central Kansas arches is intensely recrystallized, but farther down dip and in basinal areas, a simpler concentric texture predominates. Collage (intensely recrystallized) and mimetic dolomites at the crests of these arches are nearly stoichiometric whereas the concentric dolomite down dip is calcian. The collage and mimetic dolomite may, in part, derived from concentric dolomite that recrystallized when subjected to downward-moving hypersaline brines.

16. Much of the dolomitization of the Viola occurred before significant burial

in Late Mississippian time. Dolomite in the upper cherty dolomite is brecciated by karstic processes associated with the unconformity beneath Upper Devonian -- Lower Mississippian Chattanooga Shale. Fluid inclusions indicate that the dolomitization occurred at temperatures less than about 50 °C. The influence of near-surface conditions on diagenetic events that followed dolomitization is demonstrated by fresh-water inclusions in calcitized dolomites, fresh-water inclusions in quartz filling vugs that truncate the dolomite, and internal pressures of fluid inclusions in the vug-filling quartz that indicate burial less than 150 m.

17. Strontium isotopic ratios in the concentric dolomite in the Viola are consistent with dolomitization during Late Ordovician time. Dolomitization during Silurian time may be responsible for the collage and mimetic dolomite. Primary(?) fluid inclusions in the collage dolomite are hypersaline; stratigraphic relationships of this dolomite are congruent with a seepage-reflux environment. Isotopically negative oxygen in the mimetic and collage dolomites are not consistent with hypersalinity, but recrystallization may have altered their original isotopic signature. Primary(?) fluid inclusions and oxygen isotopes in the concentric dolomite indicate generally lower but variable salinities during precipitation, compatible with a mixing-zone environment.

SUGGESTIONS FOR FURTHER RESEARCH

1. The dolomite aureole on the Chautauqua arch and the associated mimetic dolomitization of the basal limestone subunit begs the question of whether other older strata subcropping on the arch are similarly dolomitized. Lithologic and well-log analysis of the Arbuckle Group and carbonate strata in the Simpson Group where they subcrop at the crest of the arch will answer this question. If these units are

dolomitized on the crest of the arch, further investigations of these units on the flanks of the arch will provide a better understanding of the geometry and extent of the dolomitized strata. More investigation is also needed to the south in Oklahoma to understand the distribution of dolomite on the south flank of the Chautauqua arch.

2. A detailed diagenetic study of the mimetically dolomitized grainstones in the vicinity of the Midcontinent Marine #1 North Hilger and #1 South Hilger cores may establish more details on how porosity and dolomite evolved in these rocks. Both dolomite cements and replacive dolomites are present in these rocks. Three additional cores in the Hilger oil field are available for study in addition to several sets of drill cuttings. Transmitted-light, cathodoluminescence, and SEM petrography could be employed. Results could indicate whether dolomitization created or destroyed porosity in this region.

3. Dolomite in the lower part of the "Hunton" group may have a similar origin to the dolomite in the Viola (i.e., a flux of hypersaline water in Silurian time). A detailed geochemical comparison of dolomite in the lower part of the "Hunton" group with that of the Viola confirm the extent and importance of the dolomitizing event. Stable isotopes, cathodoluminescence, trace elements, and fluid inclusions could be used in this comparative study. Depending on availability of samples and sampling density, likely paths of flow of the dolomitizing fluids possibly could be defined.

4. Drill cuttings could compensate for lack of core control to better define the extent of the collage and concentric dolomites in the Viola. Ancillary work with trace elements and x-ray diffraction to determine stoichiometry and crystallinity of both types of dolomite may show why the concentric dolomites may have recrystallized at the crest of the Central Kansas and Chautauqua arch and how they spatially relate to the collage and mimetic dolomites.

5. A cathodoluminescence study of selected samples of drill cuttings throughout the Viola may be the way to crack the puzzle on the spatial distribution and correlation of individual zones in the concentric dolomite. With present control, very little well-to-well correlation could be discerned, and the lack of cores that penetrate the entire Viola prohibited understanding of the vertical distribution of the concentric zonation at any given locality. If a correlatable microstratigraphy of the concentric zones in the dolomite could be established, a better understanding of the fluid inclusions in this dolomite could be achieved. In turn, fluid movement and the environment of dolomitization in the early diagenetic history of the Viola could be better understood.

6. Fluid-inclusion data on the collage dolomite in the Viola is from only one sample. Additional fluid-inclusion work concentrating on all-liquid primary inclusions in collage dolomites at the crest of the arch and the concentric dolomite farther down dip could more confidently establish the salinity of the dolomitizing fluids in addition to delineating spatial variations in salinity.

7. As more suites of modern well logs become available, they could be analyzed to better establish diagenetic and depositional patterns in the Viola. Specifically, the combination of neutron, density, and photoelectric absorption cross-section index (Pe) logs would be useful in determining the vertical distribution of dolomite, chert, and calcite in the lower and upper cherty dolomites. The intraformational breccia found between the lower cherty dolomitic limestone and the upper limestone subunits could possibly be traced with spectral gamma-ray logs in the same fashion that Carr and Lundgren (1994) used these logs to detect exposure surfaces in Mississippian strata in Kansas. If these methods are successful in defining exposure surfaces and flooding events, they could be used to establish a sequence stratigraphic framework for the Viola Formation.

8. Subcrop maps indicate the Welling Formation in Oklahoma may be the lithologic correlative to the basal limestone subunit in Kansas. Further lithostratigraphic correlation of the Viola southward into Oklahoma could establish this correlation with more confidence. Resultant correlations could lead to key outcrops and cores in the vicinity of the Arbuckle Mountains of Oklahoma that could aid in understanding the geometry and origin of these carbonate sands.

9. The internal stratigraphy established for the Viola could be extended northward toward the Transcontinental arch. This correlation exercise could establish if the grain-supported lithologies of the Viola become more dominant northward. Several cores archived at the Kansas Geological Survey from the axis of the Forest City basin could provide lithologic control for the well-log correlations.

10. A better understanding of the burial history and thermal history in central Kansas could perhaps be achieved by studying the compaction of chalks and shales in the Cretaceous and Permian systems. Porosity-depth relationships established for these units utilizing gamma ray, density, sonic, and neutron logs may be useful in estimating the total amount of Cretaceous strata deposited in central Kansas. Physical measurements on the variation of density, porosity, and permeability of chalks with depth (Scholle, 1977) indicate that well logs could be used to establish critical compaction-depth relationships in Kansas. In addition, more work needs to be done to understand the apparent discrepancy between organic maturation and fluid-inclusion temperatures recorded in saddle dolomites. A possible approach would be to study the maturation of disseminated organic material directly adjacent to vugs containing saddle dolomite to check if locally higher maturation is recorded by these materials.

11. An investigation of saddle dolomite on the northern flank of the Anadarko basin may be warranted to understand if and how basinal brines flowed out of the

Ouachita orogen. Specifically, this study could a) determine if advective flow could account for spatial pattern of salinities and temperatures recorded by these dolomites, and b) compare paleothermometry in successions of fluid-inclusion assemblages within individual crystals to ascertain if any patterns can be correlated to nearby localities. SEM microscopy and imagery would also help in determining if internal zones are present in these saddle dolomites and if these zones are correlatable, regardless of geologic formation. Stable isotopes also may record consistent changes in saddle dolomites along hypothetical advection pathways out of the Anadarko basin. A pilot study should first be done in a selected geologic formation such as the Viola, then the results of that study could be compared to saddle dolomites in other units.

REFERENCES CITED

Abbott, P.L., 1974, Calcitization of Edwards Group dolomites in the Balcones fault zone aquifer, south-central Texas: Geology, v. 2, p. 359-362.

Abed, A.M., Makhlouf, I.M., Amireh, B.S., and Khalil, B., 1993, Upper Ordovician glacial deposits in southern Jordan: Episodes, v. 16, p. 316-328.

Adams, A.E., MacKenzie, W.S., and Guilford, C., 1984, Atlas of sedimentary rocks under the microscope: John Wiley and Sons, New York, New York, 104 p.

Adkison, W.L., 1972, Stratigraphy and structure of Middle Ordovician rocks in the Sedgwick basin and adjacent areas, south-central Kansas: United States Geological Survey, Professional Paper 702, 33 p.

Adler, F.J., 1971, Future petroleum provinces of the Midcontinent, region 7, *in* Cram, I.H., ed., Future petroleum provinces of the United States -- their geology and potential: American Association of Petroleum Geologists, Memoir 15, p. 985-1,120.

Ahr, W.M., 1973, The carbonate ramp; an alternative to the shelf model: Transactions of the Gulf Coast Association of Geological Societies, v. 23, p. 221-225.

Aigner, T., 1982, Calcareous tempestites; storm-dominated stratification in Upper Muschelkalk limestones (Middle Tria, SW-Germany), *in* Einsele, G., and Seilacher, A., Cyclic and event stratification: Springer-Verlag, Berlin, Germany, p. 180-198.

Al-Hashimi, W.S., and Hemingway, J.E., 1973, Recent dolomitization and origin of Rusty Crusts of Northumberland: Journal of Sedimentary Petrology, v. 43, p. 82-91.

Al-Shaieb, Z., Beardall, G.B., Jr., Medlock, P., Matthews, F., and Manni, F., 1993, Overview of Hunton facies and reservoirs in the Anadarko basin, *in* Johnson, K.S., ed., Hunton Group core workshop and field trip: Oklahoma Geological Survey, Special Publication 93-4, p. 3-39.

Alberstadt, L.P., 1973, Articulate brachiopods of the Viola Formation (Ordovician) in the Arbuckle Mountains, Oklahoma: Oklahoma Geological Survey, Bulletin 117, 90 p.

Allan, J.R., and Wiggins, W.D., 1993, Dolomite reservoirs -- geochemical techniques for evaluating origin and distribution: American Association of Petroleum Geologists, Continuing Education Course Note Series #36, 129 p., plus appendices.

Allen, P., 1975, Ordovician glacials of the central Sahara, *in* Wright, A.E., and Mosely, F., eds., Ice ages; ancient and modern: Geological Journal, Special Issue 6, Seele House Press, Liverpool, England, p. 275-286.

Amaral, E.J., and Pryor, W.A., 1977, Depositional environment of the St. Peter Sandstone deduced by textural analysis: Journal of Sedimentary Petrology, v. 47, p. 32-52.

American Association of Petroleum Geologists, 1976, Geothermal gradient map of eastern Colorado -- Kansas (portfolio map area no. 15): Geothermal Survey of North America sponsored by American Association of Petroleum Geologists, Tulsa, Oklahoma (1:1,000,000 map).

Amsden, T.W., 1979, Welling Formation, a new name for a Late Ordovician unit in eastern Oklahoma formerly called "Fernvale": American Association of Petroleum Geologists, Bulletin, v. 63, p. 1,135-1,138.

Amsden, T.W., 1980, Hunton Group (Late Ordovician, Silurian, and Early Devonian) in the Arkoma basin of Oklahoma: Oklahoma Geological Survey, Bulletin 129, 136 p.

Amsden, T.W., and Klapper, G., 1972, Misener Sandstone (Middle-Upper Devonian), north-central Oklahoma: American Association of Petroleum Geologists, Bulletin, v. 56, p. 2,323-2,334.

Amsden, T.W., and Sweet, W.C., 1983, Upper Bromide Formation and Viola Group (Middle and Upper Ordovician) in eastern Oklahoma: Oklahoma Geological Survey, Bulletin 132, 76 p.

Anderson, T.F., and Arthur, M.A., 1983, Stable isotopes of oxygen and carbon and their application to sedimentologic and paleoenvironmental problems, *in* Arthur, M.A., Anderson, T.F., Kaplan, I.R., Veizer, J., and Land, L.S., Stable isotopes in sedimentary geology: Society of Economic Paleontologists and Mineralogists, Short Course No. 10, p.4-1-4-22.

Asquith, G.B., with Gibson, C.R., 1982, Basic well log analysis for geologists: American Association of Petroleum Geologists, Tulsa, Oklahoma, 216 p.

Autio, W., 1985, Lithofacies and depositional environments of the Simpson Group of central Kansas, *in* Adkins-Heljeson, M.D., ed., Core studies in Kansas -- sedimentology and diagenesis of economically important rock strata in Kansas: Kansas Geological Survey, Subsurface Geology Series 6, p. 1-7.

Back, W., Hanshaw, B.B., Plummer, L.N., Rahn, P.H., Rightmire, C.T., and Rubin, M., 1983, Process and rate of dedolomitization; mass transfer, and ^{14}C dating in a regional carbonate aquifer: Geological Society of America, Bulletin, v. 94, p. 1,415-1,429.

Badiozamani, K., 1973, The dorag dolomitization model -- application to the Middle Ordovician of Wisconsin: Journal of Sedimentary Petrology, v. 43, p. 965-984.

Baker, P.A, and Kastner, M., 1981, Constraints on the formation of sedimentary dolomite: Science, v. 213, p. 214-216.

Bakush, S.H., and Carozzi, A.V., 1986, Subtidal storm-influenced carbonate ramp model; Galena Group (Middle Ordovician) along Mississippi River (Iowa, Wisconsin, Illinois, and Missouri): U.S.A. Archives Science, Gèneve, v. 39, p. 141-183.

Ball, S.M., 1982, Exploration application of temperatures recorded on log headings -- an up-the-odds method of hydrocarbon-charged porosity prediction: American Association of Petroleum Geologists, Bulletin, v. 66, p. 1,108-1,123.

Banner, J.L., Hanson, G.N., and Meyers, W.J., 1988, Determination of initial Sr isotopic compositions of dolostones from the Burlington-Keokuk Formation (Mississippian); constraints from cathodoluminescence, glauconite paragenesis and analytical methods: Journal of Sedimentary Petrology, v. 58, p. 673-687.

Barker, C.E., Goldstein, R.H., Hatch, J.R., Walton, A.W., and Wojcik, K.M., 1992, Burial history and thermal maturation of Pennsylvanian rocks, Cherokee basin, southeastern Kansas, *in* Johnson, K.S., and Cardott, B.J., eds., Source rocks in the southern midcontinent: Oklahoma Geological Survey, Circular 93, p. 299-310.

Bathurst, R.G.C., 1966, Boring algae, micrite envelopes and lithification of molluscan biosparites: Geological Journal, v. 5, p. 15-32.

Bathurst, R.G.C., 1976, Carbonate sediments and their diagenesis: Developments in Sedimentology 12 (2nd edition), Elsevier Publishing Company, New York, New York, 658 p.

Bathurst, R.G.C., 1987, Diagenetically enhanced bedding in argillaceous platform limestones; stratified cementation and selective compaction: Sedimentology, v. 34, p. 749-778.

Beardall, G.B., Jr., 1984, Dolomitization stages in a regressive sequence of Hunton Group, Anadarko basin, Oklahoma (abs.): American Association of Petroleum Geologists, Bulletin, v. 68, p. 452.

Beene, D.L., 1993, 1992 oil and gas production in Kansas: Kansas Geological Survey, Oil and Gas Production Data Set 92, 267 p.

Bennacef, A., Beuf, S., Biju-Duval, B., De Charpal, O., and Rognon, P., 1971, Examples of cratonic sedimentation; Lower Paleozoic of Algerian Sahara: American Association of Petroleum Geologists, Bulletin, v. 55, p. 2,225-2,245.

Berendsen, P., and Blair, K.P., 1986, Subsurface structural maps over the Central North American rift system (CNARS), central Kansas, with discussion: Kansas Geological Survey, Subsurface Geology Series 8, 16 p.

Berendsen, P., Doveton, J.H., and Speczik, S., 1992, Distribution and characteristics of a Middle Ordovician oolitic ironstone in northeastern Kansas based on petrographic and petrophysical properties; a Laurasian ironstone case study: Sedimentary Geology, v. 76, p. 207-219.

Berner, R.A., 1971, Principles of chemical sedimentology: McGraw-Hill, New York, New York, 240 p.

Berry, W.B.N., 1976, Aspects of correlation on North American shelly and graptolitic faunas, *in* Bassett, M.G., ed., The Ordovician System: University of Wales Press, Cardiff, Wales, p. 153-169.

Berry, W.B.N., and Boucot, A.J., 1970, Correlation of the North American Silurian rocks: Geological Society of America, Special Paper 141, 289 p.

Berry, W.B.N., and Boucot, A.J., 1973, Glacio-eustatic control of Late Ordovician -- Early Silurian platform sedimentation and faunal changes: Geological Society of America, Bulletin, v. 84, p. 275-284.

Biederman, E.W., Jr., 1966, Petrology of the Viola formation, El Dorado field, Butler County, Kansas, *in* Schramm, M.W., Jr., and Chenoweth, P.A., eds., Symposium on the Viola, Fernvale and Sylvan: Tulsa Geological Society, Digest, v. 34, p. 41-60.

Blair, K.P., and Berendsen, P., 1988, Ordovician carbonate lithofacies: Kansas Geological Survey, Open-File Report 88-51B (1:1,000,000 map).

Blash, S.R., and Coveney, R.M., Jr., 1988, Goethite-bearing brine inclusions, petroleum inclusions, and the geochemical conditions of ore deposition at Jumbo mine, Kansas: Geochimica et Cosmochimica Acta, v. 52, p. 1,007-1,017.

Blatt, H., Middleton, G., and Murray, R., 1980, Origin of sedimentary rocks (2nd edition): Prentice-Hall, Inc, Englewood Cliffs, New Jersey, 782 p.

Bodnar, R.J., 1992, Revised equation and table for freezing-point depressions of the H_2O-salt fluid inclusions (abs.): PACROFI IV, Fourth Biennial Pan-American Conference on Research on Fluid Inclusions, Program and Abstracts, Lake Arrowhead, California, v. 4, p. 108-111.

Bodnar, R.J., and Bethke, P.M., 1992, Systematics of stretching of fluid inclusions; fluorite and sphalerite at 1 atm confining pressure: Economic Geology, v. 79, p. 141-161.

Bornemann, E., 1979, Well-log analysis as a tool for lithofacies determination in the Viola Limestone (Ordovician) of south-central Kansas: Ph.D. dissertation, Syracuse University, Syracuse, New York, 151 p.

Bornemann, E., Doveton, J.H., and St. Clair, P.N., 1982, Lithofacies analysis of Viola Limestone in south-central Kansas: Kansas Geological Survey, Petrophysical Series No. 3, 44 p.

Bornemann, E., and Doveton, J.H., 1983, Lithofacies mapping of Viola Limestone in south-central Kansas based on wireline logs: American Association of Petroleum Geologists, Bulletin, v. 67, p. 609-623.

Braun, M., and Friedman, G.M., 1970, Dedolomitization fabric in peels; a possible clue to unconformity surfaces: Journal of Sedimentary Petrology, v. 40, p. 417-419.

Brenchley, P.J., Marshall, J.D., Carden, G.A.F., Robertson, D.B.R., Long, D.G.F., Meidla, T., Hints, L., and Anderson, T.F., 1994, Bathymetric and isotopic evidence for a short-lived Late Ordovician glaciation in a greenhouse climate: Geology, v. 22, p. 295-298.

Brenchley, P.J., and Newall, G., 1980, A facies analysis of Upper Ordovician regressive sequences in the Oslo region, Norway -- a record of glacio-eustatic changes: Palaeogeography, Palaeoclimatology, Palaeoecology, v. 31, p. 1-38.

Brenchley, P.J., and Newall, G., 1984, Late Ordovician environmental changes and their effect on faunas, *in* Bruton, D.L., ed., Aspects of the Ordovician System: Palaeontological Contributions from the University of Oslo, no. 295, Universtetsforlaget, p. 65-79.

Brewer, J.E., 1959, Geophysical problems on Pratt anticline, Pratt County, Kansas, *in* W.W. Hambleton, ed., Symposium on geophysics in Kansas: Kansas Geological Survey, Bulletin 137, p. 275-280.

Brown, H.A, and Banta, A.D., 1993, Unusual occurrence of oil in the Viola Limestone, Pratt anticline, Kansas, *in* Johnson, K.S., and Campbell, J.A., eds., Petroleum reservoir geology in the southern Midcontinent, 1991 symposium: Oklahoma Geological Survey, Circular 95, p. 104-112.

Budai, J.M., Lohmann, K.C., and Owen, R.M., 1983, Burial dedolomite in the Mississippian Madison Limestone, Wyoming and Utah thrust belt: Journal of Sedimentary Petrology, v. 54, p. 276-288.

Bunker, B.J., Witzke, B.J., Watney, W.L., and Ludvigson, G.A., 1988, Phanerozoic history of the central midcontinent, United States, *in* Sloss, L.L., ed., Sedimentary cover -- North American craton, U.S.: Geological Society of America, The Geology of North America, v. D-2., p. 243-260.

Burke, W.H., Denison, R.E., Hetherington, E.A., Koepnick, R.B., Nelson, H.K., and Otto, J.B., 1982, Variation of seawater $^{87}Sr/^{86}Sr$ throughout Phanerozoic time: Geology, v. 10, p. 516-519.

Burruss, R.C., 1981, Hydrocarbon fluid inclusions in studies of sedimentary diagenesis, *in* Hollister, L.S., and Crawford, M.L., eds., Short course in fluid inclusions; application to petrology: Mineralogic Association of Canada, Short Course Handbook, V. 6, p. 138-156.

Burruss, R.C., 1991, Practical aspects of fluorescence microscopy of petroleum fluid inclusions, *in* Barker, C.E., and Kopp, O.C., eds., Luminescence microscopy; qualitative and quantitative applications: SEPM (Society for Sedimentary Geology), Short Course Note Series #25, p. 1-7.

Bushnag, I.O., 1989, Geological characterization of the Cunningham gas storage reservoir, Pratt and Kingman counties, Kansas: M.S. thesis, Wichita State University, Wichita, Kansas, 139 p.

Buxton, T.M., and Sibley, D.F., 1981, Pressure solution features in a shallow buried limestone: Journal of Sedimentary Petrology, v. 51, p. 19-26.

Calder, H.S., Kaufman, J., Hanson, G.N., and Meyers, W.J., 1984, Two-stage cementation of the Burlington-Keokuk Limestone in Illinois, Missouri, and Iowa (abs.): Geological Society of America Abstracts with Programs, v. 16, p. 631.

Cander, H.S., Kaufman, J., Daniels, L.D., and Meyers, W.J., 1988, Regional dolomitization of shelf carbonates in the Burlington-Keokuk Formation (Mississippian), Illinois and Missouri; constraints from cathodoluminescent zonal stratigraphy, *in* Shukla, V., and Baker, P.A., eds., Sedimentology and geochemistry of dolostones: Society of Economic Paleontologists and Mineralogists, Special Publication 43, p. 129-144.

Cantrell, D.L., and Walker, K.R., 1985, Deposition and diagenetic patterns, ancient oolite, Middle Ordovician, eastern Tennessee: American Association of Petroleum Geologists, Bulletin, v. 55, p. 518-531.

Capps, W.M., 1965, Nestcatunga field, *in*, Kansas oil and gas fields, v. 4: Kansas Geological Society, Wichita, Kansas, p. 157-162.

Caputo, M.V., and Crowell, J.C., 1985, Migration of glacial centers across Gondwana during the Paleozoic Era: Geological Society of America, Bulletin, v. 96, p. 1,020-1,036.

Carozzi, A.V., 1989, Carbonate rock depositional models; a microfacies approach: Prentice Hall, Englewood Cliffs, New Jersey, 604 p.

Carr, T.R., and Lundgren, C.E., 1994, Use of gamma ray spectral log to recognize exposure surfaces at the reservoir scale; Big Bow field (St. Louis Limestone), Kansas, *in* Dolson, J.C., Hendricks, M.L., and Wescott, W.A., eds., Unconformity-related hydrocarbons in sedimentary sequences, a guidebook for petroleum exploration and exploitation in clastic and carbonate sediments: Rocky Mountain Association of Petroleum Geologists, Denver, Colorado: p. 79-88, 281.

Cayeux, L., 1935, Les roches sédimentaires de France; roches carbonatées: Masson, Paris, France, 463 p.

Chafetz, H.S., 1972, Surface diagenesis of limestone: Journal of Sedimentary Petrology, v. 42, p. 325-329.

Chenoweth, P.A., 1966, Viola oil and gas field of the Mid-Continent, *in* Schramm, M.W., Jr., and Chenoweth, P.A., eds., Symposium on the Viola, Fernvale and Sylvan: Tulsa Geological Society, Digest, v. 34, p. 110-118.

Choquette, P.W., and Pray, L.C., 1970, Geologic nomenclature and classification of porosity in sedimentary carbonates: American Association of Petroleum Geologists, Bulletin, v. 54, p. 207-250.

Cisne, J.L., and Gildner, R.F., 1988, Measurement of sea-level change in epeiric seas; the Middle Ordovician transgression in the North American midcontinent, *in* Wilgus, C.K., Hastings, B.S., Kendall, C.G.St.C., Ross, C.A., and Van Wagoner, J.C., eds., Sea-level changes; an integrated approach: Society of Economic Paleontologists and Mineralogist, Special Publication 42, p. 217-225.

Clark, W.R., 1956, The Rhodes field, *in*, Kansas oil and gas fields, v. 1: Kansas Geological Society, Wichita, Kansas, p. 77-81.

Clementz, D.M., 1979, Effect of oil and bitumen saturation on source-rock pyrolysis: American Association of Petroleum Geologists, Bulletin, v. 63, p. 2,227-2,232.

Cole, V.B., 1975, Subsurface Ordovician rocks in Kansas: Kansas Geological Survey, Subsurface Geology Series 2, 18 p.

Coniglio, M., Sherlock, R., Williams-Jones, A.E., Middleton, K., and Frape, S.K., 1994, Burial and hydrothermal diagenesis of Ordovician carbonates from the Michigan basin, Ontario, Canada, *in* Purser, B., Tucker, M., and Zenger, D., eds., Dolomites -- a volume in honour of Dolomieu: International Association of Sedimentologists, Special Publication Number 21, p. 231-254.

Cook, T.D., and Bally, A.W, eds., 1975, Stratigraphic atlas of North and Central America: Princeton University Press, Princeton, New Jersey, 272 p.

Cooper, G.A., 1976, Early Middle Ordovician of the United States, *in* Bassett, M.G., ed., The Ordovician System: University of Wales Press, Cardiff, Wales, p. 171-194.

Coveney, R.M., Jr., Goebel, E.D., and Ragan, V.M., 1987, Pressures and temperatures from fluid inclusions in sphalerite from Midcontinent country rocks: Economic Geology, v. 82, p. 740-751.

Craig, H., 1957, Isotopic standards for carbon and oxygen and correction factors for mass spectrometric analysis of carbon dioxide: Geochimica et Cosmochimica Acta, v. 12, p. 133-149.

Cram, I.H., 1930, Early Paleozoic stratigraphy of the Wichita Mountain uplift, Oklahoma: American Association of Petroleum Geologists, Bulletin, v. 14, p. 623-626.

Cruce, J.D., 1956, Willowdale field, *in*, Kansas oil and gas fields, v. 1: Kansas Geological Society, Wichita, Kansas, p. 95-97.

Cullity, B.D., 1956, Elements of x-ray diffraction: Addison-Wesley Publishing Company, Reading, Massachusetts, 514 p.

Dapples, E.C., 1955, General lithofacies relationships of St. Peter Sandstone and Simpson Group: American Association of Petroleum Geologists, Bulletin, v. 39, p. 444-467.

Davies, G., 1979, Dolomite reservoir rocks; processes, controls, porosity development, *in* Geology of carbonate porosity: American Association of Petroleum Geologists, Continuing Education Course Note Series #11, p. C1-C17.

Davis, J.C., 1976, Contouring algorithms, *in*, AUTOCARTO II -- Proceedings of the International Symposium on Computer-Assisted Cartography: American Congress on Surveying and Mapping, p. 352-359.

Davis, J.C., 1986, Statistics and data analysis in geology (2nd edition): John Wiley and Sons, Inc., New York, New York, 646 p.

Davis, J.C., 1987, Contour mapping and Surface III: Science, v. 237, p. 669-672.

de Groot, K., 1967, Experimental dedolomitization: Journal of Sedimentary Petrology, v. 37, p. 1,216-1,220.

Decker, C.E., 1933, The Early Paleozoic stratigraphy of Arbuckle and Wichita Mountains: Tulsa Geological Society, Digest 1933, p. 55-57.

Decker, C.E., 1952, Stratigraphic significance of graptolites of Athens Shale: American Association of Petroleum Geologists, Bulletin, v. 36, p. 1-145.

Delgado, D.J., 1983, Deposition and diagenesis of the Galena Group in the upper Mississippi Valley, *in* Delgado, D.J., ed., Ordovician Galena Group; deposition, submarine and later diagenesis, and paleoecology: Society of Economic Paleontologists and Mineralogists, Great Lakes Section, 13th Annual Field Conference Guidebook, p. A1-A17.

Deming, D., and Nunn, J.A., 1991, Numerical simulations of brine migration by topographically driven recharge: Journal of Geophysical Research, v. 96, p. B2,485-B2,499.

Dennison, J.M., 1976, Appalachian Queenston delta related to eustatic sea-level drop accompanying Late Ordovician glaciation centered in Africa, *in* Bassett, M.G., ed., The Ordovician System: University of Wales Press, Cardiff, Wales, p. 121-151.

DePaolo, D.J., Kyte, F.T., Marshall, B.D., O'Neill, J.R., and Smit, J., 1983, Rb-Sr, Sm-Nd, K-Ca, O, and H isotopic study of Cretaceous-Tertiary boundary sediments, Caravaca, Spain; evidence for an oceanic impact site; Earth and Planetary Science Letters, v. 64, p. 356-373.

Dewey, J.F., and Bird, J.M., 1970, Mountain belts and the new global tectonics: Journal of Geophysical Research, v. 75, p. 2,625-2,647.

Dickas, A,B., 1986, Comparative Precambrian stratigraphy and structure along the Mid-Continent rift: American Association of Petroleum Geologists, Bulletin, v. 70, p. 225-238.

Dickson, J.A.D., 1965, A modified staining technique for carbonates in this section: Nature, no. 4971 (February 5th), p. 587.

Dickson, J.A.D., 1966, Carbonate identification and genesis as revealed by staining: Journal of Sedimentary Petrology, v. 53, p. 1,216-1,220.

Dorobek, S.L., 1987, Petrography, geochemistry, and origin of burial diagenetic facies, Siluro-Devonian Helderberg Group (carbonate rocks), central Appalachians: American Association of Petroleum Geologists, Bulletin, v. 71, p. 492-514.

Dott, R.H., Jr., Byers, C.W., Fielder, G.W., Stenzel, S.R., and Winfree, K.E., 1986, Aeolian to marine transition in Cambro-Ordovician cratonic sheet sandstones of the northern Mississippi Valley, U.S.A.: Sedimentology, v.33, p. 345-367.

Dott, R.H., Jr., and Roshardt, M.A., 1972, Analysis of cross-stratification in St. Peter Sandstone of southwestern Wisconsin: Geological Society of America, Bulletin, v. 83, p. 2,589-2,596.

Doveton, J.H., 1986, Log analysis of subsurface geology -- concepts and computer methods: John Wiley and Sons, New York, New York, 273 p.

Doveton, J.H., 1994, Geologic log interpretation: Society for Sedimentary Geology (SEPM), Short Course Notes #29, 169 p.

Doveton, J.H., Charpentier, R.R., and Metzger, E.P., 1990, Lithofacies analysis of the Simpson Group in south-central Kansas: Kansas Geological Survey, Petrophysical Series 5, 34 p.

Doveton, J.H., and Bornemann, E., 1981, Log normalization by trend surface analysis: The Log Analyst, v. 22, no. 4, p. 3-8.

Doveton, J.H., Ke-An, Zhu, and Davis, J.H., 1984, Three dimensional trend mapping using gamma-ray well logs -- Simpson Group, south-central Kansas: American Association of Petroleum Geologists, Bulletin, v. 68, p. 690-703.

Dow, W.G., and O'Connor, D.I., 1982, Kerogen maturity and type by reflected light microscopy applied to petroleum exploration, *in*, How to assess maturation and paleotemperatures: Society of Economic Paleontologists and Mineralogists, Short Course Notes #7, p. 133-157.

Driese, S.G., and Foreman, J.L., 1992, Paleopedology and paleoclimatic implications of Late Ordovician vertic paleosols, Juniata Formation, southern Appalachians: Journal of Sedimentary Petrology, v. 62, p. 71-83.

Droser, M.L., and Bottjer, D.J., 1988, Trends in depth and extent of bioturbation in Cambrian carbonate marine environments, western United States: Geology, v. 16, p. 233-236.

Duke, W.L., 1990, Hummocky cross-stratification, tropical hurricanes and intense winter storms: Sedimentology, v. 32, p. 167-194.

Duke, W.L., Arnott, R.W.C., and Cheel, R.J., 1991, Shelf sandstones and hummocky cross-stratification; new insights on a stormy debate: Geology, v. 19, p. 625-628.

Dunbar, C.O., and Rodgers, J., 1957, Principles of stratigraphy: John Wiley and Sons, New York, New York, 356 p.

Dunham, R.J., 1962, Classification of carbonate rocks according to depositional texture, *in* Ham, W.E., ed., Classification of carbonate rocks -- a symposium: American Association of Petroleum Geologists, Memoir 1, p. 108-121.

Ebers, M.L., and Kopp, O.C., 1979, Cathodoluminescent microstratigraphy in gangue dolomite, the Mascot-Jefferson City district, Tennessee: Economic Geology, v. 74, p. 908-918.

Edson, F.C., 1929, Pre-Mississippian sediments in central Kansas: American Association of Petroleum Geologists, Bulletin, v. 13, p. 441-458.

Elmore, R.D., Condon, D., Nick, K., and Coles, K., 1989, Fluid control on chemical remagnetization; the role of meteoric, hydrocarbon, and basinal fluids: Eos, Transactions of the American Geophysical Union, v. 70, p. 370.

Engelder, T., Geiser, P.A., and Alvarez, W., 1981, Role of pressure solution and dissolution in geology: Geology, v. 9, p. 44-45.

Enos, Paul, 1983, Shelf, *in* Scholle, P.A., Bebout, D.G., and Moore, C.H., Carbonate depositional environments: American Association of Petroleum Geologists, Memoir 33, p. 268-295.

Enos, Paul, 1988, Evolution of pore space in the Poza Rica trend (Mid-Cretaceous), Mexico: Sedimentology, v. 35, p. 287-326.

Enos, Paul, 1991, Sedimentary parameters for computer modeling, *in* Franseen, E.K., Watney, W.L., Kendall, C.G.St.C., and Ross, W., eds., Sedimentary modeling; computer simulations and methods for improved parameter definition: Kansas Geological Survey, Bulletin, v. 223, p. 63-99.

Enos, Paul, and Sawatsky, L.H., 1981, Pore networks in Holocene carbonate sediments: Journal of Sedimentary Petrology, v. 51, p. 961-985.

Erlenwein, S.D., 1985, Sullivan field, *in* Gerlach, P.M., and Hansen, T., Kansas oil and gas fields, v. 5: Kansas Geological Society, Wichita, Kansas, p. 279-288.

Espitalié, J., Laporte, J.L., Madec, M., Marquis, F., Leplat, P., Paulet, J., and Boutefeu, A., 1977, Méthode rapide de caractérisation des roches mères, et de leur potentiel pétrolier et de leur degré d'évolution: Revue de l'Institut Français du Pétrole, v. 32, p. 23-42.

Esslinger, B., 1983, Facies and depositional environment of the Simpson Group (Middle Ordovician) of central Oklahoma: M.S. thesis, University of Missouri, Columbia, Missouri, 72 p.

Evamy, B.D., 1967, Dedolomitization and the development of rhombohedral pores in limestones: Journal of Sedimentary Petrology, v. 37, p. 1,204-1,215.

Evamy, B.D., 1969, The precipitational environment and correlation of some calcite cements deduced from artificial staining: Journal of Sedimentary Petrology, v. 39, p. 787-793.

Evamy, B.D., and Shearman, D.J., 1965, The development of overgrowths from crinoid fragments: Sedimentology, v. 5, p. 211-233.

Fairbridge, R.W., 1971, Upper Ordovician glaciation in northwest Africa (reply): Geological Society of America, Bulletin, v. 82, p. 269-274.

Fara, D.R., and Keith, B.D., 1988, Depositional facies and diagenetic history of the Trenton limestone in northern Indiana, *in* Keith, B.D., ed., The Trenton Group (Upper Ordovician Series) of eastern North America; deposition, diagenesis, and petroleum: American Association of Petroleum Geologists, Studies in Geology 29, p. 277-298.

Feinstein, S., 1981, Subsidence and thermal history of southern Oklahoma aulacogen; implications for petroleum exploration: American Association of Petroleum Geologists, Bulletin, v. 65, p. 2,521-2,533.

Feldman, H.R., Brown, M.A., and Archer, A.W., 1993, Benthic assemblages as indicators of sediment stability; evidence from grainstones of the Harrodsburg and Salem Limestones (Mississippian, Indiana), *in* Keith, B.D., and Zuppann, C.W., Mississippian oolites and modern analogs: American Association of Petroleum Geologists, Studies in Geology 35, p. 115-128.

Filipek, L.H., 1992, Hydrodynamics of deep-basin flow; constraints on timing of MVT deposits and a mechanism for heating Pennsylvanian coal (abs.), *in* Johnson, K.S., and Cardott, B., eds., Source rocks in the southern Midcontinent: Oklahoma Geological Survey, Circular 93, p. 311-312.

Flint, R.F., 1971, Glacial and Quaternary geology: John Wiley and Sons, New York, New York, 892 p.

Folk, R.L., 1965, Some aspects of recrystallization in ancient limestones, *in* Pray, L.C., and Murray, R.C., eds., Dolomitization and limestone diagenesis; a symposium: Society of Economic Paleontologists and Mineralogists, Special Publication 13, p. 14-48.

Folk, R.L., 1974, The natural history of crystalline calcium carbonate; effect of magnesium content and salinity: Journal of Sedimentary Petrology, v. 44, p. 40-53.

Förster, A., and Merriam, D.F., 1993, Geothermal field investigation in south-central Kansas for parts of the Nemaha anticline and flanking Cherokee and Sedgwick basins: Basin Research, v. 5, p. 213-234.

Förster, A., and Merriam, D.F., 1994, Burial depth, missing stratigraphic section, and geothermics in the Cherokee basin of the midcontinent (abs.): American Association of Petroleum Geologists, Annual Convention Official Program, v. 3, p. 150-151.

Förster, A., and Merriam, D.F., in press, Burial depth, missing stratigraphic section, and geothermics in the Cherokee basin of the midcontinent: Journal of Sedimentary Research.

Fortey, R.A., 1984, Global earlier Ordovician transgressions and regressions and their biological implications, *in* Bruton, D.L., ed., Aspects of the Ordovician System: Palaeontological Contributions from the University of Oslo, no. 295, Universtetsforlaget, p. 37-50.

Fortey, R.A., Bassett, M.G., Harper, D.A.T., Hughs, R.A., Ingham, J.K., Molyneux, S.G., Owen, A.W., Owens, R.M., Rushton, A.W.A., and Sheldon, P.R., 1991, Progress and problems in the selection of stratotypes for the bases of the series in the Ordovician System of the historical type area in the U.K., *in* Barnes, C.R., and Williams, S.H., eds., Advances in Ordovician geology: Geological Survey of Canada, Paper 90-9, p. 271-282.

Fowler, M.G., and Douglas, A.G., 1984, Distribution and structure of hydrocarbons in four organic-rich Ordovician rocks: Organic Geochemistry, v. 6, p. 105-114.

Frank, J.R., Carpenter, A.B., and Oglesby, T.W., 1982, Cathodoluminescence and composition of calcite in the Taum Sauk Limestone (Upper Cambrian), southeast Missouri: Journal of Sedimentary Petrology, v. 52, p. 631-638.

Frazier, W.J., and Schwimmer, D.R., 1987, Regional Stratigraphy of North America: Plenum Press, New York, New York, 719 p.

Freeman, T., 1966, Petrology of the post-St. Peter Ordovician, northern Arkansas, *in* Schramm, M.W., Jr., and Chenoweth, P.A., eds., Symposium on the Viola, Fernvale and Sylvan: Tulsa Geological Society, Digest, v. 34, p. 82-98.

Fritz, R.D., and Medlock, P.L., 1993, Sequence stratigraphy of the Hunton Group as defined by core, outcrop, and log data, *in* Johnson, K.S., ed., Hunton Group core workshop and field trip: Oklahoma Geological Survey, Special Publication 93-4, p. 161-180.

Fritz, P., Lapcevic, P.A., Miles, M.C., Frape, S.K., Lawson, D.E., and O'Shea, K.J., 1988, Stable isotopes in sulphate minerals from the Salina Formation in southwestern Ontario: Canadian Journal of Earth Science, v. 25, p. 195-205.

Füchtbauer, H., 1974, Sediments and sedimentary rocks 1 (2nd edition): Halsted Press, New York, New York, 464 p.

Fuller, J.G.C.M., 1961, Ordovician and contiguous formations in North Dakota, South Dakota, Montana, and adjoining areas of Canada and United States: American Association of Petroleum Geologists, Bulletin, v. 45, p. 1,334-1,363.

Gardiner-Kuserk, M.A., 1988, Cyclic sedimentation patterns in the Middle and Upper Ordovician Trenton Group of central Pennsylvania, *in* Keith, B.D., ed., The Trenton Group (Upper Ordovician Series) of eastern North America; deposition, diagenesis, and petroleum: American Association of Petroleum Geologists, Studies in Geology 29, p. 55-76.

Garner, D.L., and Turcotte, D.L., 1984, The thermal and mechanical evolution of the Anadarko basin: Tectonophysics, v. 107, p. 1-24.

Garrison, R.E., 1981, Diagenesis of oceanic carbonate sediments; a review of the DSDP perspective, *in* Warme, J.E., Douglas, R.G., and Winterer, E.L., eds., The deep sea drilling project; a decade of progress: Society of Economic Paleontologists and Mineralogists, Special Publication 32, p. 181-207.

Garven, G., and Freeze, R.A., 1984a, Theoretical analysis of the role of groundwater flow in the genesis of stratabound ore deposits; 1. Mathematical and numerical model: American Journal of Science, v. 284, p. 1,085-1,124.

Garven, G., and Freeze, R.A., 1984b, Theoretical analysis of the role of groundwater flow in the genesis of stratabound ore deposits; 2. Quantitative results: American Journal of Science, v. 284, p. 1,125-1,174.

Garven, G., Ge, S., Person, M.A., and Sverjensky, D.A., 1993, Genesis of stratabound ore deposits in the midcontinent basins of North America, 1. The role of regional groundwater flow: American Journal of Science, v. 293, p. 497-568.

Ge, S., and Garven, G., 1992, Hydromechanical modeling of tectonically driven groundwater flow with application to the Arkoma foreland basin: Journal of Geophysical Research, v. 97, p. 9,119-9,144.

Ginsburg, R.N., 1957, Early diagenesis and lithification of shallow-water carbonate sediments in south Florida, *in* LeBlanc, R.J., and Breeding, J.G., eds., Regional aspects of carbonate deposition: Society of Economic Paleontologists and Mineralogists, Special Publication 5, p. 80-99.

Goebel, E.D., 1968a, Ordovician System, *in* Zeller, D.E., ed., The stratigraphic succession in Kansas: Kansas Geological Survey, Bulletin 189, p. 14-15.

Goebel, E.D., 1968b, Undifferentiated Silurian and Devonian, *in* Zeller, D.E., ed., The stratigraphic succession in Kansas: Kansas Geological Survey, Bulletin 189, p. 15-17.

Goebel, E.D., 1968c, Mississippian rocks of western Kansas: American Association of Petroleum Geologists, Bulletin, v. 52, p. 1,732-1,778.

Goldberg, M., 1967, Supratidal dolomitization and dedolomitization in Jurassic rocks of Hamakhtesh Hagatan, Israel: Journal of Sedimentary Petrology, v. 37, p. 760-773.

Goldhammer, R.K., Oswald, E.J., and Dunn, P.A., 1991, Hierarchy of stratigraphic forcing; example from Middle Pennsylvanian shelf carbonates of the Paradox basin, *in* Franseen, E.K., Watney, W.L., Kendall, C.G.St.C., and Ross, W., eds., Sedimentary modeling; computer simulations and methods for improved parameter definition: Kansas Geological Survey, Bulletin, v. 223, p. 361-414.

Goldsmith, J.R., and Graf, D.L., 1958a, Relations between lattice constants and composition of the Ca-Mg carbonates: The American Mineralogist, v. 43, p. 84-101.

Goldsmith, J.R., and Graf, D.L., 1958b, Structural and compositional variations in some natural dolomites: Journal of Geology, v. 66, p. 678-692.

Goldstein, R.H., 1986, Reequilibration of fluid inclusions in low-temperature calcium-carbonate cement: Geology, v. 14, p.p. 792-795.

Goldstein, R.H., and Reynolds, T.J. 1994, Systematics of fluid inclusions in diagenetic minerals: SEPM (Society for Sedimentary Geology), Short Course Notes #31, 199 p.

Grabau, A.W., 1905, Physical character and history of some New York formations: Science, n.s., v. 22, p. 534.

Granath, V.C., 1991, Geochemical constraints on the origin of dolomite in the Ordovician Trenton and Black River Limestones, Albion-Scipio area, Michigan (abs.): American Association of Petroleum Geologists, Bulletin, v. 75, p. 584-585.

Gregg, J.M., 1985, Regional epigenetic dolomitization in the Bonneterre Dolomite (Cambrian), southeastern Missouri: Geology, v. 13, p. 503-506.

Gregg, J.M., Howard, S.A., and Mazzullo, S.J., 1992, Early diagenetic recrystallization of Holocene (<3000 years old) peritidal dolomites, Ambergris Cay, Belize: Sedimentology, v. 39, p. 143-160.

Gregg, J.M., and Shelton, K.L., 1990, Dolomitization and dolomite neomorphism in the back reef facies of the Bonneterre and Davis Formations (Cambrian), southeastern Missouri: Journal of Sedimentary Petrology, v. 60, p. 549-562.

Gregg, J.M., Shelton, K.L., and Bauer, R.M., 1992, Geochemical and fluid inclusion evidence for regional alteration of Upper Cambrian carbonates by basinal fluids in southern Missouri: Oklahoma Geological Survey, Circular 93, p. 313-320.

Gregg, J.M., and Sibley, D.F., 1984, Epigenetic dolomitization and the origin of xenotopic dolomite texture: Journal of Sedimentary Petrology, v. 54, p. 908-931.

Gretener, P.E., and Curtis, C.D., 1982, Role of temperature and time on organic metamorphism: American Association of Petroleum Geologists, Bulletin, v. 66, p. 1,124-1,149.

Grover, G., Jr., and Read, J.F., 1983, Paleoaquifer and deep burial related cements defined by regional cathodoluminescent patterns, Middle Ordovician carbonates, Virginia: American Association of Petroleum Geologists, Bulletin, v. 67, p. 1,275-1,303.

Gussow, W.C., 1954, Differential entrapment of oil and gas; a fundamental principle: American Association of Petroleum Geologists, Bulletin, v. 38, p. 816-853.

Habicht, J.K.A., 1979, Paleoclimate, paleomagnetism, and continental drift: American Association of Petroleum Geologists, Studies in Geology, No. 9, 31 p.

Handford, C.R., and Loucks, R.G., 1993, Carbonate depositional sequence and systems tracts -- responses of carbonate platforms to relative sea-level changes, *in* Loucks, R.G., and Sarg, J.F., eds., Carbonate sequence stratigraphy, recent developments and applications: American Association of Petroleum Geologists, Memoir 57, p. 3-41.

Hardie, L.A., 1987, Dolomitization; a critical review of some current views: Journal of Sedimentary Petrology, v. 57, p. 166-183.

Hardy, R.G., and Tucker, M.E., 1988, X-ray powder diffraction of sediments, *in* Tucker, M.E., ed., Techniques in sedimentology: Blackwell Scientific Publications, London, England, p. 191-228

Harms, J.C., Southard, J.B., and Walker, R.G., 1975, Structures and sequences in clastic rocks: Society of Economic Paleontologists and Mineralogist (Society for Sedimentary Geology), Short Course No. 9, 161 p.

Harris, A., 1979, Conodont color alteration, and organo-mineral metamorphic index, and its application to Appalachian basin geology, *in* Scholle, P.A., and Schlugar, P.R., eds., Aspects of diagenesis: SEPM (Society for Sedimentary Geology), Special Publication 26, p. 17-43.

Harris, R.W., 1957, Ostracoda of the Simpson Group of Oklahoma: Oklahoma Geological Survey, Bulletin, v. 75, 333 p.

Hatch, J.R., Jacobson, S.R., Witzke, B.J., Risatti, J.B., Anders, D.E., Watney, W.L., Newell, K.D., and Vuletich, A.K., 1987, Possible late Middle Ordovician organic carbon isotope excursion; evidence from Ordovician oils and hydrocarbon source rocks, mid-Continent and east-central United States: American Association of Petroleum Geologists, Bulletin, v. 71, p. 1,342-1,354.

Haq, B.U., and Van Eysinga, W.B., 1987, Geological Time Scale (4th edition): Elsevier Science Publishers B.V., Amsterdam, The Netherlands.

Heckel, P.H., 1977, Origin of phosphatic black shale facies in Pennsylvanian cyclothems of North America: American Association of Petroleum Geologists, Bulletin, v. 61, p. 1,045-1,068.

Hemming, N.G., Meyers, W.J., and Grams, J.C., 1989, Cathodoluminescence in diagenetic calcites; the roles of Fe and Mn as deduced from electron probe and spectrophotometric measurements: Journal of Sedimentary Petrology, v. 59, p. 404-411.

Héroux, Y., Chagnon, A., and Bertrand, R., 1979, Compilation and correlation of major thermal maturation indicators: American Association of Petroleum Geologists, Bulletin, v. 63, p. 2,128-2,144.

Hiestand, T.C., 1933, Voshell field, McPherson County, Kansas: American Association of Petroleum Geologists, Bulletin, v. 17, p. 169-191.

Hilpman, P.L., 1967, Devonian stratigraphy in Kansas; a progress report: Tulsa Geological Society, Digest, v. 35, p. 88-98.

Hoffman, C.F., Foster, C.B., Powell, T.G., and Summons, R.E., 1987, Hydrocarbon biomarkers from Ordovician sediments and the fossil alga *Gloeocapsomorpha priscae* Zalessky 1917: Geochimica et Cosmochimica Acta, v. 51, p. 2,681-2,697.

Houseknecht, D.W., Hathon, L.A., and McGilvery, 1992, Thermal maturity of Paleozoic strata in the Arkoma basin: Oklahoma Geological Survey, Circular 93, p. 122-132.

Huff, W.D., Bergstrom, S.M., and Kolata, D.R., 1992, Gigantic Ordovician volcanic ash fall in North America and Europe; biological, tectonomagmatic, and event-stratigraphic significance: Geology, v. 20, p. 875-878.

Huffman, G.G., and Starke, J.M., Jr., 1960, A Chazyan faunule from the Lower Tyner, northeastern Oklahoma: Oklahoma Geological Survey, Notes, v. 20, p. 268-271.

Imbt, W.C., 1941, Zenith pool, Stafford County, Kansas, *in* Levorsen, A.I., ed., Stratigraphic Type Oil Fields: American Association of Petroleum Geologists, Tulsa, Oklahoma, p. 139-165.

Ireland, H.A., 1965, Regional depositional basin and correlation of Simpson Group, *in* Herndon, T., and Schramm, M.W., Jr., eds., Symposium on the Simpson: Tulsa Geological Society, Digest, v. 33, p. 74-89.

Ireland, H.A., 1966, Resume and setting of Middle and Upper Ordovician stratigraphy, midcontinent and adjacent regions, *in* Schramm, M.W., Jr., and Chenoweth, P.A., eds., Symposium on the Viola, Fernvale and Sylvan: Tulsa Geological Society, Digest, v. 34, p. 26-40.

Ireland, H.A., 1967, Zonation and correlation of the subsurface Hunton Group (Silurian-Devonian) in Kansas by Foraminifera and acid residues, *in* Teichert, C., and Yochelson, E.L., eds., Essays in paleontology and stratigraphy -- R.C. Moore commemorative volume: University of Kansas, Department of Geology, Special Publication 2, p. 479-502.

Jaanusson, V., 1984, Ordovician benthic macrofaunal associations, *in* Bruton, D.L., ed., Aspects of the Ordovician System: Palaeontological Contributions from the University of Oslo, no. 295, Universtetsforlaget, p. 127-139.

Jacobson, S.R., Hatch, J.R., Teerman, S.C., and Askin, R.A., 1988, Middle Ordovician organic matter assemblages and their effect on Ordovician-derived oils: American Association of Petroleum Geologists, Bulletin, v. 72, p. 1,090-1,100.

James, N.P., and Bone, Y., 1989, Petrogenesis of Cenozoic, temperate water calcarenites, South Australia; a model for meteoric/shallow burial diagenesis calcite sediments: Journal of Sedimentary Petrology, v. 59, p. 191-203.

James, N.P., Bone, Y., and Kyser, T.K., 1993, Shallow burial dolomitization and dedolomitization of mid-Cenozoic, cool-water, calcitic, deep-shelf limestones, southern Australia: Journal of Sedimentary Petrology, v. 63, p. 528-538.

Jenden, P.D., Newell, K.D., Kaplan, I.R., and Watney, W.L., 1988, Composition and stable-isotope geochemistry of natural gases from Kansas, Midcontinent, U.S.A.: Chemical Geology, v. 71, p. 117-147.

Jenkins, W.A.M., 1979, Chitinozoa from the Ordovician Sylvan Shale of the Arbuckle Mountains, Oklahoma: Palaeontology, v. 13, p. 261-288.

Jennette, D.C., and Pryor, W.A., 1993, Cyclic alternation of proximal and distal storm facies; Kope and Fairview formations (Upper Ordovician), Ohio and Kentucky: Journal of Sedimentary Petrology, v. 63, p. 183-203.

Jewett, J.M., 1951, Geologic structures in Kansas: Kansas Geological Survey, Bulletin 90, part 6, p. 105-172.

Kansas Geological Survey and Tertiary Oil Recovery Project, 1991, Zenith field -- a field demonstration project for improved efficiency for oil and gas recovery in Kansas: Final Report submitted to the Kansas Corporation Commission, 92 p., with appendices.

Kansas State Board of Agriculture, 1985, 69th annual report and farm facts: Kansas State Board of Agriculture, Topeka, Kansas, 272 p.

Kastner, M., 1982, When does dolomitization occur and what controls it? (abs.): 11th International Congress of Sedimentology, Hamilton, Ontario, Canada, p. 124.

Katz, A., and Matthews, A., 1977, The dolomitization of $CaCO_3$, an experimental study at 252-295 °C: Geochimica et Cosmochimica Acta, v. 41, p. 297-308.

Kaufman, J., Cander, H.S., Daniels, L.D., and Meyers, W.J., 1988, Calcite cement stratigraphy and cementation history of the Burlington-Keokuk Formation (Mississippian), Illinois and Missouri: Journal of Sedimentary Petrology, v. 58, p. 312-326.

Kay, G.M., 1937, Stratigraphy of the Trentonian Group: Geological Society of America, Bulletin, v. 48, p. 233-302.

Keelan, D.K., 1977, Core analysis, *in* LeRoy, L.W., LeRoy, D.O., and Raese, J.W., Subsurface geology -- petroleum, mining, construction (4th edition): Colorado School of Mines Press, Golden, Colorado, p. 114-126.

Keith, B.D., 1988a, Regional facies of Upper Ordovician Series of eastern North America, *in* Keith, B.D., ed., The Trenton Group (Upper Ordovician Series) of eastern North America; deposition, diagenesis, and petroleum: American Association of Petroleum Geologists, Studies in Geology 29, p. 1-16.

Keith, B.D., 1988b, Reservoirs resulting from facies-independent dolomitization; case histories from the Trenton and Black River carbonate rocks of the Great Lakes area, *in* Keith, B.D., ed., The Trenton Group (Upper Ordovician Series) of eastern North America; deposition, diagenesis, and petroleum: American Association of Petroleum Geologists, Studies in Geology 29, p. 267-276.

Kerans, C., 1988, Karst-controlled reservoir heterogeneity in Ellenberger Group carbonates of west Texas: American Association of Petroleum Geologists, Bulletin, v. 49, p. 1,160-1,183.

Ketner, K.B., 1968, Origin of Ordovician quartzite in the Cordilleran miogeosyncline: United States Geological Survey, Professional Paper 600-B, p. B211-B217.

King, C.R., 1965a, Alameda field, *in*, Kansas oil and gas fields, v. 4: Kansas Geological Society, Wichita, Kansas, p. 1-17.

King, C.R., 1965b, Alameda field, Sedgwick embayment "sleeper": American Association of Petroleum Geologists, Bulletin, v. 49, p. 1,562.

Knauth, L.P., 1979, A model for the origin of chert in limestone: Geology, v. 7, p. 274-277.

Kohout, F.A., 1967, Groundwater flow and the geothermal regime of the Floridian plateau: Transactions of the Gulf Coast Association of Geological Societies, v. 17, p. 339-354.

Kolata, D.R., Huff, W.D., and Frost, J.K., 1983, Correlation of K-bentonites in the Decorah Subgroup of the Mississippi Valley by chemical fingerprinting, *in* Delgado, D.J., ed., Ordovician Galena Group; deposition, submarine and later diagenesis, and paleoecology: Society of Economic Paleontologists and Mineralogists, Great Lakes Section, 13th Annual Field Conference Guidebook, p. F1-F15.

Kornfeld, J.A., 1943, Peace Creek field (Kansas), a stratigraphic trap: World Petroleum, v. 14, no. 13, p. 38-47.

Kralik, M., 1984, Effects of cation-exchange treatment and acid leaching on the Rb-Sr system of illite from Fithian, Illinois: Geochimica et Cosmochimica Acta, v. 48, p. 527-533.

Kreisa, R., 1981, Storm-generated sedimentary structures un subtidal marine facies with examples from the Middle and Upper Ordovician of southwestern Virginia: Journal of Sedimentary Petrology, v. 51, p. 823-848.

Kuhnhenn, G.L., and Carozzi, A.V., 1977, Carbonate microfacies of the Platteville Group (Middle Ordovician), Lee and LaSalle counties, Illinois: U.S.A. Archives Science, Gèneve, v. 30, p. 179-212.

Kuykendall, M.D., and Fritz, R.D., 1993, Misener sandstone; distribution and relationship to late/post-Hunton unconformities, *in* Johnson, K.S., ed., Hunton core workshop and field trip: Oklahoma Geological Survey, Special Publication 93-4, p. 117-134.

Lambert, M.W., 1992a, Lithology and geochemistry of shale members within the Devonian-Mississippian Chattanooga (Woodford) Shale, Midcontinent, USA, Ph.D. dissertation, University of Kansas, Lawrence, Kansas, 163 p.

Lambert, M.W., 1992b, Internal stratigraphy of the Chattanooga Shale in Kansas and Oklahoma, *in* Johnson, K.S., and Cardott, B., eds., Source rocks in the southern Midcontinent: Oklahoma Geological Survey, Circular 93, p. 94-103.

Land, L.S., 1973, Holocene meteoric dolomitization of Pleistocene limestones, North Jamaica: Sedimentology, v. 20, p. 411-424.

Land, L.S., 1980, The isotopic and trace element geochemistry of dolomite; the state of the art, *in* Zenger, D.H., Dunham, J.B., and Ethington, R.L., eds., Concepts and models of dolomitization: Society of Economic Paleontologists and Mineralogists, Special Publication 28, p. 87-110.

Land, L.S., 1983a, The application of stable isotopes to studies of the origin of dolomite and to problems of diagenesis of clastic sediments, *in* Arthur, M.A., Anderson, T.F., Kaplan, I.R., Veizer, J., and Land, L.S., Stable isotopes in sedimentary geology: Society of Economic Paleontologists and Mineralogists, Short Course No. 10, p.4-1-4-22.

Land, L.S., 1983b, Dolomitization: American Association of Petroleum Geologists, Continuing Education Course Note Series, #24, 20 p.

Land, L.S., 1985, The origin of massive dolomite: Journal of Geological Education, v. 33, p. 112-125.

Land, L.S., and Prezbindowski, D.R., 1981, The origin and evolution of saline formation waters, Lower Cretaceous carbonates, south-central Texas, U.S.A.: Journal of Hydrology, v. 54, p. 51-74.

Leach, D.L., Plumlee, G.S., Hofstra, A.H., Landis, G.P., Rowan, E.L., and Viets, J.G., 1991, Origin of late dolomite cement by CO_2-saturated deep basin brines; evidence from the Ozark region, central United States: Geology, v. 19, p. 348-351.

Leach, D.L., and Rowan, E.L., 1986, Genetic link between Ouachita foldbelt tectonism and the Mississippi Valley-type lead-zinc deposits of the Ozarks: Geology, v. 14, p. 931-935.

Leatherock, C., 1945, The correlation of rocks of Simpson age in north-central Kansas with the St. Peter Sandstone and associated rocks in northwestern Missouri: Kansas Geological Survey, Bulletin 60, pt. 1, p. 1-16.

LeCampion-Alsumard, T., Campbell, S.E., and Golubic, S., 1982, Endoliths and the depth of the photic zone -- discussion: Journal of Sedimentary Petrology, v. 52, p. 1,333.

Leckie, D.A., and Krystinik, L.F., 1989, Is there evidence for geostrophic currents preserved in the sedimentary record of inner to middle-shelf deposits?: Journal of Sedimentary Petrology, v. 59, p. 862-870.

Lee, J.L., 1983, Stratigraphy and depositional environments of the Plattin Limestone (Middle Ordovician), parts of Independence, Izard, and Stone counties, Arkansas, *in* Hyne, N.J., ed., Limestones of the Mid-Continent, Tulsa Geological Society, Special Publication 2, p. 307-326.

Lee, W., 1943, The stratigraphy and structural development of the Forest City basin in Kansas: Kansas Geological Survey, Bulletin 51, 142 p.

Lee, W., 1949, Subsurface geologic cross section from Barber County to Saline County, Kansas: Kansas Geological Survey, Oil and Gas Investigations 9, 16 p.

Lee, W., 1956, Stratigraphy and structural development of the Salina basin area: Kansas Geological Survey, Bulletin 121, 167 p.

Lee, W., Grohskopf, J.B., Reed, E.C., and Hershey, H.C., 1946, The structural development of the Forest City basin in Missouri, Kansas, Iowa, and Nebraska: United States Geological Survey, Oil and Gas Investigations, Preliminary Map No. 48.

Lenz, A.C., 1976, Late Ordovician -- Early Silurian glaciation and the Ordovician -- Silurian boundary in the northern Canadian cordillera: Geology, v. 3, p. 313-317.

Leutoff, A.H., and Meyers, W.J., 1984, Regional distribution of microdolomite inclusions in Mississippian echinoderms from southwestern New Mexico; Journal of Sedimentary Petrology, v. 54, p. 432-446.

Lindholm, R.C., and Finkelman, R.B., 1972, Calcite staining; quantitative determination of ferrous iron: Journal of Sedimentary Petrology, v. 42, p. 239-242.

Lippmann, F., 1973, Sedimentary carbonate minerals: Springer-Verlag, Berlin, Germany, 228 p.

Lloyd, M., 1966, Oxygen isotope enrichment of seawater by evaporation: Geochimica et Cosmochimica Acta, v. 30, p. 801-814.

Lohmann, K.C., 1983, Unraveling the diagenetic history of carbonate reservoirs -- integration of petrographic and chemical data, *in* Wilson, J.L., Wilkinson, B.H., Lohmann, K.C., and Hurley, N.F., A short course -- new ideas and methods for exploration for carbonate reservoirs: Dallas Geological Society, Short Course, Section V, 41 p.

Lohmann, K.C., and Walker, J.C.G., 1989, The $\delta^{18}O$ record of Phanerozoic abiotic marine calcite cements: Geophysics Research Letters, v. 16, p. 319-322.

Longman, M.W., 1980, Carbonate diagenetic textures from nearsurface diagenetic environments: American Association of Petroleum Geologists, Bulletin, v. 64, p. 461-487.

Longman, M.W., 1981, Carbonate diagenesis as a control on stratigraphic traps (with examples from the Williston basin): American Association of Petroleum Geologists, Educational Course Note Series #21, 159 p.

Longman, M.W., and Mench, P.A., 1978, Diagenesis of Cretaceous limestones in the Edwards aquifer system of south-central Texas; a scanning electron microscope study: Sedimentary Geology, v. 21, p. 241-276.

Longman, M.W., and Palmer, S.E., 1987, Organic geochemistry of Mid-Continent Middle and Late Ordovician oils: American Association of Petroleum Geologists, Bulletin, v. 71, p. 938-950.

Lopatin, N.V., 1971, Temperature and geologic time as factors in coalification (in Russian): Akademiya Nauk SSSR Izvestiya, Seriya Geologicheskaya, no. 3, p. 95-106.

Lucia, F.J., 1962, Diagenesis of a crinoidal sediment: Journal of Sedimentary Petrology, v. 32, p. 848-865.

Lucia, F.J., and Murray, R.C., 1967, Origin and distribution of porosity in crinoidal rocks: VIIth World Petroleum Congress, v. 2, p. 409-423.

Lukas, K.J., 1978, Depth distribution and form among common microboring algae from the Florida continental shelf (abs.): Geological Society of America, Abstracts with Programs, Toronto, Canada, p. 448.

Lumsden, D.N., 1979, Discrepancy between thin-section and x-ray estimates of dolomite in limestone: Journal of Sedimentary Petrology, v. 49, p. 429-436.

Lumsden, D.N., and Chimahusky, J.S., 1980, Relationship between dolomite nonstoichiometry and carbonate facies parameters, *in* Zenger, D.H., Dunham, J.B., and Ethington, R.L., eds., Concepts and models of dolomitization: Society of Economic Paleontologists and Mineralogists, Special Publication 28, p. 123-137.

Lyons, P.L., 1966, Trenton extent in the United States, a regional study, *in* Schramm, M.W., Jr., and Chenoweth, P.A., eds., Symposium on the Viola, Fernvale and Sylvan: Tulsa Geological Society, Digest, v. 34, p. 99-109.

Machel, H.G., Mason, R.A., Mariano, A.N., and Mucci, A., 1991, Causes and measurements of luminescence in calcite and dolomite, *in* Barker, C.E., and Kopp, O.C., eds., Luminescence microscopy and spectroscopy; qualitative and quantitative applications, SEPM (Society for Sedimentary Geology, Short Course Note Series #25, p. 9-25, 173.

Machel, H.G., and Burton, E.A., 1991, Factors governing cathodoluminescence in calcite and dolomite, and their implications for studies of diagenesis, *in* Barker, C.E., and Kopp, O.C., eds., Luminescence microscopy and spectroscopy; qualitative and quantitative applications, SEPM (Society for Sedimentary Geology, Short Course Note Series #25, p. 37-57.

Machel, H.G., and Mountjoy, E.W., 1986, Chemistry and environments of dolomitization -- a reappraisal: Earth Science Reviews, v. 23, p. 175-222.

Mackenzie, F.T., Bischoff, W.D., Bishop, F.C., Loijens, M., Schoonmaker, J., and Wollast, R., 1983, Magnesian calcites; low-temperature occurrence, solubility, and solid-solution behavior: Reviews in Mineralogy, v. 11, p. 97-144.

Magaritz, M., Goldenburg, L., Kafri, U., and Arad, A., 1980, Dolomite formation in the seawater-freshwater interface: Nature, v. 287, p. 622-624.

Martin, R.L., Winters, J.C., and Williams, J.A., 1963, Distributions of n-paraffins in crude oils and their implications to petroleum: Nature, v. 199, p. 110-113.

McCabe, C., and Elmore, R.D., 1989, The occurrence and origin of late Paleozoic remagnetization in the sedimentary rocks of North America: Reviews of Geophysics, v. 27, p. 471-494.

McCaleb, G.A., and Wheeler, J., 1965, Wil field, *in*, Kansas oil and gas fields, v. 4: Kansas Geological Society, Wichita, Kansas, p. 278-289.

McElhinny, M.W., and Briden, J.C., 1971, Continental drifting during the Paleozoic: Earth and Planetary Science Letters, v. 10, p. 407-416.

McElhinny, M.W., and Opdyke, N.D., 1973, Remagnetization hypothesis discounted; a paleomagnetic study of the Trenton Limestone, New York State: Geological Society of America, Bulletin, v. 84, p. 3,697-3,708.

McGinness, D.H., 1956, Lerado and Lerado Southwest fields, *in*, Kansas oil and gas fields, v. 4: Kansas Geological Society, Wichita, Kansas, p. 63-68.

McKee, E.D., Oriel, S.S., and fifteen others, 1967, Paleotectonic investigations of the Permian System in the United States: United States Geological Survey, Professional Paper 515, 271 p.

McKerrow, W.S., 1979, Ordovician and Silurian changes in sea level: Journal of the Geological Society, v. 136, p. 137-147.

McNeice, B.T., 1986, Clay-rich zones in Upper Pennsylvanian (Missourian-Virgilian) shelf limestones, eastern Kansas: M.S. thesis, University of Kansas, Lawrence, Kansas, 86 p.

McQueen, H.S., and Greene, F.C., 1938, Geology of northwestern Missouri: Missouri Bureau of Geology and Mines, v. 25, 2nd series, p. 40-42.

Melchin, M.J., and Mitchell, C.E., 1991, Late Ordovician extinction in the Graptoloidea, *in* Barnes, C.R., and Williams, S.H., eds., Advances in Ordovician geology: Geological Survey of Canada, Paper 90-9, p. 143-156.

Merriam, D.F., 1963, Geologic history of Kansas: Kansas Geological Survey, Bulletin 162, 317 p.

Merriam, D.F., and Atkison, W.R., 1956, Simpson-filled sinkholes in eastern Kansas: Kansas Geological Survey, Bulletin 119, pt. 2, p. 61-80.

Meyers, W.J., 1974, Carbonate cement stratigraphy of the Lake Valley Formation (Mississippian), Sacramento Mountains, New Mexico: Journal of Sedimentary Petrology, v. 44, p. 837-861.

Meyers, W.J., 1978, Carbonate cements; their regional distribution and interpretation in Mississippian limestones of southwestern New Mexico: Sedimentology, v. 25, p. 105-124.

Meyers, W.J., and Lohmann, K.C., 1978, Microdolomite-rich syntaxial cements -- proposed meteoric-marine mixing zone phreatic cements from Mississippian limestones, New Mexico: Journal of Sedimentary Petrology, v. 48, p. 475-488.

Miall, A.D., 1984, Principles of sedimentary basin analysis: Springer-Verlag, New York, New York, 490 p.

Mišík, M., 1993, Carbonate rhombohedra in nodular cherts; Mesozoic of the West Carpathians: Journal of Sedimentary Petrology, v. 63, p. 275-281.

Morrow, D.W., 1982a, Diagenesis I. Dolomite -- part I; the chemistry of dolomitization and dolomite precipitation: Geoscience Canada, v. 9. p. 5-13.

Morrow, D.W., 1982b, Diagenesis II. Dolomite -- part II; dolomitization models and ancient dolostones: Geoscience Canada, v. 9. p. 95-107.

Murray, R.C., 1960, Origin of porosity in carbonate rocks: Journal of Sedimentary Petrology, v. 30, p. 59-84.

Murray, R.C., and Lucia, F.J., 1967, Cause and control of dolomite distribution by rock selectivity: Geological Society of America, v. 78, p. 21-36.

Mussman, W.J., and Read, J.F., 1986, Sedimentology and development of a passive- to convergent-margin unconformity; Middle Ordovician Knox unconformity, Virginia Appalachians: Geological Society of America, Bulletin, v. 97, p. 282-295.

Neuman, R.B., 1976, Ordovician of the eastern United States, *in* Bassett, M.G., ed., The Ordovician System: University of Wales Press, Cardiff, Wales, p. 121-151.

Newell, K.D., 1986, Pre-Pennsylvanian subcrop map of Rice and Ellsworth counties, Kansas: Kansas Geological Survey, Open-File Report 86-6 (1:100,000 map).

Newell, K.D., 1987a, Pre-Pennsylvanian subcrop map of Salina basin, Kansas: Kansas Geological Survey, Open-File Report 87-3 (1:500,000 map).

Newell, K.D., 1987b, Pre-Chattanooga subcrop map of Salina basin, Kansas: Kansas Geological Survey, Open-File Report 87-4 (1:500,000 map).

Newell, K.D., 1989, Distribution of Upper Devonian-Lower Mississippian Misener sandstone in Salina basin, Kansas: Kansas Geological Survey, Open-File Report 89-18 (1:500,000 map with discussion).

Newell, K.D., 1990, Lindsborg field--U.S.A., Salina basin, Kansas; *in* Beaumont, E.A. and Foster, N.H., eds., American Association of Petroleum Geologists, Treatise of Petroleum Geology, Atlas of Oil and Gas Fields, Structural Trap IV, p. 347-382: American Association of Petroleum Geologists, Tulsa, Oklahoma.

Newell, K.D., 1991, Databases for Zenith oil field: Kansas Geological Survey Open-File Report 91-30, 11 p., with data diskette.

Newell, K.D., Cunningham, K.J., Wong, J.-C., Watney, W.L., and Weatherbie, W.J., 1991, Large- and small-scale geological features of the Zenith field and their bearing on planning for enhanced oil recovery operations: Proceedings of the 9th Tertiary Oil Recovery Conference, Wichita, KS; Tertiary Oil Recovery Project, University of Kansas, p. 99-130.

Newell, K.D., Watney, W.L., Cheng, S.W.L., and Brownrigg, R.L., 1987, Spatial and stratigraphic distribution of Kansas oil and gas production: Kansas Geological Survey, Subsurface Geology Series 9, 86 p.

Newell, K.D., Watney, W.L., Stephens, B.P., and Hatch, J.R., 1987b, Hydrocarbon potential in Forest City basin: Oil and Gas Journal, v. 88 (October 19th), p. 58-62.

Nielson, P., Swennen, R., and Keppens, E., 1994, Multiple-step recrystallization within massive ancient dolomite units; an example from the Dinantian of Belgium: Sedimentology, v. 41, p. 567-584.

Northrop, D.A., and Clayton, R.N., 1966, Oxygen-isotope fractionations in systems containing dolomite: Journal of Geology, v. 74, p. 174-196.

Nuffield, E.W., 1966, X-ray diffraction methods: John Wiley and Sons, New York, New York, 409 p.

Oros, M.O., 1965, Albion and Albion North fields, Reno County, Kansas, *in*, Kansas oil and gas fields, v. 4: Kansas Geological Society, Wichita, Kansas, p. 18-34.

O'Neil, J.R., Clayton, R.N., and Mayeda, T.K., 1969, Oxygen isotope fractionation in divalent metal carbonates: Journal of Chemistry and Physics, v. 51, p. 5,547-5,548.

O'Shea, K.J., Miles, M.C., Fritz, P., Frape, S.K., and Lawson, D.E., 1988, Oxygen-18 and carbon-13 in the carbonates of the Salina Formation of southwestern Ontario: Canadian Journal of Earth Science, v. 25, p. 182-194.

Paddleford, J.T., 1941, The Zenith pool of Stafford and Reno counties, Kansas: Mines Magazine, v. 31, p. 445-448, 454, 470, 472.

Page, J.H., 1940, Larger gas fields in Kansas: American Association of Petroleum Geologists, Bulletin, v. 24, p. 1,779-1,797.

Palmer, A.R., compiler, 1983, The Decade of North American Geology 1983 Geologic Time Scale: Geology, v. 11, p. 503-504.

Perkins, R.D., 1968, Primary rhombic calcite in sedimentary carbonates: Journal of Sedimentary Petrology, v. 38, p. 1,371-1,374.

Peters, K.E., 1986, Guidelines for evaluating petroleum source rock using programmed pyrolysis: American Association of Petroleum Geologists, Bulletin, v. 70, p. 318-329.

Plummer, L.N., 1977, Defining reactions and mass transfer in part of the Floridian Aquifer: Water Resources Research, v. 13, p. 801-812.

Plummer, L.N., and Back, W., 1980, The mass balance approach; applications to interpreting the chemical evolution of hydrologic systems: American Journal of Science, v. 280, p. 130-142.

Popp, B.N., Anderson, T.F., and Sandberg, P.A., 1986, Brachiopods as indicators of original isotopic compositions in some Paleozoic limestones: Geological Society of America, Bulletin, v. 97, p. 1,262-1,269.

Potter, R.W., II, Clynne, M.A., and Brown, D.L., 1978, Freezing point depression of aqueous sodium chloride solutions: Economic Geology, v. 73, p. 283-285.

Prezbindowski, D.R., and Larese, R.E., 1987, Experimental stretching of fluid inclusions in calcite -- implications for diagenetic studies: Geology, v. 15, p. 333-336.

Prezbindowski, D.R., and Tapp, J.B., 1991, Dynamics of fluid inclusions alteration in sedimentary rocks; a review and discussion; Organic Geochemistry, v. 17, p. 131-142.

Price, L., 1980, Shelf and shallow basin oil as related to hot-deep origin of petroleum: Journal of Petroleum Geology, v. 3, p. 91-116.

Purser, B.H., Brown, A., and Aissaoui, D.M., 1994a, Nature, origins and evolution of porosity in dolomites, *in* Purser, B., Tucker, M., and Zenger, D., eds., Dolomites -- a volume in honour of Dolomieu: International Association of Sedimentologists, Special Publication Number 21, p. 283-308.

Purser, B.H., Tucker, M.E., and Zenger, D.H., 1994b, Problems, progress and future research concerning dolomites and dolomitization, *in* Purser, B., Tucker, M., and Zenger, D., eds., Dolomites -- a volume in honour of Dolomieu: International Association of Sedimentologists, Special Publication Number 21, p. 3-20.

Quinlan, J.F., 1972, Karst-related mineral deposits and possible criteria for the recognition of paleokarsts; a review of preservable characteristics of Holocene and older karst terranes: 24th International Geological Congress, v. 6, p. 156-167.

Radke, B.M., and Mathis, R.L., 1980, On the formation and occurrence of saddle dolomite: Journal of Sedimentary Petrology, v. 50, p. 1,149-1,168.

Railsback, L.B., 1993a, Contrasting styles of chemical compaction in the Upper Pennsylvanian Dennis Limestone in the Midcontinent region, U.S.A.: Journal of Sedimentary Geology, v. 63, p. 61-72.

Railsback, L.B., 1993b, Lithologic controls on morphology of pressure-dissolution surfaces (stylolites and dissolution seams) in Paleozoic carbonate rocks from the mideastern United States: Journal of Sedimentary Geology, v. 63, p. 513-522.

Rast, N., 1989, The evolution of the Appalachian chain, *in* Bally, A.W., and Palmer, A.R., eds., The geology of North America -- an overview: Geological Society of America, The Geology of North America, v. A., p. 323-348.

Reed, J.D., Illich, H.A., and Horsfield, B., 1986, Biochemical evolutionary significance of Ordovician oils and their sources, *in* Leythaeuser, D., and Rullkotter, J., eds., Advances on organic geochemistry 1985: Pergamon Press, Oxford, England, p. 347-358.

Reeder, R.J., 1981, Electron optical investigations of sedimentary dolomites: Contributions in Mineralogy and Petrology, v. 76, p. 148-157.

Reeves, J.R., 1929, El Dorado oil field, Butler County, Kansas, *in*, Structure of typical American oil fields, v. 2: American Association of Petroleum Geologists, Tulsa, Oklahoma, p. 160-167.

Retallack, G.J., 1988, Field recognition of paleosols, *in* Reinhardt, J., and Sigleo, W.R., eds., Paleosols and weathering through geologic time: Geological Society of America, Special Paper 216, p. 1-20.

Rich, J.L., 1933, Distribution of oil pools in Kansas in relation to pre-Mississippian structure and areal geology: American Association of Petroleum Geologists, Bulletin, v. 17, p. 793-815.

Rock Color Chart Committee, 1984, Rock color chart: Geological Society of America, Boulder, Colorado.

Roedder, E., 1970, Application of an improved crushing stage to study gases in fluid inclusions: Schweizerische Mineralogische und Petrographische Mitteilungen, v. 50, p. 41-58.

Roedder, E., 1984, Fluid inclusions: Mineralogical Society of America, Reviews in Mineralogy, v. 12, 644 p.

Ross, C.G., 1991, LEO II -- automated legal and geographic reference system conversion in Kansas: Kansas Geological Survey, Open-File Report 91-54 (revised 1992), 68 p.

Ross, R.J., Jr., 1976, Ordovician sedimentation in the western United States, *in* Bassett, M.G., ed., The Ordovician System: University of Wales Press, Cardiff, Wales, p. 73-105.

Rowan, E.L., 1986, Cathodoluminescent zonation in hydrothermal cements; relation to Mississippi Valley-type Pb-Zn mineralization in southern Missouri and northern Arkansas, *in* Hagni, R.D., ed., Process Mineralogy VI: Metallurgical Society, Warrenville, Pennsylvania, p. 69-87.

Rowley, D.B., and Kidd, W.S.F., 1981, Stratigraphic relationships and detrital composition of the Medial Ordovician flysch of western New England; implications for the tectonic evolution of the Taconic orogeny: Journal of Geology, v. 89, p. 199-218.

Rutledge, R.B., and Bryant, H.S., 1937, Cunningham field, Kingman and Pratt counties, Kansas: American Association of Petroleum Geologists, Bulletin, v. 21, p. 500-524.

St. Clair, P.N., 1982, Depositional history and diagenesis of the Viola Limestone in south-central Kansas: M.S. thesis, University of Kansas, Lawrence, Kansas, 66 p.

St. Clair, P.N., 1985, Core studies of the Viola Limestone in Barber and Pratt counties, *in* Watney, W.L., Doveton, J.H., and Walton, A.W., comps., Core studies in Kansas -- sedimentology and diagenesis of economically important rock strata in Kansas: Kansas Geological Survey, Subsurface Geology Series 6, p. 8-16.

Salgat, B., 1983, Scully field -- Marion County, Kansas: American Association of Petroleum Geologists, Bulletin, v. 67, p. 1,327.

Salvador, A., 1985, Chronostratigraphic and geochronometric scales in COSUNA stratigraphic correlation charts of the United States: American Association of Petroleum Geologists, Bulletin, v. 69, p. 181-189.

Sampson, R.J., 1988, SURFACE III user's manual: Interactive Concepts Incorporated, Surface III Office, Kansas Geological Survey, Lawrence, Kansas, 277 p.

Schlumberger, 1987, Log interpretation principals/applications, volume I: Schlumberger Educational Services, Houston, Texas, 198 p.

Schmidt, V., 1965, Facies, diagenesis, and related reservoir properties in the Gigas beds (upper Jurassic), northwestern Germany, *in* Pray, L.C., and Murray, R.C., eds., Dolomitization and limestone diagenesis; a symposium: Society of Economic Paleontologists and Mineralogists, Special Publication 13, p. 124-168.

Schneider, H., 1976, The progressive crystallization and ordering of low-temperature dolomites: Mineralogical Magazine, v. 40, p. 579-587.

Schneidermann, N., and Harris, P.M., eds., 1985, Carbonate cements: Society of Economic Paleontologists and Mineralogists, Special Publication 36, 379 p.

Scholle, P.A., 1977, Chalk diagenesis and its relation to petroleum exploration; oil from chalks, a modern miracle?: American Association of Petroleum Geologists, Bulletin, v. 61, p. 982-1,009.

Scholle, P.A., 1978, A color illustrated guide to carbonate rock constituents, cements, and porosities: American Association of Petroleum Geologists, Memoir 27, 241 p.

Schramm, M.W., Jr., 1964, Paleogeologic and quantitative lithofacies analysis, Simpson Group, Oklahoma: American Association of Petroleum Geologists, Bulletin, v. 48, p. 1,164-1,195.

Schramm, M.W., Jr., 1965a, Resume of Simpson (Ordovician) stratigraphy, *in* Herndon, T., and M.W. Schramm, M.W., Jr., eds., Symposium on the Simpson: Tulsa Geological Society, Digest, v. 33, p. 26-34.

Schramm, M.W., Jr., 1965b, Distribution of Simpson production, central mid-continent region, *in* Herndon, T., and Schramm, M.W., Jr., eds., Symposium on the Simpson: Tulsa Geological Society, Digest, v. 33, p. 130-133.

Scotese, C.R., and McKerrow, W.S., 1991, Ordovician plate reconstructions, *in* Barnes, C.R., and Williams, S.H., eds., Advances in Ordovician geology: Geological Survey of Canada, Paper 90-9, p. 271-282.

Shaver, R.H., and others, 1985, Midwestern basins and arches region, *in* Childs, O.E., and others, eds., Correlation of stratigraphic units of North America: American Association of Petroleum Geologists, COSUNA Chart MBA.

Sheats, C., Jr., 1956, Enlow pool, *in*, Kansas oil and gas fields, v. 1: Kansas Geological Society, Wichita, Kansas, p. 36-37.

Sheehan, P.M., 1973, The relation of Late Ordovician glaciation to the Ordovician-Silurian changeover in North American brachiopod faunas: Lethaia, v. 6, p. 147-154.

Sheehan, P.M., 1975, Brachiopod synecology in a time of crisis (Late Ordovician -- Early Silurian): Paleobiology, v. 1, p. 205-212.

Shelton, K.L., Bauer, R.M., and Gregg, J.M., 1992, Fluid-inclusion studies of regionally extensive epigenetic dolomites, Bonneterre Dolomite (Cambrian), southeast Missouri; evidence of multiple fluids during dolomitization and lead-zinc mineralization: Geological Society of America, Bulletin, v. 104, p. 675-683.

Shinn, E.A., 1968, Practical significance of birdseye structures in carbonate rocks: Journal of Sedimentary Petrology, v. 38, p. 215-223.

Shinn, E.A., Ginsburg, R.N., and Lloyd, R.M., 1965, Recent supratidal dolomite from Andros Island, Bahamas, *in* Pray, L.C., and Murray, R.D., eds., Dolomitization and limestone diagenesis, a symposium: Society of Economic Paleontologists and Mineralogists, Special Publication 13, p. 112-113.

Sibley, D.F., 1990, Unstable to stable transformations during dolomitization: Journal of Geology, v. 98, p. 739-748.

Sibley, D.F., and Gregg, J.M., 1987, Classification of dolomite rock texture: Journal of Sedimentary Petrology, v. 75, p. 967-975.

Simms, M., 1984, Dolomitization by groundwater-flow systems in carbonate platforms: Transactions of the Gulf Coast Association of Geological Societies, v. 34, p. 411-420.

Simo, J.A., Johnson, C.M., Vandrey, M.R., Brown, P.E., Castrogiovanni, E., Drzewiecki, P.E., Valley, J.W., and Boyer, J., 1994, Burial dolomitization of the Middle Ordovician Glenwood Formation by evaporitic brines, Michigan basin, *in* Purser, B., Tucker, M., and Zenger, D., eds., Dolomites -- a volume in honour of Dolomieu: International Association of Sedimentologists, Special Publication Number 21, p. 169-186.

Skelly Oil Company Geological Department, 1956, Cunningham field, *in*, Kansas oil and gas fields, v. 1: Kansas Geological Society, Wichita, Kansas, p. 25-28.

Sloan, R.E., 1987, An Ordovician time scale, *in* Sloan, R.E., ed., Middle and Late Ordovician lithostratigraphy and biostratigraphy of the upper Mississippi Valley: Minnesota Geological Survey, Report of Investigations 35, p. 232.

Sloss, L.L., 1963, Sequences in the cratonic interior of North America: Geological Society of America, Bulletin, v. 74, p. 93-114.

Sloss, L.L., 1988, Tectonic evolution of the craton in Phanerozoic time, *in* Sloss, L.L., ed., Sedimentary cover -- North American craton, U.S.: Geological Society of America, The Geology of North America, v. D-2., p. 25-51.

Sperber, C.M., Wilkinson, B.H., and Peacor, D.R., 1984, Rock composition, dolomite stoichiometry, and rock/water reactions in dolomitic carbonate rock: Journal of Geology, v. 92, p. 609-622.

Spjeldnaes, N., 1976, Ordovician climates, *in* Bassett, M.G., ed., The Ordovician System: University of Wales Press, Cardiff, Wales, p. 67-69.

Spötl, C., Houseknecht, D.W., and Longstaff, F.J., 1994, Authigenic chlorites in sandstones as indicators of high-temperature diagenesis, Arkoma foreland basin, USA: Journal of Sedimentary Research, v. A64, p. 553-556.

Statler, A.T., 1965, Stratigraphy of the Simpson Group in Oklahoma, *in* Herndon, T., and Schramm, M.W., Jr., eds., Symposium on the Simpson: Tulsa Geological Society Digest, v. 33, p. 162-211.

Stavnes, S.A., 1982, A preliminary study of the subsurface temperature distribution in Kansas and its relationship to the geology: M.S. thesis, University of Kansas, Lawrence, Kansas, 311 p.

Stavnes, S.A., and Steeples, D.W., 1982, Geothermal resources of Kansas: Division of Geothermal Energy, United States Department of Energy (1:500,000 map with text and subsidiary maps; map also available at Kansas Geological Survey).

Steeples, D.W., 1989, Structure of the Salina-Forest City interbasin boundary from seismic studies, *in* Steeples, D.W., ed., Geophysics in Kansas: Kansas Geological Survey, Bulletin 226, p. 31-52.

Steincamp, H.L., 1965, Lerado pool, *in*, Kansas oil and gas fields, v. 4: Kansas Geological Society, Wichita, Kansas, p. 114-122.

Sumner, D.Y., and Grotzinger, J.P., 1993, Numerical modeling of ooid size and the problem of Neoproterozoic giant ooids: Journal of Sedimentary Petrology, v. 63, p. 974-982.

Swanson, R.G., 1981, Sample examination manual: Methods in Exploration Series, Association of Petroleum Geologists, Tulsa, Oklahoma.

Sweet, W.C., 1984, Graphic correlation of upper Middle and Upper Ordovician rocks, North American midcontinent province, U.S.A., *in* Bruton, D.L., ed., Aspects of the Ordovician System: Palaeontological Contributions from the University of Oslo, no. 295, Universtetsforlaget, p. 23-35.

Sweet, W.C., and Bergstrom, S.M., 1976, Conodont biostratigraphy of the Middle and Upper Ordovician of the United States midcontinent, *in* Bassett, M.G., ed., The Ordovician System: University of Wales Press, Cardiff, Wales, p. 121-151.

Sweet, W.C., 1992, Middle and Late Ordovician conodonts from southwestern Kansas and their biostratigraphic significance, *in* Chaplin, J.R., and Barrick, J.E., eds., Special papers in paleontology; a tribute to Thomas W. Amsden: Oklahoma Geological Survey Bulletin 145, p. 181-191.

Swinchatt, J.P., 1969, Algal boring; a possible depth indicator in carbonate rocks and sediments: Geological Society of America, Bulletin, v. 80, p. 1,391-1,396.

Taff, J.A., 1902, Description of the Atoka quadrangle [Indian Territory]: United States Geological Survey, Geological Atlas, Folio 79, 8 p.

Taff, J.A., 1904, Preliminary report on the geology of the Arbuckle and Wichita Mountains in Indian Territory and Oklahoma: United States Geological Survey, Professional Paper No. 31, (republished as Oklahoma Geological Survey, Bulletin 12, 1928).

Taylor, M.H., Jr., 1946, Siluro-Devonian strata in central Kansas: American Association of Petroleum Geologists, Bulletin, v. 30, p. 1,221-1,254.

Taylor, M.H., Jr., 1947a, Upper Ordovician shales in central Kansas: American Association of Petroleum Geologists, Bulletin, v. 31, p. 1,594-1,607.

Taylor, M.H., Jr., 1947b, Middle Ordovician limestones in central Kansas: American Association of Petroleum Geologists, Bulletin, v. 31, p. 1,242-1,282.

Templeton, J.S., and Willman, H.B., 1963, Champlainian Series (Middle Ordovician) in Illinois: Illinois Geological Survey, Bulletin 89, 260 p.

Thompson, J.W., 1956, Cairo North pool, *in*, Kansas oil and gas pools, v. 1, Kansas Geological Society, Wichita, Kansas, p. 16-17.

Tissot, B.P., and Welte, D.H., 1984, Petroleum formation and occurrence (2nd edition): Springer-Verlag, Berlin, Germany, 699 p.

Towe, K.M., 1967, Echinoderm calcite; single crystal or polycrystalline aggregate: Science, v. 157, p. 1,048-1,050.

Tucker, M., 1990, Dolomites and dolomitization models, *in* Tucker, M.E., and Wright, V.P., Carbonate sedimentology: Blackwell Scientific Publications, Oxford, England, p. 365-400.

Tucker, V.M., 1956, Deerhead pool, *in*, Kansas oil and gas pools, v. 1, Kansas Geological Society, Wichita, Kansas, p. 29-31.

Twenhofel, W.H. (chairman), and fourteen others, 1954, Correlation of the Ordovician formations of North America: Geological Society of America, Bulletin, v. 65, p. 247-298.

Vail, P.R., Mitchum, R.M., Jr., Thompson, S., III, 1977, Global cycles of relative changes of sea level, *in* Payton, C.E., ed., Seismic stratigraphy -- applications to hydrocarbon exploration: American Association of Petroleum Geologists, Memoir 26, p. 83-98.

van Gijzel, P., 1982, Characterization and identification of kerogen and bitumen and determination of thermal maturation by means of qualitative and quantitative microscopical techniques: SEPM (Society for Sedimentary Geology), Short Course Notes #7, p. 159-216.

Van Wagoner, J.C., Mitchum, R.M., Campion, K.M., and Rahmanian, V.D., 1990, Siliciclastic sequence stratigraphy in well logs, cores, and outcrops: American Association of Petroleum Geologists, Methods in Exploration Series 7, 55 p.

Van Schmus, W.R., Green, J.C., and Halls, H.C., 1982, Geochronology of Keweenawan rocks of the Lake Superior region, *in* Wold, R.J., and Hinze, W.J., eds., Geology and tectonics of the Lake Superior basin: Geological Society of America, Memoir 156, p. 165-172.

Veizer, J., and Compston, W., 1974, $^{87}Sr/^{86}Sr$ composition of seawater during the Phanerozoic: Geochimica et Cosmochimica Acta, v. 38, p. 1,461-1,484.

Veizer, J., Fritz, P., and Jones, B., 1986, Geochemistry of brachiopods, oxygen and carbon isotopic records of Paleozoic oceans: Geochimica et Cosmochimica Acta, v. 50, p. 1,679-1,696.

Ver Wiebe, W.A., 1947, Zones of the Viola Formation in western Kansas (abs.): Geological Society of America, Bulletin, v. 58, p. 1,236.

Ver Wiebe, W.A., 1948, So-called Maquoketa of Barber County, Kansas: American Association of Petroleum Geologists, Bulletin, v. 32, p. 126-128.

Von der Borch, C.C., and Jones, J.B., 1976, Spherular modern dolomite from the Coorong area, South Australia: Sedimentology, v. 23, p. 587-591.

Voss, R.L., and Hagni, R.D., 1985, The application of cathodoluminescence microscopy to the study of sparry dolomite from the Viburnum Trend, southeastern Missouri, *in* Hausen, O.C., and Kopp, O.C., eds., Mineralogy -- applications to the mineral industry: American Institute of Mining and Metallurgy, and Society of Mining Engineers, New York, New York, p. 51-68.

Walter, L.M., 1983, New data on the relative stability of carbonate minerals; implications for diagenesis and stability (abs.): American Association of Petroleum Geologists, Bulletin, v. 67, p. 566.

Walters, R.F., 1958, Differential entrapment of oil and gas in Arbuckle dolomite of central Kansas: American Association of Petroleum Geologists, Bulletin, v. 42, p. 2,133-2,173.

Walther, J., 1894, Einleitung in die Geologie als historische Wissenschaft: Jena, Fischer Verlag, v. 3, 1,055 p.

Walton, A.W., Wojcik, K.M, Goldstein, R.H., and Barker, C.E., 1995, Diagenesis of Upper Carboniferous rocks in the Ouachita foreland shelf in mid-continent USA; an overview of widespread effects of a Variscan-equivalent orogeny: Geologishes Rundschau, v. 84, p. 535-551.

Wanless, H.R., 1979, Limestone response to stress; pressure solution and dolomitization: Journal of Sedimentary Petrology, v. 49, p. 437-462.

Waples, D.W., 1980, Time and temperature in petroleum generation; application of Lopatin's technique to petroleum exploration: American Association of Petroleum Geologists, Bulletin, v. 64, p. 916-926.

Waples, D.W., 1981, Organic geochemistry for exploration geologists: Burgess Publishing Company, Minneapolis, Minnesota, 151 p.

Wardlaw, N.C., 1976, Pore geometry of carbonate rocks as revealed by pore casts and capillary pressure: American Association of Petroleum Geologists, Bulletin, v. 60, p. 245-267.

Watney, W.L., Wong, J.-C., and French, J.A., 1991, Computer simulation of Upper Pennsylvanian (Missourian) carbonate-dominated cycles in western Kansas, *in* Franseen, E.K., Watney, W.L., Kendall, C.G.St.C., and Ross, W., eds., Sedimentary modeling; computer simulations and methods for improved parameter definition: Kansas Geological Survey, Bulletin, v. 223, p. 415-430.

Weber, J.N., 1969, The incorporation of magnesium into skeletal calcites of echinoderms: American Journal of Science, v. 267, p. 537-566.

Wengerd, S.A., 1948, Fernvale and Viola limestones in south-central Oklahoma: American Association of Petroleum Geologists, Bulletin, v. 32, p. 2,183-2,254.

Wentworth. C.K., 1922, A scale of grade class terms for clastic sediments: Journal of Geology, v. 30, p. 377-392.

Weyl, P.K., 1960, Porosity through dolomitization -- conservation-of-mass requirement: Journal of Sedimentary Petrology, v. 30, p. 85-90.

Wigley, T.M.L., and Plummer, L.N., 1976, Mixing of carbonate waters: Geochimica et Cosmochimica Acta, v. 40, p. 989-995.

Wigley, T.M.L., Plummer, L.N., and Pearson, F.J., Jr., 1978, Mass transfer and carbon isotope evolution of natural water systems: Geochimica et Cosmochimica Acta, v. 42, p. 1,117-1,139.

Williams, D.F., 1988, Evidence for and against sea-level changes from the stable isotope record of the Cenozoic, *in* Wilgus, C.K., Posamentier, H., Ross, C.A., and Kendall, C.G.St.C., eds., Sea-level changes -- an integrated approach: Society of Economic Paleontologists and Mineralogists, Special Publication 42, p. 31-36.

Willman, H.B., and Kolata, D.R., 1978, The Platteville and Galena groups in northern Illinois: Illinois Geological Survey, Circular 502, 75 p.

Wilson, J.L., 1975, Carbonate rocks in geologic history: Springer-Verlag, New York, New York, 471 p.

Winter, B.L., Johnson, C.M., Simo, J.A., and Valley, J.W., 1995, Paleozoic fluid history of the Michigan basin; evidence from dolomite geochemistry in the Middle Ordovician St. Peter Sandstone: Journal of Sedimentary Research, v. A65, p. 306-320.

Wise, S.W., and Weaver, F.M., 1974, Chertification of oceanic sediments, *in* Hsu, K.J., and Jenkyns, H.C., eds., Pelagic sediments; on land and under the sea: International Association of Sedimentologists: Special Publication 1, p. 301-326.

Witzke, B.J., 1980, Ordovician paleogeography of the Transcontinental arch, *in* Fouch, T.D., and Magathan, E.R., eds., Paleozoic paleogeography of the west-central United States: The Rocky Mountain Section of the Society of Economic Paleontologists and Mineralogists, Rocky Mountain Paleogeography, Symposium 1, p. 1-18.

Witzke, B.J., 1983, Ordovician Galena Group in Iowa subsurface, *in* Delgado, D.J., ed., Ordovician Galena Group; deposition, submarine and later digenesis, and paleoecology: Society of Economic Paleontologists and Mineralogists, Great Lakes Section, 13th Annual Field Conference Guidebook, p. D1-D26.

Witzke, B.J., 1990, Palaeoclimatic constraints for Palaeozoic palaeolatitudes of Laurencia and Euramerica, *in* McKerrow, W.S., and Scotese, eds., Palaeozoic palaeogeography and biogeography: Geological Society, Special Memoir 12, p. 57-74.

Wojcik, K.M., 1991, Diagenesis of Pennsylvanian sandstones and limestones, Cherokee basin, southeastern Kansas; importance of regional flow: Ph.D dissertation, University of Kansas, Lawrence, Kansas, 349 p.

Wojcik, K.M., Goldstein, R.H., and Walton, A.W., 1994, History of diagenetic fluids in a distant foreland area, Middle and Upper Pennsylvanian, Cherokee basin, Kansas, USA; fluid inclusion evidence: Geochimica et Cosmochimica Acta, v. 58, p. 1,175-1,191.

Wojcik, K.M., McKibben, M.E., Goldstein, R.H., and Walton, A.W., 1992, Diagenesis, thermal history, and fluid migration, Middle and Upper Pennsylvanian Rocks, southeastern Kansas, *in* Johnson, K.S., and Cardott, B.J., eds., Source rocks in the southern midcontinent: Oklahoma Geological Survey, Circular 93, p. 144-159.

Woods, J.J., Bohling, G.C., McElwee, C.D., and Newell, K.D., 1988, Thermal basin modeling and analysis using the time-temperature index: Kansas Geological Survey, Open-File Report 88-28, 153 p.

Wright, B.J., 1960, Valley Center field, *in* Curtis, G.R., ed., Kansas oil and gas fields, v. 3 (northeastern Kansas), Kansas Geological Society, Wichita, Kansas, p. 149-156.

Wright, R.P., and Meyers, W.C., 1981, Organic-walled microplankton in the subsurface Ordovician of northeastern Kansas: Kansas Geological Survey, Subsurface Geology Series 4, 53 p.

Yarger, H.L., 1981, Aeromagnetic survey of Kansas: Eos, v. 62, no. 17, p. 173-178.

Yarger, H.L., 1983, Regional interpretation of Kansas aeromagnetic data: Kansas Geological Survey, Geophysical Series 1, 35 p.

Zeff, M.L., and Perkins, R.D., 1979, Microbial alteration of Bahamian deep-sea carbonates: Sedimentology, v. 26, p. 175-201.

Zeller, D.E., ed., 1968, The stratigraphic succession in Kansas: Kansas Geological Survey, Bulletin, v. 189, 81 p.

APPENDIX I -- TOPS OF SUB-UNITS OF VIOLA FORMATION, SOUTH-CENTRAL KANSAS (TAKEN FROM 1,709 WIRELINE LOGS)

KEY

A = upper cherty dolomitic limestone
B = upper limestone
C = lower cherty dolomitic limestone
D = basal limestone
E = Simpson Formation

abs -- unit not present because of erosion or nondeposition

(no value) -- unit not penetrated or logged

???? -- unit cannot be picked with confidence with present data

---- = no datum (i.e., surface, drill floor, or kelly bushing elevation) given for well

(all depths are in feet; wells listed first by northernmost townships and eastern ranges, then western ranges)

OPERATOR	WELL NAME	LOCATION S.	T.	R.	SPOT	DEPTHS A	B	C	D	E	DATUM
Adair et al.	#1 Carpenter-Simmons	25	17S	1E	NE NE NW	abs	3188	3203	3230	3274	1463
Booth	#1 Wedel	34	17S	1E	NW SW SE	abs	3174	3190	3224	3269	1458
Diamond Shamrock	#1-26A60 Scully	26	17S	2E	NE SE	abs	3112	3121	3162	3206	1464
Diamond Shamrock	#133 A78 Scully	33	17S	2E	SW SW SE	abs	3120	3130	3160	3204	1462
Geodessa	#1-A Rundberg	19	17S	3E	SW SE	3412	3422	3436	3456	3494	----
Kan-Go	#3 Novak	30	17S	5E	SW	abs	2732	2745	2781	2820	1480
Oil Property Mgmt.	#1 Fahrney	9	17S	6E	SE SE SW	abs	2216	2220	2255	2302	----
BMG	#1-22 Randle	22	17S	6E	SW NE	abs	1958	1960	2004	2040	1342
BMG	#1-32 Eckland	32	17S	6E	E2 SW NW	abs	2104	2108	2152	2188	1463
Conoco	#1 Elythe	13	17S	7E	SE SE SE	abs	3168	3176	3208	3228	1433
Berrong Enterprises	#2 Mulvane	36	17S	7E	SW SW	abs	2478	2490	2528	2548	1405
Diamond Shamrock	#1-9 Scully 181	9	18S	1E	SE SE	abs	3147	3154	3192	3234	1439
R.J. Walker	#1-11 Oberlander	11	18S	1E	SW SW NW	abs	3106	3114	3162	3206	1428
Pickrell Drlg.	#1-A Donahue	19	18S	1E	NW SE	abs	3274	3278	3318	3356	1485
Cobra	#1-3 Scully	3	18S	2E	NE NW NW	abs	3086	3089	3124	3170	1450
Hunt Oil	#1 Krispense	9	18S	2E	SE NE	abs	abs	3065	3104	3146	1424
George Reed	#2-M Scully	29	18S	2E	SW NW NE	abs	abs	3020	3068	3107	1409
Wildcat Resources	#1-34 Scully	34	18S	2E	S2 SW NW	abs	abs	2918	2964	2999	1371
Hunt Oil	#1 Vanier	16	18S	3E	N2 NE NW	abs	2933	2944	2982	3018	1389
McCown	#3 Klenda	36	18S	3E	SE NW SE	abs	abs	2794	2845	2878	1377
Sunflower	#1 Utting	34	18S	4E	SW SE NW	abs	2688	2710	2744	2777	1369
Burns Corp.	#1 Lehman	15	18S	5E	SE SE	abs	2236	2241	2285	2316	1410
BMG	#1-26 Symes	26	18S	5E	SW NE	abs	abs	abs	2076	2100	1446
Mack	#1 Frick	33	18S	5E	SE	abs	2530	2542			1470
Berrong Enterprises	#1 Mulvane	2	18S	7E		abs	2440	2450	2488	2506	1481
Berrong Enterprises	#5 Mulvane	26	18S	7E	SW NW	abs	2726	2751	2786	2800	1371
Aladdin Petrol.	#1 Weyand	22	19S	1E	SE SE NW	abs	abs	3290	3352	3380	1550
Anderson-Prichard	#1 Hett	3	19S	2E	SW NE SW	abs	abs	2920	2950	2982	1402
G.A. Reed	#1 Penner	17	19S	2E	NW NE NE	abs	3094	3096	3136	3174	1450
Wildcat Resources	#2 Jost	22	19S	2E	SE NW SW	abs	abs	2966	3016	3047	1397
Wildcat Resources	#1-28 Scully	28	19S	2E	N2 NW NE	abs	abs	2980	3020	3049	1407

APPENDIX I (continued)

OPERATOR	WELL NAME	LOCATION S.	T.	R.	SPOT	DEPTHS A	B	C	D	E	DATUM
F. Hawn	#1 Melcher	8	19S	3E	SE SW SW	abs	abs	2808	2850	2882	1339
Oil Property Mgmt.	#3 Vogel	11	19S	3E	SW NE SW	abs	abs	2761	2805	2834	----
Wildcat Resources	#1 Olsen	34	19S	3E	SW SE	abs	abs	2658	2696	2723	1329
J.T. Hannah	#1-SWD Wight	1	19S	4E	NW NW	abs	2672	2685	2722	2757	----
Nat'l Assoc. Pet.	#1 Baxter	28	19S	4E	NE NE SW	abs	2619	2640	2670	2704	1404
Cimarron Petrol.	#1 Hilsenbeck	36	19S	4E	NW NW	abs	2560	2570			1445
Raymond	#1 Stika	17	19S	5E	NW NW SE	abs	2570	2586	2622	2653	1444
Anderson-Prichard	#1 Church	24	19S	5E	SE SW SE	abs	2177	2198	2230	2260	1454
Anderson-Prichard	#1 Koegeboehn	19	19S	6E	NE NE NE	abs	2052	2072	2114	2144	1370
Brandt	#1 Reehling	29	19S	6E	SW SW NE	abs	abs	2147	2180	2210	1465
Stanolind	#1 N. Kline	10	19S	7E	SW SW NE	abs	abs	2188	2230	2262	1207
R.J. Walker	#1-15 Unruh	15	20S	1E	NW SW SE	abs	abs	3204	3220	3254	1485
R.J. Walker	#1-18 Goering	18	20S	1E	SE NE SE	abs	abs	abs	3385	3410	1566
McGinness	#1 Wiens	33	20S	2E	NE SE SW	abs	abs	2940	????	2998	1432
Cities Service	#1-D Loewen	36	20S	2E	SW SW SW	abs	abs	2883	2912	2934	1429
Anderson-Prichard	#1 Schaeffler	4	20S	3E	E2 E2 NE	abs	2676	2690	2715	2746	1343
Rains & Williamson	#1 Siebert	11	20S	3E	NW NW NE	abs	2607	2628	2648	2678	1348
Anadarko	#1-A Suderman	31	20S	3E	NE NW NW	abs	abs	2890	2930	2951	1401
E.H. Adair	#1 Ely	36	20S	3E	NE NE NW	abs	abs	2655	2672	2701	1372
Herndon Drlg.	#1 Skinner	4	20S	4E	NW SW SW	abs	2542	2570	2592	2624	1360
Herndon Drlg.	#1 Eliza Hett	23	20S	4E	NW NW SW	abs	2532	2570	2588	2618	1329
Patton	#1 Vogel	9	20S	5E	SE	abs	2444	2460	2496		1421
Range	#1 Schroeder	8	20S	6E	SE SE	abs	2288	2299	2332	2363	1432
Jay Boy	#1 Hettenbach	35	20S	6E	SE SW NW	abs	abs	abs	2572	2590	1414
B.C. Resources	#33-14 Williams	33	20S	7E	NW SE SW	2732	2754	2773	2803	2836	1479
Lone Star	#1 Koehn	2	21S	1E	SW NE	abs	abs	abs	3332	3364	1499
Shawver & Armour	#1 Goertzen	16	21S	1E	NW NE SW	abs	abs	abs	3426	3462	1550
Phillips	#1 Bernhard	24	21S	1E	SE SE SW	abs	abs	abs	3336	3370	1531
Glickman	#1 Voth	28	21S	1E	SE SE NW	abs	abs	abs	3458	3490	1538
Jay Boy	#1 Penner	3	21S	2E	SE SE	abs	abs	abs	2856	2894	1427
Raymond	#1 G. Hodges	5	21S	2E	NW NW SE	abs	abs	abs	3145	3178	1459
Cities Service	#1 Depler	26	21S	2E	SE NE NW	abs	abs	abs	3136	3180	1472
Round Table Invest.	#1-28 Suderman	28	21S	2E	SW	abs	abs	abs	3172	3212	1450
Cities Service	#3 Loewen	8	21S	3E	SW SE SW	abs	abs	abs	2870	2915	1401
Cascade	#1 Mott	10	21S	3E	SE SE	abs	abs	abs	2829	2872	1403
Anderson-Prichard	#1 Davis	21	21S	3E	NW NW NW	abs	abs	2939	2950	3004	1436
W. Osborn	#1 Slater	34	21S	3E	SE NE SW	abs	abs	2834	2852	2902	1394
Raymond	#1 Keirns	5	21S	4E	NE SW SW	abs	abs	abs	2560	2600	1371
Morris	#1 Bibler	24	21S	4E	NE NW NW	abs	abs	2382	2394	2440	1329
Toklan Prod.	#5 Stovall	29	21S	4E	SW NE NE	abs	abs	abs	2380	2414	1314
Pendleton	#8 Strait Ranch	8	21S	5E	S2 N2 SE	abs	abs	abs	2268	2302	1266
Murfin Drlg.	#1-29 Strait	29	21S	5E	SE SW NW	abs	2456	2476	2494	2528	1407
Conoco	#1 M.P. Berns	24	21S	6E	SE NW SE	abs	abs	abs	3042	3076	1444
Time Petrol.	#1 Wyckkoff	11	22S	1E	SW SE SW	abs	abs	abs	3396	3420	1514
G.L. Reasor	#1 Hudson	33	22S	1E	SW SE NE	abs	abs	3470	3490	3530	1470
Aladdin Petrol.	#1 Winsor	1	22S	2E	SW NW NE	abs	abs	abs	3105	3152	1463
E.H. Adair	#1 Wallace	6	22S	2E	SW SW NE	abs	abs	abs	2968	3014	1436
Herndon Drlg.	#1 Orpin	26	22S	2E	SE SE NW	abs	abs	3190	3226	3246	1466
Round Table Invest.	#1-3 Potter	3	22S	3E	SE	abs	abs	2880	2911	2953	1358
E.H. Adair	#1 Wallace	6	22S	3E	SW SW NE	abs	abs	abs	2968	3014	1436
Adair & L. Phillips	#1-B Wiebe	34	22S	3E	SW SE SW	abs	abs	3014	3036	3053	1458
Drillers & Prod.	#4 Faylor	4	22S	4E	SW SW	abs	abs	2484	2510	2538	1425
Hammer & MacLean	#3 Clark	15	22S	4E	SW NE SE	abs	abs	2596	????	2645	----
Adair & L. Phillips	#1 Meyer	21	22S	5E	SE SE NE	abs	abs	2628	2676	2704	1450
Pure	#1-A Langenegger	28	22S	5E	SW NE	abs	abs	2620	2654	2679	1476
Nat'l Assoc. Pet.	#1 Becker	32	22S	5E	SE SW NW	abs	abs	2658	2676	2700	1474
White & Ellis	#1 Chisholm	15	22S	6E	NW NW SW	abs	2988	3005	3026	3066	1736
Bay Petrol.	#1 Sauder	3	23S	1E	SE SW SW	abs	abs	3476	3486	3526	1466

APPENDIX I (continued)

OPERATOR	WELL NAME	LOCATION S.	T.	R.	SPOT	DEPTHS A	B	C	D	E	DATUM
Ingling at al.	#1 Krehbiel	14	23S	2E	SE SE NW	abs	abs	3255	3265	3287	1454
Charles Carlock	#1 Walton	19	23S	2E	SE NE NE	abs	abs	abs	3440	3472	1501
Husky	#1 Balzer	26	23S	2E	SW SE SW	abs	abs	3218	3230	3256	1418
E.H. Adair	#1 Regier	18	23S	3E	NE	abs	abs	abs	3134	3170	1448
E.H. Adair	#3 Schrivner	24	23S	3E	NW SW SW	abs	abs	abs	2735	2762	----
Adair & L. Phillips	#1 Decker	13	23S	4E	NW NW SE	abs	abs	2762	2792	2810	1441
CRA	#21 Lathrop	17	23S	4E	SW NE SW	abs	abs	abs	2436	2462	1363
Branine & Goering	#2 Everett	29	23S	4E	NW NE NW	abs	abs	abs	2016	2035	----
Rex & Morris	#1 Stucky	6	23S	5E	NW NW NE	abs	abs	abs	2723	2754	1465
Beaumont Petrol.	#1 O. Shields	34	23S	5E	NW NE SW	abs	abs	2540	2566	2590	1429
White & Ellis	#1 Classen	5	23S	6E	SE SE NW	abs	abs	3224	3234	3260	1465
B.C. Resources	#9-15 Olberding	9	23S	6E	SW SE	abs	abs	3334	3360	3378	1451
Gear Petrol.	#1-6 Spangler	6	24S	1E	SE NW	abs	abs	3508	3520	3531	1430
Bedell-Catt	#1 Fluke	11	24S	1E	NW NW SW	abs	abs	abs	3462	3484	1462
Conoco	#1 Hickerson	27	24S	1E	SW SE SW	abs	abs	abs	3536	3562	1453
Don Slawson	#2-B Ulmer	11	24S	2E	W2 W2 NW	abs	abs	abs	3250	3274	1417
Renfro Drlg.	#1 Nattier	30	24S	2E	SE SW SW	abs	abs	abs	3424	3446	1425
Sunshine	#1-A Mellor	12	24S	3E	NE NW	abs	abs	2762	2786	2800	1385
Anderson-Prichard	#1 Wiebe	33	24S	3E	NE NW NE	abs	abs	3223	3238	3256	1383
Range	#2 Bohlin	6	24S	4E	NE SW	abs	abs	abs	2670	2703	1338
Selkirk	#1 Pickett	10	24S	4E	NW SE NE	abs	abs	abs	2760	2785	1392
Raymond	#2 Claassen	18	24S	4E	SE NE NW	abs	abs	abs	2785	2807	1330
Reach Petrol.	#1-17 Joseph	17	24S	5E	NE NE SE	abs	abs	2684	2700	2715	1431
Range	#4-A Weber	19	24S	5E	SW SE	abs	abs	2774	2780	2797	1428
Allied Material	#1 Rukert	15	24S	6E	SE SW NE	abs	3157	3160	3190	3208	1378
Sierra Petrol.	#1 Entz	3	25S	1E	SW SW NE	abs	abs	abs	3541	3566	1463
Bennett & Gould	#1 Mann	18	25S	1E	SE NE SE	abs	abs	abs	3460	3470	1385
Sutton et al.	#1 Kallenbach	28	25S	1E	NE NE SW	abs	abs	abs	3515	3538	1415
Quaker Drlg.	#1 Carey	34	25S	1E	NW NW NE	abs	abs	abs	3466	3490	1401
Renfro Drlg.	#1 DuBois	3	25S	2E	SW NE NW	abs	abs	3298	3319	3337	1373
B & R Drlg.	#1 Mosiman	24	25S	2E	SW SW SW	abs	abs	abs	3205	3220	1340
Renfro Drlg. et al.	#1 Jackson	28	25S	2E	SW SE SW	abs	abs	abs	3336	3348	1392
White & Ellis	#1 Ulmer	6	25S	3E	SW NW SW	abs	abs	3248	3267	3298	1356
Raymond	#1 Paul	26	25S	3E	NW NW NE	abs	abs	3140	3150	3169	1341
Kathol Petrol.	#3 Hamilton	33	25S	3E	SW SE NE	abs	abs	3100	3105	3123	1299
Abderhalden	#5 Mitchell	25	25S	4E	SE NE SW	abs	abs	abs	2537	2548	1389
Baker	#1 Pierce	33	25S	4E	NW NW SE	abs	abs	abs	2590	2604	1317
Adair	#1 Entz	1	25S	5E	SE SE NW	abs	abs	2920	2950	2968	1400
Cities Service	#51-A Knox	15	25S	5E	S2 S2 SW	abs	abs	2595	2612	2620	1344
Skelly	#6 Hill	34	25S	5E	SE SW SW	abs	abs	abs	2533	2551	----
Pet-Ex Petrol.	#1-8 Zebold	8	25S	7E	NW NW SE	abs	abs	3156	3180	3192	1425
Nat'l Assoc. Pet.	#1 Buckman	11	25S	7E	NE NE NW	abs	3107	3112	3136	3154	1474
Pet-Ex Petrol.	#1 Orion	19	25S	7E	NE NE SW	abs	abs	3139	3159	3172	1394
J.P. Gaty	#1 Clark	2	26S	1E	SE NW SE	abs	abs	abs	3477	3494	1414
Eagle	#1-5 Fuson	5	26S	1E	W2 NW SW	abs	abs	abs	3431	3444	1346
Gabbert-Jones	#1 Berthole	26	26S	1E	SW NE	abs	abs	abs	3435	3444	1379
Ash O&G	#2 Timmercamp	8	26S	2E	NE SW SW	abs	abs	abs	3341	3348	1426
Kennedy & Mitchell	#50-790 Ressurrection	19	26S	2E	NE SW SW	abs	abs	abs	3385	3402	1411
Avanti	#3 Jefferies	22	26S	2E	SE NE NW	abs	abs	abs	3206	3220	1405
Cities Service	#1 Thacker	27	26S	3E	NE SW	abs	abs	3104	3116	3130	1361
Stelbar	#1 Colburn	36	26S	3E	SE NW	abs	abs	3038	3050	3057	1345
Rex & Morris	#19 Rice	5	26S	4E	SW SE NW	abs	abs	abs	2532	2551	1311
Aladdin Petrol.	#1 Oliver	19	26S	4E	NE SW SW	abs	abs	3008	3026	3038	1326
Bedell-Catt	#1 Schreve	25	26S	4E	NW NW SW	abs	abs	abs	2714	2732	1329
Burton	#1-B Sluss	26	26S	5E	SE SE	abs	abs	abs	3292	3303	1344
Martin	#1-B Hogoboom	32	26S	5E	NE NE	abs	abs	abs	2639	2652	----
Nat'l Assoc. Pet.	#1 Webb	11	26S	6E	NE NE NW	abs	abs	3159	3169	3180	1385
Nat'l Assoc. Pet.	#1-A Falkenburg	18	26S	6E	SE SE NW	abs	abs	3304	3310	3316	1368
Kennedy & Mitchell	#11-992 Carver	27	26S	6E	SE SE SW	abs	abs	abs	3222	3233	1433
Kennedy & Mitchell	#1-911 Reeves	30	26S	6E	NW SW NE	abs	abs	abs	3184	3195	1359

APPENDIX I (continued)

OPERATOR	WELL NAME	LOCATION S.	T.	R.	SPOT	DEPTHS A	B	C	D	E	DATUM
El Dorado Refining	#9-B Young	27	26S	7E	NE SW NE	abs	abs	abs	3068	3072	----
Pickrell Drlg.	#1 Johns	3	27S	1E	NW NW NW	abs	abs	abs	3359	3374	1325
Blair	#2 Reed	11	27S	2E	NE NW NW	abs	abs	abs	3192	3206	1373
Silver Creek	#2 Hart	15	27S	2E	NE NE NE	abs	abs	abs	3170	3186	1360
Chapman Energy	#1 Ballew	1	27S	3E	NW SW SW	abs	abs	abs	3028	3034	1307
Charles Carlock	#1 Corbin	6	27S	4E	NW NE NE	abs	abs	abs	2921	2940	1275
Siegel	#1 Currier	6	27S	5E	SE NE SE	abs	abs	abs	3062	3070	1255
Hammer & MacLean	#3-B Stearns	22	27S	6E	SW SE SW	abs	abs	abs	3095	3102	1368
Glickman	#1 Becker	13	17S	1W	NE NE SE	abs	3404	3416	3456	3500	1545
Sun Range Resources	#1 B. Warnock	28	17S	1W	SE NW	abs	3094	3105	3138	3180	1337
Aladdin Petrol.	#1 Olson	3	17S	2W	SW SW NW	abs	3549	3572	3600	3640	1515
Aladdin Petrol.	#1 Jacobson	20	17S	2W	NW NE SW	abs	3564	3580	3600	3636	1442
Walker	#1-35 Gillberg	35	17S	2W	SW	3466	3473	3486	3510	3546	1465
Bay Petrol.	#2 Fagerberg	8	17S	3W	NE NW	abs	abs	3376	3410	3456	1336
T. Brown	#1 Sandell	15	17S	3W	SW SE SE	abs	3368	3377	3396	3442	1332
McPherson	#1 Lillian	30	17S	3W	NW SW	abs	abs	3420	3444	3496	----
Anschutz Drlg.	#1 Malm	36	17S	3W	NE NE SE	abs	abs	3604	3620	3662	1461
Nat'l Assoc. Pet.	#1 Knackstedt	8	17S	4W	SE SW NE	abs	abs	3690	3715	3759	1522
Hanco	#1 Dahlstein	10	17S	4W	SE SW SE	abs	3740	3763	3791	3834	1525
Globe	#1 Bean	25	17S	4W	W2 NE SW	abs	abs	3467	3492	3540	----
Rupp-Ferguson	#1 Johnson	33	17S	4W	SW NW	abs	abs	3553	3566	3604	1368
Bay Petrol.	#1 Bjorn	17	17S	5W	W2 SW NW	abs	3390	3406	3432	3472	1336
Gore	#1 Janssen	23	17S	6W	NW NE NE	abs	abs	abs	3547	3602	1527
Cities Service	#1-C Roelfs	16	17S	7W	NE SE NE	abs	abs	abs	3580	3611	1672
Amber	#1 Rush	28	17S	7W	NE NW NW	abs	abs	abs	3489	3530	1712
Bennett & Roberts	#1 Handlin	2	17S	8W	NE NE NE	abs	abs	abs	3525	3560	1719
Leben Drlg. et al.	#1 Andrews	4	17S	8W	NW NE SE	abs	abs	abs	3254	3300	1769
El Dorado Refining	#3 Gray	26	17S	8W	SW SE SE	abs	abs	abs	3185	3238	1722
CRA	#3 Paden	10	18S	1W	NW SW SE	abs	3209	3232	3263	3300	1451
Glickman	#2-C State	21	18S	1W	SE NE SE	abs	3280	3303	3325	3360	1422
Nat'l Assoc. Pet.	#2 Peterson	17	18S	2W	SE SW NE	abs	abs	3600	3628	3660	1514
Deep Rock	#1 A. Miller	27	18S	2W	NE SE	abs	abs	3434	3448	3484	1491
CRA	#3 Gustavson	30	18S	2W	NE NE NW	abs	abs	3173	3194	3232	----
Sierra Petrol.	#2-B Landgren	6	18S	3W	W2 SW	abs	abs	3460	3478	3512	1378
Time Petrol.	#1 Johnson	13	18S	3W	NE SE SE	abs	abs	3626	3642	3680	1492
Rex & Morris	#1 Thompson	19	18S	3W	SW SE	abs	abs	abs	3571	3619	1484
Texas Company	#1 Hedlund	26	18S	3W	NE NW	abs	abs	3614	3627	3665	1532
White & Ellis	#1 Neufeldt	5	18S	4W	SE SE NW	abs	abs	abs	3568	3610	1378
Anschutz Drlg.	#1 Priddy	12	18S	4W	SE SE SE	abs	abs	3508	3516	3550	1411
Sohio Petrol.	#1 Kumle	20	18S	4W	SW SW SE	abs	abs	abs	3644	3686	1427
F&M	#1-A Swanson	22	18S	4W	NE SE NE	abs	abs	3662	3676	3708	1521
Trans Era	#1 John Myers	8	18S	5W	SE SE SE	abs	abs	abs	3754	3796	1592
J.A. Melland	#1 Christenson	12	18S	5W	NE NE NW	abs	abs	3635	3642	3684	1409
Hummon	#1 Bruce	29	18S	5W	SW SE	abs	abs	abs	3760	3806	1581
Compressor Systems	#1 DeWitt	5	18S	6W	SE NE	abs	abs	abs	3803	3845	1687
Black Petrol.	#1 Olander	29	18S	6W	NE SE NE	abs	abs	abs	3492	3535	1698
A.D. Allison	#1-A Click	3	18S	7W	NW SW SE	abs	abs	abs	3315	3363	1711
Graves Drlg.	#1 Grey	9	18S	7W	NE NE NE	abs	abs	abs	3298	3340	1695
Solar	#1 Sellers	27	18S	7W	SE NE NE	abs	abs	abs	3321	3363	1646
Meyer	#1 Manwarren	32	18S	7W	SE NW SE	abs	abs	abs	3296	3340	1687
Graves Drlg.	#1 Splitter	5	18S	8W	SW NW	abs	abs	abs	3306	3356	1754
Adair	#1 Archibald	27	18S	8W	NW NW	abs	abs	abs	3330	3382	1739
Woodman et al.	#1 Baldwin	29	18S	8W	SW NE	abs	abs	abs	3323	3378	1732
Edmiston	#1 Bronleewee	1	18S	9W	NE SE NW	abs	abs	abs	3198	3208	1763
Walker	#1-6 Hawley	6	19S	1W	SE NE	abs	abs	3524	3538	3570	1589
Producers	#1-A Decker	20	19S	1W	SW SW	abs	abs	3436	3446	3475	----
Ingling et al.	#1 Leon	22	19S	1W	SE SE NW	abs	abs	3667	3680	3704	1507

APPENDIX I (continued)

OPERATOR	WELL NAME	LOCATION S.	T.	R.	SPOT	DEPTHS A	B	C	D	E	DATUM
Nat'l Assoc. Pet.	#1 Swanson	8	19S	2W	NE NE SE	abs	abs	3464	3470	3512	1550
Tom Kat	#3 Dunkelburger	11	19S	2W	SE SE	abs	abs	3362	3374	3402	1558
Nat'l Assoc. Pet.	#5 Robertson	27	19S	2W	S2 N2 NW	abs	abs	3444	3450	3488	1554
Ackerson	#1 Ackerson	33	19S	2W	SE NE SW	abs	abs	3450	3460	3494	1547
Time Petrol.	#1 Henrickson-Mathes	5	19S	3W	NE NE NE	abs	abs	abs	3639	3681	1522
NCRA	#1 Anderson	15	19S	3W	SE SE NW	abs	abs	abs	3668	3703	1501
Natural G&O	#1 Quantius	31	19S	3W	NE NE SW	abs	abs	abs	3747	3776	1500
Anschutz Drlg.	#1 Schrag	27	19S	4W	SE SE NE	abs	abs	abs	3760	3790	1488
NCRA	#1 LPG SWD	29	19S	4W	NE NW SE	abs	abs	abs	3824	3860	1561
R. Brooks	#1 Fisher	5	19S	5W	SW SW NW	abs	abs	abs	3866	3902	1666
Trans Era	#1 Myers	19	19S	5W	SW SW SE	abs	abs	abs	3838	3870	1644
Mid American	#1 Disposal	24	19S	5W	NW SW SW	abs	abs	abs	3899	3932	1591
Little River Co.	#1 Wolf	7	19S	6W	NE NE SW	abs	abs	abs	3404	3442	1627
F.G. Holl	#1-11-B Nelson	11	19S	6W	SE SE	abs	abs	abs	3896	3929	1621
GRB Resources	#1 Smith	26	19S	6W	N2 SE NW	abs	abs	abs	3537	3572	1615
Atlantic Refining	#1 Hardy	30	19S	6W	SW SW SW	abs	abs	abs	3545	3578	1635
M&R	#1 Shrader	1	19S	7W	NW SW	abs	abs	abs	3383	3420	1611
R.G. Smith	#1 Le Clere	7	19S	7W	NE SE	abs	abs	abs	3466	3507	1764
F&M	#1 Father Flanagon	26	19S	7W	SE SW SW	abs	abs	abs	3516	3550	1741
I.O. Miller	#1 Bacon	8	19S	8W	NE NE	abs	abs	abs	3359	3407	1703
Aladdin Petrol.	#1-C LeClerc	13	19S	8W	SW NE SW	abs	abs	abs	3440	3468	1750
Northern Natural	#26-01	26	19S	8W	NW SE SW	abs	abs	abs	3412	3454	1724
Sutton	#2 Good	29	19S	8W	NE SW	abs	abs	abs	3362	3406	1700
Spencer Drlg.	#1 Saint	12	19S	9W	SE SE	abs	abs	abs	3351	3402	1752
Raymond	#1 Molsder	25	19S	9W	S2 SE SE	abs	abs	abs	3275	3327	1712
Kewanee	#1 Becker	4	20S	1W	NE NE NW	abs	abs	3450	3458	3492	1569
Bay Petrol.	#1 Banman	24	20S	1W	SE SE SW	abs	abs	abs	3420	3460	1546
Veeder Supply	#1 John	29	20S	1W	NE NE NE	abs	abs	3446	3452	3490	1547
Jay Boy	#1 Goering	16	20S	2W	NW NW	abs	abs	3444	3452	3487	1515
Ingling	#1-A Lumley	20	20S	2W	NW NW NW	abs	abs	3446	3448	3488	1491
Lewis & Durbin	#1 Moddelmog	24	20S	2W	SW SW SE	abs	abs	3397	3408	3443	1542
Aladdin Petrol.	#1 Schrag	8	20S	3W	NE NE NW	abs	abs	abs	3712	3744	1496
Texas Pacific	#2 Krehbiel	11	20S	3W	NW SW SE	abs	abs	3470	3480	3509	1497
Hinkle et al.	#1 Goering	27	20S	3W	SW NW NW	abs	abs	3195	3207	3235	1475
Shelley-Miller	#1 Neufeldt	30	20S	3W	NE NE SW	abs	abs	abs	3745	3774	1470
Anschutz Drlg.	#1 Stitts	4	20S	4W	SW SW SE	abs	abs	abs	3785	3813	1487
Anschutz Drlg.	#1 Fleming	10	20S	4W	SE SE NE	abs	abs	abs	3734	3765	1480
Thunderbird Drlg.	#1 Bukey	26	20S	4W	SE SE NE	abs	abs	abs	3759	3788	1483
Glenwil Energy	#1 Smith	28	20S	4W	NW SW	abs	abs	abs	3805	3826	1487
R.W. Shade	#1 Lindell	22	20S	5W	SW NE NW	abs	abs	abs	3930	3958	1570
Green Energy	#2 Nelson	29	20S	5W	SW SW NE	abs	abs	abs	3756	3781	1560
NCRA	#1 Johannson	7	20S	6W	NE SW	abs	abs	abs	3664	3697	1682
Braden Drlg.	#1 Conrad-Brucker	11	20S	6W	NE SW NW	abs	abs	abs	3586	3610	1594
Rains & Williamson	#1 Hunter	3	20S	7W	NE NW SW	abs	abs	abs	3563	3600	1704
Lario	#1 Monroe	7	20S	7W	NW NE	abs	abs	abs	3472	3500	1728
Brown et al.	#2 Cherpital	8	20S	8W	NW NE SW	abs	abs	abs	3456	3502	1662
Northern Natural	#11-09 Edwards	11	20S	8W	SW SE SE	abs	abs	abs	3275	3312	1662
Kaiser-Francis	#1 Cowdery	19	20S	8W	SW NE	abs	abs	abs	3473	3518	1672
Isern-Wells	#1 Bundy	23	20S	8W	SE NW	abs	abs	abs	3458	3498	1650
Lebsack et al.	#1 Shuler	11	20S	9W	NW SW SE	abs	abs	abs	3278	3328	1672
Raymond	#1 Ploog	26	20S	9W	SE NE NW	abs	abs	abs	3274	3322	1682
Petroleum Mgmt.	#1 Schroeder	8	21S	1W	SW SE NE	abs	abs	abs	3414	3451	1505
Anderson-Prichard	#4 Goossen	12	21S	1W	NE NE NE	abs	abs	abs	3474	3506	1540
Ingling et al.	#1 Krehbiel	26	21S	1W	SW NE	abs	abs	abs	3473	3487	1511
Conoco	#12 Huxman	29	21S	1W	SW NE NW	abs	abs	abs	3370	3402	1485
Source Petrol.	#1-A Mercy	2	21S	2W	NE NE NW	abs	abs	3410	3416	3452	1508
Fred Ayesh	#1 Goering	20	21S	2W	NW NW SE	abs	abs	abs	3563	3592	1474
Barbara	#1 Young	26	21S	2W	NE NE NE	abs	abs	abs	3478	3501	1491
Trans America	#1-B Stucky	3	21S	3W	W2 NW NW	abs	abs	3314	3330	3360	1450
Source Petrol.	#1-E Goering	12	21S	3W	SW SE NW	abs	abs	3562	3578	3610	1478
Jay Boy	#1 Ediger	16	21S	3W	NE SE SW	abs	abs	abs	3354	3383	1468
Source-Jay Boy	#1-B Zerger	23	21S	3W	SE SE NW	abs	abs	abs	3640	3666	1457
Sutton	#1 Krehbiel	30	21S	3W	SW NE SW	abs	abs	abs	3908	3928	1520

APPENDIX I (continued)

OPERATOR	WELL NAME	LOCATION S.	T.	R.	SPOT	DEPTHS A	B	C	D	E	DATUM
Pickrell Drlg.	#1-C Wiens	11	21S	4W	NE NW SW	abs	abs	abs	3814	3837	1468
Walker	#1-16 Friesen	16	21S	4W	NW NW SW	abs	abs	abs	3911	3934	1531
Wakefield	#1 Plett	19	21S	4W	NW NW NW	abs	abs	abs	3931	3948	1542
Mayfield & Smith	#1 DuBois	22	21S	4W	SE NE	abs	abs	abs	3822	3842	1446
R.P. Nixon	#2 Lindholm	5	21S	5W	SW SE NW	abs	abs	abs	3783	3810	1534
Carey	#1 Friesen	36	21S	5W	NE NE SE	abs	abs	abs	3928	3947	1546
Kansas Horizon	#1 Sand Hills	2	21S	6W	S2 S2 SW	abs	abs	abs	3754	3786	----
Edwards	#1 Ball Wilson	7	21S	7W	N2 N2 NE	abs	abs	abs	3632	3667	1630
Lassiter	#1 Theede	11	21S	7W	NW SE NE	abs	abs	abs	3632	3667	1632
Jayhawk	#1 Gross	30	21S	7W	NW NE	abs	abs	abs	3727	3772	1622
Kanoco	#1 Blackhall	8	21S	8W	NE NW SE	abs	abs	abs	3484	3533	1658
Sanders	#1 Gibson	11	21S	8W	SW NE	abs	abs	abs	3600	3643	1640
Pure	#2 Thode	26	21S	8W	SW SE	abs	abs	abs	3648	3692	1629
Buick Drlg.	#1 Yeakel	32	21S	8W	NE NE NE	abs	abs	abs	3498	3541	1646
Allen Drlg.	#1 Schafer	2	21S	9W	NW SE SE	abs	abs	abs	3305	3350	1675
Champlin	#1 G.C. Frederick	3	21S	9W	SW NW	abs	abs	3334	3340	3379	1696
H-30 Drlg.	#1 Brown	14	21S	9W	NW SE	abs	abs	abs	3534	3576	1667
Petro-Pak	#1 Fair	15	21S	9W	NW SE NW	abs	abs	abs	3380	3420	1677
Tom Palmer	#1 Schoepflin	17	21S	9W	SW SW NW	abs	abs	abs	3298	3369	1687
Jay Bee	#1 Wellman	28	21S	9W	NW NE NW	abs	abs	abs	3420	3478	1680
Cities Service	#1 Fair-Beck	30	21S	9W	SW SE	abs	3360	3370	3396	3417	1711
Helmerich & Payne	#1 Harp	24	21S	10W	NW NW SE	abs	abs	abs	3373	3395	1708
Braden Drlg.	#1 Proffits	29	21S	10W	NW NW NW	abs	abs	abs	3374	3397	1738
Nadel & Gussman	#1 Sleeper	35	21S	10W	SW SW	abs	abs	abs	3437	3456	1731
Alpine & Royalty	#1 U.S. Government	26	21S	11W	SE SE SE	abs	abs	3392	????	3428	1751
Allan et al.	#1 Widener	26	21S	12W	NW NE SE	abs	abs	3549	????	3592	1828
Anschutz Drlg.	#3 Fischer	31	21S	12W	SW SE SW	abs	abs	3550	????	3589	1870
Abercrombie Drlg.	#2 Linke	27	21S	13W	S2 N2 NW	abs	abs	abs	3616	3630	1888
K&E Drlg.	#1 Brown	30	21S	13W	NE NE NE	abs	abs	3624	????	3664	1914
Bi States	#1-A Drew	8	21S	14W	SW SW NE	abs	abs	3582	????	3615	1941
Hilton Drlg.	#1 Boese	11	21S	14W	SW NW NW	abs	abs	3578	????	3617	1922
Petroleum, Inc.	#1 McGinty	26	21S	14W	NW SW SW	abs	abs	3691	????	3734	1935
Kedco	#1 Weirauch	29	21S	14W	NE NW	abs	abs	3686	????	3723	1949
Vickers Expl.	#1 Sweeny	8	21S	15W	NW NW NE	abs	abs	abs	3786	3792	1955
A. Scott Ritchie	#1-A Fisher	11	21S	15W	NE SW NW	abs	abs	abs	3634	3653	1937
Zenith Drlg.	#1 Melchert	26	21S	15W	SE NE SE	abs	abs	3763	????	3790	1953
Lebco	#1 Unruh	29	21S	15W	N2 NW SW	abs	abs	3860	????	3890	1992
Hupfer	#1-A Powers	14	21S	16W	NW NE SE	abs	abs	3718	????	3779	1975
Glenn Byars	#1 Dyck	2	22S	1W	NE SW NE	abs	abs	abs	3480	3504	1490
Petroleum, Inc.	#1 Dirks	8	22S	1W	SW SE NW	abs	abs	abs	3430	3458	1468
Charles Carlock	#1 Dilts	19	22S	1W	NE NE NE	abs	abs	3446	3458	3482	1456
Beardmore Drlg.	#1 Schrag	4	22S	2W	SW SW SW	abs	abs	abs	3648	3684	1473
Ash O&G	#1 Wedel	12	22S	2W	SW NE SE	abs	abs	3406	3418	3454	1456
El Dorado Refining	#1 Nickell	26	22S	2W	NW NW NE	abs	abs	abs	3380	3409	----
C.W. Sanders	#1 Drier	29	22S	2W	N2 SE NW	abs	abs	abs	3654	3694	1433
Aladdin Petrol.	#5 Neufeld	8	22S	3W	NW SE NW	abs	abs	abs	3561	3580	1450
Trans America	#1 Preheim	12	22S	3W	NE SE SE	abs	abs	3666	3672	3697	1451
Krehbiel-Buller	#1 Randall	26	22S	3W	NE NE NE	abs	abs	3660	3673	3696	1426
Aladdin Petrol.	#1 Franz	30	22S	3W	N2 N2 NW	abs	abs	abs	3499	3520	1447
Quintin Little	#1 Franz	1	22S	4W	NW NW NW	abs	abs	abs	3826	3844	1459
Walker	#1-8 Goertzen	8	22S	4W	SE NW SW	abs	abs	abs	3916	3930	1535
Messman-Rinehart	#1-A Siemans	24	22S	4W	E2 SE SE	abs	abs	abs	3808	3828	1444
Beardmore-Sutton	#1 Rice	5	22S	5W	NE NE SE	abs	abs	abs	3926	3948	1534
Jantz	#1 Bontrager	12	22S	5W	SW NE	abs	abs	abs	3914	3932	1531
Skelly	#3 L. Robinson	24	22S	5W	W2 SW SE	abs	abs	abs	3845	3863	1505
Petroleum Mgmt.	#1 Nelson	34	22S	6W	NE SE NE	abs	abs	abs	3952	3982	1555
Texas	#1 McVay	21	22S	7W	SW SW NW	abs	abs	abs	3775	3806	1597
Anschutz et al.	#1 Short	3	22S	8W	NE NE SE	abs	abs	3947	3952	3982	1663
Skelly	#1 Gossage	17	22S	8W	SW SE	abs	abs	abs	3710	3750	1603
Eagle	#1 Rupp	19	22S	8W	NW SW	abs	abs	abs	3830	3871	1720
Sterling Drlg.	#1 Osenbaugh	34	22S	8W	SW SW	abs	abs	abs	3929	3961	1658

APPENDIX I (continued)

OPERATOR	WELL NAME	LOCATION S.	T.	R.	SPOT	DEPTHS A	B	C	D	E	DATUM
Trans-Era Petrol.	#1 S. Fair	3	22S	9W	NW NW SW	abs	abs	abs	3662	3716	1720
Barnett	#1 Drake	5	22S	9W	NE SW	abs	abs	3540	3581	3602	1752
Sterling Drlg.	#1 Proffitt	12	22S	9W	SW NW	abs	abs	abs	3730	3772	1718
Globe	#1-A Drake	17	22S	9W	NW NW NW	abs	3526	3546	3582	3603	1733
Kinetic	#1 Schweitzer	26	22S	9W	NE NW	abs	abs	abs	3818	3857	1716
Sanders	#1 Cantwell	28	22S	9W	SW NE	abs	3704	3710	3762	3782	1717
TDR Expl.	#1-A Sleeper	30	22S	9W		abs	3584	3610	3658	3676	1751
Lee Phillips	#1 Stout	1	22S	10W	SE SE NE	abs	3454	3476	3517	3540	1754
Dozier	#1 Titus	4	22S	10W	SE SE SE	abs	abs	3458	????	3490	1757
Mid-Continent	#1 Starr	7	22S	10W	SE SE NW	abs	abs	abs	3477	3495	1767
Dudley & Heath	#1 Greighton	13	22S	10W	SE NW SE	abs	3536	3578	3615	3637	1748
Lindas	#1 Smith-Taylor	18	22S	10W	SW SW NW	abs	abs	abs	3520	3532	1777
Duke Drlg.	#1 Schweitzer	21	22S	10W	SE SE SE	abs	abs	3558	????	3594	1762
Jay Bee	#1-B Sleeper	25	22S	10W	SW SE NE	abs	3556	3584	3628	3647	1748
Russell-Schwinn	#1 Moore	28	22S	10W	NE NW	abs	abs	3568	????	3594	1769
Musgrove et al.	#1 Miller	30	22S	10W	NE NE SW	abs	abs	3550	????	3581	1779
Ainsworth	#1-B Hammeke	8	22S	11W	S2 S2 NW	abs	abs	3496	????	3530	1801
Aspen Drlg.	#1 McKay	11	22S	11W	NE SW NE	abs	abs	3456	????	3481	1764
W.C. McBride et al.	#1 Richardson	26	22S	11W	SW SW NE	abs	abs	3566	????	3588	1789
Anderson-Prichard	#1 Nolte	30	22S	11W	NW NW NW	abs	abs	3556	????	3606	1852
Atlantic Refining	#1-A Fisher	8	22S	12W	S2 SW NW	abs	abs	3575	????	3618	1876
Armer	#1 Voight	11	22S	12W	SW SE NE	abs	abs	3540	????	3575	1843
Shelley-Miller	#4 Spangenberg	26	22S	12W	SE SW SE	abs	abs	3539	????	3582	1839
Hutchinson	#1-29 Hitz	29	22S	12W	SW NE SW	abs	abs	3625	????	3689	1870
El Dorado Refining	#1 Schmidt	8	22S	13W	NE NW NE	abs	abs	3702	????	3738	1909
Edmiston	#4 Sittner	11	22S	13W	SW NW SW	abs	abs	3665	????	3722	1893
Brooks Pierce	#1 Spatz	26	22S	13W	N2 SE	abs	abs	3654	????	3697	1887
Clinton	#1-V H.V. Riddle	29	22S	13W	NW SE NW	abs	abs	3773	????	3806	1909
Muir-Thompson	#1 Unruh	8	22S	14W	NW SE SE	abs	abs	3804	????	3844	1955
Sunray-Midcon	#1 Mitchell	11	22S	14W	SW SW NW	abs	abs	3706	????	3742	1936
Petroleum, Inc.	#1 Ross	25	22S	14W	SW SW NW	abs	abs	3734	????	3769	1928
Lauck & Sunray	#1 Garvin	27	22S	14W	SW NW NW	abs	abs	3812	????	3850	1947
Hilton Drlg.	#1 McMillan	29	22S	14W	NE NE NE	abs	abs	3864	3916	3928	1958
Nat'l Development	#1 Horner	8	22S	15W	SW NW	abs	abs	3874	????	3907	1985
Great Bend	#1 Crane OWWO	11	22S	15W	N2 NE	abs	abs	3855	????	3892	1970
Lauck	#1 Barstow	25	22S	15W	SW SW NE	abs	abs	3930	3977	3990	1983
F&M	#1 Dunbar	27	22S	15W	NE NE SE	abs	abs	3973	????	4000	1996
F&M	#1-C Barstow	29	22S	15W	NW NW SE	abs	abs	3890	????	3957	2014
Gramehart-Miller	#1 Boyd	12	22S	16W	NW NW NE	abs	abs	3854	????	3874	1992
Anschutz Drlg.	#1 Barstow	26	22S	16W	NE NE NE	abs	abs	abs	3998	4015	2011
Texas O&G	#1 Kirchgassner	30	22S	16W	SE SE NE	abs	abs	4150	4203	4210	2053
Amerada	#1 Odell	15	22S	17W	SW SW NW	abs	abs	4090	4108	4143	2034
Honaker	#1 Lupfer	17	22S	17W	NE NE SE	abs	abs	4105	????	4132	2040
Real Petrol.	#1-V Lowrey	25	22S	17W	NW NW NE	abs	abs	4081	4136	4148	2036
Wakefield	#1 Ewing	29	22S	17W	NE NE NE	abs	abs	4180	4243	4280	2055
Shawver-Graham	#1 Pierce	21	23S	1W	SW SW SE	abs	abs	abs?	3544	3582	1416
Little George	#1 Grove	27	23S	1W	SW SW NW	abs	abs	abs	3531	3566	1415
Jay Boy	#1 Unruh	11	23S	2W	NW NW	abs	abs	3320	3333	3367	1442
Iron Drlg.	#1 Clark	18	23S	2W	SE SE SE	abs	abs	3797	3804	3840	1423
Gruenerwald at al.	#1 Brown	22	23S	2W	NW SE	abs	abs	abs	3395	3435	1399
F & B	#1-A-C Sizemore	4	23S	3W	N2 NW NE	abs	abs	abs	3783	3811	1465
Westgate-Greenland	#1 Hurty	12	23S	3W	SE NW SW	abs	abs	3797	3814	3836	1456
Adair	#1 McElwain	24	23S	3W	SW NE	abs	abs	abs	3830	3854	1441
Sierra Petrol.	#1 Wilson	33	23S	3W	NE NE SW	abs	abs	abs	3845	3870	1441
Virginia Drlg.	#1 Frederick	8	23S	4W	SW SW SW	abs	abs	abs	3974	4000	1588
Sunray-Midcon	#2-B Sabin	11	23S	4W	SW SW NE	abs	abs	abs	3668	3692	1492
Woffard & Clark	#1 Hale	21	23S	4W	NE NW NW	abs	abs	abs	3850	3866	1492
S & K	#6-B Base Twin	26	23S	4W	NW NW SE	abs	abs	abs	3705	3727	1471
Leben Drlg.	#1 Gagnebin	2	23S	5W	NE SE	abs	abs	abs	3962	3982	1604
Jedco	#1 Whited	22	23S	5W	NE NE	abs	abs	abs	3855	3873	1516
National	#1 Brawner	26	23S	5W	NE SW NE	abs	abs	abs	3842	3860	1500
Cities Service	#1 Hamilton	22	23S	6W	SW SW SW	abs	abs	abs	4006	4031	1560
Anschutz Drlg.	#1 Wiegel	9	23S	7W	SE SE SE	abs	abs	abs	3944	3978	1596
Braden Drlg.	#1 Russell	30	23S	7W	SE SE NW	abs	abs	abs	3988	4010	1604
Atlantic Refining	#1 Love	33	23S	7W	SE SE SW	abs	abs	abs	4077	4097	1632
Atlantic Refining	#1 Short	14	23S	8W	NE NE NE	abs	abs	abs	3960	3980	1638

APPENDIX I (continued)

OPERATOR	WELL NAME	LOCATION S.	T.	R.	SPOT	DEPTHS A	B	C	D	E	DATUM
Iron	#1 Ramsey	16	23S	8W	SW SW SW	abs	abs	abs	4013	4025	1672
Bell O&G	#1 Schmucker	32	23S	8W	NE NE NW	abs	abs	abs	4024	4046	1675
Ambassador	#1 Roth	2	23S	9W	SE SE NW	abs	abs	abs	3777	3809	1718
Energy	#1 Harley	7	23S	9W	SE NW	abs	3746	3778	3840	3856	1745
Manhart et al.	#1 Snay	18	23S	9W	SE SE SE	abs	3800	3820	3880	3897	1750
Manhart et al.	#1 Beck	24	23S	9W	SW NE NW	abs	abs	abs	4011	4026	1705
Richardson et al.	#1 Stiggins	30	23S	9W	NE NW NE	abs	3862	3866	3950	3966	1746
Kathol Petrol.	#1 Dion	3	23S	10W	NE NW SW	abs	abs	3595	3633	3662	1759
Carter	#4 A. Tonn	11	23S	10W	SW SW SE	abs	3742	3747	3825	3842	1760
E.F. Wakefield	#1 Moeckel	13	23S	10W	SE SE	abs	3780	3799	3880	3895	1753
Wilkinson	#1 Hinshaw	16	23S	10W	SW SW NW	abs	abs	3644	3679	3696	1781
Fell	#1-B Yust	20	23S	10W	SE NE	abs	abs	3639	3706	3725	1785
Plains Expl.	#1 Paine	26	23S	10W	NE SW	abs	abs	3825	3900	3922	1765
Stelbar	#1 Bowen	29	23S	10W	SW NW NW	abs	3654	3667	3728	3748	1798
Armer	#1 Tretbar	1	23S	11W	NW NW NE	abs	abs	3592	????	3632	1788
Rains & Williamson	#1 Hill	5	23S	11W	SE SE NW	abs	abs	3580	????	3620	1810
Henderson	#1 Krey	13	23S	11W	SE SE NE	abs	abs	3644	????	3678	1792
Ritchie	#1-A Hornbaker	15	23S	11W	SW NE NW	abs	abs	3636	????	3677	1802
Barnett	#1 Hornbaker	18	23S	11W	NW NE NW	abs	abs	3612	????	3644	1824
PanCanadian	#2-14-28 Riley	28	23S	11W	W2 SW	abs	abs	3633	????	3664	1817
CRA & Hawley	#1-E Allen	30	23S	11W	SW SW NE	abs	abs	3680	????	3747	1831
Stanolind	#1 Figger	1	23S	12W	NE NE	abs	abs	3454	????	3486	1820
Lowenstein et al.	#1 Allen	3	23S	12W	SE SW SW	abs	abs	abs	3648	3668	1841
JFW	#1 Salem	6	23S	12W	SW SE	abs	abs	3696	????	3749	1863
Edwards	#1 Hughes-Ritt	13	23S	12W	SE SW NE	abs	abs	3655	????	3694	1828
Armer	#1 McGill	15	23S	12W	SE NE SW	abs	abs	3700	????	3749	1850
Patton	#1 McCune	17	23S	12W	NW NW SW	abs	abs	3748	????	3802	1850
F&M	#1 Fritzmeier	25	23S	12W	NW SE NW	abs	abs	3750	????	3796	1848
Gas Marketing	#2 Heyen	28	23S	12W	NE NW	abs	abs	3712	????	3760	1862
ROC	#1 Rice	29	23S	12W	SE SE NE	abs	abs	3732	????	3780	1872
Petroleum, Inc.	#1-G Witt	1	23S	13W	NE NE NE	abs	abs	3678	????	3720	1856
Vac Petrol.	#1 Fisher	3	23S	13W	NE NE	abs	abs	3756	????	3792	1869
Inger	#1 Corn	6	23S	13W	NE SE SE	abs	abs	3811	????	3854	1922
Hilton Drlg.	#1 Russell	14	23S	13W	SW SW NE	abs	abs	3807	3843	3855	1879
Petroleum, Inc.	#1 Ward	15	23S	13W	NE SW NE	abs	abs	3721	????	3760	1883
Aylward Drlg.	#1 Batchman	17	23S	13W	SE SE NE	abs	abs	3848	????	3882	1899
Phillips	#1 Detweiler	26	23S	13W	SW SW SW	abs	abs	3850	????	3900	1894
Skelly	#1 Geiginghagen	29	23S	13W	SE NE SE	abs	abs	3887	3936	3948	1899
Rains & Williamson	#1 Mason	1	23S	14W	SE NW SE	abs	abs	3787	????	3820	1924
Oil Producers	#2-C Devore	3	23S	14W	SW NW	abs	abs	3888	????	3920	1966
Boger Bros.	#2 Miller	5	23S	14W	E2 E2	abs	3913	3924	3973	3990	1964
Allen Drlg.	#1 Eppley	13	23S	14W	NE SE NW	abs	abs	3894	????	3926	1912
Kathol Petrol.	#1 Copeland	15	23S	14W	W2 NW NW	abs	abs	3914	????	3952	1950
K & E Drlg.	#1 Cornwell	17	23S	14W	NW SE SE	abs	abs	3930	????	3979	1965
Alpine	#1 Radke	25	23S	14W	NE SW SW	abs	abs	3952	????	4012	1950
Reach Petrol.	#1-A Getty	28	23S	14W	NE NE	abs	abs	3964	????	4002	1952
Natural G&O	#1 Gilmore	29	23S	14W	SW SE NE	abs	abs	3970	????	4014	1923
Natural G&O	#1 McComas	1	23S	15W	NE SW SW	abs	abs	3944	????	3994	1991
Alma	#1 Irma	3	23S	15W	NW NW SE	abs	abs	4003	????	4028	2002
Pickrell Drlg.	#1 Curtis	6	23S	15W	SE SW NW	abs	abs	3996	????	4044	2019
CXY	#1 Petro	15	23S	15W	SW NW NW	abs	abs	4006	4065	4080	2019
Lario	#1 Wilcox	18	23S	15W	SE SE SW	abs	abs	abs	4000	4028	2038
Loffland Brothers	#1 Grizzell	23	23S	15W	SW SW SE	abs	abs	3992	4060	4076	2013
Alpine	#2 English	25	23S	15W	NE NE NW	abs	abs	4076	4107	4116	1989
Anschutz Drlg.	#1 English	28	23S	15W	NW NW SE	abs	abs	4050	4082	4113	2017
Stanolind	#1-B W. Riley	30	23S	15W	SW NE SW	abs	abs	4034	4050	4072	2054
Hershberger Expl.	#1 Schertz	1	23S	16W	NW NW NW	abs	abs	4020	4060	4077	2022
Halliburton	#1 H.C. Colglazier	4	23S	16W	SW SE	abs	abs	4172	????	4109	2050
Halliburton	#1 Schwartz	8	23S	16W	SW SW SW	abs	abs	4268	4316	4332	2065
Alpine	#1 Buhrer	14	23S	16W	NW NW	abs	abs	4040	4069	4085	2042
Rupe & Ash	#1 Horton	16	23S	16W	NE SW SW	abs	abs	4169	4232	4266	2054
G-M-R	#1 Thomas	19	23S	16W	NE NE SE	abs	4120	4152	4236	4280	2066
R.F. White	#1 Curtis	25	23S	16W	SE NE NE	abs	abs	abs	4082	4102	2048
Barnett	#1 Hawes	28	23S	16W	SW SE	abs	abs	4168	4182	4207	2070
Leben Drlg.	#1-B Hawes	29	23S	16W	SW SE	abs	abs	4269	4350	4393	2072
Colorado	#1 Schwartz	1	23S	17W	NW NW SW	abs	abs	4177	4258	4304	2076
Clark Knight Drlg.	#1 Hutchinson	3	23S	17W	NW NW NW	abs	abs	4260	4300	4344	2061
Todd Drlg.	#1 Morrow	5	23S	17W	NW SW SE	abs	abs	4266	4342	4385	2062
Kewanee	#1-X Parramore	13	23S	17W	SE SE NE	abs	abs	4182	4242	4266	2083
Sohio Petrol.	#1 Slepeke	15	23S	17W	NW NW NE	abs	abs	4304	4366	4392	2100
Blackhawk	#1-A Chicago	17	23S	17W	W2 E2 NW	abs	abs	4398	4458	4498	2096
C.U. Bay	#1 Fischer	26	23S	17W	NW NE NW	abs	4374	4380	4480	4507	2087
Sohio Petrol.	#1 Aldrich	32	23S	17W	NE SE NW	4376	4445	4462	4542	4568	2116

APPENDIX I (continued)

OPERATOR	WELL NAME	LOCATION S.	T.	R.	SPOT	DEPTHS A	B	C	D	E	DATUM
Brougher	#2 Wagner	33	23S	17W	NE NE NE	abs	4380	4384	4495	4525	2104
Cherry Drlg.	#1 Briggs	12	24S	1W	SE SE SE	abs	abs	3548	3561	3576	1416
Adair	#1 Chavez	26	24S	1W	SE SE	abs	abs	3623	3635	3650	1424
Jay Boy	#1 Foster	3	24S	2W	NW NW NE	abs	abs	abs	3758	3788	1397
F&M	#1 Baalman	7	24S	2W	SE SE NE	abs	abs	abs	3864	3886	1424
Anadarko	#1-B Krauss	31	24S	2W	NW SW SW	abs	abs	abs	3930	3939	1415
Kewanee	#1 Richer	1	24S	3W	SW SE SE	abs	abs	abs	3877	3895	1430
Cities Service	#1 McNew	8	24S	3W	SE SE NE	abs	abs	abs	3890	3908	1447
Renfro Drlg.	#1 Stutzman	22	24S	3W	NE NE NE	abs	abs	3944	3954	3970	1435
Shell	#1 Noskinson	9	24S	4W	E2	abs	abs	abs	3753	3767	1472
Ram Petrol.	#1 Kincaid	13	24S	4W	SW NW NW	abs	abs	abs	3862	3875	1461
Buffalo & B&R	#1 Morgan	24	24S	4W	NW NW SW	abs	abs	abs	3862	3880	1454
APC	#1 Stroud	3	24S	5W	NE NE NE	abs	abs	abs	3828	3838	1498
Lion et al.	#1 Bontrager	8	24S	5W	SE SW SE	abs	abs	abs	3893	3914	1555
Lochiel	#1 Schrock	27	24S	5W	SE NW SE	abs	abs	abs	3837	3857	1545
Osage O&G	#1 Benton	6	24S	6W	NW NW SE	abs	abs	abs	4034	4067	1583
T&M Oil	#1 Haines	10	24S	6W	NW NW NW	abs	abs	abs	4037	4065	1559
Lotus	#1 Durpser	7	24S	7W	NE NE NW	abs	abs	abs	4054	4076	1625
Sanders	#1 Haskard	12	24S	7W	SE SE	abs	abs	abs	4055	4087	1586
Rex et al.	#1 Evalyn	21	24S	7W	NW NW SW	abs	abs	4085	4092	4118	1600
Virginia Drlg.	#1 Thompson	27	24S	7W	SE SE	abs	abs	abs	4076	4112	1559
Barbour Drlg.	#1 Rothenberg	3	24S	8W	NW NE SE	abs	abs	abs	4083	4092	1645
Denver Energy	#1 Gagnebin	5	24S	8W	NW NW	abs	abs	abs	4084	4110	1679
Woodman et al.	#1 Birkett	20	24S	8W	NW NE NE	abs	abs	abs	3811	3817	1648
W.R. Justice	#1 Guyer	35	24S	8W	NE NW NW	abs	abs	abs	4132	4145	1617
Trans-Era Petrol.	#1 Wagler	3	24S	9W	NE NE SE	abs	abs	4076	4100	4114	1712
Midcontinent Energy	#1 Demuth	11	24S	9W	SE SW	abs	abs	4075	4102	4116	1677
Smitherman	#1 Dion	15	24S	9W	NE SW NW	abs	abs	4050	4118	4132	1690
Manhart et al.	#1 Hinshaw	17	24S	9W	NW NW SW	abs	abs	3986	4048	4063	1663
Apache	#1 Horton	30	24S	9W	SE NW	abs	abs	4063	4130	4144	1720
Raymond	#1 Cole	35	24S	9W	NE NE NE	abs	abs	4109	4154	4170	1670
Stearns & Johnson	#1 Schultz	3	24S	10W	NW NW NE	abs	abs	3848	3915	3932	1767
Schermerhorn	#1 F. Miller	12	24S	10W	SW SW SE	abs	abs	3986	4064	4080	1710
Lee Phillips	#1 McVey	19	24S	10W	SE SE SW	abs	3916	3935	4025	4040	1773
Artnell	#1 Fassnacht	28	24S	10W	SW SW NE	abs	3978	3984	4068	4082	1715
Demier	#2 Brownlee	31	24S	10W	NE NW SW	abs	3929	3948	4034	4050	1757
Graves Drlg.	#1 Figger	4	24S	11W	NE SW SW	abs	3754	3770	3852	3871	1829
Alma	#1 G. Figger	8	24S	11W	NE SE NW	abs	3760	3790	3860	3879	1831
Striker Petrol.	#ZU-14	12	24S	11W	W2 W2 NW	3735	3766	3784	3836	3854	1813
Time Petrol.	#1 Hartnett	13	24S	11W	N2 N2 NW	3783	3814	3824	3882	3900	1805
Harms-Burt	#1 Allen	19	24S	11W	NW NW SW	abs	3904	3917	3994	4014	1842
Case	#1 McComb	22	24S	11W	N2 N2 NE	abs	3830	3852	3936	3952	1819
Halliburton	#1 McComb	26	24S	11W	SE SW NW	3821	3843	3860	3946	3962	1793
Weslch	#1 Hogan	27	24S	11W	E2 NW NW	3840	3858	3887	3972	3986	1811
CRA	#1-A McMillan	30	24S	11W	SW NE NW	abs	3903	3908	3996	4013	1836
Case	#1 Allen	1	24S	12W	NW NE SW	abs	3798	3812	3889	3910	1853
Huber et al.	#1 Bartlett	3	24S	12W	NE NE SW	abs	3837	3850	3922	3944	1867
Ash O&G	#1 Knoche	5	24S	12W	E2 SE SE	3808	3822	3840			1881
Int'l. Hydrocarb.	#1 Tretbar	5	24S	12W	NE SW NE	abs	abs	3840	3904	3925	1887
C. Clagett	#1 Seifkes	15	24S	12W	NE	abs	3814	3838	3927	3948	1877
Anschutz Drlg.	#1 Byer	17	24S	12W	NW NW SE	3884	3897	3915	4009	4017	1887
W. Hartman	#1 Kissling	25	24S	12W	SW SW NW	abs	3922	3932	4008	4026	1854
CRA	#1-B Byer	27	24S	12W	SE SE NW	abs	3921	3942	4030	4049	1878
Anschutz Drlg.	#1 Budde	29	24S	12W	NW NW SW	abs	3960	4000	4064	4084	1897
Musgrove Petrol.	#1 Manke	2	24S	13W	SW SW NE	abs	abs	3886	3948	3967	1902
Nat'l Assoc. Pet.	#1 W. Davis	3	24S	13W	NW SE NE	abs	abs	3852	????	3902	1901
Abercrombie Drlg.	#1 McMillan	5	24S	13W	NE SW SW	abs	abs	3977	4033	4050	1924
Sunray-Midcon.	#1 Sutton	9	24S	13W	NW NE NW	abs	3890	3920	3984	4006	1916
Allison	#1 Roohms	14	24S	13W	SE NE NW	3875	3900	3922	3998	4010	1918
Sterling Drlg.	#1-A Soden	15	24S	13W	SW SE NW	3913	3944	3970	4034	4056	1922
Beacon Resources	#1 Harrison	17	24S	13W	SW SW SW	abs	abs	4037	4100	4115	1937
F&M	#1-B Kachelman	21	24S	13W	NE SW SE	abs	3992	4014	4076	4100	1934
Sunray-Midcon.	#1 Cline	25	24S	13W	NE SW SE	abs	3966	3989	4055	4076	1910
Arco	#5-B McNaghten	27	24S	13W	SW SW NW	abs	abs	3945	4000	4011	1935
Aurora Gas	#1 Hoover	29	24S	13W	SE NE SE	3988	4024	4046	4112	4135	----
Altman	#1 Brehm-Burke	2	24S	14W	SE SW NE	abs	abs	4036	4074	4100	1963
Abercrombie Drlg.	#1 Jerel	3	24S	14W	NW NW SW	abs	4054	4082	4144	4170	1973
Musgrove Drlg.	#1 Krause	5	24S	14W	SW SW SW	abs	abs	3982	4030	4048	1995

APPENDIX I (continued)

OPERATOR	WELL NAME	LOCATION S.	T.	R.	SPOT	DEPTHS A	B	C	D	E	DATUM
Abercrombie Drlg.	#1 Cotton	9	24S	14W	N2 N2 SE	abs	abs	4124	4184	4208	1986
Atlantic Refining	#2 Weise	13	24S	14W	SE NW NW	3971	4010	4042	4110	4131	1925
Abercrombie Drlg.	#1 Morris	15	24S	14W	N2 SE NE	abs	abs	4090	4152	4164	1951
Anschutz Drlg.	#1 Laundrick	17	24S	14W	SE SE SW	abs	abs	4181	4240	4266	1987
Kaiser-Francis	#1 Suiter	21	24S	14W	NW NW NE	4130	4143	4162	4220	4240	1975
Hilton Drlg.	#1 Koelsch	25	24S	14W	NE SE SW	3994	4031	4057	4120	4144	1945
Natural G&O et al.	#1 Koelsch-Oswald	27	24S	14W	SE SW SW	abs	4158	4162	4226	4238	1977
Pickrell Drlg.	#1-C Sparks	29	24S	14W	SW SW SW	abs	4205	4226	4289	4315	1999
Murfin Drlg.	#1-C Southwestern	1	24S	15W	SE NW NE	abs	abs	4040	4079	4089	2003
Wallingford	#1 Cornwall	3	24S	15W	W2 SE NW	abs	abs	4025	????	4069	2020
Musgrove Drlg.	#1 Hoover	5	24S	15W	NE NE NE	abs	abs	4025	4102	4110	2028
Leben Drlg.	#1 Birdsell	9	24S	15W	SE SE NW	abs	abs	4005	????	4040	2040
Rex & Morris	#1 Hardten	11	24S	15W	SE NE SE	abs	abs	abs	4004	4018	2004
Murfin Drlg.	#1-B English-Reid	13	24S	15W	W2 SE	4134	4186	4210	4260	4290	2012
Lauck	#1-A Suiter	15	24S	15W	SE SE SE	4124	4180	4202	4270	4296	2020
Arizona	#1 Thurow	15	24S	15W	NE NE SW	abs	abs	4118	????	4144	2022
F.G. Holl	#2-18 Young	18	24S	15W	SW SE	abs	4205	4237	4296	4323	2054
J.O. Farmer	#1 Steward	19	24S	15W	SW NE	4214	4275	4298	4372	4400	2055
Natural G&O	#1 Carpenter	25	24S	15W	SW SW SW	4202	4226	4250	4304	4330	2016
Musgrove Drlg.	#1 Dykes	27	24S	15W	NE SE	abs	4316	4332	4374	4401	2025
Arrowhead	#1 Graybill	28	24S	15W	NW SE SE	4330	4355	4382	4438	4466	2036
Anschutz Drlg.	#1 Ackerman	29	24S	15W	NW NW SW	abs	4338	4352	4395	4412	2048
Etal Inc.	#1 Hammeke	1	24S	16W	NW NW NE	abs	abs	abs	4060	4074	2056
Natural G&O	#1 Hahn	4	24S	16W	NW SE SW	abs	4188	4225	4314	4347	2081
Imperial	#1 Doll	5	24S	16W	NW SE NE	4261	4294	4330			2083
Helmerich & Payne	#1 Hawley	7	24S	16W	SW SW NE	abs	abs	4370	4436	4486	2091
Imperial	#1 Smith	8	24S	16W	NE NE NE	abs	abs	4352	4430	4463	2082
Helmerich & Payne	#1 Coppoc	9	24S	16W	NE NE SW	abs	abs	4268	4350	4382	2075
Natural G&O	#1 Campbell	18	24S	16W	SE SW SW	4380	4402	4424	4512	4563	2093
Sunray	#1 Embry	24	24S	16W	NW NW SW	4284	4362	4388	4455	4486	2064
Armer	#1 Elmore	25	24S	16W	SE SE NW	4338	4416	4435	4506	4536	2064
Morrison	#1 Fisher	27	24S	16W	SW SW NW	4401	4440	4478	4563	4598	2079
Bennett & Roberts	#1 Laremore	33	24S	16W	SW SW SW	4450	4504	4547	4618	4661	2099
Conoco	#1 Meyer	34	24S	16W	SW SE SW	abs	abs	4374	4458	4500	2081
Aurora Gas	#1 Enlow	36	24S	16W	SW SW SE	4282	4338	4369	4434	4466	2059
F.G. Holl	#8-13 Hawley	13	24S	17W	NE NE NE	abs	abs	4450	4526	4565	2101
NCRA	#1 Lovette	17	24S	17W	SE SE NW	4437	4500	4540	4615	4646	2123
Lauck et al.	#1 Cross	28	24S	17W	NE NE NE	4477	4498	4546	4634	4675	2116
Sutton	#1 Vogt	17	25S	1W	SW SW NW	abs	abs	abs	3842	3856	1376
Allison	#1 Devore	19	25S	1W	NE SW NW	abs	abs	abs	3855	3878	1378
Catron	#1 Royal	36	25S	1W	S2 S2 SE	abs	abs	abs	3461	3480	1349
Allison et al.	#1 Williams	18	25S	2W	SW NE	abs	abs	3916	3938	3953	1405
Champlin	#1 Caple	19	25S	2W	SE SE NW	abs	abs	3921	3930	3938	1405
Charles Carlock	#1 Basore	25	25S	2W	SW SW SW	abs	abs	abs	3879	3894	1375
APC	#1 Smith	35	25S	2W	NE NE SW	abs	abs	abs	3896	3918	1382
Rupp et al.	#1 Jorgenson	10	25S	3W	NW NE NE	abs	abs	3955	3965	3990	1430
Texstar Petrol.	#1 Gilmore	3	25S	4W	SE NW	abs	abs	abs	3916	3932	1461
Kenwood	#1 Kinast	4	25S	4W	NE NE NW	abs	abs	3872	3883	3896	1465
Aurora Gas	#1 Tonn	21	25S	4W	NW NW NW	abs	abs	abs	4002	4014	1509
R. Godfrey	#1 Smith	23	25S	4W	NE NE NE	abs	abs	abs	4030	4034	1469
Shawver & Armour	#1 Elling	2	25S	5W	NW SW	abs	abs	abs	3858	3878	1536
Hummon	#1 Woodruff	17	25S	5W	NW NE	abs	abs	3824	3833	3844	1501
Wentworth	#1 Stuckey	20	25S	5W	SW SW SW	abs	abs	abs	3865	3868	1468
Texstar Petrol.	#1 Blocker-Tunn	24	25S	5W	SE SE	abs	abs	abs	4030	4045	1543
F&M	#1 Smythe	10	25S	6W	SE SE	abs	abs	abs	3980	4006	1518
Cities Service	#1 Zimmerman	21	25S	6W	NW NW SE	abs	abs	3922	3936	3950	1475
Petroleum, Inc.	#1 Binford	22	25S	6W	SW SE SE	abs	abs	3930	3937	3954	1456
F&M	#1-J Miller	35	25S	6W	NW NW	abs	abs	3963	3970	3989	1497
Stearns	#1 Burling	3	25S	7W	SE SE SW	abs	abs	4117	4122	4149	1586
Thunderbird Drlg.	#1 Trembley	18	25S	7W	SE SE NE	abs	abs	abs	4156	4164	1573
Shawver et al.	#1 Linscheid	2	25S	8W	NW NW NE	abs	abs	abs	4131	4144	1613
Allison et al.	#1 Miller	8	25S	8W	SE SE	abs	abs	4088	4111	4120	1649
Gear Petrol.	#1 Layman	26	25S	8W	SW SW	abs	abs	abs	4121	4134	1571
Aurora Gas	#1 Breidenstein	1	25S	9W	NE NE NE	abs	abs	4128	4164	4178	1671
Time Petrol.	#1 Nixon	7	25S	9W	SW SW SE	abs	abs	4144	4217	4232	1722
Murfin Drlg.	#1 Benson	19	25S	9W	S2 SE	abs	abs	4139	4218	4230	1712
Hendrick	#1 Catte	22	25S	9W	SW SE	abs	4065	4068	4145	4158	1617
El Dorado Refining	#1 McAtee	26	25S	9W	SE SE SE	abs	abs	4114	4192	4204	1618
Kaiser et al.	#1 Yar Mar	1	25S	10W	SE SE SE	abs	4154	4160	4234	4250	1724

APPENDIX I (continued)

OPERATOR	WELL NAME	LOCATION S.	T.	R.	SPOT	DEPTHS A	B	C	D	E	DATUM
Schermerhorn	#1 Brownlee	6	25S	10W	SE SE SW	abs	4046	4062	4150	4164	1757
Midstates	#1 Nies	15	25S	10W	NW SW	abs	abs	4140	4227	4240	1752
Schermerhorn	#1 Nies	20	25S	10W	SE NW NW	abs	abs	4168	4243	4258	1800
Rex & Morris	#1 Linder	23	25S	10W	NE NE NW	abs	abs	4143	4218	4234	1736
Colorado	#1 Nies	28	25S	10W	SW NE	abs	abs	4174	4246	4260	1755
Smitherman	#1 Zink	31	25S	10W	NE NE NE	abs	abs	4194	4274	4288	1787
Honey	#1 Brownlee	1	25S	11W	NW NE SE	abs	3972	3994	4080	4097	1771
American	#1 McCune	3	25S	11W	NW SE SW	abs	3907	3921	4000	4017	1795
Aylward Drlg.	#1 Newell	6	25S	11W	NW NW NE	3890	3936	3950	4027	4046	1827
Nixon	#1 Cravens	15	25S	11W	NW NW NE	abs	abs	3934	4022	4038	1799
Lawson & Skelly	#1 Dickson	17	25S	11W	NW SE NW	abs	3998	4020	4077	4094	1829
Huber & Lewis Drlg.	#1 Bargdill	25	25S	11W	NE NE NE	abs	4174	4180	4264	4279	1806
Pan Western	#1-28SRM Hodgins	28	25S	11W	W2 NE SE	abs	abs	4018	4105	4120	1838
Champlin	#1 Thomas	29	25S	11W	N2 NW SW	abs	abs	4124	4187	4203	1834
Bonanza	#1 Fritzemeier	3	25S	12W	SW SE	abs	3965	4002	4066	4082	1877
F&M	#1 McCune	5	25S	12W	SE NW SW	abs	4010	4044	4109	4126	1906
American Lariat	#1 McFadden	12	25S	12W	SE SE SE	abs	3958	3994	4060	4076	1838
Goodin	#1-5 Staton Farms	15	25S	12W	NW NW NW	abs	3964	3986	4052	4071	1873
Aurora Gas	#1 McCune	17	25S	12W	SW SW NE	abs	abs	4034	4086	4102	1893
Brandt	#1 Slade	23	25S	12W	NE SW SW	4014	4037	4065	4128	4146	1854
Pure	#1 Brock	25	25S	12W	SE NW NE	abs	4010	4035	4099	4116	1838
Energy Expl.	#1 EnEx-Weller	28	25S	12W	E2 SE SW	abs	abs	4070	4120	4135	1874
F&M	#1 Christie	30	25S	12W	NE NE SW	abs	abs	4094	4154	4172	1902
F&M	#1 Fort	2	25S	13W	SE SW NW	abs	4025	4050	4113	4136	1922
Brougher	#1-A Bell	3	25S	13W	NW NE NW	abs	4080	4094	4158	4180	1940
Petroleum, Inc.	#1 Barstow	5	25S	13W	NW NE NW	abs	4096	4114	4180	4203	1943
Conoco	#2 Russell	13	25S	13W	SE NW NE	abs	abs	3950	4013	4030	1912
Artnell	#1 Shank	15	25S	13W	NE NE	abs	abs	4126	4194	4214	1931
El Dorado Refining	#2 Lyon	17	25S	13W	NW NW NW	abs	abs	4167	4210	4225	1958
Dunne-Gardner	#1 Russell	25	25S	13W	NW SW NW	abs	abs	4095	????	4157	1916
F&M	#1 Dudrey	27	25S	13W	S2 SW NE	abs	abs	4168	4216	4232	1931
Dunne-Gardner	#1 Curtis	29	25S	13W	SE NE NE	abs	abs	4200	4278	4294	1951
Alco	#6 Sanders	1	25S	14W	SE NE NW	4115	4140	4166	4228	4252	1956
Helmerich & Payne	#1 Dykes	3	25S	14W	SW SE NE	abs	4104	4150	4224	4248	1955
Falcon	#1 Wilson	5	25S	14W	NW NE SW	abs	abs	4250	4282	4300	2001
Gear Petrol.	#2-6 Wilson	6	25S	14W	SW SW NW	abs	abs	4296	4356	4380	2005
Apache	#1 Bear	8	25S	14W	NW NW SW	abs	abs	4266	4326	4348	1993
Dean & Clark	#1 Kachelman	13	25S	14W	NW NW SE	abs	abs	4206	4252	4262	1971
Allison	#1 Fox	15	25S	14W	SW SE NE	abs	abs	4192	4226	4232	1978
Alpine	#1 Hall	17	25S	14W	SW SW NE	4239	4270	4290	4346	4368	1988
Zenith Drlg.	#2 Goodman	25	25S	14W	NW NW NE	abs	abs	4224	4283	4305	1969
Knighton	#1 Toland	27	25S	14W	N2 NE NW	abs	abs	4193	????	4230	1986
Texas	#1-29 English	29	25S	14W	SW SW	4278	4314	4344	4416	4442	2005
Gulf	#1 Lynn Reese	1	25S	15W	NE NE NW	abs	abs	4276	4310	4333	2017
Dunne-Gardner	#1 Barstow	3	25S	15W	SW NW NW	4250	4260	4287	4337	4366	2042
Aylward Drlg.	#1 Knudson	6	25S	15W	NE NE SW	abs	abs	4374	4430	4460	2055
Dunne-Gardner	#1 Wilson	13	25S	15W	NW NW SE	abs	abs	4418	4440	4446	2016
Sierra & Houston	#1 Wiles	15	25S	15W	NW SE NW	4250	4268	4302	4391	4418	2030
Strata Drlg.	#1 Childs	17	25S	15W	NE NE	4304	4376	4408	4448	4476	2043
Charles Hulme	#1 Piland	18	25S	15W	SE SE SE	4447	4467	4486	4516	4544	2054
Lauck & Sunray	#1 Frack	20	25S	15W	NE SW	4344	4414	4458	4510	4540	2045
Nadel & Gussman	#1 Stambaugh	24	25S	15W	SW SW	abs	abs	4376	4430	4455	2001
White & Ellis	#2 Waddle	26	25S	15W	SE NW	abs	4398	4427	4481	4502	2009
Lauck & Sunray	#1 Frack	27	25S	15W	SW SW SW	4384	4404	4456	4493	4516	2022
Chief Drlg.	#1 Lamb	30	25S	15W	SW SW SW	abs	4340	4356			2053
Alpine & Royalty	#1 Stambaugh	33	25S	15W	SW SW NE	abs	abs	4470	4507	4531	2029
Birmingham-Bartlett	#1 Frack	35	25S	15W	NE NE SW	abs	4444	4462	4511	4535	2022
Lauck	#1-A Breitenbach	5	25S	16W	N2 SE SE	4327	4372	4398	4498	4533	2085
Harms-Burt	#1 Breitenbach	10	25S	16W	NE NE NW	abs	4400	4442	4536	4570	2075
Skelly	#1 Miller	12	25S	16W	NE NW NE	4305	4390	4409	4468	4502	2065
Lauck	#1 Palmitir	16	25S	16W	SW SW	abs	4516	4538	4620	4648	2081
Natural G&O	#1 Johnston	18	25S	16W	NE NW SE	abs	abs	4500	4577	4616	2096
Lauck	#1 Ansel	23	25S	16W	SE SE NE	4397	4435	4488	4576	4607	2062
Lauck	#1 Johnson	25	25S	16W	NW NW	abs	4460	4489	4573	4606	2053
Lauck	#1 Parker	30	25S	16W	NW NW	abs	4551	4564	4647	4690	2090
Smitherman	#1 Mayhew	33	25S	16W	NW SE SE	4530	4557	4594	4673	4708	2084
Lauck	#1 Johnson	1	25S	17W	NE SE SW	abs	abs	4557	4657	4704	2108
Twin Drlg.	#1 Britton	9	25S	17W	SW SW NW	abs	abs	4602	4688	4725	2139
Cities Service	#1 Wokaty	25	25S	17W	NE SE NE	abs	abs	4562	4664	4710	2093
Sherrod & Apperson	#1 Huff	31	25S	17W	SE NE NW	4627	????	????	4784	4822	2146
Braden Drlg.	#1 Gatterman	34	25S	17W	NE NE NW	abs	abs	4607			2124
Halliburton et al.	#1 Burge	4	26S	1W	SE SE NE	abs	abs	3764	3776	3780	1348
Catron	#3 Wilson	12	26S	1W	E2 E2 SE	abs	abs	3360	3370	3382	1343
Allison	#1 Hitt	32	26S	1W	NE NW NE	abs	abs	abs	3882	3888	1370

APPENDIX I (continued)

OPERATOR	WELL NAME	LOCATION S.	T.	R.	SPOT	DEPTHS A	B	C	D	E	DATUM
Amerada	#1 A. Kessler	34	26S	1W	SW SW	abs	abs	abs	3834	3844	1333
Shawver & Armour	#1 Hyde	11	26S	2W	NW NW NE	abs	abs	abs	3902	3910	1375
Barbara	#1 Seiwart	18	26S	2W	SW SW SW	abs	abs	abs	3987	3996	1408
Aurora Gas	#1 Baalman	21	26S	2W	SE SE NW	abs	abs	3939	3954	3962	1372
Sun	#1-A Lies	12	26S	3W	SW SW	abs	abs	abs	3972	3981	1420
Skelly	#1 Biermann	26	26S	3W	NE NE NE	abs	abs	abs	4052	4058	1463
Gabbert-Jones	#1 Schmidt	1	26S	4W	SW NW	abs	abs	abs	4116	4120	1526
Eagle	#1 Reussner	4	26S	4W	NW SE SW	abs	abs	abs	4000	4012	1555
Shawver & Armour	#1 Schmitz	22	26S	4W	SW SE SE	abs	abs	abs	4099	4106	1492
Wilkinson	#1 Longsdorf	29	26S	4W	NE NW SW	abs	abs	abs	4020	4027	1428
Ritchie	#1 Popp	11	26S	5W	NE NW SW	abs	abs	3924	3930	3944	1550
Mizel	#1 Blocker	23	26S	5W	NE NE SE	abs	abs	4006	4018	4024	1432
Brad's Petrol.	#1 White	31	26S	5W	NW NE	abs	abs	4108	4122	4125	1515
Stickle Drlg.	#1 Graham	8	26S	6W	NE NE SW	abs	abs	4072	4086	4095	1565
Petroleum Oper.	#1 Collingwood	11	26S	6W	NW SW	abs	abs	4027	4050	4055	1541
Aylward Drlg.	#1 Krehbiel	26	26S	6W	NW NW NW	abs	abs	abs	4086	4091	1572
Plains	#1 Sieb	32	26S	6W	SW	abs	abs	abs	4174	4185	1572
Messman-Rinehart	#1 Larson	8	26S	7W	SE SE SE	abs	abs	abs	4244	4254	1607
H-30 Drlg.	#1 Graber	13	26S	7W	NE SE	abs	abs	abs	4070	4082	1576
K&E Drlg.	#1 Snapp	25	26S	7W	SE NE NW	abs	abs	abs	4147	4156	1595
Pickrell Drlg.	#1-E Bruch	31	26S	7W	SE NW	abs	abs	abs	4306	4312	1591
Anschutz Drlg.	#1 Gardner	5	26S	8W	NE NE SW	abs	abs	4202	4235	4245	1639
Tomlinson-Kathol	#1 Brooks	10	26S	8W	SW SW	abs	abs	4234	4245	4257	1619
Cinco Expl.	#1 Brooks	17	26S	8W	NE SW	abs	abs	4231	4273	4282	1655
K&E Drlg.	#1 Peek	21	26S	8W	NE NE	abs	abs	4281	4305	4314	1658
Aylward Drlg.	#1 Hay	25	26S	8W	SE SE SE	abs	abs	4316	4336	4339	1608
Texas	#1 Foss	27	26S	8W	NE NE SE	abs	abs	4280	4303	4310	1631
Huber	#2 Reese	11	26S	9W	SW NE SW	abs	abs	4120	4188	4202	1668
Sohio Petrol.	#1 Wells	18	26S	9W	SW NW NW	abs	abs	4196	4270	4285	1664
NCRA	#1 Woodson	22	26S	9W	NW NW SW	abs	abs	4176	4242	4255	1701
Harms-Burt	#1 Jones	26	26S	9W	NE NE SE	abs	abs	4211	4278	4287	1670
Durbin Bond	#1 foster	29	26S	9W	NE NE NE	abs	abs	4188	4253	4260	1717
Armer	#1 Geesling	3	26S	10W	SE SE SE	abs	abs	4216	4284	4297	1733
T.O. Lillystrand	#1 Flukes	15	26S	10W	NE NW NW	abs	abs	4204	4271	4285	1727
Aylward Drlg.	#1 Tredway	34	26S	10W	SW NW NE	abs	abs	4263	4330	4343	1709
Deep Rock	#1 Slater	1	26S	11W	SW SW NE	abs	abs	4224	4299	4314	1809
Helmerich & Payne	#1 Jorns	5	26S	11W	SW SW NW	abs	abs	4123	4200	4218	1853
Imperial	#1 Deniston	6	26S	11W	W2 SW NE	abs	4100	4128	4190	4204	1855
Allison	#1 McOsker	9	26S	11W	SE NW NW	abs	abs	4242	4326	4340	1856
Vickers Expl.	#1 Walker	13	26S	11W	NW NW SE	abs	abs	4252	4324	4338	1803
Natural G&O	#1 Schriver	16	26S	11W	SW SE NW	abs	abs	4254	4324	4336	1841
APC	#1 Stark	18	26S	11W	SW SE NW	abs	4195	4208	4282	4298	1866
Rains & Williamson	#1 Shanline	27	26S	11W	SW NW	abs	abs	4297	4376	4391	1817
Herndon & Flynn	#1 Simon	32	26S	11W	N2 NE NE	abs	abs	4282	4362	4376	1830
Texas Energies	#1-35 Huff	35	26S	11W	SE SW	abs	4288	4290	4370	4394	1791
Abercrombie Drlg.	#1 Stewart	3	26S	12W	NW	abs	abs	4100	4156	4169	1878
Mercury et al.	#1 Hawver	5	26S	12W	NW NW NE	abs	abs	4117	4176	4182	1886
Murfin et al.	#1 Stalcup	11	26S	12W	SW NE SW	abs	abs	4126	4180	4192	----
Texas Energies	#1-13 Rundell	13	26S	12W	SE SE NW	abs	4146	4155	4225	4242	1879
Argonaut	#1 Hartsell	14	26S	12W	SE SE	abs	4186	4200	4262	4280	1884
Musgrove Drlg.	#1 Trimpe	17	26S	12W	SW SW SW	abs	abs	4238	4292	4309	1911
Aladdin Petrol.	#2 Holme	20	26S	12W	SE SW SW	abs	4109	4125	4189	4197	1911
B.F. Brack	#1 Knop	21	26S	12W	SW SW SW	abs	abs	4154	4206	4208	1920
NCRA	#1 Burkner	25	26S	12W	SE SE SW	4292	4308	4315	4383	4390	1862
Nate Appleman	#1 Stead	27	26S	12W	SW SW NE	abs	abs	4247	4300	4307	1911
CRA	#3-B Brown	29	26S	12W	NE SW SE	abs	abs	4094	4148	4156	1909
Armer	#1 Fincham	3	26S	13W	SW SW NW	abs	abs	4274	4314	4330	1936
Skelly	#1 Russell	5	26S	13W	SE NE NE	abs	abs	4222	4260	4276	1942
F&M	#1-G Keller	11	26S	13W	NE SW SE	abs	abs	4203	4268	4286	1913
F&M	#1-D Keller	14	26S	13W	NW NW NE	abs	abs	4236	4285	4296	1919
Lauck	#1 Schrack	15	26S	13W	SE SE NE	abs	abs	4268	4308	4311	1919
F&M	#1-A Craig	17	26S	13W	NE NE NW	abs	abs	4340	4388	4402	1953
Hill	#1 Dodson	21	26S	13W	SW SE NE	abs	abs	4336	4390	4411	1941
Beardmore Drlg.	#6 Lunt	25	26S	13W	NW NW	abs	abs	4153	????	4226	1935
Rine Drlg.	#1 Hoener	27	26S	13W	SW SW SW	abs	abs	4226	????	4323	1953
Moore	#2 Williams	29	26S	13W	SW SE NW	abs	abs	4344	4401	4419	1948
F&M	#1-C Tobias	30	26S	13W	SW SW SE	abs	abs	4372	4434	4452	1968
Deep Rock	#1 McCandless	1	26S	14W	S2 NW	abs	4282	4290	4342	4352	1985
Armer	#1 Henderson	2	26S	14W	NE NW SE	abs	abs	4234	4307	4326	1993

APPENDIX I (continued)

OPERATOR	WELL NAME	LOCATION S.	T.	R.	SPOT	DEPTHS A	B	C	D	E	DATUM
Dunne-Gardner	#1 Collins	3	26S	14W	SW SW SW	abs	4276	4295	4338	4361	1999
Dunne-Gardner	#1 Henderson	4	26S	14W	SE SE SE	abs	abs	4310	4362	4386	2003
Skelly	#1 A.E. Randle	5	26S	14W	NW NE SW	abs	abs	4291	4320	4339	2013
Imperial	#1 Elliott	6	26S	14W	SW SW NW	4309	4362	4380	4443	4468	2023
Rine Drlg.	#1-B Gereke	7	26S	14W	NE NE NE	4310	4353	4365	4422	4444	2019
Petroleum, Inc.	#1-E Gereke	8	26S	14W	NE NE NW	4348	4360	4379	4440	4452	2018
F&M	#1-B Hutchins	9	26S	14W	NE SE SW	4337	4370	4394	4448	4471	2016
Champlin	#1-B Henderson	10	26S	14W	NE SE SE	4302	4318	4340	4400	4422	1995
Champlin	#1 Henderson	11	26S	14W	SW NE NW	abs	abs	4279	4344	4360	1991
F&M	#1-A Henderson	12	26S	14W	SE NE NW	abs	4312	4322	4386	4404	1974
Raymond	#1 Warren	14	26S	14W	NW NE NE	abs	4330	4340	4400	4424	1980
F&M	#1-B Henderson	15	26S	14W	S2 SW	abs	abs	4380	4437	4460	1997
Dunne-Gardner	#1 Carr Farms	22	26S	14W	NW NW SE	abs	abs	4382	4412	4419	1991
Par Petrol.	#1 Hensley	23	26S	14W	NW NE	abs	4388	4396	4455	4476	1979
Cities Service	#1 Bennett	24	26S	14W	NE NE SE	abs	abs	4356	4404	4420	1958
TXO	#1 McMannis	25	26S	14W	S2 N2 NE	abs	abs	4362	4419	4438	1870
Murfin Drlg.	#1-26 Hoener	26	26S	14W	SE NW	abs	4404	4414	4475	4497	1996
Messman-Rinehart	#1-A Berg	27	26S	14W	SE SE NW	abs	abs	4380	4450	4466	1985
K&E & Musgrove	#1 Thompson	28	26S	14W	NW NW SE	abs	abs	4496	4528	4532	2005
Strata Drlg.	#1 Schoonover	29	26S	14W	NE NW	abs	abs	4452	4498	4502	2017
National	#1 Berry	32	26S	14W	NW NE	abs	4420	4438	4496	4514	2013
Lion	#1 Callahan	33	26S	14W	NW NW SE	abs	abs	4450	4499	4505	2005
Sierra Petrol.	#1 McMannis	36	26S	14W	SW SW NW	abs	4386	4402	4462	4478	1967
Rex & Morris	#1 Childs	1	26S	15W	SE NW	4350	4427	4446	4498	4522	2027
Rex & Morris	#1 Binger	2	26S	15W	SW NE	abs	4389	4419	4484	4510	2024
Anschutz Drlg.	#1 Leming	3	26S	15W	S2 NE NE	abs	4455	4476	4532	4558	2032
Sunray	#1 Neelly	5	26S	15W	NW SE NE	abs	4496	4525	4572	4597	2052
WTA	#2-A Curtis	8	26S	15W	SE NE SE	4466	4504	4534	4604	4627	2066
Anderson-Prichard	#1 Long	11	26S	15W	SW SW NE	abs	4378	4382	4450	4464	2034
Rine Drlg.	#1 Gereke	12	26S	15W	SW NE SE	4328	4380	4400	4462	4486	2038
Deep Rock	#1 Lutes	13	26S	15W	NE NE NW	abs	4442	4450	4510	4535	2029
Pickrell Drlg.	#1 Smith O-O	14	26S	15W	SE SW SE	4386	4448	4482	4542	4566	2044
Mull Drlg.	#1 Doggett	17	26S	15W	NE NE SW	4416	4489	4514	4570	4596	2046
Twin Drlg.	#1 Bisel	19	26S	15W	NE NW SW	4442	4510	4523	4599	4628	2064
Stickle Drlg.	#1 Curtis	20	26S	15W	NW SE	4410	4503	4520	4572	4598	2055
Lion	#1 Elliott	21	26S	15W	SE SE SW	4420	4508	4523	4576	4600	2055
Texas Energies	#1-23 Curtis	23	26S	15W	S2 SE NW	4418	4482	4516	4570	4594	2058
Texas Energies	#1-25 Thomas	25	26S	15W	NW NE	abs	abs	4464	4527	4552	2037
Strata Drlg.	#3 Curtis	26	26S	15W	SW SE NW	4373	4436	4457	4510	4532	2044
Texas Energies	#1-27 State of Kansas	27	26S	15W	NE NE SW	4380	4456	4484	4534	4561	2065
Anschutz Drlg.	#1 Tatlock	28	26S	15W	NE NE NW	4416	4498	4516	4568	4591	2053
Texas Energies	#1-29 State of Kansas	29	26S	15W	SE	4412	4504	4510	4568	4592	2059
Aladdin Petrol.	#2 Tatlock	30	26S	15W	NE SW NW	4400	4488	4515	4577	4602	2070
Bell et al.	#1-A Tatlock	32	26S	15W	NE NE NW	4430	4480	4512	4567	4592	2062
Texas Energies	#1-34 State of Kansas	34	26S	15W	W2 E2 NE	4397	4460	4480	4532	4557	2053
Texas Energies	#1-36 Lutes	36	26S	15W	S2 NW	abs	4522	4527	4576	4600	2042
Robert-Gay	#1 R.G. Fouse	1	26S	16W	SW NW	4452	4492	4526			2055
Oil Prop.	#1 Bryant	3	26S	16W	NE NE	4472	4534	4570	4648	4678	2075
Benson	#4 Gibson	10	26S	16W	SE NE	4419	4470	4498	4592	4622	2063
Amerada	#1 Schultz	11	26S	16W	NE SE NE	abs	4505	4508	4604	4630	2066
F.K. Johnson	#1 Salser	12	26S	16W	SW SW NW	abs	abs	4538	4626	4652	2066
Ambassador	#1-A Wood	13	26S	16W	SW NW NW	abs	abs	4452	4543	4552	2067
Aurora Gas	#1 Schultz	21	26S	16W	SE SE NW	abs	abs	4666	4734	4770	2103
Cinco Expl.	#1 Doggett	24	26S	16W	SW SE	abs	abs	4552	4624	4656	2092
F.K. Johnson	#1 E.D. Wood	26	26S	16W	NE NE NE	abs	abs	4560	4636	4654	2079
Sinclair	#1 Mellor	28	26S	16W	SW SW SE	abs	abs	4622	4716	4748	2091
Sunray	#1 King	33	26S	16W	NE NE SW	abs	abs	4636	4720	4750	2091
Aurora Gas	#1 Fatzer	9	26S	17W	SE SE SE	abs	abs	4695	4774	4793	2131
Trans-Era Petrol.	#1 Sherman	12	26S	17W	NW NW SW	abs	4646	4651	4765	4782	2116
Phillips	#1 Newsom	13	26S	17W	SW SW SW	4626	4632	4671	4768	4782	2107
Anschutz Drlg.	#1 Fatzer	15	26S	17W	SE SE SE	abs	abs	4676	4756	4774	2124
Anschutz & Aurora	#1 Fisher	35	26S	17W	NE NE NE	4675	4699	4722	4816	4834	2109
Aladdin Petrol.	#1 Woods	32	27S	1W	SE SW NE	abs	abs	abs	3661	3670	1313
Adair	#1 Strunk	5	27S	2W	NW NW NW	abs	abs	4088	4096	4105	1457
F&M	#1 Falkowski	15	27S	2W	SW SE SE	abs	abs	abs	4030	4041	1401
Ben Brack	#1 Siggs	20	27S	2W	NW SW NE	abs	abs	4084	4088	4093	1419
Aurora Gas	#1 Klausmeyer	14	27S	3W	NE NE NE	abs	abs	abs	4143	4156	1471
Amerada	#1 Becker	18	27S	3W	SE NE SE	abs	abs	abs	4200	4204	1485
Ferguson	#1 Scheer	22	27S	3W	SE SE SW	abs	abs	abs	4177	4186	1500
Aylward Drlg.	#1 Wells	26	27S	3W	NE NW	abs	abs	abs	4192	4197	1493
Ritchie	#1 Rosenhagen	8	27S	4W	SE SW NW	abs	abs	4026	4032	4038	1381
Sanders & Con-Am	#1 Rosenhagen	26	27S	4W	NW NW SW	abs	abs	abs	4235	4238	1447
Huber et al.	#1 Webb	29	27S	4W	SW SW NE	abs	abs	abs	4182	4186	1388
Lauck	#1 Teimeyer	8	27S	5W	SE SE SE	abs	abs	4168	4179	4188	1505

APPENDIX I (continued)

OPERATOR	WELL NAME	LOCATION S.	T.	R.	SPOT	DEPTHS A	B	C	D	E	DATUM
Armer	#1 Ambler	15	27S	5W	NE NW NW	abs	abs	4209	4216	4220	1523
Skelly	#1 Bonjour	26	27S	5W	NW NW NE	abs	abs	abs	4177	4192	1496
F&M	#1 Reno	29	27S	5W	NE SE	abs	abs	4191	4197	4214	1459
Trans Era	#1 Goering	1	27S	6W	NE NE NW	abs	abs	4184	4194	4204	1556
Mack	#1 Hampel	8	27S	6W	NW SE	abs	abs	4107	4113	4120	1498
Commercial	#1 Knight	26	27S	6W	NE NE NW	abs	abs	4112	4122	4133	----
Mack	#1 Wolf	29	27S	6W	NE SW	abs	abs	abs	4248	4272	1566
Sutton	#1 Endicott	33	27S	6W	NW NW NW	abs	abs	abs	4260	4268	1563
Osage O&G	#1 Hyde	1	27S	7W	NE NE SE	abs	abs	abs	4190	4195	1524
Silver Creek	#1 McCutchen	3	27S	7W	SE SE SW	abs	abs	abs	4124	4133	1547
Heathman-Seeligson	#1 Wooldridge	16	27S	7W	SW SE NE	abs	abs	abs	4156	4170	1554
South Ranch	#1 Hamblin	17	27S	7W	SE NE	abs	abs	abs	4266	4280	1567
Texas O&G	#1-A Schwartz	27	27S	7W	SE NW	abs	abs	abs	4264	4280	1603
Mack	#1 Van Sickle	29	27S	7W	SW NE	abs	abs	abs	4314	4334	1600
Anschutz Drlg.	#1 Dondelinger	35	27S	7W	SE SE SW	abs	abs	abs	4227	4250	1526
Alpha	#1 Stucky	1	27S	8W	NW NW NE	abs	abs	4264	4270	4302	1592
Collins	#1 Keller	6	27S	8W	NE NE NE	abs	abs	4298	4363	4374	1692
Rupe	#1 Geesling	17	27S	8W	SE NW	abs	abs	4319	4379	4388	1680
Leben Drlg.	#1 Dutton	21	27S	8W	NW NE	abs	abs	4332	4383	4392	1663
Mack	#1 Freeland	24	27S	8W	SW SW	abs	abs	4352	4354	4381	1631
Leben Drlg.	#1 Funke	25	27S	8W	SE SE	abs	abs	abs	4328	4354	1613
Wentworth & Sons	#1 McClure	31	27S	8W	NW NE NW	abs	abs	4321	4368	4376	1625
Ferguson	#1 Sears	33	27S	8W	SE SE	abs	abs	4317	4380	4390	1639
Brown-Woolsey	#1 Oak	4	27S	9W	SW NE	abs	abs	4208	4276	4288	1700
Lauck	#1 Bradshaw	5	27S	9W	NW NE SE	abs	abs	4222	4300	4310	1720
Jay Boy	#1 Boswell	20	27S	9W	E2 E2 SW	abs	abs	4338	4398	4410	1734
Pickrell Drlg.	#1-C Stitts	27	27S	9W	SW NW	abs	abs	4287	4360	4370	1650
Pickrell Drlg.	#1-H Tjaken	29	27S	9W	NE NW	abs	abs	4328	4390	4399	1713
Gulf	#1 Calista State	35	27S	9W	NW NE NE	abs	abs	4270	4330	4340	----
Aylward Drlg.	#1 Tonn	3	27S	10W	NE NE SW	abs	abs	4307	4372	4386	1743
Time Petrol.	#1 Bradshaw	12	27S	10W	SW SE	abs	abs	4270	4341	4354	1745
Lion	#2 McMichael	13	27S	10W	SE SE SW	abs	abs	4275	4340	4354	1729
Amerada	#1 McNamee	21	27S	10W	NW NW SE	abs	abs	4313	4376	4390	1749
Texas Energies	#1-27 Alley	27	27S	10W	W2 W2 SE	abs	abs	4242	4303	4316	1639
Ingling et al.	#1 Schwartz	36	27S	10W	NE NW	abs	abs	4294	4354	4364	1684
Larsen et al.	#1 Maas	7	27S	11W	NW NW	abs	4330	4332	4404	4420	1835
A & A	#1-A Holland	8	27S	11W	SE NW	abs	4300	4302	4378	4395	1829
D&M	#1 Cannon	12	27S	11W	NE SW SE	abs	4291	4294	4368	4380	1769
Trans-Pacific	#1-A Park	14	27S	11W	SE NE	abs	abs	4321	4396	4411	1793
GMR	#1 Bradley	16	27S	11W	SW SW SE	abs	abs	4344	4424	4438	1820
Woolsey	#2 Lehrling	19	27S	11W	NE NW	abs	abs	4360	4443	4456	1863
Kirkland	#1 Fitzsimmons	27	27S	11W	NW NW NW	abs	abs	4277	4338	4354	1772
Southwestern Expl.	#1 Lion	29	27S	11W	E2 NE NW	abs	abs	4323	4406	4420	1817
Kirkman	#1-35B Fitzsimmons	35	27S	11W	SE NW	abs	4104	4110	4185	4204	1706
Hummon & Ropfogel	#1 Fisher	1	27S	12W		abs	4332	4340	4402	4417	1869
D&D	#2-A Lathrop	3	27S	12W	NW	abs	4405	4422	4483	4499	1892
Studer	#2 Studer	4	27S	12W	SE SE SW	abs	abs	4300	4364	4372	1867
Skelly	#2-G Helmke	5	27S	12W	NW NE NW	abs	abs	4130	4202	4212	1893
Skelly	#5-H Helmke	6	27S	12W	NW NW NE	abs	abs	4118	4151	4162	1905
Skelly	#6-A Beck	7	27S	12W	NE NE NW	abs	abs	4118	4147	4160	----
Raymond	#1 Konold	8	27S	12W	SE SE SE	abs	abs	4189	4250	4264	1862
Black	#4-A Studer	9	27S	12W	NE SW NW	abs	abs	4272	4320	4336	1846
Leben Drlg. et al.	#1 Whitman	10	27S	12W	SW SE NE	abs	4360	4378	4434	4450	1879
Falcon Seaboard	#1 Elwood	12	27S	12W	NW NW NW	abs	4346	4350	4416	4430	1866
Texas Energies	#1-14-B Barnes	14	27S	12W	N2 NW	abs	4342	4356	4412	4430	1858
Osage O&G	#1 Hoeme	17	27S	12W	SW SW NW	abs	4214	4226	4286	4303	1870
Skelly	#4 Siedel	18	27S	12W	SE SE NE	abs	abs	4166	4236	4249	1869
Stableford	#1 Helmke	19	27S	12W	NW NW SW	abs	4186	4198	4278	4284	1877
Rex & Morris et al.	#1 Maas	20	27S	12W	SE SE SW	abs	4320	4330	4400	4415	1858
Republic Nat. Gas	#1 Maas	21	27S	12W	SE SE SW	abs	4286	4302	4361	4374	1827
Merchant	#1 Roberts	22	27S	12W	SW SW	abs	abs	4332	4368	4376	1791
Black	#1-G Studer	23	27S	12W	N2 SW NW	abs	4337	4350	4407	4418	1817
Hummon & Ropfogel	#1 Carver	24	27S	12W	NW NW SW	abs	abs	4301	4361	4371	1790
Texas Energies	#2-25 Barnes	25	27S	12W	W2 W2 NE	abs	abs	4298	4354	4364	1764
Kern-Landes	#1 Elmer	28	27S	12W	NW NE SW	abs	abs	4306	4367	4376	1915
McAlester Fuel	#1 Lunt	29	27S	12W	SE SE	abs	abs	4333	4392	4396	1832
Palmer & Colorado	#2 Rollinson	30	27S	12W	NW SW SW	abs	4224	4236	4295	4302	1902
Colorado	#1-A Humphrey	31	27S	12W	SW NW	abs	abs	4372	4413	4420	1882
Lauck	#1 Stull	32	27S	12W	SE NW NE	abs	4304	4320	4380	4390	1827
Kern-Landes	#1 Lunt	33	27S	12W	NW NW	abs	abs	4298	4338	4346	1789
Bowers	#1 Bergner	35	27S	12W	W2 SE NE	abs	4246	4252	4315	4329	1761
Bowers	#1-A Bergner	36	27S	12W	W2 SW NW	abs	4242	4256	4317	4330	1746
Getty	#1 Dean	1	27S	13W	NW NE NW	abs	4176	4194	4253	4260	1914
Lion	#2 Chance	4	27S	13W	E2 NW NW	abs	abs	4255	????	4335	1965

APPENDIX I (continued)

OPERATOR	WELL NAME	LOCATION S.	T.	R.	SPOT	DEPTHS A	B	C	D	E	DATUM
Eagle	#1 McGuire	5	27S	13W	SE NW	abs	abs	4327	4376	4380	1978
Lindsley Drlg.	#4-A Luders	13	27S	13W NE	SW NW	abs	4200	4217	4280	4290	1890
Hinkle	#1 Carver	15	27S	13W NE	NW SE	abs	abs	4320	4362	4380	1950
Cinco Expl.	#1 Pratt Airport	17	27S	13W	NW SE	abs	abs	4362	4407	4424	1958
Palmer et al.	#1 Bergner	25	27S	13W SE	NE SE	abs	abs	4257	4306	4309	1905
Beardmore & Lario	#1 Barnes	28	27S	13W NE	NE NE	abs	abs	4370	4410	4414	1948
NCRA	#1 Honeman	29	27S	13W SE	SE NW	abs	4336	4358	4408	4412	1926
Dunne-Gardner	#1 Hoener	1	27S	14W NW	SW SW	abs	abs	4428	4470	4490	1994
Lion	#1-B Ewbank	4	27S	14W NW	NW NW	abs	4417	4428	4484	4509	2004
Aurora Gas	#1 Jones	5	27S	14W SW	SW SW	abs	abs	4508	4544	4560	2019
Lario	#1 Moon	13	27S	14W SW	NE SW	4374	4396	4432	4502	4523	1982
Anadarko	#1-A Logue	15	27S	14W	SW NW	abs	4468	4470	4535	4555	2014
Musgrove & Seminole	#1 Reed	27	27S	14W NE	NE NW	abs	abs	4477	4534	4548	2000
Parker Petrol.	#1 I. Adams	29	27S	14W NW	NW SE	abs	4507	4512	4566	4588	2011
H-30 Drlg.	#1 Krueger	35	27S	14W	NW NE	abs	4446	4468	4528	4538	1973
Tennessee Gas	#1 Stotts	3	27S	15W	SE NE	abs	4460	4472	4516	4542	2060
Musgrove Drlg.	#1 Tatlock	6	27S	15W NE	NE NE	4538	4581	4599	4678	4707	2073
Aegis-Maxwell	#1 Halper Twin	12	27S	15W SE	NE SE	abs	4474	4480	4535	4557	2031
Anschutz Drlg.	#1 Jones	13	27S	15W SW	SW SW	4487	4518	4560	4618	4641	2050
Osage O&G	#1 Thompson	15	27S	15W NW	NW SE	abs	4608	4620	4689	4694	2064
TXO	#1-AC Miller	17	27S	15W W2	SE NE	abs	4620				2066
Braden Drlg.	#1 Lemon	27	27S	15W SE	NW NW	abs	4589	4608	4693	4720	2076
Musgrove Drlg.	#1 Bryant	32	27S	15W SW	SW NE	abs	abs	4674	4756	4759	2063
Murfin Drlg.	#1 White	35	27S	15W	NE NE	abs	4581	4592	4660	4682	2059
Sunray	#1 L. French	4	27S	16W	NE SW	abs	4613	4636			2105
Murfin Drlg.	#1 Matthews	7	27S	16W SE	SE NE	abs	4712	4740	4832	4854	2109
Jones & Campbell	#1 Baker	9	27S	16W	NE NE	abs	4616	4641	4723	4746	2094
Imperial	#1-12 Winklepleck	12	27S	16W SE	SE SE	abs	4593	4614	4711	4736	2075
Imperial	#1-13 Hoff	13	27S	16W	SE NE	abs	abs	4643	4733	4758	2073
Richardson	#1-C Clark	15	27S	16W SW	SW SW	abs	4712	4724	4820	4836	2107
Hilton-Sun-Tatlock	#1 Warren	16	27S	16W	NW NW	abs	4708	4730			2102
Richardson	#1-B Clark	21	27S	16W NE	NE NE	abs	abs	4698	4792	4823	2099
Armer & NCRA	#1 Reeder	22	27S	16W NW	NW NW	abs	abs	4729	4794	4820	2091
Pawnee	#1 Burns	25	27S	16W	SW SE	4646	4682	4716	4782	4802	2102
Jones et al.	#1 Fruit	28	27S	16W SW	SW SW	abs	abs	4746	4834	4852	2113
Case	#1 Whitney	31	27S	16W	W2 W2	abs	abs	4796	4903	4920	2140
Rock Island O&R	#1 Woodard	32	27S	16W	NW SE	4727	4754	4766	4850	4872	2177
Case	#1 November	35	27S	16W N2	NE NW	4750	4762	4768	4828	4846	2096
Dunne-Gardner	#1 Curtis	15	27S	17W	SW SW	4700	4766	4794	4886	4903	2149
Aurora Gas	#1 Campbell	17	27S	17W SE	SE SW	4807	4842	4859	4938	4959	2147
Katex Energies	#2 Taylor	20	27S	17W NE	NE SW	4802	4840	4874	4960	4988	2163
Jones-Gebert	#1 Thome	2	28S	2W	SE SW	abs	abs	abs	3958	3972	1385
Pickrell Drlg.	#1 Miles	9	28S	2W NW	NW NE	abs	abs	abs	4081	4090	1395
Sutton	#1 Puetz	6	28S	3W NE	NE SW	abs	abs	abs	4261	4268	1459
Cities Service	#1 Ritchie	2	28S	5W SW	SW SE	abs	abs	abs	4145	4157	1410
Lochiel	#1 Clause	7	28S	5W	NW NE	abs	abs	4195	4207	4233	1437
Drillers	#2 Kostner	30	28S	5W NW	SE NE	abs	abs	abs	4255	4276	1434
Lauck	#1 Bollinger	34	28S	5W SW	SE NW	abs	abs	4298	4308	4320	1379
Pickrell Drlg.	#1 Meng	1	28S	6W	SE NE	abs	abs	4158	4164	4184	1429
Ingling et al.	#1 Calkin	9	28S	6W	NE NE	abs	abs	abs	4339	4356	1554
Rains & Williamson	#1 Greenleaf	20	28S	6W	NW NW	abs	abs	abs	4353	4365	1555
Comet Petrol.	#3 Hedrick	25	28S	6W	SW NW	abs	abs	4235	4240	4254	1425
Energy 3	#1 Ewy	2	28S	7W	NW NW	abs	abs	abs	4225	4244	1532
Lochiel	#1 Harper	3	28S	7W	SW NW	abs	abs	4200	4206	4217	1497
Pickrell Drlg.	#1 Bock	7	28S	7W	SW NW	abs	abs	abs	4356	4368	1583
Petroleum, Inc.	#1 Bomholt	14	28S	7W	NW SW	abs	abs	abs	4406	4412	1603
Mack	#1 Rich	15	28S	7W	NW	abs	abs	4374	4380	4386	1577
Mack	#1 Gonzales	17	28S	7W	NE NW	abs	abs	4426	4441	4447	1625
Walters	#1 Rosenkranz	26	28S	7W	NW SW	abs	abs	4368	4378	4382	1588
Texaco	#5 Alameda Tract 6	27	28S	7W	NW	abs	abs	abs	4354	4358	1611
Mack	#1 Lord	30	28S	7W	SE NW	abs	abs	abs	4426	4430	1621
Pentagon	#1 Hoskins	2	28S	8W	SE NW	abs	abs	4306	4356	4365	1582
Graybol	#1 McKenna	3	28S	8W	NW SE	abs	abs	4331	4363	4370	1604
Graybol	#1 Stead	6	28S	8W	SW NE	abs	abs	4280	4324	4333	1560
Green	#16-1 McKenna	16	28S	8W	NW SE	abs	abs	4330	4362	4369	1590
Petro Quest	#57-18 Gillen	18	28S	8W		abs	abs	4350	4396	4404	1607
Petroleum, Inc.	#1 Dillon	23	28S	8W SW	SW SW	abs	abs	4424	4460	4465	1626
Texas O&G	#1-C Henning	25	28S	8W	NW	abs	abs	4446	4456	4461	1659
Reading & Bates	#1 Covington	27	28S	8W	SW SE	abs	abs	4465	4500	4504	1654
Utica Southern	#1 Boch	29	28S	8W	NW NE	abs	abs	4354	4400	4407	1589
Mercury Drlg.	#1 Dunne	3	28S	9W	SW SW	abs	abs	4286	4336	4344	1597

APPENDIX I (continued)

OPERATOR	WELL NAME	LOCATION S.	T.	R.	SPOT	DEPTHS A	B	C	D	E	DATUM
Midwest	#1 Sears	5	28S	9W	NE NE NE	abs	abs	4342	4404	4416	1679
Bachus & Prime	#1 Hay	11	28S	9W	E2 NE NW	abs	abs	4326	4370	4379	1623
Kaiser-Francis	#1 Sisters	14	28S	9W	SE SW	abs	abs	4416	4470	4478	1690
Anadarko	#1-A Merton	16	28S	9W	SW SW	abs	abs	4360	4416	4428	1667
MTM	#1 Sternecker	20	28S	9W	N2 NE SE	abs	abs	4387	4443	4454	1683
Phillips	#2 Darlington	29	28S	9W	NW NW NW	abs	abs	4406	4463	4474	1715
National	#1 Isley	33	28S	9W	NE SW SE	abs	abs	4464	4508	4514	1715
Pickrell Drlg.	#1-C Beat	36	28S	9W	NW SE	abs	abs	4472	4518	4530	1673
Mercury Drlg.	#1 Hayes	1	28S	10W	NW SW	abs	abs	4301	4360	4373	1664
Mack	#1 Clayton	4	28S	10W	SW NE	abs	abs	4323	4380	4392	1715
Pabco Drlg.	#1 Spain	5	28S	10W	SW SW SW	abs	abs	4357	4407	4418	1741
Kimbark	#1-19 Zrubeck	19	28S	10W	SW SW	abs	abs	4450	4514	4527	1792
Barbara	#1 Doan	23	28S	10W	NW NW NW	abs	abs	4395	4447	4456	1695
Midcontinent Energy	#1 Fenn	31	28S	10W	NW NW SE	abs	abs	4517	4583	4595	1804
Aylward Drlg.	#1 Steffin	33	28S	10W	SW SW SW	abs	abs	4529	4586	4595	1783
Anschutz Drlg.	#1 Adelhardt	36	28S	10W	SW NE	abs	abs	4473	4528	4542	1731
Midcontinent Energy	#1 House	2	28S	11W	NE NE SE	abs	4216	4230	4304	4318	1763
Rocket Drlg.	#1 Bucklin	6	28S	11W	NE NE SE	abs	4300	4305	4380	4395	1758
Toklan et al.	#1 Bucklin	10	28S	11W	SW NW SE	abs	4252	4264	4336	4350	1781
Kimbark	#1-20-A Thompson	20	28S	11W	NW NE NE	abs	4340	4350	4420	4432	1837
Kimbark	#1-22 Brenton	22	28S	11W	SW SE	abs	4338	4347	4426	4436	1786
Kimbark	#1 KOG Whitmore	24	28S	11W	SE SE	abs	abs	4433	4499	4510	1774
Aurora Gas	#1 Dyche	25	28S	11W	SW SW SW	abs	4488	4502	4565	4578	1800
Aurora & Trans Era	#1 Rose	27	28S	11W	NW NW NE	abs	4328	4340	4420	4431	1777
Cities Service	#1 Tipton	29	28S	11W	SW SE SW	abs	4375	4382	4456	4468	1829
Stickle Drlg.	#1 Crosley	1	28S	12W	SE SE SE	abs	4353	4370	4437	4450	1813
Halliburton	#1 Barker	3	28S	12W	SW SW NE	abs	4368	4386	4446	4458	1847
Lindas	#1 Lunt	5	28S	12W	NW NE NW	abs	4318	4330	4393	4401	1808
Masters	#1-7.5-5 Rosenbaum	14	28S	12W	W2 SW SE	abs	4281	4299	4364	4376	1869
Kirkman	#1-D Rosenbaum	15	28S	12W	SE SW NE	abs	4386	4403	4472	4485	1887
Allison	#1 Bailey	17	28S	12W	SW NW	abs	4400	4416	4480	4492	1870
Vincent	#1 Megaffin	26	28S	12W	SE SW	abs	4396	4403	4479	4490	1868
Bennett & Roberts	#1 Petrie	28	28S	12W	SE SE NE	abs	4343	4358	4436	4451	1888
Wilkinson Drlg.	#1 Dietz Estate	31	28S	12W	SW NE NE	abs	4422	4450	4522	4539	1899
Raymond	#2 Hillard	1	28S	13W	NW NW	abs	abs	4247	4298	4308	1858
Phelps-Dodge	#22-3-2 Green	2	28S	13W	SW SE NW	abs	abs	4253	4299	4312	1838
Woolsey	#1 Randle	3	28S	13W	SE NE SE	abs	abs	4276	4310	4320	1854
Phillips	#1-A Fannie	6	28S	13W	N2 NE NW	abs	abs	4333	4387	4394	1918
Amerada	#1 Dietz Trust	7	28S	13W	SE SW	abs	abs	4370	4427	4434	1936
Virginia Drlg.	#1 Buckner	9	28S	13W	SE SE SE	abs	abs	4353	4407	4414	1898
Tomlinson-Kathol	#1 Country	10	28S	13W	SE NE	abs	abs	4348	4404	4419	1906
Vac Petrol.	#1 Withers	11	28S	13W	N2 N2 NW	abs	abs	4343	4382	4396	1881
Phelps	#31-4-12 Fincham	12	28S	13W	SE NW NE	abs	abs	4360	4416	4420	1822
Texas	#2-P Jones	13	28S	13W	NW SW	abs	abs	4395	4436	4448	1878
Imperial	#1 Gilliam	14	28S	13W	NW SE	abs	abs	4421	4476	4483	1920
Woolsey	#1 Lawton	15	28S	13W	W2 SW	abs	abs	4370	4440	4459	1922
Virginia Drlg.	#1 Smith	17	28S	13W	SE SE NE	abs	4384	4398	4458	4462	1936
Texas Energies	#1-19 Lemon	19	28S	13W	SE NW	abs	4434	4440	4500	4504	1988
Texas Energies	#1-20 Letholt	20	28S	13W	NE NE NE	abs	4410	4414	4486	4506	1973
Sterling et al.	#1 Herthein	22	28S	13W	NE NE NE	abs	abs	4448	4500	4508	1939
Landes Expl.	#1 Dietz Estate	23	28S	13W	SW NW SE	abs	abs	4466	4504	4506	1939
Conoco	#1 Brehm	26	28S	13W	SW NW SE	abs	abs	4445	4486	4490	1947
Tomlinson	#1 Taylor	27	28S	13W	NW NE SE	abs	abs	4395	4432	4440	1939
Edmiston	#1 Gates	28	28S	13W	NW NE SE	abs	abs	4350	4400	4404	1940
Tilco et al.	#1 Brehm	29	28S	13W	W2 SW SW	abs	abs	4415	4476	4482	1878
Petrie	#1 Ryan	30	28S	13W	S2 S2 NE	abs	abs	4418	4479	4494	1958
Braden Drlg.	#1 Hertlein	31	28S	13W	SW SW SW	abs	abs	abs	4509	4516	1985
Lion	#1 McMinn	32	28S	13W	SE SE NE	abs	4414	4430	4472	4482	1961
American Energies	#1-A Eubank	33	28S	13W	NW SW SW	abs	4410	4426	4478	4484	1949
TXO	#1 Peachy	35	28S	13W	SW SE	abs	abs	4557	4619	4634	1935
F&M	#1 Stoops	36	28S	13W	SW NE SW	abs	abs	4522	4594	4612	1920
Pickrell Drlg.	#1-A Lavelle	1	28S	14W	SE NW	abs	4380	4392	4458	4477	1966
Texas Energies	#1-2 Lavelle	2	28S	14W	NW NE SE	abs	abs	4412	4478	4498	1996
Lario	#1 Patterson	4	28S	14W	SE NW SE	abs	abs	4546	4596	4612	2022
Lee Phillips	#1 Hall	5	28S	14W	SW NW	abs	abs	4545	4573	4590	2013
Tomlinson-Kathol	#1 Moore	6	28S	14W	NE NW NW	abs	abs	4564	4608	4617	2022
Crescent	#1 Hoimuller	9	28S	14W	NE SW	abs	4550	4554	4617	4634	2033
EOC	#1-11 Lavelle	11	28S	14W	NE NE SE	4390	4394	4412	4468	4487	1967
Graybol	#1 Becker	12	28S	14W	NE SW	abs	4378	4388	4443	4462	1941
Kan-Ex	#1 Roberts	13	28S	14W	NE SW	4367	4370	4387	4455	4476	1936
Three G	#1 Woolfolk	15	28S	14W	NW NE SE	abs	abs	4416	4452	4461	1995
Rock Island O&R	#1 Michael	20	28S	14W	NW NW NE	abs	4540	4548	4606	4612	2005
NCRA	#1 Leake	21	28S	14W	SE NW	abs	abs	4540	4580	4585	1981
Armer	#1 Biddenger	23	28S	14W	NE NE NE	4352	4392	4409	4468	4490	1934
Lohmann & Johnson	#1 Thompson	24	28S	14W	SE SE SE	4415	4424	4440	4510	4527	1966
Texas	#1-A McGuire	25	28S	14W	NW NE	abs	4444	4456	4514	4532	1976
Coppinger	#1 Woolfolk	26	28S	14W	SE SE SE	abs	abs	4448	????	4486	1977

APPENDIX I (continued)

OPERATOR	WELL NAME	LOCATION S.	T.	R.	SPOT	DEPTHS A	B	C	D	E	DATUM
Musgrove Drlg.	#1 Thompson	27	28S	14W	NE NE NW	4446	4460	4468	4530	4548	1963
CRA	#1 Spines	28	28S	14W	NE NW NW	abs	4488	4498	4550	4568	1977
Texas Energies	#1-29 Barbee	29	28S	14W	NE SW SW	abs	4615	4626	4676	4700	2044
Lario	#1-A Eubank Estate	30	28S	14W	NE SE NW	abs	abs	4593	4652	4667	2039
Crescent	#1 Davis	32	28S	14W	NE NE	abs	4593	4608	4680	4689	2039
Vincent	#1 Omo	35	28S	14W	S2 SW SE	abs	abs	4533	4550	4564	1984
Lauck	#1 Schenck	36	28S	14W	SW NE NE	abs	abs	4446	4484	4498	1981
Robert Gay	#4-RG Cosby	1	28S	15W	NE SE	abs	4556	4570	4636	4657	2035
Leben Drlg.	#1 Betschart	4	28S	15W	SW SW NW	abs	abs	4654	4709	4732	2081
Leben Drlg.	#1 Swafford	5	28S	15W	SW SW SE	abs	4684	4698	4770	4784	2091
Wenert Trich	#1 Ross	7	28S	15W	NW SW	abs	abs	4630	4667	4690	2117
Sunwest	#1 Williams	8	28S	15W	N2 NW SE	abs	4694	4698	4782	4796	2103
Imperial	#1-10 Seyfert	10	28S	15W	NW NW SW	abs	abs	4654	4686	4716	2084
Lauck	#1 Seyfert	14	28S	15W	SE SE SE	abs	abs	4641	4677	4696	2070
Imperial	#1-15 Vaught	15	28S	15W	SE SE	abs	abs	4630	4702	4714	2078
Imperial	#1-17 Hinshaw	17	28S	15W	SE SE	4696	4715	4735	4800	4818	2101
Imperial	#1-20 Chubb	20	28S	15W	SE SE SE	abs	4682	4694	4764		2085
Texas Energies	#1-22 Spines	22	28S	15W	NW SE NW	abs	abs	4600	4668	4690	2058
Crescent	#1 Miller	23	28S	15W	SW NW	4592	4614	4633	4691	4711	2072
Twin Drlg.	#1 Johnson	25	28S	15W	SW SW SE	abs	4616	4619	4677	4696	2049
Ainsworth	#2 Poovey	28	28S	15W	SE NW NW	abs	abs	4690	4743	4765	2074
Braden Drlg.	#1 Thompson	29	28S	15W	SW SW SW	4684	4730	4750	4800	4824	2055
Vac Petrol.	#1 Moore	33	28S	15W	SW SW SE	abs	abs	4655	4719	4738	2041
Case	#1 Fankhauser	8	28S	16W	SW SE SE	4762	4802	4828	4907	4932	2162
Schafer Drlg.	#1 Peoples Bank	12	28S	16W	SE SE SE	abs	4748	4755	4836	4848	2114
Southwestern Expl.	#1 Heath	20	28S	16W	SE SW SE	abs	abs	4850	4950	4960	2177
Murfin Drlg.	#1 Bowman	31	28S	16W	SE SW SE	4792	4814	4836	4921	4952	2139
KWB	#1 E.M. Davis	2	28S	17W	SW SW	abs	abs	4830	4914	4938	2147
Aurora Gas	#1 Fatzer	9	28S	17W	SE SE SE	abs	4683	4703	4774	4794	2131
K&E Drlg.	#1 Kemp	12	28S	17W	SE SE SE	4812	4836	4858	4940	4965	2169
Robert-Gay	#1-RG Bevan	13	28S	17W	NE NW	abs	abs	4884	4966	4980	2167
Sun	#1 Ross	14	28S	17W	SW SW NW	4868	4881	4902	5000	5014	2181
Midco Expl.	#1 Wheeler	35	28S	17W	NW NE	abs	4824	4842	4928		2112
Rains & Williamson	#1 Kinkaid	8	29S	5W	SW NW NW	abs	abs	abs	4274	4291	1425
Texaco	#1 C. Ward	29	29S	5W	NE SW	abs	abs	abs	4514	4530	1487
Campbell	#2 Zerger	8	29S	6W	NE NW	abs	abs	abs	4462	4470	1555
Drillers	#1 Sours	14	29S	6W	NE SW	abs	abs	abs	4454	4468	1524
Aylward Drlg.	#1 Bently	24	29S	6W	SE SE SW	abs	abs	abs	4440	4446	1511
Armer	#1 Maple	30	29S	6W	NE NE NE	abs	abs	abs	4517	4521	1551
Sunray	#1 Voth	4	29S	7W	NW NW SE	abs	abs	4456	????	4472	1613
Mack	#1 Weniger	7	29S	7W	NE NE	abs	abs	abs	4541	4546	1631
Murfin Drlg.	#1 Mary Brown	12	29S	7W	SE SE	abs	abs	4524	4540	4546	1592
Coppinger	#1 Voran	13	29S	7W	NE SE	abs	abs	4534	4552	4556	1576
Mack	#1 Castle	17	29S	7W	SW SW	abs	abs	abs	4514	4522	1581
Drilling & Expl.	#1-A Calkin	30	29S	7W	NW SE SW	abs	abs	abs	4509	4512	1534
Conoco	#1 Shepard	3	29S	8W	NE SW	abs	abs	4503	4520	4524	1680
Leben Drlg.	#1 Specht	5	29S	8W	NE NW	abs	abs	4465	4502	4510	1648
Mack	#1 Huey	12	29S	8W	SE SE	abs	abs	4530	4554	4557	1638
Sutton	#1 Van Gieson	13	29S	8W	SE NW	abs	abs	4450	4482	4485	1562
Mack	#1 Hibbs	16	29S	8W	NE NW	abs	abs	4483	4520	4522	1660
Leben Drlg.	#1 Bock	17	29S	8W	SW NE	abs	abs	4490	4534	4538	1671
Texaco	#1 Plush	26	29S	8W	NW NW	abs	abs	4549	4570	4574	1617
Rupp-Ferguson	#1 Shepard	30	29S	8W	NE NE SE	abs	abs	4467	4506	4512	1589
Pickrell Drlg.	#1 Tiesmeyer	1	29S	9W	NE NE SE	abs	abs	4517	4566	4571	1700
Walters	#1 Becker	3	29S	9W	SE NW	abs	abs	4470	4522	4533	1690
Anadarko	#1-A Schwartz	5	29S	9W	SW SE	abs	abs	4508	4571	4576	1727
Cities Service	#1-C Mueller	14	29S	9W	NE NW NW	abs	abs	4475	4513	4520	1696
Cities Service	#1-B Arensdorf	16	29S	9W	NE SE SW	abs	abs	4492	4539	4546	1690
Cities Service	#1 Schreiner	17	29S	9W	SE SE SE	abs	abs	4478	4526	4536	1663
Herndon Drlg.	#1 Gilbert	25	29S	9W	NW NW SW	abs	abs	4530	4586	4596	1650
Brack	#1 Goetz	27	29S	9W	NE NE SW	abs	abs	4466	4522	4530	1595
Cities Service	#1 Reuter	29	29S	9W	NE SW NW	abs	abs	4440	4501	4507	1692
Phil-Han	#1 Allbriten	6	29S	10W	SW SW	abs	abs	4533	4601	4613	1793
Pickrell Drlg.	#1-A Komerek	11	29S	10W	SE SE	abs	abs	4526	4588	4596	1747
Time Petrol.	#1 Twyman	20	29S	10W	SE SE SE	abs	4552	4558	4620	4630	1744
National	#1 Simon	21	29S	10W	SE NE SE	abs	abs	4557	4618	4628	1733
Petroleum, Inc.	#1 Spade	23	29S	10W	NE NE NW	abs	abs	4502	4555	4562	1689
Herndon Drlg.	#1 Gilbert	25	29S	10W	NW NW SW	abs	abs	4530	4591	4598	1650
Anadarko	#1-A Spade	27	29S	10W	NW NW	abs	abs	4566	4626	4636	1748
Berwick et al.	#1 Cirkel	30	29S	10W	NW NE	abs	abs	4554	4615	4628	1747
Musgrove Petrol.	#1 Mowbroy	4	29S	11W	SW SW SW	abs	4444	4446	4520	4530	1842
Cities Service	#1-B Lynch	6	29S	11W	SW SW NE	abs	abs	4426	4506	4519	1849

APPENDIX I (continued)

OPERATOR	WELL NAME	LOCATION S.	T.	R.	SPOT	DEPTHS A	B	C	D	E	DATUM
Kern Drlg.	#1 Murry	11	29S	11W	NW SW	abs	abs	4534	4596	4610	1805
F.G. Holl	#1-14A Ford	14	29S	11W	SW NW SE	abs	abs	4560	4608	4620	1783
F.G. Holl	#1-15 Blackwelder	15	29S	11W	SW SW SE	abs	abs	4595	4655	4666	1802
Lauck	#1 Miller	20	29S	11W	NW SE SE	abs	abs	4638	4696	4711	1856
Drilling & Expl.	#1-A Titus	27	29S	11W	SW NW	abs	abs	4601	4664	4681	1811
Austral	#1 J. Collett	30	29S	11W	SW NW	abs	abs	4514	4582	4594	1876
Phillips	#1-J Thompson	35	29S	11W	NE NW	abs	abs	4610	4677	4692	1811
Comet Petrol.	#1 Wheatley	1	29S	12W	SW NW	abs	4445	4450	4523	4536	1875
F&M	#1-A Terry	3	29S	12W	NE SE	abs	4457	4471	4548	4560	1898
Burch Expl.	#1 Hearn	5	29S	12W	SE NW	abs	4424	4442	4524	4539	1895
Rupp-Ferguson	#1 Thompson	13	29S	12W	NE NE SW	abs	4496	4498	4572	4584	1886
Beren	#1 Killingsworth	18	29S	12W	NW SW	abs	4468	4496	4562	4578	1916
Conoco	#1 J.R. Dauner	21	29S	12W	SW SW NW	4478	4490	4513	4573	4586	1898
Lion	#1 Curry	25	29S	12W	NW NW NW	abs	4512	4527	4587	4602	1876
F.G. Holl	#1-29 Hirt	29	29S	12W	SE SE NW	abs	4500	4524	4592	4604	1902
Cities Service	#1-D Fincham	1	29S	13W	SE SE NW	abs	4487	4518	4594	4609	1915
American Lariat	#1 Riffey	3	29S	13W	SE SE	abs	4550	4559	4628	4643	1944
APC	#1 Hertline	5	29S	13W	SW SE NE	abs	4464	4484	4532	4548	1957
Texas Company	#1 Thompson	13	29S	13W	SW SE NW	4484	4492	4520	4586	4600	1925
Black	#4-A Mason	15	29S	13W	SE NE SE	abs	4482	4508	4570	4586	1884
Kansas Shallow Ltd.	#1 Shriver	17	29S	13W	NW SW	4602	4609	4633	4690	4713	1972
Texas O&G	#1-B Wray	25	29S	13W	E2 SE SE	4516	4537	4565	4621	4636	1905
Cities Service	#2-D Harrel	27	29S	13W	SE SE SE	4390	4392	4424	4489	4505	1828
F.G. Holl	#1-29 Lambert	29	29S	13W	S2 S2 SW	4578	4584	4610	4676	4699	1967
Lario	#2 Moore	1	29S	14W	NE NE NW	abs	abs	4488	4532	4536	1990
Lion	#1 Omo	2	29S	14W	NW NW NW	abs	abs	4506	4551	4556	1993
Lewis Drlg.	#1 Grace Eads	3	29S	14W	NE NE NW	4484	4492	4512	4568	4584	2014
Twin Drlg.	#1 Moore	4	29S	14W	SE SE SE	abs	4518	4526	4576	4592	2017
Aurora Gas	#1 Jenkins	5	29S	14W	NE NE SW	abs	4574	4584	4638	4656	2032
Lauck	#1 Stelzer	7	29S	14W	NE SW	abs	abs	4720	4781	4798	2031
Tilco et al.	#1 Hutchins	8	29S	14W	SE NW	abs	4562	4568	4622	4637	2010
Aurora Gas	#1 Morrell	10	29S	14W	SW SW NE	abs	abs	4520	4554	4570	2012
Amerada	#1 Lee	11	29S	14W	NW NW NE	abs	abs	4538	4584	4594	1990
Lario	#1 Schriver Estate	12	29S	14W	NW SW SE	abs	4487	4496	4555	4576	1993
Plano	#2 Schrepel	13	29S	14W	SW NE SW	abs	4462	4470	4530	4546	1965
Reach Petrol.	#2 Shriver	14	29S	14W	SE NE SE	abs	abs	4447	4506	4514	1955
Rains & Williamson	#1 Luther	15	29S	14W	NW SW	abs	abs	4504	4556	4576	2006
Lario	#1 Schrepel	16	29S	14W	NW NW SE	abs	abs	4548	4598	4612	2018
Aurora Gas	#1 Morrell	19	29S	14W	SW SW NE	abs	abs	4520	4555	4572	2012
Musgrove Drlg.	#1 Schrepel	20	29S	14W	SW SW SW	abs	abs	4600	4640	4657	2035
Hummon	#1-21 Eubank	21	29S	14W	SW SE NW	abs	abs	4532	4556	4560	1982
Texas Energies	#2-22 Eads	22	29S	14W	NE SW NE	abs	abs	4535	4570	4584	1996
Nadel & Gussman	#2 Moss	23	29S	14W	NE SW NE	abs	abs	4454	4506	4526	1949
Lario	#1 Christain	24	29S	14W	NW SW NW	abs	abs	4454	4512	4529	1943
Raymond	#1 Kerr	27	29S	14W	NE NE NW	abs	abs	4514	4546	4558	1978
Raymond	#1 N&W Farms	28	29S	14W	NE SW SE	abs	abs	4574	4594	4600	1982
Ultramar	#1 Schrepel	30	29S	14W	NE NW	abs	abs	4600	4636	4657	2045
Graybol	#1 Howell	31	29S	14W	NW SE	abs	abs	4590	4626	4634	2005
Skelly	#1 Eubank	32	29S	14W	NW NW SE	abs	abs	4580	4620	4632	2005
Mastin	#1 Osborne	34	29S	14W	NW NW SE	abs	abs	4456	4498	4515	1936
Imperial	#1 Bergner	35	29S	14W	S2 NE NW	abs	abs	4510	4549	4560	1980
Imperial	#1-36 Benson	36	29S	14W	SE NW	4510	4519	4542	4600	4614	1949
Rupp-Ferguson	#1 Brown	3	29S	15W	SW SW NE	abs	4600	4620	4683	4700	2013
Robert-Gay	#7-RG Bolser	4	29S	15W	E2 SW SW	abs	abs	4643	4686	4700	2011
TXO	#8-C Bryant	8	29S	15W	SW NW SE	abs	abs	4726	4778	4794	2046
TXO	#5-C Bryant	9	29S	15W	SW NW NW	4582	4594	4605	4668	4688	2000
Raymond	#1-B Fincham	10	29S	15W	SW NW NW	abs	abs	4596	4661	4678	1985
C.R. King	#1 Winkley	11	29S	15W	SW NW	abs	4650	4662	4710	4730	2019
Skelly	#1 Hogard	15	29S	15W	NE SE NW	abs	4615	4622	4671	4692	1968
Vac Petrol.	#1-17 Howell	17	29S	15W	NE NE SW	abs	abs	4782	4832	4842	2046
Vac Petrol.	#3-18 Howell	18	29S	15W	NW NE NE	4732	4746	4748	4818	4838	2065
Imperial	#1-20 Howell	20	29S	15W	SW NE	abs	abs	4810	4827	4830	2035
Vac Petrol.	#1-23 Howell	23	29S	15W	N2 N2 NE	4606	4652	4670	4717	4739	2014
Aylward Drlg.	#1-A Kerr	29	29S	15W	NE NE SW	abs	abs	4804	4839	4842	2040
Berexco	#1 Gilliam	32	29S	15W	S2 S2 SE	4674	4708	4723	4800	4816	2038
Imperial	#1-33 Gilliam	33	29S	15W	SE SW	4595	4634	4650	4724	4737	1983
Imperial	#1-A Howell	11	29S	16W	SW SW NW	abs	abs	4786	4880	4904	2058
Cinco Expl.	#1 Bundren	18	29S	16W	SW SE	4815	4850	4876			2090
Imperial	#1-24 Piester-Howell	24	29S	16W	NE NW	abs	4746	4765	4863	4872	2012
Graves Drlg.	#1 Piester	25	29S	16W	SW NE	4704	4740	4764	4878	4898	2003
Imperial	#1-26 Piester-Howell	26	29S	16W	NE SW	abs	4702	4718	4830	4846	1973
Rupp-Ferguson	#1 Millar	29	29S	16W	SW SW SE	4635	4675	4710			1897
Gramehart-Miller	#2 Betzer	34	29S	16W	NW NW NE	abs	4652	4666	4727	4750	1931
Tilco et al.	#1 Douglas	36	29S	16W	NE NE NE	4707	4770	4783	4858	4878	1978
Rupp-Ferguson	#1 Morford	5	29S	17W	SW NW SW	5014	5021	5040	5124	5142	2176
Barbara	#1 Conklin	11	29S	17W	SW SW SW	4844	4864	4894	4991	5007	2068

APPENDIX I (continued)

OPERATOR	WELL NAME	LOCATION S.	T.	R.	SPOT	DEPTHS A	B	C	D	E	DATUM
Pickrell Drlg.	#1 Fink	8	30S	5W	SW SW	abs	abs	abs	4544	4563	1436
Pickrell Drlg.	#1-E Feiser	18	30S	5W	NW SE	abs	abs	abs	4547	4564	1406
Rains & Williamson	#1 Sparr	32	30S	5W S2	S2 NW	abs	abs	abs	4545	4557	1351
Rains & Williamson	#1 Messinger	8	30S	6W	SW SW	abs	abs	abs	4477	4487	1399
Clements	#1 Smith	14	30S	6W	SE NE	abs	abs	abs	4534	4546	1401
Energy O&G	#1 D&L Farm	27	30S	7W SE	SW NE	abs	abs	abs	4730	4734	1594
Mack	#1 Flowers	32	30S	7W	NE SW	abs	abs	4755	4773		1631
Pickrell Drlg.	#1 Bertholf	3	30S	8W SE	SE NE	abs	abs	4547	4584	4590	1541
Vickers Expl.	#1 Rall	8	30S	8W	SW NW	abs	abs	4484	4538	4545	1531
Petroleum, Inc.	#1 Sauvage	11	30S	8W SW	SW NW	abs	abs	4508	4537	4542	1522
NCRA	#4-A Tjaden	13	30S	8W SW	NW SE	abs	abs	4522	4553	4558	1501
Magnolia et al.	#1 Holcomb-Rall	17	30S	8W NW	SW NE	abs	abs	4472	4509	4515	1526
Stanolind	#1-SWD Rall	22	30S	8W E2	SE NE	abs	abs	4535	4570	4578	1526
Pickrell Drlg.	#1-A Boyle	27	30S	8W SW	SE NE	abs	abs	4593	4641	4647	1562
NCRA & Beardmore	#1 Carrick	29	30S	8W NW	SW NE	abs	abs	4624	4666	4672	1637
Chapman	#1 Liebl	6	30S	9W	SW SW	abs	abs	4562	4614	4620	1729
Deep Rock	#1 Whitmer	10	30S	9W NW	NW SE	abs	abs	4604	4652	4658	1689
Gulf	#1 Piehl	19	30S	9W NW	SW SE	abs	abs	4686	4732	4745	1741
Cities Service	#1 Depenbusch	23	30S	9W NE	NE SE	abs	abs	4516	4570	4580	1569
Skelly	#1 Cornelius	29	30S	9W NW	NW NW	abs	abs	4655	4709	4716	1701
Magnolia	#1-B Morris-Wolf	35	30S	9W SW	NE SE	abs	abs	4684	4738	4750	1691
Bachus	#1 Bertholf	1	30S	10W	SW SW	abs	abs	4562	4614	4624	1718
Welch & Olsson	#1 Liebl	3	30S	10W NE	NE SW	abs	abs	4590	4648	4657	1698
Sunray & Skelly	#1 Morisse Ut.	14	30S	10W NW	NW SE	abs	abs	4618	4674	4684	1747
Barbour & Aurora	#1 Campbell	15	30S	10W NE	NE SW	abs	abs	4630	4685	4694	1759
Rupp-Ferguson	#1 Rolf	18	30S	10W SE	SE NE	abs	abs	4660	4725	4737	1887
Southwestern Expl.	#1-B Allen	28	30S	10W W2	SW SW	abs	abs	4650	4710	4718	1751
Duncan Oper.	#1 Oak	29	30S	10W	NW NW	abs	abs	4672	4742	4750	1774
Coppinger	#1 Meeks	4	30S	11W SE	SE SE	abs	abs	4652	4719	4737	1824
Wakefield	#1 Rolf	5	30S	11W NW	NW SW	abs	abs	4610	4682	4694	1842
Bay Petrol.	#1 Dolbow	13	30S	11W NE	NE NE	abs	4666	4672	4736	4749	1809
Edmiston	#1 Ferrel	15	30S	11W	NW NE	abs	abs	4656	4726	4739	1810
Lauck	#1 Coss	16	30S	11W NW	NW NW	abs	abs	4694	4767	4779	1827
Kirkman	#1 Wolf	19	30S	11W SW	SW SE	abs	abs	4690	4762	4778	1832
Rains & Williamson	#1 Laverentz	21	30S	11W	NW NW	abs	abs	4642	4718	4732	1823
Texas & Natural Gas	#1 Poland	22	30S	11W SW	SE NW	abs	abs	4625	4695	4710	1806
Edmiston	#1 Massoni	24	30S	11W	SE NE	abs	4667	4680	4742	4753	1797
Edmiston	#1 Westerman	25	30S	11W NW	SE NE	abs	4760	4771	4827	4838	1770
Aylward Drlg.	#1 Wehling	26	30S	11W NE	NE NE	abs	4688	4691	4754	4766	1793
Aylward Drlg.	#1 Keimig	28	30S	11W SW	SW SE	abs	4650	4655	4726	4741	1799
Schafer Drlg.	#1 Mease	36	30S	11W NE	NE NE	abs	4675	4683	4751	4762	1751
Beacon Resources	#1 Knop	1	30S	12W	SW NW	abs	4544	4554	4612	4624	1845
W.C. Payne	#1 Gibson	3	30S	12W	NE SW	4468	4480	4502	4564	4577	1812
Federal Petrol.	#1 Chance	4	30S	12W	SW SW	4524	4548	4562	4628	4642	1875
Roger Williams Co.	#1 Ball	5	30S	12W NW	NW NE	abs	4489	4522	4590	4604	----
Ferguson	#1 Rose	7	30S	12W	SW SE	4500	4534	4553	4605	4620	1871
F.G. Holl	#1-8 Rose	8	30S	12W NE	NE SW	4466	4490	4503	4560	4574	1809
Texas Energies	#1-10 Boyd	10	30S	12W	N2 SW	4524	4541	4565	4630	4644	1866
Helmerich & Payne	#1 Kumberg	11	30S	12W NW	NW SW	abs	4470	4482	4540	4554	1797
Shell	#1 Hull	12	30S	12W	SW SE	abs	abs	4595	4658	4670	1851
Carter-Mandel	#1 McIntire	13	30S	12W NW	SE NW	abs	abs	4553	4616	4628	1817
Wilkinson	#1 Kumberg	15	30S	12W	NW SE	abs	4506	4522	4582	4597	1806
F.G. Holl	#1-18 Cook	18	30S	12W	NW NW	4469	4474	4510	4568	4583	1831
Aladdin Petrol.	#1 Meairs	26	30S	12W	NW SW	abs	abs	4580	4620	4632	1725
Anadarko	#1-A Cargill	27	30S	12W NW	SE NW	abs	4484	4497	4555	4570	1776
Natural G&O	#1 Lillieovist	29	30S	12W	NE NE	abs	4446	4464	4531	4546	1674
Todd Drlg.	#3-1 Levens	1	30S	13W NW	NW NE	4455	4461	4500	4558	4572	1845
4-D Petrol.	#2-A Frame	3	30S	13W NE	SW NE	4440	4445	4472	4536	4552	1857
Graybol	#1 Lambert	5	30S	13W	NE SE	abs	4546	4574	4640	4644	1922
F.G. Holl	#1-13 Means	13	30S	13W	SE NW	4442	4453	4488	4550	4566	1787
K&E Drlg.	#1 Grigsby	15	30S	13W SE	SE NW	abs	4494	4510	4562	4572	1825
Ramco	#1-B Lambert	17	30S	13W	NW NE	4540	4550	4566	4632	4641	1906
Shenandoah	#1 Helen Smith	25	30S	13W E2	SE NW	4544	4558	4579	4643	4656	1858
Lion O&R	#1 Lemon	28	30S	13W		4527	4538	4550	4616	4629	1871
Graves Drlg.	#1 Mickey	31	30S	13W NW	SE SE	4487	4504	4530	4598	4616	1781
F.G. Holl	#1-1 Shriver	1	30S	14W SE	SE NE	abs	4546	4565	4634	4652	1927
Ashton	#1 Alexander	2	30S	14W SE	SE SW	abs	4523	4527	4584	4594	1936
Vincent	#1 Ayres	3	30S	14W	SW SE	abs	abs	4499	4530	4536	1960
NCRA	#1 Shriver	4	30S	14W NW	NW SE	abs	abs	4528	4540	4550	1982
Anatole	#1 Lenkner	5	30S	14W	SW NE	abs	abs	4557	4591	4604	1995
Gould	#1 Weede	6	30S	14W	NE NW	abs	abs	4558	4593	4608	1981
Leben Drlg.	#1 Weede	7	30S	14W SE	NE NW	abs	abs	4518	4568	4585	1925
Brown Trust	#1-A McAdoo	9	30S	14W	NE NE	abs	abs	4514	4548	4550	1965

APPENDIX I (continued)

OPERATOR	WELL NAME	LOCATION S.	T.	R.	SPOT	DEPTHS A	B	C	D	E	DATUM
Chief Drlg.	#1 West	10	30S	14W	SW SE	abs	abs	4523	4560	4570	1938
Pet-Ex Petrol.	#1 McKenzie	14	30S	14W NE	SW NE	abs	abs	4644	4684	4700	1948
F.G. Holl	#1-15 Staats	15	30S	14W	SW	abs	4556	4560	4616	4625	1952
M. Brown	#1 Stannard	16	30S	14W	SE NW	abs	abs	4546	4580	4586	1959
Leben Drlg. et al.	#1 Basye	17	30S	14W	NW SW	abs	abs	4564	4588	4592	1952
Davis	#1-20 Mills	20	30S	14W	SE SW	abs	abs	4440	4460	4471	1799
Sterling	#1 Baker	21	30S	14W NE	NE NW	abs	abs	4525	4548	4556	1912
NCRA	#1 Lambert	23	30S	14W NE	SE SE	4491	4504	4534	4600	4607	1827
Pickrell Drlg.	#1 Shriver Trust	24	30S	14W	NE NW	4587	4602	4620	4680	4694	1925
Texas Energies	#1-25 Stanford Univ.	25	30S	14W N2	SE SW	4500	4521	4539	4605	4623	1826
Great Lakes Carbon	#1-D Werner	28	30S	14W SE	SE NW	abs	abs	4480	4532	4541	1848
R.C. Patton	#1 Werner	29	30S	14W NE	NW SE	abs	4464	4476	4548	4558	1840
Coppinger	#1 McLain	30	30S	14W N2	NE NE	abs	abs	4454	4489	4494	1799
PMI	#1 Mills	31	30S	14W	NE SW	abs	4442	4448	4512	4526	1753
Bright & Schiff	#1 Mills	32	30S	14W	SE SW	abs	4422	4427	4488	4498	1727
Hummon	#1 Tempel	33	30S	14W	SW SE	abs	abs	4512	4557	4570	1754
Graves Drlg.	#1 Thompson	36	30S	14W	NE NW	4532	4552	4578	4640	4657	1863
Gould	#1-B Lee	4	30S	15W	SW NE	4590	????	????	4730	4751	1788
Sinclair	#1 Louise	6	30S	15W SW	SW SE	4664	4688	4697	4782	4798	1982
Sabine	#1-7 Lee	7	30S	15W SE	SE SE	4602	????	????	4739	4760	1882
Texas O&G	#1-B Lee	9	30S	15W S2	SE NE	abs	abs	4678	4741	4760	1986
Monsanto et al.	#1 Hullie	10	30S	15W SE	SE SW	abs	abs	4624	4684	4702	1951
Sabine	#1-16 Lee	16	30S	15W	NW NW	4560	4602	4620	4690	4709	1894
TXO	#1-D Gibson	17	30S	15W NE	NW SE	4598	4658	4668	4742	4757	1907
Magic Circle	#1 National Gypsum	19	30S	15W	NE NE	abs	abs	4524	4546	4573	1793
TXO	#3-C Gibson	20	30S	15W	NW NE	4524	4546	4564	4646	4672	1859
Sabine	#2-21 Freeman	21	30S	15W NW	NE NE	abs	4556	4576	4660	4680	1866
Farmer	#1 Hoagland	24	30S	15W	SE NE	abs	abs	4484	4543	4548	1863
Honaker-Davis	#1-B Walker	31	30S	15W	NW SW	4755	4820	4826	4915	4919	1917
Texas Energies	#1-33 Cross	33	30S	15W	SE NE	abs	4471	4480	4560	4584	1701
Birmingham-Bartlett	#1 Mills	34	30S	15W	SW SE	4424	4476	4505			1697
Crescent	#1-A Hoagland	36	30S	15W SE	SE NW	abs	4460	4470	4530	4549	1768
Pickrell et al.	#1-E Robbins	14	30S	16W SE	SE NW	4547	4607	4620	4702	4728	1790
Gulf	#1-16 Gallup	16	30S	16W	SW SW	4796	4856	4874			1958
Gulf	#1-17 Rice	17	30S	16W	SW NE	4758	4820	4844	4944	4964	1921
Gulf	#1-P Robbins	23	30S	16W NE	SW SW	4775	4824	4845	4910	4934	1879
Pickrell Drlg.	#1 Robbins-Walker	25	30S	16W	SW	4758	4798	4826			1898
Shell & Gulf	#1 Robbins	32	30S	16W	SW NE	5017	5048	5062	5158	5184	1982
Honaker-Davis	#1 Walker	36	30S	16W	NW SE	4722	4774	4778	4890	4894	1944
Grey	#2 Wedel	33	30S	17W	NE NE	5038	5091	5116	5220	5249	2161
Pickrell Drlg.	#1-E Wolf	5	31S	7W	NW NW	abs	abs	4750	4758	4762	1629
Mack	#1 Barr	18	31S	7W	SE SE	abs	abs	4780	4801	4804	1576
Conoco	#1 L.E. Mathes	29	31S	7W NE	NW NE	abs	abs	abs	4646	4654	1513
Pickrell Drlg.	#1-D Wolf	1	31S	8W SW	NW NE	abs	abs	4744	4762	4767	1634
Magnolia	#3-745 Spivey Gas	5	31S	8W NE	SW SW	abs	abs	4720	4776	4782	1691
Petrocap & Thomas	#2 Culver	9	31S	8W	NW SE	abs	abs	4713	4760	4764	1638
Pickrell Drlg.	#1-I Jackson	13	31S	8W	NW SW	abs	abs	4796	4832	4838	1603
Deep Rock	#1 Stodder Estate	17	31S	8W SW	SW SW	abs	abs	4753	4802	4808	1634
McCoy Petrol.	#3-C Williams	22	31S	8W S2	NW NE	abs	abs	4716	4753	4760	1581
Mack	#2 Squire	26	31S	8W	SE SW	abs	abs	4693	4746	4751	1511
Mack	#1 Squire	27	31S	8W	NE SW	abs	abs	4723	4766	4770	1544
Pickrell Drlg.	#1-B Warren	32	31S	8W S2	SE SE	abs	abs	4690	4750	4757	1509
Weller	#1 Cox	5	31S	9W S2	SE SE	abs	abs	4705	4758	4766	1691
Petroleum, Inc.	#1 Best	30	31S	9W SE	SE SE	abs	abs	4714	4773	4780	1623
K&E Drlg.	#1 Morrise	9	31S	10W NE	NW NE	abs	abs	4733	4800	4808	1773
Wakefield	#1 Rankin	11	31S	10W SW	SW SW	abs	abs	4791	4846	4853	1752
Aurora Gas	#1 Rankin	13	31S	10W	SW SW	abs	abs	4736	4791	4799	1673
Musgrove Drlg.	#1 Stone	15	31S	10W NE	NE NW	abs	4786	4788	4858	4865	1746
Hummon	#1 Bertha	20	31S	10W	NE SW	abs	4758	4762	4826	4835	1759
Raymond	#1 Best	26	31S	10W SE	NW SW	abs	4803	4810	4864	4874	1718
Anschutz et al.	#1 McReynolds	30	31S	10W NE	NE NW	abs	4796	4810	4874	4886	1769
Hawkins	#1 Mease	2	31S	11W	NE SE	4760	4765	4770	4840	4850	1815
Jones-Gebert	#1 Wheat	4	31S	11W	SE SW	abs	4772	4782	4846	4861	1801
K&E Drlg.	#1 Chain	5	31S	11W	NE NW	abs	abs	4690	4762	4774	1780
Stanolind	#1 Chain	7	31S	11W	SE NE	4598	4602	4610	4680	4687	1647
Bowers	#1 Axline	9	31S	11W NW	SW SW	abs	4706	4720	4780	4790	1733
Rine Drlg.	#1 Bergner	10	31S	11W NE	NE NE	4761	4764	4772	4840	4850	1806
Skelly	#1 Louthan	11	31S	11W	SE NE	4742	4744	4758	4812	4824	1791
Coppinger	#1 Warwick	12	31S	11W	NW SE	abs	4752	4766	4824	4835	1786
Beardmore Drlg.	#1 Liebst	14	31S	11W	NE SE	abs	abs	4758	4823	4834	1770
Lario	#1 Axline	17	31S	11W NE	NW NE	abs	4724	4730	4796	4811	1757
Texas O&G	#1-A Chain Ranch	18	31S	11W NE	NE NE	abs	4575	4590	4660	4678	1612
Rupp-Ferguson	#1 Catlin	19	31S	11W SE	NE NW	abs	4578	4592	4658	4674	1588
Pickrell Drlg.	#1 Clark	26	31S	11W NW	SW NE	abs	4749	4752	4812	4823	1708

APPENDIX I (continued)

OPERATOR	WELL NAME	LOCATION S.	T.	R.	SPOT	DEPTHS A	B	C	D	E	DATUM
Aylward Drlg.	#2-A Swartz	30	31S	11W	S2 S2 SE	abs	abs	4546	4614	4627	----
Eagle Expl.	#1 E. Swartz	31	31S	11W	N2 N2 NE	abs	abs	4552	4620	4632	1526
Hummon	#1-34 Chapin	34	31S	11W	NE SE	abs	abs	4672	4738	4748	1611
Hummon	#1-36 Chapin	36	31S	11W	NW SE	abs	4707	4718			1643
Clinton	#1 Mott	1	31S	12W	NE NE	abs	4588	4600	4660	4674	1633
Presley	#1 Haas Brothers	2	31S	12W	SE SW	abs	abs	4587	4656	4670	1664
APC	#2 Haas	3	31S	12W	NE SW	abs	abs	4644	4703	4718	1757
Anschutz Drlg.	#1 Gress	6	31S	12W	SE SW	abs	4434	4444	4510	4524	1697
Source Petrol.	#2-B Elliot	9	31S	12W	SW SE	abs	4596	4602	4658	4673	1780
APC	#4 Mott	11	31S	12W	N2 SW	abs	abs	4607	4672	4686	1659
Jones	#1 Mott	12	31S	12W	NW SE	abs	4546	4550	4613	4632	1601
Clinton	#1 Mott	14	31S	12W	NE NE	abs	4588	4600	4660	4675	1633
G-M-R	#1 Updegraff	15	31S	12W	NE NE NE	abs	4638	4645	4703	4722	1688
Parker Petrol.	#1 Winters	18	31S	12W	NE NE SW	4425	4429	4444	4503	4518	1642
Beardmore Drlg.	#1 Calloway	20	31S	12W	NW NW NW	4417	4420	4427	4482	4496	1622
Aylward Drlg.	#1 Updegraff	22	31S	12W	SE SE	abs	4602	4606	4673	4688	1624
Aurora Gas	#1 Clark	30	31S	12W	NW NW NE	abs	4442	4460	4512	4527	1618
Graves Drlg.	#1 Hall	31	31S	12W	SW SW NE	abs	4400	4412	4472	4484	1510
Abercrombie Drlg.	#1 Adams	33	31S	12W	SE SW	4455	4462	4480			1541
Mull Drlg.	#1 Cargill	34	31S	12W	E2 SW NE	4566	4570	4577	4643	4663	1550
Robba	#1 Maddix	2	31S	13W	W2 SE	4482	4494	4526	4582	4596	1731
National	#1 Ketner	4	31S	13W	NW SW	4502	4519	4542	4596	4611	1764
Mustang	#1-7 Standish	7	31S	13W	NE SW NE	4546	4572	4594	4651	4660	1735
Conoco	#1 A. Smith	13	31S	13W	SE SE SW	abs	4412	4430	4486	4500	1611
Sunray DX	#1-A Smith	15	31S	13W	S2 SW SW	abs	abs	4490	4540	4544	1645
Tilco	#1 Dewitt	17	31S	13W	NW SW	4418	4433	4458	4522	4536	1645
Graybol	#1 Mills	20	31S	13W	NW SW	abs	4407	4414	4480	4495	1575
Kan-Ex	#1-25 Catlin	25	31S	13W	SW SW	abs	4412	4422	4483	4498	1535
Colorado	#1 Hartley	28	31S	13W	SE NW	abs	4477	4497	4548	4566	1557
Barbara	#1 M. Mills	30	31S	13W	NW NW NE	4437	4460	4465	4528	4542	1591
Graves Drlg.	#1 Kay	1	31S	14W	S2 S2 N2	4420	4452	4472	4529	4547	1731
Kirkman	#1 Nittler	4	31S	14W	SW SW NE	abs	4453	4464	4526	4544	1730
National & Kewanee	#1 Mills	5	31S	14W	SW SE	4373	4412	4432	4486	4504	1663
Rains & Williamson	#1 Lake	13	31S	14W	NW SE	4350	4379	4396	4440	4468	1600
Huber	#1 Skinner	17	31S	14W	W2 NW NW	4356	4399	4420	4478	4506	1653
Deep Rock	#1 Skinner	21	31S	14W	NW SW	4535	4580	4596	4660	4678	1738
Coppinger	#1 Russel Lake	26	31S	14W	SE SE NE	4546	4560	4581	4646	4662	1716
Deep Rock	#1-C Skinner	28	31S	14W	W2 SW NW	4587	4613	4647	4713	4733	1796
Lauck	#1 Skinner	33	31S	14W	NW SE	4558	4582	4610	4676	4694	1729
Superior	#1 Ward	2	31S	15W	NW SE	4422	4453	4470	4530	4556	----
K&E Drlg.	#1 Lenkner	3	31S	15W	SE NW	4403	4482	4488	4556	4577	----
Aylward Drlg.	#1 Lenkner	4	31S	15W	NW SW	abs	4572	4594	4682	4703	1776
Jones et al.	#1 Moad	5	31S	15W	NE NE NW	4657	4694	4704	4788	4810	1875
Fleet Drlg.	#1 National Gypsum	9	31S	15W	NW SE	4658	4688	4698	4780	4788	1850
Skelly	#1 Reed	10	31S	15W	SE NE	4503	4566	4580	4640	4660	1750
Kirkman	#1 Riepe	11	31S	15W	NE NW NE	4430	4491	4502	4564	4586	1706
Cities Service	#1 Riepe	12	31S	15W	NW SW NW	4506	4556	4569	4628	4646	1737
Vincent	#1 Thompson	13	31S	15W	NW NW SE	4495	4528	4542	4602	4620	1676
Graybol	#1 Hull	14	31S	15W	NE NE	4611	4647	4662	4722	4739	1778
Resources Invest.	#1 Harmon	15	31S	15W	NE NW NW	4808	4835	4848	4926	4936	1888
Petrol. Technol.	#16-1A Bray	16	31S	15W	SE SW	4690	4740	4752	4840	4860	1803
Aurora Gas	#1 Kaminska	17	31S	15W	NW NW SW	4822	4882	4892	4982	5007	1915
Rupp-Ferguson	#1 Dickerson	22	31S	15W	NE NE NE	4620	4673	4684	4761	4780	1752
Texas O&G	#1-F Hull	24	31S	15W	N2 SW	4617	4638	4663	4724	4738	1730
Texas O&G	#1-C Hull	25	31S	15W	NW NE NE	4720	4752	4757	4814	4830	1858
Herndon & Flynn	#1 Dickerson	26	31S	15W	NE NE NE	abs	4846	4848	4924	4942	1752
Petrol. Technol.	#28-1 Bray	28	31S	15W	SE NW	4845	4897	4905	4996	5018	1907
Murjo	#1-C Rusk	29	31S	15W	NE NE SW	5004	5050	5068	5153	5175	2013
Great Lakes Carbon	#3 Welsh	32	31S	15W	SW NE	4898	4940	4958	5042	5065	1879
Aylward Drlg.	2-D Skinner	34	31S	15W	SW NE SE	4889					1914
Graves Drlg.	#2 Alexander	36	31S	15W	N2 NW NE	4745	4772	4780	4840	4866	1885
Barbara	#1-8 Robbins	23	31S	16W	SW	5194	5234	5249	5336	5348	2041
Barbara	#1 Kaminska	24	31S	16W	SW	5050	5100	5105	5218	5229	2010
Aylward Drlg.	#1 Parker	6	32S	7W	NE NE NE	abs	abs	4724	abs	4748	1469
Sunray-Midcon.	#1 Muir	9	32S	7W	W2 SW NE	abs	abs	abs	4743	4752	1435
Aurora Gas	#1 Garber	17	32S	7W	SW SW NE	abs	abs	4736	4761	4768	1418
Shenandoah	#1 Reynolds	23	32S	7W	SW NE	abs	abs	abs	4800	4806	1428
Musgrove Drlg.	#1 Moldenhauer	27	32S	7W	SW SW SW	abs	abs	abs	4822	4828	1405
Beardmore Drlg.	#1 Berg	29	32S	7W	SW SW SE	abs	abs	abs	4758	4766	1369
Hellar Drlg.	#1 Osborn	12	32S	8W	NW NW	abs	abs	4893	4942	4953	1478
Colorado	#1 Naffziger	13	32S	8W	SW SW	abs	abs	4824	4876	4884	1434
Rupp-Ferguson	#1 Bebermeyer	15	32S	8W	SE SE NW	abs	abs	4792	4834	4844	1423
Anadarko	#1-A Robinson	17	32S	8W	NE	abs	abs	4698	4745	4754	1467
Texas O&G	#1 Antrim	30	32S	8W	SW	abs	abs	4743	4796	4802	1450
NCRA	#1 Catlin	33	32S	8W	NW NE	abs	abs	4788	4842	4845	1414

APPENDIX I (continued)

OPERATOR	WELL NAME	LOCATION S.	T.	R.	SPOT	DEPTHS A	B	C	D	E	DATUM
F&M	#1-B Mathes	36	32S	8W	NW NW	abs	abs	4822	4840	4852	1391
Hummon	#1 Yocam	13	32S	9W	SE SW	abs	4756	4759	4816	4823	1510
Aylward Drlg.	#1 Holcomb	17	32S	9W	SW SW NW	abs	4634	4644	4705	4714	1447
Pickrell Drlg.	#1-A Bowerman	21	32S	9W	NE NW	abs	4662	4670	4724	4734	1431
Beardmore Drlg.	#1 Black	28	32S	9W	NE NE NE	abs	4735	4742	4800	4809	1476
Clinton	#1-V F. Williams	31	32S	9W	SE SW	abs	abs	4730	4736	4740	
Anschutz Drlg.	#16-32 Zuercher	32	32S	9W	SE SE SE	abs	4716	4732	4780	4790	1400
Pickens	#1 Sullivan	36	32S	9W	NE NE	abs	4704	4710	4765	4770	1411
Martin & Keller	#1 Garrett	5	32S	10W	SW NW	abs	4750	4761	4814	4824	1624
Conoco	#1 Gersner	9	32S	10W	NW SW NW	abs	4683	4692	4754	4764	1530
Vincent	#1-B Schreiner	11	32S	10W	NE SE	abs	4672	4682	4742	4752	1516
Jones et al.	#1 McKeever	13	32S	10W	SE SE SE	abs	4638	4649	4706	4716	1444
Molz	#1 Blahut	16	32S	10W	NW NW SW	4669	4672	4689	4743	4760	1475
Molz	#2 Schiff	20	32S	10W	SE NE SE	abs	4680	4690	4747	4760	1463
Ferguson	#1 McDaniel	25	32S	10W	SE NE	abs	4659	4670	4724	4736	1430
Westpan	#1 Pelton	27	32S	10W	SW SW SE	4677	4680	4689	4748	4758	1426
Globe et al.	#1 Goeman	29	32S	10W	SW SW SE	abs	4693	4714	4766	4775	1463
Hummon	#2 Ketzner	1	32S	11W	SW NW NW	abs	abs	4638	4684	4702	1686
Lario	#1 Reginier	6	32S	11W	NW NE NW	abs	4512	4522	4588	4602	1502
Beardmore & Barbara	#1 Stewart	14	32S	11W	SW SW SW	abs	4670	4673	4732	4744	1513
Brown	#1 Woolsey	15	32S	11W	SW SE	4638	4644	4656	4720	4736	1573
Mull Drlg.	#1 Peace Treaty Grnds.	17	32S	11W	SW NW	4608	4614	4624	4674	4686	1517
Jackson et al.	#1 Lukens	28	32S	11W	NW NW	abs	4687	4692	4762	4774	1516
Eagle	#1-B Lukens	29	32S	11W	N2 N2 NW	abs	4715	4725	4789	4800	1549
Page & Beardmore	#1 Benifield	2	32S	12W	SW NW NW	4525	4536	4548	4600	4618	1517
Mull Drlg.	#1 Wheelock	3	32S	12W	SW NW	4500	4514	4533	4590	4604	1496
Pryor et al.	#1 Wilson	6	32S	12W	NW NW	abs	4452	4465	4517	4532	1504
Brown	#1 Krehbiel	13	32S	12W	NE SW	abs	4561	4573	4628	4642	1454
Cecil	#1 Gillespie	15	32S	12W	NW NW	4612	4623	4640	4694	4711	1551
Underwood	#1 Elsea	18	32S	12W	SW NE NW	abs	4644	4670	4722	4737	1620
Patton	#1 Bloom	25	32S	12W	NW NW NW	abs	4625	4640	4689	4700	1508
Kewanee	#1 Tedrow	28	32S	12W	NW NW SE	4684	4703	4717	4774	4792	1608
Parker Petrol.	#1 Barthelow	33	32S	12W	SW SW SW	4709	4716	4730	4788	4806	1606
Honaker-Davis	#1 Gant	3	32S	13W	NW NW NW	abs	4580	4608	4660	4674	1646
Peel-Hardman et al.	#1 Brook	5	32S	13W	SW NE	abs	4610	4640	4698	4712	1643
Aylward Drlg.	#1 Brooks	7	32S	13W	SW SW NE	4740	4760	4786	4838	4856	1771
Avanti	#1 Lonker	14	32S	13W		abs	4752	4779	4831	4848	1693
Sunray	#1-A Palmer	16	32S	13W	W2 NW NW	4795	4805	4831	4884	4904	1792
TXO	#2 Tedrow	17	32S	13W	NE NW	abs	4782	4808	4874	4892	1789
Mull Drlg.	#1 Palmer	19	32S	13W	SW NW NE	4743	4763	4786	4850	4870	1741
Sinclair	#1 Youngers	22	32S	13W	NE NE SW	abs	4738	4767	4823	4837	----
Lion	#1 Brooks-Younger	23	32S	13W	NE NE SW	abs	4744	4763	4828	4846	1662
Anschutz Drlg.	#1 Lonker	25	32S	13W	NE NE NE	abs	4748	4773	4824	4839	1653
Skelly	#1 Hopkins	29	32S	13W	NW NW NW	abs	4826	4860	4930	4942	1796
Gulf	#1 Hopkins	30	32S	13W	SE NW	4876	4897	4922	4982	5000	1846
Sunray	#1 Hopkins	31	32S	13W	NE NE NW	4815	4832	4860	4920	4934	----
Aurora Gas	#1 Baier	32	32S	13W	SW SW SW	4815	4832	4854	4914	4928	1748
Bowers Drlg. & NCRA	#1 Lonker	35	32S	13W	NE SE	4782	4788	4800	4858	4870	1646
Skelly	#4 Lonker	36	32S	13W	SW SE	4825	4835	4852	4910	4924	1699
Century Expl.	#3 Mills	4	32S	14W	W2 SW NW	4605	4654	4670	4733	4751	1763
Conoco	#1 L. Mills	5	32S	14W	SW SE SE	4707	4746	4762	4828	4846	1833
Isern Drlg.	#1 Ely-Lytle	6	32S	14W	NE NW	4704	4740	4760	4817	4836	1860
NCRA	#2 Stumph-Smith	7	32S	14W	SW NE SW	4820	4856	4863	4928	4945	1922
Purcell & Mull	#1 Barkley	10	32S	14W	SE SE NE	4657	4676	4708	4765	4779	1740
Purcell & Mull	#1 Mull	12	32S	14W	NW SW NW	4610	4634	4655	4712	4722	1650
Colorado	#1 Lake	13	32S	14W	SE NW	4785	4815	4836	4896	4912	1801
Bowers Drlg.	#1 Elsea	14	32S	14W	SW NW	4701	4716	4732	4813	4821	1722
Aylward Drlg.	#1-F Stumph-Smith	17	32S	14W	NE NE NE	4872	4915	4930	5000	5018	1902
George Reed	#1-A Stumph	18	32S	14W	SE SW	4965	5002	5009	5074	5092	1980
Sands Drlg.	#2 Marsh	21	32S	14W	NE NW	5130	5148	5170	5244	5260	1928
Texas Energies	#1-22 Hoagland	22	32S	14W	NW NW SW	4933	4970	4990	5052	5070	1905
Olson	#1 Canfield	24	32S	14W	NE NE	4837	4860	4883	4942	4957	1852
Aurora Gas	#1 Rinke	25	32S	14W	SE SE SE	4854	4879	4900	4960	4977	1814
Wild Boys	#1 Hood Top Deal	32	32S	14W	W2 NE NE	5113	5150	5164	5232	5249	1950
Kan-Ex	#1 Allen	33	32S	14W	SE SE	5056	5092	5105	5180	5194	1925
Graves Drlg.	#1 Alexander	1	32S	15W	NE SW	4800	4835	4840	4902	4922	1938
NCRA	#1 Skinner	2	32S	15W	NW NW NE	4966	5010	5018	5071	5088	1927
Spring	#1-5 Marsh	5	32S	15W	NE SW NE	5100	5125	5132	5228	5250	2026
Aylward Drlg.	#1-A Welsh	7	32S	15W	NE NE NE	5075	5108	5122	5205	5226	1968
H. Spring	#1-8 Marsh	8	32S	15W	SE NE	5103	5128	5142	5226	5249	1987
NCRA	#1-E Skinner	12	32S	15W	SE NW NE	4896	4932	4940	5002	5022	2000
Aylward Drlg.	#1-B Stumph-Smith	13	32S	15W	NE NE SE	abs	abs	4804	4854	4870	2000
Dynamar	#14-2 Larkin	14	32S	15W	SE SE	4939	4964	4968	5032	5050	2001
Aylward Drlg.	#1-A Moores	19	32S	15W	NE NE	5089	5107	5125	5210	5230	1888
Sands Drlg.	#2 Marsh	21	32S	15W	NE NW	5130	5149	5164	5250		1928

APPENDIX I (continued)

OPERATOR	WELL NAME	LOCATION S.	T.	R.	SPOT	DEPTHS A	B	C	D	E	DATUM
Thunderbird Drlg.	#1 Larkin	23	32S	15W	SW NE SE	4928	4956	4962	5030	5051	1940
Champlin	#5 Hildebrand	26	32S	15W	S2 NE SE				5104	5122	1984
Raymond	#1-B Carr	27	32S	15W	E2 SW SW	4873	4882	4904	4982	5006	1818
Northern Natural	#1-B Davis	29	32S	15W	NE NE	5170	5198	5215	5294	5316	1938
Sunray DX	#1 DeGeer	32	32S	15W	SW NW NE	5121	5160	5172	5255	5277	1841
Time Petrol.	#1-A DeGeer	33	32S	15W	NW NW	4963	4998	5008	5086	5108	1848
Vincent	#1 DeGeer	34	32S	15W	SE NW	4954	4974	4990	5066	5090	1921
Sinclair	#1-D DeGeer	35	32S	15W	SE SW SW	5390	5407	5422	5480	5498	----
Graves & Beacon	#1 Carr	36	32S	15W	NE NE SW	5169	5200	5211	5270	5288	1974
Kern Drlg.	#1 Schutte	2	32S	16W	SW NE	5106	5128	5136	5238	5246	1920
Wentworth & Sons	#1 Price	4	32S	16W	SE SE SE	5083	5100	5120	5204	5225	1856
Rupp-Ferguson	#1 Schuette	9	32S	16W	SW SW NE	5128	5162	5189	5265	5289	1926
Wild Boys	#1 Eatin' Dust	12	32S	16W	SE	5080	5114	5134	5234	5255	1939
Zink & Trumbo	#1-30 Lenhart	30	32S	16W	SE NE NE	5432	5476	5498	5571	5594	2011
United Producing	#1 L. York	6	32S	17W	SE NW	5632	5656	5696	5764	5792	2120
Graves Drlg.	#1 Peoples	17	32S	17W	NW NE	5620	5651	5682	5750	5775	2075
Cities Service	#1-A Belcher	21	32S	17W	NE NE	5552	5595	5611	5689	5715	2099
Cities Service	#1-A Dove	22	32S	17W	NW NW	5556	5596	5622	5706	5732	2104
Petroleum, Inc.	#1-B Gregg Unit	27	32S	17W	NE NE	5543	5595	5621			2061
Parker Petrol.	#1 Cary	30	32S	17W	SE SW	5696	5736	5763	5842	5866	2002
Musgrove Petrol.	#1 Hayter	6	33S	6W	NE NE NE	abs	abs	abs	4795	4800	1343
Norbla Oil	#1 Mattimore	28	33S	6W	SE NW	abs	abs	abs	4931	4941	1332
Amerada	#1 Steward	31	33S	6W	NE NW	abs	abs	abs	4934	4944	1308
National Oil	#2 Burgmeier	36	33S	6W	SW SE SE	abs	abs	abs	4986	4995	1273
Sinclair	#1 Sechler	3	33S	7W	SE SE NW	abs	abs	5048	5069	5075	1381
Imperial Kansas	#1 Stout	12	33S	7W	SW SW NE	abs	abs	5050	5073	5076	1393
Lee Phillips	#1 Blasdel	16	33S	7W	NE NE	abs	abs	4928	4953	4960	1345
Pickrell Drlg.	#1 Tysor	17	33S	7W	NW SE	abs	abs	4944	4957	4965	1343
Anschutz Drlg.	#1 Mollohan	34	33S	7W	SW NE	abs	abs	abs	4974	4988	1313
Robinson	#1-A Powell	35	33S	7W	SW NW	abs	abs	abs	4970	4978	1334
B & B Oil	#2 Barker	6	33S	8W	SE SE NW	abs	4734	4742	4794	4800	1379
Skelly	#1 Alfred Miller	12	33S	8W	NW NW SW	abs	abs	4902	4952	4958	1374
Mack	#1 McKenny	16	33S	8W	SW SW	abs	4856	4860	4921	4926	1372
Cherokee	#1 McKenny	17	33S	8W	N2 N2 SE	abs	4829	4832	4888	4896	1370
McCoy Petrol.	#1-C Dalrymple	24	33S	8W	NE SW	abs	abs	5060	5086	5096	1396
Rupp-Ferguson	#1 Kastens	28	33S	8W	W2 W2	abs	abs	4938	4988	4997	1359
McCoy Petrol.	#1-A Lonker	30	33S	8W	NE SE SW	abs	abs	4814	4872	4882	1312
Mack	#1 Heath	6	33S	9W	SW SW	abs	4688	4696	4749	4759	1386
F&M	#1-A Winans	9	33S	9W	NW SE	abs	4750	4763	4816	4826	1364
Gruenerwald	#1 Enderud	15	33S	9W	SE SE SE	abs	abs	4780	4811	4819	1342
K & E Drlg.	#1 Cristfield Townsite	17	33S	9W	SW SE SE	abs	4729	4738	4797	4806	1371
Cities Service	#1-D Tucker	29	33S	9W	NW NE	abs	4795	4804	4862	4872	1327
Mack	#1 Patterson	33	33S	9W	NE NE	abs	4872	4882	4937	4946	1328
George Jones	#1 Curtis	1	33S	10W	NW NE SW	abs	4699	4703	4762	4772	1399
Magnolia	#1 Traffas	6	33S	10W	NW NW SE	abs	4878	4893	4956	4968	1592
Davidor & Davidor	#1 Dunkin	14	33S	10W	NE NE NW	abs	4759	4766	4827	4843	1402
Smith & Toto	#1 McReynolds	16	33S	10W	NW SW	abs	4885	4907			1514
Trans-Era Petrol.	#1 Stewart	17	33S	10W	NE SE SE	4862	4868	4881	4940	4948	1488
Jones et al.	#1 Washburn	29	33S	10W	SW SW SW	abs	4910	4928	4987	4998	1472
Ambassador	#1 Page	36	33S	10W	N2 NE SW	abs	4904	4922	4980	4990	1366
Musgrove Drlg.	#1 Early	4	33S	11W	SE SE SW	abs	4740	4750	4813	4828	1526
Patton	#1 McClure	6	33S	11W	SW SW SW	abs	4624	4641	4695	4706	1408
Sinclair	#3 Newkirk	16	33S	11W	SE NE NW	abs	4806	4814	4880	4887	1482
Gulf	#1 Newkirk	17	33S	11W	SE NE SE	abs	4758	4768	4835	4846	1427
Todd Drlg.	#1-A Burns	24	33S	11W	NE NE NE	4900	4910	4928	4977	4991	1505
Oilwell Operators	#1 Cathy	25	33S	11W	NE NE	abs	4961	4974	5037	5047	1541
Barbara	#1 Forrester	28	33S	11W	SW NW NE	4752	4763	4777	4837	4847	1372
Honaker-Davis	#1 Newkirk	31	33S	11W	NE NE SW	4916	4932	4958	5013	5024	1463
Skelly	#1-E Boggs	2	33S	12W	NW NW SW	4704	4719	4728	4785	4800	1526
Conoco	#1 Colborn	3	33S	12W	NW NW SE	abs	4692	4716	4773	4786	1516
Rine Drlg.	#8-F Bartholow	8	33S	12W	SE NW NE	4777	4791	4808	4863	4879	1611
Skelly	#1-C Harbaugh	13	33S	12W	SE SW SE	abs	4776	4796	4850	4861	1422
Magnolia	#1 Bartholow	16	33S	12W	W2 NW NW	abs	4721	4748	4804	4820	1542
Skelly	#1-C Boggs	17	33S	12W	SW NE NE	abs	4701	4728	4781	4797	1515
Bachus	#1 McKanna	25	33S	12W	N2 NW	4897	4908	4926	4980	4992	1480
Bowers Drlg.	#1 Groendycke	27	33S	12W	SW SW SE	abs	5073	5102	5154	5169	1582
Dunne-Gardner	#1 Smith Estate	29	33S	12W	NE SW	abs	4800	4820	4876	4893	1521
Reach Petrol.	#1 Hospital	1	33S	13W	SE SE	abs	4974	5007	5063	5077	1824
Aylward Drlg.	#1 Warwick	2	33S	13W	W2 NE SW	4834	4852	4869	4923	4933	1686
Wakefield	#1 Baler	5	33S	13W	NE NE NE	4968	4980	4999	5068	5083	1877
Shenandoah	#1 Hoefle	8	33S	13W	N2 SW SW	5012	5031	5054	5116	5134	1862
Barbara	#2-13 Alexander	13	33S	13W	NW SW	4754	4775	4787	4848	4866	1545

APPENDIX I (continued)

OPERATOR	WELL NAME	LOCATION S.	T.	R.	SPOT	DEPTHS A	B	C	D	E	DATUM
Barbara	#1 Storm	18	33S	13W	NW NW	5026	5052	5074	5135	5150	1873
McElvain	#1 Bell	19	33S	13W	NE NW	4990	5020	5037	5100	5116	1781
Conoco	#1 B.E. Holmes	35	33S	13W NE	NE NW	4872	4881	4900	4960	4980	1551
Kachina	#4 Angel	2	33S	14W E2	W2 SE	5018	5053	5070			1900
Anschutz Drlg.	#1 Mills	5	33S	14W	NE SE	4937	4985	5005	5062	5082	1755
Bolyard	#1 Angel	11	33S	14W	SE SE	5023	5050	5075	5140	5156	1875
Shell	#1 Gentry	19	33S	14W	SE NW	5051	5103	5125	5180	5200	1735
Barbara	#1 Ott	22	33S	14W	NE NW	4924	4962	4976	5042	5055	1702
Gramehart-Miller	#1 Lenker	24	33S	14W SE	NE SW	5070	5102	5118	5181	5198	1856
Champlin	#1-D Davis	33	33S	14W	NW NW	4997	5032	5058	5110	5130	1712
Champlin	#1 Wheat	34	33S	14W	NE NW	4972	5000	5024	5086	5102	1660
Lion	#1 Liles	1	33S	15W NW	NW NW	5176	5209	5224	5276	5294	1991
Sunray DX	#1-A DeGeer	2	33S	15W S2	SW NW	5222	5242	5252	5320	5338	2016
Sinclair-Prairie	#1-B V. DeGeer	3	33S	15W	NE SE	5226	5232	5255	5332	5352	2002
Champlin	#1 Brass	4	33S	15W	NW SW	4952	4982	4996	5070	5089	1843
Sunray DX	#1-D Lendon	5	33S	15W SW	NW SW	4696	4737	4760	4844	4858	1729
Sunray DX	#1-B Lendon	7	33S	15W NE	NE SE	4692	4732	4750	4834	4850	1775
Champlin	#1 Winter	8	33S	15W NE	SE NW	4875	4908	4921	5000	5019	1814
Fisher Oil	#1 Brass	9	33S	15W W2	SW SW	5154	5174	5191	5259	5273	1848
Raymond	#1 Cline	14	33S	15W	SE NW	5235	5270	5277	5351	5370	1922
Superior	#1 Mitchell	15	33S	15W	NW SW	5187	5207	5226	5299	5318	1849
Aylward Drlg.	#1 Platt	17	33S	15W SW	SW SW	4953	4988	5006	5078	5094	1744
Sunray DX	#1 R. Platt	18	33S	15W	NE NE	4840	4885	4907	4980	5001	1705
Jack Expl.	#1-19 Brass	19	33S	15W	SW NE	4998	5025	5044	5117	5135	1725
Petrosil	#1-A Platt	20	33S	15W	NE NE	5099	5123	5146	5213	5237	1770
Petrosil	#1 Beck	21	33S	15W	NW SE	5174	5206	5222	5289	5308	1822
Edmiston	#1 Bundren	28	33S	15W	SW NE	5144	5178	5200	5263	5284	1776
Mull Drlg.	#1 Platt	30	33S	15W SE	SE NE	4972	5007	5027	5098	5117	1645
Shenandoah	#1-A Merrill	13	33S	16W	NE SW	5216	5245	5272	5350	5366	1782
NCRA	#1 Merrill	24	33S	16W E2	NE NE	5066	5100	5123	5201	5220	1668
Shenandoah	#2-B Merrill	26	33S	16W	SW SW	5355	5396	5420	5496	5520	1759
Sunray DX	#1 M. Gregg	31	33S	16W	NW SE	5453	5486	5510	5580	5614	1712
Conoco	#1 C. Einsel	2	33S	17W	NW NE	5594	5670	5696	5766	5794	2012
J.M. Huber	#1 Einsel	11	33S	17W SW	NW NW	5530	5604	5622	5694	5720	1960
Conoco	#1 C.F. Biddle	13	33S	17W	NE NE	5474	5502	5527	5596	5621	1862
Source Petrol.	#1-A Einsel	19	33S	17W SW	NW NW	5690	5750	5774	5814	5840	1894
Gould	#1 Jobe	21	33S	17W	NW NW	5738	5752	5776	5812	5834	1904
Huber	#1 Warren	25	33S	17W	SE	5499	5534	5558	5616	5646	1767
AFG Energy	#2-A Haper	32	33S	17W	SE NW	5662	5708	5730	5766	5795	1864
Continental	#1 Huck & Hall	33	33S	17W SW	NW SW	5508	5530	5554	5589	5617	1835
Gould	#1 Carlile	34	33S	17W	SE SW	5614	5656	5684	5728	5755	1838
PMI	#1 Warren Ranch	35	33S	17W	SE SE	5562	5606	5626	5672	5698	1742
Alpine & Roy	#1 Brownback	5	34S	2W NE	NE SW	abs	abs	abs	4528	4538	1146
Elledge & Meese	#1-18 Fuhrmann	18	34S	2W SW	NW NW	abs	abs	abs	4626	4641	1160
Natural G&O	#1 Neal	20	34S	2W NE	NW SE	abs	abs	abs	4606	4621	1142
Time Petrol.	#1 Kerr	34	34S	2W	NW NE	abs	abs	abs	4600	4608	----
Sanders & Con-Am	#1 Baker	1	34S	3W NE	NW SW	abs	abs	abs	4582	4587	1137
Pendleton	#1 Turek	3	34S	3W SE	NW SW	abs	abs	abs	4651	4670	1199
F&M	#1 Berka	19	34S	3W NE	SW SE	abs	abs	abs	4764	4778	1164
Herndon Drlg.	#5 Subera	22	34S	3W NW	NW SW	abs	abs	abs	4720	4733	1200
Texaco	#1 Anton	21	34S	5W	SE SE	abs	abs	abs	5093	5100	1222
Texas Company	#1 Baker	24	34S	5W NE	SW NW	abs	abs	abs	4876	4885	1217
Allison	#1 Jelenik	25	34S	5W	NW SW	abs	abs	abs	4909	4921	1192
Prime & Benedict	#1 Hallman	9	34S	6W	SE SW	abs	abs	abs	5032	5044	1300
Worsham	#4 Wilcox	15	34S	6W	W2 NW	abs	abs	abs	4994	5003	1273
Aurora Gas	#1 Barrett	20	34S	6W SW	SW SE	abs	abs	5150	5174	5180	1308
Huber	#1 Denton-Fox	30	34S	6W	SW NE	abs	abs	5177	5195	5202	1332
Gulf	#1 Birchenough	1	34S	7W	SW NW	abs	abs	4990	5043	5047	1302
Hamilton	#1 Carr	14	34S	7W	NE SE	abs	abs	5108			1352
Huber	#1 Cather	16	34S	7W NE	SE NE	abs	abs	5153	5168	5174	1404
McCoy Petrol.	#1-A Ritter	2	34S	8W W2	SW SE	abs	abs	5070	5111	5116	1395
Ferguson	#1 Patterson	7	34S	8W	SW NW	abs	abs	4960	5009	5020	1333
Mull Drlg.	#1 Dusenbury	10	34S	8W SE	SE NW	abs	abs	5012	5055	5059	1346
Anschutz Drlg.	#13-20 Croft	20	34S	8W SW	SW SW	abs	abs	5084	5125	5135	1265
Falcon-Seaboard	#1 Schupbach	7	34S	9W SW	SW NW	abs	4865	4876	4930	4940	----
Oil Capitol	#1 Woodworth	16	34S	9W	NE SE	abs	abs	4982	5035	5046	1292
Phillips-Ferguson	#1 Dumler	18	34S	9W	SE NE	abs	4946	4960	5015	5028	1309
Gruenerwald	#1 Hibbard	23	34S	9W NW	NW SW	abs	abs	4978	5012	5020	1290
APC	#1 Chain-Burke	35	34S	9W	SW NW	abs	5088	5097	5148	5157	1280
Mull Drlg.	#1 Griffin	7	34S	10W SE	SE SE	abs	4982	4998	5057	5066	1415

APPENDIX I (continued)

OPERATOR	WELL NAME	LOCATION S.	T.	R.	SPOT	DEPTHS A	B	C	D	E	DATUM
Berexco	#1 Norman	12	34S	10W	S2 SW SW	abs	4930	4950	5008	5018	1309
Champlin	#1 Skaggs	13	34S	10W	SE SW NW	abs	4916	4937	4994	5004	1295
Prime Drlg.	#1 Garner	21	34S	10W	NE NE SE	abs	5070	5082	5142	5154	1355
Thunderbird Drlg.	#1 McClure	26	34S	10W	NE NE SE	abs	5114	5131	5185	5198	1362
Conoco	#1 Porterfield	32	34S	10W	SE NE SW	abs	5140	5152	5212	5226	1302
Mack	#1 Swartz	1	34S	11W	SW NE	abs	4940	4957	5020	5030	1426
Gulf	#1 Groendyke	6	34S	11W	NW NW NW	4975	4994				1499
Wood Drlg. et al.	#1 Schupbach	15	34S	11W	N2 NW NW	4881	4894	4906	4962	4976	1334
Honaker-Davis	#1 Stolebarger	25	34S	11W	NE NE NE	abs	5100	5110	5176	5191	1336
Aurora Gas	#1 Goldman	32	34S	11W	NW NW SW	abs	5090	5106	5172	5187	1365
Atlantic Refining	#1 V. Cook	8	34S	12W	W2 SW NW	abs	5128	5148	5204	5222	----
Dunne-Gardner	#1 Andrews	11	34S	12W	NE SW	abs	5080	5110	5166	5180	1498
Aurora Gas	#1 Humphrey	24	34S	12W	SE SE NE	abs	5078	5108	5161	5170	1450
Molz	#2 Molz Farm	26	34S	12W	NW SW	abs	5154	5174	5231	5245	1449
Aurora & Barbour	#1 Rathegaber	31	34S	12W	NE SE	5266	5274	5285	5345	5359	1480
Wild Boys	#1 No Time To Reload	1	34S	13W	NW NW	4950	4955	4970	5030	5046	1558
Harper Oil	#1 Donovan	3	34S	13W	NW NW	abs	5078	5097	5160	5181	1648
Imperial Drlg.	#1 Blunk	5	34S	13W	NE SW SW	5226	5245	5261	5323	5340	1860
K & E Drlg.	#1 Ott	6	34S	13W	NW NW NE	5189	5212	5223	5287	5302	1876
Jones	#1 Clark	7	34S	13W	N2 SW	5147	5166	5181	5243	5262	1761
Graham et al.	#1 Donovan	9	34S	13W	NE NE SE	5148	5166	5176	5238	5260	1730
Aylward Drlg.	#1-D Donovan	11	34S	13W	SW SE	abs	5044	5068	5117	5134	1584
Magnolia	#1 Donovan	12	34S	13W	SE NW NE	5012	5019	5030	5083	5098	1603
Pickrell Drlg.	#1-A Diel	14	34S	13W	SW NE	abs	5050	5072	5132	5148	1586
Palmer Oil	#1 Schupbach	15	34S	13W	SE SW NE	5018	5033	5052	5121	5139	1574
Petroleum, Inc.	#1-D Sterling	27	34S	13W	SE SE	abs	5113	5134	5197	5214	1493
Messman-Rinehart	#1-A Holmes	2	34S	14W	NE NW SE	4967	4971	4992	5052	5068	1580
Aladdin Petrol.	#1 Kincaid	15	34S	14W	SW NE NW	5176	5226	5236	5288	5307	1694
Adair et al.	#1-B Graves	24	34S	14W	S2 S2 NE	5136	5160	5178	5240	5256	1638
Deep Rock	#1 McBrayer	26	34S	14W	SE SW NW	5174	5208	5224	5280	5299	1574
Gruenerwald	#1 Farley	32	34S	14W	NW NW	5187	5231	5249	5298	5319	1520
Honaker-Davis	#1 Platt	6	34S	15W	SE NE	5082	5130	5150	5220	5242	1612
Chicago Corp.	#1-B Davis Ranch	9	34S	15W	SE SE	5053	5125	5140	5196	5220	1601
Barbara	#1 Brack	17	34S	15W	NE NE SW	5113	5170	5188	5254	5276	1597
Honaker-Davis	#1 Davis	18	34S	15W	NE NE SW	5135	5195	5214	5283	5303	1582
Gruenerwald	#1 Ballet	27	34S	15W	NE NW	5142	5216	5232	5282	5302	1500
Champlin	#1 Huck	22	34S	16W	SW SE	5416	5466	5494	5550	5581	1823
Yucca Petrol.	#1 Guss	16	34S	17W	NW NE SE	5747	5790	5826	5860	5900	1764
Olympic Petrol.	#1 Haas	19	34S	17W	NW NW	5818	5884	5908	5943	5974	1790
Expl. & Devel.	#1 Ehrlich	20	34S	17W	E2 NE SW	5845	5894	5924	5962	5998	1846
Sunray-Midcon.	#1 Jackson	28	34S	17W	SW SE	6025	6057	6114			1847
Forney	#1-6 Schwarz	6	35S	2W	NW SE SE	abs	abs	abs	4754	4774	1131
MidStates	#1 Hudson	3	35S	3W	SW NW SE	abs	abs	abs	4788	4799	1123
Rine	#1-7 Jenista	7	35S	3W	NE SW NE	abs	abs	abs	4859	4870	1160
Trans-Pacific	#1 Dombaugh	7	35S	5W	SE SE SW	abs	abs	5232	5240	5248	1256
MidAmerica Petrol.	#1-15 Williams	15	35S	5W	SE SE	abs	abs	abs	5215	5222	1229
Texaco	#1 Bush	17	35S	5W	SW SW	abs	abs	5236	5245	5253	1223
Denver Energy	#1-A Bollman	3	35S	6W	SW NW	abs	abs	5210	5230	5236	1332
TXO	#1 KU Endowment	5	35S	6W	SE SE	abs	abs	5170	5180	5186	1310
Sanders	#1 Smith	11	35S	6W	SW NW	abs	abs	5274	5294	5302	1264
Jones et al.	#1 Livengood	14	35S	6W	W2 NW SW	abs	abs	5334	5368	5370	1258
Provincial	#1 Burchfield	3	35S	7W	NE NE SE	abs	abs	5286	5336	5342	1336
Conoco	#1 McKee	6	35S	7W	SE SW NW	abs	abs	5254	5290	5296	1312
NCRA	#1 K. Meyer	12	35S	7W	SW SW	abs	abs	5325	5334	5348	1359
Mull Drlg.	#1 Burchfield	15	35S	7W	NW NE	abs	abs	5276	5286	5310	1264
Aurora Gas	#1 Zellers	10	35S	8W	SW SW SW	abs	5278	5284	5330	5337	1268
Anschutz Drlg.	#1 Carroll	2	35S	9W	N2 NW NW	abs	5188	5201	5248	5258	1253
Geo Dan	#1 Carroll	3	35S	9W	NW NW	abs	abs	5215	5268	5277	1264
Sinclair	#1 Helmley	3	35S	10W	N2 NW NW	abs	5150	5170	5222	5233	1284
Aurora Gas	#1 Gudeman	10	35S	10W	NW NW NE	abs	5150	5172	5230	5241	1287
Vickers Expl.	#1 Schupbach	16	35S	10W	NW NW NW	abs	abs	5320	5372	5382	1349
Molz	#1 Blond-Goldman	5	35S	11W	N2 NW NW	abs	5129	5153	5217	5229	----
Jones et al.	#1-B Warshburne	10	35S	11W	NW NW SW	abs	5189	5210	5274	5290	1330
Molz	#1-A Yates	1	35S	12W	N2 NE NE	abs	5161	5184	5240	5248	1409
McGinness	#1-A Lohmann	3	35S	12W	SW SE SE	abs	5222	5244	5301	5314	1498

APPENDIX I (continued)

OPERATOR	WELL NAME	LOCATION S.	T.	R.	SPOT	DEPTHS A	B	C	D	E	DATUM
Aurora Gas	#1-C Ohlson	8	35S	12W	NW NW	abs	5270	5286			1419
Sands Drlg.	#2 Platt	1	35S	13W	N2 SW NE	abs	5254	5274	5333	5345	1397
City Prod. et al.	#1 Walsh	4	35S	13W	SW NW NW	5300	5308	5324	5390	5410	1636
Huber	#1 Achenbach	11	35S	13W	NW SW	5280	5300	5324	5383	5405	1480
Gruenerwald	#1 Molz	8	35S	14W	NW NW NW	5254	5332	5350	5400	5424	1491
City Products	#1 Wolgamott	16	35S	14W	S2 S2 S2	5348	5397	5417	5468	5486	1491
Chicago Corp.	#1-A Davis Ranch	3	35S	15W	NW NW NW	5321	5408	5426	5474	5492	1630
Midwest	#4 Ballet Ranch	6	35S	15W	SE SE	5593	5664	5692	5744	5764	1807
Chicago Corp.	#1 Davis Ranch	11	35S	15W	NE NE	5400	5490	5508	5554	5576	1609
Petroleum, Inc.	#1 Beely Ut.	7	35S	16W	N2 NE SE	5783	5865	5890	5930	5960	1905
Texas O&G	#1 McMoran	8	35S	16W	SE NW	5696	5768	5800	5840	5871	1870
Smith et al.	#1 McMoran	16	35S	16W	S2 SE NW	5640	5713	5738	5771	5802	1904

APPENDIX II -- ROCK-EVAL MATURATION DATA FOR ORDOVICIAN STRATA IN NORTHEASTERN AND NORTH-CENTRAL KANSAS.

Formation Key

ABCK -- Arbuckle Gp.
CHAT -- Chattanooga Sh.
CHER -- Cherokee Gp.
DGLS -- Douglas Gp.
HEEB -- Heebner Sh.
HUSH -- Hushpuckney Sh.
LANS -- Lansing Gp.
LKC -- Lansing-Kansas City gps.
MARM -- Marmaton Gp.
MQKT -- Maquoketa Sh.
SMPS -- Simpson Gp.
STRK -- Stark Sh.
VIOL -- Viola Fm.

OPERATOR AND WELL NAME (LOCATION)

SAMPLE INTERVAL (ft)	FM.	LITH.	SAMPLE TYPE	TOC* (wt. %)	S_1 (kg/tn)	S_2 (kg/tn)	S_3 (kg/tn)	HI**	OI***	T_{MAX} (°C)	TR****	S_1+S_2 (kg/tn)	DATA SOURCE
Dallas Group #1-83 Rift (NE SE NW, 08-T.01S.-R.01E.)													
3160-3170	SMPS	shale	cuttings	0.29	0.18	0.22	0.61	76	210	409	0.45	0.40	DGSI
Mallard Drlg. #1 Broeckelman (N2 NE NE, 15-T.01S.-R.10W.)													
4130-4160	SMPS	shale	cuttings	0.18	0.09	0.31	----	172	----	----	----	0.40	Sohio
4130-4160	SMPS	shale	cuttings	7.14	0.23	10.92	----	153	----	439	0.02	11.15	Sohio
Roxy Resources #1-14 Schneider (NW SE SW, 14-T.01S.-R.14E.)													
3410-3430	MQKT	shale	cuttings	3.07	0.28	2.18	0.51	71	17	430	0.11	2.46	DGSI
3480-3490	VIOL	ls	cuttings	2.89	0.20	2.00	0.54	69	19	432	0.09	2.20	DGSI
3700-3720	SMPS	shale	cuttings	8.15	1.74	66.39	0.88	815	11	441	0.03	68.13	DGSI
Pemsco #1 Schou (NE SE NE, 23-T.04S.-R.02W.)													
3100-3110	MQKT	shale	cuttings	0.27	----	----	----	----	----	----	----	----	DGSI
3420-3430	SMPS	shale	cuttings	0.20	----	----	----	----	----	----	----	----	DGSI
3430-3440	SMPS	shale	cuttings	0.36	0.36	0.75	0.74	208	206	428	0.32	1.11	DGSI
Producers Eng. et al. #1-4 Finn (S2 S2 NE, 04-T.04S.-R.07E.)													
2050-2100	SMPS	shale	cuttings	0.06	----	----	----	----	----	----	----	----	DGSI
2090-2110	SMPS	shale	cuttings	0.27	0.10	0.10	0.63	37	233	----	----	0.20	DGSI
2110-2130	SMPS	shale	cuttings	0.25	----	----	----	----	----	----	----	----	DGSI
Pendleton #1 Hermesch (NW SE SE, 09-T.05S.-R.13E.)													
3580-3590	MQKT	shale	cuttings	0.13	----	----	----	----	----	----	----	----	DGSI
3720-3800	SMPS	shale	cuttings	0.20	0.34	0.26	0.62	130	310	422	0.57	0.60	DGSI

APPENDIX II (continued)

SAMPLE INTERVAL (ft)	FM.	LITH.	SAMPLE TYPE	TOC* (wt. %)	S_1 (kg/tn)	S_2 (kg/tn)	S_3 (kg/tn)	HI**	OI***	T_{MAX} (°C)	TR****	S_1+S_2 (kg/tn)	DATA SOURCE
OPERATOR AND WELL NAME (LOCATION)													
Pendleton #1 Steinlage (SE NE, 27-T.05S.-R.12E.)													
2310-2320	MQKT	shale	cuttings	0.14	----	----	----	----	----	----	----	----	DGSI
2580-2630	SMPS	shale	cuttings	0.44	0.13	0.39	0.11	89	25	432	0.25	0.52	DGSI
Texaco #1 Poersch (SW SW, 31-T.05S.-R.05E.)													
2490-2520	MQKT	shale	cuttings	0.30	0.03	0.19	0.39	63	130	----	----	0.22	DGSI
2704	SMPS	shale	core	0.37	0.02	0.64	0.22	173	59	429	0.03	0.66	DGSI
2722	SMPS	shale	core	0.33	0.00	0.28	0.11	85	33	423	0.00	0.28	DGSI
2744	SMPS	shale	core	0.42	0.02	0.71	0.15	169	36	430	0.03	0.73	DGSI
2782	SMPS	shale	core	0.57	0.01	0.81	0.14	142	25	429	0.01	0.82	DGSI
2798	SMPS	shale	core	0.27	0.01	0.05	0.19	19	70	----	----	0.06	DGSI
Producers Eng. et al. #1-8 Freiderich (S2 SE SE, 08-T.07S.-R.05E.)													
2630-2650	SMPS	shale	cuttings	0.18	----	----	----	----	----	----	----	----	DGSI
Wakefield #1 Nelson (SE SW SW, 06-T.09S.-R.03W.)													
3510-3520	MQKT	shale	cuttings	0.23	0.03	0.06	0.23	26	100	----	----	0.09	DGSI
3713-3727	SMPS	shale	cuttings	0.19	0.01	0.02	0.07	11	37	----	----	0.03	DGSI
Kosarek #1 Lessor (SW SE SE, 11-T.11S.-R.09W.)													
3595-3600	MQKT	shale	cuttings	0.74	0.08	0.32	0.23	43	31	432	0.20	0.40	DGSI
3860-3865	SMPS	shale	cuttings	0.37	0.08	0.28	0.20	76	54	430	0.22	0.36	DGSI
Kosarek #1 Nielson (NE NE, 16-T.11S.-R.09W.)													
3300-3310	MQKT	shale	cuttings	0.34	0.10	0.22	0.41	65	121	416	0.31	0.32	DGSI
3600-3620	SMPS	shale	cuttings	0.16	----	----	----	----	----	----	----	----	DGSI
Sunflower #1 Wohler (NW NE NE, 02-T.11S.-R.10W.)													
3718-3730	MQKT	shale	cuttings	0.27	----	----	----	----	----	----	----	----	DGSI
3940-3960	SMPS	shale	cuttings	0.20	----	----	----	----	----	----	----	----	DGSI
3985-3990	SMPS	shale	cuttings	0.50	0.02	0.76	0.21	152	42	432	0.03	0.78	DGSI
Ogle #1 Stanley (SE SW, 15-T.12S.-R.03W.)													
3530-3535	MQKT	shale	cuttings	0.42	0.09	0.14	0.07	33	17	----	----	0.23	DGSI
3675-3680	SMPS	shale	cuttings	0.29	0.11	0.31	0.12	107	41	425	0.26	0.42	DGSI
Carter #2-A Davis (SW NE SW, 33-T.13S.-R.10E.)													
3200	MQKT?	shale	core	0.26	0.00	0.23	0.14	88	54	425	0.00	0.23	USGS

APPENDIX II (continued)

SAMPLE INTERVAL (ft)	FM.	LITH.	SAMPLE TYPE	TOC* (wt. %)	S_1 (kg/tn)	S_2 (kg/tn)	S_3 (kg/tn)	HI**	OI***	T_{MAX} (°C)	TR****	S_1+S_2 (kg/tn)	DATA SOURCE
OPERATOR AND WELL NAME (LOCATION)													
Carter #2-A Davis (SW NE SW, 33-T.13S.-R.10E.) (continued)													
3200	MQKT?	shale	core	0.25	----	----	----	----	----	----	----	----	DGSI
3298.5	SMPS	shale	core	0.61	0.27	1.35	0.15	221	25	432	0.17	1.62	USGS
3313.5	SMPS	shale	core	15.82	2.98	148.00	0.65	936	4	444	0.02	150.98	USGS
3314.8	SMPS	shale	core	1.02	0.21	3.69	0.27	362	26	443	0.05	3.90	USGS
3315.5	SMPS	shale	core	1.43	0.30	3.73	0.33	261	23	440	0.07	4.03	USGS
3320.4	SMPS	shale	core	0.77	0.14	1.17	0.15	152	19	438	0.11	1.31	USGS
3321	SMPS	shale	core	0.95	0.21	3.51	0.27	369	28	437	0.06	3.72	USGS
3321	SMPS	shale	core	0.76	0.73	2.12	0.39	279	51	437	0.26	2.85	DGSI
3322.5	SMPS	shale	core	0.69	0.40	1.24	0.22	180	32	433	0.24	1.64	USGS
3323.5	SMPS	shale	core	0.53	0.45	1.24	0.37	234	70	452	0.27	1.69	USGS
3326.2	SMPS	shale	core	0.76	0.72	2.91	0.29	383	38	436	0.20	3.63	USGS
Heller #1 Stice (NW, 11-T.14S.-R.08E.)													
2162-2165	MQKT	shale	cuttings	1.52	0.08	0.92	----	61	----	----	0.08	1.00	Sohio
2165-2170	SMPS	shale	cuttings	1.20	0.11	0.91	----	76	----	----	0.11	1.02	Sohio
2220-2225	SMPS	shale	cuttings	1.03	0.10	0.38	----	37	----	----	0.21	0.48	Sohio
Range #1 Winslow (N2 S2, 05-T.14S.-R.02W.)													
3100-3110	MQKT	shale	cuttings	0.93	<0.10	0.13	0.23	14	25	----	----	----	B&R
3100-3100	MQKT	shale	cuttings	1.63	<0.10	0.36	0.27	22	17	431	<0.27	----	B&R
3140-3150	MQKT	shale	cuttings	0.66	<0.10	0.20	0.28	30	42	428	<0.50	----	B&R
3140-3150	MQKT	shale	cuttings	0.78	<0.10	0.13	0.26	17	33	----	----	----	B&R
Diamond-Shamrock #1-9 Skully 181 (SE SE, 09-T.18S.-R.01E.)													
3080-3090	MQKT	shale	cuttings	0.56	0.04	0.09	----	16	----	----	----	0.13	Sohio
3133-3133	MQKT	shale	cuttings	0.52	0.05	0.16	----	31	----	----	----	0.21	Sohio
3141-3141	VIOL	dol	cuttings	0.24	0.06	0.40	----	167	----	----	----	0.46	Sohio
3230-3245	SMPS	shale	cuttings	0.72	0.08	1.51	----	210	----	----	----	1.59	Sohio
3265-3270	SMPS	slst	cuttings	7.29	2.67	71.49	----	981	----	451	0.04	74.16	Sohio
3270-3280	SMPS	shale	cuttings	0.44	0.19	1.15	----	261	----	----	----	1.34	Sohio
3280-3290	SMPS	shale	cuttings	0.88	0.00	0.00	----	----	----	----	----	----	Sohio
Brandt #10 Dunsford (23-T.19S.-R.02W.)													
3370-3380	SMPS	shale	cuttings	0.72	<0.10	0.22	0.16	31	22	434	<0.45	----	B&R
3410-3425	SMPS	shale	cuttings	0.73	0.19	1.15	0.23	158	32	440	0.14	1.34	B&R
3440-3460	SMPS	shale	cuttings	0.75	0.17	1.14	0.12	152	16	441	0.13	1.31	B&R
3460-3480	SMPS	shale	cuttings	0.63	0.13	0.88	0.07	140	11	438	0.13	1.01	B&R

APPENDIX II (continued)

SAMPLE INTERVAL (ft)	FM.	LITH.	SAMPLE TYPE	TOC* (wt. %)	S_1 (kg/tn)	S_2 (kg/tn)	S_3 (kg/tn)	HI**	OI***	T_{MAX} (°C)	TR****	S_1+S_2 (kg/tn)	DATA SOURCE
Champlin #1 Kottman (NE SW, 19-T.19S.-R.08W.)													
3378.5	SMPS	shale	core	8.72	2.23	75.96	0.99	871	11	442	0.03	78.19	USGS
3380.5	SMPS	shale	core	0.60	0.00	0.62	0.32	103	53	426	0.00	0.62	USGS
3383.3	SMPS	shale	core	0.30	0.01	0.48	0.40	160	133	424	0.02	0.49	USGS
3385.2	SMPS	shale	core	0.35	0.12	0.35	0.96	100	274	427	0.26	0.47	USGS
3385.7	SMPS	shale	core	7.05	2.46	41.94	2.39	595	34	444	0.06	44.40	USGS
3386.4	SMPS	shale	core	0.28	0.01	1.29	0.24	461	86	426	0.01	1.30	USGS
NNG #1 Madsen (NE SE, 35-T.19S.-R.08W.)													
3266.5	SMPS	shale	core	0.79	0.16	1.56	0.49	197	62	430	0.09	1.72	USGS
3268.5	SMPS	shale	core	0.63	0.03	1.37	0.21	217	33	434	0.02	1.40	USGS
3270.5	SMPS	shale	core	0.13	0.02	0.05	0.14	38	108	----	----	0.07	USGS
3272	SMPS	shale	core	0.27	0.02	0.16	0.13	59	48	----	----	0.18	USGS
3274	SMPS	shale	core	0.29	0.02	0.28	0.10	97	34	423	0.07	0.30	USGS
3275.5	SMPS	shale	core	0.19	0.03	0.17	0.09	89	47	----	----	0.20	USGS
NNG #35-9 Pulliam (N2 S2 N2, 35-T.19S.-R.08W.)													
3276	SMPS	shale	core	0.83	0.12	5.31	0.10	640	12	430	0.02	5.43	USGS
3287	SMPS	shale	core	0.17	----	----	----	----	----	----	----	----	USGS
Champlin #8 Speck (07-T.20S.-R.08W.)													
3446	SMPS	shale	core	0.64	0.06	2.46	0.26	384	41	434	0.02	2.52	USGS
3449	SMPS	shale	core	0.22	----	----	----	----	----	----	----	----	USGS
NNG #1 Caldwell (NE NE, 02-T.20S.-R.08W.)													
3279.5	SMPS	shale	core	0.56	0.16	5.01	0.12	895	21	432	0.03	5.17	USGS
3333	SMPS	shale	core	0.33	0.01	0.33	0.39	100	118	424	0.03	0.34	USGS
3334.5	SMPS	shale	core	0.77	0.08	1.18	0.12	153	16	421	0.06	1.26	USGS
3336	SMPS	shale	core	1.07	0.12	1.99	0.15	186	14	420	0.06	2.11	USGS
3338	SMPS	shale	core	0.38	0.04	0.62	0.10	163	26	422	0.06	0.66	USGS
3343.8	SMPS	shale	core	0.23	0.01	0.16	0.10	70	43	----	----	0.17	USGS
Walker #1 Baerg (SE NW, 25-T.20S.-R.04W.)													
3770-3780	MQKT	shale	cuttings	0.66	0.00	0.15	1.07	23	162	----	0.00	0.15	Sohio
3800-3810	SMPS	shale	cuttings	0.67	0.00	0.14	1.20	21	179	----	0.00	0.14	Sohio
3830-3840	SMPS	shale	cuttings	0.13	0.00	0.00	1.21	0	931	----	----	----	Sohio
3830-3840	SMPS	shale	cuttings	0.81	0.01	0.17	2.84	21	351	----	----	0.18	Sohio
3850-3860	SMPS	shale	cuttings	0.65	0.00	0.16	2.19	25	337	----	0.00	0.16	Sohio

APPENDIX II (continued)

SAMPLE INTERVAL (ft)	FM.	LITH.	SAMPLE TYPE	TOC* (wt. %)	S_1 (kg/tn)	S_2 (kg/tn)	S_3 (kg/tn)	HI**	OI***	T_{MAX} (°C)	TR****	S_1+S_2 (kg/tn)	DATA SOURCE
OPERATOR AND WELL NAME (LOCATION)													
Walker #1-15 Unruh (NW SW SE, 15-T.20S.-R.01E.)													
3260-3320	SMPS	shale	cuttings	0.25	----	----	----	----	----	----	----	----	DGSI
Shell #1 A.C. Gordon (W2 W2 NE, 21-T.21S.-R.10W.)													
3416	SMPS	shale	core	0.23	0.10	1.17	0.20	509	87	426	0.08	1.27	USGS
3418	SMPS	shale	core	0.69	0.05	1.58	0.05	229	7	----	0.03	1.63	USGS
3426	SMPS	shale	core	0.56	0.03	0.67	0.01	120	2	----	0.04	0.70	USGS
Derby #1 Rainbow (SE, 33-T.22S.-R.07W.)													
3839	SMPS	shale	core	0.28	----	----	----	----	----	----	----	----	USGS
3903.5	SMPS	shale	core	0.23	----	----	----	----	----	----	----	----	USGS
3909	SMPS	shale	core	0.12	----	----	----	----	----	----	----	----	USGS
3918	SMPS	shale	core	0.60	0.11	2.46	0.26	410	43	430	0.04	2.57	USGS
3920	SMPS	shale	core	0.20	----	----	----	----	----	----	----	----	USGS
3932	SMPS	shale	core	2.26	0.13	10.36	0.34	458	15	433	0.01	10.49	USGS
Derby #1 Wood (SW NE, 36-T.22S.-R.05W.)													
3885	MQKT	shale	core	0.56	0.14	0.85	0.82	152	146	434	0.14	0.99	DGSI
Walker #1-08 Goertzen (SE NW SW, 08-T.22S.-R.04W.)													
3970-3990	SMPS	shale	cuttings	0.53	<0.10	0.34	0.30	64	57	435	<0.29	----	B&R
Quinoco #1 Zenith Unit (W2 SW, 12-T.24S.-R.11W.)													
3900-3910	SMPS	shale	cuttings	0.36	0.08	0.14	0.20	39	56	----	----	0.22	DGSI
3940-3950	SMPS	shale	cuttings	0.63	0.04	0.19	0.18	30	29	----	----	0.23	DGSI
Moore #1 Secrest (S2 SE NW, 21-T.25S.-R.11W.)													
4080-4090	SMPS	shale	cuttings	0.44	0.06	0.02	0.56	5	127	----	----	0.08	DGSI

* Cuttings samples were handpicked and washed with distilled water to remove impurities. In samples analyzed by DGSI, total organic carbon (TOC) content is determined by grinding samples and passing them through a 60 mesh sieve to assure homogeneity. Each sample (approximately 0.2 grams) is treated with concentrated hydrochloric acid to remove carbonate minerals and the residue is in turn removed by filtration and analyzed with a LECO EC-12 carbon analyzer. Instrumentation used by Sohio, USGS (United States Geological Survey), and B&R (Brown and Root) is unknown. Pyrolysis data are obtained by a Rock-Eval II instrument. Approximately 0.1 gram of sample is used but sample size may vary according to organic content. No pyrolysis is attempted if TOC content of the sample is less than 0.20 weight

APPENDIX II (continued)

percent. T_{max} data are not considered reliable if S_2 is less than 0.20 (Peters, 1986).

** Hydrogen Index = S_2/TOC X 100 (units are mg HC/g TOC)

*** Oxygen Index = S_3/TOC X 100 (units are mg HC/g TOC)

**** Transformation ratio = $S_1/(S_1 + S_2)$, TRs are not listed for samples with S_2 <0.20

APPENDIX III -- ROCK-EVAL AND VITRINITE-REFLECTANCE MATURATION DATA FOR WELLS IN AND NEAR McPHERSON COUNTY, KANSAS.

Formation Key

ABCK -- Arbuckle Gp.
CHAT -- Chattanooga Sh.
CHER -- Cherokee Gp.
DGLS -- Douglas Gp.
HEEB -- Heebner Sh.
HUSH -- Hushpuckney Sh.
LANS -- Lansing Gp.
LKC -- Lansing-Kansas City gps.
MARM -- Marmaton Gp.
MQKT -- Maquoketa Sh.
SMPS -- Simpson Gp.
STRK -- Stark Sh.
VIOL -- Viola Fm.

OPERATOR AND WELL NAME (LOCATION)

SAMPLE INTERVAL (ft)	AGE	FM.	LITH.	SAMPLE TYPE	TOC* (wt. %)	S_1 (kg/tn)	S_2 (kg/tn)	S_3 (kg/tn)	T_{MAX} (°C)	TR**	R_o	DATA SOURCE
Range #1 Winslow (N2 S2, 05-T.14S.-R.02W., datum elev. 1213)												
1950-1960	Penn. (Missour.)	LKC	shale	cuttings	0.62	<0.10	0.16	0.26	----	----	----	B&R
1950-1960	Penn. (Missour.)	LKC	shale	cuttings	0.72	<0.10	<0.10	0.24	----	----	----	B&R
1980-2000	Penn. (Missour.)	LKC	shale	cuttings	0.64	<0.10	<0.10	0.24	----	----	----	B&R
1980-2000	Penn. (Missour.)	LKC	shale	cuttings	0.67	<0.10	<0.10	0.26	----	----	----	B&R
2100-2110	Penn. (Missour.)	LKC	shale	cuttings	0.73	<0.10	0.18	0.24	----	----	----	B&R
2100-2110	Penn. (Missour.)	LKC	shale	cuttings	0.74	<0.10	0.24	0.21	427	<0.42	----	B&R
2120-2130	Penn. (Missour.)	LKC	shale	cuttings	15.07	1.19	42.72	7.37	422	0.03	----	B&R
2120-2130	Penn. (Missour.)	LKC	shale	cuttings	15.31	1.36	46.88	7.86	424	0.03	----	B&R
2210-2220	Penn. (Missour.)	LKC	shale	cuttings	14.27	2.40	60.31	1.91	424	0.04	----	B&R
2210-2220	Penn. (Missour.)	LKC	shale	cuttings	13.78	2.44	59.24	1.83	423	0.04	----	B&R
2260-2280	Penn. (Missour.)	LKC	shale	cuttings	2.81	<0.10	3.09	0.93	429	<0.03	----	B&R
2260-2280	Penn. (Missour.)	LKC	shale	cuttings	2.23	<0.10	2.25	0.91	430	<0.04	----	B&R
2300-2310	Penn. (Missour.)	LKC	shale	cuttings	1.33	<0.10	0.95	0.38	428	<0.11	----	B&R
2300-2310	Penn. (Missour.)	LKC	shale	cuttings	1.75	0.11	1.72	0.40	428	0.06	----	B&R
2320-2330	Penn. (Missour.)	LKC	shale	cuttings	0.92	<0.10	0.34	0.39	426	<0.29	----	B&R
2320-2330	Penn. (Missour.)	LKC	shale	cuttings	1.11	<0.10	0.57	0.46	427	<0.17	----	B&R
2410-2420	Penn. (Desmoin.)	CHER	shale	cuttings	0.97	<0.10	0.44	0.35	428	<0.23	----	B&R
2410-2420	Penn. (Desmoin.)	CHER	shale	cuttings	1.09	<0.10	0.55	0.36	426	<0.18	----	B&R
2480-2500	Penn. (Desmoin.)	CHER	shale	cuttings	0.72	<0.10	0.18	0.31	----	----	----	B&R
2480-2500	Penn. (Desmoin.)	CHER	shale	cuttings	0.73	<0.10	0.18	0.40	----	----	----	B&R
2540-2550	Penn. (Desmoin.)	CHER	shale	cuttings	3.30	0.11	3.29	1.62	429	0.03	----	B&R
2540-2550	Penn. (Desmoin.)	CHER	shale	cuttings	0.71	<0.10	0.27	0.26	382	<0.37	----	B&R

APPENDIX III (continued)

SAMPLE INTERVAL (ft)	AGE	FM.	LITH.	SAMPLE TYPE	TOC* (wt. %)	S_1 (kg/tn)	S_2 (kg/tn)	S_3 (kg/tn)	T_{MAX} (°C)	TR**	R_o	DATA SOURCE
OPERATOR AND WELL NAME (LOCATION)												
2560-2580	Penn. (Desmoin.)	CHER	shale	cuttings	1.23	<0.10	0.30	0.29	430	<0.33	----	B&R
2560-2580	Penn. (Desmoin.)	CHER	shale	cuttings	1.38	<0.10	0.42	0.29	429	<0.24	----	B&R
2620-2630	Mssp.		shale	cuttings	0.86	<0.10	0.28	0.19	429	<0.36	----	B&R
2620-2630	Mssp.		shale	cuttings	0.97	<0.10	0.12	0.26	----	----	----	B&R
2720-2750	Dev.-Mssp.	CHAT	shale	cuttings	1.87	<0.10	0.40	0.59	432	<0.25	----	B&R
2720-2750	Dev.-Mssp.	CHAT	shale	cuttings	1.74	<0.10	0.31	0.64	431	<0.32	----	B&R
2830-2850	Dev.-Mssp.	CHAT	shale	cuttings	1.24	<0.10	0.28	0.29	430	<0.36	----	B&R
2830-2850	Dev.-Mssp.	CHAT	shale	cuttings	1.04	<0.10	0.18	0.31	----	----	----	B&R
2880-2890	Dev.-Mssp.	CHAT	shale	cuttings	0.71	<0.10	<0.10	0.31	----	----	----	B&R
2880-2890	Dev.-Mssp.	CHAT	shale	cuttings	0.80	<0.10	<0.10	0.26	----	----	----	B&R
2900-2910	Dev.-Mssp.	CHAT	shale	cuttings	0.78	<0.10	<0.10	0.26	----	----	----	B&R
2900-2910	Dev.-Mssp.	CHAT	shale	cuttings	1.17	<0.10	0.35	0.26	433	<0.29	----	B&R
2920-2930	Dev.-Mssp.	CHAT	shale	cuttings	0.70	<0.10	<0.10	0.25	----	----	----	B&R
2920-2930	Dev.-Mssp.	CHAT	shale	cuttings	0.75	<0.10	<0.10	0.28	----	----	----	B&R
2970-2980	Dev.-Mssp.	CHAT	shale	cuttings	1.05	<0.10	0.17	0.29	----	----	----	B&R
2970-2980	Dev.-Mssp.	CHAT	shale	cuttings	1.02	<0.10	0.14	0.25	----	----	----	B&R
3100-3110	U. Ord.	MQKT	shale	cuttings	1.63	<0.10	0.36	0.27	431	<0.28	----	B&R
3100-3110	U. Ord.	MQKT	shale	cuttings	0.93	<0.10	0.13	0.23	430	----	----	B&R
3140-3150	U. Ord.	MQKT	shale	cuttings	0.78	<0.10	0.13	0.26	436	----	----	B&R
3140-3150	U. Ord.	MQKT	shale	cuttings	0.66	<0.10	0.20	0.28	428	<0.50	----	B&R
Damac #1 Allen (SW, 7-T.17S.-R.03W., datum elev. 1360)												
3140	Dev.-Mssp.	CHAT	shale	core	0.36	----	----	----	----	----	----	DGSI
3353.9	Dev.-Mssp.	CHAT	shale	core	0.50	----	----	----	439	----	----	ARCo
3355	Dev.-Mssp.	CHAT	shale	core	0.47	----	----	----	----	----	----	DGSI
3367.9	Dev.-Mssp.	CHAT	shale	core	1.36	0.42	3.58	0.32	435	0.11	----	DGSI
Diamond-Shamrock #1-9 Skully 181 (SE SE, 09-T.18S.-R.01E., datum elev. 1439)												
1900-1920	Penn. (Virgil.)	HEEB	shale	cuttings	0.92	0.04	0.42	0.28	432	0.09	----	Sohio
2160-2170	Penn. (Missour.)	LANS	shale	cuttings	4.78	0.59	12.66	0.52	434	0.04	0.61	Sohio
2270-2290	Penn. (Missour.)	LANS	shale	cuttings	0.69	0.01	0.15	0.33	----	----	----	Sohio
2400-2410	Penn. (Missour.)	LANS	shale	cuttings	10.71	2.91	53.00	1.42	430	0.05	----	Sohio
2440-2450	Penn. (Missour.)	HUSH	shale	cuttings	13.55	3.69	72.03	1.67	432	0.05	0.56	Sohio
2460-2480	Penn. (Missour.)	LANS	shale	cuttings	1.68	0.15	2.03	0.42	433	0.07	----	Sohio
2480-2490	Penn. (Missour.)	LKC	cshale	cuttings	0.23	0.03	0.14	0.23	----	----	----	Sohio
2580-2590	Penn. (Desmoin.)	MARM	cshale	cuttings	0.96	0.05	0.27	0.33	437	0.16	----	Sohio
2610-2620	Penn. (Desmoin.)	MARM	cshale	cuttings	0.08	----	----	----	----	----	----	Sohio

APPENDIX III (continued)

SAMPLE INTERVAL (ft)	AGE	FM.	LITH.	SAMPLE TYPE	TOC* (wt. %)	S_1 (kg/tn)	S_2 (kg/tn)	S_3 (kg/tn)	T_{MAX} (°C)	TR****	R_o	DATA SOURCE
OPERATOR AND WELL NAME (LOCATION)												
2630-2640	Penn. (Desmoin.)	MARM	cshale	cuttings	0.69	0.12	0.18	----	----	----	----	Sohio
2630-2640	Penn. (Desmoin.)	MARM	cshale	cuttings	0.09	----	----	----	----	----	----	Sohio
2630-2640	Penn. (Desmoin.)	MARM	cshale	cuttings	0.07	----	----	----	----	----	----	Sohio
2660-2670	Penn. (Desmoin.)	MARM	ls	cuttings	0.06	----	----	----	----	----	0.54	Sohio
2660-2670	Penn. (Desmoin.)	CHER	shale	cuttings	0.68	0.32	0.22	----	407	0.59	----	Sohio
2820-2840	Mssp.		shale	cuttings	0.53	0.26	0.03	----	----	----	----	Sohio
2900-2910	Dev.-Mssp.	CHAT	shale	cuttings	0.24	0.15	0.42	----	----	----	----	Sohio
2970-3000	Dev.-Mssp.	CHAT	shale	cuttings	0.67	0.08	0.19	----	----	----	----	Sohio
2980-3000	Dev.-Mssp.	CHAT	shale	cuttings	0.17	0.04	0.16	----	----	----	----	Sohio
3030-3040	Dev.-Mssp.	CHAT	shale	cuttings	1.00	0.23	1.73	----	440	0.12	----	Sohio
3080-3090	U. Ord.	MQKT	shale	cuttings	0.56	0.04	0.09	----	----	----	----	Sohio
3133-3133	U. Ord.	MQKT	shale	cuttings	0.52	0.05	0.16	----	----	----	0.66	Sohio
3141-3141	U. Ord.	VIOL	dol	cuttings	0.24	0.06	0.40	----	----	----	----	Sohio
3230-3245	M. Ord.	SMPS	shale	cuttings	0.72	0.08	1.51	----	----	----	----	Sohio
3265-3270	M. Ord.	SMPS	slst	cuttings	7.29	2.67	71.49	----	451	0.04	----	Sohio
3270-3280	M. Ord.	SMPS	shale	cuttings	0.44	0.19	1.15	----	----	----	----	Sohio
3280-3290	M. Ord.	SMPS	shale	cuttings	0.88	0.00	0.00	----	----	----	----	Sohio
3320-3330	Camb.-Ord.	ABCK	dol	cuttings	0.06	0.01	0.01	----	----	----	----	Sohio
Brandt #10 Dunsford (SW, 23-T.19S.-R.02W., datum elev. approx. 1550)												
2895-2900	Penn. (Desmoin.)	CHER	shale	cuttings	0.78	<0.10	0.27	0.15	428	<0.37	----	B&R
2910-2920	Penn. (Desmoin.)	CHER	shale	cuttings	1.05	<0.10	0.20	0.12	429	<0.50	----	B&R
3370-3380	M. Ord.	SMPS	shale	cuttings	0.72	<0.10	0.22	0.16	434	<0.45	----	B&R
3410-3425	M. Ord.	SMPS	shale	cuttings	0.73	0.19	1.15	0.23	440	0.14	----	B&R
3440-3460	M. Ord.	SMPS	shale	cuttings	0.75	0.17	1.14	0.12	441	0.13	----	B&R
3460-3480	M. Ord.	SMPS	shale	cuttings	0.63	0.13	0.88	0.07	438	0.13	----	B&R
Walker #1-15 Unruh (NW SW SE, 15-T.20S.-R.01E., datum elev. 1485)												
1992-1996	Penn. (Virgil.)	HEEB	shale	cuttings	1.54	0.28	2.53	0.61	430	0.10	0.48	DGSI
2478-2480	Penn. (Missour.)	STRK	shale	cuttings	0.70	0.16	0.22	0.37	427	0.42	----	DGSI
3090-3140	Dev.-Mssp.	CHAT	shale	cuttings	1.01	0.18	0.61	0.37	430	0.23	0.52	DGSI
3260-3320	M. Ord.	SMPS	shale	cuttings	0.25	----	----	----	----	----	----	DGSI
3190-3200	Dev.-Mssp.	CHAT	shale	cuttings	0.15	----	----	----	----	----	----	DGSI
3260-3270	Dev.-Mssp.	CHAT	shale	cuttings	0.87	0.07	0.23	0.21	430	0.23	----	DGSI
3530-3535	U. Ord.	MQKT	shale	cuttings	0.42	----	----	----	----	----	----	DGSI
3675-3680	M. Ord.	SMPS	shale	cuttings	0.29	----	----	----	----	----	----	DGSI

APPENDIX III (continued)

SAMPLE INTERVAL (ft)	AGE	FM.	LITH.	SAMPLE TYPE	TOC* (wt. %)	S_1 (kg/tn)	S_2 (kg/tn)	S_3 (kg/tn)	T_{MAX} (°C)	TR**	R_o	DATA SOURCE
Walker #1 Baerg (SE NW, 25-T.20S.-R.04W., datum elev. 1472)												
2330-2340	Penn. (Virgil.)	HEEB	shale	cuttings	12.00	1.96	56.92	----	429	0.03	0.6	Sohio
2380-2390	Penn. (Virgil.)	DGLS	shale	cuttings	0.72	0.02	0.19	----	----	----	----	Sohio
2430-2440	Penn. (Virgil.)	DGLS	shale	cuttings	0.84	0.03	0.36	----	436	0.08	----	Sohio
2540-2550	Penn. (Virgil.)	DGLS	shale	cuttings	0.67	0.00	0.07	----	----	----	----	Sohio
2880-2890	Penn. (Missour.)	STRK	shale	cuttings	0.65	0.08	0.25	----	314	0.24	0.69	Sohio
2910-2930	Penn. (Missour.)	LANS	shale	cuttings	0.81	0.00	0.09	----	----	----	----	Sohio
3040-3050	Penn. (Desmoin.)	MARM	shale	cuttings	2.34	0.18	3.30	----	438	0.05	0.65	Sohio
3070-3080	Penn. (Desmoin.)	MARM	shale	cuttings	0.53	0.07	0.22	----	441	0.24	----	Sohio
3090-3110	Penn. (Desmoin.)	MARM	shale	cuttings	0.97	0.01	0.05	----	----	----	----	Sohio
3140-3150	Penn. (Desmoin.)	CHER	shale	cuttings	1.04	0.00	0.05	----	----	----	----	Sohio
3560-3570	Dev.-Mssp.	CHAT	shale	cuttings	0.33	----	----	----	----	----	----	Sohio
3590-3600	Dev.-Mssp.	CHAT	shale	cuttings	0.65	0.01	0.18	----	----	----	----	Sohio
3720-3730	Dev.-Mssp.	CHAT	shale	cuttings	0.49	----	----	----	----	----	----	Sohio
3770-3770	U. Ord.	MQKT	shale	cuttings	0.66	0.00	0.15	1.07	----	----	----	Sohio
3800-3810	M. Ord.	SMPS	shale	cuttings	0.67	0.00	0.14	1.20	----	----	----	Sohio
3830-3840	M. Ord.	SMPS	shale	cuttings	0.13	----	----	----	----	----	----	Sohio
3830-3840	M. Ord.	SMPS	shale	cuttings	0.81	0.01	0.17	2.84	----	----	0.82	Sohio
3850-3860	M. Ord.	SMPS	shale	cuttings	0.65	0.00	0.16	2.19	----	----	----	Sohio
Mabee-Shell #1 Friessen (NW SW SE, 33-T.21S.-R.03W., datum elev. unknown)												
3476-3476	Dev.-Mssp.	CHAT	shale	core	0.40	----	----	----	----	----	----	DGSI
Walker #1-08 Goertzen (SE NW SW, 08-T.22S.-R.04W., datum elev. 1535)												
3330-3350	Penn. (Missour.)	LKC	shale	cuttings	0.90	<0.10	0.46	0.35	432	<0.21	----	B&R
3380-3400	Penn. (Missour.)	LKC	shale	cuttings	0.55	<0.10	0.22	0.23	431	<0.45	----	B&R
3670-3690	Dev.-Mssp.	CHAT	shale	cuttings	0.92	0.10	0.53	0.41	430	0.16	----	B&R
3720-3740	Dev.-Mssp.	CHAT	shale	cuttings	0.77	<0.10	0.43	0.25	430	<0.23	----	B&R
3760-3780	Dev.-Mssp.	CHAT	shale	cuttings	0.84	<0.10	0.47	0.39	431	<0.21	----	B&R
3860-3870	Dev.-Mssp.	CHAT	shale	cuttings	0.85	0.10	1.20	0.28	434	0.08	----	B&R
3970-3990	M. Ord.	SMPS	shale	cuttings	0.53	<0.10	0.34	0.30	435	<0.29	----	B&R

* Cuttings samples were handpicked and washed with distilled water to remove impurities. In samples analyzed by DGSI, total organic carbon (TOC) content is determined by grinding samples and passing them through a 60 mesh sieve to assure homogeneity. Each sample (approximately 0.2 grams) is treated with concentrated hydrochloric acid to remove carbonate minerals and the residue is in turn removed

APPENDIX III (continued)

by filtration and analyzed with a LECO EC-12 carbon analyzer. Instrumentation used by Sohio, USGS (United States Geological Survey), and B&R (Brown and Root) is unknown.

The analyses performed by Atlantic Richfield (ARCo) are taken from Lambert (1992). Pyrolysis data are obtained by a Rock-Eval II instrument. Approximately 0.1 gram of sample is used but sample size may vary according to organic content. No pyrolysis is attempted if TOC content of the sample is less than 0.20 weight percent. T_{max} data are not considered reliable if S_2 is less than 0.20 (Peters, 1986).

Kerogens inspected for vitrinite reflectance are concentrated by successively treating samples of ground rock with hydrochloric, hydrofluoric, and hot hydrochloric acids. Kerogen concentrates are mounted on glass slides and microscopic analysis is done with a tungsten light source. A xenon light source is utilized for blue-light fluorescence. Vitrinite-like material was utililized for reflectance measurements in pre-Devonian age rocks (Irene Penfield -- Sohio Oil Company, personal communication, 1985).

** Transformation ratio = $S_1/(S_1 + S_2)$, TRs are not listed for samples with $S_2 < 0.20$

APPENDIX IV -- LITHOLOGIC DESCRIPTIONS FOR VIOLA CORES

Various lithologic characteristics and sedimentary structures are summarized in several columns in the core report form. The Sedimentary Structures (Graphic) column is available as a column for free-form artistry by the geologist, in which key features of the core can be sketched for general appearance and later reference. Some of these same features are also represented symbolically in the Lithology column, as are various fossil and diagenetic features. Many symbols for fossils, lithologies, and sedimentary features are taken from a more general lithologic description form provided by Dr. Paul Enos, University of Kansas. Quantitative estimates (percentages) and semi-quantitative estimates (i.e., R = rare, C = common, A = abundant) of other features are allowed in some columns, as are comments. The Viola subunit being described is in italics (usually on the right side of the description form) where room permits. In the column in which particle or crytal size is described, fine and very-fine sand (crystal) size were usually left blank because these grains (crystals) were usually always present in both the packstones. These size-classes were usually not present in finer grained wackestones and mudstones, or were obscured by dolomitization.

Cores are ordered by their legal location -- township, then range, then section.

KEY TO CORE DESCRIPTIONS

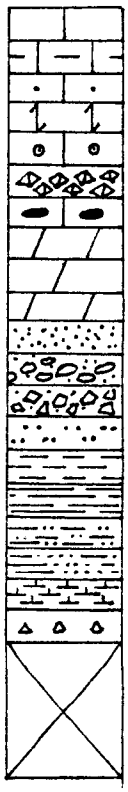

LITHOLOGIES

- LIMESTONE
  - argillaceous
  - sandy
  - dolomitic
  - oolitic
  - lithoclastic breccia
  - cherty
- DOLOMITE
  - *(descriptors above can apply)*
- SANDSTONE
- CONGLOMERATE
- BRECCIA
- SILTSTONE
- SHALE
  - platy
  - silty
  - sandy
  - calcareous
- BEDDED CHERT
- MISSING CORE

STRUCTURES

- fenestral por.
- burrow (vert.)
- burrow (horiz.)
- mudcrack
- planar lam.
- wavy lam.
- discont. lam.
- cross lam.

PARTICLES

- peloid
- intraclast
- lithoclast
- ooid
- coated grain
- shells

DIAGENETIC FEATURES

- pyrite
- fractures
- stylolites
- vug
- dol. burrow

FOSSILS

- spicule
- horn coral
- bryzoan *(general & fenestral)*
- bryzoan *(ramose)*
- brachiopod
- bivalve
- gastropod
- crinoid frag.
- ostracode
- trilobite frag.

CONTACTS *(in class col.)*

- unknown
- transition
- sharp

Textural Chart[1]

SILICICLASTIC ROCKS		GRAIN SIZE MILLIMETERS		GRAIN SIZE MICRONS	CARBONATE ROCKS	
Boulder (Bld)		256	256		Extremely Coarse (xc)	
Cobble (Cbl)		64	64			
Pebble (Pbl)		4	4			
Granule (Gran)		2	2	2000		
Sand	Very Coarse (vc)	1	1	1000	Very Coarse (vc)	
	Coarse (c)	.5	1/2	500	Coarse (c)	
	Medium (m)	.25	1/4	250	Medium (m)	
	Fine (f)	.125	1/8	125	Fine (f)	
	Very Fine (vf)	.062	1/16	62	Very Fine (vf)	
Silt		.020	1/50	20	Mud: Silt/lite	Extremely Fine (xf)
Mud					Mud	Micro-grained/crystalline (Lithographic/mat)

1) For practical reasons Wentworth's division of the lutites into clay and silt at the 4μ (1/256 mm) boundary has been replaced by the above subdivision into mud and silt at the 20μ boundary.

from Swanson (1981)

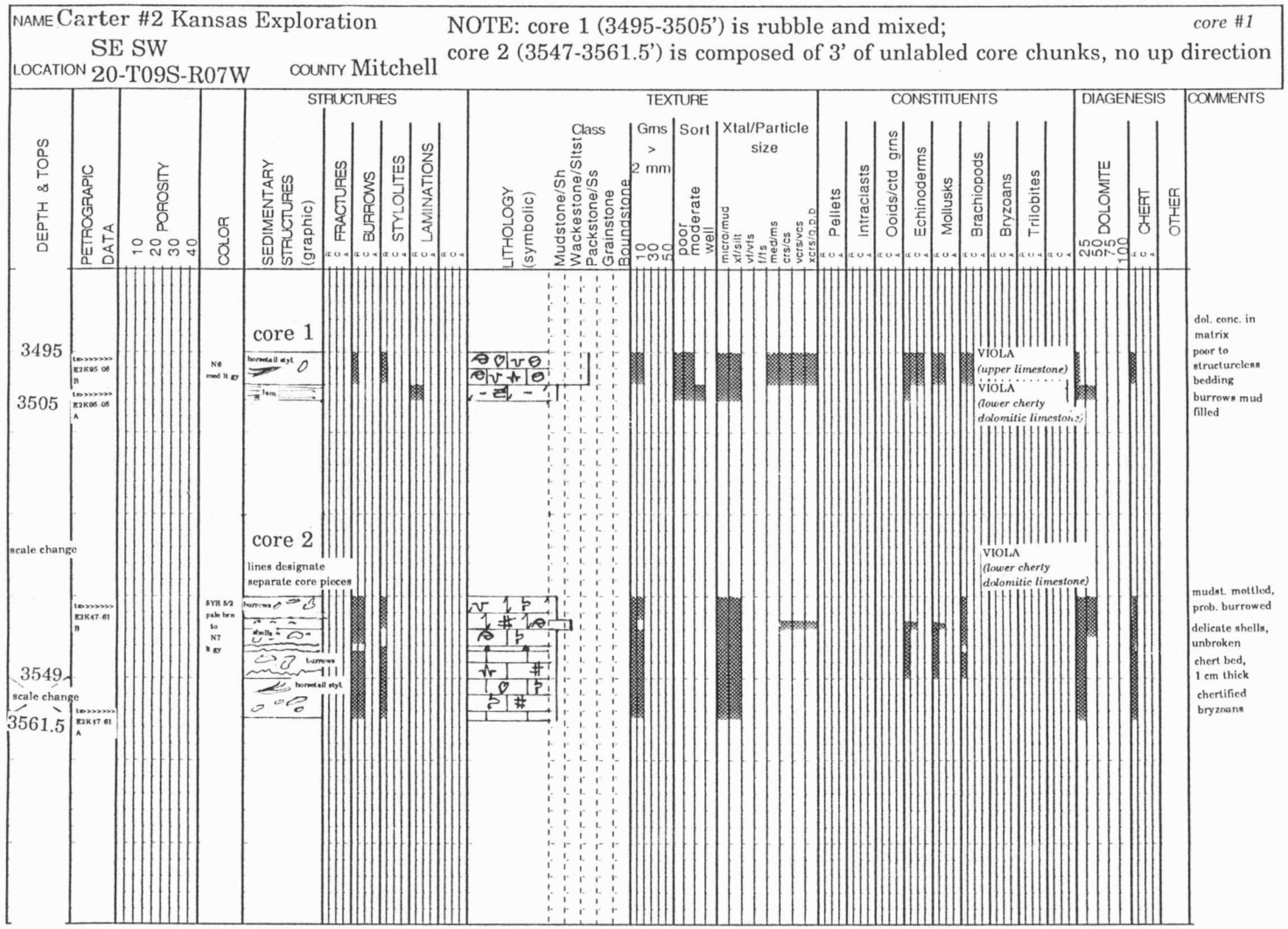
NAME Carter #2 Kansas Exploration
SE SW
LOCATION 20-T09S-R07W
COUNTY Mitchell
NOTE: core 1 (3495-3505') is rubble and mixed;
core 2 (3547-3561.5') is composed of 3' of unlabled core chunks, no up direction
core #1
STRUCTURES
TEXTURE
CONSTITUENTS
DIAGENESIS
COMMENTS
DEPTH & TOPS
PETROGRAPIC DATA
POROSITY
COLOR
SEDIMENTARY STRUCTURES (graphic)
FRACTURES
BURROWS
STYLOLITES
LAMINATIONS
LITHOLOGY (symbolic)
Class
Mudstone/Sh
Wackestone/Sltst
Packstone/Ss
Grainstone
Boundstone
Gms > 2 mm
Sort
poor
moderate
well
Xtal/Particle size
micro/mud
xf/silt
vf/vfs
f/fs
med/ms
crs/cs
vcrs/vcs
xcrs/g.p.p
Pellets
Intraclasts
Ooids/ctd grns
Echinoderms
Mollusks
Brachiopods
Bryzoans
Trilobites
DOLOMITE
CHERT
OTHER
core 1
3495
3505
N6 med lt gy
hornetail styl
core 2
scale change
lines designate separate core pieces
5YR 5/2 pale brn to N7 lt gy
burrows
shells
hornetail styl
3549
scale change
3561.5
VIOLA (upper limestone)
VIOLA (lower cherty dolomitic limestone)
VIOLA (lower cherty dolomitic limestone)
dol. conc. in matrix
poor to structureless bedding
burrows mud filled
mudst. mottled, prob. burrowed
delicate shells, unbroken
chert bed, 1 cm thick
chertified bryzoans

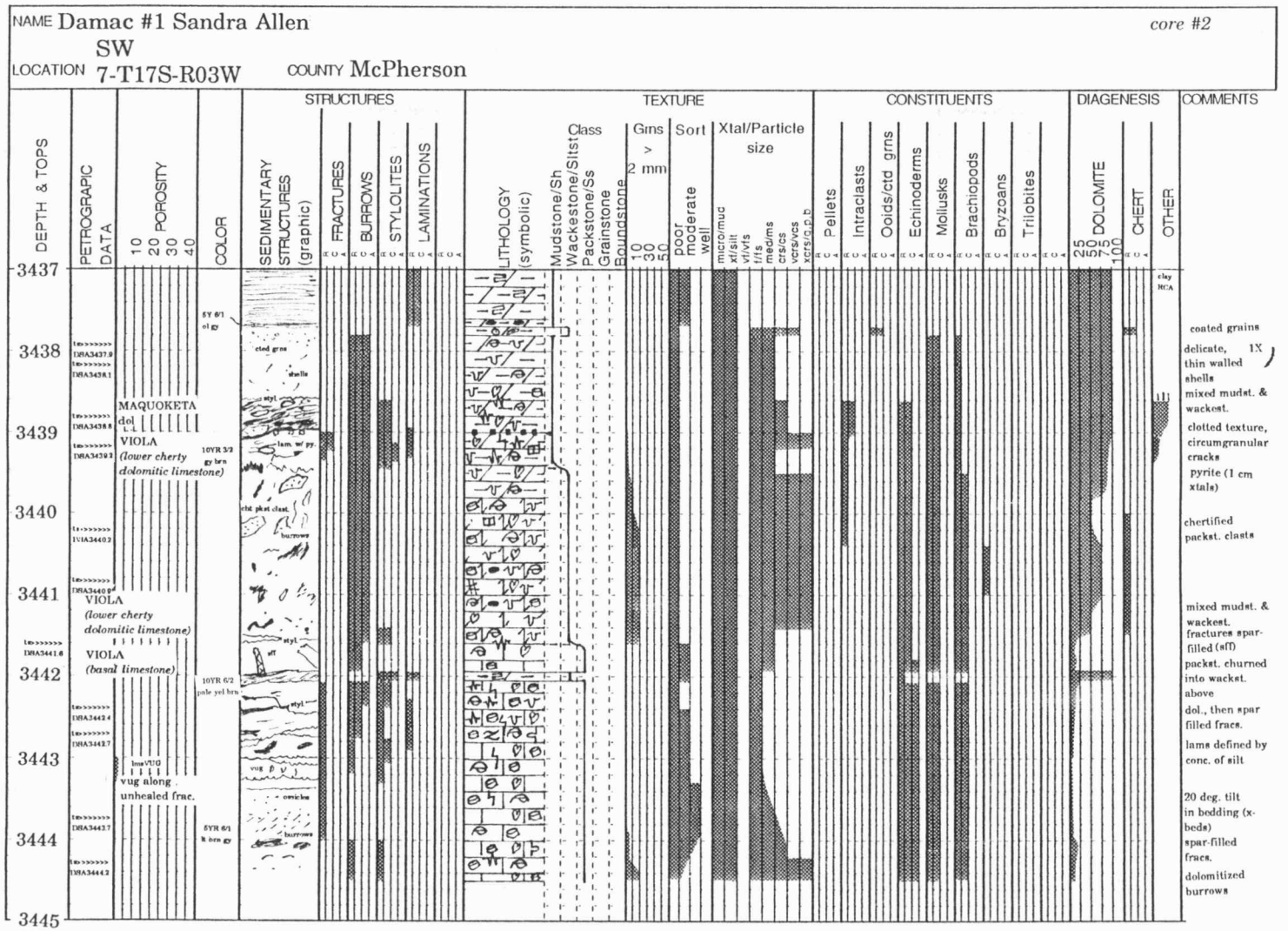
NAME Damac #1 Sandra Allen
SW
LOCATION 7-T17S-R03W
COUNTY McPherson
core #2
STRUCTURES
TEXTURE
CONSTITUENTS
DIAGENESIS
COMMENTS
DEPTH & TOPS
PETROGRAPIC DATA
10 20 POROSITY 30 40
COLOR
SEDIMENTARY STRUCTURES (graphic)
FRACTURES
BURROWS
STYLOLITES
LAMINATIONS
LITHOLOGY (symbolic)
Class
Mudstone/Sh
Wackestone/Siltst
Packstone/Ss
Grainstone
Boundstone
Grns > 2 mm
10 30 50
Sort
poor moderate well
Xtal/Particle size
micro/muc
xf/silt
vf/vfs
f/fs
med/ms
crs/cs
vcrs/vcs
xcrs/g,p,b
Pellets
Intraclasts
Ooids/ctd grns
Echinoderms
Mollusks
Brachiopods
Bryzoans
Trilobites
25 50 75 100
DOLOMITE
CHERT
OTHER
clay
RCA
3437
3438
3439
3440
3441
3442
3443
3444
3445
MAQUOKETA
dol
VIOLA
(lower cherty dolomitic limestone)
VIOLA
(lower cherty dolomitic limestone)
VIOLA
(basal limestone)
5Y 6/1 ol gy
10YR 3/2 gy brn
10YR 6/2 pale yel brn
5YR 6/1 lt brn gy
vug along unhealed frac.
cted grns
shells
styl
lam. w/ py.
cht. phat clast
burrows
vf
styl
styl
vug
burrows
coated grains
delicate, thin walled shells
1X
mixed mudst. & wackest.
clotted texture, circumgranular cracks
pyrite (1 cm xtals)
chertified packst. clasts
mixed mudst. & wackest. fractures spar-filled (sff)
packst. churned into wackst. above dol., then spar filled fracs.
lams defined by conc. of silt
20 deg. tilt in bedding (x-beds)
spar-filled fracs.
dolomitized burrows

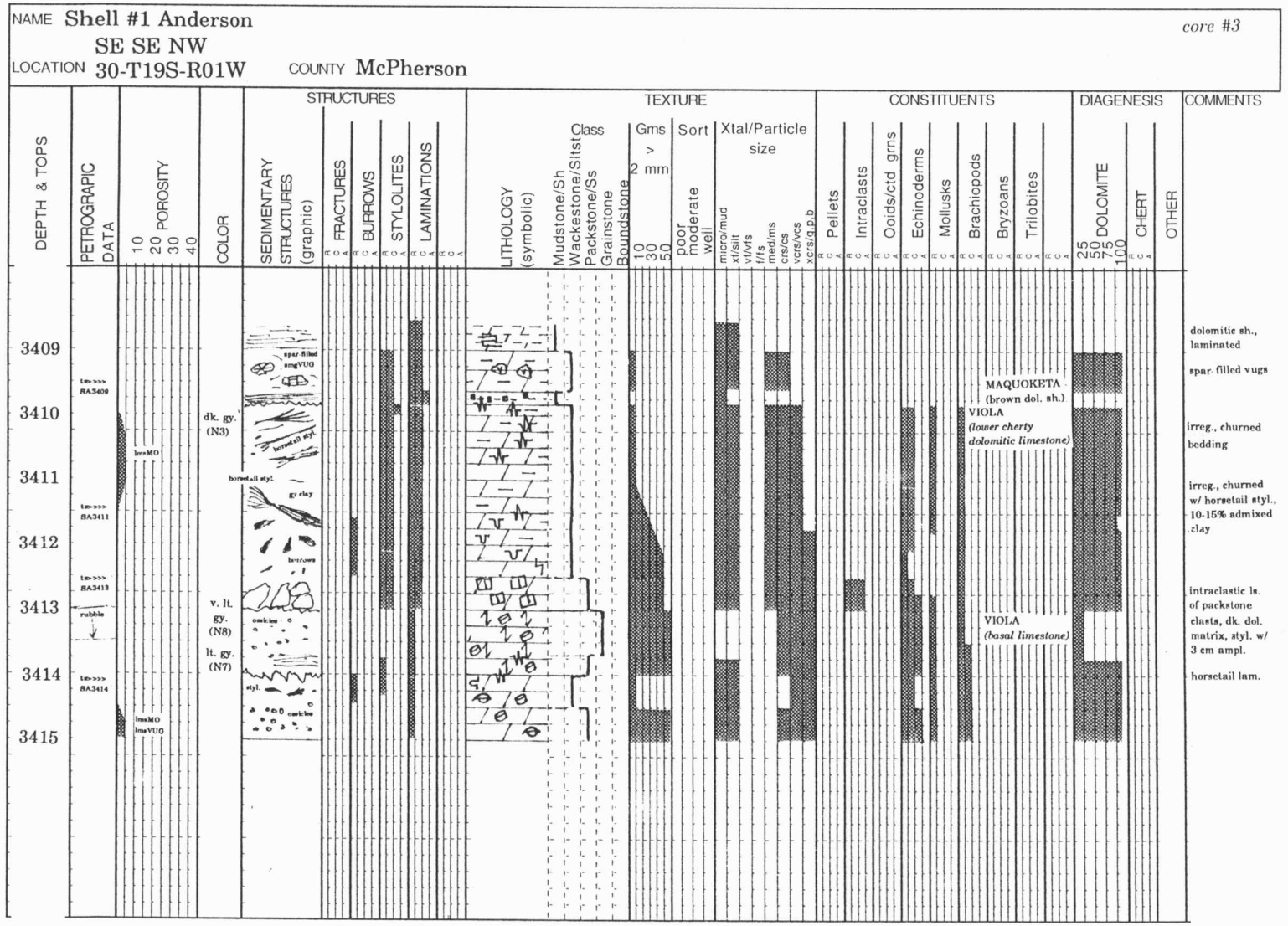
NAME Shell #1 Anderson
SE SE NW
LOCATION 30-T19S-R01W
COUNTY McPherson
core #3
STRUCTURES
TEXTURE
CONSTITUENTS
DIAGENESIS
COMMENTS
DEPTH & TOPS
PETROGRAPIC DATA
10 20 POROSITY 30 40
COLOR
SEDIMENTARY STRUCTURES (graphic)
FRACTURES
BURROWS
STYLOLITES
LAMINATIONS
LITHOLOGY (symbolic)
Class
Mudstone/Sh
Wackestone/Sltst
Packstone/Ss
Grainstone
Boundstone
Gms > 2 mm
10 30 50
Sort
poor moderate well
Xtal/Particle size
micro/mud
xf/silt
vf/vfs
f/fs
med/ms
crs/cs
vcrs/vcs
xcrs/g.p.b
Pellets
Intraclasts
Ooids/ctd grns
Echinoderms
Mollusks
Brachiopods
Bryzoans
Trilobites
25 50 75 100
DOLOMITE
CHERT
OTHER
3409
3410
3411
3412
3413
3414
3415
dk. gy. (N3)
v. lt. gy. (N8)
lt. gy. (N7)
spar filled smgVUG
horsetail styl.
gy clay
burrows
oosicles
styl.
rubble
lmsMO
lmsVUG
MAQUOKETA (brown dol. sh.)
VIOLA (lower cherty dolomitic limestone)
VIOLA (basal limestone)
dolomitic sh., laminated
spar filled vugs
irreg., churned bedding
irreg., churned w/ horsetail styl., 10-15% admixed clay
intraclastic ls. of packstone clasts, dk. dol. matrix, styl. w/ 3 cm ampl.
horsetail lam.

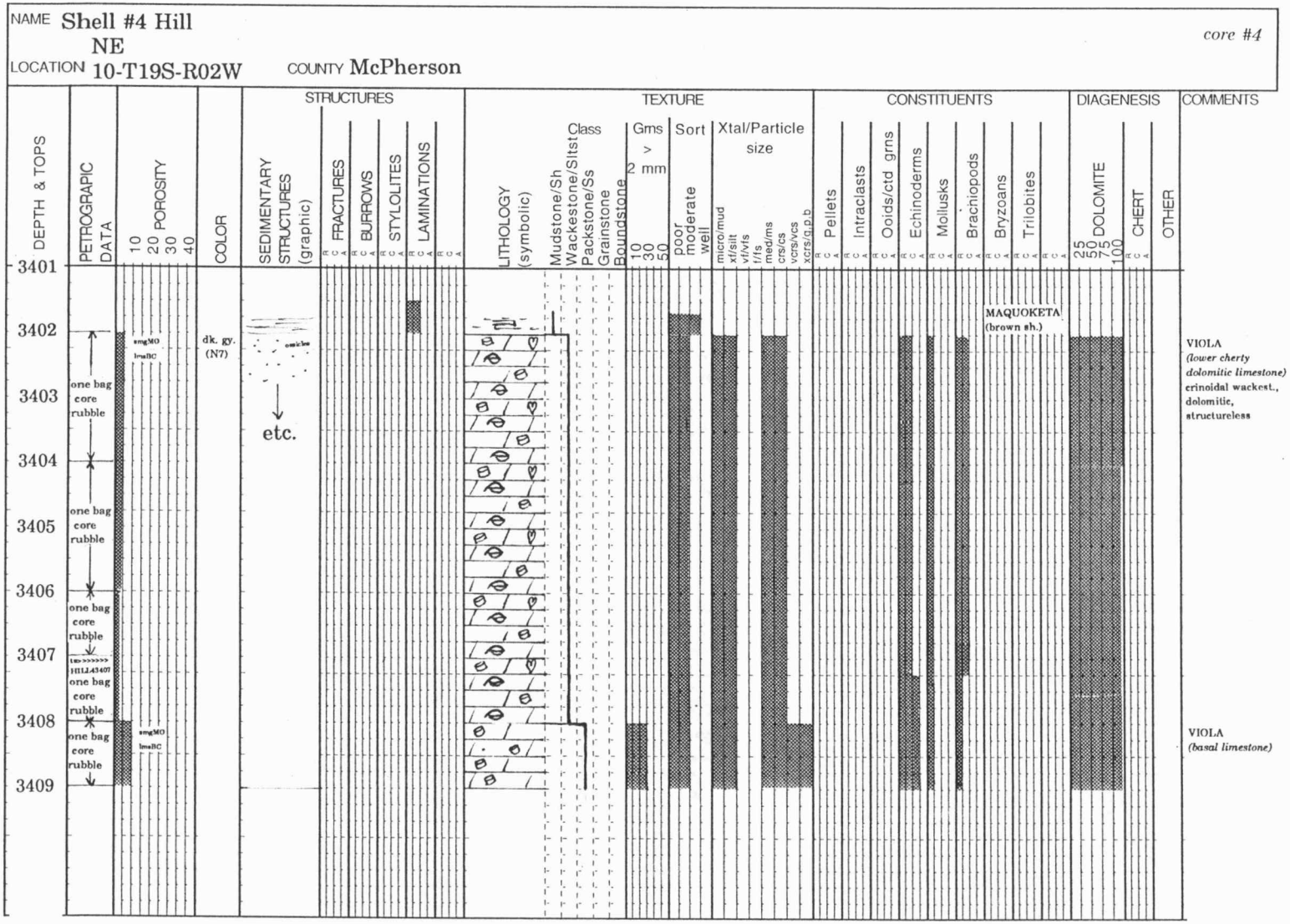
NAME Shell #4 Hill
NE
LOCATION 10-T19S-R02W
COUNTY McPherson
core #4
STRUCTURES
TEXTURE
CONSTITUENTS
DIAGENESIS
COMMENTS
DEPTH & TOPS
PETROGRAPIC DATA
POROSITY
COLOR
SEDIMENTARY STRUCTURES (graphic)
FRACTURES
BURROWS
STYLOLITES
LAMINATIONS
LITHOLOGY (symbolic)
Class
Mudstone/Sh
Wackestone/Sltst
Packstone/Ss
Grainstone
Boundstone
Grns > 2 mm
Sort
poor
moderate
well
Xtal/Particle size
micro/mud
vf/silt
vf/vfs
f/fs
med/ms
crs/cs
vcrs/vcs
xcrs/g.p.b
Pellets
Intraclasts
Ooids/ctd grns
Echinoderms
Mollusks
Brachiopods
Bryzoans
Trilobites
DOLOMITE
CHERT
OTHER
3401
3402
3403
3404
3405
3406
3407
3408
3409
dk. gy. (N7)
etc.
one bag core rubble
MAQUOKETA (brown sh.)
VIOLA
(lower cherty dolomitic limestone)
crinoidal wackest., dolomitic, structureless
VIOLA
(basal limestone)

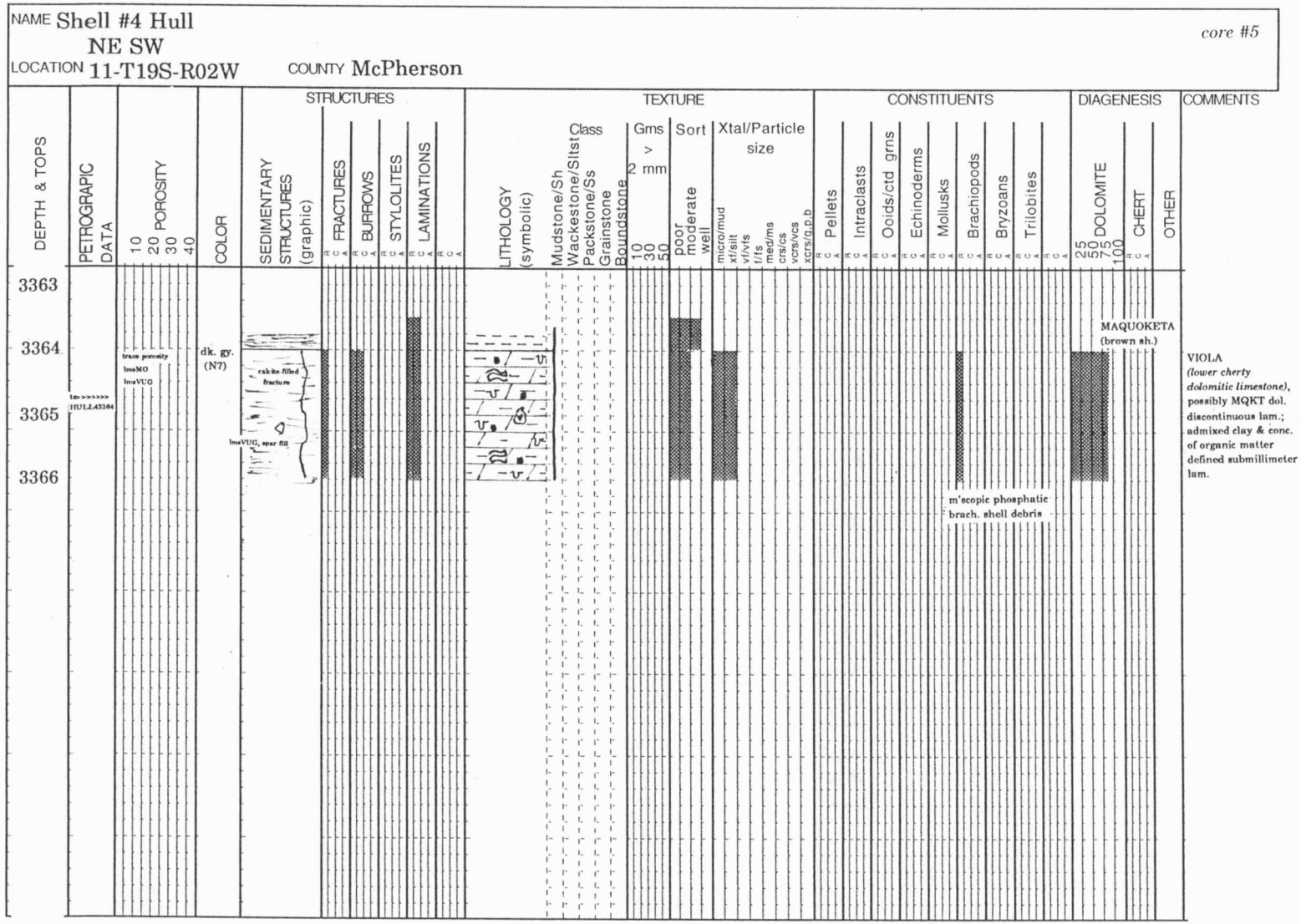
NAME Shell #4 Hull
NE SW
LOCATION 11-T19S-R02W
COUNTY McPherson
core #5
STRUCTURES
TEXTURE
CONSTITUENTS
DIAGENESIS
COMMENTS
DEPTH & TOPS
PETROGRAPIC DATA
POROSITY
COLOR
SEDIMENTARY STRUCTURES (graphic)
FRACTURES
BURROWS
STYLOLITES
LAMINATIONS
LITHOLOGY (symbolic)
Class
Mudstone/Sh
Wackestone/Sltst
Packstone/Ss
Grainstone
Boundstone
Gms > 2 mm
Sort
poor
moderate
well
Xtal/Particle size
micro/mud
xf/silt
vf/vfs
f/fs
med/ms
crs/cs
vcrs/vcs
xcrs/g,p,b
Pellets
Intraclasts
Ooids/ctd grns
Echinoderms
Mollusks
Brachiopods
Bryzoans
Trilobites
DOLOMITE
CHERT
OTHER
3363
3364
3365
3366
trace porosity
lmsMO
lmsVUG
dk. gy. (N7)
calcite filled fracture
lmsVUG, spar fill
HULL43364
MAQUOKETA (brown sh.)
m'scopic phosphatic brach. shell debris
VIOLA (lower cherty dolomitic limestone), possibly MQKT dol. discontinuous lam.; admixed clay & conc. of organic matter defined submillimeter lam.

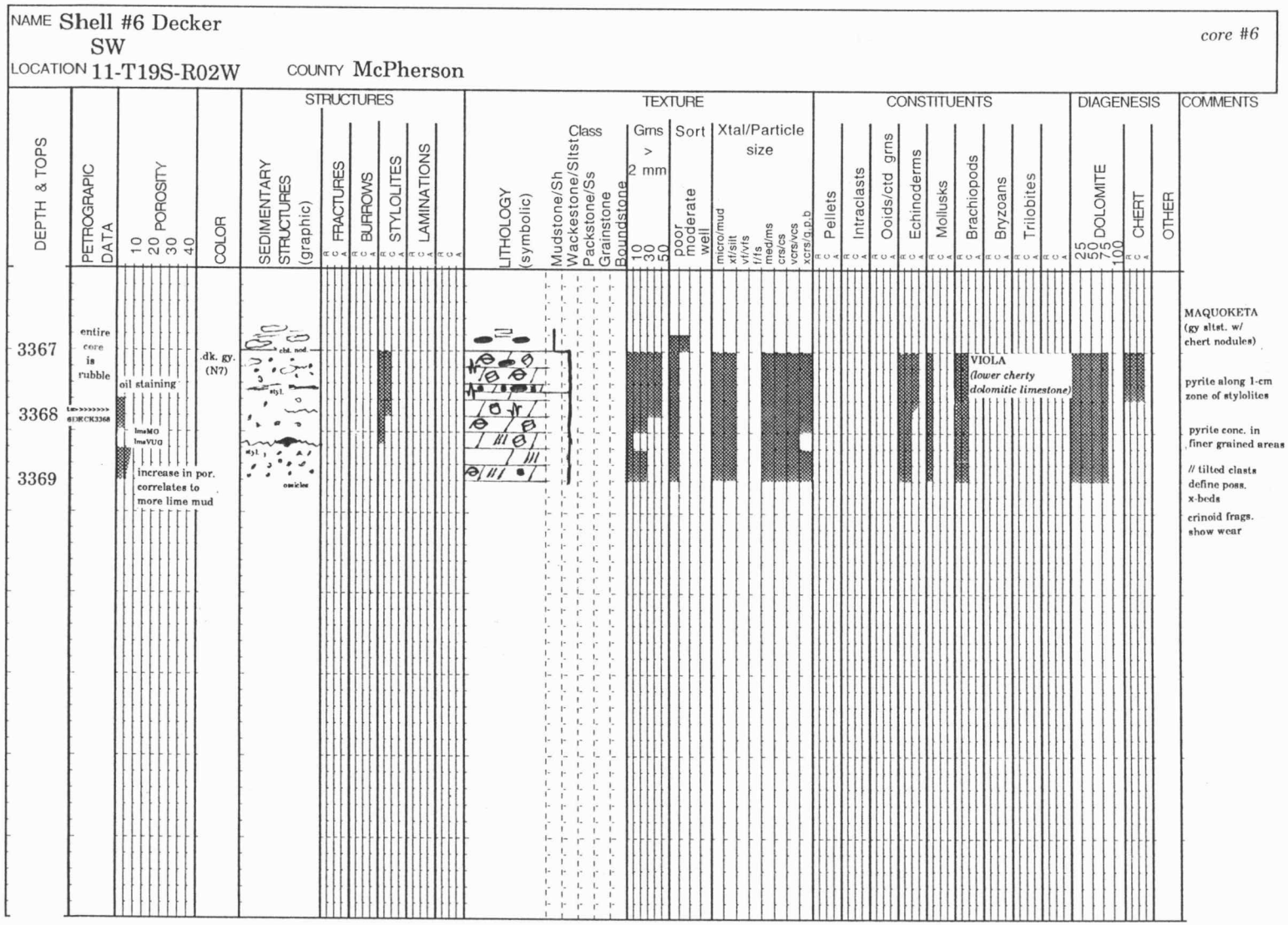
NAME Shell #6 Decker SW
LOCATION 11-T19S-R02W
COUNTY McPherson
core #6
STRUCTURES
TEXTURE
CONSTITUENTS
DIAGENESIS
COMMENTS
DEPTH & TOPS
PETROGRAPIC DATA
POROSITY
COLOR
SEDIMENTARY STRUCTURES (graphic)
FRACTURES
BURROWS
STYLOLITES
LAMINATIONS
LITHOLOGY (symbolic)
Class
Mudstone/Sh
Wackestone/Siltst
Packstone/Ss
Grainstone
Boundstone
Grns > 2 mm
Sort
poor
moderate
well
Xtal/Particle size
micro/mud
vf/silt
vf/vfs
f/fs
med/ms
crs/cs
vcrs/vcs
xcrs/g,p,b
Pellets
Intraclasts
Ooids/ctd grns
Echinoderms
Mollusks
Brachiopods
Bryzoans
Trilobites
DOLOMITE
CHERT
OTHER
3367
3368
3369
entire core is rubble
oil staining
dk. gy. (N7)
chtl. nod.
styl.
omicles
increase in por. correlates to more lime mud
VIOLA
(lower cherty dolomitic limestone)
MAQUOKETA (gy siltst. w/ chert nodules)
pyrite along 1-cm zone of stylolites
pyrite conc. in finer grained areas
// tilted clasts define poss. x-beds
crinoid frags. show wear

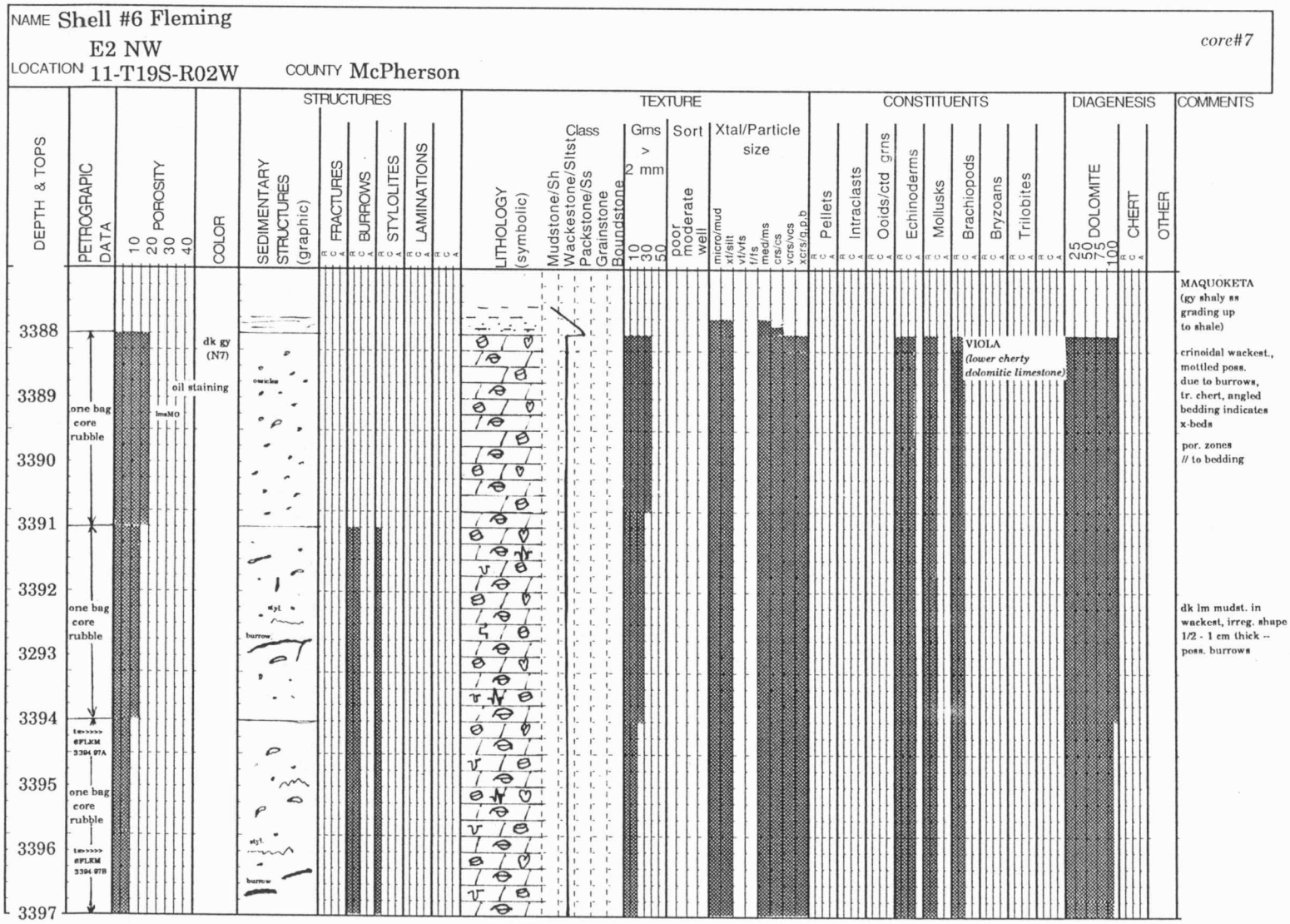
NAME Shell #6 Fleming
E2 NW
LOCATION 11-T19S-R02W
COUNTY McPherson
core#7
DEPTH & TOPS
PETROGRAPIC DATA
POROSITY
COLOR
STRUCTURES
SEDIMENTARY STRUCTURES (graphic)
FRACTURES
BURROWS
STYLOLITES
LAMINATIONS
TEXTURE
LITHOLOGY (symbolic)
Class
Mudstone/Sh
Wackestone/Sltst
Packstone/Ss
Grainstone
Boundstone
Grns > 2 mm
Sort
poor
moderate
well
Xtal/Particle size
micro/mud
xf/silt
vf/vfs
f/fs
med/ms
crs/cs
vcrs/vcs
xcrs/g.p.b
CONSTITUENTS
Pellets
Intraclasts
Ooids/ctd grns
Echinoderms
Mollusks
Brachiopods
Bryzoans
Trilobites
DIAGENESIS
DOLOMITE
CHERT
OTHER
COMMENTS
3388
3389
3390
3391
3392
3293
3394
3395
3396
3397
dk gy (N7)
oil staining
lmsMO
one bag core rubble
one bag core rubble
one bag core rubble
VIOLA
(lower cherty dolomitic limestone)
MAQUOKETA
(gy shaly ss grading up to shale)
crinoidal wackest., mottled poss. due to burrows, tr. chert, angled bedding indicates x-beds
por. zones // to bedding
dk lm mudst. in wackest, irreg. shape 1/2 - 1 cm thick -- poss. burrows

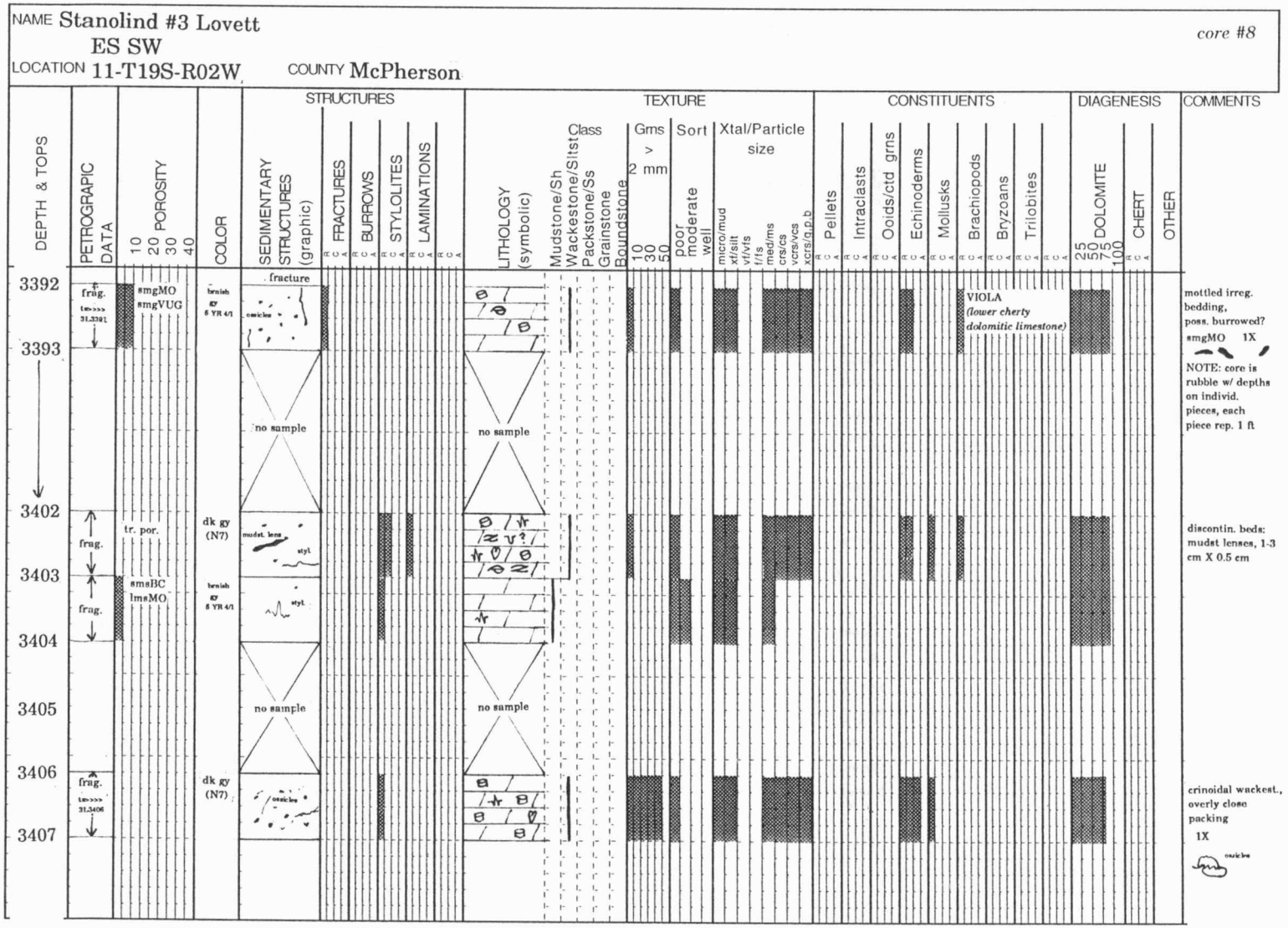
NAME Stanolind #3 Lovett
ES SW
LOCATION 11-T19S-R02W
COUNTY McPherson
core #8
DEPTH & TOPS
PETROGRAPHIC DATA
10 20 POROSITY 30 40
COLOR
STRUCTURES
SEDIMENTARY STRUCTURES (graphic)
FRACTURES
BURROWS
STYLOLITES
LAMINATIONS
TEXTURE
LITHOLOGY (symbolic)
Mudstone/Sh
Wackestone/Slstst
Packstone/Ss
Grainstone
Boundstone
Class
Gms > 2 mm
Sort
poor
moderate
well
Xtal/Particle size
micro/mud
xf/silt
vf/vfs
f/fs
med/ms
crs/cs
vcrs/vcs
xcrs/g,p,b
CONSTITUENTS
Pellets
Intraclasts
Ooids/ctd grns
Echinoderms
Mollusks
Brachiopods
Bryzoans
Trilobites
DIAGENESIS
DOLOMITE
CHERT
OTHER
COMMENTS
3392
3393
3402
3403
3404
3405
3406
3407
frag.
smgMO
smgVUG
tr. por.
smsBC
lmsMO
fracture
no sample
mudst. lens
styl
dk gy (N7)
brnish gy 5 YR 4/1
VIOLA
(lower cherty dolomitic limestone)
mottled irreg. bedding, poss. burrowed?
smgMO 1X
NOTE: core is rubble w/ depths on individ. pieces, each piece rep. 1 ft
discontin. beds; mudst lenses, 1-3 cm X 0.5 cm
crinoidal wackest., overly close packing
1X

NAME **Shell #4 Griffin 'B'**
W2 W2 NE
LOCATION **11-T19S-R02W** COUNTY **McPherson**

core #9

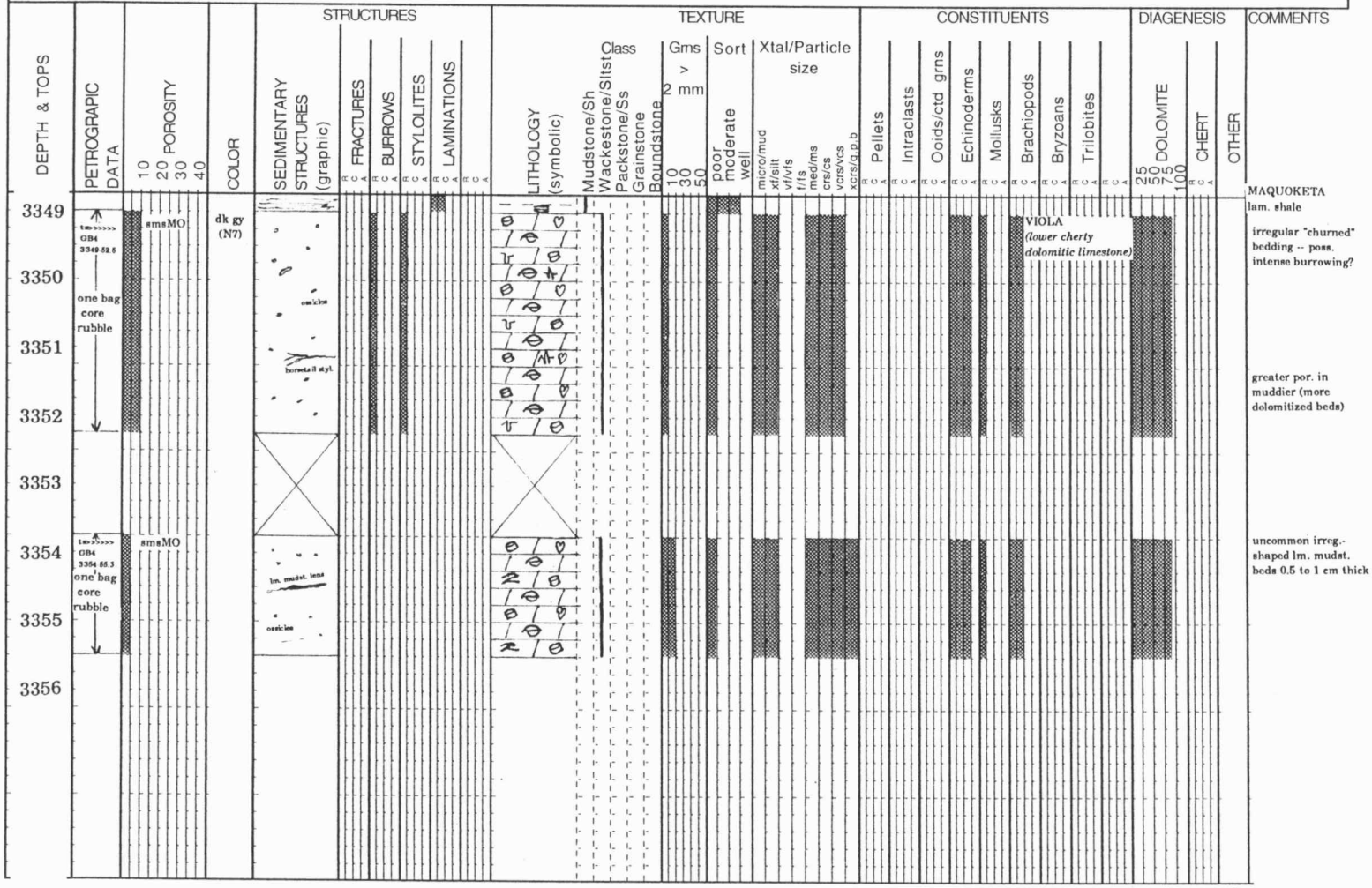

NAME **Champlin #8 Speck**
NW NW
LOCATION **18-T19S-R08W** COUNTY **Rice**

core #10

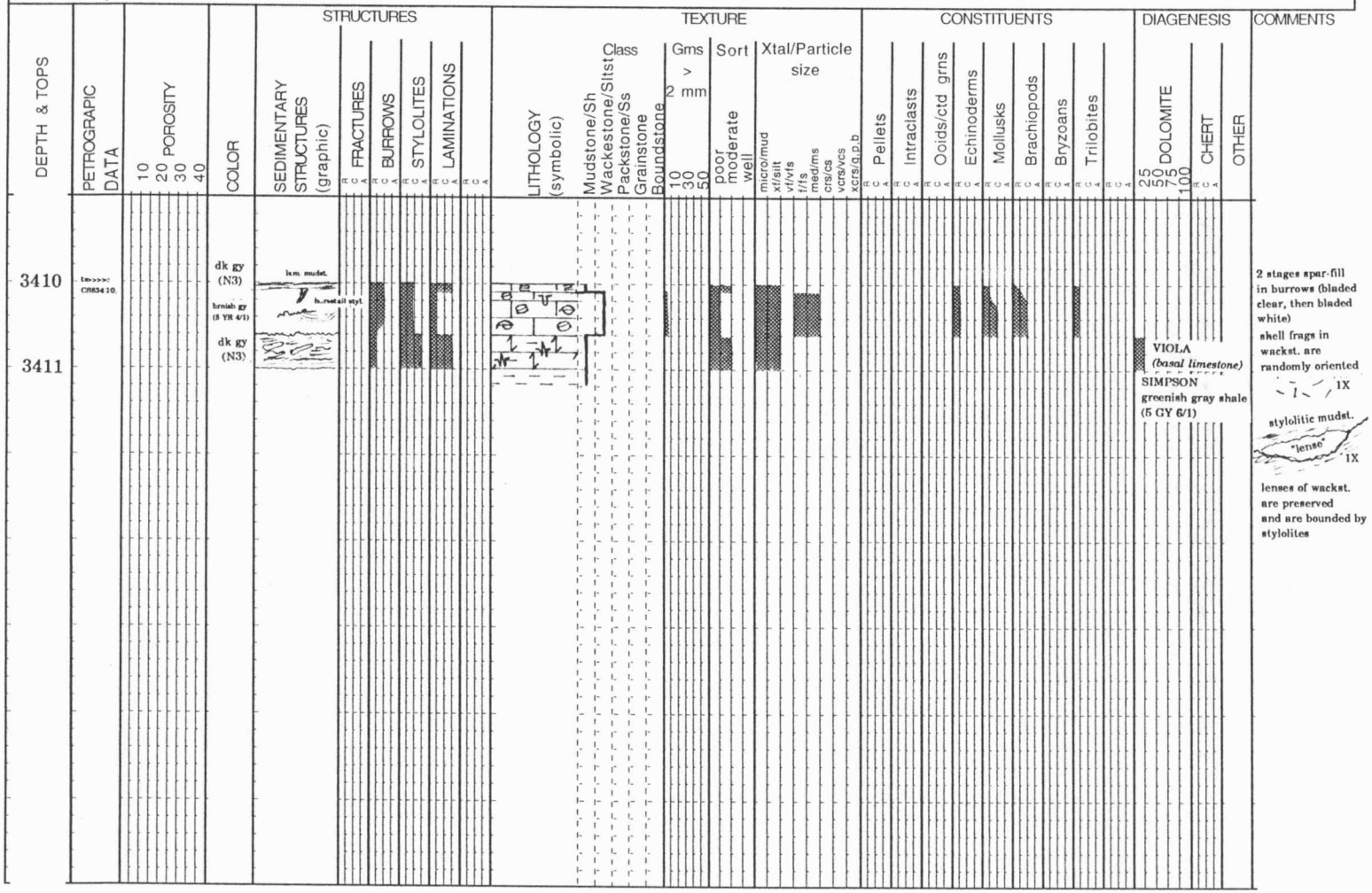

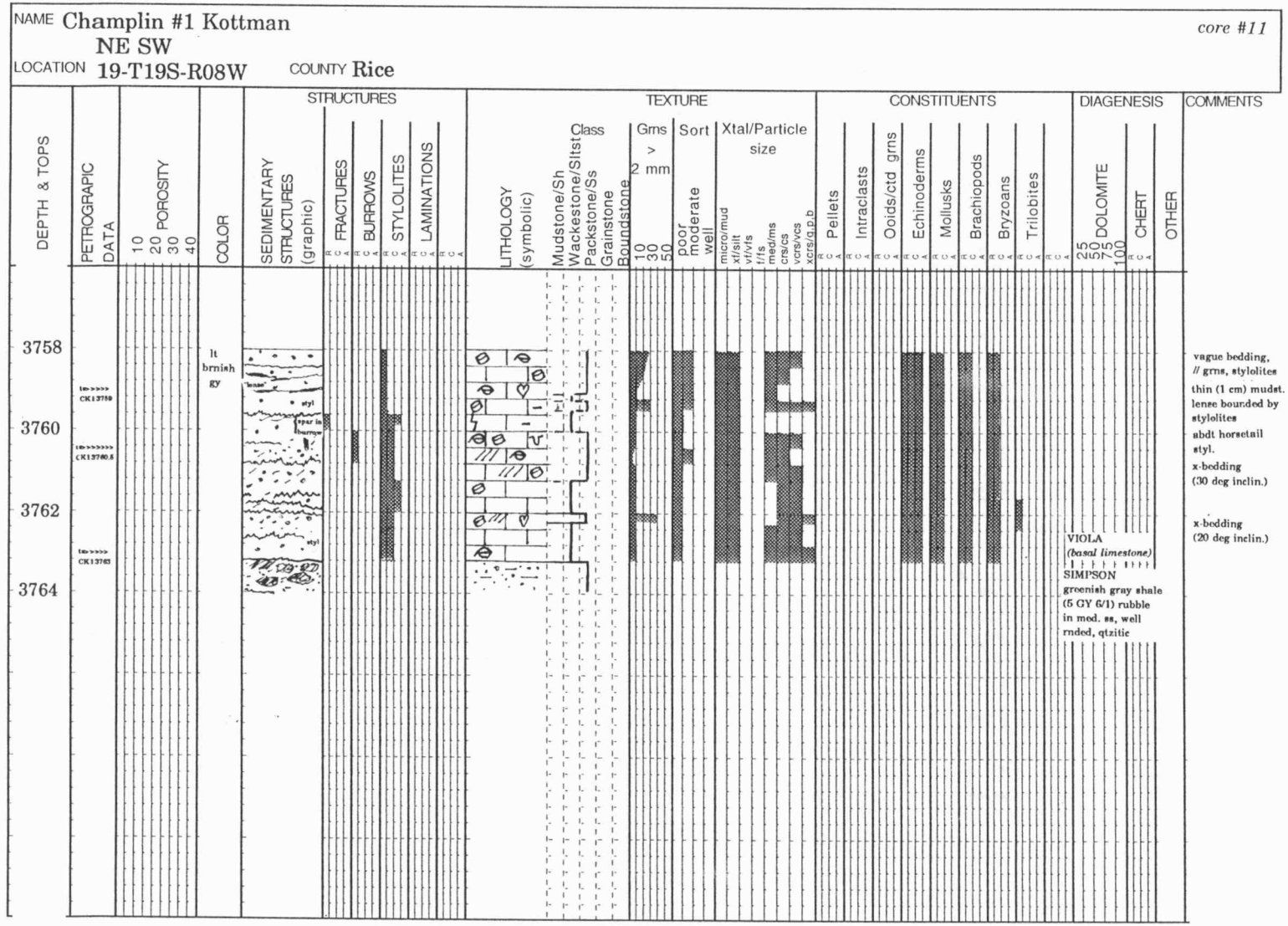
NAME Champlin #1 Kottman
NE SW
LOCATION 19-T19S-R08W
COUNTY Rice
core #11
DEPTH & TOPS
PETROGRAPHIC DATA
10 20 POROSITY 30 40
COLOR
STRUCTURES
SEDIMENTARY STRUCTURES (graphic)
FRACTURES
BURROWS
STYLOLITES
LAMINATIONS
TEXTURE
LITHOLOGY (symbolic)
Class
Mudstone/Sh
Wackestone/Sltst
Packstone/Ss
Grainstone
Boundstone
Grns > 2 mm
10 30 50
Sort
poor moderate well
Xtal/Particle size
micro/mud
xf/silt
vf/vfs
f/fs
med/ms
crs/cs
vcrs/vcs
xcrs/g.p.b
CONSTITUENTS
Pellets
Intraclasts
Ooids/ctd grns
Echinoderms
Mollusks
Brachiopods
Bryzoans
Trilobites
DIAGENESIS
25 50 75 100
DOLOMITE
CHERT
OTHER
COMMENTS
3758
3760
3762
3764
lt brnish gy
styl
spar in burrow
styl
VIOLA
(basal limestone)
SIMPSON
groenish gray shale (5 GY 6/1) rubble in med. ss, well rnded, qtzitic
vague bedding, // grns, stylolites
thin (1 cm) mudst. lense bounded by stylolites
abdt horsetail styl.
x-bedding (30 deg inclin.)
x-bedding (20 deg inclin.)

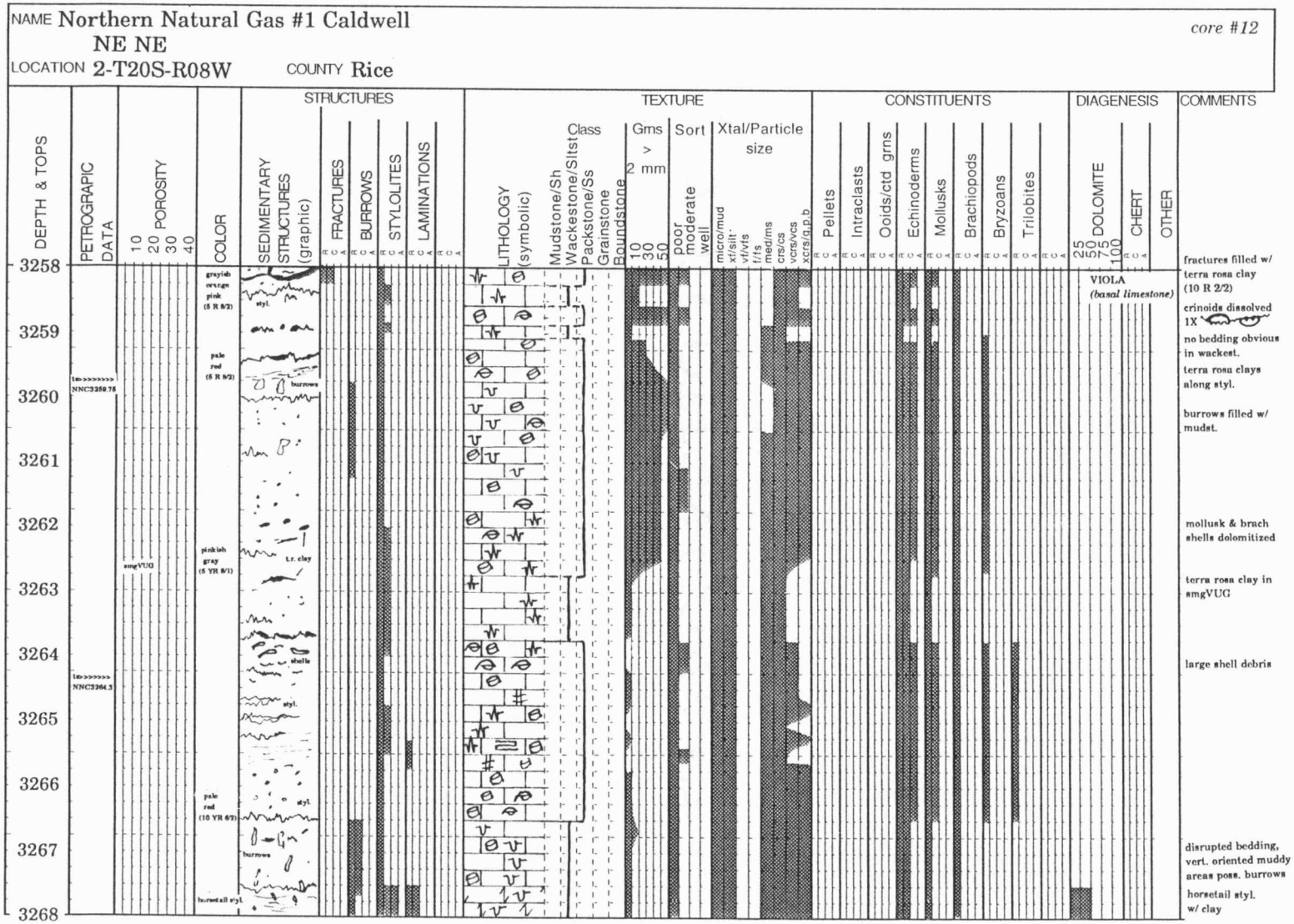
NAME Northern Natural Gas #1 Caldwell
NE NE
LOCATION 2-T20S-R08W
COUNTY Rice
core #12
STRUCTURES
TEXTURE
CONSTITUENTS
DIAGENESIS
COMMENTS
DEPTH & TOPS
PETROGRAPHIC DATA
POROSITY
COLOR
SEDIMENTARY STRUCTURES (graphic)
FRACTURES
BURROWS
STYLOLITES
LAMINATIONS
LITHOLOGY (symbolic)
Class
Mudstone/Sh
Wackestone/Sltst
Packstone/Ss
Grainstone
Boundstone
Grns > 2 mm
Sort
poor
moderate
well
Xtal/Particle size
micro/mud
xf/silt
vf/vfs
f/fs
med/ms
crs/cs
vcrs/vcs
xcrs/g,p,b
Pellets
Intraclasts
Ooids/ctd grns
Echinoderms
Mollusks
Brachiopods
Bryzoans
Trilobites
DOLOMITE
CHERT
OTHER
3258
3259
3260
3261
3262
3263
3264
3265
3266
3267
3268
VIOLA
(basal limestone)
fractures filled w/ terra rosa clay (10 R 2/2)
crinoids dissolved 1X
no bedding obvious in wackest. terra rosa clays along styl.
burrows filled w/ mudst.
mollusk & brach shells dolomitized
terra rosa clay in smgVUG
large shell debris
disrupted bedding, vert. oriented muddy areas poss. burrows
horsetail styl. w/ clay

NAME **Northern Natural Gas #1 Caldwell (continued)**

NE NE

LOCATION **2-T20S-R08W** COUNTY **Rice**

core #12

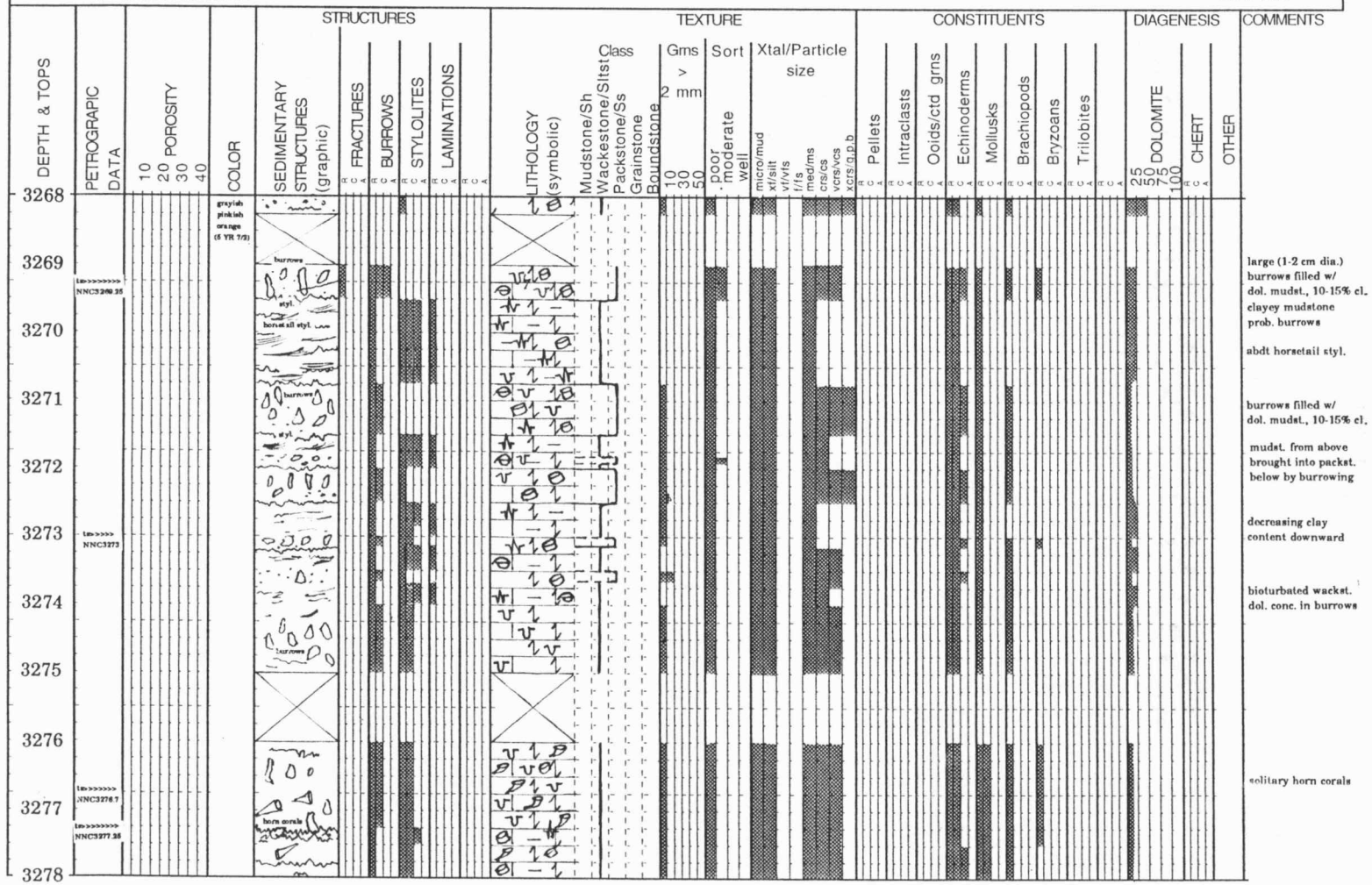

NAME **Northern Natural Gas #1 Caldwell (continued)**

NE NE

LOCATION **2-T20S-R08W** COUNTY **Rice**

core #12

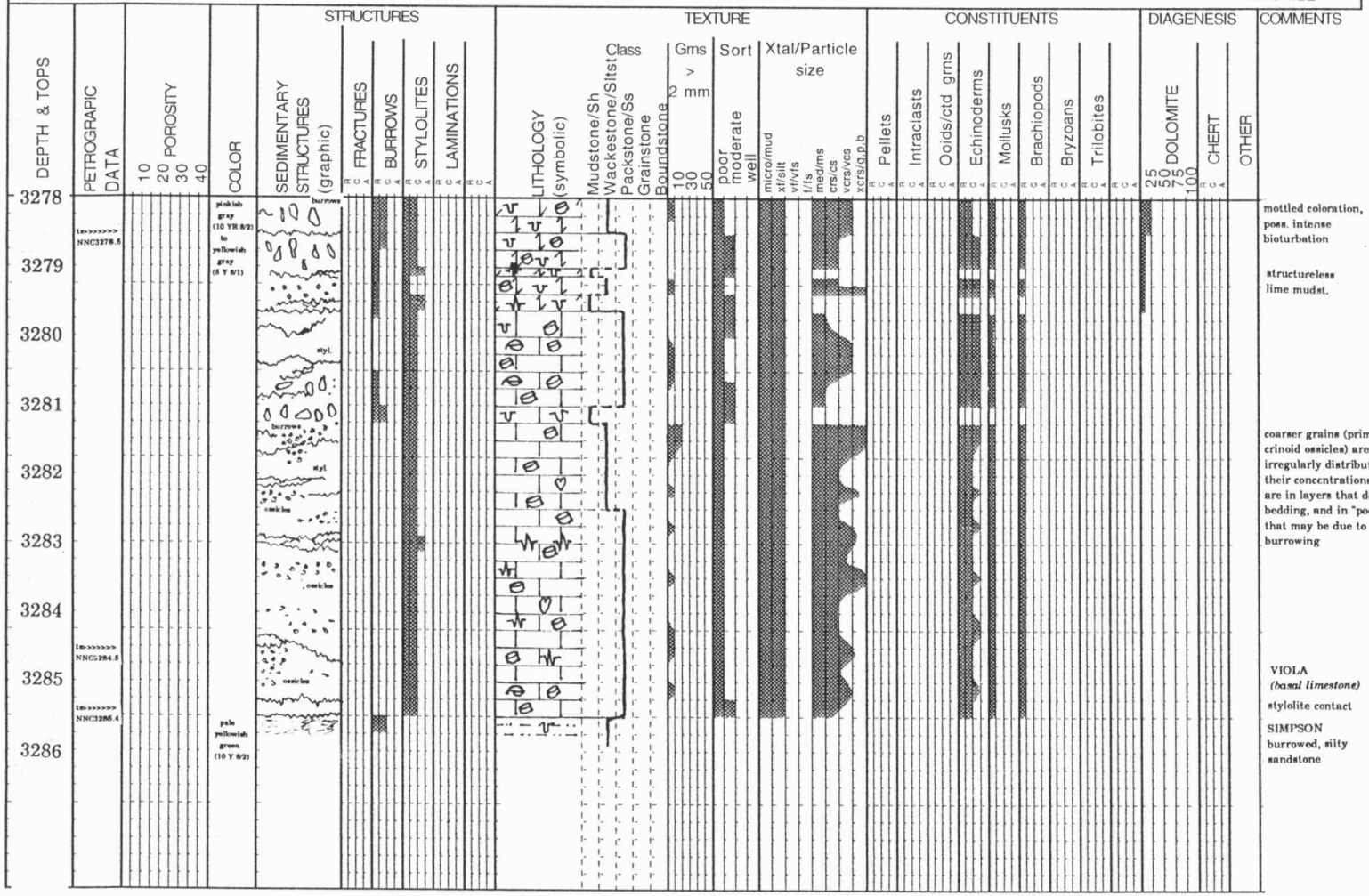

mottled coloration, poss. intense bioturbation

structureless lime mudst.

coarser grains (primarily crinoid ossicles) are irregularly distributed, their concentrations are in layers that define bedding, and in "pods" that may be due to burrowing

VIOLA
(basal limestone)

stylolite contact

SIMPSON
burrowed, silty sandstone

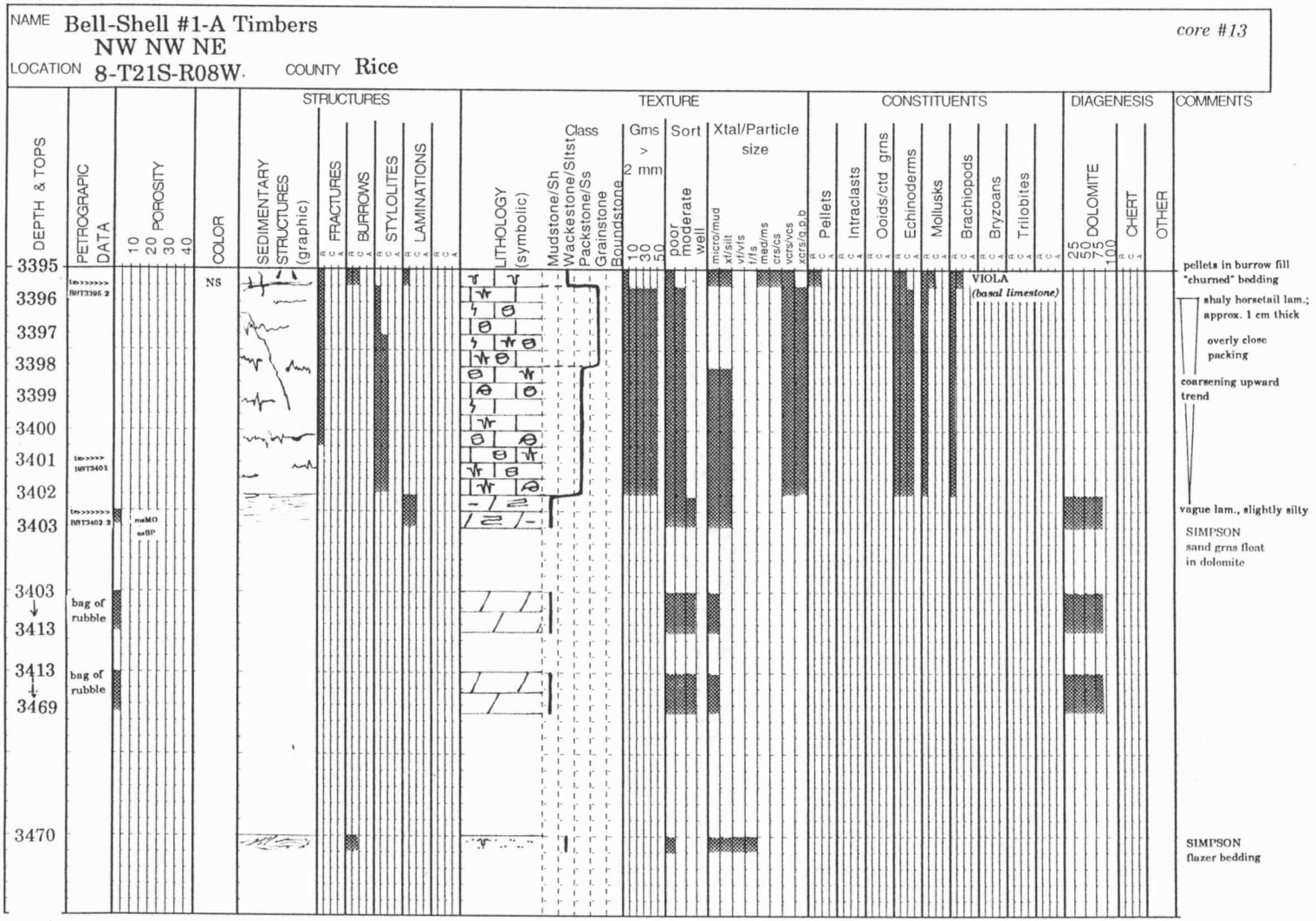
NAME Bell-Shell #1-A Timbers
NW NW NE
LOCATION 8-T21S-R08W. COUNTY Rice
core #13
STRUCTURES
TEXTURE
CONSTITUENTS
DIAGENESIS
COMMENTS
DEPTH & TOPS
PETROGRAPHIC DATA
POROSITY
COLOR
SEDIMENTARY STRUCTURES (graphic)
FRACTURES
BURROWS
STYLOLITES
LAMINATIONS
LITHOLOGY (symbolic)
Class
Mudstone/Sh
Wackestone/Sltst
Packstone/Ss
Grainstone
Boundstone
Gms > 2 mm
Sort
poor
moderate
well
Xtal/Particle size
micro/mud
xf/silt
vf/vfs
f/fs
med/ms
crs/cs
vcrs/vcs
xcrs/g.p.b
Pellets
Intraclasts
Ooids/ctd grns
Echinoderms
Mollusks
Brachiopods
Bryzoans
Trilobites
DOLOMITE
CHERT
OTHER
3395
3396
3397
3398
3399
3400
3401
3402
3403
3403
3413
3413
3469
3470
NS
naMO
naBP
bag of rubble
bag of rubble
VIOLA
(basal limestone)
pellets in burrow fill "churned" bedding
shaly horsetail lam.; approx. 1 cm thick
overly close packing
coarsening upward trend
vague lam., slightly silty
SIMPSON
sand grns float in dolomite
SIMPSON
flazer bedding

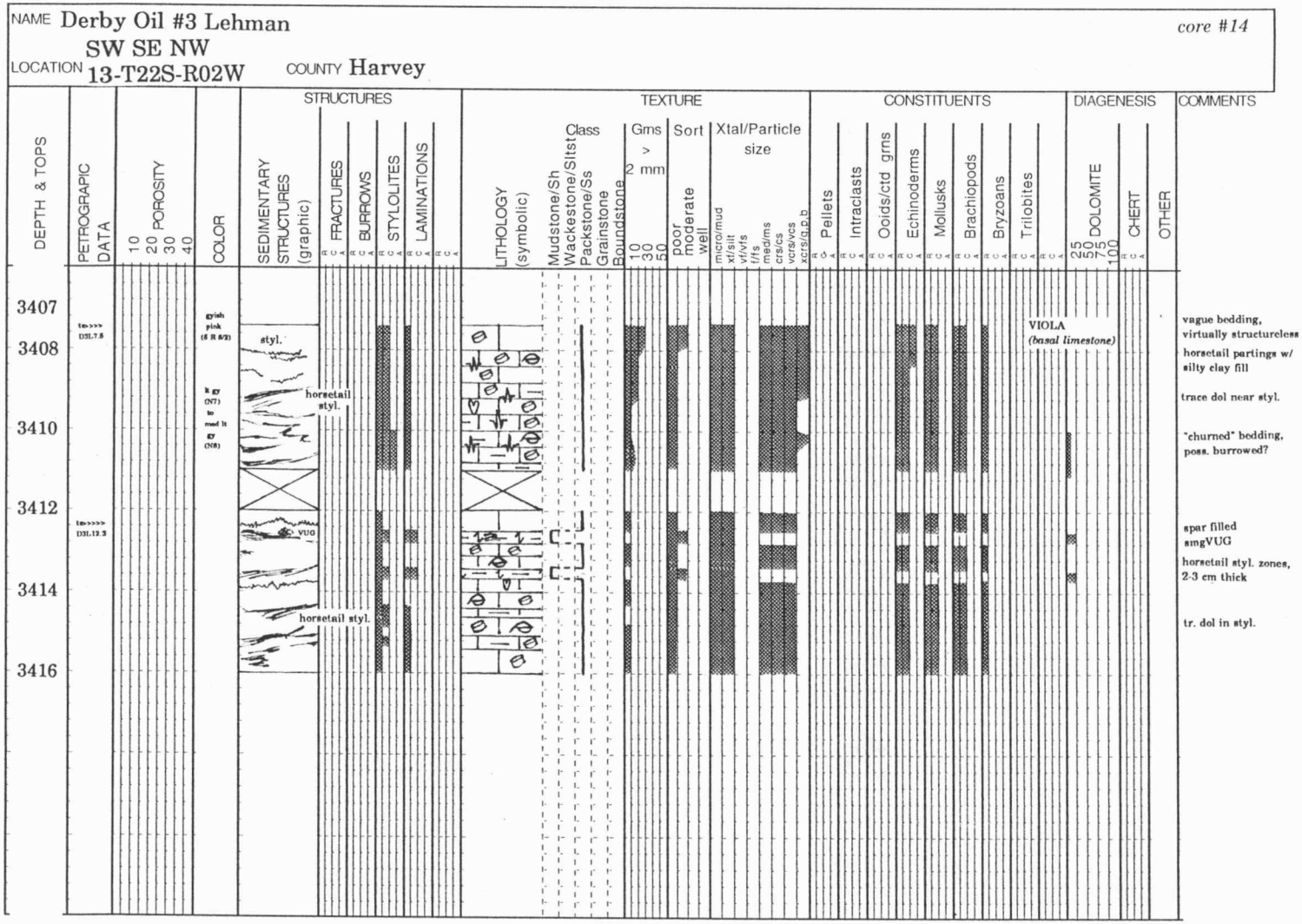
NAME Derby Oil #3 Lehman
SW SE NW
LOCATION 13-T22S-R02W
COUNTY Harvey
core #14
DEPTH & TOPS
PETROGRAPHIC DATA
POROSITY
COLOR
STRUCTURES
SEDIMENTARY STRUCTURES (graphic)
FRACTURES
BURROWS
STYLOLITES
LAMINATIONS
TEXTURE
LITHOLOGY (symbolic)
Mudstone/Sh
Wackestone/Sltst
Packstone/Ss
Grainstone
Boundstone
Class
Gms > 2 mm
Sort
Xtal/Particle size
CONSTITUENTS
Pellets
Intraclasts
Ooids/ctd grns
Echinoderms
Mollusks
Brachiopods
Bryzoans
Trilobites
DIAGENESIS
DOLOMITE
CHERT
OTHER
COMMENTS
3407
3408
3410
3412
3414
3416
styl.
horsetail styl.
VUG
horsetail styl.
VIOLA
(basal limestone)
vague bedding, virtually structureless
horsetail partings w/ silty clay fill
trace dol near styl.
"churned" bedding, poss. burrowed?
spar filled smgVUG
horsetail styl. zones, 2-3 cm thick
tr. dol in styl.

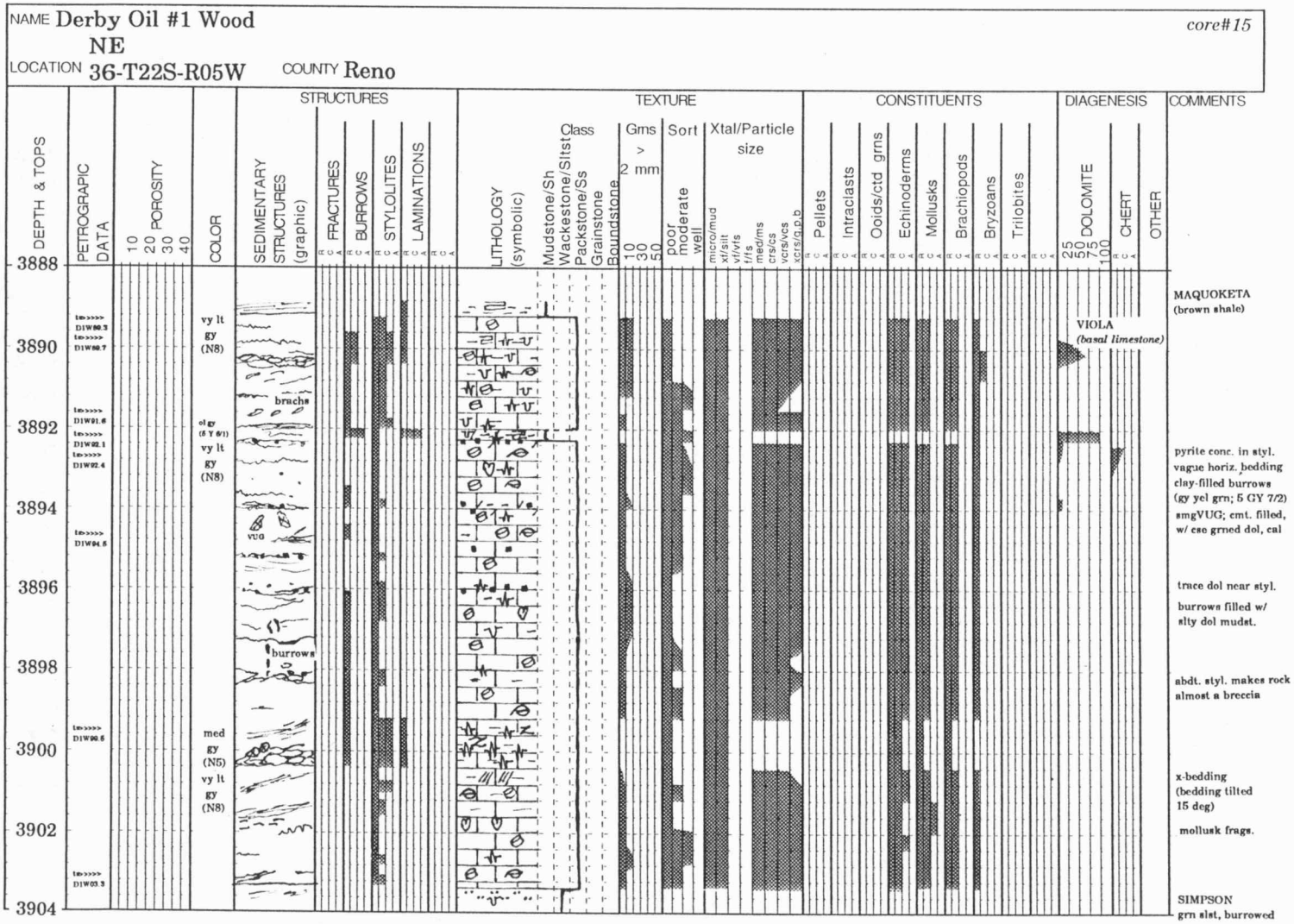
NAME Derby Oil #1 Wood
NE
LOCATION 36-T22S-R05W
COUNTY Reno
core#15
STRUCTURES
TEXTURE
CONSTITUENTS
DIAGENESIS
COMMENTS
DEPTH & TOPS
PETROGRAPHIC DATA
POROSITY
COLOR
SEDIMENTARY STRUCTURES (graphic)
FRACTURES
BURROWS
STYLOLITES
LAMINATIONS
LITHOLOGY (symbolic)
Class
Mudstone/Sh
Wackestone/Sltst
Packstone/Ss
Grainstone
Boundstone
Gms > 2 mm
Sort
poor
moderate
well
Xtal/Particle size
micro/mud
xf/silt
vf/fs
med/ms
crs/cs
vcrs/vcs
vcrs/g,p,b
Pellets
Intraclasts
Ooids/ctd grns
Echinoderms
Mollusks
Brachiopods
Bryzoans
Trilobites
DOLOMITE
CHERT
OTHER
3888
3890
3892
3894
3896
3898
3900
3902
3904
vy lt gy (N8)
brachs
ol gy (5 Y 6/1)
vy lt gy (N8)
VUG
burrows
med gy (N5)
vy lt gy (N8)
VIOLA
(basal limestone)
MAQUOKETA
(brown shale)
pyrite conc. in styl.
vague horiz. bedding
clay-filled burrows
(gy yel grn; 5 GY 7/2)
smgVUG; cmt. filled,
w/ cse grned dol, cal
trace dol near styl.
burrows filled w/
slty dol mudst.
abdt. styl. makes rock
almost a breccia
x-bedding
(bedding tilted
15 deg)
mollusk frags.
SIMPSON
grn slst, burrowed

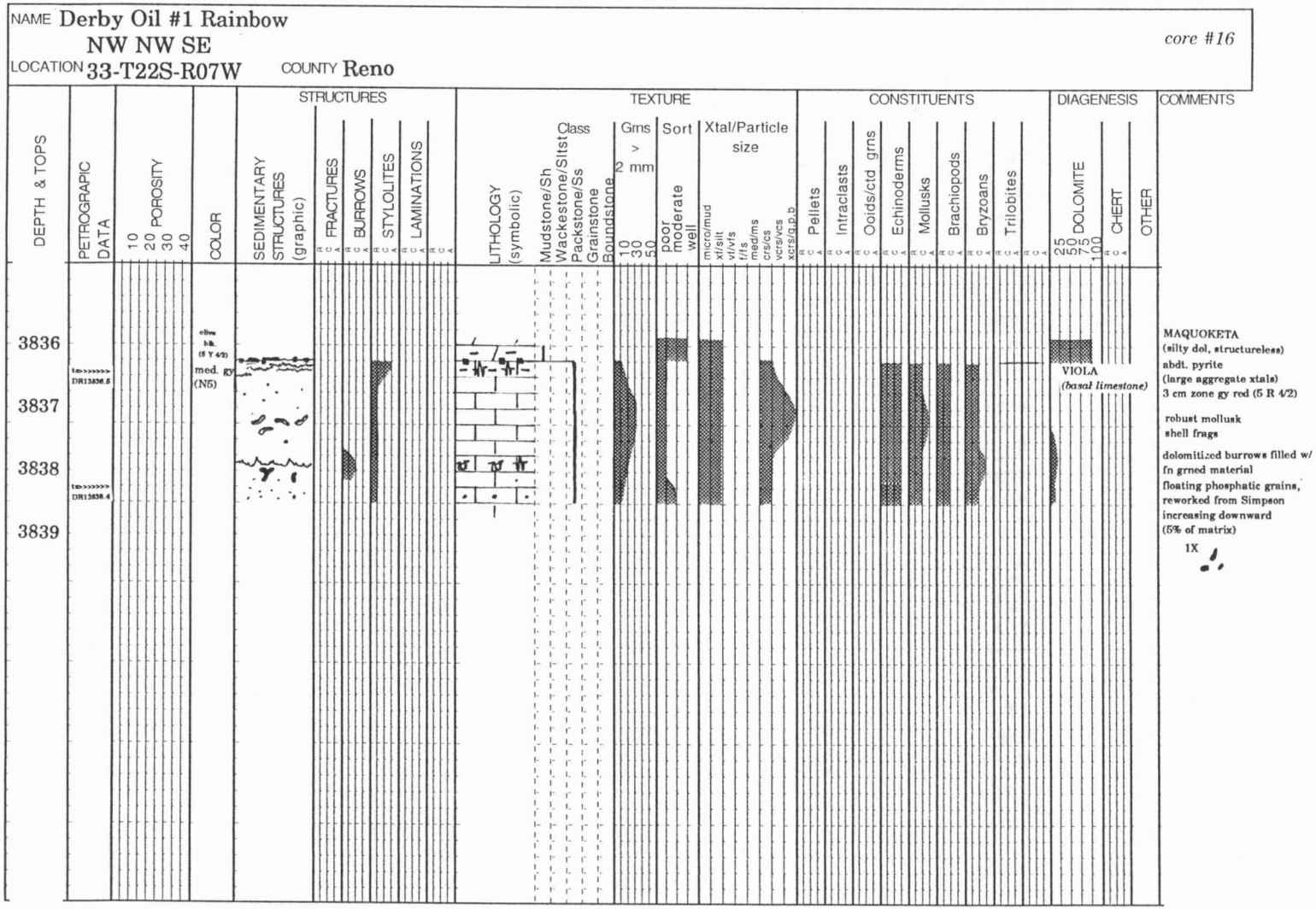
NAME Derby Oil #1 Rainbow
NW NW SE
LOCATION 33-T22S-R07W
COUNTY Reno
core #16
DEPTH & TOPS
PETROGRAPIC DATA
10 20 POROSITY 30 40
COLOR
STRUCTURES
SEDIMENTARY STRUCTURES (graphic)
FRACTURES
BURROWS
STYLOLITES
LAMINATIONS
TEXTURE
LITHOLOGY (symbolic)
Class
Mudstone/Sh
Wackestone/Sltst
Packstone/Ss
Grainstone
Boundstone
Grns > 2 mm
10 30 50
Sort
poor moderate well
Xtal/Particle size
micro/mud
xf/slt
vf/vfs
f/fs
med/ms
crs/cs
vcrs/vcs
xcrs/gp,b
CONSTITUENTS
Pellets
Intraclasts
Ooids/ctd grns
Echinoderms
Mollusks
Brachiopods
Bryzoans
Trilobites
DIAGENESIS
25 50 75 100 DOLOMITE
CHERT
OTHER
COMMENTS
3836
3837
3838
3839
olive blk. (5 Y 4/2)
med. gy (N5)
DR13838.5
DR13838.4
VIOLA
(basal limestone)
MAQUOKETA
(silty dol, structureless)
abdt. pyrite
(large aggregate xtals)
3 cm zone gy red (5 R 4/2)
robust mollusk
shell frags
dolomitized burrows filled w/
fn grned material
floating phosphatic grains,
reworked from Simpson
increasing downward
(5% of matrix)
1X

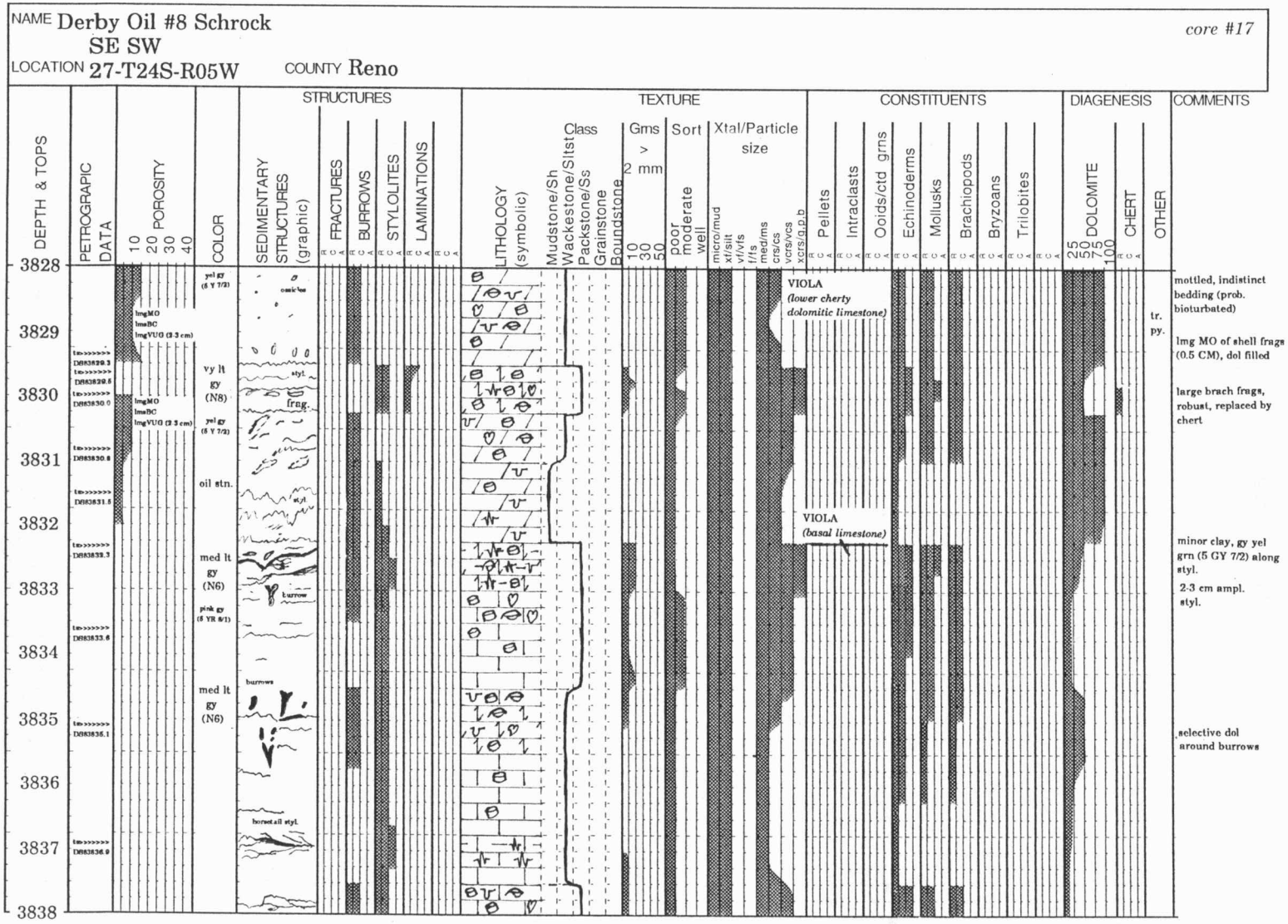
NAME Derby Oil #8 Schrock
SE SW
LOCATION 27-T24S-R05W
COUNTY Reno
core #17
STRUCTURES
TEXTURE
CONSTITUENTS
DIAGENESIS
COMMENTS
DEPTH & TOPS
PETROGRAPHIC DATA
POROSITY
COLOR
SEDIMENTARY STRUCTURES (graphic)
FRACTURES
BURROWS
STYLOLITES
LAMINATIONS
LITHOLOGY (symbolic)
Class
Mudstone/Sh
Wackestone/Sltst
Packstone/Ss
Grainstone
Boundstone
Gms > 2 mm
Sort
poor
moderate
well
Xtal/Particle size
micro/mud
xf/silt
vf/vfs
f/fs
med/ms
crs/cs
vcrs/vcs
xcrs/g,p,b
Pellets
Intraclasts
Ooids/ctd grns
Echinoderms
Mollusks
Brachiopods
Bryzoans
Trilobites
DOLOMITE
CHERT
OTHER
3828
3829
3830
3831
3832
3833
3834
3835
3836
3837
3838
VIOLA
(lower cherty dolomitic limestone)
VIOLA
(basal limestone)
mottled, indistinct bedding (prob. bioturbated)
tr. py.
lmg MO of shell frags (0.5 CM), dol filled
large brach frags, robust, replaced by chert
minor clay, gy yel grn (5 GY 7/2) along styl.
2-3 cm ampl. styl.
selective dol around burrows

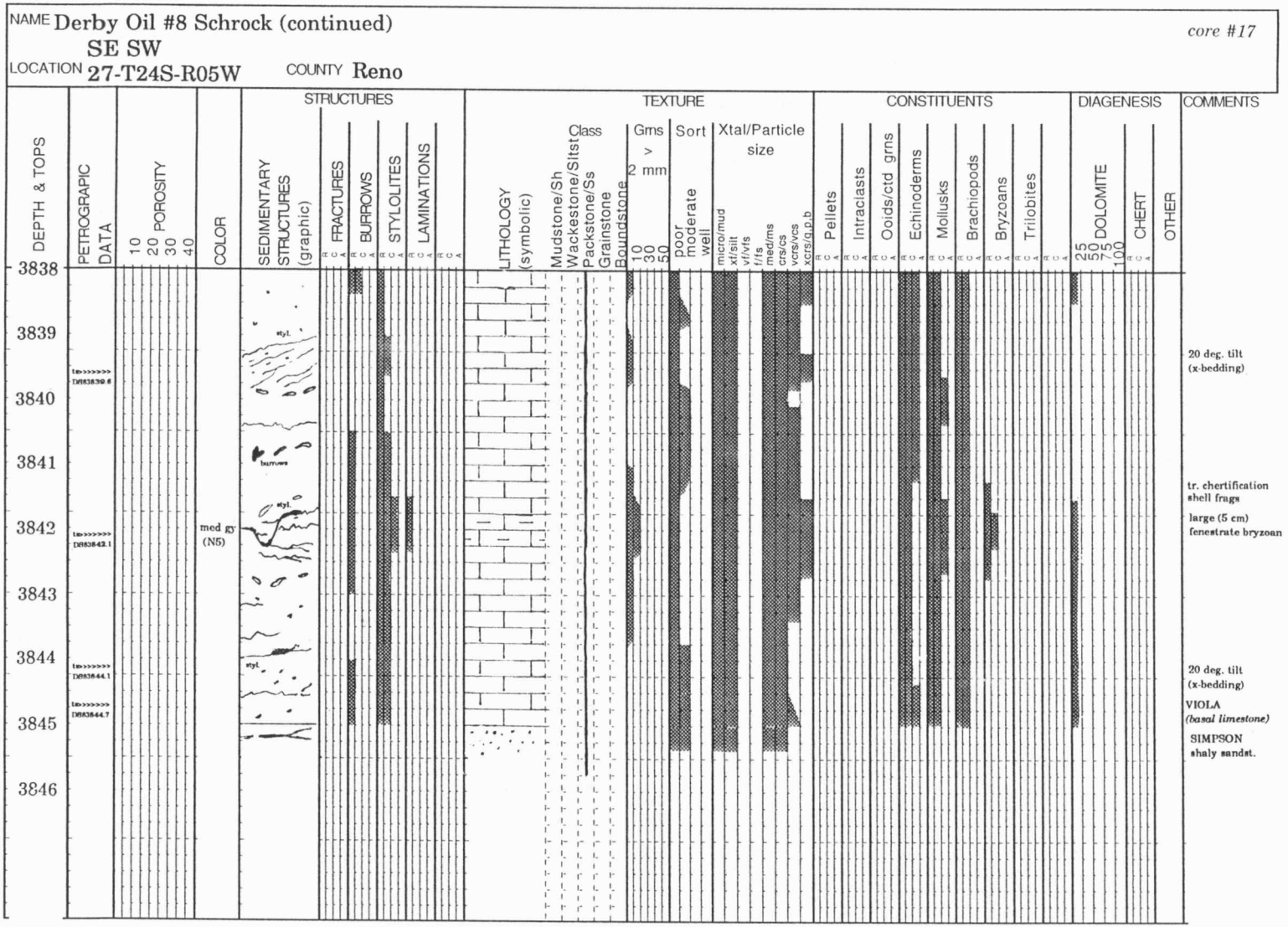
NAME Derby Oil #8 Schrock (continued)
SE SW
LOCATION 27-T24S-R05W
COUNTY Reno
core #17
DEPTH & TOPS
PETROGRAPHIC DATA
POROSITY
COLOR
STRUCTURES
SEDIMENTARY STRUCTURES (graphic)
FRACTURES
BURROWS
STYLOLITES
LAMINATIONS
TEXTURE
LITHOLOGY (symbolic)
Class
Mudstone/Sh
Wackestone/Sltst
Packstone/Ss
Grainstone
Boundstone
Gms > 2 mm
Sort
poor
moderate
well
Xtal/Particle size
micro/mud
xf/silt
vf/vfs
f/fs
med/ms
crs/cs
vcrs/vcs
xcrs/g.p.b
CONSTITUENTS
Pellets
Intraclasts
Ooids/ctd grns
Echinoderms
Mollusks
Brachiopods
Bryzoans
Trilobites
DIAGENESIS
DOLOMITE
CHERT
OTHER
COMMENTS
3838
3839
3840
3841
3842
3843
3844
3845
3846
med gy (N5)
20 deg. tilt (x-bedding)
tr. chertification
shell frags
large (5 cm) fenestrate bryzoan
20 deg. tilt (x-bedding)
VIOLA
(basal limestone)
SIMPSON
shaly sandst.

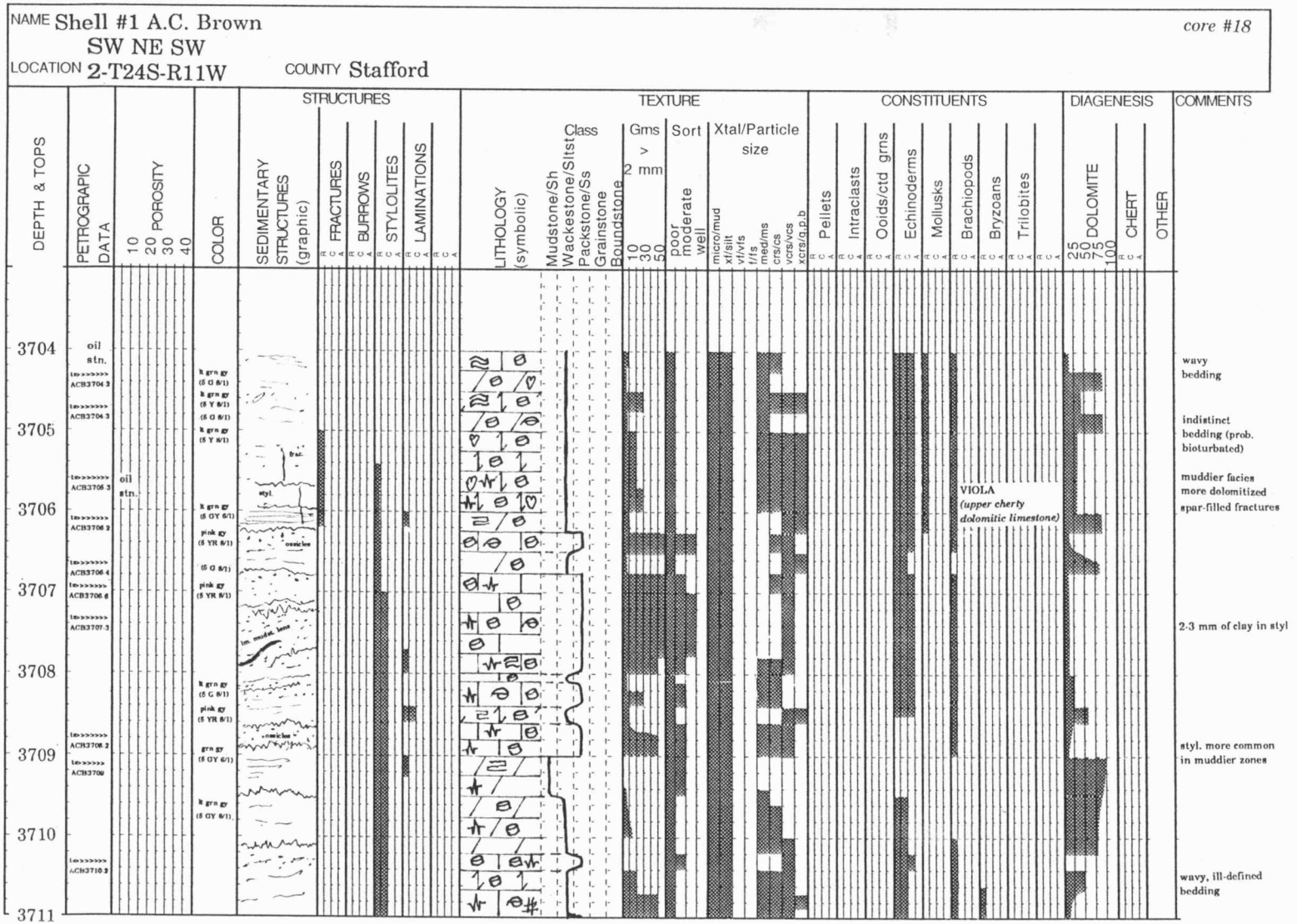
NAME Shell #1 A.C. Brown
SW NE SW
LOCATION 2-T24S-R11W
COUNTY Stafford
core #18
DEPTH & TOPS
PETROGRAPHIC DATA
POROSITY
COLOR
STRUCTURES
SEDIMENTARY STRUCTURES (graphic)
FRACTURES
BURROWS
STYLOLITES
LAMINATIONS
TEXTURE
LITHOLOGY (symbolic)
Mudstone/Sh
Wackestone/Sltst
Packstone/Ss
Grainstone
Boundstone
Class
Gms > 2 mm
Sort
poor
moderate
well
Xtal/Particle size
micro/mud
xf/silt
vf/vfs
f/fs
med/ms
crs/cs
vcrs/vcs
xcrs/g,p,b
CONSTITUENTS
Pellets
Intraclasts
Ooids/ctd grns
Echinoderms
Mollusks
Brachiopods
Bryzoans
Trilobites
DIAGENESIS
DOLOMITE
CHERT
OTHER
COMMENTS
3704
3705
3706
3707
3708
3709
3710
3711
oil stn.
VIOLA
(upper cherty dolomitic limestone)
styl.
bioturb.
ostracles
wavy bedding
indistinct bedding (prob. bioturbated)
muddier facies more dolomitized spar-filled fractures
2-3 mm of clay in styl
styl. more common in muddier zones
wavy, ill-defined bedding

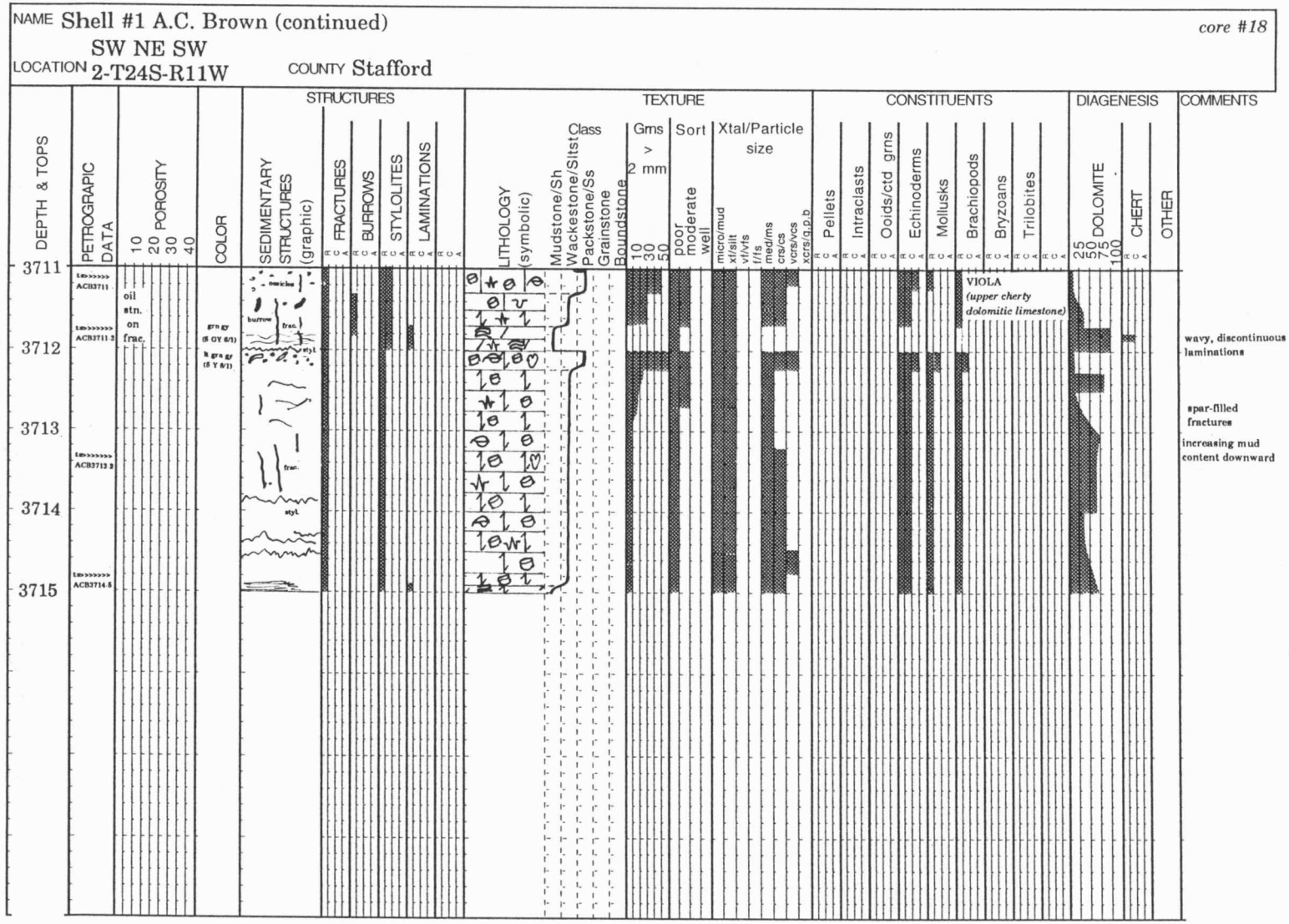
NAME Shell #1 A.C. Brown (continued)
core #18
SW NE SW
LOCATION 2-T24S-R11W
COUNTY Stafford
STRUCTURES
TEXTURE
CONSTITUENTS
DIAGENESIS
COMMENTS
DEPTH & TOPS
PETROGRAPHIC DATA
POROSITY
COLOR
SEDIMENTARY STRUCTURES (graphic)
FRACTURES
BURROWS
STYLOLITES
LAMINATIONS
LITHOLOGY (symbolic)
Class
Mudstone/Sh
Wackestone/Siltst.
Packstone/Ss
Grainstone
Boundstone
Grns > 2 mm
Sort
poor
moderate
well
Xtal/Particle size
micro/mud
xf/silt
vf/vfs
f/fs
med/ms
crs/cs
vcrs/vcs
xcrs/g.p.b
Pellets
Intraclasts
Ooids/ctd grns
Echinoderms
Mollusks
Brachiopods
Bryzoans
Trilobites
DOLOMITE
CHERT
OTHER
3711
3712
3713
3714
3715
oil stn. on frac.
VIOLA
(upper cherty dolomitic limestone)
wavy, discontinuous laminations
spar-filled fractures
increasing mud content downward

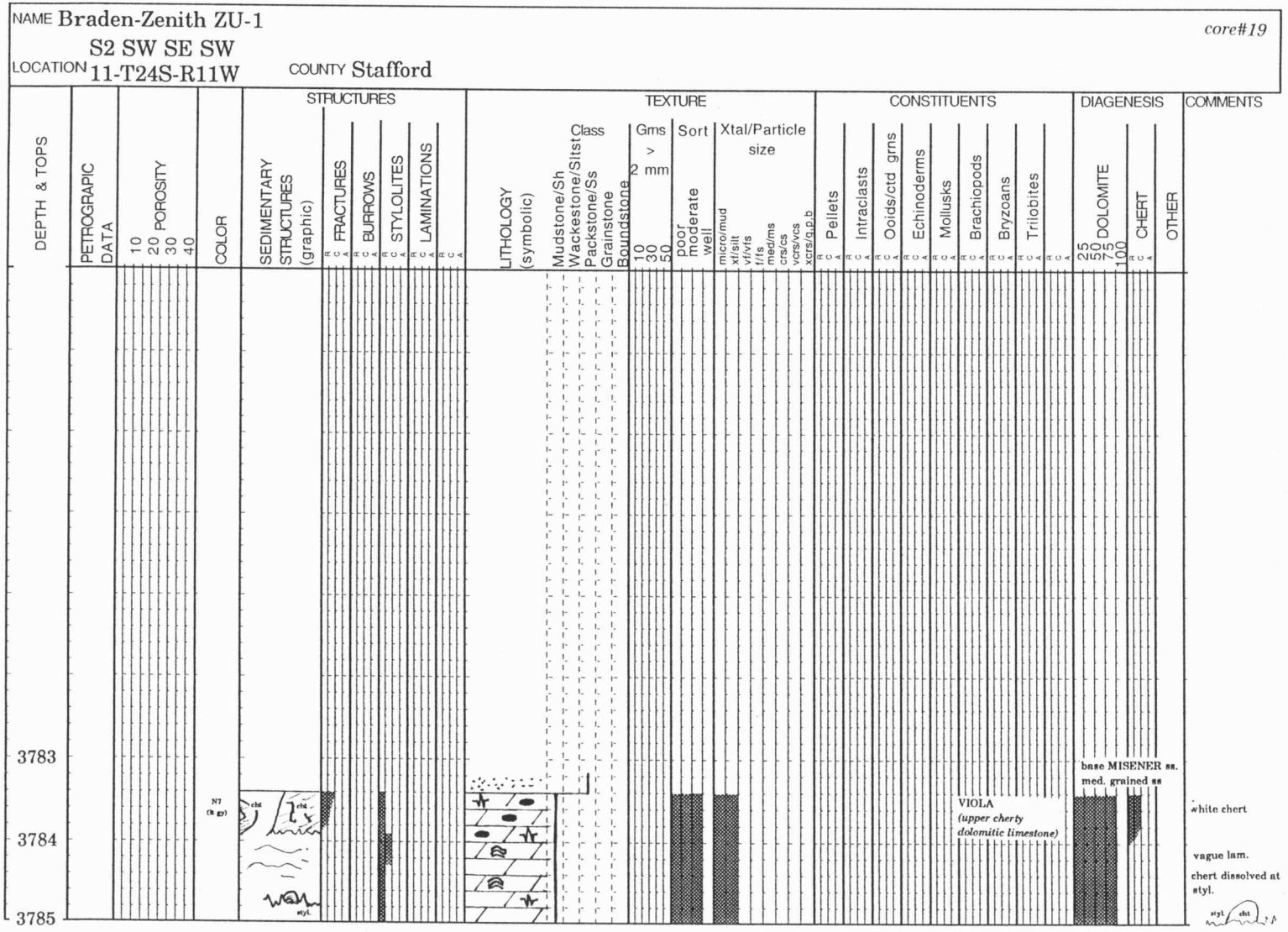
NAME Braden-Zenith ZU-1
S2 SW SE SW
LOCATION 11-T24S-R11W
COUNTY Stafford
core#19
DEPTH & TOPS
PETROGRAPIC DATA
10 20 POROSITY 30 40
COLOR
STRUCTURES
SEDIMENTARY STRUCTURES (graphic)
FRACTURES
BURROWS
STYLOLITES
LAMINATIONS
TEXTURE
LITHOLOGY (symbolic)
Class
Mudstone/Sh
Wackestone/Sltst
Packstone/Ss
Grainstone
Boundstone
Grns > 2 mm
10 30 50
Sort
poor moderate well
Xtal/Particle size
micro/mud
xf/silt
vf/vfs
f/fs
med/ms
crs/cs
vcrs/vcs
xcrs/g.p.b
CONSTITUENTS
Pellets
Intraclasts
Ooids/ctd grns
Echinoderms
Mollusks
Brachiopods
Bryzoans
Trilobites
DIAGENESIS
25 50 75 100
DOLOMITE
CHERT
OTHER
COMMENTS
3783
3784
3785
N7 (lt gy)
chd
styl.
base MISENER ss.
med. grained ss
VIOLA
(upper cherty dolomitic limestone)
white chert
vague lam.
chert dissolved at styl.
styl
cht

NAME Braden-Zenith ZU-1 (continued) *core #19*

LOCATION S2 SW SE SW 11-T24S-R11W COUNTY Stafford

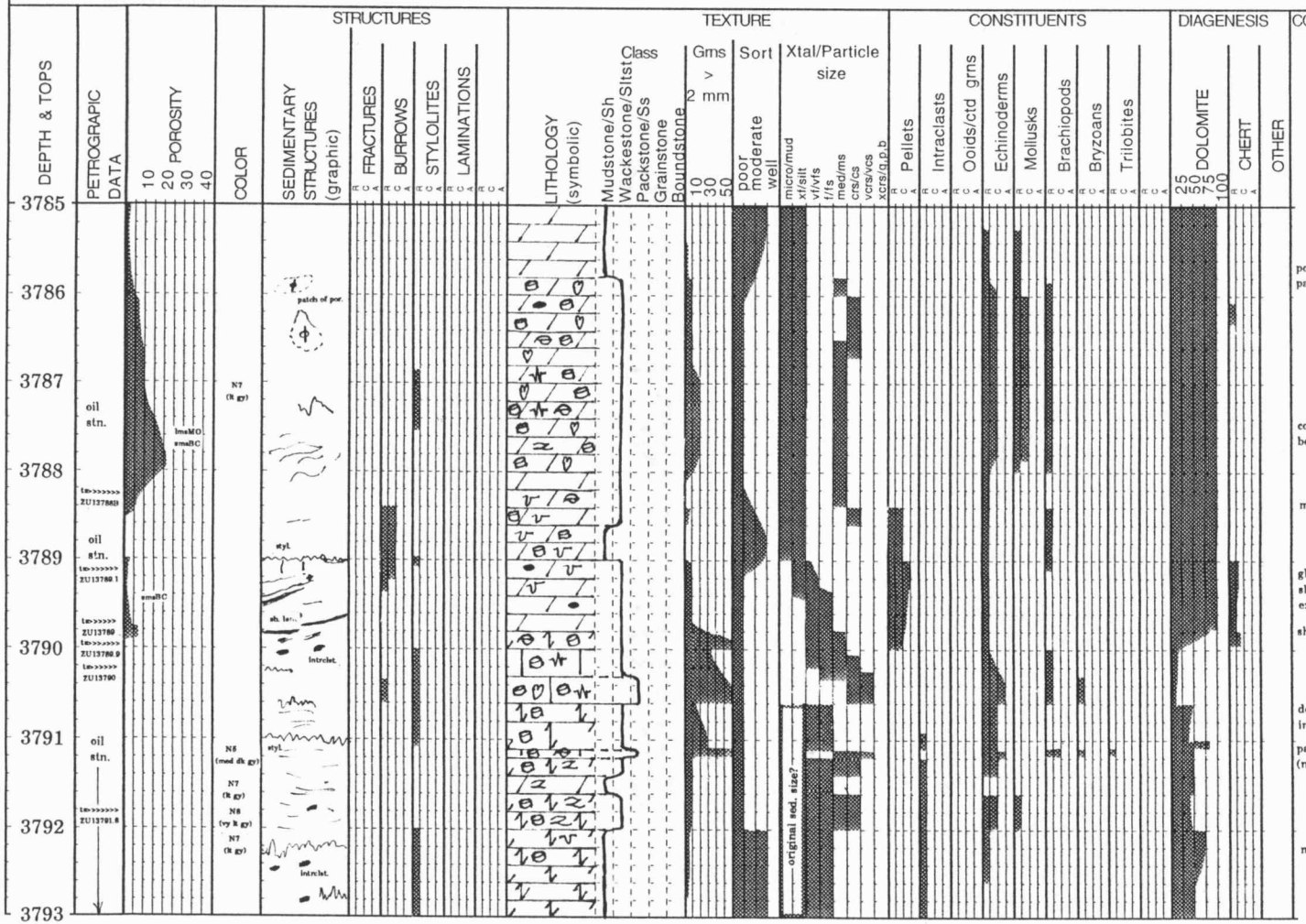

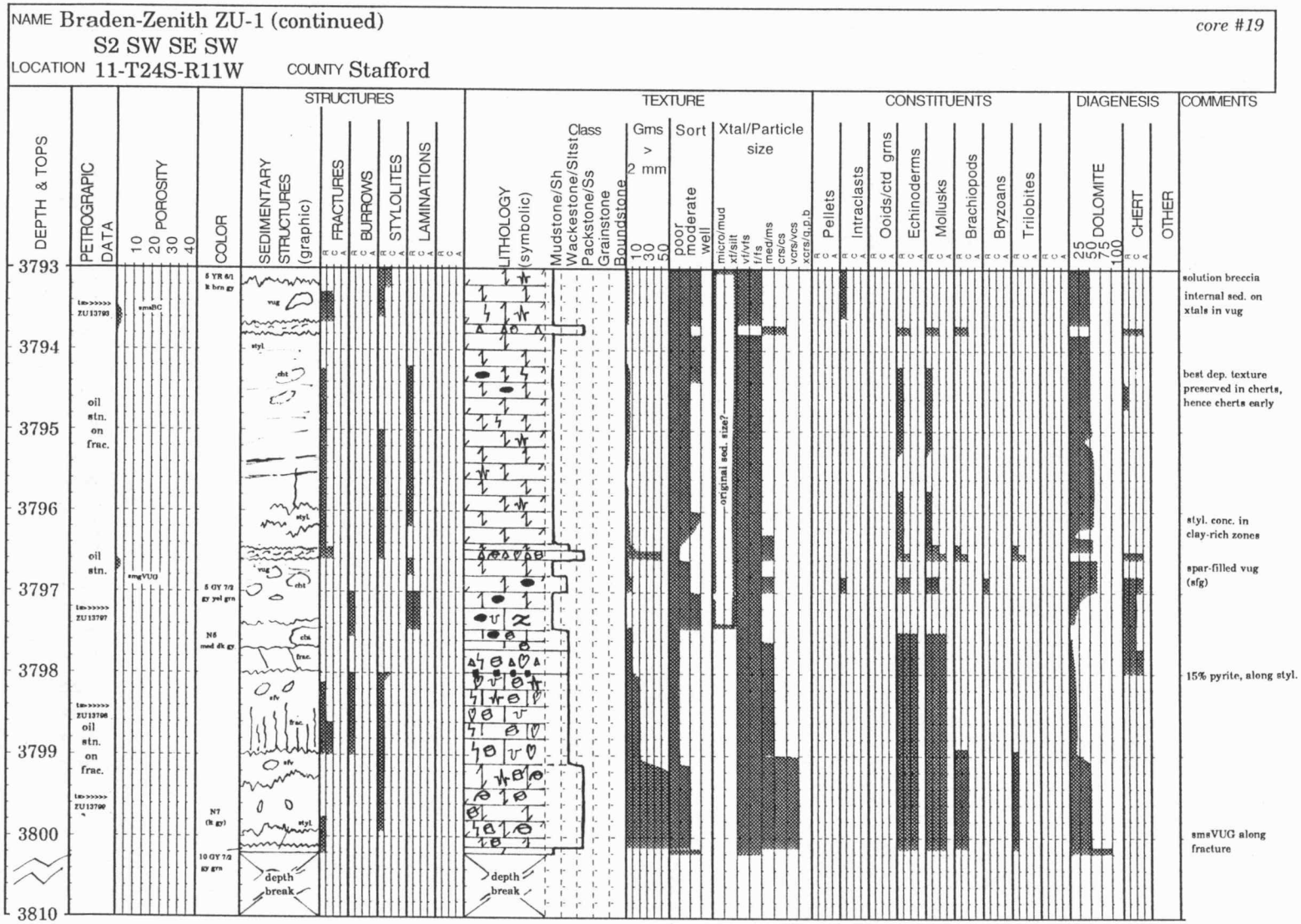
NAME Braden-Zenith ZU-1 (continued)
S2 SW SE SW
LOCATION 11-T24S-R11W
COUNTY Stafford
core #19
STRUCTURES
TEXTURE
CONSTITUENTS
DIAGENESIS
COMMENTS
DEPTH & TOPS
PETROGRAPHIC DATA
POROSITY
COLOR
SEDIMENTARY STRUCTURES (graphic)
FRACTURES
BURROWS
STYLOLITES
LAMINATIONS
LITHOLOGY (symbolic)
Class
Mudstone/Sh
Wackestone/Slt
Packstone/Ss
Grainstone
Boundstone
Gms > 2 mm
Sort
poor
moderate
well
Xtal/Particle size
micro/mud
xf/silt
vf/vfs
f/fs
med/ms
crs/cs
vcrs/vcs
xcrs/g.p.b
Pellets
Intraclasts
Ooids/ctd grns
Echinoderms
Mollusks
Brachiopods
Bryzoans
Trilobites
DOLOMITE
CHERT
OTHER
3793
3794
3795
3796
3797
3798
3799
3800
3810
oil stn. on frac.
oil stn.
oil stn. on frac.
smsBC
smsVUG
5 YR 6/1 lt brn gy
5 GY 7/2 gy yel grn
N6 med dk gy
N7 (lt gy)
10 GY 7/2 gy grn
vug
styl
cht
frac.
sfv
depth break
original sed. size?
solution breccia
internal sed. on xtals in vug
best dep. texture preserved in cherts, hence cherts early
styl. conc. in clay-rich zones
spar-filled vug (sfg)
15% pyrite, along styl.
smsVUG along fracture

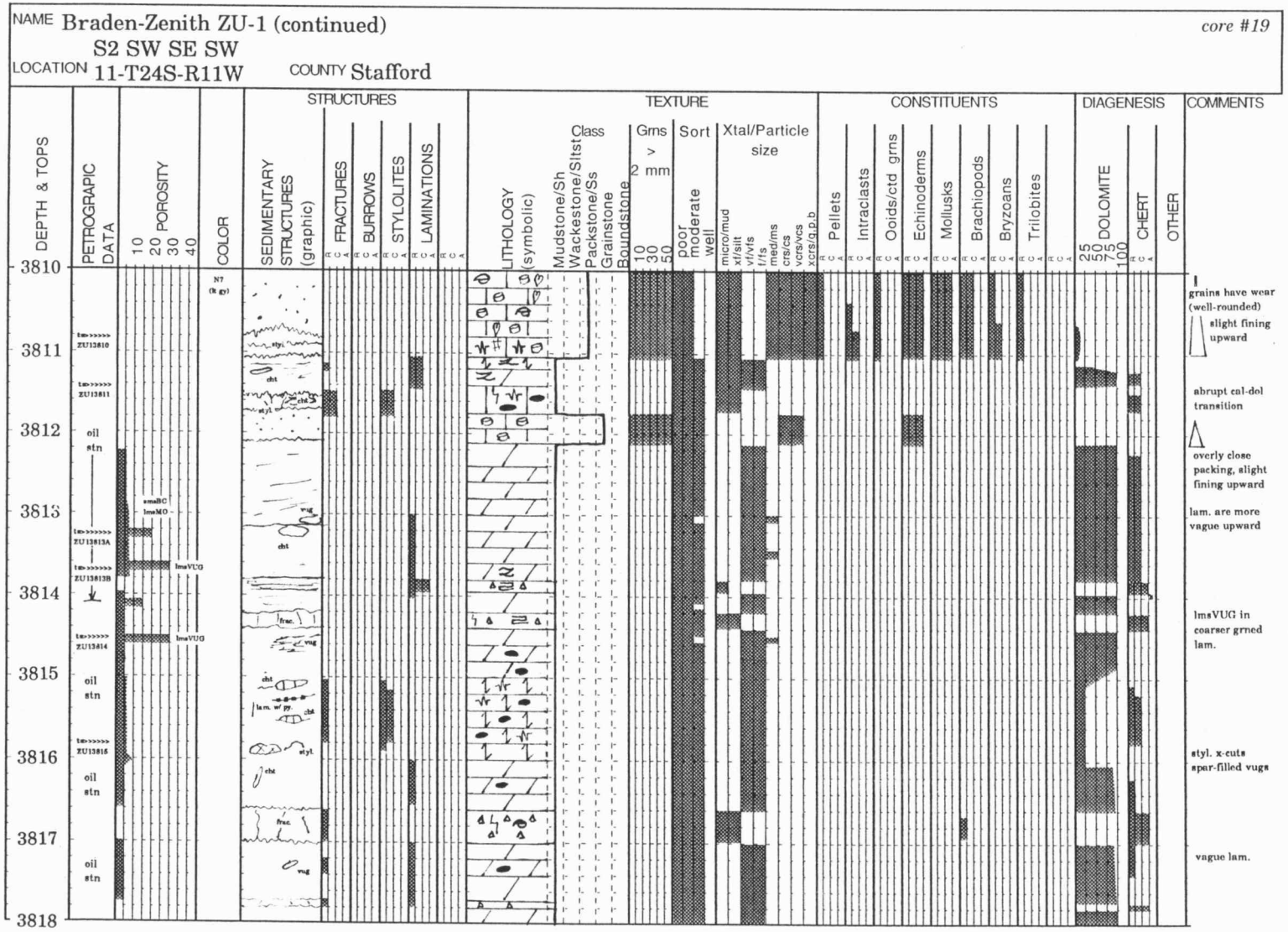
NAME Braden-Zenith ZU-1 (continued)
core #19
S2 SW SE SW
LOCATION 11-T24S-R11W
COUNTY Stafford
STRUCTURES
TEXTURE
CONSTITUENTS
DIAGENESIS
COMMENTS
DEPTH & TOPS
PETROGRAPHIC DATA
POROSITY
COLOR
SEDIMENTARY STRUCTURES (graphic)
FRACTURES
BURROWS
STYLOLITES
LAMINATIONS
LITHOLOGY (symbolic)
Mudstone/Sh
Wackestone/Sltst
Packstone/Ss
Grainstone
Boundstone
Class
Grns > 2 mm
Sort
poor
moderate
well
Xtal/Particle size
micro/mud
vf/silt
vf/vfs
f/fs
med/ms
crs/cs
vcrs/vcs
xcrs/g.p.b
Pellets
Intraclasts
Ooids/ctd grns
Echinoderms
Mollusks
Brachiopods
Bryzoans
Trilobites
DOLOMITE
CHERT
OTHER
3810
3811
3812
3813
3814
3815
3816
3817
3818
oil stn
smaBC
lmsMO
lmsVUG
ZU13810
ZU13811
ZU13813A
ZU13813B
ZU13814
ZU13815
styl.
cht
frac.
vug
lam. w/ py
grains have wear (well-rounded)
slight fining upward
abrupt cal-dol transition
overly close packing, slight fining upward
lam. are more vague upward
lmsVUG in coarser grned lam.
styl. x-cuts spar-filled vugs
vague lam.

NAME **Braden-Zenith ZU-1 (continued)** *core #19*

S2 SW SE SW

LOCATION **11-T24S-R11W** COUNTY **Stafford**

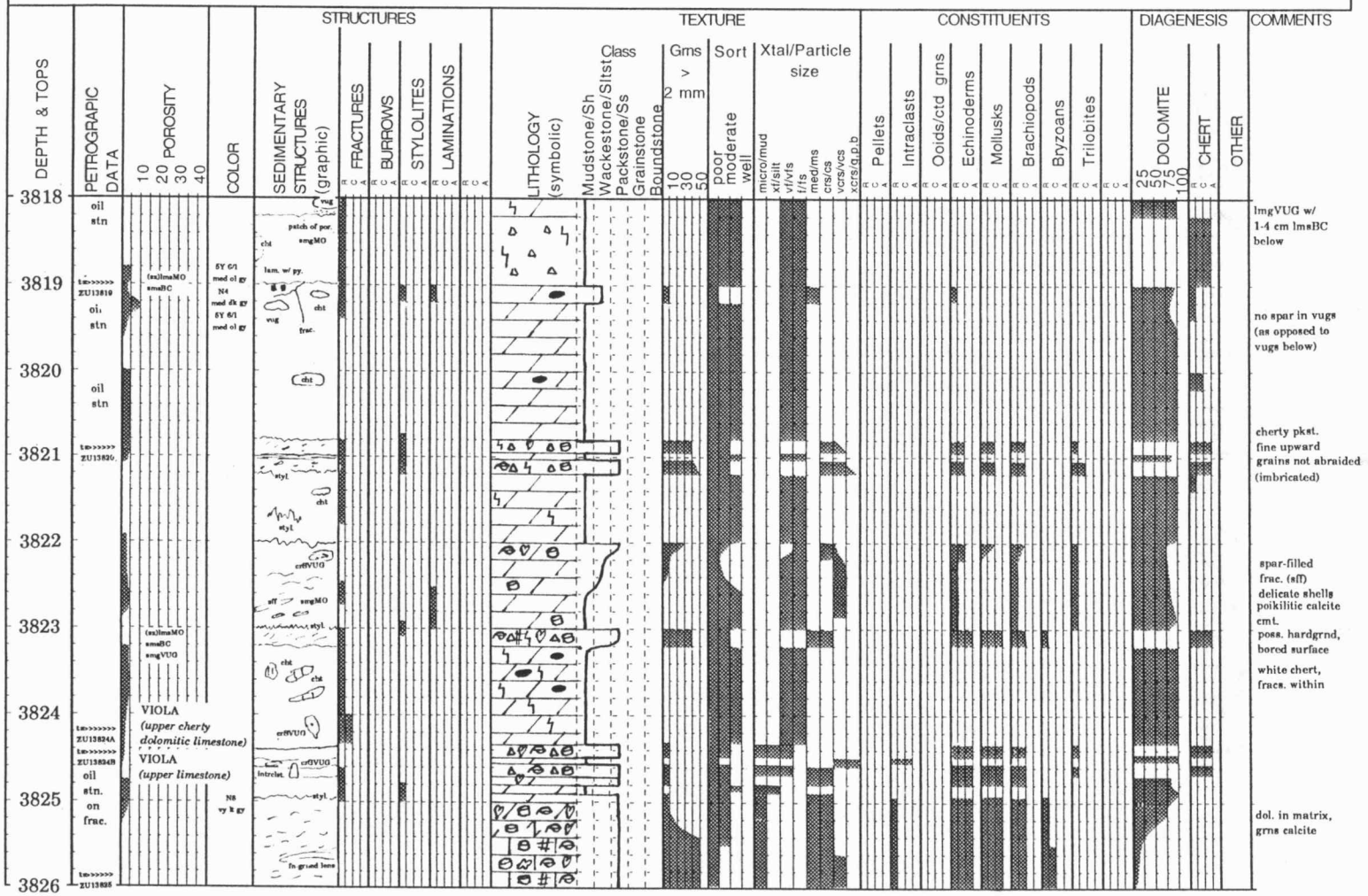

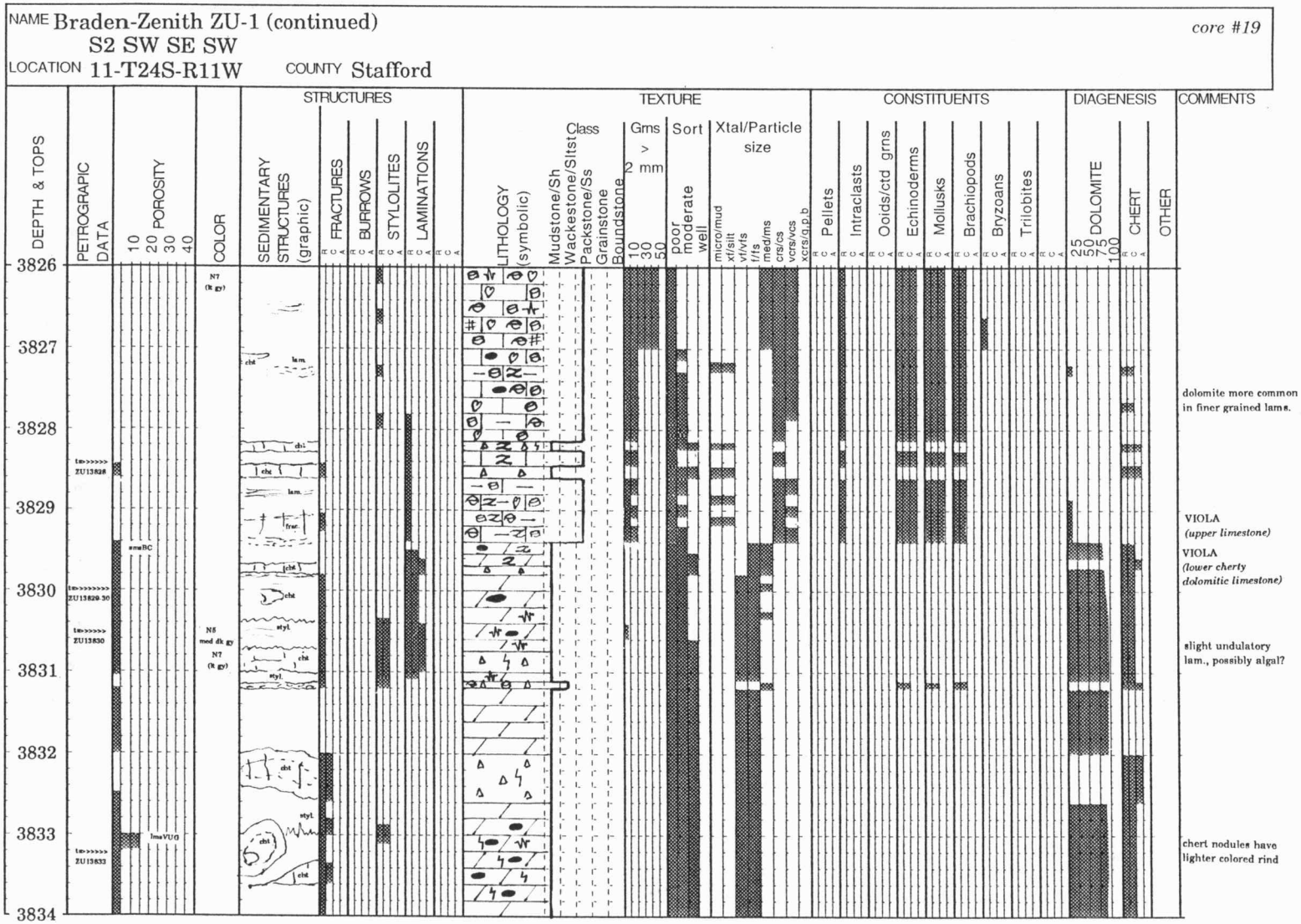
NAME Braden-Zenith ZU-1 (continued)
S2 SW SE SW
LOCATION 11-T24S-R11W
COUNTY Stafford
core #19
STRUCTURES
TEXTURE
CONSTITUENTS
DIAGENESIS
COMMENTS
DEPTH & TOPS
PETROGRAPHIC DATA
POROSITY
COLOR
SEDIMENTARY STRUCTURES (graphic)
FRACTURES
BURROWS
STYLOLITES
LAMINATIONS
LITHOLOGY (symbolic)
Class
Mudstone/Sh
Wackestone/Sltst
Packstone/Ss
Grainstone
Boundstone
Grns > 2 mm
Sort
poor
moderate
well
Xtal/Particle size
micro/mud
xf/silt
vf/vfs
f/fs
med/ms
crs/cs
vcrs/vcs
xcrs/g,p,b
Pellets
Intraclasts
Ooids/ctd grns
Echinoderms
Mollusks
Brachiopods
Bryzoans
Trilobites
DOLOMITE
CHERT
OTHER
3826
3827
3828
3829
3830
3831
3832
3833
3834
ZU13828
ZU13829-30
ZU13830
ZU13833
smsBC
lmsVUG
N7 (lt gy)
N8 med dk gy
lam.
frac.
styl.
dolomite more common in finer grained lams.
VIOLA (upper limestone)
VIOLA (lower cherty dolomitic limestone)
slight undulatory lam., possibly algal?
chert nodules have lighter colored rind

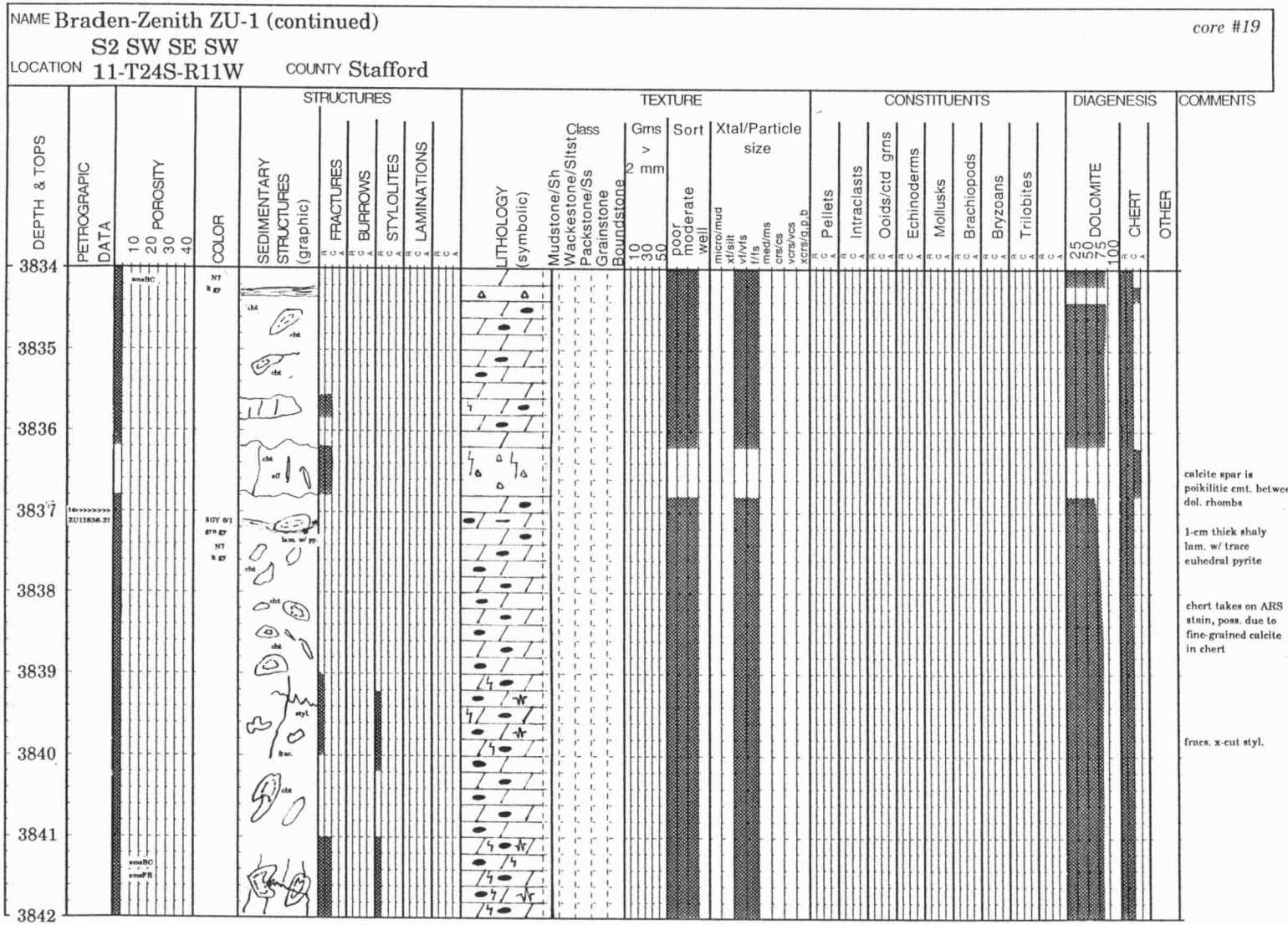
NAME Braden-Zenith ZU-1 (continued)
core #19
S2 SW SE SW
LOCATION 11-T24S-R11W
COUNTY Stafford
DEPTH & TOPS
PETROGRAPHIC DATA
POROSITY
COLOR
STRUCTURES
SEDIMENTARY STRUCTURES (graphic)
FRACTURES
BURROWS
STYLOLITES
LAMINATIONS
TEXTURE
LITHOLOGY (symbolic)
Class
Mudstone/Sh
Wackestone/Sltst
Packstone/Ss
Grainstone
Boundstone
Grns > 2 mm
Sort
poor
moderate
well
Xtal/Particle size
micro/mud
xf/silt
vf/vfs
f/fs
med/ms
crs/cs
vcrs/vcs
xcrs/g_p_b
CONSTITUENTS
Pellets
Intraclasts
Ooids/ctd grns
Echinoderms
Mollusks
Brachiopods
Bryzoans
Trilobites
DIAGENESIS
DOLOMITE
CHERT
OTHER
COMMENTS
3834
3835
3836
3837
3838
3839
3840
3841
3842
calcite spar is poikilitic cmt. between dol. rhombs
1-cm thick shaly lam. w/ trace euhedral pyrite
chert takes on ARS stain, poss. due to fine-grained calcite in chert
fracs. x-cut styl.

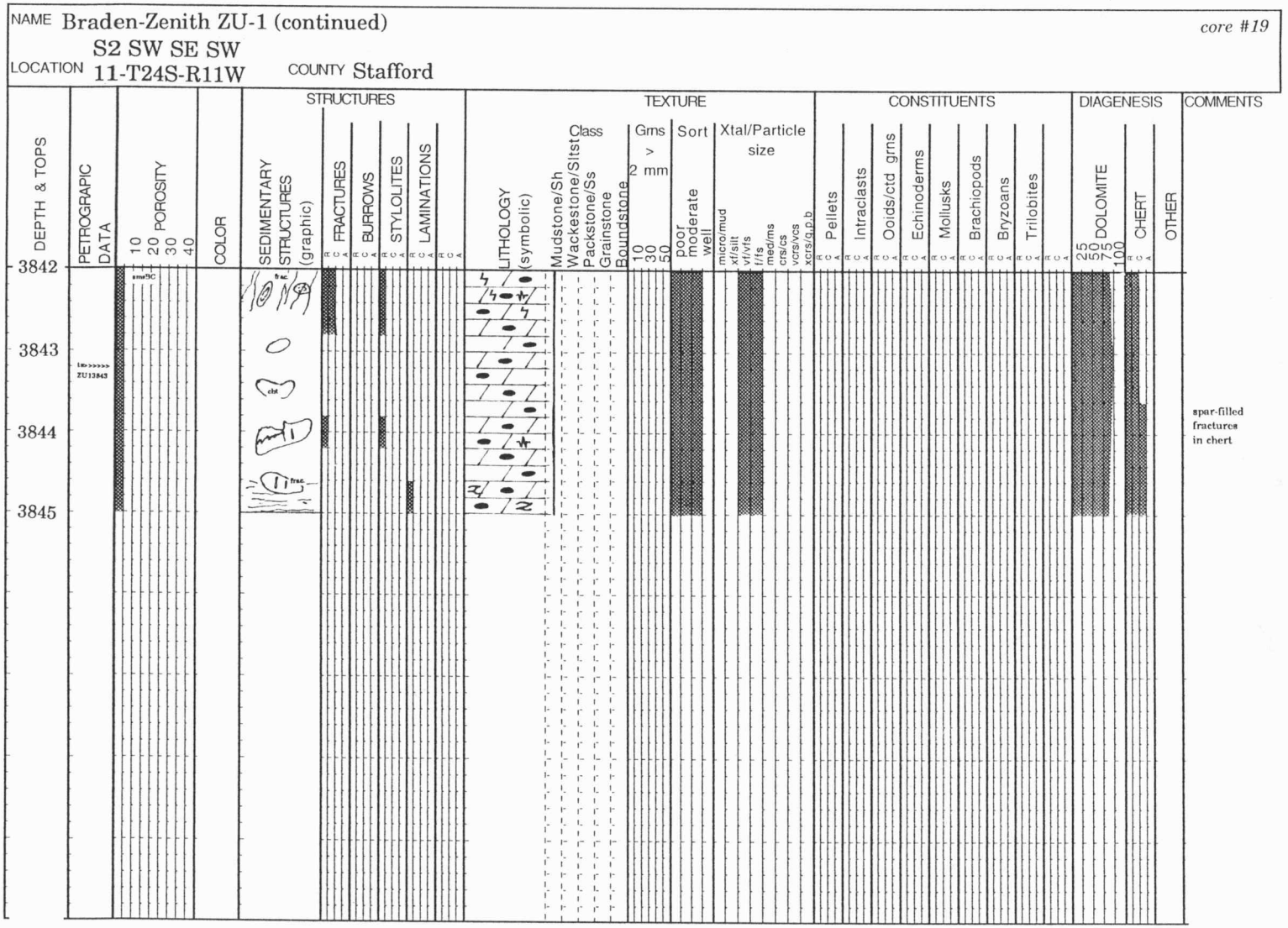
NAME Braden-Zenith ZU-1 (continued)
core #19
S2 SW SE SW
LOCATION 11-T24S-R11W
COUNTY Stafford
DEPTH & TOPS
PETROGRAPHIC DATA
POROSITY
10
20
30
40
COLOR
STRUCTURES
SEDIMENTARY STRUCTURES (graphic)
FRACTURES
BURROWS
STYLOLITES
LAMINATIONS
TEXTURE
LITHOLOGY (symbolic)
Mudstone/Sh
Wackestone/Sltst
Packstone/Ss
Grainstone
Boundstone
Class
Grns > 2 mm
10
30
50
Sort
poor
moderate
well
Xtal/Particle size
micro/mud
xf/silt
vf/vfs
f/fs
med/ms
crs/cs
vcrs/vcs
xcrs/g,p,b
CONSTITUENTS
Pellets
Intraclasts
Ooids/ctd grns
Echinoderms
Mollusks
Brachiopods
Bryzoans
Trilobites
DIAGENESIS
25
50
75
100
DOLOMITE
CHERT
OTHER
COMMENTS
3842
3843
3844
3845
ZU13843
frac
cht
spar-filled fractures in chert

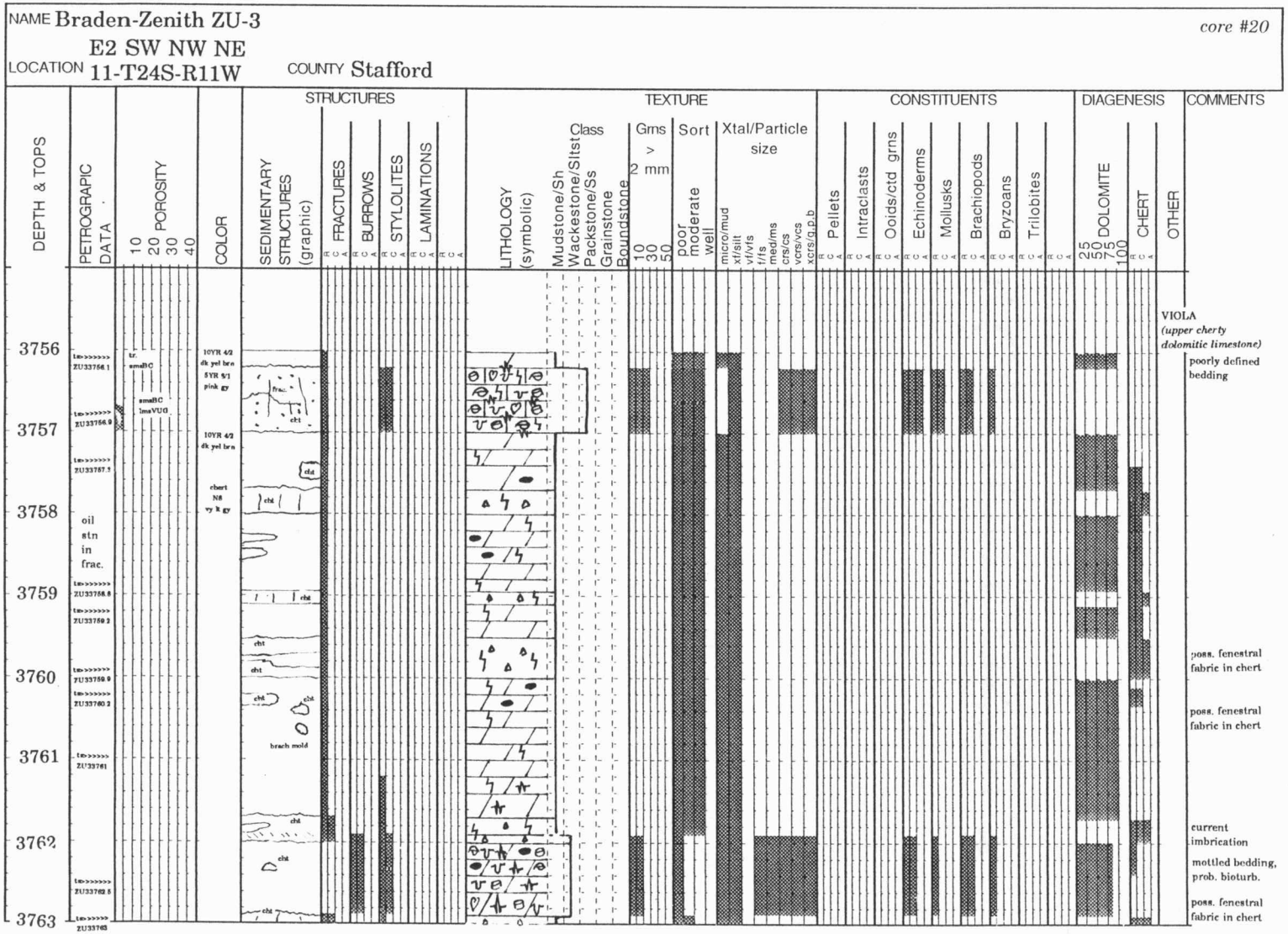
NAME Braden-Zenith ZU-3
E2 SW NW NE
LOCATION 11-T24S-R11W
COUNTY Stafford
core #20
DEPTH & TOPS
PETROGRAPIC DATA
10 20 POROSITY 30 40
COLOR
STRUCTURES
SEDIMENTARY STRUCTURES (graphic)
FRACTURES
BURROWS
STYLOLITES
LAMINATIONS
TEXTURE
LITHOLOGY (symbolic)
Class
Mudstone/Sh
Wackestone/Sltst
Packstone/Ss
Grainstone
Boundstone
Grns > 2 mm
10 30 50
Sort
poor moderate well
Xtal/Particle size
micro/mud
xf/silt
vf/vfs
f/fs
med/ms
crs/cs
vcrs/vcs
xcrs/g,p,b
CONSTITUENTS
Pellets
Intraclasts
Ooids/ctd grns
Echinoderms
Mollusks
Brachiopods
Bryzoans
Trilobites
DIAGENESIS
25 50 75 100
DOLOMITE
CHERT
OTHER
COMMENTS
3756
3757
3758
3759
3760
3761
3762
3763
oil stn in frac.
VIOLA
(upper cherty dolomitic limestone)
poorly defined bedding
poss. fenestral fabric in chert
poss. fenestral fabric in chert
current imbrication
mottled bedding, prob. bioturb.
poss. fenestral fabric in chert

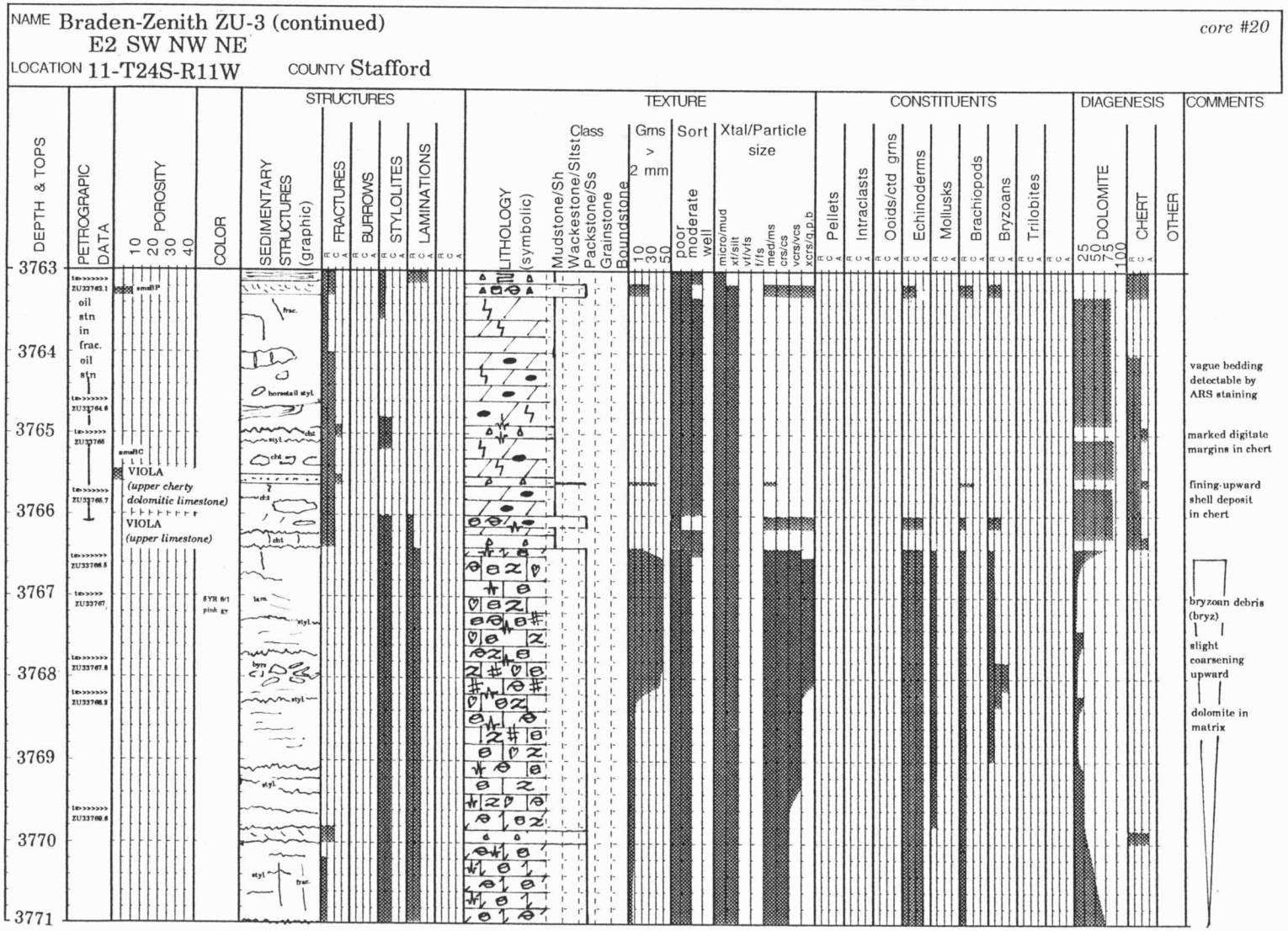
NAME Braden-Zenith ZU-3 (continued)
E2 SW NW NE
LOCATION 11-T24S-R11W
COUNTY Stafford
core #20
DEPTH & TOPS
PETROGRAPHIC DATA
POROSITY
COLOR
STRUCTURES
SEDIMENTARY STRUCTURES (graphic)
FRACTURES
BURROWS
STYLOLITES
LAMINATIONS
TEXTURE
LITHOLOGY (symbolic)
Class
Mudstone/Sh
Wackestone/Slst
Packstone/Ss
Grainstone
Boundstone
Gms > 2 mm
Sort
poor
moderate
well
Xtal/Particle size
micro/mud
xf/silt
vf/vfs
f/fs
med/ms
crs/cs
vcrs/vcs
xcrs/g.p.b
CONSTITUENTS
Pellets
Intraclasts
Ooids/ctd grns
Echinoderms
Mollusks
Brachiopods
Bryzoans
Trilobites
DIAGENESIS
DOLOMITE
CHERT
OTHER
COMMENTS
3763
3764
3765
3766
3767
3768
3769
3770
3771
oil stn in frac.
oil stn
VIOLA
(upper cherty dolomitic limestone)
VIOLA
(upper limestone)
vague bedding detectable by ARS staining
marked digitate margins in chert
fining-upward shell deposit in chert
bryzoan debris (bryz)
slight coarsening upward
dolomite in matrix

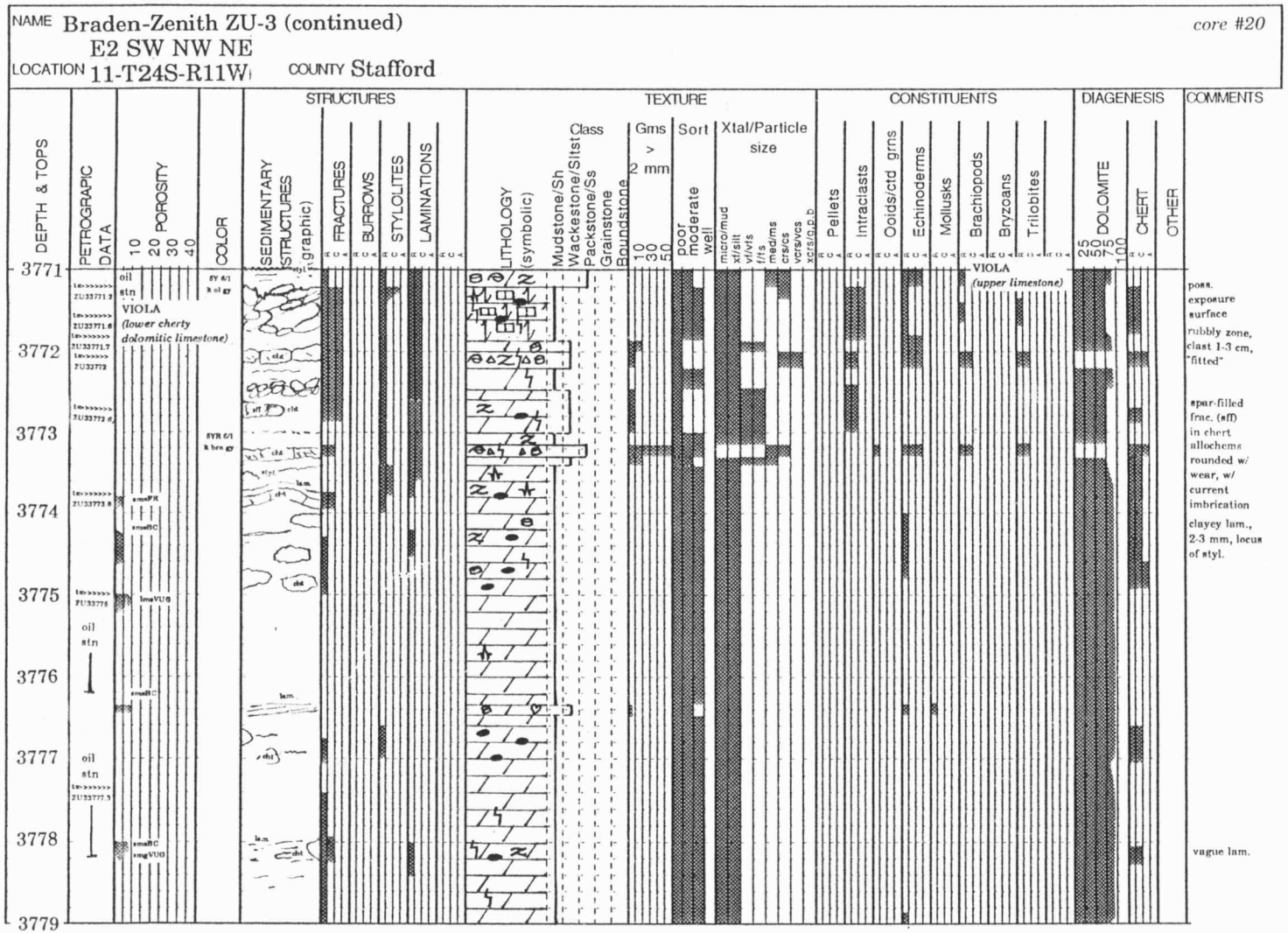
NAME Braden-Zenith ZU-3 (continued)
E2 SW NW NE
LOCATION 11-T24S-R11W COUNTY Stafford
core #20
DEPTH & TOPS
PETROGRAPHIC DATA
POROSITY
COLOR
STRUCTURES
SEDIMENTARY STRUCTURES (graphic)
FRACTURES
BURROWS
STYLOLITES
LAMINATIONS
TEXTURE
LITHOLOGY (symbolic)
Class
Mudstone/Sh
Wackestone/Sltst
Packstone/Ss
Grainstone
Boundstone
Gms > 2 mm
Sort
poor
moderate
well
Xtal/Particle size
micro/mud
vf/silt
vl/vfs
f/fs
med/ms
crs/cs
vcrs/vcs
xcrs/cp,b
CONSTITUENTS
Pellets
Intraclasts
Ooids/ctd grns
Echinoderms
Mollusks
Brachiopods
Bryozoans
Trilobites
DIAGENESIS
DOLOMITE
CHERT
OTHER
COMMENTS
3771
3772
3773
3774
3775
3776
3777
3778
3779
oil stn
VIOLA
(lower cherty dolomitic limestone)
VIOLA
(upper limestone)
5Y 6/1 ol gy
5YR 6/1 lt brn gy
poss. exposure surface
rubbly zone, clast 1-3 cm, "fitted"
spar-filled frac. (sff) in chert allochems rounded w/ wear, w/ current imbrication
clayey lam., 2-3 mm, locus of styl.
vague lam.

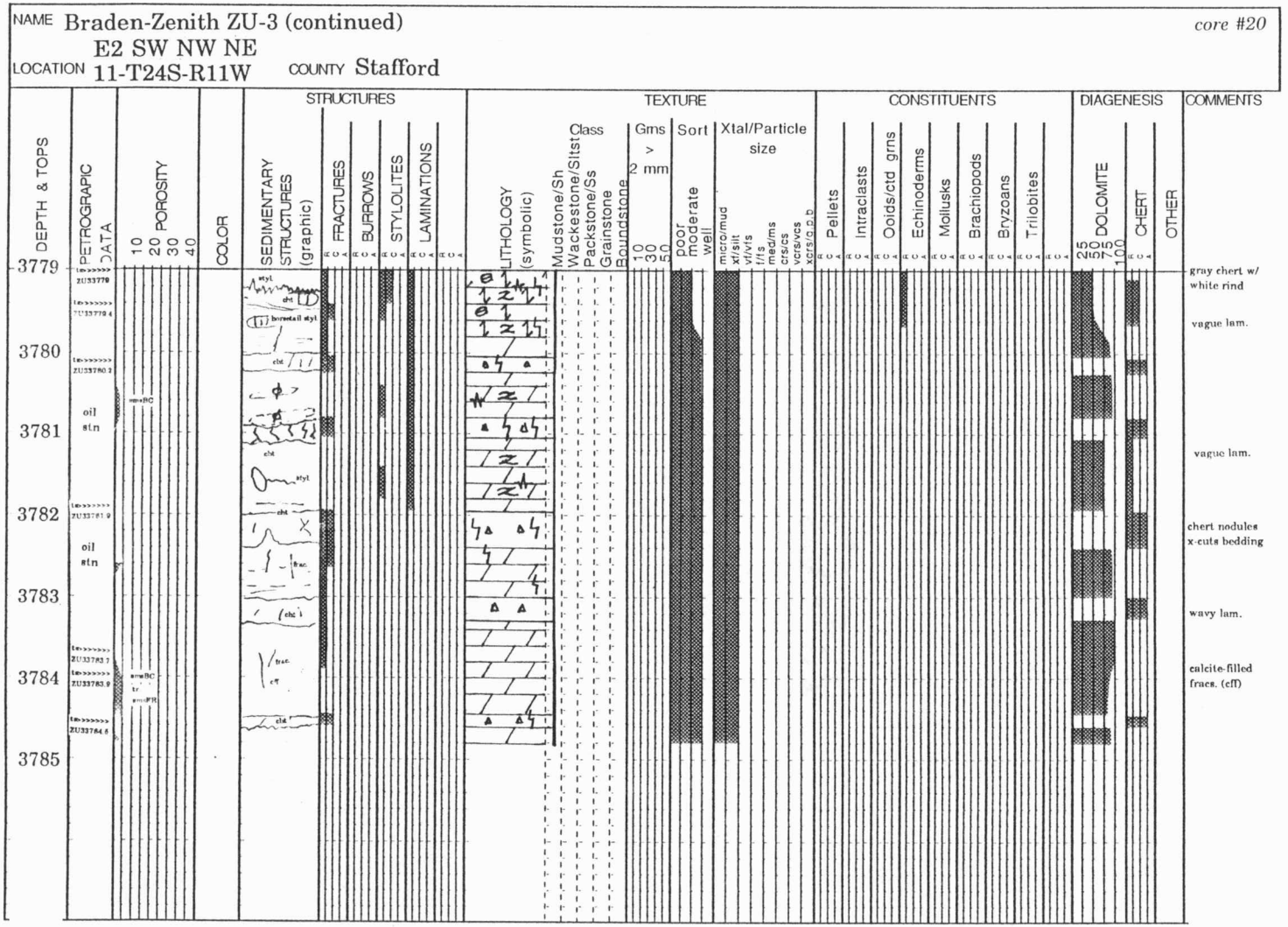
NAME Braden-Zenith ZU-3 (continued)
core #20
E2 SW NW NE
LOCATION 11-T24S-R11W
COUNTY Stafford
DEPTH & TOPS
PETROGRAPHIC DATA
POROSITY
COLOR
STRUCTURES
SEDIMENTARY STRUCTURES (graphic)
FRACTURES
BURROWS
STYLOLITES
LAMINATIONS
TEXTURE
LITHOLOGY (symbolic)
Class
Mudstone/Sh
Wackestone/Sltst
Packstone/Ss
Grainstone
Boundstone
Gms > 2 mm
Sort
poor
moderate
well
Xtal/Particle size
micro/mud
vf/slt
vf/vfs
f/fs
med/ms
crs/cs
vcrs/vcs
xcrs/g,p,b
CONSTITUENTS
Pellets
Intraclasts
Ooids/ctd grns
Echinoderms
Mollusks
Brachiopods
Bryzoans
Trilobites
DIAGENESIS
DOLOMITE
CHERT
OTHER
COMMENTS
3779
3780
3781
3782
3783
3784
3785
oil stn
oil stn
gray chert w/ white rind
vague lam.
vague lam.
chert nodules x-cuts bedding
wavy lam.
calcite-filled fracs. (cff)

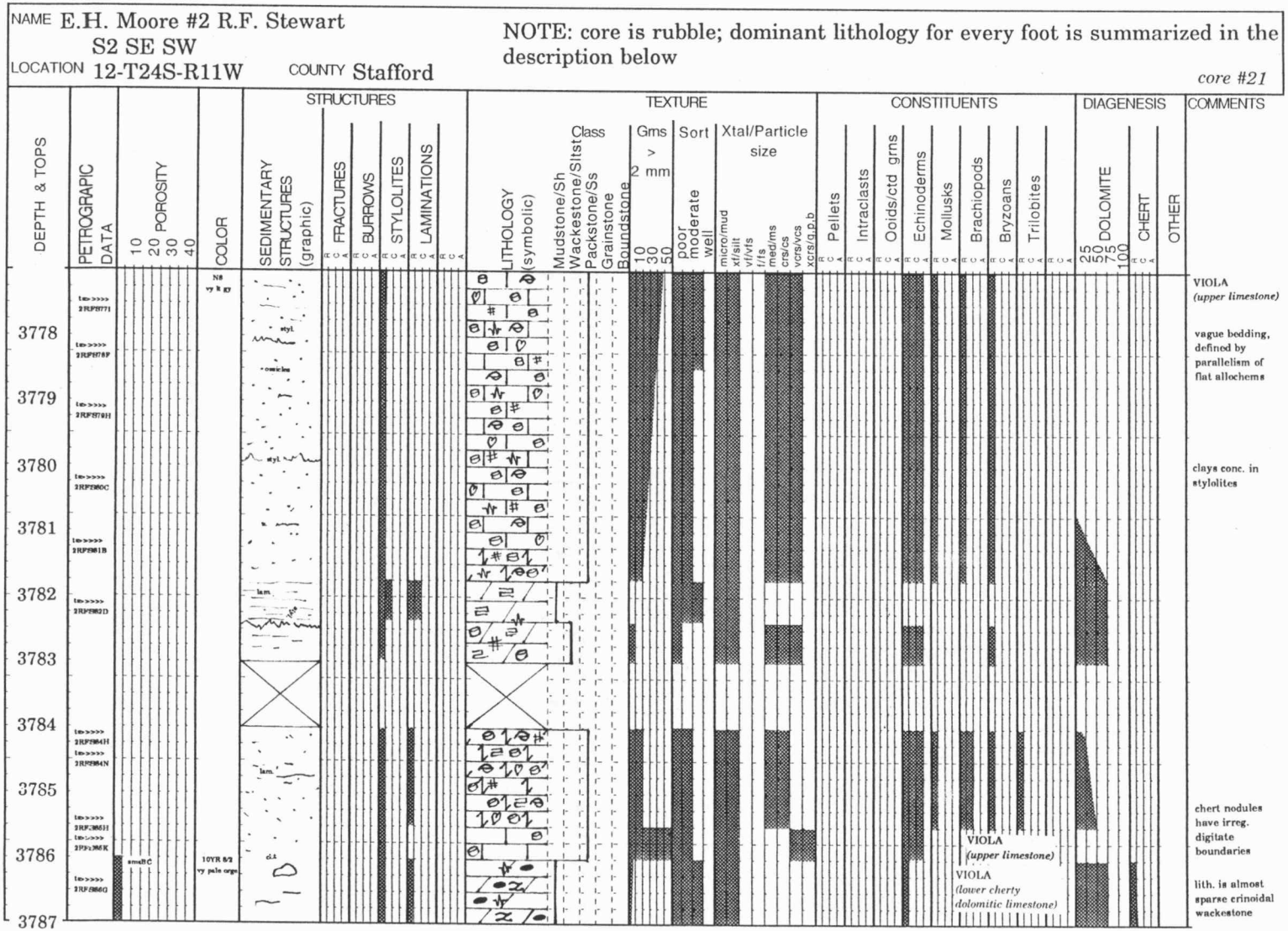
NAME E.H. Moore #2 R.F. Stewart
S2 SE SW
LOCATION 12-T24S-R11W
COUNTY Stafford
NOTE: core is rubble; dominant lithology for every foot is summarized in the description below
core #21
DEPTH & TOPS
PETROGRAPHIC DATA
POROSITY
COLOR
STRUCTURES
SEDIMENTARY STRUCTURES (graphic)
FRACTURES
BURROWS
STYLOLITES
LAMINATIONS
TEXTURE
LITHOLOGY (symbolic)
Class
Mudstone/Sh
Wackestone/Sltst
Packstone/Ss
Grainstone
Boundstone
Gms > 2 mm
Sort
poor
moderate
well
Xtal/Particle size
micro/mud
xf/silt
vf/vfs
f/fs
med/ms
crs/cs
vcrs/vcs
xcrs/g.p.b
CONSTITUENTS
Pellets
Intraclasts
Ooids/ctd grns
Echinoderms
Mollusks
Brachiopods
Bryzoans
Trilobites
DIAGENESIS
DOLOMITE
CHERT
OTHER
COMMENTS
3778
3779
3780
3781
3782
3783
3784
3785
3786
3787
VIOLA
(upper limestone)
VIOLA
(lower cherty dolomitic limestone)
VIOLA
(upper limestone)
vague bedding, defined by parallelism of flat allochems
clays conc. in stylolites
chert nodules have irreg. digitate boundaries
lith. is almost sparse crinoidal wackestone

NAME E.H. Moore #2 R.F. Stewart (continued) *core #21*

S2 SE SW

LOCATION 12-T24S-R11W COUNTY Stafford

DEPTH & TOPS

3787

3788

PETROGRAPHIC DATA

10 20 POROSITY 30 40

COLOR

STRUCTURES

SEDIMENTARY STRUCTURES (graphic)

FRACTURES

BURROWS

STYLOLITES

LAMINATIONS

TEXTURE

LITHOLOGY (symbolic)

Class

Mudstone/Sh

Wackestone/Sltst

Packstone/Ss

Grainstone

Boundstone

Grns > 2 mm

10 30 50

Sort

poor moderate well

Xtal/Particle size

micro/mud

xf/silt

vf/vfs

f/fs

med/ms

crs/cs

vcrs/vcs

xcrs/g,p,b

CONSTITUENTS

Pellets

Intraclasts

Ooids/ctd grns

Echinoderms

Mollusks

Brachiopods

Bryzoans

Trilobites

DIAGENESIS

25 50 75 100 DOLOMITE

CHERT

OTHER

COMMENTS

wavy lam.

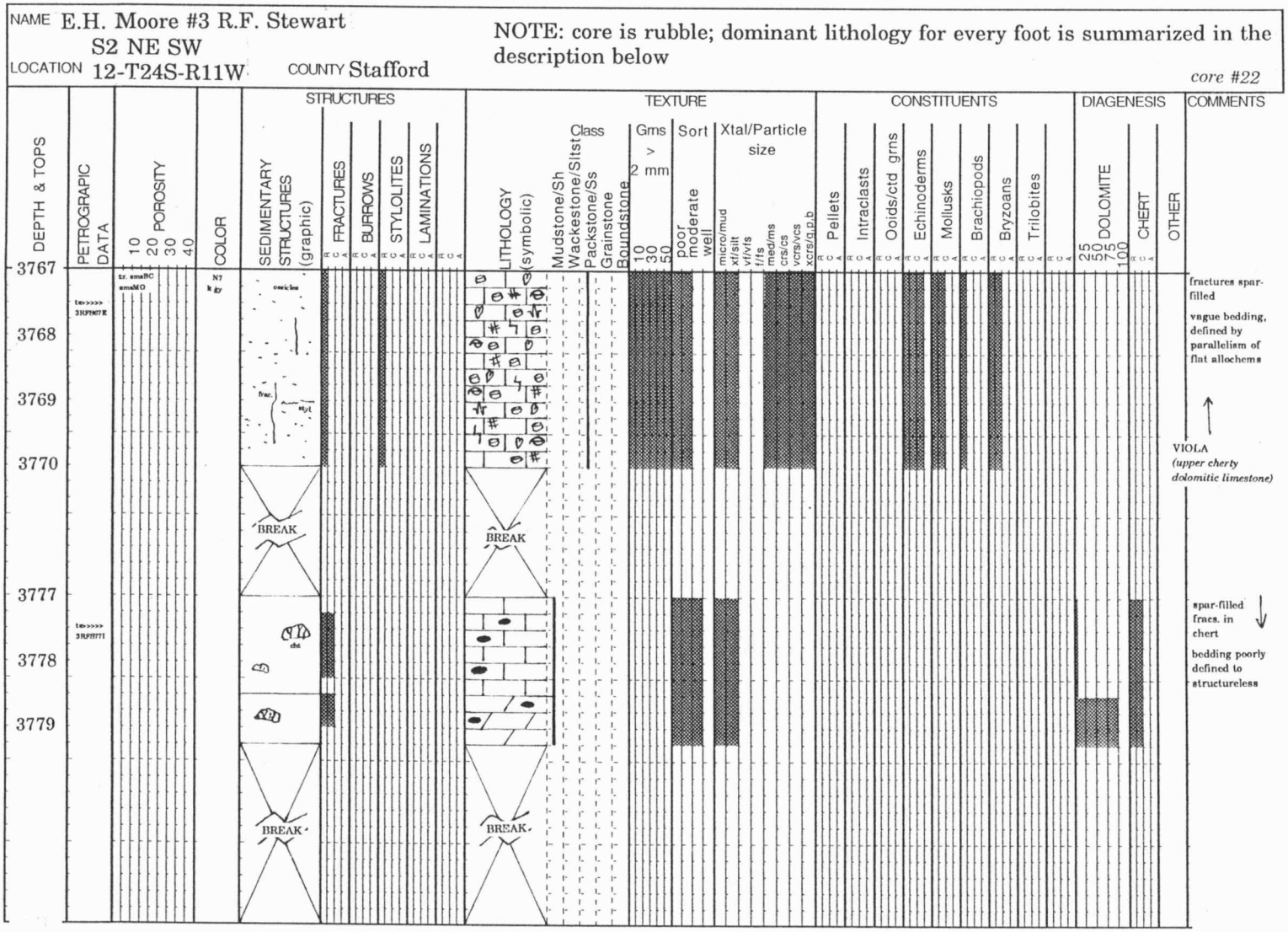
NAME E.H. Moore #3 R.F. Stewart
S2 NE SW
LOCATION 12-T24S-R11W
COUNTY Stafford
NOTE: core is rubble; dominant lithology for every foot is summarized in the description below
core #22
STRUCTURES
TEXTURE
CONSTITUENTS
DIAGENESIS
COMMENTS
DEPTH & TOPS
PETROGRAPHIC DATA
POROSITY
COLOR
SEDIMENTARY STRUCTURES (graphic)
FRACTURES
BURROWS
STYLOLITES
LAMINATIONS
LITHOLOGY (symbolic)
Class
Mudstone/Sh
Wackestone/Sitst
Packstone/Ss
Grainstone
Boundstone
Gms > 2 mm
Sort
poor
moderate
well
Xtal/Particle size
micro/mud
xf/silt
vf/vfs
f/fs
med/ms
crs/cs
vcrs/vcs
xcrs/cl,p,b
Pellets
Intraclasts
Ooids/ctd grns
Echinoderms
Mollusks
Brachiopods
Bryzoans
Trilobites
DOLOMITE
CHERT
OTHER
3767
3768
3769
3770
3777
3778
3779
BREAK
fractures spar-filled
vague bedding, defined by parallelism of flat allochems
VIOLA
(upper cherty dolomitic limestone)
spar-filled fracs. in chert
bedding poorly defined to structureless

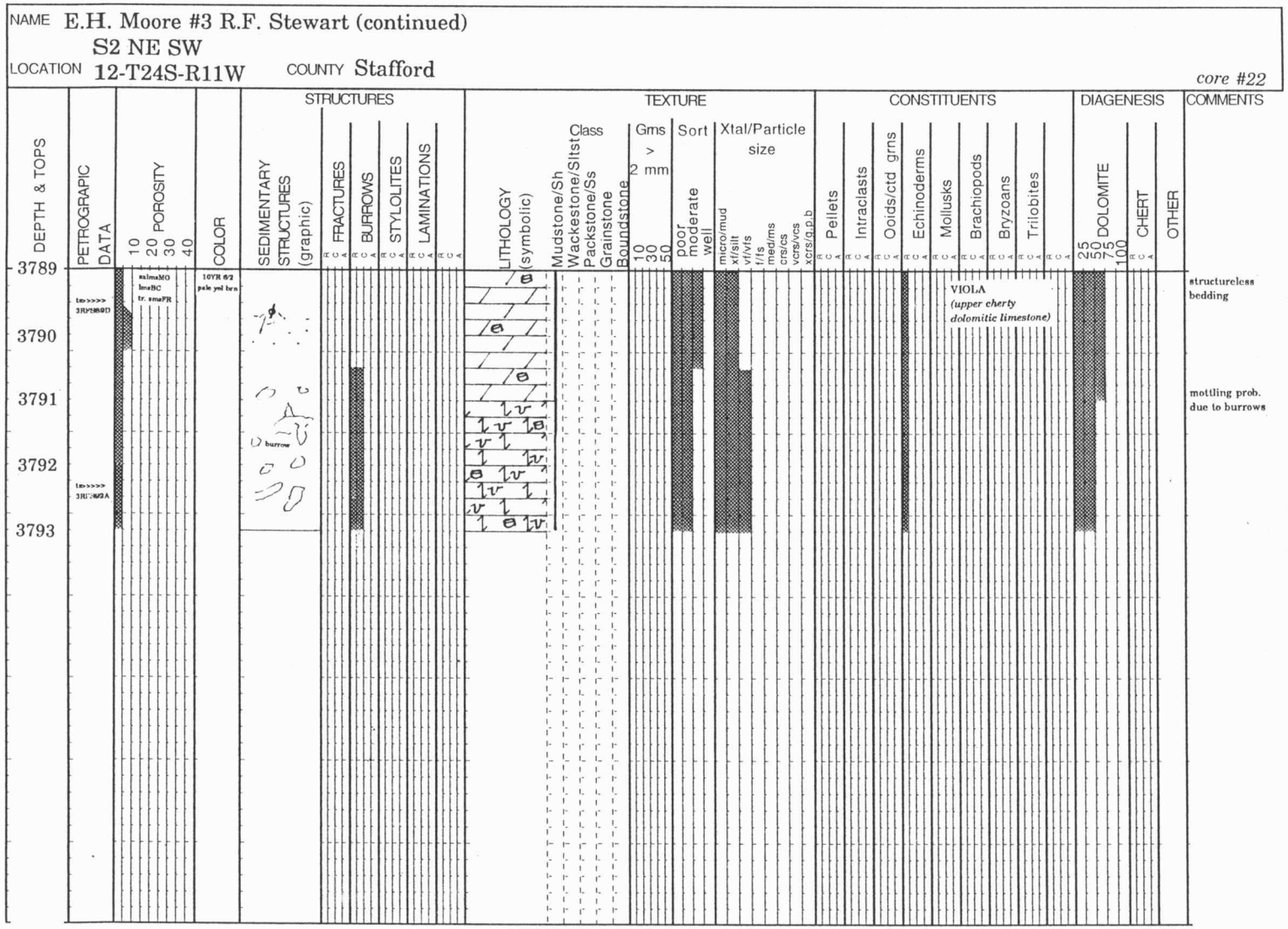
NAME E.H. Moore #3 R.F. Stewart (continued)
S2 NE SW
LOCATION 12-T24S-R11W
COUNTY Stafford
core #22
STRUCTURES
TEXTURE
CONSTITUENTS
DIAGENESIS
COMMENTS
DEPTH & TOPS
PETROGRAPIC DATA
10 20 POROSITY 30 40
COLOR
SEDIMENTARY STRUCTURES (graphic)
FRACTURES
BURROWS
STYLOLITES
LAMINATIONS
LITHOLOGY (symbolic)
Class
Mudstone/Sh
Wackestone/Sltst
Packstone/Ss
Grainstone
Boundstone
Gms > 2 mm
10 30 50
Sort
poor moderate well
Xtal/Particle size
micro/mud
xf/silt
vf/vfs
f/fs
med/ms
crs/cs
vcrs/vcs
xcrs/g,p,b
Pellets
Intraclasts
Ooids/ctd grns
Echinoderms
Mollusks
Brachiopods
Bryzoans
Trilobites
25 50 75 100
DOLOMITE
CHERT
OTHER
3789
3790
3791
3792
3793
10YR 6/2
pale yel brn
burrow
VIOLA
(upper cherty
dolomitic limestone)
structureless
bedding
mottling prob.
due to burrows

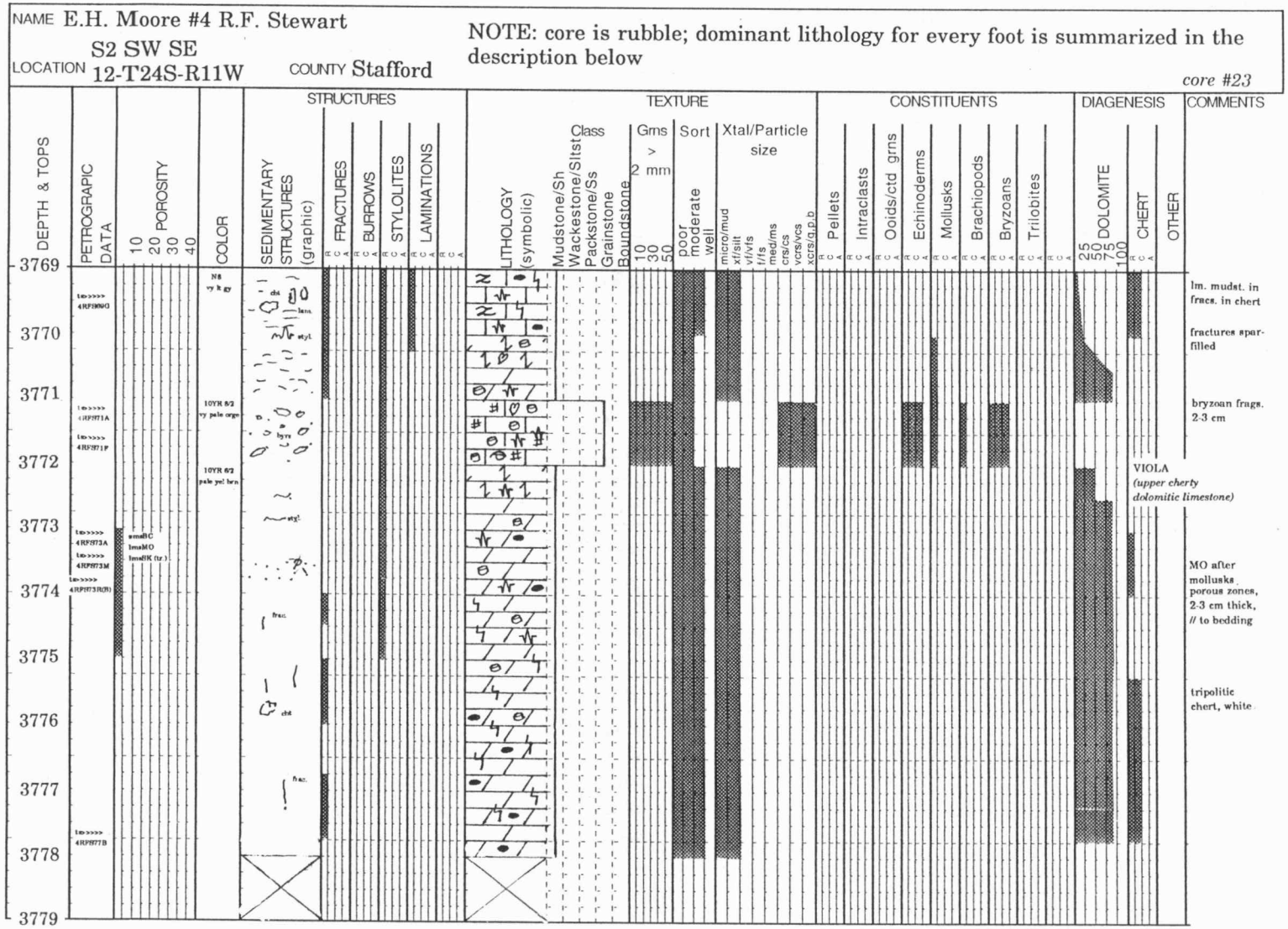
NAME E.H. Moore #4 R.F. Stewart
LOCATION S2 SW SE 12-T24S-R11W
COUNTY Stafford
NOTE: core is rubble; dominant lithology for every foot is summarized in the description below
core #23
DEPTH & TOPS
PETROGRAPHIC DATA
POROSITY
COLOR
STRUCTURES
SEDIMENTARY STRUCTURES (graphic)
FRACTURES
BURROWS
STYLOLITES
LAMINATIONS
TEXTURE
LITHOLOGY (symbolic)
Class
Mudstone/Sh
Wackestone/Sltst
Packstone/Ss
Grainstone
Boundstone
Gms > 2 mm
Sort
poor
moderate
well
Xtal/Particle size
micro/mud
xf/silt
vf/vfs
f/fs
med/ms
crs/cs
vcrs/vcs
xcrs/g,p,b
CONSTITUENTS
Pellets
Intraclasts
Ooids/ctd grns
Echinoderms
Mollusks
Brachiopods
Bryzoans
Trilobites
DIAGENESIS
DOLOMITE
CHERT
OTHER
COMMENTS
3769
3770
3771
3772
3773
3774
3775
3776
3777
3778
3779
lm. mudst. in fracs. in chert
fractures spar-filled
bryzoan frags. 2-3 cm
VIOLA
(upper cherty dolomitic limestone)
MO after mollusks, porous zones, 2-3 cm thick, // to bedding
tripolitic chert, white

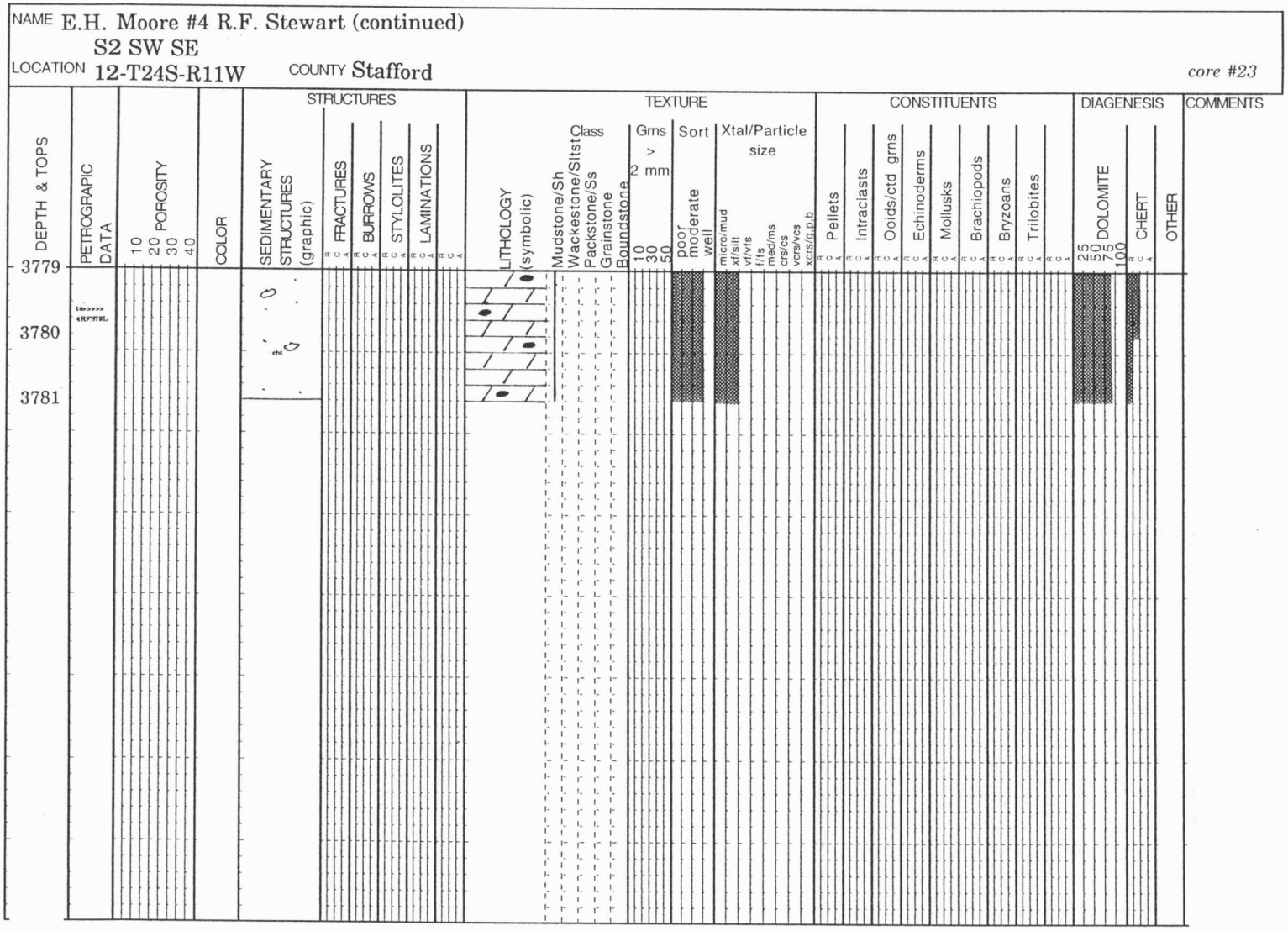
NAME E.H. Moore #4 R.F. Stewart (continued)
S2 SW SE
LOCATION 12-T24S-R11W
COUNTY Stafford
core #23
STRUCTURES
TEXTURE
CONSTITUENTS
DIAGENESIS
COMMENTS
DEPTH & TOPS
PETROGRAPIC DATA
10 20 POROSITY 30 40
COLOR
SEDIMENTARY STRUCTURES (graphic)
FRACTURES
BURROWS
STYLOLITES
LAMINATIONS
LITHOLOGY (symbolic)
Class
Mudstone/Sh
Wackestone/Slt
Packstone/Ss
Grainstone
Boundstone
Grns > 2 mm
10 30 50
Sort
poor moderate well
Xtal/Particle size
micro/mud
xf/silt
vf/vfs
f/fs
med/ms
crs/cs
vcrs/vcs
xcrs/g,p,b
Pellets
Intraclasts
Ooids/ctd grns
Echinoderms
Mollusks
Brachiopods
Bryzoans
Trilobites
25 50 75 100
DOLOMITE
CHERT
OTHER
3779
3780
3781

NAME E.H. Moore #1 N.W. Johnson

LOCATION SW NW NE 13-T24S-R11W COUNTY Stafford

NOTE: core is rubble; dominant lithology for every foot is summarized in the description below

core #24

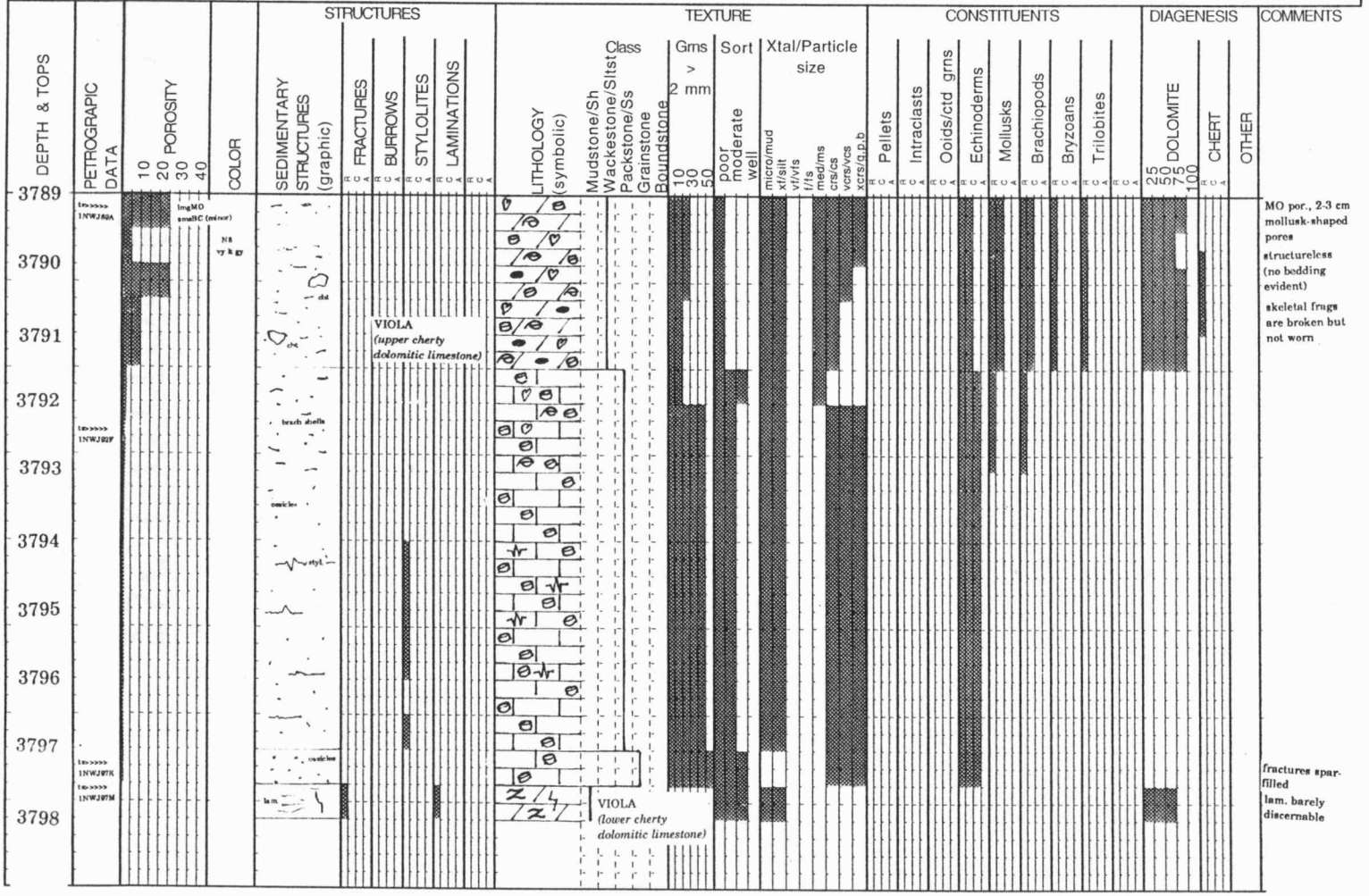

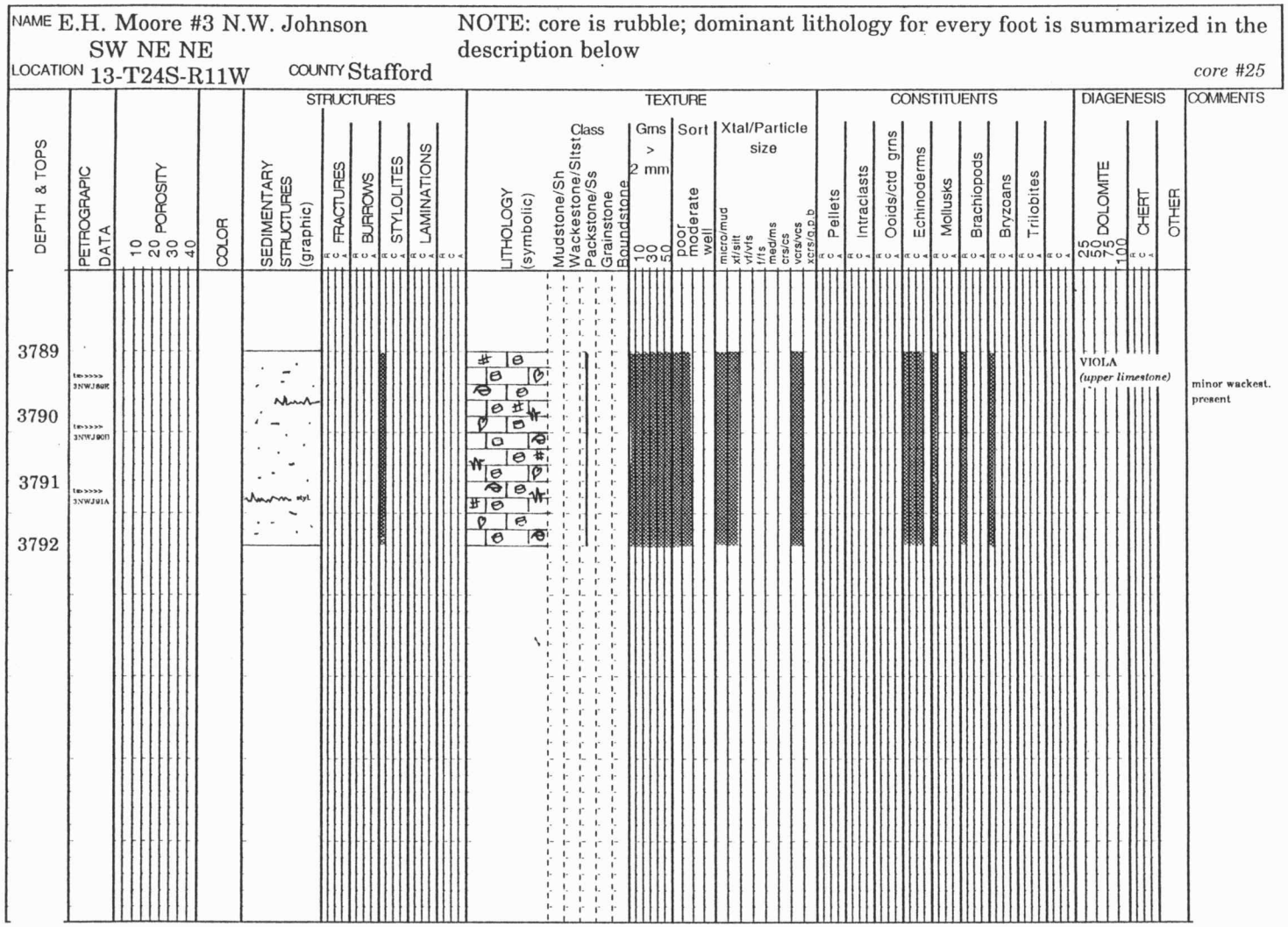
NAME E.H. Moore #3 N.W. Johnson
SW NE NE
LOCATION 13-T24S-R11W
COUNTY Stafford
NOTE: core is rubble; dominant lithology for every foot is summarized in the description below
core #25
DEPTH & TOPS
PETROGRAPHIC DATA
POROSITY
10
20
30
40
COLOR
STRUCTURES
SEDIMENTARY STRUCTURES (graphic)
FRACTURES
BURROWS
STYLOLITES
LAMINATIONS
TEXTURE
LITHOLOGY (symbolic)
Class
Mudstone/Sh
Wackestone/Sltst
Packstone/Ss
Grainstone
Boundstone
Gms > 2 mm
10
30
50
Sort
poor
moderate
well
Xtal/Particle size
micro/mud
xf/silt
vf/vfs
f/fs
med/ms
crs/cs
vcrs/vcs
xcrs/g,p,b
CONSTITUENTS
Pellets
Intraclasts
Ooids/ctd grns
Echinoderms
Mollusks
Brachiopods
Bryzoans
Trilobites
DIAGENESIS
25
50
75
100
DOLOMITE
CHERT
OTHER
COMMENTS
3789
3790
3791
3792
VIOLA
(upper limestone)
minor wackest.
present

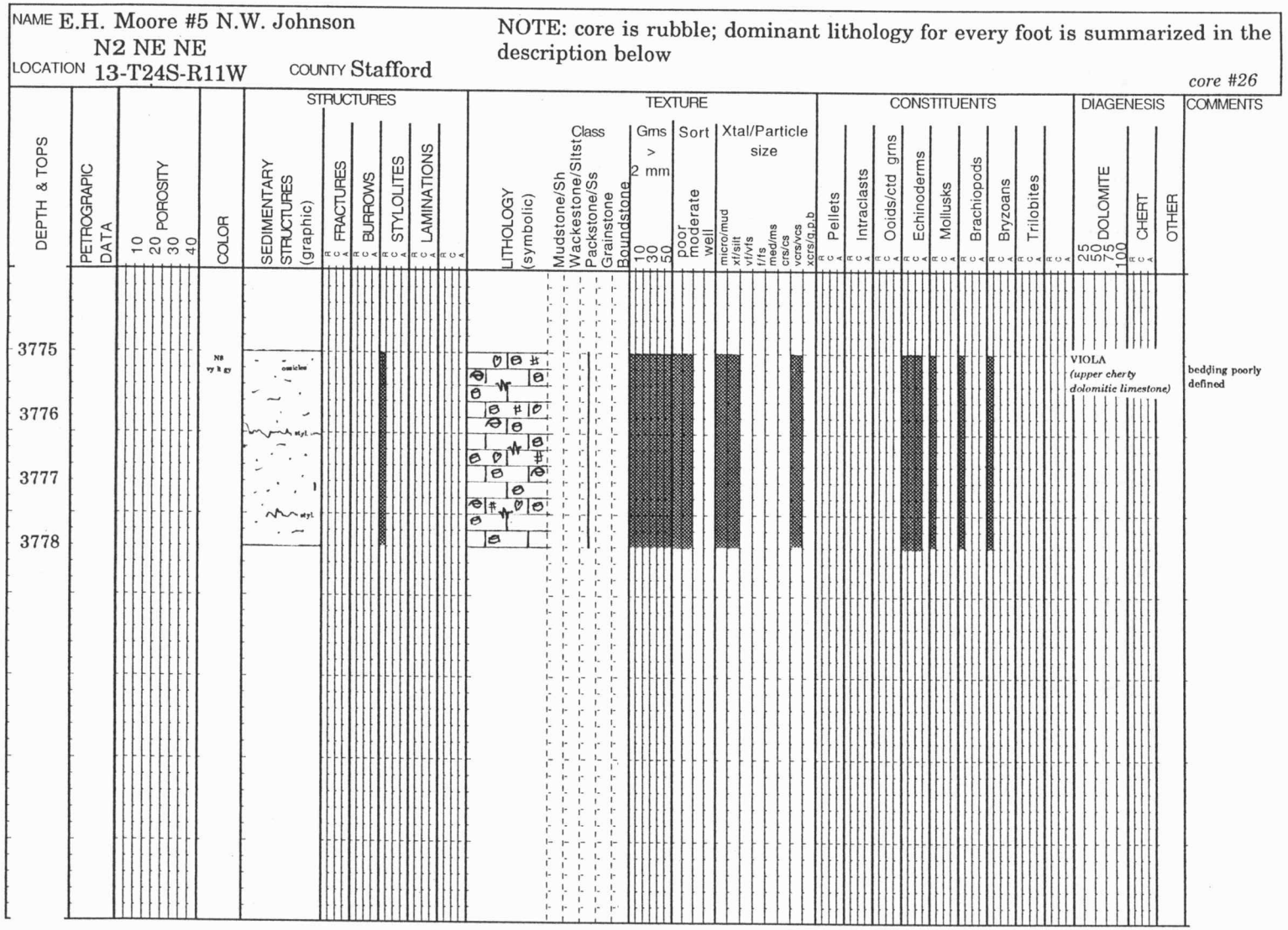
NAME E.H. Moore #5 N.W. Johnson
N2 NE NE
LOCATION 13-T24S-R11W
COUNTY Stafford
NOTE: core is rubble; dominant lithology for every foot is summarized in the description below
core #26
DEPTH & TOPS
PETROGRAPHIC DATA
POROSITY
COLOR
STRUCTURES
SEDIMENTARY STRUCTURES (graphic)
FRACTURES
BURROWS
STYLOLITES
LAMINATIONS
TEXTURE
LITHOLOGY (symbolic)
Class
Mudstone/Sh
Wackestone/Sltst
Packstone/Ss
Grainstone
Boundstone
Gms > 2 mm
Sort
poor
moderate
well
Xtal/Particle size
micro/mud
xf/silt
vf/vfs
f/fs
med/ms
crs/cs
vcrs/vcs
xcrs/g,p,b
CONSTITUENTS
Pellets
Intraclasts
Ooids/ctd grns
Echinoderms
Mollusks
Brachiopods
Bryzoans
Trilobites
DIAGENESIS
DOLOMITE
CHERT
OTHER
COMMENTS
3775
3776
3777
3778
VIOLA
(upper cherty dolomitic limestone)
bedding poorly defined

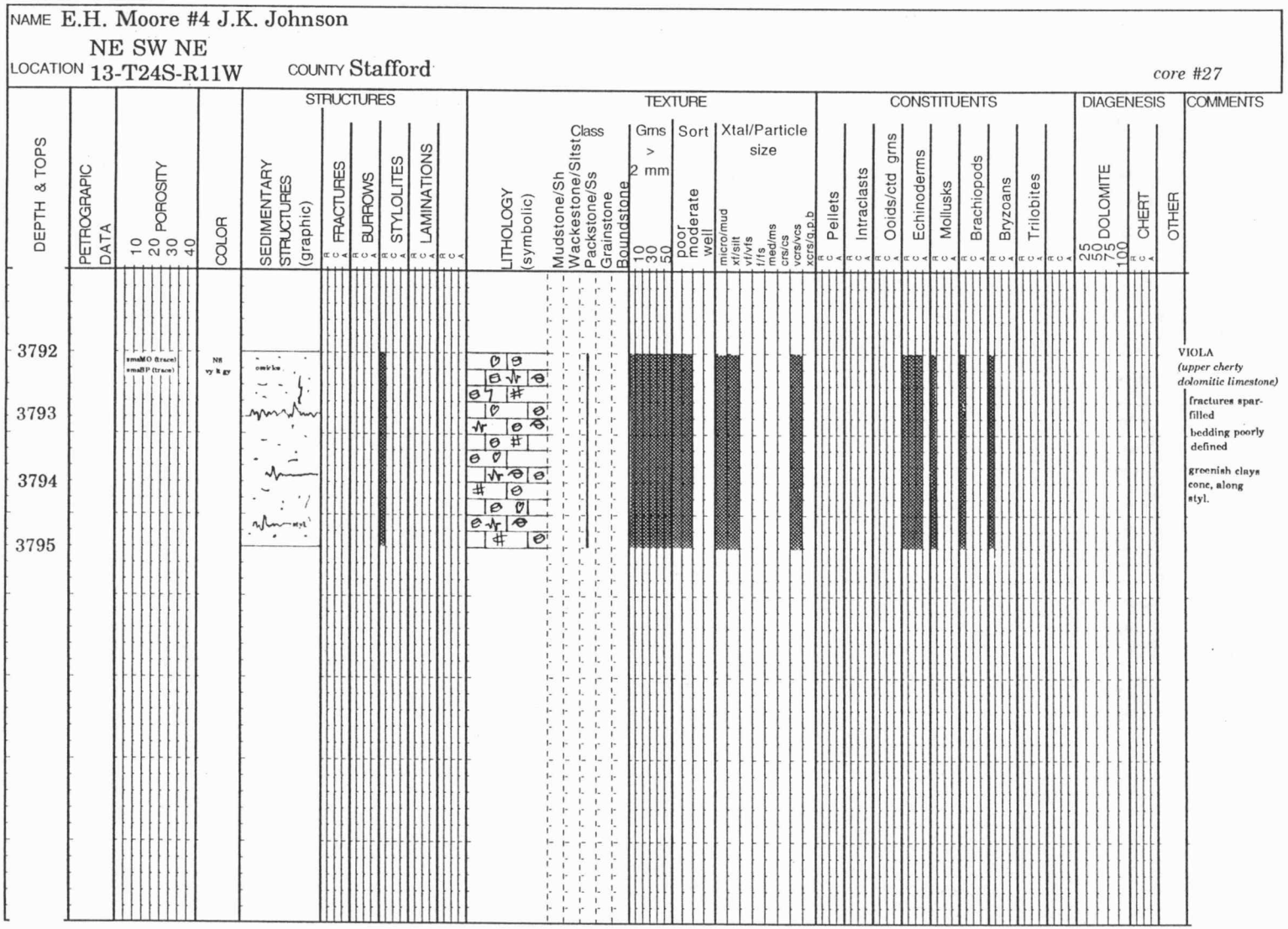
NAME E.H. Moore #4 J.K. Johnson
NE SW NE
LOCATION 13-T24S-R11W
COUNTY Stafford
core #27
DEPTH & TOPS
PETROGRAPIC DATA
POROSITY
COLOR
STRUCTURES
SEDIMENTARY STRUCTURES (graphic)
FRACTURES
BURROWS
STYLOLITES
LAMINATIONS
TEXTURE
LITHOLOGY (symbolic)
Class
Mudstone/Sh
Wackestone/Sltst
Packstone/Ss
Grainstone
Boundstone
Gms > 2 mm
Sort
poor
moderate
well
Xtal/Particle size
micro/mud
xf/silt
vf/vls
f/ls
med/ms
crs/cs
vcrs/vcs
xcrs/g,p,b
CONSTITUENTS
Pellets
Intraclasts
Ooids/ctd grns
Echinoderms
Mollusks
Brachiopods
Bryzoans
Trilobites
DIAGENESIS
DOLOMITE
CHERT
OTHER
COMMENTS
3792
3793
3794
3795
VIOLA
(upper cherty dolomitic limestone)
fractures spar-filled
bedding poorly defined
greenish clays cone, along styl.

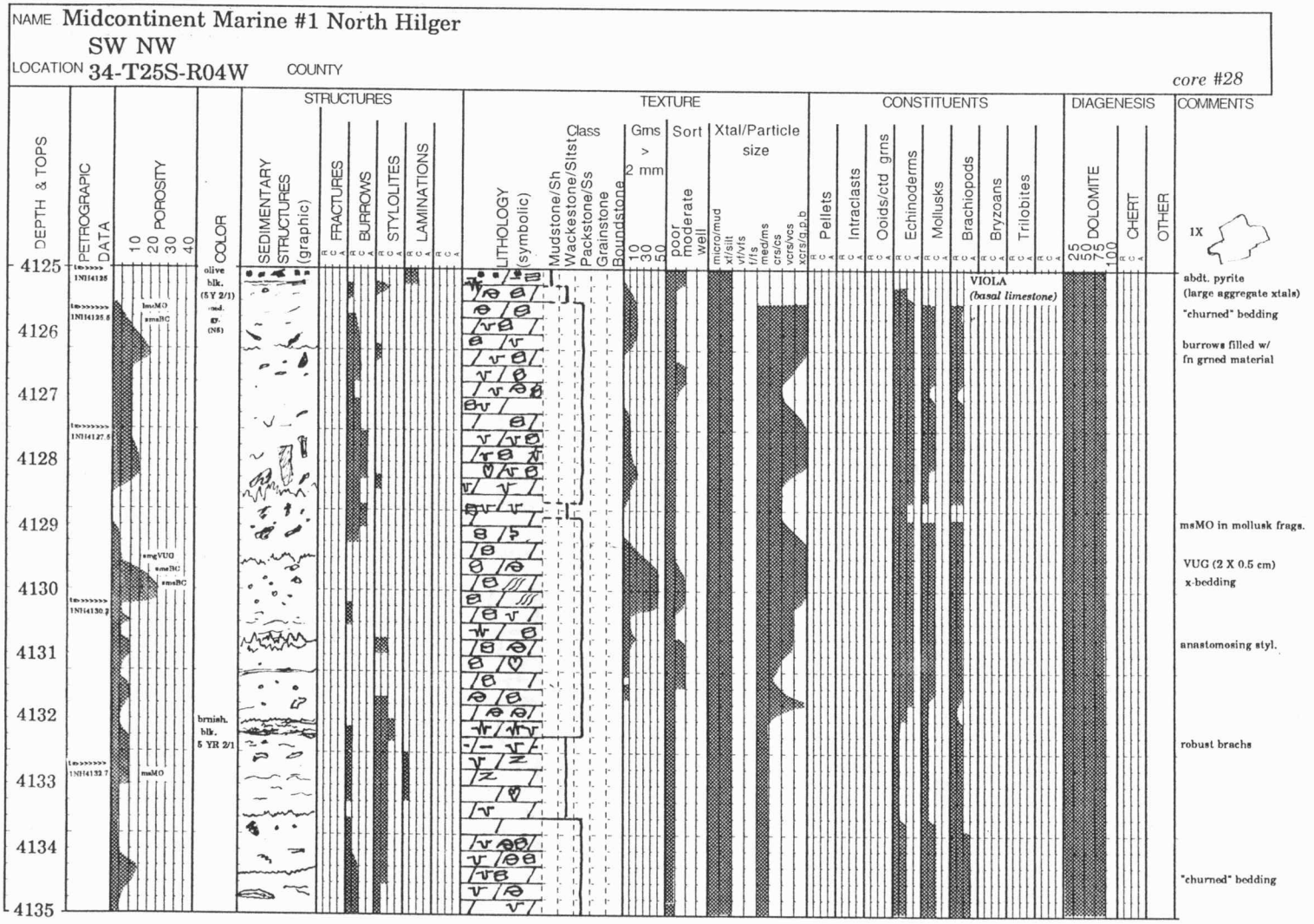
NAME Midcontinent Marine #1 North Hilger
SW NW
LOCATION 34-T25S-R04W
COUNTY
core #28
STRUCTURES
TEXTURE
CONSTITUENTS
DIAGENESIS
COMMENTS
DEPTH & TOPS
PETROGRAPHIC DATA
10 20 POROSITY 30 40
COLOR
SEDIMENTARY STRUCTURES (graphic)
FRACTURES
BURROWS
STYLOLITES
LAMINATIONS
LITHOLOGY (symbolic)
Class
Mudstone/Sh
Wackestone/Siltst
Packstone/Ss
Grainstone
Boundstone
Gms > 2 mm
10 30 50
Sort
poor moderate well
Xtal/Particle size
micromud
xf/silt
vf/vfs
f/fs
med/ms
crs/cs
vcrs/vcs
xcrs/g,p,b
Pellets
Intraclasts
Ooids/ctd grns
Echinoderms
Mollusks
Brachiopods
Bryzoans
Trilobites
25 50 75 100 DOLOMITE
CHERT
OTHER
1X
4125
4126
4127
4128
4129
4130
4131
4132
4133
4134
4135
olive blk. (5 Y 2/1) mod. br. (N8)
brnish. blk. 5 YR 2/1
1N14125
1N14125.5
1N14127.5
1N14130.2
1N14132.7
lmsMO
smsBC
smgVUG
smsBC
msMO
VIOLA
(basal limestone)
abdt. pyrite (large aggregate xtals)
"churned" bedding
burrows filled w/ fn grned material
msMO in mollusk frags.
VUG (2 X 0.5 cm)
x-bedding
anastomosing styl.
robust brachs
"churned" bedding

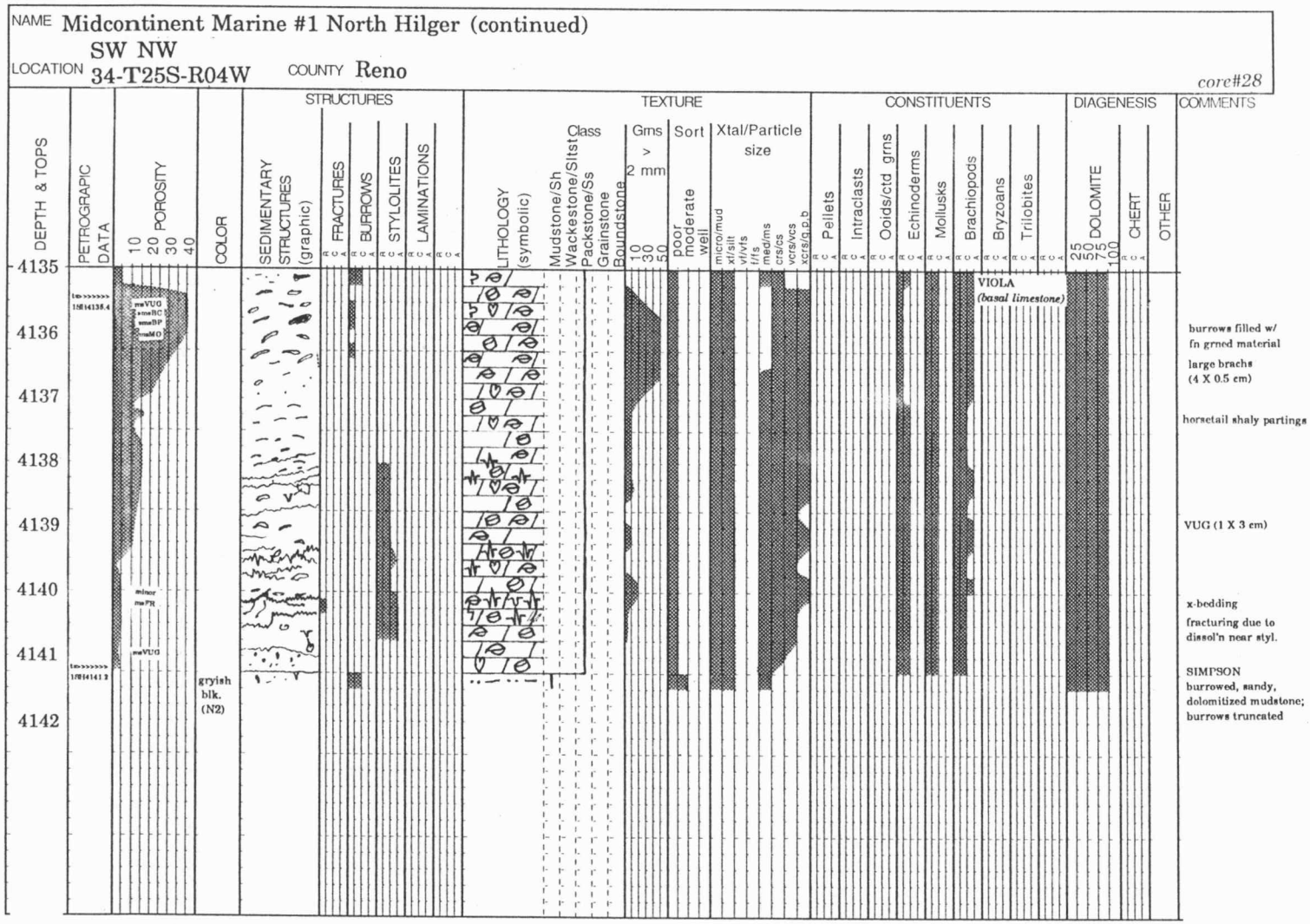
NAME Midcontinent Marine #1 North Hilger (continued)
LOCATION SW NW 34-T25S-R04W
COUNTY Reno
core#28
STRUCTURES
TEXTURE
CONSTITUENTS
DIAGENESIS
COMMENTS
DEPTH & TOPS
PETROGRAPIC DATA
10 20 POROSITY 30 40
COLOR
SEDIMENTARY STRUCTURES (graphic)
FRACTURES
BURROWS
STYLOLITES
LAMINATIONS
LITHOLOGY (symbolic)
Class
Mudstone/Sh
Wackestone/Sltst
Packstone/Ss
Grainstone
Boundstone
Gms > 2 mm
10 30 50
Sort
poor moderate well
Xtal/Particle size
micro/mud
xf/silt
vf/vfs
f/fs
med/ms
crs/cs
vcrs/vcs
xcrs/g,p,b
Pellets
Intraclasts
Ooids/ctd grns
Echinoderms
Mollusks
Brachiopods
Bryzoans
Trilobites
25 50 75 100 DOLOMITE
CHERT
OTHER
4135
4136
4137
4138
4139
4140
4141
4142
VIOLA
(basal limestone)
gryish blk. (N2)
burrows filled w/ fn grned material
large brachs (4 X 0.5 cm)
horsetail shaly partings
VUG (1 X 3 cm)
x-bedding
fracturing due to dissol'n near styl.
SIMPSON
burrowed, sandy, dolomitized mudstone; burrows truncated

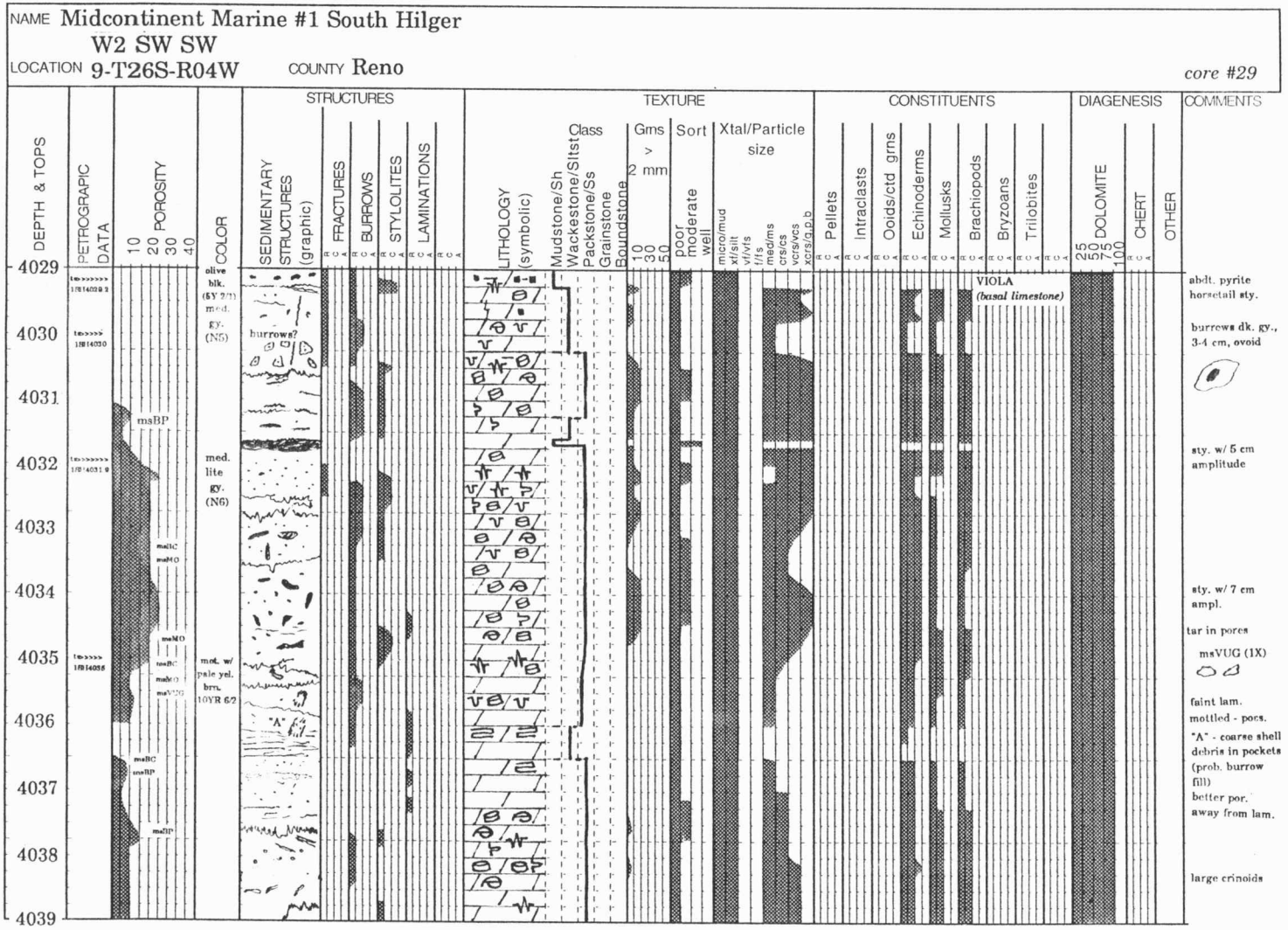
NAME Midcontinent Marine #1 South Hilger
W2 SW SW
LOCATION 9-T26S-R04W
COUNTY Reno
core #29
DEPTH & TOPS
PETROGRAPHIC DATA
POROSITY
COLOR
STRUCTURES
SEDIMENTARY STRUCTURES (graphic)
FRACTURES
BURROWS
STYLOLITES
LAMINATIONS
TEXTURE
LITHOLOGY (symbolic)
Class
Mudstone/Sh
Wackestone/Sltst
Packstone/Ss
Grainstone
Boundstone
Gms > 2 mm
Sort
poor
moderate
well
Xtal/Particle size
micro/mud
xf/silt
vf/vfs
f/fs
med/ms
crs/cs
vcrs/vcs
xcrs/g,p,b
CONSTITUENTS
Pellets
Intraclasts
Ooids/ctd grns
Echinoderms
Mollusks
Brachiopods
Bryzoans
Trilobites
DIAGENESIS
DOLOMITE
CHERT
OTHER
COMMENTS
4029
4030
4031
4032
4033
4034
4035
4036
4037
4038
4039
olive blk. (5Y 2/1) med. gy. (N5)
med. lite gy. (N6)
mot. w/ pale yel. brn. 10YR 6/2
burrows?
msBP
msMO
msBC
msVUG
msBP
VIOLA
(basal limestone)
abdt. pyrite horsetail sty.
burrows dk. gy., 3-4 cm, ovoid
sty. w/ 5 cm amplitude
sty. w/ 7 cm ampl.
tar in pores
msVUG (1X)
faint lam. mottled - pors.
"A" - coarse shell debris in pockets (prob. burrow fill)
better por. away from lam.
large crinoids

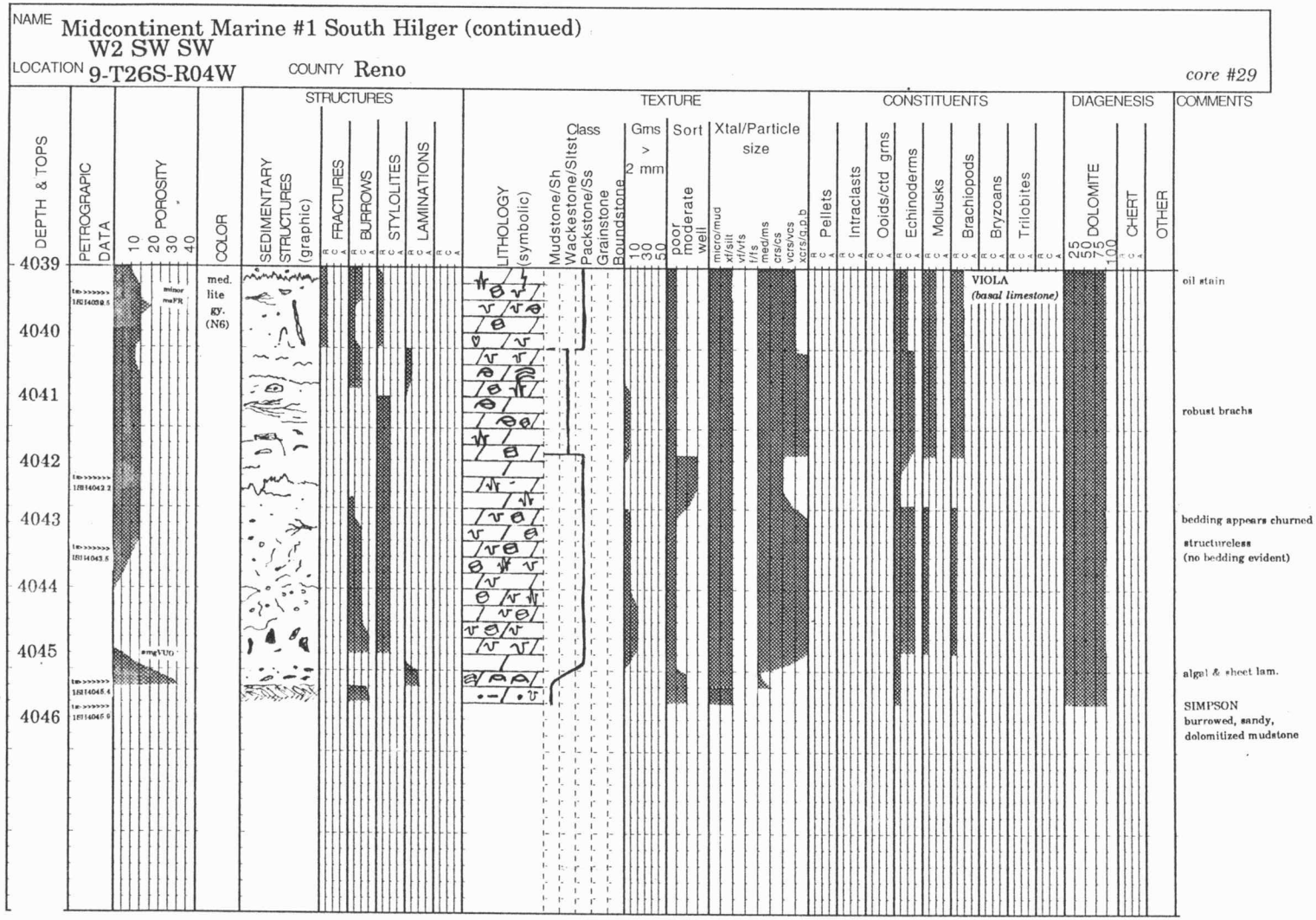
NAME Midcontinent Marine #1 South Hilger (continued)
W2 SW SW
LOCATION 9-T26S-R04W
COUNTY Reno
core #29
STRUCTURES
TEXTURE
CONSTITUENTS
DIAGENESIS
COMMENTS
DEPTH & TOPS
PETROGRAPHIC DATA
POROSITY
COLOR
SEDIMENTARY STRUCTURES (graphic)
FRACTURES
BURROWS
STYLOLITES
LAMINATIONS
LITHOLOGY (symbolic)
Class
Mudstone/Sh
Wackestone/Siltst
Packstone/Ss
Grainstone
Boundstone
Grns > 2 mm
Sort
poor
moderate
well
Xtal/Particle size
micr/mud
vf/silt
f/s
med/ms
crs/cs
vcrs/vcs
Pellets
Intraclasts
Ooids/ctd grns
Echinoderms
Mollusks
Brachiopods
Bryzoans
Trilobites
DOLOMITE
CHERT
OTHER
4039
4040
4041
4042
4043
4044
4045
4046
med. lite gy. (N6)
VIOLA
(basal limestone)
oil stain
robust brachs
bedding appears churned
structureless
(no bedding evident)
algal & sheet lam.
SIMPSON
burrowed, sandy,
dolomitized mudstone

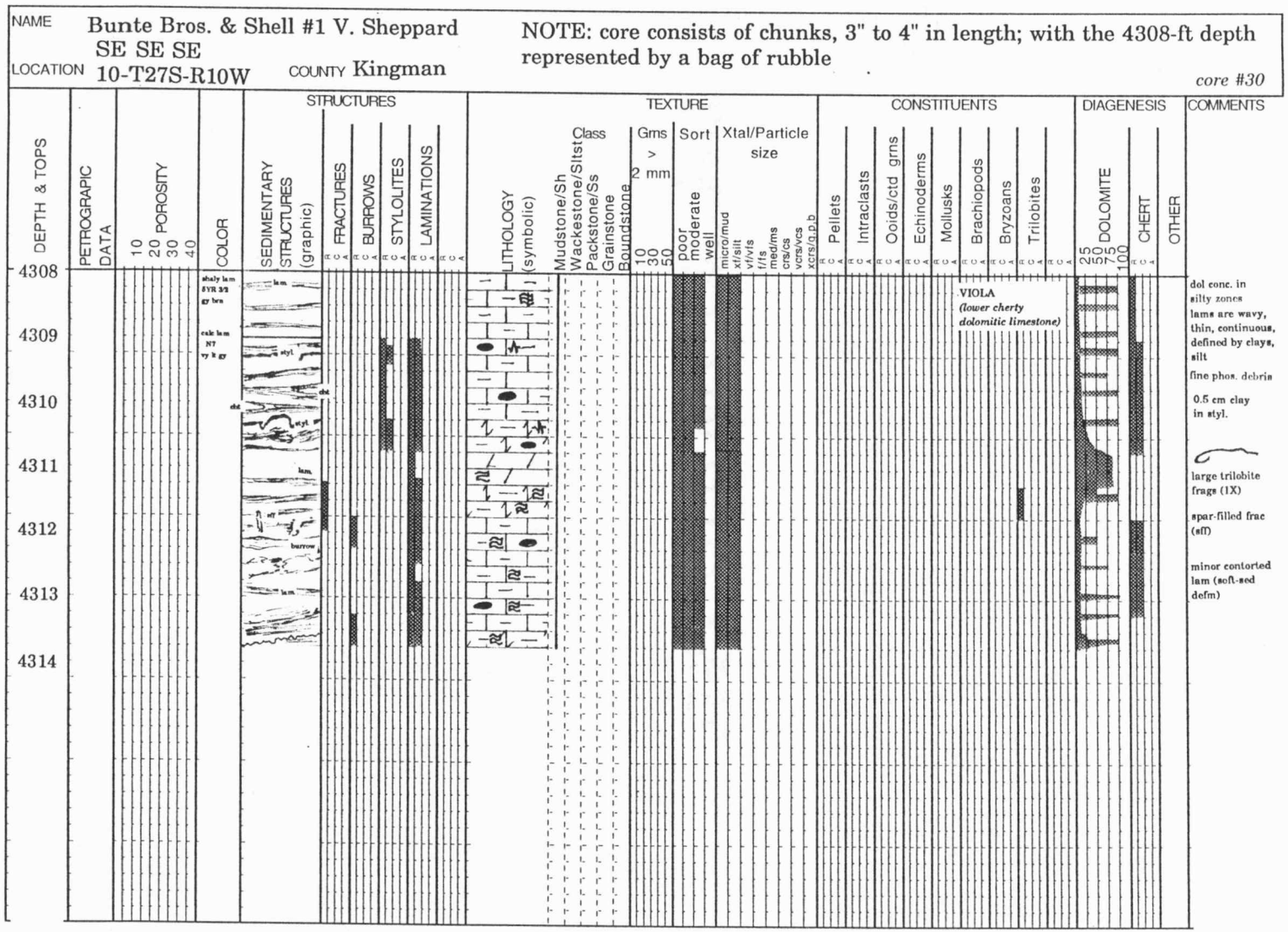
NAME Bunte Bros. & Shell #1 V. Sheppard
SE SE SE
LOCATION 10-T27S-R10W COUNTY Kingman
NOTE: core consists of chunks, 3" to 4" in length; with the 4308-ft depth represented by a bag of rubble
core #30
DEPTH & TOPS
PETROGRAPHIC DATA
10 20 POROSITY 30 40
COLOR
STRUCTURES
SEDIMENTARY STRUCTURES (graphic)
FRACTURES
BURROWS
STYLOLITES
LAMINATIONS
TEXTURE
LITHOLOGY (symbolic)
Class
Mudstone/Sh
Wackestone/Sltst
Packstone/Ss
Grainstone
Boundstone
Gms > 2 mm
10 30 50
Sort
poor moderate well
Xtal/Particle size
micro/mud
xf/silt
vf/vfs
f/fs
med/ms
crs/cs
vcrs/vcs
xcrs/g.p.b
CONSTITUENTS
Pellets
Intraclasts
Ooids/ctd grns
Echinoderms
Mollusks
Brachiopods
Bryzoans
Trilobites
DIAGENESIS
25 50 75 100 DOLOMITE
CHERT
OTHER
COMMENTS
4308
4309
4310
4311
4312
4313
4314
shaly lam 5YR 3/2 gy brn
calc lam N7 vy lt gy
lam
styl
cht
burrow
VIOLA
(lower cherty dolomitic limestone)
dol conc. in silty zones
lams are wavy, thin, continuous, defined by clays, silt
fine phos. debris
0.5 cm clay in styl.
large trilobite frags (1X)
spar-filled frac (sff)
minor contorted lam (soft-sed defm)

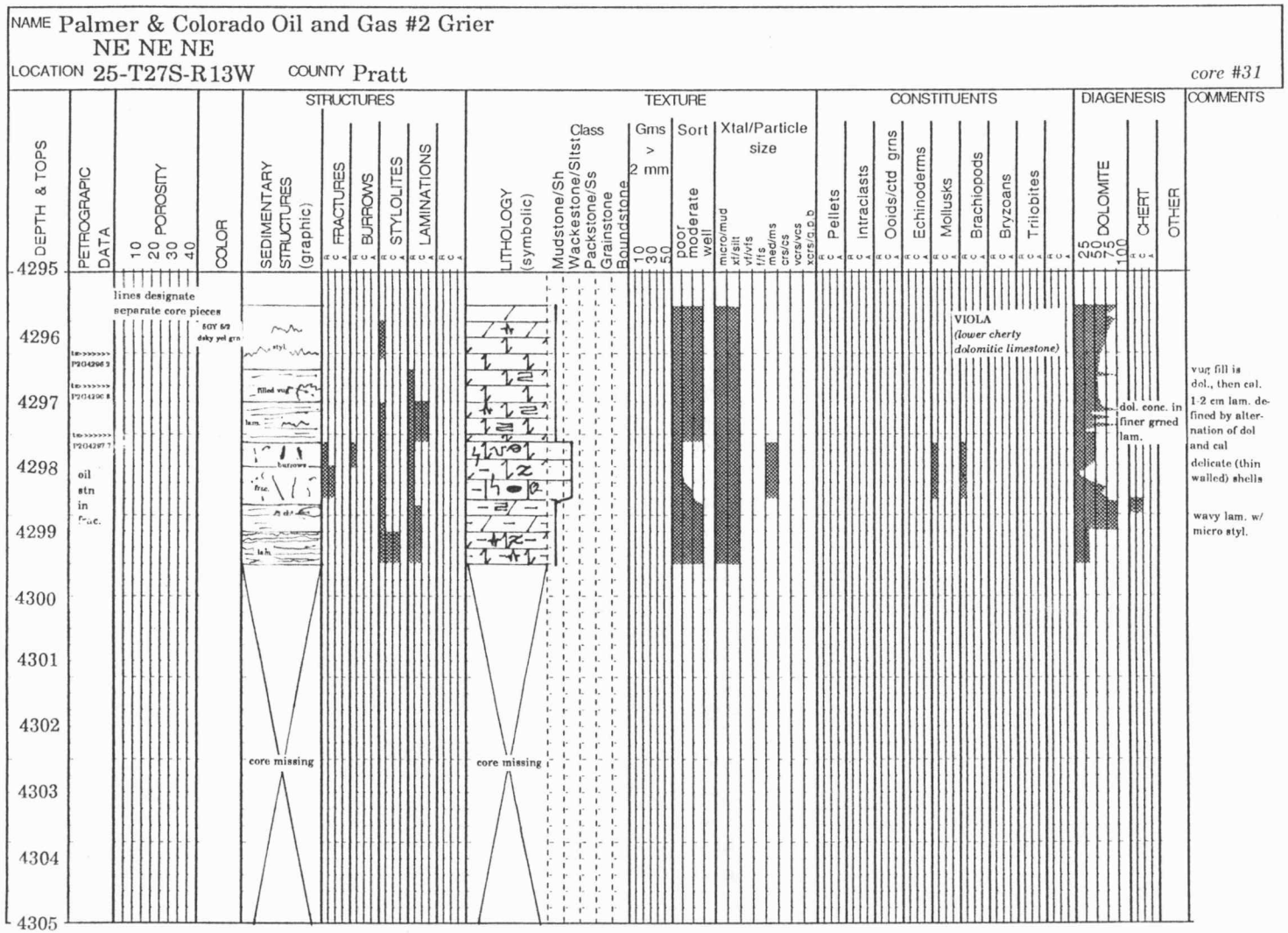
NAME Palmer & Colorado Oil and Gas #2 Grier
NE NE NE
LOCATION 25-T27S-R13W
COUNTY Pratt
core #31
DEPTH & TOPS
PETROGRAPHIC DATA
POROSITY
10 20 30 40
COLOR
STRUCTURES
SEDIMENTARY STRUCTURES (graphic)
FRACTURES
BURROWS
STYLOLITES
LAMINATIONS
TEXTURE
LITHOLOGY (symbolic)
Class
Mudstone/Sh
Wackestone/Sltst
Packstone/Ss
Grainstone
Boundstone
Grns > 2 mm
10 30 50
Sort
poor moderate well
Xtal/Particle size
micro/mud
xf/silt
vf/vfs
f/fs
med/ms
crs/cs
vcrs/vcs
vcrs/g.p.b
CONSTITUENTS
Pellets
Intraclasts
Ooids/ctd grns
Echinoderms
Mollusks
Brachiopods
Bryzoans
Trilobites
DIAGENESIS
25 50 75 100
DOLOMITE
CHERT
OTHER
COMMENTS
4295
4296
4297
4298
4299
4300
4301
4302
4303
4304
4305
lines designate separate core pieces
5GY 6/2 dsky yel grn
styl.
filled vug
lam.
burrows
frac.
lam.
oil stn in frac.
core missing
core missing
VIOLA
(lower cherty dolomitic limestone)
vug fill is dol., then cal.
1-2 cm lam. defined by alternation of dol and cal
delicate (thin walled) shells
dol. cone. in finer grned lam.
wavy lam. w/ micro styl.

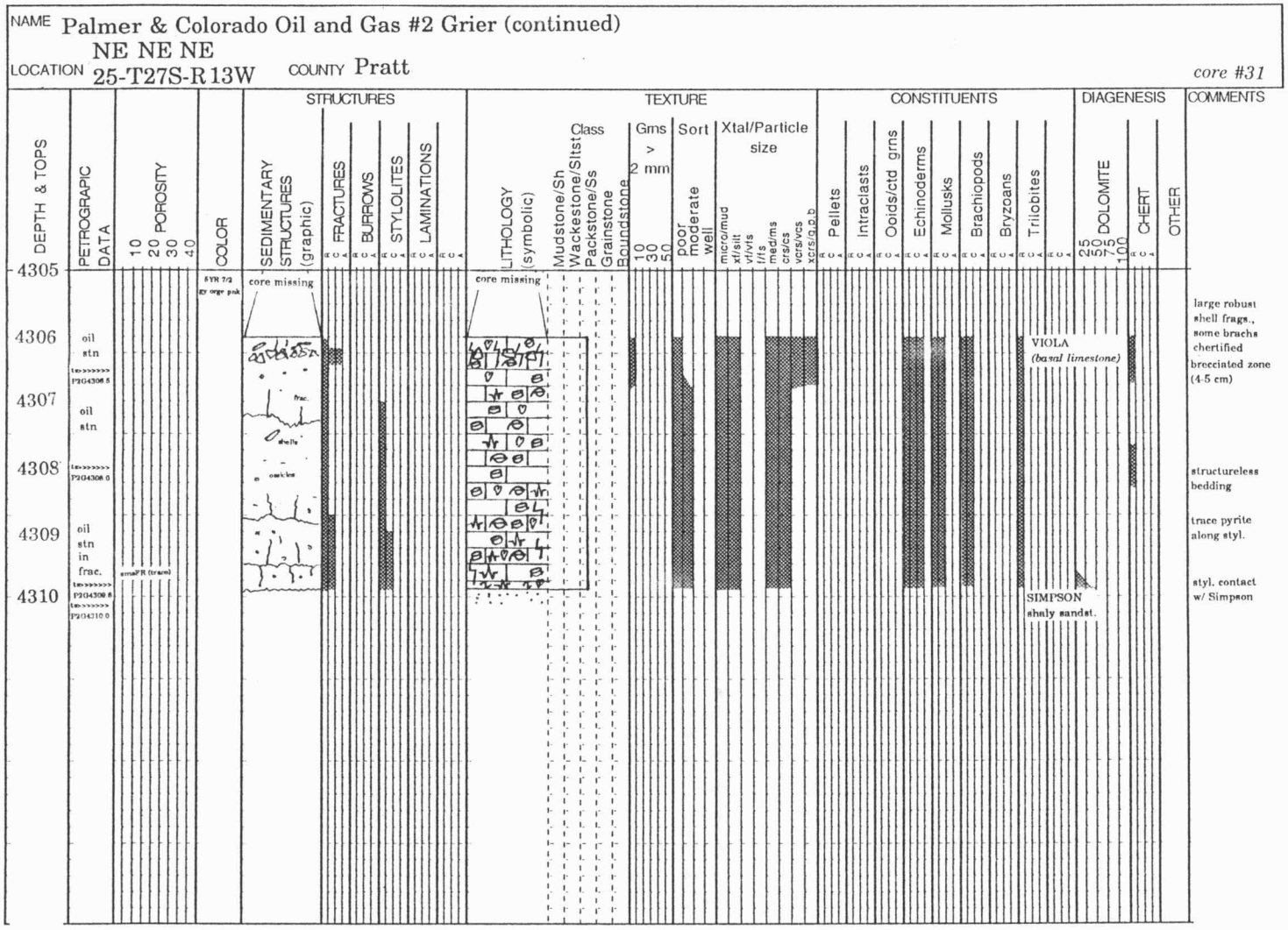
NAME Palmer & Colorado Oil and Gas #2 Grier (continued)
LOCATION NE NE NE 25-T27S-R13W
COUNTY Pratt
core #31
STRUCTURES
TEXTURE
CONSTITUENTS
DIAGENESIS
COMMENTS
DEPTH & TOPS
PETROGRAPHIC DATA
10 20 POROSITY 30 40
COLOR
SEDIMENTARY STRUCTURES (graphic)
FRACTURES
BURROWS
STYLOLITES
LAMINATIONS
LITHOLOGY (symbolic)
Class
Mudstone/Sh
Wackestone/Sltst
Packstone/Ss
Grainstone
Boundstone
Gms > 2 mm
10 30 50
Sort
poor moderate well
Xtal/Particle size
micr/mud
vf/slt
vf/vls
f/fs
med/ms
crs/cs
vcrs/vcs
xcrs/g,p,b
Pellets
Intraclasts
Ooids/ctd grns
Echinoderms
Mollusks
Brachiopods
Bryzoans
Trilobites
25 50 75 100 DOLOMITE
CHERT
OTHER
4305
4306
4307
4308
4309
4310
oil stn
oil stn
oil stn in frac.
5YR 7/2 gy orge pnk
core missing
core missing
frac.
shelly
oolicles
VIOLA
(basal limestone)
SIMPSON
shaly sandst.
large robust shell frags., some brachs chertified brecciated zone (4-5 cm)
structureless bedding
trace pyrite along styl.
styl. contact w/ Simpson

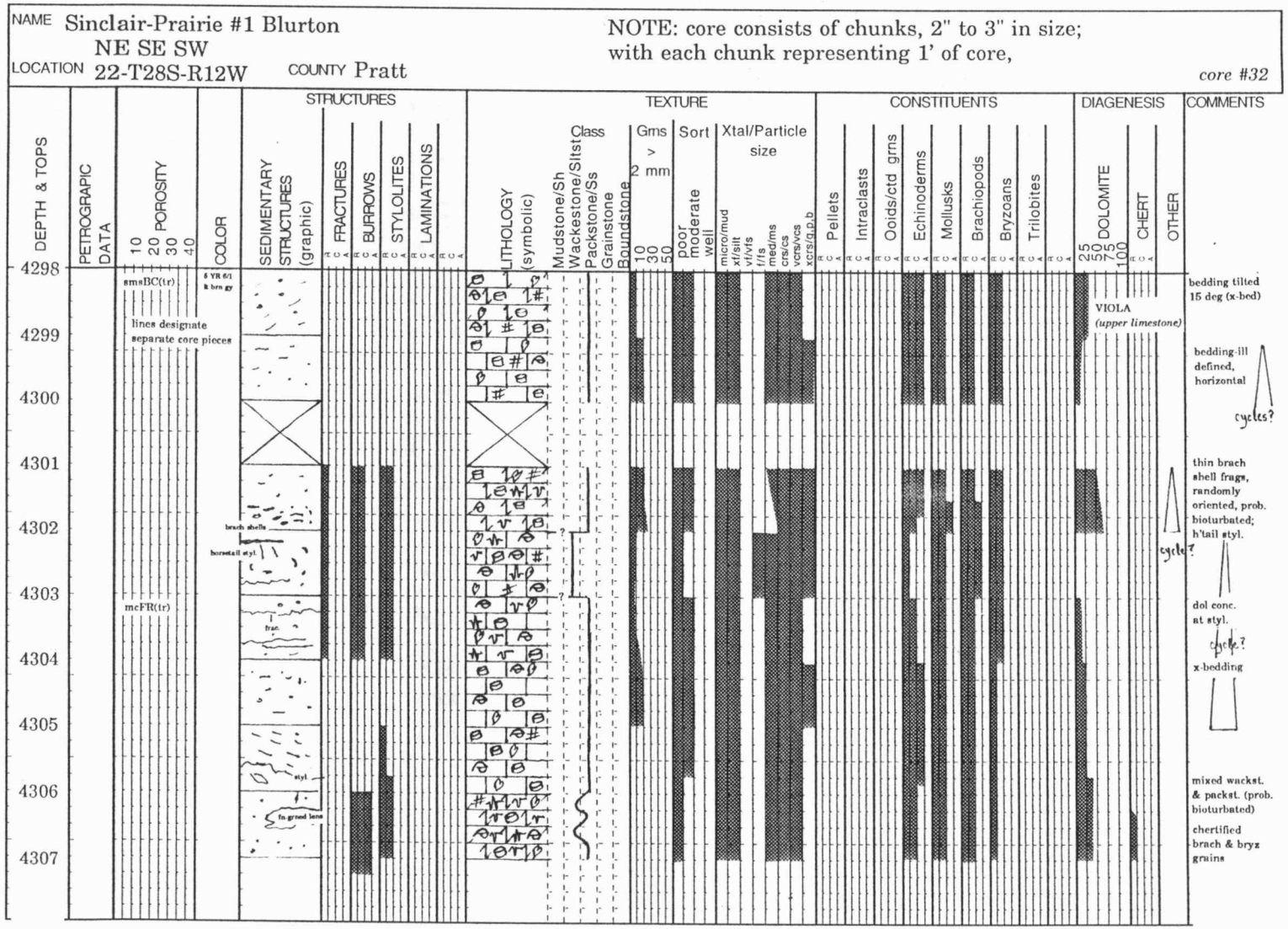
NAME Sinclair-Prairie #1 Blurton
NE SE SW
LOCATION 22-T28S-R12W
COUNTY Pratt
NOTE: core consists of chunks, 2" to 3" in size; with each chunk representing 1' of core,
core #32
DEPTH & TOPS
PETROGRAPHIC DATA
POROSITY
COLOR
STRUCTURES
SEDIMENTARY STRUCTURES (graphic)
FRACTURES
BURROWS
STYLOLITES
LAMINATIONS
TEXTURE
LITHOLOGY (symbolic)
Class
Mudstone/Sh
Wackestone/Slts
Packstone/Ss
Grainstone
Boundstone
Gms > 2 mm
Sort
poor
moderate
well
Xtal/Particle size
micro/mud
xf/silt
vf/vfs
f/fs
med/ms
crs/cs
vcrs/vcs
xcrs/g,p,b
CONSTITUENTS
Pellets
Intraclasts
Ooids/ctd grns
Echinoderms
Mollusks
Brachiopods
Bryzoans
Trilobites
DIAGENESIS
DOLOMITE
CHERT
OTHER
COMMENTS
4298
4299
4300
4301
4302
4303
4304
4305
4306
4307
smsBC(tr)
lines designate separate core pieces
mcFR(tr)
5 YR 6/1 lt brn gy
brach shells
horsetail styl
frac
styl
fn grned lens
VIOLA
(upper limestone)
cycle?
bedding tilted 15 deg (x-bed)
bedding-ill defined, horizontal
cycles?
thin brach shell frags, randomly oriented, prob. bioturbated; h'tail styl.
dol conc. at styl.
cycle?
x-bedding
mixed wackst. & packst. (prob. bioturbated)
chertified brach & bryz grains

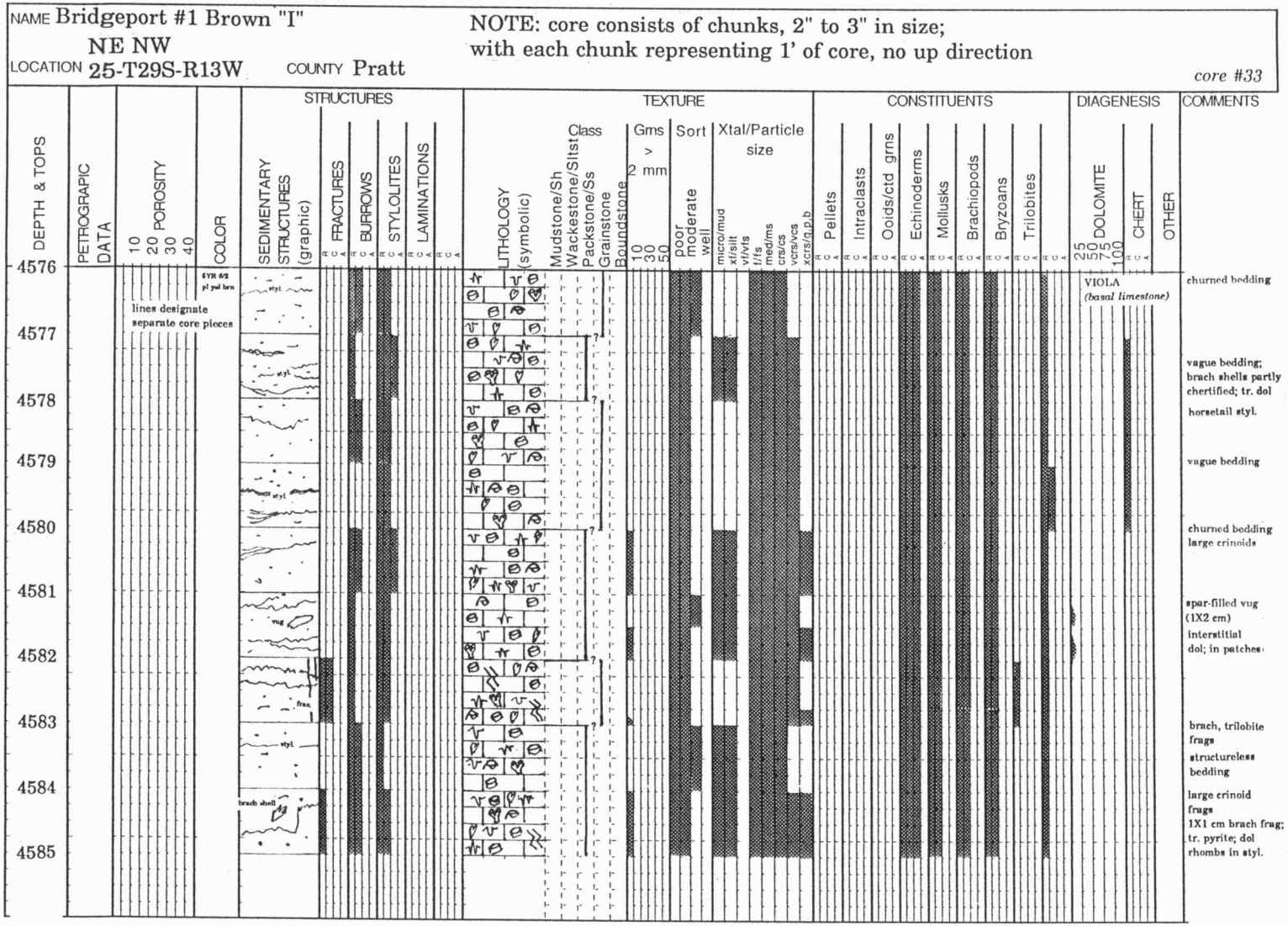
NAME Bridgeport #1 Brown "I"
NE NW
LOCATION 25-T29S-R13W
COUNTY Pratt
NOTE: core consists of chunks, 2" to 3" in size;
with each chunk representing 1' of core, no up direction
core #33
DEPTH & TOPS
PETROGRAPHIC DATA
POROSITY
COLOR
STRUCTURES
SEDIMENTARY STRUCTURES (graphic)
FRACTURES
BURROWS
STYLOLITES
LAMINATIONS
TEXTURE
LITHOLOGY (symbolic)
Class
Mudstone/Sh
Wackestone/Sltst
Packstone/Ss
Grainstone
Boundstone
Gms > 2 mm
Sort
poor
moderate
well
Xtal/Particle size
micro/mud
vf/silt
vf/vfs
f/fs
med/ms
crs/cs
vcrs/vcs
xcrs/g.p.b
CONSTITUENTS
Pellets
Intraclasts
Ooids/ctd grns
Echinoderms
Mollusks
Brachiopods
Bryzoans
Trilobites
DIAGENESIS
DOLOMITE
CHERT
OTHER
COMMENTS
4576
4577
4578
4579
4580
4581
4582
4583
4584
4585
lines designate separate core pieces
6YR 6/2 pl yel brn
styl.
vug
frac.
brach shell
VIOLA
(basal limestone)
churned bedding
vague bedding; brach shells partly chertified; tr. dol
horsetail styl.
vague bedding
churned bedding large crinoids
spar-filled vug (1X2 cm) interstitial dol; in patches
brach, trilobite frags
structureless bedding
large crinoid frags
1X1 cm brach frag; tr. pyrite; dol rhombs in styl.

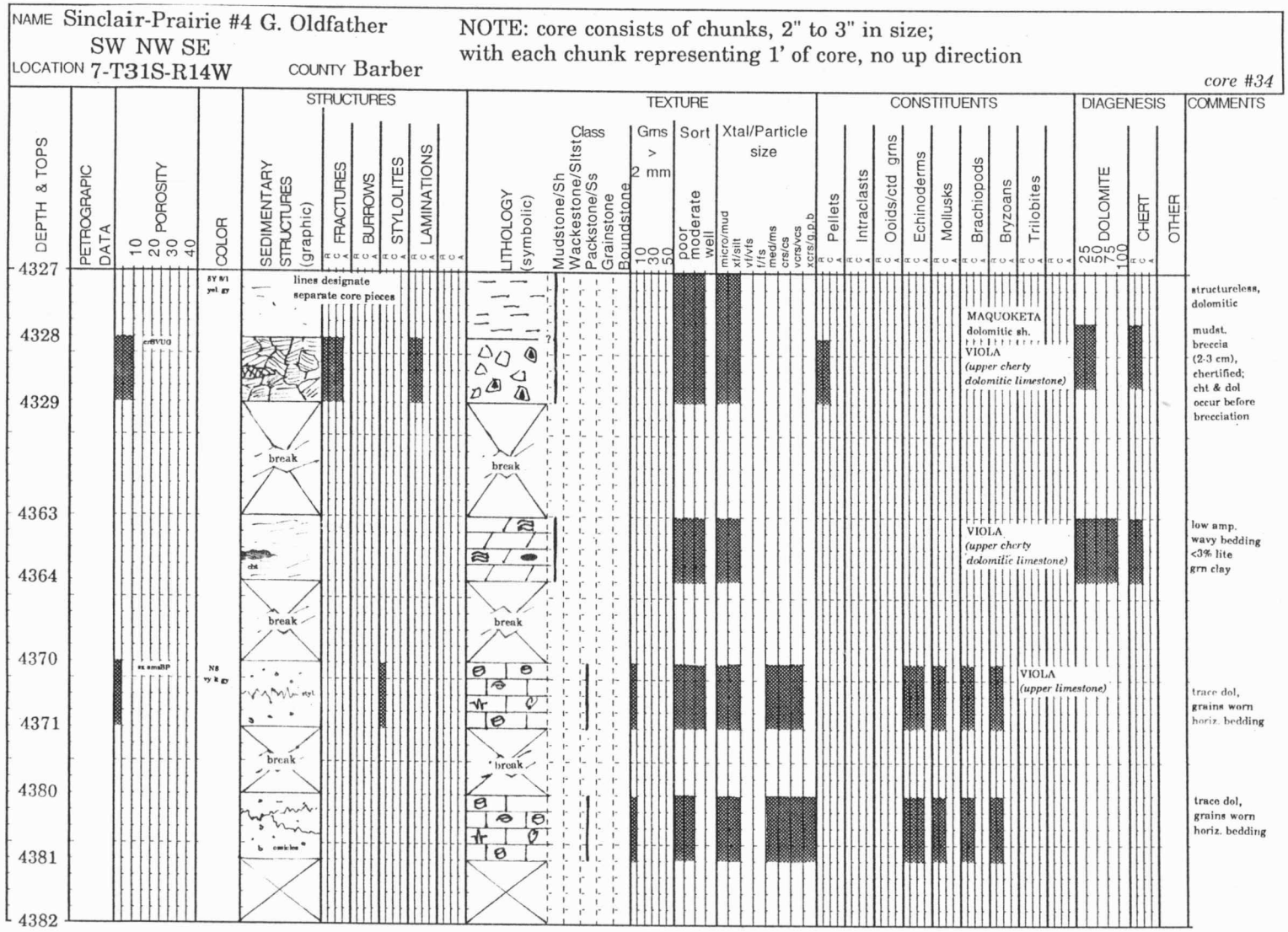
NAME Sinclair-Prairie #4 G. Oldfather
SW NW SE
LOCATION 7-T31S-R14W
COUNTY Barber
NOTE: core consists of chunks, 2" to 3" in size;
with each chunk representing 1' of core, no up direction
core #34
DEPTH & TOPS
PETROGRAPHIC DATA
POROSITY
COLOR
STRUCTURES
SEDIMENTARY STRUCTURES (graphic)
FRACTURES
BURROWS
STYLOLITES
LAMINATIONS
TEXTURE
LITHOLOGY (symbolic)
Class
Mudstone/Sh
Wackestone/Sltst
Packstone/Ss
Grainstone
Boundstone
Gms > 2 mm
Sort
poor
moderate
well
Xtal/Particle size
micro/mud
xf/silt
vf/vfs
f/fs
med/ms
crs/cs
vcrs/vcs
xcrs/g,p,b
CONSTITUENTS
Pellets
Intraclasts
Ooids/ctd grns
Echinoderms
Mollusks
Brachiopods
Bryzoans
Trilobites
DIAGENESIS
DOLOMITE
CHERT
OTHER
COMMENTS
4327
4328
4329
4363
4364
4370
4371
4380
4381
4382
lines designate
separate core pieces
break
MAQUOKETA
dolomitic sh.
VIOLA
(upper cherty
dolomitic limestone)
VIOLA
(upper cherty
dolomitic limestone)
VIOLA
(upper limestone)
structureless,
dolomitic
mudst.
breccia
(2-3 cm),
chertified;
cht & dol
occur before
brecciation
low amp.
wavy bedding
<3% lite
grn clay
trace dol,
grains worn
horiz. bedding
trace dol,
grains worn
horiz. bedding

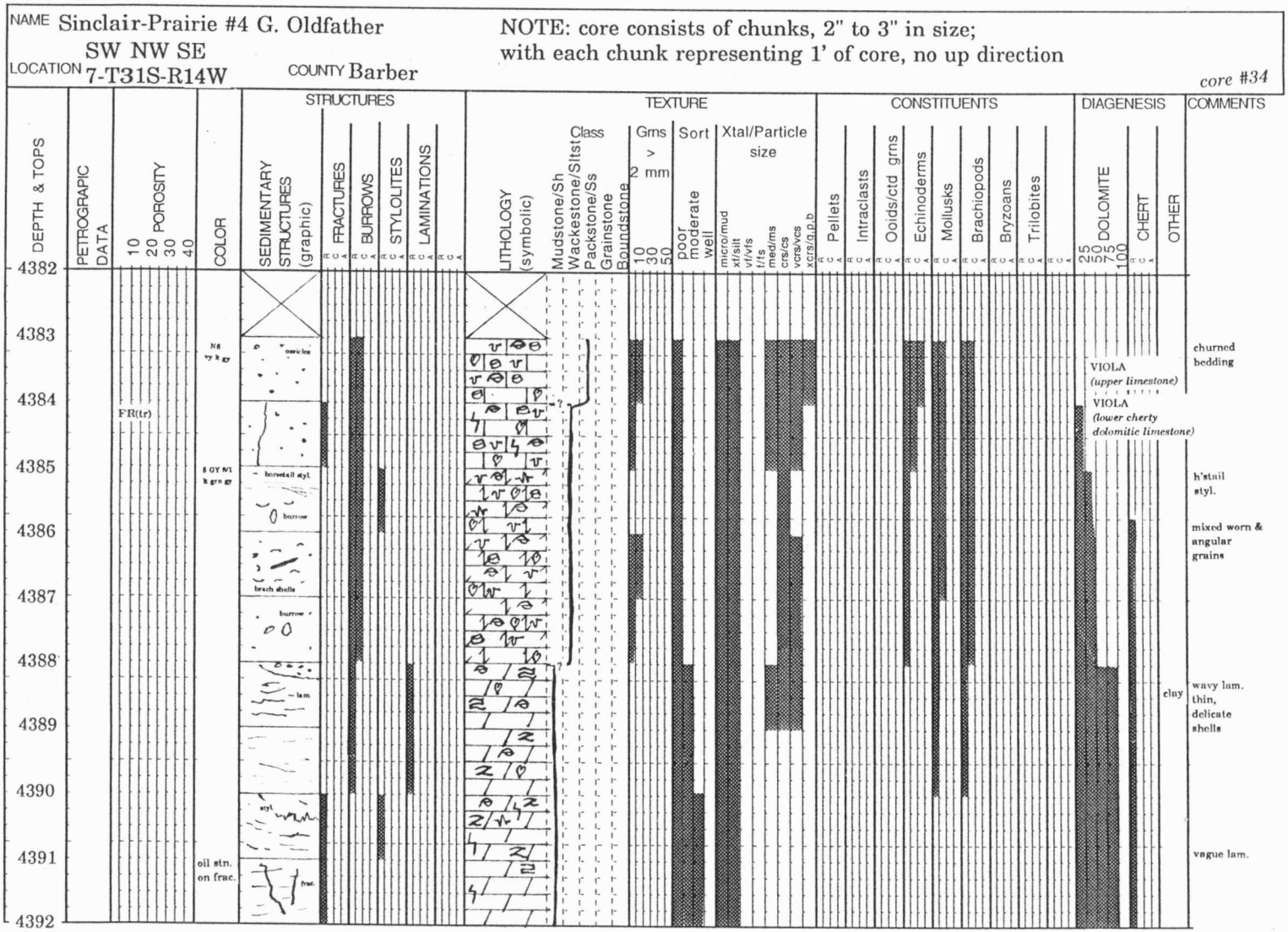
NAME Sinclair-Prairie #4 G. Oldfather
SW NW SE
LOCATION 7-T31S-R14W
COUNTY Barber
NOTE: core consists of chunks, 2" to 3" in size;
with each chunk representing 1' of core, no up direction
core #34
DEPTH & TOPS
PETROGRAPHIC DATA
POROSITY
COLOR
STRUCTURES
SEDIMENTARY STRUCTURES (graphic)
FRACTURES
BURROWS
STYLOLITES
LAMINATIONS
TEXTURE
LITHOLOGY (symbolic)
Class
Mudstone/Sh
Wackestone/Slst
Packstone/Ss
Grainstone
Boundstone
Grns > 2 mm
Sort
poor
moderate
well
Xtal/Particle size
micro/mud
xf/silt
vf/vfs
f/fs
med/ms
crs/cs
vcrs/vcs
xcrs/g,p,b
CONSTITUENTS
Pellets
Intraclasts
Ooids/ctd grns
Echinoderms
Mollusks
Brachiopods
Bryzoans
Trilobites
DIAGENESIS
DOLOMITE
CHERT
OTHER
COMMENTS
4382
4383
4384
4385
4386
4387
4388
4389
4390
4391
4392
FR(tr)
oil stn. on frac.
oosicles
horsetail styl.
burrow
brach shells
burrow
lam.
styl.
frac.
VIOLA
(upper limestone)
VIOLA
(lower cherty
dolomitic limestone)
clay
churned bedding
h'stail styl.
mixed worn & angular grains
wavy lam. thin, delicate shells
vague lam.

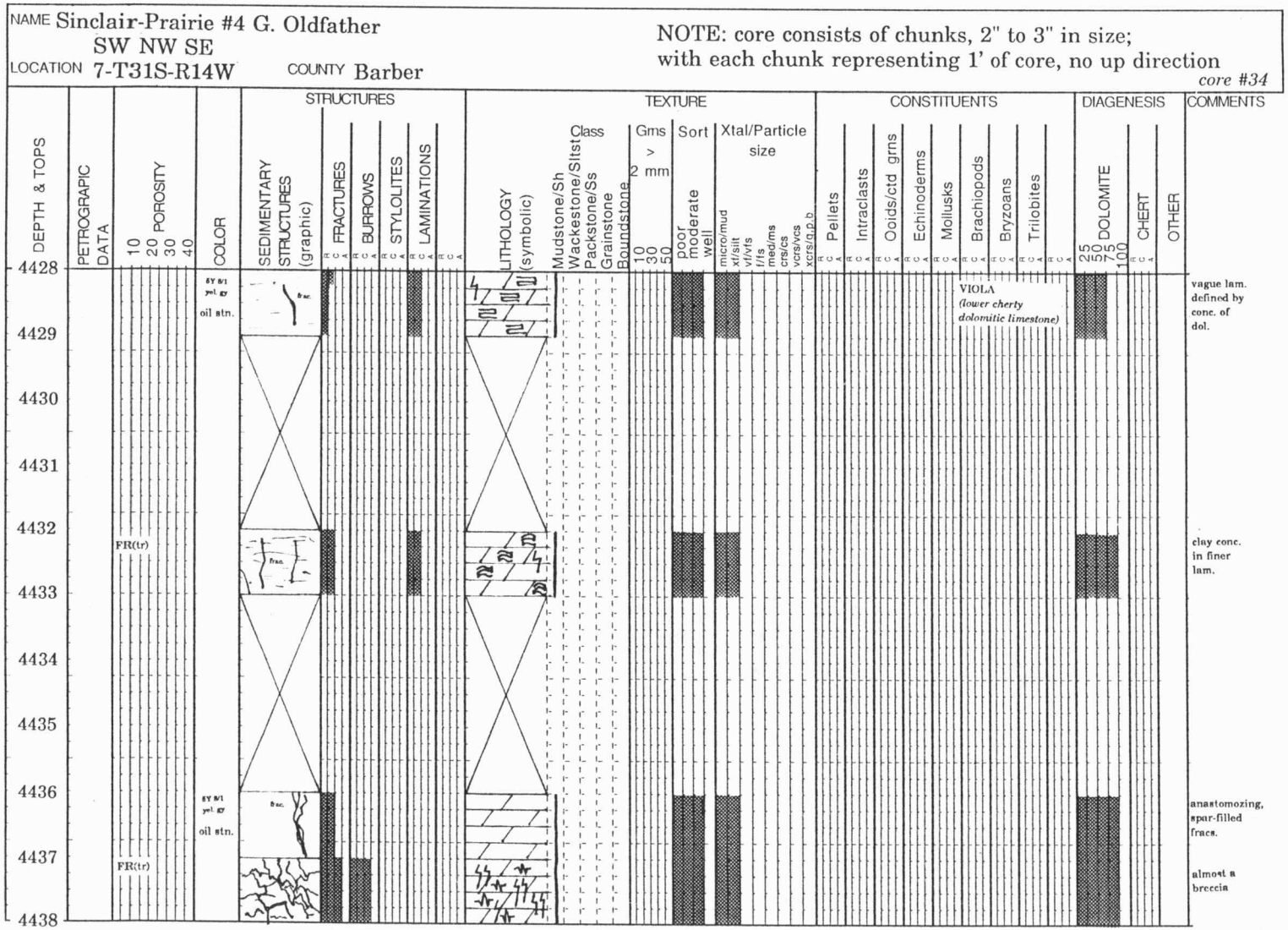
NAME Sinclair-Prairie #4 G. Oldfather
SW NW SE
LOCATION 7-T31S-R14W
COUNTY Barber
NOTE: core consists of chunks, 2" to 3" in size;
with each chunk representing 1' of core, no up direction
core #34
DEPTH & TOPS
PETROGRAPIC DATA
POROSITY
COLOR
STRUCTURES
SEDIMENTARY STRUCTURES (graphic)
FRACTURES
BURROWS
STYLOLITES
LAMINATIONS
TEXTURE
LITHOLOGY (symbolic)
Class
Mudstone/Sh
Wackestone/Sltst
Packstone/Ss
Grainstone
Boundstone
Gms > 2 mm
Sort
poor
moderate
well
Xtal/Particle size
micro/mud
xf/silt
vf/vfs
f/fs
med/ms
crs/cs
vcrs/vcs
xcrs/g.p.b.
CONSTITUENTS
Pellets
Intraclasts
Ooids/ctd grns
Echinoderms
Mollusks
Brachiopods
Bryzoans
Trilobites
DIAGENESIS
DOLOMITE
CHERT
OTHER
COMMENTS
4428
4429
4430
4431
4432
4433
4434
4435
4436
4437
4438
oil stn.
oil stn.
FR(tr)
FR(tr)
VIOLA
(lower cherty dolomitic limestone)
vague lam. defined by conc. of dol.
clay conc. in finer lam.
anastomozing, spar-filled fracs.
almost a breccia

NAME Sinclair-Prairie #4 G. Oldfather
SW NW SE
LOCATION 7-T31S-R14W COUNTY Barber

NOTE: core consists of chunks, 2" to 3" in size; with each chunk representing 1' of core, no up direction

core #34

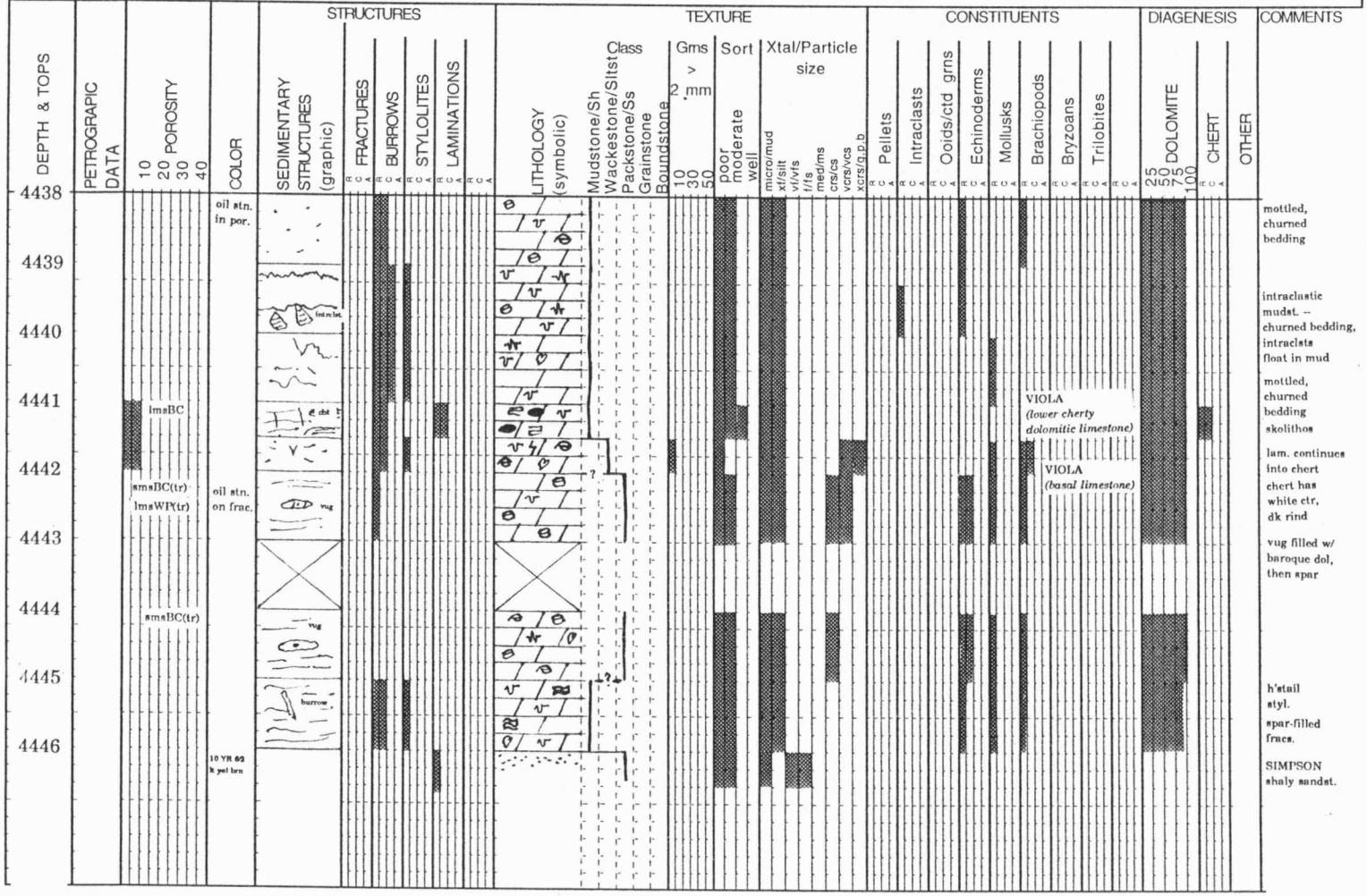

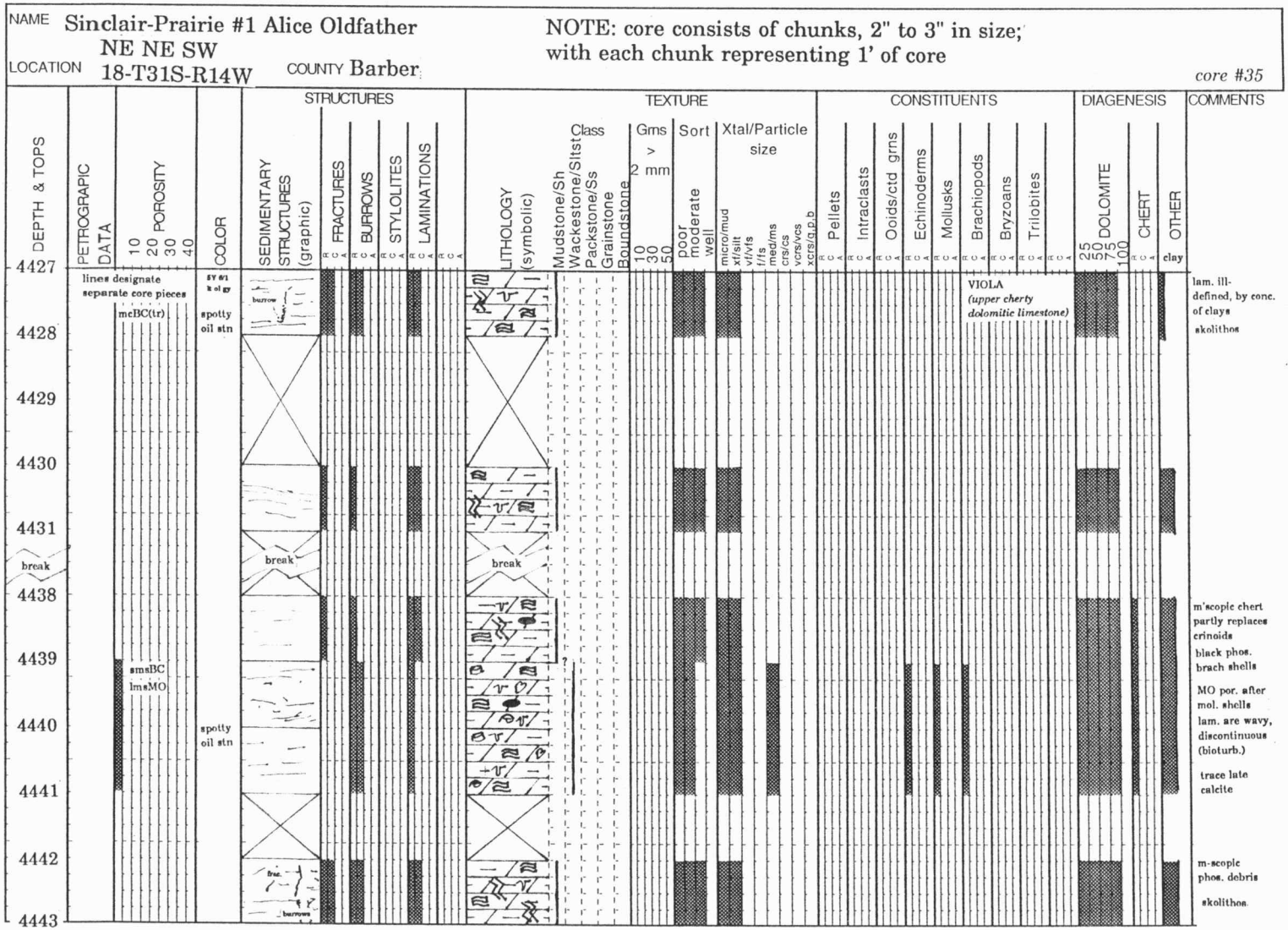
NAME Sinclair-Prairie #1 Alice Oldfather
LOCATION NE NE SW 18-T31S-R14W
COUNTY Barber
NOTE: core consists of chunks, 2" to 3" in size; with each chunk representing 1' of core
core #35
STRUCTURES
TEXTURE
CONSTITUENTS
DIAGENESIS
COMMENTS
DEPTH & TOPS
PETROGRAPIC DATA
POROSITY
COLOR
SEDIMENTARY STRUCTURES (graphic)
FRACTURES
BURROWS
STYLOLITES
LAMINATIONS
LITHOLOGY (symbolic)
Class
Mudstone/Sh
Wackestone/Sltst
Packstone/Ss
Grainstone
Boundstone
Grns > 2 mm
Sort
poor
moderate
well
Xtal/Particle size
micro/mud
vf/slt
vf/vs
f/fs
med/ms
crs/cs
vcrs/vcs
xcrs/g.p.b
Pellets
Intraclasts
Ooids/ctd grns
Echinoderms
Mollusks
Brachiopods
Bryzoans
Trilobites
DOLOMITE
CHERT
OTHER
clay
4427
4428
4429
4430
4431
break
4438
4439
4440
4441
4442
4443
lines designate separate core pieces
mcBC(tr)
smsBC
lmsMO
spotty oil stn
spotty oil stn
burrow
break
break
VIOLA
(upper cherty dolomitic limestone)
lam. ill-defined, by conc. of clays
skolithos
m'scopic chert partly replaces crinoids
black phos. brach shells
MO por. after mol. shells
lam. are wavy, discontinuous (bioturb.)
trace late calcite
m-scopic phos. debris
skolithos

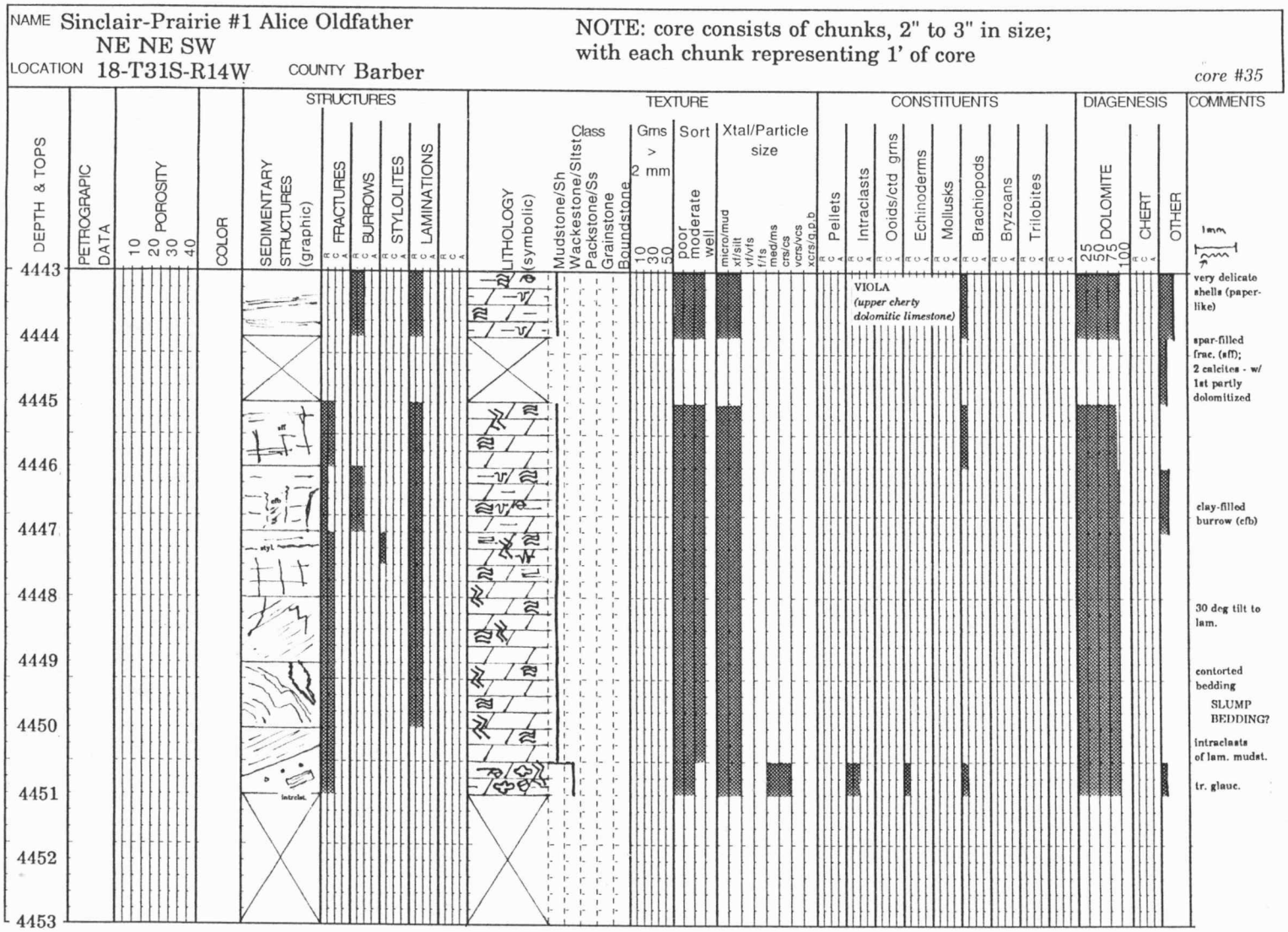
NAME Sinclair-Prairie #1 Alice Oldfather
NE NE SW
LOCATION 18-T31S-R14W
COUNTY Barber
NOTE: core consists of chunks, 2" to 3" in size; with each chunk representing 1' of core
core #35
DEPTH & TOPS
PETROGRAPHIC DATA
10 20 POROSITY 30 40
COLOR
STRUCTURES
SEDIMENTARY STRUCTURES (graphic)
FRACTURES
BURROWS
STYLOLITES
LAMINATIONS
TEXTURE
LITHOLOGY (symbolic)
Class
Mudstone/Sh
Wackestone/Sltst
Packstone/Ss
Grainstone
Boundstone
Gms > 2 mm
10 30 50
Sort
poor moderate well
Xtal/Particle size
micro/mud
vf/slt
vf/vfs
f/fs
med/ms
crs/cs
vcrs/vcs
xcrs/g,p,b
CONSTITUENTS
Pellets
Intraclasts
Ooids/ctd grns
Echinoderms
Mollusks
Brachiopods
Bryzoans
Trilobites
DIAGENESIS
25 50 75 100
DOLOMITE
CHERT
OTHER
COMMENTS
1mm
4443
4444
4445
4446
4447
4448
4449
4450
4451
4452
4453
VIOLA
(upper cherty dolomitic limestone)
intrclst.
very delicate shells (paper-like)
spar-filled frac. (sff); 2 calcites - w/ 1st partly dolomitized
clay-filled burrow (cfb)
30 deg tilt to lam.
contorted bedding
SLUMP BEDDING?
intraclasts of lam. mudst.
tr. glauc.

NAME Sinclair-Prairie #1 Alice Oldfather (continued)
NE NE SW
LOCATION 18-T31S-R14W COUNTY Barber

NOTE: core consists of chunks, 2" to 3" in size; with each chunk representing 1' of core

core #35

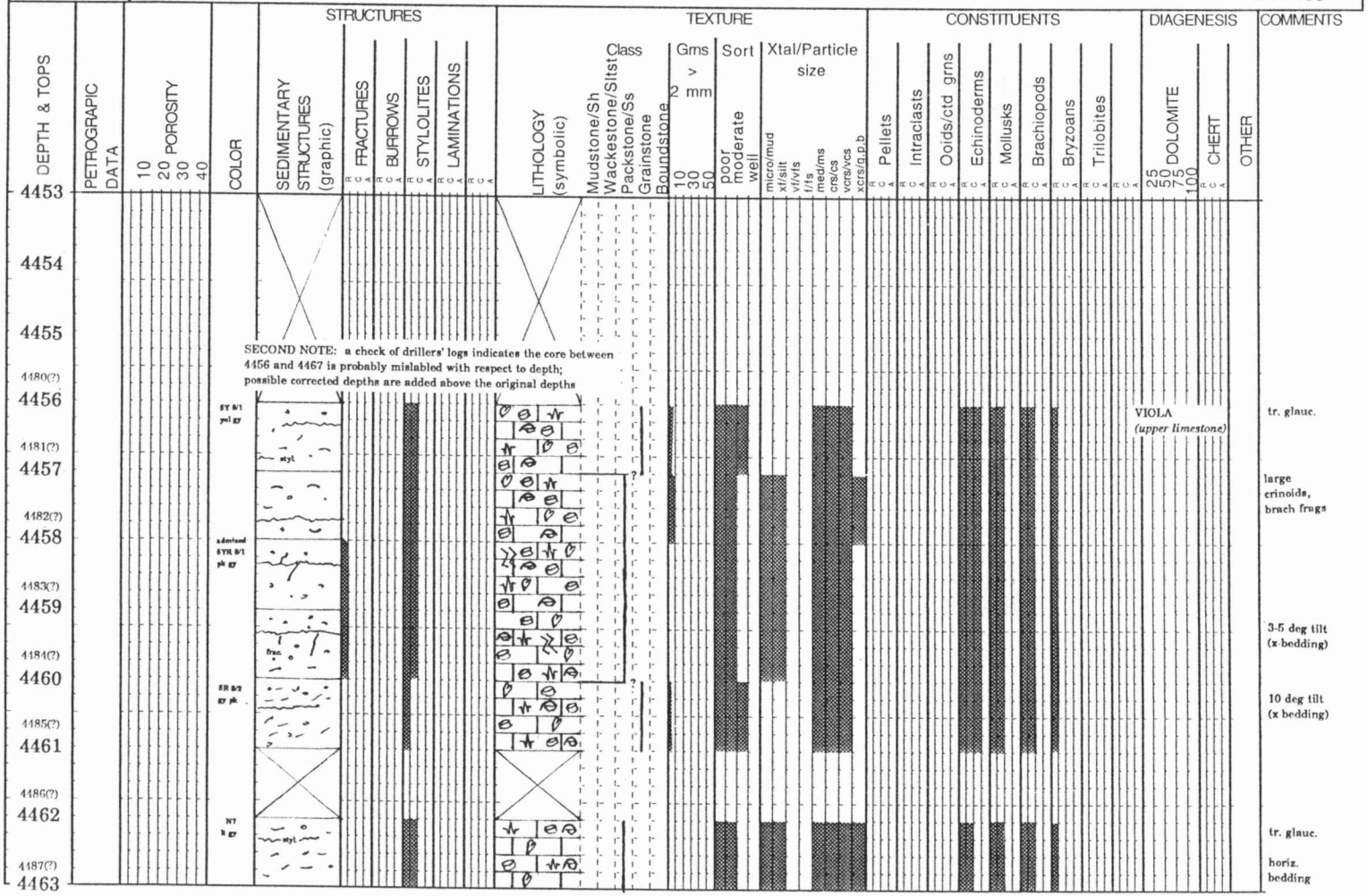

SECOND NOTE: a check of drillers' logs indicates the core between 4456 and 4467 is probably mislabled with respect to depth; possible corrected depths are added above the original depths

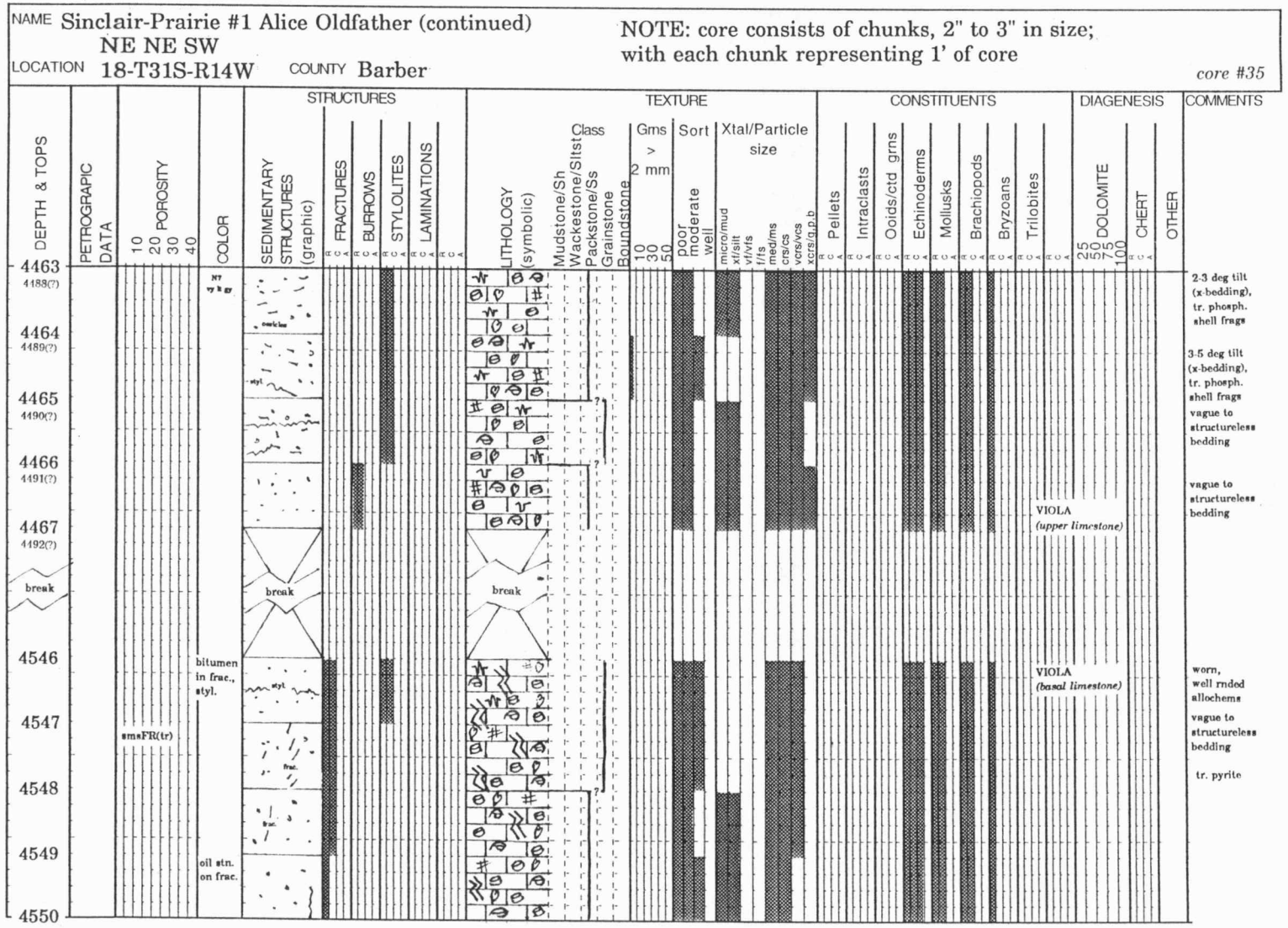
NAME Sinclair-Prairie #1 Alice Oldfather (continued)
NE NE SW
LOCATION 18-T31S-R14W COUNTY Barber
NOTE: core consists of chunks, 2" to 3" in size; with each chunk representing 1' of core
core #35
DEPTH & TOPS
PETROGRAPHIC DATA
POROSITY
COLOR
STRUCTURES
SEDIMENTARY STRUCTURES (graphic)
FRACTURES
BURROWS
STYLOLITES
LAMINATIONS
TEXTURE
LITHOLOGY (symbolic)
Class
Mudstone/Sh
Wackestone/Sltst
Packstone/Ss
Grainstone
Boundstone
Gms > 2 mm
Sort
poor
moderate
well
Xtal/Particle size
micro/mud
xl/silt
vf/vfs
f/fs
med/ms
crs/cs
vcrs/vcs
xcrs/g,p,b
CONSTITUENTS
Pellets
Intraclasts
Ooids/ctd grns
Echinoderms
Mollusks
Brachiopods
Bryzoans
Trilobites
DIAGENESIS
DOLOMITE
CHERT
OTHER
COMMENTS
4463
4188(?)
4464
4489(?)
4465
4490(?)
4466
4491(?)
4467
4492(?)
break
4546
4547
4548
4549
4550
smsFR(tr)
bitumen in frac., styl.
oil stn. on frac.
styl
frac.
VIOLA (upper limestone)
VIOLA (basal limestone)
2-3 deg tilt (x-bedding), tr. phosph. shell frags
3-5 deg tilt (x-bedding), tr. phosph. shell frags vague to structureless bedding
vague to structureless bedding
worn, well rnded allochems
vague to structureless bedding
tr. pyrite

NAME Sinclair-Prairie #1 Alice Oldfather (continued)

LOCATION NE NE SW 18-T31S-R14W COUNTY Barber

NOTE: core consists of chunks, 2" to 3" in size; with each chunk representing 1' of core

core #35

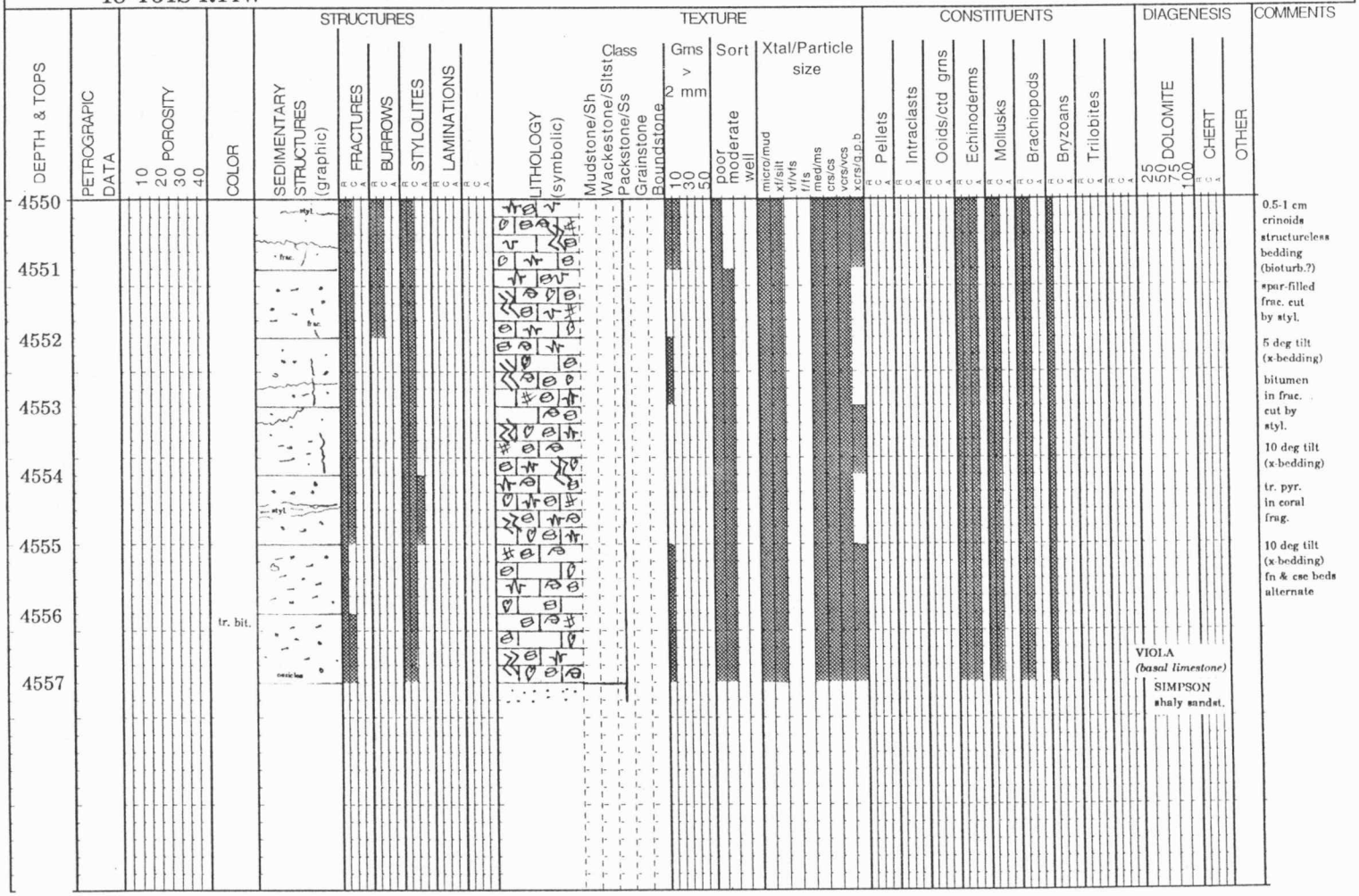

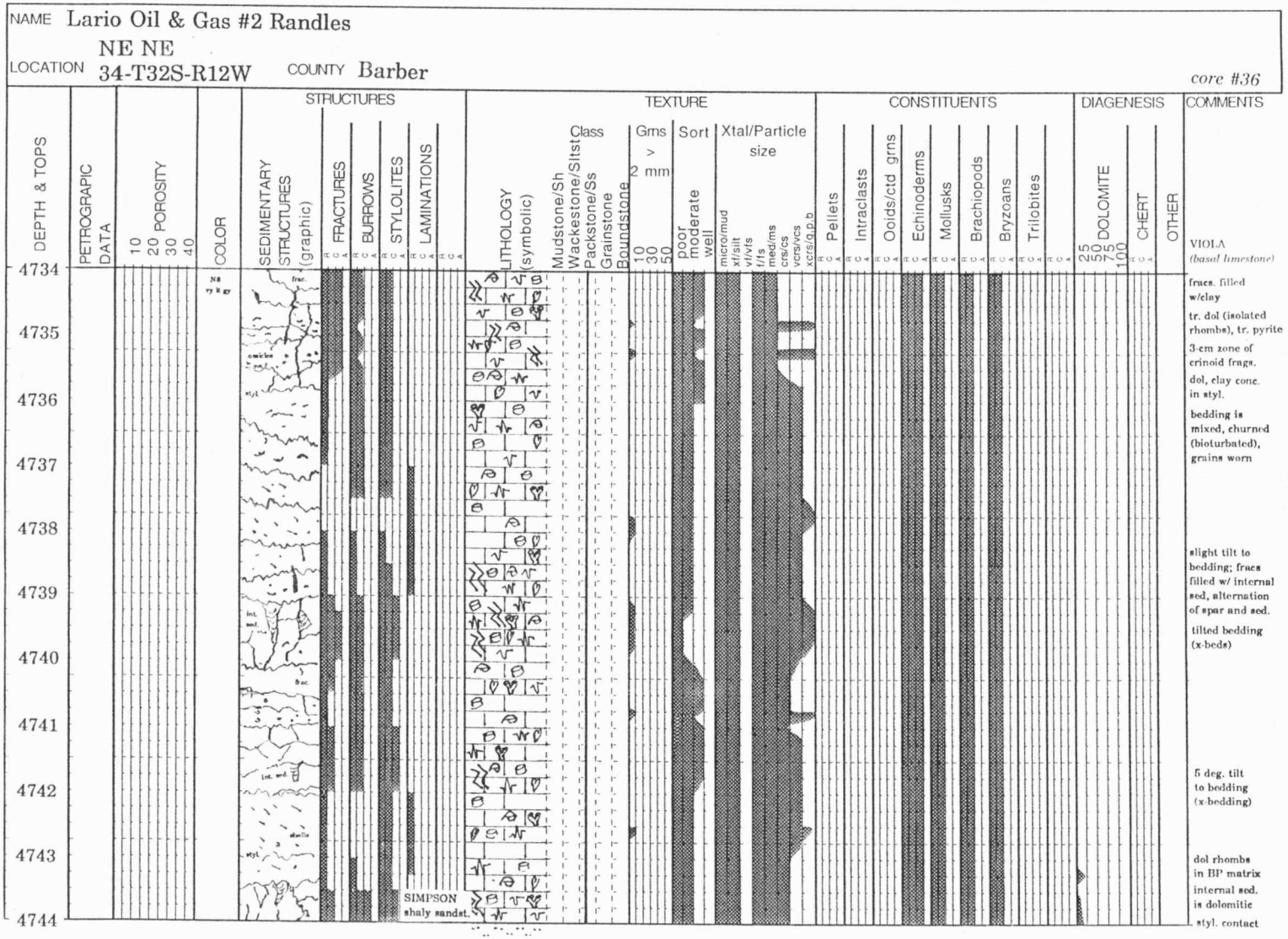
NAME Lario Oil & Gas #2 Randles
LOCATION NE NE 34-T32S-R12W
COUNTY Barber
core #36
DEPTH & TOPS
PETROGRAPHIC DATA
POROSITY
COLOR
STRUCTURES
SEDIMENTARY STRUCTURES (graphic)
FRACTURES
BURROWS
STYLOLITES
LAMINATIONS
TEXTURE
LITHOLOGY (symbolic)
Class
Mudstone/Sh
Wackestone/Sltst
Packstone/Ss
Grainstone
Boundstone
Grns > 2 mm
Sort
poor
moderate
well
Xtal/Particle size
micr/mud
xf/silt
vf/vfs
f/fs
med/ms
crs/cs
vcrs/vcs
xcrs/g,p,b
CONSTITUENTS
Pellets
Intraclasts
Ooids/ctd grns
Echinoderms
Mollusks
Brachiopods
Bryzoans
Trilobites
DIAGENESIS
DOLOMITE
CHERT
OTHER
COMMENTS
4734
4735
4736
4737
4738
4739
4740
4741
4742
4743
4744
SIMPSON
shaly sandst.
VIOLA
(basal limestone)
fracs. filled w/clay
tr. dol (isolated rhombs), tr. pyrite
3-cm zone of crinoid frags.
dol, clay conc. in styl.
bedding is mixed, churned (bioturbated), grains worn
slight tilt to bedding; fracs filled w/ internal sed, alternation of spar and sed.
tilted bedding (x-beds)
5 deg. tilt to bedding (x-bedding)
dol rhombs in BP matrix
internal sed. is dolomitic
styl. contact

NAME Sinclair #1 M. Binning

LOCATION SE SE SW 26-T32S-R13W COUNTY Barber

NOTE: core consists of chunks, 2" to 3" in size; with each chunk representing 1' of core

core #37

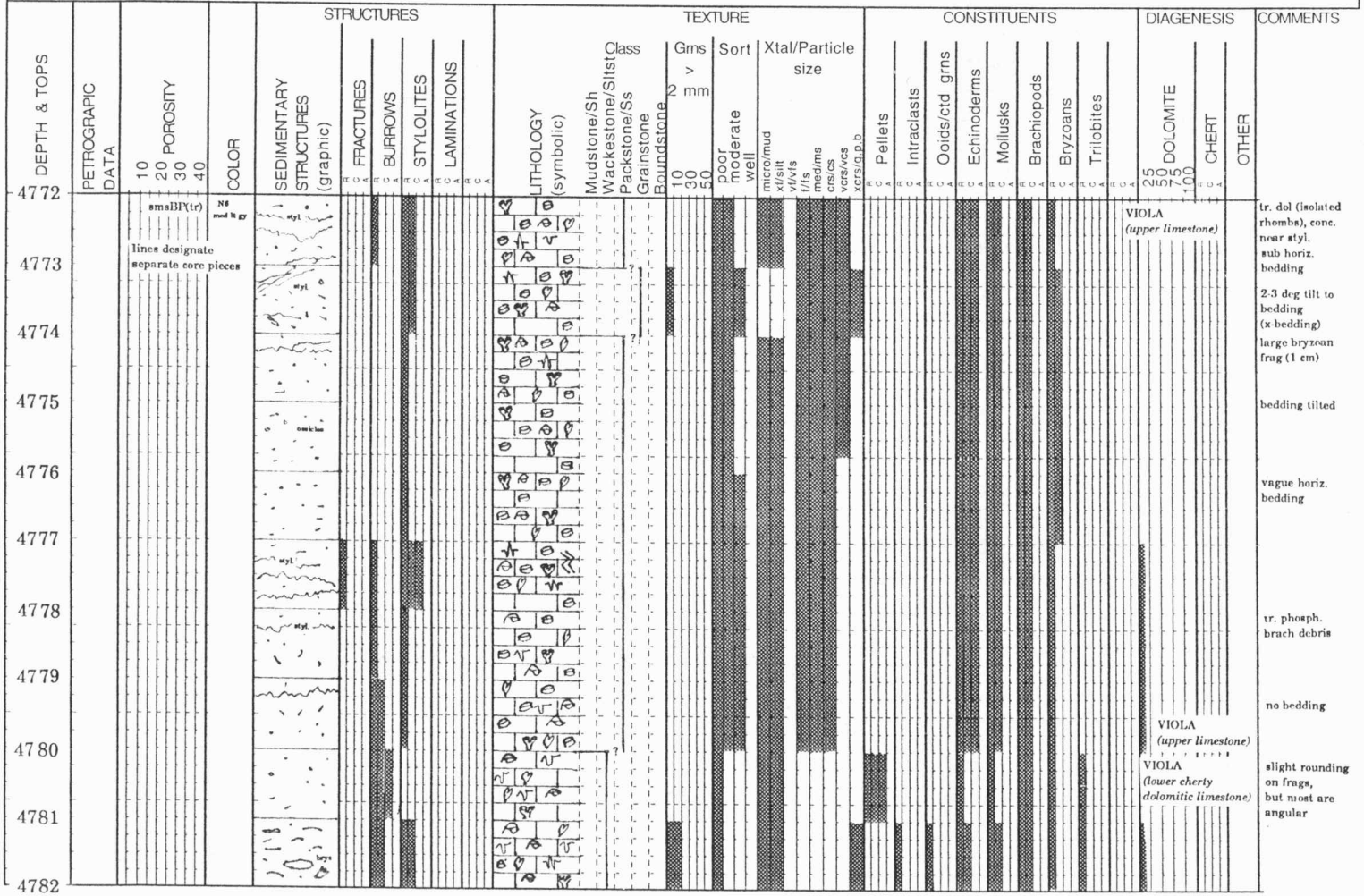

NAME Sinclair #1 M. Binning (continued)
SE SE SW
LOCATION 26-T32S-R13W COUNTY Barber

NOTE: core consists of chunks, 2" to 3" in size; with each chunk representing 1' of core

core #37

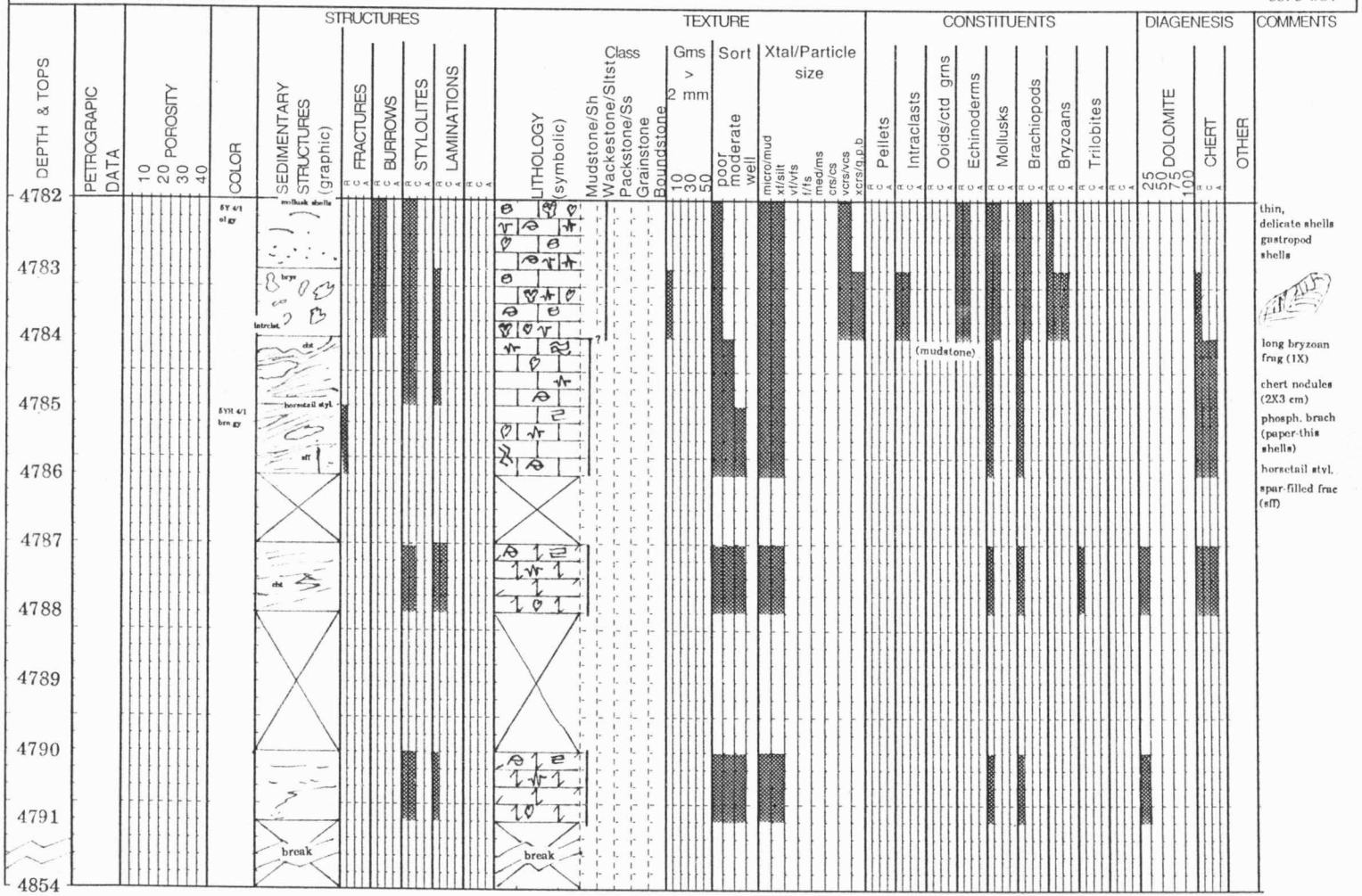

thin, delicate shells gastropod shells

long bryzoan frag (1X)

chert nodules (2X3 cm)

phosph. brach (paper-thin shells)

horsetail styl.

spar-filled frac (sff)

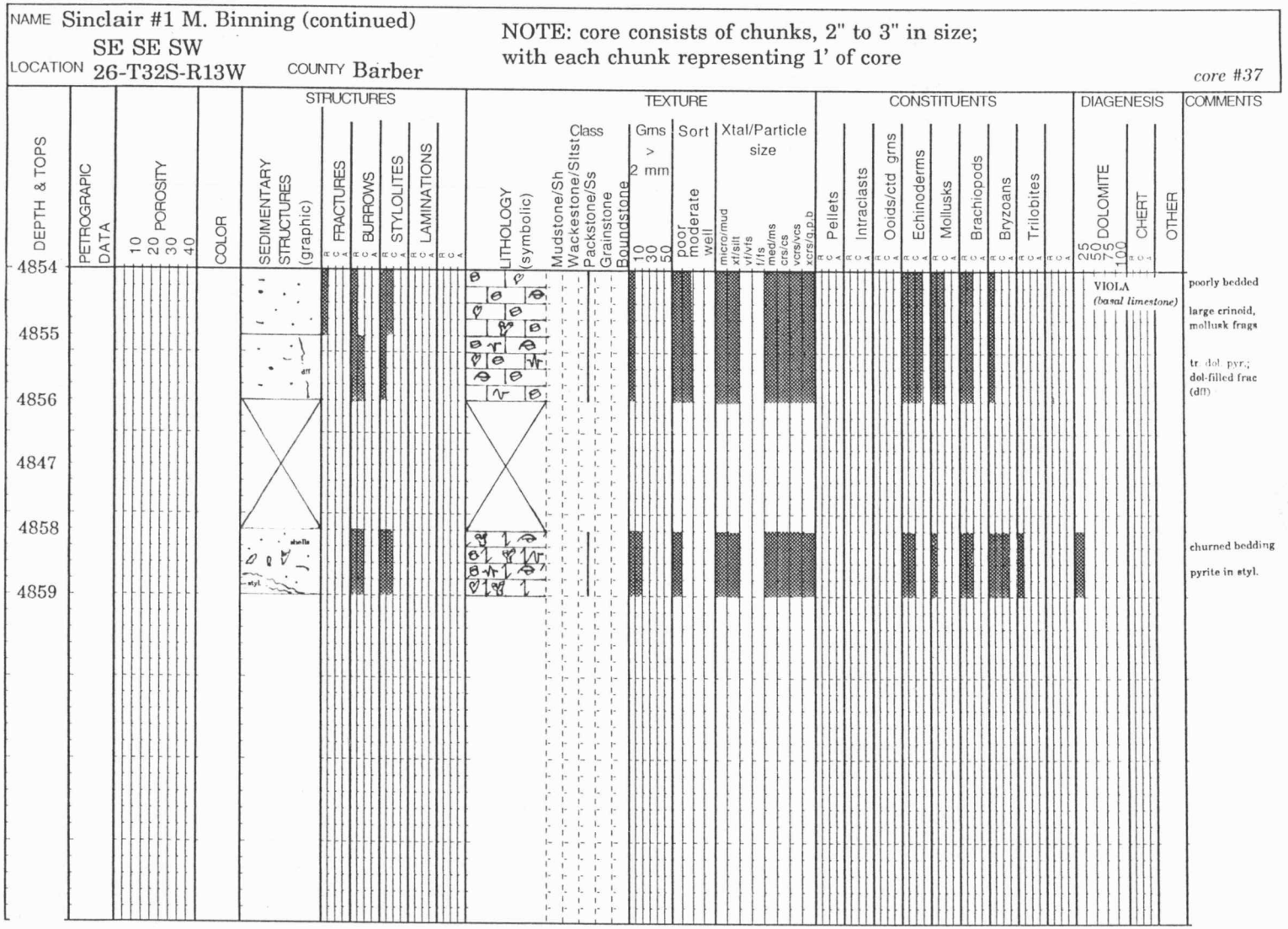
NAME Sinclair #1 M. Binning (continued)
LOCATION SE SE SW 26-T32S-R13W
COUNTY Barber
NOTE: core consists of chunks, 2" to 3" in size; with each chunk representing 1' of core
core #37
DEPTH & TOPS
PETROGRAPIC DATA
10 20 POROSITY 30 40
COLOR
STRUCTURES
SEDIMENTARY STRUCTURES (graphic)
FRACTURES
BURROWS
STYLOLITES
LAMINATIONS
TEXTURE
LITHOLOGY (symbolic)
Class
Mudstone/Sh
Wackestone/Slstst
Packstone/Ss
Grainstone
Boundstone
Grns > 2 mm
10 30 50
Sort
poor moderate well
Xtal/Particle size
micromud
xf/silt
vf/vfs
f/fs
med/ms
crs/cs
vcrs/vcs
xcrs/g.p.b
CONSTITUENTS
Pellets
Intraclasts
Ooids/ctd grns
Echinoderms
Mollusks
Brachiopods
Bryzoans
Trilobites
DIAGENESIS
25 50 75 100 DOLOMITE
CHERT
OTHER
COMMENTS
4854
4855
4856
4847
4858
4859
dff
shells
styl
VIOLA
(basal limestone)
poorly bedded
large crinoid, mollusk frags
tr dol pyr.; dol-filled frac (dff)
churned bedding
pyrite in styl.

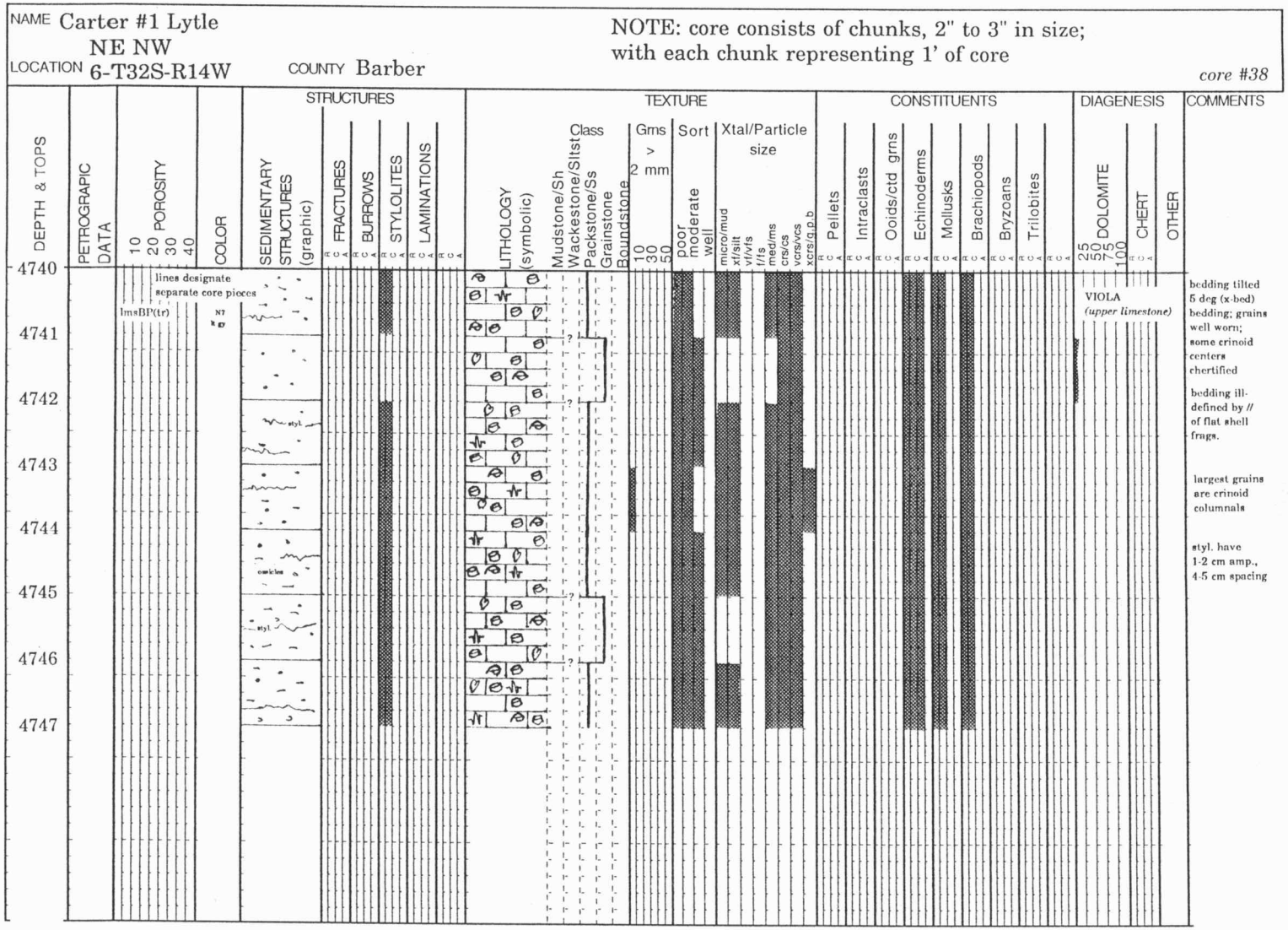
NAME Carter #1 Lytle
NE NW
LOCATION 6-T32S-R14W
COUNTY Barber
NOTE: core consists of chunks, 2" to 3" in size; with each chunk representing 1' of core
core #38
STRUCTURES
TEXTURE
CONSTITUENTS
DIAGENESIS
COMMENTS
DEPTH & TOPS
PETROGRAPIC DATA
POROSITY
COLOR
SEDIMENTARY STRUCTURES (graphic)
FRACTURES
BURROWS
STYLOLITES
LAMINATIONS
LITHOLOGY (symbolic)
Mudstone/Sh
Wackestone/Sltst
Packstone/Ss
Grainstone
Boundstone
Class
Gms > 2 mm
Sort
poor
moderate
well
Xtal/Particle size
micro/mud
xf/silt
vf/vfs
f/fs
med/ms
crs/cs
vcrs/vcs
xcrs/gran/b
Pellets
Intraclasts
Ooids/ctd grns
Echinoderms
Mollusks
Brachiopods
Bryzoans
Trilobites
DOLOMITE
CHERT
OTHER
4740
4741
4742
4743
4744
4745
4746
4747
lines designate separate core pieces
lmsBP(tr)
VIOLA
(upper limestone)
bedding tilted 5 deg (x-bed) bedding; grains well worn; some crinoid centers chertified
bedding ill-defined by // of flat shell frags.
largest grains are crinoid columnals
styl. have 1-2 cm amp., 4-5 cm spacing

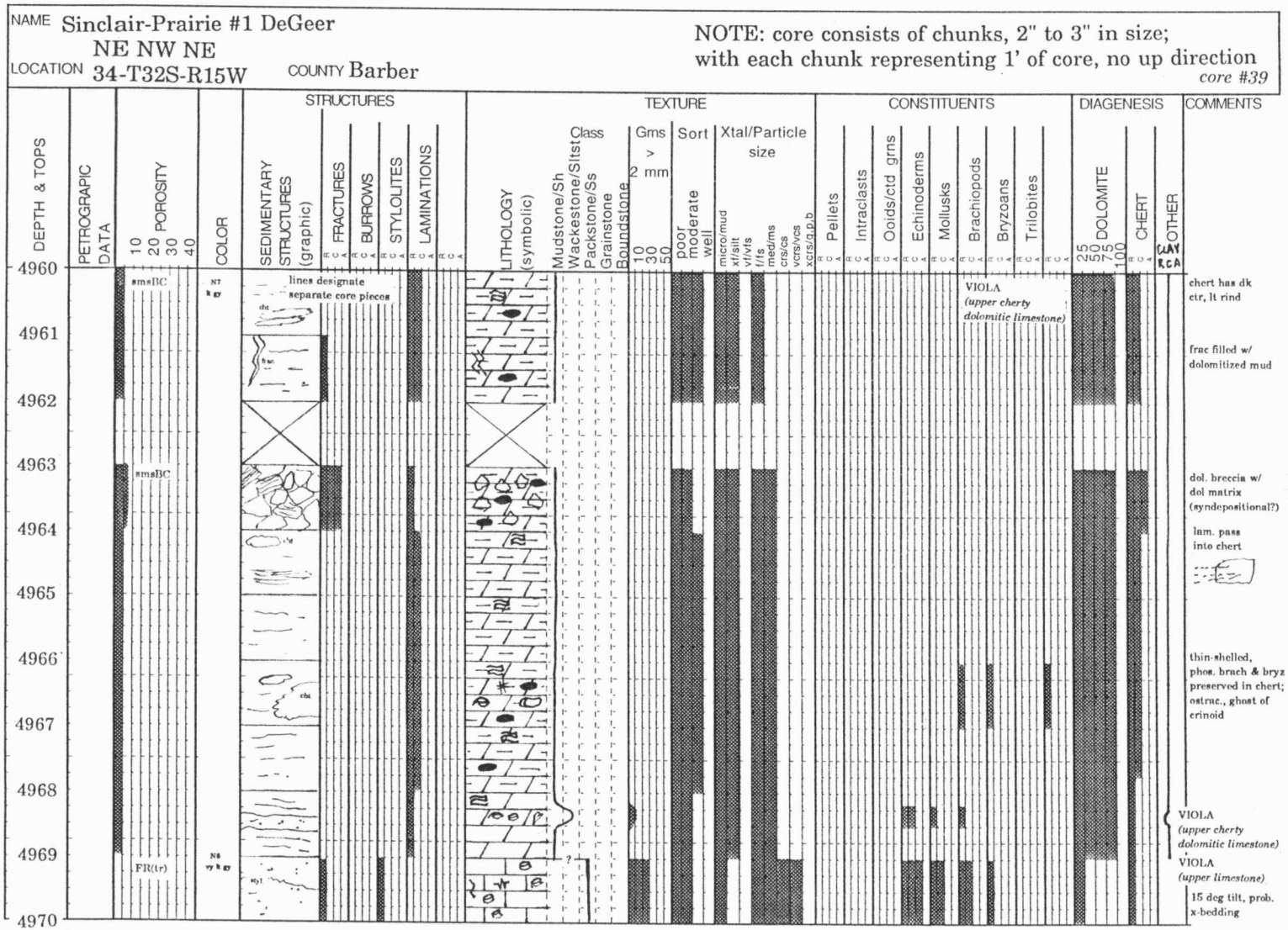
NAME Sinclair-Prairie #1 DeGeer
NE NW NE
LOCATION 34-T32S-R15W
COUNTY Barber
NOTE: core consists of chunks, 2" to 3" in size; with each chunk representing 1' of core, no up direction
core #39
DEPTH & TOPS
PETROGRAPHIC DATA
POROSITY
COLOR
STRUCTURES
SEDIMENTARY STRUCTURES (graphic)
FRACTURES
BURROWS
STYLOLITES
LAMINATIONS
TEXTURE
LITHOLOGY (symbolic)
Class
Mudstone/Sh
Wackestone/Sltst
Packstone/Ss
Grainstone
Boundstone
Gms > 2 mm
Sort
poor
moderate
well
Xtal/Particle size
micro/mud
xf/silt
vf/vfs
f/fs
med/ms
crs/cs
vcrs/vcs
xcrs/g,p,b
CONSTITUENTS
Pellets
Intraclasts
Ooids/ctd grns
Echinoderms
Mollusks
Brachiopods
Bryzoans
Trilobites
DIAGENESIS
DOLOMITE
CHERT
OTHER
CLAY
COMMENTS
4960
4961
4962
4963
4964
4965
4966
4967
4968
4969
4970
smsBC
FR(tr)
lines designate separate core pieces
VIOLA
(upper cherty dolomitic limestone)
chert has dk ctr, lt rind
frac filled w/ dolomitized mud
dol. breccia w/ dol matrix (syndepositional?)
lam. pass into chert
thin-shelled, phos. brach & bryz preserved in chert; ostrac., ghost of crinoid
VIOLA
(upper cherty dolomitic limestone)
VIOLA
(upper limestone)
15 deg tilt, prob. x-bedding

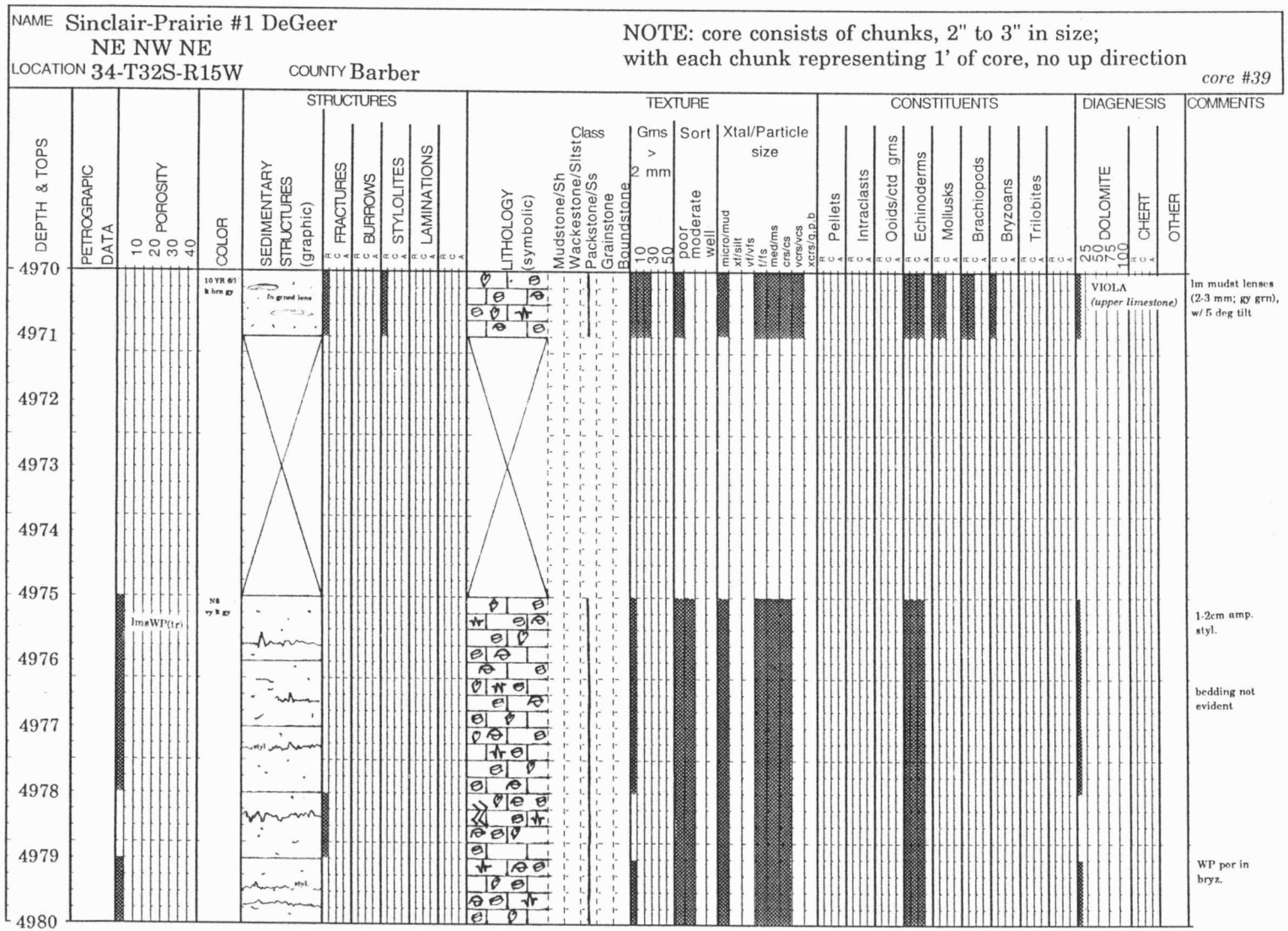
NAME Sinclair-Prairie #1 DeGeer
NE NW NE
LOCATION 34-T32S-R15W
COUNTY Barber
NOTE: core consists of chunks, 2" to 3" in size;
with each chunk representing 1' of core, no up direction
core #39
STRUCTURES
TEXTURE
CONSTITUENTS
DIAGENESIS
COMMENTS
DEPTH & TOPS
PETROGRAPHIC DATA
POROSITY
COLOR
SEDIMENTARY STRUCTURES (graphic)
FRACTURES
BURROWS
STYLOLITES
LAMINATIONS
LITHOLOGY (symbolic)
Class
Mudstone/Sh
Wackestone/Sltst
Packstone/Ss
Grainstone
Boundstone
Grns > 2 mm
Sort
poor
moderate
well
Xtal/Particle size
micro/mud
xf/silt
vf/vfs
f/fs
med/ms
crs/cs
vcrs/vcs
Pellets
Intraclasts
Ooids/ctd grns
Echinoderms
Mollusks
Brachiopods
Bryzoans
Trilobites
DOLOMITE
CHERT
OTHER
4970
4971
4972
4973
4974
4975
4976
4977
4978
4979
4980
lmsWP(tr)
VIOLA
(upper limestone)
lm mudst lenses (2-3 mm; gy grn), w/ 5 deg tilt
1-2cm amp. styl.
bedding not evident
WP por in bryz.

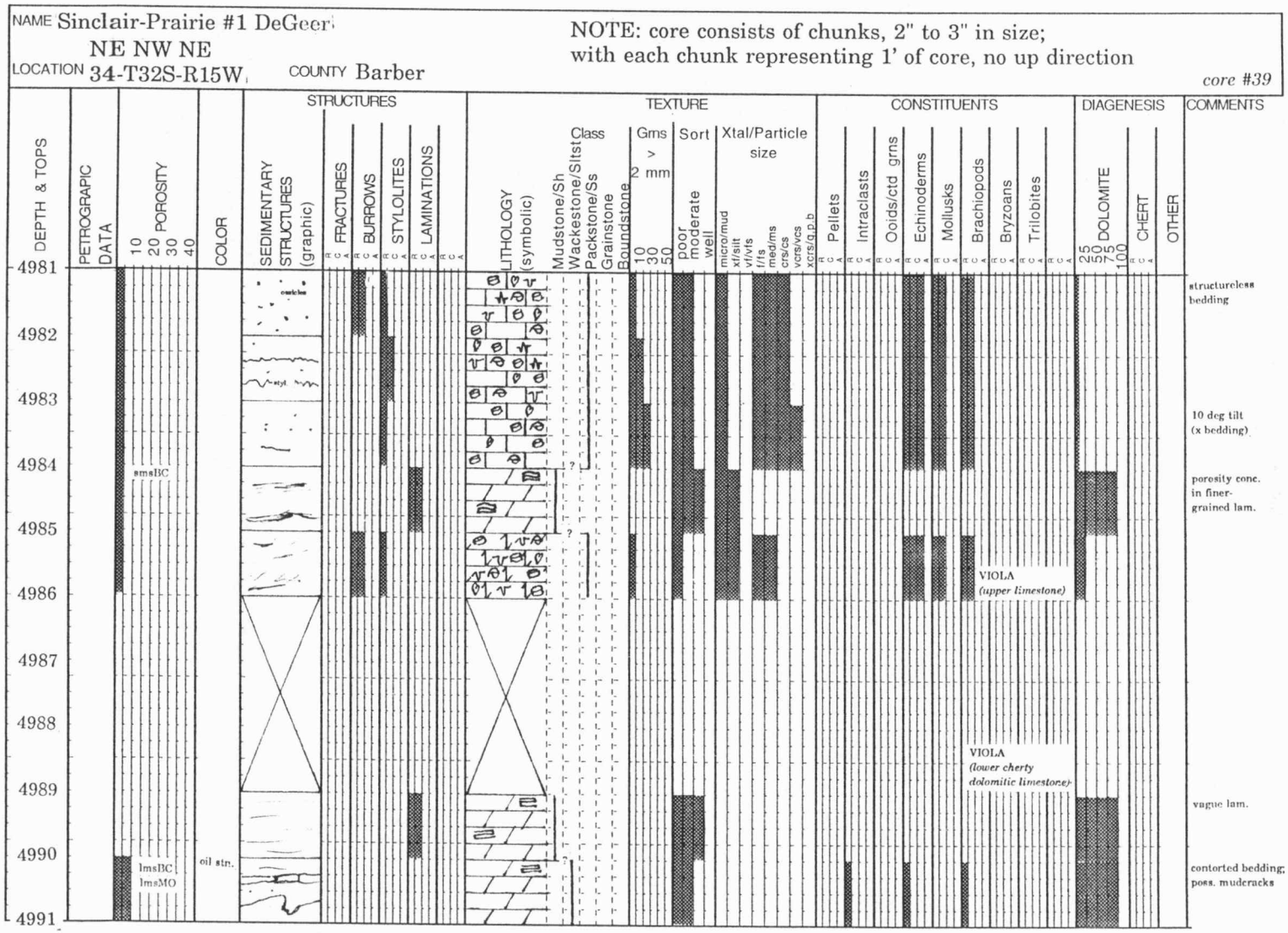
NAME Sinclair-Prairie #1 DeGeer
NE NW NE
LOCATION 34-T32S-R15W, COUNTY Barber
NOTE: core consists of chunks, 2" to 3" in size;
with each chunk representing 1' of core, no up direction
core #39
STRUCTURES
TEXTURE
CONSTITUENTS
DIAGENESIS
COMMENTS
DEPTH & TOPS
PETROGRAPHIC DATA
10 20 POROSITY 30 40
COLOR
SEDIMENTARY STRUCTURES (graphic)
FRACTURES
BURROWS
STYLOLITES
LAMINATIONS
LITHOLOGY (symbolic)
Mudstone/Sh
Wackestone/Slts
Packstone/Ss
Grainstone
Boundstone
Class
Gms > 2 mm
10 30 50
Sort
poor moderate well
Xtal/Particle size
micro/mud
xf/silt
vf/vfs
f/fs
med/ms
crs/cs
vcrs/vcs
xcrs/g.p.b
Pellets
Intraclasts
Ooids/ctd grns
Echinoderms
Mollusks
Brachiopods
Bryzoans
Trilobites
25 50 75 100 DOLOMITE
CHERT
OTHER
4981
4982
4983
4984
4985
4986
4987
4988
4989
4990
4991
smslBC
lmsBC
lmsMO
oil stn.
VIOLA
(upper limestone)
VIOLA
(lower cherty
dolomitic limestone)
structureless bedding
10 deg tilt (x bedding)
porosity conc. in finer-grained lam.
vague lam.
contorted bedding; poss. mudcracks

NAME Sinclair-Prairie #1 DeGeer
NE NW NE
LOCATION 34-T32S-R15W COUNTY Barber

NOTE: core consists of chunks, 2" to 3" in size;
with each chunk representing 1' of core, no up direction

core #39

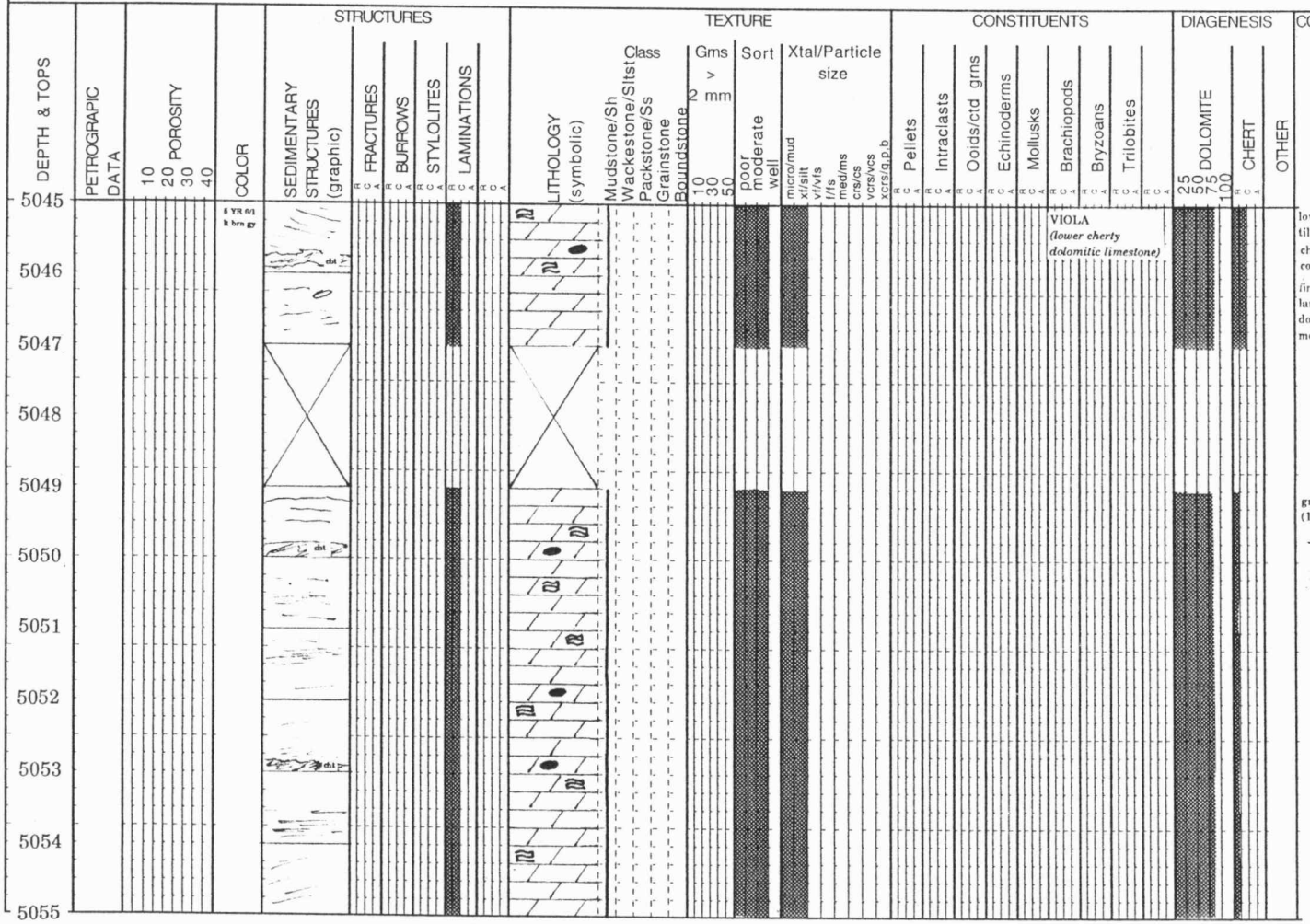

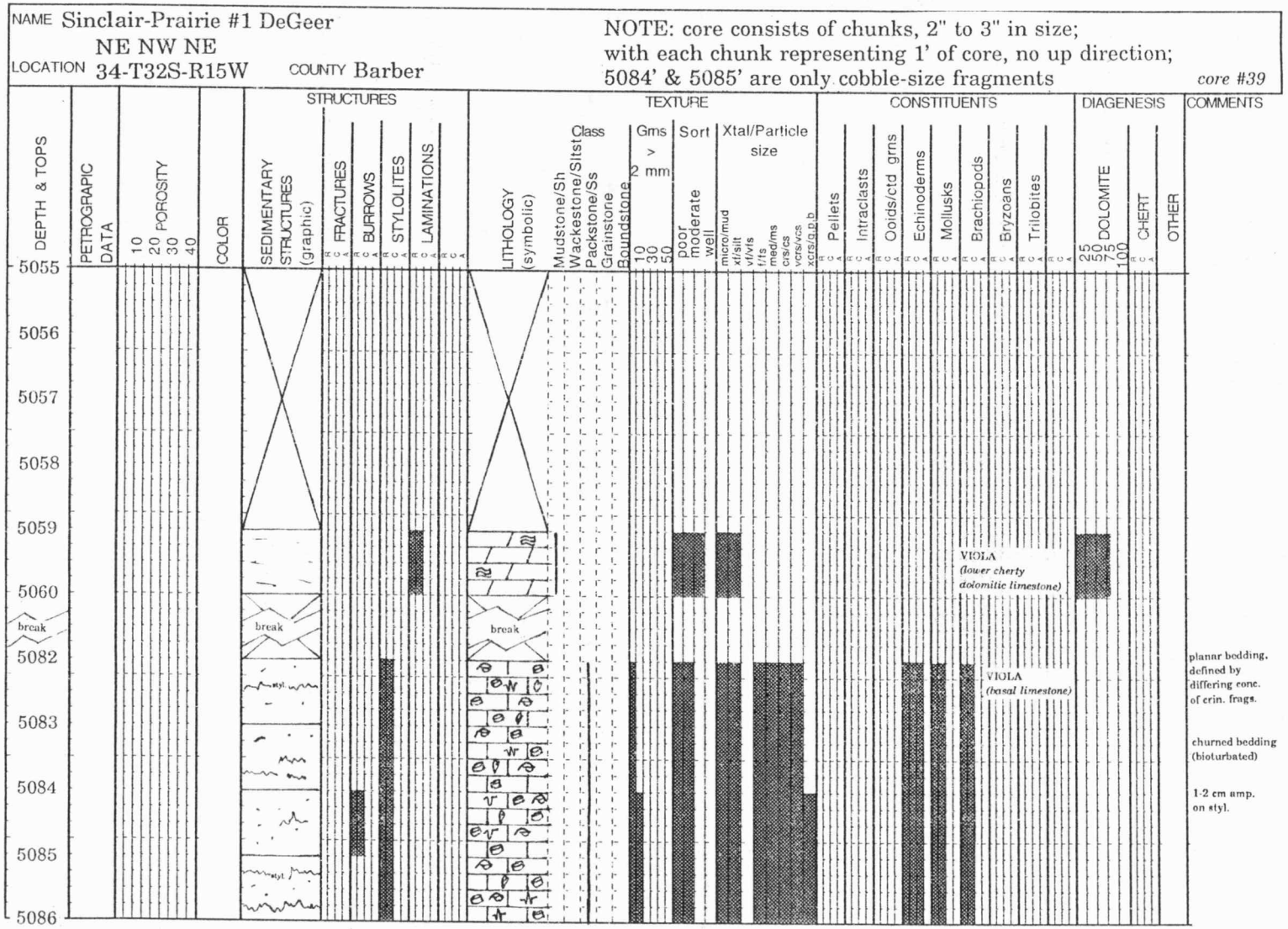
NAME Sinclair-Prairie #1 DeGeer
NE NW NE
LOCATION 34-T32S-R15W
COUNTY Barber
NOTE: core consists of chunks, 2" to 3" in size;
with each chunk representing 1' of core, no up direction;
5084' & 5085' are only cobble-size fragments
core #39
DEPTH & TOPS
PETROGRAPHIC DATA
POROSITY
COLOR
STRUCTURES
SEDIMENTARY STRUCTURES (graphic)
FRACTURES
BURROWS
STYLOLITES
LAMINATIONS
TEXTURE
LITHOLOGY (symbolic)
Class
Mudstone/Sh
Wackestone/Siltst
Packstone/Ss
Grainstone
Boundstone
Gms > 2 mm
Sort
poor
moderate
well
Xtal/Particle size
micro/mud
xf/silt
vf/vfs
f/fs
med/ms
cs/cs
vcrs/vcs
xcrs/g.p.b
CONSTITUENTS
Pellets
Intraclasts
Ooids/ctd grns
Echinoderms
Mollusks
Brachiopods
Bryzoans
Trilobites
DIAGENESIS
DOLOMITE
CHERT
OTHER
COMMENTS
5055
5056
5057
5058
5059
5060
5082
5083
5084
5085
5086
break
VIOLA
(lower cherty dolomitic limestone)
VIOLA
(basal limestone)
planar bedding, defined by differing conc. of crin. frags.
churned bedding (bioturbated)
1-2 cm amp. on styl.

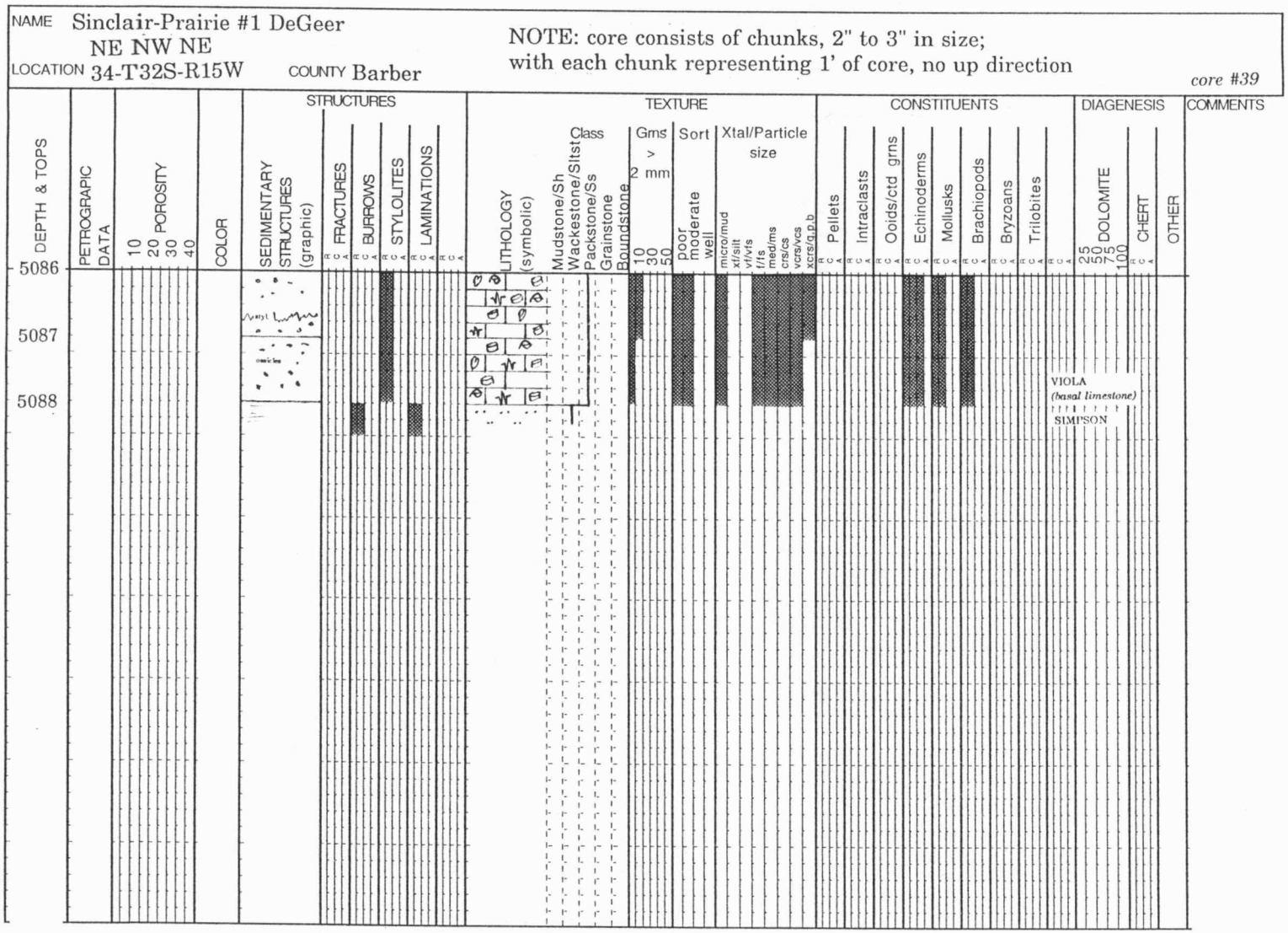
NAME Sinclair-Prairie #1 DeGeer
NE NW NE
LOCATION 34-T32S-R15W
COUNTY Barber
NOTE: core consists of chunks, 2" to 3" in size;
with each chunk representing 1' of core, no up direction
core #39
DEPTH & TOPS
PETROGRAPHIC DATA
POROSITY
10
20
30
40
COLOR
STRUCTURES
SEDIMENTARY STRUCTURES (graphic)
FRACTURES
BURROWS
STYLOLITES
LAMINATIONS
TEXTURE
LITHOLOGY (symbolic)
Class
Mudstone/Sh
Wackestone/Sltst
Packstone/Ss
Grainstone
Boundstone
Gms > 2 mm
10
30
50
Sort
poor
moderate
well
Xtal/Particle size
micro/mud
xf/silt
vf/vfs
f/fs
med/ms
crs/cs
vcrs/vcs
xcrs/g,p,b
CONSTITUENTS
Pellets
Intraclasts
Ooids/ctd grns
Echinoderms
Mollusks
Brachiopods
Bryzoans
Trilobites
DIAGENESIS
25
50
75
100
DOLOMITE
CHERT
OTHER
COMMENTS
5086
5087
5088
VIOLA
(basal limestone)
SIMPSON

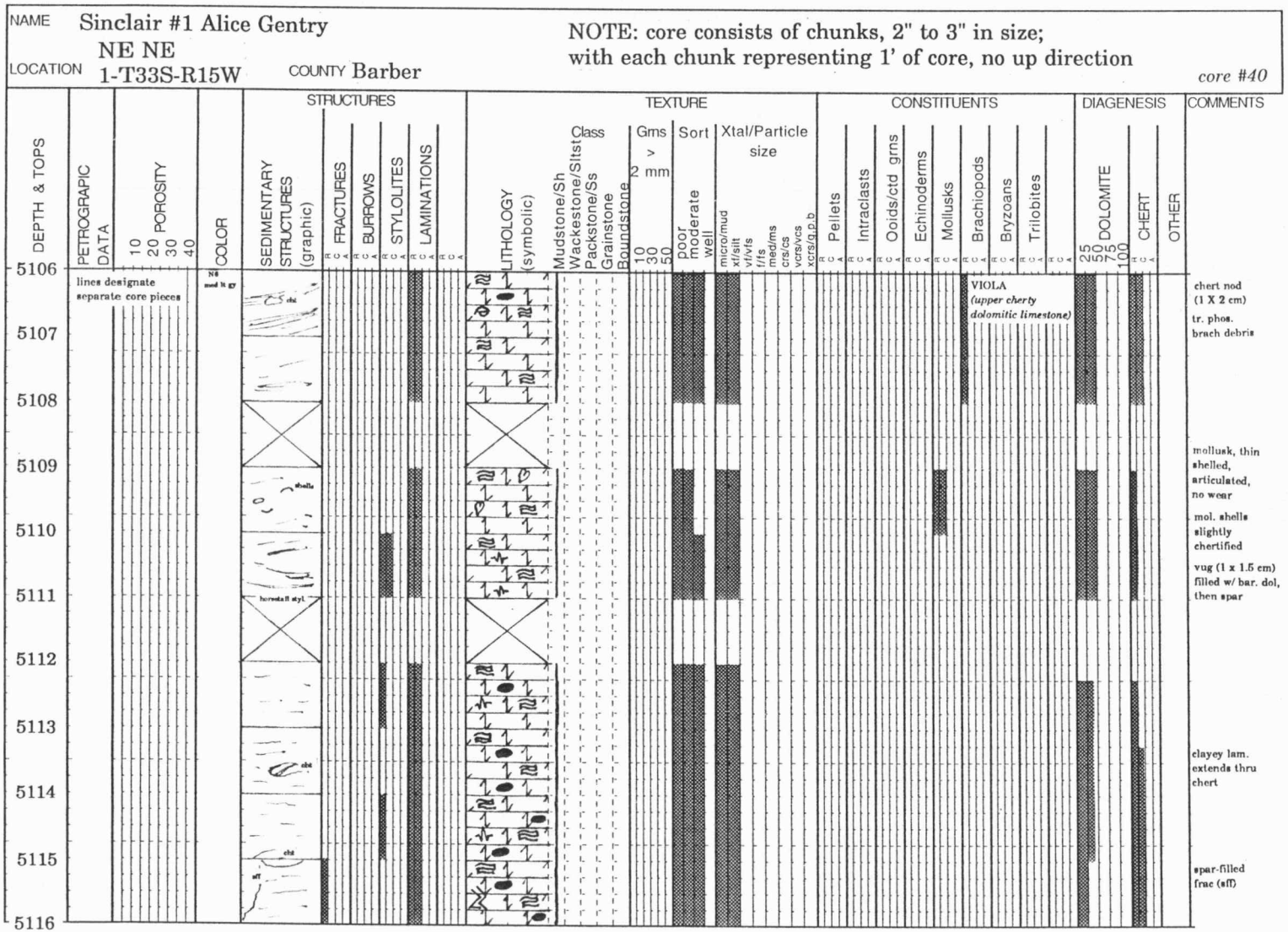
NAME Sinclair #1 Alice Gentry
LOCATION NE NE 1-T33S-R15W
COUNTY Barber
NOTE: core consists of chunks, 2" to 3" in size; with each chunk representing 1' of core, no up direction
core #40
DEPTH & TOPS
PETROGRAPHIC DATA
POROSITY
COLOR
STRUCTURES
SEDIMENTARY STRUCTURES (graphic)
FRACTURES
BURROWS
STYLOLITES
LAMINATIONS
TEXTURE
LITHOLOGY (symbolic)
Class
Mudstone/Sh
Wackestone/Slstst
Packstone/Ss
Grainstone
Boundstone
Gms > 2 mm
Sort
poor moderate well
Xtal/Particle size
micro/mud
xf/silt
vf/vfs
f/fs
med/ms
crs/cs
vcrs/vcs
xcrs/g.p.b
CONSTITUENTS
Pellets
Intraclasts
Ooids/ctd grns
Echinoderms
Mollusks
Brachiopods
Bryzoans
Trilobites
DIAGENESIS
DOLOMITE
CHERT
OTHER
COMMENTS
5106
5107
5108
5109
5110
5111
5112
5113
5114
5115
5116
lines designate separate core pieces
N8 med lt gy
chts
shells
horsetail styl.
chts
sff
VIOLA
(upper cherty dolomitic limestone)
chert nod (1 X 2 cm)
tr. phos. brach debris
mollusk, thin shelled, articulated, no wear
mol. shells slightly chertified
vug (1 x 1.5 cm) filled w/ bar. dol, then spar
clayey lam. extends thru chert
spar-filled frac (sff)

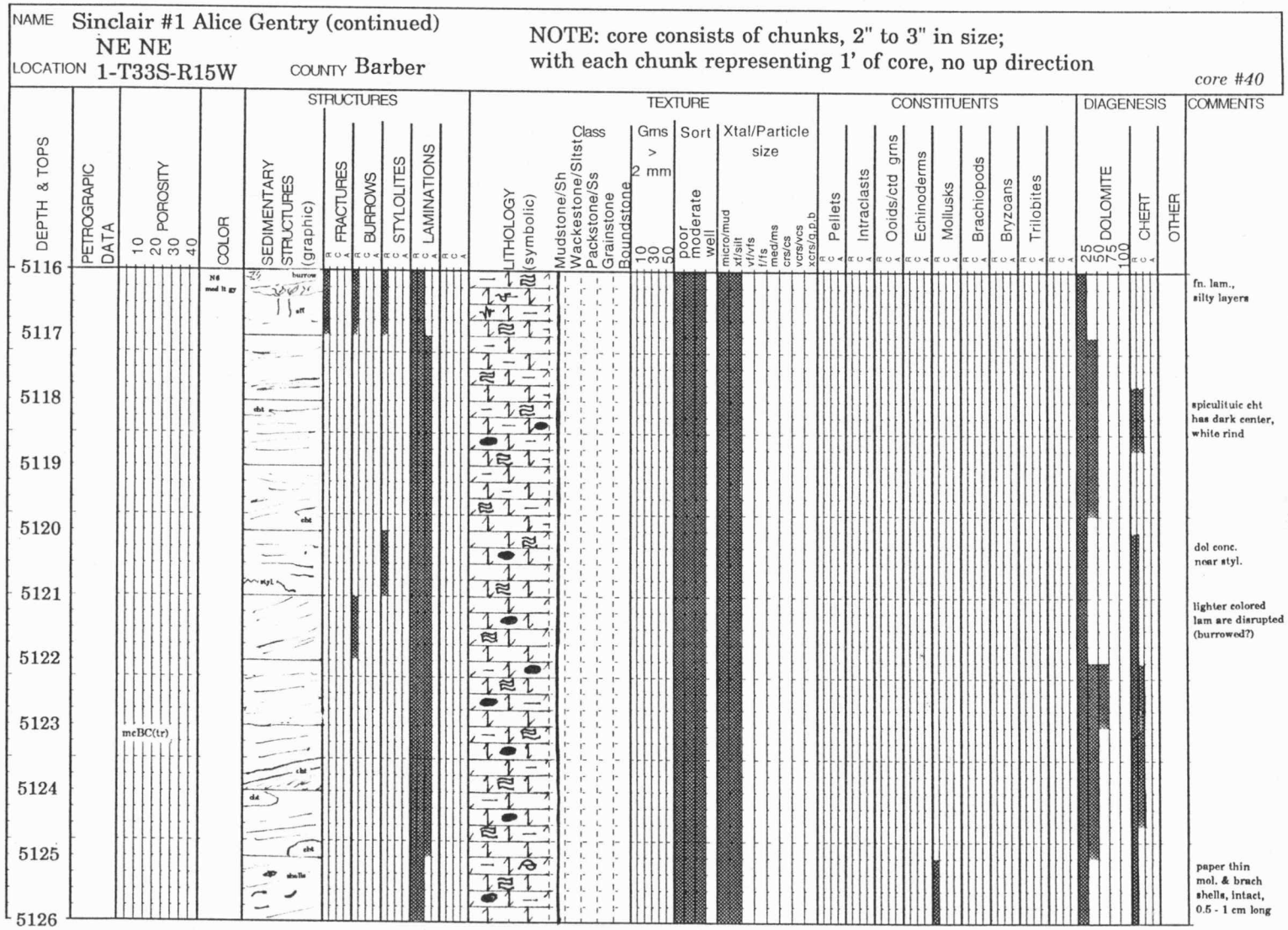
NAME Sinclair #1 Alice Gentry (continued)
NE NE
LOCATION 1-T33S-R15W
COUNTY Barber
NOTE: core consists of chunks, 2" to 3" in size;
with each chunk representing 1' of core, no up direction
core #40
DEPTH & TOPS
PETROGRAPHIC DATA
POROSITY
COLOR
STRUCTURES
SEDIMENTARY STRUCTURES (graphic)
FRACTURES
BURROWS
STYLOLITES
LAMINATIONS
TEXTURE
LITHOLOGY (symbolic)
Class
Mudstone/Sh
Wackestone/Sltst
Packstone/Ss
Grainstone
Boundstone
Gms > 2 mm
Sort
poor
moderate
well
Xtal/Particle size
micro/mud
vf/silt
vf/vfs
f/fs
med/ms
crs/cs
vcrs/vcs
xcrs/gran
CONSTITUENTS
Pellets
Intraclasts
Ooids/ctd grns
Echinoderms
Mollusks
Brachiopods
Bryzoans
Trilobites
DIAGENESIS
DOLOMITE
CHERT
OTHER
COMMENTS
5116
5117
5118
5119
5120
5121
5122
5123
5124
5125
5126
mcBC(tr)
fn. lam., silty layers
spiculituic cht has dark center, white rind
dol conc. near styl.
lighter colored lam are disrupted (burrowed?)
paper thin mol. & brach shells, intact, 0.5 - 1 cm long

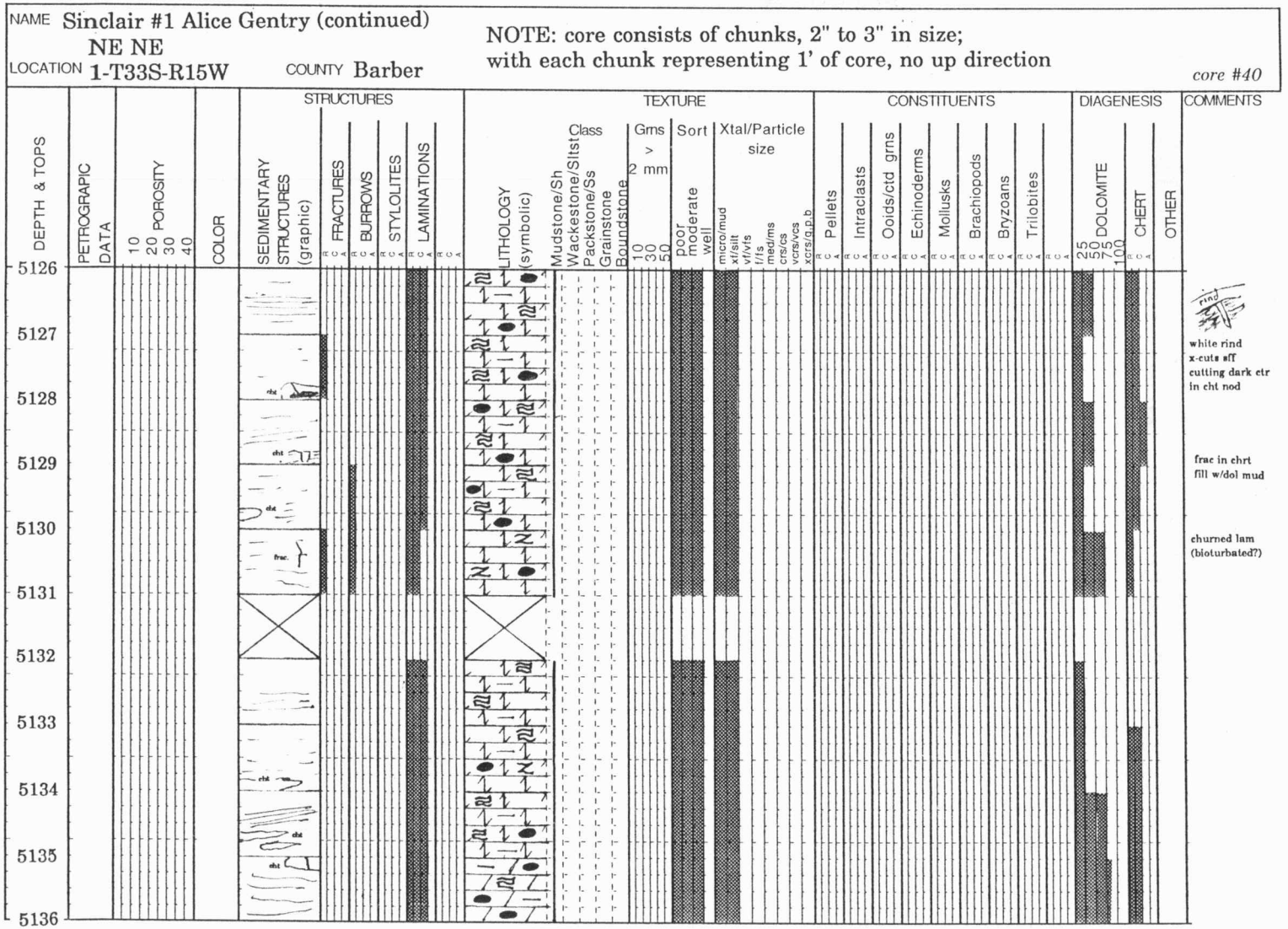
NAME Sinclair #1 Alice Gentry (continued)
NE NE
LOCATION 1-T33S-R15W
COUNTY Barber
NOTE: core consists of chunks, 2" to 3" in size;
with each chunk representing 1' of core, no up direction
core #40
DEPTH & TOPS
PETROGRAPHIC DATA
POROSITY
COLOR
STRUCTURES
SEDIMENTARY STRUCTURES (graphic)
FRACTURES
BURROWS
STYLOLITES
LAMINATIONS
TEXTURE
LITHOLOGY (symbolic)
Class
Mudstone/Sh
Wackestone/Sltst
Packstone/Ss
Grainstone
Boundstone
Grns > 2 mm
Sort
poor
moderate
well
Xtal/Particle size
micro/mud
xf/silt
vf/vfs
f/fs
med/ms
crs/cs
vcrs/vcs
xcrs/g.p.b
CONSTITUENTS
Pellets
Intraclasts
Ooids/ctd grns
Echinoderms
Mollusks
Brachiopods
Bryzoans
Trilobites
DIAGENESIS
DOLOMITE
CHERT
OTHER
COMMENTS
5126
5127
5128
5129
5130
5131
5132
5133
5134
5135
5136
white rind
x-cuts aff
cutting dark etr
in cht nod
frac in chrt
fill w/dol mud
churned lam
(bioturbated?)

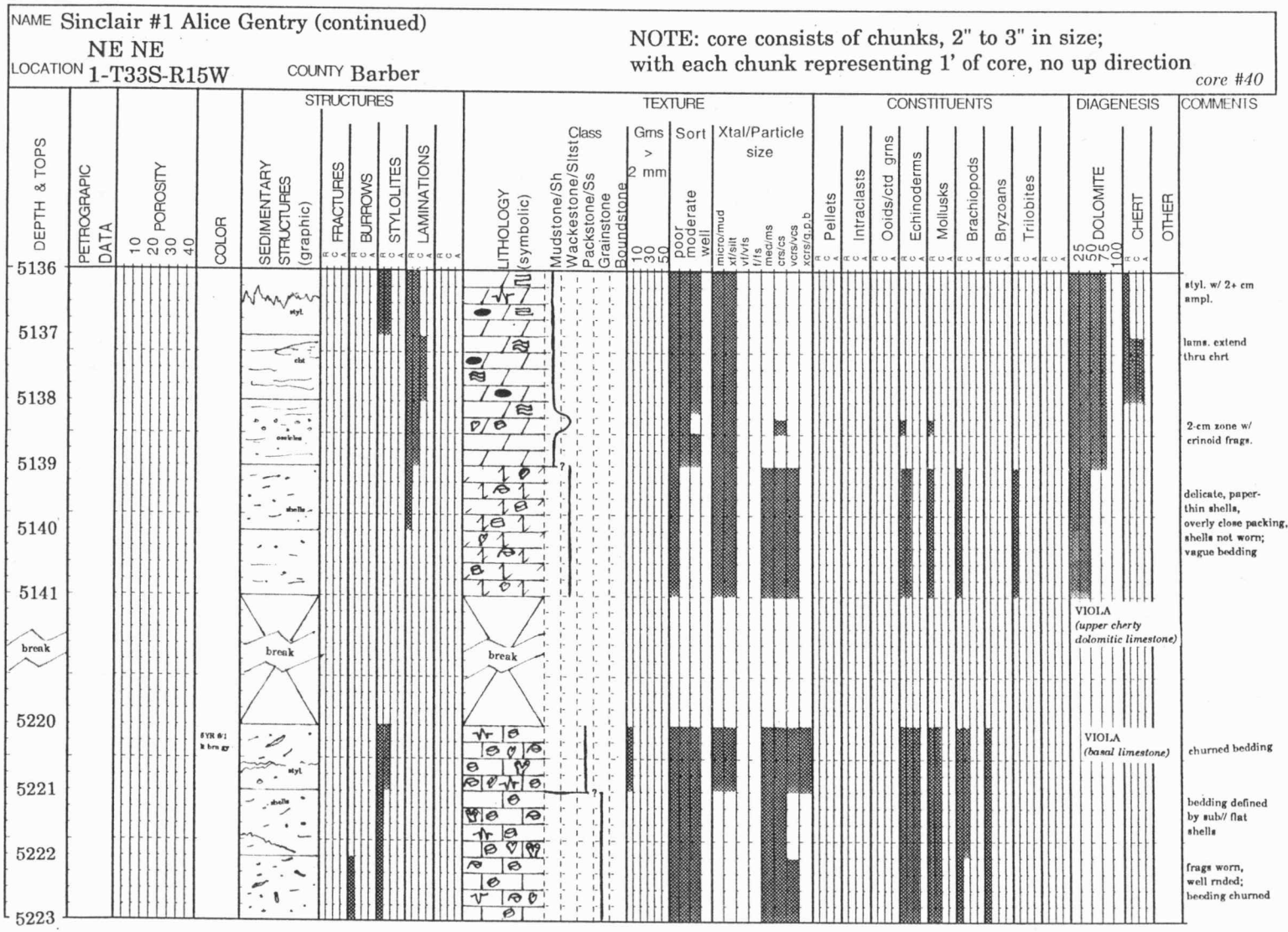
NAME Sinclair #1 Alice Gentry (continued)
NE NE
LOCATION 1-T33S-R15W
COUNTY Barber
NOTE: core consists of chunks, 2" to 3" in size; with each chunk representing 1' of core, no up direction
core #40
DEPTH & TOPS
PETROGRAPIC DATA
10 20 POROSITY 30 40
COLOR
STRUCTURES
SEDIMENTARY STRUCTURES (graphic)
FRACTURES
BURROWS
STYLOLITES
LAMINATIONS
TEXTURE
LITHOLOGY (symbolic)
Class
Mudstone/Sh
Wackestone/Siltst
Packstone/Ss
Grainstone
Boundstone
Gms > 2 mm
10 30 50
Sort
poor moderate well
Xtal/Particle size
micro/mud
xf/silt
vf/vfs
f/fs
med/ms
crs/cs
vcrs/vcs
xcrs/g.p.b
CONSTITUENTS
Pellets
Intraclasts
Ooids/ctd grns
Echinoderms
Mollusks
Brachiopods
Bryzoans
Trilobites
DIAGENESIS
25 50 75 100
DOLOMITE
CHERT
OTHER
COMMENTS
5136
5137
5138
5139
5140
5141
break
5220
5221
5222
5223
5YR 6/1 lt brn gy
styl.
chrt
conglom
shells
break
styl.
shells
VIOLA
(upper cherty dolomitic limestone)
VIOLA
(basal limestone)
styl. w/ 2+ cm ampl.
lams. extend thru chrt
2-cm zone w/ crinoid frags.
delicate, paper-thin shells, overly close packing, shells not worn; vague bedding
churned bedding
bedding defined by sub// flat shells
frags worn, well rnded; beeding churned

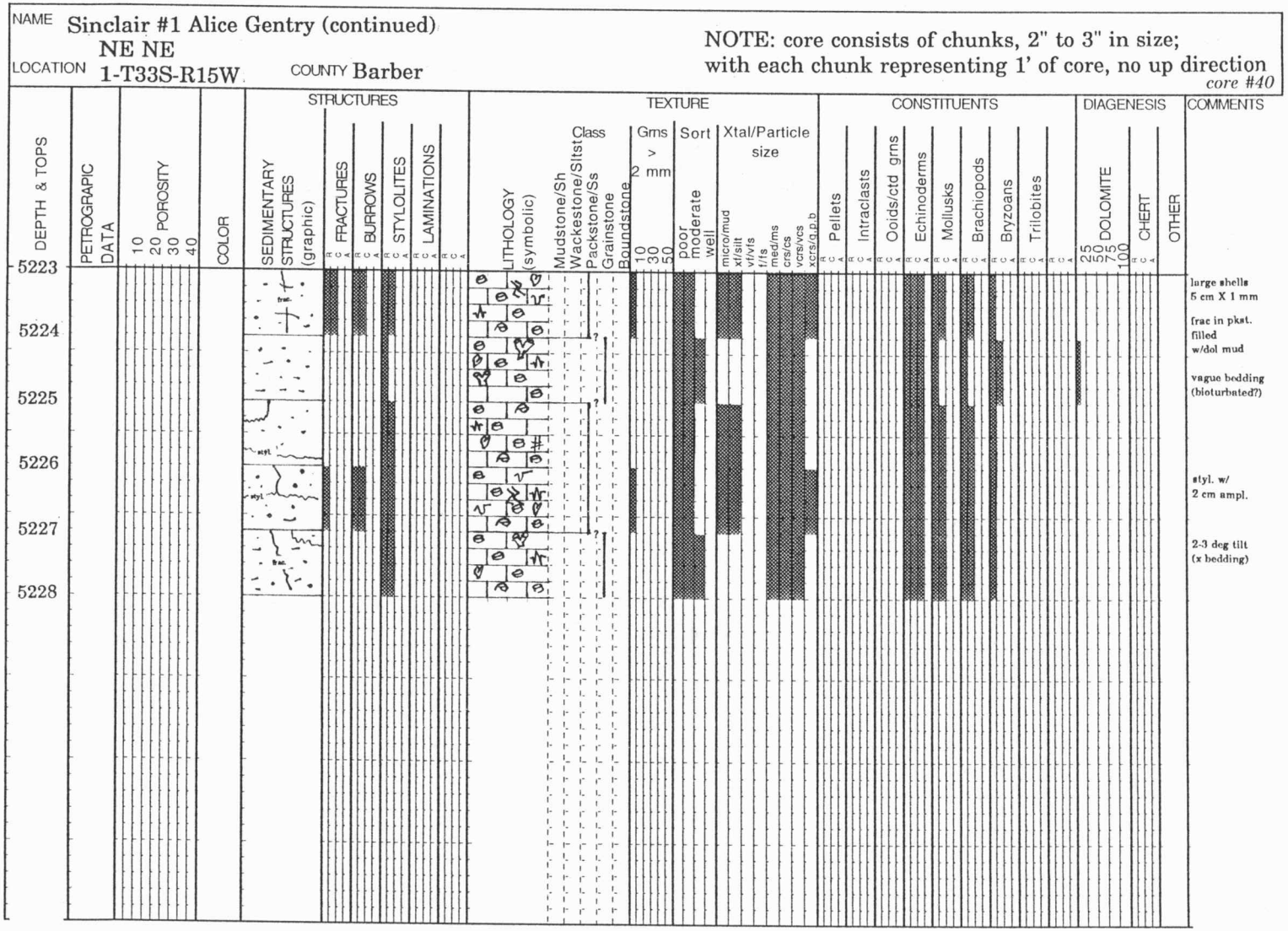
NAME Sinclair #1 Alice Gentry (continued)
LOCATION NE NE 1-T33S-R15W
COUNTY Barber
NOTE: core consists of chunks, 2" to 3" in size; with each chunk representing 1' of core, no up direction
core #40
DEPTH & TOPS
PETROGRAPHIC DATA
10 20 POROSITY 30 40
COLOR
STRUCTURES
SEDIMENTARY STRUCTURES (graphic)
FRACTURES
BURROWS
STYLOLITES
LAMINATIONS
TEXTURE
LITHOLOGY (symbolic)
Mudstone/Sh
Wackestone/Sltst
Packstone/Ss
Grainstone
Boundstone
Class
Grns > 2 mm
10 30 50
Sort
poor moderate well
Xtal/Particle size
micro/mud
xf/silt
vf/vfs
f/fs
med/ms
crs/cs
vcrs/vcs
xcrs/g,p,b
CONSTITUENTS
Pellets
Intraclasts
Ooids/ctd grns
Echinoderms
Mollusks
Brachiopods
Bryzoans
Trilobites
DIAGENESIS
25 50 75 100
DOLOMITE
CHERT
OTHER
COMMENTS
5223
5224
5225
5226
5227
5228
large shells 5 cm X 1 mm
frac in pkst. filled w/dol mud
vague bedding (bioturbated?)
styl. w/ 2 cm ampl.
2-3 deg tilt (x bedding)

APPENDIX V -- LITHOLOGY OF SUBUNITS OF VIOLA FORMATION, SOUTH-CENTRAL KANSAS (TAKEN FROM DAVIES'S SAMPLE LOGS)

KEY

A = upper cherty dolomitic limestone
B = upper limestone
C = lower cherty dolomitic limestone
D = basal limestone

abs -- unit not present because of erosion or nondeposition

d -- dolomite (presence or absence of chert ignored)

dwl -- dolomite with limestone (i.e., dolomite with minor limestone; presence or absence of chert ignored)

lwd -- limestone with dolomite (i.e., limestone with minor dolomite, "dolomitic limestone"; presence or absence of chert ignored)

l -- limestone (presence or absence of chert ignored)

c -- chert, chert breccia

(no value) -- unit not penetrated or logged

(wells listed first by northernmost townships and eastern ranges, then western ranges)

OPERATOR	WELL NAME	LOCATION S.	T.	R.	SPOT	DEPTHS A	B	C	D
Booth	#1 Wedel	6	17S	1E	NW NE	abs	l	d	l
White Eagle	#1 Ucker	24	17S	2E		abs	l	d	l
Rex & Morris	#1 Pankratz	21	17S	3E	NW SW SE	dwl	l	lwd	l
Smitherman	#1 Schlehuber	13	18S	1E	NW NW SW	abs	d	dwl	lwd
White Eagle	#1 Cline	28	18S	3E	SE NW SE	abs	abs	d	l
Augusta	#1 Albright	15	18S	4E	SW SE NW	abs	dwl		
Aladdin Petrol.	#1 Weyand	22	19S	1E	SE SE NW	abs	abs	d	l
Anderson-Prichard	#1 Hett	3	19S	2E	SW NE SW	abs	abs	dwl	l
Wildcat Resources	#2 Jost	22	19S	2E	SE NW SW	abs	abs	d	l
Crest	#1 Turner	34	19S	3E	SW SW NW	abs	abs	d	l
Nat'l Assoc. Pet.	#1 Baxter	28	19S	4E	NE NE SW	abs	l	d	l
Raymond	#1 Stika	17	19S	5E	NW NW SE	abs	dwl	d	l
Anderson-Prichard	#1 Koegeboehn	19	19S	6E	NE NE NE	abs	d	d	d
Stanolind	#1 N. Kline	10	19S	7E	SW SW NE	abs	abs	d	d
Mull	#1 C. Hiebert	33	20S	2E	SE SE NW	abs	abs	d	d
Cities Service	#1-D Loewen	36	20S	2E	SW SW SW	abs	abs	l	l
Anderson-Prichard	#1 Schaeffler	4	20S	3E	E2 E2 NE	abs	d	d	l

OPERATOR	WELL NAME	LOCATION S.	T.	R.	SPOT	DEPTHS A	B	C	D
Renfro	#1 Suderman	3	21S	2E	SW SW NW	abs	abs	abs	d
Raymond	#1 G. Hodges	5	21S	2E	NW NW SE	abs	abs	abs	dwl
Cities Service	#1 Depler	26	21S	2E	SE NE NW	abs	abs	abs	l
Anderson-Prichard	#1 Davis	21	21S	3E	NW NW NW	abs	abs	l	dwl
Bedell-Catt	#1 Coleman	19	21S	4E	SW NE NE	abs	abs	abs	dwl
G.L. Reasor	#1 Hudson	33	22S	1E	SW SE NE	abs	abs	d	d
Aladdin Petrol.	#1 Winsor	1	22S	2E	SW NW NE	abs	abs	abs	d
Herndon Drlg.	#1 Orpin	26	22S	2E	SE SE NW	abs	abs	d	d
Round Table Invest.	#1-3 Potter	3	22S	3E	SE	abs	abs	d	d
E.H. Adair	#1 Wallace	6	22S	3E	SW SW NE	abs	abs	abs	d
Phillips	#1 Clark	15	22S	4E	NE NW SE	abs	abs	d	d
Adair & L. Phillips	#1 Meyer	21	22S	5E	SE SE NE	abs	abs	d	d
Pure	#1-A Langenegger	28	22S	5E	SW NE	abs	abs	d	d
White & Ellis	#1 Chisholm	15	22S	6E	NW NW SW	abs	d	d	d
Bay Petrol.	#1 Sauder	3	23S	1E	SE SW SW	abs	abs	d	d
Ingling et al.	#1 Krehbiel	14	23S	2E	SE SE NW	abs	abs	d	d
Charles Carlock	#1 Walton	19	23S	2E	SE NE NE	abs	abs	abs	d
Husky	#1 Balzer	26	23S	2E	SW SE SW	abs	abs	d	d
E.H. Adair	#1 Regier	18	23S	3E	NE	abs	abs	abs	d
Adair & L. Phillips	#1 Decker	13	23S	4E	NW NW SE	abs	abs	d	d
Phillips	#23 Skully	17	23S	4E	SW NE NE	abs	abs	abs	d
Rex & Morris	#1 Phillips	28	23S	5E	NE SE NW	abs	abs	d	d
Adair	#1 Breinning	7	23S	6E	SW SW SE	abs	abs	d	d
Adair	#1 Kurr	23	24S	1E	SW SW SW	abs	abs	abs	d
Renfro Drlg.	#1 Nattier	30	24S	2E	SE SW SW	abs	abs	abs	d
Anderson-Prichard	#1 Wiebe	33	24S	3E	NE NW NE	abs	abs	d	d
Frontier	#1 Skully	11	24S	4E	SE SE SW	abs	abs	abs	d
Adair	#1 Wiebe	5	24S	5E	NW NW SE	abs	abs	d	d
Allied Material	#1 Rukert	15	24S	6E	SE SW NE	abs	d	d	d
Sutton et al.	#1 Kallenbach	28	25S	1E	NE NE SW	abs	abs	abs	d
Quaker Drlg.	#1 Carey	34	25S	1E	NW NW NE	abs	abs	abs	d
Renfro Drlg.	#1 DuBois	3	25S	2E	SW NE NW	abs	abs	d	d
B & R Drlg.	#1 Mosiman	24	25S	2E	SW SW SW	abs	abs	abs	d
Renfro Drlg. et al.	#1 Jackson	28	25S	2E	SW SE SW	abs	abs	abs	d
Gaty	#1 Harder	19	25S	3E	NE SW SE	abs	abs	d	d
Branine & Goering	#1 Joseph	12	25S	5E	SW SE SE	abs	abs	abs	d
Nat'l Assoc. Pet.	#1 Buckman	11	25S	7E	NE NE NW	abs	d	d	d
J.P. Gaty	#1 Clark	2	26S	1E	SE NW SE	abs	abs	abs	d
Gaty	#1 Beech	9	26S	2E	SW NE NE	abs	abs	abs	d
Cities Service	#1 Thacker	27	26S	3E	NE SW	abs	abs	d	d
Bay	#1 Hazen	36	26S	3E	SW SW SE	abs	abs	d	d
Aladdin Petrol.	#1 Oliver	19	26S	4E	NE SW SW	abs	abs	d	d
Huber	#1 Strait	28	26S	6E	SE SW SE	abs	abs	abs	d
Derby Ref.	#1 Derby Ref.	4	27S	1E	SE SE	abs	abs	abs	d
Allison	#1 Faulk	11	27S	2E	SE SW SE	abs	abs	abs	d
Gaty	#1 James	5	27S	3E	NE SE NE	abs	abs	abs	d
Crowe	#1 Wallace	22	27S	6E	SE SE NE	abs	abs	abs	d
Casebeer	#1 Hugoton	35	17S	2W	SE SE SE	dwl	dwl	d	l

OPERATOR	WELL NAME	LOCATION S.	T.	R.	SPOT	DEPTHS A	B	C	D
Petroleum Inc.	#1 Nelson	33	17S	3W	NW SE SW NW	abs	abs	lwd	1
Nat'l Assoc. Pet.	#1 Knackstedt	8	17S	4W	SE SW NE	abs	abs	dwl	1
Hanco	#1 Dahlstein	10	17S	4W	SE SW SE	abs	1	1	1
Rupp-Ferguson	#1 Johnson	33	17S	4W	SW NW	abs	abs	lwd	1
Raymond	#1 Hokr	7	17S	7W	NW NW NW	abs	abs	abs	1
Vickers	#1 Staatz	24	17S	8W	SW SE SE	abs	abs	abs	1
Time	#1 Berggren	26	18S	3W	NW NW NE	abs	abs	d	dwl
White & Ellis	#1 Neufeldt	5	18S	4W	SE SE NW	abs	abs	abs	d
Sohio Petrol.	#1 Kumle	20	18S	4W	SW SW SE	abs	abs	abs	dwl
Trans Era	#1 John Myers	8	18S	5W	SE SE SE	abs	abs	abs	dwl
J.A. Melland	#1 Christenson	12	18S	5W	NE NE NW	abs	abs	d	dwl
Solar	#1 Sellers	27	18S	7W	SE NE NE	abs	abs	abs	1
Skiles	#1 Skiles	8	18S	8W	NE NE SW	abs	abs	abs	1
NCRA	#1 Anderson	15	19S	3W	SE SE NW	abs	abs	abs	dwl
Natural G&O	#1 Quantius	31	19S	3W	NE NE SW	abs	abs	abs	dwl
NCRA	#1 LPG SWD	29	19S	4W	NE NW SE	abs	abs	abs	dwl
Durban	#1 Durland	5	19S	5W	SW SW NE	abs	abs	abs	dwl
Fortier	#1 Cain	27	19S	7W	NE NW SW	abs	abs	abs	lwd
Birmingham-Bartlett	#1 Wieland	13	19S	8W	NW SW SE	abs	abs	abs	lwd
Veeder Supply	#1 John	29	20S	1W	NE NE NE	abs	abs	d	dwl
Lewis & Durbin	#1 Moddelmog	24	20S	2W	SW SW SE	abs	abs	d	1
Anschutz Drlg.	#1 Stitts	4	20S	4W	SW SW SE	abs	abs	abs	dwl
Thunderbird Drlg.	#1 Bukey	26	20S	4W	SE SE NE	abs	abs	abs	d
Glenwil Energy	#1 Smith	28	20S	4W	NW SW	abs	abs	abs	d
Cherry	#1 Rose	9	20S	6W	NE NE SE	abs	abs	abs	d
Carlock	#1 Leonard	16	20S	7W	NW NW SE	abs	abs	abs	dwl
Lauck	#1 Schumway	20	20S	8W	NW NW SE	abs	abs	abs	1
Sutton	#1 Dirkson	27	21S	1W	NE NE NE	abs	abs	abs	dwl
Gaty	#1 Scott	2	21S	2W	NW NW NW	abs	abs	d	1
Barbara	#1 Young	26	21S	2W	NE NE NE	abs	abs	abs	dwl
Wakefield	#1 Plett	19	21S	4W	NW NW NW	abs	abs	abs	d
Brunson-Spines	#1 Emma	31	21S	3W	SE NE NW	abs	abs	abs	dwl
Carey	#1 Friesen	36	21S	5W	NE NE SE	abs	abs	abs	1
Pure	#2 Thode	26	21S	8W	SW SE	abs	abs	abs	1
Thunderbird Drlg.	#1 Faler	2	21S	9W	SE NW NE	abs	abs	lwd	1
Braden Drlg.	#1 Proffits	29	21S	10W	NW NW NW	abs	abs	abs	c
Vickers Expl.	#1 Sweeny	8	21S	15W	NW NW NE	abs	abs	abs	1
Lebco	#1 Unruh	29	21S	15W	N2 NW SW	abs	abs	c	c
Glenn Byars	#1 Dyck	2	22S	1W	NE SW NE	abs	abs	abs	1
Charles Carlock	#1 Dilts	19	22S	1W	NE NE NE	abs	abs	lwd	lwd
El Dorado Refining	#1 Nickell	26	22S	2W	NW NW NE	abs	abs	abs	lwd
IMO	#1 Sperling	23	22S	2W		abs	abs	abs	1
C.W. Sanders	#1 Drier	29	22S	2W	N2 SE NW	abs	abs	abs	dwl
Coppinger	#1 Wall	25	22S	3W	SE SE SE	abs	abs	abs	1
Leben	#1 Schroeder	6	22S	4W	SW SW SE	abs	abs	abs	1
Osage	#1 Unruh	7	22S	4W	NW NW SW	abs	abs	abs	1
Beardmore-Sutton	#1 Rice	5	22S	5W	NE NE SE	abs	abs	abs	1
Lario	#1 Shepherd	18	22S	5W	SW SW NW	abs	abs	abs	1
Phillips	#1 Rowland	21	22S	5W	NE NE NE	abs	abs	abs	dwl
Penquin	#1 Phillips	23	22S	6W	NE SW NW	abs	abs	abs	1

OPERATOR	WELL NAME	LOCATION S.	T.	R.	SPOT	DEPTHS A	B	C	D
Skelly	#1 Gossage	17	22S	7W	SW SE	abs	abs	abs	l
Marathon	#5 Van Sickle	23	22S	8W	SW SW	abs	abs	abs	l
Globe	#1 Drake	7	22S	9W	SE NW NW	abs	abs	abs	l
Stag	#1 Schumaker	24	22S	9W	SW SW SE	abs	abs	abs	l
Dozier	#1 Titus	4	22S	10W	SE SE SE	abs	abs	c	d
Mid-Continent	#1 Starr	7	22S	10W	SE SE NW	abs	abs	abs	c
Dudley & Heath	#1 Greighton	13	22S	10W	SE NW SE	abs	l	l	l
Russell-Schwinn	#1 Moore	28	22S	10W	NE NW	abs	abs	c	l
Musgrove et al.	#1 Miller	30	22S	10W	NE NE SW	abs	abs	c	l
Mallonee	#1 Isern	2	22S	11W	SE SE SW	abs	abs	c	c
Ainsworth	#1-B Hammeke	8	22S	11W	S2 S2 NW	abs	abs	c	c
Aspen Drlg.	#1 McKay	11	22S	11W	NE SW NE	abs	abs	c	c
W.C. McBride et al.	#1 Richardson	26	22S	11W	SW SW NE	abs	abs	c	c
Monsanto	#1 Krankenberg	19	22S	12W	SW SW SE	abs	abs	c	c
Shelley-Miller	#4 Spangenberg	26	22S	12W	SE SW SE	abs	abs	c	c
Hutchinson	#1-29 Hitz	29	22S	12W	SW NE SW	abs	abs	c	c
Thunderbird	#1 Purdue	7	22S	13W	SW SW SE	abs	abs	c	c
Alpen	#1 Ukens	24	22S	13W	SW SW NW	abs	abs	abs	c
Clinton	#1-V H.V. Riddle	29	22S	13W	NW SE NW	abs	abs	c	c
Petroleum Inc.	#1 Stoble 'B'	9	22S	14W	N2 NW SW	abs	abs	c	c
Hilton Drlg.	#1 McMillan	29	22S	14W	NE NE NE	abs	abs	l	l
Great Bend	#1 Crane OWWO	11	22S	15W	N2 NE	abs	abs	c	c
Lauck	#1 Barstow	25	22S	15W	SW SW NE	abs	abs	c	l
F&M	#1-C Barstow	29	22S	15W	NW NW SE	abs	abs	l	l
Gramehart-Miller	#1 Boyd	12	22S	16W	NW NW NE	abs	abs	c	c
Anschutz Drlg.	#1 Barstow	26	22S	16W	NE NE NE	abs	abs	abs	l
JSF	#1 Eikmeir	18	22S	17W	NW NW SE	abs	abs	dwl	l
Hilton	#1 Zook	26	22S	17W	SW SE SW	abs	abs	dwl	l
Wakefield	#1 Ewing	29	22S	17W	NE NE NE	abs	abs	lwd	l
Cherry	#1 Mayle	17	23S	1W	NE NE SW	abs	abs	abs	d
Hannum	#1 Moreshead	24	23S	1W		abs	abs	abs	dwl
Anderson-Prichard	#1 Nachitgal	3	23S	2W	SW NW NW	abs	abs	dwl	l
Iron Drlg.	#1 Clark	18	23S	2W	SE SE SE	abs	abs	dwl	dwl
A & P	#1 Will	10	23S	3W	SW NW NE	abs	abs	dwl	dwl
Virginia Drlg.	#1 Frederick	8	23S	4W	SW SW SW	abs	abs	abs	dwl
Union Texas	#1 Hill	27	23S	4W	NW NW SW	abs	abs	abs	d
El Dorado	#1 Swanson	1	23S	5W	NE NW SW	abs	abs	abs	lwd
GMR	#1 Teterer	11	23S	5W	SW SE NE	abs	abs	abs	l
Jedco	#1 Whited	22	23S	5W	NE NE	abs	abs	abs	l
Cities Service	#1 Hamilton	22	23S	6W	SW SW SW	abs	abs	abs	l
Anschutz Drlg.	#1 Wiegel	9	23S	7W	SE SE SE	abs	abs	abs	l
Comet	#1 Griffin	17	23S	7W	SW SW	abs	abs	abs	l
Braden Drlg.	#1 Russell	30	23S	7W	SE SE NW	abs	abs	abs	l
Atlantic Refining	#1 Short	14	23S	8W	NE NE NE	abs	abs	abs	l
Iron	#1 Ramsey	16	23S	8W	SW SW SW	abs	abs	abs	l
Bell O&G	#1 Schmucker	32	23S	8W	NE NE NW	abs	abs	abs	lwd
Manhart	#1 Prettyman	2	23S	9W	NE NE NW	abs	abs	abs	d
Manhart et al.	#1 Beck	24	23S	9W	SW NE NW	abs	abs	abs	dwl
Wilkinson	#1 Hinshaw	16	23S	10W	SW SW NW	abs	abs	dwl	l
Cities	#1 Kreie	27	23S	10W	E2 W2 NW	abs	abs	d	l
Henderson	#1 Krey	13	23S	11W	SE SE NE	abs	abs	c	l
CRA & Hawley	#1-E Allen	30	23S	11W	SW SW NE	abs	abs	c	l
Stanolind	#1 Figger	1	23S	12W	NE NE	abs	abs	c	c
JFW	#1 Salem	6	23S	12W	SW SE	abs	abs	c	c
Edwards	#1 Hughes-Ritt	13	23S	12W	SE SW NE	abs	abs	c	l
Patton	#1 McCune	17	23S	12W	NW NW SW	abs	abs	d	l
Texas	#1 McGerdes	34	23S	12W	NE NE NE	abs	abs	abs	l
Petroleum, Inc.	#1-G Witt	1	23S	13W	NE NE NE	abs	abs	c	c
Hilton Drlg.	#1 Russell	14	23S	13W	SW SW NE	abs	abs	c	c
Phillips	#1 Detweiler	26	23S	13W	SW SW SW	abs	abs	c	l
Nat'l O&G	#1 Smith	30	23S	13W	SE SE NW	abs	abs	c	l

OPERATOR	WELL NAME	LOCATION S.	T.	R.	SPOT	DEPTHS A	B	C	D
Boger Bros.	#2 Miller	5	23S	14W	E2 E2	abs	c	dwl	1
Natural G&O	#1 Gilmore	29	23S	14W	SW SE NE	abs	abs	c	c
Natural G&O	#1 McComas	1	23S	15W	NE SW SW	abs	abs	c	c
Alma	#1 Irma	3	23S	15W	NW NW SE	abs	abs	c	c
Pickrell Drlg.	#1 Curtis	6	23S	15W	SE SW NW	abs	abs		c
CXY	#1 Petro	15	23S	15W	SW NW NW	abs	abs	c	1
Lario	#1 Wilcox	18	23S	15W	SE SE SW	abs	abs	abs	c
Loffland Brothers	#1 Grizzell	23	23S	15W	SW SW SE	abs	abs	c	1
Alpine	#2 English	25	23S	15W	NE NE NW	abs	abs	c	c
Anschutz Drlg.	#1 English	28	23S	15W	NW NW SE	abs	abs	c	c
Stanolind	#1-B W. Riley	30	23S	15W	SW NE SW	abs	abs	c	c
Halliburton	#1 H.C. Colglazier	4	23S	16W	SW SE	abs	abs	c	1
Halliburton	#1 Schwartz	8	23S	16W	SW SW SW	abs	abs	dwl	1
Alpine	#1 Buhrer	14	23S	16W	NW NW	abs	abs	c	1
Rupe & Ash	#1 Horton	16	23S	16W	NE SW SW	abs	abs	c	1
R.F. White	#1 Curtis	25	23S	16W	SE NE NE	abs	abs	abs	c
Barnett	#1 Hawes	28	23S	16W	SW SE	abs	abs	dwl	c
Colorado	#1 Schwartz	1	23S	17W	NW NW SW	abs	abs	c	dwl
Clark Knight Drlg.	#1 Hutchinson	3	23S	17W	NW NW NW	abs	abs	dwl	1
C.U. Bay	#1 Fischer	26	23S	17W	NW NE NW	abs	dwl	dwl	1
Sohio Petrol.	#1 Aldrich	32	23S	17W	NE SE NW	dwl	dwl	dwl	1
Cherry Drlg.	#1 Briggs	12	24S	1W	SE SE SE	abs	abs	d	d
Anderson-Prichard	#1 Gingrass	36	24S	1W	SW SW NE	abs	abs	abs	d
F&M	#1 Baalman	7	24S	2W	SE SE NE	abs	abs	abs	d
Messman-Rinehart	#1 Bradenberger	18	24S	2W	NW SW SW	abs	abs	abs	d
Cities Service	#1 McNew	8	24S	3W	SE SE NE	abs	abs	abs	lwd
Renfro Drlg.	#1 Stutzman	22	24S	3W	NE NE NE	abs	abs	1	1
GMR	#1 Baird	34	24S	3W	SW SW SW	abs	abs	1	1
McBride	#1 Popp	24	24S	4W		abs	abs	abs	1
Stanolind	#1 Sprowel	1	24S	5W	NE NE NE	abs	abs	abs	1
Lion et al.	#1 Bontrager	8	24S	5W	SE SW SE	abs	abs	abs	dwl
Lochiel	#1 Schrock	27	24S	5W	SE NW SE	abs	abs	abs	1
Osage O&G	#1 Benton	6	24S	6W	NW NW SE	abs	abs	abs	1
T&M Oil	#1 Haines	10	24S	6W	NW NW NW	abs	abs	abs	lwd
Tomlinson	#1 Coffey	31	24S	6W		abs	abs	abs	dwl
Rex et al.	#1 Evalyn	21	24S	7W	NW NW SW	abs	abs	d	1
Grant	#1 Foster 'B'	21	24S	8W	SE SE SW	abs	abs	abs	1
Trans-Era Petrol.	#1 Wagler	3	24S	9W	NE NE SE	abs	abs	d	1
Smitherman	#1 Dion	15	24S	9W	NE SW NW	abs	abs	d	1
Manhart et al.	#1 Hinshaw	17	24S	9W	NW NW SW	abs	abs	dwl	1
L. Phillips	#1 McVey	19	24S	9W	SE SE SW	abs	abs	d	1
Stearns & Johnson	#1 Schultz	3	24S	10W	NW NW NE	abs	abs	d	1
Lee Phillips	#1 McVey	19	24S	10W	SE SE SW	abs	d	d	1
Artnell	#1 Fassnacht	28	24S	10W	SW SW NE	abs	d	dwl	1
Demier	#2 Brownlee	31	24S	10W	NE NW SW	abs	d	dwl	1
CRA	#1-A McMillan	30	24S	11W	SW NE NW	abs	dwl	d	1
Veeder	#1 Bennett	7	24S	12W	NE NE NW	abs	dwl	dwl	1
Sunray-Midcon.	#1 Cline	25	24S	13W	NE SW SE	abs	1	d	1
Arco	#5-B McNaghten	27	24S	13W	SW SW NW	abs	abs	dwl	1
Aurora Gas	#1 Hoover	29	24S	13W	SE NE SE	d	1	dwl	1
Altman	#1 Brehm-Burke	2	24S	14W	SE SW NE	abs	abs	dwl	1
Musgrove Drlg.	#1 Krause	5	24S	14W	SW SW SW	abs	abs	c	c
Chief & Sunray	#1 Snyder	28	24S	14W	SE SW NW	c	dwl	dwl	1
Murfin Drlg.	#1-C Southwestern	1	24S	15W	SE NW NE	abs	abs	c	c
Musgrove Drlg.	#1 Hoover	5	24S	15W	NE NE NE	abs	abs	c	1
Musgrove Drlg.	#1 Dykes	27	24S	15W	NE SE	abs	d	dwl	1
Anschutz Drlg.	#1 Ackerman	29	24S	15W	NW NW SW	abs	dwl	dwl	1
Imperial	#1 Doll	5	24S	16W	NW SE NE	dwl	dwl		
Helmerich & Payne	#1 Coppoc	9	24S	16W	NE NE SW	abs	abs	lwd	1
Natural G&O	#1 Campbell	18	24S	16W	SE SW SW	dwl	lwd	lwd	1
Sunray	#1 Embry	24	24S	16W	NW NW SW	dwl	dwl	dwl	1
Conoco	#1 Meyer	34	24S	16W	SW SE SW	abs	abs	lwd	1
NCRA	#1 Lovette	17	24S	17W	SE SE NW	dwl	d	dwl	1
Lauck et al.	#1 Cross	28	24S	17W	NE NE NE	dwl	dwl	dwl	1

OPERATOR	WELL NAME	LOCATION S.	T.	R.	SPOT	DEPTHS A	B	C	D
Sutton	#1 Vogt	17	25S	1W	SW SW NW	abs	abs	abs	d
Champlin	#1 Caple	19	25S	2W	SE SE NW	abs	abs	dwl	dwl
Kenwood	#1 Kinast	4	25S	4W	NE NE NW	abs	abs	dwl	1
Aurora Gas	#1 Tonn	21	25S	4W	NW NW NW	abs	abs	abs	1
R. Godfrey	#1 Smith	23	25S	4W	NE NE NE	abs	abs	abs	d
Wentworth	#1 Stuckey	20	25S	5W	SW SW SW	abs	abs	abs	d
Cities Service	#1 Zimmerman	21	25S	6W	NW NW SE	abs	abs	d	1
Stearns	#1 Burling	3	25S	7W	SE SE SW	abs	abs	d	1
Shawver et al.	#1 Linscheid	2	25S	8W	NW NW NE	abs	abs	abs	lwd
Aurora Gas	#1 Breidenstein	1	25S	9W	NE NE NE	abs	abs	dwl	1
Time Petrol.	#1 Nixon	7	25S	9W	SW SW SE	abs	abs	dwl	1
El Dorado Refining	#1 McAtee	26	25S	9W	SE SE SE	abs	abs	dwl	1
Schermerhorn	#1 Brownlee	6	25S	10W	SE SE SW	abs	d	dwl	1
Schermerhorn	#1 Nies	20	25S	10W	SE NW NW	abs	abs	d	1
Rex & Morris	#1 Linder	23	25S	10W	NE NE NW	abs	abs	dwl	1
Colorado	#1 Nies	28	25S	10W	SW NE	abs	abs	dwl	1
Lawson & Skelly	#1 Dickson	17	25S	11W	NW SE NW	abs	dwl	dwl	1
Aurora Gas	#1 McCune	17	25S	12W	SW SW NE	abs	abs	dwl	1
Pure	#1 Brock	25	25S	12W	SE NW NE	abs	1	dwl	dwl
Petroleum, Inc.	#1 Barstow	5	25S	13W	NW NE NW	abs	abs	dwl	dwl
Artnell	#1 Shank	15	25S	13W	NE NE	abs	abs	dwl	1
Alpine	#1 Hall	17	25S	14W	SW SW NE	1	1	1	1
Sierra & Houston	#1 Wiles	15	25S	15W	NW SE NW	1	1	dwl	1
Strata Drlg.	#1 Childs	17	25S	15W	NE NE	1	1	1	1
Lauck & Sunray	#1 Frack	27	25S	15W	SW SW SW	1	1	1	1
Birmingham-Bartlett	#1 Frack	35	25S	15W	NE NE SW	abs	dwl	dwl	1
Harms-Burt	#1 Breitenbach	10	25S	16W	NE NE NW	abs	1	lwd	1
Skelly	#1 Miller	12	25S	16W	NE NW NE	dwl	dwl	dwl	1
Lauck	#1 Palmitir	16	25S	16W	SW SW	abs	dwl	dwl	1
Natural G&O	#1 Johnston	18	25S	16W	NE NW SE	abs	abs	dwl	1
Lauck	#1 Johnson	1	25S	17W	NE SE SW	abs	abs	dwl	1
Cities Service	#1 Wokaty	25	25S	17W	NE SE NE	abs	abs	dwl	1
Sherrod & Apperson	#1 Huff	31	25S	17W	SE NE NW	dwl	dwl	dwl	dwl
Halliburton et al.	#1 Burge	4	26S	1W	SE SE NE	abs	abs	d	d
Catron	#3 Wilson	12	26S	1W	E2 E2 SE	abs	abs	d	d
Allison	#1 Hitt	32	26S	1W	NE NW NE	abs	abs	abs	d
Amerada	#1 A. Kessler	34	26S	1W	SW SW	abs	abs	abs	d
Barbara	#1 Seiwart	18	26S	2W	SW SW SW	abs	abs	abs	d
Aurora Gas	#1 Baalman	21	26S	2W	SE SE NW	abs	abs	d	d
Sun	#1-A Lies	12	26S	3W	SW SW	abs	abs	abs	d
Aylward Drlg.	#1 Krehbiel	26	26S	6W	NW NW NW	abs	abs	abs	d
H-30 Drlg.	#1 Graber	13	26S	7W	NE SE	abs	abs	abs	d
Anschutz Drlg.	#1 Gardner	5	26S	8W	NE NE SW	abs	abs	dwl	1
K&E Drlg.	#1 Peek	21	26S	8W	NE NE	abs	abs	d	1
Sohio Petrol.	#1 Wells	18	26S	9W	SW NW NW	abs	abs	dwl	1
Harms-Burt	#1 Jones	26	26S	9W	NE NE SE	abs	abs	dwl	1
Durbin Bond	#1 foster	29	26S	9W	NE NE NE	abs	abs	dwl	1
Armer	#1 Geesling	3	26S	10W	SE SE SE	abs	abs	dwl	1
T.O. Lillystrand	#1 Flukes	15	26S	10W	NE NW NW	abs	abs	d	1
Deep Rock	#1 Slater	1	26S	11W	SW SW NE	abs	abs	dwl	1
Helmerich & Payne	#1 Jorns	5	26S	11W	SW SW NW	abs	abs	dwl	1
Vickers Expl.	#1 Walker	13	26S	11W	NW NW SE	abs	abs	dwl	1
Natural G&O	#1 Schriver	16	26S	11W	SW SE NW	abs	abs	dwl	1
Mercury et al.	#1 Hawver	5	26S	12W	NW NW NE	abs	abs	dwl	1
Musgrove Drlg.	#1 Trimpe	17	26S	12W	SW SW SW	abs	abs	dwl	1
NCRA	#1 Burkner	25	26S	12W	SE SE SW	c	dwl	d	1
Champlin	#1 Henderson	11	26S	14W	SW NE NW	abs	abs	dwl	1
Cities Service	#1 Bennett	24	26S	14W	NE NE SE	abs	abs	c	1
K&E & Musgrove	#1 Thompson	28	26S	14W	NW NW SE	abs	abs	c	1

OPERATOR	WELL NAME	LOCATION S.	T.	R.	SPOT	DEPTHS A	B	C	D
Sierra Petrol.	#1 McMannis	36	26S	14W	SW SW NW	abs	l	dwl	l
Rine Drlg.	#1 Gereke	12	26S	15W	SW NE SE	dwl	dwl	lwd	l
Mull Drlg.	#1 Doggett	17	26S	15W	NE NE SW	dwl	dwl	dwl	l
Anschutz Drlg.	#1 Tatlock	28	26S	15W	NE NE NW	dwl	dwl	dwl	l
Bell et al.	#1-A Tatlock	32	26S	15W	NE NE NW	lwd	lwd	lwd	l
F.K. Johnson	#1 Salser	12	26S	16W	SW SW NW	abs	abs	dwl	l
Ambassador	#1-A Wood	13	26S	16W	SW NW NW	abs	abs	dwl	l
Aurora Gas	#1 Schultz	21	26S	16W	SE SE NW	abs	abs	dwl	l
F.K. Johnson	#1 E.D. Wood	26	26S	16W	NE NE NE	abs	abs	c	l
Sinclair	#1 Mellor	28	26S	16W	SW SW SE	abs	abs	dwl	l
Sunray	#1 King	33	26S	16W	NE NE SW	abs	abs	dwl	dwl
Trans-Era Petrol.	#1 Sherman	12	26S	17W	NW NW SW	abs	dwl	dwl	l
Phillips	#1 Newsom	13	26S	17W	SW SW SW	d	dwl	d	l
Anschutz Drlg.	#1 Fatzer	15	26S	17W	SE SE SE	abs	abs	d	dwl
Anschutz & Aurora	#1 Fisher	35	26S	17W	NE NE NE	dwl	dwl	d	l
Adair	#1 Strunk	5	27S	2W	NW NW NW	abs	abs	abs	d
Aurora Gas	#1 Klausmeyer	14	27S	3W	NE NE NE	abs	abs	abs	d
Amerada	#1 Becker	18	27S	3W	SE NE SE	abs	abs	abs	d
Ferguson	#1 Scheer	22	27S	3W	SE SE SW	abs	abs	abs	d
Aylward Drlg.	#1 Wells	26	27S	3W	NE NW	abs	abs	abs	d
Armer	#1 Ambler	15	27S	5W	NE NW NW	abs	abs	abs	d
Mack	#1 Van Sickle	29	27S	7W	SW NE	abs	abs	abs	d
Anschutz Drlg.	#1 Dondelinger	35	27S	7W	SE SE SW	abs	abs	abs	d
Rupe	#1 Geesling	17	27S	8W	SE NW	abs	abs	d	l
Leben Drlg.	#1 Funke	25	27S	8W	SE SE	abs	abs	abs	d
Wentworth & Sons	#1 McClure	31	27S	8W	NW NE NW	abs	abs	d	l
Pickrell Drlg.	#1-H Tjaken	29	27S	9W	NE NW	abs	abs	d	l
Aylward Drlg.	#1 Tonn	3	27S	10W	NE NE SW	abs	abs	dwl	l
Amerada	#1 McNamee	21	27S	10W	NW NW SE	abs	abs	dwl	l
Southwestern Expl.	#1 Lion	29	27S	11W	E2 NE NW	abs	abs	d	l
Falcon Seaboard	#1 Elwood	12	27S	12W	NW NW NW	abs	l	dwl	dwl
Merchant	#1 Roberts	22	27S	12W	SW SW	abs	abs	dwl	l
Aurora Gas	#1 Jones	5	27S	14W	SW SW SW	abs	abs	dwl	l
Lario	#1 Moon	13	27S	14W	SW NE SW	l	l	dwl	dwl
Parker Petrol.	#1 I. Adams	29	27S	14W	NW NW SE	abs	dwl	dwl	l
Musgrove Drlg.	#1 Tatlock	6	27S	15W	NE NE NE	dwl	dwl	dwl	l
Anschutz Drlg.	#1 Jones	13	27S	15W	SW SW SW	dwl	l	dwl	dwl
Musgrove Drlg.	#1 Bryant	32	27S	15W	SW SW NE	abs	abs	dwl	l
Sunray	#1 L. French	4	27S	16W	NE SW	abs	l	l	
Murfin Drlg.	#1 Matthews	7	27S	16W	SE SE NE	abs	dwl	d	l
Dunne-Gardner	#1 Curtis	15	27S	17W	SW SW	dwl	d	d	l
Aurora Gas	#1 Campbell	17	27S	17W	SE SE SW	dwl	dwl	dwl	dwl
Jones-Gebert	#1 Thome	2	28S	2W	SE SW	abs	abs	abs	d
Pickrell Drlg.	#1 Meng	1	28S	6W	SE NE	abs	abs	d	d
Rains & Williamson	#1 Greenleaf	20	28S	6W	NW NW	abs	abs	abs	d
Mack	#1 Gonzales	17	28S	7W	NE NW	abs	abs	d	d
Graybol	#1 McKenna	3	28S	8W	NW SE	abs	abs	d	l
Graybol	#1 Stead	6	28S	8W	SW NE	abs	abs	d	l
Petroleum, Inc.	#1 Dillon	23	28S	8W	SW SW SW	abs	abs	d	l
Reading & Bates	#1 Covington	27	28S	8W	SW SE	abs	abs	d	d
Utica Southern	#1 Boch	29	28S	8W	NW NE	abs	abs	dwl	l
Kaiser-Francis	#1 Sisters	14	28S	9W	SE SW	abs	abs	d	l
Pickrell Drlg.	#1-C Beat	36	28S	9W	NW SE	abs	abs	dwl	l
Anschutz Drlg.	#1 Adelhardt	36	28S	10W	SW NE	abs	abs	dwl	l
Aurora Gas	#1 Dyche	25	28S	11W	SW SW SW	abs	d	dwl	l
Aurora & Trans Era	#1 Rose	27	28S	11W	NW NW NE	abs	d	dwl	l
Cities Service	#1 Tipton	29	28S	11W	SW SE SW	abs	d	dwl	l
Lindas	#1 Lunt	5	28S	12W	NW NE NW	abs	dwl	dwl	l
Raymond	#2 Hillard	1	28S	13W	NW NW	abs	abs	dwl	l

OPERATOR	WELL NAME	LOCATION S.	T.	R.	SPOT	DEPTHS A	B	C	D
Imperial	#1 Gilliam	14	28S	13W	NW SE	abs	abs	c	c
Lion	#1 McMinn	32	28S	13W	SE SE NE	abs	dwl	dwl	1
Pickrell Drlg.	#1-A Lavelle	1	28S	14W	SE NW	abs	dwl	dwl	1
Tomlinson-Kathol	#1 Moore	6	28S	14W	NE NW NW	abs	abs	c	c
NCRA	#1 Leake	21	28S	14W	SE NW	abs	abs	dwl	dwl
Lohmann & Johnson	#1 Thompson	24	28S	14W	SE SE SE	dwl	dwl	dwl	1
CRA	#1 Spines	28	28S	14W	NE NW NW	abs	dwl	dwl	1
Lario	#1-A Eubank Estate	30	28S	14W	NE SE NW	abs	abs	dwl	1
Lauck	#1 Seyfert	14	28S	15W	SE SE SE	abs	abs	dwl	1
Schafer Drlg.	#1 Peoples Bank	12	28S	16W	SE SE SE	abs	dwl	dwl	dwl
Murfin Drlg.	#1 Bowman	31	28S	16W	SE SW SE	d	d	d	dwl
KWB	#1 E.M. Davis	2	28S	17W	SW SW	abs	abs	dwl	d
K&E Drlg.	#1 Kemp	12	28S	17W	SE SE SE	dwl	dwl	d	1
Sun	#1 Ross	14	28S	17W	SW SW NW	dwl	dwl	d	dwl
Drillers	#1 Sours	14	29S	6W	NE SW	abs	abs	abs	d
Armer	#1 Maple	30	29S	6W	NE NE NE	abs	abs	abs	d
Sunray	#1 Voth	4	29S	7W	NW NW SE	abs	abs	d	d
Murfin Drlg.	#1 Mary Brown	12	29S	7W	SE SE	abs	abs	d	d
Conoco	#1 Shepard	3	29S	8W	NE SW	abs	abs	dwl	d
Leben Drlg.	#1 Specht	5	29S	8W	NE NW	abs	abs	dwl	dwl
Mack	#1 Huey	12	29S	8W	SE SE	abs	abs	d	d
Leben Drlg.	#1 Bock	17	29S	8W	SW NE	abs	abs	dwl	dwl
Rupp-Ferguson	#1 Shepard	30	29S	8W	NE NE SE	abs	abs	d	d
Pickrell Drlg.	#1 Tiesmeyer	1	29S	9W	NE NE SE	abs	abs	dwl	1
Anadarko	#1-A Schwartz	5	29S	9W	SW SE	abs	abs	dwl	d
Time Petrol.	#1 Twyman	20	29S	10W	SE SE SE	abs	d	dwl	dwl
Petroleum, Inc.	#1 Spade	23	29S	10W	NE NE NW	abs	abs	d	1
Cities Service	#1-B Lynch	6	29S	11W	SW SW NE	abs	abs	dwl	1
Drilling & Expl.	#1-A Titus	27	29S	11W	SW NW	abs	abs	dwl	1
Rupp-Ferguson	#1 Thompson	13	29S	12W	NE NE SW	abs	dwl	dwl	1
Conoco	#1 J.R. Dauner	21	29S	12W	SW SW NW	dwl	dwl	dwl	1
Texas Company	#1 Thompson	13	29S	13W	SW SE NW	dwl	dwl	dwl	1
Aurora Gas	#1 Morrell	10	29S	14W	SW SW NE	abs	abs	dwl	1
Amerada	#1 Lee	11	29S	14W	NW NW NE	abs	abs	dwl	1
Lario	#1 Schriver Estate	12	29S	14W	NW SW SE	abs	c	dwl	1
Lario	#1 Schrepel	16	29S	14W	NW NW SE	abs	abs	dwl	1
Lario	#1 Christain	24	29S	14W	NW SW NW	abs	abs	1	1
Imperial	#1 Bergner	35	29S	14W	S2 NE NW	abs	abs	c	1
C.R. King	#1 Winkley	11	29S	15W	SW NW	abs	dwl	dwl	1
Skelly	#1 Hogard	15	29S	15W	NE SE NW	abs	dwl	dwl	1
Aylward Drlg.	#1-A Kerr	29	29S	15W	NE NE SW	abs	abs	c	d
Imperial	#1-A Howell	11	29S	16W	SW SW NW	abs	abs	abs	1
Gramehart-Miller	#2 Betzer	34	29S	16W	NW NW NE	abs	dwl	dwl	1
Rupp-Ferguson	#1 Morford	5	29S	17W	SW NW SW	lwd	lwd	dwl	1
Pickrell Drlg.	#1-E Feiser	18	30S	5W	NW SE	abs	abs	abs	d
Rains & Williamson	#1 Sparr	32	30S	5W	S2 S2 NW	abs	abs	abs	d
Clements	#1 Smith	14	30S	6W	SE NE	abs	abs	abs	d
Pickrell Drlg.	#1 Bertholf	3	30S	8W	SE SE NE	abs	abs	dwl	dwl
NCRA	#4-A Tjaden	13	30S	8W	SW NW SE	abs	abs	d	d
Chapman	#1 Liebl	6	30S	9W	SW SW	abs	abs	d	1
Gulf	#1 Piehl	19	30S	9W	NW SW SE	abs	abs	dwl	1
Cities Service	#1 Depenbusch	23	30S	9W	NE NE SE	abs	abs	d	1
Welch & Olsson	#1 Liebl	3	30S	10W	NE NE SW	abs	abs	d	dwl
Sunray & Skelly	#1 Morisse Ut.	14	30S	10W	NW NW SE	abs	abs	d	1
Southwestern Expl.	#1-B Allen	28	30S	10W	W2 SW SW	abs	abs	dwl	1
Coppinger	#1 Meeks	4	30S	11W	SE SE SE	abs	abs	dwl	1
Edmiston	#1 Ferrel	15	30S	11W	NW NE	abs	abs	dwl	1
Lauck	#1 Coss	16	30S	11W	NW NW NW	abs	abs	dwl	1
Aylward Drlg.	#1 Wehling	26	30S	11W	NE NE NE	abs	d	dwl	1
Schafer Drlg.	#1 Mease	36	30S	11W	NE NE NE	abs	d	dwl	1
W.C. Payne	#1 Gibson	3	30S	12W	NE SW	dwl	dwl	dwl	1

OPERATOR	WELL NAME	LOCATION S.	T.	R.	SPOT	DEPTHS A	B	C	D
Ferguson	#1 Rose	7	30S	12W	SW SE	d	dwl	dwl	l
Carter-Mandel	#1 McIntire	13	30S	12W NW	SE NW	abs	abs	dwl	l
Natural G&O	#1 Lillieovist	29	30S	12W	NE NE	abs	d	dwl	l
Sterling	#1 Baker	21	30S	14W NE	NE NW	abs	abs	dwl	l
Pickrell Drlg.	#1 Shriver Trust	24	30S	14W	NE NW	dwl	dwl	dwl	l
Great Lakes Carbon	#1-D Werner	28	30S	14W SE	SE NW	abs	abs	d	l
R.C. Patton	#1 Werner	29	30S	14W NE	NW SE	abs	dwl	d	l
PMI	#1 Mills	31	30S	14W	NE SW	abs	dwl	dwl	l
Farmer	#1 Hoagland	24	30S	15W	SE NE	abs	abs	dwl	l
Birmingham-Bartlett	#1 Mills	34	30S	15W	SW SE	dwl			
Gulf	#1-P Robbins	23	30S	16W NE	SW SW	d	dwl	dwl	l
Shell & Gulf	#1 Robbins	32	30S	16W	SW NE	dwl	dwl	dwl	dwl
Honaker-Davis	#1 Walker	36	30S	16W	NW SE	d	dwl	dwl	l
Mack	#1 Barr	18	31S	7W	SE SE	abs	abs	d	dwl
McCoy Petrol.	#3-C Williams	22	31S	8W S2	NW NE	abs	abs	d	d
Mack	#2 Squire	26	31S	8W	SE SW	abs	abs	d	d
K&E Drlg.	#1 Morrise	9	31S	10W NE	NW NE	abs	abs	dwl	l
Aurora Gas	#1 Rankin	13	31S	10W	SW SW	abs	abs	dwl	l
Musgrove Drlg.	#1 Stone	15	31S	10W NE	NE NW	abs	d	d	l
Jones-Gebert	#1 Wheat	4	31S	11W	SE SW	abs	l	dwl	l
K&E Drlg.	#1 Chain	5	31S	11W	NE NW	abs	abs	dwl	l
Coppinger	#1 Warwick	12	31S	11W	NW SE	abs	dwl	dwl	l
Beardmore Drlg.	#1 Liebst	14	31S	11W	NE SE	abs	abs	dwl	l
Lario	#1 Axline	17	31S	11W NE	NW NE	abs	l	dwl	l
Pickrell Drlg.	#1 Clark	26	31S	11W NW	SW NE	abs	c	dwl	dwl
Anschutz Drlg.	#1 Gress	6	31S	12W	SE SW	abs	dwl	dwl	l
G-M-R	#1 Updegraff	15	31S	12W NE	NE NE	abs	dwl	dwl	l
Parker Petrol.	#1 Winters	18	31S	12W NE	NE SW	dwl	dwl	dwl	l
Beardmore Drlg.	#1 Calloway	20	31S	12W NW	NW NW	c	dwl	dwl	l
Aylward Drlg.	#1 Updegraff	22	31S	12W	SE SE	abs	l	dwl	l
Aurora Gas	#1 Clark	30	31S	12W NW	NW NE	abs	l	dwl	l
Colorado	#1 Hartley	30	31S	13W	SE NW	abs	dwl	dwl	l
Barbara	#1 M. Mills	30	31S	13W NW	NW NE	dwl	dwl	dwl	l
K&E Drlg.	#1 Lenkner	3	31S	15W	SE NW	dwl	dwl	d	l
Aylward Drlg.	#1 Lenkner	4	31S	15W	NW SW	abs	dwl	dwl	dwl
Skelly	#1 Reed	10	31S	15W	SE NE	dwl	d	d	l
Petrol. Technol.	#16-1ABray	16	31S	15W	SE NW	dwl	dwl	d	l
Aurora Gas	#1 Kaminska	17	31S	15W NW	NW SW	d	dwl	dwl	l
Rupp-Furguson	#1 Dickerson	22	31S	15W NE	NE NE	dwl	dwl	d	l
Barbara	#1-8 Robbins	23	31S	16W	SW	dwl	lwd	d	d
Barbara	#1 Kaminska	24	31S	16W	SW	dwl	dwl	dwl	l
Aylward Drlg.	#1 Parker	6	32S	7W NE	NE NE	abs	abs	d	abs
Aurora Gas	#1 Garber	17	32S	7W SW	SW NE	abs	abs	d	d
Musgrove Drlg.	#1 Moldenhauer	27	32S	7W SW	SW SW	abs	abs	abs	d
Beardmore Drlg.	#1 Berg	29	32S	7W SW	SW SE	abs	abs	abs	d
Hellar Drlg.	#1 Osborn	12	32S	8W	NW NW	abs	abs	d	l
Colorado	#1 Naffziger	13	32S	8W	SW SW	abs	abs	d	l
Rupp-Ferguson	#1 Bebermeyer	15	32S	8W SE	SE NW	abs	abs	d	l
NCRA	#1 Catlin	33	32S	8W	NW NE	abs	abs	d	l
Aylward Drlg.	#1 Holcomb	17	32S	9W SW	SW NW	abs	dwl	dwl	l
Beardmore Drlg.	#1 Black	28	32S	9W NE	NE NE	abs	d	d	dwl
Conoco	#1 Gersner	9	32S	10W NW	SW NW	abs	dwl	lwd	l
Mull Drlg.	#1 Wheelock	3	32S	12W	SW NW	d	dwl	dwl	l
Pryor et al.	#1 Wilson	6	32S	12W	NW NW	abs	dwl	dwl	l
Patton	#1 Bloom	25	32S	12W NW	NW NW	abs	dwl	dwl	l
Honaker-Davis	#1 Gant	3	32S	13W NW	NW NW	abs	dwl	dwl	dwl
Aylward Drlg.	#1 Brooks	7	32S	13W SW	SW NE	dwl	dwl	dwl	l
Lion	#1 Brooks-Younger	23	32S	13W NE	NE SW	abs	l	dwl	dwl
Anschutz Drlg.	#1 Lonker	25	32S	13W NE	NE NE	abs	dwl	l	l
Conoco	#1 L. Mills	5	32S	14W SW	SE SE	l	l	l	l
Aylward Drlg.	#1-F Stumph-Smith	17	32S	14W NE	NE NE	dwl	l	l	l
Olson	#1 Canfield	24	32S	14W	NE NE	dwl	dwl	l	l
Kern Drlg.	#1 Schutte	2	32S	16W	SW NE	dwl	dwl	dwl	dwl
Wentworth & Sons	#1 Price	4	32S	16W SE	SE SE	dwl	l	dwl	l
Rupp-Ferguson	#1 Schuette	9	32S	16W SW	SW NE	dwl	l	dwl	l

OPERATOR	WELL NAME	LOCATION S.	T.	R.	SPOT	DEPTHS A	B	C	D
Petroleum, Inc.	#1-B Gregg Unit	27	32S	17W	NE NE	d	d	dwl	l
Parker Petrol.	#1 Cary	30	32S	17W	SE SW	dwl	dwl	dwl	l
Musgrove Petrol.	#1 Hayter	6	33S	6W	NE NE NE	abs	abs	abs	d
Anschutz Drlg.	#1 Mollohan	34	33S	7W	SW NE	abs	abs	abs	d
Rupp-Ferguson	#1 Kastens	28	33S	8W	W2 W2	abs	abs	dwl	l
Cities Service	#1-D Tucker	29	33S	9W	NW NE	abs	d	d	dwl
Mack	#1 Patterson	33	33S	9W	NE NE	abs	d	d	dwl
Magnolia	#1 Traffas	6	33S	10W	NW NW SE	abs	dwl	lwd	l
Davidor & Davidor	#1 Dunkin	14	33S	10W	NE NE NW	abs	l	lwd	l
Smith & Toto	#1 McReynolds	16	33S	10W	NW SW	abs	l	dwl	
Trans-Era Petrol.	#1 Stewart	17	33S	10W	NE SE SE	dwl	dwl	dwl	l
Jones et al.	#1 Washburn	29	33S	10W	SW SW SW	abs	lwd	dwl	l
Ambassador	#1 Page	36	33S	10W	N2 NE SW	abs	d	dwl	l
Todd Drlg.	#1-A Burns	24	33S	11W	NE NE NE	dwl	dwl	lwd	l
Barbara	#1 Forrester	28	33S	11W	SW NW NE	d	l	dwl	l
Skelly	#1-C Harbaugh	13	33S	12W	SE SW SE	abs	d	lwd	l
Wakefield	#1 Baler	8	33S	13W	NE NE NE	l	l	dwl	l
Conoco	#1 B.E. Holmes	35	33S	13W	NE NE NW	lwd	lwd	dwl	l
Anschutz Drlg.	#1 Mills	5	33S	14W	NE SE	dwl	dwl	dwl	l
Gramehart-Miller	#1 Lenker	24	33S	14W	SE NE SW	d	l	dwl	l
Fisher Oil	#1 Brass	9	33S	15W	W2 SW SW	dwl	dwl	dwl	l
Aylward Drlg.	#1 Platt	17	33S	15W	SW SW SW	l	l	dwl	l
Mull Drlg.	#1 Platt	30	33S	15W	SE SE NE	dwl	dwl	dwl	l
Sunray DX	#1 M. Gregg	31	33S	16W	NW SE	dwl	l	dwl	l
J.M. Huber	#1 Einsel	11	33S	17W	SW NW NW	d	l	l	l
Conoco	#1 C.F. Biddle	13	33S	17W	NE NE	d	d	d	l
Huber	#1 Warren	25	33S	17W	SE	l	l	l	l
PMI	#1 Warren Ranch	35	33S	17W	SE SE	lwd	lwd	lwd	l
Alpine & Roy	#1 Brownback	5	34S	2W	NE NE SW	abs	abs	abs	d
Natural G&O	#1 Neal	20	34S	2W	NE NW SE	abs	abs	abs	l
F&M	#1 Berka	19	34S	3W	NE SW SE	abs	abs	abs	l
Texas Company	#1 Baker	24	34S	5W	NE SW NW	abs	abs	abs	l
Prime & Benedict	#1 Hallman	9	34S	6W	SE SW	abs	abs	abs	d
Aurora Gas	#1 Barrett	20	34S	6W	SW SW SE	abs	abs	l	l
Gulf	#1 Birchenough	1	34S	7W	SW NW	abs	abs	dwl	dwl
Hamilton	#1 Carr	14	34S	7W	NE SE	abs	abs	dwl	dwl
Huber	#1 Cather	16	34S	7W	NE SE NE	abs	abs	l	l
Mull Drlg.	#1 Dusenbury	10	34S	8W	SE SE NW	abs	abs	dwl	l
Oil Capitol	#1 Woodworth	16	34S	9W	NE SE	abs	abs	dwl	l
Gruenerwald	#1 Hibbard	23	34S	9W	NW NW SW	abs	abs	dwl	l
Mull Drlg.	#1 Griffin	7	34S	10W	SE SE SE	abs	l	dwl	l
Prime Drlg.	#1 Garner	21	34S	10W	NE NE SE	abs	l	l	l
Conoco	#1 Porterfield	32	34S	10W	SE NE SW	abs	l	l	l
Gulf	#1 Groendyke	6	34S	11W	NW NW NW	l	l	lwd	l
Honaker-Davis	#1 Stolebarger	25	34S	11W	NE NE NE	abs	dwl	dwl	l
Aurora Gas	#1 Goldman	32	34S	11W	NW NW SW	abs	l	dwl	l
Aurora Gas	#1 Humphrey	24	34S	12W	SE SE NE	abs	l	dwl	l
Imperial Drlg.	#1 Blunk	5	34S	13W	NE SW SW	l	l	dwl	l
K & E Drlg.	#1 Ott	6	34S	13W	NW NW NE	l	dwl	dwl	l
Graham et al.	#1 Donovan	9	34S	13W	NE NE SE	l	l	dwl	l
Palmer Oil	#1 Schupbach	15	34S	13W	SE SW NE	l	l	dwl	l
Adair et al.	#1-B Graves	24	34S	14W	S2 S2 NE	l	l	l	l
Deep Rock	#1 McBrayer	26	34S	14W	SE SW NW	l	l	lwd	l
Gruenerwald	#1 Farley	32	34S	14W	NW NW	l	l	l	l
Honaker-Davis	#1 Platt	6	34S	15W	SE NE	dwl	l	dwl	l
Chicago Corp.	#1-B Davis Ranch	9	34S	15W	SE SE	dwl	lwd	lwd	l
Honaker-Davis	#1 Davis	18	34S	15W	NE NE SW	dwl	l	lwd	l
Yucca Petrol.	#1 Guss	16	34S	17W	NW NE SE	dwl	l	lwd	l

OPERATOR	WELL NAME	LOCATION S.	T.	R.	SPOT			DEPTHS A	B	C	D
Olympic Petrol.	#1 Haas	19	34S	17W		NW	NW	lwd	lwd	lwd	l
Midcon.	#1 Erlich	28	34S	17W	NE	SW	NW	lwd	lwd	lwd	l
Forney	#1-6 Schwarz	6	35S	2W	NW	SE	SE	abs	abs	abs	l
MidStates	#1 Hudson	3	35S	3W	SW	NW	SE	abs	abs	abs	l
Jones et al.	#1 Livengood	14	35S	6W	W2	NW	SW	abs	abs	lwd	lwd
Provincial	#1 Burchfield	3	35S	7W	NE	NE	SE	abs	abs	lwd	l
Conoco	#1 McKee	6	35S	7W	SE	SW	NW	abs	abs	d	lwd
Mull Drlg.	#1 Burchfield	15	35S	7W		NW	NE	abs	abs	lwd	l
Aurora Gas	#1 Zellers	10	35S	8W	SW	SW	SW	abs	l	dwl	l
Anschutz Drlg.	#1 Carroll	2	35S	9W	N2	NW	NW	abs	l	dwl	d
Carlock	#1 Carroll	3	35S	9W		NW	NW	abs	abs	dwl	l
Aurora Gas	#1 Gudeman	10	35S	10W	NW	NW	NE	abs	d	dwl	l
Vickers Expl.	#1 Schupbach	16	35S	10W	NW	NW	NW	abs	abs	d	l
Aurora	#1 Washburne 'B'	10	35S	11W	NW	NW	SW	abs	l	d	l
Aurora Gas	#1-C Ohlson	8	35S	12W		NW	NW	abs	l	dwl	l
Gruenerwald	#1 Molz	8	35S	14W	NW	NW	NW	dwl	l	lwd	l
City Products	#1 Wolgamott	16	35S	14W	S2	S2	S2	d	l	dwl	l
Chicago Corp.	#1 Davis Ranch	11	35S	15W		NE	NE	dwl	l	dwl	l
Petroleum Inc.	#1 Beely Ut.	7	35S	16W	N2	NE	SE	dwl	l	dwl	l
Texas O&G	#1 McMoran	8	35S	16W		SE	NW	dwl	l	dwl	l
Smith et al.	#1 McMoran	16	35S	16W	S2	SE	NW	dwl	l	dwl	l

APPENDIX VI -- POROSITY-THICKNESS RELATIONSHIPS FOR VIOLA SUBUNITS ON PRATT ANTICLINE

Inasmuch as porosity was observed to be quite variable in hand specimens, and both spatially and vertically within the Viola Formation, it was decided to initially investigate the distribution of porosity in the Viola subunits in a small area, The area chosen was, by convenience, the small map area on the Pratt anticline (Figure 5.3) that was used to examine the depositional geometry of the Viola subunits. Hopefully, a reasonable understanding of the complex depositional and diagenetic influences in porosity development and preservation in this small area could, by inductive logic, be applicable to the Viola subunits in other parts of the study area.

Average porosities for each of the Viola subunits in the small map area (see Figures 5.18 - 5.22) are posted by each well for which they were available. Porosity measurements were calculated from either sonic, neutron, or combination neutron-density logs. Sonic-derived porosities were obtained by the Sonic Porosity Formula (from Schlumberger, 1987) in which matrix velocities for limestone and dolomite were respectively assumed to be 47.6 and 43.5 microseconds per foot. Interval transit time for fluid in the well bore was assumed to be that of salt mud, 185 microseconds per foot, if salinities were not stated on the log heading. Porosities on older neutron logs (i.e., those before establishment the unified API calibration scale) were taken using tool-response-to-porosity conversion templates provided on the logs. None of the wells considered produced hydrocarbons so a lowering of neutron porosity by "gas effect" (Asquith and Gibson, 1982, p. 67; Doveton, 1986, p. 112) was assumed to be negligible. Footage intervals over which a given porosity was characteristic were selected by visual estimates, rather than using a strict mathematical method such as calculating a porosity for every two-foot interval. Porosities derived from newer neutron-density logs with common calculated porosity scales were determined by use of the root mean square formula (see Asquith with Gibson, 1982, p. 68). If porosity varied over the stratigraphic interval being examined, an arithmetic average porosity was determined for that interval on the basis of footages.

No trends are evident either laterally or with depth in porosities in the subunits isopached in Figures 5.18 through 5.22. However, a crossplot of porosity measurements versus thickness for the basal limestone and the part of the cherty dolomitic limestone below the "intermediate" limestone (Figure VI.1) indicates porosity decreases slightly with increasing thickness in the basal limestone. A weak increase in porosity with thickness also may be manifest for the lower cherty dolomitic limestone (Figure VI.1). Comparing porosity to thickness of all three crinoidal limestones (basal, "intermediate", and upper) yields a stronger indication of decreasing porosity with increasing thickness, although the correlation is still weak (Figure VI.2). Although both thick and thin crinoidal limestones may be characterized by low porosity, some of the thinner limestones develop significant porosity. The range in porosity for a limestone of a given thickness is greater for the thinner limestones.

The increase in porosity with decreasing thickness in the crinoidal limestones of the Viola suggests that post-depositional modification of porosity may be, in part, dependent on factors related to depositional environment. The depositional environment, in turn, is expressed by the original texture and composition of the sediments. The geometry of the crinoidal limestones according to their detailed isopachs is reminiscent of shoals or sediment lobes that have been influenced by currents. The thicker shoals may be subject to more current agitation, particularly at

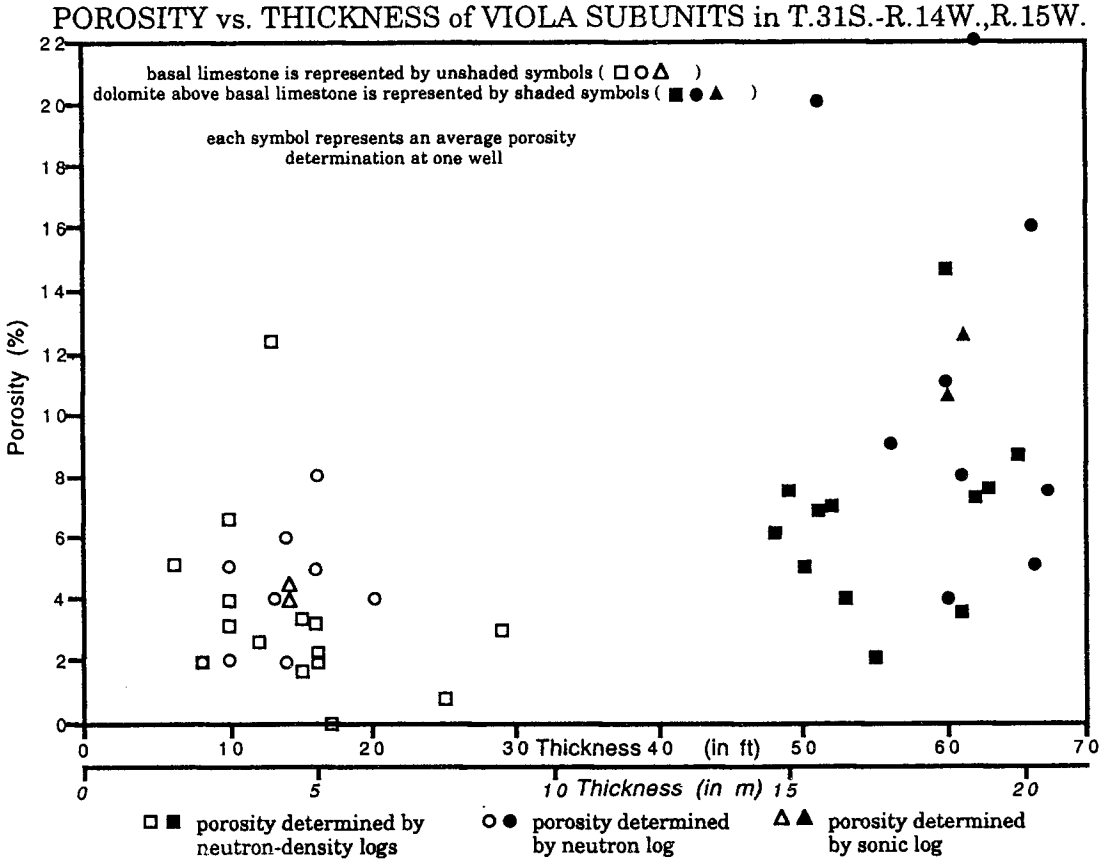

Figure VI.1 Porosity vs. thickness of the basal limestone and the portion of the lower cherty dolomitic limestone between the basal and "intermediate" limestone. Data was gathered in the small map area depicted in Figures 5.18 through 5.22 (see text for discussion). The basal limestone displays a slight decrease in porosity with increasing thickness, whereas the lower cherty dolomitic limestone displays possibly a weak increase in porosity with increasing thickness. No consistent differences in porosity with tool response (i.e., data from sonic vs. neutron vs. neutron-density tools) is noted with this limited data set.

or near their crests. These thicker shoals may contain less carbonate mud than thinner deposits of crinoidal debris, or even the flanks of the shoals that are presumably deposited in quieter and deeper water. Bornemann (1979) and St. Clair (1982) surmised that porosity-occluding syntaxial cements common in these crinoidal limestones are inhibited by the presence of interstitial mud, and invoked similar observations by Lucia (1962), Lucia and Murray (1967), and Evamy and Shearman (1965) for Devonian and Mississippian crinoidal limestones. The presence of more interstitial mud in the thinner deposits of the crinoidal limestone could also encourage subsequent development of diagenetic porosity inasmuch as this mud would be more prone to post-depositional dissolution by virtue of its significant surface area (Bathurst, 1975, p. 254; Longman, 1981). A significant aragonitic

POROSITY vs. THICKNESS of VIOLA CRINOIDAL LIMESTONES in T.31S.-R.14W., R.15W.

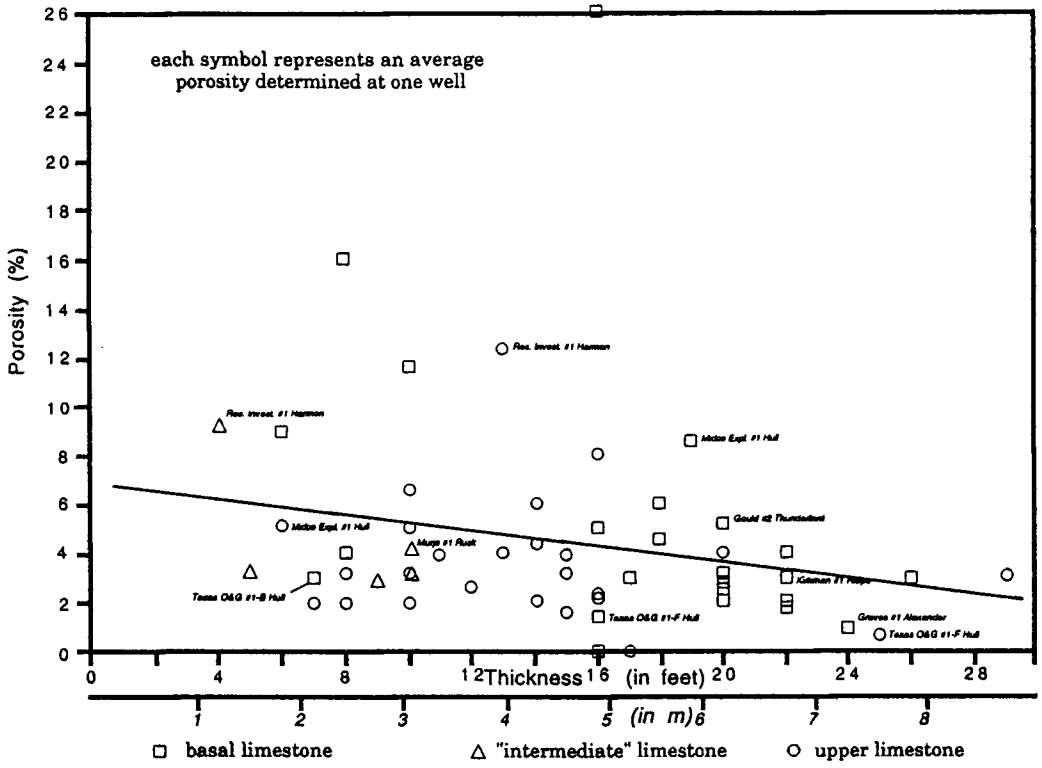

Figure VI.2 Porosity vs. thickness of the crinoidal limestones (basal, "intermediate", and upper limestones) in the small map area depicted in Figures 5.18 through 5.22. The data for the basal limestone is that depicted in Figure VI.1. A general trend of increasing porosity with decreasing thickness is evident. A regression line with an R^2 of 0.047 (0.22 goodness-of-fit) is superimposed on the plotted data. Wells used in the neutron-density crossplot in Figure VI.3 are shown to the right of their average porosities.

component, it originally present, would also be subject to preferential dissolution.

Localized thinning of the basal limestone occurs over the Pratt anticline (see Figures 5.7 and 5.10), indicating that the Pratt anticline was present during deposition of the basal limestone. Most likely, structural culminations along the Pratt anticline were expressed as bathymetric highs. In turn, the bathymetric highs probably were subject to stronger or more frequent current agitation. Bornemann (1979) and Doveton and Bornemann (1981), in fitting trend-surfaces to a four-county array of neutron-, sonic-, and density-porosity measurements from the basal limestone of the Viola, noted a 2 to 3% decrease in porosity of this unit down the flanks of the Pratt anticline. Their trend-surface analysis supports the relationship of lower porosity being associated with thicker accumulations of the crinoidal limestones and not the thinner accumulations as suggested in Figures VI.1 and VI.2. The apparent contradiction may be attributable to an over-simplified difference in scale of

investigation. Resolution of this paradox requires more investigation than the isopachous studies and porosity determinations presently considered. Supplemental trend-surface studies may help in understanding the distribution of porosity in the basal limestones in that a spatial association of positive trend-surface residuals with areas of lower porosity would support the depositional model in which porosity is least likely to be preserved in the cleaner crinoidal grainstones.

Ultimately, the reasons for the association of greater porosity with thinner intervals of the basal and upper limestone (Figure VI.2) are circumstantial. Although regional mapping indicates the basal and upper limestone subunits generally are thicker over large-scale structural uplifts such as the Central Kansas arch and the Pratt anticline (see Figures 5.7 and 5.14), local isopach thins could have developed over small structures that grew during deposition. Locally shallow areas, which could have developed over growing structures, were perhaps environmentally more favorable for accumulation of coarser-grained crinoidal and skeletal debris.

Carbonate sediments deposited over these structural highs also could be more prone to subsequent diagenesis and dolomitization than structurally lower adjacent strata, particularly if these structural highs are partly eroded and preferentially subject to fluxes of meteoric waters. Subsequent dolomitization could therefore also augment the pattern of higher porosity that is associated with some thinner packstone units. In order to ascertain if there is any association of dolomitization with porosity, neutron-density crossplots were constructed for the basal and upper limestone subunits from selected wells in the small map area on the Pratt anticline (see Figures 5.3, 5.18 - 5.22). The neutron-density crossplots for the basal limestone and upper limestone (Figure VI.3) show a general increase in porosity with increasing dolomitization in both of these Viola subunits. The greatest crossplotted porosity of 8-12% (i.e, the Midco Exploration #1 Hull well) occurs in the basal limestone where this subunit is almost completely dolomitized (Figure VI.3). Partial dolomitization of both subunits generally yields lesser amounts of porosity.

A noticeable compositional-porosity trend in the neutron-density crossplot (Figure VI.3) extends between nonporous pure limestone to dolomite with 8 to 12% porosity. No cores penetrate any dolomitized packstone in the area studied, so the nature of the porosity in the dolomitized rocks cannot be directly observed. However, the porosity is probably a type of secondary porosity (e.g., moldic or vuggy), or an intercrystalline porosity developed between dolomite rhombs.

Although the majority of pure limestones depicted in Figure VI.1 and VI.2 have little porosity (generally less than 5%), some pure limestones have up to approximately 10% porosity by wireline log analysis (Figure VI.3). The type of porosity in these pure limestones cannot be conclusively known because no cores are available from any well shown in Figure VI.3. Similarly, cores that are available are from wells that do not have suitable logging suites. However, cores recovered from the basal and upper limestone subunits in the vicinity of the wells that were crossplotted in Figure VI.3 have undolomitized crinoidal packstones with minor observable primary porosity. The undolomitized crinoidal packstones with the most porosity are coarser grained than other undolomitized packstones (Figure VI.4). Furthermore, although some of the finer grained, undolomitized packstones contain minor amounts of micrite, this material has not significantly inhibited precipitation of the calcite cement that has occluded the primary interparticle porosity. Thin-section examination of the preserved porosity in the coarser grained packstones indicates it is principally intergranular (BP) porosity that has been partly occluded by syntaxial spar cement (Figure VI.5).

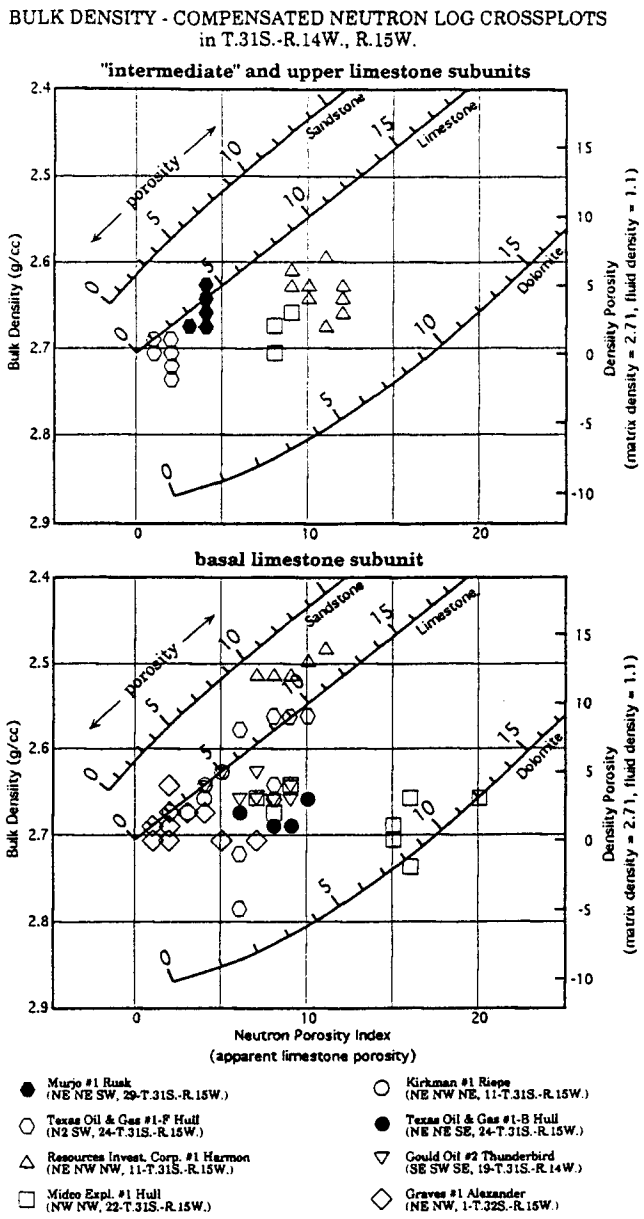

Figure VI.3 Neutron-density crossplot of the basal limestone and upper limestone from wells shown from the small map area straddling T.31S., T.32S. and R.14W., R.15W. (see Figures 5.18 - 5.22). Wells selected for crossplotting are those spanning a range of thickness and porosities (see Figure VI.1), and from which neutron and density logs are available. An increase in porosity with increasing dolomitization is evident. Each individual symbol represents a porosity determination for a 2-ft thickness interval. Compositional lines are from Schlumberger (1987, p. 56).

Figure VI.4 Comparison of porous and nonporous crinoidal packstones from the upper limestone subunit from the small map area straddling T.31S., T.32S. and R.14W., R.15W. (see Figures 5.18 - 5.22). Porous samples from the Sinclair-Prairie #4 G. Oldfather well (*#34*, 7-T.31S.-R.14W.; at left) are coarser grained than the nonporous samples from the Sinclair-Prairie #1 Alice Oldfather (*#35*, 18-T.31S.-R.14W.; at right). These porous samples are coarser grained than all other crinoidal packstones observed in either well.

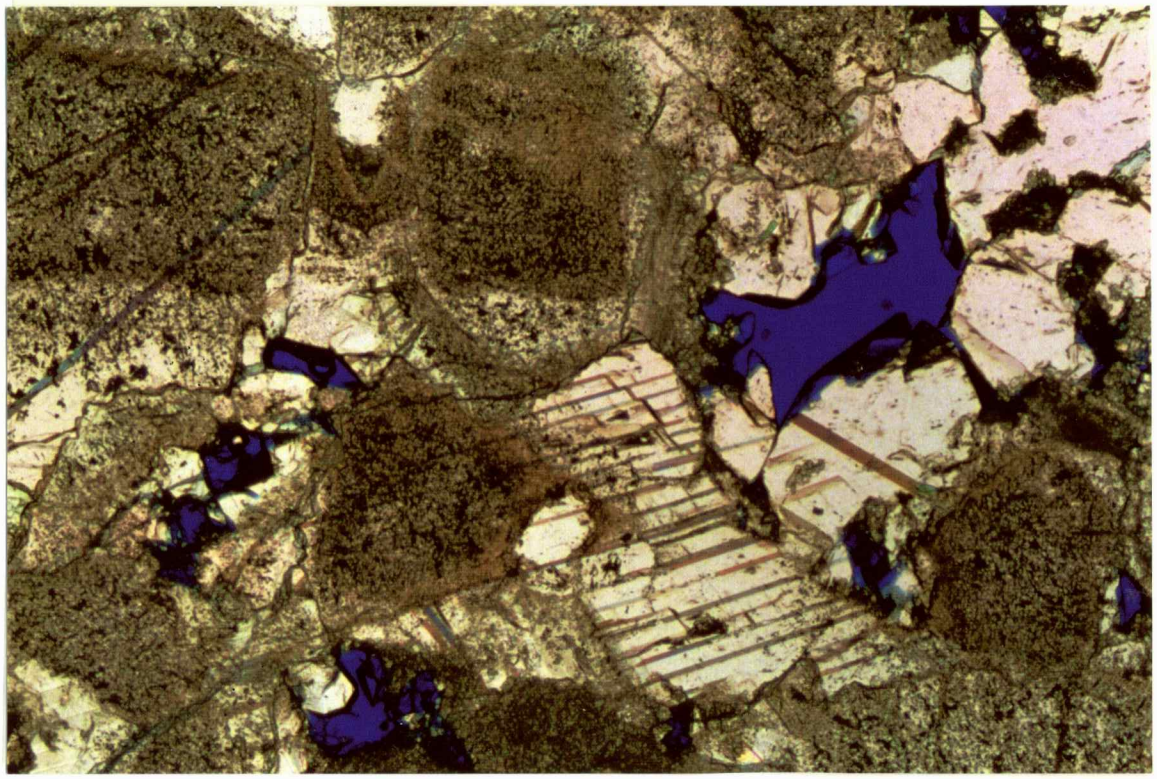

Figure VI.5. Thin-section photomicrograph of porosity (impregnated with blue epoxy) in a crinoidal packstone from the upper limestone subunit (4370-ft depth) in the Sinclair-Prairie #4 G. Oldfather well (*#34*, 7-T.31S.-R.14W.) shown in Figure VI.4. The dominant porosity is cement-reduced interparticle porosity (BP), with minor cement-reduced partial molds (MO), located primarily within crinoid grains.

APPENDIX VII -- REQUISITE CHEMICAL AND PHYSICAL CONDITIONS NECESSARY FOR REGIONAL DOLOMITIZATION

Extensive dolomitization is usually assumed to require an open system that is characterized by a high fluid/rock ratio. A flow of this fluid is necessary for dolomitization in order to both import Mg^{2+} and simultaneously export Ca^{2+} by the following chemical reaction:

$$2CaCO_3 + Mg^{2+} \rightleftharpoons CaMg(CO_3)_2 + Ca^{2+}$$

An implication of this reaction is that in a replacement process in which pre-existing limestone is converted to dolomite with conservation of carbonate (see Weyl, 1960; Murray, 1960; Blatt and others, 1980, p. 530), an increase in porosity will occur because dolomite has a smaller molar volume than that of calcite. Specifically, Davies (1979) stated that the increase in porosity would be between 6% and 13%, depending if the precursor limestone is composed of aragonite or calcite, respectively. Development of secondary porosity in association with dolomitization is common because the molar volume of the mineral dolomite is 12 to 13% smaller than that of calcite (Weyl, 1960; Blatt and others, 1980, p. 530). In a closed system in which the quantity of carbonate is fixed (i.e., locally sourced by the dissolution of calcite to the benefit of the precipitating dolomite), 12 to 13% porosity would hence develop. Seawater and groundwater also typically contain low concentrations of carbonate as compared to Mg^{+2} and Ca^{+2} (Weyl, 1960), therefore carbonate is most likely to be locally supplied from what is available with the rock itself.

A criticism of the dolomitization process implied by the above reaction is the requirement that only Mg^{2+} is brought into the system and only Ca^{2+} is removed (Tucker, 1990, p. 367), otherwise the Mg/Ca ratio would decrease until the reaction would not go forward. However, if new Mg^{2+} and CO_3^{2+} are brought into the system, instead of a mole-for-mole replacement of calcium by magnesium, the following additional dolomitizing reaction can occur (from Lippmann, 1973, p. 150):

$$Ca^{2+} + Mg^{2+} + 2CO_3^{2+} \rightleftharpoons CaMg(CO_3)_2$$

This reaction implies direct precipitation of dolomite and provides an uptake for the excess Ca^{2+} released by the previous reaction; a decrease in rock volume (i.e., increase in porosity) is therefore not necessary with dolomitization. The reaction that combines the processes of the above reactions is represented by the following equation from Lippmann (1973, p. 179)

$$CaCO_3 + Mg^{2+} + CO_3^{2+} \rightleftharpoons CaMg(CO_3)_2$$

In this reaction both the Mg^{2+} and CO_3^{2+} are supplied by the dolomitizing fluid, and all Ca^{2+} ions from the precursor limestone are incorporated into the dolomite. The degree to which porosity decreases or increases will therefore depend on how much Mg^{2+} and CO_3^{2+} can be brought into the system. Morrow (1982a) gave a dolomitizing reaction

$$(2\text{-}X)CaCO_3 + Mg^{2+} + XCO_3^{2+} \rightleftharpoons CaMg(CO_3)_2 + (1\text{-}X)Ca^{2+}$$

where X = 0.11 for an aragonitic precursor limestone, and 0.25 for a calcitic precursor limestone, **if** a volume-per-volume replacement occurs. If porosity increases with dolomitization in a calcite-dominated limestone such as the Viola, then X would have to be less than 0.25. Inasmuch as core and engineering data (Figures 8.1 and 8.2), and wireline log analysis (Figures 8.6, 8.7, and 8.10) indicates porosity increases with increasing dolomite content in the Viola, this suggests little CO_3^{2+} was probably brought into the system by the dolomitizing fluids. Although porosity appears to increase with increasing dolomitization in the Viola, this does not necessarily mean that the dolomitization created this porosity during the transformation of the precursor limestone to dolomite. It is also possible that the dolomitization could have merely played a passive role and merely rearranged the preexisting porosity system(s) of the precursor limestone (see Purser and others, 1994a). The basal limestone near its pinchout on the crest of the Chautauqua arch has porosity approaching 10 to 15% where it is most dolomitized (Figures 8.6 and 8.7), and this is consistent with a mole-for-mole replacement of $CaCO_3$, rather than a volume-for-volume replacement. Nevertheless, the pinchout of the basal limestone could have also been subject to partial dissolution by calcite-undersaturated water prior to dolomitization. Moldic and vugular porosity, which is dominant in this area (see Midcontinent Marine #1 North Hilger [*#28*] and #1 South Hilger [*#29*] core descriptions in Appendix IV) are not necessarily types of porosity directly related to the process of dolomitization. If this limestone was largely nonporous before dolomitization, perhaps intercrystalline porosity would be the dominant pore type if the dolomitization was controlled by conservation of carbonate. In areas where the lower and upper cherty dolomitic limestones are dolomitized and possess greater than 13% porosity (see Figure 8.2), the original limestone presumably had over 12-13% porosity before it was dolomitized. Most likely this precursor porosity was microscopic intergranular porosity contained within the partly lithified lime mudstone and moldic porosity.

Only a minor dolomitization can take place without an external source of magnesium. An echinoderm-rich limestone, composed of high-magnesium calcite (~15-19 mole % $MgCO_3$), would yield a rock composed of approximately 27-30% dolomite (Cander and others, 1988; Tucker, 1990, p. 367) if no more magnesium was brought into the system. The dolomite present in the basal and upper limestones (i.e., 10 to 25%, see Appendix IV) where these units are only partly dolomitized could therefore conceivably be accounted for by the magnesium that was already contained within them. Nonetheless, studies of the Lake Valley Formation in New Mexico (Leutoff and Meyers, 1984) indicate formation of microdolomite inclusions within echinoderm grains may shunt off as much as 75% of the available intraformational magnesium from participating in dolomitization of the at-large stratigraphic formation, hence extraformational magnesium may still be required for the minor dolomitization in the basal and upper limestones.

PLATE 1. EAST-WEST STRATIGRAPHIC CROSS-SECTION OF VIOLA FORMATION (V.E. = 195)

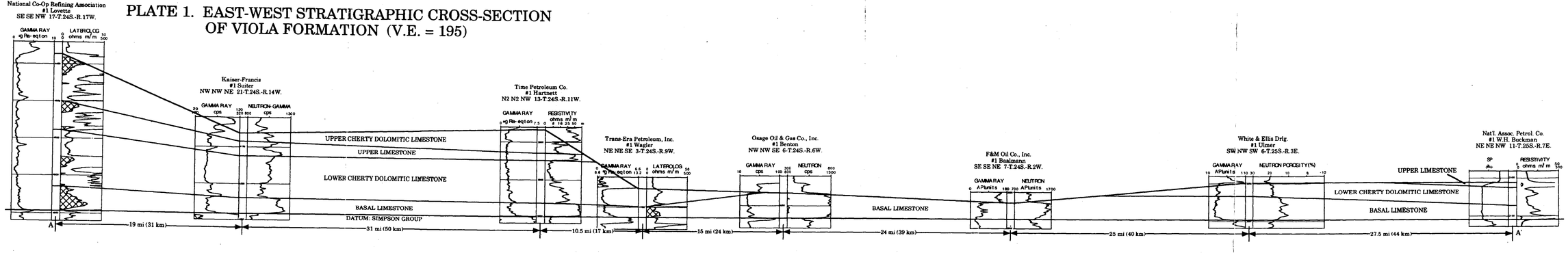

PLATE 2. SSW-NNE STRATIGRAPHIC CROSS-SECTION OF VIOLA FORMATION (V.E. = 195)